# NATURE ENVIRONMENT & POLLUTION TECHNOLOGY

*A Multidisciplinary, International Journal on Diverse Aspects of Environment*

## Technoscience Publications
website: www.neptjournal.com

# Nature Environment and Pollution Technology
**(An International Quarterly Scientific Research Journal)**

### INSTRUCTIONS TO AUTHORS

## Scope of the Journal

The Journal publishes original research/review papers covering almost all aspects of environment like monitoring, control and management of air, water, soil and noise pollution; solid waste management; industrial hygiene and occupational health hazards; biomedical aspects of pollution; conservation and management of resources; environmental laws and legal aspects of pollution; toxicology; radiation and recycling etc. Reports of important events, environmental news, environmental highlights and book reviews are also published in the journal.

## Format of Manuscript

- The manuscript (mss) should be typed in double space leaving wide margins on both the sides.
- First page of mss should contain only the title of the paper, name(s) of author(s) and name and address of Organization(s) where the work has been carried out along with the affiliation of the authors.

# Nature Environment and Pollution Technology
## Vol. 22, No. (4), December 2023

# CONTENTS

## The Journal is Currently **Abstracted and Indexed** in:

- CNKI Scholar (China National Knowledge Infrastructure)
- Scopus Cite Score (2022) 0.90
- Scopus®, SJR (2022) 0.191
- Index Copernicus (2022) = 128.35
- Indian Science Abstracts, New Delhi, India
- Chemical Abstracts, U.S.A.
- Pollution Abstracts, U.S.A.
- Elsevier Bibliographic Databases
- Paryavaran Abstract, New Delhi, India
- Zoological Records
- CAB Abstracts, U.K.
- Electronic Social and Science Citation Index (ESSCI)
- Indian Citation Index (ICI)
- CrossRef (DOI)
- EBSCO: Environment Index™
- ProQuest, U.K.
- Google Scholar
- DOAJ
- Zetoc
- J-Gate
- Environment Abstract, U.S.A.
- Centre for Research Libraries
- Elektronische Zeitschriftenbibliothek (EZB)
- CSA: Environmental Sciences and Pollution Management
- Access to Global Online Research in Agriculture (AGORA)
- Present in UGC-CARE List (Group II)

- WorldCat (OCLC)
- British Library
- Connect Journals (India)
- Indian Science
- JournalSeek
- Research Bible (Japan)
- SHERPA/RoMEO
- Directory of Science
- AGRIS (UN-FAO)
- Ulrich's (Refereed) database

- UDL-EDGE (Malaysia) Products like i-Journals, i-Focus and i-Future

**www.neptjournal.com**

# Nature Environment and Pollution Technology

# Overview of Helminths in Land Vertebrates from the Mordovia Nature Reserve, European Russia

**N. Yu. Kirillova\*** (iD)**, A. B. Ruchin\*\*†** (iD)**, A. A. Kirillov\*** (iD)**, I. V. Chikhlyaev\* and M. A. Alpeev\*\***

\*Laboratory of Biodiversity, Institute of Ecology of Volga River basin of RAS, Samara Federal Research Center of RAS, Togliatti 445003, Russia

\*\*Joint Directorate of the Mordovia State Nature Reserve and National Park "Smolny", Saransk 430005, Russia

†Corresponding author: Alexander B. Ruchin; ruchin.alexander@gmail.com

## ABSTRACT

In this study, we summarized our own and literature data on the helminth fauna in amphibians, reptiles, birds, and mammals inhabiting the Mordovia Nature Reserve (European Russia). The history of research on parasitic worms in vertebrates has more than 70 years here. Nowadays, 242 species of helminths have been identified in vertebrates in this protected area: 54 cestodes, 87 trematodes, 98 nematodes, and 3 acanthocephalans. Of these, 169 helminth species have an indirect life cycle, while 73 develop directly. 217 revealed parasite species use vertebrates as definitive hosts and 21 as intermediate and/or parathenic hosts. Three species of trematodes, *Gorgoderina vitelliloba*, *Haplometra cylindracea*, and *Opisthioglyphe ranae* combine the larval and mature lifestyle stages in amphibians. The most diverse helminth fauna is in rodents (41 species), birds (38), artiodactyls (37), and insectivores (35). Less rich in amphibians (32), bats (32), reptiles (26), and carnivores (19). Only six parasite species are found in hares. Most of the helminth species recorded in the vertebrates of the Mordovia Nature Reserve belong to the Palearctic faunistic complex – 107 species. Fifty-eight species are cosmopolitan. The range of 39 species covers the Holarctic. The distribution of 37 species of helminths is limited to Europe. Seventy-three of 242 species found in the nature reserve's vertebrates have medical and veterinary importance as potential pathogens of dangerous zoonoses.

## INTRODUCTION

Population growth, industrialization, expansion of transport communications, and tourism, combined with intensive agriculture, have led to increased exploitation of natural resources and loss of biodiversity caused by human activity. Nowadays, almost no natural ecosystems are left in Europe that have not been affected by anthropogenic activity (Poulin & Morand 2004, Kirillov et al. 2012). Protected areas are characterized by the undisturbed structure of biocenoses and minimal anthropogenic impact on them. Natural ecosystems with rich fauna and flora are often preserved only in nature reserves (Pringle 2017, Ghosh-Harihar et al. 2019, Afonina & Tashlykova 2021, Kaicheen & Mohd-Azlan 2022, Vasenkova et al. 2022). In this context, research in protected areas has always attracted the attention of parasitologists as areas where helminths can freely carry out their life cycles (Turner & Getz 2010, Kouassi et al. 2015, Herczeg, et al. 2016, Chikhlyaev et al. 2020, Kononova & Prisniy 2020, Bhat et al. 2022, Ieshko et al. 2022, Martinez-Sotelo et al. 2022).

An extensive study of the helminth fauna of different species of wild vertebrates is of general biological significance from the ecological, biocenotic, and zoogeographic aspects. Helminths, like other parasites, are a necessary component of a sustainable natural ecosystem, an integral part of the world's biodiversity (Poulin & Morand 2004, Horwitz & Wilcox 2005, Dobson et al. 2008).

The disappearance of parasites in biocenoses can lead to extensive and unforeseen consequences that will affect the condition and abundance of most animal species (Dobson et al. 2008, Orlova & Orlov 2019). On the other hand, interest in wild vertebrates from an applied aspect is determined primarily by their epidemiological and epizootological role as involvement in the preservation and distribution of natural focal zoonoses dangerous to humans, domestic and game animals (Georgopoulou & Tsiouris 2008, Froeschke & Matthee 2014, Bordes et al. 2015, Krucken et al. 2017, Recht et al. 2020, Romashov et al. 2021). As a rule, protected areas are surrounded by agricultural landscapes, livestock farms, and settlements. Wild vertebrates can move freely

from the reserve to the surrounding areas. The movement freedom of animals creates the possibility, if there are foci of zoonoses in the territory of reserves, to spread them to the surrounding territories. The reverse case is also possible. However, the main role in preserving and distributing natural focal helminthic zoonoses belongs to wild vertebrates.

The first helminthological studies in the Mordovia Nature Reserve began with the work of Nizhny Novgorod parasitologists in the late 1940s. The results of these studies were published in only a few publications on helminths in rodents, insectivores, bats, lagomorphs, carnivores, and ungulates (Shaldybin 1957, 1964, Matevosyan 1964a, 1964b, Shtarev 1967, 1971, Machinsky & Semov 1974, Nazarova 1974a, 1974b, Shtarev et al. 1978). Most attention was paid to the helminth fauna of introduced animals such as *Bison bonasus*, *Cervus nippon*, *Cervus elaphus*, and *Nyctereutes procyonoides*. Oliger (1952, 1957) published information on helminths of the tetraonid birds in European Russia, including data on this Nature Reserve. Since 2003, data about the parasitic worms in the animals of the protected area have increased quickly as a result of the partnership between staff of the Mordovia Nature Reserve, Mordovia State University (Saransk), and the Institute of Ecology of the Volga Basin of RAS (Togliatti). The first data on helminths of amphibians of Mordovia (Ryzhov et al. 2004, Chikhlyaev et al. 2009, Ruchin & Chikhlyaev 2013, Ivanov et al. 2019), reptiles (Ruchin & Kirillov 2012, Kirillov et al. 2015a), birds (Kirillov et al. 2023), and bats (Kirillov et al. 2015b) were published. Some parasitological manuscripts-reports are stored in the Mordovia Reserve, which began to be published only recently as Oliger's works (2016a, 2016b). Data on helminths in vertebrates of the reserve were partially included in some reviews and regional summaries (Bykhovskaya-Pavlovskaya 1962, Gvozdev et al. 1970, Ryzhikov et al. 1978, 1979, Kostyunin 2010, Kirillov et al. 2012, Chikhlyaev & Ruchin 2014, Chikhlyaev et al. 2015). In 2016, we published the first monographic summary of parasitic worms in terrestrial vertebrates of the Mordovia Nature Reserve, which contains information on helminth fauna of amphibians, reptiles, birds, and mammals (Ruchin et al. 2016). Nowadays, data on parasitic worms of vertebrates are contained in 41 papers and reviews.

The Mordovia Nature Reserve, one of the oldest in Russia, was organized in 1936. The territory of the protected area is part of the Temnikovsky district of the Republic of Mordovia, and currently, its area is 321.62 km$^2$. Its main task is to preserve the natural landscapes of the southern woodlands, extending along the border of mixed broadleafed forests and forest-steppe (Ruchin et al. 2016).

The Mordovia Nature Reserve is located in the northwestern part of the Volga Upland and occupies the wooded right bank of the Moksha River. From the North, the border runs along the Satis River, the right tributary of the Moksha River, and further to the East – along the Arga River, which flows into the Satis River. The western border goes along the Chernaya, Satis, and Moksha Rivers. Forest-steppe approaches from the south, naturally limiting the boundary of this protected area (Gafferberg 1960, 2015). In terms of climate, the territory of the reserve is included in the Atlantic-continental region of the temperate zone (Ruchin et al. 2016, Gafferberg 1960, 2015).

The water network of the nature reserve is represented by small rivers Pushta, Bolshaya Malaya Chernaya, Arga, and streams flowing into the Moksha River. Most of the territory is included in the catchment area of the Pushta River, which flows into the Satis River at the border of the protected area. The hydrology of rivers is significantly affected by beaver dams, which flood large areas. In dry years, the riverbed dries up to the very lower reaches. There are about two dozen lakes in the southwestern part of the nature reserve. These are the oxbows of the Moksha River, sometimes large and deep like Picherki, Bokovoe, Taratinskoe, Inorki, and Valza (Ruchin et al. 2016, Grishutkin 2013, Artaev & Grishutkin 2014). The fauna of the Mordovia Nature Reserve includes 10 species of amphibians, 7 reptiles, 219 birds, and 63 mammals (Ruchin et al. 2016, Artaev et al. 2012, Artaev & Smirnov 2016).

This work is based on the analysis of literature data and the results of our own studies of the helminth fauna of vertebrates in this protected area. Own material on helminths of amphibians, reptiles, insectivores, bats, birds and myomorph rodents, collected by the authors from various sites in the Mordovia Nature Reserve in 2008, 2009, 2011, 2014, 2021 and 2022. Fig. 1 shows the study localities of the helminth fauna in land vertebrates.

Helminthological studies of vertebrates were carried out in the vicinity of the Pushta village, on the cordons of the Nature Reserve and their vicinities. Only amphibians, insectivores, and myomorph rodents that fell into the pitfall traps of our fellow entomologists were studied in sites called "compartments". In site "440th compartment", only amphibians and reptiles were studied. In the works by Shaldybin (1964) and Oliger (1952, 1957, 2016a, 2016b), the study sites of the helminth fauna of vertebrates in the Mordovia Nature Reserve were not specified.

The international databases Scopus, Web of Science Core Collection, Google Scholar, and Russian scientific electronic library (eLIBRARY.ru) were used to search scientific literature on the helminths fauna in vertebrates from the Mordovia State Nature Reserve. We used both Russian and
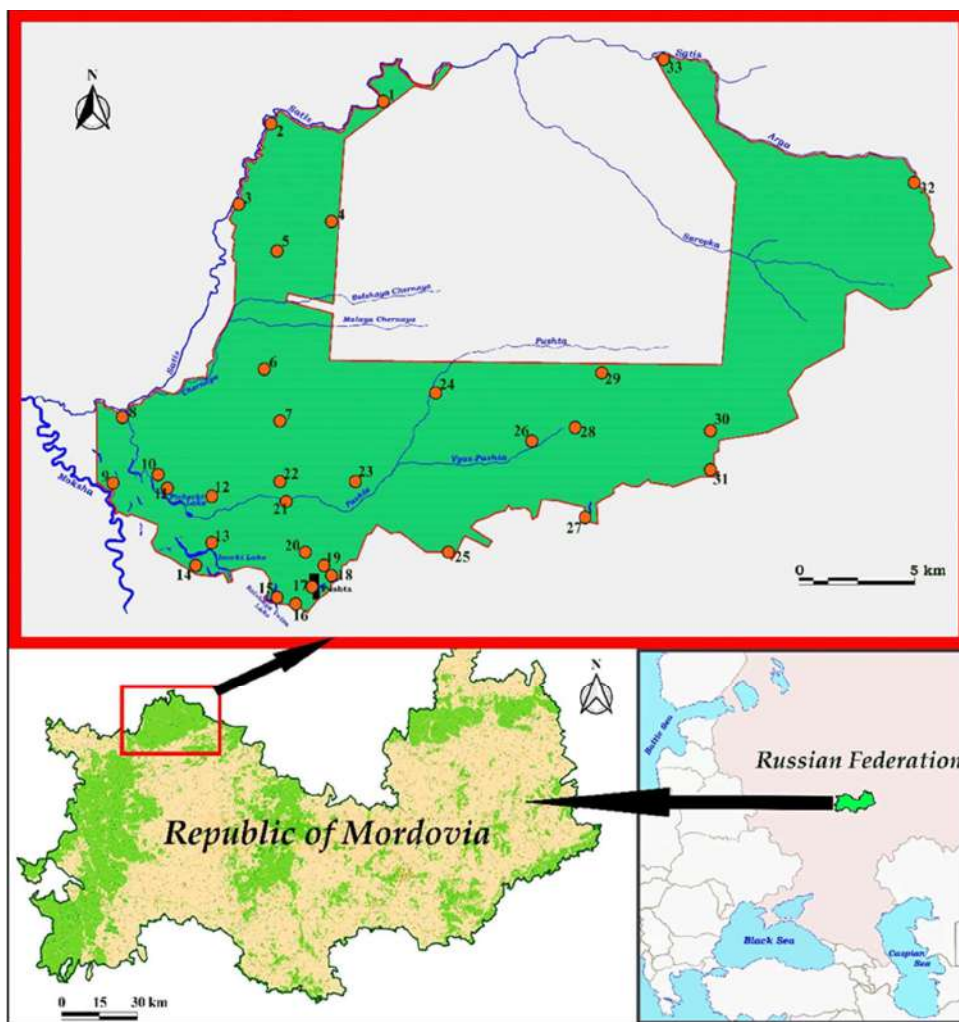
Fig. 1: A schematic map of the helminth studying sites in the Mordovia State Nature Reserve. Red circles in the map showed the places, where animal helminths were studied. 1 – Cordon "Srednyay Melnitsa", 2 – Cordon "Plotomoyka", 3 – Cordon "Pilna", 4 – 145th compartment, 5 – 170th compartment, 6 – 276th compartment, 7 – 330th compartment,  8 – Vorovskoy cordon, 9 – Taratinskiy cordon, 10 – 378th compartment, 11 – Picherki Lake, 12 – 405th compartment, 13 – Inorskiy cordon, 14 – 443rd compartment, 15 – Bolshaya Valza Lake, 16 – Novenkiy cordon, 17 – Pushta village, 18 – Valzenskiy cordon, 19 – 441st  compartment, 20 – 440th compartment, 21 – Cordon "Dolgiy Most", 22 – 383rd compartment, 23 – 386th compartment, 24 – 308th compartment, 25 – Drozhdenovskiy cordon, 26 – Zhegalovskiy cordon, 27 – Pavlovskiy cordon, 28 – 342nd compartment, 29 – 290th compartment, 30 – 347th compartment, 31 – Polyanskiy cordon, 32 – Steklyanniy cordon, 33 – Novenkovskiy cordon.

English characters to enter our search strings in the Russian database eLIBRARY.ru. Most of the literature sources, including those not indexed in electronic databases, were taken from the library of the Mordovia Nature Reserve. The analysis of parasitological literature was conducted between 1950 and 2022.

The helminth taxonomy is based on the Fauna Europaea (https://fauna-eu.org) and the Global Cestode Database (http://tapewormdb.uconn.edu). The voucher specimens of parasitic worms are stored in the Parasitological collection at the Institute of Ecology of Volga Basin of RAS, Togliatti, Russia.

## PARASITIC WORMS OF VERTEBRATES IN THE MORDOVIA NATURE RESERVE

Nowadays, taking into account recent concepts on the helminth taxonomy, the list of parasitic worms in land vertebrates of the Mordovia Nature Reserve includes 242 species: 54 cestodes, 87 trematodes, 98 nematodes, and 3 acanthocephalans.

### Helminths of Amphibians (Amphibia)

The helminth fauna in amphibians of the protected area includes 32 species: 25 trematodes and 7 nematodes

(Ryzhov et al. 2004, Ruchin et al. 2016, Chikhlyaev et al. 2009, Ruchin & Chikhlyaev 2013, Kirillov et al. 2012, Chikhlyaev & Ruchin 2014, Chikhlyaev et al. 2015) (Table 1).

Twenty-one helminth species in mature forms parasitize amphibians and use them as definitive hosts. While eight trematode species occur in amphibians at the larval stage. Three species (trematodes *Gorgoderina vitelliloba*,

Table 1: The list of helminths in amphibians (Amphibia) from the Mordovia Nature Reserve.

| Species | D[1] | *Pelophylax ridibundus* | *Pelophylax lessonae* | *Rana arvalis* | *Rana temporaria* | *Bufo bufo* | *Pelobates vespertinus* | *Bombina bombina* | *Lissotriton vulgaris* | *Triturus cristatus* |
|---|---|---|---|---|---|---|---|---|---|---|
| **Trematoda** | | | | | | | | | | |
| *Halipegus ovocaudatus* | E | | + | | + | | | | | |
| *Diplodiscus subclavatus* | P | | + | + | + | | + | | + | + |
| *Gorgodera cygnoides* | P | | + | + | | + | | + | | |
| *Gorgodera microovata* | E | | + | + | + | + | | | | |
| *Gorgodera pagenstecheri* | P | | + | | | | | | | |
| *Gorgoderina vitelliloba* | P | | | + | + | + | | | | |
| *Haplometra cylindracea* | P | | | + | | | | | | |
| *Haematoloechus abbreviatus* | E | | | | | | | + | | |
| *Haematoloechus asper* | E | | + | | | | | | | |
| *Haematoloechus variegatus* | P | | + | | | | | | | |
| *Skrjabinoeces similis* | P | | + | | | | | | | |
| *Paralepoderma cloacicola*, mtc. | P | | + | + | | | + | | | |
| *Opisthioglyphe ranae* | P | + | + | + | | | | | | |
| *Pleurogenes claviger* | C | + | + | | + | + | | | | |
| *Pleurogenes intermedius* | P | | | + | | | | | | |
| *Pleurogenoides medians* | P | | + | + | | + | | | | |
| *Brandesia turgida* | P | | + | | | | | | | |
| *Prosotocus confusus* | P | + | + | | | | | | | |
| *Strigea falconis*, mtc. | C | | | + | | | | | | |
| *Strigea sphaerula*, mtc. | P | | + | + | | | | | | |
| *Strigea strigis*, mtc. | P | | + | + | + | | + | | | |
| *Alaria alata*, msc. | C | | + | + | | + | + | | | |
| *Neodiplostomum spathoides*, mtc. | P | | | + | | | + | | | |
| *Tylodelphys excavata*, mtc. | E | | + | | | | | + | | |
| *Astiotrema monticelli*, mtc. | E | | + | | | + | + | | | |
| **Nematoda** | | | | | | | | | | |
| *Amphibiocapillaria tritonispunctati* | E | | | | | | | | | + |
| *Rhabdias bufonis* | P | | + | + | + | + | + | | | |
| *Oswaldocruzia filiformis* | H | | + | + | + | + | + | | | |
| *Megalobatrachonema terdentatum* | E | | | | | | | | + | |
| *Cosmocerca ornata* | E | | + | + | + | + | + | + | | |
| *Oxysomatium brevicaudatum* | H | | | | | + | + | | | |
| *Icosiella neglecta* | C | + | + | + | + | | | | | |
| Total | | 4 | 23 | 18 | 10 | 11 | 10 | 4 | 2 | 2 |

[1] Here and in Tables 2–9, D – distribution, E – Europe, C – Cosmopolitan, H – Holarctic, P – Palaearctic.

*Haplometra cylindracea,* and *Opisthioglyphe ranae*) combine the larval and adult development stages in amphibians and characterize them as amphixenic hosts.

All found helminth species are obligate parasites of amphibians. According to the degree of host specificity, 30 species of trematodes and nematodes belong to parasites-generalists occurring in various amphibian species. Of these, 21 species are polyhostal parasites of amphibians. Nine more species (trematodes *Gorgodera pagenstecheri*, *G. microovata*, *Haplometra cylindracea*, *Haematoloechus asper*, *Skrjabinoeces similis*, *Pleurogenes intermedius*, *Brandesia turgida*, *Neodiplostomum spathoides*, mtc. and nematode *Icosiella neglecta*) are oligohostal parasites of frogs

from the family Ranidae. The nematodes *Amphibiocapillaria tritonispunctati* and *Megalobatrachonema terdentatum* are host-specific parasites of newts from the genera *Triturus* and *Lissotriton*, respectively.

No helminth species was found to parasitize the entire range of infected amphibian species in the Mordovia Nature Reserve (Table 1). The trematode *Diplodiscus subclavatus* and the nematode *Cosmocerca ornata* have the widest host ranges (6 amphibian species each). Two nematodes *Rhabdias bufonis* and *Oswaldocruzia filiformis* were revealed in five amphibian species each. The trematodes *Gorgodera cygnoides*, *G. microovata*, *Pleurogenes claviger*, *Strigea strigis*, mtc., *Alaria alata*, msc. and the nematode

Table 2: The list of helminths in reptiles (Reptilia) from the Mordovia Nature Reserve.

| Species | D | Lacerta agilis | Zootoca vivipara | Anguis fragilis | Natrix natrix | Vipera berus |
|---|---|---|---|---|---|---|
| Cestoda | | | | | | |
| *Spirometra erinaceieuropaei*, plc. | P | | | | + | |
| *Ophiotaenia europaea* | E | | | | + | |
| Trematoda | | | | | | |
| *Plagiorchis elegans* | H | + | + | | | |
| *Plagiorchis molini* | P | + | + | | | |
| *Leptophallus nigrovenosus* | P | | | | + | + |
| *Astiotrema monticelli* | E | | | | + | |
| *Telorchis assula* | P | | | | + | |
| *Macrodera longicollis* | P | | | | + | |
| *Paralepoderma cloacicola* | P | | | | + | |
| *Opisthioglyphe ranae* | P | | | | + | |
| *Strigea falconis*, mtc. | C | | | | + | |
| *Strigea sphaerula*, mtc. | P | | | | + | + |
| *Strigea strigis*, mtc. | P | | | | + | + |
| *Alaria alata*, msc. | C | | | | + | + |
| *Neodiplostomum spathoides*, mtc. | P | | | | + | |
| Nematoda | | | | | | |
| *Rhabdias fuscovenosa* | H | | | | + | + |
| *Strongyloides mirzai* | P | | | | + | |
| *Oswaldocruzia filiformis* | H | + | + | + | | + |
| *Entomelas entomelas* | P | | | + | | |
| *Entomelas dujardini* | P | | | + | | |
| *Oxysomatium brevicaudatum* | H | | | + | | |
| *Physocephalus sexalatus*, juv. | C | | | | + | |
| *Physaloptera clausa*, juv. | H | + | + | | | + |
| *Agamospirura minuta*, juv. | E | | | + | + | + |
| Acanthocephala | | | | | | |
| *Centrorhynchus aluconis*, juv. | P | | | | | + |
| *Sphaerirostris picae*, juv. | P | | + | | | |
| Total | | 4 | 5 | 5 | 17 | 9 |

*Icosiella neglecta* were found in four host species each. The trematodes *Gorgoderina vitelliloba*, *Paralepoderma cloacicola*, larvae, *Opisthioglyphe ranae*, *Pleurogenoides medians*, *Astiotrema monticelli*, mtc. parasitize amphibians of three species each. For five trematode species (*Halipegus ovocaudatus*, *Prosotocus confusus*, *Strigea sphaerula*, mtc., *Neodiplostomum spathoides*, mtc., *Tylodelphys excavata*, mtc. and the nematode *Oxysomatium brevicaudatum*) the host range is limited to two species of anurans. Other 11 helminth species were found only in one host species (Table 1).

The most number of helminth species was found in *Pelophylax lessonae* (23 species). The helminth fauna of *Rana arvalis* (18), *Bufo bufo* (11), *Rana temporaria,* and *Pelobates vespertinus* (10 each) is less diverse. The smallest number of helminth species was identified in *Pelophylax ridibundus* and *Bombina bombina* (4 each), *Lissotriton vulgaris,* and *Triturus cristatus* (2 each) (Table 1).

Four species of parasitic worms found in amphibians in the Mordovia State Nature Reserve are cosmopolitans. Seventeen species of helminths have a Palearctic distribution. Two nematode species are distributed in the Holarctic. The distribution of nine species of trematodes and nematodes is limited to the territory of Europe (Table 1).

## Helminths of Reptiles (Reptilia)

A total of 26 species of helminths were revealed in the reptiles of the Nature Reserve: 2 cestodes, 13 trematodes, 9 nematodes, and 2 acanthocephalans (Kirillov et al. 2012, 2015a, Ruchin & Kirillov 2012, Ruchin et al. 2016) (Table 2).

Fifteen species of helminths use reptiles as definitive hosts. Reptiles are paratenic hosts for other 11 species of parasites found at the larval stages. Most helminth species recorded are obligate parasites of reptiles. Only two species, the trematodes *Plagiorchis elegans* and *Opisthioglyphe ranae*, belong to occasional and facultative parasites of reptiles. The finding in *Natrix natrix* of a host-specific parasite of the amphibians, *O. ranae* is a case of post-cyclic parasitism. This trematode can be considered as a temporary transit inhabitant of the snake intestine, where the parasite came from tailless amphibians swallowed by reptiles. *Plagiorchis elegans* is a generalist parasite found in many vertebrates of different classes (birds, mammals, and reptiles), more common in passerine birds. The metacestode *Spirometra erinaceieuropaei* are parasitizing fish, amphibians, and reptiles. Seven species of parasitic worms (nematodes *Oswaldocruzia filiformis*, *Oxysomatium brevicaudatum*, trematodes *Strigea falconis*, mtc., *S. sphaerula*, mtc., *S. strigis*, mtc., *Neodiplostomum spathoides*, mtc. and *A. alata*, msc.) belong to amphibian and reptile generalists. Juveniles of nematodes *Physocephalus sexalatus*, *Physaloptera clausa*,

*Agamospirura minuta,* and acanthocephalans *Centrorhynchus aluconis*, *Sphaerirostris picae* are reptile generalists. The cestode *Ophiotaenia europaea*, the trematodes *Leptophallus nigrovenosus*, *Astiotrema monticelli*, *Telorchis assula*, *Macrodera longicollis*, *Paralepoderma cloacicola*, the nematodes *Rhabdias fuscovenosa* and *Strongyloides mirzai* are generalist parasites in colubride snakes. The trematode *Plagiorchis molini* is a specific parasite of lacertid lizards, while *Entomelas entomelas* and *E. dujardini* belong to parasite specialists in *Anguis* slowworms.

We did not find a single helminth species that would be parasitized in all five studied reptile species in the Mordovia Nature Reserve. The nematode *Oswaldocruzia filiformis* was identified in four species of reptiles. The nematodes *Physaloptera clausa*, juv., *Agamospirura minuta* were found in three host species (Table 2). The trematodes *Plagiorchis elegans*, *P. molini*, *Leptophallus nigrovenosus*, *Strigea sphaerula*, mtc., *S. strigis*, mtc., *Alaria alata*, msc. and nematode *Rhabdias fuscovenosa* found in two host species each. Another 16 helminth species were registered only in one host species (Table 2).

The greatest helminth diversity was revealed in *Natrix natrix* – 17 species. The list of *Vipera berus* helminths includes 9 species. The helminth fauna of lizards is less diverse. So, in *Zootoca vivipara* and *Anguis fragilis*, five parasites were found, and in *Lacerta agilis* four helminth species were found (Table 2).

Most of the helminths of reptiles belong to the Palearctic complex (15 species). Five species of helminths are common in the Holarctic. Three parasite species are cosmopolitans. Distribution of three more species of parasitic worms restricted to Europe (Table 2).

Taxonomic remarks. *Agamospirura minuta*, juv. is a specific parasite of reptiles, usually parasitizing the slowworm *Anguis fragilis* and less common in other lizards and snakes (Sharpilo 1976). The final host is unknown. Lewin (1990) found similar nematode larvae in reptiles of Poland and identified them as Protostrongylidae sp. In his opinion, the identification by Sharpilo (1976) of *Agamospirura* larva as Spirurida is erroneous.

## Helminths of Birds (Aves)

A total of 38 species of parasitic worms were revealed in the birds of the Mordovia Nature Reserve: 16 cestodes, 14 trematodes, and 8 nematodes (Oliger 1952, 1957, 2016a, Bykhovskaya-Pavlovskaya 1962, Kirillov et al. 2012, 2023, Ruchin et al. 2016) (Tables 3 and 4).

All of them parasitize birds at the mature stage and are their obligate parasites, with the exception of

Table 3: The list of helminths in passerine birds (Aves, Passeriformes) from the Mordovia Nature Reserve.

| Species | D | Turdus philomelos | Turdus viscivorus | Turdus merula | Parus major | Cyanistes caeruleus | Fringilla coelebs | Carduelis carduelis | Pyrrhula pyrrhula | Sylvia nisoria | Ficedula hypoleuca | Muscicapa striata | Hippolais icterina | Phylloscopus collybita | Erithacus rubecula | Motacilla alba | Hirundo rustica |
|---|---|---|---|---|---|---|---|---|---|---|---|---|---|---|---|---|---|
| **Cestoda** | | | | | | | | | | | | | | | | | |
| *Dilepis undula* | H | + | + | + | | | | | | | | | | | | | |
| *Emberizotaenia reductorhyncha* | P | | | | + | + | | | | | | | | | | | |
| *Passerilepis crenata* | H | + | + | | | | + | + | | + | + | | | | + | | |
| *Wardium farciminosa* | C | | | | | | | | | | + | | + | | | | |
| *Monorcholepis dujardini* | P | + | | | | | | | | | | | | | | | |
| **Trematoda** | | | | | | | | | | | | | | | | | |
| *Urogonimus macrostomus* | H | + | | | + | | + | | + | | | + | | | | | + |
| *Leucochloridium holostomum* | C | | | + | | | | | | | | | | | | | |
| *Leucochloridium phragmitophila* | P | | | | | | | | | | | | | | + | | |
| *Mosesia amplavaginata* | P | | | | | | + | | | | | | | | | | |
| *Plagiorchis elegans* | H | | | | + | | | | | | | | | + | | | |
| *Plagiorchis maculosus* | C | | | | | | | | | | | | + | | | + | |
| *Morishitium polonicum* | P | + | | + | | | | | | | | | | | | | |
| *Brachylecithum fringillae* | P | | | | | | + | | | | | | | | | | |
| *Brachylecithum attenuatum* | P | | | + | | | | | | | | | | | | | |
| **Nematoda** | | | | | | | | | | | | | | | | | |
| *Aonchotheca exilis* | H | + | + | | | | | | | | | | | | | | |
| *Acuaria subula* | P | | | | | | | | | | | | + | | | | |
| *Hadjelia truncata* | P | + | + | | | | | | | | | | | | + | | |
| *Porrocaecum ensicaudatum* | H | + | + | | | | | | | | | | | | | | |
| *Physocephalus sexalatus*, juv. | C | | + | | | | | | | | | | | | | | |
| *Diplotriaena henryi* | P | | | | | + | | | | | | | | | | | |
| Total | | 8 | 6 | 4 | 3 | 2 | 4 | 1 | 1 | 1 | 2 | 1 | 3 | 1 | 3 | 1 | 1 |

the nematode *Physocephalus sexalatus*. Birds serve as paratenic hosts for these nematode larvae. The trematode *Plagiorchis elegans* is a parasite generalist found in a wide range of vertebrates (birds, mammals and reptiles) and more common in passerines. The cestodes *Dilepis undula*, *Passerilepis crenata*, trematodes *Mosesia amplavaginata*, *Plagiorchis maculosus*, *Prosthogonimus ovatus*, *Eumegacetes triangularis*, *Cotylurus cornutus* s.l., nematodes *Acuaria subula*, *Hadjelia truncata* and *Diplotriaena henryi* are bird generalists, parasitising a wide range of birds from different orders. Six species (the cestodes *Emberizotaenia reductorhyncha*, *Wardium farciminosa*, trematodes *Urogonimus macrostomus*, *Phaneropsolus micrococcus*, are specific parasites of Passeriformes birds. The cestodes *Liga crateriformis* and *Raillietina frontina*

are helminths specialists of woodpeckers. The trematodes *Brachylecithum attenuatum*, *Morishitium polonicum,* and cestode *Monorcholepis dujardini* are specialist parasites in thrushes. Only waders are parasitized by the cestodes *Anomolepis glareola*, *Anomotaenia citrus*, *Kowalewskiella cingulifera*, and the trematode *Leucochloridium perturbatum*. The trematode *Leucochloridium holostomum* is a specific parasite of Rallidae birds, less common in waders and thrushes. The trematode *Leucochloridium phragmitophila* is a specialist parasite of birds from the family Passeridae, and the trematode *Brachylecithum fringillae* is a specific parasite of finches. Eight species of helminths (the cestodes *Choanotaenia infundibulum*, *Paroniella urogalli*, *Raillietina penetrans*, *Skrjabinia cesticillus*, *S. polyuterina*, *Rhabdometra tomica*, nematodes *Trichostrongylus medius*

Table 4: The list of helminths in non-passerine birds from the Mordovia Nature Reserve.

| Species | D | Lyrurus tetrix | Tetrao urogallus | Tetrastes bonasia | Actitis hypoleucos | Dendrocopos major | Picus canus | Caprimulgus europaeus |
|---|---|---|---|---|---|---|---|---|
| **Cestoda** | | | | | | | | |
| *Dilepis undula* | H | | | | | + | | |
| *Choanotaenia infundibulum* | C | + | | | | | | |
| *Anomolepis glareola* | P | | | | + | | | |
| *Anomotaenia citrus* | H | | | | + | | | |
| *Kowalewskiella cingulifera* | P | | | | + | | | |
| *Liga crateriformis* | P | | | | | + | + | |
| *Passerilepis crenata* | H | | | | | + | | |
| *Monorcholepis dujardini* | P | | | | | | | |
| *Paroniella urogalli* | H | + | + | | | | | |
| *Raillietina frontina* | P | | | | | + | | |
| *Raillietina penetrans* | P | | + | | | | | |
| *Skrjabinia cesticillus* | C | + | + | + | | | | |
| *Skrjabinia polyuterina* | P | + | + | | | | | |
| *Rhabdometra tomica* | P | + | | | | | | |
| **Trematoda** | | | | | | | | |
| *Urogonimus macrostomus* | H | | | | | + | | |
| *Leucochloridium perturbatum* | H | | | | + | | | |
| *Phaneropsolus micrococcus* | P | | | | | | | + |
| *Plagiorchis elegans* | H | | | | | | | + |
| *Eumegacetes triangularis* | P | | | | | | | + |
| *Morishitium polonicum* | P | | | | | | | |
| *Prosthogonimus ovatus* | C | + | | | | | | |
| *Cotylurus cornutus* s.l. | C | | | | + | | | |
| **Nematoda** | | | | | | | | |
| *Aonchotheca exilis* | H | | | | | + | | |
| *Trichostrongylus medius* | E | + | | | | | | |
| *Porrocaecum ensicaudatum* | H | | | | | | + | |
| *Ascaridia compar* | C | + | + | + | | | | |
| *Hadjelia truncata* | P | | | | | | | |
| Total | | 8 | 5 | 2 | 5 | 6 | 2 | 3 |

and *Ascaridia compar*) are specialist parasites in galliform birds.

No helminths were found in 8 of 31 studied bird species in the Mordovia Nature Reserve: *Anthus trivialis*, *Aegithalos caudatus*, *Alcedo atthis*, *Carduelis chloris*, *Poecile montanus*, *Sylvia atricapilla*, *Luscinia luscinia* and *Phoenicurus phoenicurus*. No parasite species would be identified in all five studied bird species in the protected area (Tables 3 and 4). The cestode *Passerilepis crenata* and the

trematode *Urogonimus macrostomus* have the widest range of hosts, parasitizing 8 and 7 bird species, respectively. The cestode *Dilepis undula* was identified in four species of birds. The host range of the cestode *Skrjabinia cesticillus*, the trematode *Plagiorchis elegans*, and the nematodes *Aonchotheca exilis*, *Ascaridia compar* and *Hadjelia truncata* includes 3 bird species each. Eight parasite species (*Emberizotaenia reductorhyncha*, *Wardium farciminosa*, *Morishitium polonicum*, *Liga crateriformis*, *Paroniella*

Table 5: The list of helminths in insectivores (Eulipotyphla) from the Mordovia Nature Reserve.

| Species | D | Desmana moschata | Sorex araneus | Sorex minutus | Crocidura suaveolens | Neomys fodiens | Neomys anomalus | Erinaceus roumanicus |
|---|---|---|---|---|---|---|---|---|
| Cestoda | | | | | | | | |
| Dilepis undula | H | | + | | | | | |
| Hymenolepis erinacei | E | | | | | | | + |
| Ditestolepis diaphana | P | | + | + | | + | | |
| Insectivorolepis infirma | P | | + | + | | | | |
| Molluscotaenia crassiscolex | P | | + | + | | + | | |
| Neomylepis magnirostellata | P | | | | | + | | |
| Neoskrjabinolepis schaldybini | P | | + | + | | + | | |
| Pseudobothrialepis mathevossianae | P | | + | + | | | | |
| Spasskylepis ovaluteri | P | | + | + | | + | | |
| Staphylocystis brusatae | E | | | | + | | | |
| Staphylocystis furcata | P | | + | + | | | | |
| Staphylocystoides stefanskii | P | | + | | | | | |
| Vigisolepis spinulosa | P | | + | + | | | | |
| Trematoda | | | | | | | | |
| Brachylaima fulvum | P | | + | + | | + | | |
| Pseudoleucochloridium soricis | P | | + | + | | + | | |
| Metorchis bilis | H | | | | | + | | |
| Rubenstrema exasperatum | H | | + | + | | + | + | |
| Rubenstrema opisthovitellinus | P | | | | | + | | |
| Neoglyphe locellus | H | | | | | + | | |
| Neoglyphe sobolevi | H | | + | + | | | | |
| Omphalometra desmanae | E | + | | | | | | |
| Nematoda | | | | | | | | |
| Soboliphyme soricis | P | | | | | + | | |
| Paracrenosoma skrjabini | P | | | + | | | | |
| Aonchotheca erinacei | P | | | | | | | + |
| Aonchotheca kutorii | P | | + | + | | + | | |
| Calodium soricicola | P | | + | | | | | |
| Eucoleus oesophagicola | P | | + | | | + | | |
| Liniscus incrassatus | P | | + | | | + | + | |
| Longistriata paradoxi | P | | + | + | | | | |
| Longistriata neomi | E | | | | | + | + | |
| Physaloptera clausa | H | | + | | | | | + |
| Pseudophysaloptera soricina | H | | | + | | | | |
| Porrocaecum depressum, juv. | C | | + | | | | | |
| Hadjelia truncata, juv. | P | | + | | | | | |
| Acanthocephala | | | | | | | | |
| Centrorhynchus aluconis, juv. | P | | + | | | | | |
| Total | | 1 | 23 | 16 | 1 | 16 | 3 | 3 |

*urogalli*, *Skrjabinia polyuterina*, *Plagiorchis maculosus* and *Porrocaecum ensicaudatum*) were each found in two host species. Another 22 species of parasitic worms were found only in a single bird species (Tables 3 and 4).

Among birds, the most diverse fauna of helminths is in *Turdus philomelos* and *Lyrurus tetrix*, in which 8 species of parasites each were found. The helminth fauna of *Turdus viscivorus* and *Dendrocopos major* has six species of helminths each, while *Tetrao urogallus* and *Actitis hypoleucos* have five species of parasitic worms each. Fewer helminth species were found in *Turdus merula* and *Fringilla coelebs* (4 species each); *Parus major*, *Hippolais icterina*, *Erithacus rubecula* and *Caprimulgus europaeus* (3 species each). Two species of parasites were noted in *Tetrastes bonasia*, *Picus canus*, *Cyanistes caeruleus*, and *Ficedula hypoleuca*. Another six species of birds have only one helminth species each (Tables 3 and 4).

Half of the helminth species found in the birds of the protected area have a Palearctic distribution – 19 species. The Holarctic faunistic complex includes 9 species of parasitic worms. Also, 9 species of parasites have a cosmopolitan distribution. The distribution range of one helminth species is limited to Europe (Tables 3 and 4).

### Helminths of Insectivores (Eulipotyphla)

The helminth fauna in insectivores of the reserve includes 35 species: 13 cestodes, 8 trematodes, 13 nematodes, and one acanthocephalan (Shaldybin 1964, Kostyunin 2010, Kirillov et al. 2012, Ruchin et al. 2016) (Table 5).

Most parasites (32 species) use insectivores as final hosts. Insectivores serve as paratenic hosts for two species (acanthocephalan *Centrorhynchus aluconis* and nematode *Porrocaecum depressum*). The nematode juveniles of *Hadjelia truncata* is an occasional parasite of insectivores. This nematode is a specific avian parasite that only transits the intestinal tract of shrews and does not reach maturity in these hosts. The trematode *Metorchis bilis* is an occasional and facultative parasite of insectivores.

Thirty-two species of helminths use insectivores as obligate hosts and are their specialist parasites. The cestode *Dilepis undula* is a generalist parasite in bird insectivores and less common in rodents. The nematodes *Calodium soricicola*, *Eucoleus oesophagicola*, *Liniscus incrassatus*, and *Physaloptera clausa* are specialist parasites in insectivores, found in a wide range of species. Sixteen species of helminths, namely the cestodes *Molluscotaenia crassiscolex*, *Neoskrjabinolepis schaldybini*, *Spasskylepis ovaluteri*, *Staphylocystis furcata*, *Staphylocystoides stefanskii*, *Vigisolepis spinulosa*, trematodes *Brachylaima fulvum*, *Pseudoleucochloridium soricis*, *Rubenstrema exasperatum*,

*R. opisthovitellinus*, *Neoglyphe locellus*, *N. sobolevi*, nematodes *Soboliphyme soricis*, *Aonchotheca kutorii*, *Longistriata paradoxi* and *Pseudophysaloptera soricina*, are specific parasites in mammals of the family Soricidae, while the cestodes *Ditestolepis diaphana*, *Molluscotaenia crassiscolex*, *Pseudobothrialepis mathevossianae* and nematode *Paracrenosoma skrjabini* are specialist parasites in *Sorex* shrews. The cestode *Hymenolepis erinacei* and the nematode *Aonchotheca erinacei* are host-specific parasites of hedgehogs of the genus *Erinaceus*. The cestode *Staphylocystis brusatae* parasitizes only shrews of the genus *Crocidura*. The cestode *Neomylepis magnirostellata* and nematode *Longistriata neomi* are specific parasites in *Neomys* shrews. The trematode *Omphalometra desmanae* is a host-specific parasite of *Desmana moschata* and is a threatened species like its host.

We did not identify a single parasite species that would be found in all seven studied species of Eulipotyphla in the Mordovia Nature Reserve (Table 5). The trematode *Rubenstrema exasperatum*, revealed in four animal species, is most often found in the insectivores of the reserve. The host range of cestodes *Molluscotaenia crassiscolex*, *Neoskrjabinolepis schaldybini*, *Spasskylepis ovaluteri*, *Ditestolepis diaphana*, trematodes *Brachylaima fulvum*, *Pseudoleucochloridium soricis*, nematodes *Aonchotheca kutorii* and *Liniscus incrassatus* includes three species of insectivores. The cestodes *Insectivorolepis infirma*, *Pseudobothrialepis mathevossianae*, *Staphylocystis furcata*, *Vigisolepis spinulosa*, trematode *Neoglyphe sobolevi*, nematodes *Eucoleus oesophagicola*, *Longistriata paradoxi*, *L. neomi* and *Physaloptera clausa* use as hosts two insectivore species each. Another 17 helminth species were identified only in one host species (Table 5).

Among the studied species of insectivores, the largest number of helminths was found in *Sorex araneus* (23 species). The helminth fauna of *Neomys fodiens* and *Sorex minutus* is less diverse, with 16 species of parasites each. The helminth fauna in *Neomys anomalus* and *Erinaceus roumanicus* is poor (3 species each). *Desmana moschata* and *Crocidura suaveolens* have only one helminth species each (Table 5).

Most of the helminths (23 species) in insectivores belong to the Palearctic complex. Seven species are distributed in the Holarctic. For four species of parasites, distribution is limited to Europe. And only one species is cosmopolitan (Table 5).

Taxonomic remarks. The article by Shaldybin (1964) should be considered the first essential work on helminths in vertebrate animals from the Mordovia Nature Reserve. This work contains several problematic helminth species. Shaldybin (1964) described nematode *Capillaria reni*

Shaldybin, 1964, from the kidneys of *Neomys fodiens*. But since the time of the original description, no one else has found this helminth species. Therefore, we classify this nematode as a species inquirenda. The species *Aonchotheca petrovi*

Table 6: The list of helminths in bats (Chiroptera) from the Mordovia Nature Reserve.

| Species | D | Myotis daubentonii | Myotis dasycneme | Myotis brandtii | Myotis nattereri | Vespertilio murinus | Nyctalus noctula | Nyctalus leisleri | Pipistrellus nathusii | Pipistrellus pygmaeus |
|---|---|---|---|---|---|---|---|---|---|---|
| Cestoda | | | | | | | | | | |
| *Vampirolepis balsaci* | P | | | + | | | | | | |
| *Vampirolepis spasskii* | P | | | | | + | + | + | | |
| Trematoda | | | | | | | | | | |
| *Plagiorchis elegans* | H | + | | | | | + | | | |
| *Plagiorchis koreanus* | C | + | + | + | | + | + | + | + | |
| *Plagiorchis muelleri* | H | | | | | | + | | | |
| *Plagiorchis vespertilionis* | P | + | + | | | + | + | + | | |
| *Lecithodendrium linstowi* | P | + | | | | | + | | + | |
| *Lecithodendrium rysavyi* | E | | | | | + | + | + | + | + |
| *Lecithodendrium skrjabini* | E | | | | | + | + | + | + | + |
| *Paralecithodendrium skrjabini* | E | | | | | + | | | | |
| *Prosthodendrium ascidia* | P | + | + | + | | | | | + | |
| *Prosthodendrium chilostomum* | C | + | + | + | | + | + | + | | |
| *Prosthodendrium hurkovaae* | P | + | + | | | | | | | |
| *Prosthodendrium ilei* | E | | | | | | + | | | |
| *Prosthodendrium longiforme* | C | + | + | + | | | | | | |
| *Parabascus duboisi* | P | + | + | + | | | | | | |
| *Parabascus joannae* | E | | | | | | | | + | |
| *Parabascus lepidotus* | P | + | + | | | + | + | + | + | |
| *Parabascus semisquamosus* | E | | | | | | + | + | + | + |
| *Gyrabascus amphoraeformis* | E | + | + | | | | | | | |
| *Gyrabascus oppositus* | E | | | | | | + | + | + | |
| *Pycnoporus heteroporus* | P | | | | | + | + | | + | + |
| *Pycnoporus megacotyle* | P | | | | | | | + | | |
| *Symmetricatesticula symmetrica* | E | + | + | + | | + | | | | |
| Nematoda | | | | | | | | | | |
| *Aonchotheca eubursata* | P | | | | | | + | | | |
| *Pterothominx neopulchra* | P | + | + | | + | | + | | + | |
| *Molinostrongylus skrjabini* | P | | + | | | + | + | | + | |
| *Molinostrongylis spasskii* | P | + | | | | | | | | |
| *Molinostrongylis vespertilionis* | P | | | | | | | + | + | |
| *Litomosa filaria* | P | | | | | + | | | | |
| *Physaloptera clausa*, juv. | H | | | | | | | | + | |
| *Physocephalus sexalatus*, juv. | C | | + | | | | + | | | |
| Total | | 14 | 13 | 7 | 1 | 12 | 18 | 11 | 14 | 4 |

(Ruchljadeva 1946) (= *Capillaria petrovi* Ruchljadeva, 1946) is a synonym of *Aonchotheca kutorii* (Ruchlyadeva 1946). The finding by Shaldybin (1964) of the muskrat parasite *Eucoleus marii* (= *Thominx marii*) in the nasal cavity of shrews was erroneous. Most likely, the author dealt with the unusual localization of the common parasite of the shrew' esophagus the nematode *Eucoleus oesophagicola*. The species *Longistriata paradoxi* Schaldybin, 1964 described by Shaldybin (1964) from the shrew intestine is close to *Longistriata pseudodidas* Vaucher et Durette-Desset, 1973. In accordance with Genov (1984), they are identical species. At the same time, the finding by Shaldybin (1964) of *L. paradoxi* in *Neomys fodiens* is erroneous. The author dealt with a specific parasite of *Neomys* spp. *Longistriata neomi* Lubarskaja, 1962. The cestode species *Vampirolepis heleni* described by Shaldybin (1964) from *Neomys fodiens* is a synonym of *Neomylepis magnirostellata* (Baer, 1931). According to Genov (1984), *Ditestolepis secunda* Shaldybin, 1964 from shrews is a synonym for *Insectivorolepis infirma* Zarnovski, 1955.

## Helminths of Bats (Chiroptera)

A total of 32 species of helminths were identified in bats of the protected area: 2 cestodes, 22 trematodes, and 8 nematodes (Shaldybin 1964, Kostyunin 2010, Kirillov et al. 2012, 2015b, Ruchin et al. 2016) (Table 6).

Of these, only two species of nematodes, *Physaloptera clausa,* and *Physocephalus sexalatus* were recorded in bats at larval stage. Bats are paratenic hosts for these parasites. Adult forms represent all other species of parasites. Most of the helminth species (29 species) recorded are bat specialists. Of these, the trematodes *Plagiorchis vespertilionis* and *Prosthodendrium chilostomum* can facultatively parasitize other species of mammals. Three helminth species, *Plagiorchis elegans*, *Physaloptera clausa*, juv. and *Physocephalus sexalatus*, juv. are generalist parasites, occurring in a wide range of vertebrate hosts from different classes.

No helminth species was found to parasitize the entire range of bat species in this protected area (Table 6). The species diversity of helminths is greater in *Nyctalus noctula*, in which 18 species of parasites are revealed in the nature reserve. The helminth communities of *Myotis daubentonii* (14), *Myotis dasycneme* (13), and *Pipistrellus nathusii* (14) are also representative. In *Vespertilio murinus* and *Nyctalus leisleri* were recorded 12 and 11 species of helminths, respectively. The fauna of the helminths of Brandt's bat (7) and the *Pipistrellus pygmaeus* (4) is less diverse. *Myotis nattereri* has only one species of helminth (Table 6).

Three species of parasites have a wide host range in the nature reserve, namely *Plagiorchis koreanus* which is found in

8 bat species: *Prosthodendrium chilostomum* and *Parabascus lepidotus* – each in six species of bats. Four helminth species, *Plagiorchis vespertilionis*, *Lecithodendrium skrjabini*, *Lecithodendrium rysavyi,* and *Pterothominx neopulchra* each have five bat species (Table 6).

The host ranges of trematodes *Symmetricatesticula symmetrica*, *Prosthodendrium ascidia*, *Pycnoporus heteroporus,* and the nematode *Molinostrongylus skrjabini* include four bat species each. The cestode *Vampirolepis spasskii* and the trematodes *Lecithodendrium linstowi*, *Prosthodendrium longiforme*, *Parabascus duboisi,* and *Gyrabascus oppositus* recorded in three bat species each are relatively rare in the bats of the nature reserve. The trematodes *Plagiorchis elegans*, *Prosthodendrium hurkovaae*, *Gyrabascus amphoraeformis*, nematodes *Molinostrongylis vespertilionis* and *Physocephalus sexalatus*, juv. revealed in two host species. The other 10 helminth species are recorded in one bat species each (Table 6). No helminths were found in the Mordovia Nature Reserve in one of 10 studied bat species, *Plecotus auritus*.

Half of the helminth species (16 species) found in the bats of the protected area are distributed in the Palearctic. The distribution ranges of nine parasite species are limited to Europe. Four helminth species have a cosmopolitan distribution. Three species of helminths belong to the Holarctic faunistic complex (Table 6).

## Helminths of Rodents (Rodentia)

A total of 41 species of helminths were revealed in rodents from the protected area: 14 cestodes, 11 trematodes, and 16 nematodes (Shaldybin 1964, Ryzhikov et al. 1978, 1979, Kostyunin 2010, Kirillov et al. 2012, Ruchin et al. 2016) (Table 7).

Of these, 36 species parasitize rodents at the mature stage, and four cestode species are revealed at the larval stage. For them, rodents serve as the main intermediate hosts. All helminths found in rodents are their obligate parasites, with the exception of the trematode *Echinostoma revolutum*, which parasitizes micromammals facultatively.

The cestode *Dilepis undula* and the trematode *Plagiorchis elegans* are generalist parasites in a wide range of vertebrates from different classes, while the metacestodes *Taenia laticollis*, *Taenia martis*, *Versteria mustelae* и *Hydatigera taeniaeformis* s.l. the trematodes *Brachylaima recurva*, *Skrjabinoplagiorchis polonicus*, *Brachylecithum rodentini*, *Corrigia vitta*, nematodes *Mastophorus muris* and *Rictularia cristata* are rodent generalists. The nematodes *Aonchotheca murissylvatici*, *Carolinensis minutus* and *Heligmosomum*

Table 7: The list of helminths in rodents (Rodentia) and lagomorphs (Lagomorpha) from the Mordovia Nature Reserve.

| Species | D | Castor fiber | Arvicola amphibius | Microtus cf arvalis | Microtus agrestis | Microtus oeconomus | Clethrionomys glareolus | Apodemus flavicollis | Apodemus uralensis | Apodemus agrarius | Sicista betulina | Dryomys nitedula | Lepus europaeus | Lepus timidus |
|---|---|---|---|---|---|---|---|---|---|---|---|---|---|---|
| **Cestoda** | | | | | | | | | | | | | | |
| *Mosgovoyia pectinata* | H | | | | | | | | | | | | | + |
| *Anoplocephaloides dentata* | H | | | + | + | + | + | | | | | | | |
| *Paranoplocephala omphalodes* | P | | + | + | | + | + | | | | | | | |
| *Eurotaenia gracilis* | E | | | | | | + | | | | | | | |
| *Hymenolepis procera* | H | | + | | | | | | | | | | | |
| *Rodentolepis asymmetrica* | E | | | | + | | | | | | | | | |
| *Spasskijela lobata* | P | | | | | | | + | + | + | | | | |
| *Catenotaenia henttoneni* | E | | | | | | + | | | | | | | |
| *Catenotaenia* sp. | E | | | | | | | | | | | + | | |
| *Dilepis undula* | H | | | | | | | | | + | | | | |
| *Armadolepis dryomi* | E | | | | | | | | | | | + | | |
| *Taenia laticollis*, larva | C | | | | | | | | | | | | | |
| *Taenia martis*, larva | H | | | | | | + | | + | | | | | |
| *Versteria mustelae*, larva | H | | | | | | + | | | | | | | |
| *Hydatigera taeniaeformis* s.l., larva | C | | | | | | | + | + | | | | | |
| **Trematoda** | | | | | | | | | | | | | | |
| *Brachylaima recurva* | P | | | | | + | + | | | | | | | |
| *Stichorchis subtriquetrus* | H | + | | | | | | | | | | | | |
| *Psilotrema castoris* | E | + | | | | | | | | | | | | |
| *Echinostoma revolutum* | C | | | + | | | | | | | | | | |
| *Notocotylus noyeri* | P | | | + | | | + | | | | | | | |
| *Plagiorchis elegans* | H | | | | | | + | | + | | | | | |
| *Plagiorchis arvicolae* | P | | | + | | | | | | | | | | |
| *Skrjabinoplagiorchis polonicus* | E | | | | | | | + | + | | | | | |
| *Dicrocoelium dendriticum* | C | | | | | | | | | | | | | + |
| *Brachylecithum rodentini* | P | | | | | | + | | | | | | | |
| *Corrigia vitta* | P | | | | | | | | + | | | | | |
| *Macyella apodemi* | E | | | | | | | | + | | | | | |
| **Nematoda** | | | | | | | | | | | | | | |
| *Aonchotheca murissylvatici* | P | | | | | | + | | + | | | | | |
| *Trichuris arvicolae* | E | | | + | + | + | + | | | | | | | |
| *Trichostrongylus colubriformis* | C | | | | | | | | | | | | + | |
| *Trichostrongylus retortaeformis* | C | | | | | | | | | | | | | + |
| *Carolinensis minutus* | P | | | | + | | + | | | | | | | |
| *Heligmosomoides polygyrus* | P | | | | | | | + | + | + | | | | |
| *Heligmosomoides glareoli* | P | | | | | | + | | | | | | | |
| *Heligmosomoides laevis* | P | | | + | + | + | | | | | | | | |

Table cont....

| Species | D | Castor fiber | Arvicola amphibius | Microtus cf arvalis | Microtus agrestis | Microtus oeconomus | Clethrionomys glareolus | Apodemus flavicollis | Apodemus uralensis | Apodemus agrarius | Sicista betulina | Dryomis nitedula | Lepus europaeus | Lepus timidus |
|---|---|---|---|---|---|---|---|---|---|---|---|---|---|---|
| *Heligmosomum mixtum* | P | | | | | | + | | | | | | | |
| *Protostrongylus kamenskyi* | P | | | | | | | | | | | | | + |
| *Protostrongylus terminalis* | E | | | | | | | | | | | | + | + |
| *Heterakis spumosa* | ▯ | | | | | | | | + | | | | | |
| *Syphacia agraria* | E | | | | | | | | | + | | | | |
| *Syphacia obvelata* | C | | | | | | | + | + | | | | | |
| *Syphacia nigeriana* | H | | | + | + | | | | | | | | | |
| *Syphacia stroma* | P | | | | | | | + | + | | | | | |
| *Syphacia petrusewiczii* | H | | | | | | + | | | | | | | |
| *Mastophorus muris* | C | | | | | | | + | + | + | | | | |
| *Rictularia proni* | P | | | | | | | + | + | | | | | |
| *Rictularia cristata* | E | | | | | | | | | | | + | | |
| Total | | 2 | 5 | 5 | 6 | 5 | 17 | 8 | 14 | 4 | 1 | 2 | 2 | 5 |

*mixtum* are specialist parasites in rodents of the families Cricetidae and Muridae, and the cestodes *Anoplocephaloides dentata*, *Paranoplocephala omphalodes*, *Eurotaenia gracilis*, *Hymenolepis procera*, *Rodentolepis asymmetrica*, trematodes *Notocotylus noyeri*, *Plagiorchis arvicolae*, nematodes *Trichuris arvicolae* and *Heligmosomoides laevis* are specialist parasites in members of the subfamily Arvicolinae. The cestode *Spasskijela lobata*, trematode *Macyella apodemi*, nematodes *Heligmosomoides polygyrus* and *Rictularia proni* are specific parasites of mice from the family Muridae. The nematode *Syphacia agraria* parasitizes only *Apodemus agrarius*, while the nematodes *Syphacia obvelata* and *Syphacia stroma* parasitize only wood mice *Apodemus flavicollis* and *A. uralensis*. The trematodes *Stichorchis subtriquetrus* and *Psilotrema castoris* are host-specific parasites of beavers.

A number of rodent helminths have a high degree of specificity. Thus, the nematode *Syphacia nigeriana* is *Microtus* voles' specialist, the cestode *Catenotaenia henttoneni*, nematodes *Heligmosomoides glareoli* and *Syphacia petrusewiczii* are *Clethrionomys* voles' specialist and the cestode *Armadolepis dryomi* is a host-specific parasite of *Dryomis nitedula*.

We did not find a single helminth species that would parasitize all studied rodent species (Table 7). The cestode *Anoplocephaloides dentata* and the nematode *Trichuris arvicolae* have the widest host range among rodent parasites, found in four host species each. The cestode

*Spasskijela lobata*, nematodes *Heligmosomoides polygyrus*, *Heligmosomoides laevis,* and *Mastophorus muris* each parasitize three rodent species. For 12 helminth species (the cestodes *Taenia martis*, larva, *Hydatigera taeniaeformis* s.l., larva, trematodes *Brachylaima recurva*, *Notocotylus noyeri*, *Plagiorchis elegans*, *Skrjabinoplagiorchis polonicus*, nematodes *Aonchotheca murissylvatici*, *Carolinensis minutus*, *Syphacia obvelata*, *S. nigeriana*, *S. stroma* and *Rictularia proni*) two species of rodents were recorded as hosts. Another 21 species of parasitic worms were revealed in a single host species (Table 7). No parasitic worms in the nature reserve were found in two of the 13 studied rodent species (*Rattus norvegicus* and *Micromys minutus*).

Among all the studied rodents, the largest trematode species were recorded in the bank vole *Clethrionomys glareolus* (17 species). *Apodemus uralensis* has 14 species of parasites. The helminth fauna of *Apodemus flavicollis* (8), *Microtus agrestis* (6), *M.* cf *arvalis* (5), *M. oeconomus* (5), *Arvicola amphibius* (5), and *Apodemus agrarius* (4) is less diverse. The parasite communities of *Castor fiber* (2), *Dryomis nitedula* (2), and *Sicista betulina* (1) are poor (Table 7).

Most of the helminth species (15) revealed in rodents have a Palearctic distribution. In Europe and the Holarctic, 11 and 9 species are distributed, respectively. Six species of parasitic worms are cosmopolitan (Table 7).

Taxonomic remarks. The nematode *Trichuris muris* was identified in *Microtus agrestis* by Schaldybin (1964)

erroneously, just like the findings of the cestode *Catenotaenia pusilla* in *Clethrionomys glareolus* and *Sicista betulina*.

Recent studies of *Trichuris* spp. from European mice and voles have revealed that arvicoline rodents parasitize by

Table 8: The list of helminths in artiodactyls (Artiodactyla) from the Mordovia Nature Reserve.

| Species | D | *Cervus nippon* | *Cervus elaphus* | *Bison bonasus* | *Alces alces* |
|---|---|---|---|---|---|
| Cestoda | | | | | |
| *Moniezia autumnalis* | P | | | + | |
| *Moniezia benedeni* | C | | | + | + |
| *Taenia hydatigena*, larva | C | + | | + | |
| Trematoda | | | | | |
| *Fasciola hepatica* | C | + | | + | |
| *Parafasciolopsis fasciolaemorpha* | P | + | | | + |
| *Paramphistomum cervi* | C | + | + | + | + |
| *Dicrocoelium dendriticum* | C | + | | + | + |
| Nematoda | | | | | |
| *Aonchotheca bilobata* | C | | | + | |
| *Aonchotheca bovis* | C | + | | + | |
| *Trichuris ovis* | C | | | + | + |
| *Camelostrongylus lyratus* | C | | | + | |
| *Cooperia oncophora* | H | | | + | |
| *Cooperia pectinata* | C | + | | | |
| *Cooperia punctata* | C | | | + | |
| *Cooperia zurnabada* | P | | | + | |
| *Haemonchus contortus* | C | | | + | |
| *Marshallagia marshalli* | C | + | | | |
| *Ostertagia ostertagi* | C | | + | + | + |
| *Spiculopteragia alicis* | E | | | | + |
| *Spiculopteragia asymmetrica* | C | + | | + | |
| *Spiculopteragia spiculoptera* | C | + | | | |
| *Spiculopteragia panticola* | P | + | | | |
| *Spiculopteragia schulzi* | P | + | | | |
| *Trichostrongylus axei* | C | + | | | |
| *Dictyocaulus viviparus* | C | | | + | |
| *Nematodirella longissimespiculata* | H | + | | | + |
| *Nematodirus helvetianus* | C | | | + | |
| *Chabertia ovina* | C | | | + | |
| *Oesophagostomum asperum* | C | + | | | + |
| *Oesophagostomum radiatum* | C | + | | + | |
| *Oesophagostomum sikae* | C | + | | | |
| *Oesophagostomum venulosum* | C | | | + | |
| *Schulzinema miroljubovi* | P | + | | | |
| *Bunostomum phlebotomum* | C | | | + | |
| *Elaphostrongylus panticola* | P | + | + | | + |
| *Setaria labiatopapillosa* | C | | | + | + |
| *Thelazia rhodesi* | C | | | + | |
| Total | | 19 | 3 | 24 | 11 |

*Trichuris arvicolae* Feliu et al., 2000 (Feliu et al. 2000, Cutillas et al. 2002). Studies of the morphological and genetic variability of *Trichuris* spp. have revealed that *T. arvicolae* parasitizes in rodents of the subfamily Arvicolinae, and *T. muris* parasitizes in mice (Feliu et al. 2000, Cutillas et al. 2002). Therefore, the nematodes found by Shaldybin (1964) in *Microtus agrestis* we assigned to *T. arvicolae*.

Recent studies have shown that *Catenotaenia* spp. possess a high degree of specificity. *Catenotaenia pusilla* is a host-specific parasite of *Mus musculus* and does not parasitize other rodent species (Haukisalmi et al. 2010). Therefore, the cestode found by Shaldybin (1964) in *Sicista betulina* is considered *Catenotaenia* sp. 1. Here, molecular genetic studies are needed to identify cestode from *S. betulina*. And *Clethrionomys glareolus* is parasitized by *Catenotaenia hentonneni*, a specific parasite of *Clethrionomys* voles (Haukisalmi et al. 2010).

The metacestode *H. taeniaeformis* s. l. is a common parasite of various rodent species. According to recent concepts, the cestode *H. taeniaformis* is a complex of species. There are three differentiated clades A (*H. taeniaformis* s.str.), B (*Hydatigera kamiyai* Iwaki 2016) and C (*Hydatigera* sp.) based on the results of molecular-based studies (Lavikainen, et al. 2015, Lavikainen et al. 2016).

## Helminths of Lagomorphs (Lagomorpha)

In two species of lagomorphs of the reserve' fauna, a total of six species of helminths were found: one cestode, one trematode, and four nematodes (Shaldybin 1964, Gvozdev et al. 1970, Kirillov et al. 2012, Ruchin et al. 2016) (Table 7). Mature forms represent all of them. The trematode *Dicrocoelium dendriticum* and the nematode Trichostrongylus colubriformis are generalist parasites in mammals from various orders. *Dicrocoelium dendriticum* parasitizes mainly ungulates. The cestode *Mosgovoyia pectinata*, nematodes *Trichostrongylus retortaeformis*, *Protostrongylus kamenskyi,* and *Protostrongylus terminalis* are host-specific parasites of hares.

In both studied hare species, the nematode *P. kamenskyi* was found (Table 7). Only *Lepus timidus* is the host for the cestode *Mosgovoyia pectinata*, the trematode *Dicrocoelium dendriticum*, the nematodes *Trichostrongylus retortaeformis* and *P. terminalis*. The nematode *Trichostrongylus colubriformis* is identified only in *Lepus europaeus*. Thus, five species of helminths are registered in *Lepus timidus*, and two species in *L. europaeus* (Table 7).

Three species of parasites found in the hares of the reserve are cosmopolitan. Three more species are distributed in the Holarctic, Palearctic, and Europe (Table 7).

## Helminths of Artiodactyls (Artiodactyla)

The list of the helminth fauna in artiodactyls of the nature reserve includes 37 species: 3 cestodes, 4 trematodes and 30 nematodes (Matevosyan, 1964a, Shaldybin 1964, Shtarev 1967, 1971, Machinsky & Semov 1974, Nazarova 1974a, 1974b, Shtarev et al. 1978, Kirillov et al. 2012, Oliger 2016b, Ruchin et al. 2016) (Table 8).

All helminth species found in ungulates use artiodactyls as definitive hosts, with the exception of the cestode *Taenia hydatigena*. For this metacestode, ungulates serve as the main intermediate hosts. All species of helminths identified in ungulates of the protected area are their obligate parasites.

The trematodes *Fasciola hepatica*, *Dicrocoelium dendriticum*, nematodes *Haemonchus contortus*, *Trichostrongylus axei,* and *Setaria labiatopapillosa* are generalist parasites in mammals from various orders. The nematode *Thelazia rhodesi* is a generalist parasite occurring in various species of the orders Artiodactyla and Perissodactyla. The nematodes *Aonchotheca bilobata*, *Ostertagia ostertagi,* and *Oesophagostomum venulosum* are specialist parasites in mammals from order Artiodactyla. *Ostertagia ostertagi* can also be found in primates. The cestodes *Moniezia autumnalis*, *M. benedeni*, nematodes from genus *Cooperia*, *Marshallagia marshalli*, *Spiculopteragia schulzi*, *Trichuris ovis*, *Camelostrongylus lyratus*, *Nematodirus helvetianus*, *Dictyocaulus viviparous*, *Bunostomum phlebotomum* and *Chabertia ovina* are specialist parasites in ungulates of the suborder Ruminantia.

Seven species of helminths (the trematodes *Parafasciolopsis fasciolaemorpha*, *Paramphistomum cervi*, nematodes *Aonchotheca bovis*, *Nematodirella longissimespiculata, Spiculopteragia spiculoptera*, *Oesophagostomum asperum* and *O. radiatum*) specific parasites of members from the families Cervidae and Bovidae, while six nematode species (*Oesophagostomum sikae*, *Spiculopteragia alicis*, *S. asymmetrica*, *S. panticola*, *Elaphostrongylus panticola* and *Schulzinema miroljubovi*) are specialist parasites in cervids.

Among four species of artiodactyls studied in the protected area, the largest number of helminths was found in *Bison bonasus* (24 species). Nineteen species of parasites were revealed in *Cervus nippon*. Less diverse is the helminth fauna of *Alces alces*, in which 11 species of helminths were registered. Only three helminth species were recorded in *Cervus elaphus* (Table 8).

The trematode *Paramphistomum cervi* found in all studied species of ungulates is the most common among hoofed mammals in the Mordovia Nature Reserve (Table 8). The trematode *Dicrocoelium dendriticum*,

nematodes *Elaphostrongylus panticola,* and *Ostertagia ostertagi* were revealed in three species of ungulates. The host range of ten helminth species (cestode *Moniezia benedeni*, trematodes *Fasciola hepatica*, *Parafasciolopsis fasciolaemorpha*, nematodes *Aonchotheca bovis*, *Trichuris ovis*, *Spiculopteragia asymmetrica*, *Nematodirella longissimespiculata*, *Oesophagostomum asperum*, *O. radiatum* and *Setaria labiatopapillosa*) includes two species of hoofed mammals each. Another 23 species of parasites were registered in one species of ungulates (Table 8).

Most of the helminth species recorded in artiodactyls from the Mordovia Nature Reserve are widely distributed in the world. Thus, 27 helminth species of 37 identified are cosmopolitan. The range of seven parasite species covers the Palearctic. In the Holarctic and Europe, two and one species of helminths are common, respectively (Table 8).

### Helminths of Carnivores (Carnivora)

A total of 19 species of helminths were identified in carnivore mammals of the protected area: 6 cestodes, 2 trematodes, 10 nematodes, and one acanthocephalan (Shaldybin 1957, 1964, Matevosyan, 1964b, Kirillov et al. 2012, Ruchin et al. 2016) (Table 9).

All helminths found in carnivores parasitize at the mature stage and are obligate parasites of carnivores. The cestodes *Taenia multiceps*, *T. polyacantha*, trematode *Alaria alata,* and nematode *Uncinaria stenocephala* are specialist parasites in carnivores from the family Canidae, while the cestodes *Taenia krabbei*, *T. serialis*, *T. hydatigena*, nematodes *Toxascaris leonina* host-specific parasites in canids and felids. The nematodes *Skrjabingylus nasicola* and *Molineus patens* are specialist parasites in mammals from the family Mustelidae, and the nematode *Spirocerca lupi* is a specific parasite in canids, less common in Mustelids. The cestode *Mesocestoides lineatus*, trematode *Pseudamphistomum truncatum,* and nematodes *Aonchotheca putorii*, *Eucoleus aerophilus*, *Pearsonema plica*, *Toxocara canis,* and *Crenosoma vulpis* are generalist parasites in a wide range of carnivores from different families.

Table 9: The list of helminths in carnivores (Carnivora) from the Mordovia Nature Reserve.

| Species | D | *Vulpes vulpes* | *Canis lupus* | *Mustela nivalis* | *Nyctereutes procyonoides* |
|---|---|---|---|---|---|
| Cestoda | | | | | |
| *Taenia hydatigena* | C | | + | | |
| *Taenia krabbei* | H | | + | | |
| *Taenia multiceps* | C | + | + | | |
| *Taenia polyacantha* | H | | + | | |
| *Taenia serialis* | C | + | + | | |
| *Mesocestoides lineatus* | P | | + | | |
| Trematoda | | | | | |
| *Pseudamphistomum truncatum* | H | + | | | |
| *Alaria alata* | C | + | + | | |
| Nematoda | | | | | |
| *Aonchotheca putorii* | H | | | + | |
| *Eucoleus aerophilus* | H | | + | | |
| *Pearsonema plica* | H | + | + | | |
| *Molineus patens* | C | | | | + |
| *Uncinaria stenocephala* | H | + | + | | |
| *Crenosoma vulpis* | H | + | + | | |
| *Skrjabingylus nasicola* | H | | | + | |
| *Spirocerca lupi* | C | | + | | |
| *Toxascaris leonina* | C | | + | | |
| *Toxocara canis* | C | + | | | |
| Acanthocephala | | | | | |
| *Macracanthorhynchus catulinus* | P | + | | | |
| Total | | 9 | 13 | 2 | 1 |

Among the carnivores of the Mordovia Nature Reserve, the most diverse helminth fauna is *Canis lupis*, listed by 13 species of parasitic worms (Table 9). The less diverse parasite fauna of *Vulpes vulpes* includes nine helminth species. *Mustela nivalis* and *Nyctereutes procyonoides* have only two and one species of helminths, respectively. For six species of helminths (the cestodes *Taenia multiceps*, *Taenia serialis*, trematode *Alaria alata*, nematodes *Pearsonema plica*, *Uncinaria stenocephala*, and *Crenosoma vulpis*), two species of carnivores were recorded as hosts each. Another 13 helminth species parasitized one carnivore species in the Mordovia Nature Reserve (Table 9).

Most of the helminth species identified in the carnivores of the nature reserve are widespread and have a cosmopolitan and Holarctic distribution, with eight and nine species, respectively. Two species of parasites belonging to the Palearctic faunistic complex (Table 9).

Taxonomic remarks. Shaldybin (1964) described nematode *Metathelazia petrovi* Schaldybin, 1950 from the bronchi of *Canis lupus*. Since the time of the original description, no one else has found this parasite, as in the case of the shrew parasite *Capillaria reni*. We classify *Metathelazia petrovi* and *Capillaria reni* as species inquirenda.

## STRUCTURE OF HELMINTH FAUNA IN VERTEBRATE ANIMALS IN THE MORDOVIA NATURE RESERVE

The fauna of nematodes represented by adult and larval forms is the most diverse in the Mordovia Nature Reserve vertebrates. Nematodes account for 40.5% of the parasite fauna in all studied animal species. Ninety-three species of nematodes were recorded at the mature stage and three species (*Physocephalus sexalatus*, *Porrocaecum depressum*, and *Agamospirura minuta*) only at the larval stage. The nematodes *Hadjelia truncata* and *Physaloptera clausa* parasitize animals in the protected area at the mature and larval stages. *Physaloptera clausa*, found in reptiles, insectivores, and bats, has the widest host range (Tables 2, 5 and 6). *Physocephalus sexalatus*, juv. was identified in reptiles, birds, and bats (Tables 2, 3, and 5); *Hadjelia truncata* occurs in birds and insectivores (Tables 3, 4, and 5); *Oswaldocruzia filiformis* and *Oxysomatium brevicaudatum* are common to the amphibians and reptiles in the nature reserve (Tables 1 and 2). Another 93 helminth species are identified only within one taxonomic group of vertebrates.

Trematodes represent 36.0% of the total helminth species in vertebrates from the reserve's fauna. Both marites and larval forms represent trematodes. Seventy-six species of

trematodes were revealed only in the adult stage. Five species (*Strigea falconis*, *S. sphaerula*, *S. strigis*, *Neodiplostomum spathoides*, and *Tylodelphys excavata*) were found only in the larval stage. Six species of trematodes (*Gorgoderina vitelliloba*, *Haplometra cylindracea*, *Opisthioglyphe ranae*, *Paralepoderma cloacicola*, *Alaria alata*, and *Astiotrema monticelli*) use vertebrates both as intermediate and definitive hosts. The trematodes *Plagiorchis elegans* (reptiles, birds, bats, and rodents) (Tables 2, 3, 4, 6, and 7) and *Alaria alata* (in amphibians, reptiles, and carnivores) have the widest range of hosts (Tables 1, 2 and 9).

Seven species of trematodes (*Paralepoderma cloacicola*, *Astiotrema monticelli*, *Opisthioglyphe ranae*, *Strigea falconis* mtc., *S. sphaerula* mtc., *S. strigis* mtc. and *Neodiplostomum spathoides*) parasitize both amphibians and reptiles (Tables 1 and 2). The trematode *Dicrocoelium dendriticum is* found in ungulates and hares (Tables 7 and 8). Another 77 trematode species parasitize within the same taxonomic group of vertebrates.

The cestodes account for 22.3% of the helminth fauna of the studied vertebrate species in the reserve, found in vertebrates as adult forms and larval stages. Forty-eight cestode species were identified at the mature stage, while five species (*Taenia laticollis*, *T. martis*, *Versteria mustelae*, and *Hydatigera taeniaeformis* s.l., *Spirometra erinaceieuropaei*) only as metacestodes. One species, *Taenia hydatigena*, was recorded in adult and larval stages in vertebrates.

*Dilepis undula* has the widest host range among the recorded cestode species and occurs in birds, insectivores, and rodents (Tables 3, 4, 5, and 7). *Taenia hydatigena* is a common species for carnivores and ungulates (Tables 8 and 9). Another 52 species parasitize within the same systematic group of vertebrates-hosts.

Only three species of acanthocephalans (1.2%) were recorded in the studied vertebrate species in the reserve. Two acanthocephalan species parasitize at the larval stage, and one occurs in adulthood. *Centrothynchus aluconis* is a common species for insectivores and reptiles (Tables 2 and 5). *Macracanthorhynchus catulinus* parasitizes only carnivores (Table 9), while *Sphaerirostris picae* is found only in reptiles (Table 2).

The helminth communities are represented in reptiles, insectivores, and carnivores. All taxonomic groups of parasites are recorded in reptiles: Trematoda-Nematoda-Cestoda-Acanthocephala (Fig. 2).

The predominance of trematodes is due to feeding mainly on anurans (snakes) and terrestrial invertebrates (lizards). The helminth fauna of insectivores is dominated equally by cestodes and nematodes: Cestoda-Nematoda-Trematoda-
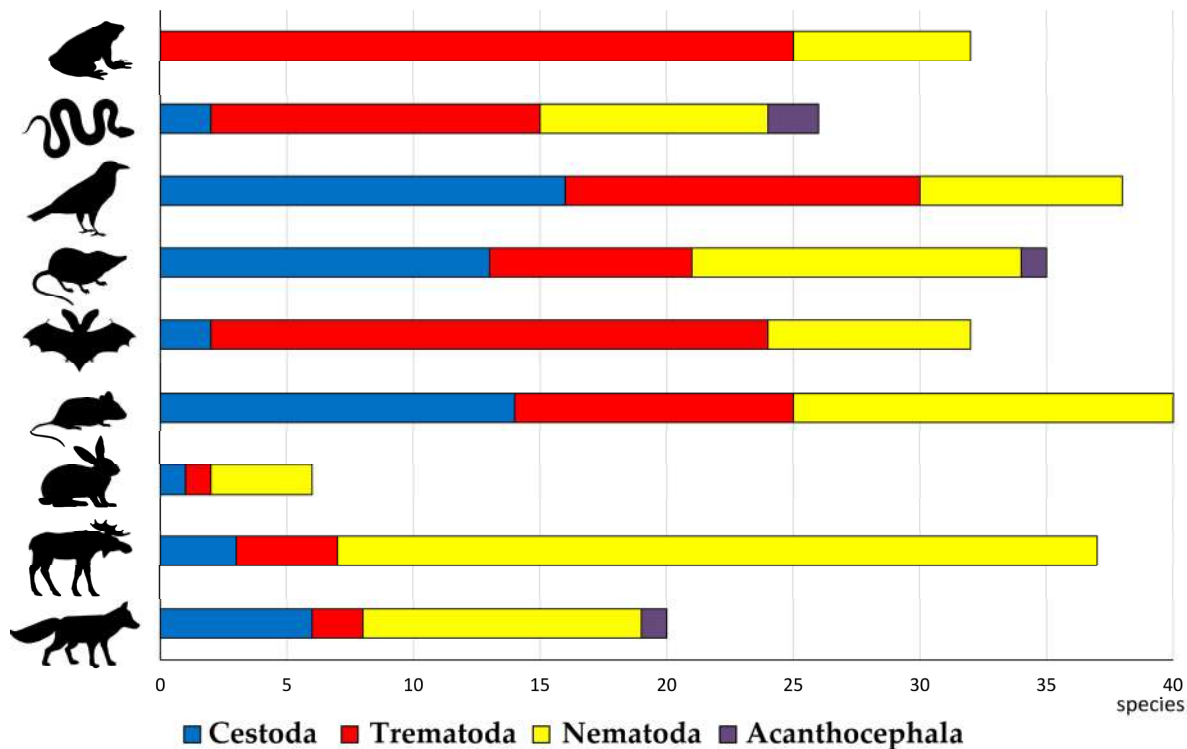
Fig. 2: The diversity of different taxonomic groups of helminths in vertebrates of the Mordovia Nature Reserve.

Acanthocephala. Feeding on terrestrial invertebrates and close contact of insectivores with soil litter play an important role here. The structure of the helminth fauna of carnivore animals is similar to insectivores: Nematoda-Cestoda-Trematoda-Acanthocephala, but with a predominance of nematodes, among which half of the species have an indirect life cycle. Birds, rodents, bats, hares, and artiodactyls do not have acanthocephalans in the helminth fauna. In the structure of the community of bird parasites, cestodes and trematodes prevail: Cestoda-Trematoda-Nematoda (Fig. 2), which is primarily due to feeding on terrestrial and semi-aquatic invertebrates.

In rodents, hares, and artiodactyls, the structure of the helminth fauna is similar in the dominance of nematodes (mainly with a direct life cycle) due to the nutrition of plant food, along with which animals obtain invasive eggs and larvae of nematodes. In rodents and hares, the helminth community structure looks like Nematoda-Cestoda-Trematoda, and in artiodactyls Nematoda-Trematoda-Cestoda. In bats, the predominance of trematodes in the helminth fauna (Trematoda-Nematoda-Cestoda) is due to feeding mainly on peri-aquatic insects. The structure of the helminth fauna of amphibians is represented only by nematodes and trematodes, with a predominance of the latter (Trematoda-Nematoda), which is also associated with feeding on aquatic and semi-aquatic insects and gastropods.

Thus, the helminth species composition in vertebrates is strongly influenced by the diet and lifestyle of animals. Vertebrates obtain most of the parasite species through food. Thus, 169 of 242 parasite species recorded in the nature reserve's vertebrates have an indirect life cycle. Infection of animals with them occurs through various food objects intermediate and paratenic hosts of helminths. If animals' dietary range is more varied, their helminth fauna is more varied, too. Thus, the largest number of helminth species with a complex life cycle was recorded in birds, 35 of 38 (92.1%). Fewer helminth species with indirect lifestyle were found in bats – 27 of 32 recorded (84.4%), in insectivores – 28 of 35 (80.0%), in amphibians – 25 of 32 (78.1%), in reptiles – 20 of 26 (76.9%), in carnivores – 14 of 19 (73.7%). %), in rodents – 28 of 41 (68.3%), and in hares – 4 of 6 (66.7%). The smallest number of helminth species with an indirect life cycle was found in ungulates (10 of 37, 27.0%), whose diet includes animal food only occasionally swallowed together with plant food.

Another 73 species of parasites found in the reserve's vertebrates have a direct life cycle. Infection with helminths occurs directly from the environment. In the infection of

different vertebrates with the soil-transmitted helminths, feeding on plant foods and the degree of contact of the animals with wet forest litter play a decisive role. The largest number of helminth species with a direct lifestyle is observed in animals whose diet includes mainly green parts of plants. Thus, 27 such species of 37 recorded (73.0%) were found in ungulates of the reserve, 2 of 6 (33.3%) in hares, and 13 of 41 (31.7%) in rodents. Fewer helminths with an indirect life cycle were recorded in amphibians of the reserve, 7 of 32 (21.9%), and in reptiles, 6 out of 26 (23.1%). And in carnivores, 5 out of 19 (26.3%). The least number of parasites with a complex lifestyle is in bats (5 of 32, 15.6%) and birds (3 of 38, 7.9%), animals with minimal contact with the soil litter.

Only 21 of 242 helminths found in vertebrates were revealed at the larval stage. A greater number of larval stages of helminths was recorded in reptiles (11 species) and amphibians (8), which are, in most cases, the paratenic hosts of parasites (Tables 1 and 2). Significantly fewer helminth larvae were observed in rodents (4), insectivores (3), and bats (2) (Tables 5, 6 and 7). One helminth species, the metacestode *Taenia hydatigena*, was found in ungulates, the second intermediate host of this parasite (Table 8). No larval helminth forms were found because the carnivore mammals complete the trophic chains.

The findings of helminth larvae in amphibians, reptiles, small mammals, and ungulates indicate an important role of these vertebrates in the circulation of parasites in animals at the highest trophic levels – birds of prey and carnivores. On the other hand, the findings of many larval forms in vertebrates indicate the biocenosis's integrity and the stability of parasitic systems in the study area. The involvement of paratenic hosts in the helminth life cycles plays an important role in the distribution and preservation of parasites in the wild. It increases the infection probability of the definitive hosts.

It should be noted that the nematode juveniles of *Hadjelia truncata* (in insectivores), *Physocephalus sexalatus* (in bats and birds), *Physaloptera clausa* (in bats and insectivores), *Agamospirura minuta* (in reptiles) are occasional parasites in these hosts. The probability of their transmission to the final hosts is extremely low. These vertebrate hosts represent a kind of "ecological dead end" for nematodes. While parasitisation of larvae of *Physocephalus sexalatus* and *Physaloptera clausa* in reptiles (parathenic hosts) provides an opportunity to complete their life cycle since reptiles are included in the diet of the final hosts of these nematodes (Bakiev 2007).

Comparison of the helminth fauna in vertebrates of different taxonomic groups according to the Jaccard index ($Cj$) showed a low degree of similarity in the composition of helminths (Table 10).

The helminth communities in amphibians and reptiles are the most similar (10 common species), which is primarily due to the use of trophic chains between these vertebrates by trematodes; to a lesser extent – by inhabiting the same habitats, which leads to infection of amphibians and reptiles by nematodes with a direct life cycle. In other cases, extremely low values of the Jaccard index are recorded, or there is no similarity of helminth fauna. In all pairs (where the Jaccard index is greater than 0), with the exception of Artyodactyla-Carnivora, the similarity in the parasite faunas in different taxonomic groups of vertebrates is associated with feeding (possibly occasional) on the same invertebrates, which are intermediate or paratenic hosts of parasites. It should be noted that these were single findings of common parasite species in vertebrates of various taxonomic groups. In the pair Artyodactyla-Carnivora, the trophic chain is used by the cestode *T. hydatigena*.

The similarity level between vertebrates of various taxonomic groups expected by us was not noted; for example,

Table 10: Similarity of helminth fauna in land vertebrates from the Mordovia Nature Reserve ($Cj$).

| | Amphibia | Reptilia | Aves | Eulipotyphla | Chiroptera | Rodentia | Lagomorpha | Artyodactyla | Carnivora |
|---|---|---|---|---|---|---|---|---|---|
| Amphibia | 1 | 0.21 | 0 | 0 | 0 | 0 | 0 | 0 | 0.02 |
| Reptilia | 0.21 | 1 | 0.06 | 0.03 | 0.06 | 0.02 | 0 | 0 | 0.02 |
| Aves | 0 | 0.06 | 1 | 0.03 | 0.03 | 0.03 | 0 | 0 | 0 |
| Eulipotyphla | 0 | 0.03 | 0.03 | 1 | 0.02 | 0.01 | 0 | 0 | 0 |
| Chiroptera | 0 | 0.06 | 0.03 | 0.02 | 1 | 0.01 | 0 | 0 | 0 |
| Rodentia | 0 | 0.02 | 0.03 | 0.01 | 0.01 | 1 | 0 | 0 | 0 |
| Lagomorpha | 0 | 0 | 0 | 0 | 0 | 0 | 1 | 0.02 | 0 |
| Artyodactyla | 0 | 0 | 0 | 0 | 0 | 0 | 0.02 | 1 | 0.02 |
| Carnivora | 0.02 | 0.02 | 0 | 0 | 0 | 0 | 0 | 0.02 | 1 |
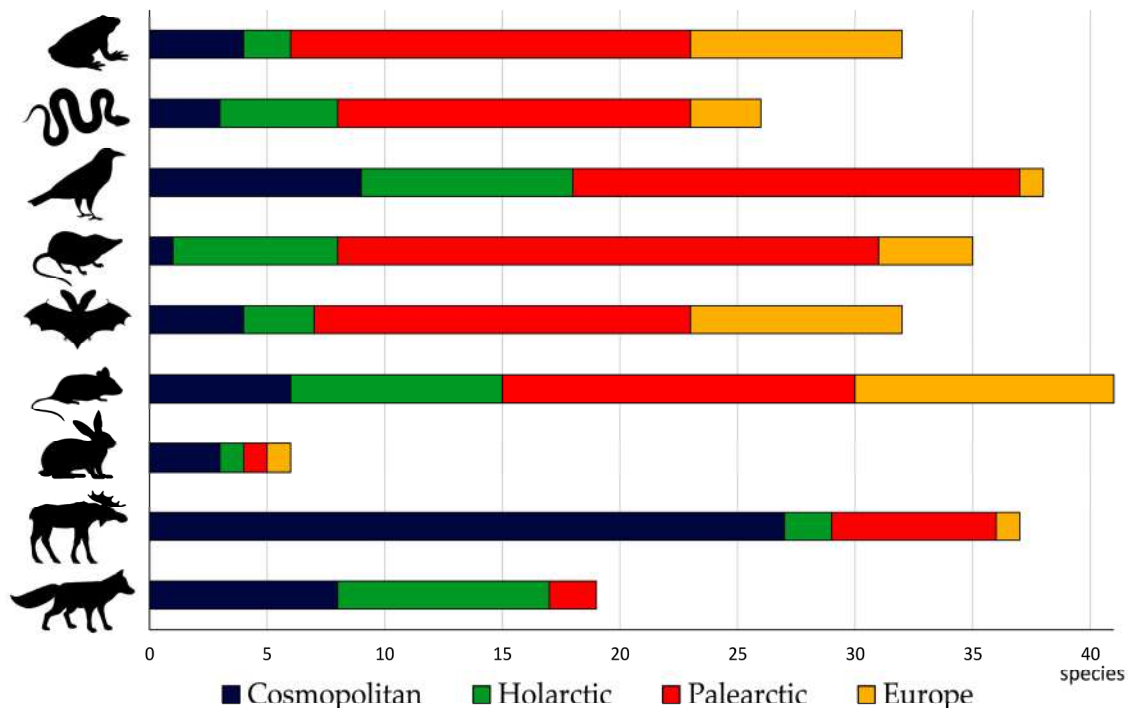
Fig. 3: The zoogeographical distribution of helminths found in vertebrate animals in the Mordovia Nature Reserve.

between rodents and carnivores, rodents and birds, ungulates, lagomorphs, and rodents. This is due to the insufficient knowledge of helminths in various taxonomic groups and species of vertebrates in the Mordovia Nature Reserve. In particular, the helminth fauna of ungulates, lagomorphs, and mustelids have been poorly studied, and the parasite study of birds of prey has not yet been carried out. This caused a low similarity of the helminth fauna of vertebrates from separate taxonomic groups.

The helminth fauna of land vertebrates in the Mordovia Nature Reserve is heterogeneous and is represented by parasites of different zoogeographic regions (Tables 1-9 and Fig. 3).

The broad distribution of parasites depends not so much on environmental conditions as on the distribution of their hosts, as in the case of ungulate helminths. The wider distribution range of those helminths that have adapted to habitation in several species or groups of hosts (intermediate or final) with different ranges, such as the trematodes *Fasciola hepatica*, *Dicrocoelium dendriticum*, *Alaria alata*, and nematode *Physocephalus sexalatus*. The bulk of the helminth fauna of the land vertebrates in the nature reserve are parasites belonging to the Palearctic complex (107 of 242 identified species). Most Palearctic species of helminths parasitize amphibians, reptiles, birds, insectivores, bats, and rodents (Fig. 3). The parasites of

these taxonomic groups of vertebrates have a high degree of specificity for host species, genera, or subfamilies. Fifty-eight species of vertebrate helminths have a cosmopolitan distribution. About half of them are parasites of ungulates (Fig. 3). The number of helminths cosmopolitan is much less in other studied vertebrate groups. The Holarctic complex is represented by 39 species of helminths among the vertebrates of the Mordovia Nature Reserve. The parasite fauna of birds, rodents, and predators is more represented here (Fig. 3). The distribution of 37 helminth species, most found in amphibians, bats, and rodents, was limited to Europe and represented by species specialists.

## CONCLUSION

Thus, 242 species of helminths were identified in the studied land vertebrates in the Mordovia Nature Reserve: 54 cestodes, 87 trematodes, 98 nematodes, and 3 acanthocephalans. Of these, 169 parasite species have an indirect life cycle, and 72 develop directly. Two hundred seventeen species of parasitic worms use vertebrates as definitive hosts and 21 as intermediate and/or parathenic hosts. Three more species of trematodes (*Gorgoderina vitelliloba*, *Haplometra cylindracea*, and *Opisthioglyphe ranae*) combine the larval and adult stages of the life cycle in amphibians and characterize them as amphixenic hosts. Seventy-three of 242 species found in the reserve's vertebrates are of

medical and veterinary importance as potential pathogens of zoonoses.

An analysis of the helminth fauna in vertebrates showed that it is the richest in rodents (41 species), birds (38), artiodactyls (37), and insectivores (35). Less diverse in amphibians (32), bats (32), reptiles (26), and carnivores (19). Very few species of parasites were found in the hares of the Nature Reserve – six species. Here, the degree of helminthological knowledge of individual vertebrate groups and species is of great importance. In addition, the diversity of various systematic vertebrate groups in the study area is important. Thus, the helminth fauna of 85 out of 299 species of land vertebrates inhabiting the Mordovia Nature Reserve were studied to some extent. The helminth fauna of bats, hares, amphibians, and reptiles were studied more fully and in detail. So, among bats, all 10 species of bats inhabiting the reserve and from lagomorphs, both species were studied. Also, 9 of 10 species of amphibians and 5 of 7 species of reptiles were subjected to parasitological research. To a lesser extent, rodents (13 out of 20), artiodactyls (4 out of 7), and predators (4 out of 13) have been studied. Of the vertebrate fauna of the reserve, birds are the most poorly studied. They harbored only 32 of 219 species of helminths found in vertebrates in the protected area.

Most of the helminth species (107) identified in the vertebrates from the Mordovia Nature Reserve belong to the Palearctic faunistic complex. Fifty-eight species of parasitic worms have a cosmopolitan distribution. The range of 39 species of parasites covers the Holarctic. The distribution of 37 species of helminths is limited to Europe.

Sixty-eight of 242 helminth species of recorded in vertebrates of the protected area are of epidemiological and epizootological significance, since they are potential pathogens of dangerous helminthiases in humans, wild and domestic animals: the trematodes *Fasciola hepatica*, *Paraphasciolopsis fasciolaemorpha*, *Paramphistomum cervi*, *Stichorchis subtriquetrus*, *Dicrocoelium dendriticum*, *Metorchis bilis*, *Pseudamphistomum truncatum*, *Alaria alata*, *Echinostoma revolutum*, *Prosthogonimus ovatus*, cestodes of genera *Taenia* and *Moniezia*, *Mosgovoyia pectinata*, *Versteria mustelae*, *Hydatigera taeniaeformis* s.l., *Mesocestoides lineatus*, acanthocephalan *Macracanthorhynchus catulinus*, nematodes of genera *Cooperia*, *Trichostrongylus*, *Spiculopteragia*, *Oesophagostomum*, *Protostrongylus*, *Ascaridia compar*, *Aonchotheca bilobata*, *A. bovis*, *A. putorii*, *Eucoleus aerophilus*, *Pearsonema plica*, *Trichuris ovis*, *Camelostrongylus lyratus*, *Haemonchus contortus*, *Marshallagia marshalli*, *Ostertagia ostertagi*, *Dictyocaulus viviparus*, *Molineus patens*, *Nematodirella longissimespiculata*, *Nematodirus helvetianus*, *Bunostomum phlebotomum*, *Chabertia ovina*, *Crenosoma vulpis*, *Uncinaria stenocephala*, *Elaphostrongylus panticola*, *Skrjabingylus nasicola*, *Physocephalus sexalatus*, *Spirocerca lupi*, *Setaria labiatopapillosa*, *Thelazia rhodesi*, *Toxascaris leonina*, *Toxocara canis* and *Syphacia obvelata*.

The data obtained help the implementation of prevention and the development of measures to combat natural focal helminthiases, in the maintenance of which wild vertebrates play an important role. When taking into account the epidemiological significance of parasites, it is necessary to know that the spread of a particular zoonosis is associated with the spread of its pathogens. These helminth diseases may not occur in this territory despite the presence of their pathogens.

The parasites found in the examined animals of the Mordovia Nature Reserve do not reflect overall helminth diversity in land vertebrates since a great number of animal species were not subjected to parasitological studies. In particular, there is still little data on helminths of birds and carnivore mammals and no information about fish parasites in the protected area. From the perspective of further research, on the one hand, the identification of the helminth fauna of unstudied species of vertebrates. On the other hand, the extension of research sites in the Mordovia Nature Reserve will greatly expand the list of helminth fauna in vertebrate animals.

## ACKNOWLEDGEMENT

## REFERENCES

Afonina, E.Yu. and Tashlykova, N.A. 2021. Torey Lakes, Daursky State Nature Biosphere Reserve, Russia: Long-term changes in environmental parameters. Nat. Conserv. Res., 6(2): 42-52. https://dx.doi.org/10.24189/ncr.2021.024

Artaev, O.N. and Grishutkin, O.G. 2014. Lakes of Mordovia. Mord. Res., 6: 20-23.

Artaev, O.N. and Smirnov, D.G. 2016. Bats (Chiroptera; Mammalia) of Mordovia: Specific structure and features of distribution. Nat. Conserv. Res., 1(1): 38-51. https://doi.org/10.24189/ncr.2016.004

Artaev, O.N., Ruchin, A.B., Bugaev, K.E., Grishutkin, G.F., Potapov, S.K. and Spiridonov, S.N. 2012. Vertebrates of the Mordovia State Nature Reserve. Flora and Fauna of Reserves, Vol. 120. Committee of RAS for the Conservation of Biological Diversity, pp. 64.

Bakiev, A.G. 2007. Snakes of the Volga River basin as nutrition objects for vertebrates. Cur. Stud. Herpetol., 7(1/2): 124-132.

Bhat, R.A., Tak, H., Bhat, B.A., Dar, J.A. and Ahmad, R. 2022. Gastrointestinal helminth parasites of wild ungulates in Hirpora Wildlife Sanctuary, Kashmir, India. J. Parasit. Dis., 46(3): 804–810. https://dx.doi.org/10.1007/s12639-022-01493-3

Bordes, F., Blasdell, K. and Morand, S. 2015. Transmission ecology of rodent-borne diseases: New frontiers. Integr. Zool., 10: 424-435. https://dx.doi.org/10.1111/1749-4877.12149

Bykhovskaya-Pavlovskaya, I.E. 1962. Trematodes of birds of the fauna of the USSR. Academy of Sciences of the USSR Publishers, Moscow, pp. 407.

Chikhlyaev, I.V. and Ruchin, A.B. 2014. The helminth fauna study of the European common brown frog (*Rana temporaria* Linnaeus, 1758) in the Volga basin. Acta Parasit., 59(3): 459-471.

Chikhlyaev, I.V., Ruchin, A.B. and Lukiyanov, S.V. 2009. Helminthofauna of *Bufo bufo* (Amphibia: Anura) in Mordovia. Cur. Stud. Herpetol., 9(3/4): 153-158.

Chikhlyaev, I.V., Ruchin, A.B. and Fayzulin, A.I. 2015. Helminths of tailless amphibians (Amphibia, Anura) in the Mordovia State Nature Reserve. Proc. Mord. St. Nat. Res., 14: 376-388.

Chikhlyaev, I.V., Ruchin, A.B. and Kirillov, A.A. 2020. Ecological analysis of the helminth fauna of European common toad *Bufo bufo* (Amphibia: Anura) from various habitats. Nat. Conserv. Res., 5(2): 1-10. https://dx.doi.org/10.24189/ncr.2020.026

Cutillas, C., Oliveros, R., Rojas, M. and Guevarra, D.C. 2002. Determination of *Trichuris muris* from murid hosts and *T. arvicolae* (Nematoda) from arvicolid rodents by amplification and sequestration of the ITS1-5.8SITS2 segment of the ribosomal DNA. Parasitol. Res., 88: 574–582. https://doi.org/10.1007/s00436-002-0596-5

Dobson, A., Lafferty, K.D., Kuris, A.M., Hechinger, R.F. and Jetz, W. 2008. Homage to Linnaeus: How many parasites? How many hosts? Proc. Nat. Acad. Sci. USA, 105(1): 11482-11489. http://dx.doi.org/10.1073/pnas.0803232105

Feliu, C., Spakulova, M., Casanova, J.C., Renaud, F., Morand, S., Hugot, J.P., Santalla, F. and Durand, P. 2000. Genetic and morphological heterogeneity in small rodent whipworms in southwestern Europe: Characterization of *Trichuris muris* and description of *Trichuris arvicolae* n. sp. (Nematoda: Trichuridae). J. Parasitol., 86: 442-449. https://doi.org/10.1645/0022-3395(2000)086[0442:GAMHIS]2.0.CO;2

Froeschke, G. and Matthee, S. 2014. Landscape characteristics influence helminth infestations in a peri-domestic rodent - implications for possible zoonotic disease. Parasit. Vect., 7: 393. https://doi.org/10.1186/1756-3305-7-393

Gafferberg, I.G. 1960. Mordovia State Nature Reserve: A brief physical and geographical review of the nature in the Mordovia Reserve. Proc. Mord. St. Nat. Res., 1: 5-24.

Gafferberg, I.G. 2015. Climate of the Mordovia State Nature Reserve. 1938. Proc. Mord. St. Nat. Res., 13: 5-20.

Genov, T. 1984. Helminths of Insectivores and Rodents in Bulgaria. Bulg. Acad. Sci., 16: 348.

Georgopoulou, I. and Tsiouris, V. 2008. The potential role of migratory birds in the transmission of zoonoses. Vet. Ital., 44(4): 671-677.

Ghosh-Harihar, M., An, R., Athreya, R., Borthakur, U., Chanchani, P., Chetry, D., Datta, A., Harihar, A., Karanth, K.K., Mariyam, D., Mohan D., Onial M., Ramakrishnan U., Robin V.V., Saxena A., Shahabuddin Gh., Thatte P., Vijay V., Wacker K., Mathur V.B., Pimm S.L. and Price T.D. 2019. Protected areas and biodiversity conservation in India. Biol. Conserv., 237: 114-124. https://doi.org/10.1016/j.biocon.2019.06.024

Grishutkin, O.G. 2013. Patterns of the distribution of swamps depending on the absolute marks of the relief on the territory of the Mordovia State Nature Reserve. Proc. Mord. St. Nat. Res., 11: 259-263.

Gvozdev, E.V., Kontrimavichus, V.L., Ryzhikov, K.M. and Shaldybin L.S. 1970. Keys to the helminths of lagomorphs of the USSR. Nauka, 11: 232.

Haukisalmi, V., Hardman, L.M. and Henttonen, H. 2010. Taxonomic review of cestodes oft the genus *Catenotaenia* Janicki, 1904 in Eurasia and molecular phylogeny of the Catenotaeniidae (Cyclophyllidea). Zootaxa, 2489: 1-33.

Herczeg, D., Vörös, J., Vegvari, Z., Kuzmin, Y. and Brooks, D.R. 2016. Helminth parasites of the *Pelophylax esculentus* complex (Anura: Ranidae) in Hortobágy National Park (Hungary). Comp. Parasitol., 83(1): 36–48. https://doi.org/10.1654/1525-2647-83.1.36

Horwitz, P. and Wilcox, B. 2005. Parasites, ecosystems and sustainability: An ecological and complex systems perspective. Int. J. Parasitol., 35: 725-732. https://doi.org/10.1016/J.IJPARA.2005.03.002

Ieshko, E.P., Lebedeva, D.I., Anikieva, L.V., Gorbach, V.V. and Ilmast, N.V. 2022. Helminth communities of *Coregonus lavaretus* (Salmonidae: Coregoninae) from Lake Kamennoye (Kostomuksha State Nature Reserve, Russia). Nat. Conserv. Res., 7(3): 75-87. https://dx.doi.org/10.24189/ncr.2022.032

Ivanov, A.Y., Ruchin, A.B., Fayzulin, A.I., Chikhlyaev, I.V., Litvinchuk, S.N., Kirillov, A.A., Svinin, A.O. and Ermakov, O.A. 2019. The first record of the natural transfer of mitochondrial DNA from *Pelophylax cf. bedriagae* into *P. lessonae* (Amphibia, Anura). Nat. Conserv. Res., 4(2): 125-128. https://dx.doi.org/10.24189/ncr.2019.020

Kaicheen, S.S. and Mohd-Azlan, J. 2022. Community structures of mid-sized to large-bodied mammals in tropical lowland and lower montane forests in Gunung Pueh National Park, Western Sarawak, Borneo. Nat. Conserv. Res., 7(1): 70-79. https://dx.doi.org/10.24189/ncr.2022.009

Kirillov, A.A., Kirillova, N.Y. and Chikhlyaev, I.V. 2012. Trematodes of land vertebrates of the Middle Volga region. Cassandra, 11: 329.

Kirillov, A.A., Ruchin, A.B., Fayzulin, A.I. and Chikhlyaev, I.V. 2015a. Helminths of reptiles in Mordovia: preliminary data. Proc. Mord. St. Nat. Res., 14: 243-255.

Kirillov, A.A., Ruchin, A.B. and Artaev, O.N. 2015b. Helminths of bats (Chiroptera) from Mordovia. Bull. Univ. Tatishch., 4: 319-328.

Kirillov, A.A., Kirillova, N.Y. and Spiridonov, S.N. 2023. Trematodes of land birds from the Republic of Mordovia with a checklist of avian trematodes of the Middle Volga region (European Russia). Diversity, 15: 330. https://doi.org/10.3390/d15030330

Kononova, M.I. and Prisniy, Yu.A. 2020. Helminthes of mouse-like rodents in the Belogorye State Nature Reserve (Russia). Nat. Conserv. Res., 5(2): 11-18. https://doi.org/10.24189/ncr.2020.036

Kostyunin, V.M. 2010. Helminth fauna of land vertebrates in the Middle Volga region. Nizhny Novgorod State Pedagogical University, pp. 225.

Kouassi, R.Y.W., McGraw, S.W., Yao, P.K., Abou-Bacar, A., Brunet, J., Pesson, B., Bonfoh, B., N'goran, E.K. and Candolfi, E. 2015. Diversity and prevalence of gastrointestinal parasites in seven non-human primates of the Taï National Park, Côte d'Ivoire. Parasite, 22: 1. https://dx.doi.org/10.1051/parasite/2015001

Krucken, J., Blumke, J., Maaz, D., Demeler, J., Ramunke, S., Antolova, D., Schaper, R. and von Samson-Himmelstjerna, G. 2017. Small rodents as paratenic or intermediate hosts of carnivore parasites in Berlin, Germany. PLoS ONE, 12: e0172829. https://dx.doi.org/10.1371/journal.pone.0172829

Lavikainen, A., Iwaki, T., Nakao, M. and Konyaev, S.V. 2015. Genetic Diversity of the Cryptic *Hydatigera taeniaformis* complex. In: Yurlova, N.I, and Konyaev, S.V. (eds.) New knowledge about parasites. Parasitological research in Siberia and the Far East. Materials of the V Interregional conference, Garamond.

Lavikainen, A., Iwaki, T., Haukisalmi, V., Konyaev, S.V., Casiraghi, M.; Dokuchaev, N.E., Galimberti, A., Haljian, A., Henttonen, H., Ichikawa-Seki, M., Itagaki T., Krivopalov AV., Meri S., Morand S., Näreaho A.,

Olsson G.E., Ribas A., Terefe Y. and Nakao M. 2016. Reappraisal of *Hydatigera taeniaeformis* (Batsch, 1786) (Cestoda: Taeniidae) sensu lato with description of *Hydatigera kamiyai* n. sp. Int. J. Parasitol., 46(5-6): 361-374.

Lewin, J. 1990. Parasitic worms in a slowworm (*Anguis fragilis* L.) population from the Bieszczady Mountains (Poland). Acta Parasitol. Polon., 35(3): 207-215.

Machinsky, A.P. and Semov, V.N. 1974. On the fauna of helminths of the sika deer in the Mordovia State Nature Reserve. Proc. Mord. St. Nat. Res., 6: 169-173.

Martinez-Sotelo, J., Sanchez-Jasso, J.M., Ibarra-Zimbron, S. and Sanchez-Nava, P. 2022. Zoonotic intestinal parasites in free-ranging dogs (*Canis lupus familiaris*): A risk to public health in a Mexican protected area. Nat. Conserv. Res., 7(2): 21-31. https://dx.doi.org/10.24189/ncr.2022.015

Matevosyan, E.M. 1964a. Helminth fauna of bison in the Mordovia State Nature Reserve. Proc. Mord. St. Nat. Res., 2: 181-189.

Matevosyan, E.M. 1964b. To the knowledge of the helminth fauna in the common raccoon dog *Nyctereutes procyonoides* Gray. Proc. Mord. St. Nat. Res., 2: 233-235.

Nazarova, N.S. 1974a. Helminth fauna of the sika deer of the Mordovia State Nature Reserve and its change depending on the host age. Proc. Mord. St. Nat. Res., 6: 174-179.

Nazarova, N.S. 1974b. Helminths of complicated hybrids of bison of the Mordovia Nature Reserve. Proc. Mord. St. Nat. Res., 6: 180-185.

Oliger, I.M. 1952. Parasite fauna of the tetraonid birds from the forest area of the European part of the RSFSR. Proc. Helminthol. Lab. Acad. Sci., 6: 411-412.

Oliger, I.M. 1957. Fauna of the parasites of the family Tetraonidae in the forest zone of the European part of the RSFSR. Zool. Zhurn., 36(4): 493-503.

Oliger, I.M. 2016a. Parasite fauna of wild galliform birds in the Mordovia State Nature Reserve. Report of 1941. Proc. Mord. St. Nat. Res., 16: 34-42.

Oliger, I.M. 2016b. Parasite fauna of acclimatized ungulates in the Mordovia State Reserve. 1941. Proc. Mord. St. Nat. Res., 16: 43-52.

Orlova, M.V. and Orlov, O.L. 2019. Conservation of animals' parasite species: problems and prospects. Nat. Conserv. Res., 4(1): 1-21. http://dx.doi.org/10.24189/ncr.2019.011

Poulin, R. and Morand, S. 2004. Parasite Biodiversity. Smithsonian Institution Press, Washington DC., pp. 216.

Pringle, R. 2017. Upgrading protected areas to conserve wild biodiversity. Nature, 546: 91-99. https://doi.org/10.1038/nature2290

Recht, J., Schuenemann, V.J. and Sanchez-Villagra, M.R. 2020. Host diversity and origin of zoonoses: The ancient and the new. Animals, 10(9): 1672. https://doi.org/10.3390/ani10091672

Romashov, B.V., Odoevskaya, I.M., Romashova, N.B. and Golubova, N.A. 2021. Ecology of trichinellosis transmission in the Voronezh State Nature Reserve and adjacent areas, Russia. Nat. Conserv. Res., 6(2): 51-65. https://dx.doi.org/10.24189/ncr.2021.023

Ruchin, A.B. and Chikhlyaev, I.V. 2013. Helminth fauna of the moor frog *Rana arvalis* Nilsson (Amphibia: Anura) in the Republic of Mordovia. Rus. J. Parasitol., 3: 27-34.

Ruchin, A.B. and Kirillov, A.A. 2012. The helminth fauna of the grass snake *Natrix natrix* L. from Republic of Mordovia. Biol. Sci. Kazakh., 4: 30-37.

Ruchin, A.B., Kirillov, A.A., Chikhlyaev, I.V. and Kirillova, N.Y. 2016. Parasitic worms of land vertebrates of the Mordovia State Nature Reserve. Flora and Fauna of Reserves. Vol. 124. Committee of RAS for the Conservation of Biological Diversity, pp. 72.

Ryzhikov, K.M., Gvozdev, E.V., Tokobaev, M.M., Shaldybin, L.C., Matsaberidze, G.V., Merkusheva, I.V., Nadtochiy, E.V., Khokhlova, I.G. and Sharpilo, L.D. 1978. Keys to the helminths of rodents in the USSR fauna: Cestodes and Trematodes. Nauka, 7: 232.

Ryzhikov, K.M., Gvozdev, E.V., Tokobaev, M.M., Shaldybin, L.C., Matsaberidze, G.V., Merkusheva, I.V., Nadtochiy, E.V., Khokhlova, I.G. and Sharpilo, L.D. 1979. Keys to the helminths of rodents in the USSR fauna: Nematodes and Acanthocephalans. Nauka, 14: 272.

Ryzhov, M.K., Chikhlyaev, I.V. and Ruchin, A.B. 2004. About helminths of the marsh frog (*Pelophylax ridibundus*) in Mordovia. Act. Probl. Herpetol. Toxinol., 7: 119-121.

Shaldybin, L.S. 1957. Parasitological worms of wolves in the Mordovia ASSR. Proc. Gorky St. Ped. Inst., 19: 65-71.

Shaldybin, L.S. 1964. Helminth fauna of mammals in Mordovia State Nature Reserve. Proc. Mord. St. Nat. Res., 2: 135-180.

Sharpilo, V.P. 1976. Parasitic worms of the reptilian fauna of the USSR. Naukova Dumka, 11: 376.

Shtarev, Y.F. 1967. The results of the acclimatization of the sika deer in the Mordovia ASSR. Proc. Mord. St. Nat. Res., 3: 55-125.

Shtarev, Y.F. 1971. The results of the acclimatization of the red deer in the Mordovia ASSR. Proc. Mord. St. Nat. Res., 5: 137-170.

Shtarev, Y.F., Potapov, S.K., Astradamov, V.I. and Machinsky, A.P. 1978. Ecology and Helminth Fauna of the Sika Deer in the Conditions of the Mordovia State Nature Reserve. In: Antsiferova, T.A. (ed.) Ecological and Faunistic Research in the Non-Chernozem Zone of the European Part of the USSR. Vol. 1. Mordovia State University.

Turner, W.C. and Getz, W.M. 2010. Seasonal and demographic factors influencing gastrointestinal parasitism in ungulates of Etosha National Park. J. Wildl. Dis., 46(4): 1108-1119. https://dx.doi.org/10.7589/0090-3558-46.4.1108

Vasenkova, N.V. and Kuznetsova, N.A. 2022. A multiscale approach to evaluate the structure of diversity of Collembola in boreo-nemoral forests of the Russian Plain. Nat. Conserv. Res., 7(1): 38-51. https://dx.doi.org/10.24189/ncr.2022.019

## ORCID DETAILS OF THE AUTHORS

N. Yu. Kirillova: https://orcid.org/0000-0002-4585-8970
A. B. Ruchin: https://orcid.org/0000-0003-2653-3879
A. A. Kirillov: https://orcid.org/0000-0002-4374-8858

# State-of-the-art Overview of Biological Treatment of Polluted Water from Rice Mills and Imminent Technologies with Green Energy Retrieval

## R. K. Singh† and S. Bajpai

Department of Civil Engineering, National Institute of Technology, Raipur, Chhattisgarh, India
†Corresponding author: R. K. Singh; rksingh.phd2019.ce@nitrr.ac.in

## ABSTRACT

Rice milling involves shelling and polishing paddy grains to produce rice- both raw and parboiled. Parboiled rice production requires a massive quantity of freshwater for soaking, which, in turn, generates a large amount of wastewater. If this wastewater is not properly ameliorated, it can cause tremendous troubles of surface water pollution, land pollution, and, ultimately, groundwater pollution. Therefore, proper treatment of polluted water from rice mills (PWRM) as per the effluent discharge norms is necessary to protect the surface and subsurface water resources for sustainable development. There are two methods for remediating rice mill wastewater- physicochemical and biological. The biological methods produce comparatively less sludge and are cost-effective. Moreover, these processes are capable of retrieving green energy in the form of biomethane, biohydrogen, and bioelectricity to augment bio-fuel production, aiming to meet the ever-increasing fuel demands caused by rapid industrialization, motorization, and urbanization. The focus on green energy production is gaining momentum day by day due to the adverse effects of conventional energy derived from fossil fuel combustion in terms of enhanced Air Pollution Index (API) in the ambient atmosphere. In this paper, anaerobic biodegradation, phytoremediation, phyco-remediation, and microbial fuel cell techniques adopted by various researchers for remediating the polluted water from rice mills have been well addressed and critically discussed. The pros and cons of these biological methods have been well addressed to assess the socio-techno-economic feasibility of each method.

## INTRODUCTION

Rice is the prime food-grain crop of India. India is the next biggest paddy grower on the planet, with an annual production of 118.9 million tons (MT), followed by China with an annual production of 146.7 MT (Statistica 2021). Rice is produced from paddy, usually in a rice mill. As per the consumer market's demand, stakeholders in the agro-industrial sector produce two types of rice: parboiled rice and raw rice. The parboiled rice is produced by soaking and steaming the paddy in the parboiling unit, drying the paddy to a moisture content of 14%, and ultimately milling the dried paddy to produce parboiled rice. The raw rice is directly produced from paddy by milling after cleaning and drying to the moisture content of 14% (Araullo et al. 1976).

The production of edible rice is a fast-growing industry that has a pivotal role in the country's economic growth. There are about 1,30,000 rice mills in India (FNB News 2022) and more than 1,500 rice mills in Chhattisgarh, including modern rice mills (Department of Commerce & Industries Chhattisgarh 2022). The parboiled rice mills generate a huge amount of wastewater in the soaking operation of the paddy. Industrial wastewater has a deleterious effect on biological diversity, mainly due to its pollution potential . Due to this, wastewater can have severe adverse effects when discharged into natural water bodies without proper treatment (Galvez et al. 2003, Alderson et al. 2005).

Rice constitutes a vital component of the dietary regime for nearly 50% of the world's demography. It provides nearly 21% of the world's food intake and 15% of each protein. Three basic steps to prepare partially boiled rice are soaking, boiling, and drying the paddy before milling. Preference for parboiled rice includes traditional flavor, non-sticky grain structure, and enriched nutrients (Kato et al. 1983, Unnikrishnan & Bhattacharya 1987, Heinemann et al. 2005). However, the paddy from the crop area flooded during harvesting results in breakdown during shelling and polishing operations (Bhattacharya 2011). To tide over this problem, partial boiling of paddy is done to reduce breakage and optimize the production of whole rice grains during these operations.

The quantity of water used for soaking paddy during parboiling is approximately 1.25 times the quantity of paddy to be soaked. The liquid rice mill effluent is produced at nearly 1.0-1.2 liters per kilogram of milled paddy (Rajesh et al. 1999). Continued disposal of this polluted water causes the degradation of water bodies, where algal blooms and eutrophication thrive. Thick layers of algal blooms block sun rays from entering the water in depth, resulting in the drooping of these plants. The drooped plants are degraded by bacteria that utilize large amounts of dissolved oxygen (DO) from the polluted water. As a result, the polluted water is rendered to an oxygen starvation condition for a while. This oxygen starvation condition promotes the microbial species that release toxins. The oxygen starvation state and accumulation of toxic residues in the water eventually result in the death of water creatures like fish and zooplankton (Karul et al. 2000).

The rice mill industry produces several forms of pollution that transit from air to water, soil, and, ultimately, groundwater pollution due to contaminants transported from soil capillaries. Rice husk ash (RHA), disposed of in low-lying terrestrial cavities, also causes severe damage to the groundwater due to contaminant transport, which can seriously affect public and animal health (Santos et al. 2012).

The polluted water from rice mills primarily contains organic materials, total suspended solids (TSS), total dissolved solids (TDS), nutrients, pesticides, lignin, phenol, and pigment, which are attributable to large chemical oxygen demand (COD) values (Behera et al. 2010, Kumar et al. 2015). Lignin is a complicated, bio-refractory, and antagonistic substance in rice mill wastewater. Therefore, it creates problems in biological treatments of polluted water from rice mills (PWRM). The other substance contained in PWRM is phenol, which is also deleterious even at a low level and hampers the microorganisms (Kumar et al. 2015).

The amount of wastewater generated from a parboiled rice mill is nearly $20 \times 10^6$ liters annually in India (Varshney 2012). Thus, approximately 57,850 rice mills producing parboiled rice in India generate polluted water, approximately equal to $1,157 \times 10^9$ liters per year (CPCB 2008). Indian rice mills are of various types according to their production strength (Choudhary et al. 2015). Therefore, regulatory agencies of India for pollution control have furnished stringent guidelines about disposal standards of liquid rice mill effluent (CPCB 2008).

It is imperative to meet disposal standards set by CPCB for industrial wastewater. Hence, the essential treatment of the wastewater must be performed before discharging into water bodies (Mukherjee et al. 2015). According to India's Environment (Protection) Act (1986), each rice mill must establish a completely operational wastewater treatment plant (WWTP). The rice mill should also be accompanied by a biological remediation unit (CPCB 2007). However, owing to the investment required in establishing and maintaining WWTP, most stakeholders in this sector ignore the norms of CPCB (Business Standard 2015, Paul et al. 2015).

Several studies on research findings of the previous researchers on biological treatments of PWRM have been performed; each treatment technique has its own merits and demerits, and the acceptability of each method depends on various parameters viz., expenditures incurred, characteristics of the wastewater and the intended use of the treated water. In the present paper, efforts have been made to explicitly analyze their strategies and evaluate their research outcomes in terms of applicability, sustainability, feasibility, and techno-economic viability. This paper highlights anaerobic digestion, dark fermentation, microbial fuel cells, phytoremediation, and phycoremediation of wastewater from rice mills with the recovery of biomethane, biohydrogen, and bioelectricity as well as the removal of the organic and inorganic pollutants as well as nutrients like nitrogen and phosphorus.

## PARBOILING PROCESS AND SOURCE OF POLLUTED WATER

Conventional techniques of partial boiling of paddy depend on the engineered operations adopted and range from one topographical vicinity to the other (Hettiarachchy et al. 2000). Parboiled edible rice is produced in rice mills and sold overseas from various international locations in Asia. They usually use partial boiling to avoid under-nourishment, food shortages, and wastage (Tomlins et al. 2005).

Parboiled rice production comprises some crucial stages. First, the paddy is soaked in water up to 23-31% moisture content. Heat treatment imparts gelatinization and enables dehydration of the paddy to an appropriate moisture stage suitable for milling operation. Different levels of heat treatment are needed for different partial boiling technologies, leading to parboiled rice production with different properties. The process must be improved to attain high yields and modify the quality of the product before establishing a rice mill (Bhattacharya 1985, Oli et al. 2014). Partially boiled rice is usually brown to yellow due to color dispersion from paddy husks. Moreover, it has high granular rigidity, making the least breakage during shelling and polishing operations difficult. It also has an enriched vitamin B content (Oli et al. 2014).

Paddy is screened to eliminate foreign substances such as grit, pebbles, and stones, as illustrated in Fig.1. The
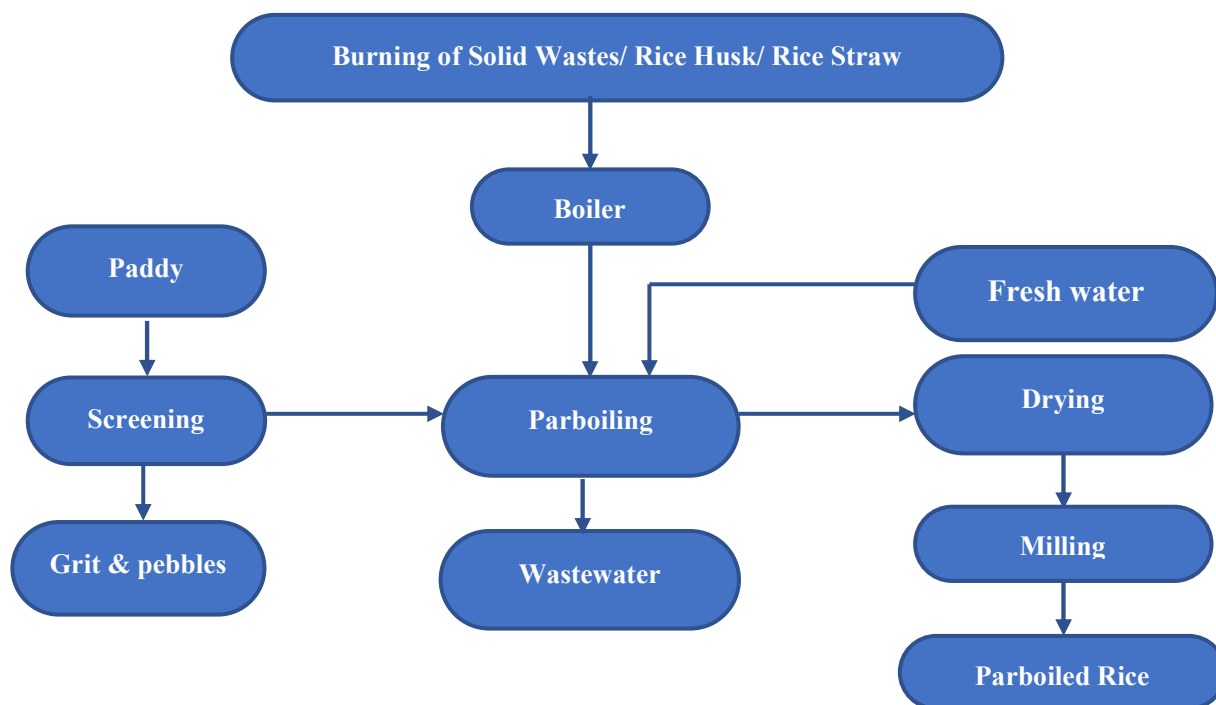
Fig. 1: Flow Diagram of parboiled rice mill processing and origin of PWRM (Asati 2013).

cleaned paddy is then placed into a drum-like vessel for partial boiling. Hot water vapor (steam) is introduced into the drum vessel, and the regenerated hot water is reused continually to ascertain a temperature of 70-100°C for 4 hours (Asati 2013). The parboiling process depends on seasonal variations. It is performed at 92-102°C during the humid rainy season and 72-82°C during summer's dry spell (Araullo et al. 1976). When partial boiling of the paddy is complete, the remaining water is extracted from the drum container. This water extracted from the parboiling unit is the PWRM. It contains organic and inorganic contaminants, including nutrients like nitrogen and phosphorus and bio-refractory organics like lignin and phenol.

Thus, the parboiling unit is the origin of PWRM. Though boiler blowdown is extracted from the same pipeline used for the liquid effluent discharge, its contribution is minimal, as boiler blowdown is generally accomplished every 2-3 months. Thus, the extracted wastewater from the parboiling unit is highly polluted and must be remediated before its discharge either into water bodies or onto the land surface. Where rice mills are far away from the surface water bodies like streams, lakes, and rivers, the wastewater is generally discharged onto the land surface. The source of wastewater generated from the rice milling industry and the processing technology of the parboiled rice mill are shown in Fig. 1.

## Characterization of PWRM

The wastewater generated from rice mills contains various toxic organic materials and inorganic pollutants.

Table 1. illustrates the wastewater characterization of rice mills as previously quoted. The pH variation (4.5-8.5) is encountered due to the different characteristics of the paddy, the partial boiling procedure, and the water quality being adopted. However, the turbidity caused by the total suspended solids (0.3-166 mg.L$^{-1}$) enhances both chemical oxygen demand (COD) and biochemical oxygen demand (BOD), which presents a significant challenge for water creatures by blocking sun rays and interfering with the photosynthetic process (Choudhury et al. 2010).

The wastewater produced primarily contains starch and other carbohydrates, lignin, phenol ($C_6H_5OH$), sulfates, chlorides, nitrates, total Kjeldahl nitrogen (TKN), phosphates, and some pigmenting substances that increase the BOD and COD of the wastewater (Behera et al. 2010). Lignin is a complicated and recalcitrant organic contaminant present in wastewater that hinders the biochemical reactions in the biological treatment of wastewater (Kumar et al. 2015). Phenol is also a virulent aromatic compound, even at small concentrations. Phytotoxicity testing of contaminated water from the rice mill has been performed on *Vigna radiata* (mung bean seeds), which have shown blocked roots and dwarf length of shoots (Kumar & Deswal 2020). Vigorous

toxicological assays have been accomplished in *Lebistes reticulatus*-a, a fish variety, in terms of $LC_{50}$ (deleterious concentration enough to take the life of half of the number of people residing in the affected area). The bioassay test reveals that the toxicity of PWRM to *L. reticulatus* depends upon the exposure time and strength of the wastewater. The anaerobically remediated PWRM is less toxic compared to raw wastewater. During the bio-assay test, the movement of *L. reticulatus* was drastically hindered (Giri et al. 2016). In addition, polluted water from rice mills has been reported to reduce the quality of sperm of zebrafish and, accordingly, lower reproductivity rates (Gerber et al. 2016). Consequently, the efficient and effective bioremediation of PWRM is necessary for safeguarding environmental and ecological sustainability.

## ADVERSE IMPACT OF PWRM ON VARIOUS ECOSYSTEMS

The significant pollutions attributable to the rice mill industry

are to the surface water, groundwater, soil, and air, but this paper emphasizes water pollution. The wastewater from rice mills has inverse impacts on the aquatic, terrestrial, and, ultimately, marine ecosystems. Accordingly, it has the potential to adversely influence the food chain as the pollutants may enter into aquatic and marine ecosystems. Moreover, pollutants added to surface water bodies like rivers and streams and terrestrial land due to untreated and undertreated rice mill wastewater disposal may worsen the water quality of surface and groundwater resources. The direct mixing of pollutants hampers surface water quality, whereas groundwater quality is rendered polluted due to contaminant transport. The wastewater produced by parboiled rice mills comprises high organic matter, nutrients, soluble solvents, pesticides, and phenolic contents (Gil de los Santos et al. 2012). The fish in the aquatic ecosystem may uptake these toxic contaminants. Eventually, they may enter the human and animal bodies in enlarged quantities due to biomagnification when they eat fish. Paul et al. (2015) assessed the impact of PWRM on surface water bodies. They obtained the concentrations of COD and

Table 1: Characterization of PWRM by previous researchers.

| Sl. No. | pH | BOD [mg.L⁻¹] | COD [mg.L⁻¹] | TDS [mg.L⁻¹] | TSS [mg.L⁻¹] | Lignin [mg.L⁻¹] | Phenol [mg.L⁻¹] | Nitrogen [mg.L⁻¹] | References |
|---|---|---|---|---|---|---|---|---|---|
| 1. | 8.00 | 484 | 690 | - | - | - | 47 | 0.53 | Pradhan and Sahu (2004) |
| 2. | 4.22-5.51 | - | 2,578-6,480 | - | - | - | - | 25-95 | Queiroz et al. (2007) |
| 3. | 8.40 | 1,136 | 1,400 | 464 | - | - | - | - | Manogari et al. (2008) |
| 4. | - | - | 5,020 | - | - | - | - | - | Karnaratne (2009) |
| 5. | 4.00-4.30 | - | 2,200-2,250 | - | - | 80-88 | 15-17 | - | Behera et al. (2010) |
| 6. | 7.50 | 1,200 | 1,350 | 700 | 1,100 | - | - | - | Asati (2013) |
| 7. | 4.98 | - | 2,200 | 768 | - | - | - | - | Karichappan et al. (2013) |
| 8. | 4.56 | 2,401 | 2,886 | 1,773 | - | - | - | - | Choudhary et al. (2015) |
| 9. | 7.60 | - | 2,578-5,022 | - | - | - | - | 25.40-50.40 | Bastos et al. (2015) |
| 10. | 4.70 | 1,089 | 1,931 | 3,010 | - | - | - | 36.70 | Mukherjee et al. (2015) |
| 11. | 4.80 | - | 1,708 | 1,578 | - | 182 | 16.21 | - | Kumar et al. (2016) |
| 12. | 4.67-4.90 | 3,968-4,464 | 6,400-7,200 | 1,386-2,340 | 4,187-5,134 | - | - | 62-80 | Giri et al. (2016) |
| 13. | 5.10 | 6,900 | 18,600 | 4,720 | - | - | - | 31 | Ramprakash & Muthukumar (2018) |
| 14. | 6.30 | 9,600 | 19,800 | 8,500 | - | - | - | 39 | Rambabu et al. (2019) |
| 15. | 7.20 | 538 | 1,620 | - | - | - | - | 85 | Keerthana et al. (2020) |
| 16. | 4.51-5.10 | 2,550-2,950 | 4,250-5,120 | 2,030-2,460 | 850-1,170 | - | - | 44-71 | Sadhasivam & Jayanthi (2021) |
| 17. | 5.40 | 1,450 | 3,150 | 3,300 | 220 | 417 | 4.97 | - | Raychoudhuri & Behera (2022) |
| 18. | 5.30 | 3,435 | 5,279 | 4,327 | - | - | - | 45 | Anuf et al. (2022) |
| 19. | 5.40 | 1,350 | 2,800 | 3,300 | - | - | 4.95 | - | Raychoudhuri et al. (2022) |

BOD significantly more in downstream and drainage zones than in upstream samples.

Pradhan and Sahu (2011) examined the application of PWRM to irrigate rice fields. The wastewater was naturally alkaline (pH=8) and enriched with TSS, phenol, and BOD contents of 530, 35, and 450 mg.L$^{-1}$, respectively, with intermediate concentrations of TDS, COD, and phosphate of 670, 630, and 21 mg.L$^{-1}$, respectively. In this examination, the biomass growth, population, and reproduction of the earthworm *Drawida willsi* (Michaelsen) were assessed for 105 days with a sample time of 15 days. There are four main categories of earthworms prevailing in the cultivable land of India, but among them, *D. willsi* predominates, with greater than 80% concentration in biosolids (Pani 1986). The researchers found that the field irrigated by polluted rice mill water contained 22% fewer larvae than the field irrigated by normal river water.

Moreover, there was a diminution of 46% in the cocoon population. The researchers also revealed that the reproduction of cocoons diminishes by about 25% in the experimental plot compared to the control plot. The cocoon and worm populations diminished by about 41% and 26% in the experimental plot compared to the control plot.

## BIOLOGICAL TREATMENT OF PWRM

The primary purpose of the biological treatment of PWRM is to reduce biodegradable organics, nutrients like nitrogen and phosphorus, and other contaminants to meet the effluent discharge standards of CPCB. Its secondary purpose is to achieve bioenergy in the form of biomethane, biohydrogen, and bioelectricity from agriculture-based industrial wastewater. Suppose bioenergy is exploited from agro-industrial effluents and other biomass at full capacity with the help of biological treatment. In that case, it can substantially reduce the dependency of energy requirements on fossil fuel-based thermal power plants. The global carbon footprint from the combustion of fossil fuels like coal, oil, and gas in 2021 is 36.4 billion metric tons, a major contributor to greenhouse gas (GHG) and global warming (USEPA 2022). Thus, biological treatment of biodegradable organic wastes with green energy retrieval is the probable domain that can generate wealth from wastes, diminish pollution loads in major environmental matrices- air, soil, and water, curtail global carbon emissions due to lesser dependence on thermal power plants for energy requirements and save the environment and ecological balance. Biological treatment may be categorized into three types:

- Microbial treatment
- Phytoremediation and
- Phyco-remediation

### Microbial Treatment

A microorganism or microbe is a microscopic organism that is unicellular or multicellular. Microorganisms can be categorized as eukaryotes, prokaryotes, and viruses. The eukaryotes include protozoa, algae, fungi, and bacteria, whereas the prokaryotes include only bacteria and blue-green algae, also called cyanobacteria (Obayashi & Gaudy 1973). Thus, prokaryotes and bacteria are similar terms. Bacteria are unicellular, whereas algae and fungi are usually multicellular. Microbial treatment is a cumbersome process in which microbes, specifically bacteria, slowly degrade biodegradable and harmful organics and nutrients like nitrogen and phosphorus. Some protozoa and fungi also participate in the biodegradation process- aerobic and anaerobic. Microorganisms, except fungi, are generally sensitive to the substrate's pH, temperature, and alkalinity. Fungi are insensitive to pH variation and significantly survive even at diminished pH and low nitrogen levels.

Consequently, fungi are considered in wastewater treatment (Dadrasnia et al. 2017). Microbial treatment is currently quite common because of its simplicity in installation and operation and its generation of minimal toxic substances. It is a more efficacious and low-cost process as compared to physicochemical methods. It is mainly of three types: aerobic, anaerobic, and facultative. The aerobic process works in the presence of oxygen, the anaerobic process functions in the strict absence of oxygen, and the facultative process works both in the presence and absence of oxygen.

Microbial treatment of the polluted water emanating from rice mills may be subdivided into two categories:

- Anaerobic degradation
- Bioremediation with cyanobacteria and yeast

**Anaerobic degradation (AD):** Anaerobic degradation occurs in a strict anaerobic condition by anaerobic and facultative microorganisms. It is a biochemical reaction in four paramount stages: solubilization, acidogenesis, acetogenesis, and methanogenesis (Anukam et al. 2019).

*Solubilization*: Complex organic molecules (carbohydrates, proteins, and lipids) are solubilized into monosaccharides (normal sugars), higher (long-chain) fatty acids, and amino acids.

Chemistry of solubilization-

$$(C_6H_{10}O_5)n + nH_2O \longrightarrow nC_6H_{12}O_6 + nH_2 \quad ...(1)$$
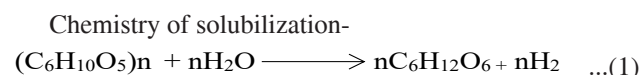
The solubilization of complex organic polymers takes place slowly. The rate and degree at which the polymers are solubilized depend on the following parameters:

- pH of the substrate
- Operational temperature of the anaerobic digester
- Particle size of the food
- Ingredients of the substrate, viz. carbohydrate, protein, lipids, and lignin contents
- The concentration of solubilization products viz. volatile fatty acids (VFA)
- Ammonia nitrogen ($NH_4^+$-N) concentration
- Hydraulic retention time (HRT) and solids retention time (SRT) of the substrate in the digester

*Acidogenesis*: It is the fermentative phase, in which the simple and soluble molecules obtained in solubilization are decomposed into carbon dioxide and hydrogen gas by acidogenic bacteria. The essential acid in this phase is acetic acid ($CH_3COOH$), the most important organic acid used as a substrate by bacteria that generate methane ($CH_4$) gas.

Chemistry of acidogenesis:

$$C_6H_{12}O_6 + 2H_2 \longleftrightarrow 2CH_3CH_2COOH + 2H_2O \quad \ldots(2)$$

$$C_6H_{12}O_6 \longrightarrow 3CH_3COOH \quad \ldots(3)$$

$$C_6H_{12}O_6 \longleftrightarrow 2CH_3CH_2OH + 2CO_2 \quad \ldots(4)$$
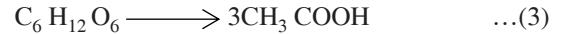
a. Hydrolytic bacteria

b. Fermentative bacteria

c. $H_2$- producing acetogenins

d. $H_2$- utilizing homoacetogens

e. Acetoclastic methanogens

f. $CO_2$- reducing methanogens
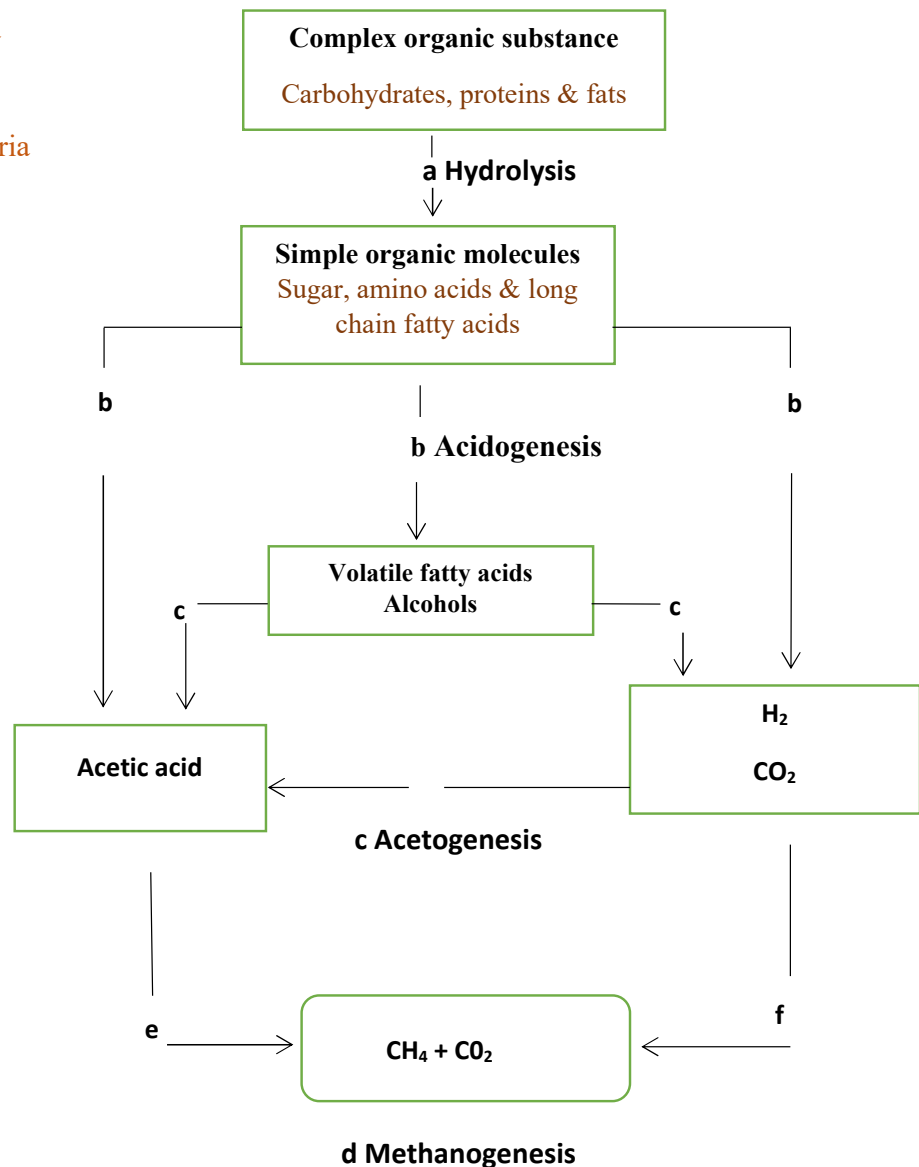


Fig. 2: Flow chart of the anaerobic digestion process (Anukam et al. 2019).

*Acetogenesis***:** In this phase, simpler molecules made by the acidogenic bacteria are converted into acetic acid, $CO_2$, and $H_2$ gases by acetogenic bacteria. This phase is also referred to as dehydrogenation, as the waste of acetogenesis is $H_2$ gas formed in the acidogenic phase.

Chemistry of acetogenesis -

$$C_6H_{12}O_6 + 2H_2O \longleftrightarrow 2CH_3COOH + 2CO_2 + 4H \qquad …(5)$$

$$CH_3CH_2OH + 2H_2O \longleftrightarrow CH_3COO^- + 3H_2 + H^+ \qquad …(6)$$

$$CH_3CH_2COO^- + 3H_2O \longleftrightarrow CH_3COO^- + H^+HCO_3^- + 3H \qquad …(7)$$
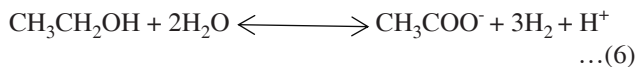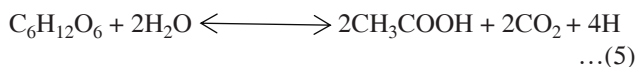
*Methanogenesis***:** It is the final stage of the anaerobic degradation procedure, in which methanogenic bacteria convert intermediate products of the previous phase, namely acetic acid and hydrogen gas, into methane, $CO_2$, and water. Methanogens are frequently anaerobes, and their vulnerability is exceptionally high to little oxygen.

Chemistry of Methanogenesis -

$$CO_2 + 4H_2 \longrightarrow CH_4 + 2H_2O \qquad …(8)$$

$$CH_3COOH \longrightarrow CH_4 + CO_2 \qquad …(9)$$

$$2CH_3CH_2OH + CO_2 \longrightarrow CH_4 + 2CH_3COOH \qquad …(10)$$
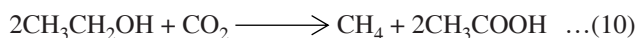
The methanogenic stage is highly vulnerable to high and low pH and strictly takes place in between a pH range of 6.5 to 8.

The anaerobic digestion process is illustrated in Fig. 2.

Rajesh et al. (1999) examined the effectiveness of bioreactors for remediating PWRM. The biodigester used a two-phase bio-methanation procedure employing up-flow anaerobic sludge blanket (UASB) digesters. The efficiencies of removal of BOD and COD were 89% and 78% in the organic loading rate (OLR) of 3 kg $COD.m^{-3}.day^{-1}$. However, this strategy requires further research to be applied in this field.

Lopes et al. (2001) conducted successful experimentation on the denitrification of parboiled rice mill wastewater over a UASB reactor, which creates an anoxic environment. It eradicated the need for an extra digester for denitrifying the wastewater. In addition, the digestion procedure exhibited 80% removal of total nitrogen.

Saini et al. (2016) performed anaerobic treatment of PWRM at room temperature in a lab-scale cylindrical glass UASB reactor with a 2.4-liter reaction volume. The length and diameter of the reactor were 60 cm and 24 cm, respectively. The target substrate was co-digested with filtrate of biogas plant sludge and distilled water in the ratio of 2:1:1. The researcher observed COD removal efficiencies to be more than 97%, 89%, and 86% in phases I, II, and III, respectively, along with the production of biomethane. Studies show that anaerobic digestion is an excellent option to treat rice mill wastewater since 86% COD removal was attained even with a high dose of organic loading, i.e., 100% influent concentration and HRT of 10 hrs.

Sadhasivam & Jayanthi (2021) performed anaerobic treatment of rice mill wastewater (75%) co-digested with distillery sludge (25%) in a lab-scale setup of a constantly stirred anaerobic tank reactor at ambient temperature. The researchers observed that % COD reduction efficiency of 91% was attained at an HRT of 32 days and an OLR of 3.75 kg $COD.day^{-1}.m^{-3}$. The researchers suggest that anaerobic degradation is an appropriate method for the abatement of polluted rice mill water with substantial diminution in COD and resource recovery as methane gas. Studies reveal that a small OLR and considerable HRT provide excellent BOD and COD removal efficiencies as well as continuous and high biomethane yields.

**Bioremediation with cyanobacteria and yeast:** Cyanobacteria are photosynthetic and aquatic. They produce their food in sunlight and live in water. They are tiny and often do not coalesce as bacteria, although they usually grow into colonies large enough to be visible. They differ from prehistoric fossils, dating approximately 3500 million years ago (Whitton & Potts 2012). Since they are water-living microorganisms and photosynthetic, they are often called "blue-green algae." However, there is no correlation between cyanobacteria and other aquatic microorganisms like algae.

Queiroz et al. (2007) treated the PWRM with the help of cyanobacteria *Aphanothece microscopica Nageli* in an agitated biodigester in the batch mode. The dynamic analysis is assessed by 83.44% and 72.74% removal of COD and total nitrogen (Total-N), respectively, after 15 h of HRT. Santos et al. (2012) treated the PWRM with a methylotrophic yeast *Pichiapastoris X-33* in a growth media of 15 grams per liter ($g.L^{-1}$) of biodiesel-derived glycerol. It exhibited a 55%, 45%, and 52% reduction in COD, TKN, and orthophosphate phosphorus ($PO_4^{3-}$- P) and recovered 2.1 $g.L^{-1}$ of the useful biomass.

Manogari et al. (2008) carried out an appraisal investigation on the PWRM by using immobilized cells of a cyanobacterial strain, namely *Pseudomonas species*, belonging to the family Pseudomonadacea, in a packed bed reactor. The investigation exhibited a reduction of 86.44%, 55.34%, 78.07%, 76.36%, and 76.51%, respectively, in COD, BOD, electrical conductivity (EC), salinity, and TDS, in an HRT of 24 hours.

## Merits of Microbial Treatment

a. Cost-effective and minimal energy requirement

b. Biodegradability of the substrate depends upon the BOD/COD ratio

c. Eco-friendly and non-lethal

d. Substantial diminution in hazardous components of the wastewater

e. Recovery of biomethane as a by-product

## Demerits of Microbial Treatment

a. The operation time of the bioreactor is high

b. Nuisance and odor problems in anaerobic digestion

c. High dependency on pH, temperature, alkalinity, and presence of VFA

d. Contaminant reduction largely depends on carbon-nitrogen (C/N) and phosphorus-nitrogen (P/N) ratios

## Phytoremediation

Phytoremediation is a growing technology for the treatment of polluted water. The process requires plants to degrade, mitigate, transport, or stabilize the pollution potential in water, soil, and sludge (Kumar & Deswal 2020). Certain plants diminish organic matter, heavy metals, and nutrients from water and wastewater (Pavlineri et al. 2017). It is an inexpensive and power-efficient procedure that effectively removes contaminants from contaminated water.

Mukherjee et al. (2015) investigated the treatment of PWRM and concluded that the proliferation of *Pistia stratiotes L.* (water lettuce) was hindered in the wastewater without dilution. Subsequently, the researchers diluted the PWRM with fresh water in a ratio of 1:1. They found that removal efficiencies of BOD, total phosphorus (Total-P), and nitrate nitrogen ($NO_3$-N) were 83–85%, 71–73%, and 68–70%, respectively with an HRT of 15 days after adopting the dilution strategy.

Kumar & Deswal (2020) conducted an extensive study on the treatment of PWRM with the help of four water plants, salvinia, water lettuce, duckweed, and water hyacinth, and got an inspiring outcome. The plants diminished COD and Total-P to 75% and 80% during the investigation for 15 days. As a result, some investigators are exploring the actual application of water plants to remediate contaminated water, in which they have obtained motivating outcomes.

Ajayi & Ogunbayio (2012) used water hyacinth to eliminate contaminants from wastewater from the textile, pharmaceutical, and metal industries. Lead elimination by duckweed was studied by Singh et al. (2012). Azeez & Sabbir (2012) also studied the strength of duckweed in removing pollutants from polluted water of petrochemical industries. Favas & Pratas (2013) conducted a comprehensive study on removing uranium through water plants. The elimination of heavy metals from polluted water of paper mills by aquatic plants was evaluated by Mishra et al. (2013). Abu Bakar et al. (2013) studied the elimination of arsenic, aluminum, and zinc from polluted water of goldmines using water plants. The elimination of pollutants from polluted water of sugar mills by water plants was explored by Reddy et al. (2015). The potential use of water hyacinth in removing chromium from sewage was explored by Saha et al. (2017). An extensive study on the bioremediation of landfill leachate by duckweed was conducted by Daud et al. (2018).

## Merits of Phytoremediation

a. It can be applied at the micro level, even in a water tub, as a pilot project

b. Sustainable, cheaper, and simpler biological method

c. Biomass can be harvested and applied in other aerobic and anaerobic reactors

d. Eco-friendly and zero energy-consuming method

## Demerits of Phytoremediation

a. Large operation time, as the plants need time to grow and absorb the pollutants of the wastewater

b. Plants' growth is hindered in the PWRM without dilution since high concentrations of hazardous materials may be toxic to the plants.

c. The depth of the treatment zone is determined by the root zone depth of the plants used in the phytoremediation process.

## Phycoremediation

Phycoremediation is the utilization of microalgae or macroalgae to reduce or bio-transform the contaminants, inclusive of hazardous synthetics as well as nutrients from contaminated water. It is considered an eco-friendly technique in the bioremediation of polluted water. In wastewater, ammonia is the predominant inorganic nitrogen, and algae help convert inorganic nitrogen into organically bound nitrogen by physiological ingestion. The functioning of algae in the bioremediation of polluted water depends on various factors, namely features of wastewater, the intensity of solar insolation, ambient $CO_2$ gas, and N/P & C/N ratios (Hongyang et al. 2011). The bioremediation of wastewater by microalgae was first investigated during the 1950s (Johansen 2012). After this investigation, the correlation between microalgae and bacteria was found in 1957 (Oswald et al. 1957).

Phycoremediation incorporates algal treatment as a biological method to sustainably facilitate the treatment of polluted water with green energy retrieval. Microalgae, the heterotrophic and photosynthetic microorganisms, can remediate polluted water by taking excessive pollutants and nutrients (Wang et al. 2012, Solovchenko et al. 2014). Phycoremediation is a cost-effective and efficacious method for remediating nutrient-laden wastewater from industries such as tanneries, textiles, carpet milling, and food processing, where a substantial elimination of nutrients and biomass production is visualized to occur (Pathak et al. 2014, Fazal et al. 2018).

A lot of investigators have investigated the capability of microalgae/algae to remediate polluted water. Abinandan et al. (2015) studied bioremediation of the PWRM by *Chlorella pyrenoidosa* and *Scenedesmus abundans* in a 500-mL Erlenmeyer flask comprising 300 mL of contaminated water under irradiation of a flashlight having an intensity

of illumination of 1800 lux. The outcomes achieved in this investigation illustrated a significant elimination of $PO_4^{3-}$- P and $NH_3$-N to 97% and 91%, respectively. Kim et al. (2010) carried out an extensive study on nutrient removal from the PWRM by a species of green microalgae *Chlorella vulgaris* in a batch reactor with an HRT of 9 days and obtained 55.8% of $NH_3$-N removal. The biodegradation of secondary effluent by Cyanobacterium *Phormidium bohneri* was accomplished in a batch reactor for an HRT of 5 days (Laliberte et al. 1997). The researchers found that the cyanobacterium removed $PO_4^{3-}$- P and NH3-N, 1.6-13.8 $mg.L^{-1}.day^{-1}$ and 2.4-19.9 $mg.L^{-1}.day^{-1}$, respectively.

Umamaheshwari & Shanthakumar (2020) studied the growth of five microalgal species using response surface methodology (RSM) in the PWRM viz. *Chlorella vulgaris* (Cv), *Chlorella pyrenoidosa* (Cp), *Spirulina* sp. (Ss), *Scenedesmus obliquus* (So) and *Scenedesmus abundans* (Sa). Better biomass production and substantial wastewater

Table 2: Evaluation of various biological treatment processes for PWRM.

| Sl. No. | Method | Brief-description | Result | Reference |
|---|---|---|---|---|
| 1. | Phycoremediation (*Chlorella pyrenoidosa*) | Research works performed on raw PWRM and autoclaved PWRM. Light illuminance = 1800 lumen/m$^2$ | Pollutants reduction: Raw PWRM = 97.5% Autoclaved PWRM = 97.7% $NH_3$-N reduction: Raw PWRM = 90.3% Autoclaved PWRM= 91.4% | Abinandan et al. (2015) |
| 2. | Phyco-remediation (*Scenedesmus abundans*) | Research works performed on raw PWRM and autoclaved PWRM. Light illuminance = 1800 lumen.m$^{-2}$ | Pollutants reduction: Raw PWRM = 98.3% Autoclaved PWRM = 98.7% $NH_3$-N reduction: Raw PWRM = 92% Autoclaved PWRM = 90% | Abinandan et al. (2015) |
| 3. | Phytoremediation | Water lettuce (*Pistia Stratiotes*) applied in 1:1 diluted PWRM with tap water; plant growth hindered in undiluted ww | Pollutants reduction: COD = 65% $NH_3$-N = 98% $NO_3$-N = 70% Phosphates = 65% | Ramprakash & Muthukumar (2015) |
| 4. | Phytoremediation | Four hydrophytic plants, viz., water lettuce, water hyacinth, salvinia, and duckweed, were applied in 1:1diluted PWRM with tap water | Pollutants reduction: Total-P = 80% COD = 75% Operation time = 15 days Max. removal efficiency shown by water lettuce | Kumar & Deswal (2020) |
| 5. | Dark fermentation | Nickel oxide (NiO) and cobalt oxide (CoO) nanoparticles included in the dark fermentation process of PWRM | NiO NPs (nanoparticles) increased biohydrogen production by 2.1 to 2.4 times; CoO NPs increased biohydrogen production by 1.9 to 2.0 times | Rambabu et al. (2021) |
| 6. | Dark fermentation | Combined methods of dark fermentation and Electro-fermentation adopted for PWRM | 41% more hydrogen production compared with dark fermentation alone | Ramprakash et al. (2021) |
| 7. | Anaerobic digestion | 75% PWRM+ 25% distillery sludge used in an anaerobic batch reactor | COD reduction = 91% | Sadhasivam & Jayanthi (2021) |

Table 3: Economic efficiency and suitability of different biological treatment methods for PWRM.

| Sl. No. | Method | Capital Requirement | HRT | Value addition | Effluent Quality |
|---------|--------|---------------------|-----|----------------|------------------|
| 1. | Microbial treatment | Medium | Large | Biomethane in anaerobic process<br>Biohydrogen in the dark fermentation process<br>Bioelectricity in microbial fuel cells | Medium to good |
| 2. | Phytoremediation | Small | Large | Biomass | Inferior |
| 3. | Phyco-remediation | Small | Large | Biomass | Inferior |

abatement were obtained by 30% inoculum size at 25°C. *Chlorella pyrenoidosa* showed a high content of dry biomass (831 mg.L$^{-1}$) and over 90% uptake of $PO_4^{3-}$- P and $NH_3$-N out of all chosen microalgae. Similar results were obtained for *Chlorella vulgaris* and *Scenedesmus obliquus,* with a more than 80% removal potential. Moreover, *Chlorella pyrenoidosa* showed the best result at a higher temperature. In contrast, other species failed to sustain biomass generation and the elimination of $PO_4^{3-}$-P and $NH_3$-N. The growth pattern for microalgae was in the descending order of Cp > Cv > So > Sa > Ss in the PWRM. This study has justified that phycoremediation may be an effective wastewater treatment method while selecting the appropriate species and conditions indispensable for grade-up applications.

**Merits of Phycoremediation**

a. Retrieval of valuable by-product

b. Biodegradability is significantly achieved

c. Eco-friendly and non-toxic

d. There is no requirement for any chemical to be added

e. Low installation and operation cost

**Demerits of Phycoremediation**

a. High dependency on pH, temperature, alkalinity, and the presence of VFA

b. Large operation time

c. Pollutant removal is highly dependent on light, C/N, and P/N ratios.

According to the literature on the biological treatment methods of PWRM, we can conclude that each method has its own merits and demerits. Hence, the adoption of the appropriate method depends on the use of the treated effluent. If the treated effluent is proposed for irrigation, slightly inferior-quality effluent may be used. On the contrary, if the effluent is intended to be used for cattle farming or recycling for the parboiling operation unit in the rice mill itself, we may go for physicochemical treatment methods, viz., adsorption by chitosan and electrocoagulation, where effluent quality is superior. However, physicochemical treatment methods have their drawbacks of being costly and generating a huge amount of sludge, whose safe disposal is a big concern. Table. 3.

reveals the criteria for economic efficiency and suitability of different biological treatment methods of PWRM. The following inferences can be concluded from the literature.

• Phytoremediation is favorable for small enterprises and household wastewater treatment systems. It is an energy-saving and non-polluting biological method advantageous for countryside areas, where sufficient land is not a big problem. It is a time-consuming method and requires a sizable land area. The growth of the hydrophytic plants in undiluted PWRM is impeded due to excessive concentration of the pollutants and low pH value. Therefore, it is suggested that the wastewater must be blended with fresh tap water before treatment by phytoremediation technique. However, this technique is unable to treat wastewater containing radioactive pollutants.

The quality of the effluent by this technique is a bit inferior. Consequently, treated effluent by this method is not safe for cattle farming. Rather, it is quite safe for irrigating crops. The researchers should open new avenues for integrating microorganisms with phytoremediation to improve effluent quality.

• Phycoremediation is also efficacious for micro-industrial and household wastewater remediation. Like phytoremediation, it is an environment-friendly, non-polluting, and non-toxic method. The microalgae and algae are chlorophyll-rich, photosynthetic, and single-celled tiny hydrophytes. They significantly reduce nutrients like nitrogen and phosphorus, BOD, COD, and other toxic contaminants, but they moderately enhance total solids (TS) by the microalgal growth. The nutrient removal efficiency of phytoremediation is 78% to 99%, whereas BOD and COD removal efficiencies are 40% to 65%. However, overall effluent quality by this method is slightly inferior. Consequently, effluent from this technique should also be encouraged for irrigation purposes.

• Microbial treatment is a cost-effective, environment-friendly, and non-lethal method. It facilitates enhanced efficiency in removing volatile substances (organic materials) and leaves a smaller carbon footprint. Anaerobic digestion depends upon pH, temperature,

alkalinity, VFA, C/N ratio, and P/N ratio. Aerobic digestion is an energy-intensive biodegradable process requiring energy for aerating the bioreactor. Anaerobic digestion is an energy-saving process in which aeration is not required as anaerobes strictly work without oxygen. Anaerobic digestion contributes to the value addition in the form of biomethane as a by-product. The effluent quality of microbial treatment is medium to good. Therefore, the effluent from the microbial treatment process may be used for cattle farming and recycling to the parboiling unit in the rice mill after slight physicochemical treatment, like adsorption by chitosan or electrocoagulation.

## VALUE ADDITION FROM PWRM

Technology has radically changed in treating polluted water from various industries, including rice mills and other agro-industries. However, the stakeholders of this pertinent sector in previous times merely intended to eliminate pollutants from wastewater. But nowadays, this notion has changed. They aspire to create wealth from waste. They are trying to restore value-added products with reduced energy consumption due to breakthroughs in microbiological science and biotechnology. These retrieval techniques are referred to as water resource recovery facilities (WRRFs), according to Gude et al. (2016).

The concerns for the environment emphasize recycling industrial wastes along with the retrieval of valuable products. Recycling waste is also essential for a sustainable environment and the economy since it compensates the expenditures incurred on the operation and maintenance of WWTP by generating green energy. Therefore, the future use of polluted water for retrieving enormous amounts of valuable products is gaining momentum day by day.

The prime purpose of traditional treatment plants for polluted water is to eliminate impurities from the wastewater aimed at meeting disposal regulations and stabilizing the sludge aftermath. However, the ongoing decline in conventional energy sources, the ecological imbalance caused by enhanced pollution load on the environment, and the insufficient availability of water resources necessitate appropriate endeavors to achieve sustained ecosystems. The conversion of wastewater and sludge into bioenergy is an innovative technology of non-conventional energy sources with the help of microorganisms, whose ultimate aim is to diminish the discharge of non-reclaimed wastes into the environment.

### Microbial Fuel Cell (MFC)

MFC is a modern technology that generates bioelectricity with the aid of exoelectrogen bacteria while removing pollutants from medium to high-strength wastewaters (Pant et al. 2010, He et al. 2015). It is an electro-biochemical device in which electrical energy is generated by microbes that accomplish the anaerobic degradation of organic materials. Microbes oxidize organic materials to generate protons and electrons in the anodic chamber, and bioelectricity is generated due to the release of electrons. Carbon dioxide ($CO_2$) gas and biomass are also released due to the biochemical reactions involved in this bio-assay procedure. Behera et al. (2010) have used PWRM as a viable substrate to prepare MFC for generating bioelectricity and removing pollutants from wastewater. Researchers have achieved remarkable outcomes of earthen container MFC concerning bioelectricity generation and abatement of organics from the PWRM.

Raychoudhury & Behera (2020) revealed that the main hurdle in achieving higher production from MFC is the loss of organics due to methanogenesis. Hence, coulombic efficiency (CE) can be increased by regulating methanogenesis. The researchers compared the effect of three inoculum treatment techniques viz. thermal treatment ($MFC_t$), ultrasonic treatment ($MFC_u$), and aeration ($MFC_a$) for controlling methanogenesis using PWRM as the substrate of MFC. $MFC_t$, $MFC_u$, and $MFC_a$ gave power densities of 309.19 mW.m$^{-3}$, 525.62 mW.m$^{-3}$ and 656.10 mW.m$^{-3}$ respectively. Thus, $MFC_u$ and $MFC_a$ gave 1.7 and 2.1 times higher power densities than $MFC_t$. Similarly, $MFC_t$, $MFC_u$, and $MFC_a$ exhibited CE of 9.27%, 14.14%, and 17.21%, respectively. The researchers concluded that intermittent aeration by air exposure of inoculum was observed to be more beneficial for bioelectricity generation in MFC.

Raychoudhury & Behera (2021) explored acidogenic pretreatment to the PWRM to increase the generation of bioelectricity as well as substrate removal efficiency of the MFC. The researchers acidified the PWRM in the acidogenic chamber to promote the biodegradation of complex organics before feeding it to MFC. They compared the performance of the acidogenic chamber-MFC unit (MFC-Acid.) with a conventional dual-chambered MFC (MFC-Con.) for an HRT of 15 days. The average COD removal efficiency for MFC-Acid. And MFC-Con. HRT of 15 days was 74.96 ± 0.98% and 70.71 ± 1.24%, respectively, under steady-state conditions. The higher COD removal efficiency in the former case was achieved due to acidogenic pretreatment, which facilitated the conversion of complex organics into simpler compounds. Similarly, the maximum volumetric power density was obtained in MFC-Acid. MFC-Con. were 2.34 ± 0.07 W.m$^{-3}$ and 2.11 ± 0.04 W.m$^{-3,}$ respectively under the steady-state condition.

### Biohydrogen and Methane Generation

Hydrogen is an eco-friendly, energetic, non-conventional, and

reclaimable propellant with tremendous energy. According to Demirbas et al. (2011), hydrogen burns vigorously to produce 2.75 times more energy than petrochemicals, and, in this combustion, water is the only final product. Hydrogen gas is considered a superior alternative to fossil fuels due to its specific characteristics of the highest gravimetric energy density (i.e., $120 \, kJ.g^{-1}$), zero carbon emission on the ignition, and substantial energy-transmitting efficiency (Rambabu et al. 2019). Wang et al. (2011) generated hydrogen gas ($H_2$) and $CH_4$ from industrial wastewater and municipal sewage by fermentation techniques in two phases, along with contaminants removal aimed at providing economic development potential for waste management.

PWRM comprises a large amount of biodegradable organic materials like starch, cellulose, and hemicellulose, so it is one of the efficient and renewable bioresources for the generation of biohydrogen (Ramprakash & Muthukumar 2014). Peixoto et al. (2012) produced hydrogen and methane from PWRM by fermenting wastewater with microflora in two phases.

Ramprakash & Muthukumar (2015) produced bio-hydrogen from starch-rich PWRM using *Klebsiella aerogenes* (also known as *Enterobacter aerogenes*) and *Citrobacter freundii* (a species of *Enterobacteriaceae* family). The results reveal effective enzymatic hydrolysis with a reduction in COD of 71.8%. In addition, a substantial amount of hydrogen was produced through a combination of acid and enzymatic processes. Furthermore, the researchers ameliorated bio-hydrogen generation through a mutant strain of *Enterobacter aerogenes* compared with the indigenous species.

Rambabu et al. (2021) investigated that biohydrogen production was enhanced by introducing nickel oxide (NiO/26 nm) and cobalt oxide (CoO/50 nm) nanoparticles (NPs) at a concentration of $1.5 \, mg.L^{-1}$ to dark fermentation of PWRM using *Clostridium beijerinckii* DSM 791- a gram-positive, rod-shaped and motile bacteria of the genus *Clostridium*. Biohydrogen generation was enhanced by 2.09 and 1.9 times for optimum dosage ($1.5 \, mg.L^{-1}$) of NiO and CoO, respectively, compared with the control run without NPs. COD removal efficiencies of 77.6% and 69.5% were obtained for NiO and CoO nanoparticles (NPs), significantly more than the control run without NPs (57.5%). Thus, including NiO and CoO NPs in wastewater fermentation is a good technique for enhanced biohydrogen production.

In the future, there is enormous potential to remove pollutants from wastewater and, at the same time, produce bioenergy by dint of biological treatments. However, obtaining significant levels of efficiency and productivity are major threats to be tided over to allow for effective implementation.

## CONCLUSION

The rice milling industry must comply with the strict effluent discharge standards and maintain human health and environmental sustainability. Effective wastewater treatment and safe disposal of the sludge produced are essential for this. However, the rice millers are not complying with the effluent discharge norms of CPCB satisfactorily due to the excessive expenditures incurred on it. So, the current challenge is to enunciate an economical and affordable method for the sustainable treatment of PWRM. The favorable results of biological treatment techniques remain in generating fewer wastes, reducing harmful chemicals, and converting waste into valuable resources. This paper discusses three techniques for the biological treatment of PWRM: microbial treatment, phytoremediation, and phycoremediation. Phytoremediation and phycoremediation have also emerged as cost-effective and non-polluting techniques for the remediation of PWRM. Phycoremediation may be encouraged in a small community at grass root levels. The treated water by biological treatment methods may be used for irrigating crops, fisheries, and other aquacultural practices for sustainable water management. The authors conclude that future research should focus on developing novel and innovative biological treatments for wastewater, including PWRM. In addition, it should focus on reducing massive sludge production, retrieving precious by-products, and conserving ecological balance.

## ACKNOWLEDGEMENT

## REFERENCES

Abinandan, S., Bhattacharya, R. and Shanthakumar, S. 2015. Efficacy of chlorella pyrenoidosa and *Scenedesmus abundans* for nutrient removal in rice mill effluent (paddy-soaked water). Int. J. Phytoremed., 17(4): 377-381.

Abu Bakar, A.F., Yusoff I., Fatt, N.T., Othman, F. and Ashraf, M.A. 2013. Arsenic, zinc, and aluminum removal from gold mine wastewater effluents and accumulation by submerged aquatic plants (*Cabomba piauhyensis*, *Egeria denser*, and *Hydrilla verticillata*). Biomed. Res. Int., 13: 890803.

Ajayi, T.O. and Ogunbayio, A.O. 2012. Achieving environmental sustainability in wastewater treatment by phytoremediation with water hyacinth (*Eichhornia crassipes*). J. Sustain. Dev., 5(7): 8.

Alderson, M.P., Santos, A.B.D. and Filho, C.R.M. 2015. Reliability analysis of low-cost, full-scale domestic wastewater treatment plants for reuse in aquaculture and agriculture. Ecol. Eng., 82: 6-14.

Anuf, A.R., Ramaraj, K., Sivasankarapillai, V.S., Dhanusuraman, R., Maran, J.P., Rajeshkumar, G. and Díez-Pascual, A.M. 2022. Optimization of electrocoagulation process for treatment of rice mill effluent using response surface methodology. J. Water Process Eng., 49: 103074.

Anukam, A., Mohammadi, A., Naqvi, M. and Granstrom, K. 2019. A review of the chemistry of anaerobic digestion: Methods of accelerating and optimizing process efficiency. Processes, 7(8): 504.

Araullo, E.V., De Pauda, D.B. and Graham, M. 1976. Rice: Post Harvest Technology. International Development Research Centre, Ottawa, Canada, pp. 163-204.

Asati, S.R. 2013 Treatment of wastewater from parboiled rice mill unit by coagulation/flocculation. Int. J. Life Sci. Biotechnol. Pharm. Res., 2: 264-277.

Azeez, N.M. and Sabbir, A.A. 2012. Efficiency of duckweed (Lemna minor L.) in phytoremediation of wastewater pollutants from Basrah oil refinery. J. Appl. Phytotechnol. Environ. Sanit., 1(4):163-172.

Bastos, R.G., Bonini, M.A., Zepka, L.Q., Jacob-Lopes, E. and Queiroz, M.I. 2015. Treatment of rice parboiling wastewater by cyanobacterium Aphanothece microscopica Nägeli with potential for biomass products. Desal. Water Treat., 56(3): 608-614.

Behera, M., Jana, P.S., More, T.T. and Ghangrekar, M.M. 2010. Rice mill wastewater treatment in microbial fuel cells fabricated using proton exchange membrane and earthen pot at different pH. Bioelectrochemistry, 79: 228-233.

Bhattacharya, K.R. 1985. Parboiling of rice. In: Juliano, B.O. (ed), Rice: Chemistry and Technology, Second Edition, American Association of Cereal Chemists, St. Paul, pp. 289-348.

Bhattacharya, K.R. 2011. Rice Quality. Woodhead Publishing Limited, Cambridge, UK.

Business Standard 2015. Rice Mills: HC Refuses to Extend Deadline for Getting Pollution. Press Trust of India, Chennai (Accessed on 29.01.2022).

Central Pollution Control Board (CPCB) New Delhi 2007. Guidelines on Effluent Characteristics (Accessed on 17.01.2022).

Central Pollution Control Board (CPCB) 2008. Comprehensive Industry Documents On The Pulse, Wheat, And Rice Mills. Ministry of Environment and Forest. Govt. of India Report, New Delhi, p. 76.

Choudhary, M., Majumder, S. and Neogi, S. 2015. Studies on the treatment of rice mill effluent by electrocoagulation. Sep. Sci. Technol., 50: 505-51.

Chowdhury, P., Viraraghavan, T. and Srinivasan, A. 2010. Biological treatment processes for fish processing wastewater: A review. Bioresour. Technol., 101: 439-449.

Dadrasnia, A., Usman, M. M., Lim, K. T., Velappan, R. D., Shahsavari, N., Vejan, P. and Ismail, S. 2017. Microbial Aspects in Wastewater Treatment–A Technical. Environmental Pollution and Protection, 2(2): 75-84.

Daud, M.K., Ali, S., Abbas, Z., Zaheer, I.E., Riaz, M.A., Malik, A., Hussain, A., Rizwan, M., Zia-ur-Rehman, M. and Zhu, S.J. 2018. The potential of duckweed (Lemna minor) for the phytoremediation of landfill leachate. J Chem., 2018: 1-9.

Demirbas, A., Balat, M. and Balat, H. 2011. Biowastes-to-biofuels. Energy. Convers. Manage 52: 1815-1828.

Department of Commerce & Industries, Chhattisgarh 2022. https://industries.cg.gov.in

Favas, P.J.C. and Pratas, J. 2013. Uptake of uranium by native aquatic plants: potential for bioindication and phytoremediation. E3S Web Conf 1: 2-4.

Fazal, T., Mushtaq, A., Rehman, F., Khan, A. Ullah, Rashid, N., Farooq, W., Rehman, M.S.U. and Xu J. 2018. Bioremediation of textile wastewater and successive biodiesel production using microalgae. Renewable Sustainable Energy Rev., 82 (Feb): 3107-3126.

FNB (Food and Beverages) News 2022. Rice Processing and Value Addition in India FB http://www.fnbnews.com

Galvez, J.M., Gomez, M.A., Hontoria, E. and Gonzalez-Lopez, J. 2003. Influence of hydraulic loading and air flow rate on urban wastewater nitrogen removal with the submerged fixed-film reactor. J. Hazard. Mater., 101(2): 219-229.

Gerber, M.D., Junior, A.S.V., Caldas, J.S., Corcini, C.D., Lucia, T. Jr., Correa, L.B. and Correa É.K. 2016. Toxicity evaluation of parboiled rice effluent using sperm quality of zebrafish as bioindicator. Ecol. Indic., 61: 214-218.

Gil de los Santos, D., Gil Turnes, C. and Rochedo Conceição, F. 2012. Bioremediation of parboiled rice effluent supplemented with biodiesel-derived glycerol using Pichia pastoris X-33. Sci. World J., 2: 1-5.

Giri, D.R., Singh, E. and Satyanarayan, S. 2016. Comparative study on toxicity evaluation of anaerobically treated parboiled rice manufacturing wastewater through fish bioassay. Water Sci Technol., 73(8): 1825-1831.

Gude, V.G. 2016. Wastewater treatment in microbial fuel cells e an overview. J. Clean. Prod., 122: 287-307.

He, C., Mu, Z., Yang, H., Wang, Y., Mu, Y. and Yu, H. 2015. Electron acceptors for energy generation in microbial fuel cells fed with wastewaters: A mini-review. Chemosphere, 140: 12-17.

Heinemann, R.J.B., Fagundes, P.L., Pinto, E.A., Penteado, M.V.C. and Lanfer-Marquez, U.M. 2005. Comparative study of the nutrient composition of commercial brown, parboiled, and milled rice from Brazil. J. Food Comp. Anal., 18: 287-296.

Hettiarachchy, N.S., Ju, Z.Y., Siebenmorgen, T. and Sharp, R.N. 2000. Rice: Production, Processing, and Utilization. Handbook Cereal Sci. Technology, 203-221.

Hongyang, S., Yalei, Z., Chunmin, Z., Xuefei, Z. and Jinpeng, L. 2011. Cultivation of Chlorella pyrenoidosa in soybean processing wastewater. Bioresour Technol., 102(21): 9.

Johansen, M.N. (ed). 2012. Microalgae: Biotechnology, Microbiology, and Energy. Nova Science, New York.

Karichappan, T., Venkatachalam, S., Jeganathan, P. M. and Sengodan, K. 2013. Treatment of rice mill wastewater using continuous electrocoagulation technique: optimization and modeling. J. Korean Chem. Soc., 57(6): 761-768.

Karul, C., Soyupak, S., Çilesiz, A.F., Akbay, N. and Germen, E. 2000. Case studies on the use of neural networks in eutrophication modeling. Ecol. Model., 134(2-3): 145-152.

Karunaratne, H.W.G.I. and Gunasekera, M.Y. 2010. Removal of Pollutants In Soak Water Resulting from Parboiling of Paddy. M. Tech. Thesis. Department of Chemical and Process Engineering of the University of Moratua, Sri Lanka.

Kato, H., Ohta, T., Tsugita, T. and Hosaka, Y. 1983. Effect of parboiling on texture and flavor components of cooked rice. J. Agri. Food Chem., 31(4): 818-823.

Keerthana, S., Sekar, S., Kumar, S.D., Santhanam, P., Divya, M., Krishnaveni, N., Arthikha R. and Kim, M.K. 2020. Scenedesmus pecsensis cultivation in rice mill effluent using commercial scale nutrient sources. Bioresour. Technol. Rep., 9: 100379.

Kim, J., Lingaraju, B.P., Rheaume, R., Lee, J. and Siddiqui, K.F. 2010. Removal of ammonia from wastewater effluent by Chlorella vulgaris. Tsinghua Sci. Technol., 15(4): 391-396.

Kumar, A., Priyadarshinee, R., Roy, A., Dasgupta, D. and Mandal, T. 2016. Current techniques in rice mill effluent treatment: emerging opportunities for waste reuse and waste-to-energy conversion. Chemosphere, 164: 404-412.

Kumar, A., Singha, S., Dasgupta, D., Datta, S. and Mandal, T. 2015. Simultaneous recovery of silica and treatment of rice mill wastewater using rice husk ash: An economic approach. Ecol. Eng., 84: 29-37.

Kumar, S. and Deswal, S. 2020. Phytoremediation capabilities of Salvinia molesta, water hyacinth, water lettuce, and duckweed to reduce

phosphorus in rice mill wastewater. Int. J. Phytoremed., 22(11): 1097-1109.

Laliberte, G., Lessard, P., De La Noüe, J. and Sylvestre, S. 1997. Effect of phosphorus addition on nutrient removal from wastewater with the Cyanobacterium *Phormidium bohneri*. Bioresour. Technol., 59(2-3): 227-233.

Lopes, L.F., Koetz, P.R. and Santos, M.S. 2001. Denitrification on the top of UASB reactors of rice wastewater. Water Sci. Technol., 44(4): 79-82.

Manogari, R., Daniel, D. and Krastanov, A. 2008. Biodegradation of rice mill effluent by immobilized *Pseudomonas* sp. cells. Ecol. Eng. Environ. Protect., 1: 30-35.

Mishra, S., Mohanty, M., Pradhan, C., Patra, H.K., Das, R. and Sahoo, S. 2013. Physicochemical assessment of paper mill effluent and its heavy metal remediation using aquatic macrophytes - A case study at JK Paper mill, Rayagada, India. Environ. Monit. Assess., 185(5): 4347-4359.

Mukherjee, B., Majumdar, M., Gangopadhyay, A., Chakraborty, S. and Chatterjee, D. 2015. Phytoremediation of parboiled rice mill wastewater using water lettuce (Pistia Stratiotes). Int. J. Phytoremed., 17(7): 651-656.

Obayashi, A.W. and Gaudy Jr., A.F. 1973. Aerobic digestion of extracellular microbial polysaccharides. J. Water Pollut. Contr. Fed., 174: 1584-1594.

Oli, P., Ward, R., Adhikari, B. and Torley, P. 2014. Parboiled rice: understanding from a materials science approach. J. Food Eng. 124: 173-183.

Oswald, W.J., Gotaas, H.B., Golueke, C.G., Kellen, W.R., Gloyna, E.F. and Hermann, E.R. 1957. Algae in waste treatment (with discussion). Sewage Ind. Waste, 29(4): 437-457.

Pani, S.C. 1986. Aspects of Ecological Studies on Tropical Earthworms in the Irrigated Agricultural System of Orissa, India. Ph.D. Thesis, Sambalpur University, p. 232.

Pant, D., Van Bogaert, G., Diels, L. and Vanbroekhoven, K. 2010. A review of the substrates used in microbial fuel cells (MFCs) for sustainable energy production. Bioresour. Technol., 101: 1533-1543.

Pathak, V.V., Singh, D.P., Kothari R. and Chopra, A.K. 2014. Phycoremediation of textile wastewater by unicellular microalga *Chlorella pyrenoidosa*. Cell. Mol. Biol., 60(5): 35-40.

Paul, J., Abhijith, D., Vr, A.R., Joy, J. and Latheef, S. 2015. Environmental impact of rice mills on groundwater and surface water. Int. J. Civ. Struct. Eng. Res., 3(1): 11-15.

Pavlineri, N., Skoulikidis, N.T. and Tsihrintzis, V.A. 2017. Constructed floating wetlands: a review of research, design, operation and management aspects, and data meta-analysis. Chem. Eng. J., 308: 1120-1132.

Peixoto, G., Pantoja-Filho, J.L.R., Agnelli, J.A.B., Barboza, M. and Zaiat, M. 2012. Hydrogen and methane production, energy recovery, and organic matter removal from effluents in a two-stage fermentative process. Appl. Biochem. Biotechnol., 168(3): 651-671.

Pradhan, A. and Sahu, S.K. 2004. Process details and effluent characteristics of a rice mill in the Sambalpur district of Orissa. I Contr. Pollut., 20(1): 414-436.

Pradhan, A. and Sahu, S.K. 2011. Effect of rice mill wastewater on population, biomass, rate of reproduction, and secondary production of *Drawida willsi* (Oligochaeta) in rice field agroecosystem. Int. J. Res. Rev. Appl. Sci., 6(2): 138-146.

Queiroz, M.I., Lopes, E.J., Zepka, L.Q., Bastos, R.G. and Goldbeck, R. 2007. The kinetics of the removal of nitrogen and organic matter from parboiled rice effluent by cyanobacteria in a stirred batch reactor. Bioresour. Technol., 98(11): 2163-2169.

Rajesh, G., Bandyopadhyay, M. and Das, D. 1999. Some studies on UASB bioreactors for the stabilization of low-strength industrial effluents. Bioprocess Eng., 21(2): 113-116.

Rambabu, K., Bharath, G., Thanigaivelan, A., Das, D.B., Show, P.L. and Banat, F. 2021. Augmented biohydrogen production from rice mill wastewater through nano-metal oxides assisted dark fermentation. Bioresour. Technol., 319: 124243.

Rambabu, K., Show, P.L., Bharath, G., Banat, F., Naushad, M. and Chang, J.S. 2019. Enhanced biohydrogen production from date seeds by *Clostridium thermocellum* ATCC 27405. Int. J. Hydrog. Energy, 45: 22271-22280.

Ramprakash, B. and Muthukumar, K. 2014. Comparative study on the production of biohydrogen from rice mill wastewater. Int. J. Hydrog. Energy, 39(27): 14613-14621.

Ramprakash, B. and Muthukumar, K. 2015. Comparative study on the performance of various pretreatment and hydrolysis methods for the production of biohydrogen using *Enterobacter aerogenes* RM 08 from rice mill wastewater. Int. J. Hydrog. Energy, 40(30): 9106-9112.

Ramprakash, B. and Muthukumar, K. 2016. Biohydrogen production from rice mill wastewater using mutated *Enterobacter aerogenes*. Eng. Agric. Environ. Food, 9(1): 109-115.

Ramprakash, B. and Muthukumar, K. 2018. Influence of sulfuric acid concentration on biohydrogen production from rice mill wastewater using pure and coculture of *Enterobacter aerogenes* and *Citrobacter freundii*. Int. J. Hydro. Energy, 43(19): 9254-9258.

Ramprakash, B., Lindblad, P., Eaton-Rye, J.J. and Incharoensakdi, A. 2022. Current strategies and future perspectives in biological hydrogen production: A review. Renew. Sustain. Energy Rev., 168: 112773.

Raychaudhuri, A. and Behera, M. 2020. Comparative evaluation of methanogenesis suppression methods in microbial fuel cell during rice mill wastewater treatment. Environ. Technol. Innov., 17: 100509.

Raychaudhuri, A. and Behera, M. 2021. Enhancement of bioelectricity generation by integrating acidogenic compartment into a dual-chambered microbial fuel cell during rice mill wastewater treatment. Process Biochem., 105: 19-26.

Raychaudhuri, A. and Behera, M. 2022. Effect of operating parameters on rice mill wastewater treatment in an acidogenic chamber and MFC coupled system. Bioresour. Technol. Rep., 10: 249.

Raychaudhuri, A., Sahoo, R.N. and Behera, M. 2022. Sequential anaerobic-aerobic treatment of rice mill wastewater and simultaneous power generation in the microbial fuel cell. Environ. Technol., 16: 1-7.

Reddy, S.S.G., Raju, A.J.S. and Kumar, B.M. 2015. Phytoremediation of sugar industrial water effluent using various hydrophytes. Int. J. Environ. Sci., 5(6): 1147.

Sadhasivam, S. and Jayanthi, S. 2021. An experimental study on biogas production by anaerobic digestion of rice mill wastewater. Glob. NEST J., 23(1): 27-34.

Saha, P., Shinde, O. and Sarkar, S. 2017. Phytoremediation of industrial mines wastewater using water hyacinth. Int. J. Phytoremed., 19(1): 87-96.

Saini, J.K., Saini, A. and Lohchab, R.K. 2016. Rice mill wastewater treatment by up-flow anaerobic sludge blanket reactor. Int. J. Plant Anim. Environ. Sci., 6(3): 128-134.

Singh, D., Gupta, R. and Tiwari, A. 2012. Potential of Duckweed (Lemna minor) for removal of lead from wastewater by phytoremediation. J. Pharm. Res., 5(3):1578-1582.

Solovchenko, A., Pogosyan, S., Chivkunova, O., Selyakh, I., Semenova, L., Voronova, E. and Lobakova, E. 2014. Phyco-remediation of alcohol distillery wastewater with a novel *Chlorella sorokiniana* strain cultivated in a photobioreactor monitored online via chlorophyll fluorescence. Algal Res., 6: 234-241.

Statistica 2021. Production volume of rice in India FY 2010-2022- Statistica. https://www.statistica.com₅statistics

Tomlins, K.I., Manful, J.T., Larwer, P. and Hammond, L. 2005. Urban consumer preferences and sensory evaluation of locally produced and imported rice in West Africa. Food. Qual. Pref., 16 (1): 79-89.

Umamaheswari, J. and Shanthakumar, S. 2020. Optimization of temperature and inoculum size for phyco-remediation of paddy-soaked rice mill wastewater. J. Environ. Eng., 146(1): 04019091.

Unnikrishnan, K.R. and Bhattacharya, K.R. 1987. Influence of varietal difference on properties of parboiled rice. Cereal Chem., 65(4): 315-321.

USEPA 2022. Global Greenhouse Gas Emission Data. US Environmental Protection Agency

Varshney, C.K. 2012. All India Rice Exporters Association Event. Available online at: http://www.airea.net/Events-Rice (Accessed on 17.12.2021).

Wang, H., Xiong, H., Hui, Z. and X. Zeng. 2012. Mixotrophic cultivation of *Chlorella pyrenoidosa* with diluted primary piggery wastewater to produce lipids. Bioresour. Technol., 104: 215–220.

Wang, W., Xie, L., Chen, J., Luo, G. and Zhou, Q. 2011. Biohydrogen and methane production by co-digestion of cassava stillage and excess sludge under thermophilic conditions. Bioresour. Technol., 102: 3833-3839.

Whitton, B.A. and Potts, M. 2012. Introduction to the Cyanobacteria. Ecology of Cyanobacteria II: Their Diversity in Space and Time. Springer, NY, 1-13.

# Optimization of Supply Chain Network in Solid Waste Management Using a Hybrid Approach of Genetic Algorithm and Fuzzy Logic: A Case Study of Lagos State

**O. J. Oyebode†** (iD) **and Z. O. Abdulazeez**

Civil and Environmental Engineering Department, Afe Babalola University, Ado-Ekiti, Ekiti State, Nigeria

†Corresponding Author: O. J. Oyebode; oyebodedare@yahoo.co

## ABSTRACT

A strategic shift towards sustainable, appropriate supply chain networks and data-driven decision-making in solid waste management in rural and urban areas can drastically reduce environmental pollution. This study utilizes a hybrid strategy of genetic algorithms and fuzzy logic to improve the supply chain network in solid waste management in Lagos State. In this research, four local governments in Lagos State are taken as a case study to help Identify solid waste in those selected areas, acquire data to better understand the supply chain network in solid waste management, and use the data acquired to model for the algorithm. A series of 30 iterations were carried out using a fitness parameter of frequency, price range, and means of disposal to determine who should be given utmost importance in the chain. Supply chains often exhibit inadequacies that may be enriched using Artificial Intelligence (AI) tools. The optimization model is flexible and useful, so everyone involved in the chain can coexist harmoniously. One of the reasons causing these inadequacies in proper waste management is a poorly planned supply chain network. It was concluded that the scavengers must be recognized as major participants in the movement of waste from houses to these provided refuse bins, with their frequency increased to 6 times daily with dustbins ranging from 9-20 be provided on each street which the private service participants (PSP).

## INTRODUCTION

Solid waste management is becoming more than just an environmental concern, with the world's solid waste estimated at 2.01 billion tons and Lagos at 14,000 metric tonnes daily. One of the most significant environmental issues, air pollution, is mostly a concern in urban areas. It is challenging to monitor atmospheric pollution, especially particulate matter and nitrogen oxides, and this problem must be solved for both health and wealth. Waste is defined as any material that has been discarded and is no longer useful to humans. Waste can be made up of any material, including solid, liquid, organic, toxic, or biodegradable. While some garbage can be recycled, other garbage cannot. The term "solid waste" refers to a collection of trash from a variety of sources, including household, institutional, industrial, commercial, and demolition sites (as well as waste from public spaces and hazardous waste) (British Columbia Government 2018). The options include house-to-house collection, community bins, curbside pickup, self-delivery, and hired or delegated service (Olberg et al. 2018). All

of these factors contribute to the rapid accumulation of municipal solid waste in every state's waste management system due to uncontrolled population growth, rapid industrial growth, and rising community living standards. 1.3 billion tons of municipal solid waste (MSW) are generated every day, according to Singh et al. (2011) an estimate that is equivalent to two-thirds of a kilogram or ten times the weight of an adult's body in a year. As of February 2021, more than 50 million tons of hazardous chemicals have been disposed of worldwide. Global garbage production is expected to reach 3.4 billion tons by 2050, according to current projections. According to a survey of 151 large cities worldwide, insufficient solid waste disposal is the community's second most serious issue after unemployment (Elahi 2009).

Waste management is an important part of any developing or industrial society, and its generation and disposal are influenced by factors such as population growth, societal awareness, and the government's response and approach. It could be argued that the amount of waste produced does not always equate to a problem, but rather the

government's, individual's, and waste management force's response to the accumulated waste. Compilation of almost all waste produced globally isn't technically difficult, but it is mostly solid, and one of the issues that arise in this regard is organizational issues. For example, the means of waste collection and transportation are weighed in societies where proper and adequate structured management companies are present. Chemical, physical, and product analyses are also performed regularly on appropriate waste samples. But in places like Nigeria, especially Lagos state, the management of waste disposal isn't good enough; meanwhile, the problem with solid waste has reached an alarming level. Lagos, Nigeria's most populous state, is home to a large percentage of the country's population. In 2021, the population of Lagos' metropolitan area was 14,862,000, an increase of 3.44 percent from 2020. As of 2020, Lagos' metro area had a population of 14,368,000, an increase of 3.34 percent from 2019. Lagos State's population is expected to rise, and with it, an efficient waste management system is needed. This is because poor solid waste management has many undesirable characteristics that our society cannot tolerate.

## EARLIER STUDIES

One of the most significant and newly emerging potential difficulties in the majority of large cities is the availability of land for effective trash disposal. Landfill dumping remains the primary method of trash disposal despite some efforts to reduce and reclaim garbage (Ramu et al. 2023). Owing to this problem, some researchers conduct research and experiment to recover waste heat from any resources to be combined with an application to decrease energy usage (Ramadan et al. 2017). Every household or commercial space may employ air conditioning for thermal comfort and to maintain indoor air quality (Wu et al. 2020). In developing nations, improper municipal solid waste disposal poses serious environmental and health risks (Ayomoh et al. 2008). The life cycle analysis

(LCA) approach is useful for estimating greenhouse gas emissions from different waste management activities (Ali et al. 2016). The promotion of waste management laws and regulations was done to help with guidance and to lessen the continual dumping of waste into rivers, waterways, and illegal dump sites (Abila & Kantola 2013). Environmental quality is a prerequisite for an increase in per capita well-being over time, and the sustainable management of waste approach seeks to achieve this (Bari et al. 2012, Ayininuola & Muibi 2008). Human beings are exposed to toxic chemicals through various pathways (Ogarekpe et al. 2023).

There is a global need for effective waste management, necessitating intensive research and development efforts to examine innovative applications for sustainable and environmentally sound management (Oyebode 2013, Oyebode & Otoko 2022). Engineering intervention and strategic groundwater monitoring surrounding landfills are required for environmental sustainability, pollution reduction, and public health as urbanization and population growth continue in the megacity (Oyebode et al. 2023). Waste is a byproduct of life that can be produced by municipal, industrial, familial, individual, and developmental activities like civil engineering construction projects. To promote public health, economic prosperity, and effective energy systems, the management of solid wastes must be effective (Oyebode 2018, 2019). Waste incineration is the principal method for managing medical waste in poor nations like Nigeria, with the pathogen removal from the waste stream and trash volume and reactivity reduction having positive economic effects (Oyebode et al. 2022, Oyebode & Coker 2021). A key assurance of social and economic sustainability is the availability of water resources. Enhancing water's ecological carbon sequestration capacity directly reacts to the double carbon objective. Water quality evaluation significantly impacts human life and development (Guojiao et al. 2023).
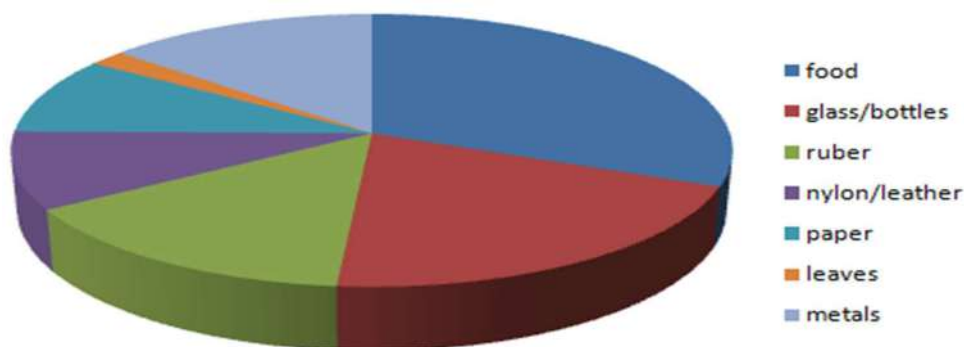


Source: (Khair et al. 2019)

Fig. 1: Compositions of household wastes.

In general, waste can be classified as solid, liquid, or gaseous (Javourez et al. 2021). Solid wastes: Urban wastes, industrial wastes, agricultural wastes, biomedical wastes, and radioactive wastes are all examples of these (Samson et al. 2011). Fig. 1 gives the Compositions of household wastes.

## Solid Waste Management

The system that oversees the collection, source separation, storage, transportation, treatment, and disposal of solid waste is known as solid waste management (Ahsan et al. 2014). The selection and design of landfill sites is an important step in waste disposal because it allows landfill gas to be extracted as a source of energy that can be used for various energy-producing purposes, generating revenue for the landfill (Kofoworola 2007). We have no choice but to seek a technical method of solid waste management system by using a modern and integrated concept of SC due to the amount of waste generated in Lagos state and Nigeria's inability to collect proper data due to various factors. As a result, waste reduction, recycling, and recovery, as well as appropriate waste treatment methods, more environmentally friendly technology, and appropriate final disposal, should all be considered and encouraged when designing SWM systems (Kofoworola 2007). Fig. 2 presents the waste management cycle.

## Solid Waste Management in Lagos State

The Lagos State Waste Disposal Board, now known as the Lagos State Waste Management Agency (LAWMA), was founded by Lagos State (Afon 2007). The organization is tasked with properly managing the garbage of the state's 14 million citizens and providing a clean environment through transportation, waste disposal site management, and, more recently, recycling. As a result, LAWMA embarked on a public-private partnership project to manage the system. It is open to the public in the sense that LAWMA regulates both residents and private partners. While the PSP is in charge of service delivery, the LAWMA sets rates for households and businesses. Charges for garbage collection are based on direct charges to families and other businesses; the amount to be paid for rubbish collection is determined by the location and kind of households and establishments rather than the volume of waste generated (Anestina et al. 2014). Under state legislation, all Lagos citizens are required to use the services to keep the state clean. Due to financial constraints, this scenario has been exacerbated by some resident households' unwillingness to pay for garbage disposal services. One of the reasons why people in the country, particularly in Lagos State, are unwilling to pay is that the Waste Management Board was founded as a non-profit organization, and its services are considered a public good that attracts little or no cost (Anestina et al. 2014)

The state government has contracted solid waste collection and disposal to private sector operators to maintain a clean Lagos at no additional expense to the government (Idowu et al. 2011). Conservation efforts can only be a long-term success if local people embrace their goals and actions (Anestina et al. 2014).

The supply chain (SC) is the network that connects purchasing, shipping, and processing of raw materials and distributing and delivering goods to customers (Nan et al. 2021). The primary goal of a supply chain is to improve a system's operating efficiency (Gu et al. 2021). SC design is a strategic problem whose solution significantly impacts the SC's performance. It includes decisions about the number and location of production facilities, the amount



Source: (Alli et al. 2016)

Fig. 2: Waste management cycle.

of capacity at each facility, the assignment of each market region to one or more locations, and sub-entity, component, and material supplier selection (Ambe 2012). Supply chain optimization uses the most efficient methods for collecting and transporting solid waste. Transporting raw materials, commodities, and information from start to finish is critical for global trade, as is reverse logistics (moving waste) (MacArthur 2016).

**Network of Supply Chain**

The term "network" is important since it implies that most SCs are more sophisticated than a chain and that flows between entities are an integral feature of the SC (Santabarbara-Ruiz et al. 2015). Managers in a supply chain network (SCN) are responsible for making sustainable strategic decisions for the system. Supply chain management is the process of developing, executing, and operating a supply chain network system to fulfill consumer demand while lowering the total cost of the network's operations (Gurtu & Johny 2021).

**Elements of a Supply Chain**

All of the functions that begin with receiving an order and end with satisfying the customer's request are included in the elements of a supply chain. These responsibilities include planning, sourcing, manufacturing, delivering, and returning (Santabarbara-Ruiz et al. 2015).

**Design and Modeling of a Supply Chain**

Multi-stage supply chain design and analysis models may be separated into four groups by modeling technique. The nature of the inputs and the study's goal influence the modeling technique in the situations shown below.

The four categories are as follows:
- Deterministic analytical models, which have known and stated variables,
- Analytical stochastic models, in which at least one variable is unknown and is assumed to follow a certain probability distribution,
- business models
- A simulation model aims to determine which tactics are the most successful in smoothing demand fluctuations (Fayezi & Zomorrodi, 2015).

**Optimization (Mathematical Optimization)**

Mathematical optimization is selecting the optimal element from a group of alternatives based on criteria. It is frequently utilized when a choice incorporating several factors must be made quickly and efficiently.

The Main Components of Mathematical Optimization Decision variables are physical quantities the decision-maker may control and represent by mathematical symbols.

The objective function defines the criterion for assessing the solution. It is a mathematical function of the choice variables that transforms a solution into a numerical evaluation.

Constraints are a collection of functional equality or inequalities that indicate physical, economic, technological, legal, ethical, or other limitations on the numerical values that can be assigned to decision variables.

The inefficiency of MSW management in Nigeria can be attributed to an improper supply chain, which includes how waste is generated, collected, separated, sorted, distributed, processed, renewed, if necessary, reused, and re-disposed (Sabbas et al. 2003), as the efficiency of MSW management can be improved by supply chain management technique optimization (Mamashli & Javadian 2021).

**Optimization of the Supply Chain Network**

Supply chain optimization uses technology and resources such as blockchain, artificial intelligence, and the Internet of Things to improve supply chain efficiency and performance (Kadad et al. 2020). Silos (data visibility), client demands, competitive advantages, agility, and sustainability are all addressed in a well-designed supply chain (IBM). Within a successful supply chain optimization, there are three stages.

- Supply chain design describes network design activities such as where facilities are situated, how waste and products flow between them, and strategic objectives such as demand forecasting, supply establishment, and industrial operations planning and scheduling.
- Supply chain management involves making a comprehensive plan for supply chain development, planning inventory, and coordinating assets to get customers the most products, services, and information as quickly as possible.
- Managing the supply chain is focused on execution-oriented applications and systems, such as real-time decision support, supply chain visibility, other management systems, warehouse and inventory management, global trade management, and other execution-oriented applications.

**Genetic Algorithm (GA)**

The genetic algorithm is a stochastic optimization approach derived from natural selection and the survival of the fittest (Ray et al. 2021). A genetic algorithm (GA) is a meta-heuristic inspired by natural selection that belongs to the

wider family of evolutionary algorithms in computer science and operations research (EA). Genetic algorithms depend on biologically inspired operators, including mutation, crossover, and selection, to develop high-quality solutions to optimization and search problems. A population of potential solutions to an optimization issue is developed toward superior answers in a genetic algorithm (Joshi 2021).

## Genetic Algorithm Working Principle

GA falls within the category of evolutionary algorithms based on Darwin's theory of evolution. Initially, the genetic algorithm has a population of solutions (represented by chromosomes) (Crowl et al. 1991). A population's solutions are chosen and processed to create a new population. The belief that the new population would perform better than the previous one motivates the planned development of a new population. The fitness of the solutions chosen to create new solutions (offspring) is determined. They will be more capable of passing on their traits to the following generation if they are better suited. It is repeated until a pre-defined criterion (for example, the number of populations or the best solution improvement) is met (Gupta et al. 2019).

## Genetic Algorithm Applications and Uses

a) Engineering design, traffic, and shipping routing, and robotics are just a few real-world uses of genetic algorithms (Suman et al. 2018).

b) Engineering design to make the design cycle quicker and more cost-effective, engineering designs rely on modeling and simulations.

c) Many sales-based organizations employ traffic and shipment routing to save time and money.

d) Robotics, GA, is being utilized to develop learning robots that will act like people and do tasks like preparing our meals and doing our washing.

e) Financial markets are used to forecast the performance of publicly traded stocks in the future.

f) System engineering is the process of doing multi-objective activities, such as developing turbines that generate electricity.

g) Aeronautical engineering to create supersonic aircraft wing shapes that minimize aerodynamic drag at supersonic cruising speeds, subsonic drag, and aerodynamic load.

## The Benefits and Drawbacks of Genetic Algorithms (GAs)

The Benefits of Genetic Algorithms:

1. GAs are capable of addressing issues with a large number of viable solutions.

2. GAs investigate all of their options before deciding on the greatest fit.

3. Genetic algorithms are adaptable and can rapidly adjust to changes.

4. GA's selection process is non-biased and open-minded.

The Drawbacks of Genetic Algorithms:

1. Finding the best way out of hard, high-dimensional, multimodal situations often requires expensive fitness function assessments.

2. Genetic algorithms do not scale effectively as the complexity of the problem increases.

3. The "better" answer is just superior to the alternatives. As a result, the stop condition isn't always obvious.

4. GAs often tend toward local optima or random places instead of the problem's global optimum.

5. GAs can't handle issues if the only fitness criterion is a single right or wrong answer.

6. Other optimization methods may work better than genetic algorithms regarding how quickly they find the best solution to an optimization problem or issue.

## Supply Chain Network Optimization Using a Genetic Algorithm

A genetic algorithm is employed in SC to help filter out all the undesired disruptions that would lead to the SC's ineffectiveness by selecting the best ways to address a given problem using a "survival of the fittest" strategy.

## Fuzzy Logic-Meaning and History

The truth value of variables in fuzzy logic can be any real number between 0 and 1, making it a type of many-valued logic. It deals with partial truth, where the true value might be between true and false. The truth values of variables in Boolean logic, on the other hand, can only be the integer values 0 or 1. The concept of fuzzy logic is founded on individuals making judgments based on inexact and non-numerical data. Fuzzy models or sets are mathematical representations of ambiguity and imprecise data (hence the term "fuzzy"). These models can identify, express, manipulate, understand, and utilize ambiguous and uncertain facts and information.

## Fuzzy Logic's History

With Lotfi Zadeh's proposal of fuzzy set theory in 1965, the term fuzzy logic was coined. However, fuzzy logic has been

investigated as infinite-valued since the 1920s, especially by Ukasiewicz and Tarski.

## Applications of Fuzzy Logic

It's utilized in control systems to allow specialists to input broad guidelines like "raise the train's brake pressure if you're close to the target station and traveling rapidly," which can then be quantitatively improved within the system.

Japan was home to several of the first effective uses of fuzzy logic. The first prominent use was on the Sendai metro train, where fuzzy logic improved the ride's economy, comfort, and accuracy (Emokhare & Igbape 2015). It's also been used by the Institute of Seismology Bureau of Meteorology in Japan for handwriting recognition in Sony pocket computers, helicopter flight aids, subway system controls, improving automobile fuel efficiency, single-button washing machine controls, automatic power controls in vacuum cleaners, and early earthquake detection.

### Artificial Intelligence

When studied, AI and fuzzy logic are the same things. Neural networks have a hazy logic at their core (Bechtler et al. 2001). A neural network will take several valuable inputs, weigh them differently concerning one another, and arrive at a decision that is usually also valuable. There are no sequences of either-or judgments in that process, which describes non-fuzzy mathematics, practically all computer computerized systems of programming, and digital electronics. In the 1980s, academics were split on whether "common sense" models or neural networks were the most successful method of machine learning. The former method necessitates massive decision trees and binary logic compatible with the hardware. Although physical devices are confined to binary logic, AI can do computations via software. This is how neural networks function, resulting in more accurate simulations of complicated situations. A wide range of electrical devices quickly used neural networks.

### Medical Decision-Making

In medical decision-making, fuzzy logic is a crucial notion. Because medical and healthcare data might be subjective or ambiguous, fuzzy logic-based techniques in this sector have a lot of promise to help (Wang et al. 2017).

F fuzzy logic may be employed in various ways within the medical decision-making framework. Medical image analysis, biomedical signal analysis, or signals, and feature extraction selection of images or signals are examples of such aspects.

### Computer-Assisted Diagnosis Using Images

In medicine, image-based computer-aided diagnosis (CAD) is one of the most prevalent domains where fuzzy logic is used. CAD is a computerized system of interconnected tools that can help doctors make better diagnostic decisions. For example, if a clinician discovers an aberrant lesion still in its early stages of development, they may employ a CAD method to describe and identify the lesion's nature. Fuzzy logic can be a good way to characterize the major features of this lesion (Yanase & Evangelos 2019).

### Fuzzy Logic for Supply Chain Optimization

The necessary flow is established in the supply chain regardless of the connection, proving the most effective method for achieving the desired result.

### Supply Chain Network Optimization Using a Hybrid Approach

Because of the intricacy of their hybridization and the inadequacies of each system, the hybridization of multiple functions associated with an ideal supply chain network has not been adequately discussed in earlier research publications. This justifies the urgent need to create a model to address these flaws.

### Fuzzy Logic Hybridization Genetic Algorithm Working Principle

Even though some systems are very complicated and can't be described well with just one AI tool, it's becoming more common to use a combination of fuzzy logic, neuro-computing, and evolutionary algorithms to get a better picture.

State and local government environmental protection organizations in Nigeria are grappling with a growing problem: waste management. A rapid increase in the amount of solid waste produced has outpaced the agencies' ability to increase their financial and technological resources to keep up with it (Ogwueleka 2009).

## MATERIALS AND METHODS

### Description of Area of Study

Lagos is Nigeria's most populous metropolis, with about 20 million people. According to population, it is Nigeria's most populous state but is Nigeria's smallest state by area; it is located in the southwest and covers 3577 square miles. Lagos has a population density of approximately 5032 people per square kilometer and is one of the world's

fastest-growing metropolitan areas, growing at an annual average rate of around 4 percent (Ayeni 2017). About 70% of Nigeria's commercial activity occurs here, and it has an excellent location, which explains the state's large population (ibid). Approximately 37% of Lagos' total land area is devoted to the city's 20 Local Government Areas (LGAs). However, over 85% of the population lives in these areas.

Alimosho LGA, Eti-Osa LGA, Oshodi-Isolo LGA, and Ibeju-Lekki LGA families were surveyed in this study. Two years ago, 11,456,783 people lived in Alimosho LGA, the state's largest and most populous LGA. Now, there are 287,958, 1,621,789, and 288,743 people in Eti-Osa LGA, Oshodi-Isolo LGA, and Ibeju-Lekki LGA (Lagos Bureau of Statistics, 2010). Private operators are located in Alimosho, whereas garbage disposal sites and scavengers are found within Ibeju-Lekki Local Government Area. As a result, all the homes in the city were represented by those who responded. Fig. 3 presents the map of the location of the study in Lagos State.

**Methodological Framework**

An example of a case study methodology is used to describe how this research was conducted. Data collection is an organized collection of data about an individual or individuals, a social situation, or issues through various means and organized in a way that provides a better understanding of the study topic. In addition to being used to study complex phenomena, it also serves as a way for theories

to be applied. For a more thorough understanding of the research topic, it's the systematic gathering and analysis of information about a specific individual or individuals, as well as a social situation or issues. Due to its focus on solid waste management in Lagos State (Nigeria), the case study method is appropriate for this study. Data were gathered for the study using a variety of methods. Because Lagos is Nigeria's most populous city, it was chosen as a case study for this research. Researchers looking to better manage garbage collected from city residents could serve as a model for similar work being done in other cities across the country, as the state appears to be setting an example for development initiatives elsewhere. While many studies have focused on the state's solid waste disposal issues, the sector's major players have received insufficient attention. Characterization and supply chain analysis of solid waste for all trash generated are both included in this study. Hybrid genetic algorithms and fuzzy logic algorithms are proposed to help with the supply chain.

**Data Collection and Methodology**

The approach used in this research is essentially a qualitative method that focuses on the quality of data obtained and analyzed rather than the quantity of study to help find answers to research questions by studying society and its inhabitants to achieve its associated goals. Primary and secondary data were collected from various sources, including field observation and interviews with various stakeholders in Lagos, including homes, private operators, LAWMA staff,



Fig. 3: Map of Lagos State (Google Maps).

Fig. 4: Household waste.



Fig. 5: Scavengers on the site.

and scavengers. A thorough review of relevant literature gathered secondary data. Fig. 4 presented various Household Waste, and Fig. 5 presented typical Scavengers on Site.

## Materials

To collect data from interviews in the field, researchers often use a tape recorder, which allows them to focus on the interviewee's response and follow up on points of interest; they can also identify any inconsistencies in the interviewee's answers if necessary. A camera and the same method were used to monitor the garbage disposal site. A camera and a pair of gloves were used to spy on the house. This study

relied heavily on a camera to capture visual representations of its subject matter and findings to aid in its presentation and comprehension. Photographing various interesting things in the field, including domestic solid waste storage, collection, disposal, and landfill activities, was possible. After completing the fieldwork, all recorded responses and photographs were categorized for analysis.

**Data Analysis**

Qualitative data analysis can be approached in a variety of ways. An in-depth examination of data to discover and interpret trends is known as content analysis. Content analysis is the detailed and in-depth examination of data to identify and interpret trends. A Google questionnaire form was utilized for the household interviews in this study, with graphs and charts created for each respondent's response. A PSP and LAWMA operator reply Excel spreadsheet was employed to tabulate the responses for the scavengers. Following the receipt of the responses, a C++ program was utilized to assist in the execution of the Fuzzy logic and Genetic algorithm iterations.

**Modeling with Fuzzy Logic**

A fuzzy-genetic algorithm is employed in providing suitable optimized solutions.

The fuzzy inference system (FIS) and genetic algorithm are synergized such that the fuzzy inference takes the members of the population as input values and provides an output value that serves as the fitness of the individuals in the population.

The FIS serves the fitness function; hence, it must be built within the boundaries of the definition of a good or poor solution. The Matlab fuzzy logic designer was used to build the fuzzy inference system for each local government area. However, these were implemented in C++ for the benefit of computational speed while continuously iterating through generations of the genetic algorithm.

It is important to define all linguistic variables and the boundaries of the membership functions before building the FIS. This leads to the following:

- The input variables and linguistic variables
- The boundaries of the membership functions
- The Fuzzy Inference System

Input variables and linguistic variables:

To optimize waste management, the genetic algorithm seeks to provide a good solution consisting of the number of refuse bins required to manage the waste produced and how frequently the waste should be removed.

Hence, the input variables to the FIS are 'frequency' and 'number of refuse bins.' The genetic algorithm represents the genotypes using real numbers. Therefore, no conversion is required before passing individuals through the FIS.

Boundaries of the membership function:

a. The frequency input variable consists of two membership functions, namely, poor and good.

b. This variable ranges from 1 to 7 since it describes the number of times the waste is removed in a week.

c. The frequency is 100% poor at the point for which, after the consecutive value of frequency, the waste generated in the remaining days of the week fills up the provided refuse bin.

    If the waste distribution at 'the max' number of refuse bins is 25 bags per day, and the capacity of the refuse bin is 100 bags. It will take 4 days to fill up the bin. Hence, the frequency value '3' is 100% poor. This is because after taking out the refuse for 3 consecutive days, the refuse bin gets full before the next week. Though this consecutive combination is only a probability, it is considered.

d. The input variable, 'number of refuse bins,' has 2 membership functions, namely, poor and good.

e. The number of refuse bins required is 100% poor when the distribution of daily generated waste exceeds or fills the provided bins in a single day, considering the capacity of the bins provided.

    If the total generated waste is 250 bags daily, and the capacity of the bin is 100 bags. If only 2 bins are provided, the daily distribution is 125 bags, which exceeds the capacity of the bin. Hence, the input value 2 is 100% poor.

f. The number of refuse bins required is 100% good at the point where the daily distributed waste takes 5 consecutive days to exceed or fill the bin.

    If the total generated waste is 250 bags daily and the capacity of the bin is 100 bags. It will take 5 days to exceed the capacity using 10 bins.

g. The output value, the fitness value, spans a scale of 1-10, having 2 membership functions, namely, poor and good. They span from end-to-end meetings at 50%.

Fuzzy Inference System:

Generally, there are three popular types of fuzzy inference methods: Mamdani fuzzy inference, Sugeno fuzzy inference, and Tsukamoto fuzzy inference. Fuzzifying the crisp input values into membership values according to appropriate fuzzy sets is the same in all three types. However,

differences occur in integrating rules into a single precise value.

The Mamdani inference is widely used, as it is straightforward and less complex and is used in this project to build fuzzy inference systems. In this inference type, the consequent of the IF-THEN rule is defined by a fuzzy set, and a corresponding value reshapes the output fuzzy set of each rule.

Mamdani-Type Fuzzy Inference Process:

The Mamdani-type fuzzy inference process consists of five steps:

- Fuzzify input variables
- Apply fuzzy operator
- Apply implication method
- Apply aggregation method
- Defuzzification

The input variables and output variables both have 2 membership functions. Hence, complete and symmetric rules are used to avoid disturbance from rules.

IF-THEN rules:

a. If (frequency is poor) and (the number of refuse bins is poor) then (fitness is poor)

b. If (frequency is good) and (the number of refuse bins is good), then (fitness is good.)

The THEN-part (implication) of the fuzzy operator reshapes the fuzzy set of the consequent part according to the result associated with the antecedent. The AND method is set to 'min,' and the aggregation method is set to 'max.' The mean of the maximum defuzzification method is chosen, as it has the characteristic of spanning through to the ends of the output range.

Due to the difference in the population of the considered local government areas, and thus the difference in waste generated, different fuzzy inference systems were built for each local government area.
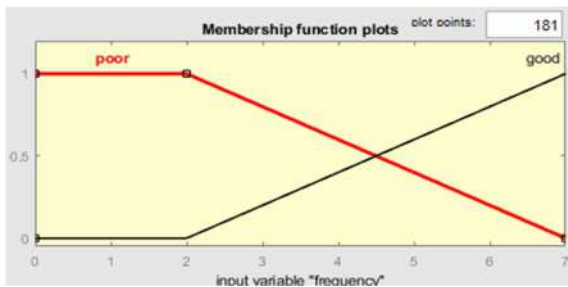


Fig. 6: Frequency membership function plot.
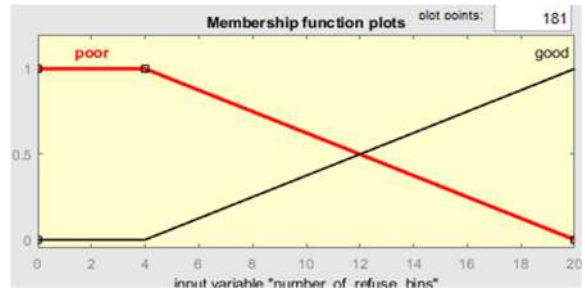


Fig. 7: Number of refuse bins' membership function plot.
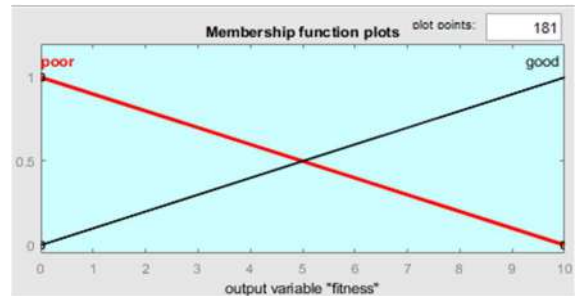


Fig. 8: Output (fitness) membership function plot.
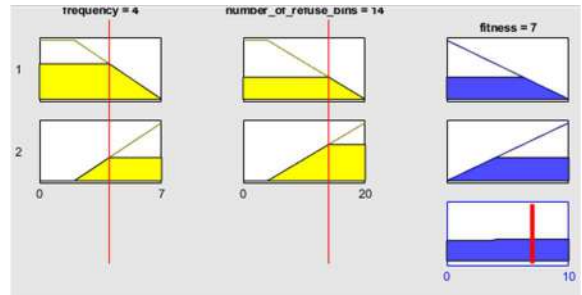


Fig. 9: Implication and aggregation process.
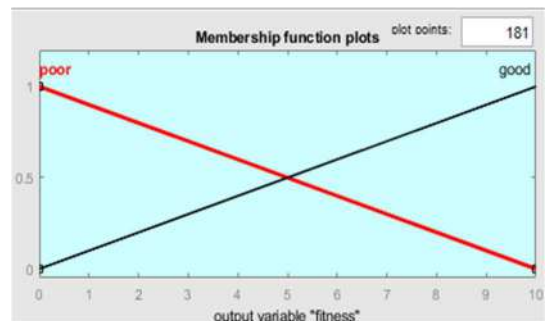


Fig. 10: Output (fitness) membership function plot.

Fig. 6 presents the frequency membership function plot, Fig. 7 presents the Number of refuse bins' membership
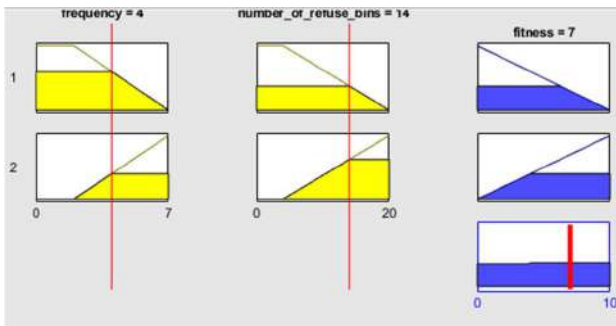
Fig. 11: Implication and aggregation process.



Fig. 14: Implication and aggregation process.

function plot, Fig. 8 presents the Output (fitness) membership function plot, Fig 9: Implication and aggregation process, Fig. 10 presents the Output (fitness) membership function plot and Fig. 11 presents the Implication and aggregation process. It indicates the membership function plots for the inputs, outputs, implication, aggregation, and input-output surface peculiar to each LGA. The membership function plot for frequency input is the same for all LGAs and the output membership function plot. The Fuzzy Inference System
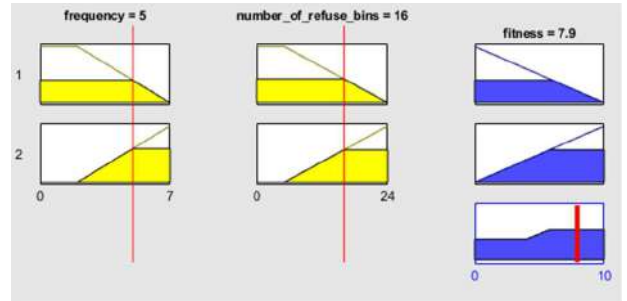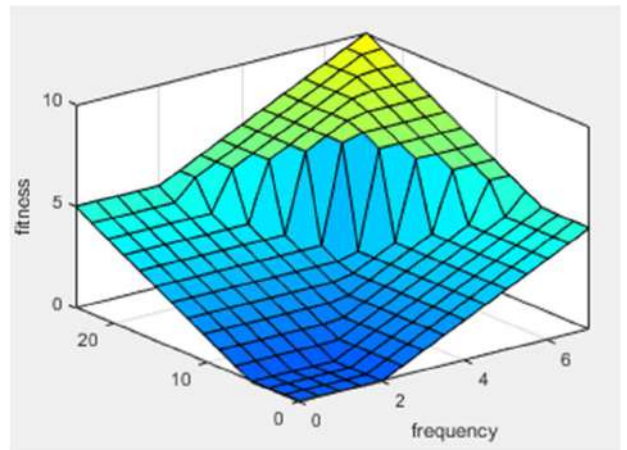


Fig. 15: Input-Output surfaces.
(Fuzzy Inference System For Eti-Osa LGA: Population-287958, Average daily waste-30 bags)
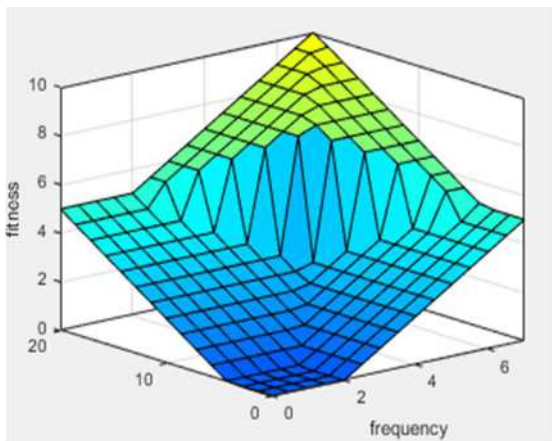
for Alimosho LGA has a population of 11,456,783 and an average daily waste of 212 bags.

Fig. 12 presents Input-Output Surfaces. The Fuzzy Inference System for Oshodi-Isolo LGA: Population-1621789, Average daily waste-48 bags. Fig. 13 presents the Number of Refuse Bins' Membership Function Plot. Fig. 14 presents the Implication and Aggregation Process, and Fig. 15 presents the Input-Output surfaces for the Fuzzy Inference System For



Fig. 12: Input-Output Surfaces.
(Fuzzy Inference System for Oshodi-Isolo LGA: Population-1621789, Average daily waste-48 bags)
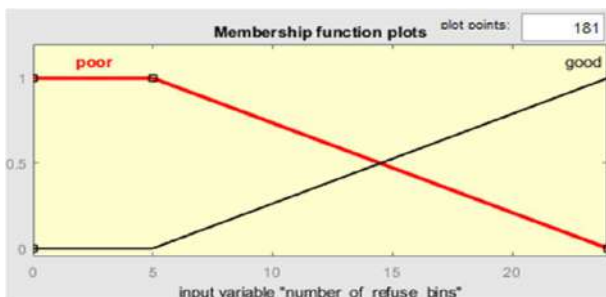


Fig. 13: 'Number of Refuse Bins' Membership Function Plot.
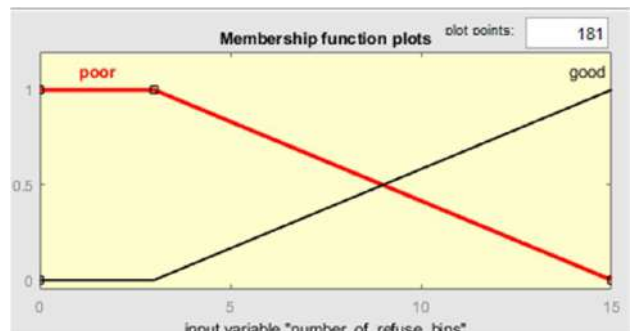


Fig. 16: 'Number of Refuse Bins' Membership Function Plot.
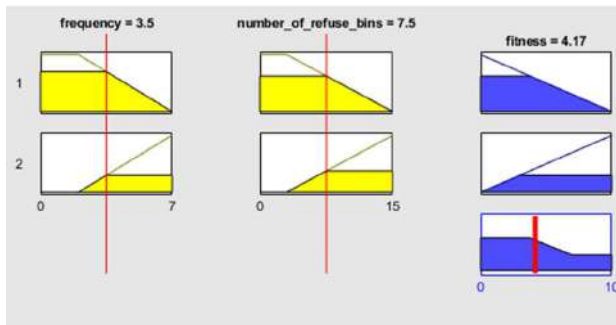
Fig. 17: Implication and Aggregation Process.
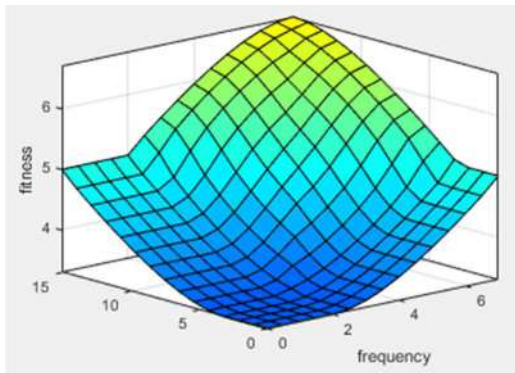


Fig. 18: Input-Output Surface.
(Fuzzy Inference System For Ibeju-Lekki LGA: Population-288,743,
Average daily waste-21 bags)
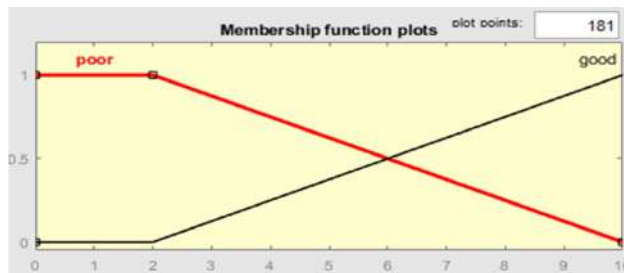


Fig. 19: 'Number of refuse bins' membership function plot.

Eti-Osa LGA: Population-287958, Average daily waste-30 bags.

Fig. 16 presents the number of Refuse Bins' Membership Function Plot, Fig. 17 presents Implication and Aggregation Process, Fig. 18 presents the Input-Output Surface for the Fuzzy Inference System For Ibeju-Lekki LGA: Population-288,743, Average daily waste-21 bags and Fig. 19 presents the Number of refuse bins' membership function plot for various aspects of the study area.

While the FIS provides the fitness of each solution (members of the population), the genetic algorithm selects the best solutions (individuals) in the entire population through a

selection process, performs crossover to create new solutions (offspring), and mutates randomly selected members of the population to maintain diversity. This process is recursively for a specified number of iterations or until some other criteria are attained. In this case, the GA is allowed to run until convergence is attained.

The GA used in this project follows the outlined steps:

- Population Initialization
- Obtain fitness
- Selection process
- Crossover
- Mutation

The GA is manually initialized with 10 random individuals whose fitness is evaluated by the FIS. Selection is carried out using the rank selection method. Beginning at the top, individuals are selected according to their expected count. The size of the population is maintained; hence, once the number of individuals required is reached, the remaining individuals are removed from the population. The best individuals in this new generation are selected, and a randomly selected genotype is exchanged (crossed over) to create offspring that replace the parents. Finally, individuals are randomly selected from the resulting population, and a randomly selected genotype is changed to maintain diversity and prevent premature convergence. Genotypes are represented as real numbers; therefore, mutation is achieved by simply increasing or decreasing a random genotype within the boundaries of its membership function. The GA was implemented in C++ for the benefit of computational speed.

## RESULTS AND DISCUSSION

Data obtained from the field with regard to their different solid waste management practice was analyzed, and the results generated are presented in this section using charts and graphs.

### Composition of Household Waste in Selected Neighborhoods in Lagos State

From the questions carried out during the research work, each household has approximately at least 25% food, 20% glass/bottles, 15% rubber, 15% metals, 10% papers, 10% nylon/leather, and 5% leaves (Fig. 20).

### The Supply Chain Network in the Selected Areas

Any households interviewed did not recycle, although some reuse their waste, and no segregation is done before disposal. Some households prefer to give their waste to scavengers
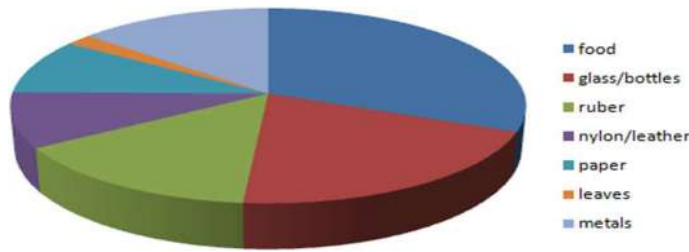
Source: (Mukhtar et al. 2019)

Fig. 20: Composition of Household Waste.
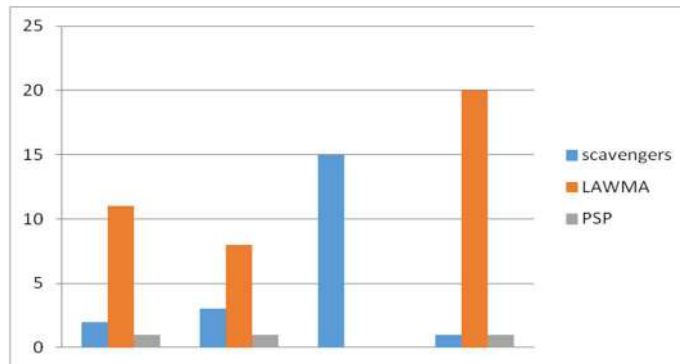


Fig. 21: Preferences of households on personnel for waste disposal.

because it can be sold to itinerant scavengers at a fair price. In addition to selling at a fair price, the scavengers revealed that the metals were piled up, sent to local fabrications, and converted to new items such as metal pots and kettles. While some individuals don't even know what the PSP operators are, those with an idea have no interest in them. Some say it is due to the prices allocated to their waste or their frequency of appearance (Fig. 21).

The GAs were set to stop if the change in average fitness was negligible after several iterations. The Fuzzy-GA provided the following solutions after converging (Fig. 22). The solution consists of how frequently waste should be removed from the provided bin, the number of bins required in the LGA, and the fitness value of each proffered solution (Figs. 23-25, Tables 1-4).

Table 1: Alimosho LGA Fitness Variables.

| Frequency of waste removal | Number of bins required | Fitness |
|---|---|---|
| 7 | 16 | 8.75 |
| 6 | 20 | 9 |
| 6 | 18 | 9 |
| 7 | 18 | 9.4 |
| 7 | 19 | 9.7 |
| 7 | 20 | 10 |
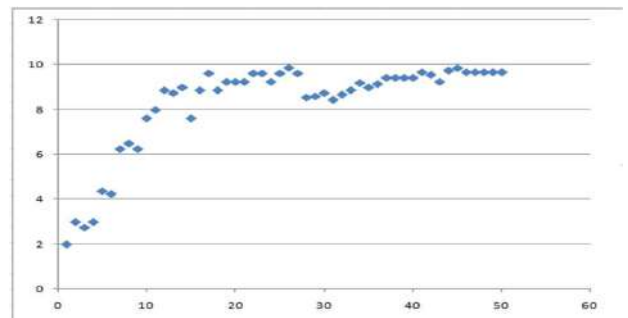


Fig. 22: Scatter plot of Average Fitness for Alimosho.

Table 2: Oshodi-Isolo LGA Fitness Variables.

| Frequency of waste removal | Number of bins required | Fitness |
|---|---|---|
| 6 | 20 | 9 |
| 7 | 24 | 10 |
| 7 | 19 | 8.7 |
| 7 | 21 | 9.25 |
| 6 | 19 | 8.7 |

## CONCLUSIONS

While carrying out the research, it was observed that the bulk of the waste produced in households was 25% food, 20% glass/bottles, 15% rubber, 15% metals, 10% papers,
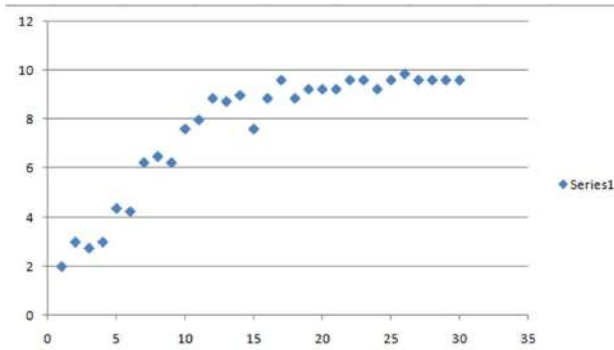
Fig. 23: Scatter plot of Average Fitness for Oshodi-Isolo.

Table 3: Eti-Osa Fitness LGA Variables.

| Frequency of waste removal | Number of bins required | Fitness |
|---|---|---|
| 5 | 10 | 7.95 |
| 7 | 15 | 10 |
| 6 | 13 | 9 |
| 7 | 14 | 9.6 |
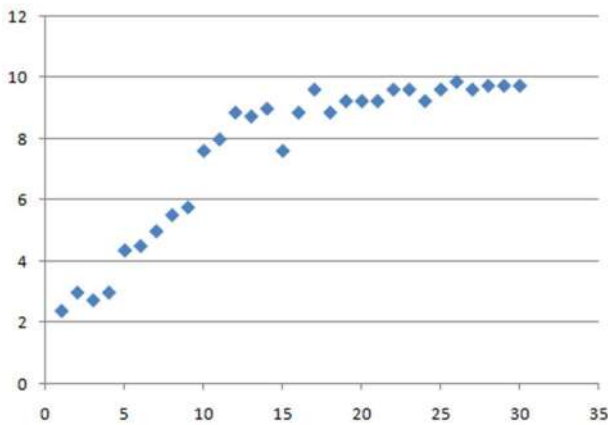


Fig. 24: Scatter Plot of Average Fitness for Eti-Osa.

Table 4: Ibeju-Lekki Fitness Variables.

| Frequency of waste removal | Number of bins required | Fitness |
|---|---|---|
| 7 | 10 | 10 |
| 5 | 7 | 8 |
| 6 | 8 | 8.75 |
| 6 | 9 | 9 |
| 7 | 9 | 9.4 |

10% nylon/leather, and 5% leaves. Of which the household does no proper sorting. Also, most correspondents prefer the inclusiveness of the scavengers due to various reasons ranging from frequency of appearance to price. Some households do not know what the PSP is about, and the data



Fig. 25: Scatter plot of average fitness for Ibeju-Lekki.

was then used in modeling the Fuzzy-GA. The Fuzzy-GA used in this optimization exercise performed efficiently, iterating for at least 30 generations for each LGA. The proffered solutions are peculiar to each LGA and are all options for optimized solutions within the boundaries of the objectives. These solutions not only optimize but preserve the existing waste management supply chain, such that the scavengers can participate by moving the waste from houses to these provided refuse bins. The PSP is involved in moving the waste from the provided bins to the already existing dump sites, where LAWMA handles it with just the appropriate number of workers and materials required for the work allotted to it. Though the provided solutions stand out by fitness values, the best solution should be chosen based on other objectives such as feasibility, cost of implementation, and so on.

## RECOMMENDATIONS

The households that are the major waste generators do not practice waste segregation and recycling. Waste segregation is fundamental for successful management, but due to the probability of financial constraints, the most basic starting point will be the separation of the household itself. This could be done by imploring the household to have at least two waste receptacles, such as wheelie bins, so that organic wastes are put in one, and inorganic waste is put in the order. The LAWMA, as a way of encouragement, could probably provide these waste bins so that if the rules are not followed, sanctions and fines should be placed on those who fail to obey. These methods not only help to separate the waste but also make the job of the workers easier. From the analysis carried out results gathered, it is obvious that all the personnel involved in the waste management have no proper relationships, resulting in improper waste management. For sustainable waste management to occur, all the individuals have to play a strategic role in the sense that the scavengers playing the key roles in this link must

be properly inculcated into the flow by formally employing the scavengers to work hand in hand with the PSP and in-turn the PSP works with the LAWMA official so that the supply chain leaves no loopholes for mismanagement. Scavengers available in Lagos state should be properly integrated into the system. Such that an association is created for them where it is easier to take a record of the areas each of the scavengers belongs to so when issues arise in those areas, they will be attended to efficiently and easily.

## ACKNOWLEDGMENT

## REFERENCES

Abila, B. and Kantola, J. 2013. Municipal solid waste management problems in Nigeria: Evolving knowledge management solution. Int. J. Environ. Ecol. Eng., 7(6): 303-308.

Afon, A. O. 2007. Informal sector initiative in the primary sub-system of urban solid waste management in Lagos, Nigeria. Habitat International, 31(2): 193-204.

Ahsan, A., Alamgir, M., El-Sergany, M. M., Shams, S., Rowshon, M. K. and Daud, N. N. 2014. Assessment of municipal solid waste management system in a developing country. Chinese J. Eng., 11: 561935.

Ali, M., Wang, W. and Chaudhry, N. 2016. Application of life cycle assessment for hospital solid waste management: A case study. J. Air Waste Manag. Assoc., 66(10): 1012-1018.

Ambe, I. M. 2012. Determining an optimal supply chain strategy. Journal of Transport and Supply Chain Management, 6(1): 126-147.

Anestina, A.I., Adetola, A. and Odafe, I.B. 2014. Performance assessment of solid waste management following private partnership operations in Lagos State, Nigeria. J. Waste Manag., 11: 201.

Ayeni, A. O. 2017. Increasing population, urbanization and climatic factors in Lagos State, Nigeria: The nexus and implications on water demand and supply. Kennesaw State University, pp. 69-87.

Ayininuola, G.M. and Muibi, M.A. 2008. An engineering approach to solid waste collection system: Ibadan North as a case study. Waste Manag., 28(9): 1681-1687.

Ayomoh, M.K.O., Oke, S.A., Adedeji, W.O. and Charles-Owaba, O.E. 2008. An approach to tackling the environmental and health impacts of municipal solid waste disposal in developing countries. J. Environ. Manag., 88(1): 108-114.

Bari, Q.H., Hassan, K.M. and Haque, M.E. 2012. Solid waste recycling in Rajshahi City of Bangladesh. Waste Manag., 32(11): 2029-2036.

Bechtler, H., Browne, M. W., Bansal, P. K. and Kecman, V. 2001. New approach to dynamic modeling of vapour-compression liquid chillers: artificial neural networks. Applied Thermal Engineering, 21(9): 941-953.

Crowl, R. M., Stoller, T. J., Conroy, R. R. and Stoner, C. R. 1991. Induction of phospholipase A2 gene expression in human hepatoma cells by mediators of the acute phase response. Journal of Biological Chemistry, 266(4): 2647-2651.

Elahi, K. Q. I. 2009. UNDP on good governance. International Journal of Social Economics, 36(12): 1167-1180.

Emokhare, B.O. and Igbape, E.M. 2015. Fuzzy Logic-based approach to early diagnosis of ebola hemorrhagic fever. Proceed. World Congr. Eng. Comp. Sci., 2: 1-6.

Fayezi, S., and Zomorrodi, M. 2015. The role of relationship integration in supply chain agility and flexibility development: An Australian perspective. Journal of Manufacturing Technology Management, 26(8): 1126-1157.

Guojiao, L., Baohui, M. and Lehao, W. 2023. Water quality assessment of Wenyu River with variable weight cloud model. Nat. Environ. Pollut. Technol., 22(1).

Gupta, S., Soni, U. and Kumar, G. 2019. Green supplier selection using multi-criterion decision making under fuzzy environment: A case study in automotive industry. Computers and Industrial Engineering, 136: 663-680.

Gurtu, A., and Johny, J. 2021. Supply chain risk management: Literature review. Risks, 9(1): 16.

Idowu, O. B., Omirin, M. M. and Osagie, J. U. 2011. Outsourcing for sustainable waste disposal in Lagos metropolis: Case study of Agege Local Government, Lagos. Journal of Sustainable Development, 4(6): 116.

Javourez, U., O'Donohue, M. and Hamelin, L. 2021. Waste-to-nutrition: A review of current and emerging conversion pathways. Biotechnol. Adv., 53: 107857.

Joshi, D. 2021. Genetic algorithm and its applications. A brief study. Asian J. Converg. Technol., 7(3): 8-12.

Kadad, I. M., Kandil, K. M. and Alzanki, T. H. 2020. Impact of UVB Solar radiation on ambient temperature for Kuwait desert climate. Smart Grid and Renewable Energy, 11(8): 103-125.

Khair, H., Rachman, I. and Matsumoto, T. 2019. Analyzing household waste generation and its composition to expand the solid waste bank program in Indonesia: A case study of Medan City. J. Mater. Cycl. Waste Manag., 21(4): 1027-1037.

Kofoworola, O.F. 2007. Recovery and recycling practices in municipal solid waste management in Lagos, Nigeria. Waste Manag., 27(9): 1139-1143.

Li, P., Karunanidhi, D., Subramani, T. and Srinivasamoorthy, K. 2021. Sources and consequences of groundwater contamination. Arch. Environ. Contam. Toxicol., 80: 1-10.

MacArthur, E. 2013. Towards the circular economy. Journal of Industrial Ecology, 2(1): 23-44.

Mamashli, Z. and Javadian, N. 2021. Sustainable design modifications municipal solid waste management network and better optimization for risk reduction analyses. J. Clean. Prod., 279: 123824.

Mukhtar, G., Retno, I., Fajar, N. and Satria, A. 2019. The reduction of COD levels in domestic wastewater using a combination of activated sludge method-activated carbon continuously. J. PConf. Ser., 1295: 012040.

Nan, M. A., Lun, Y. A. N. G., Qingwen, M. I. N., Keyu, B. and Wenhua, L. 2021. The significance of traditional culture for agricultural biodiversity—Experiences from GIAHS. Journal of Resources and Ecology, 12(4): 453-461.

Ogarekpe, N.M., Nnaji, C.C., Oyebode, O.J., Ekpenyong, M.G., Ofem, O.I., Tenebe, I.T. and Asitok, A.D. 2023. Groundwater quality index and potential human health risk assessment of heavy metals in water: A case study of Calabar metropolis, Nigeria. Environ. Nanotechnol. Monit. Manag., 17: 100780.

Ogwueleka, T. 2009. Municipal solid waste characteristics and management in Nigeria. J. Environ. Health Sci. Eng., 6(3): 173-180.

Olberg, H. K., Eide, G. E., Cox, R. J., Jul-Larsen, Å., Lartey, S. L., Vedeler, C. A. and Myhr, K. M. 2018. Antibody response to seasonal influenza vaccination in patients with multiple sclerosis receiving immunomodulatory therapy. European Journal of Neurology, 25(3): 527-534.

Oyebode, O.J. 2013. Solid waste management for sustainable development and public health: A case study of Lagos State in Nigeria. Univ. J. Pub. Health, 16: 456.

Oyebode, O.J. 2018. Evaluation of municipal solid waste management for improved public health and environment in Nigeria. Europ. J. Adv. Eng. Technol., 11: 1215-1236.

Oyebode, O.J. 2019. Design of engineered sanitary landfill for efficient solid waste management in Ado–Ekiti, South-Western Nigeria. J. Multidiscip. Eng. Sci. Stud., 5: 47-63.

Oyebode, O.J. and Coker, A.O. 2021. Management of infrastructures in the water sector: a veritable tool for healthcare and sustainable development in Nigeria. IOP Conf. Ser. Mater. Sci. Eng., 1036: 012008.

Oyebode, O.J. and Otoko, J. A. 2022. Medical waste management and design of a low-cost incinerator for reduction of environmental pollution in a multi-system hospital. Nat. Environ. Pollut. Technol., 21(4): 56.

Oyebode, O.J., Coker, A.O., Sridhar, M.K.C. and Ogarekpe, N.M. 2022. Biomedical Waste Management Practices in Sub-Saharan Africa: Insights of Its Impacts and Strategies for Its Mitigation. In Ayeni, A.O., Oladokun, O. and Orodu, O.D. (eds), Advanced Manufacturing in Biological, Petroleum, and Nanotechnology Processing: Application Tools for Design, Operation, Cost Management, and Environmental Remediation, Cham: Springer International Publishing, Cham, pp. 249-256.

Oyebode, O. J., Jimoh, F. O., Ajibade, S. M., Afolalu, S. A. and Oyebode, F. A. 2023. Strategic Monitoring of Groundwater Quality Around Olusosun Landfill in Lagos State for Pollution Reduction and Environmental Sustainability. Nature Environment and Pollution Technology, 22(2): 565-577.

Ramadan, M., Ali, S., Bazzi, H. and Khaled, M. 2017. A new hybrid system combining TEG, condenser hot air, and exhaust airflow of all-air HVAC systems. Case Stud. Therm. Eng., 10: 154-160. doi: 10.1016/j. csite.2017.05.007.

Ramu, P., Santosh, B.S. and Praveen, S. 2023. An Integrated GIS-AHP Approach for Municipal Solid Waste Landfill Siting in Srikakulam District, Andhra Pradesh. Nat. Environ. Pollut. Technol., 22(1): 3-18.

Ray, P., Bera, D.K. and Rath, A.K. 2021. Genetic Algorithm: An Innovative Technique for Optimizing a Construction Project. In Das, B.B., Barbhuiya, S., Gupta, R. and Sah, P. (eds), Recent Developments in Sustainable Infrastructure. Springer, Singapore, pp. 843-854.

Sabbas, T., Polettini, A., Pomi, R., Astrup, T., Hjelmar, O., Mostbauer, P., Cappai, G., Magel, G., Salhofer, S., Speiser, C. and Heuss-Assbichler, S. 2003. Management of municipal solid waste incineration residues. Waste Management, 23(1): 61-88.

Samson, O., Oluwole, A. and Abimbola, S. 2011. On the physical composition of solid wastes in selected dumpsites of Ogbomosoland, South-Western Nigeria. J. Water Resour. Protect., 2: 011.

Santabarbara-Ruiz, P., Lopez-Santillan, M., Martinez-Rodriguez, I., Binagui-Casas, A., Perez, L., Milán, M., Corominas, M. and Serras, F. 2015. ROS-induced JNK and p38 signaling is required for unpaired cytokine activation during Drosophila regeneration. PLoS Genetics, 11(10): e1005595.

Singh, R. P., Tyagi, V. V., Allen, T., Ibrahim, M. H., and Kothari, R. 2011. An overview for exploring the possibilities of energy generation from municipal solid waste (MSW) in Indian scenario. Renewable and Sustainable Energy Reviews, 15(9): 4797-4808.

Suman, J., Uhlik, O., Viktorova, J., and Macek, T. 2018. Phytoextraction of heavy metals: A promising tool for clean-up of polluted environment? Frontiers in Plant Science, 9: 1476.

Suman, S.K., Kumar, A. and Giri, V.K. 2018. An application of a genetic algorithm for real-life problems. Invertis J. Sci. Technol., 11(4): 178-188.

Wang, H., Xu, Z. and Pedrycz, W. 2017. An overview on the roles of fuzzy set techniques in big data processing: Trends, challenges, and opportunities. Knowl. Based Syst., 118: 15-30.

Wu, H., Skye, M and Domanski, P.A. 2020. Selecting HVAC systems to achieve comfortable and cost-effective residential net-zero energy buildings. Appl. Energy, 212: 577-591. doi: 10.1016/j. apenergy.2017.12.046.

## ORCID DETAILS OF THE AUTHORS

O. J. Oyebode: https://orcid.org/0000-0003-2792-146X

# Abundance, Characteristics, and Microplastics Load in Informal Urban Drainage System Carrying Intermixed Liquid Waste Streams

**K. Upadhyay† and S. Bajpai**

Department of Civil Engineering, National Institute of Technology, Raipur-492010, Chhattisgarh, India
†Corresponding author: K Upadhyay; kshitij.upadhyay111@gmail.com

## ABSTRACT

This first-of-its-kind study systematically assesses the abundance and characteristics of Microplastics (MPs) in different categories of informal open drains (nallas) carrying different liquid waste streams from different functional areas of an Indian city. Such drains are part of the informal urban drainage system that carries wastewater, stormwater, industrial effluent, and rural runoff. Logistical and locational limitations of traditional wastewater (WW) sampling methods severely limit their application in open drains. To overcome sampling challenges owing to complex geography, vast drainage network spread across different functional areas of the entire city, and local challenges, appropriately modified sampling strategies were adopted to collect samples from 35 open WW drains (small/local, intermediatory, and large). MPs (50µm-5mm) were present in a bucket, and net samples obtained from all 35 WW drains. The average MP concentration in WW drains was 4.20 ± 1.40 particles/L (bucket samples) and 5.19 ± 1.32 particles/L (net samples). A declining trend of MPs abundance was observed from larger to smaller drains, confirming that smaller and intermediatory drains (carrying WW from different functional areas of the city) are discharging their MP loads into larger drains. Intermixing different WW streams (municipal WW, stormwater surface runoff, agricultural runoff, and industrial WW) increases MP levels in drains. The local riverine ecosystem is being put at risk by a daily MPs load of $12.6 \times 10^8$ particles discharged from 9 larger drains into the local river Kharun. To protect the riverine ecosystem, controlling the high daily MPs load from such drains is important. Diversion of WW drains through constructed wetlands built near river banks can be a cost-effective solution. Because the entire Indian subcontinent and parts of Africa rely mainly on such drains having similar characteristics and local conditions, the findings of this study reflect the status and pattern of MPs pollution in informal drains of the entire Indian subcontinent and can be used by stakeholders and governments to take mitigative and preventive measures to manage the MPs pollution and protect the local riverine ecosystem.

## INTRODUCTION

### Microplastics (MPs) Distribution in Different Types of Liquid Waste Streams

Microplastics (plastic particles with sizes between 1 µm-5 mm) are an emerging class of pollutants and multi-dimensional environmental stressors, capable of transboundary migration (Jong et al. 2022), threaten the local, regional, national, and global ecosystems due to their diverse characteristics, ubiquity, and ecotoxicological effects (Rochman 2019). Different types of liquid waste (LW) streams originate from different anthropogenic and natural activities in any semi-urban area or urban agglomerate. These include – municipal wastewater (MWW) from residential dwellings, institutions, and public places, stormwater (SW) runoff, industrial wastewater (IWW) (treated and untreated depending upon local regulations), and rural WW (agricultural wastewater (AWW) and rural runoffs from other non-point sources). Characteristics of these streams differ, and their management may be done separately or together. Wastewater (WW) management practices vary locally, regionally, and nationally, influencing the fate of WW-associated MPs and traditionally involve – the collection of liquid waste (LW), their conveyance through drainage systems, treatment, disposal, and reuse. Conveyance conduits are designed as a separate, partial, and combined system based on the provision of SW collection.

Wastewater treatment plants (WWTPs) are a major pathway of MPs to ecosystems where effluent and sludge are disposed of or reused. High MPs levels are present in WWTPs influents, effluents, sludge, and treatment units. MPs (10-5000 µm) concentration in effluent of 79

WWTPs varied between 0.004 to 450 particles/L with an average of around 6.4 particles/L (Schmidt et al. 2020). The observation that WWTPs are a pathway for MPs comes from studies conducted in developed nations. To our knowledge, their presence in WW conveyance systems has not been explored. Until 2019, MP levels have only been assessed in 121 WWTPs located in 17 nations spread across Europe (53%), USA and Canada (24%), Asia (18%), and Australia (5%). Among Asian WWTPs, most studies originate from China and Korea, and one from Iran, Thailand, and Turkey (Yaseen et al. 2022). No study (either in WWTPs or in WW conveyance systems) has been conducted within developing nations of the Indian subcontinent, one of the most densely populated regions with similar geographic, climatic, and social characteristics.

The type of sewerage system and functional areas of the city from where WW originated influence the distribution of MPs (Yang et al. 2022). In water conduits, those flowing through commercial and residential areas are more abundant with MPs than on campus and highways (Sang et al. 2021). SW conveyance conduits and management sites are abundant with MPs (Shruti et al. 2021). Combined sewerage systems and SW collection networks have a high fraction of larger MPs, including tire wear MPs mainly relating to road dust (RD)-associated MPs (Wang et al. 2022). In separate sewerage systems carrying MWW from residential areas, fibrous MPs from laundry activity and microbeads from personal care products (PCPs) are the most abundant shapes of MPs (Hamidian et al. 2021, Ziajahromi et al. 2016).

High levels of MPs are observed in IWW (Yuan et al. 2022), and a strong positive correlation exists between MPs in WWTPs influent and several plastic industries in the study area (Long et al. 2019). MPs concentration is reportedly twice as high in IWW than in MWW of urban habitat (Franco et al. 2020). WWTPs treating MWW & IWW in highly industrialized areas report higher levels of MPs than less industrialized areas (Wei et al. 2022). Elsewhere, MPs abundance in MWW, IWW, and AWW is of the same magnitude (Wang et al. 2020). Due to the extensive use of plastic products and MPs ladened biosolids as soil conditioners in agroecosystems, rural runoff from point (rural WW (RWW), and agricultural wastewater (AWW)) and non-point sources are also abundant with MPs (Yano et al. 2021).

Given the ubiquity of MPs in MWW, IWW, SW, and rural runoff as reported in the literature, we hypothesize that if such streams intermix together, it will significantly increase MPs load and change MPs composition in intermixed WW stream. A lack of study deals with intermixing four such LW streams, limiting the scientific understanding of the implications of intermixing. Before conducting any study,

it's important to understand scenarios and reasons for intermixing LW streams.

**Informal Urban Drainage Systems as a Carrier of MPs**

In developing economies like India, habitats lacking centralized WW management systems (underground pipes, pumping stations, and treatment plants) and sewage collection systems typically use onsite sanitation systems (OSS) in the form of individual septic tanks (ST). Households have built-in STs to treat black water. The supernatant of ST and sullage from households is discharged into nearby WW surface drains or nallas (closest translation will be natural or man-made WW brook or WW drain or WW canal or WW channel), relying mainly on the natural drainage system. Such drains or nallas can be natural or man-made, and they are basically of two types- *Kucha* (unlined) and *Pucca* (lined) (CPCB 2020). A vast network of small and large earthen and man-made drains across different functional areas connects entire cities. Lager drains discharge WW to local aquatic sources or treatment facilities (Fig. 1).

IWW, particularly from the small industries or unregulated and informal industries, is also sometimes transported and discharged and mixed with MWW drains, despite strict governmental regulations forbidding intermixing of IWW and MWW or IWW discharge without treatment (Amerasinghe et al. 2013). Like the absence of the WW collection system, the SW collection network is also deficient; such WW drains collect both SW and WW, somewhat similar to the combined sewerage system. Intermixing of SW (Shukla et al. 2020) and IWW makes MWW more toxic with organic pollutants and heavy metals, thus threatening the ecosystems where they are being discharged (Vaid et al. 2022). Household gardens, public gardens, and agriculture farms in peri-urban areas discharge agricultural runoff, which also reaches these drains and mixes with the combined WW.

Most WW drains are not covered, and such natural drains or man-made kaccha nallas flow in the open and follow the natural gradient (Fig. 1). Only small portions of pucca nallas are covered, mostly in residential areas. However, even these covered stretches are opened at frequent intervals to facilitate cleaning. Planned residential colonies and gated communities may have underground sewerage, but they eventually meet with open drains. Certain kaccha nallas get lined, or sometimes they are merged with pucca nallas to prevent nallas from changing their course. Open drains flowing through the city become prone to anthropogenic pollution. Garbage and MSW disposal, littering, disposal of construction and demolition waste, and disposal of PW generated from food and catering activities, households, and public places, into the drains, cause obstruction and

Fig. 1: Different types of informal urban drains carrying liquid waste streams.

choking (Fig. 2). This, coupled with negligence in cleaning and maintenance hinders the natural flow of LW and is partly responsible for waterlogging and urban flooding in Indian cities.

Considering the huge gap in management infrastructure, intermixing of LW streams, susceptibility to receive MPs from atmospheric deposits, the volume of untreated WW discharged daily, encroachment, rampant dumping and littering of MSW and PW in the drains, and absence of preventive maintenance, informal urban open drains carrying intermixed WW can be a significant pathway of MPs pollution in an urban environment, which has been overlooked till date (Veerasingam et al. 2020). Though it's difficult to assess the quantity of MPs originating from separate LW streams (due to the mixed land use pattern of unplanned cities) and external inputs (MSW and PW disposal and atmospheric deposition of MPs), we can

generate scientific understanding on levels of MPs pollution in open drains conveying intermixed LW streams (domestic WW, industrial, stormwater and agricultural runoff) which receives plastics/MPs from illegal dumping and littering. Such understanding will help plan mitigating measures for MPs and design future studies to quantify the contribution of separate streams and external inputs.

Additionally, scientific findings mainly attribute to WWTP effluent discharge points upstream of the waterbodies for the high levels of MPs observed in downstream sampling locations in waterbodies (Woodward et al. 2021). With small numbers of WWTP discharge points, the MPs' pollution can be addressed adequately. In the absence of a sewerage system and WWTPs, multiple WW drains discharge untreated WW (Intermixed with IWW, SW, and rural runoff and loaded with disposed plastic waste) at multiple locations in local waterbodies. This substantially

Fig. 2: Informal urban drains choked with solid waste.

impacts the quantity and distribution of MPs discharged into local waterbodies. So, knowledge of the quantity of MPs being released from such drains of a particular city is urgently needed to ascertain the risk to the receiving ecosystem.

To fill this knowledge gap regarding MPs pollution in the open, informal drainage system, this study addresses the following objectives – 1) propose sampling strategies to collect samples from different types of open drains with different geographical and channel characteristics, 2) assess the levels of MPs pollution (abundance and characteristics) in such drains, and 3) estimate the daily and annual MPs loads being discharged by these drains in the local river.

## MATERIALS AND METHODS

### Study Area

The study was conducted in the old residential-industrial capital of Chhattisgarh state of India, Raipur. Raipur is the most populous city in the state and one of central India's important industrial hubs. According to the 2011 census, the population of Raipur City was 1048112. The revenue boundary of Raipur city lies between 22º33' to 2114°'N latitude and 8206°' to 81° 38'E longitudes. Raipur district is spread across a 490.43 km$^2$ geographical area, with Raipur municipality having an area of 226 km$^2$ with 70 revenue wards and 7 villages, and the Birgaon municipality governs the remaining area.

## Description of Liquid Waste Management in Study Area and Sample Collection Strategy

Currently, the city lacks a planned sewerage system and WW treatment facilities. WW generated from households (1,77,334), institutions, public places, and industries is collected through natural and man-made local (small), intermediatory, and large drains, which are part of the natural drainage system. 144,882 households have OSS-based ST that collect black water. House drains are connected with local drains (RMC 2014).

According to RMC, the city's total water consumption is 246 MLD (Million Liter Per Day), and 150-170 MLD of WW is generated daily, collected, and transported through surface drains, locally known as nallas. Location, discharge data, and other relevant details were obtained from RMC. Sullage and supernatant of ST are discharged in local drains.

A vast network of local nallas meets 11 intermediatory nallas and 9 large nallas that cover the entire city. These drains receive MWW, SW IWW, and RWW depending upon location, season, and functional areas from where LW streams originate. Nine large nallas discharge the entire LW of the city in the Kharun River at 9 different locations. Smaller nallas also emit their load in local urban ponds and agricultural lands.

To assess the influence and behavior of MPs from various functional areas of the city and to identify the influences of human activities, WW samples were obtained from 35 locations that covered local nallas, intermediatory nallas, and all larger nallas. Nine sampling stations (WW1-WW9) were located at outfalls of nine large nalla to the river, 11 sampling stations were selected from 11 intermediary nallas that flow through different functional areas of the city, and 14 sampling stations were selected at local nallas. A large
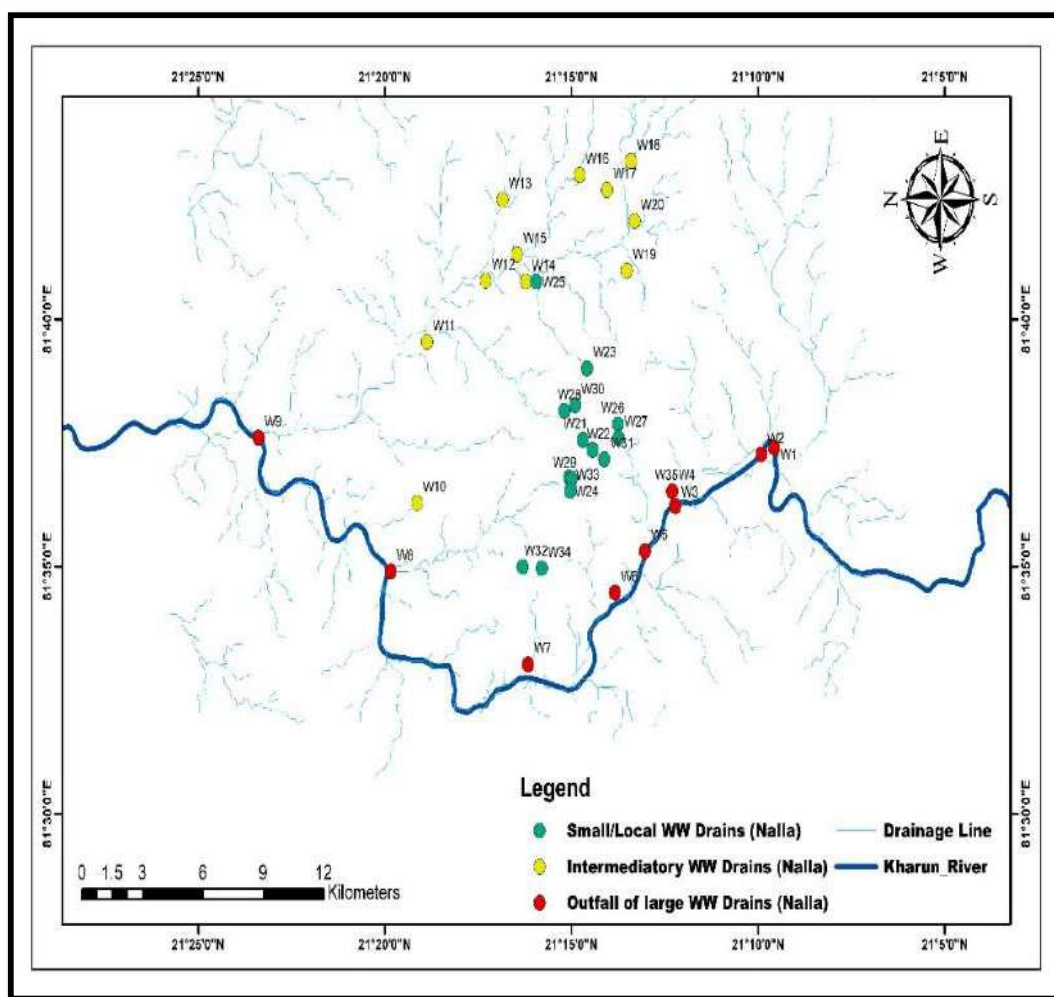


Fig. 3: Study area map depicting 35 nallas sampled in the present study.

Fig. 4: Images of some informal urban drains sampled in the present study.

nalla, the Govardhan drain, passes through a natural wetland spread over 500 m$^2$ before discharging into the river. To understand the removal efficiency of wetlands, samples were collected from the inflow area (WW35) of the wetland and wetland outfall (WW4) in the river. Samples were collected directly from three smaller nallas (WW32, WW33 & WW34) receiving the MWW from residential dwellings. The study area map is illustrated in Fig. 3, and Fig. 4 depicts images of some drains sampled here.

## Sample Collection Methodology

The sample collection was performed using two strategies. In the bucket, rope, and sieve strategy, we used a 5 L steel bucket, 50 μm mesh steel sieve, and 20 m of rope. As the access to the sampling locations became challenging – drains below the roads, drain aqueducts crossing the underpass and roadside nallas, and drains through marshy terrain –buckets and rope were necessary.

**Bucket sampling strategy:** The bucket was used to collect (through hand or through cotton and jute rope to avoid contamination of samples from plastic ropes) samples from the flowing WW. 5 L of WW was collected from drains and sieved through the steel mesh by slowly pouring the WW from the top. The steel bucket was rinsed with prefiltered double distilled water (DDW) thrice and sieved through the same mesh, which ensured a complete transfer of the sample material. The same process was done 10 times at 15-minute intervals, and a total of 50 L of WW was collected and sieved at each sampling station. The time interval allowed us to address sample heterogeneity and temporal variability, and we obtained a homogeneous and composite sample representative of the WW flowing in the drain.

For roadside drains, samples were collected by drawing the bucket in the opposite direction of the WW flow. Many sampling stations were located near overhead bridges, aqueducts, and underpasses that were not directly or easily

accessible. The elevation between the sampling surface and the nallas varied from 5 to 30 meters, so direct sampling was impossible. So, a sufficient length of rope was used to pull the bucket containing WW samples. The handle of the bucket was tied with rope, and the bucket was slowly lowered till it reached the surface of WW flow.

Using a high-weight steel bucket ensured that the bucket did not get carried with the flow. The WW sample was collected in the bucket by maneuvering the rope, and the bucket was lifted by drawing the rope using hands. Using motor pumps was impossible due to geographical, economic, and logistical constraints. The collected WW was sieved and rinsed using the procedure described earlier. The process was repeated 10 times at 15-minute intervals, and a total of 50 L of WW was collected and sieved at each sampling station.

At stations, WW32-WW34, the WW coming directly from the residential dwellings was collected by placing the bucket below the outfall of the plumbing system. The collected WW was sieved and rinsed using the procedure described earlier. The process was repeated 10 times at 15-minute intervals, and a total of 50 L of WW was collected and sieved at each sampling station.

Once the sampling was complete, the residue on the sieves was washed into a jar using DDW. The rinsing process was repeated three times, and finally, the DDW jet was sprayed from the bottom end, which allowed the capture of the MPs clogged in the sieve pores in the collection jar. To overcome clogging and subsequent retention of WW in the sieve due to high suspended impurities in the WW, the bottom portion of the sieve was gently tapped, and the bottom surface of the mesh was tapped using fingers. This unclogged the sieve and allowed WW to pass. Aluminum foil was placed on top of the jar, and the lid of the jar was tightly closed.

**Net sampling strategy:** The plankton net, rope, and rod strategy involved using a plankton net (mesh size – 50 μm, mouth opening – 13.5 cm, length – 100 cm including the cod end attached to a glass collection jar), tied with a rope and the rope tied to a stick. A mechanical flowmeter (Hydro-Bios) was attached to calculate the volume of WW passing through the net.  The length of the rope varied depending on the difference in elevation between the ground surface and the flowing WW in the drain.

The roadside drains, having small level differences, were easily accessible. The net was placed in the drain opposite the WW flow. The flowing WW continued to pass through the net, and the residue was collected in a glass jar. In drains with a small flow, the net was dragged using the stick to sample a sufficient volume of WW.  The net was lowered from the

roads lying overhead, aqueducts, and underpasses, with high elevation differences, until it reached the surface of the WW flowing in the drain below. The net was suspended in a fixed position for the entire sampling duration at a particular station where the flow was steady. However, the flow was very low or very high at many stations. When there was practically little flow through the net due to the substantially low WW flow, the net was dragged in the transverse direction of the drain by moving the stick from left to right direction, right to left direction, and opposite to flow direction. This was repeated until a sufficient volume of WW passed through the net.

At stations with high WW flow, the net started to flow away due to high velocity. In such a situation, the net was allowed to move with the flow until the entire length of the rope was stretched. When the rope was completely stretched, we dragged the net against the flow using the stick and the rope. This was repeated until a sufficient volume of WW passed through the net. At station WW32-WW34, the WW coming from the residential dwellings was collected directly by placing the mouth of the net below the outfall of the house sewer system such that the WW fell directly into the net. The sample collection continued till a sufficient volume of WW passed through the net.

After sample collection, the net was carefully lifted and placed in a steel tub. The suspended solids in the jar attached to the cod end were transferred into a sample storage jar. The cod jar was rinsed three times in the storage jar using DDW. Then, the inside of the net was turned outward, which allowed the captured suspended solids to fall into the tub. The inside portion of the net was washed into the tub using DDW. The process was repeated three times. Lastly, we jet spray the outer portion of the net mesh using DDW to transfer the clogged impurities in the mesh to the tub.

The material collected in the tub was sieved through a 50-μm mesh sieve, and the residue captured on the sieve was transferred to the previously used sample collection jar using a DDW jet. The process was repeated until the entire residue was collected. Finally, the steel tub was washed three times using DDW and sieved through the same sieve to ensure no suspended solids remained attached to the tub's surface. To overcome the problem of a clogged sieve, we followed the strategy used in the case of bucket sampling. The top of the sample storage jar was covered with aluminum foil, and the lid was tightly closed. The duration of net sampling varied between 20 min and 60 min, depending on the flow velocity. The flowmeter reading at each station was noted to calculate the volume of WW sampled at each station. The WW samples were collected from all the sampling stations following the same procedure.

## Microplastics Extraction Methodology

Samples stored in the freezer were brought back to room temperature, and wet sieving was performed to segregate MPs present in samples into 3 size groups – 5 mm to 1 mm, 1 mm to 500 μm, and 500 μm to 50 μm. The organic matter digestion protocol using Fenton's reagent (FR) recommended by MPs studies (Hurley et al. 2018, Tagg et al. 2017) was modified to neutralize the organic contaminants present in the sample matrix while ensuring no damage to MPs. FR is very effective for WW samples (Horton et al. 2021) which generates a strong oxidative and exothermic reaction using hydrogen peroxide ($H_2O_2$) in the presence of a strong ferrous catalyst (Bretas Alvim et al. 2020). Ideally, an exothermic reaction should not require external heating; however, many studies have employed additional external heating to increase efficacy and shorten digestion (Al-Azzawi et al. 2020). Studies report varying digestion temperatures, but recently it has been highlighted that certain polymers tend to exhibit alteration in morphological properties when reaction temperature (RT) reaches above 60°C (Munno et al. 2018).

So, to avoid any alteration, we ensured that the RT should be allowed to reach 60°C at no point during the extraction procedure. This was achieved by putting the reaction vessel in a cold water bath as soon as RT neared 60°C and, in extreme cases, adding cold double distilled water. Here we used multiple aliquots of 20 mL of acidified ferrous sulfate heptahydrate ($FeSO_4.7H_2O$) and 20 mL of 30% $H_2O_2$, and digestion was performed in multiple steps.

After organic matter digestion, vacuum filtration was performed to extract MPs in the digested suspension on filter paper (Whatman mixed cellulose ester, pore size - 0.45 μm, diameter - 50 mm, type – white/black grid). Filter papers were transferred into the labeled glass Petri dishes, covered with aluminum foil, and stored for further processing.

## Morphological and Chemical Characterization of Extracted MPs

Filter papers were visually examined with the naked eye and stereomicroscope (Leica S9D) for morphological characterization. Images were acquired using a handheld digital microscope (QSCOPE). Besides particle count, the suspected MPs were morphologically categorized by shape and color. The criteria for ascribing any shape and color to the suspected MPs was based on the recommendations from the literature. The suspected MPs in the size range (50μm- 5mm) were categorized as beads, spheres, fragments, films, foams, lines, and fibers. We encountered black, white/transparent, green, yellow, pink, orange, red, purple, and blue-colored MPs. The remaining MPs' colors were grouped under the umbrella of 'others. The particle count shapes, and colors were recorded for each size class.

A subset of MPs (50) was pooled from the separated MPs and chemically analyzed through FTIR (Fourier Transform Infrared Spectroscopy)- Attenuated Total Reflectance (ATR) for polymeric identification of the MPs. The particles were randomly selected from all three-size classes to avoid selection bias. Due to the limited accessibility to the instrument, it was impossible to select particles from each filter. Hence the polymer distribution reflects the distribution of MPs in the entire drains of the city rather than reflecting the distribution for all individual drains as done in the case of MPs morphology distribution. The particles were picked manually, cleaned using ethanol, air-dried in a desiccator, and placed manually on the FTIR platform for analysis.

The FTIR spectra were generated by combining 64 scans in the mid-infrared range at a set resolution of 4 cm$^{-1}$ by Bruker ALPHA-II spectrometer having ZnSe crystal. The spectra obtained were compared with the reference library of Openspecy (Cowger et al. 2021) and Bruker. The similarity cutoff was set at 70% to ascribe polymer ID to the spectra obtained from FTIR.

## Contaminant Control, Quality Assurance, and Data Analysis

During the sample collection, storage, and analysis procedures for MPs, there is the possibility of sample contamination by the MPs from the atmosphere and consumables and instruments used, leading to an overestimation of MPs (Prata et al. 2021). To avoid this, strict contaminant control and quality assurance steps and precautions were meticulously followed. Field, procedural, and analytical blanks were used to produce reliable results by adopting the recommendations of previous studies (Horton et al. 2021, Miller et al. 2021). Many blanks were contaminated with MPs (1 to 5 particles), and the results reported here are based on the field data as the MPs present in the blank samples were negligible compared to the MPs abundance in the field samples.

During polymer identification, 3 particles were identified as organic matter, bringing down the efficiency of visual identification to 94%. We didn't use this to correct the final results of MPs, as the analysis was performed on the subsamples. The reader may like to consider this factor while interpreting the results.

The data analysis was conducted in Microsoft Excel-2019, plots were prepared in Origin-2023, and the study area map was prepared in ArcGIS. One-way ANOVA was performed to test the significance of the results.

## RESULTS

### Abundance of MPs

Samples obtained from all 35 drains were abundant with MPs (Fig. 5) which varied between smaller, intermediatory, and larger drains. The average MPs concentration from net samples ($5.19 \pm 1.32$ particles/L) was greater than bucket samples ($4.20 \pm 1.40$ particles/L). For bucket samples, maximum and minimum concentration was observed in W2 (6.68 particles/L) and W33 (0.72 particles/L). For net samples, maximum and minimum concentration was observed in W9 (7.53 particles/L) and W34 (1.92 particles/L).

Among different drain categories, the highest average abundance was in larger drains (B: $4.83 \pm 1.04$ particles/L, N: $5.76 \pm 1.17$ particles/L), and we observed (Fig. 6) a clear declining trend ($p < 0.05$) for average MPs concentration in intermediatory drains (B: $4.51 \pm 0.93$ particles/L, N: $5.69 \pm 0.95$ particles/L) and smaller drains (B: $3.56 \pm 1.68$ particles/L, N: $4.43 \pm 1.35$ particles/L) in both bucket samples and net samples. This trend is due to the basin characteristics, flow volume, intermixing of different LW streams, and

functional areas where drains are located, which allows MPs to dilute or accumulate.

Smaller and intermediatory drains that carry WW generating from different functional areas of the city are discharging their MP loads into larger drains, leading to high MPs abundance. Higher MPs concentrations in intermediatory drains are due to incoming MP loads from households, intermixing of SW and IWW, and disposal and littering of MSW and PW into open drains. However, all drains are susceptible to disposal and littering of MSW and PW. It's the magnitude of the disposal that is affecting MP concentration. Within the same drain category, at a particular drain, we did not necessarily observe a similar trend of MPs concentration for both bucket and net sample, indicating that MPs captured are dependent on the sampling techniques. For instance, in smaller drains, maximum MPs concentration was observed in W31 for net samples and in W27 for bucket samples, while minimum MPs concentration was observed in W34 for net samples and in W33 for bucket samples.

WW from residential dwellings (smaller drains – WW32, WW33 & WW34) were least abundant. Drains (W18-W20)
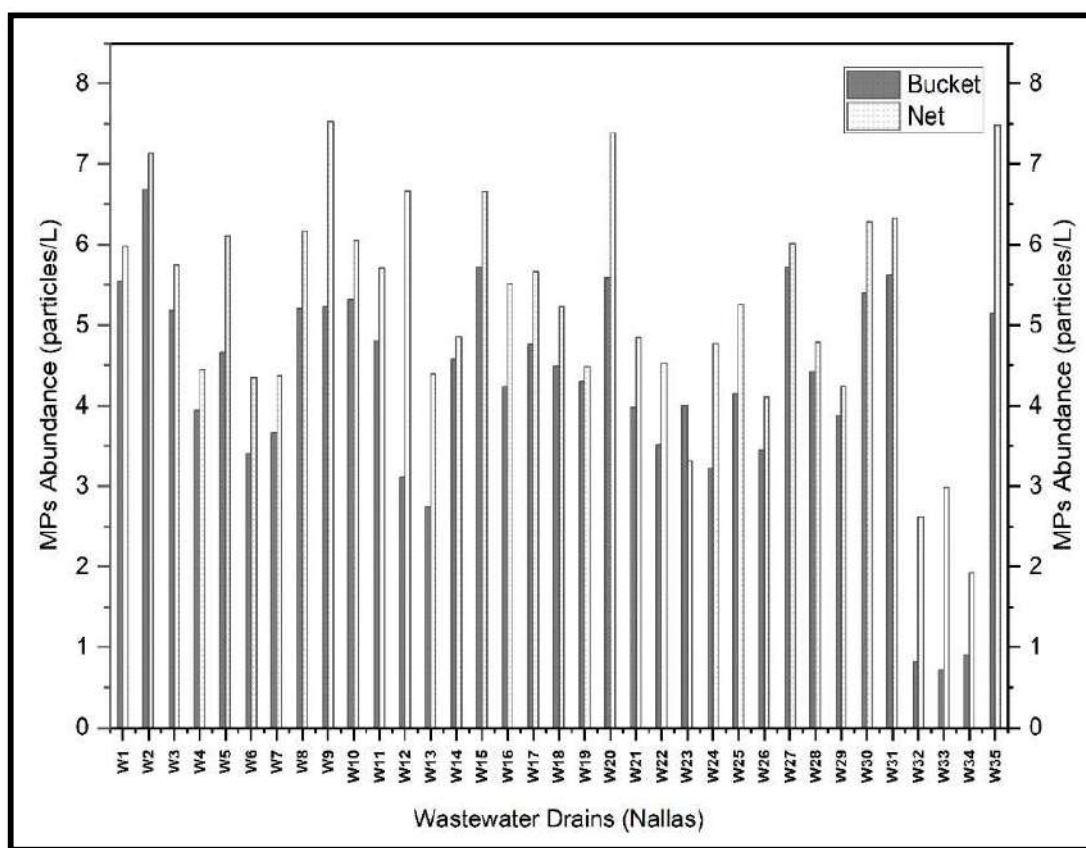


Fig. 5: Abundance of MPs in drains of study area sampled through bucket strategy and net strategy.

carrying agricultural runoff from semi-urbanized zones were comparatively higher than other drains. *Govardhan nalla* (W35) flows through a small natural wetland before being discharged into the river, and the wetland reduced MPs load in the drain by 40 %, thereby limiting the daily MPs load discharged into the river. Small wetland size, high WW volume, and disposal of MSW in the catchment areas of wetland could be the reason for lower MPs removal efficiency (Long et al. 2022). Nonetheless, even a 40 % reduction is significant considering the drain's higher average daily discharge capacity. Construction of wetlands between WW drains and local aquatic sources in locations where the commissioning of WWTPs is not feasible can significantly reduce WW-related MPs load to water bodies.

Only one study from Lahore, Pakistan (Irfan et al. 2020) reports MPs load (16.15 ±0.008 particles/L) in an untreated WW stream of open drain (*nalla*). This is the only reference available for directly comparing our results, as both study areas lie in the Indian subcontinent, having similar environmental, social, and basin characteristics. Drains in both cities are susceptible to disposal and littering of MSW and PW and are clogged in many locations with visible PW floating in drains. As sampling was conducted using a bucket, the MP concentration is twice higher than the maximum concentration observed in drain W2 while greatly higher than the average concentration in all drains. Nearshore sampling was performed in Lahore, which could be the reason for increased MPs levels, as dumping and littering majorly happen near shores that remain accessible to residents. Further, the WW drain was more polluted than freshwater streams, canals, and the *Ravi* River making open WW drains a significant source of terrestrial MP pollution.
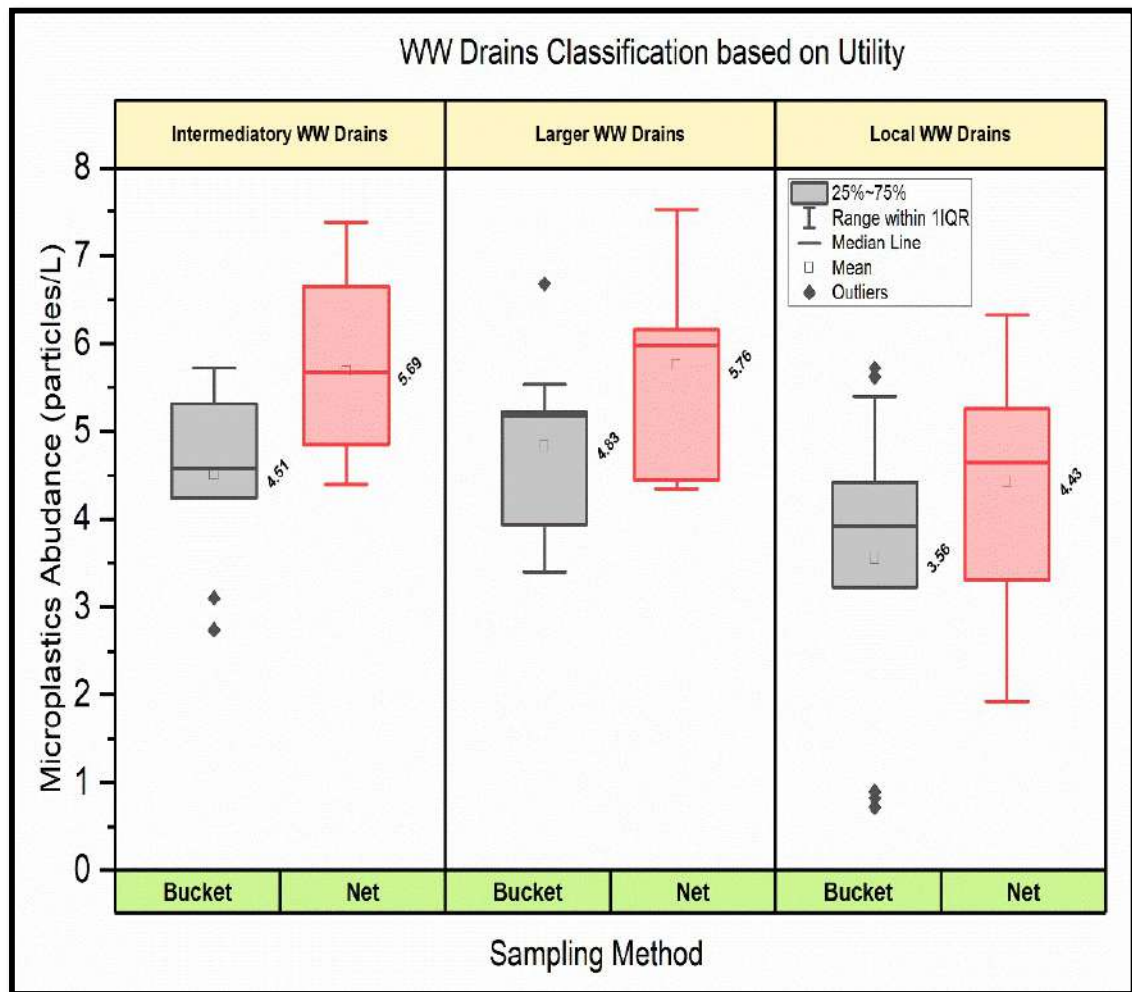


Fig. 6: MPs abundance (average) in different types of WW drains of the study area.

Another study that highlights the extent of MPs distribution in the urban drainage systems of developing areas similar to Raipur City was conducted in Da Nang City. In the drainage channel of the city, the reported high MPs concentration in surface water ((1.48 ± 1.06 particles/L) is indicative of the extraordinary impact of the discharge of urban LW streams on the MPs distribution as the channel receives MWW and landfill leachate from the city (Tran-Nguyen et al. 2022).

In the canal conveying IWW and effluent of Al-Hayer WWTP (Riyadh, Saudi Arabia) to an artificial pond, the average MPs abundance (3.2±0.2 particles/L) is lower than Raipur, mainly due to the absence of intermixing of SW with WWTP's effluent in canal (Picó et al. 2021). In 4 WW ditches (Bahir Dar City, Ethiopia), MPs concentration (1670 580± to 4300 ± 1580 particles/L) is four magnitudes higher than Raipur (Mhiret Gela & Aragaw 2022). Annual

discharge of 0.27 billion tons of municipal and industrial effluent from Yenagoa, Nigeria, into Ox-Bow Lake is the primary source of fibrous MPs in the lake (Oni et al. 2020).

Saigon River is connected to Ho Chi Minh City, Vietnam, by four large canals that carry WW of the city. MPs concentration in these canals varies from 270 to 519 particles/L, mostly comprising anthropogenic fibers originating from households WW (Lahens et al. 2018). Wet weather overflow (WWF) of urban agglomeration in Shanghai, China, mainly comprises MPs associated with MWW and road dust, discharges 130 ± 30 to 8500 ± 1241 MPs particles/L into local aquatic sources daily (Chen et al. 2020).

MPs abundance observed in drains of unsewered areas of the present study is lower than the influence of many WWTPs in Europe, the USA, and China (Wu et al. 2022). Moderately higher MPs concentration was observed in WW drains when
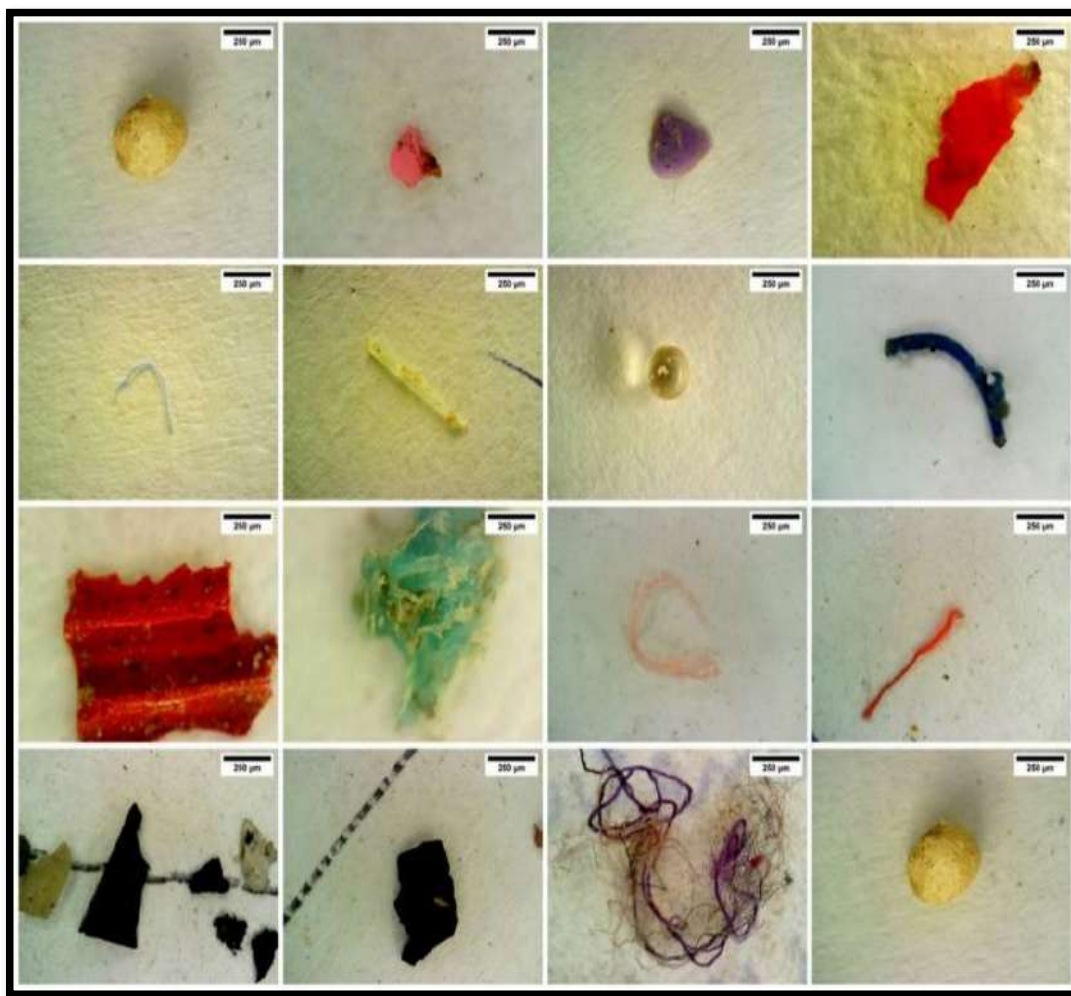


Fig. 7: Micrographs of different MPs extracted from drains in the present study.

compared with the effluent of WWTPs. As the WWTPs are highly effective in removing MPs loads from influent, lower reported MPs concentration is understandable. However, the WWTP effluent of many locations also reports higher levels of MPs, especially from Netherlands – 39 to 81 particles/L (Leslie et al. 2017), Finland - 100 – 13.50 particles/L (Lares et al. 2018), and Denmark – 19 to 447 particles/L (Simon et al. 2018). This suggests that despite WWTPs effectively removing MPs from influent, the lower MPs concentration in WW of Raipur in comparison to WWTPs effluent is mainly due to variation in volume of WW, MPs concentration in influent, difference in sampling and analysis strategy, and difference in the social, economic, and environmental factors.

**Characteristics of MPs**

Various microplastics were identified in the samples obtained from the drains of Raipur City, and micrographs of a few MPs are presented in Fig. 7. The different characteristics of MPs are discussed below.

**MPs size distribution:** The size distributions of MPs in 3 size classes – size class I (5 mm to 1 mm), size class II (1

mm to 500 μm), and size class III (500 μm to 50 μm) – in different drains sampled from the bucket and net method is shown in Fig. 8.

We observed that MPs are equally distributed across 3 size classes for both bucket and net samples suggesting input from multiple MPs sources. In MWW coming directly from households (W32. W33, & W34), large MPs prevailed followed by smaller sized MPs, while size class- II was found to be the least Fig. 9. As fibrous MPs from laundry activity were dominant in these drains, we can infer that release of MPs from laundry activity generates varying sized MPs. Additionally, floor wiping is done mostly using wet wipes or cloth rags, and wash water from wiping and washing of rags becomes part of sullage, adding MPs settled from indoor dust into the drains. Drains carrying agricultural runoff (W18-W20) were abundant with large-sized films and foams.

In choked drains, where the flow is either absent or very low, the smaller MPs will remain in suspension, while larger MPs will tend to settle (Jiang et al. 2020). The intermixing of WW streams and atmospheric deposition contributes to varying-sized MPs altering the size distribution in the WW
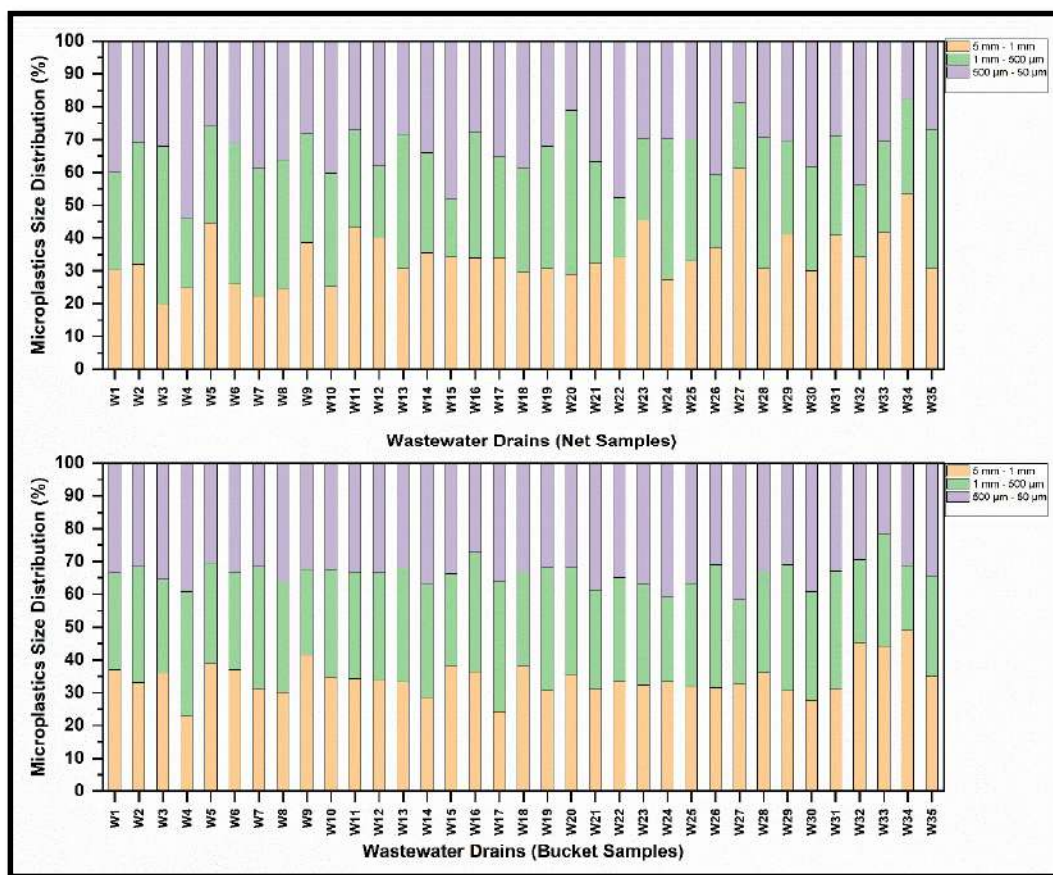


Fig. 8: Size distribution of MPs in the drains sampled in the present study.
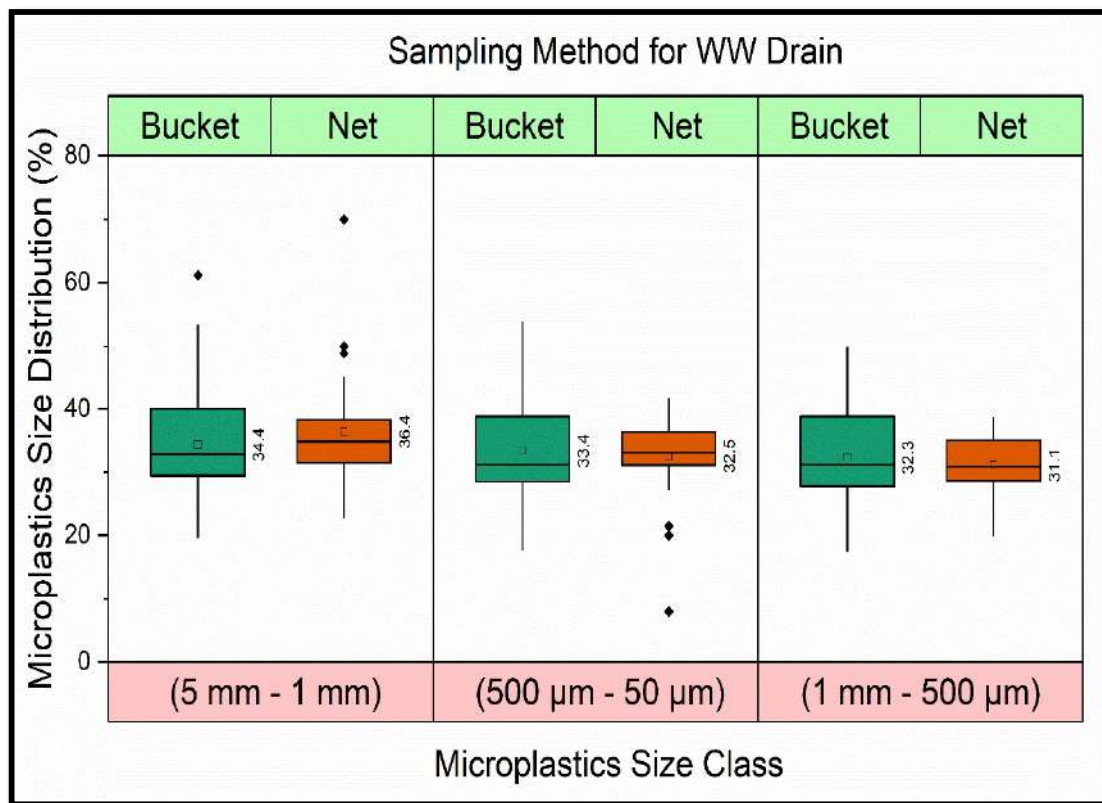
Fig. 9: Average MPs size distribution in the drains sampled in this study.

drains. For instance, larger-sized MPs associated with road dust dominate stormwater (Stang et al. 2022). Large MPs are abundant in agricultural soils and runoff (He et al. 2022). Small-sized (<100 µm) MPs prevail in atmospheric deposits (Sun et al. 2022). Laundry activity also generates smaller fibrous MPs, which mostly end up in the WW (Kelly et al. 2019). The size distribution of MPs is also governed by the shape of MPs which is discussed in the next section.

**MPs shape distribution:** MPs from both sampling techniques exhibited diverse shapes across all drains (Fig. 10) within the drain category and size class. Overall, fibrous MPs were dominant in all drains, followed by foams, films, and fragments in bucket samples; and fragments, films, and foams in net samples (Fig. 11). Collectively, these four shapes accounted for more than 96% of total MPs. Line-type MPs accounted for approximately 2 % of the MPs, while beads and spheres were observed at least (1% each).

Fibers were also dominant within all three-drain categories in bucket and net samples, followed by fragments in net and films in bucket samples. Interestingly, foams were observed in the highest numbers in larger drains, which confirms our hypothesis that smaller and intermediatory drains, which are more susceptible to obstructions, accumulate SUPs, where

they start to fragment and release secondary MPs, which flow with the WW and mix with the larger drains. The distribution of fragments was somewhat uniform across all three-drain categories, understandable so, as all drain categories are susceptible to receiving stormwater. Fibers, films, foams, and fragments were distributed consistently in all three-size classes with small variation (less than 10%). For net samples - the fragments were observed highest in size class I, films in size class III, foams in size class III, lines in size class I, and fibers in size class III. For bucket samples, the fragments were observed highest in size class III, films in size II, foams in size III, lines in size 1, and fibers in size class I.

Our results are consistent with MPs shape distribution in WWTPs. In WW, fibers are the dominant MPs shape, followed by fragments (Yaseen et al. 2022). High variation in MPs shape distribution was observed among individual drains, though fibers prevailed in each drain, suggesting the inflow of fibers from laundry (Kelly et al. 2019a) and atmospheric fallout (Napper et al. 2023) as major contributors to MPs in drains. In addition, the fraction of fibrous MPs in the WW drains W32, W33, and W34 were as high as 90.00%. Since these drains receive sullage from residential dwellings and supernatant from ST, they are abundant with
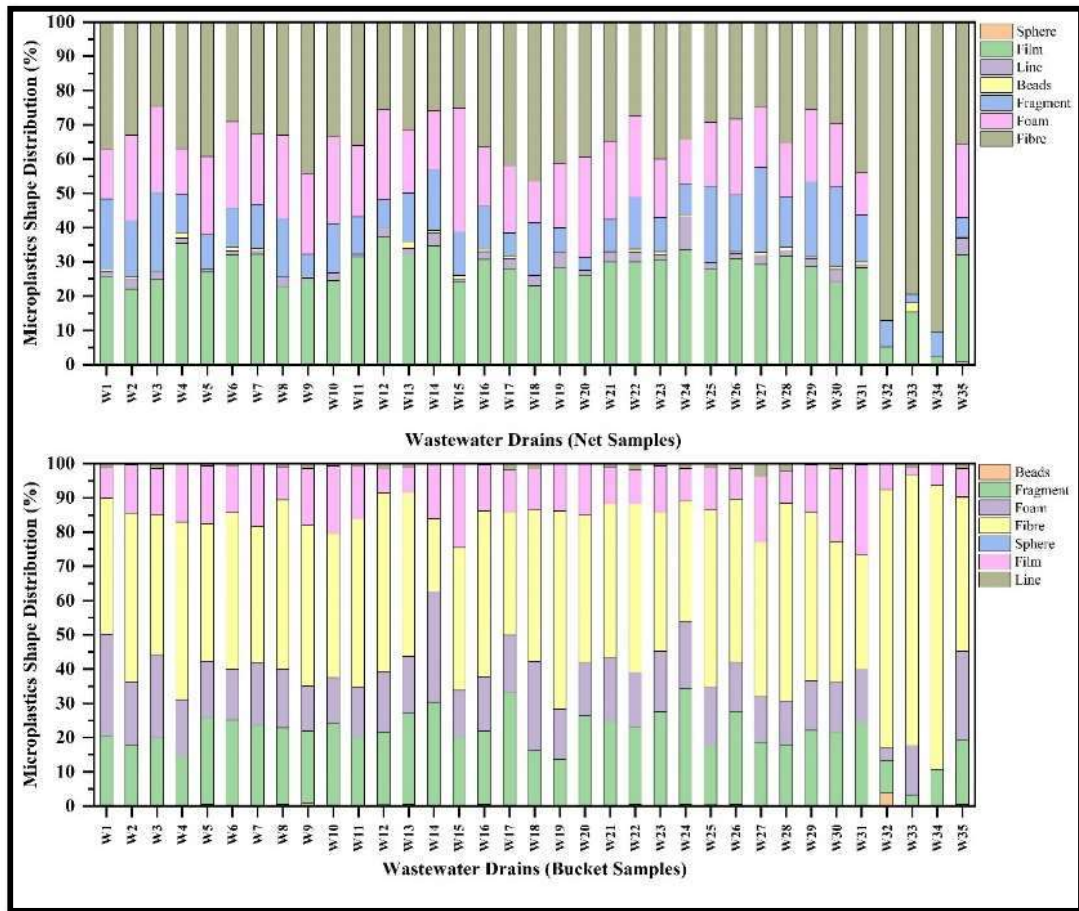
Fig. 10: Shape distribution (%) of MPs in the drains sampled in the present study.

textile fibers from laundry and indoor dust deposition. These drains are not susceptible to PW littering, MSW disposal and absence of SW intermixing, which is why there is no foam, line, and fragments.

With the inflow of MWW occurring in all drains, other varying factor influencing MPs distribution in drains is intermixing of other LW streams. This inference is supported by the observation that a substantial quantity of foam, line, and fragments are present in other drains. The consistent occurrence of rubbery fragments, such as tire wear across the remaining drains, leads to the logical conclusion that SW is transporting RD-associated MPs from the surface to the drains (Monira et al. 2021). The low distribution of beads and spheres highlights that variations in lifestyle and urbanization levels influence microbeads' release in MWW (Ziajahromi et al. 2021).

Foams were the second most abundant MPs shape in drains, followed by film. This observation helps us recognize a new source of MPs relating to WW, overlooked

by previous WW studies. The vast network of open and mostly earthen natural drains runs through various functional areas throughout the city. Poor SWM practices, which vary among functional areas, lead to the disposal of SW & PW in these drains. Channel properties (depth, width, location, and elevation) vary throughout the entire course, leading to accumulation of the disposed SW & PW at various portions in the drains having narrow channels and low depth of flow with low elevation difference, especially near LIG residential areas and recreational areas of the city.

Disposed PW in drains were composed of SUPs and polyethylene bags. Overtime, accumulated PW in drains undergoes a fragmentation process (environmental, chemical, and biological processes) and starts generating secondary MPs in drains, which get mixed with LW. SUPs from the eateries, food joints, and party halls, along with foams used in packaging food items and consumer goods, decorative items, plastic bags, FMCG wraps, and other film covers used on beverage bottles, were observed floating in all the sampled drains.
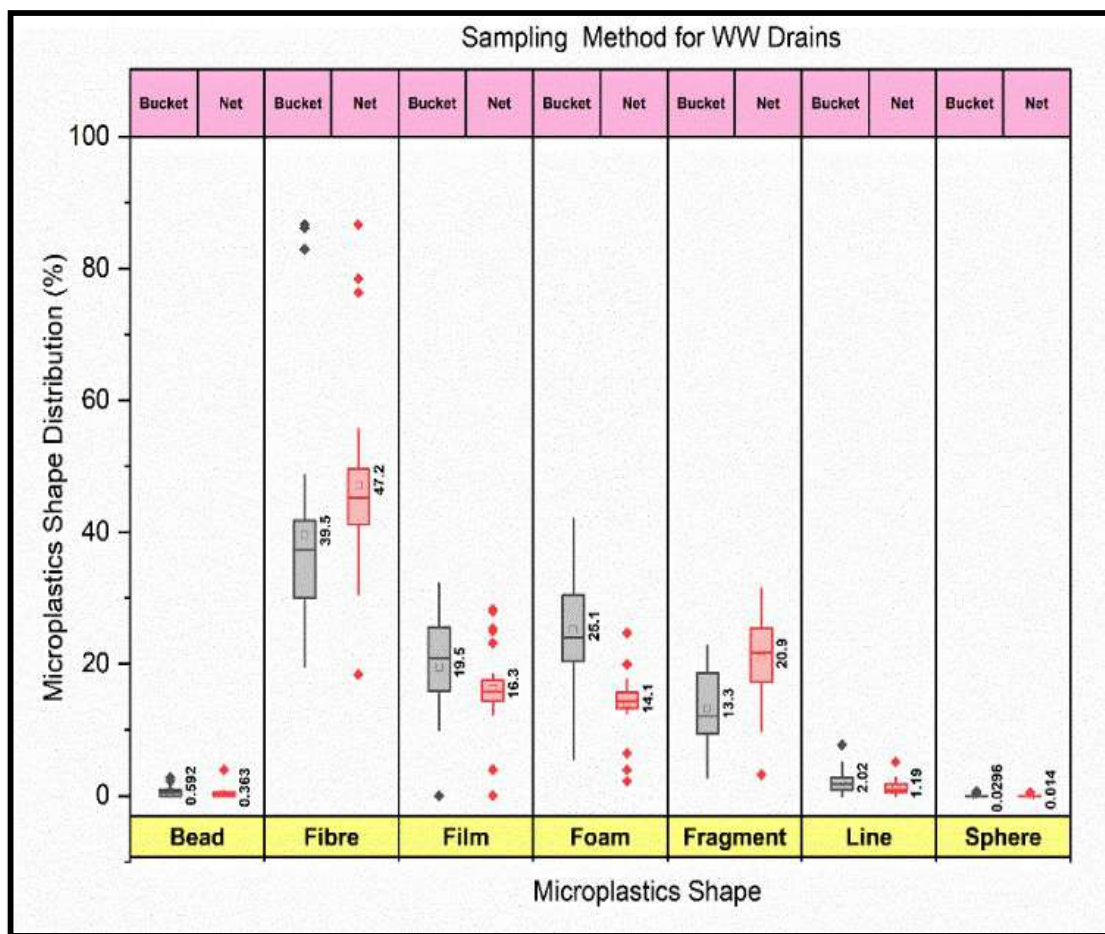
Fig. 11: Overall shape distribution (%) of MPs.

Even though the primary purpose of using two sampling strategies was to collect samples from different types of drains with different channel characteristics and logistical challenges, variation in shape distribution between the bucket and net samples highlights the importance of using at least two sampling strategies while planning any WW-related study. Regardless of the sampling technique, every sampling technique will have a bias that may not produce reliable results.

For instance, we observed that nets were not best suited to collect foams and films, which due to their low density, escaped the mouth of the net, while fibers and fragments were collected efficiently. So, if any WW drain appears to be abundant with floating foams and films during the preliminary survey, we recommend using the bucket sampling technique, and for other shapes, net sampling will work well. We understand the resources required for adopting two sampling strategies are quite higher, and the research laboratories should choose the strategy best suited for the drains of the study

area. Another approach can be to conduct a pre-experiment by collecting samples from a few drains using both strategies and analyzing the MPs diversity in the samples. Based on this, an optimum sampling strategy can be adopted.

**MPs Color Distribution:** The extracted MPs from both sampling techniques exhibited diverse spectrum of colors with low diversity, as black and white colored MPs were prevalent in all samples (Fig. 12). Average distribution (%) of colored MPs across all the drains is shown in Fig. 13. White/transparent MPs accounted for 40 -50% of all MPs in both bucket and net samples, followed by black (25-30%) and green (4-7%) MPs. Collectively, these three-color categories accounted for 74.44% (B) and 82.84% (N) of all the colors.

Particular dominance of any color or color distribution is observed to be independent of the sampling method. Blue (B-4.32%, N-5.07%) colored MPs were the fourth most observed color of MPs, followed by yellow (B-4.68%, N-2.03%) colored MPs. The percentage distribution of pink, purple, red, and orange MPs were less than 2.5 % each.
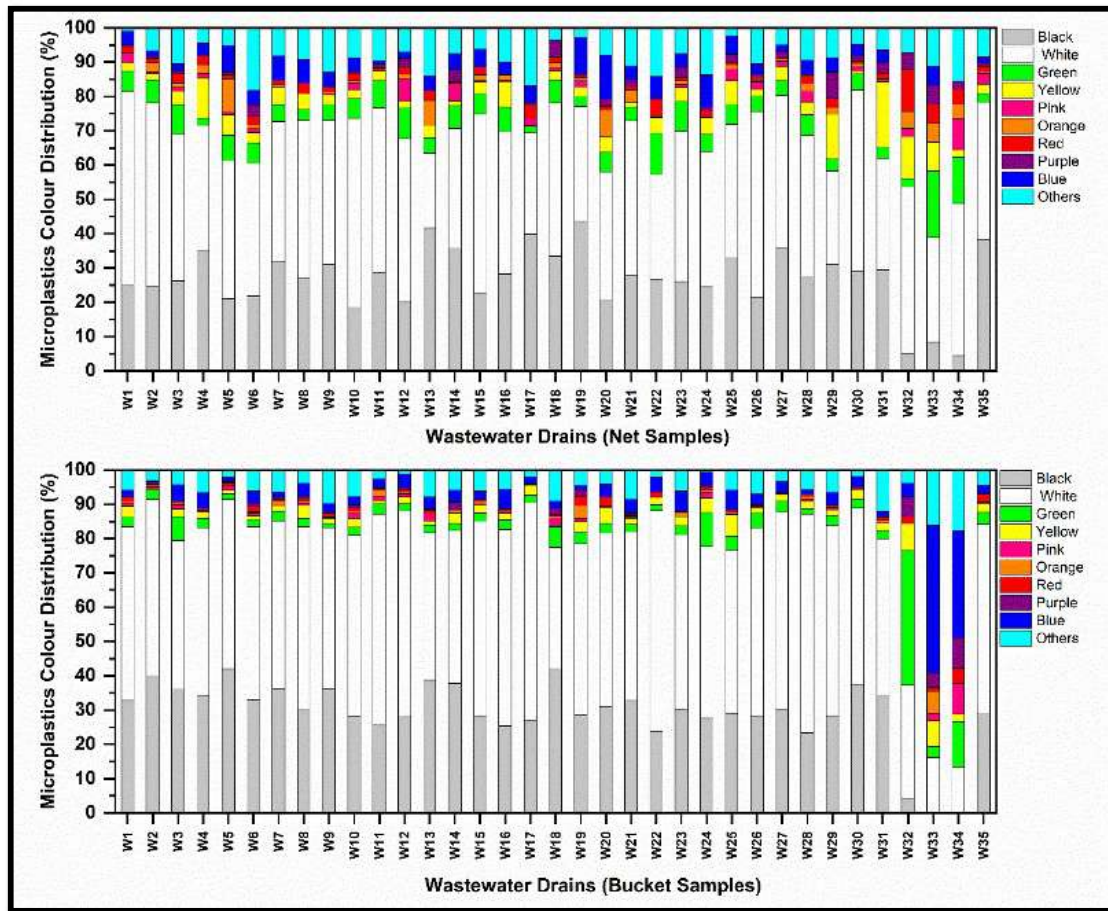
Fig. 12: Color distribution (%) of MPs in the drains sampled in the present study.

Color distribution trend (white/transparent>black> others>green>blue>yellow) with white/transparent, black, and green being dominant was similar in all three drain categories – larger WW drains (N -87.80%, B- 77.58%), intermediatory WW drains (N -86.24%, B- 76.85 %), and smaller WW drains (N -84.84%, B- 74.64%).

The remaining colors were less than 2.5% each. Color distribution trend and percentage distribution are similar in individual drains, within drain categories, and combinedly in all drains. This suggests that the sources of MPs in the drains do not vary, and different LW streams are intermixed in all the drains.  However, the lower distribution of black fragments and the prevalence of fibers in drains (W32, W33 & W34) carrying MWW (coming directly from residential dwellings) suggests that intermixing other LW streams is absent. The higher distribution of black-colored MPs in other drains (where intermixing of SW with other LW streams is occurring) makes SW a major source of MPs in drains. The dominance of black-colored MPs in SW is mainly due

to rubbery MPs generated from the wear and tear of the vehicular tire (Werbowski et al. 2021)

Comparatively, white MPs were prevalent in smaller and black MPs in larger drains. Smaller drains connected with households mostly receive MWW (mainly comprising of laundry, hygiene (wet wipes), sullage, and other WW from residential dwellings), and being narrow, open, and accessible, are more susceptible to receive SUPs, bags, FMCG scathes, and wraps, choking and accumulating PW which leads to their fragmentation into secondary fibrous, foam and film MPs.

In addition, these drains being open channels may also receive substantial amounts of white and transparent fibrous MPs from atmospheric fallouts (Sun et al. 2022). Further, the foam MPs generated from accumulated SUPs' breakdown are majorly white in color (Chen et al. 2020). Sources of colored MPs are laundry fibers, fibers from atmospheric deposits, films from the packaging of food items and consumer goods, decorative items, plastic bags, FMCG wraps, and other film
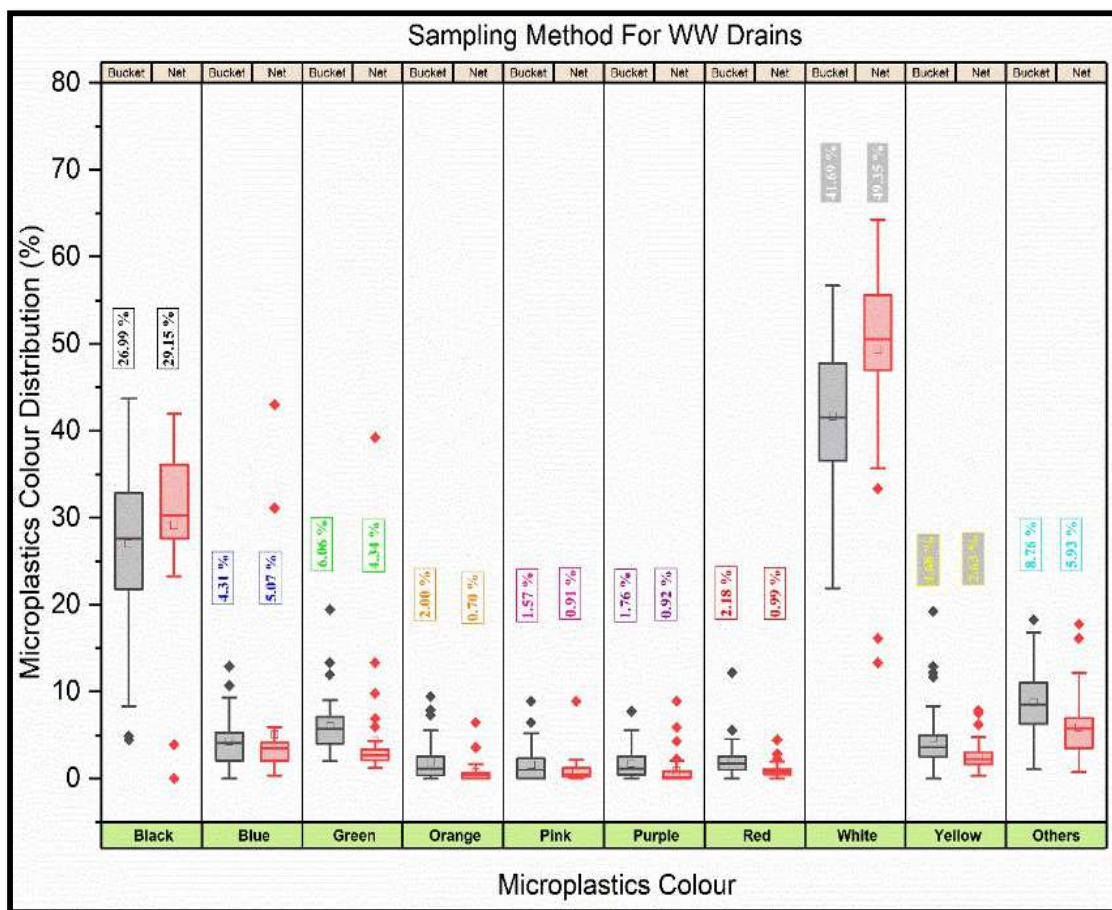
Fig. 13: Overall color distribution (%) of MPs.

covers used on beverage bottles, and colored fragments from disintegration and fragmentation of disposed PW

**MPs Polymer Distribution**

Out of 50 particles analyzed using FTIR-ATRA, only 3 were residues of undigested organic matter, and 11 types of polymers were identified. No identity could be assigned to rubbers due to the limitation of the FTIR-ATR in the analysis of black rubbery MPs. However, based on their appearance, they were categorized as rubber and not considered for assessing the polymer distribution.

The polymer distribution observed through FTIR analysis is depicted in Fig. 14, and FTIR spectra are presented in Fig. 15. Polyethylene (PE) dominated the polymeric distribution, followed by Polypropylene (PP) and Polystyrene (PS). Combinedly, these three accounted for 54% of all the particles analyzed. The distribution of other polymers was below 16 %, and their occurrence can be traced to the SW disposal in the drains. The polymer distribution in the urban drainage system of the current study follows the polymer

demand trend and plastic waste generation observed globally (PlasticsEurope 2021) in India and Raipur (CPCB 2015).

Other freshwater studies conclude that PE, PP, and PS are the most produced and demanded single-use plastics, and their low density hinders settling in the water column (Irfan et al. 2020). The polymer distribution in WW samples can assist in identifying MPs sources in the drains. Since WW drains receiving different WW streams affected the MPs' shape, size, and color distribution, it's highly likely that polymer type and their distribution are also influenced by intermixing. This is the reason that we observed high polymer diversity in the samples.

Most of the PE material appeared to be film and foam. While the films from FMCG products, wraps, mulching sheets, and plastic bags are mainly made of PE, the observation that many foams are of PE origin was interesting. Contrary to popular belief that foams are mainly manufactured from PS, SUPs, which majorly contributed to the foam MPs, are also made from PE. Interestingly, few foams were composed of styrene allyl alcohol (4%) and
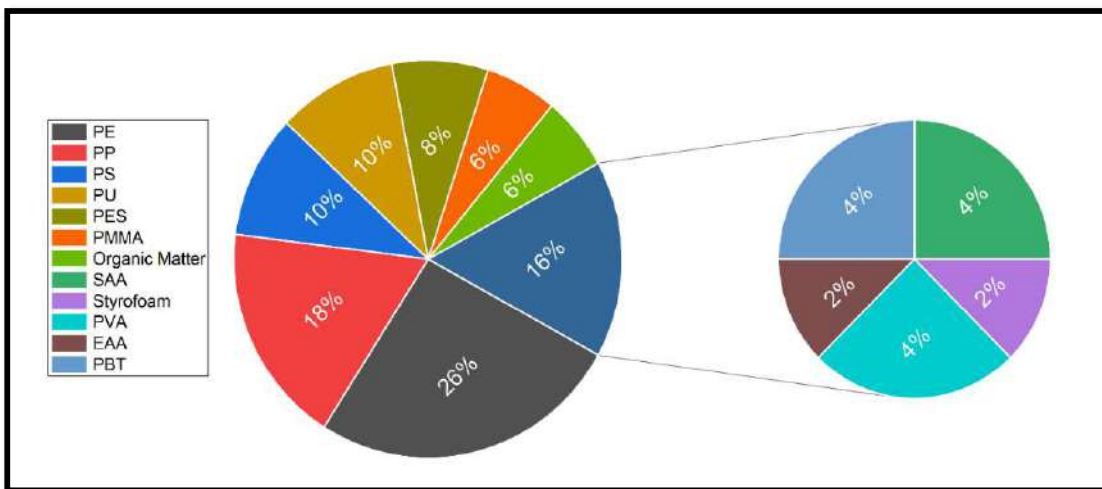
Fig. 14: Polymer distribution of the 50 MPs (subsample) analyzed through FTIR.
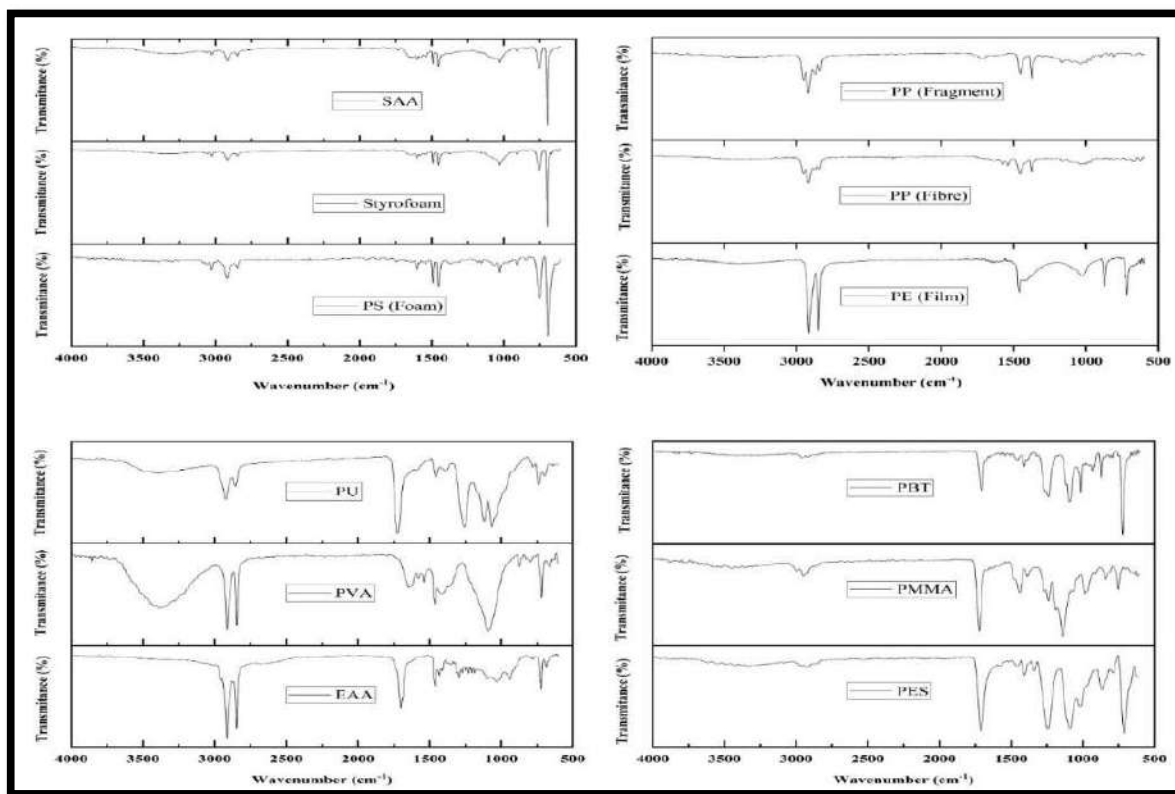


Fig. 15: FTIR spectra of MPs analyzed through FTIR-ATR.

styrofoam (2%), while polyurethane (PU) was observed to be 10%, highlighting that the disposal of PW into the drains or the MWW is contributing to the foam type of MPs in the drainage system. The disposal of electronic waste into the drains is primarily responsible for the occurrence of polybutylene terephthalate (PBT).

Synthetic fibers were mainly polyamide (PA) and polyester (PES), which also agrees with the literature and confirms the entry of fibrous MPs from laundry activity, those disintegrated from discarded textiles in the drains, and atmospheric deposits into the drains. Despite the fact that the fibers were the dominant shape category observed

here, their polymeric composition is influenced by their distribution in the subsample used for FTIR analysis, and polymeric distribution may vary due to extrapolation error from lack of homogenization, highlighting the need for an appropriate subsampling strategy for stereoscopic analysis. Nonetheless, all the fibers subsampled for FTIR comprised PP, PA, and PES.

Due to the wide range of polymers currently being produced, their wide distribution in the environment as waste, and the complex nature of informal urban drainage systems carrying intermixed liquid, coupled with instrumental limitations and lack of enough resources to analyze plentiful particles, its challenging to assess the polymeric distribution in different liquid waste streams. However, given that the majority (72%) of MPs analyzed here were composed of PE, PP, PS, PES, and PU, it is possible to use them as an indicator for assessing the MPs' pollution in informal urban drainage systems as these polymers are associated with all for LW streams being intermixed and conveyed by the drains.

## DISCUSSION

### Total MPs Burden and Daily Emission Load from Urban Drains

The total daily microplastic load (L) being discharged into the local Kharun river through 9 larger drains is calculated by formulae below and expressed as the number of particles

$$L = \sum_{n=1}^{9} Cn * Qn$$

where Cn is the MP concentration being discharged by

the WW drains, expressed as Particles/L, Qn is the daily discharge capacity of WW drains in liters per day, and n =1 to 9 for the nine wastewater drains discharging daily.

For net samples, TDML discharged by drains varied between $0.90 \times 10^8$ particles (W7) to $5.6 \times 10^8$ particles (W9), with combined TDML of $12.6 \times 10^8$ particles being discharged in the Kharun river from the entire city (all 9 larger drains) daily. The quantity of MPs emitted daily by any particular drain directly depends upon the discharge capacity of that drain. 75 MLD of liquid waste is emitted daily by drain W9 which is nearly ten times higher than drain W1 (8 MLD). Hence such a large variation in the TDML. The TDML of individual drains and discharge capacity are summarized in Table 1.

Due to limited studies conducted in the urban informal drainage systems, TDML being discharged from different WWTPs around the globe (Table 2) is used for comparative assessment. Studies report both lower and higher TDML than that observed in our study. Lower TDML in drains of Raipur in contrast with TDML of WWTPs effluent highlights the influence of variations in sources of MPs contributing to the LW, sampling, and extraction protocol, lowest size of the MPs studied, the efficacy of WWTPs, and other socioeconomic factors such as level of urbanization, and difference in lifestyle.

Higher TDML in untreated WW of the present study than TDML of WWTPs effluent is expected since WWTPs effectively reduce MPs load of the WW (Yaseen et al. 2022). Three important reasons for higher TDML from Raipur city that are absent elsewhere are intermixing of waste streams (MWW, SW runoff, agricultural runoff, industrial runoff, and secretly disposed of IWW), MSW and PW litter reaching the open drains, and atmospheric deposition in open drains.

Table 1: Total daily MPs load of nine larger drains emitting their load in the local river.

| WW Drain | Discharge capacity (MLD) | Daily discharge capacity (Liters) | MPs Concentration Net (particles/L) | MPs Concentration Bucket (particles/L) | Daily MPs load in the WW drains (net) | Daily MPs load in the WW drains (bucket) | Daily MPs load in the WW drains (Average of bucket & Net) |
|---|---|---|---|---|---|---|---|
| W1 | 8 | 8000000 | 5.979 | 5.540 | 47835897.44 | 44320000 | 46077948.72 |
| W2 | 12 | 12000000 | 7.139 | 6.680 | 85668016.19 | 80160000 | 82914008.1 |
| W3 | 18.9 | 18900000 | 5.746 | 5.180 | 108597902.1 | 97902000 | 103249951 |
| W4 | 32 | 32000000 | 4.441 | 3.940 | 142097902.1 | 126080000 | 134088951 |
| W5 | 15 | 15000000 | 6.109 | 4.660 | 91628959.28 | 69900000 | 80764479.64 |
| W6 | 9 | 9000000 | 4.347 | 3.400 | 39125874.13 | 30600000 | 34862937.06 |
| W7 | 2.07 | 2070000 | 4.371 | 3.660 | 9048351.648 | 7576200 | 8312275.824 |
| W8 | 28.43 | 28430000 | 6.167 | 5.200 | 175337516.9 | 147836000 | 161586758.4 |
| W9 | 75 | 75000000 | 7.527 | 5.220 | 564560439.6 | 391500000 | 478030219.8 |
| Total | 200.4 | 200400000 | - | - | 1263900859 | 995874200 | 1129887530 |

Table 2: Total daily MPs load from WWTPs reported in the literature.

| S. No. | Type of treatment facility | Country | TDML | Reference |
|--------|---------------------------|---------|------|-----------|
| 1. | 1 WWTP | China | $9.1 \times 10^{10}$ | (Tang et al. 2020) |
| 2. | 1 WWTP | USA | $3.56 \times 10^{10}$ | (Mason et al. 2016) |
| 3. | 1 WWTP | Germany | $1.91 \times 10^{10}$ | (Schmidt et al. 2020) |
| 4. | 7 WWTPs of Xiamen, a typical coastal city | China | $0.065 \times 10^{10}$ | (Long et al. 2019) |
| 5. | 1 WWTP near Vancouver, British Columbia | China | $0.008 \times 10^{10}$ | (Gies et al. 2018) |
| 6. | 1 WWTP of Sari | Iran | $0.009 \times 10^{10}$ | (Alavian Petroody et al. 2020), |
| 7. | 3 WWTPs in Mersin Bay | Turkey | $0.018 \times 10^{10}$ | (Akarsu et al. 2020) |
| 8. | 1 WWTP located in Wuxi | Eastern China | $0.1 \times 10^{10}$ | (Lv et al. 2019) |
| 9. | 1 tertiary WWTP in Gumi | South Korea | $0.79 \times 10^{10}$ | (Kim et al. 2022), |
| 10. | Secondary WWTP in Istanbul | Turkey | $0.0293 \times 10^{10}$ | (Vardar et al. 2021) |
| 11. | 2 WWTPs in Adana city | Turkey | $0.16 \times 10^{8}$ | (Gündoğdu et al. 2018) |
| 12. | 1 WWTP of northern Italy | Italy | $0.016 \times 10^{10}$ | (Magni et al. 2019), |
| 13. | Choneibe WWTP, located in Ahvaz City of Khuzestan province | Iran | $0.24 \times 10^{8}$ | (Takdastan et al. 2021), |
| 14. | 3 WWTPs in the Canterbury region | New Zealand | $0.24 \times 10^{6}$ | (Ruffell et al. 2021), |
| 15. | 12 WWTPs in Lower Saxony | Germany | $0.24 \times 10^{6}$ to $0.109 \times 10^{8}$ | (Mintenig et al. 2017), |
| 16. | Xi'an city | China | $0.34 \times 10^{10}$ | (Yang et al. 2021), |
| 17. | WWTP of Tokyo | Japan | $4.6 \times 10^{10}$ | (Sugiura et al. 2021) |
| 18. | 3 WWTPs Charleston Harbor | USA | $0.05 \times 10^{10}$ to $01 \times 10^{10}$ | (Conley et al. 2019) |
| 19. | 1 Conventional WWTP | Bangkok | $12.80\ 10^{8}$ | (Tadsuwan & Babel 2022) |
| 20. | 1 WWTP of Helsinki | Finland | $0.011 \times 10^{10}$ | (Talvitie et al. 2017) |
| 21. | 1 WWTP of Glasgow | Scotland | $0.006 \times 10^{10}$ | (Murphy et al. 2016) |

MPs originating from households are quite different in developed countries with higher living standards. Limited use of PCPs by residents of Raipur resulted in a negligible quantity of beads and microspheres in drains, while they remain abundant in WW of developed countries (Hu et al. 2022). Further, in ST-based OSS and Indian-style toilets with built-in laundry and bathing areas, a fraction of sullage gets disposed into the toilets and ends up in ST. A fraction of household-related MPs probably gets retained in the ST. Higher consumption and disposal of wet wipes, PCPs, and other hygiene-related products directly into the toilet (flushing) generates substantial MPs in Western countries (Ó Briain et al. 2020). Such practices are not observed in India, which explains lower MPs in the domestic WW directly emitted from households.

Globally, treated effluent disposal can add around $1.47 \times 10^{15}$ MPs annually, whereas discharge of untreated effluent is likely to add a staggering $10 \times 3.85^{16}$ MPs annually to aquatic environments (Uddin et al. 2020). Saigon River system disposes $1.1\text{-}1.6 \times 10^{14}$ fibrous MPs annually into coastal zones, and besides atmospheric fallout, MWW and IWW discharge from the city into the river is mainly responsible for fibrous MPs (Strady et al. 2020). In Malaysia,

95% of untreated WW and effluent of the WWTPs treating 5% of the WW are discharging $5.45 \times 10^{8}$ MPs particles daily in the aquatic environment (Praveena et al. 2018). The poor performance of WWTP located in the Bandar Abbas City of Iran led to the release of $1.2 \times 10^{8\ \text{MPs}}$ through 60 MLD of WW in the Persian Gulf (Naji et al. 2021). In the port of Durban, the highest MPs concentration was observed at the site located in in front of SW drains, and the authors report that due to frequent blockage occurring at the sewage pumping station, sewage overflows into SW drains result in higher MPs concentration at this site (Preston-Whyte et al. 2021). TDML from WWF to local aquatic sources was $(2.32 \times 10^{12})$, six times higher than MPs loads discharged from local WWTP. This highlights the significance and influence of WWF (intermixing of MWW and SW) mainly on the distribution of MPs in drains and ecosystems (Chen et al. 2020).

A WW drain from Lahore, Pakistan, with characteristics exactly similar to the drains studied here, discharges $7 \times 10^{9}$ MPs particles daily into the Ravi River (Irfan et al. 2020). In contrast, the collective TDML of nine larger drains of Raipur is one order less than a single drain of Lahore, suggesting that even in open drains of the Indian subcontinent with

mostly the same characteristics and sources, variation in the distribution of MPs occurs, which is mainly due to different sampling strategies, extraction and analysis techniques, and LoD. The findings stress the urgency of standardization of MPs sampling and analysis protocols for WW. Untreated WW from Longyearbyen, a smaller town with approximately 2,500 inhabitants in Svalbard, a Norwegian archipelago, emits $0.33 \times 10^8$ fibrous MPs particles daily into the fjord system. This emphasizes the importance of commissioning WWTPs even at the community level, as evident even smaller communities with low populations generate a significant number of MPs (Herzke et al. 2021).

Laundry activity from washing machines releases a significant quantity (in order of $10^6$) of microfibers (Kelly et al. 2019), and they are an important source of MPs. The primary laundry mode in Raipur is manual, unlike West, where laundry machines are prevalent. Hand washing of garments has not been studied in detail. However, hand washing is also done with detergents and fabric softeners like machine washing. Hand washing process involves constant abrasion, swishing, scrubbing, twisting, rubbing, and throwing the garment on the surface either through hand or some laundry scrub generating enough mechanical and chemical stress to release fibrous MPs from the garments, becoming part of the sullage and introduce fibrous MPs in WW drains of Raipur.

Atmospheric deposits are a significant source of fibrous MPs whose concentration (several orders higher than that emitted from WWTPs) varies between dry and wet periods (Napper et al. 2023). In Paris, the annual MPs load from atmospheric fallout is estimated to be between 3 to 10 tons, and the highest deposits occurred during the wet period in the urban zone, and atmospheric deposition in catchment areas increases the distribution of MPs (Dris et al. 2018). Hence atmospheric deposits can be a significant contributor of MPs in WW drains of Raipur for two reasons – first, unlike covered sewers limiting the entry of fallouts, WW drains, mostly natural and unlined channels, are open and prone to receive MPs from atmospheric fallout. Second, Raipur City has a tropical climate receiving a substantial portion of high annual precipitation, mostly during the three monsoon months, increasing the MPs deposition during this period. Additionally, MPs deposited from fallouts in catchment areas also enter the WW drains through urban runoff.

## CONCLUSION

This study presents the first evidence of the presence and characteristics of MPs in urban informal (open and natural) drainage systems carrying intermixed liquid waste streams originating from a residential habitat. Urban informal drainage systems are a significant source of MPs pollution discharged into aquatic environments. MPs sampling techniques were appropriately modified for logistical and locational challenges. The sampling methodology adopted here can be employed to investigate the distribution of MPs in urban informal drainage systems across the Indian subcontinent and Africa. The bucket strategy best suits the local or smaller drains and drains on the roadside, while the Net strategy suits larger drains where flow is higher.

MPs concentration and characteristics vary in different types of drains carrying liquid waste streams from different city functional areas. Moreover, we also estimated the total daily MPs emission from intermixed liquid waste streams discharged to local rivers. To protect local aquatic ecosystems that receive liquid waste streams from urban areas, constructed wetlands can be a cost-effective solution to protect the local aquatic ecosystems.

Our results establish that besides MPs emitted from households, atmospheric deposition, and SW disposal are also contributing to MPs in urban open drainage systems and must be considered when adopting preventive measures. Such potential sources warrant detailed investigation into how they influence the overall distribution of MPs associated with liquid waste streams, as these sources are not recognized as associated with wastewater. Local environmental regulations on MSW, plastic waste, MPs and microbeads, etc., and their enforcement will govern the quantity of MPs in drainage systems. We observed that WW drains in LIG and slum areas with poor SWM practices were more abundant with floating PW than those near the HIG area. By providing better municipal services and conducting educational and awareness campaigns to communicate best practices to manage MSW and PW at the household level, the entry of SW & PW can be restricted.

## ACKNOWLEDGMENTS

# REFERENCES

Akarsu, C., Kumbur, H., Gökdağ, K., Kıdeyş, A.E. and Sanchez-Vidal, A. 2020. Microplastics composition and load from three wastewater treatment plants discharging into Mersin Bay, north eastern Mediterranean Sea. Mar. Pollut. Bull., 150: 110776. https://doi.org/10.1016/j.marpolbul.2019.110776

Alavian Petroody, S.S., Hashemi, S.H. and Gestel, C.A.M. 2020. Factors affecting microplastic retention and emission by a wastewater treatment plant on the southern coast of the Caspian Sea. Chemosphere, 261: 128179. https://doi.org/10.1016/j.chemosphere.2020.128179

Al-Azzawi, M.S.M., Kefer, S., Weißer, J., Reichel, J., Schwaller, C., Glas, K., Knoop, O. and Drewes, J.E. 2020. Validation of sample preparation methods for microplastic analysis in wastewater matrices: Reproducibility and standardization. Water, 12: 2445. https://doi.org/10.3390/w12092445

Amerasinghe, P.H., Bhardwaj, R.M., Scott, C., Jella, K. and Marshall, F. (eds). 2013. Urban Wastewater and Agricultural Reuse Challenges in India (IWMI Research Report., International Water Management Institute (IWMI), Hyderabad, India. https://doi.org/10.22004/ag.econ.158342

Bretas Alvim, C., Mendoza-Roca, J.A. and Bes-Piá, A. 2020. Wastewater treatment plant as microplastics release source: Quantification and identification techniques. J. Environ. Manag., 255: 109739. https://doi.org/10.1016/j.jenvman.2019.109739

Central Pollution Control Board (CPCB). 2015. Assessment & Characterisation of Plastic Waste Generation in 60 Major Cities. CIPET & CPCB, New Delhi, India.

Central Pollution Control Board (CPCB). 2020. Annual Report 2020-21. CPCB, New Delhi, India.

Chen, B., Fan, Y., Huang, W., Rayhan, A.B.M.S., Chen, K. and Cai, M. 2020. Observation of microplastics in mariculture water of Longjiao Bay, southeast China: Influence by human activities. Mar. Pollut. Bull., 160: 111655. https://doi.org/10.1016/j.marpolbul.2020.111655

Chen, H., Jia, Q., Zhao, X., Li, L., Nie, Y., Liu, H. and Ye, J. 2020. The occurrence of microplastics in water bodies in urban agglomerations: Impacts of drainage system overflow in wet weather, catchment land-uses, and environmental management practices. Water Res., 183: 116073. https://doi.org/10.1016/j.watres.2020.116073

Conley, K., Clum, A., Deepe, J., Lane, H. and Beckingham, B. 2019. Wastewater treatment plants as a source of microplastics to an urban estuary: Removal efficiencies and loading per capita over one year. Water Res., 3:100030. https://doi.org/10.1016/j.wroa.2019.100030

Cowger, W., Steinmetz, Z., Gray, A., Munno, K., Lynch, J., Hapich, H. and Herodotou, O. 2021. Microplastic spectral classification needs an open source community: open specy to the rescue! Anal. Chem., 93: 7543-7548.

Dris, R., Gasperi, J., Rocher, V. and Tassin, B. 2018. Synthetic and non-synthetic anthropogenic fibers in a river under the impact of Paris Megacity: Sampling methodological aspects and flux estimations. Sci. Total Environ., 618: 157-164. https://doi.org/10.1016/j.scitotenv.2017.11.009

Franco, A.A., Arellano, J.M., Albendín, G., Rodríguez-Barroso, R., Zahedi, S., Quiroga, J.M. and Coello, M.D. 2020. Mapping microplastics in Cadiz (Spain): Occurrence of microplastics in municipal and industrial wastewaters. J. Water Process Eng., 38: 101596. https://doi.org/10.1016/j.jwpe.2020.101596

Gies, E.A., LeNoble, J.L., Noël, M., Etemadifar, A., Bishay, F., Hall, E.R. and Ross, P.S. 2018. Retention of microplastics in a major secondary wastewater treatment plant in Vancouver, Canada. Mar. Pollut. Bull., 133: 553-561. https://doi.org/10.1016/j.marpolbul.2018.06.006

Gündoğdu, S., Çevik, C., Güzel, E. and Kilercioğlu, S. 2018. Microplastics in municipal wastewater treatment plants in Turkey: a comparison of the influent and secondary effluent concentrations. Environ. Monit. Assess., 190: 626. https://doi.org/10.1007/s10661-018-7010-y

Hamidian, A.H., Ozumchelouei, E.J., Feizi, F., Wu, C., Zhang, Y. and Yang, M. 2021. A review on the characteristics of microplastics in wastewater treatment plants: A source for toxic chemicals. J. Clean. Prod., 295: 126480. https://doi.org/10.1016/j.jclepro.2021.126480

He, L., Ou, Z., Fan, J., Zeng, B. and Guan, W. 2022. Research on the non-point source pollution of microplastics. Front. Chem., 10: 956547. https://doi.org/10.3389/fchem.2022.956547

Herzke, D., Ghaffari, P., Sundet, J.H., Tranang, C.A. and Halsband, C. 2021. Microplastic fiber emissions from wastewater effluents: abundance, transport behavior and exposure risk for biota in an Arctic Fjord. Front. Environ. Sci., 9: 116.

Horton, A.A., Cross, R.K., Read, D.S., Jürgens, M.D., Ball, H.L., Svendsen, C., Vollertsen, J. and Johnson, A.C. 2021. Semi-automated analysis of microplastics in complex wastewater samples. Environ. Pollut., 268: 115841. https://doi.org/10.1016/j.envpol.2020.115841

Hu, E., Sun, C., Yang, F., Wang, Y., Hu, L., Wang, L., Li, M. and Gao, L. 2022. Microplastics in 48 wastewater treatment plants reveal regional differences in physical characteristics and shape-dependent removal in the transition zone between North and South China. Sci. Total Environ., 834: 155320. https://doi.org/10.1016/j.scitotenv.2022.155320

Hurley, R.R., Lusher, A.L., Olsen, M. and Nizzetto, L. 2018. Validation of a Method for Extracting Microplastics from Complex, Organic-Rich. Environmental Matrices. Environ. Sci. Technol 52, 7409–7417. https://doi.org/10.1021/acs.est.8b01517

Irfan, M., Qadir, A., Mumtaz, M. and Ahmad, S.R. 2020. An unintended challenge of microplastic pollution in the urban surface water system of Lahore, Pakistan. Environ. Sci. Pollut. Res., 27: 16718-16730. https://doi.org/10.1007/s11356-020-08114-7

Jiang, J., Wang, X., Ren, H., Cao, G., Xie, G., Xing, D. and Liu, B. 2020. Investigation and fate of microplastics in wastewater and sludge filter cake from a wastewater treatment plant in China. Sci. Total Env., 746: 141378.

Jong, M.C., Tong, X., Li, J., Xu, Z., Chng, S.H.Q., He, Y. and Gin, K.Y.H. 2022. Microplastics in equatorial coasts: Pollution hotspots and spatiotemporal variations associated with tropical monsoons. J. Hazard. Mater., 424: 127626. https://doi.org/10.1016/j.jhazmat.2021.127626

Kelly, M.R., Lant, N.J., Kurr, M. and Burgess, J.G. 2019. Importance of Water-Volume on the Release of Microplastic Fibers from Laundry. Environ. Sci. Technol 53: 11735-11744. https://doi.org/10.1021/acs.est.9b03022

Kim, M.J., Na, S.H., Batool, R., Byun, I.S. and Kim, E.J. 2022. Seasonal variation and spatial distribution of microplastics in tertiary wastewater treatment plant in South Korea. J. Hazard. Mater., 438: 129474. https://doi.org/10.1016/j.jhazmat.2022.129474

Lahens, L., Strady, E., Kieu-Le, T.-C., Dris, R., Boukerma, K., Rinnert, E., Gasperi, J. and Tassin, B. 2018. Macroplastic and microplastic contamination assessment of a tropical river (Saigon River, Vietnam) transversed by a developing megacity. Environ. Pollut., 236: 661-671. https://doi.org/10.1016/j.envpol.2018.02.005

Lares, M., Ncibi, M.C., Sillanpää, M. and Sillanpää, M. 2018. Occurrence, identification and removal of microplastic particles and fibers in conventional activated sludge process and advanced MBR technology. Water Res., 133: 236-246. https://doi.org/10.1016/j.watres.2018.01.049

Leslie, H.A., Brandsma, S.H., Velzen, M.J.M. and Vethaak, A.D. 2017. Microplastics en route: Field measurements in the Dutch river delta and Amsterdam canals, wastewater treatment plants, North Sea sediments and biota. Environ. Int., 101: 133-142. https://doi.org/10.1016/j.envint.2017.01.018

Long, Y., Zhou, Z., Yin, L., Wen, X., Xiao, R., Du, L., Zhu, L., Liu, R., Xu, Q., Li, H., Nan, R. and Yan, S. 2022. Microplastics removal and characteristics of constructed wetlands WWTPs in rural area of Changsha, China: A different situation from urban WWTPs. Sci. Total Environ., 811: 152352. https://doi.org/10.1016/j.scitotenv.2021.152352

Long, Z., Pan, Z., Wang, W., Ren, J., Yu, X., Lin, L., Lin, H., Chen, H. and Jin, X. 2019. Microplastic abundance, characteristics, and removal in

wastewater treatment plants in a coastal city of China. Water Res., 155: 255-265. https://doi.org/10.1016/j.watres.2019.02.028

Lv, X., Dong, Q., Zuo, Z., Liu, Y., Huang, X. and Wu, W.M., 2019. Microplastics in a municipal wastewater treatment plant: Fate, dynamic distribution, removal efficiencies, and control strategies. J. Clean. Prod., 225: 579-586. https://doi.org/10.1016/j.jclepro.2019.03.321

Magni, S., Binelli, A., Pittura, L., Avio, C.G., Della Torre, C., Parenti, C.C., Gorbi, S. and Regoli, F. 2019. The fate of microplastics in an Italian Wastewater Treatment Plant. Sci. Total Environ 652, 602-610. https://doi.org/10.1016/j.scitotenv.2018.10.269

Mason, S.A., Garneau, D., Sutton, R., Chu, Y., Ehmann, K., Barnes, J., Fink, P., Papazissimos, D. and Rogers, D.L. 2016. Microplastic pollution is widely detected in US municipal wastewater treatment plant effluent. Environ. Pollut., 218: 1045-1054. https://doi.org/10.1016/j.envpol.2016.08.056

Mhiret Gela, S. and Aragaw, T.A. 2022. Abundance and Characterization of Microplastics in Main Urban Ditches Across the Bahir Dar City, Ethiopia. Front. Environ. Sci., 1: 10.

Miller, E., Sedlak, M., Lin, D., Box, C., Holleman, C., Rochman, C.M. and Sutton, R. 2021. Recommended best practices for collecting, analyzing, and reporting microplastics in environmental media: Lessons learned from comprehensive monitoring of San Francisco Bay. J. Hazard. Mater., 409: 124770. https://doi.org/10.1016/j.jhazmat.2020.124770

Mintenig, S.M., Int-Veen, I., Löder, M.G.J., Primpke, S. and Gerdts, G. 2017. Identification of microplastic in effluents of waste water treatment plants using focal plane array-based micro-Fourier-transform infrared imaging. Water Res., 108: 365-372. https://doi.org/10.1016/j.watres.2016.11.015

Monira, S., Bhuiyan, M.A., Haque, N., Shah, K., Roychand, R., Hai, F.I. and Pramanik, B.K. 2021. Understanding the fate and control of road dust-associated microplastics in stormwater. Process Saf. Environ. Prot., 152: 47-57. https://doi.org/10.1016/j.psep.2021.05.033

Munno, K., Helm, P.A., Jackson, D.A., Rochman, C. and Sims, A. 2018. Impacts of temperature and selected chemical digestion methods on microplastic particles. Environ. Toxicol. Chem., 37: 91-98. https://doi.org/10.1002/etc.3935

Murphy, F., Ewins, C., Carbonnier, F. and Quinn, B. 2016. Wastewater Treatment Works (WwTW) as a source of microplastics in the aquatic environment. Environ. Sci. Technol., 50: 5800–5808. https://doi.org/10.1021/acs.est.5b05416

Naji, A., Azadkhah, S., Farahani, H., Uddin, S. and Khan, F.R. 2021. Microplastics in wastewater outlets of Bandar Abbas city (Iran): A potential point source of microplastics into the Persian Gulf. Chemosphere, 262: 128039. https://doi.org/10.1016/j.chemosphere.2020.128039

Napper, I.E., Parker-Jurd, F.N.F., Wright, S.L. and Thompson, R.C. 2023. Examining the release of synthetic microfibres to the environment via two major pathways: Atmospheric deposition and treated wastewater effluent. Sci. Total Environ., 857: 159317. https://doi.org/10.1016/j.scitotenv.2022.159317

Ó Briain, O., Marques Mendes, A.R., McCarron, S., Healy, M.G. and Morrison, L. 2020. The role of wet wipes and sanitary towels as a source of white microplastic fibres in the marine environment. Water Res., 182: 116021. https://doi.org/10.1016/j.watres.2020.116021

Oni, B.A., Ayeni, A.O., Agboola, O., Oguntade, T. and Obanla, O. 2020. Comparing microplastics contaminants in (dry and raining) seasons for Ox- Bow Lake in Yenagoa, Nigeria. Ecotoxicol. Environ. Saf., 198: 110656. https://doi.org/10.1016/j.ecoenv.2020.110656

Picó, Y., Soursou, V., Alfarhan, A.H., El-Sheikh, M.A. and Barceló, D. 2021. First evidence of microplastics occurrence in mixed surface and treated wastewater from two major Saudi Arabian cities and assessment of their ecological risk. J. Hazard. Mater., 416: 125747. https://doi.org/10.1016/j.jhazmat.2021.125747

PlasticsEurope. 2021. Plastics–The Facts: An analysis of European Plastics Production, Demand and Waste Data. PE, Brussels.

Prata, J.C., Reis, V., Costa, J.P., Mouneyrac, C., Duarte, A.C. and Rocha-Santos, T. 2021. Contamination issues as a challenge in quality control and quality assurance in microplastics analytics. J. Hazard. Mater., 403: 123660. https://doi.org/10.1016/j.jhazmat.2020.123660

Praveena, S.M., Shaifuddin, S.N.M. and Akizuki, S. 2018. Exploration of microplastics from personal care and cosmetic products and its estimated emissions to marine environment: An evidence from Malaysia. Mar. Pollut. Bull., 136: 135-140. https://doi.org/10.1016/j.marpolbul.2018.09.012

Preston-Whyte, F., Silburn, B., Meakins, B., Bakir, A., Pillay, K., Worship, M., Paruk, S., Mdazuka, Y., Mooi, G., Harmer, R., Doran, D., Tooley, F. and Maes, T. 2021. Meso- and microplastics monitoring in harbour environments: A case study for the Port of Durban, South Africa. Mar. Pollut. Bull., 163: 111948. https://doi.org/10.1016/j.marpolbul.2020.111948

RMC. 2014. Sector Wise Slip Template: Storm Water Drainage. Municipal Corporation, Raipur, Chattisgarh, India.

Rochman, C.M. 2019. Rethinking microplastics as a diverse contaminant suite. Environ. Toxicol. Chem., 38: 703-711. https://doi.org/10.1002/etc.4371

Ruffell, H., Pantos, O., Northcott, G. and Gaw, S. 2021. Wastewater treatment plant effluents in New Zealand are a significant source of microplastics to the environment. NZ J. Mar. Freshw. Res., 1: 1-17. https://doi.org/10.1080/00288330.2021.1988647

Sang, W., Chen, Z., Mei, L., Hao, S., Zhan, C., Zhang, W.B., Li, M. and Liu, J. 2021. The abundance and characteristics of microplastics in rainwater pipelines in Wuhan, China. Sci. Total Environ., 755: 142606. https://doi.org/10.1016/j.scitotenv.2020.142606

Schmidt, C., Kumar, R., Yang, S. and Büttner, O. 2020. Microplastic particle emission from wastewater treatment plant effluents into river networks in Germany: Loads, spatial patterns of concentrations and potential toxicity. Sci. Total Environ., 737: 139544. https://doi.org/10.1016/j.scitotenv.2020.139544

Shruti, V.C., Pérez-Guevara, F., Elizalde-Martínez, I. and Kutralam-Muniasamy, G. 2021. Current trends and analytical methods for evaluation of microplastics in stormwater. Trends Environ. Anal. Chem., 30: 00123. https://doi.org/10.1016/j.teac.2021.e00123

Shukla, P., Singh, S. and Gour, A. 2020. Study of trapping and intermixing of Delhi drains for rejuvenation of the river Yamuna. Int. J. Adv. Res. Innov., 8(2): 106-109.

Simon, M., Alst, N. and Vollertsen, J. 2018. Quantification of microplastic mass and removal rates at wastewater treatment plants applying Focal Plane Array (FPA)-based Fourier Transform Infrared (FT-IR) imaging. Water Res., 142: 1-9. https://doi.org/10.1016/j.watres.2018.05.019

Stang, C., Mohamed, B.A. and Li, L.Y. 2022. Microplastic removal from urban stormwater: Current treatments and research gaps. J. Environ. Manag., 317: 115510. https://doi.org/10.1016/j.jenvman.2022.115510

Strady, E., Kieu-Le, T.C., Gasperi, J. and Tassin, B. 2020. Temporal dynamic of anthropogenic fibers in a tropical river-estuarine system. Environ. Pollut., 259: 113897. https://doi.org/10.1016/j.envpol.2019.113897

Sugiura, M., Takada, H., Takada, N., Mizukawa, K., Tsuyuki, S. and Furumai, H. 2021. Microplastics in urban wastewater and estuarine water: Importance of street runoff. Environ. Monit. Contam. Res 1, 54-65. https://doi.org/10.5985/emcr.20200006

Sun, J., Peng, Z., Zhu, Z.R., Fu, W., Dai, X. and Ni, B.J. 2022. The atmospheric microplastics deposition contributes to microplastic pollution in urban waters. Water Res., 225: 119116. https://doi.org/10.1016/j.watres.2022.119116

Tadsuwan, K. and Babel, S., 2022. Microplastic abundance and removal via an ultrafiltration system coupled to a conventional municipal wastewater treatment plant in Thailand. J. Environ. Chem. Eng 10, 107142. https://doi.org/10.1016/j.jece.2022.107142

Tagg, A.S., Harrison, P., J. and Yang, C. 2017. Fenton's reagent for the rapid and efficient isolation of microplastics from wastewater. Chem. Commun., 53: 372-375. https://doi.org/10.1039/C6CC08798A

Takdastan, A., Niari, M.H., Babaei, A., Dobaradaran, S., Jorfi, S. and Ahmadi, M. 2021. Occurrence and distribution of microplastic particles and the concentration of Di 2-ethyl hexyl phthalate (DEHP) in microplastics and wastewater in the wastewater treatment plant. J. Environ. Manag., 280: 111851. https://doi.org/10.1016/j.jenvman.2020.111851

Talvitie, J., Mikola, A., Setälä, O., Heinonen, M. and Koistinen, A. 2017. How well is microlitter purified from wastewater? – A detailed study on the stepwise removal of microlitter in a tertiary level wastewater treatment plant. Water Res., 109: 164-172. https://doi.org/10.1016/j.watres.2016.11.046

Tang, N., Liu, X. and Xing, W. 2020. Microplastics in wastewater treatment plants of Wuhan, Central China: Abundance, removal, and potential source in household wastewater. Sci. Total Environ., 745: 141026. https://doi.org/10.1016/j.scitotenv.2020.141026

Tran-Nguyen, Q.A., Vu, T.B.H., Nguyen, Q.T., Nguyen, H.N.Y., Le, T.M., Vo, V.M. and Trinh-Dang, M. 2022. Urban drainage channels as microplastics pollution hotspots in developing areas: A case study in Da Nang. Vietnam. Mar. Pollut. Bull., 175: 113323. https://doi.org/10.1016/j.marpolbul.2022.113323

Uddin, S., Fowler, S.W. and Behbehani, M. 2020. An assessment of microplastic inputs into the aquatic environment from wastewater streams. Mar. Pollut. Bull 160, 111538. https://doi.org/10.1016/j.marpolbul.2020.111538

Vaid, M., Sarma, K., Kala, P. and Gupta, A. 2022. The plight of Najafgarh drain in NCT of Delhi, India: assessment of the sources, statistical water quality evaluation, and fate of water pollutants. Environ. Sci. Pollut. Res., 7: 1-21. https://doi.org/10.1007/s11356-022-21710-z

Vardar, S., Onay, T.T., Demirel, B. and Kideys, A.E. 2021. Evaluation of microplastics removal efficiency at a wastewater treatment plant discharging to the Sea of Marmara. Environ. Pollut., 289: 117862. https://doi.org/10.1016/j.envpol.2021.117862

Veerasingam, S., Ranjani, M., Venkatachalapathy, R., Bagaev, A., Mukhanov, V., Litvinyuk, D., Verzhevskaia, L., Guganathan, L. and Vethamony, P. 2020. Microplastics in different environmental compartments in India: Analytical methods, distribution, associated contaminants, and research needs. TrAC Trends Anal. Chem., 133: 116071. https://doi.org/10.1016/j.trac.2020.116071

Wang, C., O'Connor, D., Wang, L., Wu, W.-M., Luo, J. and Hou, D. 2022. Microplastics in urban runoff: Global occurrence and fate. Water Res., 225: 119129. https://doi.org/10.1016/j.watres.2022.119129

Wang, F., Wang, B., Duan, L., Zhang, Y., Zhou, Y., Sui, Q., Xu, D., Qu, H. and Yu, G. 2020. Occurrence and distribution of microplastics in domestic, industrial, agricultural and aquacultural wastewater sources: A case study in Changzhou, China. Water Res., 182: 115956. https://doi.org/10.1016/j.watres.2020.115956

Wei, F., Xu, C., Chen, C., Wang, Y., Lan, Y., Long, L., Xu, M., Wu, J., Shen, F., Zhang, Y., Xiao, Y. and Yang, G. 2022. Distribution of microplastics in the sludge of wastewater treatment plants in Chengdu, China. Chemosphere, 287: 132357. https://doi.org/10.1016/j.chemosphere.2021.132357

Werbowski, L.M., Gilbreath, A.N., Munno, K., Zhu, X., Grbic, J., Wu, T., Sutton, R., Sedlak, M.D., Deshpande, A.D. and Rochman, C.M. 2021. Urban Stormwater Runoff: A major pathway for anthropogenic particles, black rubbery fragments, and other types of microplastics to urban receiving waters. ACS EST Water, 1: 1420-1428. https://doi.org/10.1021/acsestwater.1c00017

Woodward, J., Li, J., Rothwell, J. and Hurley, R. 2021. Acute riverine microplastic contamination due to avoidable releases of untreated wastewater. Nat. Sustain., 4: 793-802. https://doi.org/10.1038/s41893-021-00718-2

Wu, X., Zhao, X., Chen, R., Liu, P., Liang, W., Wang, J., Teng, M., Wang, X. and Gao, S. 2022. Wastewater treatment plants act as essential sources of microplastic formation in aquatic environments: A critical review. Water Res., 221: 118825. https://doi.org/10.1016/j.watres.2022.118825

Yang, F., Li, D., Zhang, Z., Wen, L., Liu, S., Hu, E., Li, M. and Gao, L. 2022. Characteristics and the potential impact factors of microplastics in wastewater originated from different human activities. Process Saf. Environ. Prot., 166: 78-85. https://doi.org/10.1016/j.psep.2022.07.048

Yang, Z., Li, S., Ma, S., Liu, P., Peng, D., Ouyang, Z. and Guo, X. 2021. Characteristics and removal efficiency of microplastics in sewage treatment plant of Xi'an City, northwest China. Sci. Total Environ., 771: 145377. https://doi.org/10.1016/j.scitotenv.2021.145377

Yano, K.A., Geronimo, F.K., Reyes, N.J. and Kim, L.H. 2021. Characterization and comparison of microplastic occurrence in point and non-point pollution sources. Sci. Total Environ., 797: 148939. https://doi.org/10.1016/j.scitotenv.2021.148939

Yaseen, A., Assad, I., Sofi, M.S., Hashmi, M.Z. and Bhat, S.U. 2022. A global review of microplastics in wastewater treatment plants: Understanding their occurrence, fate and impact. Environ. Res., 212: 113258. https://doi.org/10.1016/j.envres.2022.113258

Yuan, F., Zhao, H., Sun, H., Sun, Y., Zhao, J. and Xia, T. 2022. Investigation of microplastics in sludge from five wastewater treatment plants in Nanjing, China. J. Environ. Manag., 301: 113793. https://doi.org/10.1016/j.jenvman.2021.113793

Ziajahromi, S., Neale, P.A. and Leusch, F.D.L. 2016. Wastewater treatment plant effluent as a source of microplastics: A review of the fate, chemical interactions and potential risks to aquatic organisms. Water Sci. Technol., 74: 2253-2269. https://doi.org/10.2166/wst.2016.414

Ziajahromi, S., Neale, P.A., Telles Silveira, I., Chua, A. and Leusch, F.D.L. 2021. An audit of microplastic abundance throughout three Australian wastewater treatment plants. Chemosphere, 263: 128294. https://doi.org/10.1016/j.chemosphere.2020.128294

# Assessment of Water Quality During 2018-2022 in the Vam Co River Basin, Vietnam

**N. T. Phong*(**), P. T. Vinh***, N. D. Luan***, P. H. Dung***, A. H. Tanim****, A. S. Gagnon*****,**
**W. Lohpaisankrit******, P. T. Hoa*******, P. N. Truong******** and N. D. Vuong***†**

*Laboratory of Environmental Sciences and Climate Change, Institute for Computational Science and Artificial Intelligence, Van Lang University, Ho Chi Minh City, Vietnam
**Faculty of Environment, School of Technology, Van Lang University, Ho Chi Minh City, Vietnam
***Southern Institute of Water Resources Research, Ho Chi Minh City, Vietnam
****Department of Civil and Environmental Engineering, University of South Carolina, Columbia, SC 29208, USA
*****School of Biological and Environmental Science, Liverpool John Moores University, Liverpool L3 3AF, U.K.
******Department of Civil Engineering, Faculty of Engineering, Khon Kaen University, Thailand
*******School of Earth and Planetary Sciences, Spatial Sciences Discipline, Curtin University, Perth, Australia
********Computational Biology and Bioinformatics Laboratory, Department of Integrative Biotechnology,
College of Biotechnology and Bioengineering, Sungkyunkwan University, Suwon 16419, Gyeonggi-do, Republic of Korea
†Corresponding author: N. D. Vuong; dinhvuongkhtlmn@gmail.com

## ABSTRACT

Water pollution in the Vam Co River basin is becoming more complicated due to untreated wastewater being directly discharged into rivers and canals from agricultural, industrial, and domestic activities. To assess the water quality in this area, this study conducted monitoring at ten sampling locations (S1-S10) from 2018 to 2022, calculated the Water Quality Index (WQI) for each parameter, and simulated water quality in 2022 using the 1D- MIKE 11 model developed by DHI with two main modules including HD and AD. The findings showed that most parameters did not surpass the allowable limits per QCVN 08-MT:2015/BTNMT on Vietnam National Technical Regulation on Surface Water Quality. However, organic and microbial pollution led to certain parameters, such as $BOD_5$, COD, and Coliform, exceeding the limits. The lowest water quality was recorded in Long An province, especially at sampling locations S3, S4, and S6, with the average WQI for nine water quality parameters from February to July 2022 being 58.4, 67.8, and 21.1, respectively. Additionally, the simulation outcomes of the MIKE 11 model salinity, $BOD_5$, DO, and $NH_4$ aligned with the real measurements taken. It has been observed that the southern area of the Vam Co River Basin possesses poorer water quality than the northern part, with Long An province located downstream of the Vam Co River basin being the primary source of pollution. The development of this hydraulic model signifies a crucial milestone in comprehending and regulating the effects of pollution in monitoring and managing water management systems, controlling saline intrusion, and ensuring water supply for agricultural production and daily use in the Vam Co River basin.

## INTRODUCTION

Water is an essential resource for human life as well as for all industrial and agricultural processes. Over the past few decades, the rapid growth of industrial and agricultural development, along with a surge in population growth, has significantly increased the demand for freshwater (Ramakrishnaiah et al. 2009, Thu Minh et al. 2020, Duc et al. 2021). However, quality water is one of the most sensitive components of the environment (Das & Acharya 2003). Thus, contamination has become more serious over time, mainly due to the growth mentioned above generating

domestic waste and residual fertilizer pollution (Girbaciu et al. 2015). Moreover, the varied characteristics of water levels and flows due to climate change also affect water quality (Thanh Giao et al. 2021). Thus, water quality assessments have attracted more attention worldwide (Bilgin 2018, Wu et al. 2018, Li et al. 2020).

Water quality assessments can be done based on their physical, chemical, and biological properties (Loukas 2010). However, in practice, a WQI has been commonly used to summarize the overall water quality of an area in a single term and aid in selecting the appropriate treatment technology

to address related issues (Tyagi et al. 2013). Based on the WQI, the assessments can be implemented at the station and regional/basin scale. The latter is more challenging due to the in-situ sampling cost and the limitation of remote sensing technologies for capturing water quality characteristics. Thus, spatial-temporal changes in water quality have been simulated by numerical models, e.g., MIKE 21 (Paliwal & Patra 2011, Tran 2017), WASP (Lai et al. 2011, Yao et al. 2015, Mbuh et al. 2019), MIKE 11 (Cheng & Zhi 2015, Girbaciu et al. 2015, Liang et al. 2015, Thu Minh et al. 2022), SWAT (Abbaspour et al. 2007, Debele et al. 2008, Qiu & Wang 2014, Epelde et al. 2015).

Many efforts have been made to use the models mentioned above to simulate water quality. For instance, Tran (2017) used the MIKE 21 model to simulate the transport of pollutants in the Dinh Vu coastal area, Hai Phong City, Vietnam, with simulation results showing a Nash of 0.96 and 0.93, and the relative and the relatively wrong number of Ecolab parameters are below 20%. Paliwal & Patra (2011) employed MIKE 21 to simulate BOD and DO in the Hoogly estuary, West Bengal, India, providing reasonable predictions. Industrial waste has a minor effect on the Hooghly River. The river mouth has effective dilution, aided by tidal mixing. As a result, BOD levels dropped to under 4 mg.L$^{-1}$, and DO levels were also found to replenish, achieving a level higher than 3 mg.L$^{-1}$.

Similarly, Gordillo et al. (2020) used WASP to simulate steady-state testing and real-life cases at the Ebro River, and Lai et al. (2011) combined IWMM and WASP models to assess the water quality of the Kaoping River. MIKE 11 was used by Cheng & Zhi (2015) and Girbaciu et al. (2015) to identify pollution sources and simulate water quantity and quality, respectively. While Qiu & Wang (2014) applied the SWAT model to assess water quality for the Neshanic River basin, United States, with reasonably simulated hydrological conditions and water quality. Besides that, SWAT is also used by Abbaspour et al. (2007) to simulate all related processes affecting water, sediment, and nutrient availability in the basin. The results show that in river basins with good quality and availability of data and relatively small model uncertainty – SWAT can be used as a flow simulation tool. Debele et al. (2008) combined SWAT and CE-QUAL-W2 to simulate water quantity and quality processes in upland and downstream basins. The study shows that the two models are compatible and can be used to assess and manage water resources in complex basins.

Although previous studies showed significant achievements, there is little agreement on the best model parameters because they heavily rely on the quality/quantity and characteristics of meteorological, hydrological, terrain, and other related factors in a particular area. Thus, there is still a need to research using the model to simulate water quality in case no previous studies have been made or input data has been updated in the area. This topic is undergoing a revolution of considerable interest, especially in the area that has been seriously contaminated.

In this context, the Vam Co River basin, located in the northeast of the Mekong Delta, in Long An and Tay Ninh, Vietnam, is one of the case studies (Fig. 1). The surface water in this region has been contaminated by many different wastewater sources from activities such as agriculture, industry, domestic activities, etc. (Dao & Bui 2016). The main contributor to pollution is the direct discharge of untreated wastewater from various activities into rivers and canals. In addition, due to tides from the East Sea affecting Go Dau and Thanh Hoa, the water supply for daily life and irrigation faces many obstacles, especially in the Tan Tru sub-region. Salinity usually reaches its highest around March-April or May if the rainy season comes slowly. However, research on water quality in the Vam Co River basin has been limited to investigations (Dao & Bui 2016, Huntjens et al. 2013) and statistical analyses (Nguyen 2019). Thus, monitoring water quality regularly for this region is deemed crucial (Ly et al. 2013, Behmel et al. 2016).

This study aims to measure and assess water quality in the Vam Co River basin based on the WQI index. Water quality indicators measured between 2018 and 2022 at ten of the most typical points for monitoring water quality are distributed on the main rivers/canals in the region according to locations with risk of water quality pollution, such as locations of rice cultivation, aquaculture, densely populated areas, locations with strong or small flows. From that, to more accurately assess the water quality changes in the river and canal system. Besides, the MIKE 11 model with two main modules simulates water quality with its stability, reliability, flexibility, and high calculation speed (Turner et al. 2009, Mama et al. 2021). The findings from this study help identify and forecast pollution and guide for sustainably using water resources.

## MATERIALS AND METHODS

### Study Area

The Vam Co River basin covers a total natural area of 205,077 hectares and is located in the Long An and Tay Ninh provinces. The Vam Co Dong River borders the area to the northeast, the Vam Co Tay River to the southwest, and the Vietnam-Cambodia border to the north (Fig. 1). The average annual temperature ranges from 27-29°C. It increases gradually from the sea to the mainland. Air humidity is positively correlated with rain and inversely

correlated with temperature, with an average annual humidity of about 78%. The region experiences two distinct seasons - a rainy season from May to October and a dry season from November to May of the following year, with the Vam Co Dong River area experiencing a longer dry season greater than 15% of the annual rainfall. Freshwater supplies become limited, and water pollution levels increase towards the end of the dry season. At the beginning of the rainy season, rainwater carries surface waste, including alum, into the water source, affecting agriculture and aquaculture's water supply.

**Collection of Water Samples**

Water samples were collected between 2018 and 2022 at ten stations in the study area, as shown in Fig. 1. Specifically, the field collection of water samples was organized twice a month between February and July in 2018 and 2022 at the locations. As a result, a total of 600 samples were obtained (120 samples/year). The field collection was performed between February and July because the period from February to April represented the dry season, while May to July was rainy. Environmental standard factors of the water samples, such as pH, $BOD_5$, COD, DO, TSS, $NH_4$, $NO_2$, $NO_3$, $PO_4$, and Coliform, were analyzed.

**Meteorological and Hydrological Data**

Rainfall and other meteorological data were collected daily at the stations of Bien Hoa, Can Dang, Dau Tieng, Dong Phu,
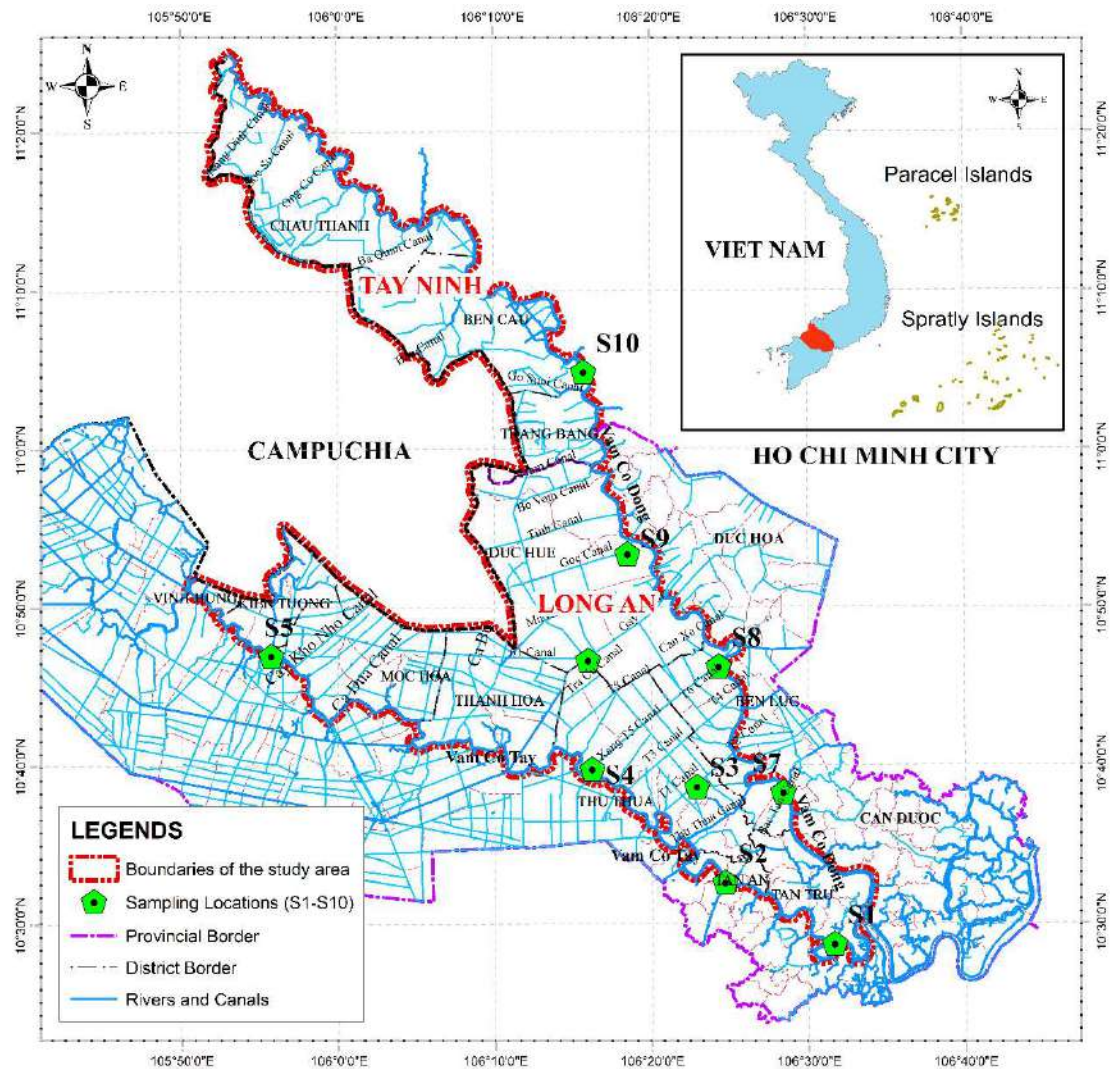


Fig. 1: Study area and sample locations (S1-S10) of the Vam Co River basin.

Go, Dau, Long Thanh, Moc Hoa, Phuoc Hoa, Tan An, Tan Son Nhat, Tay Ninh, Tri An and Vung Tau operated by the Southern Regional Hydrometeorological Center of Vietnam (Fig. 2). Hydrological daily data for 2017 and 2021 (Rainfall, discharge, and flow data) were obtained from the Vung Tau, Bien Hoa, Phu An, Nha Be, Thu Dau Mot, Ben Luc, and Tan An streamflow stations (Fig. 2) due to the Southern Regional Hydro-meteorological Center of Vietnam provides. Water level hourly data for 2017 and 2021 were generated using the global harmonic tidal model of the DHI (2019). In addition, the study also referred to the Tide Forecast Table of the Institute of Coastal and Offshore Engineering (http://www.icoe.org.vn) based on the study of Codiga (2011) and the Center for Oceanography of Vietnam (CFO 2022) annual tide table for model simulation.

### Topographic Data

For modeling the topography of rivers, measured channel cross sections of the Saigon, Dong Nai, Can Gio, Long Tau, and Soai Rap Rivers were collected from the Southern Institute of Water Resources Research under the project "Determining high shore edges."

### Water Quality Index

Water quality in the Vam Co River basin is related to various sectors such as residential, industrial, agricultural, and aquaculture. The analysis of water quality for the collected water samples was performed based on several standards and regulations of Vietnam, including TCXDVN 33:2006 on Water Supply - Distribution System and Facilities - design standard (MOC 2006), QCVN 40:2011/BTNMT on the National Technical Regulation on Industrial Wastewater (MONRE 2011), QCVN 11:2008/BTNMT (Column B) on National Technical Regulation on the effluent of aquatic products processing industry (MONRE 2008), QCVN 08-MT:2015/BTNMT on Vietnam National Technical Regulation on Surface Water Quality (MONRE 2015) and WHO standards for residential discharge. In addition, a comparison with standards and regulations will help

determine if the water meets the respective standards and regulations for safe use and discharge.

WQI is a helpful way to monitor and evaluate water quality (Nguyen & Huynh 2022). According to the MONRE of Vietnam (Nguyen & Huynh 2022), it ranges from 0 to 100. It can be categorized into six levels of water quality, namely Heavily polluted (WQI<10), Very poor (10-25), Poor (26-50), Moderate (51-75), Good (76-90), and Excellent water (91-100) (Table 1).

Besides that, based on the decision No. 1460/QD-TCMT in 2019 issued by the Ministry of Natural Resources and Environment (MONRE), which pertains to the release of technical guidelines on calculating and publication of the Vietnam Water Quality Index (VN_WQI) (MONRE 2019). The VN_WQI is divided into five parameter groups: pH (Group I), pesticide parameters (Group II), heavy metals (Group III), organic and nutrient parameters (Group IV), and microbiological parameters (Group V) (Nguyen & Huynh 2022, Thanh Giao et al. 2021). This study used the WQI to indicate the water used for agricultural production and aquaculture. Therefore, we selected three parameter groups, including pH (Group I): DO, COD, $BOD_5$, $NH_4$, $PO_4^{3-}$, $NO_3^-$, $NO_2^-$ (Group IV); and Coliform (Group V). The formula of the WQI is expressed as follows:

$$WQI = \frac{WQI_I}{100}\left[\left(\frac{1}{7}\sum_{a=1}^{7} WQI_{IV}\right)^2 \text{ x } WQI_V\right]^{\frac{1}{3}} \quad ...(1)$$

$WQI_I$, $WQI_{IV}$, and $WQI_V$ are the calculated results for groups I, IV, and V parameters, respectively.

### Calibrating and Validating the MIKE 11 Model

#### (a) MIKE 11 and the Modules Used

MIKE 11, developed by the Danish Hydraulic Institute (DHI 2017), is a one-dimensional modeling system for simulating flow, sediment transport, and water quality in canals, rivers, irrigation systems, and estuaries (Havnø et al. 1995). MIKE 11 uses finite difference diagrams to calculate unstable

Table 1: Standard rating of water quality as per WQI.

| No. | WQI range | Water quality classification | Suitable for use purpose |
|-----|-----------|------------------------------|--------------------------|
| 1. | < 10 | Heavily polluted | Contaminated water needs to be remedied and treated |
| 2. | 10-25 | Very poor | Unsuitable for agricultural and aquaculture |
| 3. | 26-50 | Poor | Used for navigation and other equivalent purposes |
| 4. | 51-75 | Moderate | It may be suitable for agricultural and aquaculture purposes with certain precautions or treatments. |
| 5. | 76-90 | Good | Suitable for agriculture and aquaculture with certain precautions or treatments |
| 6. | 91-100 | Excellent | Used good for agriculture and aquaculture |

flows. It can also describe subcritical and supercritical flow conditions through a numerical scheme that adapts to local flow conditions (in time and space) (Girbaciu et al. 2015). This study employed the hydrodynamic module (HD) and advection-dispersion module (AD) to solve water contamination problems.

**(b) Defining the River Network and Boundaries**

The river network shown in Fig. 2 comprises the Saigon River, Be River, Vam Co Dong River, and Vam Co Tay River. The hydraulic scheme of the river network included 255 river branches with a total length of 2,341,639m and 1,076 cross-sections.

The upstream boundary conditions of the river networks for the HD module were determined by using the discharge data at Tri An, Dau Tieng, Phuoc Hoa, and Can Dang stations. Regarding the downstream boundary, four water level boundaries are arranged at the sea outlet and the water

level boundary at Moc Hoa. The selection is based on the geographic condition of the study area. It is part of the Saigon-Dong Nai basin and is an almost closed basin with the main entrance to the sea at Soai Rap and some other small estuaries affected by the flow of the Mekong Delta. The data is the tidal level of Vung Tau station, which will be calibrated according to the correlation between Vung Tau and Soai Rap. The salinity concentration data collected from the survey documents were used for the salinity margin at the upstream boundary.

For the AD module, the upstream boundary conditions were set the same as in the HD module. To assign the downstream boundary of the AD model, the water quality data of Soai Rap River (outside the sea) was used, including the quality of discharge water in industrial parks, export processing zones, factories, and domestic wastewater included in the model to simulate. The concentration of waste discharged into rivers and canals is calculated to
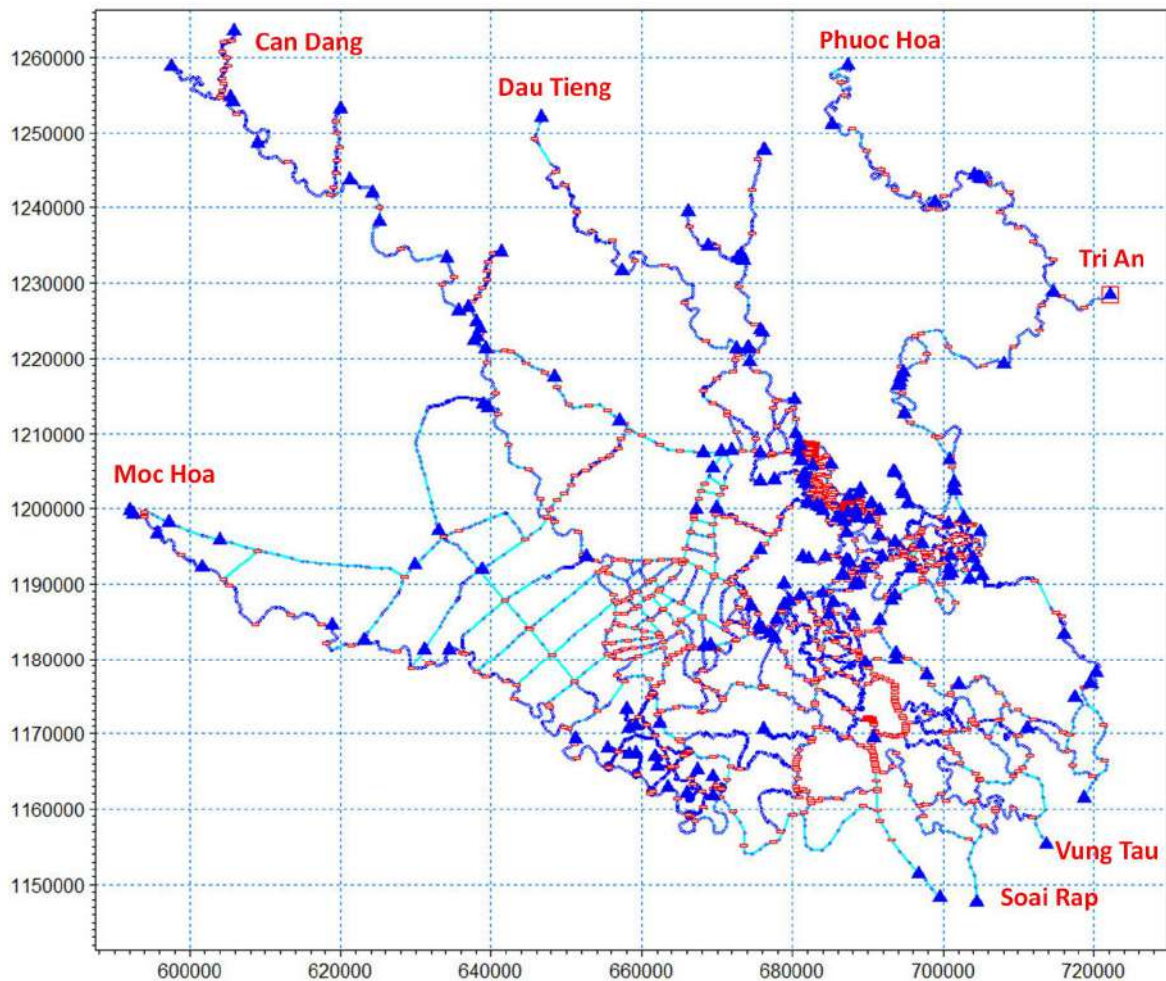


Fig. 2: River network of Vam Co River basin in MIKE 11 with cross-section (red dots) and water level (blue dots).

simulate water quality. After being calculated, the water quality indicators are the sectors' loads converted to the concentration of substances (mg.L$^{-1}$). Wastewater input data based on various sectors, namely, industrial, agricultural, and domestic zones, were computed by considering drainage areas of the river and canal sections.

### (c) Calibration, Validation, and Evaluation of the MIKE 11 Model

The MIKE 11 with the HD and AD modules underwent calibration and validation using salinity and water level data from monitoring stations at Cau Noi, Ben Luc, Tan An, Phu An, and Nha Be in 2017 and 2021. Various parameters, such as Manning's roughness coefficient (n) for the HD module and the diffusion load factor for the AD module, were adjusted to improve model accuracy. The values of the MIKE 11 model parameters were modified based on the trial-and-error method.

After calibrating and validating the model, water quality during the dry season 2022 was simulated and compared with actual measurements. The WQI was calculated using ten representative sampling locations (S1-S10) within the study area, and the results were displayed as a spatial distribution map to visualize the water quality status. The simulated data was evaluated by comparing it with the measured data, using various statistical measures such as the coefficient of determination ($R^2$), Nash-Sutcliffe efficiency (NSE), Root mean square error (RMSE), and Mean absolute error (MAE). In $R^2$ and NSE, values range from 0 to 1, where higher values closer to 1 indicate a stronger correlation between the simulated and measured data (Krause et al. 2005; McCuen et al. 2006). The RMSE and MAE values have a range from 0 to $\infty$, and lower values indicate better performance of the simulated model (Moriasi et al. 2012, 2007).

The formula used to calculate the indicators is as follows:

$$R^2 = \left( \frac{\sum_{i=1}^{n}(O_i - \overline{O})(P_i - \overline{P})}{\sqrt{\sum_{i=1}^{n}(O_i - \overline{O})^2} \sqrt{\sum_{i=1}^{n}(P_i - \overline{P})^2}} \right)^2 \quad ...(2)$$

$$NSE = 1 - \frac{\sum_{i=1}^{n}(O_i - P_i)^2}{\sum_{i=1}^{n}(O_i - \overline{O})^2} \quad ...(3)$$

$$RMSE = \sqrt{\frac{1}{n}\sum_{i=1}^{n}(O_i - P_i)^2} \quad ...(4)$$

$$MAE = \frac{1}{n}\sum_{i=1}^{n}|O_i - P_i| \quad ...(5)$$

Where $O_i$ is the observed data at the time i, $P_i$ is the simulated data at the time i, $\overline{O}$ is the mean value of the observed data and $\overline{P}$ is the mean value of the simulated data.

## RESULTS

### Calibration and Validation MIKE 11 Model

The HD module of the MIKE 11 model was calibrated by comparing its simulation results with measured water level data obtained at Tan An and Ben Luc hydrological stations during the dry season 2017. Fig. 3 shows the comparisons between the observed and simulated water levels at the hydrological stations. The simulated water levels closely resembled the measured water levels, showing similar magnitudes and tidal amplitudes. The evaluation metrics, including $R^2 = 0.990$, NSE = 0.990, RMSE = 0.002, and MAE = 0.002, indicate a high level of agreement between the simulated and measured values, falling within the optimal range of distribution (Table 2). To further confirm the effectiveness of the HD module, the validation procedures were performed with the observed water level data gathered in 2021. The results in Fig. 4 demonstrate a close agreement between the simulated and observed water levels, indicating falling within the optimal distribution range. At the Phu An station, the evaluation indices of $R^2 = 0.812$, RMSE = 0.811, NSE = 0.353, and MAE = 0.261 were obtained, while at the Nha Be station, the indices were $R^2 = 0.863$, RMSE = 0.863, NSE = 0.308, and MAE = 0.236 (Table 2). According to the calibration and validation results, the HD module of the MIKE 11 model was acceptable, and its model parameters can be utilized to simulate the pollutant propagation processes in the Vam Co River basin.

Calibrating the AD module is more challenging than the HD model due to saltwater intrusion in the Vam Co River basin, affected by factors like seasonal winds and salt control structures. The dense stream network makes it hard to determine suitable Advection-Dispersion coefficients for each section and channel leading to the basin, and the lack of continuous salinity data is also a concerning issue for

Table 2: Statistical evaluation of model performance on water level simulations.

| Station | $R^2$ | NSE | RMSE | MAE |
|---|---|---|---|---|
| I | Calibration | | | |
| Ben Luc | 0.990 | 0.990 | 0.002 | 0.002 |
| Tan An | 0.990 | 0.990 | 0.002 | 0.002 |
| II | Validation | | | |
| Nha Be | 0.863 | 0.863 | 0.308 | 0.236 |
| Phu An | 0.812 | 0.811 | 0.353 | 0.261 |
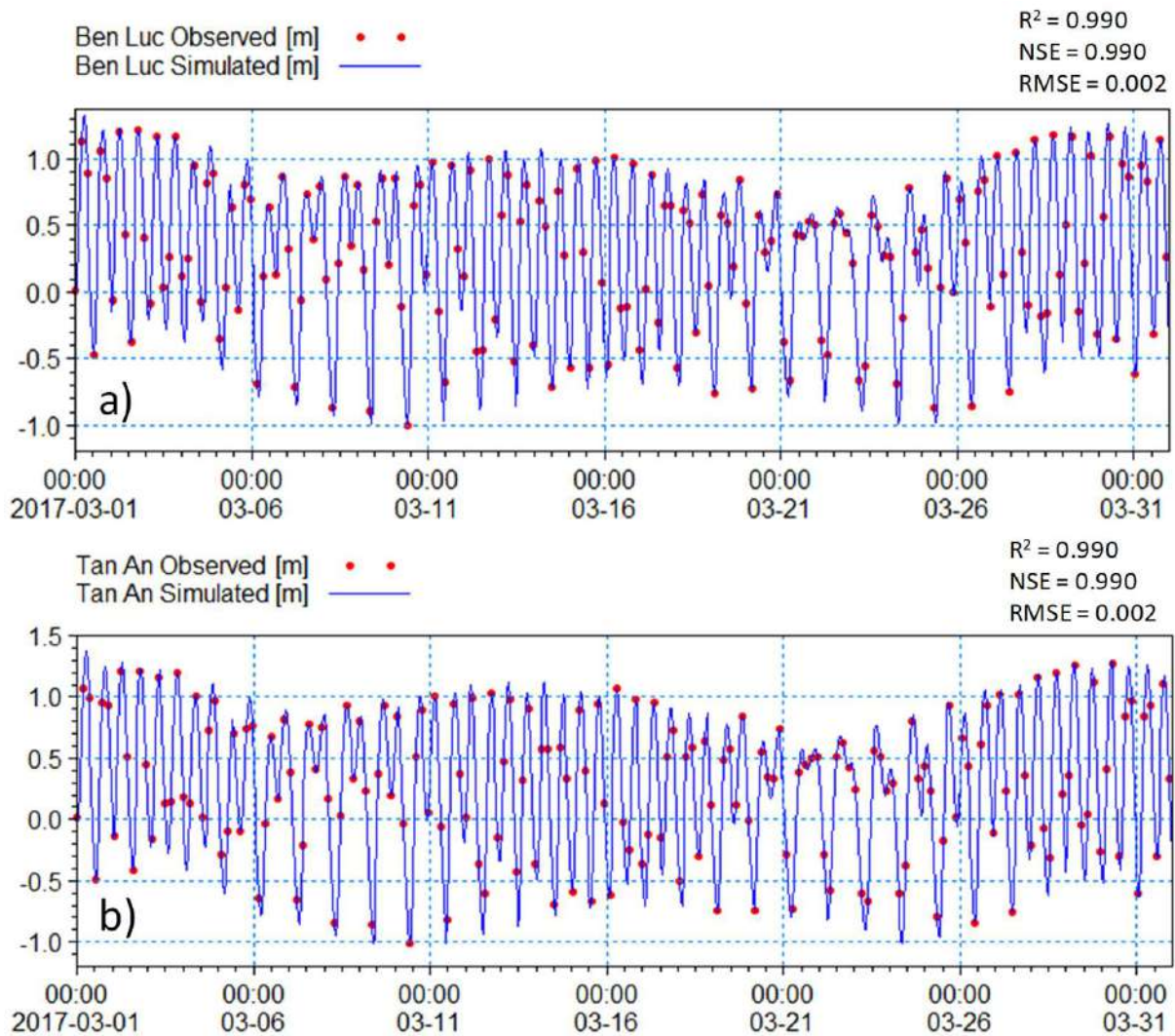
Fig. 3: Calibrated water level (a) at Ben Luc station and (b) at Tan An station.

model calibration and validation. Nonetheless, the simulated saltwater intrusion model is reasonably precise. MIKE 11 AD model was calibrated with measured salinity data between January and April 2017 at Cau Noi and Ben Luc stations. The calibration results of salinity daily at the Cau Noi and Ben Luc stations are shown in Fig. 5. The calibration results show a good agreement with the measured salinity data in terms of magnitude and tidal variation over time. The model validation results in February 2021 and March 2021 at Cau Noi and Ben Luc stations, respectively, are shown in Fig. 6. According to the comparison results between calculated and measured data, the MIKE 11 AD model was able to produce good simulations of the salinity concentration at Ben Luc and Cau Noi stations during the dry season of 2021. Therefore, the MIKE 11 model can be used to predict water quality during the dry season 2022.

**Evaluation of Water Quality Monitoring in 2018-2022**

The analysis results of water quality from 2018 to 2022 are presented in Fig. 7, with ten water quality indicators at the ten sampling locations. In Fig. 7, the results are compared to the permissible limit values of the indicators (QCVN 08-MT: 2015 / BTNMT column A1). Almost all locations had values of pH within the acceptable range ranging from 5.5 to 7.5. Excepting location S6, pH values were lower than the other sampling locations, indicating heavy iron pollution in the area, which has persisted for many years. $BOD_5$ values were higher than the allowable limit at all locations and fluctuated between 3-8 mg.$L^{-1}$. COD values showed a similar trend to $BOD_5$ measurements. Their values exceeded the permissible limit. Dissolved oxygen (DO) levels were lower than required, fluctuating between 2-3
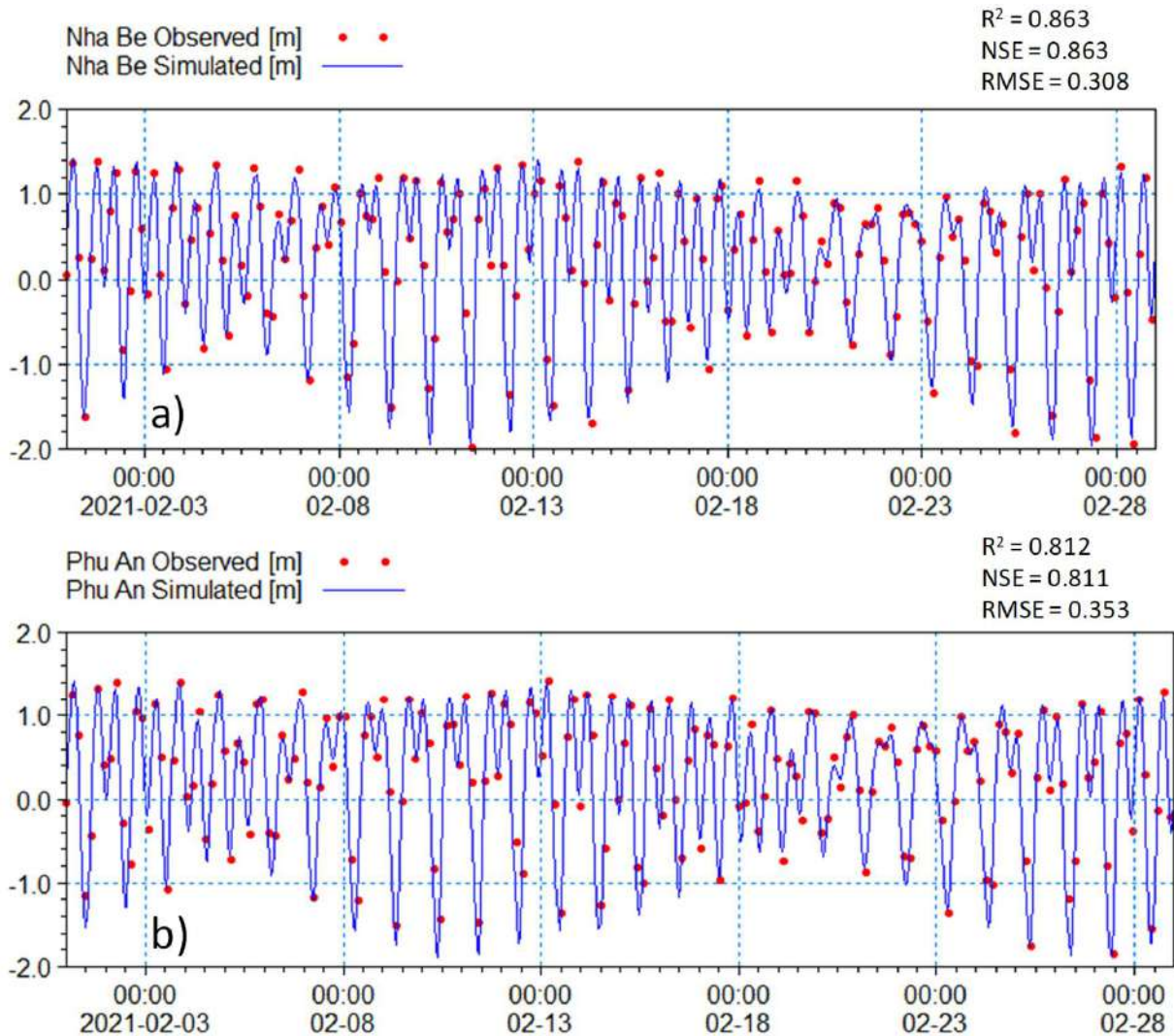
Fig. 4: Validated water level (a) at Nha Be station and (b) at Phu An station.

mg.L$^{-1}$, which can be attributed to low water exchange capacity during the dry season. TSS values showed significant variation between the minimum and maximum values but were lower than the allowable limit. Measured values of NH$_4$, NO$_2$, and PO$_4$ concentrations were lower than the permissible limit. However, the values of the Coliform concentrations were higher than the allowable limit. This indicated that the water at the study locations was unsuitable for aquaculture and crops. At location S7, the observed values of Coliform concentration greatly fluctuated, indicating long-term contamination by microorganisms in the area.

For salinity during the study period, the monitoring results in 2022, the highest salinity values at Cau Noi, Ben Luc, and Tan An stations were 14.3, 3.2, and 1.7 g.L$^{-1}$,

respectively. Their values were lower than the highest salinity in 2016, 2020, and 2021. The main reason is that 2016 and 2020 were two years of record drought in the Mekong Delta, Vietnam. In 2016, the highest salinity at 3 stations was 20.3, 12.8, and 11.8 g.L$^{-1}$, respectively, and in 2020, 21.6, 15.7, and 11.7 g.L$^{-1}$. For 2022, managers and people have been more proactive in preventing salinity due to the experience of 2 years of historical salinity drought. However, salinity in 2022 is still high, and the highest is at Cau Noi station, with a sanity value of 14.3 g.L$^{-1}$ (Fig. 8).

**Evaluating the Sampling Sites and Frequencies of the Water Quality Monitoring**

Table 3 presents an assessment of water quality based on the Water Quality Index (WQI) for 9 parameters (pH, BOD$_5$,
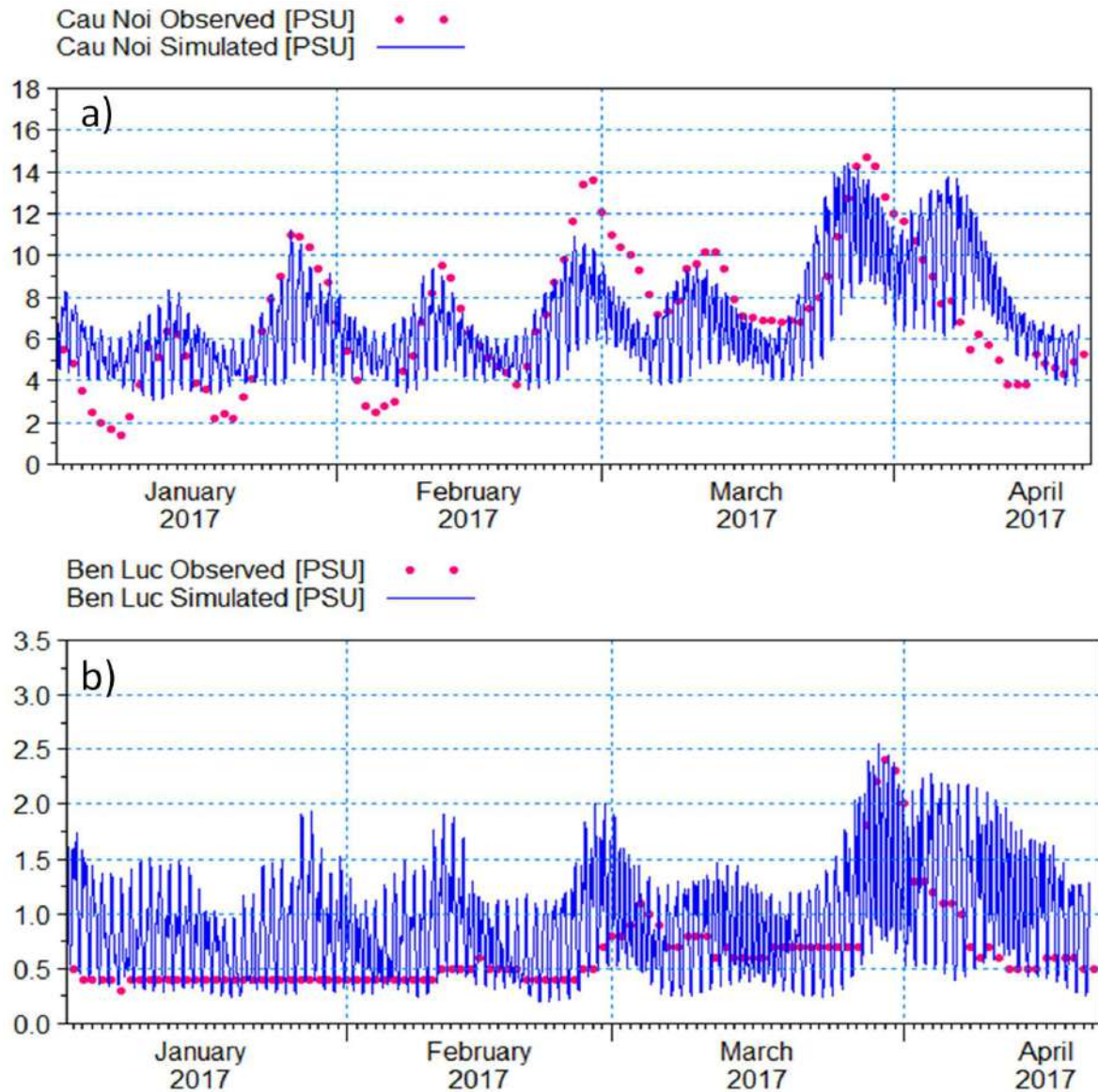
Fig. 5: Calibration results of salinity (a) at Cau Noi station and (b) at Ben Luc station.

COD, DO, TSS, NH$_4$, NO$_2$, NO$_3$, and PO$_4$) obtained from 12 sampling events conducted twice a month for 6 months from February to July 2022 at ten locations, with a total of 120 samples collected. The purpose of this assessment is to evaluate the water quality for production purposes and to monitor the production progress of the local area. At location S6, the WQI values were 25.0 for pH and NO$_3$, which has a significant impact on the total score of the WQI at this location. Additionally, the WQI values of DO at all monitoring sites range from 36.8 to 66.2 and significantly influence the total score of the WQI at all monitoring points.

According to the analysis of the WQI, it can be concluded that the water quality in the Vam Co River Basin is suitable for irrigation or other activities. Although some locations have pollution issues during the late dry and early rainy seasons, the water quality is suitable for irrigation purposes in other periods.

The water quality at location S6 was Very poor, indicated by red. The two locations (S3 and S4) had moderate water quality, and the remaining seven locations had good water quality, indicated by green. The map depicting the spatial distribution of WQI values in Fig.
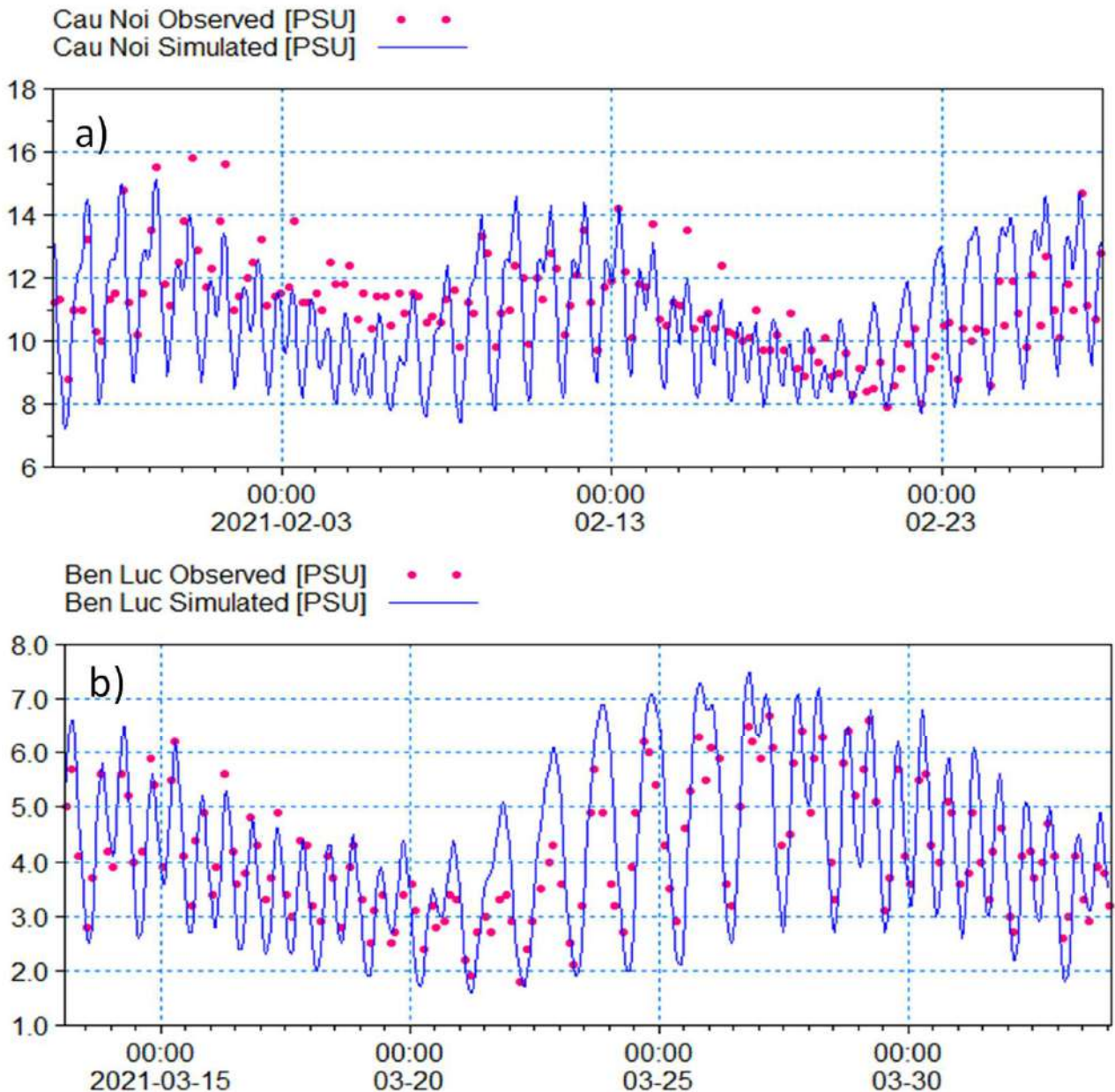
Fig. 6: Salinity validation results at (a) Cau Noi station and (b) Ben Luc station.

9 shows that Long An had the lowest water quality in 2022.

**Evaluation of Simulated Water Quality**

The study area is mainly affected by seawater intrusions from the East Sea. Thus, the salinity concentration has strongly impacted water quality in the Vam Co River Basin. Fig. 10a shows the comparison between simulated and measured values of water quality indicators, namely, salinity, $BOD_5$,

DO, and $NH_4$, at the sampling locations during the dry season of 2022. The simulated values of salinity fit well with the measured values with $R^2 = 0.961$, NSE = 0.956, RMSE = 0.023, and MAE = 0.017 (Table 4).

Fig. 10b and 10c show the comparisons between simulated and observed values of $BOD_5$ and DO, respectively. The simulated and observed values of $BOD_5$ have a good agreement with $R^2 = 0.919$, NSE = 0.911, RMSE = 0.266, and MAE = 0.170. Moreover, the simulated values of DO
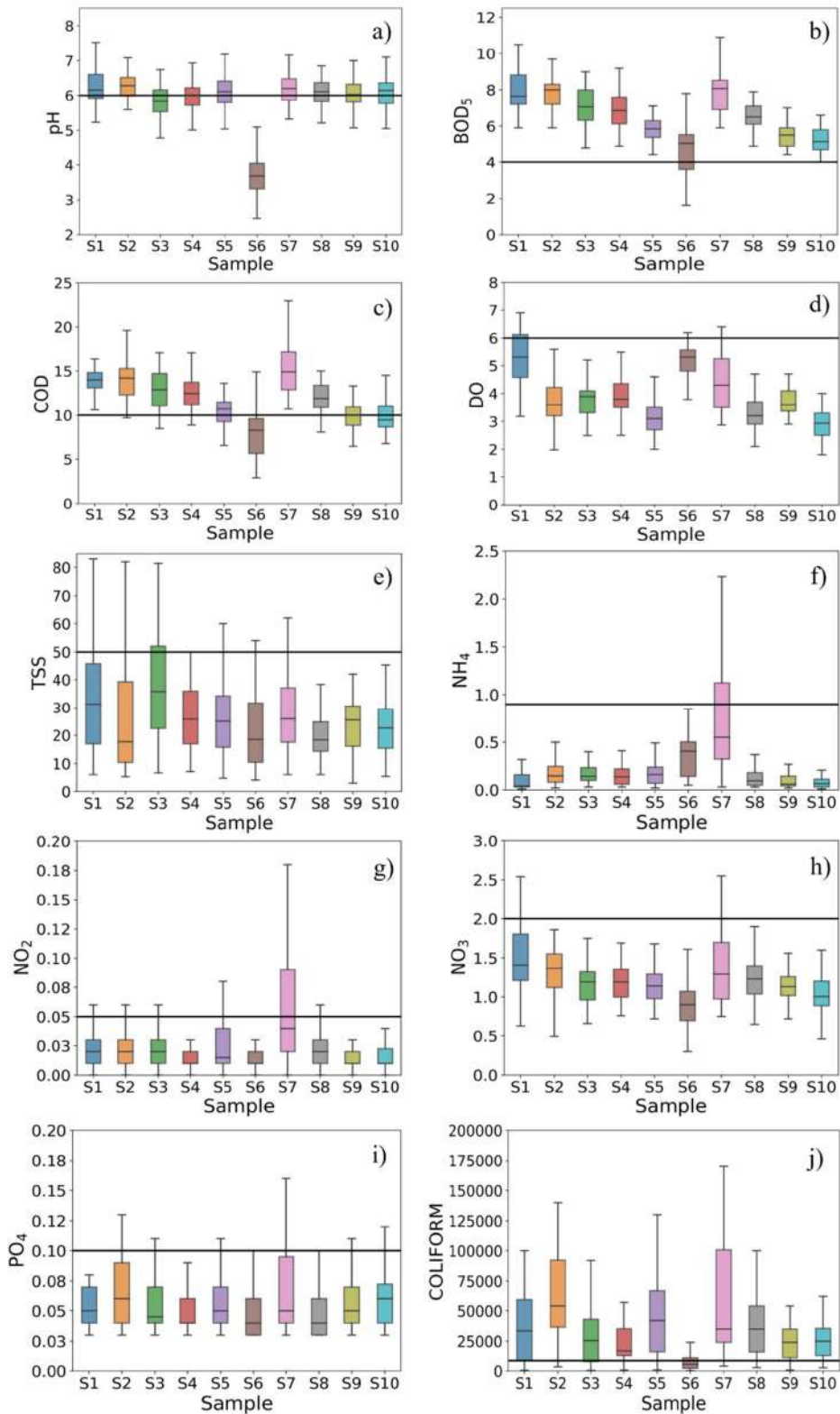
Fig. 7: Average water quality parameters were measured at ten sampling locations from February to July each year for 2018 to 2022.
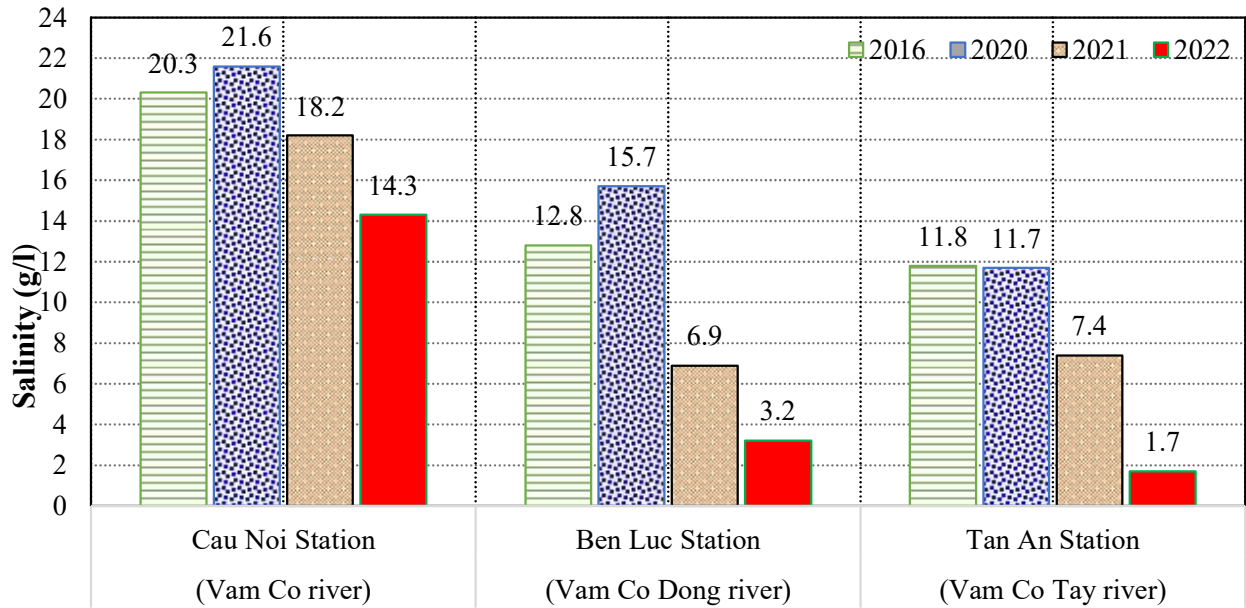
Fig. 8: The highest salinity in the dry season of 2016, 2020, 2021, and 2022

Table 3: The average WQI for each parameter from February to July 2022.

| Locations | WQI (pH) | WQI (BOD$_5$) | WQI (COD) | WQI (DO) | WQI (TSS) | WQI (NH$_4$) | WQI (NO$_2$) | WQI (NO$_3$) | WQI (PO$_4$) | WQI |
|-----------|----------|----------------|-----------|----------|-----------|---------------|---------------|---------------|---------------|------|
| S1 | 98.3 | 71.3 | 83.3 | 66.2 | 82.8 | 90.6 | 64.3 | 100.0 | 77.1 | 78.4 |
| S2 | 96.9 | 70.6 | 82.2 | 43.7 | 100.0 | 78.3 | 80.1 | 77.5 | 79.9 | 81.6 |
| S3 | 77.7 | 72.6 | 85.6 | 46.9 | 80.2 | 81.0 | 72.5 | 77.5 | 83.2 | 58.4 |
| S4 | 85.9 | 75.3 | 84.7 | 44.5 | 86.7 | 79.3 | 82.7 | 77.5 | 80.9 | 67.8 |
| S5 | 94.4 | 80.4 | 94.4 | 37.9 | 96.9 | 84.6 | 71.6 | 100.0 | 92.7 | 82.9 |
| S6 | 25.0 | 89.5 | 100.0 | 65.4 | 90.4 | 55.0 | 41.6 | 25.0 | 90.0 | 21.1 |
| S7 | 98.6 | 70.6 | 80.6 | 59.4 | 88.2 | 55.0 | 87.8 | 32.5 | 67.6 | 75.3 |
| S8 | 97.9 | 77.0 | 90.6 | 41.6 | 84.5 | 85.9 | 88.1 | 92.5 | 84.6 | 78.0 |
| S9 | 97.2 | 83.7 | 97.9 | 44.5 | 93.5 | 88.4 | 78.1 | 100.0 | 89.8 | 84.1 |
| S10 | 99.4 | 81.3 | 92.3 | 36.8 | 81.2 | 92.0 | 80.9 | 100.0 | 86.6 | 78.6 |

also fit well with observed values of DO with $R^2 = 0.995$, NSE = 0.995, RMSE = 0.054, and MAE = 0.029 (Table 4). The values of DO concentrations fluctuated because streamflow at different locations was varied.

Fig. 10d shows the comparison between the simulated and observed values of NH$_4$ at the different sampling locations in the Vam Co River Basin. The results show that the simulated values were significantly fitted to the observed values with $R^2 = 0.977$, NSE = 0.973, RMSE = 0.022, and MAE = 0.015 (Table 4). As can be seen in the figure, the simulated values of NH$_4$ were lower than the

measured ones. However, the overall results of the water quality modeling were acceptable. It can be said that the statistical indicators $R^2$, NSE, RMSE, and MAE are all within a good range, indicating a high degree of consistency and accuracy between the simulated data and the observed data.

Fig. 11 shows a spatial distribution of WQI of 2022 in the study area. The map clearly shows strong variations in the WQI values, indicating that the southern part of the Vam Co River basin has lower water quality than the northern part. According to WQI, the water quality in Thu Thua district (S3 and S4) was at a Moderate level. The water quality at
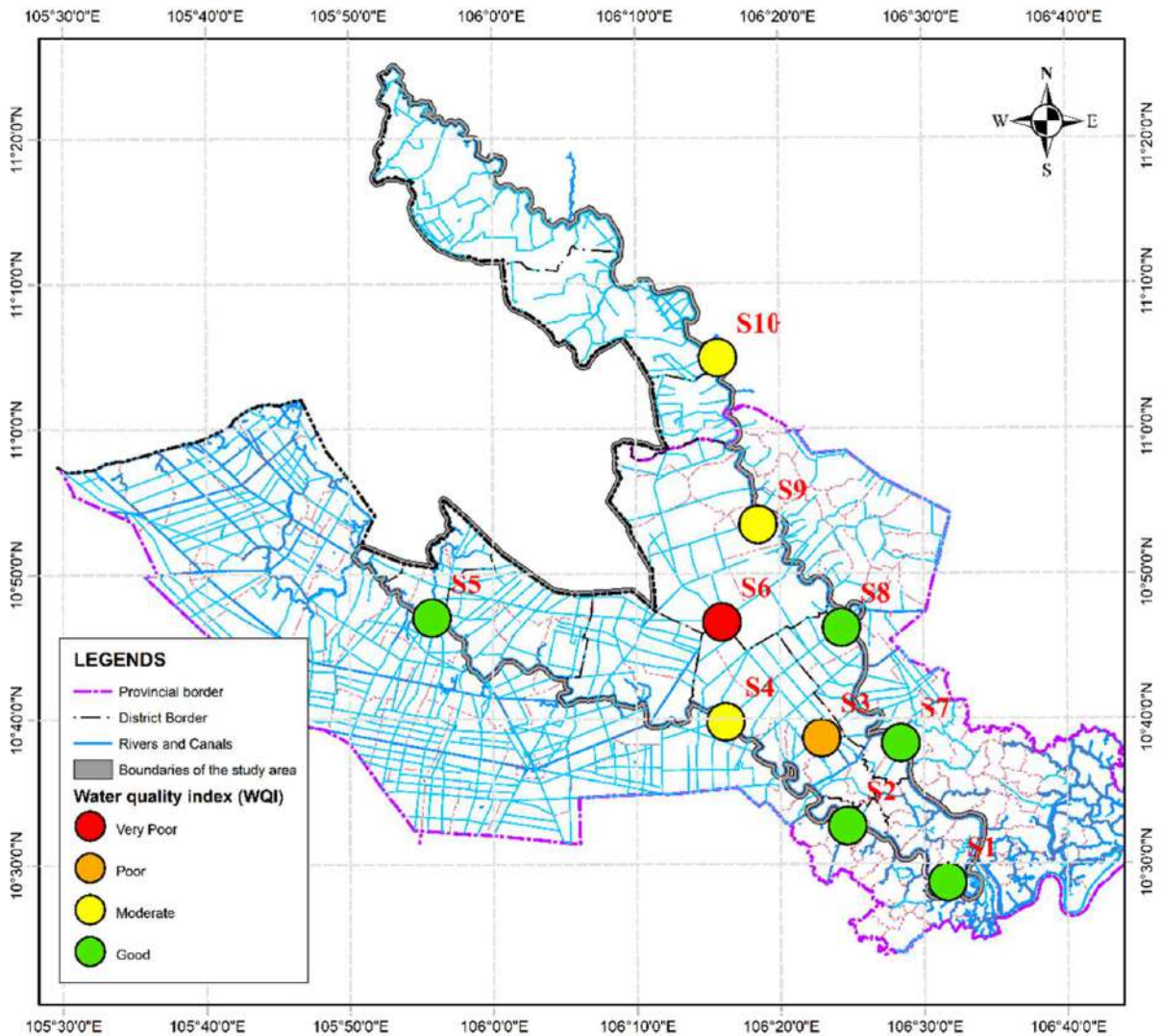
Fig. 9: Average WQI at ten sampling locations from February to July 2022.

the Moc Hoa (S5) was determined as Poor based on the WQI value, and the water quality at the Duc Hue (S6) districts of Long An province was Very poor. This is because economic and social activities in the area are intense. In addition, this area receives a significant amount of wastewater from industrial, agricultural, aquaculture, and domestic activities.

## DISCUSSION

Overall, the water quality analysis conducted between 2018 and 2022 on nine indicators shows that most of them are within limits allowed by QCVN 08-MT:2015/BTNMT, indicating stable and satisfactory water quality. However, COD, $BOD_5$, and Coliform still exceed the allowed limits due

Table 4: Statistical evaluation of model performance on water quality simulation 2022.

| Parameter | $R^2$ | NSE | RMSE | MAE |
|-----------|-------|-----|------|-----|
| Salinity | 0.961 | 0.956 | 0.023 | 0.017 |
| $BOD_5$ | 0.919 | 0.911 | 0.266 | 0.170 |
| DO | 0.995 | 0.995 | 0.054 | 0.029 |
| $NH_4$ | 0.977 | 0.973 | 0.022 | 0.015 |
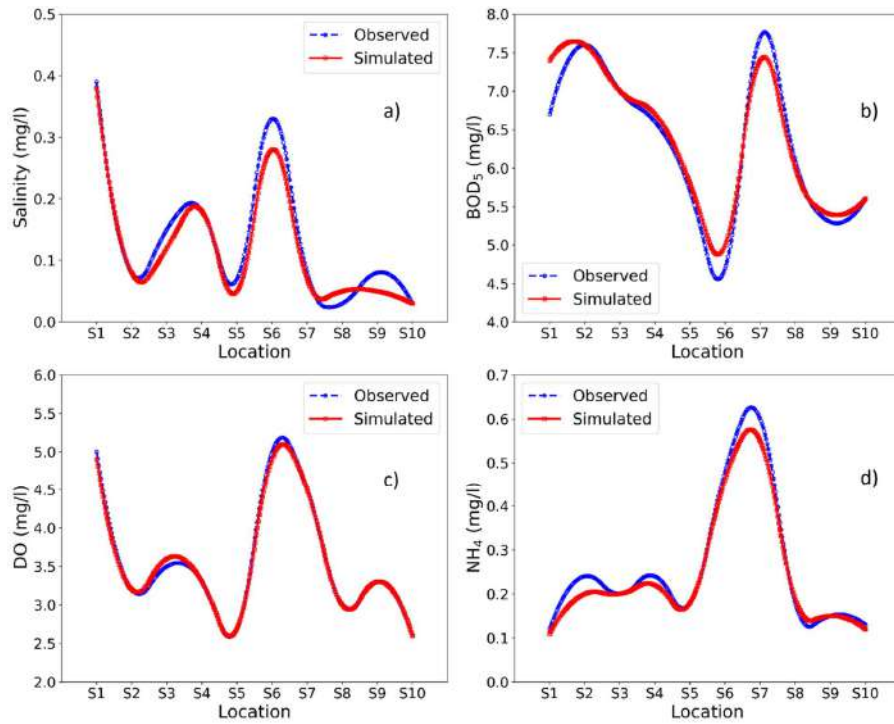
Fig. 10: Comparison of measured and forecasted water quality indicators (mg.L$^{-1}$).
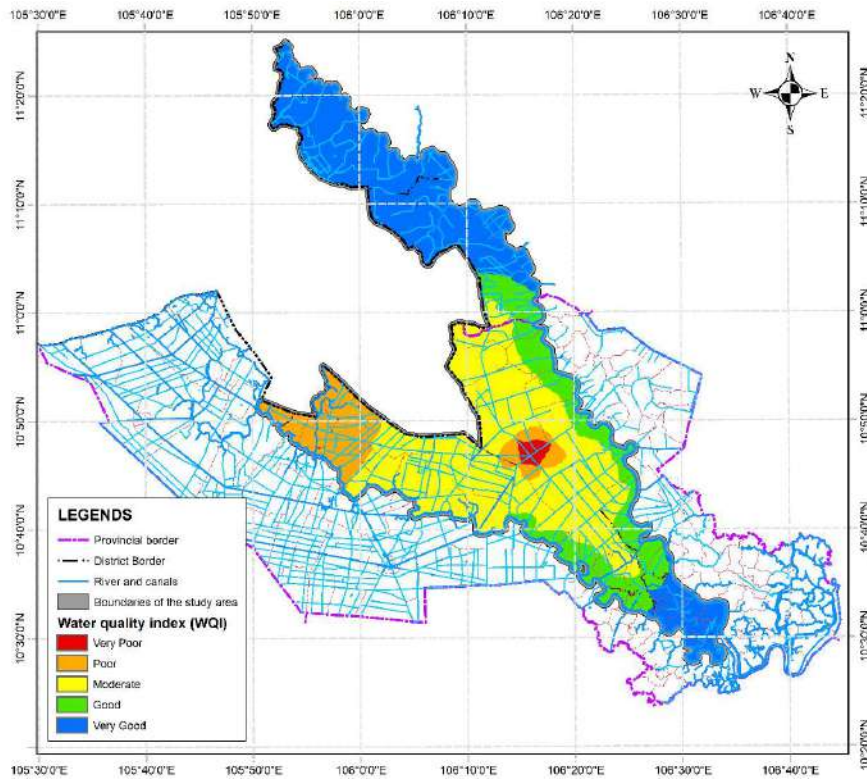


Fig. 11: Spatial distribution map of average WQI in 2022.

to mild organic and microbial contamination. This finding is corroborated by a study conducted by Nguyen and Huynh (2022), which yielded similar results. Table 3 shows that the water source in the irrigation system of the Vam Co River Basin is generally good for irrigation or other purposes. However, pollution still occurs in some locations, particularly in the late dry season and early rainy season. Earlier research conducted in the Mekong Delta also indicated that the water was contaminated with organic pollutants and exhibited fluctuations based on the season (Giao & Minh 2021, Ly et al. 2013, Nguyen 2020). Additionally, 2016 and 2020 were two years of record drought in the Mekong Delta, Vietnam (Loc et al. 2021, Park et al. 2022), so people have experienced and taken proactive preventive measures. Therefore, the salinity situation in 2022 was lower than in previous years.

The study also shows that the simulated results of water quality in 2022 are relatively good, with insignificant differences between predicted and measured salinity values. However, the predicted results were slightly lower than the measured results at some locations due to unpredictable weather conditions. The model is stable and produces results relatively close to reality based on seasonal weather conditions, simulating a similar trend to saltwater intrusion in the study area. For indicators such as $BOD_5$, DO, and $NH_4$, the simulated results differ from the actual measured values due to varying environmental factors in space and time, particularly at location S6, where there is a construction site. Abrupt fluctuations between measurement times were observed in DO and $NH_4$ values, possibly due to wastewater, dead vegetation, decomposed straw after rice harvest, mud on the bank, excess food settling on channels and rivers, and waste discharged at actual station locations. According to the research conducted by Viet and Kieu (2020), it has been evident since 2018 that the Vam Co Dong River, which passes through the Ben Luc District in Long An Province, has become incapable of sustaining acceptable levels of $BOD_5$ and DO. This is primarily attributed to the substantial discharge of untreated wastewater stemming from various sources such as industrial, agricultural, residential, and service activities. Besides that, the $NH_4$ value showed sudden changes due to production habits and excessive use of pesticides and chemical fertilizers, and this has also been demonstrated in the study of Dang et al. (2019).

However, many factors can affect the results, especially if the data sources are inaccurate or incomplete (Moges et al. 2021). Monitoring water quality every two weeks is insufficient to fully assess the fluctuations in water quality according to hydrological changes, leading to inaccurate predictions and inconsistency with reality (Asadollah et al. 2021, Rode & Suhr 2007). Pollution sources often occur locally, in areas with little flow due to drainage systems and the characteristics of the canal network and terrain. Investigating wastewater discharge into water sources still has many limitations due to difficulties accessing waste discharge units into the irrigation system, incomplete information, and scattered data from various sources.

## CONCLUSION

This study aims to evaluate the water quality status in the Vam Co River Basin by conducting sampling at ten stations during 2018-2021 and utilizing the WQI and the MIKE 11 model. At the station scale, the results of the sampling from 2018-2022 indicate that while the area has been desalinated, saltwater intrusion is still prevalent during the dry season. Besides that, indicators analysis is within acceptable limits, but some, such as $BOD_5$, COD, and Coliform, still exceed allowable limits. The WQI calculation for 2022 shows that pollution status ranges from Very poor to Moderate, concentrated mainly in Thu Thua (S3, S4), Moc Hoa (S5), and Duc Hue (S6) districts of Long An province due to active industry, agriculture, and high population density.

At the basin scale, the MIKE 11 model's simulated water quality results are relatively accurate, with little difference between the predicted and actual results. The southern part of the Vam Co River Basin has lower water quality than the northern part, with pollution mainly concentrated in Long An province. Establishing this hydraulic model is a significant step towards understanding and managing the impacts of pollution in the Vam Co River basin.

This study not only enriches the awareness of water quality in the Vam Co River Basin from 2018 to 2022 but highlights the feasibility of using the MIKE 11 model to simulate water quality and provides useful information for monitoring and forecasting water quality, controlling saltwater intrusion, and ensuring water supply for agriculture and people's livelihoods. With further refinement and improvement, this model has the potential to play a critical role in ensuring the long-term sustainability of the local environment and the communities that depend on it.

## DATA AVAILABILITY STATEMENT

The datasets generated during and/or analyzed during the current study are not publicly available but are available from the corresponding author at a reasonable request.

## REFERENCES

Abbaspour, K.C., Yang, J., Maximov, I., Siber, R., Bogner, K., Mieleitner, J., Zobrist, J. and Srinivasan, R. 2007. Modeling hydrology and water quality in the pre-alpine/alpine Thur watershed using SWAT. J. Hydrol., 333: 413–430.

Asadollah, S.B.H.S., Sharafati, A., Motta, D. and Yaseen, Z.M. 2021. River water quality index prediction and uncertainty analysis: A comparative study of machine learning models. J. Environ. Chem. Eng., 9: 104599.

Behmel, S., Damour, M., Ludwig, R. and Rodriguez, M.J. 2016. Water quality monitoring strategies—A review and future perspectives. Sci. Total Environ., 571: 1312–1329.

Bilgin, A. 2018. Evaluation of surface water quality using Canadian Council of Ministers of the Environment Water Quality Index (CCME WQI) method and discriminant analysis method: a case study Coruh River Basin. Environ. Monit. Assess., 190: 1-11.

CFO. 2022. Tide Table in 2022. Publishing House Natural Resources - Environment and Maps of Vietnam, Hanoi, Viet Nam.

Cheng, H. and Zhi, Z. 2015. Identification of the most efficient methods for improving water quality in rapidly urbanized areas using the Mike 11 modeling system. In the 2015 Seventh International Conference on Measuring Technology and Mechatronics Automation, June 13-14, 2015, Nanchang, China, IEEE, Manhattan, NY, US, pp. 545-548.

Codiga, D.L. 2011. Unified tidal analysis and prediction using the UTide Matlab functions. https://www.mathworks.com/matlabcentral/fileexchange/46523-utide-unified-tidal-analysis-and-prediction-functions

Dang, T.Q., Van, S.P., Dang, T.D. and Anh, D.T. 2019. Predicting water quality responses under climate change using coupled one-and two-dimensional models for Dong Nai River Basin. In Conference: 15th International Asian Urbanization Conference (AUC) At. Vietnamese-German University (VGU), November 27-30, 2019, Ho Chi Minh City, Vietnam, Springer, NY.

Dao, T.S. and Bui, T.N.P. 2016. Phytoplankton from Vam Co River in Southern Vietnam. Environ. Manag. Sustain. Dev., 5: 113-125.

Das, J. and Acharya, B.C. 2003. Hydrology and assessment of lotic water quality in Cuttack City, India. Water. Air. Soil Pollut., 150: 163-175.

Debele, B., Srinivasan, R. and Parlange, J.Y. 2008. Coupling upland watershed and downstream waterbody hydrodynamic and water quality models (SWAT and CE-QUAL-W2) for better water resources management in complex river basins. Environ. Model. Assess., 13: 135–153. https://doi.org/10.1007/s10666-006-9075-1

DHI. 2019. MIKE 21 - Tidal Analysis and Prediction Module, DHI, Denmark.

DHI. 2017. MIKE 11: A modeling system for Rivers and Channels. User Guide. DHI, Denmark

Duc, N.H., Avtar, R., Kumar, P. and Lan, P.P. 2021. Scenario-based numerical simulation to predict future water quality for developing robust water management plan: a case study from the Hau River, Vietnam. Mitig. Adapt. Strateg. Glob. Change, 26: 1-38.

Epelde, A.M., Cerro, I., Sánchez-Pérez, J.M., Sauvage, S., Srinivasan, R. and Antigüedad, I. 2015. Application of the SWAT model to assess the impact of changes in agricultural management practices on water quality. Hydrol. Sci. J., 60: 825-843.

Giao, N.T., Minh, V.Q. 2021. Evaluating surface water quality and water monitoring variables in Tien River, Vietnamese Mekong Delta. J. Teknol., 83: 29-36.

Girbaciu, A., Girbaciu, C., Petcovici, E. and Dodocioiu, A.M. 2015. Water quality modeling using Mike 11. Rev. Chim., 66: 1206-1211.

Gordillo, G., Morales-Hernández, M. and García-Navarro, P. 2020. Finite volume model for the simulation of 1D unsteady river flow and water quality based on the WASP. J. Hydroinform., 22: 327-345.

Havnø, K., Madsen, M.N. and Dørge, J. 1995. MIKE -11a generalized river modelling package. Comput. Model. Watershed Hydrol., 11: 733–782.

Huntjens, P., Kool, J., Lasage, R., Sprengers, C., Ottow, B. and Kerssens, P. 2013. Preferred Climate Change Adaptation Strategy for the Lower Vam Co River Basin, Viet Nam. Water Governance Center, Vietnam.

Krause, P., Boyle, D.P. and Bäse, F. 2005. Comparison of different efficiency criteria for hydrological model assessment. Adv. Geosci., 5: 89-97.

Lai, Y.C., Yang, C.P., Hsieh, C.Y., Wu, C.Y. and Kao, C.M. 2011. Evaluation of non-point source pollution and river water quality using a multimedia two-model system. J. Hydrol., 409: 583–595.

Li, X., Li, Y. and Li, G. 2020. A scientometric review of the research on the impacts of climate change on water quality during 1998–2018. Environ. Sci. Pollut. Res., 27: 14322-14341.

Liang, R., Schruff, T., Jia, X., Schüttrumpf, H. and Frings, R.M. 2015. Validation of a stochastic digital packing algorithm for porosity prediction in fluvial gravel deposits. Sediment. Geol., 329: 18-27.

Loc, H.H., Van Binh, D., Park, E., Shrestha, S., Dung, T.D., Son, V.H., Truc, N.H.T., Mai, N.P. and Seijger, C. 2021. Intensifying saline water intrusion and drought in the Mekong Delta: From physical evidence to policy outlooks. Sci. Total Environ., 757: 143919.

Loukas, A. 2010. Surface water quantity and quality assessment in Pinios River, Thessaly, Greece. Desalination, 250: 266-273.

Ly, K., Larsen, H. and Duyen, N. 2013. Lower Mekong Regional Water Quality Monitoring Report. Mekong River Commission, Vientiane, p. 205.

Mama, A.C., Bodo, W.K.A., Ghepdeu, G.F.Y., Ajonina, G.N. and Ndam, J.R.N. 2021. Understanding the seasonal and spatial variation of water quality parameters in mangrove estuary of the Nyong River using multivariate analysis (Cameroon Southern Atlantic Coast). Open J. Mar. Sci., 11: 103-128.

Mbuh, M.J., Mbih, R. and Wendi, C. 2019. Water quality modeling and sensitivity analysis using the Water Quality Analysis Simulation Program (WASP) in the Shenandoah River watershed. Phys. Geogr., 40: 127-148.

McCuen, R.H., Knight, Z. and Cutter, A.G. 2006. Evaluation of the Nash–Sutcliffe efficiency index. J. Hydrol. Eng., 11: 597-602.

MOC. 2006. TCXDVN 33:2006-Water Supply - Distribution System and Facilities Design Standard. Ministry of Construction, Hanoi, Vietnam.

Moges, E., Demissie, Y., Larsen, L., Yassin, F. 2021. Sources of hydrological model uncertainties and advances in their analysis. Water., 13: 28.

MONRE. 2019. Decision No. 1460/QD-TCMT-Technical Guidance on Calculation and Publication of Vietnam Water Quality Index (VN_WQI). Ministry of Natural Resources and Environment, Hanoi, Vietnam.

MONRE. 2015. Studying the impact of Mekong hydropower on the Mekong Delta (Project by HDR and DHI). Ministry of Natural Resources and Environment, Hanoi, Vietnam.

MONRE. 2011. National Technical Regulation on Industrial Wastewater. Minister of Natural Resources and Environment, Hanoi, Vietnam.

MONRE. 2008. National Technical Regulation on the Effluent of Aquatic Products Processing Industry. Ministry of Natural Resources and Environment, Hanoi, Vietnam.

Moriasi, D.N., Arnold, J.G., Van Liew, M.W., Bingner, R.L., Harmel, R.D. and Veith, T.L. 2007. Model evaluation guidelines for systematic quantification of accuracy in watershed simulations. Trans. ASABE, 50: 885-900.

Moriasi, D.N., Wilson, B.N., Douglas-Mankin, K.R., Arnold, J.G. and Gowda, PH 2012. Hydrologic and water quality models: Use, calibration, and validation. Trans. ASABE., 55: 1241-1247.

Nguyen, C.N. 2019. Applying Geostatistics to Predict Dissolvent Oxygen (DO) in Water on the Rivers in Ho Chi Minh City. In Context-Aware Systems and Applications, and Nature of Computation and Communication: 8th EAI International Conference, ICCASA 2019, 5th EAI International Conference, ICTCC 2019, My Tho City, Vietnam, November 28-29, 2019, Proceedings. Springer, NY, pp. 247-257.

Nguyen, G.T. 2020. Evaluating current water quality monitoring system on Hau River, Mekong Delta, Vietnam using multivariate statistical techniques. Appl. Environ. Res., 42: 14-25.

Nguyen, T.G. and Huynh, T.H.N. 2022. Assessment of surface water quality and monitoring in southern Vietnam using multicriteria statistical approaches. Sustain. Environ. Res., 32: 1-12.

Paliwal, R. and Patra, R.R. 2011. Applicability of MIKE 21 to assess temporal and spatial variation in water quality of an estuary under the impact of effluent from an industrial estate. Water Sci. Technol., 63: 1932-1943.

Park, E., Loc, H.H., Van Binh, D. and Kantoush, S. 2022. The worst 2020 saline water intrusion disaster of the past century in the Mekong Delta: Impacts, causes, and management implications. Ambio, 51: 691-699.

Qiu, Z. and Wang, L. 2014. Hydrological and water quality assessment in a suburban watershed with mixed land uses using the SWAT model. J. Hydrol. Eng., 19: 816-827.

Ramakrishnaiah, C.R., Sadashivaiah, C. and Ranganna, G. 2009. Assessment of water quality index for the groundwater in Tumkur Taluk, Karnataka State, India. E-J. Chem., 6: 523-530.

Rode, M. and Suhr, U. 2007. Uncertainties in selected river water quality data. Hydrol. Earth Syst. Sci., 11: 863-874.

Thanh Giao, N., Kim Anh, P. and Thi Hong Nhien, H. 2021. Spatiotemporal analysis of surface water quality in Dong Thap province, Vietnam using water quality index and statistical approaches. Water., 13: 336.

Thu Minh, H.V., Avtar, R., Kumar, P., Le, K.N., Kurasaki, M. and Ty, T.V. 2020. Impact of rice intensification and urbanization on surface water quality in An Giang using a statistical approach. Water, 12: 1710.

Thu Minh, H.V., Tri, V.P.D., Ut, V.N., Avtar, R., Kumar, P., Dang, T.T.T., Hoa, A.V., Ty, T.V. and Downes, N.K. 2022. A model-based approach for improving surface water quality management in aquaculture using MIKE 11: A case of the Long Xuyen Quadrangle, Mekong Delta, Vietnam. Water, 14: 412.

Tran, T.H. 2017. Application of MIKE 21 FM modeling to simulate the water quality at the coastal area Đinh Vu. VNUHCM J. Nat. Sci., 1: 282-292 (Vietnam).

Turner, S., Pangare, G. and Mather, R.J. 2009. Water governance: A situational analysis of Cambodia, Lao PDR and Viet Nam. Mekong Reg. Water Dial. Publ., 2: 47.

Tyagi, S., Sharma, B., Singh, P., Dobhal, R. 2013. Water quality assessment in terms of water quality index. Am. J. Water Resour., 1: 34-38.

Viet, L.B. and Kieu, P.T.M. 2020. Assessment of pollutant load on Vam Co Dong river in Ben Luc district, Long An province. Sci. J. Dong Nai Univ. 18: 145.

Wu, Z., Wang, X., Chen, Y., Cai, Y. and Deng, J. 2018. Assessing river water quality using water quality index in Lake Taihu Basin, China. Sci. Total Environ., 612: 914-922.

Yao, H., Qian, X., Yin, H., Gao, H. and Wang, Y. 2015. Regional risk assessment for point source pollution based on a water quality model of the Taipu River, China. Risk Anal., 35: 265-277.

# Role of Human Capital Accumulation in the Adoption of Sustainable Technology: An Overlapping Generations Model with Natural Resource Degradation

**Shilpy Verma*† and Md. Raghib Nadeem**** (iD)

*Amity School of Economics, Amity University, Noida Campus, Uttar Pradesh, India
**Department of Economics, Galgotias University, Greater Noida, Uttar Pradesh, India
†Corresponding author: S. Verma; shilpyverma1@gmail.com

## ABSTRACT

We develop an economic model to derive the conditions under which individuals will invest in human capital and move on to adopt sustainable technology instead of natural resource-intensive technology. For this purpose, we extend the overlapping generation model developed by Ikefuji & Horii as our analytical framework. Unlike Ikefuji & Horii who developed an overlapping generation model (OLG) in the context of local pollution, the authors adopted it in the context of renewable natural resources. To do this, we have introduced the production sector that relies on natural resource-intensive technology. This research extends beyond the Ikefuji & Horii model by assuming that an individual derives utility by investing in his child's education apart from utility derived from consumption when young and adult. Human capital accumulation enables individuals to participate in human capital-intensive production, which produces output through sustainable production technology. As the main result of our theoretical analysis, we find that more educated individual is less dependent on the natural resource endowment for earning their income. We also find that sustainable consumption growth requires that individuals assign a certain positive weight to investment in their child's education. A long-run steady-state equilibrium level of human capital accumulation is higher and higher than the weight assigned by the parents to the child's education. In this overlapping generation's economy, sustainable consumption growth requires that individuals assign a certain weight or give some importance to human capital accumulation. This follows from the fact that the long-run steady-state value of the income earned by an individual depends positively on the expenditure on education.

## INTRODUCTION

The human capital theory by Olaniyan & Okemakinde (2008) has emphasized how education raises efficiency as well as productivity of laborers by augmenting the cognitive skills of human ability. They argue that the productivity level of better-educated individuals is higher, a fact that will facilitate technological progress. According to Wells 1972, educated people are more willing to adopt innovative technology than less educated ones. Human capital accumulation via education facilitates the adoption and development of sustainable technologies that can reduce the extent of resource degradation. Human capital is a composite of skills accumulated by workers through learning by doing or education (Becker 1964).

The pessimistic Malthusian view that natural resource scarcity would put an end to economic growth was countered by neoclassical economics in the 1970s. In a neoclassical growth framework, natural resources are an indispensable input in production, and the consequences are in contrast with the pessimistic Malthusian predictions. However, the application of the neoclassical growth theory to resource depletion problems dismisses the possibility that natural resource scarcity can significantly constrain economic growth (Nordhaus 1992). Despite the natural resource scarcity, economies may grow if there is continuous exogenous technical progress (Dasgupta & Heal 1974, Solow 1974, Stiglitz 1974). According to this theory, technical change and substitution among production inputs that permit the replacement of depleted resources by human-made capital (people, factories, machines, etc.) or by more abundant substitutes can effectively disassociate economic growth from natural resource depletion. According to Stiglitz (1974), increasing returns to scale, technical progress, and substitution of scarce inputs by abundant inputs are some of the ways to counteract the negative effects on economic growth of natural resource scarcity.

Gylfason (2001) argued that neglecting the role of human capital can result in poor economic performance and natural resource degradation in countries rich in natural resources. This happensbecause they assumed that natural resources and education could be substituted for each other. Hence, human capital accumulation can sustain growth and development as well as mitigate natural resource degradation (Bravo-Ortega & De Gregorio 2005, Gylfason et al. 1999, Papyrakis & Gerlagh 2004).

Human capital plays a critical role in promoting sustainable growth in the presence of natural resources (Goderis & Malone 2011). In such cases, human capital is assumed to embody technological progress in workers, while natural resource stock remains a purely quantitative input.

Hence, a comprehensive analysis must be carried out to evaluate the role played by human capital in sustaining economic growth or in the adoption of more sustainable technology. Moreover, we will explore whether the investment in human capital accumulation could lead to the adoption of sustainable production technology. Since sustainable technologies are less reliant on natural resources and use human capital intensively, they have smaller impacts on natural resource degradation than technologies that use natural resources intensively. Many empirical studies support such kind of specifications. The increase in the net enrolment ratio of primary schools leads to a decrease in the annual deforestation rate (Ikefuji & Horrii 2007). The increase in human capital by way of an increase in the education level of the individual greatly encourages the use of sustainable farming practices. It reduces the likelihood of felling trees (Swinton & Quitroz 2003). Higher literacy rates improve the quality of the environment, especially in low-income countries (Torras & Boyce 1998). As the health of the individual is negatively affected by environmental degradation, improvement in environmentalquality is posited to have a positive effect on human capital accumulation (Chakrobarty & Gupta 2014). Drawing on this body of literature, this study develops and solves an analytical model of a stylized economy to examine the role of human capital in natural resource management and the adoption of sustainable technology of production.

To analyze the role of human capital accumulation in the adoption of sustainable technology of production, we need a baseline analytical model to start with. For this purpose, we extend the model developed by Ikefuji & Horii (2014) for our analytical framework. They derive the conditions under which the economy could adopt sustainable technology that helps in escaping the 'poverty-environment trap.'

This research extends beyond Ikefuji & Horii (2014) to examine the role of human capital by assuming that an individual derives utility by investing in his child's education apart from utility from consumption when young and adult. Unlike Ikefuji & Horii (2014), who developed an overlapping generation model (OLG) in the context of local pollution, we have adapted it in the context of renewable natural resources. Our focus is entirely on the extractive use of resources for production purposes, and we neglect amenity services provided by the resources.To do this, we have introduced the production sector that relies on natural resource-intensive technology. In an OLG economy, Gerlagh & Keyzer (2001) have examined the possibility of a positive, balanced growth path with natural resources, which have amenity value but are not used as an essential input into the production sector. Unlike Gerlagh & Keyzer (2001), we have incorporated natural resources as an essential input in the natural resource-intensive production sector.

The livelihood of the 'asset less' poor is dependent on the exploitation of their surrounding localnatural resources, without the availability of any alternative livelihood earning opportunities (Barrett et al. 2001). Households having a greater number of uneducated members are more reliant on unskilled paid work to obtain most of their income (Banerjee & Duflo 2007). Underinvestment in human capital is a persistent problem for low-income households, particularly in fragile environments (Barbier 2010). Our analysis rests on this premise.

In our model, all individuals are assumed to live for a two-time period. In period t-1, she/he is young, and in period t, she/he becomes an adult. At the end of period t, an adult gets old and exits the system. We assume that participation in employment activity that does not exploit natural resources requires individuals to invest in human capital, and only through human capital accumulation can individuals participate in sustainable or human capital-intensive production activity. The young agent is endowed with a certain time or labor endowment, which, when combined with theeducational expenditure fully funded by their parents, leads to the accumulation/acquisition of human capital. We further assume that each young agent receives a transfer of income from their parents, which is utilized for consumption when young and to acquire ownership rights for natural resources from the current generation of adult agents. In this setting, the initial endowment of natural resource stock belongs to the adult agents of the first generation, and they sell the natural resourceto their successor generation to provide for adult age.

Further, individuals are not concerned about the welfare of future generations. As a result, in each period, only the working generation owns the natural resource stock. This framework is borrowed from Agnani et al. (2005).

In adult age, each individual can earn their livelihood by participating in two different production activities that rely on two distinct types of technologies. One is human capital-intensive (HCI) technology, which uses human capital and unskilled labor as production inputs. The other technology is called natural resource-intensive technology (NRI), which depends on unskilled labor and exploitation of a natural resource or agricultural land, or an easily accessible common property resource. The adult agent uses their total wage income and income received from selling their natural resource endowment for consumption, transfer to their child, and fund expenditure on their child's/young agent's education.

The framework stated above helps us characterize the conditions under which the household will be caught in the low human capital accumulation and natural resource degradation trap or the conditions that will help escape this trap through human capital accumulation via investment in human capital. Specifically, the scope of the study is extended to derive the conditions under which individuals will invest in human capital accumulation and adopt sustainable or human capital-intensive technology instead of natural resource-intensive technology, and by utilizing this framework, we will examine the likely desirable policies for sustainable economic growth.

As the key results of our theoretical analyses, we find that as the investment in a child's education by the parents increases, the total earned income of the individual increases, but the income earned from the natural resource stock endowment declines. A more educated individual is less dependent on natural resources for earning their income. If the investment in education is zero, then the individual has no option but to rely completely on natural resource-intensive technology for earning their livelihood. We also find that as the investment in education increases, the output produced from sustainable technology rises, and the output produced from natural resource-intensive technology falls. However, as the extraction of natural resource stock increases, the aggregate output produced from sustainable technology decreases, and the aggregate output produced from natural resource-intensive technology increases. We also find that sustainable consumption growth requires that individuals assign a certain weight to investment in their child's education. A long-run steady-state equilibrium level of the human capital accumulation is higher, the larger the weight assigned by the parent to the child's education.

The steady-state value of income earned by an individual depends on the investment in education made by their parents. The long-run steady-state value of the income earned by an individual depends positively on the expenditure on education, the productivity of human capital-intensive technology, unskilled labor, the share of human capital in human capital-intensive output, and the productivity of human capital accumulation. The steady-state value of natural resource stock is higher when an individual assigns higher importance to education investment relative to consumption. The steady-state value of natural resource stock is higher, higher is the weight assigned by an adult agent on the investment in their child's education, higher is the productivity of human capital-intensive technology, higher is the share of human capital relative to the share of unskilled labor in human capital-intensive output lowers the price of natural resource-intensive sector output and lowers the productivity of natural resource-intensive technology.

In this overlapping generation's economy, sustainable consumption growth requires that individuals assign a certain positive weight or give some importance to human capital accumulation. This follows from the fact that the long-run steady-state value of the income earned by an individual depends positively on the expenditure on education. We now proceed with a description of the analytical framework.

## THEORETICAL MODEL FRAMEWORK

In this section, we develop the theoretical/analytical model of human capital accumulation and natural resource degradation to explain the mechanisms that lead to the adoption of sustainable technology. We have considered an overlapping generation model (OLG), where each individual is alive for two time periods: t-1 and t. Individuals are born in period t-1 and are called young agents, and in period t, individuals become older and are called adult agents. We assume that the population of each generation does not grow since each adult agent is presumed to bear a single child. Thus, the total population is stationary, and it is normalized to one.

During period t-1, young agents do not work, but they spend on consumption and buy the ownership right of a natural resource out of the transfer that they receive from their parents. When young, the individual benefits from their parent's spending on their education and builds on their human capital (through education acquisition). The young agents are endowed with a certain ability to learn, of which they devote a fraction towards learning or acquiring education, which, in turn, leads to human capital accumulation. This framework is borrowed from Ikefuji & Horii (2014). We, therefore, assume that there is no work undertaken during young age or childhood. We also assume that each adult agent in period t can earn their livelihood by participating in two different kinds of production activities that distinctly employ two different technologies: (i) production of output based on unskilled labor, such as exploitation of natural

resources or agriculture land or easily accessible common property resources, (ii) production of output that depends on skilled labor, i.e., human capital. During period t, the adult agent uses their total wage income earned from unskilled labor and skilled labor or human capital that they supply to firms and income received from selling their natural resource endowment for consumption, transfer to their child, and to fund their child's/young's agent education for human capital accumulation which will benefit to their children as they become adults in the next period of their life.

## Individual Preferences, Budget Constraints, and Labor Allocation

We assume that all the agents are identical and have rational expectations except for their age or cohort. Every period consists of individuals of two cohorts: young and adult agents. There is no population growth, and we normalize the number of agents of each generation or cohort to one. Every generation consists of $L_{t-1}$ young agents or families who live for two periods. Since the population is homogenous and normalized to unity such that, $C_{t-1}^Y = c_{t-1}^Y$, $C_t^A = c_t^A$, and aggregate consumption in each period is simply $C_t = C_{t-1}^Y + C_t^A$, $V_t = v_t$ and $L_{t-1} = l_{t-1} = l$, it also holds for other variables. More formally, individuals born in period t-1 care about consumption when young, $C_{t-1}^Y$, consumption when adult, $C_t^A$ and the amount spent or invested in a child's education in period $t$, $V_t$. We, therefore, assume that the parents enjoy giving a transfer to their children for education acquisition, as in Glomm & Ravikumar (1992). However, this bequest motive is not analyzed explicitly by us. Accordingly, the utility of an individual is represented by the following additively separable utility function:

$$U_t = lnC_{t-1}^Y + \beta lnC_t^A + (1-\beta)lnV_t. \qquad …(1)$$

Here, $0 < \beta < 1$ is the parameter that measures the weight assigned by the young agent to the future level of consumption $(C_t^A)$ as opposed to the investment that they make in their child's education $(V_t)$.

Similarly, to Ikefuji & Horii (2014), the human capital accumulation (due to education acquisition) by young agents in period $t$ is defined by

$$H_t = \psi V_{t-1}L_{t-1} = \psi V_{t-1}l. \qquad …(2)$$

Here, $\psi > 0$ is the productivity parameter associated with human capital accumulation.

Each young born in period $t$-1 is endowed with a certain endowment of labor $(L_{t-1} = l)$, which when combined with educational expenditure $(V_{t-1})$, is fully funded by their parent's or adult agents of period t-1 helps build their human capital $(H_t)$, which becomes available to the young agents in the next period of a lifetime, that is, in adult age. In period

t, the endowment of labor of the adult agents $(L_t)$ remains the same as their endowment of labor when she/he was young $(L_{t-1})$, that is, $L_{t-1} = L_t$, which, in turn, is constant $l$. Investment in the young agent's human capital by the adult agent in period t-1 can raise the young agent's productivity. It is often predicted by human capital theory that investment in education has a positive impact on cognitive and other skills. These, in turn, supplement the productivity of labor (Becker 1964, Schultz 1961). The adult agents of generation t-1 are endowed with a unit time endowment, which she/he devotes entirely to work and earns income $(Y_{t-1})$; a part of this income, that is, $\mathcal{E} Y_{t-1}$, is transferred to their child or young agent of period t-1.

We assume that the initial endowment of natural resource stock belongs to the adult agents of period t-1 and aggregate economy-wide endowment is distributed equally among all the adult agents of the time t-1. These adult agents sell their natural resources to their successors, that is, young agents of period t-1, to provide for their spending, which then sells the stock to the firms in period t. This framework is borrowed from Agnani et al. (2005). Further, we assume that individuals cannot borrow or lend as they lack access to a well-functioning credit market, and they do not work when young. In period $t$-1, each young agent receives a transfer of income from his/her parents $(\mathcal{E} Y_{t-1})$ that they utilize for consumption when young $(C^Y)$ and to acquire ownership right for natural resources from first-generation adult agents $(p_{t-1}N_{t-1})$. The budget constraint faced by young agents is given as follows:

$$C_{t-1}^Y + p_{t-1}N_{t-1} = \mathcal{E}Y_{t-1} \qquad …(3)$$

Where $\mathcal{E}$ is the exogenously assumed fraction of income earned by an adult agent of period t-1 that is transferred to young agents who are born in period t-1, $N_{t-1}$ is the endowment of the natural resource that young agent purchases from adults of generation t-1, $p_{t-1}$ is the price of the ownership right of one unit of the natural resource in terms of the consumption good.

Accordingly, in period $t$, each adult earns aggregate wage income $(Y_t)$ from their unskilled labor stock (equal to $w_{l_t} l$), skilled labor stock, or human capital stock (amounting to $w_{h_t}H_t$) and receives income from selling natural resources to the next generation young agent $(p_tN_{t-1})$. Where $w_{l_t}$ and $w_{h_t}$ are wages of unskilled and skilled labor/human capital, and $w_{l_t} < w_{h_t}$. The individual will earn $w_{l_t}$ if he does not receive education, that is, $V_{t-1}$=0. But if he receives an education, then he can earn wages from unskilled labor as well as skilled labor/human capital. The adult agent uses their total wage income and income received from selling their natural resource endowment for consumption $(C^A)$, transfer to their child $(\mathcal{E} Y_t)$, and to fund expenditure on investment in child's/young's education $(V_t)$. Thus, the budget constraint

during the second periodof an individual's life (when adult) can be written as:

$$C_t^A + V_t + \mathcal{E}Y_t = Y_t + p_t N_{t-1} \qquad \ldots(4)$$

Where $\mathcal{E}$ is the fraction of wage income earned by each adult agent in period t that is transferred totheir young, $Y_t$ is the total wage income earned by adults, $p_t$ is the unit price at which natural resource stock is sold to firms by an adult agent in period t.

The total wage income earned by an adult in period t will be as follows:

$$Y_t = w_{h_t} H_t + w_{l_t} s_t l + w_{l_t}(1 - s_t)l = w_{h_t} H_t + w_{l_t} l \qquad \ldots(5)$$

This can be explained as follows. The adult agent earns income by participating in two types of economic activities: (i) a production activity that depends on human capital-intensive technology, for which she/he earns a wage rate per unit of human capital, $w_{h_t}$, and wage rate per unit of unskilled labor, $w_{l_t}$ and where $s_t$ is the fraction of unskilled labor devoted to human capital intensive output production, and (ii) another production activity that relies on natural resources that can be exploited at zero economic cost for which they earn unskilled labor wage income (offraction, $(1 - s_t)l$), where $(1 - s_t)$ is the fraction of unskilled labor devoted to natural resource.

Intensive output production. The assumption of zero economic cost of extraction of natural resources offers mathematical tractability. A similar assumption is used by Agnani et al. (2005). Here $l$ is labor input per unit of output as the population of each generation is normalized to one ($l_t = L_t = l$).

**Production Structure and Firm's Behavior**

As mentioned earlier, there exist $N$ numbers of competitive firms producing a homogenous outputby using two different types of technologies. One type of technology is human capital-intensive, which produces output by using skilled labor/human capital and unskilled labor as inputs. There exist $N^H$ firms in this sector. We assume a Cobb-Douglas form production function wherein inputscan be substituted foreach other to produce the same output but cannot be substituted at a constantrate. This type of production function assumes constant returns to scale with respect to all the inputs for a given technology level. This production technology does not utilize natural resources, and in this sense, it is taken to be pollution-free or clean technology (Ikefuji & Horii 2014). Theaggregate output of all the $N^H$ firms producing output from human capital-intensive technology can be written as:

$$Y_t^H = N^H A^H (H^\theta)(s_t l)^{1-\theta} \qquad \ldots(6)$$

Where $A^H > 0$ is the constant measuring the productivity level of the human capital-intensive technology, $s_t$ is the fraction of the adult's stock of unskilled labor ($l$) devoted to the productionof output through human capital-intensive technology.

The other available technology of production is natural resource-intensive, which uses unskilled labor to produce goods and relies more heavily on the extraction of natural resources, $X_t$. There exist $N^R$ firms in this sector. The production function, in this case, is similar to the one given in Ikefuji & Horri's (2014) framework. Still, here, we have added the extracted natural resource stock, $X_t$, usedin production. The aggregate output of all the $N^R$ firms produced from natural resource-intensive technology in per-worker terms is expressed as:

$$Y_t^R = N^R A^R (1 - s_t) l X_t \qquad \ldots(7)$$

Where $A^R > 0$ is the constant that measures the productivity or technology level of the natural resource-intensive technology, $1 - s_t$ is the fraction of unskilled labor of an adult agent devoted to production using natural resource-degrading technology, and $X_t$ is the stock of natural resource used for production in this sector. The firm's exploitation of natural resources involves price $p_t$, and the utilization of natural resources as an input into the production depletes the stock of natural resources. Thus, the production technology in this sector is dirty.

Finally, the evolution of natural resource stock is determined by the amount of output produced from natural resource-intensive technology. This resource stock can regenerate or grow over time.

**Natural Resource Dynamics**

The natural resource stock in our model is renewable. It is used as an input in the production of natural resource-intensive output. In period t-1, the adult agents own the natural resource stock, which they sell to the young agents. These young agents are adults in period t, and they sell this stock to firms, which then decide on how much of that resource to extract and use as an input in the production of the natural resource-intensive output. The extraction of resources is costless, andthe decision on how much to extract is not modeled explicitly.

At the beginning of period t-1, the economy is initially endowed with a positive amount of the natural resource, $N_{t-1}$, which belongs to the adult agents of the first generation. In period t, the total stock of the natural resource, $N_t$, is determined by deducting resources used for current production, $X_t$, from available previous resource stock, $N_t$.

The equation governing the dynamics of natural resource stock is given by

$$N_t = (1 + \delta)N_{t-1} - \eta\, X_t \qquad \dots(8)$$

Where $0 < \delta < 1$ is the parameter referring to the natural regeneration capacity of resources and $\eta > 0$ measures the extent of natural resource degradation due to the extraction of natural resources for production in the natural-resource-intensive sector. With this apparatus, we now solve for the market equilibrium.

## SOLVING FOR THE MARKET EQUILIBRIUM

### The Firm's Optimization in the Two Production Sectors

Each firm in the human capital-intensive (HCI) sector produces the output by using human capital/skilled labor and unskilled labor by employing HCI technology that is given by the production function in equation (7). All firms in this sector share the same production technology. We assume that the human capital-intensive (HCI) sector is the numeraire, such that $p^H = 1$. In a perfectly competitive framework, the profit-maximizing firm chooses human capital/skilled labor $(H_t)$ and unskilled labor $(s_t l)$ while taking the human capital/skilled labor $(H_t)$ and unskilled labor $(s_t l)$ wage rates, $w_{h_t}$, and $w_{l_t}$ as given, that is,

$$\max_{H_t s_t l} \pi^H = A^H(H_t^\theta)(s_t l)^{1-\theta} - w_h H_t - w_l s_t l$$

The first-order conditions of the representative firm's profit maximization problem are given, in per-worker terms, by:

$$w_{h_t} = \theta A^H H_t^{\theta-1} (s_t l)^{1-\theta} ; \qquad \dots(9)$$

$$w_{l_t} = \frac{(1-\theta)A^H h_t^\theta}{(s_t l_t)^\theta} \qquad \dots(10)$$

The above profit maximization conditions state that given the return to human capital/skilled and the unskilled labor wage rate, $w_{h_t}$ and $w_{l_t}$, the demand for each type of labor is determined by equating these returns to the marginal productivity of human capital and unskilled labor respectively.

When output is produced from natural resource-intensive (NRI) technology, the representative firm hires unskilled labor $((1-s_t)l)$. It combines it with extracted natural resources $(X_t)$ to maximize profit, taking relative prices of natural resource-intensive output $(p^R)$, unskilled labor wage $(w_{l_t})$, and price of extracted natural resources used in production $(p_t)$ as given. That is,

$$\max_{x_t, s_t l} \pi^R = p^R A^R (1-s_t)lX_t - w_{l_t}(1-s_t)l - p_t\, X_t$$

Here, the firm hires unskilled labor to be employed, $(1-s_t)l$, and natural resource stock to be used in the production of output, $X_t$, which lead to the following first-order conditions:

$$w_{l_t} = p^R A^R X_t ; \qquad \dots(11)$$

$$p_t = p^R A^R (1 - s_t)l \qquad \dots(12)$$

This indicates that each firm hires unskilled labor and natural resources until their respective marginal products get equated to the factor return or price. By equating equation (10) with (11), we get that,

$$\frac{(1-\theta)A^H H_t^\theta}{(s_t l)^\theta} = p^R A^R X_t$$

$$s_t l = \left(\frac{(1-\theta)A^H}{p^R A^R X_t}\right)^{1/\theta} H_t ,$$

Where $H_t = \psi V_{t-1} l$

Equation (13) states that unskilled labor devoted to the production in the human capital-intensive (HCI) sector, $s_t l$, depends positively on the share of unskilled labor in aggregate output $(1 - \theta)$, the investment in the human capital of young agent made by the adult agent or parent, $V_{t-1}$, and the productivity of human capital-intensive technology relative to the productivity of natural resource-intensive technology, $A^H/A^R$, negatively on the price of natural resource-intensive output, $p^R$, and natural resource stock used in the production of natural resource-intensive output, $X_t$. Substituting the value of $s_t l$ from (13) into (9), we derive that

$$w_{h_t} = \theta(1-\theta)^{(1-\theta)/\theta} \frac{A^{H 1/\theta}}{(p^R A^R X_t)^{(1-\theta)/\theta}} . \qquad \dots(14)$$

**Lemma 1:** For a given value of $(1 - \theta)$, $A^H$, $p^R$ and $A^R$, as $X_t$ increases $w_{l_t}$ increases, which in turn leads to decrease in $w_{h_t}$.

**Proof:** Follows from the solution of $w_{h_t}$ (See equation (14))

This lemma states that for a given level of share of unskilled labor in the human capital-intensive sector, $(1 - \theta)$, productivity level of human capital intensive (HCI) technology $(A^H)$, productivity level of natural resource-intensive (NRI) technology $(A^R)$ and price of natural resource-intensive output $(p^R)$, as the extraction of resources increases $(X_t)$, the unskilled labor wage rate increases $(w_{l_t})$ (follows from (11)), since, from (11) we have, $w_{l_t} = p^R A^R X_t$. An increase in $w_{l_t}$ reduces the wage rate for human capital $(w_{h_t})$ (follows from equation (14)). This happens because the increase in $w_{l_t}$ will reduce the demand for unskilled labor in the human capital-intensive sector (follows from (10)), which, in turn, reduces the skilled labor/human capital wage rate (follows from (9)). This implies that as the unskilled

wage rate increases, the profitability of output produced from natural resource-intensive technology will fall. Still, the profitability of output produced from human capital-intensive technology will increase.

From (12), we have

$$p_t = p^R A^R (1 - s_t) l$$

The above equation implies that the price of the extracted natural resource used in production ($p_t$) depends on the price of natural resource-intensive output ($p^R$), productivity level of natural resource-intensive (NRI) technology ($A^R$) and the unskilled labor used in natural resource-intensive output ($(1-s_t)l$).

We next turn to substituting $s_t l$ from equation (24) into the above equation. We get that

$$p_t = p^R A^R L_t - p^R A^R \left[ \frac{(1-\theta)A^{H\ 1/\theta}}{p^R A^R\ X_t} \right]\ H_t$$

$$p_t = \frac{(p^R A^R X_t)^{1/\theta} l - ((1-\theta)A^H)^{1/\theta} H_t}{(p^R A^R)^{1-\theta/\theta}\ (X_t)^{1/\theta}}, \quad ...(15)$$

Where $H_t = \psi V_{t-1} l$.

**Lemma 2:** For a given value of $(1 - \theta)$, $A^H, p^R$ and $A^R$, as $V_{t-1}$ increases $p_t$ decreases and as $X_t$ increases $p_t$ increases.

**Proof:** Differentiating the equation (15) with respect to $V_{t-1}$, we get

$$\frac{\partial p_t}{\partial V_{t-1}} = -\frac{((1-\theta)A^H)^{\frac{1}{\theta}}\psi l_{t-1}}{(p^R A^R)^{\frac{1-\theta}{\theta}}(X_t)^{\frac{1}{\theta}}} \quad ...(16)$$
$$< 0$$

Differentiating the equation (15) with respect to $X_t$, we get

$$\frac{\partial p_t}{\partial X_t} = \frac{1}{\theta}\frac{((1-\theta)A^H)^{\frac{1}{\theta}}\psi V_{t-1}l}{(p^R A^R)^{\frac{1-\theta}{\theta}}(X_t)^{\frac{(\theta^2-\theta+1)}{\theta^2}}} \quad ...(17)$$
$$> 0$$

From equation (16), we can infer that the price that the firm will pay for the extracted natural resource and the price that adult agent will receive from selling their natural resource stock to firms ($p_t$) will decrease as the investment in the education of the young agent made by the parents ($V_{t-1}$) increases. The more educated individual will rely less on natural resource stock to earn their income; they can increase their income by working in a human capital-intensive sector. Similarly, from equation (17), we can say that $p_t$ will increase as the natural resource stock extracted for production ($X_t$) will increase.

**Consumers Optimization**

The representative agent born at period t-1 maximizes their utility function with respect to young and adult agent consumption and expenditure to be made in their child's education, taking prices as given. The two-period utility maximization problem of the adult agent (in period t) can be written as:

$$\max_{C_{t-1}^Y, C_t^A, V_t} U_t = \ln C_{t-1}^Y + \beta \ln C_t^A + (1-\beta)\ln V_t$$

Subject to budget constraints of time periods t-1 and t to be:

$$C_{t-1}^Y + p_{t-1}N_{t-1} = \mathcal{E}Y_{t-1}; \quad ...(19)$$

$$C_t^A + V_t + \mathcal{E}Y_t = Y_t + p_t N_{t-1}; \quad ...(20)$$

$$Y_t = w_{h_t}H_t + w_{l_t}s_t l + w_{l_t}(1-s_t)l \quad ...(21)$$

Given the transfer of income received by each young agent from their parents ($\mathcal{E}Y_{t-1}$ ($\mathcal{E}$ being exogenous here)) and the expenditure on education ($V_{t-1}$), the agent born in period t-1 chooses the expenditure to be done on their child's education ($V_t$), the natural resource endowment to buy ($N_{t-1}$) from first generation adults agent or adult agents who coexists with the young agent born in period t-1.

Given the human capital/skilled labor equation in (2), $H_t = \psi V_{t-1}l$. and the budget constraint in (19) and (20), the langrage an expression for the above-stated problem, with the choice variables for optimization as $V_t$ and $N_{t-1}$, can be written as:

$$\mathcal{L} = \ln(\mathcal{E}Y_{t-1} - p_{t-1}N_{t-1}) + \beta\ln((1-\mathcal{E})Y_t + p_t N_{t-1} - V_t) + (1-\beta)\ln V_t$$

Accordingly, the first-order conditions for the consumer's optimization problem take the form:

$$\frac{d\mathcal{L}}{dV_t} = \frac{\beta(-1)}{((1-\mathcal{E})Y_t + p_t N_{t-1} - V_t)} + \frac{(1-\beta)}{(V_t)} = 0; \quad ...(22)$$

$$\frac{d\mathcal{L}}{dN_{t-1}} = \frac{-p_{t-1}}{(\mathcal{E}Y_{t-1} - p_{t-1}N_{t-1})}$$
$$+ \frac{\beta p_t}{((1-\mathcal{E})Y_t + p_t N_{t-1} - V_t)} = 0 \quad ...(23)$$

By simplifying equation (22), one gets that,

$$V_t = (1-\beta)((1-\mathcal{E})Y_t + p_t N_{t-1}) \quad ...(24)$$

Equation (24) shows that investment made by an adult agent in a child's education ($V_t$) depends positively on the weight given by her/him to the investment in the child's education ($1 - \beta$), the total wage income that the adult agent will earn from their human capital and unskilled labor ($Y_t$) and positively on the income that she/he received from selling natural resource stock to firm ($p_t N_{t-1}$).

By solving equation (23), we get that each consumer equates the marginal rate of substitution between current and future consumption to the marginal rate of investment in natural resources.

$$p_{t-1}((1 - \mathcal{E})Y_t + p_t N_{t-1} - V_t) = \beta p_t(\mathcal{E}Y_{t-1} - p_{t-1}N_{t-1}) \qquad \ldots(25)$$

Substituting the value of $V_t$ from equation (24) into equation (25) yields:

$$p_{t-1}((1 - \mathcal{E})Y_t + p_t N_{t-1} - (1 - \beta)((1 - \mathcal{E})Y_t + p_t N_{t-1}))$$
$$= \beta p_t(\mathcal{E}Y_{t-1} - p_{t-1}N_{t-1})$$

By rearranging the above equation, we get the solution for the natural resource stock purchased by the young to be:

$$\beta p_{t-1}((1 - \mathcal{E})Y_t + p_t N_{t-1})$$
$$= \beta p_t(\mathcal{E}Y_{t-1} - p_{t-1}N_{t-1})$$

$$N_{t-1} = \frac{1}{2}\left[\frac{\mathcal{E}y_{t-1}}{p_{t-1}} - \frac{(1 - \mathcal{E})Y_t}{p_t}\right] \qquad \ldots(26)$$

**Lemma 3:** For a given exogenous value of $0 < \mathcal{E} < 1$, $N_{t-1}$ depends positively on $Y_{t-1}$ and $p_t$, and negatively on $Y_t$ and $p_t$.

**Proof:** The proof of this lemma follows from equation (26)

From equation (26), it is plausible that the natural resource stock that the young agent will buy from the first-generation adult agent of period t-1 ($N_{t-1}$) depends positively on the transfer that the young agent will receive from their parents ($\mathcal{E}Y_{t-1}$), negatively on the price at which they will buy the natural resource stock ($p_{t-1}$), positively on the price that they will receive by selling the natural resource stock to next generation agents ($p_t$) and negatively on the total wage income that an adult will earn from their human capital/skilled labor and unskilled labor ($Y_t$).

From equation (21), we know that the aggregate income earned by an adult in the second period (that is, period $t$ of life) is the sum of the income earned by supplying human capital in the human capital-intensive (HCI) production sector and wage income earned by supplying unskilled labor to the two sectors. Specifically,

$$Y_t = w_{h_t}H_t + w_{l_t}s_t l + w_{l_t}(1 - s_t)l = w_{h_t}H_t + w_{l_t}l$$

Next, substituting the values of $w_{h_t}$, $H_t$, and $w_{l_t}$ from equations (14), (2), and (11), respectively, we derive the following expression for aggregate income ($Y_t$) as a function of investment in young's education by the parent ($V_{t-1}$) and the unskilled labor wage rate ($w_{l_t}$).

$$Y_t = \theta(1 - \theta)^{(1-\theta)/\theta}\frac{A^{H^{1/\theta}}}{(p^R A^R X_t)^{(1-\theta)/\theta}}$$
$$\psi V_{t-1}l + p^R A^R X_t\, l$$

$$Y_t = \frac{\theta(1 - \theta)^{(1-\theta)/\theta}A^{H^{1/\theta}}\psi V_{t-1}l + (p^R A^R X_t)^{1/\theta}l}{(p^R A^R x_t)^{(1-\theta)/\theta}}$$

**Lemma 4:** The above expression states that given the constants $\theta$, $A^H$, $\psi$, $p^R$, and $A^R$, the income earned by an adult agent depends ($Y_t$) on the educational expenditure incurred by their parents ($V_{t-1}$) and the level of extraction of natural resource ($X_t$).

**Proof:** The proof of this lemma follows from equation (27).

This lemma states that the total wage income earned by adult agents ($Y_t$), that is, the sum of unskilled wage income and human capital/skilled wage income, depends positively on the educational expenditure incurred by their parents ($V_{t-1}$) and negatively on the extracted natural resource used in the production of NRI output (see equations (43) and (44)).

If $V_{t-1} = 0$, from equation (27), we get that,

$$Y_t = p^R A^R X_t\, l \qquad \ldots(28)$$

Intuitively, this can be seen from equation (28). That is, if the parent of the young does not incur any expenditure on the education of their child ($V_{t-1} = 0$), then she/he does not receive any education and remains unskilled. In the next period, when this young agent becomes an adult, their income will now depend on the wage income earned from unskilled labor by working in the natural resource-intensive sector ($p^R A^R X_t$), which in turn, depends on the extraction of the natural resource ($X_t$).

Combining the solution for $Y_t$ with the cases where $V_{t-1} = 0$ and $V_{t-1} > 0$, given by equations (28) and (27), respectively, we get the total wage income earned by an adult to be:

$$Y_t =
\begin{cases}
p^R A^R X_t l, & V_{t-1} = 0; \\
\dfrac{\theta(1 - \theta)^{(1-\theta)/\theta}A^{H^{1/\theta}}\psi V_{t-1}L_{t-1} + (p^R A^R X_t)^{1/\theta}l}{(p^R A^R X_t)^{(1-\theta)/\theta}}, & V_{t-1} > 0.
\end{cases}$$

$$\ldots(29)$$

Thus,

**Proposition 1**: In this overlapping generation (OLG) economy, as the investment in the education of the child by the parent increases, the income earned by the adult in the next period also increases (see the case for $V_{t-1} > 0$ in equation (29)). If, however, there is no investment in the child's education by the parent, then in the next period, the adult derives the entire income by working as unskilled labor in the natural resource-intensive sector (this follows from equation (29) when $V_{t-1} = 0$).

## Behavior of Outputs of the Two Sectors Along the Equilibrium Path

Given perfect competition in commodity and factor markets and constant returns to scale (CRS), the number of firms in the aggregate economy is immaterial. We exogenously assume it to $N^H$ for the firms using HCI technology and $N^R$ for the firms using NRI technology. In this setup, choosing $N^H = N^R = 1$ will not change the results qualitatively. At the economy-wide level, the aggregate output produced by $N^H$ firms from HCI technology (equation (6)) is given as:

$$N^H Y^H = N^H A^H ((H_t^\theta)(s_t l)^{1-\theta}$$

Substituting the value of $H_t$ from equation (2) and $s_t l$ from equation (13) into the above equation, we get,

$$N^H Y_t^H = N^H (A^H)^{\frac{1}{\theta}} \left( \frac{(1-\theta)}{P^R A^R X_t} \right)^{1-\theta/\theta} \psi V_{t-1} l \quad ...(30)$$

Differentiating the above equation with respect to $V_{t-1}$, we get that

$$\frac{\partial N^H Y_t^H}{\partial V_{t-1}} = N^H (A^H)^{\frac{1}{\theta}} \left( \frac{(1-\theta)}{P^R A^R X_t} \right)^{1-\theta/\theta} \psi l > 0$$

$$...(31)$$

**Lemma 5:** Equation (31) states that as the investment in education ($V_{t-1}$) increases, the aggregate output produced from HCI technology ($N^H Y_t^H$) rises for a given positive level of extracted natural resource stock ($X_t$). Similarly, from equation (30), one can infer that as the extracted natural resource stock ($X_t$) increases, the output produced from HCI technology falls.

The aggregate output produced by $N^R$ firms from NRI technology is given as:

$$N^R Y_t^R = N^R A^R (1 - s_t) l X_t$$

Next, substituting the value of $s_t l$ from equation (13) into the above equation, we get:

$$N^R Y_t^R = N^R (A^R l X_t - \frac{\left( (1-\theta)A^H \right)^{\frac{1}{\theta}} \psi V_{t-1} l^2 \right)}{(P^R)^{\frac{1}{\theta}} (A^R X_t)^{\frac{1-\theta}{\theta}}}$$

$$...(32)$$

Differentiating the above equation with respect to $V_{t-1}$, we get the following expression:

**Lemma 6:** The above equation (33) states that as the investment in education ($V_{t-1}$) increases, the aggregate output produced from NRI technology ($N^R Y^R$) decreases. Similarly, from equation (32), we can say that as the extracted natural resource stock ($X_t$) increases, the output produced from NRI technology increases. Thus,

**Proposition 2**: As investment in education increases or $dV_{t-1} > 0$, the aggregate output produced from HCI technology ($N^H Y^H$) increases, and the aggregate output produced from NRI technology ($N^R Y^R$) decreases. Similarly, as the extraction of natural resource stock ($dX_t > 0$) increases, the aggregate output produced from HCI technology decreases, and the aggregate output produced from NRI technology increases (proof follows from Lemma 5 and Lemma 6).

Intuitively, whenever investment in the education of the young agent made by the parents ($V_{t-1}$) increases, the price that the firm will pay for the extracted natural resources ($p_t$) decreases (follows from Lemma 2). We also know that as the extraction of resources increases ($X_t$), the price that the firm will pay for the extracted natural resources ($p_t$) will increase (follows from Lemma 2), and the unskilled labor wage rate increases ($w_{l_t}$), which in turn, will decrease wage rate for human capital ($w_{h_t}$) (follows from Lemma 1). An increase in ($p_t$) will reduce the profitability of output production from natural resource-intensive (NRI) technology, $Y_t^R$. This will reduce the output produced by NRI technology. Similarly, a decrease in $w_{h_t}$ will increase the profitability of output produced from human capital intensive (HCI) technology, $Y^H$. This will increase the output produced from HCI technology.

Next, let us see how the natural resource that young agents will buy from first-generation adult agents of period t-1 changes when investment in education increases. Substituting the value of $Y_t$ from equation (27) and $p_t$ from equation (15) into equation (26), we get,

$$N_{t-1} =$$

$$\frac{1}{2} \left[ \frac{\varepsilon Y_{t-1}}{p_{t-1}} - \frac{(1-\varepsilon) \left[ \frac{\theta(1-\theta)^{\frac{1-\theta}{\theta}} A^{H\frac{1}{\theta}} \psi V_{t-1} l + (p^R A^R X_t)^{\frac{1}{\theta}} l}{(p^R A^R X_t)^{\frac{1-\theta}{\theta}}} \right]}{\frac{(p^R A^R X_t)^{\frac{1}{\theta}} l - ((1-\theta)A^H)^{\frac{1}{\theta}} \psi V_{t-1} l}{(p^R A^R)^{\frac{1-\theta}{\theta}} (X_t)^{\frac{1}{\theta}}}} \right]$$

$$...(34)$$

Differentiating the above equation with respect to $V_{t-1}$, we

$$\frac{\partial N_{t-1}}{\partial V_{t-1}} =$$

$$\frac{-(1-\varepsilon)\theta(1-\theta)^{\frac{1-\theta}{\theta}}A^{H\frac{1}{\theta}}\psi(p^R A^R X_t)^{\frac{1}{\theta}} - (1-\varepsilon)X_t(p^R A^R X_t)^{\frac{1}{\theta}}((1-\theta)A^H)^{\frac{1}{\theta}}\psi}{\left((p^R A^R X_t)^{\frac{1}{\theta}}l - ((1-\theta)A^H)^{\frac{1}{\theta}}V_{t-1}l\right)^2}$$

...(35)

$$\frac{\partial N_{t-1}}{\partial V_{t-1}} < 0, \text{ as } 0 < \varepsilon, \theta < 1; p^R, A^R, X_t, A^R > 0$$

$$\text{and } V_{t-1} > 0$$

**Proposition 3**: In this OLG economy, investment by the parents in young agent's education ($V_{t-1}$) will always lower the young's reliance on natural resource stock ($N_{t-1}$) (see equation (35) for proof). This follows from the fact that in equilibrium, a more educated adult will tend to be less dependent on natural resources for earning their income in the second period (t).

**Solving for Equilibrium Consumption, Resource Use, and Associated Price**

Next, we will derive the solution for $V_t$, $C_{t-1}^Y$ and $C_t^A$ substituting the value of $N_{t-1}$ from equation (26) into (24), we get $V_t$ as:

$$V_t = \frac{(1-\beta)}{2}\left((1-\varepsilon)Y_t + \frac{\varepsilon p_t Y_{t-1}}{p_{t-1}}\right) \quad ...(36)$$

Equation (36) states that investment incurred by an adult agent in their child's education depends positively on the weight assigned by the adult agent to investment in their child's education ($1-\beta$), positively on the transfer that the adult receives when young from their parents ($\varepsilon Y_{t-1}$), positively on the total wage income that the adult agent earns from their human capital/skilled labor and unskilled labor ($Y_t$), positively on the price that she/he receives from selling the natural resource in period t relative to the price at which she/he buys it from the adult agent in period t-1, $p_t/p_t - 1$. All of which are plausible directions of impact.

Next, the consumption of the young, $C_{t-1}^Y$, is solved by rearranging equation (19), which yields that

$$C^Y{}_{t-1} = \varepsilon Y_{t-1} - p_{t-1}N_{t-1}$$

Further, substituting $N_{t-1}$ from equation (26) into the above, we get that,

$$C_{t-1}^Y = \frac{1}{2}\left(\varepsilon Y_{t-1} + \frac{p_{t-1}}{p_t}(1-\varepsilon)Y_t\right) \quad ...(37)$$

Equation (37) implies that the consumption of the young agent in period t-1 depends positively on the transfer that she/

he receives from the adult agents or their parents ($\varepsilon Y_{t-1}$), positively onthe total wage income that the adult agent will earn from their human capital/skilled labor and unskilled labor ($Y_t$), positively on the price at which they buy natural resource from an adult agent in period t-1 relative to the price that they receive from selling natural resource stock in period t ($\frac{p_{t-1}}{p_t}$).

Further, the consumption of the adult is derived by rearranging equation (20) and substituting $N_{t-1}$ from (26) and $V_t$ from (36) into equation (20), we get that

$$C_t = \frac{\beta}{2}\left((1-\varepsilon)Y_t + \frac{\varepsilon p_t Y_{t-1}}{p_{t-1}}\right) \quad ...(38)$$

Equation (38) states that the consumption by an adult in period t depends positively on the weight assigned by a young agent to the future level of consumption as opposed to the investment in theirchild's education ($\beta$), positively on the transfer she/he receives from their parents when young ($\varepsilon Y_{t-1}$), the total wage income that adult agent will earn from their human capital and unskilledlabor ($Y_t$), and the price that she/he receives from selling the natural resource in period t relative to the price at which they buy it from the adult agent in period t-1, $\frac{p_t}{p_{t-1}}$.

Further, from equation (15), we have

$$p_t = p^R A^R l - \frac{((1-\theta)A^H)^{\frac{1}{\theta}}\psi V_{t-1}l}{(p^R A^R)^{\frac{1-\theta}{\theta}}(X_t)^{\frac{1}{\theta}}} \quad ...(39)$$

From equation (39), we can say that whenever $V_{t-1} > 0$, in the above equation $p_t > 0$ when the following holds.

$$X_t > \frac{(1-\theta)A^H(\psi V_{t-1})^\theta}{(p^R A^R)} = \bar{X} \quad ...(40)$$

Where $\bar{X}$ is the threshold level of resource extraction that depends positively on the educational expenditure incurred by his/her parents, $V_{t-1}$. Further, from equation (39), we can say that,

$$p_t = 0 \text{ when } X_t = \frac{(1-\theta)A^H(\psi V_{t-1})^\theta}{(p^R A^R)} = \bar{X}$$

...(41)

From equation (41), one can infer that the natural resource stock extracted, $X_t$, for production of natural resource-intensive output, $Yt^R$, depends positively on the price that the firm will receive from natural resource-intensive production, $p^R$, positively on the productivity of

technology, $A^R$, as well as the investment in the education of the young agent made by the parents, $V_{t-1}$.

Combining the above two cases (that is, when $p_t = 0$ and $p_t > 0$), the solution for the price of the resource, $p_t$, turns out to be:

$$p_t = \begin{cases} 0, & X_t = \bar{X} \\ p^R A^R l - \dfrac{((1-\theta)A^H)^{\frac{1}{\theta}} \psi V_{t-1} l}{(p^R A^R)^{\frac{1-\theta}{\theta}} (X_t)^{\frac{1}{\theta}}}, & X_t > \bar{X} \end{cases}$$

...(42)

The above equation states that the extracted resource stock ($X_t$) used in the production of the NRI sector increases whenever the extracted resource stock, $X_t$, increases beyond a certain threshold level $\bar{X}$, The price of the extracted resource stock remains at 0 if $X_t \leq \bar{X}$, where $\bar{X}$ is given by equation (41). We rule out the case where $p_t = 0$, as young will always want a positive price when they sell natural resource to firms where natural resource is assumed to be an essential input in the production of the NRI sector. The extracted resource stock depends on the investment in the education of the young agent made by the parents ($V_{t-1}$) (see equations 40 and 41). When $X_t > \bar{X}$ As the investment made by parents in the education of young agents increases, the price of natural resource stock decreases (see Lemma 2). Whenever $V_{t-1} = 0$, the $p_t = p^R A^R l$ (from (39)) and $V_{t-1} > 0$, the $p_t$ is given by equation (39). From Lemma 2, we can say that as the extracted resource stock used in the production of the NRI output increases, the price of extracted resources increases. Hence, the profitability of production from NRI technology decreases due to an increase in the price of the extracted natural resource. Whenever $X_t > \bar{X}$ The increase in the price of extracted resources due to the increase in extraction (see equation (17)) will be more than offset by the decrease in the price of extracted resources due to the increase in investment in young agent education made by their parent (see equation (16)). We can say that higher educational attainment by an individual means she/he entails a lower dependence on natural resources to increase their income. The more educated the individual, the more options available to her/him to earn their livelihood by sustainable means.

**Proposition 4:** When the extraction of natural resources exceeds a certain minimum threshold level ($X_t > \bar{X}$), such that $p_t > 0$, the price that an individual receives from selling its natural resource stock to a firm gets lowered (42) as the investment in education made by the young agent ($V_{t-1}$) increases (16). This implies that the more educated the individual is, the less dependent on natural resources for earning his/her income (proof follows from Lemma 2).

Next, we analyze the effect of investment in the education of an agent by their parents ($V_{t-1}$) as well as the level of extracted natural resource ($X_t$) on the aggregate income of the adult agent ($Y_t$).

For this, we differentiate equation (27) with respect to $V_{t-1}$, to get:

$$\frac{\partial Y_t}{\partial V_{t-1}} = \frac{\theta(1-\theta)^{(1-\theta)/\theta} A^{H 1/\theta} \psi l}{(p^R A^R X_t)^{(1-\theta)/\theta}} > 0$$

...(43)

$$\frac{\partial Y_t}{\partial X_t} = \frac{1}{\theta} \frac{(p^R A^R)^{1/\theta}(X_t)^{1-\theta/\theta} l}{(p^R A^R X_t)^{(1-\theta)/\theta}} -$$

$$\frac{(1-\theta)}{\theta}\left( \frac{\theta(1-\theta)^{\frac{1-\theta}{\theta}} A^{H\frac{1}{\theta}} \psi v_{t-1} l_{t-1} + (p^R A^R X_t)^{\frac{1}{\theta}} l}{(p^R A^R)^{\frac{1-\theta}{\theta}}(X_t)^{\frac{1}{\theta}}} \right)$$

$$\frac{\partial Y_t}{\partial X_t} = \frac{1}{\theta}(p^R A^R l) -$$

$$\left( \frac{(1-\theta)^{\frac{1}{\theta}} A^{H\frac{1}{\theta}} \psi V_{t-1} l}{(p^R A^R)^{\frac{1-\theta}{\theta}}(X_t)^{\frac{1}{\theta}}} + \frac{(1-\theta)p^R A^R l}{\theta} \right)$$

$$\frac{\partial Y_t}{\partial X_t} = (p^R A^R l) - \left( \frac{(1-\theta)^{\frac{1}{\theta}} A^{H\frac{1}{\theta}} \psi V_{t-1} l}{(p^R A^R)^{\frac{1-\theta}{\theta}}(X_t)^{\frac{1}{\theta}}} \right)$$

This follows from equation (39), which states that

$$\frac{\partial Y_t}{\partial X_t} = p_t$$

...(44)

Equation (44) shows that the increase in the income of an adult due to an increase in extracted resources depends positively on the price the adult agent receives by selling the natural resource stock to the firm in the NRI technology sector. However, according to (16), the price that an individual receives from selling natural resources to the firm falls as the investment in a young agent's education by their parent rises. The proposition that follows from above is as follows.

**Proposition 5**: As the investment in education by parents, $V_{t-1}$, increases, the aggregate earned income of the adult increases, according to (43), but the income earned from natural resource stock declines, according to (44). This is because, from equation (16), we get that the price that the adult receives from selling natural resource stock declines when $V_{t-1}$ increases.

Intuitively, as the investment made by an adult agent in their child's education increases, $V_{t-1}$, increases the accumulation of human capital increases (as from (2), $H_t = \psi V_{t-1} l$). This, in turn, implies that young agent of period t-1 can earn wage income by working in the HCI sector from both their skilled labor/human capital as well as unskilled labor components. The young agents will supply unskilled labor ($s_t l$) and human capital ($H_t$) to the HCI sector. From equation (45), we know that whenever $V_{t-1} > 0$, $s_t l > 0$, and by assumption, we know that $w_{h_t} > w_{l_t}$. Hence, an individual's aggregate wage income will always be higher whenever an investment in their human capital is made by their parent. Moreover, the increase in total wage income ($Y_t$) due to the extraction of resources ($X_t$) is equal to the price that they will receive from selling the natural resource stock to the firm (which is $p_t$) (see equation (44)), which in turn, declines whenever the investment in human capital ($V_{t-1}$) increases (see equation (16)). The more educated individual prefers to work in the HCI sector, due to which the extraction of resources and its price decreases.

Next, from equation (13), we have

$$s_t l = \left( \frac{(1-\theta)A^H}{p^R A^R X_t} \right)^{1/\theta} H_t \qquad \text{...(45)}$$

Where $H_t = \psi V_{t-1} l$. That is, the demand for unskilled labor in the HCI technology sector (that is $s_t l$) depends positively on the share of unskilled labor in this sector (1-$\theta$) and technological productivity of the HCI sector relative to the NRI sector ($A^H/A^R$), negatively on the wage rate of unskilled labor ($p^R A^R X_t = w_{L_t}$ (from expression in (11)) and investment in education made by parents ($V_{t-1}$). The unskilled wage income depends on the extracted resource stock ($X_t$); when $X_t$ increases, the unskilled wage income in the NRI sector also increases. When $V_{t-1} = 0$, $s_t l = 0$, and the adult relies only on NRI technology for earning income (that is $p^R A^R X_t l = w_{l_t} l$), she/he will earn unskilled wages by working in the NRI sector (see equation (29)). However, when $V_{t-1} > 0$, $s_t l > 0$, in comparison, the individual will earn a higher income than the case where $V_{t-1} = 0$, which will be through sustainable means of production [again from equation (29)]. Thus, we have,

**Proposition 6**: The diversification of the income-earning source of the individual from complete reliance on the NRI sector ($s_t l = 0$) to partial reliance requires a certain positive amount of investment in the education of the young agent by the parent (this can be seen in equation (27)). From equation (28), it can be seen that when $V_{t-1} = 0$, $Y_t = w_{l_t} l$, the adult agent will earn their income only from unskilled labor ($l$). When $V_{t-1} > 0$, $s_t l > 0$ from (45), $Y_t = w_{h_t} H_t + w_{l_t} l$, individual

will earn income from both skilled labor/human capital and unskilled labor [see equation (21)].

Having derived the equilibrium solutions for young agent consumption ($C_{t-1}^Y$), adult agent consumption ($C_t^A$), expenditure to be made by adult agents in their child's education ($V_t$), natural resource endowment to buy from the adult agent ($N_{t-1}$), unskilled labor wage ($w_{l_t}$) and human capital wage income ($w_{h_t}$). As is commonly done in models of growth economics, we are interested in characterizing the steady-state values of the variables. We now characterize the long-run steady-state equilibrium for this stylized overlapping generations (OLG) economy.

## STATIONARY EQUILIBRIUM

We focus on balanced growth paths, i.e., paths that are characterized by constant growth rates of all variables. The reason for this choice is that balanced growth paths are the only kind of path that can generate long-run growth in the economy. We analyze those paths defined as follows:

Steady states are time-invariant sequences defined by $Y_{t-1} = Y_t = \bar{Y}$, $V_{t-1} = V_t = \bar{V}$, $C_{t-1}^Y$ $C_t^A = \bar{C}$, $N_{t-1} = N_t = \bar{N}$ and $p_{t-1} = p_t = \bar{p}$.

Substituting $Y_{t-1} = Y_t = \bar{Y}$ and $p_{t-1} = p_t = \bar{p}$ in equation (36), we will get the steady-state value of investment in education as given as follows. We have,

$$\bar{V} = \frac{(1-\beta)}{2}\left( (1-\mathcal{E})\bar{Y} + \frac{\mathcal{E}\bar{P}\bar{Y}}{\bar{P}} \right) = \frac{(1-\beta)}{2}\bar{Y} \qquad \text{...(46)}$$

Equation (46) represents the steady-state value of an investment in the education of the young agent. $\overline{(V)}$ depends on the weight put by the adult agent on the investment in the child's education ($1-\beta$) and half of the steady-state value of total wage income earned by the adult agent.

Next, we will solve for $\bar{Y}$ from equation (27), substituting, $Y_t = \bar{Y}$, $V_{t-1} = \bar{V}$, $X_t = \bar{X}$, $l_{t-1} = l_t = \bar{l}$ in the above equation (27), we get the steady-state value of income earned by the individual to be:

$$\bar{Y} = \frac{\theta(1-\theta)^{(1-\theta)/\theta} A^{H 1/\theta} \psi \bar{V} \bar{l}}{(P^R A^R \bar{X})^{(1-\theta)/\theta}} + P^R A^R \bar{X} \bar{l}$$

Substituting the value $\bar{X}$ of from equation (41) into the above equation and using $V_t - 1 = \overline{(V)}$ we get that,

$$X_t = \frac{(1-\theta)A^H(\psi\bar{V})^\theta}{(P^R A^R)} = \bar{X}$$

$$\bar{Y} = \frac{\theta(1-\theta)^{(1-\theta)/\theta} A^{H^{1/\theta}} \psi \bar{V} \bar{l}}{(P^R A^R \frac{(1-\theta)A^H(\psi\bar{V})^\theta}{(P^R A^R)})^{(1-\theta)/\theta}} +$$

$$P^R A^R \frac{(1-\theta)A^H(\psi\bar{V})^\theta}{(P^R A^R)} \bar{l}$$

$$\bar{Y} = \theta A^H(\psi\bar{V})^\theta \bar{l} + (1-\theta)A^H(\psi\bar{V})^\theta \bar{l}$$

$$\bar{Y} = A^H(\psi\bar{V})^\theta \bar{l} \qquad \text{...(47)}$$

Equation (47) indicates that the long-run steady-state value of the income earned by an individual depends positively on the steady-state level of expenditure on education $(\bar{V})$, the productivity of human capital-intensive technology $(A^H)$, steady-state unskilled labor ($\bar{l}$), the share of human capital in human capital-intensive output production $(\theta)$ and the productivity of the human capital accumulation $(\psi)$.

Substituting the value of $\bar{Y}$ from equation (47) into equation (46), we get

$$\bar{V} = \frac{(1-\beta)^{\frac{1}{(1-\theta)}}}{2} (A^H \bar{l})^{\frac{1}{(1-\theta)}} (\psi)^{\frac{\theta}{1-\theta}} \qquad \text{...(48)}$$

Substituting $V_{t-1} = \bar{V}$, from (47) $and\ l_{t-1} = \bar{l}$, in equation (2), we get human capital accumulation by the young agent as:

$$\bar{H} = \frac{(1-\beta)^{\frac{1}{(1-\theta)}}}{2} (A^H \bar{l})^{\frac{1}{(1-\theta)}} (\psi)^{\frac{1}{1-\theta}} (\bar{l})^{\frac{(2-\theta)}{(1-\theta)}} \qquad \text{...(49)}$$

Equation (49) indicates that investment in human capital depends on the positive productivity of human capital-intensive technology $(A^H)$, and unskilled labor. $\bar{l}$, share of human capital relative to the share of unskilled labor in HCI output production $(\theta/1-\theta)$ and the productivity of the human capital accumulation $(\psi)$, the weight given by adult agent to investment in child's education $(1-\beta)$. From this, the following proposition follows.

**Proposition 7**: Given $A^H, \bar{l}, \theta/1-\theta$ and $\psi$, a long-run steady-state equilibrium level of the human capital accumulation are higher, higher is the weight put by the parent on the child's education [the proof for this result follows from equation (49)].

Substituting the value of $N_{t-1} = N_t = \bar{N}$ and $X_t = \bar{X}$ in equation (8), we get

$$\bar{N} = \frac{\eta}{\delta}\bar{X}$$

Substituting the value of $\bar{X}$ from (41) in the above equation, we get

$$\bar{N} = \frac{\eta}{\delta}\frac{(1-\theta)A^H(\psi\bar{V})^\theta}{(P^R A^R)}$$

Substituting the value $\bar{V}$ of from equation (48) in the above equation, we get

$$\bar{N} = \frac{\eta}{\delta}\frac{(1-\theta)A^H\left(\psi\frac{(1-\beta)^{\frac{1}{(1-\theta)}}}{2}(A^H\bar{l})^{\frac{1}{(1-\theta)}}(\psi)^{\frac{\theta}{1-\theta}}\right)^\theta}{(P^R A^R)}$$

$$\bar{N} = \frac{\eta}{\delta}\frac{(1-\theta)(A^H)^{\frac{1}{(1-\theta)}}(\psi)^{\frac{\theta}{1-\theta}}\frac{(1-\beta)^{\frac{\theta}{(1-\theta)}}}{2}(\bar{l})^{\frac{\theta}{(1-\theta)}}}{(P^R A^R)} \qquad \text{...(50)}$$

Equation (50) indicates that the higher the steady-state value of natural resource stock, the higher the weight assigned by an adult agent on the investment in their child's education $(1-\beta)$, higher isthe productivity of human capital-intensive technology $(A^H)$, higher is the share of human capital relative to the share of unskilled labor in human capital-intensive output production $(\theta/1-\theta)$, the lowerthe price of NRI output $(p^R)$, and lower is the productivity of NRI technology $(A^R)$.

**Proposition 8:** Given $A^H, \frac{\theta}{1-\theta}, and\ P^R$, the steady-state value of natural resource stock is higher, higher is the weight given by adult agents to investment in a child's education $(1-\beta)$ (the formal proof follows from equation (50)).

Substituting the value of $Y_{t-1} = Y_t = \bar{Y}$ and $p_{t-1} = p_t = \bar{p}$ In equation (37), we get that,

$$C_{t-1}^Y = \frac{1}{2}\left(\mathcal{E}\bar{Y} + \frac{\bar{P}}{\bar{P}}(1-\mathcal{E})\bar{Y}\right) = \frac{1}{2}\bar{Y} \qquad \text{....(51)}$$

Substituting the value of $Y_{t-1} = Y_t = \bar{Y}$ and $p_{t-1} = p_t = \bar{p}$ In equation (38), we get

$$C_t^A = \frac{\beta}{2}\left((1-\mathcal{E})\bar{Y} + \frac{\mathcal{E}\bar{P}\bar{Y}}{\bar{P}}\right)$$

$$= \frac{\beta}{2}\bar{Y} \qquad \text{...(52)}$$

$$\frac{C_{t-1}^Y - C_t^A}{C_{t-1}^Y} = \frac{\frac{1}{2}\bar{Y} - \frac{\beta}{2}\bar{Y}}{\frac{1}{2}\bar{Y}}$$

$$= (1 - \beta) \qquad ...(53)$$

Equation (53) indicates that the consumption growth rate depends on the weight given by adult agents to investment in education $(1 - \beta)$.

Proposition 9: In this OLG economy, the continuous growth in consumption requires that individuals must assign a certain weight or give some importance to human capital accumulation $(\beta > 0)$ (the proof follows from equation (53)). This completes the characterization of our stylized OLG economy.

## CONCLUSION

In this chapter, we have developed a theoretical model to analyze the role of human capital accumulation in the adoption of natural resource technology of production. For this purpose, we extend the model developed by Ikefuji & Horii as our analytical framework. This research goes beyond the Ikefuji & Horii work by assuming that an individual derives utility by making an investment in their child's education. We have considered an overlapping generation model, where each individual is alive for two time periods, t-1 and t. She/he is born in period t-1 and is called the young agent; in period t, the individual becomes an adult and exists in the system. During a young age, an individual born in period t-1 does not work but only consumes and buys ownership rights of the natural resource out of the transfer that she/he receives from their parents. When young, the individual also benefit from the parent's education spending and builds their human capital that becomes available to him during working age in period t. We assume that an individual does not work when he is young. During the t-1 period, young agents are endowed with a certain ability to learn, which they devote entirely to learning, which, in turn, leads to human capital accumulation. During period t, an adult agent receives income from unskilled labor and human capital that they sell to the firm. Adult agent in period t also devotes an exogenous part of their income as transfer to their children for the latter's investment in education that would enable the young agent in human capital accumulation. This helps us characterize the conditions under which individuals will invest in human capital accumulation and adopt sustainable technology of production instead of natural resource-intensive technology of production.

As the main results of theoretical analyses, we find that as the investment in a child's education by the parent increases, the total earned income of the individual increases, but the income earned from the natural resource stock endowment declines. A more educated individual is less dependent on natural resources for earning their income. If the investment in education is zero, then the individual has no option but to rely completely on natural resource-intensive technology for earning their livelihood. We also find that as the investment in education increases, the output produced from sustainable technology rises, and the output produced from natural resource-intensive technology falls. Similarly, as the extraction of natural resource stock increases, the aggregate output produced from sustainable technology decreases, and the aggregate output produced from natural resource-intensive technology increases. We further find that sustainable consumption growth requires that individuals assign a certain positive weight to investment in their child's education. A long-run steady-state equilibrium level of human capital accumulation is higher; higher is the weight put by the parent on the child's education.

The steady-state value of income earned by an individual depends on the investment in education made by their parents. The long-run steady-state value of the income earned by an individual depends positively on the expenditure on education, the productivity of human capital-intensive technology, unskilled labor, the share of human capital in HCI output production, and the productivity of human capital accumulation. The steady-state value of natural resource stock is higher when an individual gives higher importance to education investment relative to consumption. The steady-state value of natural resource stock is higher, higher is the weight assigned by an adult agent on the investment in their child's education, higher is the productivity of human capital-intensive technology, higher is the share of human capital relative to the share of unskilled labor in HCI output production, lower is the price of NRI output, and lower is the productivity of NRI technology. In this overlapping generation economy, sustainable consumption growth requires that individuals assign a certain weight or give some importance to human capital accumulation. This follows from the fact that the long-run steady-state value of the income earned by an individual depends positively on the expenditure on education.

## REFERENCES

Agnani, B., Gutierrez, M.J. and Iza, A. 2005. Growth in overlapping generation economies with non-renewable resources. J. Environ. Econ. Manag., 50(2): 387-407.

Barrett, C., Reardon, T. and Webb, P. 2001. Nonfarm income diversification and household livelihood strategies in rural Africa: concepts, dynamics, and policy implications. Food Policy, 26(4): 315-331.

Banerjee, A.V. and Duflo, E. 2007. The economic lives of the poor. J. Econ. Perspect., 21(1): 141-168.

Barbier, E. 1999. Endogenous growth and natural resource scarcity. Environ. Resour. Econ., 14(1): 51-74.

Barbier, E.B. 2010. Poverty, development, and environment. Environ. Dev. Econ., 15(06): 635-660.

Becker, G.S. 1964. Human Capital: A Theoretical and Empirical Analysis, with Special Reference to Education. Columbia University Press, New York, pp. 187.

Bravo-Ortega, C. and De Gregorio, J. 2005. The relative richness of the poor? Natural resources, human capital, and economic growth. World Bank Policy Res. Work. Pap., 34: 84.

Chakrobarty, B. and Gupta, M. 2014. Human Capital Accumulation, Environmental Quality, Taxation and Endogenous Growth. In Ghosh, A. and Karmakar, A. (eds) Analytical Issues in Trade, Development and Finance, India Studies in Business and Economics, Springer, New Delhi, pp. 66-94.

Dasgupta, P. and Heal, G.M. 1974. The optimal depletion of exhaustible resources. Rev. Econ. Stud., 41(5): 3-28.

Gerlagh, R. and Keyzer, M. A. 2001. Sustainability and the intergenerational distribution of natural resource entitlements. J. Public Econ., 79(2): 315-341.

Gherghina, R. and Duca, I. 2013. The contribution of education to the economic development process of the states. J. Knowl. Manag. Econ. Inf. Technol., 3(1): 1-11.

Glomm, G. and Ravikumar, B. 1992. Public versus private investment in human capital: endogenous growth and income inequality. J. Political Econ., 100(4): 818-834.

Gutes, C.M. 1996. The concept of weak sustainability. Ecol. Econ., 17(3): 147-156.

Goderis, B. and Malone, S.W. 2011. Natural resource booms and inequality: theory and Evidence. Scand. J. Econ., 113(2): 388-417.

Gylfason, T. 2001. Natural resources, education, and economic development. Eur. Econ. Rev., 45(4-6): 847-859.

Gylfason, T., Herbertsson, T. and Zoega, G. 1999. A mixed blessing: natural resources and economic growth. Macroecon. Dyn., 3(2): 204-225.

Ikefuji, M. and Horii, R. 2007. Wealth heterogeneity and escape from the poverty-environment trap. J. Public Econ. Theory, 9(6): 1041-1068.

Ikefuji, M. and Horii, 2014. Environment and Growth. Routledge, London, pp. 25-51.

Nordhaus, W.D. 1992. Lethal model 2: the limits to growth revisited. Brookings Pap. Econ. Activity, 23(2): 1-60.

Olaniyan, D.A. and Okemakinde, T. 2008. Human capital theory: implications for educational development. Eur. J. Sci. Res., 24(2): 157-162.

Papyrakis, E. and Gerlagh, R. 2004. The resource curse hypothesis and its transmission channels. J. Comp. Econ., 32(1): 181-193

Schou, P. 2000. Polluting non-renewable resources and growth. Environ. Resour. Econ., 16(2): 211-227.

Schultz, T. W. 1961. Investment in human capital. Am. Econ. Rev., 51(1): 1-17.

Solow, R. 1974. Intergenerational equity and exhaustible resources. Rev. Econ. Stud., 41(5): 29-45.

Stiglitz, J.E. 1974. Growth with exhaustible natural resources: the competitive economy. Rev. Econ. Stud., 41(5): 139-152.

Swinton, S.M. and Quiroz, R. 2003. Is poverty to blame for soil, pasture, and forest degradation in Peru's altiplano? World Dev., 31(1): 1903-1919.

Torras, M. and Boyce, J. 1998. Income, inequality, and pollution: a reassessment of the environmental Kuznets curve. Ecol. Econ., 25(2): 147-160.

Wells, L.T. 1972. The Product Life Cycle and International Trade. Division of Research, Graduate School of Business Administration, Harvard University, Boston.

## ORCID DETAILS OF THE AUTHORS

Md. Raghib Nadeem: https://orcid.org/0000-0001-8138-3450

# A Review of Deep Transfer Learning Strategy for Energy Forecasting

**S. Siva Sankari\* and P. Senthil Kumar\*\*†**

\*School of Computer Science and Engineering, Vellore Institute of Technology, Vellore, Tamil Nadu, India

\*\*School of Computer Science Engineering and Information Systems, Vellore Institute of Technology, Vellore, Tamil Nadu, India

†Corresponding author: Senthil Kumar Paramasivan; senthilkumarpresearch@gmail.com

## ABSTRACT

Over the past decades, energy forecasting has attracted many researchers. The electrification of the modern world influences the necessity of electricity load, wind energy, and solar energy forecasting in power sectors. Energy demand increases with the increase in population. The energy has inherent characteristics like volatility and uncertainty. So, the design of accurate energy forecasting is a critical task. The electricity load, wind, and solar energy are important for maintaining the energy supply-demand equilibrium non-conventionally. Energy demand can be handled effectively using accurate load, wind, and solar energy forecasting. It helps to maintain a sustainable environment by meeting the energy requirements accurately. The limitation in the availability of sufficient data becomes a hindrance to achieving accurate energy forecasting. The transfer learning strategy supports overcoming the hindrance by transferring the knowledge from the models of similar domains where sufficient data is available for training. The present study focuses on the importance of energy forecasting, discusses the basics of transfer learning, and describes the significance of transfer learning in load forecasting, wind energy forecasting, and solar energy forecasting. It also explores the reviews of work done by various researchers in electricity load forecasting, wind energy forecasting, and solar energy forecasting. It explores how the researchers utilized the transfer learning concepts and overcame the limitations of designing accurate electricity load, wind energy, and solar energy forecasting models.

## INTRODUCTION

Nowadays, energy forecasting is the foundation for engineering and scientific researchers worldwide in energy sectors. The population increase will reach 9.8 billion in 2050; hence, the electricity demand will also exceed 38000 terawatt-hours every year (Veers et al. 2019). The energy demand increases with the increasing population. It imposes the necessity to forecast the energy demand in advance to sustain the economic growth of the country globally (Subbiah & Chinnappan 2020a). Electricity load, solar power, wind speed, and wind power forecasting are a part of energy forecasting. Many researchers have achieved this by developing various models using different technologies and considering various factors. The existing methodologies assume the dataset has sufficient data for training the model (Subbiah & Kumar 2022). In reality, sufficient data is unavailable for designing the forecast model in the newly built plants. To overcome this limitation, a transfer learning strategy is introduced that transfers the knowledge from the pre-trained model of a similar domain where sufficient data is available. It is hard to make sufficient data for energy

applications due to the two main challenges. One is the difficulty in accessing high-quality real-time data in large volumes; another is the possibility of negative knowledge transfer to the target domain from the source domain. Generally, energy forecasting is categorized into four major types: long-term, medium-term, short-term, and very short-term energy forecasting based on the forecasting duration (Subbiah & Chinnappan 2020b, Zor et al. 2017). Types of energy forecasting based on time horizon are shown in Table 1.

Energy forecasting is an important research area in the modern electric world. While searching the Scopus database with the keyword "energy forecasting" in the title, abstract, and the keyword of the documents indexed, it shows 35970 documents indexed from 2015 to 2022. It represents the number of documents indexed increases every year in Scopus 2603, 2998, 3299, 4035, 4881, 5157, 6010, and 6987 documents indexed in 2015, 2016, 2017, 2018, 2019, 2020, 2021, and 2022, respectively. Compared to 2015, there is a double of documents indexed in 2022. It represents the growing trend of research papers in the energy sector. Fig. 1 shows

Table 1: Types of energy forecasting based on time horizon.

| S. No. | Types of Energy Forecasting | Duration |
|---|---|---|
| 1. | Very Short Term Energy Forecasting | A minute to an hour |
| 2. | Short Term Energy Forecasting | An hour to a week |
| 3. | Medium Term Energy Forecasting | More than a week to a year |
| 4. | Long Term Energy Forecasting | More than a year |

the number of documents indexed in the Scopus database yearly. It demonstrates the significance and demand of energy forecasting.

In recent days, electricity load forecasting has been a trending research field. It is essential to sustain the reliability and the smooth functioning of the power system by balancing electricity demand with supply (Nazari-Heris et al. 2022). The electricity demand increases with the increase in population. Forecasting electricity demand is mandatory to satisfy the electricity demand with the supply (Fawaz et al. 2018, Subbiah et al. 2023, Weber et al. 2021). In electricity load forecasting, very short-term load forecasting represents a minute to an hour level forecasting. It is essential for controlling automatic electricity generation. Short-term load forecasting represents more than an hour to a week level forecasting (Subbiah & Chinnappan 2022b). It is useful for making the unit commitment and economical electricity dispatch plans in the power system. The medium-term load forecasting represents more than a week-to-month level of forecasting (Subbiah & Chinnappan 2022c). It is important for the preparation of effective scheduling of fuel requirements, electricity generation, electricity transmission,

and electricity maintenance (Kumar 2017). Long-term electricity load forecasting represents more than a month to a year (Subbiah & Chinnappan 2020b, Subbiah & Chinnappan 2021). It is essential for the installment of the new power plants and also for the extension of the power systems.

The accurate load forecasting of any region is achievable with the history of load demand and the correlated features to load in large volumes without any incompleteness (Yin et al. 2021). However, these details are not available completely for all the regions in the real world. In such cases, the transfer learning-like concepts can be applied to forecast the accurate load for those regions by transferring the knowledge from other models of similar regions where the complete details are available (Chen et al. 2021). The time series load has an intrinsic time-varying behavior. So, there may be much variation among the historical and new data. It has only one temporal dimension. The recorded load data from different domains can share some common features. So, the models constructed for one problem with large data can be adaptable to the different related problems with limited data in load forecasting.

In the modern era, energy from solar and wind sources is an important renewable energy source. Solar and wind energy generation increases due to its dramatic benefit of maintaining a pollution-free society and securing the environment by reducing carbon emissions and considering the depletion of fossil fuels. The developing countries also started to release a plan for future energy demand using renewable energy sources like solar and wind (Oh et al. 2022). Many governments have started investigating clean and green renewable energy sources due to the rapid global
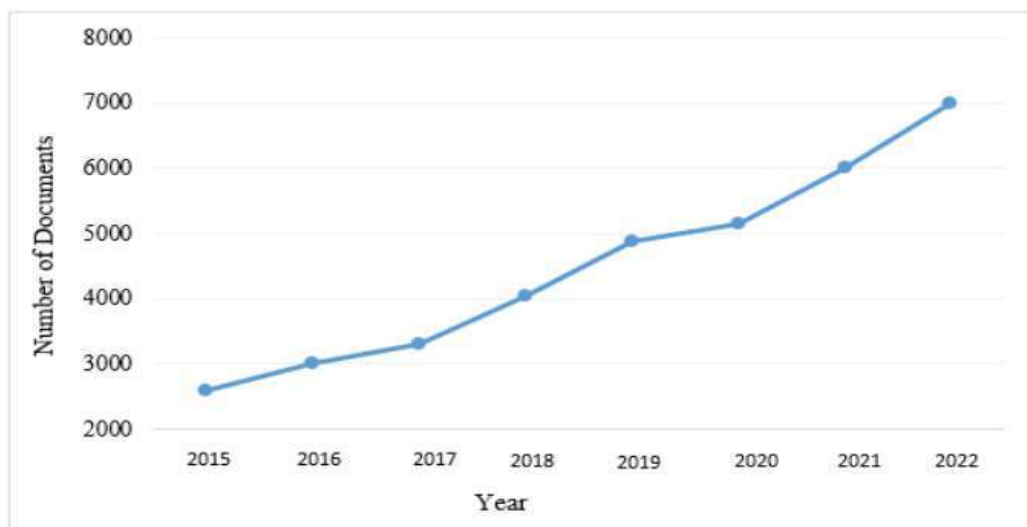


Fig. 1: Number of energy forecasting documents from 2015 to 2022.

warming and weather changes. Wind and solar energy sources got special attention for satisfying future energy demands naturally (Manandhar et al. 2023).

Wind energy is a widely utilized energy source. Wind energy has a volatile and uncertain nature. So, the accurate prediction of the wind energy depends on the accurate wind speed prediction (Yin et al. 2021). Researchers utilize physical, conventional, and artificial intelligence models for wind speed forecasting. They produced good prediction results when sufficient data was available for training the models (Ye & Dai 2018). With limited data, the performance of these models is poor. The newly built wind form has no historical data for predicting wind speed.

Similarly, some wind farms may have incomplete and less quality data. So, the researchers utilized the transfer learning concepts to forecast the wind speed for the newly built wind farm and the poor data wind farm. Transfer learning is a powerful concept used to train the new model for related real-world problems. It transfers the knowledge learned from the already trained models to build a model for another different but related problem (Hu et al. 2016).

Solar energy is a powerful alternative to conventional sources of energy nowadays. The earth receives an average of 1367 W.m$^{-2}$ of solar irradiance. It can be utilized to produce 1.74 × 1017 W yearly. This energy is sufficient for global residential, industrial, and commercial requirements. So, solar energy is important in satisfying future energy demand (Kumari & Toshniwal 2021). The planning of the solar plant photo-voltaic (PV) energy production necessitates accurate power demand in advance. People moving towards cities increases the population in urban areas. It triggers the urban areas from moving gradually into smart cities. Digitization is mandatory for automating life in smart cities. It increases the electricity demand, increasing the demand for electricity forecasting. Global warming introduces a new source like solar for electricity generation. The non-conventional solar power generation secures life in smart cities by reducing carbon emissions and utilizing solar energy for power generation. It also provides a pollution-free environment and protects human life in urban areas (Sarmas et al. 2022). Solar panels and plants can be installed easily in domestic neighborhoods to meet this energy demand with supply. The solar power plant utilizes solar radiance as an important parameter for determining photo-voltaic power. The solar radiance depends on meteorological variables (Kumari & Toshniwal 2021). Considering weather factors with PV power data guarantees improved solar power generation forecasting.

## SIGNIFICANCE OF TRANSFER LEARNING

Recently, transfer learning emerged as a powerful strategy for training the new model to related real-world problems (Hooshmand & Sharma 2019). The Scopus database shows the significance of transfer learning. The last five years data from Scopus represents the rise of research documents in energy forecasting using transfer learning every year linearly. The search was done on Scopus to find many research documents indexed with the keywords "energy forecasting" and "transfer learning" in the title, abstract, and keyword. The search result provides 327 documents indexed from 2018
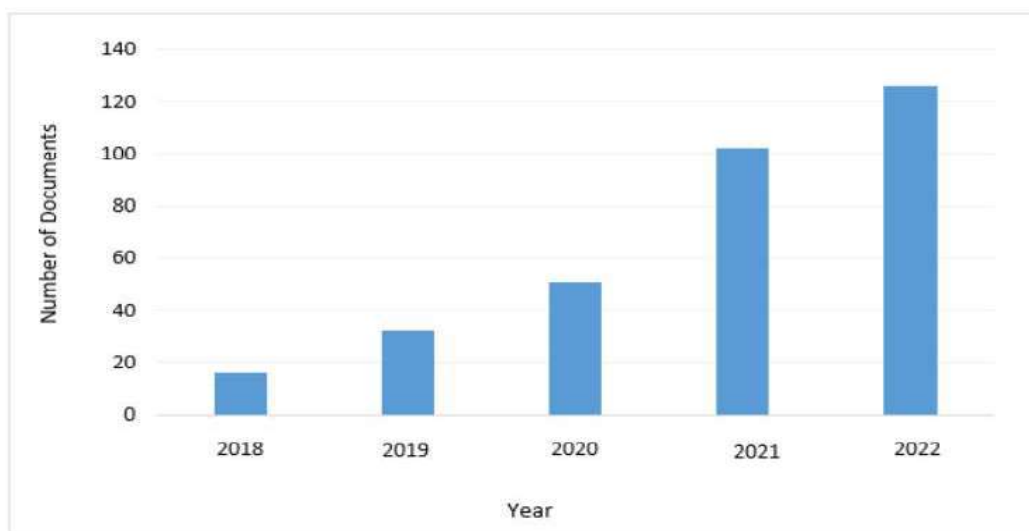


Fig. 2: Number of energy forecasting with transfer learning documents from 2018 to 2022.

to 2022. The number of papers indexed in 2018 is 16. But the papers indexed in 2019 show 32, which is the double of 2018. In 2020, 51 papers were indexed, and in 2021, 102 papers were indexed. In the last year, 2022, 126 papers were indexed. It is graphically shown in Fig. 2.

The Scopus database shows more documents published by China for energy forecasting using transfer learning, followed by the United States and India. The number of documents published by different countries is shown in Fig 3. The transfer learning strategy transfers the knowledge learned from already trained models to build a model for another different but related problem (Ye & Dai 2018, Tian et al. 2019, Qureshi et al. 2017). Fig. 4 shows the representation of transfer learning. It represents the knowledge transfer from the model developed using a large amount of data to the model that has to be trained using limited data (Peng et al. 2022). Transfer learning can be applied in two ways, namely, the pre-trained model approach and the developed model approach. These models can be applied to the new problem and attain effective predictive analysis. The pre-trained model approach helps to use the already trained model fully as it is or as part of the trained model, or it tunes the trained model for solving related other real-world problems easily. The pre-trained model approach is classified into three types: selecting the model, reusing the model, and tuning the model (Fawaz et al. 2018).

The selecting model approach selects the best model from the already trained model pool. The reusing model approach uses the already trained model of the related problem as the initial point for the next problem. It may reuse the entire or part of the model in the second problem. The tuning model approach tunes the already trained model to optimize or generalize it for the next related problem. The developed model approach identifies a similar problem with enormous data and exhibits a strong relation with the input, output, and concept. Then, it develops a better model for that problem. After that, it uses this developed model for the new problem as it is or tunes some parameters in it and then applies for the new problem. Ye & Dai (2018) utilized the transfer learning concepts in time series forecasting. Fawaz et al. (2018) used Dynamic Time Wrapping (DTW) to find the similarity between the source and target data to select and transfer knowledge from the strong source data.

The selection of transfer learning strategies relies on data availability, the task, and the application domain. The strategy selection answers what part of knowledge to be transferred, when to transfer that knowledge, and how to transfer that knowledge to a similar new problem. Traditional transfer learning is categorized into three types, namely, inductive, transductive, and unsupervised transfer learning. The inductive category of transfer learning is well applied to problems with the same source and target domains. It transfers the learned knowledge from source to target for improving the target model instead of starting the learning from scratch. Transductive learning is applied to the problem with different but interrelated source and target domains. Hence, the source domain has many labeled data, whereas the target domain only has unlabeled data. Unsupervised learning is almost the same as inductive learning. But, it
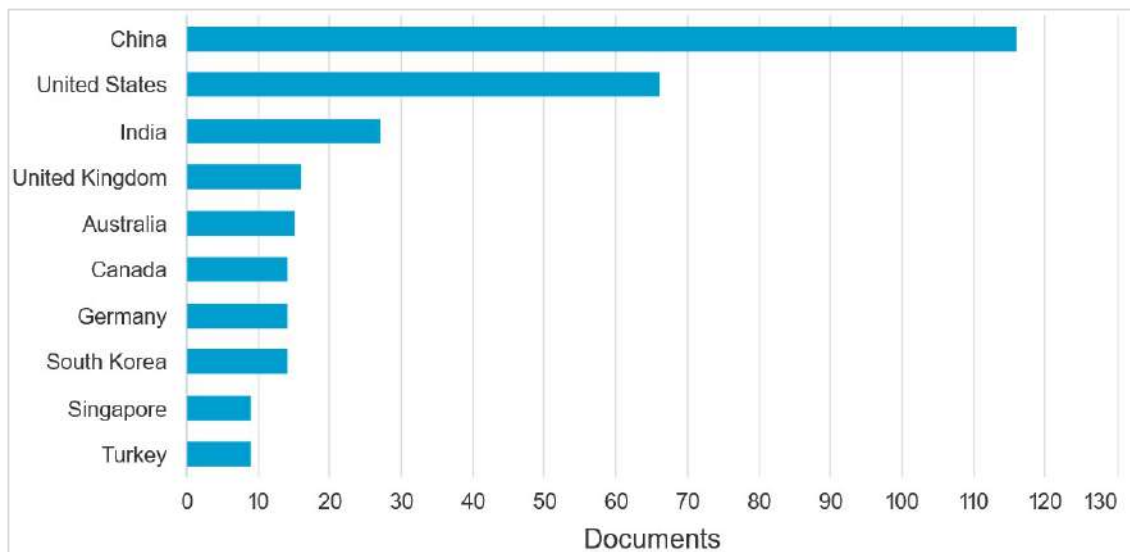


Fig. 3: Comparison of the number of energy forecasting with transfer learning documents from the Top 10 countries (2018 to 2022).
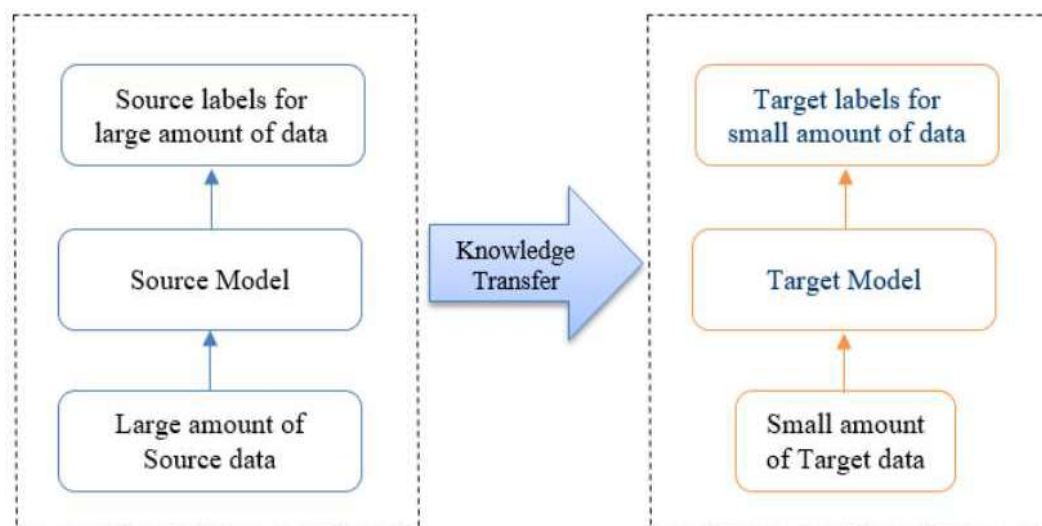
Fig. 4: Representation of transfer learning.

involves the unlabeled data in both the source and target domains (Tian et al. 2019).

Generally, there are two types of transfer learning, homogeneous and heterogeneous, depending on the dependency of the source and target domain samples and the similarity between the domains. The homogeneous type of transfer learning is applied to the domains with the same feature space but a small difference in their marginal distributions. It may follow instance transferring or parameter transferring, feature representation transferring, or rational knowledge transferring techniques from source to target for better target domain model performance. The instance transfer is done at an instance level from a source with large data and a target with limited data.

The parameter transfer is done at the model or parameter level from source to target. It creates many source learners and optimizes them by combining them like an ensemble method, and finally, it uses this learned knowledge to enhance the target learner's performance. At the feature level, the feature representation transferring is performed. It transfers the features from the source to the target or transforms the source and target features to the common feature space and then uses these features for the target domain. Rational knowledge transfer utilizes the source and target domains' relationship to transfer knowledge (Wu et al. 2022). It transfers the relationships learned from the source as a rule to the target domain. Heterogeneous transfer learning is applied to perform the interrelated or cross-domain task in the target domain (Hooshmand & Sharma 2019, Jin et al. 2022).

Machine learning with a transfer learning process enhances the learning process and model performance compared to machine learning without transfer learning (Ye & Dai 2022). The learning models are constructed by learning only the set of data provided as an input to that model. The constructed model becomes inefficient if the data is limited and incomplete (Kumar & Lopez 2016b). On the other hand, machine learning with the transfer learning concepts constructs an efficient model. First, the model with sufficient data is constructed. This is followed by the knowledge being transferred from the constructed model to the new one, which has insufficient information for training. Thus, the new model is constructed by getting information from the old model. The knowledge is transferred from the pre-trained model to the newly constructed model using the transfer learning concept. Thus, transfer learning with machine learning helps to build the electricity load forecasting, wind speed forecasting, wind power forecasting, and solar power forecasting models and also improves the performance of the forecasting models where insufficient data is available (Lu et al. 2022, Subbiah & Chinnappan 2022a).

## APPLICATIONS OF TRANSFER LEARNING

Transfer learning provides many benefits in developing machine learning and deep learning models. It is especially useful for saving resources and improving the efficiency of the model construction when a new model is trained (Gao et al. 2020, Khan et al. 2022). It can develop an efficient model with unlabeled data. Hence, every new model construction does not require a dataset with labeled data. A large volume of labeled data collection is required for accurate decision-making. But, in general, many applications in real-time suffer from limited labeled data. In such a case, transfer learning helps develop the model using sufficient labeled

data and then applies the same model to limited unlabeled data. Likewise, it helps a lot to save the training time of the model.

Similarly, constructing the learning model for complex real-time problems is tedious. Transfer learning helps to reduce this complexity by using a similar pre-trained model or simply taking it from scratch and redefining it. So, the knowledge can be transferred from the pre-trained model to the new model. Thus, the developers and decision makers take the knowledge from different models to fine-tune the model for the specific new problems easily (Jin et al. 2022). To enhance the new model, the parameters can also be transferred from the already developed models to the newly constructed ones (Hu et al. 2016).

The applications of transfer learning also include image classification, gaming, sentiment analysis, spam filtering, natural language processing, computer vision, the autonomous driving industry, the healthcare sector, the energy sector, and the e-commerce industry (Cao et al. 2018, Karmel et al. 2018, Kiruthika et al. 2014, Kumar 2019, Kumar & Lopez 2015, Kumar & Lopez 2016a, Swaroop et al. 2014). In recent research, the transfer learning concept was widely utilized in image recognition tasks. In image classification, the neural network is trained using many images to identify objects effectively. But it is a tedious and time-consuming task. The introduction of transfer learning greatly reduces the training time of the neural network by pre-training the model using ImageNet. Especially in medical image processing, kidney problems are identified from the ultrasound images by pre-training the CNN using ImageNet. Likewise, the model constructed using MR scans can be utilized for analyzing the CT scans. Transfer learning is also footprinted in gaming applications to develop new games easily by utilizing the pre-trained model of the existing game. Whenever a new game is developed, it is necessary to learn new algorithms and techniques for the new game. The transfer learning helps to understand the tactics learned from the older version or the existing game similar to the new game. In sentiment analysis, transfer learning analyzes customer behaviors and sentiments well. From the social media posting, the emotions of the customers are learned and transferred to analyze the behavior of the customer (Gomez-Rosero et al. 2021, Paramasivan 2021, Sivasankari & Baggiya Lakshmi 2016, Wang et al. 2020,). Solar panel defect detection can also be done by processing the solar panel images using MobileNetv2, ResNetv1, and inceptionv3 with pre-trained models (Zyout & Oatawneh 2020). Building the forecast model with limited samples may not provide an accurate result in energy forecasting. Similarly, the newly built plants do not have the historical data for training and building the forecast model. The transfer learning strategy is a gracious gift for the researchers to enhance the accuracy of energy forecasting with limited data.

## TRANSFER LEARNING IN LOAD FORECASTING

In the modern era, many researchers released the electricity load forecasting models for the newly built power plants using transfer learning concepts. This section reveals the research using the transfer learning concept for electricity load forecasting. Zhang & Luo (2015) presented short-term load forecasting using the Gaussian process and transfer learning. It introduces the automatic source task selection algorithm for finding the suitable source task for the target task. It experiments on the 12 nearby cities of Jiangxi province of China power load data. The presented model performs better and reduces the computational complexity by using the transferred knowledge from neighboring cities, avoiding transferring negative knowledge using the source task selection algorithm and replacing matrix inverse operations with smaller matrix orders. Lu et al. (2022) introduced the model using mixup and transfer learning concepts for short-term load forecasting. It performs the data enhancement using a mixup and avoids overfitting using transfer learning. It transfers the load of the users whose consumption load patterns are the same and enhances the generalization capability of the load forecasting model. The similarity of the load patterns is identified using the maximal information coefficient (MIC), and the forecasting was done using long short-term memory (LSTM). The simulation results showed that the deep learning-based LSTM model and a transfer learning concept proved better in forecasting the short-term load.

Jung et al. (2020) presented a monthly load forecasting model using a deep neural network. The authors enhanced the forecasting accuracy by adapting the transfer learning strategy. The experiment was done in a Tensorflow 1.13.1 environment using 14 years of monthly electricity load of 25 districts in Seoul. The population, weather, and calendar features are considered along with load data. Pearson Correlation Coefficient (PCC) extracts similar load patterns from other district datasets.

Consequently, load forecasting was done using deep neural network (DNN) with the top 10 similar domain transferred data, DNN with the top 20 similar domain transferred data, and DNN with the top 30 similar domain transferred data. The result shows that the DNN with the transfer learning attained an improved forecast compared to baseline DNN, Random Forest (RF), Multiple Linear Regression (MLR), and Extreme Gradient Boost (XGB). Jin et al. (2022) developed a model for predicting short-term

load using transfer learning concepts in deep learning. The parameter-based transfer learning is introduced in the hybrid convolution neural network-gated recurrent unit (CNN-GRU) model for improving load forecasting results. The knowledge from the model trained using the large dataset was transferred to the training model of the smaller dataset for performance enhancement. The solve-the-equation was utilized to find the data distribution bandwidth. The experiment used five years of commercial profile data from South Korea recorded hourly and one-year residential profile from the United States recorded hourly. The result shows that the CNN-GRU with transfer learning model outperformed back propagation (BP), LSTM, CNN-LSTM, Linear Regression, and GRU models.

Table 2: Transfer learning in load forecasting.

| Sl. No. | Author | Dataset | Methodology | Remarks |
|---|---|---|---|---|
| 1. | Jin et al. (2022) | Commercial profile, South Korea (Hourly), Residential profile of United States | CNN-GRU with transfer learning (Parameter-based) | Parameter-based transfer learning solved limited data issues in the CNN-GRU model and guaranteed improved accuracy and reliability. |
| 2. | Jung et al. (2020) | 25 districts monthly electric load in Seoul | Pearson correlation coefficient (PCC) + Deep neural network (DNN) | DNN with PCC transfer learning achieved better forecasting performance compared to basic DNN and other machine learning models MLR, RF, XGB |
| 3. | Zhang and Luo (2015) | Power load data of Jiangxi province of China (12 cities) | Gaussian process model with source task selection algorithm. Transfer Learning Gaussian Process (TLGP), Multi-task Gaussian Process (MTGP), Auto Regression (AR), Support Vector Machine with Particle Swarm Optimization (PSO-SVR) and Artificial Neural Network (ANN) | Achieved better accuracy with reduced time complexity using knowledge transfer from the neighboring cities, avoiding the transfer of negative knowledge using source task selection algorithm and replacing matrix inverse operations with smaller orders of matrix |
| 4. | Lu et al. (2022) | - | Mixup and Transfer learning concepts. Maximal information coefficient + long short term memory (MIC+LSTM) | LSTM with transfer learning enhanced the generalization ability and avoided the overfitting of the model |
| 5. | Gomez-Rosero et al. (2021) | Ten houses load consumption data from London-Ontario | Deep neural network with similarity-centered architecture evolution search (DNN-SCAES) | DNN-SCAES achieved an improved accuracy compared to the feed-forward neural network, LSTM one shot, and vanilla LSTM |
| 6. | Xu and Meng (2020) | USA (20 states) and Australia (5 states) electric load data | Time series decomposition-based hybrid transfer learning | A model with similar location data improved the electric load prediction by 30%. Negative transferring is also avoided by using time series seasonal decomposition. |
| 7. | Lee and Rhee (2021) | Residential dataset: Korean Non-residential dataset: substation electric load dataset - UCI repository | Deep neural network with transfer learning and Model-Agnostic Meta-Learning (MAML) | DNN with transfer learning and MAML achieved better results than ARIMA, traditional individual learning approach, and one-for-all models (MLP, XGB, LSTM, Seq2Seq, and ResNet/LSTM). |
| 8. | Ribeiro et al. (2018) | Energy consumption and weather data of 4 school buildings data for 3 years | Hephaestus- Novel transfer learning method | Hephaestus handled multi-feature time series data and improved the performance by 11.2% using other schools' data. |
| 9. | Cai et al. (2019) | ISO New England, GEFCom 2012 | Two-layer transfer-learning-based gradient boosting decision trees (TL-GBDT) | TL-GBDT achieved better forecasting results, especially with limited historical load data. |
| 10. | Mocanu et al. (2016) | Load profiles of residential and commercial buildings: Baltimore Gas and Electric Company | Reinforcement and Deep belief networks (DBN) with cross-building transfer | Cross-building transferred knowledge with Reinforcement, and DBN achieved better forecasting accuracy |
| 11. | Gaucher et al. (2021) | National Data: UK- Semi-hourly electricity, temperature and smart meter data | Generalized additive models and Random Forest | The transferring of the multi-scale information by aggregating the experts enhanced forecasting results. |

Gomez-Rosero et al. (2021) developed the model for residential load forecasting. The authors handled the challenges of residential load forecasting by expanding the demand response program and using transfer learning concepts. The multiple household electricity load consumption data was utilized to forecast the neighboring house load consumption. It uses the evolutionary algorithm named similarity-centered neural architecture search. This evolution search keeps the centremost house load consumption patterns. Then, it adjusts the weight of each other houses in the multi-house collection from their neighboring houses. The experiment used electricity load consumption data from 10 houses in London and Ontario. The simulation results showed that the developed model improved performance for the large dataset compared to the feed-forward neural network, LSTM one shot, and vanilla LSTM.

Xu & Meng (2020) presented hybrid short-term load forecasting using decomposition and transfer learning concepts. After decomposition, the seasonal and trend components are processed using machine learning methods. The irregular components are handled by using the two-stage transfer regression model. The presented model handles the issues related to transfer learning well by avoiding negative transfers. It acquires knowledge from other locations' electric load data and improves the interpretation capability of the electric load time series seasonal cycles. The model handles well the scalability issues with the dataset. The model was tested using the USA (20 States) and Australia (5 States) electric load data. The result confirms that the model attained an improvement in forecasting accuracy. Lee & Rhee (2021) designed a deep neural network model with meta-learning and transfer-learning concepts to improve the short-term load forecast outcome. The authors designed and tested the model using the residential and non-residential electricity load data. The model improved compared to Autoregressive Integrated Moving Average (ARIMA), the traditional individual learning approach, and one-for-all models (multilayer perceptron, XGB, LSTM, Seq2Seq, and ResNet/LSTM). Table 2 shows the review of transfer learning in load forecasting.

## TRANSFER LEARNING IN WIND ENERGY FORECASTING

Many researchers in the past decade developed wind speed forecasting models using physical, statistical, machine learning, and deep learning models. Hanifi et al. 2020 explored the related work done by researchers in wind power forecasting using physical, statistical, and hybrid models. Maldonado-Correa et al. (2021) reviewed the developed wind power forecasting models using artificial intelligence.

Lee et al. (2020) designed a deep neural network using long short-term memory and proved that LSTM guarantees an improvement in the wind power forecast compared to SVR and ANN. Yang et al. (2021) designed a wind power prediction model that classified the turbines by introducing the fuzzy C-means clustering algorithm and predicted the wind power generation using power curves. The model reduced complexity and improved the prediction accuracy. Researchers utilize transfer learning strategies to improve wind speed and wind power forecasting.

This section reviews the related research work done by researchers in wind speed forecasting using a transfer learning strategy. Yin et al. (2021) introduced a network-based deep transfer learning model to forecast the multi-step wind speed. The author utilized the wind and meteorological data collected from six wind farms. The model extracts the temporal and meteorological features in the pre-training stage using CNN and LSTM. It is achieved by connecting many CNNs in parallel to the LSTM in a serial manner. It forms a serio-parallel CNNs-LSTM (CL) extractor. The sound-trained CL extractor parameters are partially transferred to the target wind farm at the transfer training stage. The crisscross optimization is also implemented to fully connect layer parameters. The deep learning models CNNs-LSTM with parameter-based transfer learning achieved promising forecasting results.

Hu et al. (2016) used DNN with a transfer learning strategy for designing a short-term wind speed forecasting model. First, the model is trained using the data from an existing data-rich wind farm. Then, the author transfers the details from the data-rich wind farms to the newly built wind farm to fine-tune the deep neural network. Chen et al. (2021) developed a short-term wind speed model using bidirectional gated recurrent units and parameter-based transfer learning. First, the model is pre-trained using large volumes of source wind farm data. Then, it was fine-tuned in the target wind farm with limited data using parameter-based transfer learning. As a result, the model achieved better wind speed forecasting accuracy for the newly built target wind farm in China with less training time.

Wang et al. (2020) introduced the wind speed forecasting model using Convolutional Neural Network (CNN) and Parameter-based transfer learning. It considered the special and temporal information between three wind farms in China. The CNN migrates the fluctuation in the wind speed, and the transfer learning strategy shares the trained model parameter to the newly built wind farm (limited data) from the wind farm, which has sufficient data. The result shows that the CNN with parameter-based transfer learning offers a better wind speed forecasting result than the kernel

ridge regression, CNN, and SVR. Qureshi & Khan (2019) presented a short-term wind power forecasting model using adaptive transfer learning. The author transferred knowledge from different domains like wind speed and wind power and also from different regions. Hence, the author utilized the transferred knowledge for an effective weight initialization and better learning of the input for the deep neural network. The author proved the ATL-DNN model attained better forecasting results.

Liang et al. (2022) designed a wind speed forecasting model using the wind speed and meteorological data collected in one-hour intervals from 18 wind farms in Hebei province, China. The author constructed and trained the dilated CNN & BiLSTM model offline by fusing the multifaceted features. Then, the model was transferred to the new target wind farm, and the prediction was done online. The model performance is also improved by introducing the multi-objective grasshopper optimization algorithm during prediction. The author compared the model performance against the state-of-the-art baseline models and proved that transfer learning greatly helped improve wind speed

forecasting accuracy. Table 3 summarizes the related work done in wind speed and wind energy forecasting with transfer learning.

## TRANSFER LEARNING IN SOLAR ENERGY FORECASTING

Many researchers developed solar power forecasting models using physical and statistical models. After the introduction and advancement of artificial intelligence methods, machine learning models were introduced. Recently, deep learning-based deep neural network models were designed & forecasted for solar power generation. Researchers achieved better forecast results with deep learning models compared to other models. But still, there is a lack of achieving an accurate solar power forecast with limited data for training the models.

The transfer learning strategy strongly supports these kinds of limited data and training issues by transferring knowledge from other pre-trained models. Table 4 shows the review of transfer learning in solar power forecasting. Sarmas et al. (2022) developed a model for solar power forecasting

Table 3: Review of transfer learning in wind energy forecasting.

| Sl.No | Author | Dataset | Methodology | Remarks |
|---|---|---|---|---|
| 1. | Yin et al. (2021) | Six wind farms from Inner Mongolia and China | CNNs-LSTM with transfer learning | Spatio-temporal coupling details from the source wind form improve the forecasting performance of the target wind farm with limited training data. The deep learning model CNNs-LSTM with parameter-based transfer learning achieved promising forecasting results. |
| 2. | Hu et al. (2016) | Wind Speed data from Ningxia, Jilin, Inner Mongolia, and Gansu | Deep neural network with transfer learning | Reduced the wind speed forecasting error for a newly built wind form by transferring the details to the new wind form from an existing wind farm using transfer learning. |
| 3. | Chen et al. (2021) | Power and meteorological data from two wind farms in China (Zhejiang Province) | Bidirectional gated recurrent unit & Parameter transfer learning | Achieved a better wind speed forecasting accuracy for the newly built target wind farm in China with less training time |
| 4. | Wang et al. (2020) | Wind speed data from China (3 commercial wind farms) | CNN & Parameter-based transfer learning | CNN with Parameter transfer learning offers a better wind speed forecasting result by learning the wind speed fluctuations and transferring the trained model parameters of the wind farm with sufficient data to the newly built wind farm. |
| 5. | Cao et al. (2018) | Wind power data - China | Jaya Extreme Gradient Boosting (Jaya-XGBoost) with KNN | KNN selects highly relevant historical data from the neighboring wind farms. Jaya-XGBoost with KNN achieved better wind speed forecasting results than SVM, LASSO, and NN. |
| 6. | Qureshi and Khan (2019) | Wind power and weather data from the European-Center of Medium-range Weather-Forecasts | ATL-DNN: Adaptive Transfer Learning in Deep Neural Networks | Attained better wind power forecast by transferring knowledge from different domains and regions. |
| 7. | Liang et al. (2022) | Meteorological and wind speed data from 18 wind forms in Hebei province | CNN & BiLSTM with multifaceted feature fusion & transfer learning | The training is performed offline, and the prediction is performed online. The dilated CNN & BiLSTM learned the wind speed characteristics offline using multifaceted features, transferred the model, and improved the prediction accuracy using a multi-objective grasshopper optimization algorithm. |

using Stacked Long Short Term Memory (Stacked LSTM) and a transfer learning strategy. The author introduced three transfer learning strategies with Stacked LSTM to reduce the forecast error and improve accuracy. In the first strategy, the author fixed the network layers' weight. In the second strategy, the author utilized data from the target domain and fine-tuned the network layers' weight. The author used the target domain data in the third strategy and trained the layers' weight. Finally, the stacked LSTM model with transfer learning of three strategies is compared against the Stacked LSTM without transfer learning. The results show the Stacked LSTM with transfer learning outgunned the Stacked LSTM without transfer learning by producing a 12.6% improvement in accuracy.

Goswami et al. (2022) introduced a short-term solar energy forecast model using a Bidirectional Gated Recurrent Unit (BGRU) with transfer learning. The transfer learning-based BGRU utilizes fewer parameters by 39.6% and reduces training time by 76.1% compared to the site-specific BGRU model. The output of the photo-voltaic cells in solar panels has a proportional relationship with GHI (Global Horizontal Irradiance). The author used solar irradiation data from 6 stations (Chennai, Howrah, Guntur, Kotada Pitha, Ajmer & Dehradun) to experiment with BGRU and T-BGRU. The results show the TGRU improved the solar energy forecast output with less training time than BGRU. Sheng et al. (2022) introduced a transfer support vector regressor (Tr-SVR) for solar energy forecasting, combining SVR and transfer learning concepts to improve the solar forecast result. It also reduces the negative knowledge transfer and long-term dependencies between source and target stations by introducing a novel weighting model. Solar irradiation, temperature, wind speed, and other photovoltaic energy forecast features from four datasets were utilized for the experimental purpose. The results show the Tr-SVR outperformed ANN, SVR, Gaussian Mixture Regression (GMR), and Extreme Learning Machine (ELM) models.

Table 4: Review of transfer learning in solar energy forecasting.

| Sl. No. | Author | Dataset | Methodology | Remarks |
|---|---|---|---|---|
| 1. | Sarmas et al. (2022) | Portuguese energy community - PV production data Copernicus Atmosphere Data Store - Weather data | Stacked LSTM with a transfer learning strategy | Transfer learning was utilized for weight initialization and feature extraction for the newly built solar plant. With the transfer learning strategy stacked, LSTM attained a better solar power forecast for the target plant with the scarcity of data. |
| 2. | Manandhar et al. (2023) | ARM: Atmospheric Radiation Measurement dataset | AlexNet and ResNet-101 | The deep learning-based Alexnet and ResNet-101 extracted the required knowledge, like convolution features, from Total Sky-Imager images. It reduced the time taken for training and the resources required for modeling. |
| 3. | Goswami et al. (2022) | Solar irradiation data from 6 stations: Chennai, Howrah, Guntur, Kotada Pitha, Ajmer, and Dehradun | T-BGRU: Bidirectional Gated Recurrent Unit (BGRU) with transfer learning | T-BGRU achieved better solar energy forecasting and reduced training time of 76.1% compared to BGRU |
| 4. | Sheng et al. (2022) | Dataset D1 & D2: Nanya Technologic University-Microgrid lab Dataset D3: Nanya Technologic University of JTC CleanTech One Dataset D4: Solar Radiation Research Laboratory | Transfer Support Vector Regression (Tr-SVR) | D2, D3, and D4 are utilized as source datasets. D1 is utilized as the target dataset. Tr-SVR utilizes a novel weighting model to block negative knowledge by combining the source & target datasets and only transfers the positive knowledge from the source to the target model. The model achieved better solar energy forecasts and reduced the forecast error. |
| 5. | Luo et al. (2022) | Australia - PV plant installation parameters European Center for Medium-range Weather Forecasts - weather features | Constraint long short-term memory with parameter-based transfer learning | Transfer learning with C-LSTM improved the stability and accuracy of solar power forecast |
| 6. | Miraftabzadeh et al. (2023) | Hourly recorded photovoltaic power output, humidity, and ambient temperature of two PV plants (located within 1.25km proximity) | Long short-term memory with transfer learning | LSTM with transferred knowledge achieved a better day ahead PV power prediction. Numerical results represent the importance of transfer learning for the newly installed PV power plants for stable functioning. |

Luo et al. (2022) presented a power generation forecasting model for a newly constructed solar plant using transfer learning with deep learning-based constraint LSTM (C-LSTM). The PV plant installation parameters and weather features were utilized for the simulation. The LSTM model was designed to forecast solar power, extracting prior knowledge using the K-nearest neighbor. The parameter-transferring strategies of two categories were introduced to

Table 5: Performance Metrics for Energy Forecasting.

| Sl.No | Performance Metrics | Formula |
|---|---|---|
| 1. | Mean Absolute Error (Zor et al. 2017) | $\frac{1}{n}\sum_{t=1}^{n}|y_t - f_t|$ |
| 2. | Mean Square Error (Zor et al. 2017) | $\frac{1}{n}\sum_{t=1}^{n}(y_t - f_t)^2$ |
| 3. | Root Mean Square Error (Zor et al. 2017) | $\sqrt{\frac{1}{n}\sum_{t=1}^{n}(y_t - f_t)^2}$ |
| 4. | Percentage Error (Subbiah & Chinnappan 2020a) | $\left(\frac{y_t - f_t}{y_t}\right) * 100$ |
| 5. | Mean Percentage Error (Subbiah & Chinnappan 2020a) | $\frac{1}{n}\sum_{t=1}^{n}\left(\frac{y_t - f_t}{y_t}\right) * 100$ |
| 6. | Mean Absolute Percentage Error (Zor et al. 2017) | $\frac{1}{n}\sum_{t=1}^{n}|PE|$ |
| 7. | Normalized Root Mean Square Error (Luo et al. 2022) | $\frac{RMSE}{\sum_{t=1}^{n} y_t}$ |
| 8. | Weighted Mean Absolute Percentage Error (Miraftabzadeh et al. 2023) | $\frac{\sum_{t=1}^{n}|f_t - y_t|}{\sum_{t=1}^{n}|y_t|} \times 100\%$ |
| 9. | Coefficient of Determination $R^2$ (Sarmas et al. 2022) | $1 - \frac{\sum_{t=1}^{n}(y_t - f_t)^2}{\sum_{t=1}^{n}(y_t - \bar{y})^2}$ |
| 10. | Mean Bias Error (MBE) (Sarmas et al. 2022) | $\frac{1}{N}\sum_{t=1}^{n}(y_t - f_t)$ |
| 11. | Forecast Skill Index (Sarmas et al. 2022) | $1 - \frac{RMSE_p}{RMSE_r}$ |
| 12. | Symmetric Mean Absolute Percentage Error (Subbiah & Chinnappan 2020a) | $\frac{abs(y_t - f_t)}{abs(y_t) + abs(f_t))}$ |

enhance Strategy 1, which transfers the network parameters of Layer 1 and Layer 2 to the target model and fine-tuning the layers in the target model. In the second strategy, the parameters of layer 1 and layer 2 are fixed. It fine-tunes the remaining layer parameters only in the target model. As a result, the C-LSTM with transfer learning produces a better forecast than the C-LSTM.

Miraftabzadeh et al. (2023) developed a day-ahead photovoltaic power forecasting model using LSTM and a transfer learning strategy. The PV power and weather features are utilized for forecasting the PV power using LSTM. The performance of the LSTM is improved by utilizing a transfer learning strategy. Manandhar et al. (2023) utilized the deep neural network-based AlexNet and ResNet-101 with pre-trained models for forecasting solar irradiance. The total sky imager images from the Atmospheric Radiation Measurement dataset were utilized for the model simulation. The result shows the AlexNet and ResNet-101 with transfer learning produced better solar irradiance forecasts and reduced training time and resource requirements.

## PERFORMANCE MEASURES

A variety of performance measures are utilized for determining the performance of forecasting and proving the superiority of the developed model. It also helps to represent the significance of the specific strategy in achieving better forecast results. The commonly utilized performance metrics in energy forecasting in literature by many researchers are given in Table 5. Let 'n' represents the number of samples in the dataset, 't' represents the time period, '$y_t$' represents the real observed energy, '$f_t$' represents the forecast energy, 'p' represents the developed model, and 'r' represents the baseline persistence model.

## CONCLUSION

The rapid growth of the population requires energy forecasting globally. The modernization, digitalization, automation, and electrification mandate the energy demand to be satisfied with supply in the future. Non-conventional clean and green renewable energy sources are the powerful energy sources identified by researchers and governments to meet the energy requirement, especially in urban areas, save people's lives, and protect the environment from pollution. However, the uncertain characteristics of the electricity load, wind speed, wind energy, and solar irradiation impose complications in achieving accurate energy forecasting. Researchers have reviewed energy forecasting for a long time to overcome the challenges, especially for applications with noisy and limited data. With the advent of transfer learning strategies,

forecasting with noisy and insufficient data achieved better accuracy. This paper reviewed the role of transfer learning in load forecasting, wind speed forecasting, wind power forecasting, and solar power forecasting. Parameter-based transfer learning was utilized by many researchers in energy forecasting. Many researchers utilized correlation measures for identifying similar plants for transferring knowledge to the target plants. The exploration of the review shows that machine learning and deep learning models with transfer learning strategy greatly help to achieve better energy forecasting results.

## REFERENCES

Cai, L., Gu, J. and Jin, Z. 2019. Two-layer transfer-learning-based architecture for short-term load forecasting. IEEE Trans. Ind. Inform., 16(3): 1722-1732.

Cao, L., Wang, L., Huang, C., Luo, X. and Wang, J. H. 2018. A transfer learning strategy for short-term wind power forecasting. 2018 Chinese Automation Congress (CAC), IEEE: 3070-3075.

Chen, W., Qi, W., Li, Y., Zhang, J., Zhu, F., Xie, D., Ru, W., Luo, G., Song, M. and Tang, F. 2021. Ultra-short-term wind power prediction based on bidirectional gated recurrent unit and transfer learning. Front. Energy Res., 16: 827.

Fawaz, H.I., Forestier, G., Idoumghar, L. and Muller, P.A. 2018. Transfer learning for time series classification. 2018 IEEE Int. Conf. Big Data: 1367-1376.

Gao, Y., Ruan, Y., Fan, C. and Yin, S. 2020. Deep learning and transfer learning models of energy consumption forecasting for a building with poor information data. Energy Build., 223: 110156.

Gaucher, S., Goude, Y. and Antoniadis, A. 2021. Hierarchical transfer learning with applications for electricity load forecasting. arXiv, 11: 632

Gomez-Rosero, S., Capretz, M.A. and Mir, S. 2021. Transfer learning by similarity-centered architecture evolution for multiple residential load forecasting. Smart Cities, 4(1): 217-240. (GOMEZ)

Goswami, S., Malakar, S., Ganguli, B. and Chakrabarti, A. 2022. A novel transfer learning-based short-term solar forecasting approach for India. Neural Comput. Appl., 34(19): 16829-16843.

Hanifi, S., Liu, X., Lin, V. and Lotfian, S. 2020. A critical review of wind power forecasting methods: Past, present and future. Energies, 13: 3764.

Hooshmand, A. and Sharma, R. 2019. Energy predictive models with limited data using transfer learning. Proc. ACM Int. Conf. Future Energy Syst., pp. 12-16. (HOOSHMAND)

Hu, Q., Zhang, R. and Zhou, Y. 2016. Transfer learning for short-term wind speed prediction with deep neural networks. Renew. Energy, 85: 83-95.

Jin, Y., Acquah, M. A., Seo, M. and Han, S. 2022. Short-term electric load prediction using transfer learning with interval estimate adjustment. Energy Build., 258: 111846.

Jung, S.M., Park, S., Jung, S.W. and Hwang, E. 2020. Monthly electric load forecasting using transfer learning for smart cities. Sustainability, 12(16): 6364.

Khan, M., Naeem, M.R., Al-Ammar, E.A., Ko, W., Vettikalladi, H. and Ahmad, I. 2022. Power forecasting of regional wind farms via variational auto-encoder and deep hybrid transfer learning. Electronics, 11(2): 206.

Kiruthika, V.G., Arutchudar, V. and Kumar, P.S. 2014. Highest humidity prediction using data mining techniques. Int. J. Appl. Eng. Res., 9(16): 3259-3264.

Kumar, P.S. 2017. A review of soft computing techniques in short-term load forecasting. Int. J. Appl. Eng. Res., 12(18): 7202-7206.

Kumar, P.S. and Lopez, D. 2015. Feature selection used for wind speed

forecasting with data-driven approaches. J. Eng. Sci. Technol. Rev., 8(5): 124-127.

Kumar, P.S. and Lopez, D. 2016a. Forecasting of wind speed using feature selection and neural networks. Int. J. Renew. Energy Res., 6(3): 833-837.

Kumar, P.S. 2019. Improved prediction of wind speed using machine learning. EAI Endorsed Trans. Energy Web, 6(23): 1-7.

Kumar, P.S. and Lopez, D. 2016b. A review of feature selection methods for high-dimensional data. Int. J. Eng. Technol., 8(2): 669-672.

Kumari, P. and Toshniwa, D. 2021. Deep learning models for solar irradiance forecasting: A comprehensive review. J. Clean. Prod., 318: 128566.

Lee, E. and Rhee, W. 2021. Individualized short-term electric load forecasting with deep neural network-based transfer learning and meta-learning. IEEE Access, 9: 15413-15425.

Lee, H., Kim, K., Jeong, H., Lee, H., Kim, H. and Park, J. 2020. A study on wind power forecasting using the LSTM method. Trans. Korean Inst. Electr. Eng., 69(8): 1157-1164.

Liang, T., Chen, C., Mei, C., Jing, Y. and Sun, H. 2022. A wind speed combination forecasting method based on multifaceted feature fusion and transfer learning for centralized control center. Electr. Power Syst. Res., 213: 108765.

Lu, Y., Wang, G. and Huang, S. 2022. A short-term load forecasting model based on mixup and transfer learning. Electr. Power Syst. Res., 207: 107837.

Luo, X., Zhang, D. and Zhu, X. 2022. Combining transfer learning and constrained long-term memory for power generation forecasting of newly-constructed photovoltaic plants. Renew. Energy, 185: 1062-1077.

Maldonado-Correa, J., Solano, J. and Rojas-Moncayo, M. 2021. Wind power forecasting: a systematic literature review. Wind Eng., 45(2): 413-426.

Manandhar, P., Temimi, M. and Aung, Z. 2023. Short-term solar radiation forecast using total sky imager via transfer learning. Energy Reports, 9: 819-828

Miraftabzadeh, S. M., Colombo, C. G., Longo, M. and Foiadelli, F. 2023. A day-ahead photovoltaic power prediction via transfer learning and deep neural networks. Forecasting, 5(1): 213-228.

Mocanu, E., Nguyen, P. H., Kling, W. L. and Gibescu, M. 2016. Energy Buildings, 116: 646-655.

Nazari-Heris, M., Asadi, S., Mohammadi-Ivatloo, B., Abdar, M., Jebelli, H. and Sadat-Mohammadi, M. eds. 2022. Appl. Mach. Learn. Deep Learn. Methods Power Syst. Probl. Springer.

Oh, J., Park, J., Ok, C., Ha, C. and Jun, H.B. 2022. Wind power forecasting model transfer learning approach. Electronics, 11(24): 4125.

Paramasivan, S.K. 2021. Deep learning RNNs enhance wind energy forecasting: Rev. Intell. Artif., 35(1): 1-10.

Peng, L., Wu, H., Gao, M., Yi, H., Xiong, Q., Yang, L. and Cheng, S. 2022. TLT: Recurrent Fine-Tuning Transfer Learning Water Quality Long-Term Prediction. Water Res., 225: 119171.

Qureshi, A.S., Khan, A., Zameer, A. and Usman, A. 2017. Wind Power Prediction DNN meta-regression transfer learning. Appl. Soft Comput., 58: 742-755.

Qureshi, A.S. and Khan, A. 2019. Adaptive Transfer Learning DNN Wind Power Prediction. Comput. Intell., 35(4): 088-1112.

Ribeiro, M., Grolinger, K., ElYamany, H.F., Higashino, W.A. and Capretz, M.A. 2018. Transfer learning cross-building energy forecasting. Energy Build., 165: 352-363.

Sarmas, E., Dimitropoulos, N., Marinakis, V., Mylona, Z. and Doukas, H. 2022. Transfer learning solar power forecasting data scarcity. Sci. Rep., 12(1): 14643.

Sheng, H., Ray, B., Shao, J., Lasantha, D. and Das, N. 2022. Generalization solar power yield modeling knowledge transfer. Expert Syst. Appl., 201: 116992.

Sivasankari, S. and Baggiya Lakshmi, T. 2016. Text mining tools big data. Int. J. Pharm. Technol., 8(2): 4087-4091.

Subbiah, S.S., Paramasivan, S. K., Arockiasamy, K., Senthivel, S. and Thangavel, M. 2023. Deep Learning Wind Speed Forecasting Bi-LSTM Selected Features. Intell. Autom. Soft Comput., 35(3): 3829-3844.

Subbiah, S. S. and Chinnappan, J. 2020a. Short-term load forecasting deep learning. Int. J. Emerg. Technol., 11(2): 378-384.

Subbiah, S.S. and Chinnappan, J. 2020b. Improved short-term load forecasting ranker feature selection. J. Intell. Fuzzy Syst., 39(5): 6783-6800.

Subbiah, S.S. and Chinnappan, J. 2021. Opportunities and challenges of feature selection methods for high dimensional data: A review. Ingén. Syst. d'Inform., 26(1): 67-77.

Subbiah, S.S. and Chinnappan, J. 2022a. A Review of Bio-Inspired Computational Intelligence Algorithms in Electricity Load Forecasting. CRC Press, Boca Raton, Florida: 169-192.

Subbiah, S.S. and Chinnappan, J. 2022b. Deep learning-based short-term load forecasting with hybrid feature selection. Elect. Power Syst. Res., 210: 108065.

Subbiah, S.S. and Chinnappan, J. 2022c. Short-term load forecasting using random forest with entropy-based feature selection. Artif. Intell. Technol. Lect. Notes Electr. Eng., 806: 73-80.

Subbiah, S.S. and Kumar, P. S. 2022. Deep learning-based load forecasting with decomposition and feature selection techniques. Journal of Scientific & Industrial Research, 81(5): 505-517.

Swaroop, G., Kumar, P.S. and Selvan, T.M. 2014. An efficient model for share market prediction using data mining techniques. Int. J. Appl. Energy Res., 9(17): 3807-3812.

Tian, Y., Sehovac, L. and Grolinger, K. 2019. Similarity-based chained transfer learning for energy forecasting with big data. IEEE Access, 7: 139895-139908.

Veers, P., Dykes, K., Lantz, E., Barth, S., Bottasso, C. L., Carlson, O., Clifton, A., Green, J., Green, P. and Holttinen, H. et al. 2019. Grand challenges in the science of wind energy. Science, 366(6464): 2027.

Wang, Z., Zhang, J., Zhang, Y., Huang, C. and Wang, L. 2020. Short-term wind speed forecasting based on information of neighboring wind farms. IEEE Access, 8:16760-16770.

Weber, M., Auch, M., Doblander, C., Mandl, P. and Jacobsen, H. A. 2021. Transfer learning with time series data: a systematic mapping study. IEEE Access, 9: 165409-165432.

Wu, D., Xu, Y. T., Jenkin, M., Wang, J., Li, H., Liu, X. and Dudek, G. 2022. Short-term load forecasting with deep boosting transfer regression. IEEE Access, 110: 5530-5536.

Xu, X. and Meng, Z. 2020. A hybrid transfer learning model for short-term electric load forecasting. Electr. Eng., 102(3): 1371-1381.

Yang, M., Shi, C. and Liu, H. 2021. Day-ahead wind power forecasting based on the clustering of equivalent power curves. Energy, 218: 119515.

Ye, R. and Dai, Q. 2018. A novel transfer learning framework for time series forecasting. Knowl. Syst., 156: 74-99.

Ye, R. and Dai, Q. 2022. A relationship-aligned transfer learning algorithm for time series forecasting. Inform. Sci., 593: 17-34.

Yin, H., Ou, Z., Fu, J., Cai, Y., Chen, S. and Meng, A. 2021. A novel transfer learning approach for wind power prediction based on a serio-parallel deep learning architecture. Energy, 234: 121271.

Zhang, Y. and Luo, G. 2015. Short-term power load prediction with knowledge transfer. Inform. Syst., 53: 161-169.

Zor, K., Timur, O., Çelik, O., Yıldırım, H. and Teke, A. 2017. Interpretation of Error Calculation Methods in the Context of Energy Forecasting. In 12th Conference on Sustainable Development of Energy, Water and Environment Systems, Dubrovnik, Croatia, IEEE, NY, pp. 722-731.

Zyout, I. and Oatawneh, A. 2020. Detection of PV solar panel surface defects using transfer learning of the deep convolutional neural networks. IEEE Access, 16: 1-4.

# Distribution and Concentration of Pb, Cd, and Hg Metals Due to Land Use Influence on Sediment in Malili River, East Luwu Regency

**Nurhasmiati Nurhasmiati*†, Muhammad Farid Samawi**, Mahatma Lanuru**, Paulina Taba***, Fahruddin Fahruddin**** and M. Tumpu*****

*Department of Management of the Environment, Hasanuddin University, Makassar, Indonesia
**Department of Marine Science, Faculty of Marine Science and Fisheries, Hasanuddin University, Makassar, Indonesia
***Department of Chemistry, Faculty of Mathematics and Natural Science, Hasanuddin University, Makassar, Indonesia
****Department of Biology, Faculty of Mathematics and Natural Science, Hasanuddin University, Makassar, Indonesia
*****Disaster Management Study Program, The Graduate School, Hasanuddin University, Makassar, Indonesia
†Corresponding author: Nurhasmiati; nurhasmiatidjuma4@gmail.com

## ABSTRACT

This research was conducted in the waters of Malili River, East Luwu Regency, with 4 observation points in Malili River East Luwu Regency, namely: (a) Southeast Sulawesi Sub Das (Point 1) namely Pongkeru village bridge, Coordinate point 12126.69'8°" E; (b) Larona Sub Das Karebbe basin bridge (Point 2), Coordinate point 12115.09'9°" E; (c) The meeting point of Larona sub-dash and Pongkeru sub-dash (Point 3), coordinate point 12159.64'8°" E; (d) Upper Malili River, Malili village, Malili bridge (Point 4), Coordinate point 12147.20'5°" E. Metal concentration and distribution were analyzed descriptively with the help of images (maps), graphs, and tables. Differences in Pb, Cd, and Hg metal concentrations in sediments between point locations were tested using analysis of variance (ANOVA) through the SPSS version 22 program. The relation between grain size, organic matter, and Pb, Cd, and Hg metal concentrations was tested using linear correlation. The results showed that the sediment content of Pb and Cd metal concentrations at each point location did not exceed NOAA (1999) quality standards. In the sediment, Hg metal concentration exceeds the quality standards of NOAA (1999) at each point, namely point 1. Pongkeru 0.590 µg.g$^{-1}$, point 2. Karebbe 0.229 µg.g$^{-1}$, point 3. Kawasule 0.514 µg.g$^{-1}$ and point 4. Malili 0.358 µg.g$^{-1}$. The relation between sediment size and Pb, Cd, and Hg metal concentrations at each point location has a weak correlation. The relation does not significantly affect the content of heavy metals in the sediment. It may be due to other factors, such as the source of heavy metal pollutants in each different point location. The relation between organic matter and the concentration of Pb, Cd, and Hg metals at each point location has a weak correlation. The relation does not significantly affect the content of heavy metals in the sediment because it may be due to different sources of heavy metal pollutants in each point location.

## INTRODUCTION

River water quality can be polluted if there are activities that impact river water quality, but if there is public awareness and active participation, river water quality can be maintained. One of the areas known for its waters is Malili. It is a water area that has experienced the biggest impact due to mining activities, namely in Sorowako mining activities of PT Vale, and in Pongkeru, there is the mining of PT CLM and several southeast Sulawesi companies. Not only that, along the river flow, there are also many forest land conversion activities into pepper plantations, illegal logging, and residential settlements (Prawita et al. 2008).

According to Government Regulation No. 38/2011 on Rivers, several things must be considered in managing

rivers, one of which is river boundaries. The government has regulated that river borders should not be planted with plants other than grass, and buildings should not be erected (Yogafanny 2015). Pollution and sedimentation are high due to supplies from the watershed, especially by mining activities, agriculture, and household waste, especially supplies from the Salonoa River, Angkona River, and Malili River (Ayyub et al. 2018). The Malili River estuary is experiencing an increase in sediment in the estuary (Lanuru & Syafyudin 2018).

The higher the population activity along the watershed, the higher the possibility of pollutants in the river. The content of Hg, Pb, and Cd is very dangerous if it is in water. The number of activities around the river is the cause of polluted river waters. Pollution in the waters can be in

the form of organic and inorganic compounds. Inorganic components can be heavy metals such as Pb, Cu, Zn, Cr, Ni, Hg, etc. The presence of heavy metals in the environment is considered dangerous because of their non-degradable nature. However, they are still often used in human activities, so their production is also increasing (Sumekar et al. 2015).

The presence of heavy metals in water can negatively impact human health, accumulating in body tissues. It can cause poisoning for humans if they exceed tolerance limits and accumulate in sediments and biota through bioconcentration, bioaccumulation, and biomagnification by aquatic organisms. According to Mahardika et al. (2012), heavy metals enter the waters as part of the suspension system in water and sediment through the process of absorption, deposition, and ion exchange. Heavy metals can accumulate in solids in waters, such as sediments. Sediment quality testing, especially on heavy metal parameters, is an important stage in assessing the quality of the aquatic environment.

Heavy metals from human and natural activities are distributed on sediment particles of different sizes. The distribution of heavy metals in various particle sizes is influenced by the formation of sediments both naturally and non-naturally. Particle size plays an important role in the distribution of heavy metals in sediments (Maslukah 2013). The many activities of land use change activities such as nickel ore mining exploitation, namely at PT Vale from the upper Larona sub-dash (Sorowako) and PT CLM and Southeast Sulawesi companies from the upper Pongkeru sub-dash (Southeast Sulawesi) and the existence of forest land conversion activities into pepper plantations, illegal logging, and residential settlements are vulnerable to river pollution in Malili, East Luwu district which can cause siltation, degradation of water quality, endanger aquatic biota and human health. This is the background for the research on "Distribution and Concentration of Pb, Cd and Hg Metals Due to the Effect of Land Use on Sediments in Malili River, East Luwu Regency."

## MATERIALS AND METHODS

### Research Area

This research was conducted in the waters of Malili River, East Luwu Regency, with 4 observation point locations in Malili River, East Luwu Regency, namely: (a) Southeast Sulawesi Sub Das (Point 1) namely Pongkeru village bridge, coordinate point 121°8'26.69" E; (b) Larona Sub Das Karebbe basin bridge (Point 2), coordinate point 121°9'15.09" E; (c) Larona Sub Das and Pongkeru Sub Das meeting point (Point 3), coordinate point 121°8'59.64" E; (d) Upper Malili River, Malili village, Malili bridge (Point 4), coordinate point 121°5'47.20" E.

### Sample Preparation and Method

Sediment sampling was carried out using an Eckman Grab with a depth of ± 10 cm with the valve teeth left open. After the tool reaches the bottom, the weight is released, which causes the valve to close tightly so that the substrate that has been trapped in the Eckman Grab cavity will not be released again. Then the tool is pulled up to the surface. Then a sediment sample was taken as much as 250 grams using a plastic spoon. To avoid contamination, only the center of the sediment in the Eckman Grab was taken to analyze heavy metal content in the laboratory. The temperature and pH of the sediment were measured immediately at the time of collection. The collected sample material was put into polyethylene plastic bags, stored in an ice box, and immediately brought to the laboratory. Wet samples were air-dried for 3 days. The dried sediment samples were crushed using a porcelain mortar and pestle. Samples that have been finely weighed as much as 0.2 grams are dissolved in concentrated $HNO_3$ to a volume of 10 mL and added $HClO_4$ as much as 0.5 mL, then heated in a water bath with a temperature of 80°C for 30 min, cooled and diluted with aquabidest to a volume of 50 mL, filtered with Whatman 42 filter paper, and then analyzed with an ICP machine (Afifah et al. 2019).

### Hg, Pb, and Cd Concentration Measurement

Hg, Pb, and Cd concentrations $\mu g/g = \frac{(D-E) \; x \; Fp \; x \; V}{W}$

Where:

D = sample concentration $\mu g/l$ from the ICP reading result

E = concentration of sample blank $\mu g/l$ from the ICP reading result

Fp = dilution factor

V = Final volume of sample solution prepared (mL), must be in units of liters.

W = sample weight (g)

### Measurement of Total Organic Matter in Sediments

BOT content was analyzed using the Loss On Ignition (LOI) method. Sediment samples were dried using an oven for 2×24 h/sample to dry at 105°C. Weigh the weight of the porcelain cup (Bc). Weigh the weight of the sediment sample in the oven as much as ± 5 grams and record it as the initial weight (Baw). The cup is in the oven to ensure that there is no residual water content in the cup so that during the high-temperature exposure, the cup does not break. Heating a porcelain cup containing 5 grams of sediment samples using a furnace at 550°C for approximately 3.5 h. After reaching

3.5 h, the sediment sample in the cup was removed from the furnace. Weigh back the sample in the cup in the furnace as the final weight (Bak).

The following formula was used to calculate the organic content of sediments (Lanuru 2004).

$$\text{Organic matter } (\%) = \frac{initial\ weight\ (g) - weight\ after\ ashing\ (g)}{initial\ weight\ (g)} \times 100\%$$

**Data Analysis**

The concentration and distribution of metals will be analyzed descriptively with the help of images (maps), graphs, and tables. Heavy metal concentrations at each point location will be compared with the 1999 NOAA standard (*Sediment Quality Guidelines developed for the National Status and Trends Program)*. Differences in Pb, Cd, and Hg metal concentrations in sediments between point locations are tested using analysis of variance (ANOVA) through the SPSS version 22 program. The relation between grain size, organic matter, and Pb, Cd and Hg metal concentrations was tested using linear correlation (Steel & Torrie 1991).

## RESULTS AND DISCUSSION

**Land Use**

The following results of the land use analysis in the Malili River basin of East Luwu Regency are presented in Fig. 1.

Land use in the Malili river basin of East Luwu district has many human activities, as seen in point 1. Southeast Sulawesi sub-basin, precisely the bridge of Pongkeru Village, activities around the waters are dry land farming, forests, and mining at point 2. Larona Sub-dash, to be precise, the Laskap Karebbe bridge, activities around the waters are settlements, forests, and dry land farming at point 3. Meeting of Larona Sub-Dash and Southeast Sulawesi Sub-Dash precisely in Kawasule Village, activities around the waters are rice fields, plantations, forests, and sand mining activities that cannot be read on the map at point 4. Upper Malili River, activities around the waters are residential areas, rice fields, dry land farming, plantations, and ponds.

The fact is that the use of land maps is closely related to various purposes, including watershed management, forestry engineering, soil and water conservation, settlement architecture, road networks, reclamation of degraded lands, and many other activities that require land information. This land use map shows what activities affect the surrounding river bodies so that pollution in the waters occurs.

Land use is very important for the government to know the land used by the community where the central and regional governments will know the most potential income
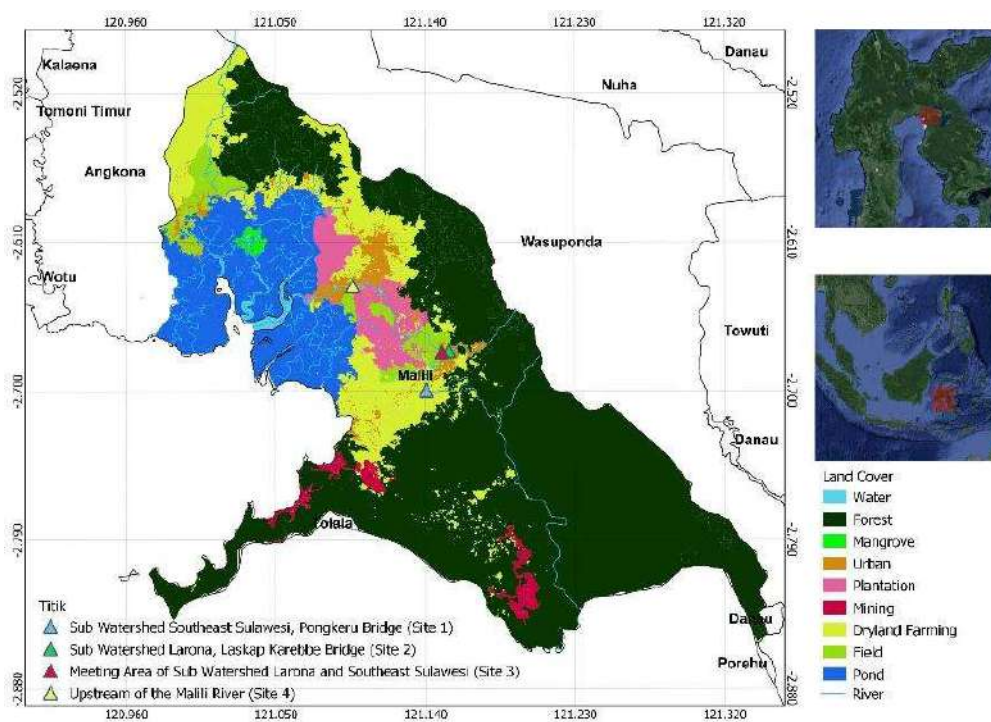


Fig. 1: Land Use Classification Map of East Luwu Regency 2022.

Table 1: Average concentration of heavy metal Pb at each location point.

| No. | Point (Repeat) | Concentration [μg.g⁻¹] | | | |
| --- | --- | --- | --- | --- | --- |
| | | Pongkeru | Karebbe | Kawasule | Malili |
| 1. | 1.1 | 1.195 | 2.847 | 2.812 | 4.419 |
| 2. | 1.2 | 4.560 | 2.567 | 2.497 | 4.612 |
| 3. | 1.3 | 5.701 | 1.672 | 2.639 | 4.479 |
| | Average | 3.819 | 2.362 | 2.694 | 4.503 |
| | Quality Standard | ERL 46.7 μg.g⁻¹ and ERM 218 μg.g⁻¹ | | | |

Source: Primary Data, 2023

in each region. The results obtained by using GIS in geo-governance studies, analyzing regional administrative maps, and combining data can be used to solve the critical environmental, social, and economic situations involved in land use management in each region.

**Concentration of Pb, Cd, and Hg Metals in Sediments**

Based on the results of the analysis of Pb, Cd, and Hg metals carried out at four points by conducting three replicates in the field can be seen in the discussion below by looking at the 1999 NOAA quality standards (*Sediment Quality Guidelines developed for the National Status and Trends Program).*

**Heavy metal lead (Pb):** Results of Pb metal testing in Malili river waters with four location points are presented in Table 1.

Based on Table 1. The average concentration of Pb metal at each point shows a concentration that does not exceed the quality standard, namely at Pongkeru 3,819 μg.g⁻¹, Karebbe 2,362 μg.g⁻¹, Kawasule 2,694 μg.g⁻¹ and Malili 4,503 μg.g⁻¹. It can be said that heavy metal Pb has not fully polluted each

point and is still far from the quality standard threshold limit of 46.7 μg.g⁻¹. The difference in each location point of heavy metal Pb can be seen in Fig. 2:

The highest result of Pb metal in each location point is in Malili, as much as 4,503 μg.g⁻¹. This Pb metal pollution is closely related to the many community activities, such as residential settlements located on the banks of the river and the existence of sales activities whose waste is discharged into the river, causing the high content of Pb in Malili. This is in accordance with the opinion of Ahmad et al. (2021), which states that heavy metal Pb pollution to the environment occurs due to a process that is closely related to the use of these metals in human activities and intentionally or unintentionally discharges various wastes containing heavy metals into the environment.

The high content of Pb in Malili is also due to the dense shipping activities of fishermen, such as painting ships on the riverbank and ships passing by also affect the high content of Pb metal in Malili. Zulfikar (2016) found that the highest value was obtained at the point 2 location with
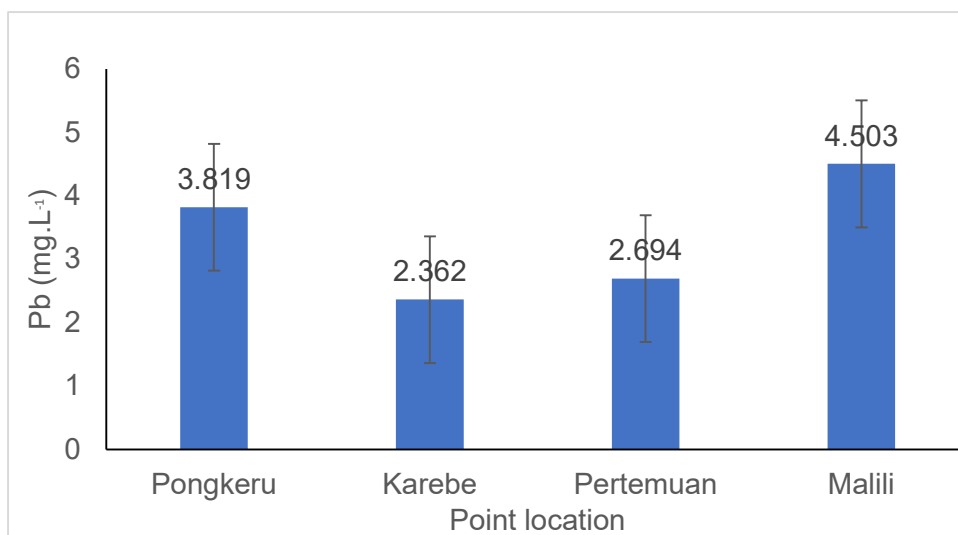


Fig. 2: Diagram of heavy metal Pb at each point.
Source: Primary data, 2023

an average Pb metal content of 22.96 μg.g$^{-1}$ due to ship and port activities, such as ship painting, ship refueling, and port waste that produces non-essential metals containing Pb elements from ship engines accidentally discharged into water bodies. According to Sumekar et al. (2015), the Pb content of the Dead River estuary is a place for fishermen who use motorized boats that may emit Pb-containing gases. Pb metal is often used as a mixture in fuel to increase octane value, although its use is starting to be reduced.

In Malili and Pongkeru, the results of Pb metal are not much different, namely 4,503 μg.g$^{-1}$ and 3,819 μg.g$^{-1}$. It can be said that the activities in Malili, namely residential areas and the number of fishing boats passing by to go to the sea, and in Pongkeru, namely the number of mining activities, are not significantly different. Based on the research of Budiastuti et al. (2016), the analysis of lead metal measurement results in Babon River sediments ranged from 4.17 mg.kg$^{-1}$ - 7.256 mg.kg$^{-1}$ of lead levels in sediments with no significant difference between sediment lead at sampling points in industrial areas and sampling points in residential areas. This is due to the nature of heavy metals that easily precipitate so that heavy metal lead has settled at the bottom of the waters. According to Putri et al. (2014), contamination from heavy metals in sediments will persist for a long period, even when the source of pollution is gone. Based on heavy metal data in sediments, past conditions can be studied and estimated the number of heavy metals accumulated in sediments.

The Pb metal content in Karebbe is low compared to other points at 2,362 μg.g$^{-1}$. The high dissolved oxygen at the location of point 2 is 6.2 ppm. The level of dissolved oxygen in the water strongly indicates pollution. Low DO values affect the toxicity of lead metal (Pb) (Budiastuti et al. 2016). In Karebbe and Kawasule, the results of Pb metal in Kawasule are also not much different, namely 2,694 μg.g$^{-1}$, because the distance between the waters of point 2 and point 3 is not too far. According to Wulandari et al. (2008), the current speed also affects the distribution of Pb and Cd metal concentrations.

**Heavy metal cadmium (Cd):** Based on the results of Cd

Table 2: Average concentration of heavy metal Cd at each location point.

| No. | Point (Repeat) | Concentration [μg.g$^{-1}$] | | | |
| --- | --- | --- | --- | --- | --- |
| | | Pongkeru | Karebbe | Kawasule | Malili |
| 1. | 1.1 | 0.021 | 0.044 | 0.020 | 0.040 |
| 2. | 1.2 | 0.044 | 0.038 | 0.023 | 0.036 |
| 3. | 1.3 | 0.068 | 0.031 | 0.019 | 0.043 |
| | Average | 0.044 | 0.038 | 0.021 | 0.040 |
| | Quality Standard | ERL 1.2 μg.g$^{-1}$ and ERM 9.6 μg.g$^{-1}$ | | | |

Source: Primary Data, 2023
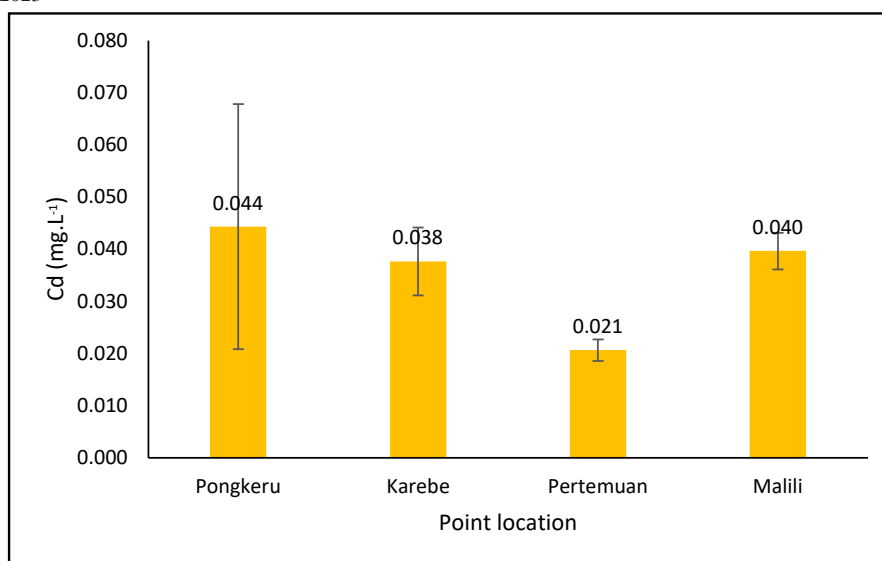


Fig. 3: Diagram of heavy metal Cd at each point.
Source: Primary Data, 2023

metal testing in Malili river waters with 4 location points, the concentration values can be seen in Table 2.

The average concentration of Cd metal at each point location shows a concentration that does not exceed the quality standard, namely at Pongkeru 0.044 $\mu g.g^{-1}$, Karebbe 0.038 $\mu g.g^{-1}$, Kawasule 0.021 $\mu g.g^{-1}$ and Malili 0.040 $\mu g.g^{-1}$. It can be said that each point has not been fully polluted by Cd heavy metal and is still far from the quality standard threshold limit of 1.2 $\mu g.g^{-1}$. The difference in each location point of heavy metal Cd can be seen in Fig. 3.

The results of Cd metal at each location point have relatively the same content and are below the quality standard. The highest Cd content at each point location is at Pongkeru, which is 0.044 $\mu g.g^{-1}$. This Pongkeru point is a mining stream, dry land agriculture such as plantations, and changes in land use from forest to pepper plantations which are thought to increase heavy metal Cd. The existence of dry land agriculture around the river using fertilizers can enter the body of water, which is thought to be the cause of the Cd metal factor. This is in line with the statement of Rachmaningrum et al. (2015), which states that phosphate fertilizers, garbage deposits, and waste from coal and oil can cause cadmium. River water and irrigation for agriculture containing cadmium (Cd) will accumulate in sediments and mud (Sudarmaji et al. 2006).

Karebbe and Malili have the same average Cd content of 0.038 $\mu g.g^{-1}$ and 0.040 $\mu g.g^{-1}$. It can be seen from the land use map Fig. 2. around the location of this point. Many residential areas, sales activities, and Malili platforms are tours around the river, causing domestic waste such as laundry detergents, plastic waste, and fecal waste from people living around the river, causing Cd content in sediment waters. The results obtained by Wulandari et al. (2008) conducted research on the Cd content in the Babon River sediment at the point 6 location, which is 0.042 ppm. The high Cd content is due to activities around the Babon River from domestic waste, such as settlements, restaurants, and hotels. The presence of Cd in the aquatic environment can come from community

activities, for example, market waste and household waste, repair, and painting of fishing boats (Alisa et al. 2020).

At Malili point, the Cd content of 0.040 $\mu g.g^{-1}$ is watering adjacent to fishery ponds that can have a dangerous impact. Based on Government Regulation No. 82 of 2001, the standard value of Cadmium heavy metal for fisheries is 0.01 $mg.L^{-1}$. According to Rachmawatie et al. (2009), the content of Cadmium parameters in the 2nd and 3rd locations, namely 0.025 $mg.L^{-1}$ and 0.075 $mg.L^{-1}$ in the estuary of the Porong River, exceeds the standard, so that the condition of these waters is not suitable for fisheries activities and marine biota habitat. The existence of fishing and harbor shipping activities around the waters causes high Cd content in the waters. This is in accordance with the opinion of Syaifullah et al. (2018) suggest that fishing port activities, and the manufacture and repair of fishing boats, are thought to be the cause of the high Cd metal content in the waters.

The low Cd content in Kawasule is 0.021 $\mu g.g^{-1}$; many sand mining activities do not affect the Cd content. This is not in line with the research of Rachmawatie et al. (2009), suggesting that the highest Cd content is found at point 3, which is 0.075 $mg.L^{-1}$ because this location is close to the sand mining area. Although the Cd metal content at each point location is low and does not exceed the quality standards, it can be toxic if accumulated in large quantities. It can have an impact on human health and aquatic organisms. According to Emilia et al. (2013), human activities can cause an increase in the amount of pollutant discharges, including heavy metal pollution such as cadmium which is a threat to the environment because it can accumulate in the body of living things through the food chain level to the highest tropical level such as humans.

**Heavy metal mercury (Hg):** Based on the results of Hg metal testing in Malili river waters with 4 location points, the concentration value can be seen in Table 3

The average concentration of Hg metal at each point shows concentrations that exceed the quality standard, namely at Pongkeru 0.590 $\mu g.g^{-1}$, Karebbe 0.229 $\mu g.g^{-1}$, Kawasule 0.514 $\mu g.g^{-1,}$ and Malili 0.358 $\mu g.g^{-1}$

Table 3: Average concentration of heavy metal Hg at each location point.

| No. | Point (Repeat) | Concentration [$\mu g.g^{-1}$] | | | |
| | | Pongkeru | Karebbe | Kawasule | Malili |
| --- | --- | --- | --- | --- | --- |
| 1. | 1.1 | 0.507 | 0.348 | 0.378 | 0.390 |
| 2. | 1.2 | 0.563 | 0.213 | 0.335 | 0.364 |
| 3. | 1.3 | 0.699 | 0.125 | 0.829 | 0.320 |
| | Average | 0.590 | 0.229 | 0.514 | 0.358 |
| | Quality Standard | ERL 0.15 $\mu g.g^{-1}$ and ERM 0.71 $\mu g.g^{-1}$ | | | |

Source: Primary Data, 2023
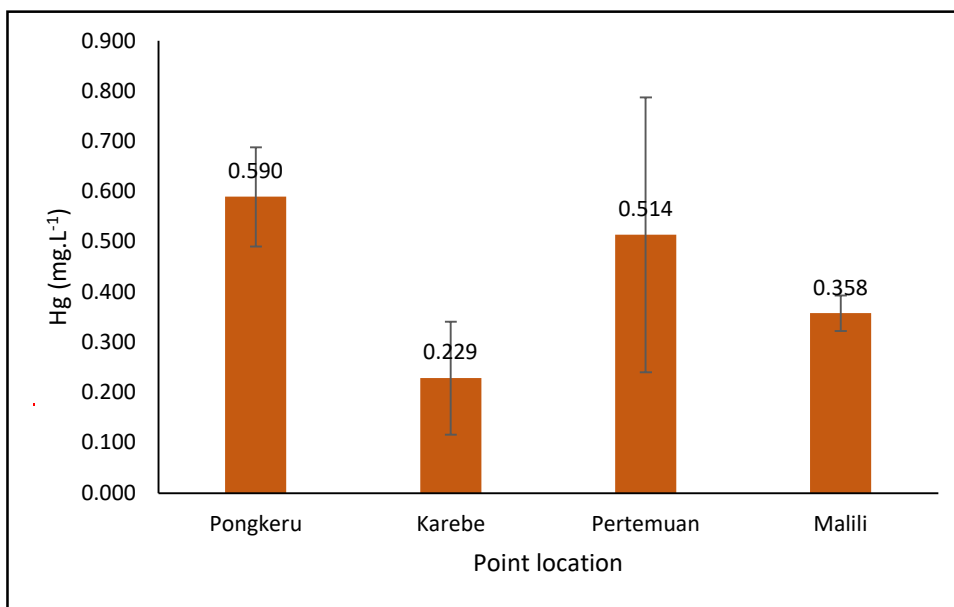
Fig. 4: Diagram of heavy metal Hg at each point.
Source: Primary Data, 2023

(Table 3). It can be said that each point is polluted by heavy metal Hg which exceeds the quality standard threshold limit of $0.15 \, \mu g.g^{-1}$. The difference in each location point of heavy metal Hg can be seen in Fig. 4.

Based on Fig. 4, the results of the Hg metal content at each point location exceed the quality standard limit. In the upper reaches of the Pongkeru sub-dash, the highest Hg metal content among each point is $0.590 \, \mu g.g^{-1}$. In Pongkeru, it can be seen on Map 1 that it is a stream from a large mine engaged in nickel, and along this stream, there is also dry land agriculture, namely the conversion of forest land into pepper plantations. This is in line with the statement of Alwan (2021), which states that sampling points closer to the mine have the potential to have a relatively large accumulation of Hg metal compared to sampling points far from the source of mining activities. Supported by Yudo's (2006) opinion, heavy metal pollution can be caused by industrial activities around the river, including the transportation industry, oil industry, mining, agriculture, and service industries that can produce waste and will increase pollution in the river. The high mercury content is also due to the sampling time during the dry season. In the dry season, mercury concentration will be greater than in the rainy season (Widodo 2008).

The results of the diagram at Kawasule, the meeting point between the upstream of the Larona sub-dash and the upstream of the Pongkeru sub-dash, also exceeded the quality standard limit of $0.514 \, \mu g.g^{-1}$. The high content of Hg metal at point 1 Pongkeru is thought to flow into

Kawasule, causing the high content of Hg metal. Activities around Kawasule waters are also illegal sand miners, agriculture, and plantations are the cause of high Hg metal. According to the opinion of Yulianti et al. (2016), mercury concentrations have increased after mining; environmental quality has decreased due to pollution due to mining and processing methods that do not follow the rules of "good mining practice." The beginning of contamination of aquatic organisms is the entry of industrial waste into water bodies (Yudo 2006).

The lowest result of Hg metal content is found in Karebbe, which is $0.229 \, \mu g.g^{-1}$. At point 2, Karebbe is the upstream river of the Larona sub-dash which is a mining stream from a large company engaged in nickel. However, these Karebbe waters already have a dam as a prevention of mine waste disposal so as not to enter the waters compared to the high Hg metal results in Pongkeru waters which also have nickel mining activities, but at this point Pongkeru there is no dam around the waters. According to Syarifuddin (2022), the solution to reduce mining waste is to make tailings dams, make a waste paste, or process waste to be returned to the ground. Tailings containing mercury directly discharged into the river can pollute aquatic biota such as fish and other aquatic plants and further damage the aquatic environment's food chain (Boky et al. 2015).

At Malili Point downstream to the sea, the Hg metal content of $0.358 \, \mu g.g^{-1}$ exceeds the NOAA quality standard. Residential activities around the river, sales, and platforms

that become community tourism in Malili are some of the factors causing Hg content in the waters. The impact of domestic waste disposal in rivers can cause pollution and reduce water quality. According to Pratiwi (2020), mercury can enter the water due to mining activities, coal combustion residues, factory waste, fungicides, pesticides, household waste, and so on. Malili waters also have shipping and weathering activities that are thought to be a source of Hg. The results of Zulfikar's research (2016) suggest that the average Hg content of 1.00 mg.kg$^{-1}$ in Karebbe is thought to be caused by ship washing activities, refueling, which is thought to be accidentally discharged into water bodies and is a port area.

Malili's proximity to fishery ponds and the sea can toxic impact water organisms. Poisoning caused by mercury generally begins with the habit of eating food from the river, such as shrimp, fish, and shellfish that have been contaminated with mercury (Yudo 2006). The high content of Hg has a toxic impact on the aquatic environment and humans. Fish or any type of food with a content of > 0.5 ppm Hg should be banned from the market and include water with a content of < 1 mg Hg.dm$^{-3}$ (Herman 2006). This is in line with the opinion of Syaifullah et al. (2018), which states that the danger of Hg metal content in waters will have an impact on the life of aquatic biota, affect aquatic biota, and pose a risk to fish eaters, such as humans and animals.

**Relation of Sediment Grain Size with Pb, Cd, and Hg**

Based on the measurement results of sediment particles at each location point, namely point 1. Pongkeru, point 2. Karebbe, point 3. Kawasule, and point 4. Malili, sediment has been classified based on the grain size listed in Table 4.

The presence of heavy metals in sediments is closely related to the size of sediment grains. Generally, sediments with finer sediment sizes contain greater concentrations of heavy metals than sediments with large sediment grain size types (Maslukah 2013). However, the Malili River waters have a medium sand grain size classification. The analysis shows that grain size and total metal concentration in sediment have a weak correlation, with correlation coefficient values of 0.0322 (Pb), 0.0065 (Cd), and 0.0511 (Hg). The weak correlation coefficient value of grain size and metals is due to the texture of medium sand grains that bind little metals. This is in line with the opinion of Miranda et al. (2018) that the sandier the texture of organic matter is, the less and heavy metals are also less, so the correlation relation is weak.

Fine sediment particles have a large surface with a more stable ion density to bind metals than larger sediment particles. So the smaller the sediment particle size, the more

Table 4: Sediment classification based on grain size (mm).

| Point location | Pb | Cd | Hg | Grain Size |
|---|---|---|---|---|
| Point 1.1 | 5.701 | 0.068 | 0.699 | 164.6 |
| Point 1.2 | 1.195 | 0.021 | 0.507 | 163.2 |
| Point 1.3 | 4.56 | 0.044 | 0.563 | 158 |
| Point 2.1 | 2.567 | 0.038 | 0.213 | 464,1 |
| Point 2.2 | 1.672 | 0.031 | 0.125 | 440.6 |
| Point 2.3 | 2.847 | 0.044 | 0.348 | 865.6 |
| Point 3.1 | 2.497 | 0.023 | 0.335 | 379.1 |
| Point 3.2 | 2.639 | 0.019 | 0.829 | 379.3 |
| Point 3.3 | 2.812 | 0.02 | 0.378 | 384 |
| Point 4.1 | 4.612 | 0.036 | 0.364 | 334.2 |
| Point 4.2 | 4.479 | 0.043 | 0.32 | 323.8 |
| Point 4.3 | 4.419 | 0.04 | 0.39 | 331.3 |

Source: Primary Data, 2023

it will have a large surface area where the process of binding heavy metals by sediments will increase (Sahara 2009). However, the results of high Hg metal content at each point location do not affect the grain size or prove the phenomenon of adsorption with this model.

The difference in sediment grain size greatly affects the physical process, namely the process of stirring and deposition strongly influenced by environmental conditions such as currents. The current will affect the deposition or sedimentation rate and the size of sediment grains deposited. According to Maslukah (2013), shallower waters and higher current velocities will affect the grain size distribution in sediments. The sand fraction mostly influences the texture of sediments contained in the waters of the Malili River.

**Relation of sediment grain size with Pb metal concentration:** The analysis shows that The relation between Pb metal and the percentage of sediment grain size has a weak correlation, with a coefficient of determination of 0.0322 (Pb). The relation between sediment grain size and Pb metal can be seen in Fig. 5.

Based on the calculation of the correlation test, the coefficient of determination is 0.0322. The magnitude of the coefficient of determination ($R^2$) 0.0322 is equal to 3.22%. This figure means that the level of influence of sediment size on Pb metal in Malili river waters at 4 location points is 3.22%, while other factors influence the remaining 96.78%.

**Relation of sediment grain size with Cd metal concentration:** The analysis shows that The relation between Cd metal and sediment grain size percentage has a weak correlation, with a coefficient of determination of 0.0065 (Cd). The relation between sediment grain size and Cd metal can be seen in Fig. 6.
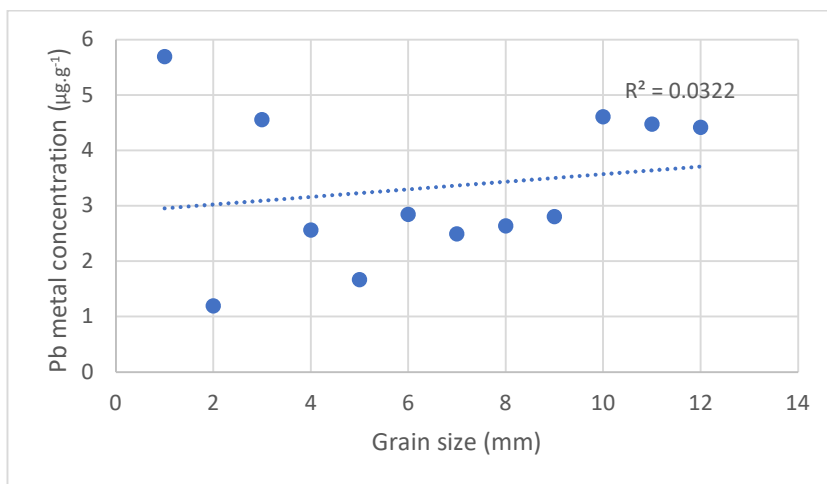
Fig. 5: The relation between sediment grain size and Pb metal concentration.
Source: Primary Data, 2023
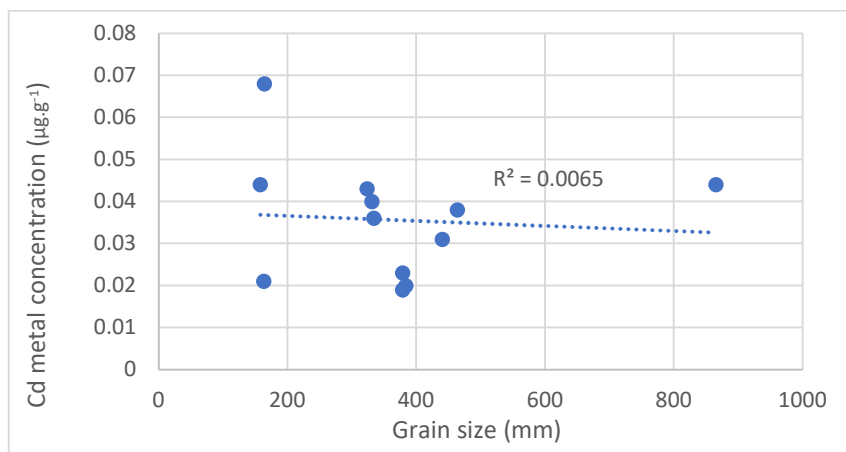


Fig. 6: The relation between sediment grain size and Cd metal concentration.
Source: Primary Data, 2023

Based on the calculation of the correlation test, it is known that the coefficient of determination is 0.0065. the magnitude of the coefficient of determination ($R^2$) 0.0065 is equal to 0.65%. This figure means that the level of influence of sediment size on Cd metal in Malili river waters at 4 location points is 0.65%, while the remaining 99.35% is influenced by other factors.

**Relation of sediment grain size with Hg metal concentration:** The analysis shows that the relation between Hg metal and sediment grain size percentage has a weak correlation, with a coefficient of determination of 0.0511 (Hg). The relation between sediment grain size and Hg metal can be seen in Fig. 7.

Based on the calculation of the correlation test, the coefficient of determination is 0.0511. The magnitude of the

coefficient of determination ($R^2$) 0.0511 is equal to 5.11%. This figure means that the level of influence of sediment size on Hg metal in Malili river waters at 4 location points is 5.11%, while other factors influence the remaining 94.89%.

**Relation of Sediment Organic Matter with Heavy Metal Concentrations of Pb, Cd, and Hg**

Based on the results of measuring sediment particles at each location point, namely point 1. Pongkeru, point 2. Karebbe, point 3. Kawasule, and point 4. Malili, the sediment has been classified based on the organic matter listed in Table 5.

Organic matter has a relation to the concentration of metal content in sediments. According to Maslukah (2013), organic matter content generally tends to be high in sediments with
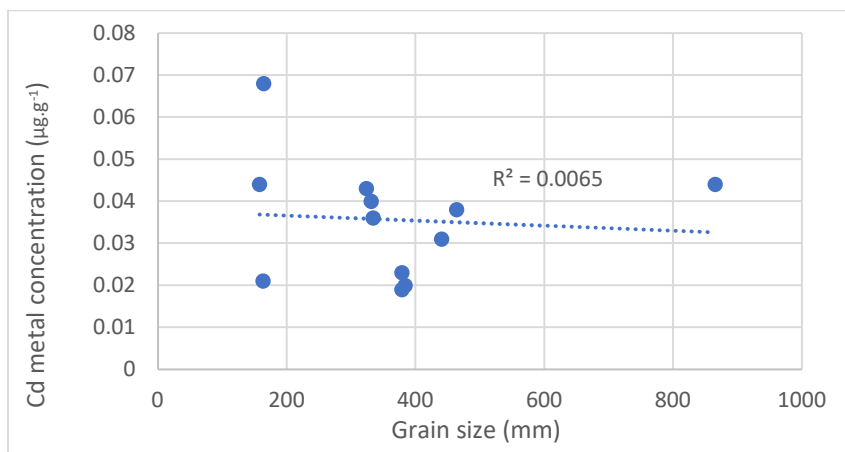
Fig. 7: The relation between sediment grain size and Hg metal concentration.
Source: Primary Data, 2023

fine grain size. Fine grain size will be followed by heavy metal concentrations that tend to be high. In Malili river waters at 4 point locations, the analysis results show that organic matter and total metal concentrations in sediments have a weak correlation The relation, with a correlation coefficient value of 0.3715 (Pb), 0.1451 (Cd), and 0.0208 (Hg). Based on the correlation test, organic matter shows a weak relation. The high Hg metal content at each point location does not affect organic matter. This is not in accordance with the opinion of Hoshika et al. (1991), which states that the content of heavy metals in sediments increases with the increase in the content of organic matter contained in water bodies and sediments. According to Thomas and Bendell (1998), organic matter is the most important geochemical component in controlling the binding of heavy metals from estuary sediments.

Table 5: Sediment classification based on organic matter (%).

| Point location | Pb | Cd | Hg | Organic Material |
|---|---|---|---|---|
| Point 1.1 | 5.701 | 0.068 | 0.699 | 7.05 |
| Point 1.2 | 1.195 | 0.021 | 0.507 | 6.92 |
| Point 1.3 | 4.56 | 0.044 | 0.563 | 8.59 |
| Point 2.1 | 2.567 | 0.038 | 0.213 | 5.05 |
| Point 2.2 | 1.672 | 0.031 | 0.125 | 5.28 |
| Point 2.3 | 2.847 | 0.044 | 0.348 | 5.79 |
| Point 3.1 | 2.497 | 0.023 | 0.335 | 2.71 |
| Point 3.2 | 2.639 | 0.019 | 0.829 | 6.82 |
| Point 3.3 | 2.812 | 0.02 | 0.378 | 2.93 |
| Point 4.1 | 4.612 | 0.036 | 0.364 | 11.47 |
| Point 4.2 | 4.479 | 0.043 | 0.32 | 10.5 |
| Point 4.3 | 4.419 | 0.04 | 0.39 | 11.74 |

Source: Primary Data, 2023

Other factors can also influence organic matter in water. According to Akbar et al. (2016), the amount of organic matter that will be deposited is also closely related to primary productivity, waves, currents, and the presence of predators and decomposers. Suspended solids are highly dependent on the physical and chemical characteristics of water. It is suspected that chemical factors other than total organic matter have a more prominent role, such as pH or sediment redox potential (Maslukah 2013). The high concentration of organic matter is influenced by the depth of the water, as well as the location of the measurement, which is close to human activities in the coastal area (Yudha et al. 2020). Given that the characteristics of the sediment itself are quite dynamic, the results obtained in this study are not necessarily the same as research conducted in different places and periods.

**The relation between organic matter and Pb metal concentration:** The analysis shows that the relation between Pb metal and the percentage of sediment organic matter has a weak correlation, with a coefficient of determination of 0.3715 (Pb). The relation between sediment organic matter and Pb metal can be seen in Fig. 8.

Based on the calculation of the correlation test, the coefficient of determination is 0.3715. The magnitude of the coefficient of determination ($R^2$) 0.3715 is equal to 37.15%. This figure means that the level of influence of sediment organic matter on Pb metal in Malili river waters at 4 location points is 37.15%, while other factors influence the remaining 62.85%.

**The relation between organic matter and Cd metal concentration:** The analysis shows that The relation between Cd metal and the percentage of sediment organic matter has a weak correlation, with a coefficient of determination of
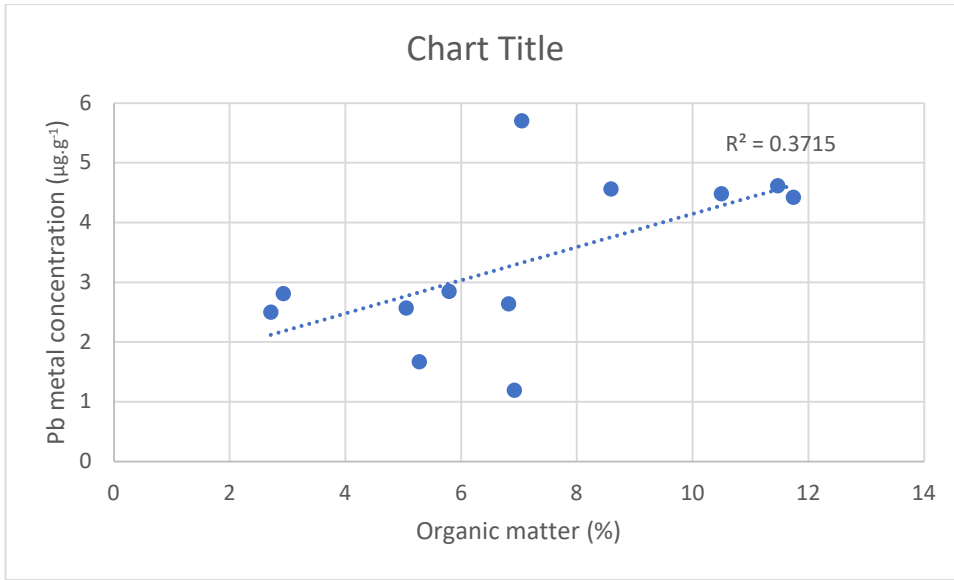
Fig. 8: The relation between sediment organic matter and Pb metal concentration.
Source: Primary Data, 2023

0.1451 (Cd). The relation between sediment organic matter and Cd metal can be seen in Fig. 9.

Based on the calculation of the correlation test, it is known that the coefficient of determination is 0.1451. the magnitude of the coefficient of determination ($R^2$) 0.1451 equals 14.51%. This Fig. 9 means that the level of influence of sediment organic matter on Cd metal in Malili river waters at 4 location points is 14.51%, while other factors influence the remaining 85.49%.

**The relation between organic matter and Hg metal concentration:** The analysis shows that The relation between Hg metal and the percentage of sediment organic matter has a weak correlation, with a coefficient of determination of 0.0208 (Hg). The relation between sediment organic matter and Hg metal can be seen in Fig. 10.

Based on the calculation of the correlation test, it is known that the coefficient of determination is 0.0208. the magnitude of the coefficient of determination ($R^2$) 0.0208
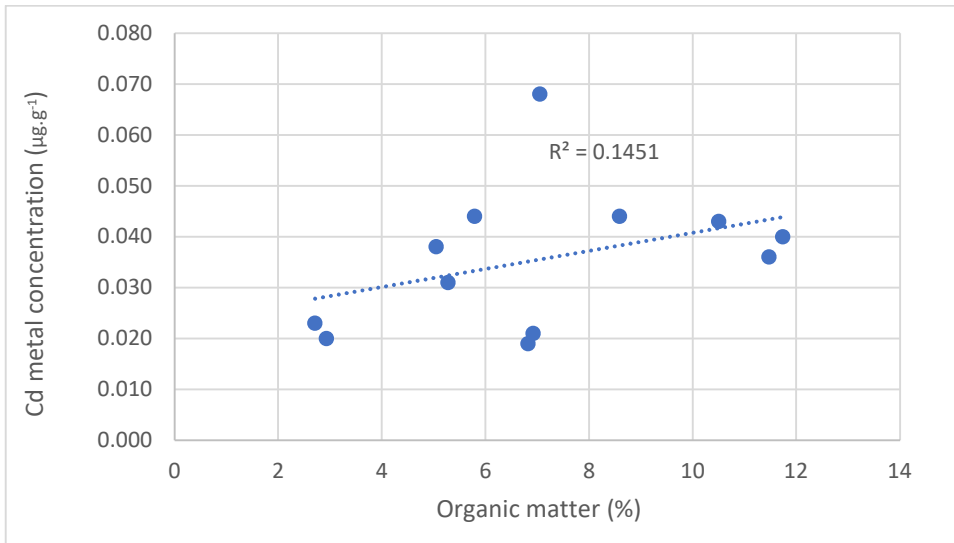


Fig. 9: The relation between sediment organic matter and Cd metal concentration.
Source: Primary Data, 2023
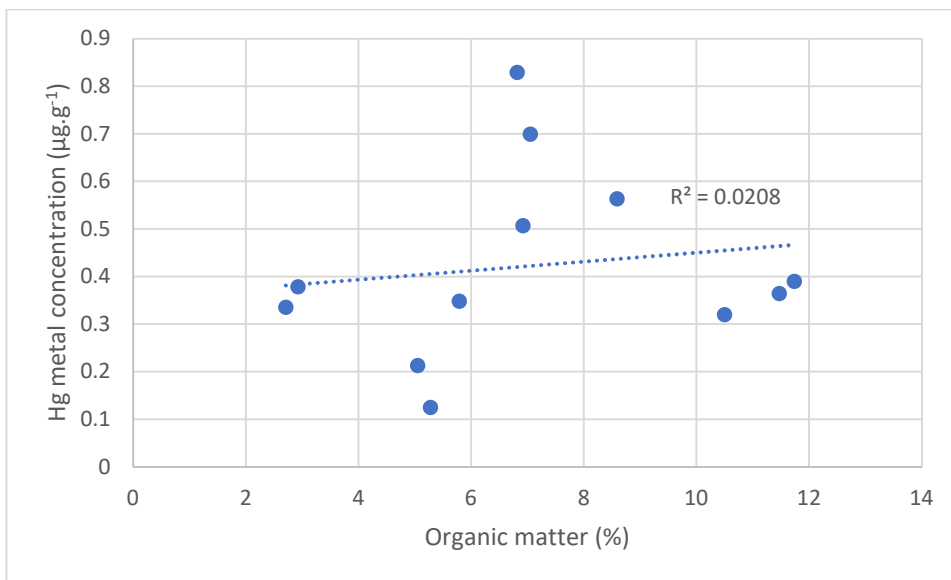
Fig. 10: The relation between sediment organic matter and Hg concentration.
Source: Primary Data, 2023

equals 2.08%. Fig. 10 shows that the level of influence of sediment organic matter on Hg metal in Malili river waters at 4 location points is 2.08%. In contrast, the remaining 97.92% is influenced by other factors.

## CONCLUSIONS

Based on the results of research and discussion, it can be concluded that:

1. The sediment content of Pb and Cd metal concentrations at each location point does not exceed NOAA (1999) quality standards. In the sediment, the concentration of Hg metal exceeds the NOAA quality standard (1999) at each point, namely Pongkeru 0.590 $\mu g.g^{-1}$, Karebbe 0.229 $\mu g.g^{-1}$, Kawasule 0.514 $\mu g.g^{-1}$ and Malili 0.358 $\mu g.g^{-1}$.

2. The relation between sediment size and Pb, Cd, and Hg metal concentrations at each point has a weak correlation. The relation does not significantly affect the content of heavy metals in sediments because it may be due to other factors, such as the source of heavy metal pollutants at each different point location.

3. The relation between organic matter and Pb, Cd, and Hg metals concentration at each point has a weak correlation. The relation does not significantly affect the content of heavy metals in the sediment because it may be due to other factors, such as different sources of heavy metal contaminants at each point.

## REFERENCES

Afifah, Z., Kurniyawan, M. and Thorikul, H. 2019. Verification of the method for determining lead (Pb) levels in ambient air samples using inductively coupled plasma optical emission spectroscopy (ICP-OES). J. Chem. Anal., 2: 74-79.

Ahmad, A., Rahman, R. and Hidayat, M. 2021. Study of lead (Pb) heavy metal content in sediment and water in Jeneberang River, Makassar City 2020. Window Pub. Health J., 2(3): 1231-1238.

Akbar, A., Sri, Y.W. and Lilik, M. 2016. Concentration of total organic matter (bot) and heavy metal lead (Pb) in sediments of Tasikagung Beach, Rembang. J. Oceanogr., 5(4): 496-504.

Alisa, C.A.G., Septyo, M.A.P. and Ibnu, F. 2020. Lead and cadmium content in water and sediments in the waters of Untung Java Island, Jakarta. Indon. J. Aqua., 5(1): 21-26.

Alwan, M.D. 2021. Analysis of Hg Concentration in River Sediment at Traditional Gold Mine Site, Kulon Progo, Yogyakarta. Thesis. Universitas Islam Indonesia Yogyakarta, Yogyakarta.

Ayyub, F.R., Abdul, R. and Andi, A. 2018. Management strategy of coral reef ecosystem in the coastal area of East Luwu Regency. J. Agric. Technol. Edu., 4: 56-65.

Boky, H., Umboh, J.M.L. and Ratag, B. 2015. Differences in mercury (Hg) content of dug well water based on distance from pollutant sources in the people's mining area of Tatelu I Village. JIKMU J., 5(1): 63-70.

Budiastuti, P., Mursid, R. and Nikie, A.Y.D. 2016. Analysis of lead heavy metal pollution in Babon River Basin, Genuk Semarang District. J. Pub. Health, 4(5): 119-125.

Emilia, I., Suheryanto, M. and Zazili, H. 2013. Distribution of Cadmium Metal in Water and Sediment in Musi River, Palembang City. J. Sci. Res., 16(2): 59-64.

Herman, D.Z. 2006. Review of tailings containing arsenic (As), mercury (Hg), lead (Pb), and cadmium (Cd) contaminants from metal ore processing residues. J. Indon. Geol., 1(1): 31-36.

Hoshika, A., Shiozawa, T., Kawana, K. and Tanimoto, T. 1991. Heavy metal pollution in sediment from the Seto Island, Sea, Japan. Marine Pollut. Bull., 23: 101-105.

Lanuru, M. 2004. The spatial and temporal patterns of erodibility of an intertidal flat in. GKSS, Berlin, Germany

Lanuru, M. and Syafyudin, Y. 2018. Bed sediment distribution in the river estuary and coastal sea of Malili (South Sulawesi, Indonesia). J. Marine Sci., 4(2): 59-62.

Mahardika, M., Dwiki, I. and Indah Rachmatiah, S.S. 2012. Distribution Profile of Heavy Metal Pollution in Water and River Sediment from Sari Mukti Landfill Leachate. Bandung Institute of Technology, Bandung.

Maslukah, L. 2013. The relation between Heavy Metal Concentrations of Pb, Cd, Cu, and Zn with Organic Matter and Grain Size in Sediments of the West Flood Canal Estuary, Semarang. Marina Oceanogr. Bull., 2: 55-62.

Miranda, F., Kurniawan, M. and Sudirman, A. 2018. Heavy Metal Content of Lead (Pb) and Cadmium (Cd) in Sediments of Pakil River in Bangka Regency. Aqua. Resour. J., 15: 84-92.

Pratiwi, D.Y. 2020. Impact of Heavy Metal Pollution (Lead, Copper, Mercury, Cadmium, Chromium) on Aquatic Organisms and Human Health. Aquatek Journal. 1 (1): 59-65.

Prawita, A., Murnitasari, D. and Darmawati, A. 2008. Heavy Metal Content of Lead (Pb), Cadmium (Cd), and Copper (Cu) in Wonokromo River Water, Surabaya. Airlangga University, Surabaya.

Putri, Z.L., Sri, Y.W. and Lilik, M. 2014. Study of the distribution of lead (Pb) heavy metal content in water and bottom sediments in the estuary waters of Manyar River, Gresik Regency, East Java. J. Oceanogr., 3(4): 589-595.

Rachmaningrum, M., Eka, W. and Kancitra, P. 2015. Cadmium (Cd) Heavy Metal Concentration in Upper Citarum River Waters of Dayeuhkolot-Nanjung Segment. Online Journal of National Institute of Technology. 3 (1): 1-11.

Rachmawatie, W., Zainul, H. and Indah, W.A. 2009. Analysis of mercury (Hg) and cadmium (Cd) concentration in Porong River Estuary as Lapindo Mud Waste Disposal Area. Marine J., 2(2): 125-134.

Sahara, E. 2009. Distribution of Pb and Cu on various sediment particle sizes in Benoa Harbor. J. Chem., 3(2): 75-80.

Steel, P.G.D. and Torrie, J.H. 1991. Principles and Procedures of Statistics a Geometric Approach. Translation B. Sumantri. PT Gramedia, Jakarta.

Sudarmaji, B., Mukono, J. and Corie, I.P. 2006. Toxicology of hazardous heavy metals and their impact on health. J. Environ. Health, 2(2): 129-142.

Sumekar, H., Iryanti, E.S. and Irdhawati, R. 2015. Metal containments of Pb and Hg in sediments in the Matik Sungai waterway, Badung, Bali. Cakra Kimia. Indon J. Appl. Chem., 3 (12): 45-49.

Syaifullah, M., Yuniar, A.C., Agoes, S. and Bambang, I. 2018. Content of non-essential metals (Pb, Cd, and Hg) and essential metals (Cu, Cr, and Zn) in sediments of Tuban, Gresik, and Sampang waters, East Java. Marine J., 11(1): 69-74.

Syarifuddin, N. 2022. The effect of the nickel mining industry on maritime environmental conditions in Morowali Regency. J. Maritime Appl. Res. Technol., 1(2): 19-23.

Thomas, C. and Bendell-Young, L.I. 1998. Linking the sediment geochemistry of an intertidal region to metal availability in the deposit feeder Tacoma Balthica. Marine Ecol. Prog. Ser., 173: 197-213.

Widodo, J. 2008. Mercury (Hg) pollution as an impact of gold ore processing in Ciliunggunung River, Waluran, Sukabumi District. J. Indon. Geol., 3(3): 139-149.

Wulandari, S.Y., Bambang, Y. and Sukristiyo, M. 2008. Patterns of Pb and Cd heavy metal distribution in the estuary of Babon and Seringin rivers, Semarang. J. Marine Sci., 13(4): 203-208.

Yogafanny, E. 2015. The effect of residents' activities in the riverbanks on the water quality of Winongo River. J. Environ, Sci. Technol., 7(1): 41-50.

Yudha, G.A., Suryono, C.A. and Santoso, A. 2020. The relation between sand sediment type and organic matter content in Kartini beach, Jepara, Central Java. J. Marine Res., 9(4): 423-430.

Yudo, S. 2006. Condition of heavy metal pollution in Jakarta river waters. JAI, 2(1): 1-15.

Zulfikar, M. 2016. Determination of Hg, Pb, and Cd Metal Levels in Sediments along Katoi Lasusua Beach. Thesis. Hasanuddin University Makassar, Makassar.

# Carbon Storage Potential of Soil in Diverse Terrestrial Ecosystems

**Shiwani Sharma\*, Pankaj Kumar Jain\* and Prama Esther Soloman\*†**

\*Department of Environmental Science, Indira Gandhi Centre for Human Ecology, Environmental and Population Studies, University of Rajasthan, Jaipur, Rajasthan, India

†Corresponding author: Prama Esther Soloman; pramaandrew@gmail.com

## ABSTRACT

Soil is one of the largest carbon reservoirs sequestering more carbon than vegetation and atmosphere. Due to the enormous potential of soil to sequester atmospheric $CO_2$, it becomes a feasible option to alleviate the current and impending effects of changing climate. Soil is a vulnerable resource globally because it is highly susceptible to global environmental problems such as land degradation, biodiversity loss, and climate change. Therefore, protecting and monitoring worldwide soil carbon pools is a complicated challenge. Soil organic carbon (SOC) is a vital factor affecting soil health since it is a major component of SOM and contributes to food production. This review attempts to summarize the information on carbon sequestration, storage, and carbon pools in the major terrestrial ecosystems and underpin soil carbon responses under climate change and mitigation strategies. Topography, pedogenic, and climatic factors mainly affect carbon input and stabilization. Humid conditions and low temperature favor high soil organic carbon content. Whereas warmer and drier regions have low SOC stocks. Tropical peatlands and mangrove ecosystems have the highest SOC stock. The soil of drylands stores 95% of the global Soil Inorganic Carbon (SIC) stock. Grasslands include rangelands, shrublands, pasturelands, and croplands. They hold about 1/5th of the world's total soil carbon stocks.

## INTRODUCTION

Soil is a major carbon reservoir with great potential to store carbon twice the potential of the atmosphere or vegetation (Schlesinger 1997, Yang et al. 2010). The stocks of soil organic carbon (SOC) act as major carbon inventories in the environment that help in sequestering atmospheric $CO_2$, acting as its prominent sink (Gomes et al. 2019) and contributing significantly to plummeting the effects of existing and impending climate change (Batjes 1998, IPCC 2014). The atmospheric $CO_2$ plays a pivotal part in sustaining the temperature of the Earth's surface globally (Dinakaran et al. 2014). Scientists have averaged the surface temperature over land and ocean in 2021 and observed an increase of 1.87°F (or 1.04°C) in comparison to the pre-industrial period (1880-1900) and at the same time, an increase of 1.51°F was observed as compared to the average of 21st century. It is also predicted to rise in mean global surface temperature by 5°C until the end of the 21st century, mostly due to increasing carbon discharges from the expanding use of fossil fuels in automobiles, industries, and alterations in land use patterns (USGCRP 2017). There was a rise in atmospheric $CO_2$ level from 280 ppm prevailing at the pre-industrial time to 397 ppm by 2014 (Ramachandran et

al. 2007, Arias et al. 2021). According to a technical report by IPCC (2021), about 2390 Gt $CO_2$ was emitted between 1850 to 2019 through anthropogenic sources only (Arias et al. 2021).

In 2020, global $CO_2$ emissions fell by 5.8%~ 2 Gt $CO_2$, which is reported to be the largest decline ever, but there was again a hike in global $CO_2$ release by 4.9% in 2021. India and China surpassed their emission rates by 13% and 4% in 2020-2021 due to the worldwide pandemic hitting the demand for coal and oil more than other energy resources (IEA 2021). With the growing intense focus on escalating climate change impacts and sustaining $CO_2$ dynamics, in the year 1992, the United Nations Framework Convention on Climatic Change (UNFCCC) was adopted, which aims to maintain the concentration of atmospheric greenhouse gases to a level that is capable of averting harmful anthropogenic intrusion with the climate. The Kyoto Protocol, an international treaty to implement the objectives of the 1992 UNFCCC, was adopted in 1997. It aims to facilitate the advancement and distribution of such mechanisms that help in developing resilience to the effects of changing climate. In its first commitment period (2008-2012), industrialized countries, economies in transition, and the European Union were bound

to accomplish the target of an average 5% emission reduction compared to 1990 levels by limiting their fossil fuel usage or by growing net sequestration of carbon in terrestrial carbon sinks (Morisada et al. 2004). An amendment to the Kyoto Protocol, named The Doha Amendment, adopted in 2012 for the second commitment period (2012-2020), aimed to reduce GHG emissions from 5% to 9%. In Article 3, the Kyoto Protocol demands serious measurement of net GHG emissions, carbon sequestration rates, changes occurring in carbon stocks, and a need to establish baseline data of carbon stock worldwide.

Consequently, it is necessary to calculate the magnitude of fluctuations in carbon pools in above- and below-ground environments (Johnson & Kern 2003, Morisada et al. 2004). It is a complicated challenge to protect and monitor carbon stocks at national and global levels (FAO 2017). Land use land-use change and forestry (LULUCF) plays a crucial part in maintaining carbon source and sink and are directly related to land cover changes and, ultimately, in the carbon stocks. LULUCF also alters the quantity of biomass and, ultimately, carbon sequestered in foliage (IPCC 2006). Soil has become one of the most susceptible resources in the world due to land degradation, biodiversity loss, and climate change. The global terrestrial carbon cycle may be affected by slight fluctuations in carbon storage in different horizons of the soil (Johnson et al. 2007, Yang et al. 2010). Anthropogenic activities can also affect and change the soil's potential to carry out sequestration of greenhouse gases.

The soil carbon pools can be augmented by carbon sequestration from the atmosphere to the soil via plant or animal biomass and microbial interface. SOC sequestration takes place in three stages:

1. Photo-autotrophic and chemo-autotrophic fixation of atmospheric $CO_2$.
2. Dead organic matter incorporated in the soil as SOM (Soil Organic Matter).
3. Microbial decomposition of SOM leads to the addition of carbon in the soil carbon pool (FAO 2017).

Microorganisms produce some extracellular enzymes, either freely present in soil or attached to the inert soil component. These enzymes decompose and break litter into simple nutrients, facilitating nutrient cycling and carbon dynamics (Hofmann 1963). SOC is a significant parameter as it indicates the health of the soil and is a chief constituent of SOM. SOC is not only a significant contributor to food production, but it also helps in moderation and adaptation to changing climatic patterns, thus favoring the attainment of sustainable development goals.

On a global level, estimated average soil organic carbon stocks are reported to be around 1500PgC in the initial 1 meter of soil with some spatial and temporal variability. SOC hot spots such as peat lands or black soil can be very helpful in mitigation and adaptation to impacts of the changing climate as they are highly efficient in sequestering large amounts of carbon in them. Therefore, the soil is a phenomenal and dynamic reservoir of carbon. The soil carbon pool depends on the equilibrium between carbon deposits and the quantity of carbon departing from the soil as $CO_2$ and $CH_4$ after decomposition (Kane 2015, FAO 2017). SOC sequestration by means of appropriate and environmentally suitable agricultural methods must be promoted to counterbalance the mounting level of $CO_2$ in the atmosphere caused due to disturbance in the terrestrial environment (Stockmann et al. 2013, Smith et al. 2016).

The current review focuses on the major aspects influencing SOC, carbon sequestration, and dynamics. The paper also outlines the importance and need to quantify carbon inventories to combat climate change by reviewing the SOC content in different ecosystems worldwide. Finally, the conclusions are summarized with recommendations for land use and effective management techniques to alleviate the climate change impacts.

## FACTORS AFFECTING SOIL ORGANIC CARBON STOCK

Significant environmental factors affect the SOC stocks in carbon dynamics involving influx and efflux of carbon. Major environmental features known as the SCORPAN factors, including- soil, climate, organisms, parent material, topography, soil information, time, and space, have a major impact on the SOC (Minasny et al. 2013, McBratney et al. 2003). These conditions strongly influence the processes that control the spatial occurrence of SOC stock, directly or indirectly, and provide an outlook to estimate actual and potential carbon inventories (Wiesmeier et al. 2019). Generally, regional climate regulates the primary productivity, and decomposition processes, influencing the sources, transfer, buildup, and breakdown of organic matter (Sutfin et al. 2016).

### Climatic Factors

Carbon reservoirs are primarily correlated with climatic features, particularly solar influx, moisture content, and temperature (Chen et al. 2013, Carvalhais et al. 2014, Ramesh et al. 2019, Wiesmeier et al. 2019). Ahirwal et al. (2021) estimated the fluctuations in biomass, C stock, and SOC stock of the Indian Himalayan region. They grouped the entire region with different ecosystem levels in three prime climatic areas, i.e., tropical, subtropical, and temperate

regions. Their study highlighted that SOC stock in temperate regions (167.77 Mg.C.ha$^{-1}$) is less than in tropical areas (178.6 Mg.C.ha$^{-1}$).

**(a) Precipitation**

In many terrestrial environments, precipitation governs the net primary productivity (NPP) and hence accumulation of C in soil. Humid conditions or moisture content in soil favors the formation of SOC by increasing the activity of soil microbes, litter disintegration, and formation of SOM and also favors stabilizing of minerals as a result of the amplified breakdown of parent material (Chaplot et al. 2010, Doetterl et al. 2015). For example, the Amazon biome within Brazil region has a humid tropical climate with mean annual precipitation (MAP) higher than 3100 mm and mean annual temperature (MAT) ranging between 25.9 to 27.7°C stores 36.1 PgC carbon stock (Gomes et al. 2019). Whereas the semi-arid eastern region of Rajasthan in India has a dry climate with average 500-1000 mm annual rainfall and an estimated carbon stock of 2129.9 Tg or 2.13 Pg (Singh et al. 2007). In arid or semi-arid conditions, shortage of water negatively affects NPP, and proportionally, SOC input is also reduced (Hobley et al. 2016, Wiesmeier et al. 2019). Low precipitation often causes soil acidification, resulting in low soil disintegration rates of organic matter (Meier & Leuschner 2010).

**(b) Temperature**

It is a significant determining aspect for storage of carbon in soil since it affects the biological disintegration of SOM in two ways: firstly, temperature affects or alters soil enzyme activities, microbial metabolism, and labile SOC content in areas with extended fertilization processes (Qi et al. 2016) and secondly it influences solubility and diffusion of carbon substrate which extrinsically depends upon temperature (Von Lützow & Kögel-Knabner 2009, Conant et al. 2011, Ramesh et al. 2019). Many studies suggest that an increase in temperature directly correlates with $CO_2$ efflux (Ramesh et al. 2019), and there is a relative importance of temperature and moisture. Both these are also two major limiting factors for SOC storage. As a result of these collective determining factors, higher stocks of SOC are found in cold-humid regions due to low evaporation/precipitation ratio and optimum temperature for microbial activity to carry out SOM degradation. In contrast, warmer and drier climatic regions have low SOC stocks globally (Post et al. 1982, Jobbagy & Jackson 2000).

**Soil Type and Texture**

Organic carbon storage is directly associated with soil type and properties in various ecosystems with varying climatic conditions (Lukina et al. 2020). Soil type is strongly influenced by parent material, which undergoes weathering to form secondary minerals such as Fe-oxides (e.g., ferrihydrite and goethite), hydroxides, and other clay minerals. These minerals determine soil reactivity, composition, and biomass production and protect SOC from biodegradation by actively forming soil aggregates. Soils with high nutrient content produce high biomass and sequester more organic carbon proportionally. Soil systems consist of different-sized particles ranging from gravels and boulders to fine fractions such as sand (0.05-2 mm), silt (0.002-0.05 mm), and clay (0.002 mm) (Dinakaran et al.
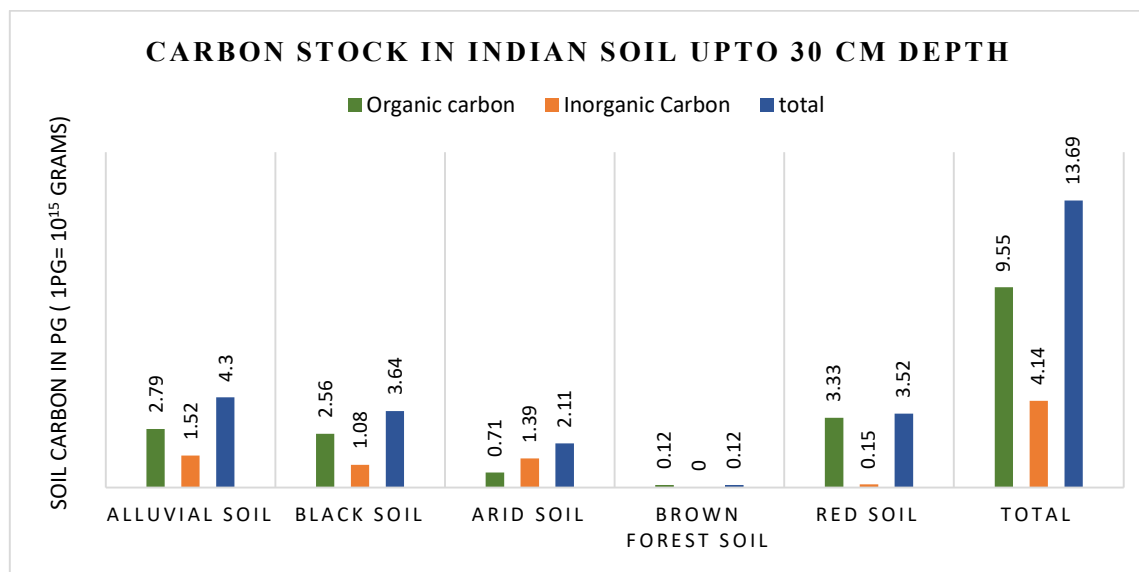


Fig. 1: Organic and Inorganic carbon stock in different soil types of the Indian subcontinent (Bhattacharya et al. 2011).

2014). Soil texture refers to the relative percentage of sand, silt, and clay particles (Kettler et al. 2001). The texture is an important soil characteristic influencing carbon sequestration and stabilization rate. Black and forest soils store high carbon as they have large fractions of clay (34.5%). In general, desert soils stock the least quantity of SOC, while tropical forest soil accumulates the maximum quantity of SOC (Batjes 2016). Drylands exhibit poor soil fertility and less organic matter content (Ramesh et al. 2019). Srinivasarao et al. (2009) examined organic carbon stocks in dominant soil types of tropical India and showed that vertisols have greater SOC stocks followed by inceptisols, alfisols, and aridisols. Bhattacharyya et al. (2009) classified Indian soil mainly into five groups, among which red soils (Alfisols and Ultisols) store the highest amount of organic carbon, followed by alluvial soils (Entisols and Inceptisols) and black soils (Vertisols). Aridisols and alluvial soils have maximum inorganic carbon content (Fig. 1).

## Vegetation Cover

Vegetation types on different landforms worldwide influence the SOC dynamics and soil carbon pool though it's a major determinant of SOC distribution. The dominant plant species have varied net primary production, litter chemistry, and rooting depth, influencing carbon input, stabilization, and losses (Gill & Burke 1999). A few studies have also suggested that in tropical forests of India, a variation in SOC storage among different vegetation systems can be seen upto 150 cm in depth. Some studies similarly show that teak plantations with deep roots can stockpile higher carbon than shallow-rooted bamboo cover deeper (Dinakaran & Krishnayya 2008). Consequently, the type of plant species profoundly impacts the deposition of SOC in forest ecosystems at global and regional scales. According to Martin et al. (2010), the type of forest and cultivation influences carbon storage as it was seen that soil of hilltop forest with the cover of *Rhododendron*, *Cedrus,* and *Quercus* plant species stored more carbon upto 30 cm soil layer as compared to carbon stored in similar soil but under agricultural land up to a depth of 150 cm. Thus, the type of cultivation done on agricultural land and varied agroecosystems also influence the SOC. Lal (2018) reported that efficient SOC sequestration is possible in about 4,900 Mha of agricultural land with about 332 Mha area and irrigation facilities. Even soils under Pinus Forest at low slope gradient were found to store less carbon (30.8 kg.m$^{-2}$) than the soils beneath *Rhododendron* and *Quercus* forests (34.7 kg.m$^{-2}$) due to high humification rate (Srivastava et al. 1994). This indicates that the forest type highly influences carbon accumulation in the soil. If we consider the cultivation system, it also follows a similar pattern in terms of carbon storage. In a study throughout tropical India, it was found that crop type has an impact on carbon storage as the soybean cultivation system (62.31 Mg C ha$^{-1}$) hoarded more carbon stock than groundnut (41.71 Mg.ha$^{-1}$) and maize (47.57 Mg.ha$^{-1}$) agriculture (Srinivasarao et al. 2009). Thus, this indicates that the nature of foliage impacts carbon accumulation in soil.

## Altitude and Topography

Altitudinal variation significantly influences SOC content through climatic variables and vegetation. In general, the global quantity of organic carbon in soil increases along with elevation (Ramesh et al. 2019, Choudhury et al. 2016), as climatic factors like mean annual rainfall (MAR) increase with height which subsequently control soil aggregation and further soil processes whereas MAT consistently decreases with elevation. Choudhury et al. (2016) conducted a study in the northern Himalayas which shows, mean rainfall, silt, and clay content increased, while MAT, sand content, and bulk density showed a decline with higher elevation. Similarly, SOC stock increased from 27.1-31.1 Mg ha$^{-1}$ at the 0-500 masl baseline to 55.8 ± 6.7 Mg ha$^{-1}$ at 2500-3500 masl altitude. Soil carbon sequestration potential of landscapes also depends upon the topography, parent materials, and regional climatic conditions. Topographical features are also important in response to SOC storage because they regulate precipitation, water flow pathways, accumulation and discharge of water significantly, and soil erosion. Sloppy areas or convex curvatures result in high water discharge, whereas low-inclined concave curvatures accumulate water. However, Soil moisture is important in controlling NPP, microbial activity, SOC input, and output (Wiesmeier et al. 2019). Bhattacharyya et al. (2009) attempted to estimate SOC stock in different physiographic regions of the Indian subcontinent. Their findings showed that the Northern mountains covering 55.3 Mha of hilly area accumulated 7.89 PgC organic carbon, which is 39% of the total SOC stock of the entire country. This is twice the SOC stock of the Great Plains (3.281 PgC) that spread over 72.4 Mha area and Peninsular Plateau (3.62 PgC) covering 105.7 Mha area.

# SOC STOCKS IN DIFFERENT ECOSYSTEMS

## Forests

Forests cover nearly 30% of Earth's land area, i.e., 4.03 billion hectares. They account for one-third of gross primary production (GPP) among terrestrial ecosystems and contribute 80% of Earth's total plant biomass (Kindermann et al. 2008). Forests approximately hoard 400 to 700 Pg of Carbon in the soil up to 1m depth (Jobbagy & Jackson 2000, Pan et al. 2011). The elevated organic material in forest soils

significantly facilitates the global carbon cycle and becomes important sinks of atmospheric carbon on Earth. The world's forests are broadly grouped into the following major biomes, i.e., tropical forests, temperate forests, and boreal forests. About 30% of the global forest area comprises boreal or taiga forest that lies at circumpolar belt/circumboreal belt across high altitude regions of Russia, Canada, and the United States. Temperate forests cover approximately 25% of the world's forest area and occur approximately between 25°-50° latitudes in both hemispheres, sharing borders with tropical forests and boreal forests in the south and north regions, respectively, and have evergreen and deciduous plant types. The carbon sink potential of this biome is currently estimated as 0.2-0.4 Pg C.year$^{-1}$ (Tyrrell et al. 2012). Tropical forests are generally found between 25° north and south of the Equator and involve predominantly rainforests, montane forests, and mangroves. The tropical domain comprises evergreen and deciduous plant species (FAO 2015, Lal 2005). Ecosystems such as tropical peatlands and mangroves act as storehouses of the highest biomass density, below-ground biomass (roots), and ultimately high soil SOC stock. There was a loss in the forested area between 1990 and 2010, which consequently led to a fall in the total carbon stock contribution of the global forest from 668 gigatonnes (Gt) in 1990 to 662 Gt in 2010, however in 2020 it remained at 662 Gt as there had been a rise in forested areas in, North and Central America, Europe and Asia (UN-DESA 2021). According to Malhi (2010), the destruction and alteration of the Tropical biome resulted in a carbon source of 1.3- 0.2 Pg C.year$^{-1}$ to the atmosphere, while undisturbed tropical biomes were predicted to act as a net carbon sink of 1.1- 0.3 Pg C.year$^{-1}$. The study also illustrates that from 2000 to 2005, the carbon absorption by tropical forests was around 12±3% of total emissions, accounting for 47% of terrestrial carbon sinks. The Boreal forests' soil carbon may constitute around 85% of the terrestrial C stock, while temperate forests have 60% and tropical rainforests have 50% C stock. The soils of the tundra, pre-tundra, and taiga regions constitute much of the total SOC stocks (Table 1).

Morisada et al. (2004) quantified stock of organic carbon in the forest soil in Japan covering a total area of 2,42,940 km$^2$

Table 1: Carbon stock estimation in major forest biomes of the world (Prentice et al. 2001; Lal 2005).

| Forest | Area [Mha] | Soil Carbon Stock [Pg] | Soil Carbon density [Mg.C.ha$^{-1}$] |
|---|---|---|---|
| Boreal Forest | 1.37 | 338 | 296 |
| Temperate Forest | 1.04 | 153 | 122 |
| Tropical forest | 1.76 | 213 | 122 |
| Total | 4.17 | 704 | - |

and found that brown forest soil (70% with Cambisols and Andisols as major components) and black soil were the second largest types (13%). The rest comprised immature, red-yellow, gleysol, and peaty soil. The estimations illustrated that the total organic carbon (TOC) in the top 30cm soil depth was 2180±50 Tg (1Tg=$10^{12}$g) which is approximately half of TOC up to 100cm depth in mineral soil, i.e., 4570±500 Tg (total ±95% confidence limit). The average value of area-weighted carbon density for the 30cm soil profile was reported to be 9.0 kg/m$^2$. In contrast, the organic carbon density for the upper 100cm depth was 18.8 kg/m$^2$, which was more than the mean global carbon density (11.3 kg.m$^{-2}$) (Sombroek et al. 1993) but larger than the carbon density of the cool temperate wet forest, i.e., 13.9 kg.m$^{-2}$ (Post et al. 1982). It is assumed that volcanic ash is responsible for such high carbon density of Japanese forest soil because it has higher efficiency in absorbing, retaining, and stabilizing organic matter. Another study done by Kyuma (1990) and Gomes et al. (2019) to estimate SOC stock in Brazilian soil revealed that Brazil is majorly covered by the Amazon biome (49.29%), having a humid tropical climate, with MAP ≥ 3100 mm and MAT of 25.9-27.7°C, Cerrado biome (22% of terrain) and Atlantic Forests. The Atlantic Forest has MAT ranging between 11-26°C and MAP between 700-1500 mm and stores 11.49 Pg of carbon in the upper 100 cm soil layer. Even though the Amazon biome has accumulated a maximum quantity of SOC (36.1 PgC), still the Atlantic Forests possesses the highest average carbon density, valued at 12.08 kg.m$^{-2}$. The stock of SOC in the protected areas was calculated in Brazil up to 100cm depth. It was found to be double the overall collective stock of SOC (11.8 PgC) estimated for the countries of Poland (1.75 PgC), Italy (0.99 PgC), Denmark (0.37 PgC), Bulgaria (0.31 PgC), Netherlands (0.30 PgC), Belgium (0.303 PgC) Slovakia (0.12 PgC), French territory (3.1 PgC) (Arrouays et al. 2001) and Great Britain (4.6 PgC) (Bradley et al. 2005, Panagos et al. 2013). Ahmad Dar (2014) assessed the SOC stock at different depths in the temperate forests of *Pinus wallichiana* and *Abies pindrow* in the Himalayan region of west Kashmir at Pahalgam (India). He reported that the mean range of SOC stock ranged between 50.37 - 55.38 Mg C ha$^{-1}$ in 30cm soil depth. Ramachandran et al. (2007) guided a study in the forested regions of Kolli Hills, a part of the Eastern Ghats, Tamil Nadu (India), to estimate carbon stock using geospatial techniques. Kolli hills are hilly terrain, situated at an altitude range of 200-1415 m above msl, and occupy an area of nearly 27,103 ha. This Reserved Forest is divided into five sub-forest types, categorized as (i) Tropical broadleaved hill forest or semi-evergreen, (ii) dry mixed deciduous forest, (iii) secondary deciduous forest, (iv) thorn forests, and (v) *Euphorbia* scrub forests.

The TOC stock in the soil of Kolli Hills was found to be 3.48 Tg. Further, the SOC stock distribution was higher in the deciduous forest as it occupied a maximum geographical area of ~ 47.7% of forest holding a SOC stock of 1.62 Tg, followed by semi-evergreen forest, which covers 14.9% of RF (Reserved Forest) having a SOC stock of 1.005 Tg. Other forests, such as the southern thorn forest, secondary deciduous, and *Euphorbia* Forest, contained 0.46, 0.35, and 0.03Tg of SOC, respectively.

## Drylands

Nearly 40% of the Earth's surface accounts for drylands, and they spread approximately 430 million ha of land in segregated form with unclear boundaries (FAO & ITPS 2015, Schlesinger 2017). Drylands are areas where the ratio of precipitation to potential evapotranspiration (PET), also known as aridity index (AI), is less than 0.65mm/mms. In other words, these areas receive lesser average rainfall than the loss of moisture via transpiration and evaporation. They are mainly categorized as hyper-arid, arid, semi-arid, and dry sub-humid regions. Scanty organic matter, nutrient content, and recurrent water-stressed conditions are major characteristics of soils of drylands (FAO & ITPS 2015). The soils of drylands store 95% of the global soil inorganic carbon (SIC) stock (Table 2), which is projected to be around 1237±15 Pg (Wang et al. 2016). This is 2 to 3 times more than organic carbon in soil (SOC) up to 100cm depth due to excessive formation of lithogenic or pedogenic carbonates (silicatic pedogenic carbonates and calcitic pedogenic carbonates) as a consequence of physical and chemical weathering of parental rock material and leaching of carbonates in soil and groundwater. The SOC stock in drylands ranges from 470 ± 7 Pg in 1m soil depth to 646 ± 9 Pg in 2 m depth. Humid regions store twice the SOC of drylands in the upper 1m soil profile (Plaza et al. 2018). Global drylands are expanding due to anthropogenic activities, conversion of natural ecosystems into agricultural lands, global warming, and rainfall patterns fluctuations. Some studies also indicate that drylands might expand up to 56% of the Earth's surface area by 2100 (Plaza et al. 2018, Lal 2019). It is reported that drylands have higher efficiency in sequestering carbon, very similar to the pine forests of Europe. 38% of the total global population lives in drylands. Hence 250 million people residing in the area can be affected by a slight increase in land degradation (Shekhawat et al. 2012).

Singh et al. (2007) estimated soil carbon stock (CS) in the arid and semi-arid areas of Rajasthan at two different depths, i.e., 0-25 and 0-100 cm. According to their estimations total carbon sock was 2129.9 Tg or 2.13 Pg. The surface layer (0–25 cm) accumulated about 31% of 0.64 Pg of total carbon. Out of the total carbon stock of the state, SOC stock comprised 58.9%, equivalent to 1230.7 Tg, while the SIC was found to be 899.2 Tg making 41.1% of the total carbon stock. Consequently, Entisols covered 43.6% of the land area and confined the highest CS of 0.72 Pg or 33.6% CS,

Table 2: Classification of drylands Soil Organic Carbon (SOC) and Soil Inorganic Carbon stocks (SIC) (mean ± standard deviation) (Plaza et al. 2018)

| Dryland | Aridity index [AI] mm/mm | Area Mkm$^2$ [Million-kilometre square] | Soil Organic Carbon [Pg] | | | Soil Inorganic Carbon [Pg] | | |
|---|---|---|---|---|---|---|---|---|
| | | | 0-30 cm | 0-100 cm | 0-200 cm | 0-30 cm | 0-100 cm | 0-200 cm |
| Hyper-arid | <0.05 | 8.6 | 11±1 | 22±1 | 31±1 | 20±2 | 65±3 | 127±5 |
| Arid | 0.05-0.2 | 20.8 | 45±3 | 91±3 | 127±3 | 63±2 | 241±5 | 487±9 |
| Semi-Arid | 0.2-0.5 | 24.1 | 100±2 | 190±3 | 259±3 | 48±2 | 207±4 | 456±7 |
| Dry sub-humid | 0.5-6.5 | 13.2 | 91±3 | 167±4 | 228±6 | 15±1 | 66±2 | 168±4 |
| Dry | >6.5 | - | 248±6 | 470±7 | 646±9 | 145±4 | 578±8 | 1237±15 |

Table 3: Soils carbon stock (in Tg) in different soil types of Rajasthan in 1992 (1000 Tg = 1 Pg) (Singh et al. 2007).

| Soil type | Area [km$^2$] | Soil Organic Carbon | | Soil Inorganic Carbon | | Total Carbon Stock | |
|---|---|---|---|---|---|---|---|
| | | 0-25cm | 0-100cm | 0-25 cm | 0-100cm | 0-25cm | 0-100 cm |
| Aridisols | 93082.6 | 42.3 | 225.2 | 43.9 | 472.1 | 86.2 | 697.3 |
| Inceptisols | 77141.8 | 81.6 | 368.2 | 22.4 | 250.6 | 104.0 | 610.8 |
| Alfisols | 2460.4 | 4.1 | 15.7 | 0.0 | 0.0 | 4.1 | 15.7 |
| Vertisols | 10212.2 | 17.3 | 56.7 | 9.9 | 49.2 | 27.2 | 105.9 |
| Entisols | 138278.4 | 205.7 | 578.4 | 56.2 | 137.7 | 261.9 | 716.1 |
| Total | 321175.0 | 337.7 | 1230.7 | 302.6 | 899.2 | 640.3 | 2129.9 |

followed by Aridisols (28.9% of total area) with 0.70 Pg or 32.7% of CS. Inceptisols covering 24.01% area had 0.61 Pg or 28.6% of CS, and the rest of the soils, like Alfisols and Verisols, were deficient in CS with 0.015 and 0.105 Pg C, respectively (Table 3).

## Grasslands

Grasslands covered approximately 3.5 billion ha in 2000, 26% of Earth's surface and $3/4^{th}$ of the agricultural area globally (Bol 2010). Grasslands commonly include shrublands, rangelands, croplands, and pasturelands used to cultivate fodder crops or as pastures. They have treasured around 20% of the entire terrestrial carbon stock (Ramankutty et al. 2008, FAOSTAT 2009, Eze et al. 2018). Integrating data from FAOSTAT (2009) and Sombroek et al. (1993), globally, SOC stock of grasslands is about 343 billion tonnes, which is 50% more as compared to forests worldwide (FAO, 2017). According to Schlesinger (1997), grasslands have high intensity to inherit soil organic matter (SOM) content, around 333 $Mg.C.ha^{-1}$. Practices supporting carbon sequestration in grasslands also enhance resilience to combat climate variability and ultimately aid in long-term adaptation towards impending climatic change. Till now, 7.5% of the total grasslands of the world have already been degraded, and in continuation, most grasslands are still vulnerable to degradation because of intensive grazing for higher livestock production. Africa's rangelands are greatly affected and face pressure to fulfill the increasing supply of milk and beef in the subcontinent (Reid et al. 2004). It has been reported that about 49% of the world's grassland and approximately 50%

of natural grassland has undergone degradation to various extent due to land mismanagement, and several countries have brought a large area of grazing and grasslands under cultivation (Gibbs & Salmon 2015). Recently, it has been indicated that 16% of rangelands, comprising 20-25% of the total area worldwide, are under threat of degradation due to cultivation which substantially credits approximately 0.8 Mg carbon from soil to the atmosphere every year (Schlesinger 1990). Thus, it is important to sustainably manage grassland ecosystems and maintain high levels of soil organic matter. In Australia, 81% of land area is rangelands and are estimated to store 34 - 48 Gt of carbon, representing a high ability of carbon sequestration, i.e., 78 Mt C/year with little upsurge of about 0.25% annually (Eady et al. 2009, Wang et al. 2018). The southern part of Brazil has a Pampas biome occupied by temperate grasslands with MAP of 1300mm – 2500mm and MAT of 14 to 20°C, which can store 1.49Pg C stock. The average carbon storage increases with depth as 1m depth soil hoards approximately 10 $kg.m^{-2}$ of organic carbon, as shown in Fig. 2.

Determination of SOC was done by Yang et al. (2008) in the Qinghai-Tibetan Plateau, situated at an average altitude of ~4000 m, covering an area of approximately 200 million hectares, which is the highest on the Earth and larger than Alaska (Li et al. 1998) having MAT of 1.61°C and MAP of 413.6 mm. The dominant ecosystems covering over 60% area are the alpine steppe and alpine meadows. The quantity of SOC accumulated in the upper 100 cm of soil in the entire alpine grasslands was calculated as 7.4 PgC, and the mean carbon density was 6.5 $kg.m^{-2}$. The SOC stock and organic
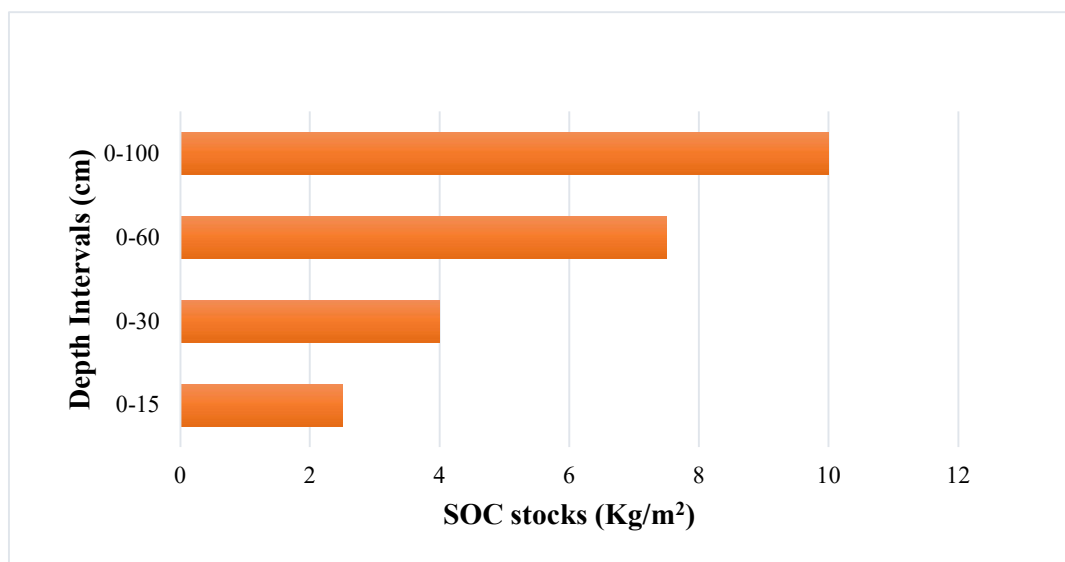


Fig. 2: Cumulative SOC stocks (kg/m$^2$) for the Pampas grasslands at different depth intervals (Gomes et al. 2019).

carbon density up to 1m soil layer in the alpine meadow were 4.68 PgC and 9.05 kg.m$^{-2}$, respectively, twice that of the alpine steppe with 2.68 PgC SOC stock and 4.38 kg.m$^{-2}$ carbon density. Upland grassland soils of Yorkshire Dales of northern England (UK) showed accumulation of a substantial amount of organic carbon that ranged between 58.93±3.50 to 100.69±8.64 Mg.ha$^{-1}$ and similarly, an average C stock of 69 Mg.ha$^{-1}$ was found to be present in grasslands of Britain up to 15cm soil depth (Carey et al. 2008). Bradley et al. (2005) also stated that England's pastures store 80 Mg ha$^{-1}$ SOC stock in 30 cm, and Ward et al. (2016) reported similar statistics of SOC stocks for grasslands of England which were intensively and extensively managed and reported about 82.6 Mg.C.ha$^{-1}$ and 84.7 Mg.C.ha$^{-1}$ respectively.

**Wetlands**

Wetlands or peatlands are distinct ecosystems that contain high amounts of peat or organic matter from dead plant materials and are saturated with water seasonally or permanently. These ecosystems are characterized by hydrological soils, vegetation, and biological features different from land and water ecosystems. They have the highest productivity and a prominent role in the global carbon cycle because of organic matter's slow decomposition, resulting in a huge carbon pool. Wetlands cover 3% of the total land area, storing almost 20-30% of global carbon stock, approximately 447 PgC of SOC up to a depth of 30cm. Wetlands are one of the most important sinks of atmospheric carbon as the anoxic conditions favor the accumulation of large amounts of carbon due to slower decomposition. The carbon seized in saline ecosystems of tidal areas is generally denoted as "blue carbon" and terrestrial carbon as "green carbon." Nahlik and Fennessy (2016) conducted a study. They revealed that the total stored carbon in the wetlands situated in the adjacent United States is 11.52 PgC, mostly in deeper layers below 30 cm (Fig. 3). According to their data, the wetlands found in Eastern mountains and upper Midwest regions of the US store about 50% of the total carbon in US and plains in the interior region had minimum carbon pools. An extensive area of freshwater inland wetland holds almost 10 times additional C compared to the tidal saline regions. However, the author refers to carbon accumulated in freshwater wetlands of inland regions as teal carbon.

Extensive anthropogenic activities, hydrological modifications, and land degradation result in a high degree of variability in carbon densities in different regions, which ranges between 195±25 tC.ha$^{-1}$ in interior plains to 539±47 tC.ha$^{-1}$ in the Upper Midwest region and Eastern Mountains up to 100 cm depth. The low precipitation area of coastal plains and west faces recurrent dry downs and slow rates of carbon sequestration, holding 198±21 and 216±30 tC.ha$^{-1}$ carbon in the soil.
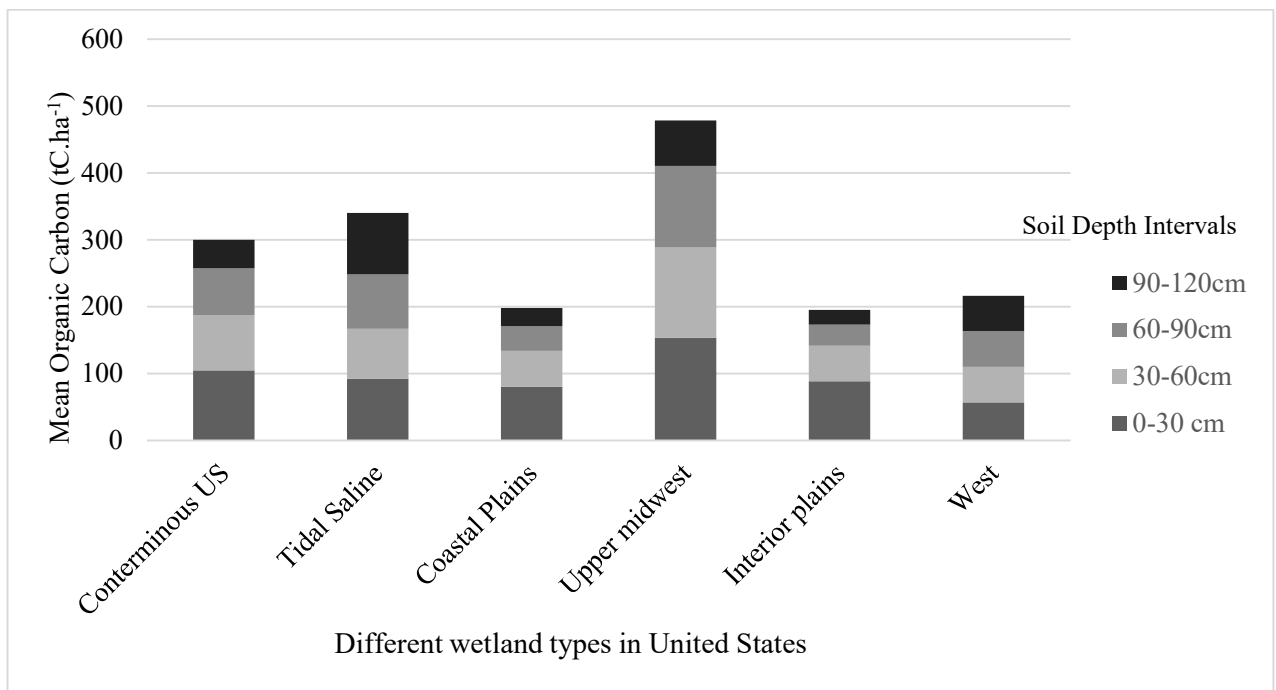


Fig. 3: Soil organic carbon (tC.ha$^{-1}$) up to 120 cm depth in diverse wetlands sites across the United States (Nahlik & Fennessy 2016).

# CONCLUSION

Global warming and climate change scenarios develop a crucial prerequisite for quantifying carbon pools and their monitoring. SOC dynamics involve the influx and efflux of carbon in the form of $CO_2$ and $CH_4$. Different phenomena like soil erosion, land use changes, and disturbances lead to the release of carbon back into the atmosphere. SOC hotspots are sensitive to temperature increase as drylands expand and SOC stocks reduce. Therefore, fortification and monitoring of SOC stocks at the global level is a challenging task. Climatic and pedogenic factors control carbon sequestration and its stabilization in deeper layers. Mainly temperature and precipitation govern carbon input in soil along with the proportion and type of vegetation in an area. As the review suggests, cold and humid areas have higher SOC stock than warm and dry regions. SOC is heterogeneously distributed due to variable soil types and climatic conditions. Forests are the major sink of $CO_2$, accumulating about 400-700 PgC in soil. Whereas grasslands cover 40 % of the area and store 343 billion tonnes of C – almost half of the carbon stock of forests (Bol 2010). Converting grasslands into cropland, deforestation, and degradation leads to loss of soil carbon, which is equal to 450–800 Gt $CO_2$, which accounts for 30-40% of collective emissions of fossil fuel (Marland et al. 2000, Olofsson & Hickler 2008, Bol 2010). Drylands store 95% of the global SIC stock, estimated as 1237±15 Pg. They have the potential to sequester more carbon. Therefore, land use management and conservation practices can foster SOC sequestration and retain carbon for longer periods in the soil. SOC is equally significant in ensuring food security because it maintains good water and nutrient-holding capacity in the soil, ultimately enhancing soil productivity and high yields. Therefore, it is crucial to study and determine the prevailing SOC stock and carbon saturation points of different ecosystems to determine the carbon sequestration potential of various soil types and ultimately manage them to combat climate change sustainably and efficiently.

# REFERENCES

Ahirwal, J., Nath, A., Brahma, B., Deb, S., Sahoo, U. and Nath, A. 2021. Patterns and driving factors of biomass carbon and soil organic carbon stock in the Indian Himalayan region. Sci. Total Environ., 770: 145292. https://doi.org/10.1016/j.scitotenv.2021.145292

Ahmad Dar, J. 2014. Soil organic carbon stock assessment in two temperate forest types of western Himalaya of Jammu and Kashmir, India. Forest Res., 03(01): 114. https://doi.org/10.4172/2168-9776.1000114.

Arias, P., Bellouin, N., Coppola, E., Jones, R., Krinner, G., Marotzke, J., Naik, V., Palmer, M., Plattner, G.K., Rogelj, J. and Rojas, M. 2021. Climate change 2021: the physical science basis. Contribution of Working Group I to the Sixth Assessment Report of the Intergovernmental Panel on Climate Change; Technical Summary.

Arrouays, D., Deslais, W. and Badeau, V. 2001. The carbon content of topsoil and its geographical distribution in France. Soil Use Manag., -7:(1)17 11. https://doi.org/10.1111/j.2743.2001-1475.tb00002.x

Batjes, N.H. 1998. Mitigation of atmospheric $CO_2$ concentrations by increased carbon sequestration in the soil. Biol. Fert. Soils, 27(3): 230-235. https://doi.org/10.1007/s003740050425

Batjes, N.H. 2016. Harmonized soil property values for broad-scale modelling (WISE30sec) with estimates of global soil carbon stocks. Geoderma, 269: 61-68. https://doi.org/10.1016/j.geoderma.2016.01.034.

Bhattacharyya, T., Ray, S.K., Pal, D.K., Chandran, P., Mandal, C. and Wani, S.P. 2009. Soil carbon stocks in India - issues and priorities. Journal of the Indian Society of Soil Science, 57(4): 461-468

Bhattacharyya, T., Pal, D.K., Chandran, P., Ray, S.K., Mandal, C., Wani, S.P. and Sahrawat, K.L. 2011. Carbon Status of Indian Soils: An Overview. Soil Carbon Sequestration for Climate Change Mitigation and Food Security, Central Research Institute for Dryland Agriculture, Hyderabad, India, pp. 11-30.

Bol, R., 2010. Challenges and opportunities for carbon sequestration in grassland system: A Technical Report on Grassland Management and Climate Change Mitigation. Compiled by Conant, R.T Rome, Italy. J. Agric. Sci., 148(6): 735-736. doi:10.1017/S0021859610000468

Bradley, R.I., Milne, R., Bell, J., Lilly, A., Jordan, C. and Higgins, A. 2005. A soil carbon and land use database for the United Kingdom. Soil Use Manag., 21: 363-369.

Carey. P.D., Wallis, S., Chamberlain, P.M., Cooper, A., Emmett, B.A., Maskell, L.C., Mccann, T., Murphy, J., Norton, L.R., Reynolds, B., Scott, W.A., Simpson, I.C., Smart, S.M. and Ullyett, J.M., 2008. Countryside Survey: UK Results from 2007. NERC/Centre for Ecology & Hydrology, UK, pp. 105.

Carvalhais, N., Forkel, M., Khomik, M., Bellarby, J., Jung, M., Migliavacca, M. and Reichstein, M., 2014. Global covariation of carbon turnover times with climate in terrestrial ecosystems. Nature, -213 :(7521)514 217.

Chaplot, V., Bouahom, B. and Valentin, C. 2010. Soil organic carbon stocks in Laos: spatial variations and controlling factors. Glob. Change Biol., 1393-1380 :(4)16.

Chen, S.T., Huang, Y., Zou, J. and Shi, Y. 2013. The mean residence time of global topsoil organic carbon depends on temperature, precipitation, and soil nitrogen. Glob. Planet Change, 100: 99-108. 10.1016/j.gloplacha.2012.10.006

Choudhury, B.U., Fiyaz, A.R., Mohapatra, K.P. and Ngachan, S., 2016. Impact of land uses, agrophysical variables and altitudinal gradient on soil organic carbon concentration of North-Eastern Himalayan Region of India. Land Degrad Dev, 27(4): 1163-1174. https://doi.org/10.1002/ldr.2338

Conant, R.T., Ryan, M.G., Agren, G.I., Birge, H.E., Davidson, E.A., Eliasson, P.E. and Bradford, M.A., 2011. Temperature and soil organic matter decomposition rates–synthesis of current knowledge and a way forward. Global change biology, 11)17): 3392-3404. https://doi.org/10.1111/j.1365-2486.2011.02496.x

Dinakaran, J., Hanief, M., Meena, A. and Rao, K.S. 2014. The chronological advancement of soil organic carbon sequestration research: A review. Proceed. National Acad. Sci. India Sec. B Biol. Sci., 84(3): 487-504. https://doi.org/10.1007/s40011-014-0320-0

Dinakaran, J. and Krishnayya, N.S.R. 2008. Variations in the type of vegetal cover and heterogeneity of soil organic carbon in affecting the sink capacity of tropical soils. Curr Sci, 94:1144-1150

Doetterl, S., Stevens, A., Six, J., Merckx, R., Van Oost, K., Casanova Pinto, M. and Boeckx, P. 2015. Soil carbon storage is controlled by interactions between geochemistry and climate. Nature Geoscience, 10)8): 780-783. 10.1038/ngeo2516

Eze, S., Palmer, S.M. and Chapman, P.J., 2018. Soil organic carbon stock and fractional distribution in upland grasslands. Geoderma, 314: 175-183. https://doi1.org/10.1016/j.geoderma.2017.11.017

Food and Agriculture Organization (FAO). 2015. Learning tool on Nationally Appropriate Mitigation Actions (NAMAs) in the agriculture, forestry, and other land use (AFOLU) sector. Food and Agriculture Organization of the United Nations Rome, Italy.

Food and Agriculture Organization (FAO) 2017. Soil Organic Carbon: The Hidden Potential. Food and Agriculture Organization of the United Nations, Rome, Italy.

Food and Agriculture Organization (FAO) and Intergovernmental Technical Panel on Soils (ITPS 2015. Status of the World's Soil Resources (SWSR) – Main Report. Food and Agriculture Organization of the United Nations and Intergovernmental Technical Panel on Soils, Rome, Italy

Food and Agriculture Organization Corporate Statistical Database (FAOSTAT). 2009. Statistical Databases. Food and Agriculture Organization of the United Nations, Rome, Italy.

Gill, R.A. and Burke, I.C. 1999. Ecosystem consequences of plant life form changes at three sites in the semi-arid United States. Oecologia, 121: 551-563. 10.1007/s004420050962

Gomes, L.C., Faria, R.M., de Souza, E., Veloso, G.V., Schaefer, C.E.G.R. and Filho, E.I.F. 2019. Modelling and mapping soil organic carbon stocks in Brazil. Geoderma, 340: 337-350. https://doi.org/10.1016/j.geoderma.2019.01.007

Gibbs, H.K. and Salmon, J.M. 2015. Mapping the world's degraded lands. Appl. Geogr., 57: 12–21.

Hobley, E.U., Baldock, J. and Wilson, B. 2016. Environmental and human influences on organic carbon fractions down the soil profile. Agric. Ecosyst. Environ., 223: 152-166. https://doi.org/10.1016/j.agee.2016.03.004

Hofmann, E. 1963. The origin and importance of enzymes in soils. Recent Prog. Microbiol., 8: 216-220.

International Energy Agency (IEA) 2021. Global Energy Review 2021 IEA Paris https://www.iea.org/reports/global-energy-review-2021

The Intergovernmental Panel on Climate Change (IPCC). 2006. IPCC Guidelines for National Greenhouse Gas Inventories. In Eggleston, H.S., Buendia, L., Miwa, K., Ngara, T., Tanabe, K. (eds), National Greenhouse Gas Inventories Programme, IGES, Japan, pp. 1114-1323.

The Intergovernmental Panel on Climate Change (IPCC). 2014. Climate Change 2014: Mitigation of Climate Change. In Edenhofer, O., Pichs-Madruga, R., Sokona, Y., Farahani, E., Kadner, S., Seyboth, K., Adler, A., Baum, I., Brunner, S., Eickemeier, P., Kriemann, B., Savolainen, J., Schlömer, S., von Stechow, C., Zwickel, T. and Minx, J.C. (eds.), Contribution of Working Group III to the Fifth Assessment Report of the Intergovernmental Panel on Climate Change. Cambridge University Press, Cambridge, UK and New York, NY, USA, pp. 450-565.

Intergovernmental Panel on Climate Change (IPCC). 2021. Technical Summary. In Masson-Delmotte, V., Zhai, P., Pirani, A., Connors, S.L., Péan, C. and Berger, S. (eds.), Climate Change 2021: The Physical Science Basis: Contribution of Working Group I to the Sixth Assessment Report of the Intergovernmental Panel on Climate Change. Cambridge University Press, Cambridge, United Kingdom and New York, NY, USA, pp. 33-144. doi:10.1017/9781009157896.002.

Jobbagy, E.G. and Jackson, R.B. 2000. The vertical distribution of soil organic carbon and its relation to climate and vegetation. Ecol. Appl., 2)10): 423-436. 10.2307/2641104

Johnson, D.W., Todd, D.E., Trettin, C.F. and Sedinger, J.S. 2007. Soil carbon and nitrogen changes in forests of Walker Branch watershed, 1972 to 2004. Soil Sci. Soc. Am. J., 71: 1639-1646. https://doi.org/10.2136/sssaj2006.0365

Johnson, M.G. and Kern, J.S. 2003. Quantifying the organic carbon held in forested soils of the United States and Puerto Rico. In: Kimble, J.S. (ed.) The Potential of US Forest Soils to Sequester and Mitigate the Greenhouse Effect, CRC Press LLC, Boca Raton, pp. 47-72.

Kane, D. 2015. Carbon Sequestration Potential on Agricultural Lands: A Review of Current Science and Available Practices. National Sustainable Agriculture Coalition, Breakthrough Strategies, and Solutions, NY, pp. 1-35.

Eady, S., Grundy, M., Battaglia, M. and Keating, B. 2009. An Analysis of Greenhouse Gas Mitigation and Carbon Biosequestration Opportunities from Rural Land Use. CSIRO, St Lucia QLD, pp. 174 https://doi.org/10.4225/08/58615c9dd6942.

Kettler, T.A., Doran, J.W. and Gilbert, T.L., 2001. Simplified method for soil particle size determination to accompany soil-quality analyses. Soil Sci. Soc. Am. J., 3)65): 849-852. http://dx.doi.org/10.2136/sssaj2001.653849x

Kindermann, G., Obersteiner, M., Sohngen, B., Sathaye, J., Andrasko, K., Rametsteiner, E. and Beach, R. 2008. Global cost estimates of reducing carbon emissions through avoided deforestation. Proceed. National Acad. Sci., 30)105): 10302-10307.

Kyuma, K. 1990. Outline of the pedogenesis of Japanese soils. In: The Committee for Soil Classification and Nomenclature, The Group of Japanese Pedologists (eds.), Explanatory Book for K.

Lal, R. 2005. Forest soils and carbon sequestration. Forest Ecol. Manag., 220(1-3): 242-258. https://doi.org/10.1016/j.foreco.2005.08.015

Lal, R. 2018. Digging deeper: A holistic perspective of factors affecting soil organic carbon sequestration in agroecosystems. Glob Change Biol., 24: 3285-3301. https://doi.org/10.1111/gcb.14054

Lal, R., 2019. Carbon Cycling in Global Drylands. Current Climate Change Reports, 3)5): 221-232. doi:10.1007/s40641-019-00132-z.

Li, W.H., Wang, Q.J., Luo, T. X., Luo, J., Zhang, X.Z. and Lin, Z.H. 1998. Biomass and Productivity of Ecosystems in Qinghai-Xizang Plateau. In Li, W.H. and Zhou, X.M. (eds.), Ecosystems of Qinghai-Xizang Plateau and Approach for Their Sustainable Management. Guangdong Science and Technology Press, Guangzhou, pp. 183-250.

Lukina, N.V., Kuznetsova, A.I., Tikhonova, E., Smirnov, V., Danilova, M., Gornov, A., Bakhmet, O., Kryshen, A., Tebenkova, D.N., Shashkov, M. and Knyazeva, S. 2020. Linking forest vegetation and soil carbon stock in Northwestern Russia. Forests, 11(979): 1-19. 10.3390/f11090979.

Marland, G., Boden, T.A. and Andres, R.J. 2000. Global, Regional and National CO$_2$ Emissions. In: Trends: A Compendium of Data on Global Change. Carbon Dioxide Information Analysis Center, Oak Ridge National Laboratory. U.S. Department of Energy, Oak Ridge, Tennesse, U.S.A.

Malhi, Y. 2010. The carbon balance of tropical forest regions, 1990-2005. Curr. Opin. Environ. Sustain., 2(4): 237-244.

Martin, D., Lal, T., Sachdev, C.B. and Sharma, J.P. 2010. Soil organic carbon storage changes with climate change, landform, and land use conditions in Garhwal hills of the Indian Himalayan mountains. Agric. Ecosyst. Environ., 138(1-2): 64-73.

McBratney, A.B., Santos, M.M. and Minasny, B. 2003. On digital soil mapping. Geoderma, 3-52 :(2-1)117.

Meier, I.C. and Leuschner, C., 2010. Variation of soil and biomass carbon pools in beech forests across a precipitation gradient. Glob. Change Biol., 3)16): 1035-1045.

Minasny, B., McBratney, A.B., Malone, B.P. and Wheeler, I. 2013. Digital mapping of soil carbon. Adv. Agron., 118: 1-47.

Morisada, K., Ono, K. and Kanomata, H. 2004. Organic carbon stock in forest soils in Japan. Geoderma, 119(1-2): 21-32. https://doi.org/10.1016/S0016-7061(03)00220-9

Nahlik, A.M. and Fennessy, M.S. 2016. Carbon storage in US wetlands. Nature Commun., 7(1): 13835. https://doi.org/10.1038/ncomms13835

Olofsson, J. and Hickler, T. 2008. Effects of human land use on the global carbon cycle during the last 6,000 years. Veg. History Archaeobot., 17: 605-615

Pan, Y., Birdsey, R.A., Fang, J., Houghton, R., Kauppi, P.E., Kurz, W.A. and Hayes, D. 2011. A large and persistent carbon sink in the world's forests. Science, 6045)333): 988-993.

Panagos, P., Hiederer, R., Van Liedekerke, M. and Bampa, F. 2013. Estimating Soil Organic Carbon in Europe Based on Data Collected

Through a European Network Ecological Indicators. Sci. Total Environ, 24: 439-450

Plaza, C., Zaccone, C., Sawicka, K., Méndez, A.M., Tarquis, A., Gascó, G., Heuvelink, G.B.M., Schuur, E.A.G. and Maestre, F.T. 2018. Soil resources and element stocks in drylands to face global issues. Sci. Rep., 8: 13788.

Post, W.M., Emanuel, W.R., Zinke, P.J. and Stangenberger, A.G. 1982. Soil carbon pools and world life zones. Nature, 5870)298): 156-159.

Prentice, I.C., Farquhar, G.D., Fasham, M.J.R., Goulden, M.L., Heimann, M., Jaramillo, V.J., Kheshgi, H.S., Le Quéré, C., Scholes, R.J. and Wallace, D.W.R. 2001. The carbon cycle and atmospheric carbon dioxide. In Houghton, J.T., Ding, Y., Griggs, D.J., Noguer, M., Linden, P.J.V.D., Dai, X., Maskell, K. and Johnson, C.A. (eds.), Climate Change 2001: The Scientific Basis, Cambridge University Press, Cambridge, pp. 183-237.

Qi, R., Li, J., Lin, Z., Li, Z., Li, Y., Yang, X., Zhang, J. and Zhao, B. 2016. Temperature effects on soil organic carbon, soil labile organic carbon fractions, and soil enzyme activities under long-term fertilization regimes. Appl. Soil Ecol., 102: 36-45. https://doi.org/10.1016/j.apsoil.2016.02.004.

Ramachandran, A., Jayakumar, S., Haroon, R.M., Bhaskaran, A. and Arockiasamy, D.I. 2007. Carbon sequestration: Estimation of carbon stock in natural forests using geospatial technology in the Eastern Ghats of Tamil Nadu, India. Curr. Sci., 92: 323-331.

Ramankutty, N., Evan, A.T., Monfreda, C. and Foley, J.A. 2008. Farming the planet: Geographic distribution of global agricultural lands in the year 2000. Glob. Biogeochem. Cycl., 1)22): 45-63. https://doi.org/10.1029/2007GB002952

Ramesh, T., Bolan, N.S., Kirkham, M.B., Wijesekara, H., Kanchikerimath, M., Rao, C.S., Sandeep, S., Rinklebe, J., Ok, Y.S., Choudhury, B.U. and Wang, H. 2019. Soil organic carbon dynamics: Impact of land use changes and management practices: A review. In: Sparks, D.L. (ed.), Advances in Agronomy, Academic Press Inc., pp. 1-107. https://doi.org/10.1016/bs.agron.2019.02.001

Reid, R., Thornton, P., McCrabb, G., Kruska, R., Atieno, F. and Jones, P. 2004. Is it possible to mitigate greenhouse gas emissions in pastoral ecosystems of the tropics? Environ. Dev. Sustain., 6: 91-109.

Schlesinger, W.H. 1990. Evidence from chronosequence studies for a low carbon storage potential of soils. Nature, 348: 232-234.

Schlesinger, W.H. 1997. Biogeochemistry: An Analysis of Global Change. Academic Press, San Diego, pp. 1-588.

Schlesinger, W.H. 2017. An evaluation of abiotic carbon sinks in deserts. Glob Chang Biol, 23: 25-27.

Shekhawat, N.S., Phulwaria, M., Rai, M.K., Kataria, V., Shekhawat, S., Gupta, A.K., Rathore, N.S., Vyas, M., Rathore, N., Vibha, J.B. and Choudhary, S.K., 2012. Bioresearches of fragile ecosystem/desert. Proceed. Nat. Acad. Sci. India Section B Biol. Sci., 82(2): 319-334.

Singh, S.K., Singh, A.K., Sharma, B.K. and Tarafdar, J.C. 2007. Carbon stock and organic carbon dynamics in soils of Rajasthan, India. J. Arid Environ., 68(3): 408-421. https://doi.org/10.1016/j.jaridenv.2006.06.005

Smith, P., Davis, S.J., Creutzig, F., Fuss, S., Minx, J., Gabrielle, B., Kato, E., Jackson, R.B., Cowie, A., Kriegler, E. and Van Vuuren, D.P. 2016. Biophysical and economic limits to negative $CO_2$ emissions. Nature Clim. Change, 6(1): 42-50.

Sombroek, W.G., Nachtergaele, F.O. and Hebel, A. 1993. Amounts, dynamics, and sequestering of carbon in tropical and subtropical soils. Ambio, 7)22): 616-623.

Srinivasarao, C., Vittal, K.P.R., Venkateswarlu, B., Wani, S.P., Sahrawat, K.L., Marimuthu, S. and Kundu, S. 2009. Carbon stocks in different soil types under diverse rainfed production systems in tropical India. Commun. Soil Sci. Plant Anal., 40(15-16): 2338-2356.

Srivastava, P.C., Martin, D. and Ghosh, D. 1994. Characteristics of soil humic substances under different forest species of Kumaon Himalayas. Chem. Environ. Res., 3: 77-84.

Stockmann, U., Adams, M.A., Crawford, J.W., Field, D.J., Henakaarchchi, N., Jenkins, M. and Zimmermann, M. 2013. The knowns, known unknowns, and unknowns of sequestration of soil organic carbon. Agric. Ecosys. Environ., 164: 80-99. https://dx.doi.org%2F 10.1016%2Fj.agee.2012.10.001

Sutfin, N.A., Wohl, E.E. and Dwire, K.A. 2016. Banking carbon: A review of organic carbon storage and physical factors influencing retention in floodplains and riparian ecosystems. Earth Surf. Process. Landforms, 41(1): 38-60. 10.1002/esp.3857

Tyrrell, M.L., Ross, J. and Kelty, M. 2012. Carbon dynamics in the temperate forest. In Liccardi, C.D., Kramer, T., Griscom, B.W. and Ashton, M.S. (eds), Managing Forest Carbon in a Changing Climate, Springer, Dordrecht, pp. 77-107.

UN-DESA, 2021. United nations department of economic and social affairs, united nations forum on forests secretariat. The Global Forest Goals Report 2021.

United States Global Change Research Program (USGCRP). 2017. Climate Science Special Report: Fourth National Climate Assessment, In Wuebbles, D.J., Fahey, D.W., Hibbard, K.A., Dokken, D.J., Stewart, B.C. and Maycock, T.K. (eds.). U.S. Global Change Research Program, Washington, DC, USA, doi: 10.7930/J0J964J6.

Von Lützow, M. and Kögel-Knabner, I. 2009. Temperature sensitivity of soil organic matter decomposition—what do we know? Biol. Fert. Soils, 1)46): 1-15. https://doi.org/10.1007/s00374-009-0413-8

Wang, B., Waters, C., Orgill, S., Cowie, A., Clark, A., Li Liu, D., Simpson, M., McGowen, I. and Sides, T. 2018. Estimating soil organic carbon stocks using different modelling techniques in the semi-arid rangelands of eastern Australia. Ecol. Indic., 88: 425-438. https://doi.org/10.1016/j.ecolind.2018.01.049

Wang, J., Monger, C., Wang, X., Serena, M. and Leinauer, B. 2016. Carbon sequestration in response to grassland–shrubland–turfgrass conversions and a test for carbonate biomineralization in desert soils, New Mexico, USA. Soil Sci. Soc. Am. J., 80(6): 1591-1603. http://dx.doi.org/10.2136/sssaj2016.03.0061

Ward, S.E., Smart, S.M., Quirk, H., Tallowin, J.R., Mortimer, S.R., Shiel, R.S., Wilby, A. and Bardgett, R.D. 2016. Legacy effects of grassland management on soil carbon to depth. Glob. Change Biol., 8: 2929-2938. https://doi.org/10.1111/gcb.13246

Wiesmeier, M., Urbanski, L., Hobley, E., Lang, B., von Lützow, M., Marin-Spiotta, E., van Wesemael, B., Rabot, E., Ließ M, Garcia-Franco, N. and Wollschläger, U. 2019. Soil organic carbon storage as a key function of soils-A review of drivers and indicators at various scales. Geoderma, 333: 149-62. doi:10.1016/j.geoderma.2018.07.026

Yang, Y., Fang, J., Tang, Y., Ji, C., Zheng, C., He, J. and Zhu, B. 2008. Storage, patterns, and controls of soil organic carbon in the Tibetan grasslands. Glob. Change Biol., 14: 1592-1599. doi: 10.1111/j.1365-2486.2008.01591.xr2008

Yang, Y., Fang, J., Ma, W., Smith, P.A., Mohammat, A.L., Wang, S. and Wang, W.E. 2010. Soil carbon stock and its changes in northern China's grasslands from 1980s to 2000s. Glob. Change Biol., 16(11): 30 36-47. https://doi.org/10.1111/j.1365-2486.2009.02123.x

# Evaluation of Cr(VI) Reducing Capability of *Bacillus licheniformis* DAS1 Using a Multifactor Experimental Approach

**Md. Saduzzaman\* , Kumari Mini\* , Shardendu Shardendu\* and S. Rehan Ahmad\*\*†**

\*Laboratory of Environment and Biotechology, Department of Botany, Patna Science College, Patna University, Patna, India
\*\*Department of Zoology, Hiralal Mazumdar Memorial College for Women, Kolkata, India
†Correspondence author: S Rehan Ahmad; zoologist.rehan@gmail.com

## ABSTRACT

The current study is about detoxifying soil and water contaminated with toxic Cr(VI). To ensure that DAS1 could develop as well as possible, the pH was changed between 4 and 10. DAS1 showed its highest growth at pH 8, and at the same pH, it had an 85% potential to remediate by converting Cr(VI) to Cr(III). Immobilized bacteria increased the reduction of Cr(VI) to Cr(III) from the culture medium to 90.4%. The impact of glucose concentrations between 0.5 and 2.5 $g.L^{-1}$ was examined. The greatest development was seen at pH 8 and 2 $g.L^{-1}$ glucose concentration. The remediation potential was improved by up to 96% when the growing medium contained 200 $mg.L^{-1}$ Cr(VI). The value of $k_s$ (0.434 $g.L^{-1}$) demonstrated the substrate's affinity for bacteria in accordance with the Monod equation, while $\mu$ max (0.090 h) demonstrated that DAS1 required 11.11 h for maximal growth. The multifactor experimental design was used to analyze mixed cultures of DAS1 and DAS2 in a 1:1 ratio, and it was determined that the X3Y2Z1 experiment design was best for completely removing Cr(VI) from the growing medium. By making pores using $Na_2EDTA$, it was determined that the cell membrane's impermeability did not cause Cr(VI) resistance in DAS1. The delayed lag phase indicated that the enzyme activity was inductive rather than constitutive.

## INTRODUCTION

India has a population of about 1.4 billion and is growing at a 1.6% annual rate. Every person utilizes leather shoes, leather clothing, and leather things from tanneries. India's tanning industry significantly pollutes the environment with Chromium. In India (at 25.6197° N, 85.1660°E), there are 1083 tanneries, according to the Central Leather Research Institute (1987). Among the states with the highest concentration of tanneries are Tamil Nadu (577 units), West Bengal (233 units), and Uttar Pradesh (147 units). These three states are home to 88% of the nation's tanneries. Most of these industries lack effluent treatment facilities, resulting in an average daily outflow of 50-60 million liters of untreated wastewater.

As per a WHO report from 2001, 90% of the 8000 tannery workers in Hazaribagh, India (25.6170° N, 85.1660° E) died before the age of 50 due to gastrointestinal, dermatological and other disorders like cancer. Chromium is the main contaminant in tannery wastewater. Both mobile and chelated forms of chromium occur. With the tannery sector, India's (25.6197° N, 85.1660° E) paper and pulp, electroplating, and

several small-scale industries located in Bihar also contribute to Chromium contamination. About a lakh weavers in Eastern India (Bihar) make a living by producing and dealing with fabric and clothing (25.6173° N, 85.1660° E). Numerous small-scale companies in the Patna metropolitan area of Bihar discharge untreated wastewater into the sewer system, contributing to chromium pollution. Every aquifer and other aquatic system is linked together in some way. In addition to the anthropogenic activities, spills, and dumping of chromium wastes, geological processes also aid in introducing chromium and its compounds into soils (Ayele & Godeto 2021). If present below 100 ppm, chromium is functional in the metabolism of lipids, carbohydrates, amino acids, and nucleic acid production (Eaton et al. 2005). Since chromium is more soluble and has a persistent oxidation property in the trivalent ($Cr^{3+}$) form, which is predominant in biological systems, it exhibits lower biotoxicity (Elahi et al. 2022, Ray 2016).

Those exposed to Cr show signs including necrosis, eardrum perforation, and skin and ear ulcers. Cr pollution is causing havoc in the ecosystem by negatively affecting the abundance and balance of microbial populations in

different ecosystem components, such as soil and water. One of the most significant ecological concerns is the effective removal of heavy metals from industrial waste, particularly from aqueous waste. Several old and typical procedures for removing heavy metals, including solvent extraction, oxidation-reduction processes, and adsorption, are generally expensive and inefficient, especially when the concentration of heavy metals reaches 1 mg.L$^{-1}$ (Elahi et al. 2022).

In water containing industrial effluent, bacteria live. These bacteria have evolved survival mechanisms to deal with the toxicity of heavy metals through processes such as metal uptake, methylation, adsorption, oxidation, and reduction. For the detoxification and eradication of Cr(VI) contaminants, bioremediation technology is a straightforward, affordable, and environmentally acceptable approach that may be used in a variety of experimental settings.

The most notable bioremediation methods include biosorption, bioaccumulation, biotransformation, and bioreduction. Out of everything said above, this study investigates the role of bio-reduction of Cr(VI) to Cr(III). Using local microbiota to remove heavy metals from contaminated environments and restore the polluted area without the addition of chemical reagents, bio-reduction, or the conversion of $Cr^{6+}$ to $Cr^{3+}$ is a potential detoxification technique (Tripti et al. 2014, Elahi et al. 2022).

In addition to microorganisms, plants like *Typha latifolia* L. and *Phragmites australis* are reported to mitigate metalloids like selenium by biotransformation (Elahi et al. 2022, Sayantan & Shardendu 2013), and certain annual plants like Raphanus sativus are reported to mitigate Cr(VI). The toxicity of Cr(VI) was reported dose-dependent. There was a gradual reduction in Cr(VI) toxicity on phosphate amendment at each increasing concentration of P amendment (Sayantan & Shardendu 2013). The enrichment of PO43- above 1 mM did, however, cause a growth reduction in *Bacillus licheniformis* DAS1, demonstrating the toxicity of phosphate (Akcil et al. 2015, Tripti & Shardendu 2016).

The current experiment uses *Bacillus licheniformis* DAS1 to bioreduce Cr(VI) at various pH and Cr concentrations. Immobilized bacterial cells on calcium alginate beads were also used to bioreduction Cr(VI) to Cr(III). Glucose was employed as a co-metabolic substrate to calculate the maximal specific growth rate (max) and ks (Shivangi et al. 2002).

The notion of microbial growth kinetics has been dominated by an empirical model first proposed by Monod (1942). The Monod model was the first to suggest the existence of a substrate that restricts growth.

$$\mu = \mu_{max}[S]/k_s+[S]$$

Specific growth rate (μ) is independent of substrate concentration if there is excess substrate present. From the hyperbolic curve generated by Monod's equation, it is impossible to accurately calculate what ks and μ max should be. Use the Line Weaver Burk plot to linearize (Double Reciprocal Plot). The formula for Monod is

$$1/\mu = K_S/\mu_{max}1/[S] +1/\mu_{max}$$

Also, an orthogonal experiment design was used in a mixed culture of DAS1 and DAS2 to maximize the reduction of Cr(VI) to Cr(III) (1:1) (Shimei et al. 2012). The mechanism underlying the resistance to Cr of DAS1 was also investigated using a permeability experiment (Batool et al. 2012).

## Objective of the Current Work

The objective of current research work is to evaluate the reduction of Cr(VI) to Cr(III) by optimizing the pH temp and inoculum concentration of bacteria *Bacillus licheniformis* DAS with a multifactor approach.

## MATERIALS AND METHODS

### Determination of MTC (Maximum Tolerable Concentration) of DAS1 for Cr(VI)

A solid nutritional agar plate was streaked with the isolated *Bacillus licheniformis* DAS1 after it had been treated with a range of Cr(VI) concentrations (50-1100 mg.L$^{-1}$). The maximum tolerated concentration of a pollutant was determined to be the level at which bacterial growth could be seen after 5 days of incubation at 37°C (Zhao et al. 2016).

### Effect of pH and Cr(VI) Concentration on Specific Growth Rate(μ) and Cr(VI) Reduction

In LB broth, the effects of various pH values (ranging from 4 to 10) and the initial Cr(VI) concentration (200 to 1000 mg.L$^{-1}$) were studied (Tripti & Shardendu 2016, Wani et al. 2019), and the specific growth rate (μ, h$^{-1}$) was estimated using the slope of the graph (Upadhyay et al. 2017, Villegas et al. 2013).

In OD/OD$_o$

where OD=optical density at the given time and OD$_o$=optical density at zeroeth h

### Effect of Glucose as Co-metabolic Substrate

Co-metabolic tests were carried out using a binary substrate system that contained bacteria, Cr(VI) at 200 mg.L$^{-1}$, and glucose in the range of 0.5-2.5 g.L$^{-1}$ to improve the specific

growth rate and reduction capacity of DAS1 (Upadhyay & Sinha 2021). The Monod kinetic parameters kS and μmax were tuned using a line weaver Burk plot.

$$\mu = \mu_{max}[S]/k_s + [S] \text{(Monod equation)}$$

$$1/\mu = K_S/\mu_{max}1/[S] + 1/\mu_{max} \text{ (Line Weaver Burk Plot)}$$

## Chromium(VI) Reduction

The concentration of hexavalent Cr becoming less hazardous was estimated using the DPC method by DAS1. A 24-h-old culture was inoculated into 50 ml of LB broth with 200–1000 mg.L$^{-1}$ of Cr VI and a pH range of 4-10. The samples were obtained by centrifuging for ten minutes at 10,000 rpm. By measuring the absorbance of the Cr(VI)-DPC complex at 540 nm with a spectrophotometer and plotting the results in the standard curve at various time intervals, it was possible to calculate the remaining Cr(VI) concentration.

The percentage reduction of Cr(VI) was calculated by using the formula (Upadhyay et al. 2017)

$$\text{Cr(VI) reduction \%} = C_0 - C_f/C_0 * 100$$

Where $C_0$ = Initial Cr(VI) concentration, $C_f$ = Final Cr(VI) concentration.

## Determination of the Ratio of Two Strains

To evaluate the effectiveness of Cr(VI) bioreduction, a mixture of the two strains, DAS1 and DAS2, in various ratios containing 1:1, 1:2, and 2:1, were used. Then, the ratio with the highest Cr(VI) reduction efficiency was chosen.

## Orthogonal Experiment Design

Compared to traditional design, orthogonal experiment design excels in optimizing the growth-related parameters, particularly temperature, pH, and inoculation amount (Table 1), and was created to find the ideal circumstances for mixed strains to remove Cr(VI).

## Effect of Immobilization of *Bacillus licheniformis* DAS1

During 24 h at 37°C, DAS1 was grown aerobically in LB broth. A 3 percent sodium alginate solution was made and autoclaved. To ensure homogeneous cell and alginate solution mixing, the bacterial culture and alginate were combined in a 1:4 ratio and shaken for 2 h. With constant shaking with a 10 mL disposable syringe, the mixture was

Table 1: Factorial Design for Orthogonal Experiment.

| Level | Temperature | pH | Inoculation amount |
|---|---|---|---|
| 1 | 25 | 7.0 | 5% |
| 2 | 30 | 8.0 | 10% |
| 3 | 35 | 9.0 | 15% |

poured dropwise into 50 mL of CaCl$_2$ solution in a beaker to create beads. For hardening, the beads were left overnight. The 3-5 mm-diameter beads were repeatedly cleaned with sterile distilled water after 24 h. Beads were kept at 4°C and were done under aseptic conditions. 50 mL LB broth with 200 mg.L$^{-1}$ Cr(VI) and 5g beads were added.

## Cell Permeability Assay and Induction Behavior

In the same buffer, cells were resuspended after being harvested at the exponential phase and once at room temperature with 0.12 Tris-Cl, pH 8.0. The suspension was incubated with $2*10-4M$ Na$_2$EDTA for two minutes at 37°C before the treatment was finished with the addition of ten volumes of growth media. Controls were diluted in the same way and added without Na$_2$EDTA.

## Instruments Used

Ultraviolet-visible (UV-Vis) Spectrophotometer is used to quantify the reduction of Cr(VI) to Cr(III) in the spiked growth medium.

## RESULTS AND DISCUSSION

### Growth Profile of DAS1 in the Presence of Cr(VI) Stress

In this investigation, *Bacillus licheniformis* DAS1 was chosen after being isolated from the rhizosphere of *A. viridis*. It was allowed to grow in LB broth that had been changed to include Cr(VI) at varying concentrations, such as 200 mg.L$^{-1}$, 400 mg.L$^{-1}$, 600 mg.L$^{-1}$, 800 mg.L$^{-1}$, and 1000 mg.L$^{-1}$ (Fig.1). The harmful effect of chromium was demonstrated by comparing the growth of cells cultured in Cr(VI) free media and Cr(VI) containing media. *Bacillus licheniformis* DAS1 grown in control (without chromium) was observed to spend the first two hs in the lag phase by remaining metabolically active and increasing only the size of cells, not the number of cells, before entering an exponential phase that lasted for nearly 26 h and saw the population growth in a logarithmic manner.

The toxic impact of the metal on DAS1 may have caused the lag phase in Cr(VI) at 200 and 400 mg.L$^{-1}$ to be significantly extended to 3 hrs.

After that, an exponential phase lasting approximately 25 h began. The specific growth rate (μ, h$^{-1}$) of DAS1 and Cr(VI) concentration was shown to be negatively correlated (Table 2), meaning that as Cr(VI) concentration climbed to 600, 800, and 1000 mg.L$^{-1}$, the lag phase also increased to 4 h, shortening the exponential phase to 22 h. With 1000 mg.L$^{-1}$, DAS1 went through a 20 h exponential phase before entering the stationary period.
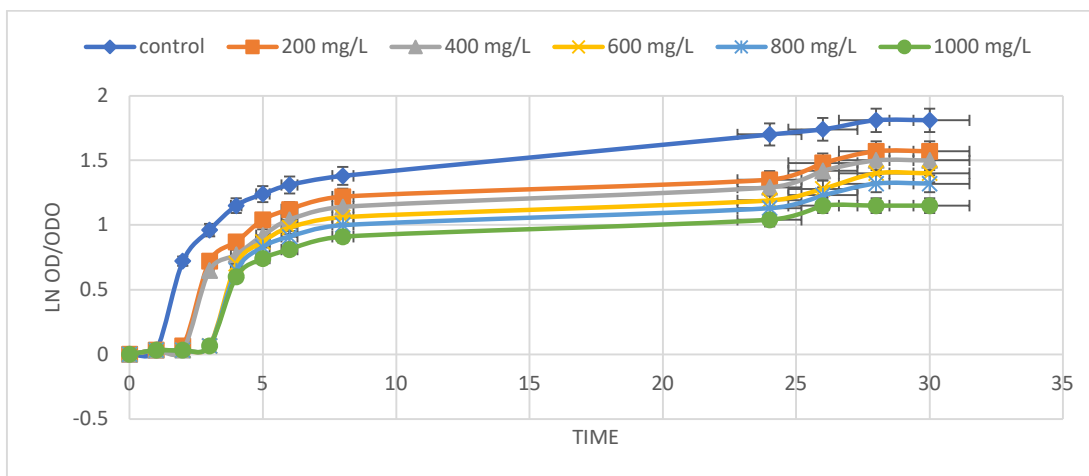
Fig. 1: Variation in growth of *Bacillus licheniformis* DAS1 at different Cr$^{6+}$ conc at neutral pH.
(All values are mean of three replicates, and standard errors (SE) are presented as error bars ($^+$.))

The specific growth rate ($\mu$, h$^{-1}$) of DAS1 calculated and presented in Table 1 vividly portrays the negative correlation between the Cr(VI) concentration and growth of DAS1.

## Effect of pH on the Growth of *Bacillus licheniformis* DAS1

*Bacillus licheniformis* DAS1's growth and development are influenced by pH. The pH limit of a cell's structural integrity and the interference of pH with cell metabolism are represented by the specific growth rate of these organisms changing with pH as a bell-shaped curve (Fig. 2 to Fig. 7

and Table 2). The highest growth was seen at pH 8 (Fig. 5 and Table 2), and it decreased as pH became more acidic and basic. The pH needed for bacteria to thrive was neutral, but up to a certain point, alkaline pH resulted in faster growth (pH 8). The growth decreased when pH 9 & pH 10 increased (Fig. 6 & Fig. 7).

## pH Modulates Toxicity of Cr(VI)

Bacillus licheniformis DAS1 may reduce Cr(VI) to chromium(III) using the chrome reductase enzyme. Each enzyme's functionality is influenced by pH and temperature
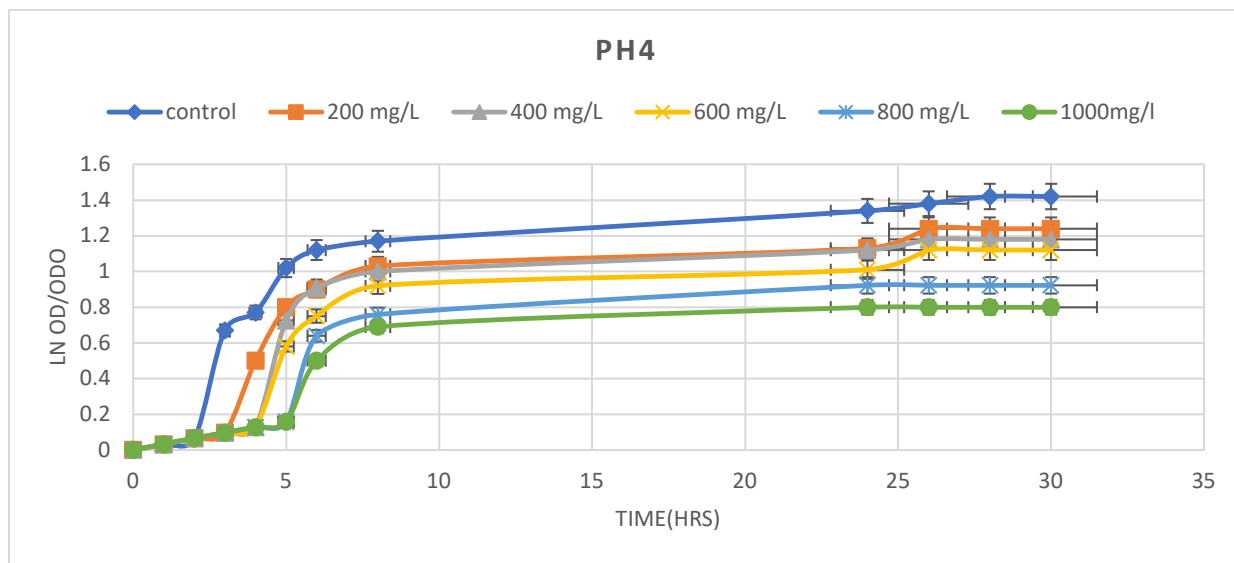


Fig. 2: *Bacillus licheniformis* DAS1 growth variation at pH 4 under different Cr$^{6+}$ conc.
(All values are the mean of three replicates, and standard errors (SE) are presented as error bars ($\pm$).)
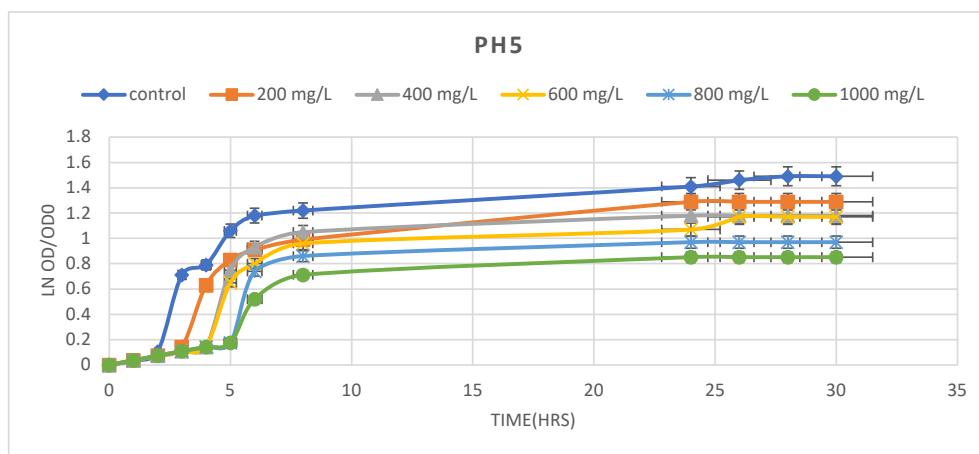
Fig. 3: *Bacillus licheniformis* DAS1 growth variation at pH 5 under different $Cr^{6+}$ conc.
(All values are the mean of three replicates, and standard errors (SE) are presented as error bars (±).
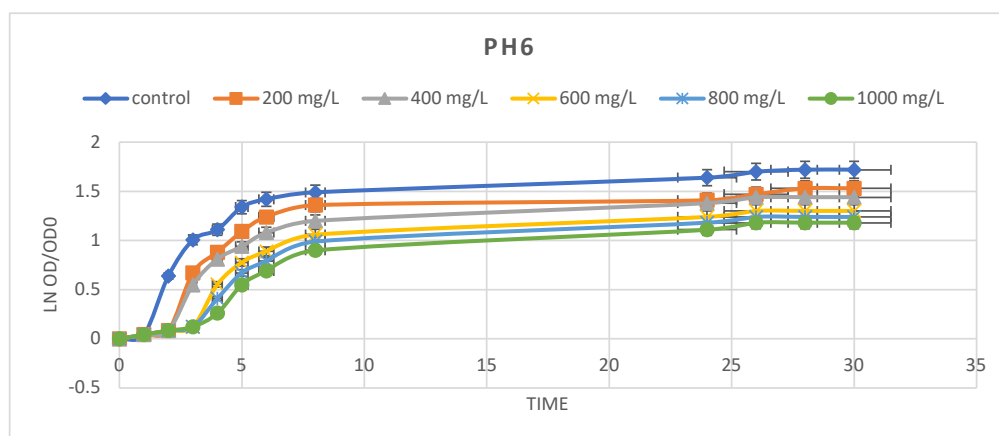


Fig. 4: *Bacillus licheniformis* DAS1 growth variation at pH 6 under different $Cr^{6+}$ conc.
(All values are the mean of three replicates, and standard errors (SE) are presented as error bars (±).
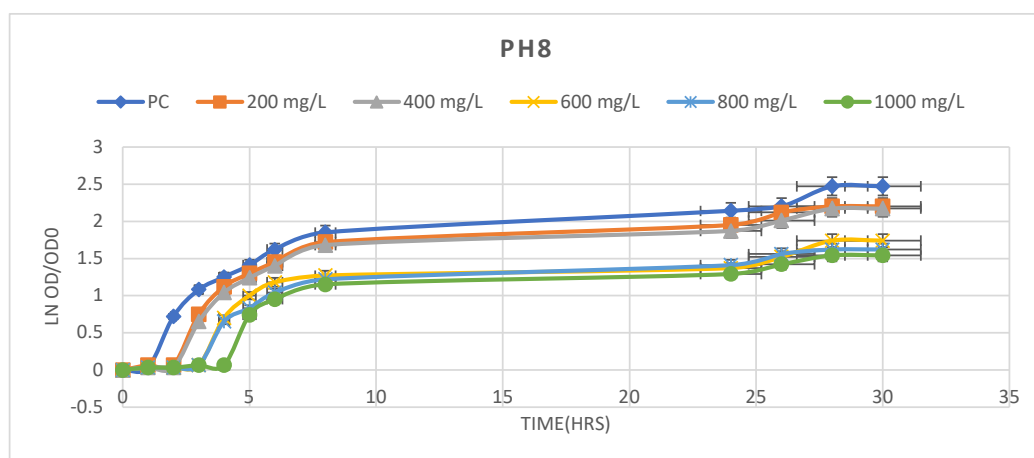


Fig. 5: The variation of *Bacillus licheniformis* DAS1 growth at pH 8 under different $Cr^{6+}$ conc.
(All values are the mean of three replicates, and standard errors (SE) are presented as error bars (±).
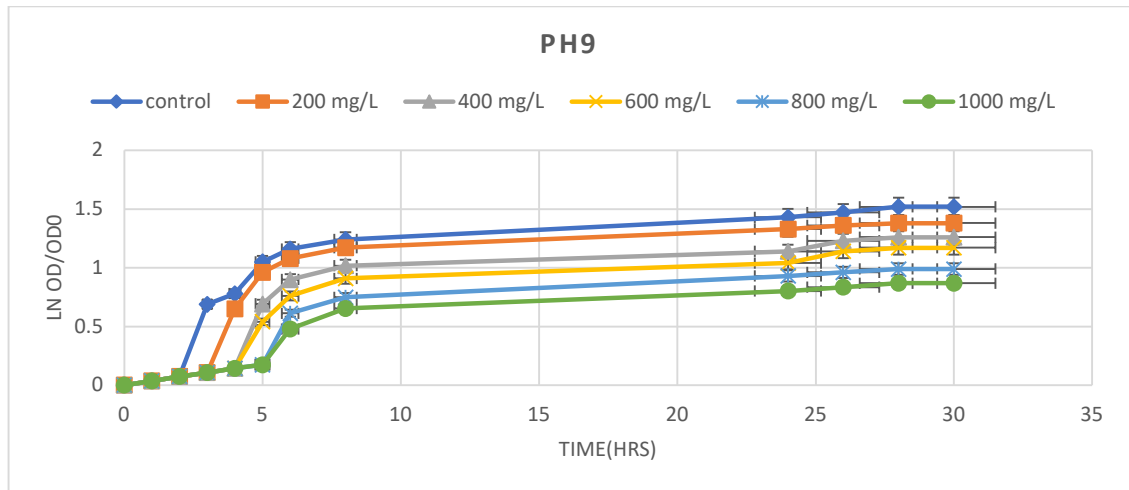
Fig. 6: *Bacillus licheniformis* DAS1 growth variation at pH 9 under different Cr$^{6+}$ conc.
(All values are the mean of three replicates, and standard errors (SE) are presented as error bars (±).
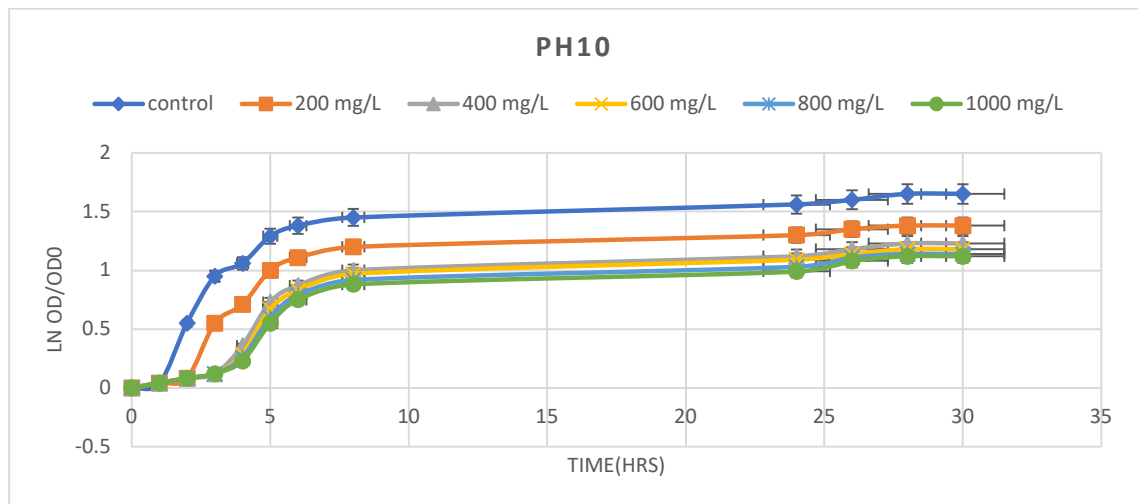


Fig. 7: *Bacillus licheniformis* DAS1 growth variation at pH 10 under different Cr$^{6+}$ conc.
(All values are the mean of three replicates, and standard errors (SE) are presented as error bars (±).

Table 2: Specific growth rate(µ): h$^{-1}$ at different pH under different Cr$^{6+}$ conentration. (Calculated from the slope of the graph)

| Specific growth rate(µ): h$^{-1}$ at different pH under different Cr$^{6+}$ conentration (Calculated from the slope of the graph) | | | | | | | |
|---|---|---|---|---|---|---|---|
| Sample | Neutral | pH 4 | pH 5 | pH 6 | pH 8 | pH 9 | pH 10 |
| Control | 0.043832 | 0.038003 | 0.039861 | 0.040187 | 0.063039 | 0.041229 | 0.038514 |
| 200 mg.L$^{-1}$ | 0.041538 | 0.037254 | 0.039173 | 0.040109 | 0.062125 | 0.040782 | 0.037286 |
| 400 mg.L$^{-1}$ | 0.040895 | 0.037360 | 0.037371 | 0.040060 | 0.061599 | 0.039774 | 0.037217 |
| 600 mg.L$^{-1}$ | 0.040603 | 0.035860 | 0.037217 | 0.039632 | 0.050483 | 0.037399 | 0.036237 |
| 800 mg.L$^{-1}$ | 0.038582 | 0.031244 | 0.032309 | 0.038830 | 0.049997 | 0.033061 | 0.035229 |
| 1000mg.L$^{-1}$ | 0.034338 | 0.026874 | 0.028604 | 0.038088 | 0.049529 | 0.028708 | 0.034739 |
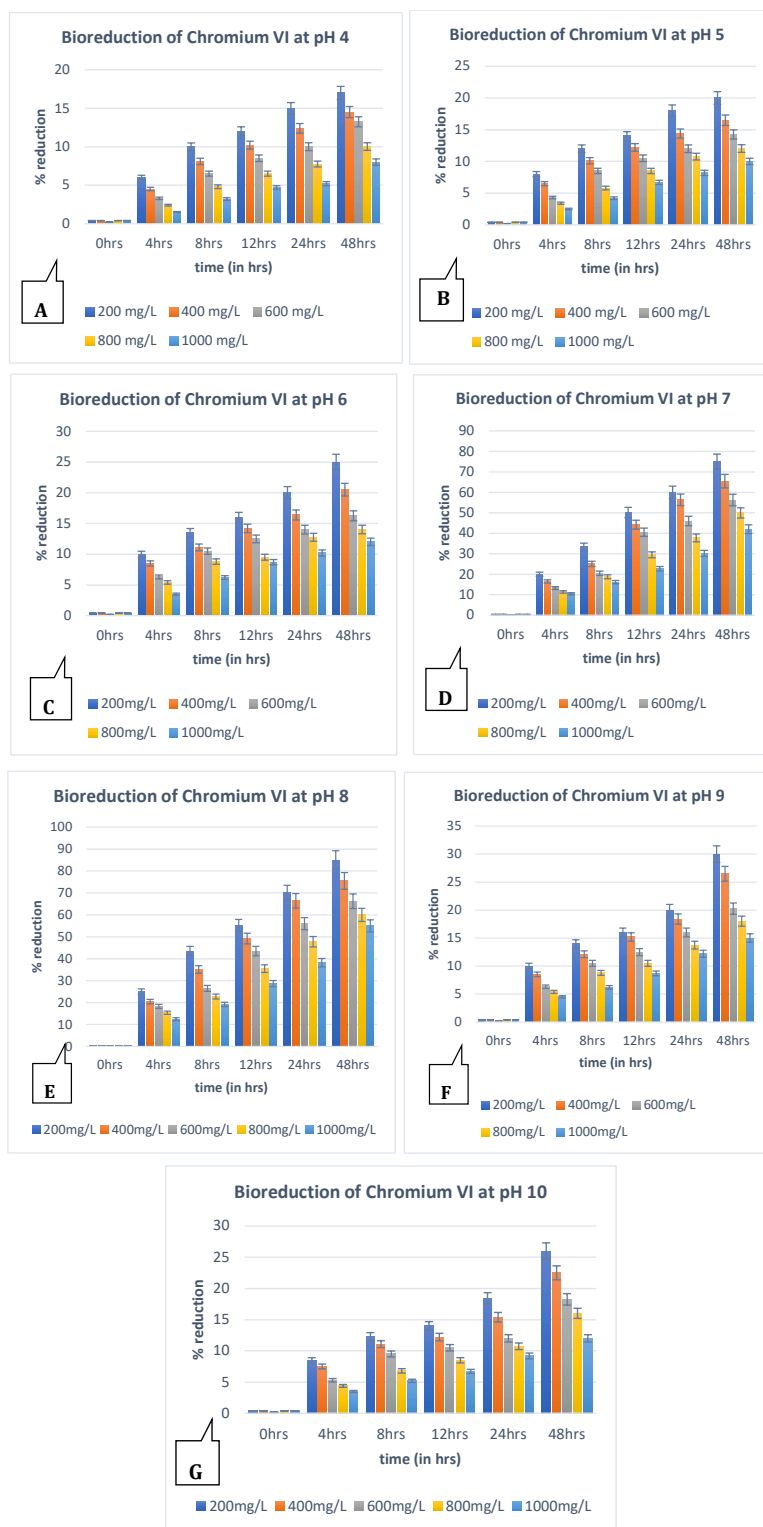
Fig. 8: Percentage reduction of Cr6+ at variable pH under different Cr $^{6+}$ Concentration.
pH4; **B**. pH5  ; **C.** pH6  ; **D**. pH7  **E**. pH8  **F.**.pH9   **G.** pH 10
(Error bars indicate the standard error of the mean reduction efficiencies from triplicate experiments with a p-value <0.05.)

Table 3: specific growth rate ($\mu$, h$^{-1}$) at pH 8 with variable glucose concentration at 200 mg.L$^{-1}$ Cr$^{6+}$. (Calculated from the slope of the graph).

| Sl. No. | Samples | Specific growth rate($\mu$): h$^{-1}$ |
|---------|---------|------------------------------------|
| 1. | control | 0.063039 |
| 2. | 0.5 g.L$^{-1}$ | 0.063039 |
| 3. | 1 g.L$^{-1}$ | 0.075187 |
| 4. | 1.5 g.L$^{-1}$ | 0.078524 |
| 5. | 2 g.L$^{-1}$ | 0.082863 |
| 6. | 2.5 g.L$^{-1}$ | 0.082863 |

(from Fig. 8A to Fig. 8G). The highest decrease of up to 85% was seen at 200 mg.L$^{-1}$ of Cr$^{6+}$ at pH 8 at roughly 48 hs (Fig. 8E), and the smallest reduction of 8.01%% was found in 1000 mg.L$^{-1}$ of Cr(VI) at pH 4. (Fig. 8A). Nonetheless, the 48 h period was consistent for all the data.

## Effect of Co-metabolic Substrate on Growth of DAS1 Reduction of Cr(VI)

Recently, cometabolism has become a potent technique for the biodegradation of refractory contaminants. Changing the substrate's carbon and energy composition may increase refractory compound degradation efficiency. The proportional relationship between a specific growth rate and a low substrate concentration is described by the Monod Equation.

$$\mu = \mu_{max}[s]/K_{s+} S$$

Three parameters are typically discovered to affect the specific growth rate of DAS1: (a) the concentration of the limiting substrate (glucose), (b) the maximal specific growth rate (max), and (c) the substrate-specific constant (Ks). The specific growth rate is independent of substrate concentration if excess substrate exists. Monod Equation yields a hyperbolic curve from which it is impossible to determine the precise values of Ks and $\mu_{max}$. The Monod equation was linearized using a line weaver-Burk plot, and the values of Ks and max were determined to be 0.44 g.L$^{-1}$ and 0.09 h$^{-1}$, respectively, using the equation below:

$$1/\mu = K_s /\mu_{max.}\ 1/s +1/\mu_{max}$$

Apart from the mathematical meaning, $k_s$ describes the affinity of microorganisms for a particular substrate. Fig. 9 to Fig. 12 illustrate the Effect of Co-metabolic substrate on the growth of DAS1 reduction of Cr(VI). Specific growth rates ($\mu$, h$^{-1}$) at pH 8 with variable glucose concentration at 200 mg.L$^{-1}$ Cr$^{6+}$ are given in Table 3.

## Determination of the Optimum Ratio of Mixed Culture for Maximum Cr(VI) Reduction

DAS1 and DAS2 were examined separately for their capacity for a reduction before being employed as mixed cultures in various ratios, including 1:1, 1:2, and 2:1. The ratio of 1:1 was chosen since it allowed for a maximum reduction of 97% (Fig. 13).

## Orthogonal Test

An experimental design known as an "orthogonal test" assures that all stated parameters may be calculated independently. The
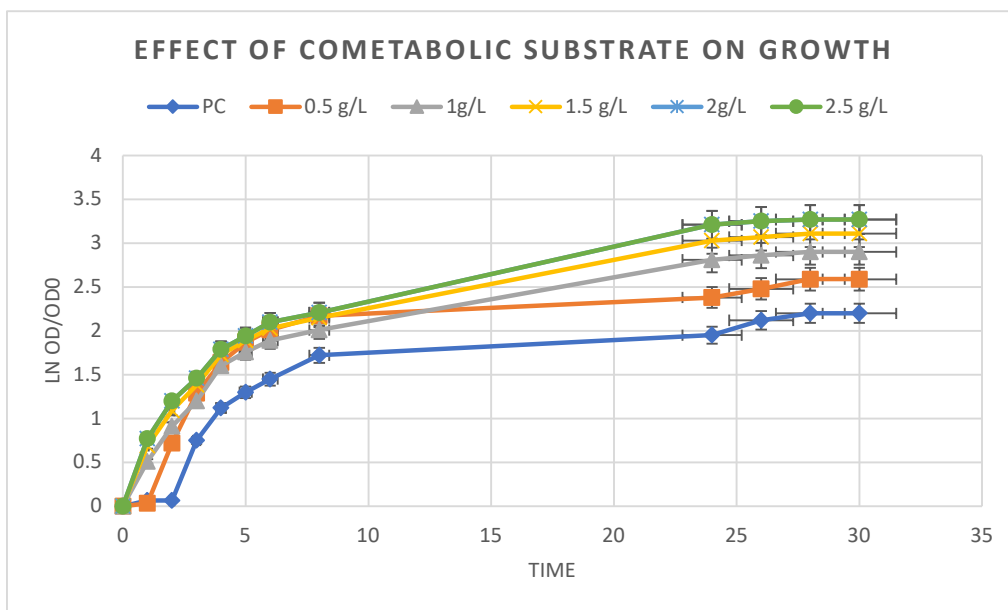


Fig. 9: *Bacillus licheniformis* DAS1 growth variation at pH 8 with variable glucose concentration at 200 mg.L$^{-1}$ Cr$^{6+}$.
(All values are the mean of three replicates, and standard errors (SE) are presented as error bars ($\pm$))

**EFFECT OF SUBSTRATE CONCENTRATION ON GROWTH OF DAS1 AT PH8.**
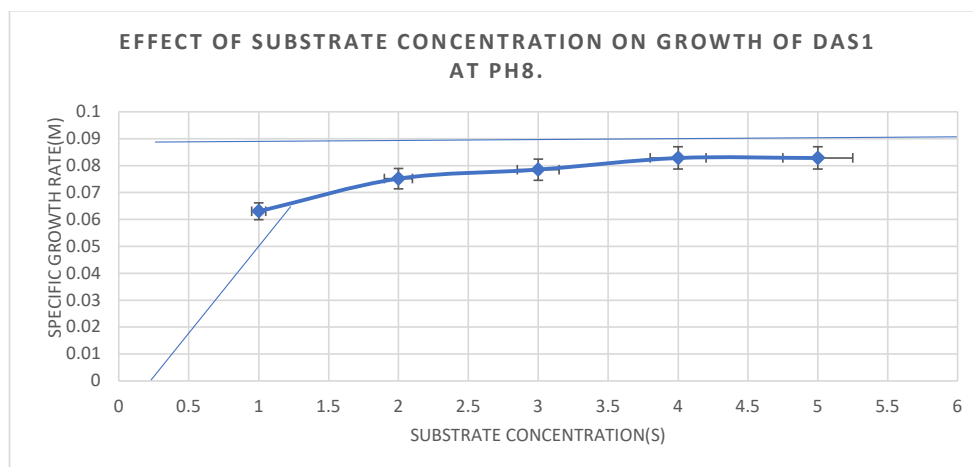
Fig. 10: Effect of substrate (glucose) conc on *Bacillus licheniformis* DAS1 growth at pH 8 measured as $k_s$ and $\mu_{max}$ by Monod equation. [All values are the mean of three replicates, and standard errors (SE) are presented as error bars (±)]

**LINE WEAVER BURK PLOT FOR KS AND MMAX**

$y = 4.831x + 10.999$
$R^2 = 0.9936$
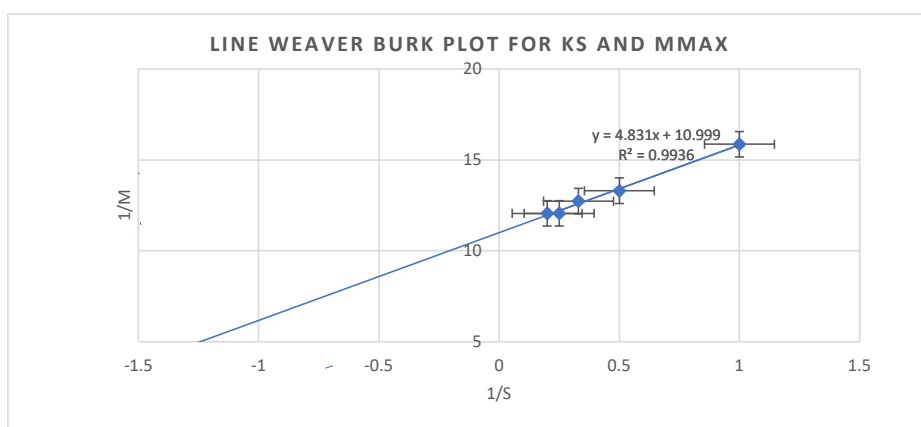
Fig. 11: Line Weaver Burk plot to Calculate k and $\mu_{max}$.
[All values are the mean of three replicates and standard errors (SE) are presented as error bars (±)]. $R^2=0.9936$

**Bioreduction of Chromium 6 at pH 8 with glucose as cometabolic substrate**
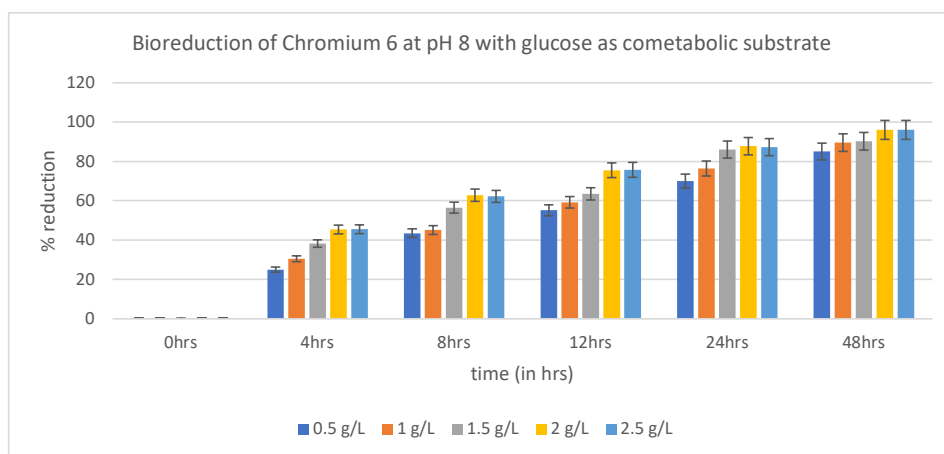
Fig. 12: percentage reduction of $Cr^{6+}$ at pH 8 & 200 mg.$L^{-1}$ $Cr^{6+}$ with glucose as Co-metabolic substrate.
(Error bars indicate the standard error of the mean reduction efficiencies from triplicate experiments with a p-value <0.05.)
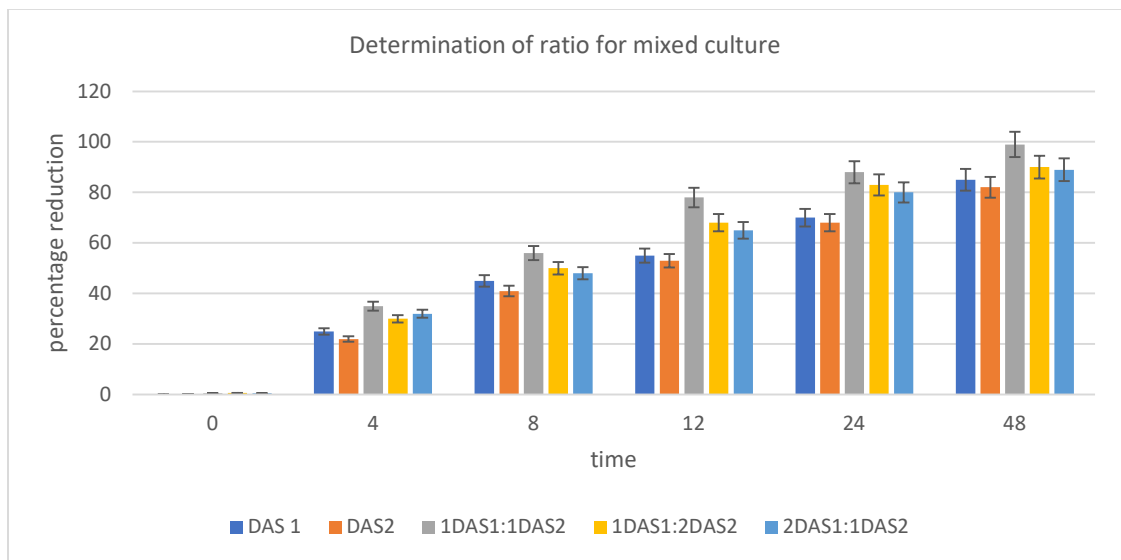
Fig. 13: Effect of mixed culture (1:1) of DAS1 and DAS2 on reduction of $Cr^{6+}$ toxicity.
(Error bars indicate the standard error of the mean reduction efficiencies from triplicate experiments with a p-value <0.05.)

Table 4: Experimental design, X-temp (X1-25° C, X2-30° C, X3-35° C) Y-pH (Y1-7.0 ,Y2-8.0, Y3-9.0) Y-Mixed inoculum of DAS1 and DAS2 in 1:1 ratio (Z1-5%,Z2-10%,Z3-15%).

| Test No. | X Temperature(°C) | Y pH | Z Inoculation Amount (%) | Combination | Cr(VI) -removal rate (%, 2d) |
|---|---|---|---|---|---|
| 1 | 2 | 1 | 2 | X2Y1Z2 | 65 |
| 2 | 1 | 2 | 2 | X1Y2Z2 | 88 |
| 3 | 3 | 1 | 3 | X3Y1Z3 | 76 |
| 4 | 1 | 1 | 1 | X1Y1Z1 | 68 |
| 5 | 2 | 3 | 1 | X2Y3Z1 | 56 |
| 6 | 3 | 3 | 2 | X3Y3Z2 | 59 |
| 7 | 1 | 3 | 3 | X1Y3Z3 | 48 |
| 8 | 2 | 2 | 3 | X2Y2Z3 | 89 |
| 9 | 3 | 2 | 1 | X3Y2Z1 | 99 |

mixed inoculum's optimal temperature, pH, and dose were determined through an orthogonal experiment design (33). The combination X3Y2Z1 demonstrated maximum efficiency, reducing 99% of 200 mg.L$^{-1}$ Cr(VI) in under 48 h. Therefore, the ideal growing conditions for DAS1 and Cr(VI) reduction were pH 8, 35°C, and a 5% inoculum concentration (Table 4).

**Effect of Bacterial Immobilization on Cr(VI) Reduction**

By immobilizing DAS1 in calcium alginate beads with a diameter of 3 to 5 mm, the Cr(VI) reduction capacities of mobile and immobile bacteria were assessed. It was discovered that after 48 hrs of incubation, immobilized bacterial cells could reduce 90.4% of Cr(VI), whereas mobile cells could only reduce up to 85% of Cr(VI) (Table 5). The findings suggest that encapsulated cells have more reduction

potential than mobile cells, which may be explained by the fact that stationary cells devote all their energy to reducing CR(VI). Encapsulated cells also provide greater benefits than mobile cells due to their increased stability, usability, etc.

**Investigation of the Mechanism of Cr(VI) % Resistance**

When DAS1 was grown with and without Cr(VI), it was noticed that there was a lag phase when the metal was present in the medium, indicating that chromium tolerance

Table 5: Cr(VI) reduction by mobile and immobile cells of DAS1.

| Sl. No. | Sample | Reduction % of Cr(VI) after 48 hrs. |
|---|---|---|
| 1. | Mobile bacteria | 85 |
| 2. | Immobile bacteria | 90.4 |

was not constitutive but rather inducible. Moreover, after treatment with Na2EDTA, DAS1 maintained its resistance to chromium salt, demonstrating that the impermeability of the outer cell membrane was not the cause of the metal tolerance.

## CONCLUSION

At pH 8 for 200 mg.L$^{-1}$ of Cr(VI), *Bacillus licheniformis* DAS1 showed maximum growth, with a specific growth rate (h-1) of 0.062125 h-1 and a bioreduction potential of 85%. Yet, when Bacillus licheniformis DAS1 was bound in calcium alginate beads, bioreduction potential rose to 90.4%. In addition to increasing the specific growth rate (h$^{-1}$) to 0.082863h-1 and bioreduction potential to 96.02%, glucose served as a metabolic substrate.

The Monod equation was used to analyze the impact of glucose on *Bacillus licheniformis* DAS1 growth, and the line weaver-Burk plot was used to compute ks and max, which were found to be 0.434 g.L$^{-1}$ and 0.090h$^{-1}$, respectively. 99% of Cr(VI) was converted to Cr using a 1:1 mixture of DAS I and DAS2 cultures (III). *Bacillus licheniformis* DAS1's resistance to Cr(VI) was not caused by the permeability of the cell membrane, and the enzyme activity was inductive rather than constitutive.

## ACKNOWLEDGMENT

## REFERENCES

Akcil, A., Erust, C., Ozdemiroglu, S., Fonti, V. and Beolchini, F. 2015. A review of approaches and techniques used in aquatic contaminated sediments: Metal removal and stabilization by chemical and biotechnological processes. J. Clean. Prod., 86: 24-36. https://doi.org/10.1016/j.jclepro.2014.08.009

Ayele, A. and Godeto, Y.G. 2021. Bioremediation of chromium by microorganisms and its mechanisms related to functional groups. J. Chem., 20: 1-21. https://doi.org/10.1155/2021/7694157

Batool, R. 2012. Hexavalent chromium reduction by bacteria from tannery effluent. J. Microbiol. Biotechnol., 22(4): 547-554. https://doi.org/10.4014/jmb.1108.08029

Eaton, A.D., Clesceri, L.S., Rice, E.W. and Greenberg, A.E. 2005. Standard Methods for the Examination of Water and Wastewater. 21st Edition, American Public Health Association (APHA) Press, Washington, DC.

Elahi, A., Rehman, A., Zajif Hussain, S., Zulfiqar, S. and Shakoori, A.R. 2022. Isolation and characterization of a highly effective bacterium, bacillus cereus B-525k, for hexavalent chromium detoxification. Saudi J. Biol. Sci., 29(4): 2878-2885. https://doi.org/10.1016/j.sjbs.2022.01.027

El-Naggar, N.E.A., El-khateeb, A.Y., Ghoniem, A.A., El-Hersh, M.S. and Saber, W.E.I. 2020. Innovative low-cost biosorption process of cr6+ by pseudomonas alcaliphila NEWG-2. Sci. Rep., 10(1): 473. https://doi.org/10.1038/s41598-020-70473-5

Ge, S., Gu, J., Ai, W. and Dong, X. 2021. Biotreatment of Pyrene and cr(vi) combined water pollution by mixed bacteria. Sci. Rep., 11(1): 800. https://doi.org/10.1038/s41598-020-80053-2

Ray, R.R. 2016. Review article. adverse hematological effects of hexavalent chromium: An overview. Interdiscip. Toxicol., 9(2): 55-65. https://doi.org/10.1515/intox-2016-0007

Sayantan, D. and Shardendu. 2013. Amendment in phosphorus levels moderate the chromium toxicity in Raphanus sativus L. as assayed by antioxidant enzyme activities. Ecotoxicol. Environ. Saf., 95: 161-170. https://doi.org/10.1016/j.ecoenv.2013.05.037

Tripti, K. and Shardendu 2016. Ph modulates arsenic toxicity in bacillus licheniformis das-2. Ecotoxicol. Environ. Saf., 130: 240-247. https://doi.org/10.1016/j.ecoenv.2016.04.029

Tripti, K., Sayantan, D., Shardendu, S., Singh, D.N. and Tripathi, A.K. 2014. Potential for the uptake and removal of arsenic [as (V) and as (iii)] and the reduction of as (V) to as (iii) by *Bacillus licheniformis* (DAS1) under different stresses. Korean J. Microbiol. Biotechnol., 42(3): 238-248. https://doi.org/10.4014/kjmb.1401.01004

Upadhyay, N., Vishwakarma, K., Singh, J., Mishra, M., Kumar, V., Rani, R., Mishra, R.K., Chauhan, D.K., Tripathi, D.K. and Sharma, S. 2017. Tolerance and reduction of chromium(vi) by *Bacillus* sp. mnu16 isolated from contaminated coal mining soil. Front. Plant Sci., 8L 778. https://doi.org/10.3389/fpls.2017.00778

Upadhyay, S. and Sinha, A. 2021. Modeling cometabolism of hexavalent chromium by iron-reducing bacteria in tertiary substrate system. Sci. Rep., 11(1): 37. https://doi.org/10.1038/s41598-021-90137-2

Villegas, L.B., Pereira, C.E., Colin, V.L. and Abate, C.M. 2013. The effect of sulphate and phosphate ions on cr(vi) reduction by streptomyces sp.. mc1, including studies of growth and pleomorphism. Int. Biodeter. Biodegrad., 82: 149-156. https://doi.org/10.1016/j.ibiod.2013.01.017

Wani, P.A., Wahid, S., Khan, M.S., Rafi, N. and Wahid, N. 2019. Investigation of the role of chromium reductase for Cr(VI) reduction by pseudomonas species isolated from Cr(VI) contaminated effluent. Biotechnol. Res. Innov., 3(1): 38-46. https://doi.org/10.1016/j.biori.2019.04.001

## ORCID DETAILS OF THE AUTHORS

Md. Saduzzaman: https://orcid.org/0000-0002-6457-4068
Kumari Mini: https://orcid.org/0000-0002-8844-6335
S. Rehan Ahmad: https://orcid.org/0000-0003-0796-5238

Original Research Paper | https://doi.org/10.46488/NEPT.2023.v22i04.011 | Open Access Journal

# An Analysis of the Effects that South Africa's Informal Settlements have had on the Country's River Systems

**B. Gqomfa\*, T. Maphanga\*† and B. S. Madonsela\***
\*Cape Peninsula University of Technology, Faculty of Applied Sciences, Department of Environmental and Occupational Studies, Corner of Hanover and Tennant Street, Zonnebloem, Cape Town, Republic of South Africa
†Corresponding author: T. Maphanga; maphangat@cput.ac.za

## ABSTRACT

The quality of surface water has a significant impact on human health and the entire ecological system. Sewer spillages from the surrounding informal settlements discharging into the river, carrying high concentrations of fecal coliforms, are one of the major causes of extreme pollution in the rivers of South Africa. These informal settlements are common in many developing countries, and they are usually located near waterways to compensate for basic demands for water, sanitation, and recreational space, where municipal infrastructure lags behind urban growth. One major problem has been poor sanitation and poor waste disposal practices in the informal settlements, which has led to the contamination of water resources. This study aims to assess the extent to which poor sanitation in informal settlements impacts the water quality of South African rivers, given the rapid rise in population and unemployment rate. The study also highlights health and environmental issues in the local regions caused by poor sanitation. Contamination of water bodies is associated with serious health problems and fatalities. Therefore, there is a need for frequent monitoring and management of waste products discharged into the neighboring aquatic environments.

## INTRODUCTION

One of society's biggest challenges is the scarcity of water which is exacerbated by the pollution of water bodies. The uneven distribution of water across the globe makes it even harder to manage water as some areas have ample water supply, while other areas may range from arid to semi-arid (Oki & Kanae 2006, Bega 2018). The issues of water supply in the latter areas are attributed to factors of low rainfall and high evaporation. Amid these issues are also environmental factors such as floods and droughts that make it hard to manage water, especially since drought and flood events are associated with exacerbating water scarcity and contamination of the water supply. These have subsequently led to the degradation of the quality of water bodies as determined by physical, chemical, and biological criteria (Strydom & King 2015). This degradation is typically measured in terms of the expected use of water, deviation from the norm, and impact on public health and ecology (Strydom & King 2015). For instance, when inefficiently treated wastewater is allowed to flow into the natural water bodies, cumulative impacts lead to the degradation of the water bodies. These impacts range from the degradation of the aquatic ecosystems to the waterborne illnesses, infections, and health complications that man is subjected to as a result of exposure to contaminated water used for irrigation, drinking, or bathing (DEADP 2011).

Contamination of water may originate from point sources or non-point sources. However, this contamination of water supply is not only limited to the direct point sources of inefficiently treated wastewater from the municipality that discharges effluents containing chemical and biological contaminants that are harmful; but it also includes non-point sources that cannot be quantified, such as the agricultural sources (Boardman et al. 2019). It is for this reason that non-point source pollution is difficult to control because it does not originate from a single, easily identifiable source that can be regulated. Instead, it is caused by the scouring effect of rainfall or snowmelt, as well as the dissolved contaminant solids that enter into the receiving water bodies (such as rivers, lakes, reservoirs, and bays) through runoff (Wang et al. 2021). Point sources and non-point sources such as sewage, garbage, and liquid waste coming from households, agricultural lands, and factories are often discharged into these lakes and rivers either directly or indirectly, especially where communities are residing next to the river, thus polluting these water bodies in the process (Barrow 2006, Maphanga et al. 2022, Gqomfa et al. 2022). This, therefore, makes sewage and household wastewater the main causes

of water pollution. Point- and non-point-source wastes may contain harmful chemicals and toxins, making the water poisonous for aquatic ecosystems. Sewage water, agricultural practices, oil spills, and radioactive substances are the most common types of water contamination (WWAP 2017). Therefore, it is clear that point sources and non-point sources are integral in the contamination of water sources. Hence, to mitigate the scarcity of water around the globe, countries have resorted to wastewater treatment plans to supplement water sources (Barceló & Petrović 2011).

South Africa's freshwater supply is under increasing pressure due to rapid urban population growth that has subsequently overloaded the wastewater systems such as sewerage, leading to the collapse of wastewater treatment infrastructure (Phungela et al. 2022) and compromising both health and the environment, given that the sewage is just flowing directly into the river (Bega 2021). Sewer spillages from the surrounding informal settlements discharging into the river, carrying high concentrations of fecal coliforms, are one of the major causes of extreme pollution in the river (Bega 2021). According to Statistics South Africa, informal settlements are "unplanned settlements on land that have not been surveyed or proclaimed as residential, consisting primarily of informal dwellings (shacks)". In 2013, it was estimated that 2.1 million South African households lacked access to basic housing services such as running water, electricity, and other amenities (Morole et al. 2022). South Africa is a semi-arid country with high water stress because of low rainfall volumes and high evaporation (Adewumi et al. 2010). Water safety measures, general health, and well-being education, and overall hygiene are prevalent issues in informal settlements. These issues go neglected because of a lack of information, support, and resources, resulting in sickness and harmful living circumstances. Greywater channels, which are wastewater streams that do not include sewage waste, pass through neighborhoods, fostering bacteria and many ailments (Radingoana et al. 2020). Toilet facilities are badly managed and filthy, resulting in a hazardous and unhygienic living environment (Cape Town Project Center 2014). Water pollution coupled with climate change makes matters around the informal settlements worse. There are also concerns that the stress on the water will worsen because of the current climate change projections. These projections tend to show uncertain after-effects for aquifer systems and the related groundwater goods and services (Knuppe 2011). The water sources and the health of the environment depend on sustainable rainfall patterns.

South Africa has an average rainfall of about 464mm per year (Mtengwana et al.2020). However, because of both local and global climate change, the country has witnessed fluctuating rainfall patterns, resulting in financial, economic, and ecological consequences, particularly when water supplies are under severe strain (Schulze 2005). Although water resources are scarce, even the available water is not evenly distributed. With changes in legislation (National Water Act 36 of 1998) from the apartheid era to the democratic dispensation, South Africa has tried to correct this anomaly. During the last decades of the apartheid period in South Africa, the Department of Water Affairs and Forestry (DWAF) was responsible for ensuring that the water needs of those chosen by the government, such as white farmers, were met. The democratic dispensation in South Africa brought change as the DWAF now ensures that all its citizens have access to safe water and basic water sanitation (Seward 2010). Despite this, South African households generally still lack adequate sanitation facilities, especially in informal settlements.

According to a Saturday Star report by Bega (2018), the Vaal River in South Africa is highly polluted, and the major contributors have been indicated as a high level of saline acid mine drainage effluent that is pumped into the river. Raw or partially treated sewage from local wastewater treatment plants is a major pollutant that creates serious health risks. The presence of $E.\ coli$ is also an indication of fecal existence in the water. $E.\ coli$ counts of 200-400 per 100 mL of water signify a major risk of gastrointestinal disorders(Bega 2017). Due to high pollution levels, the Vaal River has turned green, and a lot of fish have been found dead on the riverbanks. The community of Parys, located on the banks of the river, has suffered immensely due to such pollution (Bega 2018). The consequent water pollution poses a major threat to the well-being of both the environment and the population. Although several factors are associated with water pollution around informal settlements, insufficient studies have looked at the impacts of informal settlements on water quality in South Africa. This study aims to determine how inadequate sanitation and waste collection in informal communities affect the water quality of South African rivers. The report also emphasizes health and environmental problems in the local communities because of poor sanitation. This study is important as it will raise awareness of the impacts of informal settlements on river pollution, identify different sources of pollution, and help in understanding surface water quality such that the environment is protected and the water is safe for human use.

## LITERATURE REVIEW METHODS

The literature search included English peer-reviewed articles and relevant reports. All information used in the evaluation and review was collected from extensive project reports, published papers, and websites. The Google Scholar database and Web of Science were used to identify all the relevant

articles and reports. The criteria for selection included the following: (1) the impact of informal settlement on water quality; (2) monitoring the influence of urban sprawl on water pollution (3) the impact of rapid population and urbanization on water pollution; (4) the effect of shacks or informal settlements and different land uses on water quality; (5) contributors of surface water pollution in South Africa; and (6) the link between informal settlement and rate of water pollution just to mention few. However, the literature search focused on informal settlements, water pollution, and the destruction of river catchments around information settlements. Each article was assessed according to the accuracy of its results, and the systematic review and meta-analyses used for the selection of articles are included in our discussion.

## Causes of Water Pollution Around the Informal Settlements

Human beings are often responsible for being the main cause of water pollution, mostly due to an increase in anthropogenic activities, especially in the informal settlements where there is a general lack of basic municipal services. One of the central problems faced by residents in informal settlements is the lack of a proper system for waste management. As a result of a lack of established collection points, heaps of waste are scattered in and around residential zones, which leads to environmental and health problems. However, a minority of residents choose to burn or bury their waste near their residences(Ameyibor et al. 2003). Approximately 15 million people in South Africa lack adequate sanitation. Every citizen has a right to basic services, and municipalities are responsible for providing such services. However, the provision of basic services is a challenge and is aggravated by growing unemployment and the sprawling of unplanned informal settlements (Cousins 2004). According to a Stats SA (2016) media release, 45.6% of households in South Africa have no access to toilet facilities inside their homes, and less than 50% of households have a toilet outside of their residence.

Of the remaining 75.5% of people with access to sanitation, 12.2% have pit latrines, and 60.6% are connected to a sewerage system. In some informal settlements, toilets are shared (Stats SA 2016). As a result of these issues, residents have been forced to employ several alternative sanitation practices. Through interviews, observation, and focus group discussions in five informal settlements in the Western Cape, South Africa, 383 randomly selected respondents identified factors that shape their sanitation practices and how these practices impact access to and sustainability of sanitation services in the policy context of the Free Basic Sanitation

(FBSan) (Muanda et al. 2020). Residents utilize buckets, porta-potties, plastic bags, and existing facilities within and outside their communities for defecating or dumping bucket contents and open defecation. For instance, in the Ezindlovini informal settlement in Khayelitsha, more than 20,000 people share 380 communal toilets. Some of the residents do not have toilet facilities at all. There have been protests and cries against the local government for help in addressing this problem (Anonymous 2016). This case is similar to that of Dunoon informal settlements in Cape Town, where a large number of residents share few toilets, which are normally dirty and blocked. The residents have opted to defecate in open spaces close to the river (Gqomfa 2020).

A study conducted at the Apies River in Pretoria sampled the river at ten distinct locations (Abia 2020). These locations were upstream and downstream, exposed to various human activities. Several sewage treatment facilities damaged the river by directly discharging effluent into it. Due to system failure or overloading, the discharged effluent was sometimes not treated or partially treated. The river also receives waste from informal settlements close to the riverbank, directly through dumping or indirectly through surface runoff during heavy rains. The informal and rural settlements discharge their garbage, including feces, directly into the river (Abia 2020). The study also discovered that the number of bacteria isolated before the water traveled through informal settlements was lower than the number isolated after the river passed through the informal settlements. The residents were forced to use the river as a toilet due to a lack of facilities in the area.

## Urbanization and Poor River Systems

As stated by Worldometer (2020), South Africa's population in rural areas exceeded the population of urban areas by 10% in the year 1955. However, this is not the case anymore. In 2019, the South African population in urban areas was 66.3%, and it was estimated to rise to 66.7% in 2020(Worldometer 2020). Fig. 1 shows the rapid increase in the number of people moving from rural areas to urban areas. Although the urban population has been increasing, the rural population remained lower from 1955 to 1975 compared to the urban population. From 1980 to 2020, the urban population was higher than the rural population. In 2020, 66.7% of the population of South Africa lived in urban areas.

Urbanization is a major cause of the rapid spread of informal settlements. Many people migrating from rural areas cannot afford houses; they are compelled to construct shacks in the most vulnerable areas, such as wetlands, riverbanks, etc. Barrow (2006) corroborates that due to affordability, informal settlements are sometimes erected
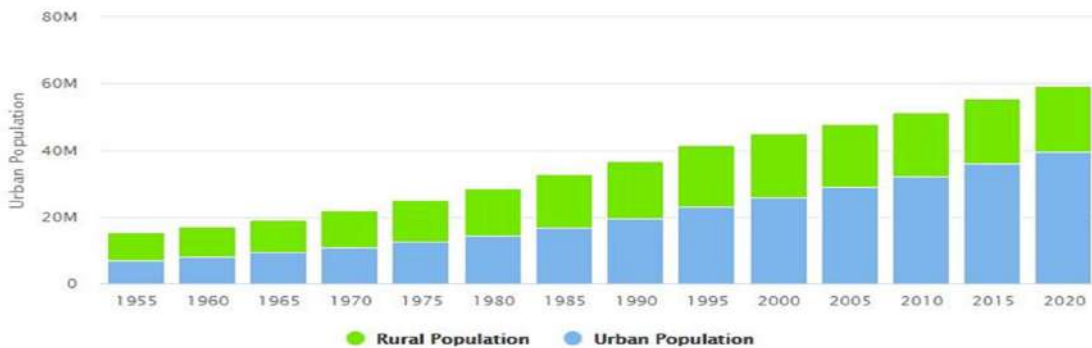
Fig. 1: South African urban vs rural population from 1955 to 2020 (Worldometer 2020).

in the most unfavorable conditions, such as those close to water bodies.

According to Barnes (2003), a study conducted in Cape Town showed that much of the water pollution is derived from human waste in informal townships where the municipality has not put appropriate sewerage systems or does not have adequate maintenance in place. In some parts of the settlements, untreated sewage leaks into storm water drains and flows into the water bodies. Barnes (2003) research work included the analysis of water samples for six years from the Plankenbrug River in Stellenbosch, which flows into the Eerste River(Barnes 2003). Samples from the river were taken, and interviews at Kayamnandi informal settlements were conducted. The results revealed that the river was excessively contaminated with hazardous levels of feces, which could adversely affect the health of all citizens who may come into contact with the water. The tests also revealed the presence of 13 million Escherichia coli per 100 ml of water. However, not all fecal contamination originated from Kayamnandi. Large amounts of fecal contamination occasionally entered the river near farming areas and Water Treatment Works areas below Kayamnandi (Barnes 2003).

**Trends on Rivers Water Quality in South Africa**

Although after 1994, revisions to South Africa's water law and regulatory frameworks were acknowledged for their emphasis on social and environmental sustainability, it is commonly acknowledged that the country's water quality is deteriorating. It is vital to comprehend what changes in water quality have occurred to analyze how management changes may have affected the resource (Abia 2020, Phungela et al. 2022). The Crocodile River in Mpumalanga and the Olifants River in Mpumalanga and Limpopo are used as examples for the investigation, which looks at trends in a number of water quality indices in these two catchments (Maphanga et al. 2022). The first is somewhat stressed and has previously been identified as water-stressed, whereas the second is severely impacted and has recently attracted a lot of attention in relation to water quality.

Overall, temporal trends frequently demonstrate declining water quality at locations in the mid to lower catchments, whereas locations in the high catchment may only experience minor changes. Sites that were impacted at the beginning of the data recording typically still exhibit that impact, though some have improved. In general, consequences are caused by increasing levels of orthophosphate (although recent studies indicate this trend has stopped at many locations), pH, salinity, and, for sites in the Olifants River, raised or increased sulfate and calcium levels. Compared to sulfate impacts, some locations displayed higher chloride levels indicative of salinization. Microbial levels were also high; however, no trend was visible (WRC Report 2014). A river system that has experienced human influence over time is the Eerste River. This study looked at the Eerste River's water quality between 1990 and 2005, looking for temporal and geographic patterns. The City of Cape Town (CCT) and the Department of Water Affairs and Forestry (DWAF) collected data at eight sample stations along the Eerste River's course and one on its tributary, the Plankenbrug, and it was analyzed to find the trends. Chemical oxygen demand (COD), pH, electrical conductivity (EC), nitrogen, and phosphorus were the water quality parameters analyzed (COD). Because they are regarded as important indicators of water quality, these measures were specifically chosen.

The lower parts of the Diep River (including the Milnerton Lagoon sites) and the Mosselbank River have declined over the past five years due to phosphorus enrichment, which has been a problem in the Diep watershed rivers historically (Gqomfa 2020, Ggomfa et al. 2022). The catchments in this area that perform the worst right now include. From 1995 to 2020, the Diep River catchment has been monitored. Fecal contamination: E. coli measurements recorded at river sites in the Sand catchment have deteriorated moderately over the monitoring period (1990-2020), indicating that conditions

are not entirely suitable for informal recreational activities (Inland 2019). Illegally establishing informal settlements on property deemed inappropriate for housing is one of the issues connected to the improper management and disposal of human waste. Due to the difficulty in providing services, homeowners often dump their domestic trash, greywater, and sewage into the environment, which leads to rapid contamination and the deterioration of occasionally significant waterbodies. Poorly maintained informal settlements and backyard residents in the Salt catchment are also sources of river water pollution (e.g., Joe Slovo, Kanana, Valhalla Park, Vygieskraal informal settlements). Additionally, backyard houses contaminate the Diep River in formal settlements like Fisantekraal as well as in informal settlements in the basin, such as Dunoon and Joe Slovo (Inland 2019).

## The Contribution of Informal Settlements in Different Provinces to River Pollution

Unplanned urbanization has contributed to the ongoing rise in informal settlements. The number of households living in informal settlements has grown since 1995, going from 1 170 902 to 1 294 904 by 2011. More than 2,700 informal settlements were nationwide (Stats SA 2016). According to government data, the number of informal settlements in South Africa increased to 2225 between 2002 and 2016 (Stats SA 2016). According to assessments and records, there were reportedly roughly 3200 informal settlements as of May. Approximately five million people live in informal settlements in and around the major urban areas (Mbanga 2020). This growing trend of informal settlements compromises the river systems. Rivers and other freshwater resources in South Africa are becoming stressed due to the country's rising economy and population. Additionally, due to increased pollution brought on by industry, urbanization, afforestation, mining, agriculture, and power generation, the water quality of these resources has deteriorated (Ashton et al. 2016).

The fast growth of informal settlements is mostly due to urbanization coupled with rapid population growth and a high unemployment rate, forcing people to migrate to urban areas (Morole et al. 2022). The most vulnerable sites, such as marshes and riverbanks, are where many people coming from rural areas establish shacks because they are unable to purchase homes. Informal settlements are sometimes in unfavorable conditions, such as those close to water bodies (Tsenkova 2010). Along South Africa's riverbanks, informal settlements dump rubbish into the rivers as well. When there is significant rainfall, this is transported by dumping and surface runoff (Maphanga et al. 2022). These informal settlements were not constructed per the necessary laws and lacked suitable waste disposal facilities (Gqomfa et al. 2022). Table 1 gives an overview of the water quality of South Africa's rivers and the informal settlements as contributors to their pollution.

The declining river water quality affects all of Africa, not just South Africa. For instance, low-income populations, especially those who reside in informal settlements, frequently use Kenya's Nairobi River as a source of water for cleaning, washing, and watering crops (Mbui 2019). Furthermore, because many homes lack toilet facilities, the river is also used to dump human and domestic waste.

## Impacts of the Environmental Pollution Caused by Informal Settlements on the South African River Systems

Table 1: Overview of the water quality of South Africa's rivers and the informal settlements as contributors to their pollution.

| Provinces | Rivers | Impacts of River Pollution & Sources |
|---|---|---|
| Kwazulu Natal | Umgeni River | The catchment areas vary in size and land use, ranging from dense informal settlements to primarily agricultural. Phosphorus input and bacterial contamination were both monitored. It was discovered that the watershed with the greatest proportion of informal settlements also had the greatest levels of non-point source pollution (Gangoo 2003). |
| Western Cape | Diep River, Black River | The informal community of Island in Site C, Khayelitsha, includes a river that is largely blocked by trash, smells noxious, and serves as a home for rats. Diep River and Black River, amongst other things, have also been polluted largely by Informal settlement waste and open defecation (Gqomfa et al. 2022, GroundUp 2018). |
| Mpumalanga/ Northern Cape/Gauteng | Olifant River | The Olifant River is close to a variety of informal settlements. Along with informal settlements polluting the catchment, sewage treatment facilities also contributed to microbiological contamination and related diseases (Ecosystem Health 2011). |
| Eastern Cape | Umtata River | According to 2001 research, contamination from residential waste from multiple riverbank informal communities is the cause of the high coliform counts and nutritional levels that are over permitted limits (Fatoki et al. 2001) |
| Gauteng | Jukskei Hennops, Klip, Apies Rivers | The rivers in Gauteng revealed that the main human activities that impact, alter, and contaminate rivers like the Jukskei, Hennops, Klip, Apies, and numerous tributaries are poorly maintained sewage systems, treatment plants, and informal settlements built along the banks of the rivers (Liebenberg 2019) |

Informal settlements in South Africa lack essential amenities and, as a result, turn to environmental degradation, such as trash dumping, the loss of vegetative cover, and water contamination. Many informal communities are located near water sources, particularly rivers (Gqomfa 2020). Due to the lack of sanitation, many people in these communities make shallow pit latrines, other natural resources, and riverbanks. As a result, the potential for water contamination is quite significant in these communities (Gangoo 2003, Kretzmann 2019). The river's water quality is impacted by pollution caused by dumping, trash, loss of vegetative cover, and raw sewage run-offs (Mbui 2019). Therefore, the pH and conductivity of the water are altered. The term "water quality" is used in this paper to express water's suitability to sustain various uses or processes. Any specific use will possess some requirements for the physical, chemical, or biological characteristics of water; for instance, limits on the concentrations of toxic substances for the use of drinking water or temperature and pH range restrictions for water that supports invertebrate communities (Bartman & Ballance 1996, Liebenberg 2019). Water quality also describes how suitable the water is for maintaining recreational, domestic, agricultural, and industrial or aquatic ecosystem processes (DEADP 2011). In general, the quality of natural water differs from one place to another, subject to seasonal changes, soil and rock type, and the surface through which it flows. The quality of water is considerably changed by various human activities like mining and recreation, urban and industrial development, and agriculture (Kretzmann 2019). The quality is also altered extensively within the spatial catchment area.

When the environment deteriorates as a result of the depletion of resources such as air, water, and soil, it leads to environmental degradation (Choudhary et al. 2015). The process of environmental degradation compromises the natural environment, reducing biological diversity and negatively impacting the general health of the environment (Mbonambi 2016). The environment may also deteriorate due to urban growth-related challenges in developing and developed countries; for example, water and air pollution, refuse disposal, and loss of farmlands and natural areas (Barrow 2006). Cape Nature compiled a river report as part of the Western Cape River Health Programme, sponsored by the Department of Water Affairs and Forestry, and aimed at investigating the quality, quantity, and ecosystem health in the Western Cape. The report revealed that, in general, only a small number of Cape Town's rivers are still in good condition (Gosling 2007). This clearly shows that the quality of water in the rivers has been deteriorating due to several reasons, amongst them being informal settlements (Gangoo 2003). The deterioration of the water quality of rivers in South Africa has brought about challenges such as microbiological contamination and eutrophication, just to name but a few (Strydom & King 2015). Microbiological pollutants from sewage often lead to contagious diseases that infect drinking water, affecting land and water life (Mbui 2019). Water supplies that have been inadequately treated will have noticeable levels of total coliform bacteria and fecal coliforms due to the presence of *E. coli*. *E.coli* indicates fecal pollution from humans and warm-blooded animals (Strydom & King 2015).

Furthermore, there is a link between fecal pollution and eutrophication. Rivers and streams are impacted by these pollutants, which cause eutrophication, move sediments, and introduce harmful bacteria when transported by rain runoff (Bianco et al. 2020). Eutrophication is excessive nutrient enrichment, increased growth of microscopic floating plants, and algae, and the formation of floating plants in water bodies (Smith & Schindler 2009, Mbonambi 2016). It also tends to cause suffocation of fish and water organisms. Eutrophication is characterized by too much plant and algal growth as a result of the increased availability of one or more limiting growth factors needed for photosynthesis, such as sunlight, carbon dioxide, and nutrient fertilizers (Schindler 2006, Bianco et al. 2020). The pH of water can also change to acidic due to sulfate particles from acid rain. This can cause damage to aquatic life, resulting in a high number of deaths within an environment (Khan & Ansari 2005, Kretzmann 2019). The growth of photosynthetic plants and microorganisms can also be disrupted because of suspended particles that tend to reduce the amount of sunlight penetrating the water (Strydom & King 2015). As the water quality has deteriorated, causing eutrophication, therefore eutrophication will cause alteration in the species composition within the aquatic ecosystem.

Informal settlements are also susceptible to ruin by the natural elements and easy to destroy by fire. Fires may cause air pollution, and, in turn, the particles from air pollution may pollute the water bodies (SERI 2018). Inadequate planning regarding drainage or sewage systems exposes informal settlements to flooding and risk of diseases because of still water and waste that is not collected but blocking drainage around the rivers or the river. This, in turn, degrades the ecosystems and their inhabitants (SERI 2018). Many rivers across the country are facing these challenges. For example, an informal settlement of Site C in Khayelitsha in South Africa is situated at the edge of the river. The river is regularly blocked with litter, and odors of toxins and has become a safe harbor for rodents. A lot of the litter is dumped by the residents of Site C into the river (Green 2018). Fig. 2 shows the Langa informal settlement constructed in the most vulnerable area, on the edge of the

Fig. 2: Langa informal settlement and pollution of Black River (Gqomfa 2020).

Black River. These settlements are prone to floods during rainy seasons. Residents dispose of their waste into the river, thus contaminating it (Mbanga 2020). Waste disposed of close to the river also enters the river, thus contaminating it through runoffs during rainy seasons.

The methods used to dispose of waste in informal settlements, such as dumping, pits, and burning waste, are harmful to the environment. The groundwater and surface water are also polluted due to the use of these disposal practices in informal settlements, as waste from the land surface can move through the soil and end up in groundwater (Mbanga 2020). As a result, pesticides, fertilizers, and waste disposed of in waste pits and landfills can pollute groundwater (Barrow 2006).

Waste management in underdeveloped nations is often characterized by unregulated dumping of waste, which is frequently accompanied by open burning (UNEP 2018). Carbon dioxide is the principal gas generated by rubbish burning, with an estimated 40 to 50 percent of waste being made up of carbon by mass. Other worldwide sources of carbon dioxide emissions, such as autos and power plants, account for just 5% of the total global $CO_2$ emissions. Dumping waste in informal settlements causes decay, leading to unpleasant odors. Consequently, dust, methane, and greenhouse gases are produced as a by-product of organisms decomposing organic waste (Ferronato & Torretta 2019).

On the other hand, the increasing amount of human involvement with the earth's climate system, caused by the continual growth in greenhouse gases, is producing imbalances in the earth's atmosphere, resulting in a variety of local and regional effects. These effects have shown themselves in a variety of ways, including changes in precipitation patterns, droughts, vegetative patterns, crop production changes, and so on. According to the IPCC (2018), the world has until 2030 to cut human-caused carbon dioxide emissions in half and reduce other greenhouse gases to have a 45% chance of avoiding the worst impacts of climate change.

## DISCUSSION AND RECOMMENDATIONS

### The impact of Erecting Informal Settlements on Water Quality

The physical disturbance of the land due to the construction of informal settlements alters land use, leading to environmental impacts (Gqomfa et al. 2022). For instance, the alteration of land use due to urbanization and agriculture causes precipitation to run off quickly, resulting in severe erosion, flash flooding, reduced groundwater, recharge, and wildly fluctuating streamflow. This poor use of land leads to nutrient over-enrichment and sediment-contaminated water, which harms fish, plankton, and aquatic plants and may slit up channels, lakes, and reservoirs (Barrow 2006, Bianco et

al. 2020). One of the major challenges that emanate from informal settlements existing along riverbanks is that people tend to do laundry in the river, as is the case with one of the Alexandra informal settlements called Stjwetla, closest to the Jukskei River in Gauteng (Mawela 2008). Phosphate salts are included in a wide variety of laundry detergents in concentrations ranging from 35 to 75%. Phosphates may contaminate water in a variety of ways, including limiting the biodegradation of organic matter. Non-biodegradable chemicals cannot be removed by either public or private wastewater treatment systems. Phosphate-based detergents can also cause eutrophication, and phosphate enrichment can cause algae and other plants to overgrow in bodies of water (Abia 2020). Eutrophication depletes available oxygen in the water, causing other species to die (Senapati 2021). The aquatic organisms are also critically impacted by pollution, erosion, and sedimentation generated by the construction of these informal settlements, which use up the dissolved oxygen content in the environment and decrease the total biodiversity of the area(Owusu-Asante & Ndiritu 2009). Furthermore, as a result of the large population, there are sewage problems time and again, which find their way into the river  (Mawela 2008).

## Sustainable Development and Water Quality

The Brundtland Commission made sustainable development popular and placed it in context, defining it as "development that meets the needs of the present without compromising the ability of future generations to meet their own needs" (Barnaby 1987). The commission focused on economic, socio-political, and ecological/environmental conditions. The concept of sustainable development advocates setting up strong measures to stimulate economic and social development, especially for people in developing countries, as well as making sure that the integrity of the environment is sustained for upcoming generations. Principles of International Environmental Law and Policymaking (e.g., Stockholm and Rio Declarations and Agenda 21) have been adopted by South Africa (Fuggle & Rabie 2015). Again, South Africa has hosted important international conferences such as the 2002 World Summit on Sustainable Development. Such summits are essential; hence, they support urban water sustainability, including access to safe drinking water, wastewater management for improved public health, and protection against flooding (Larsen et al. 2016).

The real achievements of sustainable urban development are still inadequate because of challenges, even though it has drawn interest for many years(Rathnayaka et al. 2016). Changes implemented to create greener water and improve wastewater management have drawn attention and proposals. This is because the growth of the integrated

urban water system is understood to play a key role in urban water sustainability (Capodaglio et al. 2016). Sustainable development requires that outputs, such as waste and pollution, and inputs be handled effectively in urban or rural environments. Some of the urban challenges that take priority are water supply, refuse, sewage disposal, energy, informal settlements, and transport (Barrow 2006, Abia 2020). In the transition towards sustainable development, it is important to include the public in decisions regarding water management. This helps to encourage practitioners to develop a more viable management practice (Rabadán & Sáez-Martínez 2017). The responsibility for water and waste management should be shared between government authorities and businesses. Even so, there is difficulty in determining where public responsibility ends, and corporate responsibilities begin (Rabadán & Sáez-Martínez 2017).

To attain the goal of sustainable development, precautionary and proactive measures need to be taken because humans seem to be more exposed (Barrow 2006). These measures are intended to monitor the handling and disposal of hazardous substances that could negatively and irreversibly destroy the environment. Certain substances pose major risks to the environment due to their toxicity, persistence, and capacity to bioaccumulate. In cases where the behavior of a particular substance is barely known, that substance is presumed to be a threat. A system that could be used to identify this type of pollutant has not yet been established in South Africa, particularly relative to discharge into water resources (Strydom & King 2015).

## CONCLUSION

The water demand continues to rise, and this calls for improved management of supplies. Indeed, rivers are sensitive and important ecosystems that have been extensively damaged globally and locally. This paper briefly reviewed the impact of informal settlements on the quality of water in South African rivers. The paper showed that the quality of water is affected mostly by anthropogenic activities and is declining due to the rise of urbanization, population growth, industrial production, climate change, non-compliance of wastewater treatment plants, agricultural waste, and other factors. Attempts to provide general coverage for water and sanitation continue to face challenges in South Africa, and the most vulnerable and poor communities are largely affected by this failure. The overcrowded informal settlements with inadequate sanitation are a major problem, coupled with the lack of other services like waste collection. Due to a lack of such services, human health is negatively impacted by water-related diseases as the water bodies are extensively polluted. Using polluted water from rivers for washing, swimming, drinking, and cooking

has spread water-related diseases. The subsequent water pollution poses a major threat to the well-being of both the environment and the population. Even though South African laws are meant to ensure that water resources are protected and managed sustainably and equitably to benefit all its citizens, there is a challenge with enforcement and compliance. To promote sustainable development, it is vital to incorporate the populace in decisions about water management. This may assist in encouraging experts to develop feasible management practices. Water and waste management is understood to be a mutual responsibility of government authorities, businesses, and all stakeholders.

## ACKNOWLEDGMENTS

## REFERENCES

Abia, A.L.K. 2020. River of Bacteria: A South African Study Pinpoints What's Polluting the Water. Retrieved from https://theconversation.com/river-of-bacteria-a-south-african-study-pinpoints-whats-polluting-the-water-150551 (Accessed: 23 January 2021).

Abram, N. 2021. Yes, A Few Climate Models Give Unexpected Predictions, But the Technology Remains a Powerful Tool. Retrieved from https://phys.org/news/2021-08-climate-unexpected-technology-powerful-tool.html (Accessed: 07 January 2022).

Adewumi, J.R., Ilemobade, A.A. and Van Zyl, J.E. 2010. Treated wastewater reuse in South Africa: Overview, potential and challenges. Resour. Conserv. Recycl., 55(2): 221-231.

Ameyibor, S., Basteck, T., Bierbaum, C., Frommeld, N., Giaourakis, N., Hackenbroch, K., Kirchberg, A., Kutsch, A., Mendel, M., and Schlichting, S. 2003. Informal Settlements Development on Zanzibar; A Study on the Community Based Provision of Storm Water Management. Retrieved from http://www.ips.raumplanung.tu-dortmund.de/cms/Medienpool/documents/F03_Informal_Settlements_Development_on_Zanzibar.pdf (Accessed: 17 March 2020).

Anonymous. 2016. Dying for A Pee: Khayelitsha Residents Battle for Asanitation. Retrieved from https://ewn.co.za/2016/10/12/Dying-for-a-pee-Khayelitsha-residents-battle-for-sanitation (Accessed: 17 February 2020).

Arnone, R.D. and Walling, J.P. 2007. Waterborne pathogens in urban watersheds. J. Water Health, 5(1): 149-162.

Barcelo, D. and Petrovic, M. 2011. Wastewater Treatment and Reuse in the Mediterranean Region. The Handbook of Environmental Chemistry. Springer-Verlag Berlin Heidelberg, New York.

Barnaby, F. 1987. Our Common Future: The 'Brundtland Commission' Report. Ambio., 16(4): 217-218.

Barnes, J.M. 2003. The Impact of Water Pollution from Formal and Informal Urban Developments Along the Plankenbrug River on Water Quality and Health Risk. PhD Thesis. Stellenbosch University, South Africa.

Barrow, C.J. 2006. Environmental Management for Sustainable Development, 2nd ed. Routledge, New York.

Bartman, J. and Ballance, R. 1996. Water Quality Monitoring: A practical guide to the design and implementation of freshwater quality studies and monitoring. Retrieved from https://apps.who.int/iris/bitstream/handle/10665/41851/0419217304_eng.pdf?sequence=1&isAllowed=y (Accessed: 4 April 2020).

Bega, S. 2017. Pollution of Vaal River at Crisis Point. Retrieved from http://fse.org.za/index.php/item/585-pollution-of-vaal-river-at-crisis-point (Accessed: 29 October 2019)

Bega, S. 2018. Vaal River Suffocates Under A Filthy Wave of Raw Effluent. Retrieved from https://www.iol.co.za/saturday-star/news/vaal-river-suffocates-under-filthy-wave-of-raw-effluent-16292140 (Accessed: 29 October 2019).

Bianco, K., Albano, R.M., De Oliveira, S.S., Nascimento, A.P.A., Dos Santos, T. and Clementino, M.M. 2020. Possible health impacts due to animal and human fecal pollution in water intended for the drinking water supply of Rio de Janeiro, Brazil. J. Water Supply: Res. Technol. Aqua., 69(1): 70-84.

Bisaga, I., Parikh, P. and Loggia, C. 2019. Challenges and opportunities for sustainable urban farming in South African low-income settlements: A case study in Durban. Sustainability, 11(20): 5660.

Boardman, E., Danesh-Yazdi, M., Foufoula-Georgiou, E., Dolph, C.L.and Finlay J.C. 2019. Fertilizer, landscape features, and climate regulate phosphorus retention and river export in diverse Midwestern watersheds. Biogeochemistry, 146(3): 293-309.

Bosworth, B. 2013. SA: Trust Saving an Overburdened River. Retrieved from http://nepadwatercoe.org/south-africa-saving-an-overburdened-river/ (Accessed: 08 April 2020).

Cape Town Project Center. 2014. Water, Sanitation, and Hygiene in Informal Settlements. https://wp.wpi.edu/capetown/resource-library/water-sanitation-and-hygiene-in-informal-settlements/ (Accessed 04 January 2022).

Capodaglio, A.G., Ghilardi, P. and Boguniewicz-Zablocka, J. 2016. A new paradigm to urban water management for conservation and sustainability. Water Pract. Technol., 11(1):176-186.

Choudhary, M.P., Chauhan, G.S. and Kushwah, Y.K. 2015. Environmental Degradation : Causes, Impacts, and Mitigation. In: National Seminar on Recent Advancements in Protection of Environment and Its Management Issues (NSRAPEM-2015).

City of Cape Town (COCT). 2011.City of Cape Town: Water By-law, 2010. City of Cape Town, South Africa. Retrieved from http://resource.capetown.gov.za/documentcentre/Documents/Bylaws%20and%20policies/Water%20By-law%202010.pdf (Accessed: 17 March 2020)

Conway, G.R. and Pretty, J.N.2009. Unwelcome Harvest: Agriculture and pollution. Earthscan, Sterling.

Cousins, D. 2004. Community Involvement in the Provision of Basic Sanitation Services to Informal Settlements. Master's Thesis, Cape Peninsula University of Technology, South Africa.

Department of Environmental Affairs and Development Planning, South Africa (DEADP). 2011. Land Use. Department of Environmental Affairs and Development Planning, Cape Town. Retrieved from https://pdfslide.net/download/link/western-cape-iwrm-action-plan-status-quo-report-final-draft-western-cape-iwrm. (Accessed: 03 April 2020).

Drinking Water Inspectorate (DWI). 2015. Drinking Water Quality in England: The Position After 25 Years of Regulation. Drinking Water Inspectorate, London.

Edokpayi, J.N., Rogawski, E.T., Kahler, D.M., Hill, C.L., Reynolds, C., Nyathi, E., Smith, J.A., Odiyo, J.O., Samie, A., Bessong, P. and Dillingham, R. 2018. Challenges to Sustainable Safe Drinking Water: A Case Study of Water Quality and Use across Seasons in Rural Communities in Limpopo Province, South Africa. Water, 10(159): 1-18.

Ferronato, N. and Torretta, V. 2019. Waste Mismanagement in Developing Countries: A Review of Global Issues. Int. J. Environ. Res. Public Health.,16(6): 1060.

Frayne, B., Battersby-Lennard, J., Fincham, R. and Haysom, G. 2019. Urban food security in South Africa: A case study of Cape Town, Msunduzi and Johannesburg. In Development Planning Division Working Paper Series No. 15; DBSA: Midrand, South Africa.

Fuggle, R.F. and Rabie, M.A. (eds.). 2015. Environmental Management in South Africa, 2nd ed. Juta and Company Ltd, Claremont.

Gangoo, A. 2003. Informal Communities And Their Influence on Water Quality: The Case of Umlazi. Master's Thesis, University of Durban Westville, South Africa.

General Assembly of the United Nations. 1997. Convention on the Law of the Non-navigational Uses of International Watercourses-1997. United Kingdom.

Gleick, P.H. 2002. Dirty Water: Estimated Deaths from Water-Related Diseases 2000-2020 Pacific. Pacific Institute, Oakland.

Gosling, M. 2007. Cape Town Rivers Pose A Serious Health Risk. Retrieved from https://www.iol.co.za/news/south-africa/cape-town-rivers-pose-a-serious-health-risk-318670 (Accessed 29 November 2019).

Gqomfa, B. 2020. The Impact of Informal Settlement on Water Quality of Diep River in Dunoon. Master's Thesis. Cape Peninsula University of Technology, South Africa.

Green, E. 2018. Why do informal settlements get cluttered with litter? Retrieved from https://www.groundup.org.za/article/why-do-informal-settlements-get-cluttered-litter/ (Accessed: 08 November 2018).

Gupta, A. AND Chandra, R. 2013. Impact of the effluent of River Ramganga on the hematology of freshwater fish (Heteropneustes fossilis). Int. J. Environ. Sci., 4(3): 19-22.

Global Water Partnership Technical Advisory Committee, Sweden (GWP-TAC). 2000. Integrated water resources management. Global Water Partnership, Stockholm, Sweden.

Hasan, M.M. and Alam, K. 2020. Inequality in access to improved drinking water sources and childhood diarrhea in low- and middle-income countries. Int. J. Hyg. Environ. Health., 226: 113493.

Ingwani, E., Gondo, T. and Gumbo, T. 2010. The polluter pay principle & the damage done: Controversies for sustainable development. Econ. Seria Manage., 13(1): 53-60.

Intergovernmental Panel on Climate Change (IPCC). 2018. Global Warming of 1.5 °C. Retrieved from https://www.ipcc.ch/site/assets/uploads/sites/2/2018/07/SR15_SPM_version_stand_alone_LR.pdf (Accessed: 10 January 2022).

Khan, F.A. and Ansari, A.A. 2005. Eutrophication: An ecological vision. Bot. Rev., 71(4): 449-482.

Knuppe, K. 2011. The challenges facing sustainable and adaptive groundwater management in South Africa.' Water SA., 37(1): 67-79.

Kretzmann, S. 2019. Cape Town Fails to Publish Water Quality Tests for Two Years. Retrieved from https://www.news24.com/Green/News/city-of-cape-town-fails-to-publish-water-quality-tests-for-two-years-20190212 (Accessed: 17 February 2020).

Larsen, T.A., Hoffmann, S., Lüthi, C., Truffer, B. and Maurer, M. 2016. Emerging solutions to the water challenges of an urbanizing world. Science, 352(6288): 928-933.

Maphanga, T., Madonsela, B.S., Chidi, B.S., Shale, K., Munjonji, L. and Lekata, S., 2022. The Effect of Rainfall on Escherichia coli and Chemical Oxygen Demand in the Effluent Discharge from the Crocodile River Wastewater Treatment; South Africa. Water, 14(18): 2802.

Mawela, A.S. 2008. The Level of Environmental Education Awareness Regarding Water Pollution-Related Diseases By Learners Who Live in the Stjwetla Informal Settlement Adjacent to the Jukskei River in Alexandra. Master's Thesis. University Of South Africa, South Africa.

Mbonambi, Z. 2016. An investigation into the environmental impacts of informal settlements on water: a case of Kennedy Road informal settlement in Durban, KwaZulu-Natal. Master's Thesis. University of KwaZulu-Natal, South Africa.

Mccaffrey, S. 1998. The UN Convention on the Law of the Non-Navigational Uses of International Watercourses: Prospects and Pitfalls. World Bank Technical Paper, Washington, DC, pp. 17-27.Retrieved from https://www.unece.org/fileadmin/DAM/env/water/cwc/legal/UNConvention_McCaffrey.pdf (Accessed: 19 July 2021).

Misati, A.G. 2016. Household safe water management in Kisii County, Kenya. Environ. Health Prev. Med., 21(6): 450-454.

Mpindou, G.O.M.K., Bueno, I.E. and Ramón, E.C. 2021. Review on emerging waterborne pathogens in Africa: The Case of Cryptosporidium. Water., 13(21): 2966.

Mtengwana, B., Dube, T., Mkunyana, Y.P. and Mazvimavi, D. 2020. Use of multispectral satellite datasets to improve ecological understanding of the distribution of invasive alien plants in a water-limited catchment, South Africa. Afr. J. Ecol., 58(4): 709-718.

Muanda, C., Goldin, J. and Haldenwang, R. 2020.Factors and impacts of informal settlements residents' sanitation practices on access and sustainability of sanitation services in the policy context of free basic sanitation. J. Water Sanit. Hyg. Dev., 10(2): 238-248.

Oki, T. and Kanae, S. 2006. Global hydrological cycles and world water resources. Science., 313(5790): 1068-1072.

Olaolu, T.D., Akpor, O.B. and Akor, C.O. 2014. Pollution indicators and pathogenic microorganisms in wastewater treatment: Implication on receiving water bodies. Int. J. Environ. Protect. Pollut., 2(6): 205-212.

Onda, K., LoBuglio, J. and Bartram, J. 2012. Global access to safe water: Accounting for water quality and the resulting impact on MDG Progress. Int. J. Environ. Res. Public Health., 9(3): 880-894.

Othoo, C.O., Dulo, S.O., Olago, D.O. and Ayah, R. 2020. Proximity density assessment and characterization of water and sanitation facilities in the informal settlements of Kisumu city: Implications for public health planning. J. UOEH, 42: 237-249

Owusu-Asante, Y. and Ndiritu, J. 2009. The simple modelling method for storm and grey-water quality management applied to Alexandra settlement. Water SA, 35(5): 615-626.

Patel, H.H. 2018. Water-Borne Diseases. Retrieved from https://www.news-medical.net/health/Water-Borne-Diseases.aspx (Accessed: 10 January 2022).

Paterson, A. and Kotze, L.J. 2009. Environmental Compliance and Enforcement in South Africa: Legal Perspectives. Juta Law, Cape Town.

Phungela, T.T., Maphanga, T., Chidi, B.S., Madonsela, B.S. and Shale, K. 2022. The impact of wastewater treatment effluent on Crocodile River quality in Ehlanzeni District, Mpumalanga Province, South Africa. S. Afr. J. Sci., 118(7-8):1-8.

PMG (Parliamentary Monitoring Group, South Africa). 2011. Health of Rivers: Department of Water Affairs Briefing. Retrieved from https://pmg.org.za/committee-meeting/13243/ (Accessed: 6 April 2020).

Rabadan, A. and Saez-Martinez, F.J. 2017. Why European entrepreneurs in the water and waste management sector are willing to go beyond environmental legislation. Water, 9(3): 151.

Radingoana, M.P., Dube, T. and Mazvimavi, D. 2020. An assessment of irrigation water quality and potential of reusing greywater in home gardens in water-limited environments. Phys. Chem. Earth Parts A/B/C, 116:102857.

Rathnayaka, K., Malona, H. and Arora, M. 2016. Assessment of the sustainability of Urban Water supply and demand management options: A comprehensive approach. Water, 8(12): 595.

Schindler, D.W. 2006. Recent advances in the understanding and management of eutrophication. Limnol. Oceanogr., 51(1): 356-363.

Schulze, R.E. 2005. Looking into the future: Why research impacts of possible climate change on hydrological responses in Southern Africa? In: Schulze, R.E. (ed) Climate Change and Water Resources in Southern Africa: Studies on Scenarios, Impacts, Vulnerabilities and Adaptation. WRC Report No. 1430/1/05. Water Research Commission, Pretoria.

Senapati, M.R. 2021. How Our Detergent Footprint Is Polluting Aquatic Ecosystems. Retrieved from https://www.downtoearth.org.in/blog/water/how-our-detergent-footprint-is-polluting-aquatic-ecosystems-77935 (Accessed: 05 January 2022).

SERI (Socio-Economic Rights Institute, South Africa). 2018. Informal Settlements and Human Rights in South Africa. Retrieved from https://www.ohchr.org/Documents/Issues/Housing/InformalSettlements/SERI.pdf (Accessed: 22 February 2020).

Seward, P. 2010. Challenges Facing Environmentally Sustainable Ground Water Use in South Africa.' Groundwater., 48(2), 239-245.

Smith, V.H. and Schindler D.W. 2009. Eutrophication science: where do we go from here? Trends Ecol. Evol., 24(4): 201-207.

Stats SA. 2016. Media Release: Community Survey 2016 Results. Retrieved from http://www.statssa.gov.za/?p=8150 (Accessed: 03 February 2020).

Strydom, H.A. and King, N.D. (ed.). 2015. Environmental Management in South Africa. Juta and Company Ltd, Claremont.

United Nations Environment Programme (UNEP). 2016. A Snapshot of the World's Water Quality: Towards a Global Assessment. Nairobi, Kenya. Retrieved from https://uneplive.unep.org/media/docs/assessments/unep_wwqa_report_web.pdf (Accessed: 19 March 2020).

United Nations Environment Programme (UNEP). 2018. In pictures: How Southern Africa manages its waste. Retrieved from https://www.unep.org/news-and-stories/story/pictures-how-southern-africa-manages-its-waste (Accessed: 05 January 2021).

United Nations Environment Programme (UNEP). 2021. How digital technology and innovation can help protect the planet. Retrieved from https://www.unep.org/news-and-stories/story/how-digital-technology-and-innovation-can-help-protect-planet (Accessed: 07 January 2021).

Van Abel, N., Mans, J. and Taylor, M.B. 2017. Quantitative microbial risk assessment to estimate the health risk from exposure to noroviruses in polluted surface water in South Africa. J. Water Health., 15(6): 908-922.

Villa, M., Manjón, G., Hurtado, S. and García-Tenorio R. 2011. Uranium pollution in an estuary is affected by pyrite acid mine drainage and releases of naturally occurring radioactive materials. Mar. Pollut. Bull., 62(7): 1521-1529.

Wang, R., Wang, Q., Dong, L. and Zhang, J. 2021. Cleaner agricultural production in drinking-water source areas for the control of non-point source pollution in China. J. Environ. Manage., 285: 112096.

Worldometer. 2020. South Africa Demographics: Population of South Africa (2020) - Fertility in South Africa, Life Expectancy in South Africa, Infant Mortality Rate and Deaths of Children under 5 Years Old in South Africa. Retrieved from https://www.worldometers.info/demographics/south-africa-demographics/#urb (Accessed: 23 February 2020).

World Water Assessment Programme, United Nations (WWAP). 2017. The United Nations World Water Development Report 2017. Wastewater: The Untapped Resource. UNESCO, Paris. Retrieved from https://unesdoc.unesco.org/ark:/48223/pf0000247153 (Accessed: 13 March 2021).

## ORCID DETAILS OF THE AUTHORS

T. Maphanga: https://orcid.org/0000-0002-8714-1185
B. S. Madonsela: https://orcid.org/0000-0003-3552-7470

**Original Research Paper**       **Open Access Journal**

# Quantification of Methane Emissions Rate Using Landgem Model and Estimating the Hydrogen Production Potential from Municipal Solid Waste Landfill Site

**C. Ramprasad*†** iD **, A. Anandhu\* and A. Abarna\***

\*School of Civil Engineering, Centre for Advanced Research in Environment (CARE), SASTRA Deemed to be University, Thanjavur-613 401, Tamil Nadu, India

†Corresponding author: C. Ramprasad; ramprasad@civil.sastra.edu

## ABSTRACT

In India, solid waste is deposited mostly in uncontrolled open landfills without proper segregation and handling methods. Organic wastes dumped in a landfill undergo anaerobic decomposition and emit landfill gases like methane and carbon dioxide. Landfill gases are a significant contributor to greenhouse gases and greatly impact climate change. In the interim, reducing gas emissions and controlling and recycling such gasses is important from environmental hygienic, and global perspectives. Landfill gas has tremendous potential to convert as a source of alternative fuel. The present study estimates the $CH_4$ (Methane) and $CO_2$ (Carbon dioxide) emissions and quantifies the renewable energy available and hydrogen production potential using the LandGEM 3.02 empirical models for the Kanuru, Vijayawada landfill. It was observed that methane emission peaked in 2042 with an emission rate according to the model was 2.51E+08 Metric tons $CO_2$ equivalents. The gas-recovery system is an essential component in landfills for extracting energy with 75-80% efficiency; the generation rate of greenhouse gases will reduce to around 1.78E06 Mg of $CO_2$ eq. The predicted methane emissions vary from 1.33E6-9.22E6 cu.m per year for the period of 2010-2042. It was also estimated that annual energy production from LFG emissions was from 1.8-130 GWh per year, and hydrogen production potential was 0.6-43.3 Gg per year. The study concludes that projected scientific data will assist policymakers in creating sustainable MSW management by bridging the gap between sustainable renewable energy production and protecting the environment. The basic objectives of the study include the quantification of landfill gas production using the LandGEM model for Vijayawada, assessing the electricity generation potential of the landfill methane gas emitted, methane and carbon dioxide recovery from landfills with energy conversion could reduce GHG emissions, and estimation of hydrogen generation potential from the landfill methane emissions.

## INTRODUCTION

The generation of solid and liquid waste was an unavoidable part of communal and industrial activities. Currently, waste produced is extremely complex in composition, containing a wide range of chemical, physical, biological, and recalcitrant elements. Household municipal solid wastes are classified into hazardous and non-hazardous waste based on their reactivity, chemical compositions, and the potential to affect human and environmental health (Inglezakis & Moustakas 2015, Fazzo et al. 2017, Liu et al. 2021). In developing countries, solid waste disposal is a prevalent challenge for governmental and private agencies compared to liquid waste treatment and disposal (Ramprasad & Rangabhashiyam 2021). In India, rapid urbanization and uncontrolled

population growth are the two main reasons for acute solid waste management problems. It is foreseen by researchers that; India's population will reach an ever-time high of 1,823 million by 2051 and generate nearly 300 million tons of municipal solid waste (MSW) per annum. The total land required to dispose of the generated MSW unsystematically is projected to be 1450 sq. km if the Government of India continues to rely only on landfill disposal as the better alternative for MSW management (Joshi & Ahmed 2016, Malav et al. 2020). The common scenario in Indian disposal sites is illegal or wild disposal of rubbish generated from domestic, small-scale industries and other places into open ground, low-lying regions near water bodies or over the sea. The researchers have identified that, In India, the practice of segregating domestic waste and treatment was very little

to not practiced, leading to the mixing of biodegradable, recyclable, plastic waste, hazardous e-waste, commercial wastes, and inerts (Leray et al. 2016, Joshi & Ahmed 2016) leading to many environmental and health issues.

Solid waste management is a collective incidence of public health, aesthetics, economic principles, technological advances, ecological conservation, and other environmental aspects. Waste management includes the financial, legal, planning, and technical managerial functions related to the full scope of solving the solid waste moving from the inhabitants to the disposal area (Bui et al. 2020). Apart from domestic solid waste generation, industries generate solid waste from technological and consumptive processes in sequential advancement processes as the raw material into a product. In the Indian metropolitan region, the processes of product manufacturing result in the development of solid waste due to changes in the lifestyle of people, technological advancement, and rapid economic growth. In addition, various operations within the metropolitan regions also produce solid waste, such as street/park cleaning, wastewater treatment, air pollution control measures, and other solid waste output systems (Marshall & Farahbakhsh 2013). The principles of Integrated Solid Waste Management (ISWM) is an appropriate strategy and requires an hour for Indian conditions to manage municipal solid waste. The ISWM is assimilating solid waste segregation, transportation, engaging various technologies for treatment, and management programs to address all forms of solid wastes from various sources to achieve the twin goals of (a) waste reduction and (b) effective waste management after waste reduction (Singh et al. 2020, Prajapati et al. 2021).

India is presently facing a severe problem in the management of solid waste. They are dumped openly throughout the country due to a wrong belief that it's the cheapest and the easiest disposal method. The wastes dumped openly will be more dangerous, naïve, and unavoidable pollutants in the waste will contaminate the girding natural terrain. Then they find their way to humans to affect the quality of life, health, and working conditioning. Therefore, in the ultimate run, society has to pay dearly for open jilting (Krishna et al. 2020, Khatri et al. 2021). The open dumping and burning of unscientifically managed MSW will lead to many environmental hazards like air pollution (greenhouse gaseous and particulate matter emissions), leachate generation (lead to groundwater contamination), and soil and land quality degradation due to chemical and biological activities from wastes (Cremiato et al. 2018). The major greenhouse gases (GHG) emitted from landfills are carbon dioxide, methane, nitrous oxide, water vapor, chlorofluorocarbon gases, and ozone. The MSW will attract useful and harmful bacteria, viruses, and other pathogens due to the nature of solid wastes (Fan et al. 2018) and can result in serious illnesses for living beings nearer to the site and affect wide surrounding areas (Ijaz et al. 2020). Solid waste dumpsites are the third largest source of anthropogenic methane ($CH_4$) emissions after fossil fuel burning and fermentation and are more potent in $CO_2$ emissions causing global warming (Singh et al. 2018, Chandrasekaran & Busetty 2022).

Landfill gas is a natural consequence of organic waste degradation in landfills. It highly depends on the degradable organic fraction (DOC) of wastes, waste composition, rate of degradable organics, and environmental factors like pH and temperature (Tan et al. 2014, Chalvatzaki et al. 2015, Hosseini et al. 2018). Landfill gas is made up of around 50% methane (natural gas's major component), 40% carbon dioxide ($CO_2$), and a minor quantity of non-methane chemical molecules. According to the current research, methane is 28 to 36 times more powerful than $CO_2$, which traps heat for over 100 years in the atmosphere (Ahmed et al. 2015, Bruce et al. 2017, Randazzo et al. 2020). Landfill gas, especially methane, can be trapped, processed, and used as a renewable hydrogen energy resource instead of escaping into the air (Ansari & Daigavane 2021). The landfill gas can be recovered, which reduces odors and other risks connected with their emissions, as well as the methane migration into the atmosphere, which produces local smog and climatic changes. Hydrogen production from methane is a proven and novel technology, an emerging method to use as an alternative fuel or sustainable energy.

Landfills are the non-point source emissions of methane and have high spatial variability leading to difficulty in the measurements. It is essential to estimate the landfill gas emissions to reduce GHG and meet the sustainability development goals (SDGs) (Chalvatzaki et al. 2015). Landfill gas emissions can be estimated using a few modeling approaches such as Zeroth – order kinetics model (Zheng et al. 2017), German-European Pollutant Emission Register (EPER) model, TNO model, Belgium model (Thompson et al. 2009), First order model, Landfill Gas Emission Model (LandGEM) (Sil et al. 2014, Hosseini et al. 2018, Fallahizadeh et al. 2019, Chandrasekaran & Busetty 2022), Second order generation models, Solid Waste Emission Estimation tool (SWEET), and Scholl Canyon model (Srivastava & Chakma 2020, Alexander Stege et al. 2022, Lu et al. 2022). The researchers have identified that the Belgium model, LandGEM, and Scholl Canyon provided the best result amongst the available models correlating well with field conditions. However, from the above 3 models, there are a few cons, such as lack of landfill gaseous pollutant emissions inventory, complexity in usage, small footprint, topographical features, uncertainty in available data, and

economical point of view. Henceforth, the LandGEM model of the three is considered the simplest and insensitive to uncertainties in some design parameters to estimate LFG (Hosseini et al. 2018).

Furthermore, the estimation of Landfill gas and its potential for hydrogen production or power generation over the Vijayawada dumpsite was not studied. Therefore, the present study aimed to determine the landfill gases such as methane and carbon dioxide emissions rates from the Kanuru dump yard, Vijayawada, Andhra Pradesh, India. Additionally, the hydrogen production and power generation potential are also estimated.

## MATERIALS AND METHODS

### Site Selection

The study was conducted in Vijayawada, considered the second largest city of Andhra Pradesh, with a geographical area of 61.88 sq. km. The city geographically lies in the center of Andhra Pradesh on the banks of River Krishna, within the newly formed NTR district, and also acts as the administrative headquarters of the NTR district. According to Census 2011, it is the second largest populated city in Andhra Pradesh, with a population of nearly 10.34 Lakhs with an annual growth rate of 3.05%. The GPS coordinates for the city are 16.30° N and 80.37° E, and the surface elevation is 11m (36ft) above the mean sea level. The solid

waste from the 3 divisions, namely Nandigama, Tiruvuru, and Vijayawada, was transported and dumped into one of the open landfill sites located at Kanuru. The GPS coordinates for the Kanuru dump site are 16°30'08.0" N and 80°41'35.3" E, which is more than 5km from the main city (Fig. 1). The climatic pattern is tropical wet and dry conditions, with an average annual temperature of 28.5°C and the average annual rainfall was 1066.8 mm.

### Data Collection

The data on waste generation, waste composition, per capita waste generation, the dumpsite inception year, and the design life of the dump site were obtained from the Municipal Commissioner's office, Vijayawada. The quantity of municipal solid waste generated during the year 2014-15 from the 64 municipal wards is 550 metric tons per day, of which 265 metric tons are wet, and 285 metric tons are dry. The per capita waste generation was in the range of 0.532 – 0.688 kg and is projected to increase to nearly 0.75 kg per capita per day by 2050. The governmental study report states that the average biodegradable portions like fruit, vegetables, and food wastes in the MSW collected were 55%, combustible or recyclable materials such as paper, plastics, and rubber are 35%, and inert's like glasses, sand, and silt were 10% (Unnikrishnan & Singh 2010, Niloufer & Swamy 2015). The design life of the studied landfill was estimated to be 30 years, and wastes were dumped and uniformly
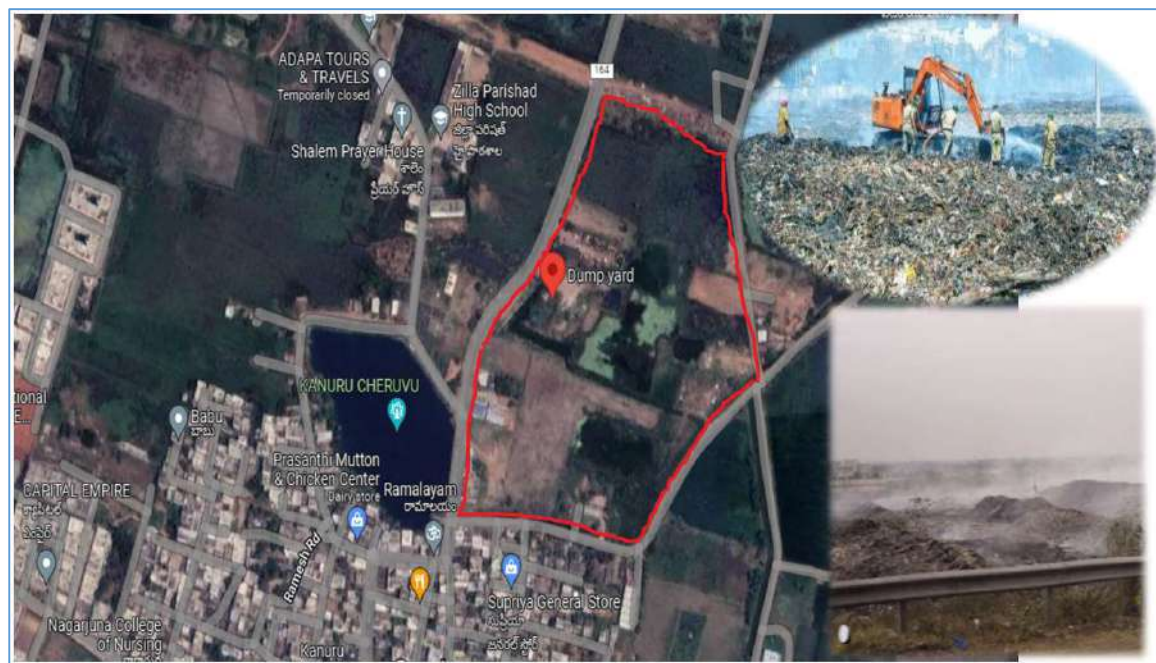


Fig. 1: The photographic view of Kanuru landfill site, Vijayawada.

Table 1: The average yearly solid waste accepted and in place at the Kanuru dump site.

| Year | Waste Acceptance [t.y$^{-1}$] | Waste In-place [Tons] |
|---|---|---|
| 2010 (Inception Year) | 0 | 0 |
| 2011 | 1,76,114 | 1,76,114 |
| 2012 | 1,81,397 | 3,57,511 |
| 2013 | 1,86,839 | 5,44,350 |
| 2014 | 1,92,444 | 7,36,794 |
| 2015 | 1,99,180 | 9,35,974 |
| 2016 | 2,04,660 | 11,40,634 |
| 2017 | 2,11,823 | 13,52,457 |
| 2018 | 2,19,237 | 15,71,694 |
| 2019 | 2,26,911 | 17,98,605 |
| 2020 | 2,30,794 | 20,29,399 |

Table 2: Physico-chemical characterization of solid waste from the Kanuru dump site.

| S. No | Parameters | Unit | Value |
|---|---|---|---|
| 1. | pH | No Unit | 6.2-8.0 |
| 2. | Moisture Content | % | 27.44-51.92 |
| 3. | C/ N ratio | No Unit | 30-43 |
| 4. | Total Organic Carbon | % | 10.64-12.03 |
| 5. | Ash Content | % | 30.17-47.74 |
| 6. | Calorific Value | kcal per kg | 2016-3216 |

rolled for compaction. The yearly solid waste generated and accepted in the dump site is tabulated in Table 1. The secondary data on the physico-chemical characterization of the MSW collected from Vijayawada is shown in Table 2. The secondary data on the solid waste characterization was obtained from Niloufer & Swamy 2015 and found that pH was 6.2 to 8.0, the carbon to nitrogen ratio was 30-43, and the calorific value was 2016-3216 Kcal per kg.

## LandGEM Model Equation

LandGEM is one of the automated tools to estimate the LFG gases like carbon dioxide, methane, non-methane organic compounds (NMOCs), etc., and their emission rate from the open and uncontrolled MSW landfills. These data, such as yearly waste acceptance, as shown in Table 1, have been entered in the LandGEM model Excel sheet, and the emission rate is determined by considering the equations' default values. The software can enter the site-specific data (if available) for a better estimation rate of LFG gases. The United States Environmental Protection Agencies (USEPA) specialists have developed and made the software universally friendly. The LandGEM model equation is as follows,

$$Q_{CH_4} = \sum_{i=1}^{n} \sum_{j=0.1}^{1} KL_0 \left(\frac{M_i}{10}\right) e^{-kt_{ij}} \quad \dots(1)$$

$Q_{CH4}$ = annual $CH_4$ generation in the calculation yr (cu.m per year)

i = 1year time increment

$M_i$ = In $i^{th}$ year waste mass accepted (Mg)

n = (year of the calculation) - (initial year of waste acceptance)

$t_{ij}$ = In the $i^{th}$ year age of the $j^{th}$ section of waste mass $M_i$ accepted

j = 0.1-year time increment

k = $CH_4$ generation rate (per year) considered as 0.05

$L_0$ = potential $CH_4$ generation capacity (cu.m per Mg) considered as 170

## Recovery of Methane and Hydrogen Estimates

Modern-day landfills need to adopt an engineered way of disposing of solid waste. The ISWM approach states that the vital component in landfills is an engineered mode of solid waste disposal. The generated solid wastes are dumped in sequences and compacted, with provisions for recovering the landfill gases. The landfill gases can be recovered to 60-85%, depending on the collection system adopted, the landfill cover material used, and the lifetime year of waste (Ansari & Daigavane 2021). The recovered methane can be converted into hydrogen gas, and thereby, electricity can be produced using the following schematic diagram. The steam reforming reaction and the shift reaction for the conversion of methane to hydrogen are also provided in Fig. 2. The clay liner cum cover has the highest recovery of methane than the other natural soils used. The recovery of methane from the landfill gases available for reforming to hydrogen is assumed to be 67%.

The electrical energy generation potential (Ep in kWh per year) from the methane emissions from the Vijayawada Kanuru landfills is estimated by the following equation (Ayodele et al. 2017, Cyril et al. 2018, Rodrigue et al. 2018),

$$E_p = \frac{0.9 \times Q_{CH4} \times LHV_{CH4} \times \eta \times \lambda}{3.6} \quad \dots(2)$$

Where $Q_{CH4}$ is the amount of methane gas emitted in cu.m per year

$LHV_{CH4}$ is the Lower Heating Value of methane and is taken as 37.2 MJ per cu.m

$\eta$ is the electrical conversion efficiency and taken as 33%

$\lambda$ is the collection efficiency of methane taken as 75%
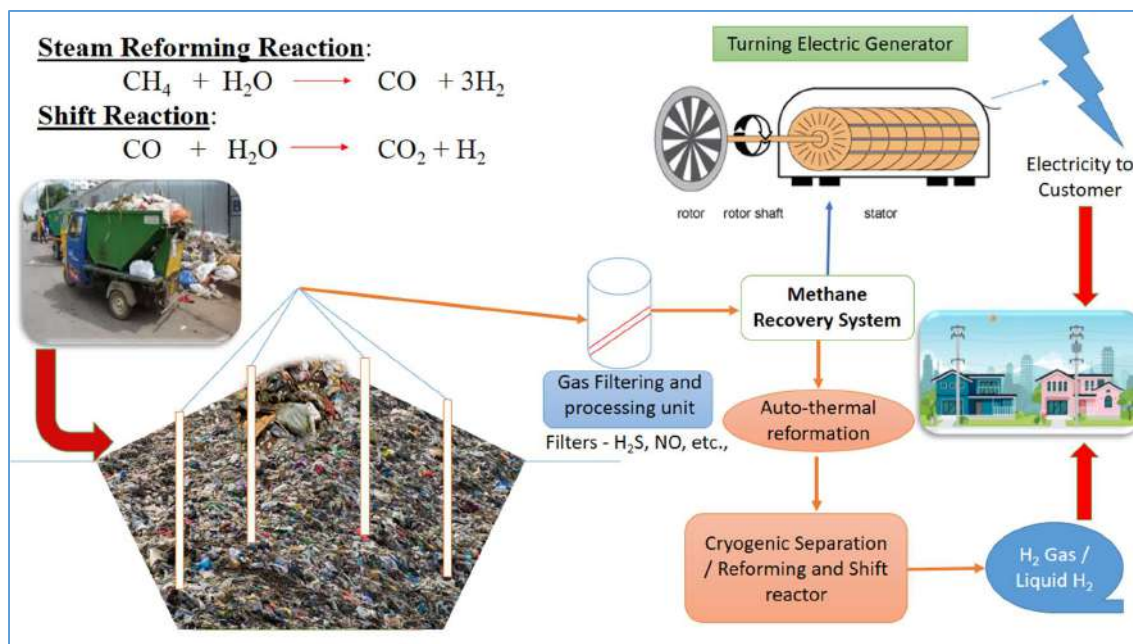
Fig. 2: Schematic representation of methane recovery and processing to obtain hydrogen.

## RESULTS AND DISCUSSION

### Waste Prediction and Disposal

The waste generation from the city of Vijayawada from 2011 to 2020 was tabulated in Table 1. The average per capita waste generation was 500-690 grams. The prediction for the years 2021 to 2041 was done based on the population growth rate and subsequently based on their per capita waste generation. Table 3 shows the geometrical mean projected population, the subsequent per capita waste generation rate, and waste produced and disposed of annually. The trend of population growth rate during the year 2011-2020 was in the range of 1.03% annually. Hence, the projection of the population for the year 2021-2041 was predicted, assuming an incremental increase for every 7 years with a three-stage growth rate of 1.04%, 1.1%, and 1.35%. The current projected population for the city of Vijayawada was in line with the already published survey report by International Urban Cooperation, European Union, 2021. The per capita waste generation also followed a three-stage growth; the per capita generation rate was 0.569 kg, 0.622 kg, and 0.808 kg. Additionally, the waste produced and disposed into the landfill at a constant collection efficiency of 85% was tabulated in tons per year and tons, respectively. The projected data was in concurrence with Niloufer & Swamy (2015), Pinupolu & Raja Kommineneni (2020) for the Vijayawada landfill site.

The authors Pinupolu & Raja Kommineneni (2020) concluded that the population projection using the geometric method for the year 2031 was 18.9 lakhs, the per capita waste generation rate was 0.66, and the total solid waste generation was 1258 tons per day. The present study results were in concurrence with the published data with less than 5% error. The authors also conclude that the land required and the cost for the disposal of the generated municipal solid waste will be 4800 sq. m and 3.20 crores, respectively. The same trend of disposing into landfills will lead to the degradation of land, soil, air, and the surrounding ecosystem. In the Kanuru landfill site, it's essential to analysis for an alternative approach to handle municipal solid waste due to the lack of land space availability. To achieve sustainability and have a circular economical approach, the cities/ municipalities/corporation should adopt Integrated Solid Waste Management (ISWM) approach (Iqbal et al. 2019, Mukherjee et al. 2020, Ramprasad & Rangabhashiyam 2021).

The ISWM approach uses various sequential techniques. It starts with door-to-door waste collection, segregation, transport of waste, treatment, and disposal (Ramprasad et al. 2019, Prajapati et al. 2021). In the treatment step, the organic fraction can be composted or anaerobically digested, whereas the recyclables, like paper, plastic, etc., can be combusted or co-processed. In this process, many valuables like compost from composting process, methane from the Bio-methanation, bio-char from the combustion process, and heat/energy/biofuel from the incineration process are obtained (Azeta et al. 2021, Harisankar et al. 2021). Whereas,

Table 3: Projected population, waste generation, and disposal for Kanuru landfill site.

| Year | Projected population | Per capita waste generation [kg/ capita/ day] | Waste produced [t.y$^{-1}$] | Waste disposed of @85% collection efficiency [Tons] |
|------|----------------------|------------------------------------------------|------------------------------|-----------------------------------------------------|
| 2021 | 13,96,853 | 0.569 | 3,19,696 | 2,71,742 |
| 2022 | 14,52,727 | 0.569 | 3,32,484 | 2,82,611 |
| 2023 | 15,10,836 | 0.569 | 3,45,783 | 2,93,916 |
| 2024 | 15,71,270 | 0.569 | 3,59,615 | 3,05,673 |
| 2025 | 16,34,120 | 0.569 | 3,73,999 | 3,17,899 |
| 2026 | 16,99,485 | 0.569 | 3,88,959 | 3,30,615 |
| 2027 | 17,67,465 | 0.569 | 4,04,518 | 3,43,840 |
| 2028 | 18,38,163 | 0.569 | 4,20,698 | 3,57,594 |
| 2029 | 19,11,690 | 0.569 | 4,37,526 | 3,71,897 |
| 2030 | 19,88,157 | 0.569 | 4,55,027 | 3,86,773 |
| 2031 | 21,86,973 | 0.622 | 5,47,152 | 4,65,080 |
| 2032 | 24,05,670 | 0.622 | 6,01,868 | 5,11,587 |
| 2033 | 26,46,237 | 0.622 | 6,62,054 | 5,62,746 |
| 2034 | 29,10,861 | 0.622 | 7,28,260 | 6,19,021 |
| 2035 | 32,01,947 | 0.622 | 8,01,086 | 6,80,923 |
| 2036 | 35,22,142 | 0.622 | 8,81,194 | 7,49,015 |
| 2037 | 38,74,356 | 0.622 | 9,69,314 | 8,23,917 |
| 2038 | 42,61,792 | 0.622 | 10,66,245 | 9,06,308 |
| 2039 | 46,87,971 | 0.808 | 12,97,322 | 11,02,724 |
| 2040 | 63,28,761 | 0.808 | 17,51,385 | 14,88,677 |
| 2041 | 85,43,827 | 0.808 | 23,64,370 | 20,09,714 |

in the disposal step, the quantity of waste and the surface area for disposal will substantially get reduced. Hence, the Kannur landfill by the year 2041 needs to dispose of/manage 20 Lakh tons of solid waste in a year in the open land if the scenario continues. Many of the developed and developing countries have practiced the ISWM approach and have succeeded, like Jaipur in India (Prajapati et al. 2021), USA (Mukherjee et al. 2020), Malaysia (Liew et al. 2021) and South Africa (Dlamini et al. 2019). Therefore, they need to adopt different alternatives, such as organics having to be composted/anaerobic digested to get methane and recyclables needing to be pyrolyzed to get bio-fuel and syngases such as hydrogen.

**Methane Emissions**

The methane emission calculated according to LandGEM model equation 1 for the Kanuru landfill site starting from 2011 was presented in Fig. 3. The methane concentration follows a gradually increasing trend. It is observed to have a peak concentration of 9.266E+07 cu.m during the year 2042. After the peak emission of methane, the concentration decreased gradually and reached a value of 5.099E+06 cu.m per year during the year 2100. Methane is a gaseous product

produced from the anaerobic bacterial decomposition of organic matter in landfills. The amount of methane gas produced is correlated to the quantity of organic waste within the landfill. Hence, higher methane concentration indicates a higher portion of organic waste presence (Ghosh et al. 2019, Sun et al. 2019, Oukili et al. 2022). There are various physical, chemical, and ecological parameters that influence the methane emissions like the waste composition, pH of the waste, average rainfall depth in the site, air temperature, pressure, topography, and microbial interactions (Fei et al. 2019, Monster et al. 2019). The ambient atmospheric temperature, relative humidity, and rainfall exhibit strong correlations with landfill gas components (Yang et al. 2015, Delkash et al. 2016). The present study site has an average annual temperature of 28.5°C and an average annual rainfall of 1066.8 mm, hence having a high potential to produce landfill gases. Similar results were projected earlier (Zhang et al. 2013). The landfills without proper gas collection systems will substantially emit methane (the most vital GHG) into the atmosphere without any control and huge spatial and seasonal variability.

The Kanuru dumpsite is in the active phase of methane production, and hence the concentration of methane was
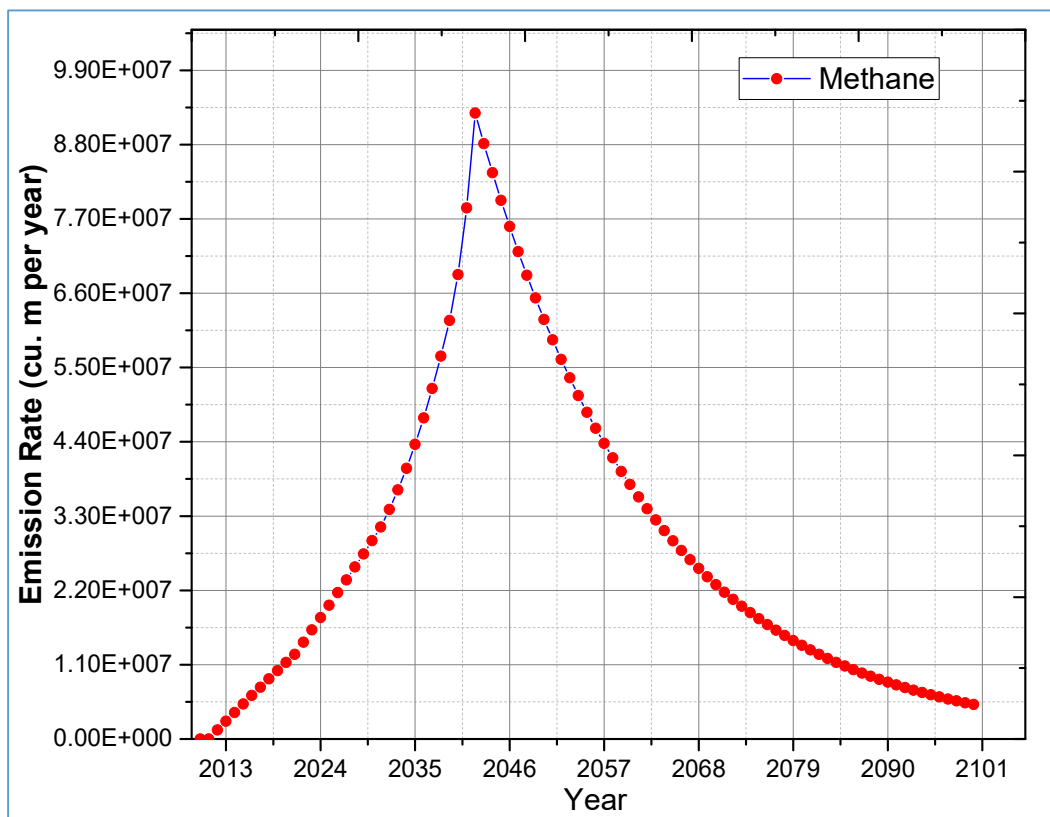
Fig. 3: Projected methane concentration from the Kanuru landfill site.

slightly higher than the other reported values. Henceforth, few remedial measures can be adopted to interlude the GHG emissions and generate/find a renewable energy source. Firstly, the Kanuru open dumpsite should be upgraded to an engineered landfill site, with a provision for a methane recovery system and proper landfill cover to avoid the escape of generated methane. Secondly, the adopting the strategy of integrated waste management and accommodating more waste from all the localities, segregation of recyclables, composting of organics, and incineration for combustible portions. Finally, the long-term strategy is to convert the methane to renewable hydrogen gas by thermocatalytic decomposition or utilization of methane for renewable electricity generation.

**Energy Potential and Hydrogen Production**

The annual electrical energy generation potential (Ep) feasible from the Kanuru dump site was calculated based on equation 2. The energy potential depends on the concentration of methane liberated in cu.m per year, the lower heating value of methane (usually in the range of 34-52 MJ per cu.m), collection, and electrical conversion efficiency

(Thema et al. 2019). During the early stages (2011-2021) of landfilling, the energy potential was 1.8-16 GWh per year and started to increase rapidly afterward. The electrical energy potential peaked during 2042 at 130.8 GWh per year. The plot showing the projected electrical energy potential trend from the Kanuru dumpsite is shown in Fig. 4. As the methane generation rate increases, the amount of electrical energy production potential also increases. A similar trend was observed for the uncontrolled Mohammedia- a Benslimane landfill (Oukili et al. 2022). The authors obtained a maximum electrical energy production 2032 valued at 35.2 GWh. The results obtained from the study conclude that improvement in waste management is a vital factor for a country like India, and the use of the energy content of waste could be one of the leading ideas for sustainable progress. The potential energy content from the solid waste can be resource recovered by either thermo-chemical processes (combustion, pyrolysis, or gasification), biological processes (anaerobic digestion), or engineered landfilling.

The biogas/methane emissions gradually increased and peaked in 2042 (9.266E+07 cu.m per year). Correspondingly, the energy potential also followed a similar trend. The carbon
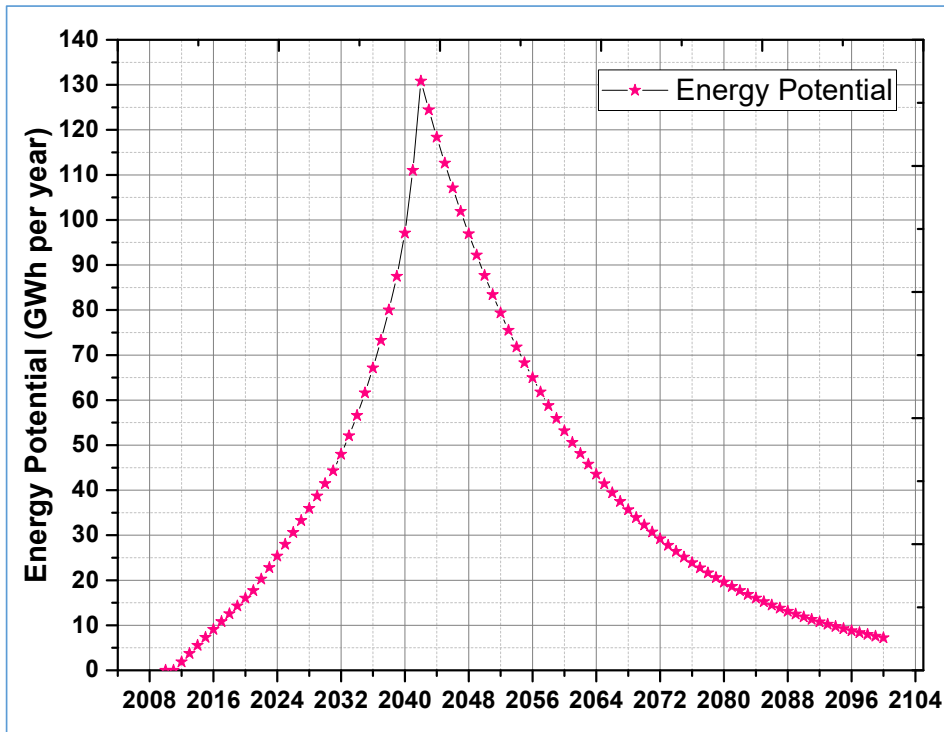
Fig. 4: Projected electrical energy potential from the Kanuru landfill site.
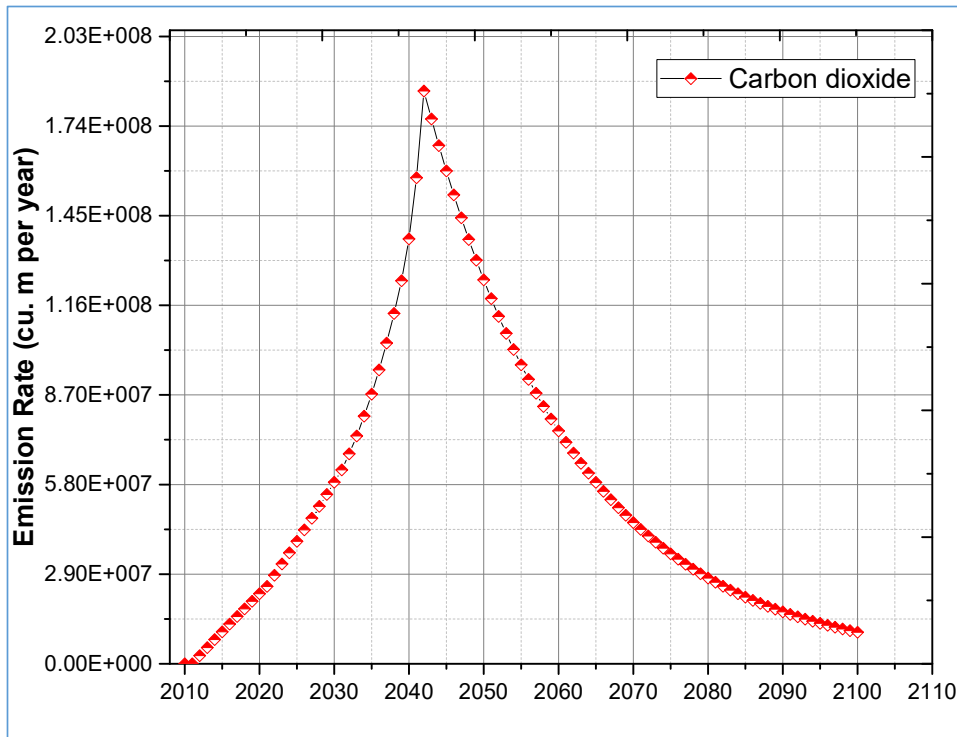


Fig. 5: Projected carbon dioxide concentration from the Kanuru Landfill Site.

dioxide equivalent's also calculated considering the global warming potential (GWP). Hence, the Kanuru landfill site contributes to 2.32E08 cu.m of $CO_2$ equivalents per year and, thereby, greenhouse effects (Fig. 5.). This significant contribution to the greenhouse effect is explained by the high organic content of the waste buried in the landfill and the meteorological conditions.

After the peak emissions and peak electrical energy potential in 2042, the contributions decreased exponentially and reached a zero value after 100 years of landfill closure. It implies that the landfills emit enormous amounts of greenhouse gases, especially methane gas, besides having the potential to convert into electrical energy. The gas recovery system installation on the landfill site will substantially reduce greenhouse emissions into the atmosphere. Similar study results were obtained by Tayyeba et al. (2011) and Villarino et al. (2020), with a GWP of 21 for methane, estimating around 80% - 90% of methane capture efficiency. The present study also concludes coherent with the reported data; the landfill gas recovery system has an achievable

GHG emission reduction of 1.78E06 Mg of $CO_2$ equivalents. In the future, the Kanuru landfill site, due to the very efficient recovery system installation and active managerial participation, will create the Kanuru, Vijayawada, a carbon green site or carbon sequestration pool.

The analysis estimates the production of renewable hydrogen using the steam methane reforming (SMR) technology with a 70% net energy efficiency. The energy conversion from methane to hydrogen depends on the higher heating value and the disposed solid waste's ultimate analysis energy level to hydrogen energy. The estimated recoverable methane in Gg per year was plotted in Fig. 6, showing a value of 13.2, 61.8, 41.4, and 11.8 Gg per year during 2025, 2042, 2050, and 2075, respectively. Subsequently, the renewable hydrogen produced from the Kanuru landfill site was about 9.3 Gg per year in 2025 and increased to 43.3 Gg per year during 2042. The value gradually exponentially decreased from the year 2042 to reach a value of 8.3 Gg per year by the end of 2075. The results were in concurrence with renewable energy produced from the California landfill site of 160-
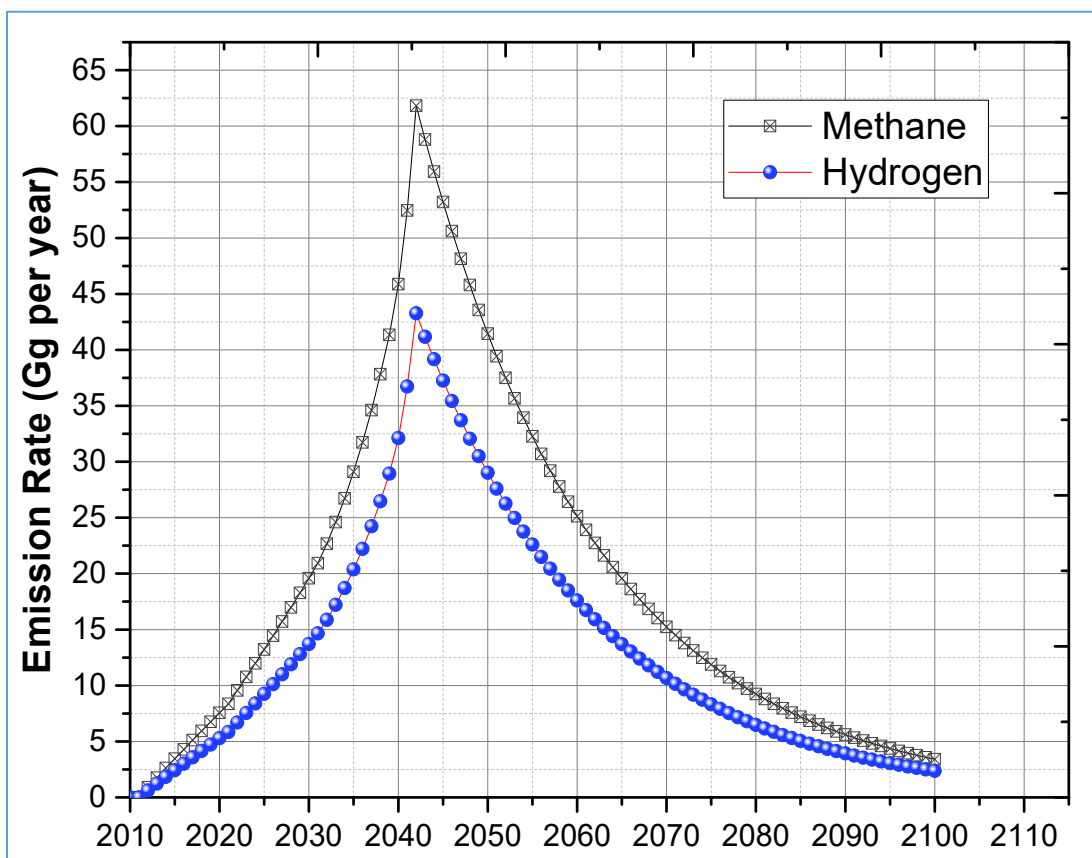


Fig. 6: Projected methane and hydrogen production potential from the Kanuru Landfill Site.

300 Gg per year (Ansari & Daigavane 2021). However, the reason for the lower hydrogen produced compared to the reported value is not evident. Still, it may be due to lower gas quality, the composition of solid waste dumped, and other meteorological conditions.

## CONCLUSION

Methane, the most vital greenhouse gas, must be monitored and controlled to combat the global crisis on climate change, as well as Landfills are one significant contributor of methane gas and a preferred disposal option in developing countries. This study is the first to estimate the quantity of methane emitted from the Kanuru landfill site, Vijayawada, and thereby project the electrical energy potential and renewable hydrogen production capacity for this landfill. The methane generation rate for the Kanuru open uncontrolled landfill site from inception (2010) to more than 100 years was projected using Landgem 3.03 model. The estimation of methane for the landfill site was based on the amount of waste disposed of every year, the methane generation rate (k), and the methane generation potential (Lo). The anaerobic decomposition of the solid waste dumped inside the Kanuru dumpsite produces methane, a good approach to protect the environment, and greenhouse gas mitigation is to generate electrical energy or to produce renewable hydrogen. Methane gas is a promising contributor to global warming and a source of green energy. It needs to be sequestered. According to the landGEM model, an exponential increase in methane emissions was observed, and the maximum methane production rate was predicted as 9.266E+07 cu.m per year during the year 2042. The year 2042 corresponds to the closure of the Kanuru landfill site, and hence the production decreased afterward. The study also concludes that the electrical energy potential of the Kanuru landfill site was 130.8 GWh per year for the year 2042.

Additionally, the Kanuru landfill site has the potential to produce renewable hydrogen based on steam reforming reaction to yield a maximum of 43.3 Gg per year during 2042. Therefore, it can be concluded that the Kanuru, Vijayawada landfill is a source of energy production and can be used as an alternative to fossil fuels. There needs to be a policy reformation to convert all the open dumpsites into engineered landfills with a gas recovery system. As well as the use of excessive liberated methane needs to be converted into electrical energy or renewable hydrogen.

## REFERENCES

Ahmed, S. I., Johari, A., Hashim, H., Mat, R., Lim, J. S., Ngadi, N. and Ali, A. 2015. Optimal landfill gas utilization for renewable energy production. Environ. Prog. Sustain. Energy, 34(1): 289-296.

Alexander Stege, G., James Law, H., Ramola, A. and Mazo-Nix, S. 2022. Mini-review of waste sector greenhouse gas and short-lived climate pollutant emissions in Tyre Caza, Lebanon, using the Solid Waste Emissions Estimation Tool ('SWEET'). Waste Management & Research, 0734242X221076295.

Ansari, A. and Daigavane, P.B. 2021. Analysis and modeling of slope failures in municipal solid waste dumps and landfills: A review. Nature Environ. Pollut. Technol., 2)20): 825-831.

Ayodele, T.R., Ogunjuyigbe, A.S.O. and Alao, M.A. 2017. Life cycle assessment of waste-to-energy (WtE) technologies for electricity generation using municipal solid waste in Nigeria. Appl. Energy, 201: 200-218.

Azeta, O., Ayeni, A.O., Agboola, O. and Elehinafe, F.B. 2021. A review on the sustainable energy generation from the pyrolysis of coconut biomass. Sci. Afr., 13: e00920.

Bruce, N., Ng, K.T.W. and Richter, A. 2017. Alternative carbon dioxide modelling approaches accounting for high residual gases in LandGEM. Environ. Sci. Pollut. Res., 24(16): 14322-14336.

Bui, T.D., Tsai, F.M., Tseng, M.L. and Ali, M.H. 2020. Identifying sustainable solid waste management barriers in practice using the fuzzy Delphi method. Resour. Conserv. Recycl., 154: 104625.

Chalvatzaki, E., Glytsos, T. and Lazaridis, M. 2015. A methodology for the determination of fugitive dust emissions from landfill sites. Int. J. Environ. Health Res., 25(5): 551-569.

Chandrasekaran, R. and Busetty, S. 2022. Estimating the methane emissions and energy potential from Trichy and Thanjavur dumpsite by LandGEM model. Environ. Sci. Pollut. Sci. Res., 66: 1-11.

Cremiato, R., Mastellone, M.L., Tagliaferri, C., Zaccariello, L. and Lettieri, P. 2018. Environmental impact of municipal solid waste management using Life Cycle Assessment: The effect of anaerobic digestion, materials recovery, and secondary fuels production. Renew. Energy, 124: 180-188.

Cyril, K.M., Essi, K., Agboue, A. and Albert, T. 2018. Characterization of the parameters and estimation of potential biogas of a Landfill in tropical area: A case study of the principal landfill of Abidjan Akouedo landfill. Res. Rev. J. Ecol. Environ. Sci., 6(1): 43-49.

Delkash, M., Zhou, B., Han, B., Chow, F.K., Rella, C.W. and Imhoff, P.T. 2016. Short-term landfill methane emissions dependency on the wind. Waste Manag., 55: 288-298.

Dlamini, S., Simatele, M.D. and Serge Kubanza, N. 2019. Municipal solid waste management in South Africa: From waste to energy recovery through waste-to-energy technologies in Johannesburg. Local Environ., 24(3): 249-257.

Fallahizadeh, S., Rahmatinia, M., Mohammadi, Z., Vaezzadeh, M., Tajamiri, A. and Soleimani, H. 2019. Estimation of methane gas by LandGEM model from Yasuj municipal solid waste landfill, Iran. MethodsX, 6: 391-398.

Fan, Y.V., Klemeš, J.J., Lee, C.T. and Ho, C.S. 2018. Efficiency of microbial inoculation for a cleaner composting technology. Clean Technol. Environ. Policy, 20(3): 517-527.

Fazzo, L., Minichilli, F., Santoro, M., Ceccarini, A., Della Seta, M., Bianchi, F. and Martuzzi, M. 2017. Hazardous waste and health impact: A systematic review of the scientific literature. Environ. Health, 16(1): 1-11.

Fei, F., Wen, Z. and De Clercq, D. 2019. Spatio-temporal estimation of landfill gas energy potential: A case study in China. Renew. Sustain. Energy Rev., 103: 217-226.

Ghosh, P., Shah, G., Chandra, R., Sahota, S., Kumar, H., Vijay, V. K. and Thakur, I.S. 2019. Assessment of methane emissions and energy recovery potential from the municipal solid waste landfills of Delhi, India. Bioresour. Technol., 272: 611-615.

Harisankar, S., Prashanth, P.F., Nallasivam, J. and Vinu, R. 2022. Optimal use of glycerol co-solvent to enhance product yield and its quality from hydrothermal liquefaction of refuse-derived fuel. Biomass Conv. Bioref., 11: 1-15.

Hosseini, S.S., Yaghmaeian, K., Yousefi, N. and Mahvi, A.H. 2018. Estimation of landfill gas generation in a municipal solid waste disposal site by LandGEM mathematical model. Glob. J. Environ. J. Sci. Manag., 4(4): 493-506.

Ijaz, M., Tabinda, A.B., Ahmad, S.R., Khan, W.U. and Yasin, N.A. 2020. Biogas synthesis from leather industry solid waste in Pakistan. Pol. J. Environ. Stud., 29(5): 3621-3628.

Inglezakis, V.J. and Moustakas, K. 2015. Household hazardous waste management: A review. J. Environ. Manage., 50: 310-321.

Iqbal, A., Zan, F., Liu, X. and Chen, G. H. 2019. Integrated municipal solid waste management scheme of Hong Kong: A comprehensive analysis in terms of global warming potential and energy use. Journal of Cleaner Production, 225: 1079-1088.

Joshi, R. and Ahmed, S. 2016. Status and challenges of municipal solid waste management in India: A review. Cogent Environmental Science, 2(1): 1139434.

Khatri, K.L., Muhammad, A.R., Soomro, S.A., Tunio, N.A. and Ali, M.M. 2021. Investigation of possible solid waste power potential for distributed generation development to overcome the power crises of Karachi city. Renewable and Sustainable Energy Rev., 143: 110882.

Krishna, R.S., Mishra, J., Meher, S., Das, S.K., Mustakim, S.M. and Singh, S.K. 2020. Industrial solid waste management through sustainable green technology: Case study insights from steel and mining industry in Keonjhar, India. Mater. Today Proceed., 33: 5243-5249.

Leray, L., Sahakian, M. and Erkman, S. 2016. Understanding household food metabolism: Relating micro-level material flow analysis to consumption practices. J. Clean Prod., 125: 44-55.

Liew, P.Y., Varbanov, P.S., Foley, A. and Klemeš, J.J. 2021. Smart energy management and recovery towards sustainable energy system optimisation with bio-based renewable energy. Renew. Sustain. Energy Rev., 135: 110385.

Liu, C., Dong, H., Cao, Y., Geng, Y., Li, H., Zhang, C. and Xiao, S. 2021. Environmental damage cost assessment from municipal solid waste treatment based on the LIME3 model. Waste Manag., 125: 249-256.

Lu, P., Cao, Q., Zhang, X., Xing, L., Yuan, Y., Wang, T. and Zhang, Z. 2022. Estimation and verification of landfill gas production by two typical prediction models in Gao Antun landfill. In Int/Cong International Conference on Statistics, Applied Mathematics, and Computing Science (CSAMCS 2021) (Vol. 12163, pp. 647-642). SPIE.

Malav, L.C., Yadav, K.K., Gupta, N., Kumar, S., Sharma, G.K., Krishnan, S. and Bach, Q. V. 2020. A review on municipal solid waste as a renewable source for waste-to-energy project in India: Current practices, challenges, and future opportunities. Journal of Cleaner Production, 277: 123227.

Marshall, R.E. and Farahbakhsh, K. 2013. Systems approach to integrated solid waste management in developing countries. Waste Manag., 33(4): 988-1003.

Mønster, J., Kjeldsen, P. and Scheutz, C. 2019. Methodologies for measuring fugitive methane emissions from landfills–A review. Waste Manag., 87: 835-859.

Mukherjee, C., Denney, J., Mbonimpa, E. G., Slagley, J. and Bhowmik, R. 2020. A review on municipal solid waste-to-energy trends in the USA. Renewable and Sustainable Energy Reviews, 119: 109512.

Niloufer, S. and Swamy, A.V.V.S. 2015. A brief assessment of municipal solid waste and its impact on leachate quality at MSW sites in Vijayawada City, India. Int. J. Innov. J. Sci. Eng. Technol, 2(6): 645-658.

Oukili, A.I., Mouloudi, M. and Chhiba, M. 2022. LandGEM biogas estimation, energy potential, and carbon footprint assessments of a controlled landfill site. Case of the controlled landfill of Mohammedia-Benslimane, Morocco. J. Ecol. Eng., 23(3).

Pinupolu, P. and Raja Kommineni, H. 2020. The best method of municipal solid waste management is through public-private partnership for Vijayawada City. Mater. Today Proceed., 33: 217-222.

Prajapati, K.K., Yadav, M., Singh, R.M., Parikh, P., Pareek, N. and Vivekanand, V. 2021. An overview of municipal solid waste management in Jaipur city, India-Current status, challenges, and recommendations. Renew. Sustain. Energy Rev., 152: 111703.

Ramprasad, C. and Rangabhashiyam, S. 2021. Recycling of Waste and Policy Frameworks in India. In Singh, P., Milshina, Y., Tian, K., Borthakur, A., Verma, P. and Kumar, A. (eds), Waste Management Policies and Practices in BRICS Nations CRC Press. pp. 231-246.

Ramprasad, C., Sona, K., Afridhi, M., Kumar, R. and Gopalakrishnan, N. 2019. Comparative Study on the Treatment of Landfill Leachate by Coagulation and Electrocoagulation Processes. Nature Environ. Pollut. Technol., 18(3): 144.

Randazzo, A., Asensio-Ramos, M., Melián, G.V., Venturi, S., Padrón, E., Hernández, P. A. and Tassi, F. 2020. Volatile organic compounds (VOCs) in solid waste landfill cover soil: Chemical and isotopic composition vs. degradation processes. Sci.of the Total Environment, 726: 138326.

Rodrigue, K., Essi, K., Cyril, K. and Albert, T. 2018. Estimation of methane emission from Kossihouen sanitary landfill and its electricity generation potential (Côte d'Ivoire). J. Power Energy Eng., 6(07): 22-31.

Sil, A., Kumar, S. and Wong, J.W. 2014. Development of correction factors for landfill gas emission model suiting Indian conditions to predict methane emission from landfills. Bioresour. Technol., 168: 97-99.

Singh, C.K., Kumar, A. and Roy, S.S. 2018. Quantitative analysis of the methane gas emissions from municipal solid waste in India. Sci. Rep., 8(1): 1-8.

Singh, N., Tang, Y. and Ogunseitan, O.A. 2020. Environmentally sustainable management of used personal protective equipment. Environ. Sci. Technol., 54(14): 8500-8502.

Srivastava, A.N. and Chakma, S. 2020. Quantification of landfill gas generation and energy recovery estimation from the municipal solid waste landfill sites of Delhi, India. Energy Sour. Part A Recov. Utiliz. Environ. Effects, 11: 1-14.

Sun, C., Liu, F., Song, Z., Wang, J., Li, Y., Pan, Y. and Li, L. 2019. Feasibility of dry anaerobic digestion of beer lees for methane production and biochar enhanced performance at mesophilic and thermophilic temperature. Bioresour. Technol., 276: 65-73.

Tan, S.T., Hashim, H., Lim, J.S., Ho, W. S., Lee, C. T. and Yan, J. 2014. Energy and emissions benefits of renewable energy derived from municipal solid waste: Analysis of a low carbon scenario in Malaysia. Applied Energy, 136: 797-804.

Tayyeba, O., Olsson, M. and Brandt, N. 2011. The best MSW treatment option by considering greenhouse gas emissions reduction: a case study in Georgia. Waste Manag. Res., 29(8): 823-833.

Thema, M., Bauer, F. and Sterner, M. 2019. Power-to-Gas: Electrolysis and methanation status review. Renew. Sustain Energy Rev., 112: 775-787.

Thompson, S., Sawyer, J., Bonam, R. and Valdivia, J.E. 2009. Building a better methane generation model: Validating models with methane recovery rates from 35 Canadian landfills. Waste management, 29(7): 2085-2091.

Unnikrishnan, S. and Singh, A. 2010. Energy recovery in solid waste management through CDM in India and other countries. Resour. Conserv. Recycl, 54(10): 630-640.

Villarino, S.H., Pinto, P., Della Chiesa, T., Jobbágy, E.G., Studdert, G.A., Bazzoni, B. and Piñeiro, G. 2020. The role of South American grazing lands in mitigating greenhouse gas emissions: A reply to Reassessing the role of grazing lands in carbon-balance estimations. Sci. Total Environ., 54: 740.

Yang, T., Li, Y., Gao, J., Huang, C., Chen, B., Zhang, L. and Li, X. 2015. Performance of dry anaerobic technology in the co-digestion of rural organic solid wastes in China. Energy, 93: 2497-2502.

Zhang, H., Yan, X., Cai, Z. and Zhang, Y. 2013. Effect of rainfall on the diurnal variations of $CH_4$, $CO_2$, and $N_2O$ fluxes from a municipal solid waste landfill. Sci. Total Environ., 442: 73-76.

Zheng, Q., Xu, W., Man, J., Zeng, L. and Wu, L. 2017. A probabilistic collocation-based iterative Kalman filter for landfill data assimilation. Adv. Water Resour., 109: 170-180.

## ORCID DETAILS OF THE AUTHORS

C. Ramprasad: https://orcid.org/0000-0002-4042-3476

# The Effect of Government Subsidies on Innovation Capability of the New Energy Vehicle Industry

**Guixing Yang\*(\*\*)†**

\*Innovation College, North-Chiang Mai University, Chiang Mai, 50230, Thailand
\*\*School of Finance and Economics, Fuzhou Technology and Business University, Fuzhou, 350175, China
†Corresponding author: Guixing Yang; g636501038@northcm.ac.th

**ABSTRACT**

Countries all over the world are paying attention to the growth of the new energy vehicle industry and implementing various subsidy policies to stimulate industry development to enhance the new energy vehicle industry's innovative capability. This study uses a network DEA model to analyze China's new energy vehicle industry's technological innovation capability, decomposing it into two stages: technology development and innovation transformation, and calculating the innovation capability level of China's new energy vehicle industry from 2012 to 2017. The findings show that due to a disconnect between the efficiency of the technology development stage and the efficiency of the innovation transformation stage, innovation technology cannot serve business operations, resulting in China's new energy vehicle industry's overall low level of innovation capability. Based on this, an IT3SLS analysis of the factors influencing innovation capability and phase-by-phase efficiency reveals that while China's new energy vehicle industry's subsidy policy has historically failed to significantly improve innovation capability, there is a complementary/substitution effect between labor input, corporate capital, and government subsidies. Based on the findings of this study, important policy recommendations are made to further develop the technological capabilities of the new energy vehicle industry in the context of China's present new energy policy.

## INTRODUCTION

The worldwide car industry is transitioning away from internal combustion engines and toward new energy sources such as pure electric and hybrid drivetrains. More and more governments around the world are discovering that a single energy mix is incompatible with national strategic security, particularly in countries with limited oil resources (Sun & Ju 2022). At the same time, some emerging developing countries believe that there is still a significant gap in internal combustion engine technology for their national automobile manufacturers to catch up to established automobile companies in developed countries, so they see the new energy vehicle revolution as a historic opportunity to develop their automobile manufacturing industries (Wang et al. 2023). The pressure from global warming, as well as the growth of business, has encouraged industrialized countries to actively create their new energy vehicle industry.

In brief, many countries aim to progressively phase out traditional fuel cars as the primary source of transportation, allowing their automobile manufacturing sectors to grow. Technological innovation activities have a degree of revenue

uncertainty and externality, and the incentive for businesses to innovate under market regulation is insufficient. It is difficult to achieve the optimal allocation of innovation resources without government intervention, guidance, and support. As a result, some nations have enacted measures to encourage the growth of the new energy vehicle industry. For example, in November 2010, the Chinese government enacted a policy designating new energy vehicles as a national strategic developing industry, and the entire industrial chain has been heavily subsidized (Liu & Kokko 2013).

Government subsidies, on the other hand, have always been a contentious policy tool for promoting the development of the new energy vehicle industry. In China, some enterprises have obtained government subsidies through rent-seeking and fraud due to insufficient policy coordination, information disclosure, supervision, and management in the new energy vehicle industry, raising questions about the rationality, effectiveness, and efficiency of government subsidies in supporting technological innovation activities (Zhang & Cai 2020). Therefore, many scholars have previously focused on the effects of government subsidies on relevant firms' innovation inputs, innovation outputs, and

firm performance and attempted to prove the mechanisms of government subsidies on firms' innovation activities using a variety of empirical methods. To some extent, this research has enriched theories about industrial policy.

However, the measures of innovation input, output, and firm performance serve only as partial indicators of firm innovation capability at a specific stage. Previous studies have rarely considered these three measures together as a comprehensive representation of innovation capability for new energy vehicle firms (Chen et al. 2021, Yang et al. 2021).

 In contrast, the government places greater emphasis on the overall enhancement of enterprise innovation capacity compared to the efficacy of these individual stages.

Many governments have made "increasing technological innovation capability" a high priority when establishing their subsidy policies, demonstrating the importance of technological innovation in the long-term development of the new energy vehicle industry. Government subsidies, according to policymakers, are designed to strengthen businesses' innovation capabilities so that they can sustain their competitiveness over time and support the seamless running of the national industrial supply chain. The success of government subsidy policies can be further debated by determining whether or not the industry's innovation capabilities have increased. By empirically analyzing the influence of government subsidy policy on enterprise innovation capability, I hope to construct innovation capability evaluation indexes for enterprises in the new energy vehicle industry, allowing them to more accurately measure innovation capability and improve the evaluation of the effectiveness of government subsidy policy.

## PAST STUDIES AND THE ORETICAL BASIS

### Past Studies

Because of the many study backgrounds, research objects, and research techniques, the relationship between government subsidies and technological innovation has yet to develop a coherent conclusion, and current studies have roughly produced the following four views: (1) Promotional function. According to this viewpoint, government subsidies can compensate for businesses' R&D deficiencies and minimize their R&D risks, allowing them to increase their innovation investment. Government subsidies have both technology-push and demand-pull impacts, lowering private costs of technological innovation and raising private investor returns (Nemet 2009). Based on data from Ireland and Northern Ireland from 1994 to 2002, Hewitt-Dundas and Roper (2010) concluded that government subsidies can enhance the share of enterprises producing innovative inputs

as well as boost incremental product innovation and new product developmental innovation behavior. (2) Disincentive function. The presence of government rent-seeking and market-oriented environments, according to this viewpoint, undermines enterprises' innovative conduct. Government subsidies, according to Beason and Weinstein (1996), weaken or eliminate the payoffs of scale and the growth impacts of enterprises to some extent. Clausen (2009) found that government subsidies have a limited crowding-out effect on firms' innovation behavior, i.e., firms may cut their own innovation inputs and lower their innovation output, implying that government subsidies have a negative impact on firms' innovation activities. (3) No significant relationship. Based on data related to the manufacturing industry in West Germany, Bönte (2004) concluded that government subsidies do not affect improving firm productivity by exploring the role of government innovation subsidies on firm productivity and the role of firm innovation inputs on firm survival. Tzelepis and Skuras (2004) analyze data on subsidies for Greek firms and find that government subsidies improve the solvency of firms and positively stimulate firm growth but have no significant effect on improving firm efficiency and profitability. (4) Non-linear relationship. According to this viewpoint, the relationship between business innovation and government subsidies is not linear but rather changes depending on the level of government subsidies. Bergstrom (2000) examined the Swedish government's subsidy to listed companies from 1987 to 1993, finding that the capital subsidy had a positive impact on the "total factor growth rate" in the first year after the subsidy. Still, then, the capital subsidy had a negative impact on the "total factor growth rate." Harris and Trainor (2005) used data from manufacturing firms in Northern Ireland from 1983 to 1998 to divide the technical level of firms. They discovered that the influence of government subsidies on total factor productivity differed depending on the technological level of firms.

Overall, most existing studies on the relationship between government subsidies and company innovation behavior focus on macro, industrial, and other levels, with less research on the new energy vehicle industry. In recent years, due to the rapid development of the new energy vehicle industry, a number of papers on the assessment of the innovation efficiency of the new energy vehicle industry have mushroomed. For example, Li et al. (2019) analyzed the panel data of 148 new energy vehicle-related firms in Zhongguancun, China, from 2005-2015, and the results showed that there was no significant effect of government subsidies on the performance of SMEs. Fang et al. (2020) explored the impact of government subsidies on innovation efficiency among 23 Chinese new energy vehicle firms during 2013-2018, using the DEA-Tobit method to not

only assess innovation efficiency but also to analyze the possible impact of government subsidies to some extent. Chen et al. (2022) analyzed the innovation efficiency of China's new energy vehicle supply chain using the NSBM method by analyzing data from 105 new energy vehicle-related listed enterprises in China from 2012 to 2019. They reorganized the way innovation efficiency is assessed in a more systematic perspective. It is easy to see that the innovation assessment efficiency methods in this field of research regarding the new energy vehicle industry have been gradually improved. However, it is worth noting that since previous studies have divergent views on the relationship between government subsidies and firm innovation, this may be due to the different understandings among academics on the relationship between the concepts of innovation inputs, innovation outputs, and firm performance. Therefore, it is necessary to adopt a new perspective to examine the innovation capability of enterprises, which in turn can explore more deeply the utility of innovation subsidies on the innovation capability of new energy vehicle enterprises.

In summary, a large number of theoretical and empirical studies have been conducted by scholars, and a certain research base has been formed as the research content continues to deepen. However, since the impact of government subsidies on innovation capability has not been discussed in detail, the existing research can be further expanded from the following perspectives: Unlike the innovation input, innovation output, and enterprise performance, the innovation capability of enterprises is the value embodiment of the enterprise innovation process, and the innovation capability of the new energy vehicle industry can be analyzed through the innovation value chain theory. Based on this, this study will examine enterprise innovation capability and the value chain theory of technological innovation in the new energy industry, investigate the impact of government subsidies on innovation capability, broaden the connotation and extension of enterprise innovation capability, and thus more thoroughly discuss the impact of government subsidies on the new energy vehicle industry's innovation capability.

## Innovation Value Chain Theory and Innovation Capability

Innovation value chain theory was first proposed by Hansen and Birkinshaw (2007), who combined technology innovation theory and value chain theory to present innovation as a process consisting of multiple stages involving idea generation, development, and concept diffusion throughout the innovation value chain. In this theoretical framework, the process of realizing the value of technological innovation in

a firm involves a complex set of activities from research to development and then from development to transformation of economic results.

Innovation capability is one of an organization's intangible assets, and the organization can also continue innovatively developing that asset. Traditional DEA approaches such as SBM-DEA and DEA-MALMQUIST have been utilized in previous research to assess organizations' innovation capacity (Guan et al. 2006, Wang & Zhang 2018). In general, it continues to break down innovation capability into innovation input, innovation output, and company performance in silos, failing to assess businesses' innovation capability holistically. In the meantime, some researchers have used questionnaires to assess firms' innovation capability (Saunila & Ukko 2014, Le & Lei 2019). While innovation capability can be measured by combining innovation inputs, innovation outputs, and firm performance, the questionnaire method is difficult to overcome due to subjectivity. To assess a firm's innovation capabilities, an integrated perspective and a combination of objective measures are required.

Innovation capability is an integrated measure of innovation inputs, innovation outputs, and business performance from the perspective of the innovation value chain. As a result, the innovation value chain perspective should be introduced in order to assess innovation capability more comprehensively, and this study combines the study of Du et al. (2019) to structure the innovation capability of the new energy vehicle industry into a technology development stage and an innovation transformation stage. The technology development stage encompasses the entire process from an enterprise's initial technology development input to the intermediate innovation output, which includes R&D funding and R&D staff. The innovation transformation stage refers to the process of applying the technology development results to the production of marketable products, commercializing the intermediate innovation results, and forming the economic benefits of the enterprise, which is the continuation of the technology development stage and the key link between the technology innovation results and the market. Its core task is to realize the market value of the intermediate innovation results output. The intermediate innovation output, as the intermediate product of the entire technological innovation activity, is not only the first result of the enterprise's initial innovation inputs but also the foundation for applying to commercial production and forming economic benefits in the later stage, connecting and promoting the mutual promotion and coordinated development of each sub-stage. The process of enterprise technology innovation value realization has apparent two-stage chain network characteristics, as can be shown. Fig. 1 depicts the specific procedure.
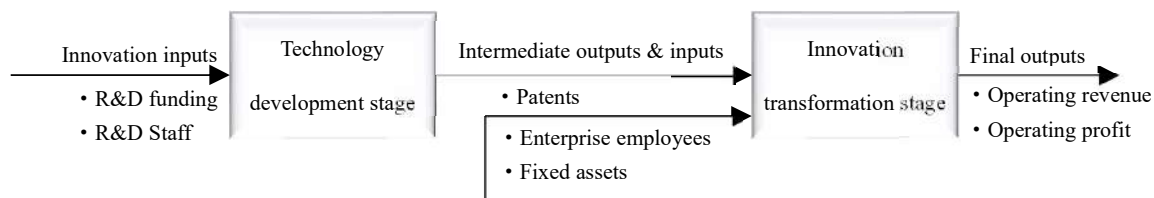
Fig. 1: Deconstruction of innovation capability of new energy vehicle industry.

## MATERIALS AND METHODS

### Two-Stage Network DEA

Traditional econometric approaches such as regression analysis and simple ratio analysis are not well suited to efficiency measurement activities. Data Envelopment Analysis (DEA) is a more powerful analytical way of testing that is better suited to efficiency measurement activities. DEA is a mathematical method that converts inputs into outputs using linear programming techniques to compare the efficiency of similar organizations or goods. Each decision-making unit (DMU) in DEA is allowed to select any combination of inputs and outputs to maximize its relative efficiency. The ratio of total weighted outputs to total weighted inputs is known as relative efficiency or efficiency score (Zhu 2009). DEA is a typical method for evaluating system efficiency in a nonparametric framework that has been popularized and extensively accepted in numerous study areas since its first application in 1978 (Cook & Seiford 2009). Traditional DEA models can only assess the efficiency of a process by putting input indicators into a "black box" and considering the efficiency of output indicators without taking into account what happens in the "black box," which used to be a benefit of DEA models. This was originally a benefit of DEA models. Still, as academic problems grew more complicated, the requirement to break down the contents of the "black box" prompted the development of network DEA models (Tone & Tsutsui 2009). The new

energy vehicle industry's innovation capability spans the entire process, from technological creation through innovation transformation. As a result, a two-stage network DEA model can aid in the "unlocking" of the "black box" of innovation capability assessment. Table 1 shows the unique explanatory factors for the network DEA model, which is based on the study by Du et al. (2019) on innovation capability.

The non-radial SBM two-stage network DEA model proposed by Tone is used to ensure the efficiency of the evaluation model to some extent because the network DEA model may cause the network DEA model to overestimate the efficiency level of the evaluation object if there is over-input or under-output in the network DEA model (i.e., there is non-zero slack). This is shown as follows.

For a set of n decision-making units $DMU_S (j = 1, ..., n)$ with $K$ nodes $(k = 1, ..., K)$. Let $m_k$ and $r_k$ be the input and output amounts for the node $k$ respectively. $(k, h)$ denotes the connection relation between nodes $k$ and $h$, and $L$ is the connection set. The observed data are $\{x_j^k \in R_+^{m_k}\}(j = 1, ..., n; k = 1, ..., K)$ ($DMU_j$ input quantity at the node), $\{y_j^k \in R_+^{r_k}\}(j = 1, ..., n; k = 1, ..., K)$ ($DMU_j$ output quantity at node $k$), and $\{z_j^{(k,h)} \in R_+^{t_{(k,h)}}\}(j = 1, ..., n; (k, h) \in L$. where $t_{(k,h)}$ is the connection relation $(k, h)$ variable number. In this paper, we adopt the assumption of variable payoffs of scale and define the set of production possibilities $\{(x^k, y^k, z^{(k,h)})\}$ as:

Table 1: Two-stage indicators for deconstructing innovation capability.

| Stage | Level 1 Indicators | Level 2 Indicators |
|---|---|---|
| Technology development stage | Innovation inputs | R&D funding (10000 yuan) |
| | | R&D staff (persons) |
| | R&D intermediate outputs | Patent applications (items) |
| | | Increase in value of intangible assets (10000 yuan) |
| Innovation transformation stage | Commercial inputs | Full-time equivalent of practitioners (persons/year) |
| | | Net value of fixed assets (10000 yuan) |
| | Commercial outputs | Revenue from main business (10000 yuan) |
| | | Operating profit (10000 yuan) |

$$\mathbf{x}^k \geq \sum_{j=1}^{n} \mathbf{x}_j^k \lambda_j^k \left(k=1,\ldots,K\right), \mathbf{y}^k \leq \sum_{j=1}^{n} \mathbf{y}_j^k \lambda_j^k \left(k=1,\ldots,K\right) \ldots(1)$$

$$\mathbf{z}^{(k,h)} = \sum_{j=1}^{n} \mathbf{z}_j^{(k,h)} \lambda_j^k \left(\forall(k,h)\right) \left(\text{as the output of node } k\right) \ldots(2)$$

$$\mathbf{z}^{(k,h)} = \sum_{j=1}^{n} \mathbf{z}_j^{(k,h)} \lambda_j^h \left(\forall(k,h)\right) \left(\text{as the input of node } h\right) \ldots(3)$$

$$\sum_{j=1}^{n} \lambda_j^k = 1 \left(\forall k\right), \lambda_j^k \geq 0 \left(\forall j,k\right) \qquad \ldots(4)$$

$\lambda^k \in R_+^n$ denotes the weight corresponding to node $k(k=1,\ldots,K)$ and $\text{DMU}_o(o=1,\ldots,n)$ and can be expressed by:

$$\mathbf{x}_o^k = \mathbf{X}^k \lambda^k + \mathbf{s}^{k-} \left(k=1,\ldots,K\right), \mathbf{y}_0^k = \mathbf{Y}^k \lambda^k - \mathbf{s}^{k+} \left(k=1,\ldots,K\right) \ldots(5)$$

$$\mathbf{e}\lambda^k = 1\left(k=1,\ldots,K\right), \lambda^k \geq 0, \mathbf{s}^{k-} \geq 0, \mathbf{s}^{k+} \geq 0, \left(\forall k\right) \quad \ldots(6)$$

$$\mathbf{X}^k = \left(\mathbf{x}_1^k,\ldots,\mathbf{x}_n^k\right) \in R^{m_k \times n}, \mathbf{Y}^k = \left(\mathbf{y}_1^k,\ldots,\mathbf{y}_n^k\right) \in R^{r_k \times n} \quad \ldots(7)$$

where $\mathbf{s}^{k-}(\mathbf{s}^{k+})$ is the input (output) slack variable. For the constraints of the connecting variables, LF is used to connect the nodes, indicating that the connecting variables are free to decide to maintain the continuity of the input and output quantities at the same time, as expressed by the following equation:

$$\mathbf{Z}^{(k,h)} \boldsymbol{\lambda}^h = \mathbf{Z}^{(k,h)} \lambda^k, \left(\forall(k,h)\right) \qquad \ldots(8)$$

$$\mathbf{Z}^{(k,h)} = \left(\mathbf{z}_1^{(k,h)},\ldots,\mathbf{z}_n^{(k,h)}\right) \in R^{l_{(k,h)} \times n} \qquad \ldots(9)$$

Considering the possible slackness of the input and output quantities, for a more accurate assessment, the undirected network model is used in this paper, as shown in the following equation.

$$\rho_o^* = \min_{\lambda^k, sk-s^{k+}} \frac{\sum_{k=1}^{K} w^k \left[1 - \frac{1}{m_k} \left(\sum_{i=1}^{m_k} \frac{s_i^k}{x_{i0}^k}\right)\right]}{\sum_{k=1}^{K} w^k \left[1 + \frac{1}{r_k} \left(\sum_{r=1}^{r_k} \frac{s_t^{k+}}{y_{t0}^k}\right)\right]} \qquad \ldots(10)$$

Here $\sum_{k=1}^{K} w^k = 1, w^k \geq 0 (\forall k)$, where $w^k$, where $w^k$ is the relative weight of node k to indicate the relative importance of that node. Meanwhile, $\rho_o^*$ is defined as the undirected efficiency of the decision unit $DMU_0$. If $\rho_o^* = 1$, it indicates the overall efficiency of the decision unit $DMU_o$, and the representation of each node is

$$\rho_k = \frac{1 - \frac{1}{m_k} \left(\sum_{i=1}^{m_k} \frac{s_i^{k-*}}{x_{ii}^k}\right)}{1 + \frac{1}{r_k} \left(\sum_{r=1}^{r_k} \frac{s_r^{k+*}}{y_{r0}^k}\right)} \left(k=1,\ldots,K\right) \qquad \ldots(11)$$

Here, $\mathbf{s}^{k-*}$ and $\mathbf{s}^{k+*}$ are the slack variables for the optimal input and optimal output, respectively.

**Model of Factors Influencing Innovation Capability**

Because the process of innovation is difficult to measure and compute, academics have been sluggish in creating methods for estimating innovation capability. Crepon et al. (1998) proposed the CDM model to solve this problem, which allows for the study of innovation capabilities using knowledge production functions; Aiello and Cardamone(2008) improved the CDM model by establishing a transcendental logarithmic production function model that includes innovation spillover effects. The transcendental logarithmic CDM model is employed as the research model in this study, based on the application of the CDM model and with reference to Aiello and Cardamone's study.

$$Cap_{it} = \alpha_i + \alpha_L \ln L_{it} + \alpha_K \ln K_{it} + \alpha_C \ln C_{it} + \alpha_R \ln R_{it} + \frac{1}{2} \beta_{LL} \left(\ln L_{it}\right)^2$$
$$+ \frac{1}{2} \beta_{KK} \left(\ln K_{it}\right)^2 + \frac{1}{2} \beta_{CC} \left(\ln C_{it}\right)^2$$
$$+ \frac{1}{2} \beta_{RR} \left(\ln R_{it}\right)^2 + \beta_{LK} \ln L_{it} \ln K_{it} + \beta_{LC} \ln L_{it} \ln C_{it} + \beta_{LR} \ln L_{it} \ln R_{it} +$$
$$\cdot \beta_{KC} \ln K_{it} \ln C_{it} + \beta_{KR} \ln K_{it} \ln R_{it} + \beta_{CR} \ln C_{it} \ln R_{it} + \varepsilon_{it} \qquad \ldots(12)$$

The following four equations, based on Aiello and Cardamone, are added to each factor input cost-sharing equation to make the above model estimation effective in avoiding multicollinearity mistakes among the parameters and control variables.

$$S_{L,it} = \alpha_L + \beta_{LL} \ln L_{it} + \beta_{LK} \ln K_{it} + \beta_{LC} \ln C_{it} + \beta_{LR} \ln R_{it} + \mu_{L,it} \qquad \ldots(13)$$

$$S_{K,it} = \alpha_K + \beta_{LK} \ln L_{it} + \beta_{KK} \ln K_{it} + \beta_{KC} \ln C_{it} + \beta_{KR} \ln R_{it} + \mu_{K,it} \qquad \ldots(14)$$

$$S_{C,it} = \alpha_C + \beta_{LC} \ln L_{it} + \beta_{KC} \ln K_{it} + \beta_{CC} \ln C_{it} + \beta_{CR} \ln R_{it} + \mu_{C,it} \qquad \ldots(15)$$

$$S_{R,it} = \alpha_R + \beta_{LR} \ln L_{it} + \beta_{KR} \ln K_{it} + \beta_{CR} \ln C_{it} + \beta_{RR} \ln R_{it} + \mu_{R,it} \qquad \ldots(16)$$

The detailed explanation and calculation of the model are shown in Table 2. The detailed explanation of the variables is as follows.

(1) Labor input. When considering labor input, we should consider not only the wages paid to employees but also other welfare and insurance expenses paid to employees, which are included in the administrative expense account.

(2) Capital investment. Referring to the unified measurement standard in the academic field, the capital input of enterprises is defined as 10% of the total assets of the year.

(3) R&D input. To calculate the cumulative effect of R&D expenditure, we take R&D input = current year R&D input + previous year R&D input × 85%.

(4) Government subsidies. The total amount of government subsidies received by the company includes financial subsidies, financial subsidies, tax reductions and refunds, and so on. The non-current profit and loss of the enterprise's financial statements and other disclosure reports are used as reconciliation information; the cumulative effect of the same R&D input is calculated by taking government subsidies = the current year's government subsidies + the previous year's government subsidies 85%.

**Data Source**

The initial sample is centered on companies that were listed on the Shanghai and Shenzhen stock exchanges prior to 2012 and whose primary industry is new energy vehicles. After eliminating ST and *ST stocks, as well as businesses with significant missing data, the balanced panel data of 39 publicly traded companies, including BYD and Shanghai Auto, is eventually chosen. Meanwhile, due to the partial absence of the database, only the dataset from 2012-2017 was used in this study to ensure the scientific accuracy of the data. The data in this study comes from the same CHOICE database, CSMAR database, State Intellectual Property Office, and each company's annual reports, with the missing individual data estimated using the interpolation approach.

The sample ends in 2017 because CSMAR's innovation data are not available after 2017.

**RESULTS**

**Evaluation of Innovation Capability of the New Energy Vehicle Industry**

The data were generated and reported in Table 3 using DeaSolver 13.0 software and the network DEA model to estimate the comprehensive efficiency of 39 new energy vehicle industry enterprises from 2012 to 2017.

Table 3 shows the three efficiency values (average efficiency from 2012 to 2017) of 39 listed new energy industry enterprises, which reflect the overall state of innovation capability as well as efficiency by stage of listed new energy vehicle industry enterprises in China over the last six years. The average value of China's enterprise innovation capability from 2012 to 2017 is 0.2246, which is a relatively low level of innovation capability overall, and the level of innovation capability varies somewhat from year to year. Although the change in innovation capability from 2015 to 2017 has increased, it has not yet achieved the level of innovation capability seen in 2012, showing that the Chinese new energy vehicle industry as a whole is still developing. There is an opportunity for improvement in terms of innovative capability.

From 2012 to 2017, the total efficiency of the innovation transformation stage of firms in China's listed new energy

Table 2: Variable selection and definition of the model.

| Variable | Definition | Definition |
|---|---|---|
| Innovation Capability | $Cap$ | Calculated by two-stage network DEA |
| Government Subsidies | $R$ | The subsidy amount of "government subsidies" in the "non-operating income" account in the annual report of the listed company for the current year + the subsidy amount of the previous year × 85% |
| Labor investment | $L$ | The sum of the enterprise's employee compensation payable and administrative expenses for the year |
| Capital investment | $K$ | Total corporate assets × 10% |
| R&D investment | $C$ | Enterprise current year R&D expenditure + previous year R&D expenditure × 85% |
| Share of labor investment | $S_L$ | $L/Cap$ |
| Share of capital investment | $S_K$ | $K/Cap$ |
| Share of R&D investment | $S_C$ | $C/Cap$ |
| Share of government subsidies | $S_R$ | $R/Cap$ |

Table 3: Innovation capacity of China's new energy vehicle industry, 2012-2017.

| | 2012 | 2013 | 2014 | 2015 | 2016 | 2017 | Mean |
|---|---|---|---|---|---|---|---|
| Innovation capability | 0.2510 | 0.1952 | 0.2085 | 0.2044 | 0.2123 | 0.2419 | 0.2189 |
| Technology development stage | 0.2637 | 0.2564 | 0.2586 | 0.2304 | 0.1975 | 0.1870 | 0.2322 |
| Innovation transformation stage | 0.2969 | 0.2119 | 0.2257 | 0.2404 | 0.2567 | 0.2948 | 0.2544 |

industry outperformed the technology development stage. The efficiency of the technology development stage is in the range [0.1870, 2637], while the efficiency of the innovation transformation stage is in the range [0.2119, 2969], with the efficiency of the innovation transformation stage being about 12.1% higher than the efficiency of the technology development stage over the last 6 years. In the past 6 years, it is easy to find that the listed Chinese enterprises in the new energy industry have emphasized the potential commercial value of enterprise technology innovation and insisted on direct market-oriented innovation transformation activities, and overall innovation transformation efficiency has remained stable. At the same time, there is a significant mismatch between the technology development stage and the innovation transformation stage of Chinese listed new energy industry enterprises, as well as a gap in efficiency between the two stages. Simultaneously, the efficiency level of the technology development stage has been steadily decreasing from 2012 to 2017, indicating that enterprise technology development activities have shifted away from solving actual technical problems and meeting market demand, lowering overall innovation capability.

## Empirical Analysis of the Impact of Government Subsidies on the Innovation Capability of the New Energy Vehicle Industry

The study is based onAiello and Cardamone (2008). It uses iterative three-stage least squares (IT3SLS) optimization to eliminate the negative impact on estimation in the absence of some cost share equations. It also examines the innovation capacity, the efficiency of the technology development stage, and the efficiency of the results of the innovation transformation stage.

Table 4 shows the statistical findings of the analysis using STATA 13.0. The factors influencing innovation capabilities and the efficiency of technology development and transformation stages in the IT3SL3 estimation pass the t-test at all three stages, and the estimated values are all negative, as can be seen from the model estimation results. Labor and capital investment are negatively correlated with innovation capability, according to the $\alpha_L$ and $\alpha_K$ Results. The results of $\alpha_L$ and $\alpha_K$ indicate that innovation capability is negatively correlated with innovation capability, indicating that innovation capability is neither labor-intensive nor capital-intensive. $\alpha_R$ Shows that the Chinese government's subsidies for new energy vehicles have not only failed to improve the innovation capability of enterprises in the past but also inhibited the improvement of innovation capability. Even though several studies have found that government subsidies have a considerable positive impact on enterprises' innovation inputs or outputs, they have mostly neglected the impact of government subsidies on innovation capability. The findings of this study imply that

Table 4: Innovation capacity and stage efficiency IT3SLS results.

| | Innovation capacity | | Technology Development Efficiency | | Innovation Transformation Efficiency | |
|---|---|---|---|---|---|---|
| | Estimated | t | Estimated | t | Estimated | t |
| $\alpha_L$ | -0.3919*** | -4.76 | -0.3501*** | -4.17 | -0.4960*** | -5.34 |
| $\alpha_K$ | -0.3429*** | -4.46 | -0.3063*** | -3.91 | -0.4177*** | -4.82 |
| $\alpha_C$ | 0.2178 | 1.44 | -0.3633** | -2.36 | 0.4360*** | 2.56 |
| $\alpha_R$ | -0.2512** | -2.52 | -0.1798* | -1.77 | -0.1939* | -1.72 |
| $\beta_{LL}$ | 0.0767 | 1.52 | -0.0991* | -1.93 | 0.1984*** | 3.49 |
| $\beta_{KK}$ | 0.0521 | 1.55 | -0.0426 | -1.24 | 0.1067*** | 2.82 |
| $\beta_{CC}$ | 0.1171*** | 3.82 | 0.0847*** | 2.71 | 0.1446*** | 4.19 |
| $\beta_{RR}$ | 0.0381* | 1.9 | 0.0374* | 1.83 | 0.0433** | 1.92 |
| $\beta_{LK}$ | 0.0199 | 0.49 | 0.0794* | 1.89 | -0.0244 | -0.53 |
| $\beta_{LC}$ | -0.0910*** | -2.66 | 0.0120 | 0.34 | -0.1640*** | -4.26 |
| $\beta_{LR}$ | 0.0525 | 1.59 | 0.0639* | 1.9 | 0.0572 | 1.54 |
| $\beta_{KC}$ | -0.0213 | -0.66 | -0.0122 | -0.37 | -0.0006 | -0.02 |
| $\beta_{KR}$ | -0.0268 | -1.44 | -0.0034 | -0.18 | -0.0544*** | -2.59 |
| $\beta_{CR}$ | -0.0376 | -1.36 | -0.0747*** | -2.65 | -0.0267 | -0.86 |
| Sample size | 227 | | 227 | | 227 | |
| $R^2$ | 0.5086 | | 0.6766 | | 0.3322 | |

Note: ***, **, * denote 1%, 5%, 10% significant levels, respectively

the current Chinese government subsidy program has a spillover impact. Government subsidy policy is not always effective due to externalities, and the Chinese new energy vehicle industry has generated a large number of fraudulent subsidies at the early stage of development. Enterprises seeking government subsidies efficiently fail to invest the funds in R&D activities, resulting in low efficiency at the technology development stage and low consumer recognition as a result of transmission to the market, resulting in low efficiency at the innovation transformation stage.

It can be noted from the results in Table 4 that the indicators of substitution complementarity associated with government subsidies, such as $\beta_{LR}$, $\beta_{CR}$, and $\beta_{KR}$, have different degrees of impact on innovation capacity and stage efficiency. As Morishima (1967) argues for the elasticity, when the elasticity value is positive (negative), the two inputs are substitutes (complementary), and it is possible to measure how the 2 input variables affect the change in output variables. $\beta_{KR}$, $\beta_{CR}$ have a negative overall impact size, demonstrating a substitution effect between government subsidies and businesses' own capital and innovation investment, implying that government subsidies have a negative influence on firms' own capital and innovation investment. This suggests that government subsidies have a crowding-out effect on firm investment and that the Chinese government's subsidy strategy for the new energy vehicle industry still has a lot of space for improvement. Government subsidies and labor investment have complimentary impacts on the technological development stage and the influence of $\beta_{LR}$ is not considerable in the innovation capability and innovation transformation stages, but the overall trend is good. This finding suggests that the success of government subsidies for improving a firm's innovation capacity is dependent on whether the firm has the necessary expertise to efficiently translate the associated innovation inputs into innovation outputs. Due to the existence of the substitution/complementarity impact, the Chinese government must and can optimize its new energy vehicle industrial policy to some extent.

## DISCUSSION

This study re-examines the innovation capability of Chinese new energy vehicle enterprises from the perspective of the innovation value chain. It analyzes the influencing factors by introducing the CDM model. The introduction of the innovation value chain theory can help to enhance the understanding of the entire innovation process of the enterprise and no longer confine the innovation capability of the enterprise to a certain stage of innovation input, innovation output, or enterprise performance. This study integrates them through a two-stage network DEA model

and conducts a systematic evaluation. Some previous studies have also noticed that the evaluation of innovation capability needs to adopt an integrated perspective. Based on this, this study further strengthens the explanatory power of enterprise innovation capability by introducing the innovation value chain theory. At the same time, the introduction of the CDM model focuses on the substitution and complementary effects between different variables, making up for the shortcomings of previous studies that only focused on linear relationships between variables (Li et al. 2019, Chen et al. 2021), and provides a certain basis for providing more policy tools.

When nations throughout the world realized the necessity of expanding the new energy vehicle industry, they made innovation capability a focal point of their industrial development. They implemented key industrial subsidy programs to help the new energy vehicle industry grow. Previous studies, on the other hand, have typically focused solely on the impact of subsidy policies on innovation inputs, innovation outputs, and enterprise performance in enterprises' innovation activities, and the inconsistency of research backgrounds has often resulted in conflicting conclusions. Firm innovation capabilities must be considered systematically; otherwise, the research perspective will be limited. This study designs a two-stage network DEA model to measure the innovation capability of organizations. It decomposes the innovation capability into the innovation development and innovation transformation stages based on the innovation value chain perspective. I develop the innovation capability measurement indexes objectively and systematically using the innovation value chain theory and DEA model, which to some extent corrects the subjectivity in previous similar studies and analyzes what is in the "black box" of innovation capability.

The total innovation capability of China's new energy vehicle industry is now weak, according to this study, and prior subsidy policies have not effectively fostered but rather impeded China's new energy vehicle industry's innovation capability. Government subsidies, when compared to market-based income distribution, are a form of income redistribution that raises transaction costs in a variety of ways, including policy design, policy implementation, policy exit, and rent-seeking costs (Wang et al. 2021). Because of these transaction expenses, government subsidies are generally ineffective in promoting the industry's innovation capability.

The Chinese government's subsidy policy for the new energy vehicle industry has begun to show a receding trend (Ye et al. 2021), indicating that the Chinese government's approach to the growth of the new energy vehicle industry is sensible, and also partially justifying the findings of this

study. In the context of the subsidy retreat, government subsidies should abandon past policy instruments that were solely aimed at expanding the scale of the industry, improve the subsidy allocation mechanism in response to China's current problems with new energy vehicle technology development, and implement a talent-oriented subsidy allocation system that focuses on the guiding and leveraging role of subsidies.

To improve their innovation capability, it is necessary to curb enterprises' motivation to cheat on subsidies from the source, stimulate their independent innovation, guide them to increase their awareness of R&D investment, focus on the output of market-oriented technological innovation results, and improve the technology conversion rate. China's new energy vehicle industry got off to a late start, and the current government subsidy monitoring mechanism has issues with information asymmetry and an ineffective supervision system (Luo et al. 2021). Simultaneously, a talent-centered subsidy mechanism should be implemented as much as feasible in accordance with the supply of talent, which corresponds to the skills required for industrial development. This is the key to effectively converting innovation inputs into innovation outputs. To achieve a talent-centered subsidy mechanism, it is critical to conduct regular assessments of new energy vehicle enterprises' innovation capabilities and to differentiate subsidies for enterprises based on their innovation capability levels in order to fully exploit the synergy between talent and government subsidies for the development of enterprises' innovation capabilities.

## ACKNOWLEDGMENTS

## REFERENCES

Aiello, F. and Cardamone, P. 2008. R&D spillovers and firms' performance in Italy: Evidence from a flexible production function. Empir. Econ., 34(1): 143-166.

Beason, R. and Weinstein, D.E., 1996. Growth, economies of scale, and targeting in Japan (1955-1990). Rev. Econ. Stat., 78(2): 286-295.

Bergstrom, F. 2000. Capital subsidies and the performance of firms. Small Bus. Econ., 14(3): 183-193.

Bönte, W. 2004. Spillovers from publicly financed business R&D: Some empirical evidence from Germany. Res. Policy, 33(10): 1635-1655.

Chen, Y., Ni, L. and Liu, K. 2021. Does China's new energy vehicle industry innovate efficiently? A three-stage dynamic network slacks-based measure approach. Technol. Forecast. Soc. Change, 173: 121161.

Chen, Y., Ni, L. and Liu, K. 2022. Innovation efficiency and technology heterogeneity within China's new energy vehicle industry: A two-stage NSBM approach embedded in a three-hierarchy meta-frontier framework. Energy Policy, 161: 112708.

Clausen, T.H. 2009. Do subsidies have positive impacts on R&D and innovation activities at the firm level? Struct. Change Econ. Dyn., 20(4): 239-253.

Cook, W.D. and Seiford, L.M. 2009. Data envelopment analysis (DEA) - Thirty years on. Eur. J. Oper. Res., 192(1): 1-17.

Crepon, B., Duguet, E. and Mairessec, J., 1998. Research, innovation, and productivity: An econometric analysis at the firm level. Econ. Innov. New Technol., 7(2): 115-158.

Du, J., Liu, Y. and Diao, W. 2019. Assessing regional differences in green innovation efficiency of industrial enterprises in China. Int. J. Environ. Res. Public. Health, 16(6): 940.

Fang, S., Xue, X., Yin, G., Fang, H., Li, J. and Zhang, Y. 2020. Evaluation and improvement of technological innovation efficiency of new energy vehicle enterprises in China based on the DEA-Tobit model. Sustainability, 12(18): 7509.

Guan, J.C., Yam, R.C.M., Mok, C.K. and Ma, N. 2006. A study of the relationship between competitiveness and technological innovation capability based on DEA models. Eur. J. Oper. Res., 170(3): 971-986.

Hansen, M.T. and Birkinshaw, J. 2007. The innovation value chain. Harv. Bus. Rev., 85(6): 121.

Harris, R. and Trainor, M. 2005. Capital Subsidies and their impact on total factor productivity: Firm-level evidence from Northern Ireland. J. Reg. Sci., 45(1): 49-74.

Hewitt-Dundas, N. and Roper, S. 2010. Output Additionality of Public Support for Innovation: Evidence for Irish Manufacturing Plants. Eur. Plan. Stud., 18(1): 107-122.

Le, P.B. and Lei, H. 2019. Determinants of innovation capability: The roles of transformational leadership, knowledge sharing, and perceived organizational support. J. Knowl. Manag. 23(3): 527-547.

Li, Y., Zeng, B., Wu, T. and Hao, H. 2019. Effects of urban environmental policies on improving firm efficiency: Evidence from Chinese new energy vehicle firms. J. Clean. Prod., 215: 600-610.

Liu, Y. and Kokko, A. 2013. Who does what in China's new energy vehicle industry? Energy Policy, 57: 21-29.

Luo, G., Liu, Y., Zhang, L., Xu, X. and Guo, Y. 2021. Do governmental subsidies improve the financial performance of China's new energy power generation enterprises? Energy, 227: 120432.

Morishima, M. 1967. A few suggestions on the theory of elasticity. Keizai Hyoron Econ. Rev., 16: 144-150.

Nemet, G.F. 2009. Demand-pull, technology-push, and government-led incentives for non-incremental technical change. Res. Policy, 38(5): 700-709.

Saunila, M. and Ukko, J. 2014. Intangible aspects of innovation capability in SMEs: Impacts of size and industry. J. Eng. Technol. Manag., 33: 32-46.

Sun, B. and Ju, Z. 2022. Research on the promotion of new energy vehicles based on multi-source heterogeneous data: Consumer and manufacturer perspectives. Environ. Sci. Pollut. Res., 6: 5-14.

Tone, K. and Tsutsui, M. 2009. Network DEA: A slacks-based measure approach. Eur. J. Oper. Res., 197(1): 243-252.

Tzelepis, D. and Skuras, D. 2004. The effects of regional capital subsidies on firm performance: An empirical study. J. Small Bus. Enterp. Dev., 11(1): 121-129.

Wang, W. and Zhang, C. 2018. Evaluation of relative technological innovation capability: Model and case study for China's coal mine. Resour. Policy, 58: 144-149.

Wang, X., Li, Z., Shaikh, R., Ranjha, A.R. and Batala, L.K. 2021. Do government subsidies promote financial performance? Fresh evidence from China's new energy vehicle industry. Sustain. Prod. Consum., 28: 142-153.

Wang, Y., Fan, R., Lin, J., Chen, F. and Qian, R. 2023. The effective subsidy policies for new energy vehicles considering both supply

and demand sides and their influence mechanisms: An analytical perspective from the network-based evolutionary game. J. Environ. Manage., 325: 116483.

Yang, T., Xing, C. and Li, X. 2021. Evaluation and analysis of new-energy vehicle industry policies in the context of technical innovation in China. J. Clean. Prod., 281: 125126.

Ye, R.K., Gao, Z.F., Fang, K., Liu, K.L. and Chen, J.W. 2021. Moving from subsidy stimulation to endogenous development: A system dynamics analysis of China's NEVs in the post-subsidy era. Technol. Forecast. Soc. Change, 168: 120757.

Zhang, H. and Cai, G. 2020. Subsidy strategy on new-energy vehicle based on incomplete information: A Case in China. Phys. Stat. Mech. Its Appl., 541: 123370.

Zhu, J. 2009. Quantitative Models for Performance Evaluation and Benchmarking: Data Envelopment Analysis with Spreadsheets. Springer, Singapore.

# Chemistry, Metabolism and Neurotoxicity of Organophosphorus Insecticides: A Review

**Ashutosh Singh\*, Abhishek Singh\*\*† [iD], Akhilesh Singh\*, Priti Singh\*, Vivek Singh\*\*\*, Yogender Singh\*\*\*\*, Hardeep Singh Tuli\*\*\*\*\* [iD], Hadi Sajid Abdulabbas\*\*\*\*\*\* and Abhishek Chauhan\*\*\*\*\*\*\*(\*) [iD]**

\*Department of Chemistry, K.S. Saket Post Graduate College, Ayodhya-224001, India
\*\*Department of Chemistry, Udai Pratap College, Varanasi-221002, India
\*\*\*Departments of Botany, Udai Pratap College, Varanasi-221002, India
\*\*\*\*Department of Chemistry, Government Degree College, B.B. Nagar, Bulandshahr-203402, India
\*\*\*\*\*Department of Bio-Sciences and Technology, Maharishi Markandeshwar Engineering College, Maharishi Markandeshwar (Deemed to be University), Mullana-Ambala 133207, India
\*\*\*\*\*\*Biology Department, College of Science, University of Babylon, Babylon Province-Hilla City, Iraq
\*\*\*\*\*\*\*Amity Institute of Environmental Toxicology, Safety, and Management, Amity University, Noida-201303, India
†Corresponding author: Abhishek Singh; abhupc@yahoo.com

## ABSTRACT

Organophosphorus compounds (OPs) are phosphoric acid derivatives represented by the formula ($R_2XP=O/S$), R as organic groups; however, they need not contain a direct carbon-phosphorus bond. The organophosphorus compounds can be categorized into three classes, *viz.*, organophosphates, carbamates nerve agents. The OPs having application as insecticides are generally phosphorothioates (i.e., containing P=S bond). These sulfur analogs are first bioactivated (*in vivo*) and converted to oxygen analogs responsible for exerting toxic action. These organophosphorus compounds are esters, fluorides, anhydrides, and amides of phosphoric, phosphorothioate, and phosphorodithioic acids. The toxicity of OPs is related to their molecular structure, metabolism in the targeted organisms, concentration, mode of decomposition, application, ingestion in organisms, etc. Exposure to OPs leads to the appearance of neurological symptoms followed by acute poisoning by targeting the target primarily, acetylcholine (AChE). However, secondary targets and other harmful effects besides nerve system problems are also reported. Organophosphates poison insects and other animals, including birds, amphibians, and mammals. These chemicals can have neural effects (Neurotoxicity), non-neuronal effects, or acute toxicity, which may also result in fatality. Their uncontrollable widespread became a significant threat to the environment; thus, corrective measures have been essential to save living beings and the environment from further damage.

## INTRODUCTION

Organophosphorus compounds (OPs) are phosphoric acid derivatives represented by the formula ($R_2XP=O/S$), R as organic groups; however, they need not contain a direct carbon-phosphorus bond. The organophosphorus compounds can be categorized into three classes: organophosphates and carbamates nerve agents. The phosphorous can have five, three, and less than three oxidation states in the compounds. Among these, pentavalent phosphorous is the most prevalent in these chemicals. These chemicals display various fuel additives, insecticides, flame retardants, lubricants, and plasticizers (Fig. 1). The OPs insecticides act as nerve agents by inhibiting acetylcholinesterase (AChE), resulting in acute toxicity. Organophosphorus-based insecticides have been used exhaustively for agriculture and other applications in the last century. Soil bacteria attack these insecticides and, upon hydrolysis in the presence of sunlight and air, may quickly degrade the insecticides (Khalid et al. 2016). However, the persistence of these moieties in food and water in small amounts is noticed (Amir et al. 2019, Akhtar et al. 2009). These have also been toxic and have led to environmental bioaccumulation (Ricardo et al. 2018, Soltaninejad & Shadnia 2014). The OPs' intoxication is a reason for sickness and death worldwide (Petroianu 2015). The wide applications of OPs and their toxicity have been
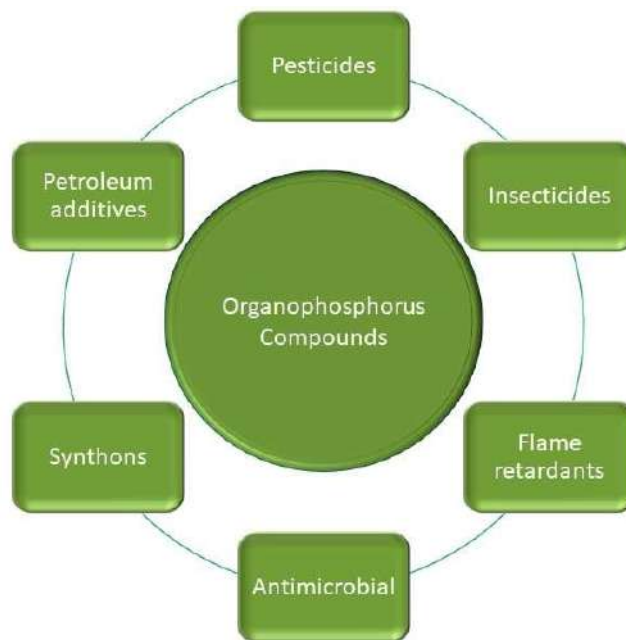
Fig. 1: Pictorial representation of applications of phosphorous compounds.

the reason for their extensive research. This encouraged us to discuss the history of organophosphorus-based insecticides, chemistry, metabolism, and neurotoxicity in the present review article.

Looking back into the past through binoculars of publication, it may be taken that the beginning of research on organic compounds containing phosphorus was marked by the work of Lassaignein 1820 (Lassaigne 1820, Thenard 1847). The scientist also investigated the alcohol and phosphoric acid interaction as well as demonstrated the presence of phosphonic derivatives. For the first time, organophosphorus compounds were described in 1847 by Thenard *via* preparation phosphines series (Hofmann et al. 2009). Hofmann was the first to prepare alkane phosphonic acids in 1872 (Michaelis et al. 1897). The German Michaelis and his coworkers are pioneers of classic but modern phosphorus ester chemistry (Lange & Krueger 1932). Although organophosphorus compounds were synthesized as early as the 19th century, their toxicity effects were reported in 1932 when the Russian scientists Arbuzov Lange and Krueger observed the potent bioactivity of organophosphorus compounds. Investigations of these compounds' biocidal effect elucidated toxicity not only in warm-blooded animals but also in insects. The development of organophosphorus compounds (OPs) was mainly the preparation of active pesticides and insecticides against insects and pests (Petroianu 2015, Soltaninejad & Shadnia 2014, Jayasinghe et al. 2012). Tetraethyl pyrophosphate (TEPP), discovered by De Clermont and Moschnine

in 1854, is the first reported organophosphorus (OPs) known for cholinesterase inhibition. During the time 1934 to1944, many OPs were developed by Schrader, namely parathion, paraoxon, soman, tabun, and sarin which were found to be nerve agents (Savage et al. 1981, Taylor et al. 2007, Squibb 2013). In 1943 parathion was introduced and widely used (Savage et al. 1981, Galli et al. 1988, IOMC & WHO 2010). After World War II, concern for public health and agricultural toxicity due to organophosphorus (Ops) pesticides rose significantly (Galli et al. 1988). The decade 1950s to the 160s showed extensive organophosphorus (OPs) pesticide use. The introduction of Malathion by Cyanamid Company in1950 (Savage et al. 1987, Taylor et al. 2007, Squibb 2013, Galli et al. 1988, WHO 2010), the development of dichlorvos, trichlorfon, and diazinon in 1952 and the creation of Vxin 1958 were marked invention the decade. Mass-produced was also started for VX by the military as a chemical warfare agent (Masson & Nachon 2017). A lot of research has been done in this field for selecting insecticides for better efficacy action, low toxicity, and activity. Current ways of plant protection are successful due to OPs. Which are far better than the chlorinated hydrocarbon insecticides, which have more bioaccumulation in the environment and humans (Galli et al. 1988, Testai et al. 2010). The drawbacks of chlorinated hydrocarbons resulted in bringing degradable organophosphates to market. Organophosphorus insecticides were found to be the only alternatives to chlorinated hydrocarbon insecticides at that time.
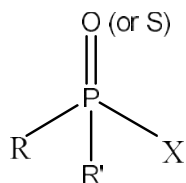
Fig. 2: General Structure of Organophosphorus (OPs).

## CHEMISTRY OF ORGANOPHOSPHORUS (OPS)

Schrader, in 1937, was the first to reveal the chemistry and general structure of organophosphorus (OPs), as shown in Fig. 2. It was observed that phosphorus was pentavalent in these compounds to which sulfur/oxygen was attached through the double bond, R & R' were either alkoxy groups or isopropyl substitutes, and X was found

Table 1: Types of Organophosphorus Compounds.



1. Phosphines

2. Phosphinites

3. Phosphonites

4. Phosphites

5. Phosphinousamides

6. Diamides

7. Triamides

8. Phosphonium salts

9. Phosphine oxides

10. Phosphinates

11. Phosphonates

12. Phosphates

to be the most crucial sensitive towards hydrolysis and was hence called leaving group (Galli et al. 1988). There are numerous subclasses of OPs, viz. phosphorothioates, phosphoramidates, phosphonates, and others (Kurt 2004, Bader 2005). These organophosphorus compounds showed their primary application as insecticides after World War II and are still in use (Kumar et al. 2016).

Most phosphorus-based insecticides are not actual organophosphorus compounds, as these do not have direct P-C bonds. These compounds are esters, amides, anhydrides, and fluorides of phosphoric, phosphorothioic, and phosphorodithioic acids (Van der Oost et al. 2003). The primary classification of organophosphorus compounds is shown in Table 1. The application of these compounds as insecticides may be due to their facile synthetic routes. The synthesis of a few essential phosphorus organo-compounds and their intermediates used as insecticides is summarized in Scheme 1. Some commercially available organophosphates registered under Section 9(3) of the Insecticides Act, 1968, for use in the country are summarized in Table 2.

## STRUCTURE-ACTIVITY RELATIONSHIPS (SAR)

The metabolic effect of Organophosphorus (OPs) insecticides was investigated between the 1950s and 1960s. The structures of OPs are related to their activity. These OPs have Oxon, i.e., P = O moiet, (e.g., dichlorvos, methamidophos, or the nerve agents sarin or soman), which is an effective inhibitor of acetylcholinesterase (Ginsberg et al. 2014). However, the maximum OPs used as insecticides are phosphorothioates and contain Thion, i.e., P=S moiety. The P=S bond needs bioactivation to form toxic oxygen analog axons to exert their harmful action. After bioactivation, OPs display their insecticidal properties via cytochrome P450 (CYPs) mediated oxidative desulfuration (Klaassen et al. 2013, ATSDR's Toxicological Profiles 2003). The formation of oxygen analogs is known as oxon during bioactivation primarily because of their toxicity. Other bioactivation, such as the formation of sulfone by cytochrome P450 (CYP) catalysis (Kurt 2004) or hydrolyticesterases (e.g., carboxylesterase, paraoxonase-1), results in metabolites with lesser or no toxicity (Bader 2005, Sakai & Matsumura 1971). The rest of the biotransformation reactions result in secondary intermediates with toxicity. Few of them are mediated by enzyme CYPs, and few esterases (e.g., paraoxonase, carboxylesterase) (Auf et al. 2007, Malina 2006).

It is mentioned in the literature that the conversion of organophosphorus esters involves metabolic enzymes like transferases, oxidase, hydrolases, etc. The sites for metabolic conversion on an OPs molecule are shown in (Fig. 3). The conversion of thion to oxon group is enzymatically mediated oxidative desulfuration, as shown in Fig. 4. This modification exemplifies intoxication because oxon analog is more potent for the inhibition of anticholinesterase. The conversion of the
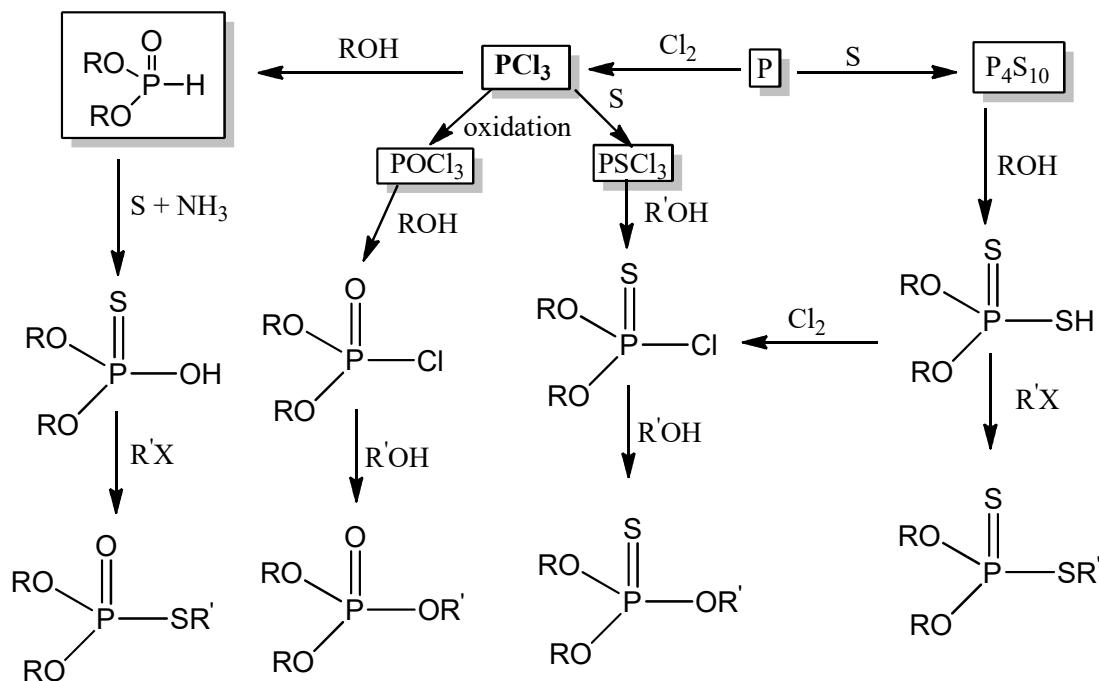


Scheme 1: Synthesis of the essential types of phosphorus ester insecticides.

Table 2: Organophosphates registered under Section 9 (3) of the Insecticides Act, 1968, for use in the country as of 31 Dec. 2014. (adopted and modified from Kumar et al. 2016, Chambers et al. 2010).

| Organophosphates | Trade Name | Molecular Formula |
|---|---|---|
| Acephate | Orthene | $C_4H_{10}NO_3PS$ |
| Chlorpyrifos | Dursban, Lorsban | $C_{13}H_{19}ClNO_2PS_3$ |
| Chlorpyrifos | Dursban, Lorsban | $C_9H_{11}Cl_3NO_3PS$ |
| Chlorpyriphos-methyl | Reldan | $C_7H_7Cl_3NO_3PS$ |
| Diazinon | Spectracide | $C_{12}H_{21}N_2O_3PS$ |
| Dichlorvos | Vapona, DDVP | $C_4H_7Cl_2O_4P$ |
| Dimethoate | Cygon, De-Fend | $C_5H_{12}NO_3PS_2$ |
| Edifenphos | Hinosan, EDDP | $C_{14}H_{15}O_2PS_2$ |
| Ethion | Ethanox, Ethiol, Hylemox, Nialate | $C_9H_{22}O_4P2S_4$ |
| Ethoprop | Mocap 2 | $C_8H_{19}O_2PS$ |
| Fenamiphos | Nemacur | $C_{13}H_{22}NO_3PS$ |
| Fenitrothion | Sumithion | $C_9H_{12}NO_5PS$ |
| Fenthion | Baytex, Tiguvon | $C_{10}H_{15}O_3PS_2$ |
| Iprobenfos | Vikita | $C_{13}H_{21}O_3PS$ |
| Malathion | Carbophos, American Cyanamide 2 | $C_{10}H_{19}O_6PS$ |
| Monocrotophos | Wankophos P | $C_7H_{14}NO_5P$ |
| Oxydemeton-methyl | Meta systox-R | $C_6H_{15}O_4PS_2$ |
| Parathion-methyl | Zofos, Azaopho | $C_{10}H_{14}NO_5PS-CH_4$ |
| Phenthoate | PAP | $C_{12}H_{17}O_4PS_2$ |
| Phorate | Thimet | $C_7H_{17}O_2PS_3$ |
| Phosalone | Zolonc | $C_{12}H_{15}ClNO_4PS_2$ |
| Phosphamidon | Dimecron | $C_{10}H_{19}ClNO_5P$ |
| Pirimiphos-methyl | Actellic | $C_{11}H_{20}N_3O_3PS$ |
| Profenofos | Dyfonate | $C_{11}H_{15}BrClO_3PS$ |
| Propetamphos | Blotic, Safrotin, and Seraphos | $C_{10}H_{20}NO_4PS$ |
| Quinalphos | Chemidor, Chemolux | $C_{12}H_{15}N_2O_3PS$ |
| Temophos | Abate | $C_{16}H_{20}O_6P_2S_3$ |
| Terbufos | Counter, Contravene | $C_9H_{21}O_2PS_3$ |
| Triazophos | Hostathion | $C_{12}H_{16}N_3O_3PS$ |
| Trichlorfon | Dylox, Neguvon | $C_4H_8Cl_3O_4P$ |
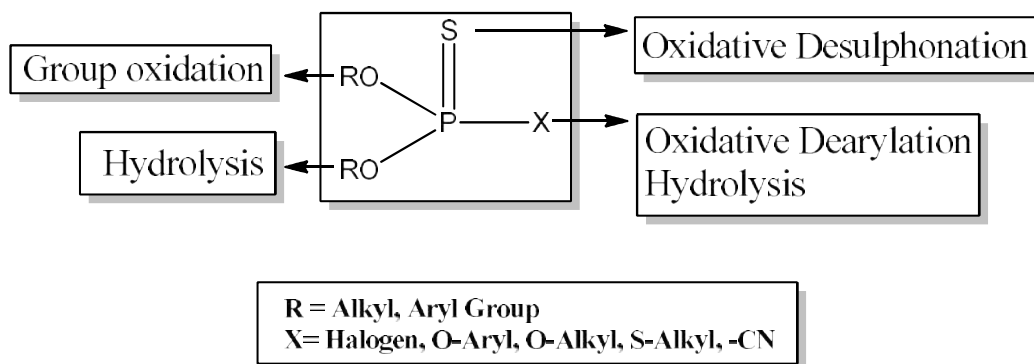
Fig. 3: Metabolic conversion sites in organophosphorus esters.
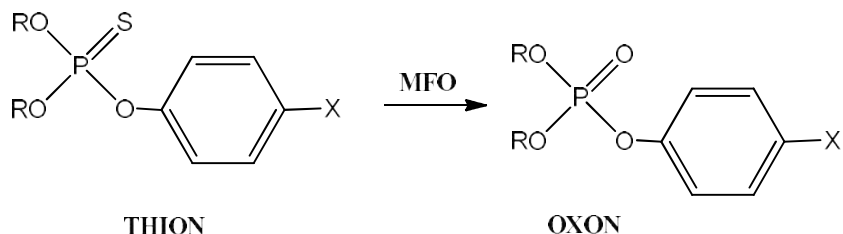
Fig. 4: Parathion: metabolic conversion activation.
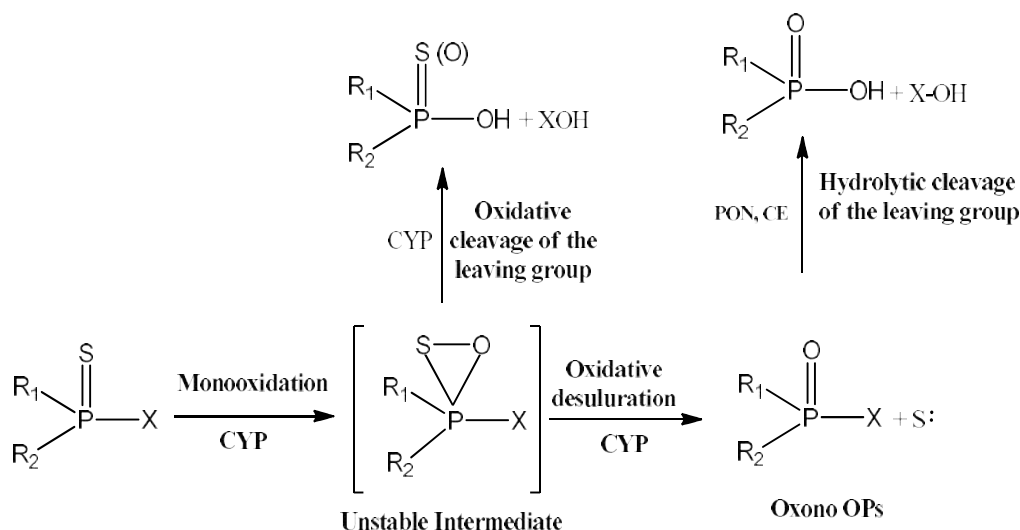


Fig. 5: Reaction of phase I OP metabolism. CYP, cytochrome $P_{450}$, PON, paraoxonase CE, carboxylesterase (Adapted from Hrejac 2009).

thion group to the oxon group has already been observed in mammals as well as in insects (News Agencies Monopolies 1900).

## METABOLISM MECHANISM OF OPs

The OP compounds are more readily absorbed in the living system leading to easy metabolism and excretion (Toxicology of Organophosphate and Carbamate Compounds, 2011). Similarly, to other xenobiotics, OPs metabolism occurs mainly in the liver and, to a lesser extent, in the lungs and intestines. Two phases of the pathway are suggested for the chemical metabolism of OPs. In phase I, the metabolic enzymes activate the OPs by functional group introduction (Maxwell et al. 1992). Phase I of OP metabolism involves oxidation and hydrolysis (Fig. 5). In phase II reactions, enzymes get attached to various hydrophilic groups, like glucuronic acid, sulfate, glycine, and glutamic acid, enabling excretion of the metabolite from the organism Metabolism of includes initial activation via oxidation followed by hydrolysis of activated metabolites (Ziegler et al. 1964).

Oxidation is the most critical reaction in activating the OP thion, leading to the formation of oxons which are active inhibitors of AchE. The sulfur atom in the thion binds to oxygen in the presence of cytochrome $P_{450}$ enzymes (CYP). This results in I formation of an unstable intermediate via oxidative desulphuration. These activated intermediates are strong inhibitors of AChE, responsible for the neurotoxic effects of OPs (Colovic et al. 2013). The influence of the active sulfur atom, as this reaction's side product, is still unclear. It may also interact with neighboring proteins, inactivating cytochrome $P_{450}$ (CYP) enzymes.

The reaction is responsible for the detoxification of OPs. OPs' paraoxonase cleaves dialkyl phosphate and (X) leaving group present on OP molecule. OPs can also be hydrolyzed by the enzyme carboxylesterase. This enzyme is different from paraoxonase in one factor: self-inactivation upon hydrolysis. Metabolism occurs in two phases. In phase I, initially, oxidative desulphuration and then hydrolysis occurs. This is followed by dealkylation or removal of leaving the group (Moser & Padilla, 2011, Grlić 1988). The process involves the intermediate formed with cytochrome P450(CYP), which

ends with a desulphurization reaction. Thus, detoxification involves desulphuration leading to activation of OPs, and then oxidation resulting in cleavage of leaving group equilibrium between desulfuration and oxidative cleavage reactions is responsible for the toxicity of OPs. In phase II metabolism, the reaction results in detoxification and excretion. The oxidation results in the hydrophilic compound, which can conjugate in phase II metabolism via enzymatic catalysis and, finally, excretion (Sogorb et al. 2008). OPs hydrolytic detoxification by phosphotriesterases is also known with a precise mechanism. The enzyme cleaves the bond between P–X of OPs (X is the leaving group), resulting in more polar and less toxic metabolites Enzyme phosphotriesterases are found in mammals, marine animals, birds, bacteria, etc. The serum and liver of mammals have shown a high level of detoxication of OPs by the enzyme (Vilanova & Sogorb 1999, Royo et al. 2007).

## TOXICOLOGY OF ORGANOPHOSPHORUS COMPOUNDS

OPs toxicity includes acute toxicity, neurotoxicity, inhibition of the enzyme AChE, etc., resulting in depression, suicide, and fatality. The toxicity of OPs is related to their molecular structure, concentration, application, decomposition, ingestion, metabolism, excretion, etc. (Camacho et al. 2022). Organophosphorus (OPs) insecticides have high acute toxicity. Organophosphates have toxic effects on insects and other animals, including birds, amphibians, and mammals. For simplicity toxicity of OPs can be studied as (i) neural effects (Neurotoxicity), (ii) non-neuronal effects, and (iii) e toxicity.

### Neurotoxicity

Two major factors, (a) AChE and (b) paraoxonase (PON1) activity levels in interaction with OPs, are responsible for their toxicity.

**Acetylcholinesterase (AChE) inhibition:** The primary reason for OPs toxicity is enzyme AChE inhibition, which hydro (Karalliedde 2001) lyses neurotransmitter acetylcholine in nervous systems. The hydrolytic degradation of AChE occurs in synaptic membranes producing choline and acetate from acetylcholine. OP cholinesterase inhibitors stop the functioning of acetylcholinesterase, leading to excessive accumulation of acetylcholine in the synaptic cleft (Fig. 6 & 7). OP compounds generally form covalent bonds between OP and the active site of AChE thus, inhibiting its functioning. Hydrolysis of OP from the active site is irreversible and slow, thus leading to long-term effects. Novel OPs are altered to accelerate spontaneous hydrolysis of the OP-AChE complex. This causes neurotoxicity and neuro-muscular paralysis (Camacho et al. 2022).

AChE inhibition causes acetylcholine accumulation at cholinergic synapses, thereby overstimulating cholinergic receptors, resulting in a "cholinergic syndrome," which includes excessive salivation, sweating, tremors, bronchial secretion, gastrointestinal motility, diarrhea, muscular
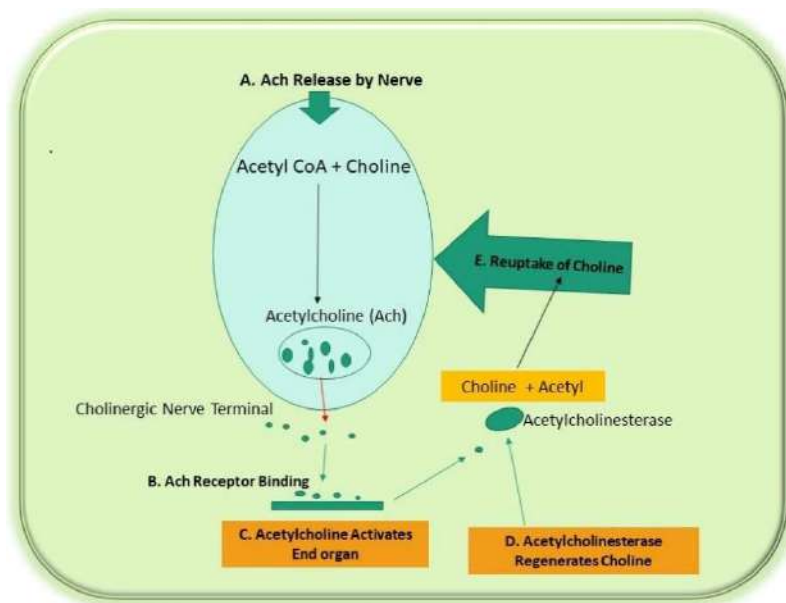


Fig. 6: Normal function of AChE esterase.
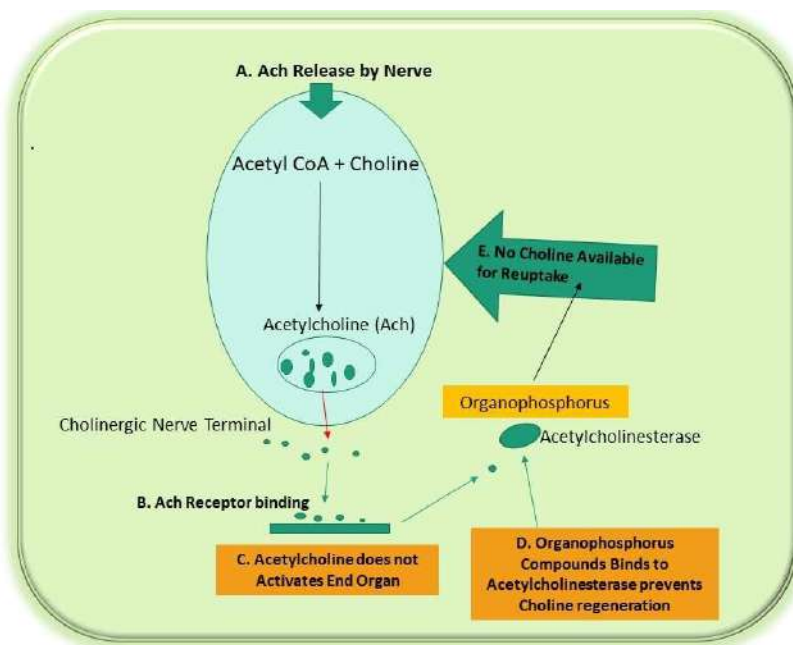
Fig. 7: AChE Esterase breaking down AChE.

twitching, etc., finally death due to respiratory failure caused by inhibition of respiratory centers in the brainstem (WHO 2006, La Du et al. 1999).

Hydrolysis of phosphorylated AChE is slow, but oximes may help accelerate the process. However, oximes may be unable to reactivate phosphorylated AChE on aging (loss of one alkyl group by nonenzymatic hydrolysis), resulting in irreversibly inhibiting enzymes. Atropine is an antidote for poisoning caused by OP and prevents the accumulation of acetylcholine on these receptors. Pralidoxime shows its application in treating OP poisoning. Diazepam is also an anti-anxiety or antagonize convulsions agent for OP toxicity (La Du et al. 1999). Prolonged cholinergic stimulation by OPs also causes acute OP poisoning (Herńandez et al. 2003), developing intermediate syndrome after a few days of exposure leading to symptoms such as marked weakness of muscles in the limb respiratory system and neck (La Du et al. 1999). Long-term CNS effects of high doses of OPs in animals and humans due to neurotoxicity (Costa et al. 2013, Ellison et al. 2012, Needham et al. 2005).

In contrast, low, chronic exposure to OPs does not result in significant neuropsychological effects, neuropsychiatric problems, or nerve dysfunction (Hoppin et al. 2006, Menini & Gugliucci 2014, Hodgson & Rose 2006, Simcox et al. 1995, Gordon et al. 1999). Young animals and children are reported to have a greater sensitivity towards acute toxicity of OPs which may be due to their low detoxication abilities (Needham et al. 2005). However, young animals show greater resistance toward delayed organophosphate-induced polyneuropathy. Pre- and/or post-natal exposure also results in the accumulation of OPs, thus causing neurotoxicity. OPs inhibit DNA replication, and neuronal survival, alter non-cholinergic processes, and enhance oxidative stress and other abnormalities (Ellison et al. 2012, Needham et al. 2005, Berlin & Yodaiken 1984, NRC 2006, La Du et al. 1999, Costa 2018, Hamblin 1960). Malathion shows a broad range against sucking and chewing insects but is less toxic to warm-blooded animals (Odinets 1971). Malathion is metabolized by its enzymatic oxidation of tomalaoxon, thus increasing the toxicity values. In the first step, hydrolysis of ester bonds by enzyme malathionase results in formation of monocarbonic acid, which is non-toxic for warm-blooded animals (Storm et al. 2000). The O,O-Dimethyl-S-(N-2-chlorophenyl-butyramido) methyl phosphorodithioate also found to be effective against many phytophagous insects (Costa et al. 2013).

**Paraoxonase (PON1):** The active metabolites of compounds such as diazinon, chlorpyrifos, and parathion may be hydrolyzed by Paraoxonase (PON1), a polymorphic enzyme. PON1 is produced in the liver and transported to plasma along with high-density lipoprotein (Menini & Gugliucc 2014, Hodsgon et al. 2006, Ellison et al. 2012, Hofmann et al. 2009, Hodgson & Rose 2006). Herńandez et al. (2003) reported decreased PON1 – 909 G/C polymorphism activity on longer exposure to OPs pesticides (Costa et al. 2013). Ellison et al. demonstrated PON1 activity influenced by PON1 55
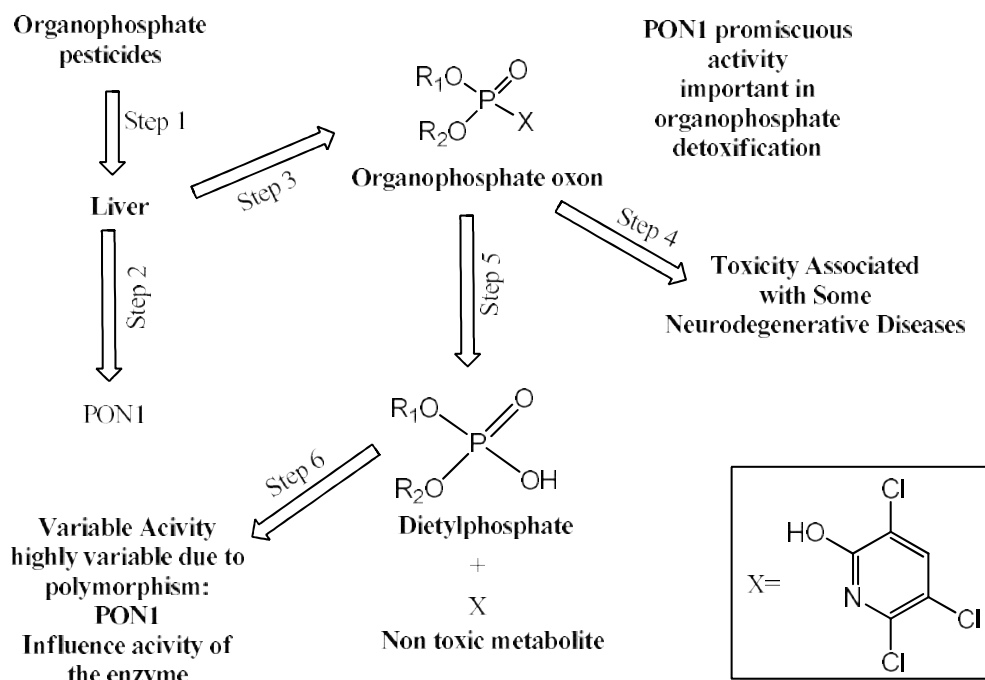
Fig. 8: Role of PON1 in Organophosphate metabolism.

and PON1 192 genotypes in agricultural workers in Egypt (Needham et al. 2005). The agricultural pesticide handlers in Washington State were studied, and it was found that lower plasma levels of PON1 activity show greater BuChE inhibition (Hodgson et al. 2006). Costa et al. (2013) found PON1 to be a crucial factor in diazinon and chlorpyrifosoxon toxicity in rats and mice (Ellison et al. 2012, Needham et al. 2005, Hoppin et al. 2006, Menini & Gugliucc 2014, Hodgson & Rose 2006, Simcox et al. 1995). (Fig. 8).

**Non-Neuronal Molecular Effects of OPs**

The non-neuronal effects of OP exposure on humans are little known (Naughton & Terry Jr. 2018, Quistad et al. 2006). A report revealed several non-neuronal tissues, upon exposure to OPs, may disturb biological processes such as carboxylase inhibition by blocking chemical transformation (Simcox et al. 1995). Xenobiotic metabolism disturbance and cytochrome P450 enzyme (CYP) inhibition by active sulfur during desulphuration (phase I metabolism) is also reported (Bomser et al. 2002). OPs also inhibit enzyme lipases and protein kinase (PKC), which are vital in cell signaling (Oral et al. 2006, Mostafalou & Abdollahi 2013). OP-induced generation of reactive oxygen species leading to oxidative stress and thus resulting apoptosis in tissues is also known, which inhibits steroid androgen (AR) receptors resulting in hormones in the organism (Than et al. 2013).

**Chronic Effects**

The toxicity of OPs at high levels may lead to cancer, cardiovascular diseases, Alzheimer's disease, congenital disabilities, reproductive disorders, Parkinson's disease, diabetes, nephropathies, chronic respiratory problems, etc. (Singh & Sharma 2000). Organophosphate exposure at certain levels leads to COPIND, i.e., chronic organophosphate-induced neuropsychiatric disorders such as hyperactivity disorder, confusion, and neurobehavioral changes (Savage et al. 1988) resulting in respiratory and cardiac diseases (Kumari. et al. 2008). The very high-level exposure may even be fatal (Kojima et al. 2004). Table 3 summarizes the WHO-recommended classifications (Galli et al. 1988) of organophosphates by a hazard registered in India (2009).

**OPs CONTAMINATION IN THE ENVIRONMENT**

OPs compounds initially replaced fewer organochlorines due to their less stable nature. Later their uncontrollable widespread became a major environmental threat, depicted in Fig. 9.

A lot of literature is available that reports the environmental contamination, particularly sediments, soil, and water, such as contamination of sediments by phorate, malathion, etc., in Tarnadmund, Nedugula, and Bison swamp wetlands of Nilgiris district (Chambers et al. 2010, Kaushik 2022, Bishnu

Table 3: Organophosphates by a hazard which are registered in India.

| Highly Toxic | | Moderately Toxic | |
|---|---|---|---|
| Organophosphates | Trade Name | Organophosphates | Trade Name |
| Azinphos-methyl | Guthion, Gusathion | Acephate | Orthene |
| Bomyl | Swat | Bensulide | Betasan, Prefar |
| Carbophenothion | Trithion | Bromophos-ethyl | Nexagan |
| Coumaphos | Co-Ral, Asuntol | Bromophos | Nexion |
| Chlorfenvinphos | Apachlor, Birlane | Chlorphoxim | Baythion-C |
| Chlormephos | Dotan | Chlorpyrifos | Dursban, Lorsban, Brodan |
| Chlorthiophos | Celathion | Crotoxyphos | Ciodrin, Cypona |
| Coumaphos | Co-Ral, Asuntol | Crufomate | Ruelene |
| Cenophosphon | Trichloronate, Agritox | Cyanophos | Cyanox |
| Cyanofenphos | Surecide | Cythioate | Proban, Cyflee |
| Demeton | Syntox | DEF | De-Green, E-Z-Off D) |
| Dalifor | Torak | Demeton-S-methyl | Duratox,  Metasystox-R |
| Dicrotophos | Bidrin | Diazinon | Spectracide |
| Dimefos | Hanane, Pestox XIV | Dichlofenthion | VC-13 Nemacide |
| Dioxathion | Delnav | Dichlorvos | DDVP, Vapona |
| Disulfoton | Disyston | Edifenphos | |
| Endothion | EPN | EPBP | S-Seven |
| Ethyl parathion | E605, Parathion, Thiophos | Ethion | Ethanox |
| Famphur | Famfos, Bo-Ana, Bash | Ethoprop | Mocap |
| Fenamiphos | Nemacur | Etrimfos | Ekamet |
| Fensulfothion | Dasanit | Fenitrothion | Accothion, Agrothion, Sumithion |
| Fonofos | Dyfonate, N-2790 | Fenthion | mercaptophos,Entex, Baytex, Tiguvon |
| Fosthietan | Nem-A-Tak | Formothion | Anthio |
| Isofenphos | Amaze, Oftanol | Heptenophos | Hostaquick |
| Mephosfolan | Cytrolane | IBP | Kitazin |
| Methamidophos | Monitor | Iodofenphos | Nuvanol-N |
| Methidathion | Supracide, Ultracide | Isoxathion | E-48, Karphos |
| Methyl parathion | E601,Penncap-M | Leptophos | Phosvel |
| Mevinphos | Phosdrin, Duraphos | Malathion | Cythion |
| Mipafox | Isopestox, Pestox XV | Merphos | Folex, Easy Off-D |
| Monocrotophos | Azodrin | Methyl trithiondimethoate | Cygon, DeFend |
| Phorate | Thimet, Rampart, AASTAR | Naled | Dibrom |
| Phosfolan | Cyolane, Cylan | Oxydemeton-methyl | Metasystox-R |
| Phosphamidon | Dimecron | Oxydeprofos | Metasystox-S |
| Prothoate | Fac | Propyl thiopyrophosphate | Aspon |
| Schradan | OMPA | Phenthoate | Dimephenthoate, Phenthoate |
| Sulfotep | Thiotepp, Bladafum, Dithione | Phosalone | Zolone |
| Terbufos | Counter, Contraven | Phosmet | Imidan, Prolate |
| Tetraethyl pyrophosphate | TEPP | Propetamphos | Safrotin |

et al. 2009), as well as detection of ethion and chlorpyrifos in tea fields' soils sample of West Bengal and South India (Bishnu et al. 2012, Sreenivasan & Muraleedharan 2011, Jacob et al. 2014) and also contamination of cardamom field of Idukki district, Kerala by chlorpyriphos, ethion, and quinalphos (Jacob et al. 2014, Mathur & Tannan 1999).
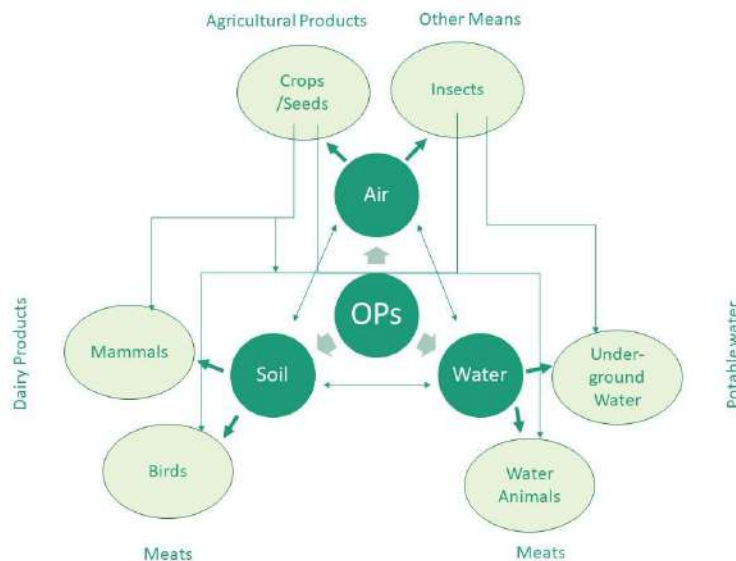
Fig. 9: Routes of exposure of humans to organophosphates (OPs).

The organophosphates are also causing water pollution due to pesticide usage in crop production of vegetables, cotton, and horticultural crops (Pujeri et al. 2008, Bhanti & Taneja 2007, Kumari et al. 2005). Agricultural products such as vegetables, fruits, tea, sugars, etc., are contaminated OPs, including big brands like Tata, Hindustan Unilever, Wagh Bakri, etc. OPs like methyl parathion, chlorpyriphos, and malathion vegetable contamination have been reported at a low level in northern India. However, long-term usage may lead to bioaccumulation may become fatal at a later stage (Lushchak et al. 2018, Leska et al. 2021, Choudhary & Sharma 2008). The presence of organophosphates residues such as malathion and chlorpyriphos residues have also been detected in other food products like butter, honey, cold drinks, etc. (CSE 2006, 2005, Sanghi et al. 2005, Srivastava et al. 2008), indicating the accumulation of these chemicals in living beings. Although OPs are degradable and thus lead to lesser bioaccumulation residues, however, these have been detected in human urine, blood, semen, breast milk, animal milk, etc. (Bajwa & Sandhu 2014, Tamaro et al. 2018, Li et al. 2020, Huen et al. 2012, Ibigbami et al. 2019, Pirsaheb et al. 2015, Lakshmi et al. 2020, Akter et al. 2020) as well as fishes and aquatic animals (Sandoval-Herrera et al. 2019, Ross et al. 2010).

## EVIDENCE FOR PSYCHOLOGICAL EFFECTS OF ORGANOPHOSPHATE COMPOUNDS

Organophosphorus compounds (OPs) are used exclusively for agricultural, industrial, and domestic purposes worldwide; therefore, developing countries correspond to public health issues. Approximately 3 million poisonings and more than 200,000 deaths occur yearly due to OP compounds. The issue of mental health is a major public health concern worldwide. 970 people worldwide are affected by mental disorders such as depression and anxiety. OP inhibits acetylcholinesterase activity and gives rise to neuropsychiatric disorders along with adverse health issues (Sandoval-Herrera et al. 2019, Harrison & Ross 2016). In addition, several studies revealed eminent depression links and associated anxiety with exposure to organochlorines, organophosphates, carbamates, pyrethroids, and herbicides like phenoxy and paraquat dichloride. After 24 h of application of OP, the most common symptoms experienced were headache, dizziness, excessive sweating, fatigue/tiredness, and skin irritation. Individuals exposed earlier are more prone to increased risk of psychiatric disorders (Koh et al. 2017, Keifer et al. 1997). Limited studies on chronic exposure to OP believe psychological dysfunction is a possible effect. Short–term memory, learning, eye-hand coordination, and reaction time in simple and complex reactions are frequently examined. The peripheral nervous system (PNS) effects of OP, which occur by inhibiting cholinesterase, include paresthesias, weakness, foot and wrist drop, and paralysis. Peripheral Neuropathy related to OP was named organophosphate-induced delayed polyneuropathy (OPIDP). It takes 2 to 5 weeks for OPIDP development after exposure to OP. Neuropathy target esterase enzyme obstruction seems to be the biochemical mechanism of the OP that caused OPIDP. The acute central nervous system (CNS) effects of OP included concentration, vigilance, memory, information

processing, psychomotor speed, language impairment, anxiety, irritability, and depression. Cognitive impairment and personality changes are the generalized changes observed in individuals exposed to OP (Keifer et al. 1997).

## CONCLUSIONS

Organophosphorus compounds (OPs) are phosphoric acid derivatives represented by the formula ($R_2XP=O/S$), R as organic groups; however, they need not contain a direct carbon-phosphorus bond. The organophosphorus compounds can be categorized into three classes: organophosphates and carbamates nerve agents. Most OPs used as insecticides are phosphorothioates (i.e., they have a P=S bond) and need to be bioactivated in vivo to their oxygen analogs to exert their toxic action. These compounds are esters, amides, anhydrides, and fluorides of phosphoric, phosphorothioate, and phosphorodithioic acids.

The toxicity of OPs is related to their molecular structure, concentration, application, decomposition, ingestion, metabolism, excretion, etc. Organophosphorus (OPs) insecticides have high acute toxicity. Organophosphates have toxic effects on insects and other animals, including birds, amphibians, and mammals. For simplicity toxicity of OPs can be studied as neural effects, non-neuronal effects, and acute toxicity. The primary reason for OPs toxicity is enzyme AchE inhibition, which hydrolyses neurotransmitter acetylcholine in nervous systems. Potential secondary targets and harmful effects outside the nerve system are also reported. Organophosphates poison insects and other animals, including birds, amphibians, and mammals. These chemicals can have neurotoxicity, non-neuronal effects, or acute toxicity, which may also result in fatality. Their uncontrollable widespread became a major threat to the environment, and thus corrective measures have been an essential requirement to save living beings and the environment from further damage.

## REFERENCES

Akhtar, W., Sengupta, D. and Chowdhury, A. 2009. Impact of pesticides use in agriculture: Their benefits and hazards. Interdisc. Toxicol., 2(1): 1-12. https://doi.org/10.2478/v10102-009-0001-7

Akter, R., Pervin, M. A., Jahan, H., Rakhi, S. F., Reza, A. H. M. and Hossain, Z. 2020. Toxic effects of an organophosphate pesticide, envoy 50 SC on the histopathological, hematological, and brain acetylcholinesterase activities in stinging catfish (Heteropneustes fossilis). J. Basic Appl. Zool., 81(1): 1-14.

ATSDR's toxicological profiles (Web version). 2003. CRC Press.

Auf der Heide, E. 2007. Cholinesterase inhibitors; including pesticides and chemical warfare nerve agents. Agency for Toxic Substances and Disease Registry.

Bader, R.F.W. 2005. Erratum to "complementarity of QTAIM and MO theory. Coord. Chem. Rev., 249(24): 3198. https://doi.org/10.1016/j.ccr.2005.05.004

Bajwa, U. and Sandhu, K. S. 2014. Effect of handling and processing on pesticide residues in food-a review. J. Food Sci. Technol., 51: 201-220.

Berlin, A.R. and Yodaiken, B. 1984. Assessment of toxic agents at the workplace. Role of ambient and biological monitoring. In: Proceedings of NIOSH-OSHA-CEC Seminar, Luxembourg, December 1980.

Bhanti, M. and Taneja, A. 2007. Contamination of vegetables of different seasons with organophosphorous pesticides and related health risk assessment in northern India. Chemosphere, 69(1): 63-68.

Bishnu, A., Chakrabarti, K., Chakraborty, A. and Saha, T. 2009. Pesticide residue level in tea ecosystems of Hill and Dooars regions of West Bengal, India. Environ. Monit. Assess., 149: 457-464.

Bishnu, A., Chakraborty, A., Chakrabarti, K. and Saha, T. 2012. Ethion degradation and its correlation with microbial and biochemical parameters of tea soils. Biol. Fert. Soils, 48: 19-29.

Bomser, J. A., Quistad, G. B. and Casida, J. E. 2002. Chlorpyrifos oxon potentiates diacylglycerol-induced extracellular signal-regulated kinase (ERK 44/42) activation, possibly by diacylglycerol lipase inhibition. Toxicol. Appl. Pharmacol., 178(1): 29-36.

Camacho-Pérez, M.R., Covantes-Rosales, C.E., Toledo-Ibarra, G.A., Mercado-Salgado, U., Ponce-Regalado, M.D., Díaz-Resendiz, K.J.G. and Girón-Pérez, M.I. 2022. Organophosphorus pesticides as modulating substances of inflammation through the cholinergic pathway. International Journal of Molecular Sciences, 23(9), 4523.

Chambers, J.E., Meek, E.C. and Chambers, H.W. 2010. The metabolism of organophosphorus insecticides. In Testai, E., Buratti, F.M. and Di Consiglio, E (eds), Hayes' Handbook of Pesticide Toxicology, Academic Press, Cambridge, MA, pp. 1407-1399.

Choudhary, A. and Sharma, D.C. 2008. Pesticide residues in honey samples from Himachal Pradesh (India). Bulletin of Environmental Contamination and Toxicology, 80(5), 417-422.

Colovic, M.B., Krstic, D.Z., Lazarevic-Pasti, T.D., Bondzic, A.M. and Vasic, V.M. 2013. Acetylcholinesterase inhibitors: pharmacology and toxicology. Current neuropharmacology, 11(3), 315-335.

Costa, L.G. 2018. Organophosphorus compounds at 80: Some old and new issues. Toxicol. Sci., 162(1): 24-35.

Costa, L.G., Giordano, G., Cole, T.B., Marsillach, J. and Furlong, C.E. 2013. Paraoxonase 1 (PON1) is a genetic determinant of susceptibility to organophosphate toxicity. Toxicology, 307: 115-122.

CSE Report 2005. Analysis of pesticide residues in blood samples from Villages of Punjab, CSE/PML/PR-21/2005. https://cdn.cseindia.org/userfiles/Punjab_blood_report.pdf

CSE Report 2006. August analysis of pesticide residues in soft drinks. http://www.indiaenvironmentportal.org.in/files/labreport2006.pdf

Ellison, C.A., Crane, A.L., Bonner, M.R., Knaak, J.B., Browne, R.W., Lein, P.J. and Olson, J.R. 2012. PON1 status does not influence cholinesterase activity in Egyptian agricultural workers exposed to chlorpyrifos. Toxicol. Appl. Pharmacol., 265(3): 308-315.

Galli, C.L., Manzo, L. and Spencer, P.S. (Eds.). 1988. Recent Advances in Nervous System Toxicology. Springer, US. https://doi.org/10.1007/978-1-4613-0887-4

Ginsberg, G., Sonawane, B., Nath, R. and Lewandowski, P. 2014. Methylmercury-induced inhibition of paraoxonase-1 (Pon1)-Implications for cardiovascular risk. Journal of Toxicology and Environmental Health, Part A, 77(17): 1004-1023. https://doi.org/10.1080/15287394.2014.919837

Gordon, S.M., Callahan, P.J., Nishioka, M.G., Brinkman, M.C., O'Rourke, M.K., Lebowitz, M.D. and Moschandreas, D.J. 1999. Residential environmental measurements in the national human exposure assessment survey (NHEXAS) pilot study in Arizona: Preliminary results for pesticides and VOCs. J. Expo. Sci. Environ. Epidemiol., 9(5): 456-470.

Grlić, L. 1988. A small chemical lexicon. Zagreb: Forward, 198 p.

Hamblin, D.O. 1960. Some phosphate ester insecticides are of lesser toxicity for man. J. Occup. Med., 2(5): 211-213.

Harrison, V. and Ross, S.M. 2016. Anxiety and depression following cumulative low-level exposure to organophosphate pesticides. Environ. Res., 151: 528-536.

Herńandez, A.F., Mackness, B., Rodrigo, L., López, O., Pla, A., Gil, F. and Mackness, M.I. 2003. Paraoxonase activity and genetic polymorphisms in greenhouse workers with long-term pesticide exposure. Hum. Exp. Toxicol., 22(11): 565-574.

Hodgson, E. and Rose, R.L. 2006. Organophosphorus chemicals: potent inhibitors of the human metabolism of steroid hormones and xenobiotics. Drug metabolism reviews, 38(1-2), 149-162.

Hofmann, J.N., Keifer, M.C., Furlong, C.E., De Roos, A.J., Farin, F.M., Fenske, R.A. and Checkoway, H. 2009. Serum cholinesterase inhibition in relation to paraoxonase-1 (PON1) status among organophosphate-exposed agricultural pesticide handlers. Environ. Health Persp., 117(9): 1402-1408.

Hoppin, J.A., Adgate, J.L., Eberhart, M., Nishioka, M. and Ryan, P.B. 2006. Environmental exposure assessment of pesticides in farmworker homes. Environmental Health Perspectives, 114(6), 929-935.

Hrejac, I. 2009. Genotoxic, cogenotoxic and potential carcinogenic activity of model organphosphorous pesticides. University of Ljubljana, Ljubljan Slovenia 2009.

Huen, K., Bradman, A., Harley, K., Yousefi, P., Barr, D.B., Eskenazi, B. and Holland, N. 2012. Organophosphate pesticide levels in blood and urine of women and newborns living in an agricultural community. Environ. Res., 117: 8-16.

Ibigbami, O.A., Aiyesanmi, A.F., Adesina, A.J. and Popoola, O.K. 2019. Occurrence and levels of chlorinated pesticides residues in cow milk: A human health risk assessment. J. Agric. Chem. Environ., 8(01): 58.

Inter-Organization Programme for the Sound Management of Chemicals (IOMC) & World Health Organization (WHO). 2010. WHO Recommended Classification of Pesticides by Hazard and Guidelines to Classification 2009. World Health Organization, Geneva, Switzerland.

Jacob, S., Resmi, G. and Mathew, P.K. 2014. Environmental pollution due to pesticide application in cardamom hills of Idukki, District, Kerala, India. Int. J. Basic. Appl. Res., 1: 27-34.

Jayasinghe, S. S., Pathirana, K. D. and Buckley, N. A. 2012. Effects of acute organophosphorus poisoning on the function of peripheral nerves: a cohort study. PloS ONE, 7(11): e49405. https://doi.org/10.1371/journal.pone.0049405

Karalliedde, L. (ed.). 2001. Organophosphates and health. World Scientific Pub. Co., India.

Kaushik, G. 2022. A review on phorate persistence, toxicity and remediation by bacterial communities. Pedosphere, 32(1): 171-183.

Keifer, M.C. and Mahurin, R.K. 1997. Chronic neurologic effects of pesticide overexposure. Occup. Med., 12(2): 291-304.

Khalid, M., Rasul, S., Hussain, J., Ahmad, R., Zia, A., Bilal, M., Pervez, A. and Naqvi, T.A. 2016. Biodegradation of organophosphorus insecticides, chlorpyrifos, by Pseudomonas putida CP-1. Pakistan Journal of Zoology, 48(5).

Klaassen, C.D., Casarett, L.J. and Doull, J. (eds). 2013. Casarett and Doull's Toxicology: The Basic Science of Poisons. Eight Edition. McGraw-Hill Education, NY.

Koh, S.B., Kim, T.H., Min, S., Lee, K., Kang, D.R. and Choi, J.R. 2017. Exposure to pesticide as a risk factor for depression: A population-based longitudinal study in Korea. Neurotoxicology, 62: 181-185.

Kojima, H., Katsura, E., Takeuchi, S., Niiyama, K. and Kobayashi, K. 2004. Screening for estrogen and androgen receptor activities in 200 pesticides by in vitro reporter gene assays using Chinese hamster ovary cells. Environmental health perspectives, 112(5), 524-531.

Kumar, S., Kaushik, G. and Villarreal-Chiu, J.F. 2016. Scenario of organophosphate pollution and toxicity in India: A review. Environ. Sci. Pollut. Res., 23: 9480-9491.

Kumari, B., Madan, V.K. and Kathpal, T.S. 2008. Status of insecticide contamination of soil and water in Haryana, India. Environmental monitoring and assessment, 136, 239-244.

Kumari, B., Singh, J., Singh, S. and Kathpal, T.S. 2005. Monitoring of butter and ghee (clarified butter fat) for pesticidal contamination from a cotton belt of Haryana, India. Environ. Monit. Assess., 105: 111-120.

Kurt, T.L. 2004. A Textbook of Modern Toxicology, E. Hodgson (ed), Wiley-Interscience, John Wiley & Sons, Hoboken, NJ. p. 557.

La Du, B.N., Aviram, M., Billecke, S., Navab, M., Primo-Parmo, S., Sorenson, R.C. and Standiford, T.J. 1999. On the physiological role (s) of the paraoxonases. Chem. Biol. Interac., 119: 379-388.

Lakshmi, J., Mukhopadhyay, K., Ramaswamy, P. and Mahadevan, S. 2020. A systematic review on organophosphate pesticide and type II diabetes mellitus. Current Diabetes Rev., 16(6): 586-597.

Lange, W. and Krueger, G. 1932. About esters of monofluorophosphoric acid. Rep. German Chem. Soc., a B Ser., 65(9): 1598-1601.

Lassaigne, I. L. 1820. Ann. Chimie. Physique., 13, Strie. 2, 294

Leska, A., Nowak, A., Nowak, I. and Górczyńska, A. 2021. Effects of insecticides and microbiological contaminants on Apis mellifera health. Molecules, 26(16): 5080.

Li, A. J., Banjabi, A. A., Takazawa, M., Kumosani, T. A., Yousef, J. M. and Kannan, K. 2020. Serum concentrations of pesticides, including organophosphates, pyrethroids, and neonicotinoids in a population with osteoarthritis in Saudi Arabia. Sci. Total Environ., 737: 139706.

Lushchak, V. I., Matviishyn, T. M., Husak, V. V., Storey, J. M. and Storey, K. B. 2018. Pesticide toxicity: a mechanistic approach. EXCLI J., 17: 1101.

Malina, D. 2006. Book review narrative medicine: Honoring the stories of illness by rita charon. Oxford University Press, NY, p. 256

Masson, P. and Nachon, F. 2017. Cholinesterase reactivators and bioscavengers for pre□and post□exposure treatments of organophosphorus poisoning. J. Neurochem., 142: 26-40.

Mathur, S.C. and Tannan, S.K. 1999. Future of Indian pesticides industry in next millennium. Pesticide information, 24(4), 9-23.

Maxwell, D.M. 1992. The specificity of carboxylesterase protection against the toxicity of organophosphorus compounds. Toxicol. Appl. Pharmacol., 114(2): 306-312. https://doi.org/10.1016/0041-008X(92)90082-4

Menini, T. and Gugliucci, A. 2014. Paraoxonase 1 in neurological disorders. Redox Report, 19(2): 49-58. https://doi.org/10.1179/1351000213Y.0000000071

Michselis, A. and Becker, T. 1897. Ueber die Constitution der phosphorigen Säure. Berichte der deutschen chemischen Gesellschaft, 30(1): 1003-1009.

Miodovnik, A., 2019. Prenatal exposure to industrial chemicals and pesticides and effects on neurodevelopment. Encyclopedia of Environmental Health, pp. 352-342, Elsevier.

Moser, V.C. and Padilla, S. 2011. Esterase metabolism of cholinesterase inhibitors using rat liver in vitro. Toxicology, 281(1–3): 56-62. https://doi.org/10.1016/j.tox.2011.01.002

Mostafalou, S. and Abdollahi, M. 2013. Pesticides and human chronic diseases: evidences, mechanisms, and perspectives. Toxicology and applied pharmacology, 268(2), 157-177.

National Research Council (NRC). 2006. Human biomonitoring for environmental chemicals. National Academies Press, NY.

Naughton, S.X. and Terry Jr, A. V. 2018. Neurotoxicity in acute and repeated organophosphate exposure. Toxicology, 408: 101-112.

Needham, L.L., Özkaynak, H., Whyatt, R.M., Barr, D.B., Wang, R.Y., Naeher, L. and Zartarian, V. 2005. Exposure assessment in the National Children's Study: introduction. Environ. Health Persp., 113(8): 1076-1082.

News Agencies. Monopolies. Inter-ocean publishing co. V. Associated press, 56 n. E. 822(Ill.). 1900. The Yale Law Journal, 9(8), 376. https://doi.org/10.2307/782184

Odinets, A.A. 1971. Toxicity of malathion for warm-blooded

animals: A review of the literature. Farmakol. Toksikol., 34(1): 113-116.

Oral, B., Guney, M., Demirin, H., Ozguner, M., Giray, S.G., Take, G. and Altuntas, I. 2006. Endometrial damage and apoptosis in rats induced by dichlorvos and the ameliorating effect of antioxidant vitamins E and C. Reprod. Toxicol., 22(4): 783-790.

Petroianu, G. 2015. History of organophosphorus cholinesterase inhibitors & reactivators. Milit. Med. Sci. Lett., 84(4): 182-185.

Pirsaheb, M., Limoee, M., Namdari, F. and Khamutian, R. 2015. Organochlorine pesticides residue in breast milk: a systematic review. Med. J. Islamic Rep. Iran., 29: 228.

Pujeri, U.S., Pujar, A.S., Hiremath, S.C. and Yadawe, M.S. 2008. The status of pesticide pollution in surface water (lakes) of Bijapur. Int. J. Appl. Biol. Pharm. Technol. 1,436-441.

Quistad, G. B., Liang, S. N., Fisher, K. J., Nomura, D. K. and Casida, J. E. 2006. Each lipase has a unique sensitivity profile for organophosphorus inhibitors. Toxicol. Sci., 91(1): 166-172.

Ricardo., A., Torres-Palma, E. and Serna-Galvis, A. 2018. Advanced Oxidation Processes for Waste Water Treatment. Elesvier, The Netherlands

Ross, S.J.M., Brewin, C.R., Curran, H.V., Furlong, C.E., Abraham-Smith, K.M. and Harrison, V. 2010. Neuropsychological and psychiatric functioning in sheep farmers exposed to low levels of organophosphate pesticides. Neurotoxicol. Teratol., 32(4): 452-459.

Royo, S., Martínez-Máñez, R., Sancenón, F., Costero, A.M., Parra, M. and Gil, S. 2007. Chromogenic and fluorogenic reagents for chemical warfare nerve agents' detection. Chemical Communications, 46, 4839. https://doi.org/10.1039/b707063b

Sakai, K. and Matsumura, F. 1971. Degradation of certain organophosphate and carbamate insecticides by human brain esterases. Toxicology and Applied Pharmacology, 19(4), 660-666. https://doi.org/10.1016/0041-008X(71)90297-3

Sandoval-Herrera, N., Mena, F., Espinoza, M. and Romero, A. 2019. Neurotoxicity of organophosphate pesticides could reduce the ability of fish to escape predation under low doses of exposure. Scie. Rep., 9(1): 1-11.

Sanghi, R., Pillai, M.K., Jayalekshmi, T.R. and Nair, A. 2003. Organochlorine and organophosphorus pesticide residues in breast milk from Bhopal, Madhya Pradesh, India. Hum. Exp. Toxicol., 22(2): 73-76.

Savage, E.P., Keefe, T.J., Mounce, L.M., Heaton, R.K., Lewis, J.A. and Burcar, P.J. 1988. Chronic neurological sequelae of acute organophosphate pesticide poisoning. Archives of Environmental Health: An International Journal, 43(1), 38-45.

Savage, E.P., Keefe, T.J., Wheeler, H.W., Mounce, L., Helwic, L., Applehans, F., Goes, E., Goes, T., Mihlan, G., Rench, J. and Taylor, D.K. 1981. Household pesticide usage in the united states. Arch. Environ. Health Int. J., 36(6): 304-309. https://doi.org/10.1080/00039896.1981.10667642

Serrano-Medina, A., Ugalde-Lizárraga, A., Bojorquez-Cuevas, M. S., Garnica-Ruiz, J., González-Corral, M.A., García-Ledezma, A. and Cornejo-Bravo, J.M. 2019. Neuropsychiatric disorders in farmers associated with organophosphorus pesticide exposure in a rural village of northwest México. Int. J. Environ. Res. Pub. Health, 16(5): 689.

Simcox, N.J., Fenske, R.A., Wolz, S.A., Lee, I.C. and Kalman, D.A. 1995. Pesticides in household dust and soil: Exposure pathways for children of agricultural families. Environ. Health Persp., 103(12): 1126-1134.

Singh, S. and Sharma, N. 2000. Neurological syndromes following organophosphate poisoning. Neurology India, 48(4), 308.

Sogorb, M.A., Garcia-Arguelles, S., Carrera, V. and Vilanova, E. 2008. Serum albumin is as efficient as paraxonase in the detoxication of paraoxon at toxicologically relevant concentrations. Chem. Res. Toxicol., 21(8): 1524-1529.

Soltaninejad, K. and Shadnia, S. 2014 History of the use and epidemiology of organophosphorus poisoning. Basic Clinic. Toxicol. Organophos. Comp., 4: 25-43.

Squibb, K. Pesticides: Program in Toxicology. Available from www.uobabylon.edu.iq/eprints/publication34640659.pdf. Accessed on October 1, 2013.

Sreenivasan, S. and Muraleedharan, N. 2011. Survey on the pesticide residues in tea in south India. Environmental monitoring and assessment, 176, 365-371.

Srivastava, S., Narvi, S.S. and Prasad, S.C. 2008. Organochlorines and organophosphates in bovine milk samples in Allahabad region.

Storm, J.E., Rozman, K.K. and Doull, J. 2000. Occupational exposure limits for 30 organophosphate pesticides based on inhibition of red blood cell acetylcholinesterase. Toxicology, 150(1-3): 1-29.

Tamaro, C.M., Smith, M.N., Workman, T., Griffith, W.C., Thompson, B. and Faustman, E. M. 2018. Characterization of organophosphate pesticides in urine and home environment dust in an agricultural community. Biomarkers, 23(2), 174-187.

Taylor, E.L., Holley, A.G. and Kirk, M. 2007. Pesticide development: A brief look at the history. South. Reg. Ext. For., 1: 1-7.

Testai, E., Buratti, F.M. and Di Consiglio, E. 2010. Hayes' Handbook of Pesticide Toxicology. Academic Press, Cambridge, MA.

Than, K. 2013. Organophosphates: a common but deadly pesticide. National Geographic.

Thenard, P. 1847. Compte. Rend., 25, 892.

Van der Oost, R., Beyer, J. and Vermeulen, N.P. 2003. Fish bioaccumulation and biomarkers in environmental risk assessment: A review. Environ. Toxicol. Pharmacol., 13(2): 57-149.

Vilanova, E. and Sogorb, M.A. 1999. The role of phosphotriesterases in the detoxication of organophosphorus compounds. Crit. Rev. Toxicology, 29(1), 21-57.

World Health Organization (WHO). 2006. Air quality guidelines: global update 2005: particulate matter, ozone, nitrogen dioxide, and sulfur dioxide. World Health Organization.

Ziegler, D.M. 1964. Metabolic oxygenation of nitrogen and sulphur compounds. In: J.K.Mitchell&M.G.Horning (eds), Drug metabolism and drug toxicity, (Raven Press, Iuew York), 33-53.

## ORCID DETAILS OF THE AUTHORS

Abhishek Singh: https://orcid.org/0000-0002-3931-1047
Abhishek Chauhan: https://orcid.org/0000-0001-6475-1266
Hardeep Singh Tuli: https://orcid.org/0000-0003-1155-0094

**Original Research Paper**

https://doi.org/10.46488/NEPT.2023.v22i04.015

**Open Access Journal**

# Palladium-Based Catalytic Treatment and a Rhizobacterial-Assisted Detoxification for the Enhanced Removal of Lindane

Rachana Sharma* and Prabhu Thangadurai**†

*BIRAC EYUVA Centre, PSGR Krishnammal College for Women, Peelamedu, Coimbatore, Tamil Nadu, India
**PSG Institute of Management, PSG College of Technology, Peelamedu, Coimbatore, Tamil Nadu, India
†Corresponding author: Prabhu Thangadurai; prabhuthangadurai@psgim.ac.in

## ABSTRACT

This study aimed to assess the efficacy of a bimetallic system consisting of $Mg^0$-$Pd^0$ and the bacterium *Acinetobacter* sp. for the complete detoxification of lindane. Our results demonstrate that palladium immobilized on activated charcoal achieved a removal rate of >99% for 100 $mg.L^{-1}$ of Lindane within 10 minutes, with the accumulation of trace amounts of intermediates. The reductive transformation of lindane followed 1st-order kinetics, with a calculated rate constant ($k_{obs}$) of 0.77 $min^{-1}$. The bimetallic system resulted in the formation of a non-toxic hydrocarbon as the end-product, indicating complete dehalogenation of lindane. Furthermore, *Acinetobacter* sp. effectively mineralized >98% of 100 $mg.L^{-1}$ of Lindane after 26 h of cultivation without any accumulation of toxic metabolite(s) in the reaction medium, demonstrating the efficiency of the biological system. Integrating both chemical and biological systems could provide significant advantages for the treatment of lindane, reducing the treatment time and overall cost. This synergistic approach can significantly enhance the overall removal efficiency of lindane from contaminated soil and water.

## INTRODUCTION

Lindane ($C_6H_6Cl_6$), also known as γ-hexachlorocyclohexane, is a synthetic organochlorine pesticide widely used in agriculture, forestry, and public health sectors for several decades. Due to its poor solubility in water and high lipophilicity, lindane accumulates in the fatty tissues of living organisms, including humans (Alsen et al. 2022). Lindane is a potent neurotoxin and has been found to have harmful effects on human health, even at low levels of exposure. Inhalation of Lindane can cause symptoms such as dizziness, headaches, and confusion, while skin contact with the pesticide can cause irritation, rashes, and seizures (Jayaraj et al. 2016). In addition to its neurological effects, lindane is toxic to the liver and kidneys, potentially leading to long-term health problems. Exposure to lindane over extended periods of time has also been linked to an increased risk of cancer, reproductive and developmental problems, and neurological disorders (Alavanja & Bonner 2012). It was classified as a Group 1 carcinogen by the WHO and IARC, indicating that it was known to cause cancer in humans. This classification was based on extensive research that had been conducted in the past, revealing that exposure to lindane was linked to an increased risk of certain types of cancer, including lymphoma and leukemia (Alsen et al. 2022).

Furthermore, lindane has been shown to have acute toxicity to a variety of animals, including mammals, birds, fish, and invertebrates. Studies have demonstrated that lindane's LD50 (median lethal dose) varies widely across different animal species. For example, the $LD_{50}$ of Lindane for rats is approximately 88 $mg.kg^{-1}$, while for rabbits, it is around 120 $mg.kg^{-1}$ (Shakur et al. 2021). The $LD_{50}$ for birds is significantly lower, ranging from 12 to 55 $mg.kg^{-1}$ (Katagi & Fujisawa 2021). Similarly, the $LD_{50}$ for fish varies depending on the species and ranges from 0.26 to 2.6 $mg.L^{-1}$ (Tao et al. 2013). The toxic effects of lindane are due to its ability to disrupt the normal functioning of the nervous system by binding to gamma-aminobutyric acid (GABA) receptors, which can lead to seizures, tremors, and convulsions (Islam & Lynch 2012). Numerous studies have highlighted the adverse effects of lindane exposure on aquatic organisms, including genotoxicity and DNA damage in fish (González-Mille et al. 2003). In addition, research has shown that lindane can negatively impact the reproductive success of birds, as evidenced by reduced clutch size, increased nest failure, and decreased egg viability (Etterson & Bennett 2013).

Understanding the fate and transport of lindane in soil, water, and air is crucial for assessing its potential impacts on human health and the environment. The combination

of low solubility and high adsorption to soil particles makes lindane persistent in the environment and difficult to degrade. Research has shown that lindane can persist in soil for many years, with the potential for leaching into groundwater and surface water. Diop et al. (2019) found that lindane residues were detected in soil samples from various agricultural fields in the Niayes zone of Dakar, Senegal, for up to 15 years after application. The study also showed that lindane was detected in groundwater samples, indicating the potential for contamination of drinking water sources. Golfinopoulos et al. (2014) measured lindane concentrations in surface water and sediment samples from the rivers of Northern Greece. The study found that lindane concentrations were higher in sediments than in surface water, suggesting that lindane can adsorb onto sediment particles and be transported downstream. In the air, lindane can be transported over long distances through atmospheric transport and deposition. Waite et al. (2005) studied the movement of lindane from the Canadian prairies to the Great Lakes, Arctic, and Rocky Mountains regions. They found that lindane traveled long distances in the atmosphere and was detected in air and precipitation samples from these regions, with peak concentrations in the summer. The study highlights the importance of monitoring and regulating POPs to prevent contaminating remote regions and ecosystems. Lindane is banned or restricted in many countries due to its harmful impact on human health and the environment. Yet, its continued presence poses significant risks, especially in developing countries with poor regulation. Developing effective technologies for removing lindane from contaminated environments is necessary to reduce its risks.

Numerous techniques, comprising physical, chemical, and biological methods, are available for the degradation of lindane in contaminated soil and water. However, the efficacy of these methods may be subject to diverse factors, such as the concentration and spatial distribution of lindane in the soil or water matrix, the physicochemical properties of the soil or water, the prevailing temperature and pH conditions, and the co-existence of other contaminants. Physical remediation, such as soil vapor extraction (SVE), has been explored to remove lindane from contaminated soils with low moisture content. For instance, De Melo Henrique et al. (2022b) successfully removed lindane from contaminated soils using SVE technology, while their subsequent study showed that electrokinetic remediation (EKR) technology was also effective for this purpose (De Melo Henrique et al. 2022a). Also, Fraiese et al. (2020) found that ultrasonic treatment was capable of removing up to 96% of lindane from contaminated water.

In recent years, the field of chemical remediation also made significant advancements, leading to the development of innovative and effective methods for removing lindane. Begum et al. (2017) reported that Fenton's reagent could effectively degrade lindane from contaminated soil, while Khan et al. (2019) demonstrated the potential of using a combination of nanocrystalline $TiO_2$ and inorganic oxidants for the photocatalytic degradation of lindane. Metal-based reduction methods have also been studied to detoxify lindane by breaking down the chlorinated bonds and converting them into less harmful products. Zinc, iron, palladium, aluminum, platinum, nickel, and copper had all been investigated for this purpose, either as supported or unsupported catalysts in various reaction systems, such as aqueous, non-aqueous, or solid-state reactions (Adriano et al. 2004, Paknikar et al. 2005, Mertens et al. 2007, Joo & Zhao 2008, Nienow et al. 2008, Singh et al. 2011, Zhao et al. 2016, Jung et al. 2018, Suresh & Thangadurai 2019, Nguyen et al. 2020, Mar-Pineda et al. 2021). Studies have demonstrated the effectiveness of metal-based reduction methods for detoxifying various recalcitrant pesticides with high conversion rates and low toxicity of the reaction products. For example, Shih et al. (2011) studied the effectiveness of Pd/Fe bimetallic nanoparticles in reducing pentachlorophenol (PCP) in water. They found that the nanoparticles were more efficient than individual Pd or Fe nanoparticles. Mohammadi & Sheibani (2019) investigated the effectiveness of a Resin-Au-Pd nanocomposite as a bimetallic photocatalyst for degrading parathion pesticides under visible light. They found that the nanocomposite showed high photocatalytic activity. Ulucan-Altuntas & Debik (2020) compared the effectiveness of Fe/Pd bimetallic nanoparticles and nZVI in degrading DDT. They found that Fe/Pd bimetallic nanoparticles were more effective and proposed a degradation mechanism and pathways. The aforementioned studies underscore the potential of metal-based reduction techniques, specifically bimetallic nanoparticles, as a viable remediation technology for sites contaminated with lindane.

Biological degradation techniques represent a potent and eco-friendly approach to the removal of lindane contamination. This degradation process can be accomplished through multiple metabolic pathways, such as aerobic and anaerobic biodegradation, co-metabolism, and co-oxidation (Singh et al. 1999, Zhang et al. 2020). Numerous bacterial and fungal strains have demonstrated the potential to degrade lindane, such as *Sphingobium indicum* (Zheng et al. 2011), *Pseudomonas putida* (Lal et al. 2008, Jaiswal et al. 2023), *Bacillus subtilis* (Hossain et al. 2018), *Rhodococcus* sp. (Sahoo & Chaudhuri 2022), *Streptomyces* sp. (Benimeli et al. 2006), *Aspergillus niger* (Asemoloye et al. 2017), *Trichoderma viride* (Satish et al. 2017), *Phanerochaete chrysosporium* (Kennedy et al. 1990), and *Pleurotus*
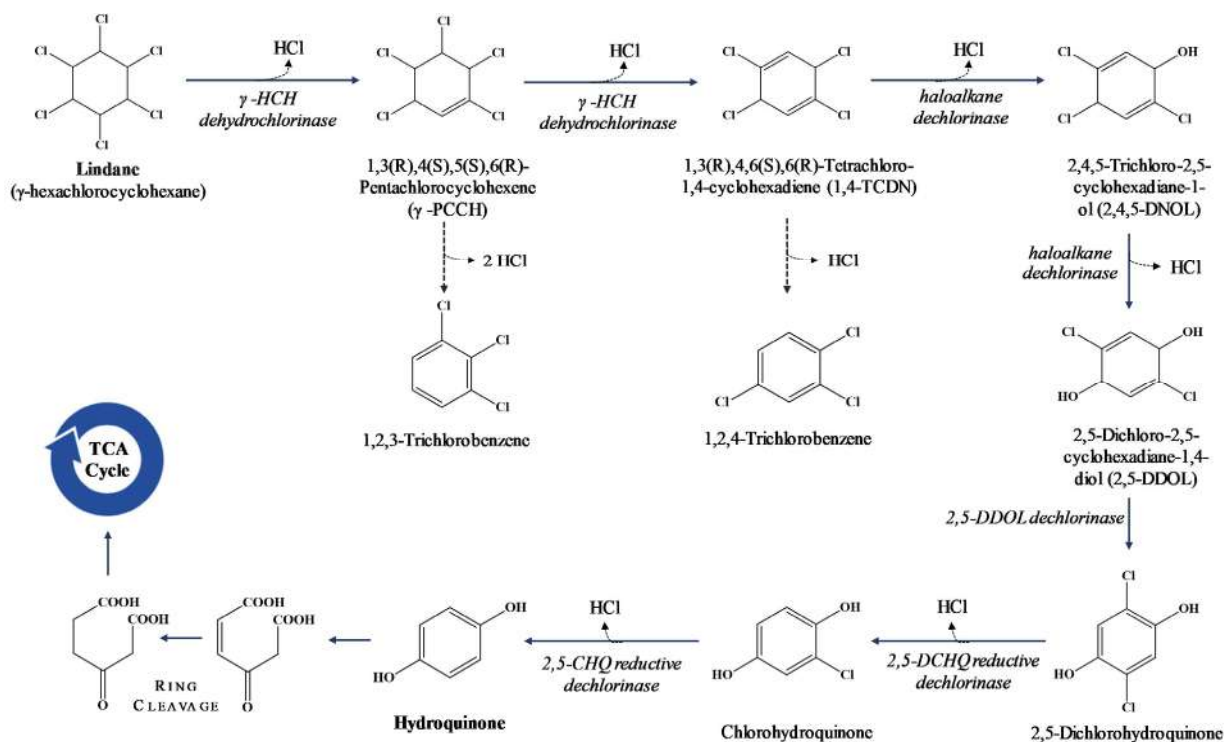
Fig. 1: Pathways involved in the biotransformation of lindane by microorganisms and associated enzymes.

*ostreatus* (Ulčnik et al. 2013). These microorganisms utilize lindane as a carbon source through the degradation pathway of enzymes, such as lindane dehydrochlorinase (Lal et al. 2008, Sowińska et al. 2018) and ligninolytic enzymes like lignin peroxidase manganese peroxidase, and laccase (Singh & Kuhad 2000, Rigas et al. 2005, Kaur et al. 2016, Zang et al. 2020). Microbial degradation of lindane typically proceeds through the formation of less toxic intermediates, namely pentachlorocyclohexene (PCCH), tetrachlorocyclohexene (TCCH), and trichlorobenzene (TCB), before reaching its ultimate degradation products such as $CO_2$. Enzymes crucial in this biodegradation process include dehydrochlorinase, γ-hexachlorocyclohexane dehydrochlorinase, and ligninolytic enzymes. Fig. 1 illustrates the metabolic pathways utilized by microorganisms for the biotransformation of lindane, along with the enzymes involved in the process. Utilizing bacteria and fungi for lindane bioremediation holds immense potential for restoring contaminated sites.

Although biological methods have proven effective in the detoxification of lindane, they are often slow and time-consuming. Conversely, chemical methods offer a more rapid solution but are costly and can lead to secondary pollution issues (Wacławek et al. 2019). In this context, due to their unique catalytic properties, bimetallic systems have emerged as an effective approach for the reductive transformation of persistent organic pollutants (POPs), such as lindane. In comparison to other chemical methods, bimetallic systems offer several advantages, including higher activity, selectivity, and stability. Bimetallic systems, which consist of two different metals on a single nanoparticle or supported catalyst, have been shown to facilitate electron transfer and enhance the surface area of the catalyst, resulting in faster reaction rates and increased efficiency. Several studies have reported successful reductive transformation of chlorinated pesticides using bimetallic systems. For example, researchers have demonstrated that magnesium-palladium bimetallic nanoparticles effectively degraded endosulfan in an aqueous solution with a high reaction rate and low energy consumption (Thangadurai & Suresh 2013).

Similarly, Nagpal et al. (2010) reported that bimetallic nanoparticles consisting of iron and palladium could degrade lindane more efficiently than individual Fe or Pd nanoparticles. Such findings indicate that bimetallic methods are a promising, cost-effective, and efficient remediation technology for treating contaminated water. Therefore, the present investigation aims to: (a) evaluate the feasibility of bimetallic systems for the reductive transformation of lindane and (b) evaluate the bacterial detoxification of lindane.

## MATERIALS AND METHODS

### Media and Chemicals

Lindane (AS, isomers ($\alpha$:$\beta$:$\gamma$:$\delta$=1:1:1:1)) was purchased from Sigma, Missouri, USA. Hexane, cyclohexane, beef extract, peptone, sodium chloride, and acetone were purchased from Merck Ltd. MSM (mineral salts medium) contained 1.5 g.L$^{-1}$ KH$_2$PO$_4$, 3.5 gL$^{-1}$ K$_2$HPO$_4$, 0.03 g.L$^{-1}$ Fe$_2$(SO$_4$)$_3$ 7H$_2$O, 0.27 g.L$^{-1}$ MgSO$_4$, 1.0 g.L$^{-1}$ NH$_4$Cl, and 0.03 g.L$^{-1}$ CaCl$_2$ and 1 mL of a solution that contained trace elements (TE). The TE stock solution had 0.136 mg.L$^{-1}$ ZnCl$_2$, 0.198 mg.L$^{-1}$ MnCl$_2$ 4H$_2$O, 0.18 mg.L$^{-1}$ CuCl$_2$.2H$_2$O, 0.025 mg.L$^{-1}$ NiCl$_2$ 6H$_2$O and 0.025 mg.L$^{-1}$ CoCl$_2$.6H$_2$O (Thangadurai & Suresh 2014). To prepare solid plates (media), agar powder was added to the aforementioned MSM at a concentration of 1.5% (w/v).

### Chemical Detoxification of Lindane Using a Bimetallic System

The experiment involved studying the reaction between Lindane and Pd°-Charcoal in a 100 mL reaction mixture, where the concentration of lindane was maintained at 100 mg.L$^{-1}$, and the concentration of Pd°-Charcoal was varied. The reactions were carried out using different amounts of palladium, ranging from 1.0 to 3.0 mg.100 mL$^{-1}$ of the reaction mixture. To initiate the reaction, 5 mg.mL$^{-1}$ of magnesium was added, and protons were provided by adding 60 µL of acetic acid to enable the corrosion of the base metal. Samples were withdrawn at different time points ranging from 0 to 30 min, and aliquots of 2 mL were taken for analysis. To perform GC-ECD analysis of lindane isomers, we used a 30 m × 0.25 mm i.d., 0.25 µm film thickness, nonpolar DB-5MS column. The injector temperature was set at 250°C, and the injection volume was 1 µL in split-less mode. The initial oven temperature was maintained at 60°C for 2 min, then ramped to 280°C at a rate of 20°C/min and held for 5 min. He (carrier gas) was used at a 1 mL.min$^{-1}$ flow rate. The electron capture detector (ECD) was operated at a temperature of 300°C with a make-up gas flow rate of 30 mL.min$^{-1}$ and a voltage of 300 V. Prior to analysis, the samples (2 mL) were extracted using a mixture of cyclohexane and acetone (3:1, v/v) and then cleaned up using solid phase extraction (SPE) with a Florisil cartridge. 0.2 µL of the pooled extracts were injected into GC-ECD to analyze residual lindane and other metabolites released during the reaction.

### Isolation of Lindane Degrading Bacteria

The isolation of bacterial strains from soil that degrade lindane specifically was performed following a rigorous protocol. Soil samples were collected from Padre village, Kerala, India, an area with a history of pesticide(s) exposure. Sampling was done by removing the top soil layer around the root zone of cashew plants. Multiple samples were combined to form a representative sample, which was transported in sterile plastic bags and stored at 4°C until processing. An enrichment culture was established using a mineral salt medium with lindane as the only carbon and energy source. Dilution and plating methods were utilized to isolate bacterial strains capable of utilizing lindane as their sole carbon and energy source. The isolated strains were then screened for their ability to degrade lindane by inoculating them into liquid media containing lindane (100 mg.L$^{-1}$) as the C source. Samples were taken at regular intervals and analyzed for lindane degradation using GC-ECD. Bacterial strains that showed significant lindane degradation were further characterized using molecular techniques such as 16s rDNA sequencing to identify the strain.

### Identification of Isolated Bacterium Using 16S r-DNA Analysis

Bangalore Genei, India, performed the 16s rDNA analysis of an isolated bacterium. The genomic DNA from the bacterial cells was isolated and purified using commercially available DNA extraction kits. The 16s rDNA gene was amplified using universal primers, and the PCR products were purified and subjected to Sanger sequencing. BLAST and NCBI GenBank were used to analyze the obtained sequences and identify the closest bacterial species. Multiple sequence alignments were performed to compare the obtained sequence with publicly available reference sequences. Phylogenetic analysis was conducted using software (MEGA 3.1) to construct a phylogenetic tree. Finally, the identity of the unknown bacterium was determined based on the results of the 16s rDNA analysis.

### Biological Degradation of Lindane Using a Bacterial Isolate

To investigate the kinetics of *Acinetobacter* sp., flasks containing sterile MSM were spiked with lindane to attain a final concentration of 100 mg.L$^{-1}$. The flasks were inoculated with 2 mL of *Acinetobacter*, which had been grown to an optical density of 0.2 at 600 nm and was subsequently placed in an orbital shaker and incubated at 30°C while agitated at a speed of 150 rpm. Samples of 2 mL were collected from each flask at different time points between 0-30 h and were analyzed for residual Lindane and bacterial OD. The samples were clarified by centrifugation and then extracted thrice with hexane. Subsequently, 2 µL of the samples were injected into GC-ECD for analysis. The experiment was continued

until complete degradation of lindane was achieved or until a plateau was reached. The progress of the degradation was monitored by comparing the GC-ECD chromatograms of the samples with that of the initial sample.

## RESULTS AND DISCUSSION

**Synergistic Effect of Bimetallic Systems in Reductive Transformation of Lindane**

In Fig. 2(a), the time-dependent profiles illustrate the removal of lindane by a bimetallic system with the Pd-Charcoal (Pd-C) catalyst at different concentrations. It is worth noting that the removal efficiency of lindane increased in proportion to the concentration of the Pd-C catalyst. Specifically, at concentrations of 10 and 20 $mg.L^{-1}$ of Pd-C, the removal percentages were approximately 72.5% and 86.6%, respectively. Moreover, using 30 $mg.L^{-1}$ of Pd-C, >99% of the 100 $mg.L^{-1}$ initial lindane concentration was
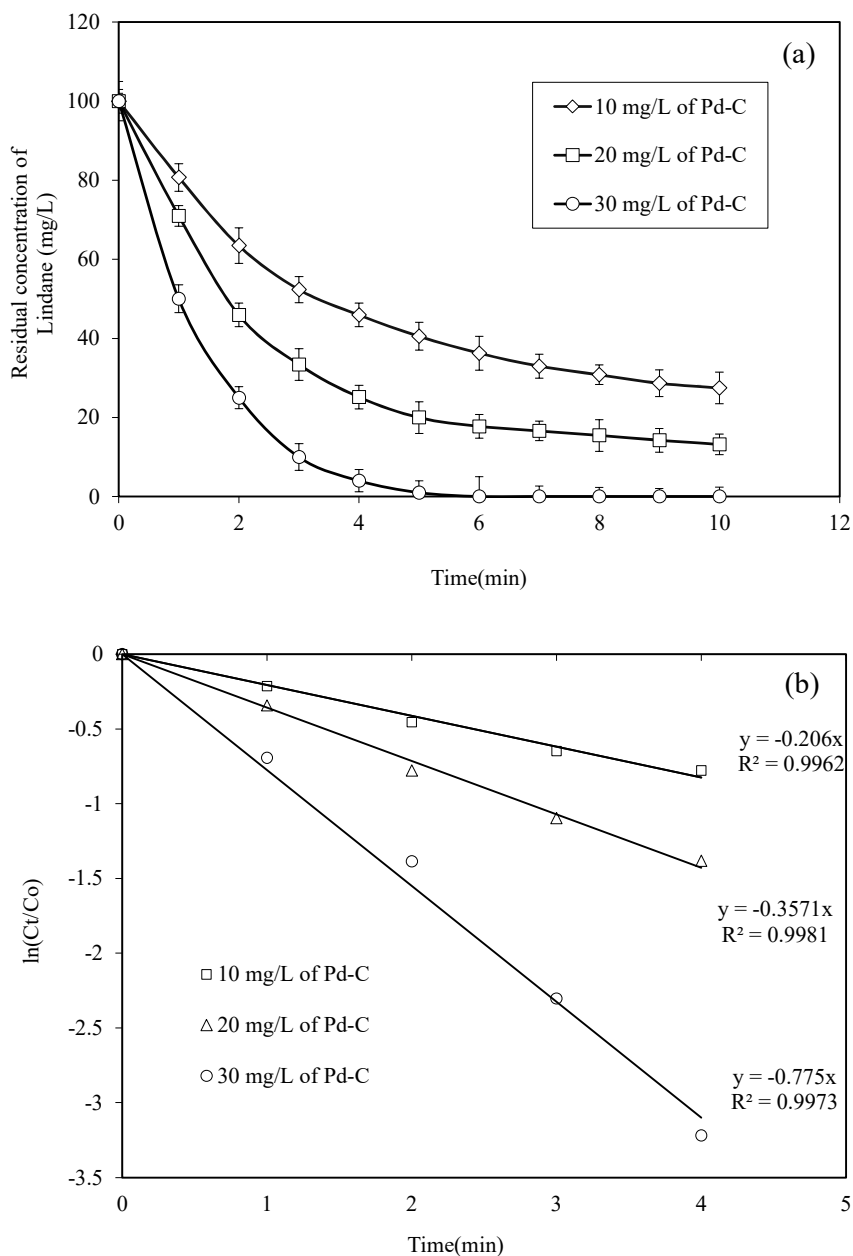


Fig. 2: (a) The time-dependent profiles illustrate the removal of lindane by a bimetallic system, with the Pd-Charcoal catalyst at different concentrations as labeled. (b) presents first-order kinetic plots that showcase the removal of lindane with different concentrations of Pd-Charcoal.
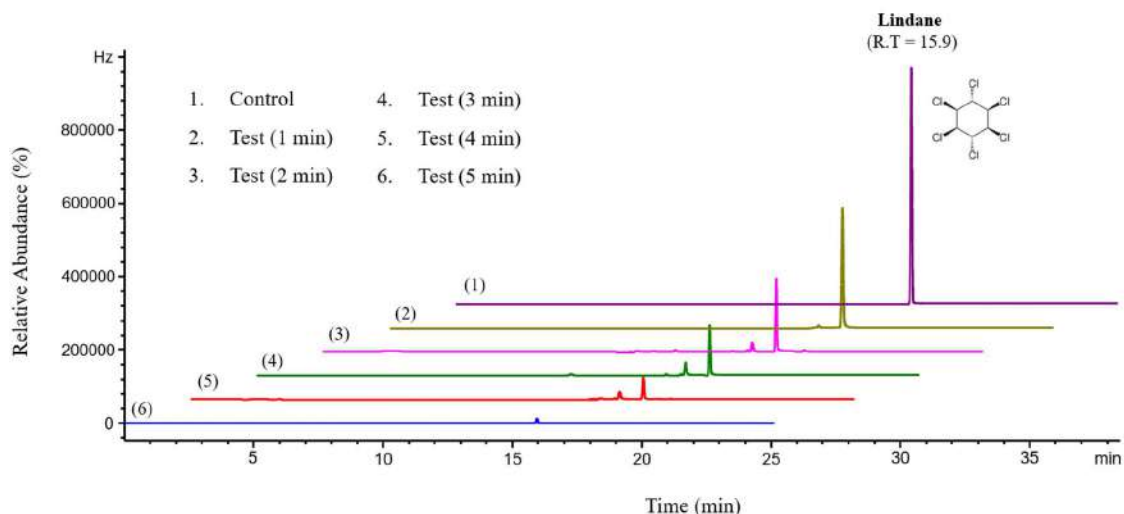
Fig. 3: Comparative analysis of GC-ECD chromatograms obtained at different time intervals for the detoxification of lindane.

removed after 10 minutes of reaction time. The initial phase of the reaction was particularly rapid, with nearly 80% of the lindane removed within 2 min of the reaction. The first-order kinetic plots presented in Fig. 2b demonstrate the removal of lindane using various concentrations of Pd-C, resulting in calculated $1^{st}$-order rate constants of 0.21 $min^{-1}$, 0.36 $min^{-1}$, and 0.77 $min^{-1}$, corresponding to the 10 20, and 30 $mg.L^{-1}$ Pd-C concentrations, respectively. The estimated $1^{st}$ order rate constant for lindane removal was calculated to be 0.77 $min^{-1}$. The GC-ECD chromatogram depicted in Fig. 3 shows successful baseline resolution of lindane at 15.9 min retention time (RT). The results highlight a clear trend, with the removal of lindane increasing over time, and corresponding partially transformed product(s) accumulating in the reaction medium at lower retention times, with the first eluting at 15.0 min. Within just 5 min of reaction, over 95% of lindane was rapidly removed. In the control experiment (using palladium and acetic acid but no magnesium), there was an insignificant change in the concentration of lindane after 15 minutes of reaction. Additionally, the control sample containing bimetals without acetic acid showed the removal of only 2% of lindane.

Various research studies have investigated the effectiveness of bimetallic systems in reducing chlorinated pesticides and pollutants. Graça et al. (2020) demonstrated that a Pd-Fe bimetallic system effectively reduced chlorpyrifos to less-toxic products, achieving complete removal within 30 min of reaction time. Similarly, Susha et al. (2012) found that a Pd-Ag bimetallic system efficiently reduced atrazine to less toxic products, achieving complete removal in only 2 h of reaction time. Venkateshaiah et al. (2022) showed that bimetallic zero-valent iron nanoparticles (BZNPs) were effective in degrading various chlorinated

organic compounds, with the Fe/Pd system displaying the highest degradation efficiency. Zhao et al. (2021) found that a bimetallic single-atom catalyst (SAC) comprising iron and palladium exhibited improved degradation efficiency for chlorinated pollutants compared to monometallic catalysts. Gunawardana et al. (2019) demonstrated that the addition of nickel coatings on zero-valent iron (ZVI) enhanced the dechlorination efficiency of pentachlorophenol (PCP), while the presence of oxygen hindered PCP dechlorination by ZVI. The various iron oxide phases present on the ZVI surface also played a crucial role in PCP dechlorination. Finally, Lokteva et al. (2023) examined the use of bimetallic Pd/Fe catalysts for the hydro dechlorination of diclofenac. They found that the choice of support material, metal deposition sequence, and reduction conditions significantly influenced the catalytic activity and selectivity of the Pd/Fe catalysts. A comparison of our results with the literature shows that the removal efficiency of lindane increases with increasing catalyst concentration and that the reaction is rapid initially.

Additionally, the estimated first-order rate constant for removing lindane is consistent with the rate constants reported in some of the other articles. The GC-ECD analysis also suggests that the reaction products are partially dechlorinated, a common observation in reducing chlorinated organic pollutants. While the specific catalysts and conditions used in this study differ from those in the other articles, the general trends and observations are consistent with the broader literature on bimetallic system-based reduction.

## Phylogenetic Identification of Bacterial Isolate Through 16S rDNA Analysis

Fig. 4 depicts a phylogenetic tree illustrating the evolutionary

relationship of lindane mineralizing bacterial isolate with other members of the *Acinetobacter* genus. This informative tree highlights the taxonomic position of the isolate and its genetic relatedness to other *Acinetobacter* species based on molecular markers such as 16S rRNA gene sequences. The analysis provides insights into the evolutionary history of the isolate and its potential ecological niche. It could contribute to our understanding of the diversity and biogeography of lindane-degrading bacteria in the environment. *Acinetobacter* is a genus of ubiquitous bacteria commonly found in various environments, including soil. Research has demonstrated that *Acinetobacter* species present in soil have numerous beneficial properties, such as plant growth promotion, bioremediation of pollutants, and biodegradation of organic compounds. For instance, Cai et al. (2021) found that *Acinetobacter* isolates from contaminated oil sludge efficiently bioremediate petroleum hydrocarbons. Furthermore, Kang (2009) demonstrated that *Acinetobacter* can enhance plant growth and development. *Acinetobacter* has also been shown to be effective in the biodegradation of pesticides and other organic pollutants, as demonstrated by Silambarasan and Vangnai (2016) and Chaudhry and Chapalamadugu (1991). Additionally, *Acinetobacter* species produce various enzymes, such as chitinase, cellulase, and protease, which have potential applications in bioremediation and other biotechnological processes (Poomai et al. 2014, Ranganath et al. 2016, Muhammed et al. 2021, Akram et al. 2022). Collectively, these studies highlight the promising potential of *Acinetobacter* in various environmental and biotechnological applications.

## Biodegradation of Lindane Using *Acinetobacter*

The bacterial culture was cultivated in a mineral salt medium (MSM) supplemented with 100 mg.L$^{-1}$ of Lindane, and the biodegradation profile was then closely monitored.

Fig. 5 depicts the growth profile of *Acinetobacter* sp., which showed a consistent rise in cell density over time. The rate of lindane degradation was initially slow until 6 h after inoculation, following which it increased rapidly. This observation is consistent with the process of bacterial acclimation to the presence of a high concentration of lindane, which is an essential prerequisite for initiating the process of biodegradation. After 30 h of bacterial growth, the concentration of lindane decreased from 100 mg.L$^{-1}$ to >1 mg.L$^{-1}$, resulting in an almost 99% reduction. The kinetics of lindane biodegradation were evaluated, and the results showed that the process followed 1$^{st}$ order kinetics, with a calculated rate constant of 0.12 h$^{-1}$. This observation implies that the rate of lindane degradation is proportional to the concentration of lindane in the medium and decreases exponentially over time. The GC-ECD analysis confirmed the complete degradation of Lindane by *Acinetobacter* sp. without the presence of any toxic intermediates or metabolites. This observation strongly suggests that the biodegradation pathway involves the complete mineralization of lindane into simpler compounds that can be efficiently utilized as a source of energy and carbon by the bacterial species. The absence of toxic intermediates or metabolites further supports the potential application of *Acinetobacter* sp. as a promising bioremediation agent. It is also important to note that the toxicity of lindane to root-associated bacteria, which perform vital ecosystem functions like nutrient cycling, nitrogen fixation, and plant growth promotion, is a significant concern. Thus, the ability of *Acinetobacter* sp., a rhizosphere resident, to degrade lindane is of great ecological significance. This claim is supported by the empirical data in Fig. 5, which provides compelling evidence of the bacterium's ability to degrade lindane. Consequently, *Acinetobacter* sp. has immense potential as a bio-augmenting agent for remediating sites contaminated with lindane,
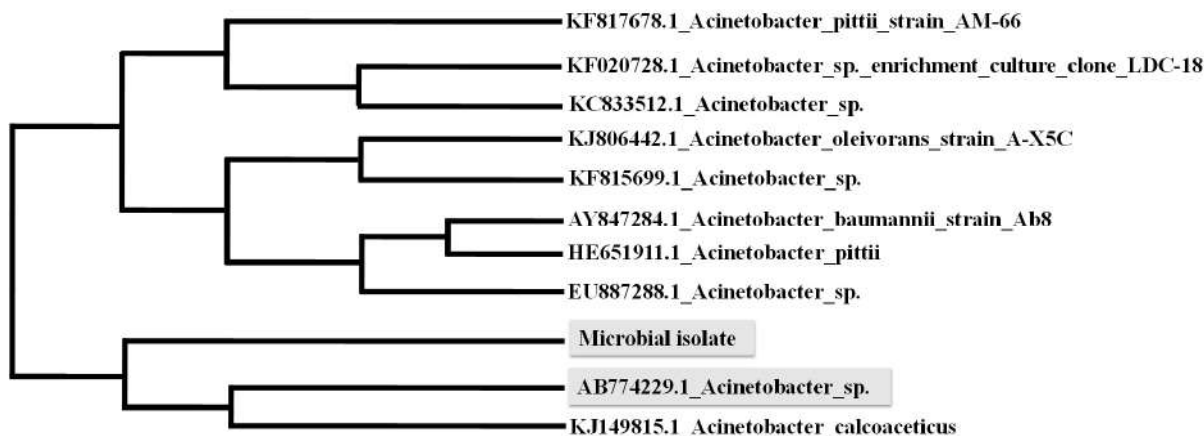


Fig. 4: Phylogenetic tree showing the relationship of lindane mineralizing bacterial isolate to other *Acinetobacter* species.
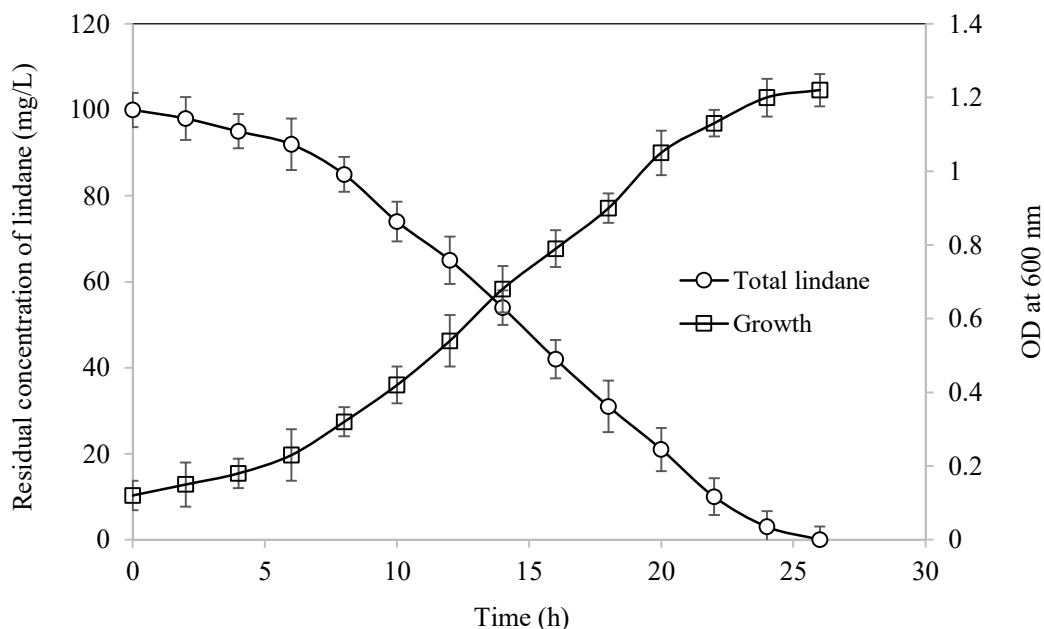
Fig. 5: Growth profile of *Acinetobacter sp*. in MSM containing 100 mg L-1 of Lindane and corresponding biodegradation profile.

making it a valuable tool for environmental restoration efforts.

The degradation of organochlorine pesticides by microorganisms is a burgeoning research area, and one group of microorganisms that shows great promise in this regard is *Acinetobacter*, which has a well-established ability to degrade diverse organic compounds. Numerous studies have explored the potential of *Acinetobacter* in biodegrading pesticides and other organic pollutants. For example, Ozdal and Algur (2022) isolated *Acinetobacter schindleri* B7 from a grasshopper species and found that it was able to degrade α-endosulfan and α-cypermethrin pesticides. Kumar et al. (2021) investigated the degradation of profenofos by *Acinetobacter* sp.33F and developed mathematical models to predict the degradation kinetics. Zhan et al. (2018) investigated the degradation of permethrin by *Acinetobacter baumannii* zh-14 and identified a novel degradation pathway. Jiang et al. (2018) studied the co-biodegradation of pyrene and other polycyclic aromatic hydrocarbons (PAHs) by *Acinetobacter johnsonii*, while Chen et al. (2018) examined the biodegradation and metabolic mechanism of cyprodinil by *Acinetobacter* sp. isolated from contaminated agricultural soil. Finally, Wu et al. (2022) isolated and characterized *Acinetobacter* sp. ZX01, which was able to efficiently degrade cyromazine. Recently, Li et al. (2022) investigated the biodegradation of dibutyl phthalate (DBP) by a newly isolated *Acinetobacter baumannii* DP-2 and found that it could degrade DBP and

identify its metabolites. *Acinetobacter* strains have been found to effectively degrade various POPs, including HCH, dioxins, PCBs, PCP, chlorpyrifos, PAHs, and benzo[a] pyrene, by producing specific enzymes. These findings suggest that *Acinetobacter* is potentially a valuable tool for bioremediation in contaminated environments. Nonetheless, further research is needed to optimize *Acinetobacter* growth conditions and activity across different contaminated environments to guarantee the successful application of this bacterium in bioremediation.

## CONCLUSIONS

Overall, this research highlights the effectiveness of bimetallic systems in reducing lindane contamination. Despite the cost implications of using palladium, the reuse of palladium immobilized on carbon offers potential economic benefits. In addition to their higher efficiency, bimetallic systems produce fewer harmful by-products than traditional treatment methods. The flexibility of the bimetallic systems to optimize various parameters also increases their potential for maximum degradation efficiency. However, further research is necessary to optimize the bimetallic system-based approach for lindane removal, particularly under varying environmental conditions. The biodegradation studies conducted in this research demonstrate that Acinetobacter sp. can be a highly effective biocatalyst for lindane remediation, with a removal rate of >99%. Further research is needed to optimize conditions for its growth and evaluate its efficacy

in large-scale bioremediation applications. Overall, this study provides valuable insights into the potential application of bimetallic systems and biocatalysts for the remediation of environmental lindane contamination.

## REFERENCES

Adriano, D.C., Wenzel, W.W., Vangronsveld, J. and Bolan, N.S. 2004. Role of assisted natural remediation in environmental cleanup. Geoderma, 122(2-4): 121-142.

Akram, F., Haq, I.U., Roohi, A. and Akram, R. 2022. *Acinetobacter indicus* ccs-12: A new bacterial source for the production and biochemical characterization of thermostable chitinase with promising antifungal activity. Waste Biomass Valor., 13(7): 3371-3388.

Alavanja, M.C.R. and Bonner, M.R. 2012. Occupational pesticide exposures and cancer risk: A review. J. Toxicol. Environ. Health, Part B, 15(4): 238-263.

Alsen, M., Vasan, V., Genden, E.M., Sinclair, C. and Van Gerwen, M. 2022. Correlation between lindane use and the incidence of thyroid cancer in the United States: An ecological study. Int. J. Environ. Res. Public Health, 19(20): 13158.

Asemoloye, M.D., Ahmad, R. and Jonathan, S.G. 2017. Synergistic rhizosphere degradation of γ-hexachlorocyclohexane (Lindane) through the combinatorial plant-fungal action. PLOS ONE, 12(8): e0183373.

Begum, A., Agnihotri, P., Mahindrakar, A.B. and Gautam, S.K. 2017. Degradation of endosulfan and lindane using Fenton's reagent. Appl. Water Sci., 7(1): 207-215.

Benimeli, C.S., Castro, G.R., Chaile, A.P. and Amoroso, M.J. 2006. Lindane removal induction by Streptomyces sp. M7. J. Basic Microbiol., 46(5): 348-357.

Cai, Y., Wang, R., Rao, P., Wu, B., Yan, L., Hu, L., Park, S., Ryu, M. and Zhou, X. 2021. Bioremediation of petroleum hydrocarbons using Acinetobacter sp. Scyy-5 isolated from contaminated oil sludge: Strategy and effectiveness study. Int. J. Environ. Res. Pub Health, 18(2): 819.

Chaudhry, G.R. and Chapalamadugu, S. 1991. Biodegradation of halogenated organic compound'. Microbiol. Rev., 55(1): 59-79.

Chen, X., He, S., Liu, X. and Hu, J. 2018. Biodegradation and metabolic mechanism of cyprodinil by strain Acinetobacter sp. From a contaminated-agricultural soil in China. Ecotoxicol. Environ. Saf., 159: 190-197.

De Melo Henrique, J.M., Isidro, J., Saez, C., Dos Santos, E.V. and Rodrigo, M.A. 2022a. Removal of Lindane using electrokinetic soil flushing coupled with air stripping. J. Appl. Electrochem., 52(9): 1317-1326.

De Melo Henrique, J., Isidro, J., Sáez, C., López-Vizcaíno, R., Yustres, A., Navarro, V., Dos Santos, E.V. and Rodrigo, M.A. 2022b. Enhancing soil vapor extraction with EKSF for the removal of HCHs. Chemosphere, 296: 134052.

Diop, A., Diop, Y.M., Sarr, S.O., Ndiaye, B., Gueye, R., Thiam, K., Cazier, F. and Delattre, F. 2019. Pesticide contamination of soil and groundwater in the vulnerable agricultural zone of the Niayes (Dakar, Senegal). Anal. Chem. Lett., 9(2): 168-181.

Etterson, M.A. and Bennett, R.S. 2013. Quantifying the effects of pesticide exposure on annual reproductive success of birds: Pesticide effects on avian reproductive success. Integr. Environ. Assess. Manage., 9(4): 590-99.

Fraiese, A., Cesaro, A., Belgiorno, V., Sanromán, M.A., Pazos, M. and Naddeo, V. 2020. Ultrasonic processes for the advanced remediation of contaminated sediments. Ultrason. Sonochem., 67: 105171.

Golfinopoulos, S.K., Nikolaou, A.D., Kostopoulou, M.N., Xilourgidis, N.K., Vagi, M.C. and Lekkas, D.T. 2003. Organochlorine pesticides in the surface waters of Northern Greece. Chemosphere, 50(4): 507-516.

González-Mille, D.J., Ilizaliturri-Hernández, C.A., Espinosa-Reyes, G.,

Costilla-Salazar, R., Díaz-Barriga, F., Ize-Lema, I. and Mejía-Saavedra, J. 2010. Exposure to persistent organic pollutants (Pops) and DNA damage as an indicator of environmental stress in fish of different feeding habits of Coatzacoalcos, Veracruz, Mexico. Ecotoxicology, 19(7): 1238-1248.

Graça, C.A.L., Mendes, M.A., Teixeira, A.C.S.C. and Velosa, A.C.D. 2020. Anoxic degradation of chlorpyrifos by zero-valent monometallic and bimetallic particles in solution. Chemosphere, 244: 125461.

Gunawardana, B., Swedlund, P.J. and Singhal, N. 2019. Effect of O2, Ni0 coatings, and iron oxide phases on pentachlorophenol dechlorination by zero-valent iron. Environ. Sci. Pollut. Res., 26(27): 27687-27698.

Ozdal, O. and Algur, O.F. 2022. Biodegradation α-endosulfan and α-cypermethrin by *Acinetobacter schindleri* B7 isolated from the microflora of grasshopper (*Poecilimon tauricola*). Arch. Microbiol., 204(3): 159.

Hossain, M.S., Akhter, M.Z., Hossain, M.M., Shishir, M.A., Khan, S.N. and Hoq, M.M. 2018. Complete genome sequence of bacillus subtilis strain mh1, which has a high level of bacteriocin-like activity, isolated from soil in Bangladesh. Genome Announc., 6(25): e00516-18.

Islam, R. and Lynch, J.W. 2012. Mechanism of action of the insecticides, lindane, and fipronil, on glycine receptor chloride channels: Inhibition of glycine receptors by insecticides. Br. J. Pharmacol., 165(8): 2707-2720.

Jaiswal, S., Singh, D.K. and Shukla, P. 2023. Degradation effectiveness of hexachlorohexane (ϒ-hch) by bacterial isolate Bacillus cereus SJPS-2, its gene annotation for bioremediation and comparison with Pseudomonas putida KT2440. Environ. Pollut., 318: 120867.

Jayaraj, R., Megha, P. and Sreedev, P. 2016. Review Article. Organochlorine pesticides, their toxic effects on living organisms, and their fate in the environment. Interdiscip. Toxicol., 9(3-4): 90-100.

Jiang, Y., Zhang, Z. and Zhang, X. 2018. Co-biodegradation of pyrene and other PAHs by the bacterium Acinetobacter johnsonii. Ecotoxicol. Environ. Saf., 163: 465-470.

Joo, S.H. and Zhao, D. 2008. Destruction of lindane and atrazine using stabilized iron nanoparticles under aerobic and anaerobic conditions: Effects of catalyst and stabilizer. Chemosphere, 70(3): 418-25.

Jung, H.J., Koutavarapu, R., Lee, S., Kim, J.H., Choi, H.C. and Choi, M.Y. 2018. Enhanced photocatalytic degradation of lindane using metal-semiconductor Zn@ZnO and ZnO/Ag nanostructures. J. Environ. Sci., 74: 107-115.

Kang, S.M., Joo, G.J., Hamayun, M., Na, C.I., Shin, D.H., Kim, H.Y., Hong, J.K. and Lee, I.J. 2009. Gibberellin production and phosphate solubilization by newly isolated strain of *Acinetobacter calcoaceticus* and its effect on plant growth. Biotechnol. Lett., 31(2): 277-281.

Katagi, T. and Fujisawa, T. 2021. Acute toxicity and metabolism of pesticides in birds. J. Pestic. Sci., 46(4): 305-321.

Kaur, H., Kapoor, S. and Kaur, G. 2016. Application of ligninolytic potentials of a white-rot fungus *Ganoderma lucidum* for degradation of lindane. Environ. Monit. Assess., 188(10): 588.

Kennedy, D.W., Aust, S.D. and Bumpus, J.A. 1990. Comparative biodegradation of alkyl halide insecticides by the white rot fungus, *Phanerochaete chrysosporium* (BKM-F-1767). Appl. Environ. Microbiol., 56(8): 2347-2353.

Khan, S., Han, C., Sayed, M., Sohail, M., Jan, S., Sultana, S., Khan, H.M. and Dionysiou, D.D. 2019. Exhaustive photocatalytic lindane degradation by combined simulated solar light-activated nanocrystalline tio2 and inorganic oxidants. Catalysts, 9(5): 425.

Kumar, V., Sharma, N. and Vangnai, A. 2021. Modeling degradation kinetics of profenofos using *Acinetobacter* sp.33F. Environ. Technol. Innov., 21: 101367.

Lal, R., Dadhwal, M., Kumari, K., Sharma, P., Singh, A., Kumari, H., Jit, S., Gupta, S.K., Nigam, A., Lal, D., Verma, M., Kaur, J., Bala, K. and Jindal, S. 2008. *Pseudomonas* sp. to *Sphingobium indicum*: A journey of microbial degradation and bioremediation of Hexachlorocyclohexane. Indian J. Microbiol., 48(1): 3-18.

Li, C., Liu, C., Li, R., Liu, Y., Xie, J. and Li, B. 2022. Biodegradation of dibutyl phthalate by the new strain *Acinetobacter baumannii* dp-2. Toxics, 10(9): 532.

Lokteva, E.S., Shishova, V.V., Maslakov, K.I., Golubina, E.V., Kharlanov, A.N., Rodin, I.A., Vokuev, M.F., Filimonov, D.S. and Tolkachev, N.N. 2023. Bimetallic PdFe catalysts in hydrodechlorination of diclofenac: Influence of support nature, metal deposition sequence, and reduction condition. Appl. Surf. Sci., 613: 156022.

Mar-Pineda, C.G., Poggi-Varaldo, H.M., Ponce-Noyola, M.T., Estrada-Bárcenas, D.A., Ríos-Leal, E., Esparza-García, F.J., Galíndez-Mayer, J. and Rinderknecht-Seijas, N.F. 2021. Effect of zero-valent iron nanoparticles on the remediation of a clayish soil contaminated with γ-hexachlorocyclohexane (Lindane) in a bioelectrochemical slurry reactor. Can. J. Chem. Eng., 99(4): 915-931.

Mertens, B., Blothe, C., Windey, K., De Windt, W. and Verstraete, W. 2007. Biocatalytic dechlorination of lindane by nano-scale particles of Pd(0) deposited on *Shewanella oneidensis*. Chemosphere, 66(1): 99-105.

Mohammadi, P. and Sheibani, H. 2019. Evaluation of the bimetallic photocatalytic performance of Resin-Au-Pd nanocomposite for the degradation of parathion pesticide under visible light. Polyhedron, 170: 132-137.

Muhammed, N.S., Hussin, N., Lim, A.S., Jonet, M.A., Mohamad, S.E. and Jamaluddin, H. 2021. Recombinant production and characterization of an extracellular subtilisin-like serine protease from Acinetobacter baumannii of fermented food origin. Protein J., 40(3): 419-435.

Nagpal, V., Bokare, A.D., Chikate, R.C., Rode, C.V. and Paknikar, K.M. 2010. Reductive dechlorination of γ-hexachlorocyclohexane using Fe–Pd bimetallic nanoparticles. J. Hazard. Mater., 175(1-3): 680-687.

Nguyen, T.H., Nguyen, T.T.L., Pham, T.D. and Le, T.S. 2020. Removal of Lindane from aqueous solution using aluminum hydroxide nanoparticles with surface modification by anionic surfactant. Polymers, 12(4): 960.

Nienow, A.M., Bezares-Cruz, J.C., Poyer, I.C., Hua, I. and Jafvert, C.T. 2008. Hydrogen peroxide-assisted UV photodegradation of lindane. Chemosphere, 72(11): 1700-1705.

Paknikar, K.M., Nagpal, V., Pethkar, A.V. and Rajwade, J.M. 2005. Degradation of Lindane from aqueous solutions using iron sulfide nanoparticles stabilized by biopolymers. Sci. Technol. Adv. Mater., 6(3-4): 370-374.

Poomai, N., Siripornadulsil, W. and Siripornadulsil, S. 2014. Cellulase enzyme production from agricultural waste by Acinetobacter sp. Kku44. Adv. Mater. Res., 931-932: 1106-1110.

Ranganath, R. 2016. Antimicrobial sensitivity pattern of Acinetobacter species isolated from clinical specimens. Int. J. Curr. Microbiol. Appl. Sci., 5(12): 519-523.

Rigas, F., Dritsa, V., Marchant, R., Papadopoulou, K., Avramides, E.J. and Hatzianestis, I. 2005. Biodegradation of Lindane by *Pleurotus ostreatus* via central composite design. Environ. Int., 31(2): 191-196.

Sahoo, B. and Chaudhuri, S. 2022. Lindane removal in contaminated soil by defined microbial consortia and evaluation of its effectiveness by bioassays and cytotoxicity studies. Int. Microbiol., 25(2): 365-378.

Satish, G.P., Ashokrao, D.M. and Arun, S.K. 2017. Microbial degradation of pesticide: A review. Afr. J. Microbiol. Res., 11(24): 992-1012.

Shakur, A.M., Garba, N.A., Ahmadu, I., Apollos, D., Asani, M.O. and Aliyu, I. 2021. Accidental poisoning with aluminum phosphide presenting with excessive cholinergic symptoms with response to atropine: A case report. Avicenna J. Med., 11(01): 58-61.

Shih, Y., Chen, M.Y. and Su, Y.-F. 2011. Pentachlorophenol reduction by Pd/Fe bimetallic nanoparticles: Effects of copper, nickel, and ferric cations. Appl. Catal. B Environ., 105(1-2): 24-29.

Silambarasan, S. and Vangnai, A.S. 2016. Biodegradation of 4-nitroaniline by plant-growth-promoting Acinetobacter sp. AVLB2 and toxicological analysis of its biodegradation metabolites. J. Hazard. Mater., 302: 426-436.

Singh, B.K. and Kuhad, R.C. 2000. Degradation of insecticide Lindane (Γ-hch) by white-rot fungi Cyathus bulleri and *Phanerochaete sordida*. Pest Manag. Sci., 56(2): 142-146.

Singh, B.K., Kuhad, R.C., Singh, A., Lal, R. and Tripathi, K.K. 1999. Biochemical and molecular basis of pesticide degradation by microorganisms. Crit. Rev. Biotechnol., 19(3): 197-225.

Singh, R., Singh, A., Misra, V. and Singh, R.P. 2011. Degradation of Lindane contaminated soil using zero-valent iron nanoparticles. J. Biomed. Nanotechnol., 7(1): 175-176.

Sowińska, A., Vasquez, L., Żaczek, S., Manna, R.N., Tuñón, I. and Dybala-Defratyka, A. 2020. Seeking the source of catalytic efficiency of Lindane dehydrochlorinase, Lina. J. Phys. Chem. B, 124(46): 10353-10364.

Suresh, S. and Thangadurai, P. 2019. Coupling of zero-valent magnesium or magnesium-palladium-mediated reductive transformation to bacterial oxidation for the elimination of endosulfan. Int. J. Environ. Sci. Technol., 16(3): 1421-1432.

Thangadurai, P. and Suresh, S. 2013. Reductive transformation of endosulfan in the aqueous phase using magnesium-palladium bimetallic systems: A comparative study. J. Hazard. Mater., 246-247: 245-256.

Thangadurai, P. and Suresh, S. 2014. Biodegradation of endosulfan by soil bacterial cultures. Int. Biodeterior. Biodegrad., 94: 38-47.

Ulčnik, A., Kralj Cigić, I. and Pohleven, F. 2013. Degradation of Lindane and endosulfan by fungi, fungal, and bacterial laccases. World J. Microbiol. Biotechnol., 29(12): 2239-2247.

Ulucan-Altuntas, K. and Debik, E. 2020. Dechlorination of dichlorodiphenyltrichloroethane (DDT) by Fe/Pd bimetallic nanoparticles: Comparison with nZVI, degradation mechanism, and pathways. Front. Environ. Sci. Eng., 14(1): 17.

Venkateshaiah, A., Silvestri, D., Wacławek, S., Ramakrishnan, R.K., Krawczyk, K., Saravanan, P., Pawlyta, M., Padil, V.V.T., Černík, M. and Dionysiou, D.D. 2022. A comparative study of the degradation efficiency of chlorinated organic compounds by bimetallic zero-valent iron nanoparticles. Environ. Sci. Water Res. Technol., 8(1): 162-172.

Wacławek, S., Silvestri, D., Hrabák, P., Padil, V.V.T., Torres-Mendieta, R., Wacławek, M., Černík, M. and Dionysiou, D.D. 2019. Chemical oxidation and reduction of hexachlorocyclohexanes: A review. Water Res., 162: 302-319.

Waite, D.T., Hunter, F.G. and Wiens, B.J. 2005. Atmospheric transport of Lindane (Γ-hexachlorocyclohexane) from the Canadian prairies—A possible source for the Canadian Great Lakes, Arctic, and Rocky Mountains. Atmos. Environ., 39(2): 275-282.

Wu, Q., Li, F., Zhu, X., Ahn, Y. and Zhu, Y. 2022. Isolation and characterization of cyromazine degrading *Acinetobacter* sp. ZX01 from Chinese ginger cultivated soil. Environ. Sci. Pollut. Res., 29(45): 67765-67775.

Zhan, H., Wang, H., Liao, L., Feng, Y., Fan, X., Zhang, L. and Chen, S. 2018. Kinetics and novel degradation pathway of permethrin in *Acinetobacter baumannii* zh-14. Front. Microbiol., 9: 98.

Zhang, W., Lin, Z., Pang, S., Bhatt, P. and Chen, S. 2020. Insights into the biodegradation of Lindane (γ-hexachlorocyclohexane) using a microbial system. Front. Microbiol., 11: 522.

Zhao, K., Quan, X., Su, Y., Qin, X., Chen, S. and Yu, H. 2021. Enhanced chlorinated pollutant degradation by the synergistic effect between dechlorination and hydroxyl radical oxidation on a bimetallic single-atom catalyst. Environ. Sci. Technol., 55(20): 14194-14203.

Zhao, X., Liu, W., Cai, Z., Han, B., Qian, T. and Zhao, D. 2016. An overview of preparation and applications of stabilized zero-valent iron nanoparticles for soil and groundwater remediation. Water Res., 100: 245-266.

Zheng, G., Selvam, A. and Wong, J.W.C. 2011. Rapid degradation of Lindane (γ-hexachlorocyclohexane) at low temperature by Sphingobium strains. Int. Biodeterior. Biodegrad., 65(4): 612-618.

# Heavy Metal Contamination Assessment in Sediments, Soils and Surface Waters in Agriculture-Based Rural Chhattisgarh, India, and Evaluation of Irrigation Water Quality

**Manash Protim Baruah†\* , Subhajit Das\*, Monjil Rajkonwar\*\* and Mahesh Thirumala\***

*Geological Survey of India, State Unit-Chhattisgarh, Raipur, India
**Department of Applied Geology, Dibrugarh University, Assam, India
†Corresponding author: Manash Protim Baruah; manashprotim.baruah@gsi.gov.in

## ABSTRACT

Regional geochemical mapping was carried out in Bilaspur and Korba Districts of Chhattisgarh, and stream sediments/slope wash, soil, and water samples were analyzed for concentration of heavy metals. The study contributes to understanding heavy metals contamination of sediments, soils, and water due to anthropogenic activity, mainly in agriculture-based rural areas. The study reveals that high geochemical anomalies observed for heavy metals like Ni, Cr, As, and Zn in sediments and soil samples are due to the extensive uses of phosphatic fertilizer and soil amendments in the form of poultry and swine manure. Water quality assessment of major streams in the study areas shows that the water is suitable for domestic and agricultural uses. Correlation analysis reveals that the chemical weathering of rock-forming minerals doesn't control the surface water chemistry of the study area and is also an anthropogenic source of sodium in water. This study also shows the importance of the country's geochemical mapping database, which will have much broader applications than conventional mineral exploration and geological mapping.

## INTRODUCTION

Rapid urbanization, industrialization, and intensified agriculture in the recent past have increased undesirable environmental pollutants, including heavy metals. Increased concentrations of heavy metals, including Cr, Cu, Co, Cd, and Pb, in soils brought on by the use of agrochemicals and polluted irrigation water resulted in a decline in the health of the soil (Rayment et al. 2002, Kaur et al. 2014). Heavy metals are elements with metallic properties, a density of >5 g cm$^{-3}$, and an atomic mass of >20 (Bakshi et al. 2018). According to He et al. (2015), the most prevalent heavy metals in the environment include arsenic (As), cadmium (Cd), chromium (Cr), copper (Cu), mercury (Hg), lead (Pb), and zinc (Zn), among others. Heavy metal contamination of agricultural soils and crops is a concern because it could impact human health and the viability of food production systems in contaminated areas.

These metals persist in the environment for a very long time. Half-lives for Cu are 310-1500 years, for Zn are 70-510 years, for Cd are 13-1100 years, and for Pb are 740-5900 years (Iimura et al. 1977), whereas the estimated residence times (in years) of 75-380 for Cd, 500-1000 for

Hg and 1000-3000 for Cu, Ni, Pb and Zn under temperate climatic conditions (Kabata-Pendias 2011). Owing to their high residence periods, heavy metals tend to accumulate in soil and sediments and thus increase the toxic level of the biosphere (Chopra 2009). Heavy metals can be added to the environment through a variety of sources, which includes air that contains mining, smelting, and refining of fossil fuels; water having domestic sewage and industrial effluents; and soil like agricultural and animal wastes, municipal and industrial sewage, coal ashes, fertilizers, and pesticides. Heavy metal pollution often results in the degradation of soil health (Kools et al. 2005, Abdu et al. 2017), the contamination of surface and groundwater (Hashim et al. 2011, Mohankumar et al. 2016) and food chain pollution (Hapke 1996, Notten et al. 2005, Tchounwou et al. 2012), and consequently is a threat to human health (Pepper 2013, Jovanović et al. 2015, Oliver & Gregory 2015, Sarwar et al. 2017, Yang et al. 2017). Contrary to the pollution brought on by excessive levels of heavy metals in the soil, it has been documented in numerous regions of the world that agricultural lands are deficient in one or more micronutrients, including heavy metals/metalloids. This includes Cu, Mn, and Zn, which are essential for plants

and animals, and Co, Cr, and Se, which are necessary for animals.

Extensive studies of soil, stream sediment, and vegetation samples are done for mineral exploration due to the rising demand for metals and the need to find reserves for new ore minerals. Although originally developed for mineral exploration, stream sediment reconnaissance studies are particularly important for highlighting geochemical anomalies of importance to agriculture and showing regional soil pollution patterns. One such ambitious program launched by the Geological Survey of India, Ministry of Mines is the National Geochemical Mapping Program (NGCM) in 2001-2002. National Geochemical Mapping aims at mapping the country geochemically by sampling and analyses of stream sediment, soil, water, etc., intending to generate geochemical baseline data for multi-purpose uses like managing and developing natural resources, environmental management, agriculture, forestry, land use, and many aspects of human and animal health. As a part of this program, geochemical mapping was carried out for an area of 728 sq km in and around Kudri-Pasan in Bilaspur and Korba Districts of Chhattisgarh, India.

The study area falls in toposheet no.64J/01 and is bounded by latitudes 22°45' N to 23°00' N and longitudes 82°00' E to 82°15' E and forms parts of Bilaspur and Korba Districts of Chhattisgarh state (Fig. 1). Physiographically, the study area can be divided into three parts, viz. hilly terrain/dense forest, plantation/cultivated land and rivers/water bodies. The eastern part of the area has a rugged topography occupied by the sedimentary sequence of Lower Gondwana Formations. In contrast, the southwestern part is more or less a flat terrain with soil cover. The Sukhad and the Bamni nadi, along with
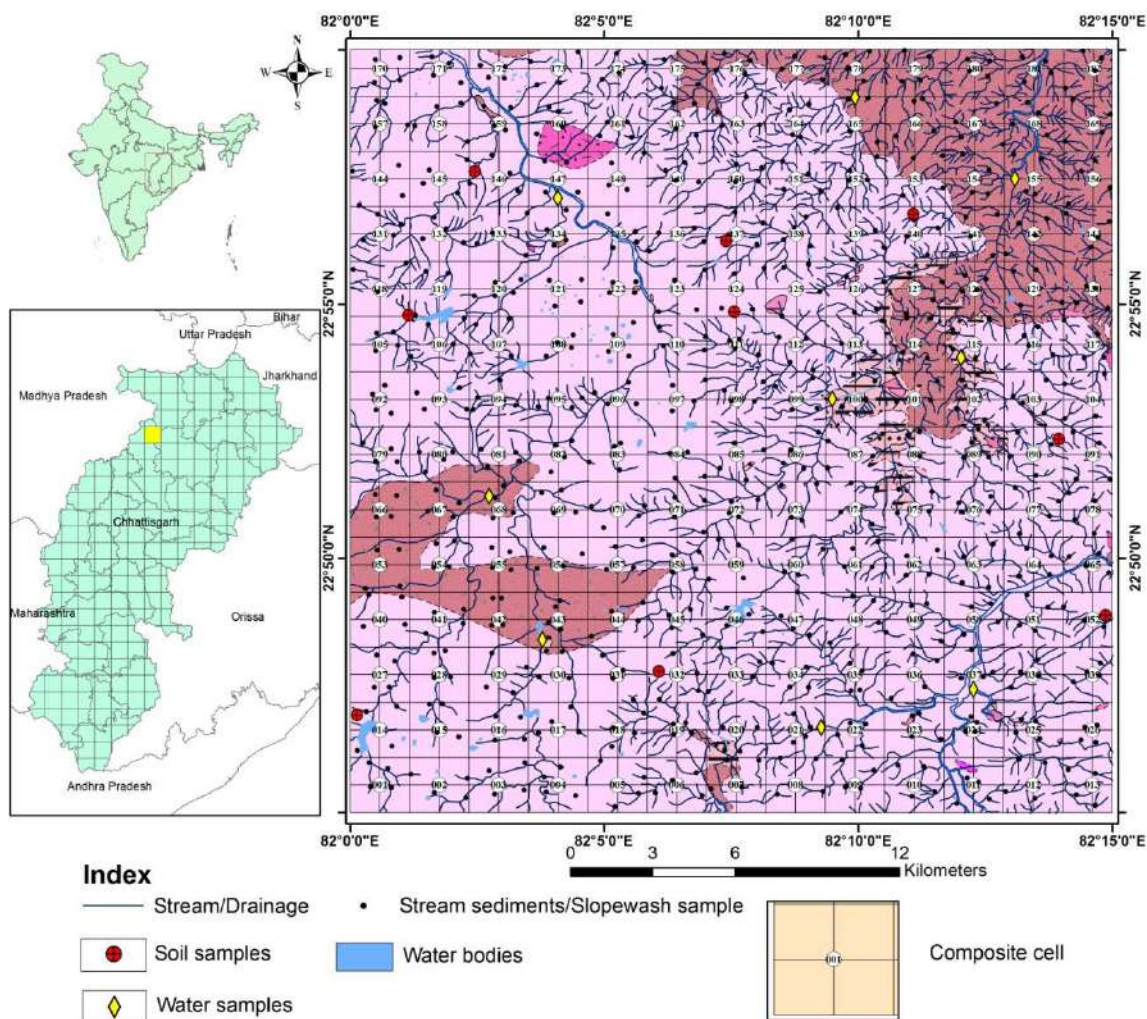


Fig. 1: Gridded geological map showing the location of the study area with stream sediments or slope wash, soil, and water sample location points.

their numerous tributaries, form the main drainage system in the eastern part of the area (Fig 1). The Son River drains the western part of the area. These are non-perennial streams; thus, rainfall is the main recharge source for surface and groundwater. The area receives an average annual rainfall of 1329 mm (CGWB 2013). The rainfall is mostly confined to July and September; the remaining months will be dry. Due to this reason, most of the agricultural activity in the low-lying cultivation areas largely depends upon the surface water sources. These agricultural lands comprised 40 to 50% of the present-day land use pattern in the area, as shown in Fig. 2. The remaining portions are occupied by forest cover (62%) and settlements and water bodies (6%).

The main objective of the present study is to assess the concentrations of heavy metals in the stream sediments and surface water bodies located in the study area, depth-wise geochemical characteristics and distribution of heavy metals in the soil profile, and finally, to assess the irrigation water quality of the surface water bodies present in the area.

## GEOLOGICAL SETTING

The area mainly forms part of the central Indian peninsular shield, exposes rocks of the Chhotanagpur gneissic complex, metasediments of the Bilaspur-Raigarh-Surguja Belt, and sedimentary sequences of the Lower Gondwana Group. Chhotanagpur gneissic complex (Peninsular Gneiss) of Archaean-Proterozoic age forms the basement in this area. This mainly consists of granite gneiss with its variant biotite gneiss, grey biotite hornblende gneiss, and porphyritic granite gneiss containing amphibolite enclaves. Granite gneiss are medium to coarse-grained, consisting of quartz, feldspar, and biotite, and are generally foliated. These rocks are traversed by basic dykes, pegmatite, and quartz veins. These gneisses are intruded by granite of various textural, mineralogical characters, such as massive porphyritic to coarse-grained and pink to grey. Granite is the most predominant rock type in the area. It is generally medium to coarse-grained, pink and grey, and composed essentially of quartz, potash feldspar, sodic plagioclase, and subordinate biotite. High muscovite-rich
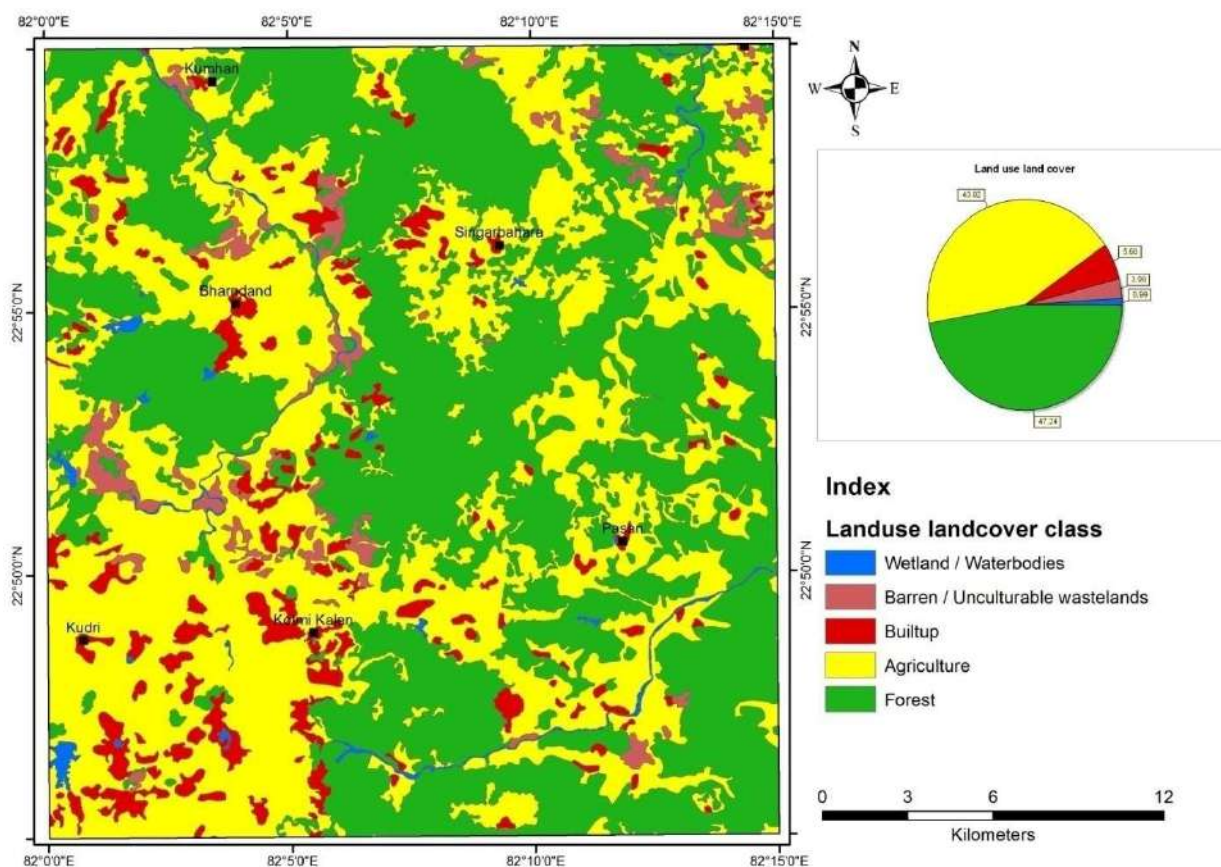


Fig. 2: Land-use land cover map of the study area.

granite is found in the southeastern part of the area, mainly south of Pasan. Muscovite, in association with biotite, occurs in granite in the northwestern part of the area.

The Bilaspur Raigarh Surguja belt (BRS) belt of Archaean-lower Proterozoic age overlying the Chotanagpur Gneissic Complex comprises low to medium-grade metasedimentary rocks, mainly phyllite, quartzite, calc gneiss, calc granulite, garnetiferous mica schist, quartz schist, mica schist, talc schist, biotite schist, marble, and amphibolite. Phyllite is fine-grained, buff, khaki green to green in color with distinct phyllitic sheen. In association with quartz chlorite-schist and quartzite, the phyllite is
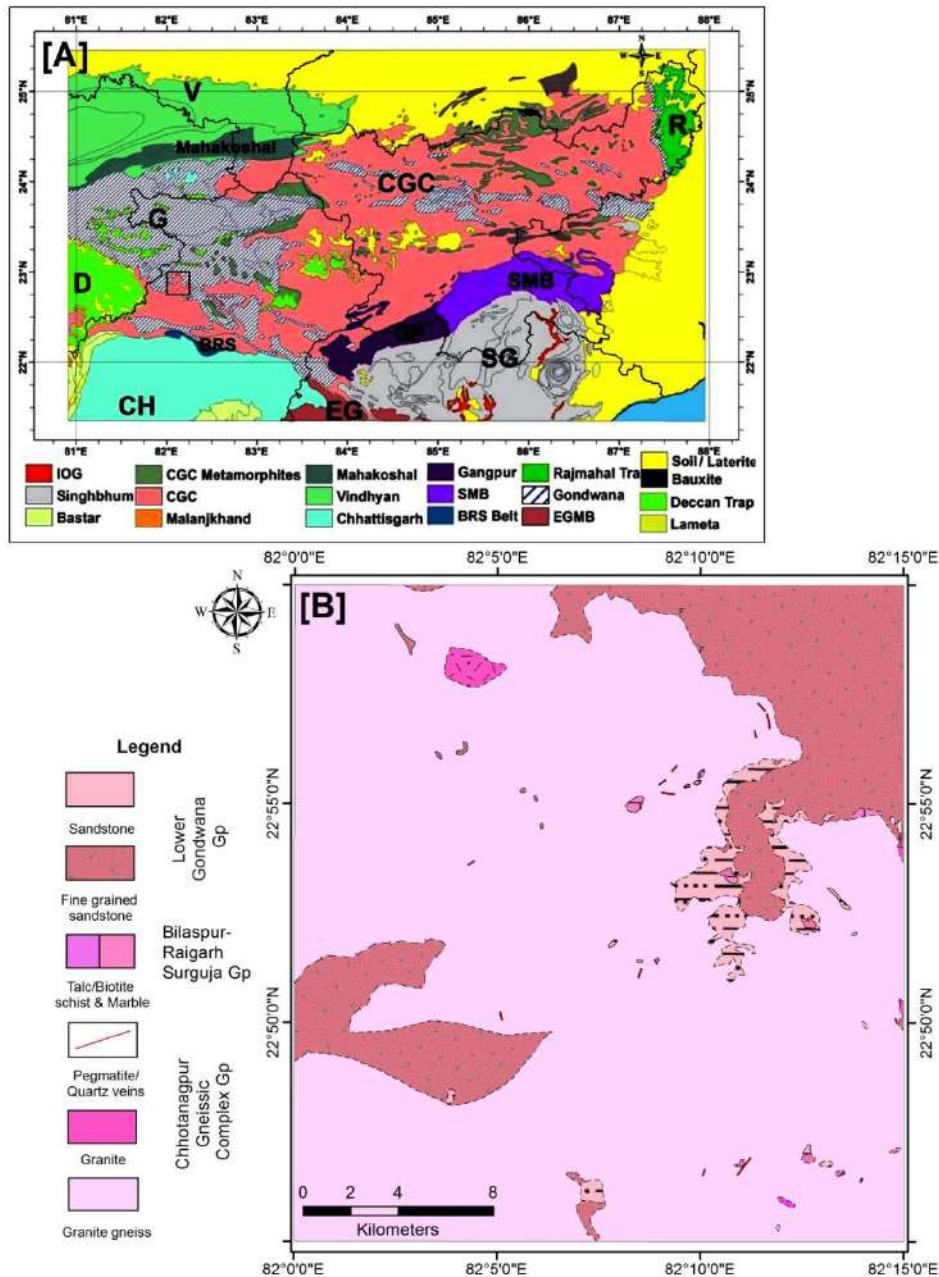


Fig. 3: (A) Regional geological map of Chotanagpur Granite Gneissic Complex (modified after Archaryya 2003, Maji et al. 2008) and (B) geological map of the area in toposheet no 64J/01 in parts of Bilaspur and Korba districts of Chhattisgarh.

seen gradually grading into biotite-gneiss. Quartz schist is fine to medium-grained, purple, and massive to schistose. Garnetiferous mica schists are greyish green to Khakhi grey in color and fine-grained with porphyroblasts of garnet. The mica schist is a fine to medium-grained, well-foliated rock comprising biotite, muscovite, quartz, and feldspars. Talc schist is greenish and fine-grained with a splintery character. The major mineral constituents are actinolite, tremolite, quartz, and plagioclase. Biotite schist consists essentially of quartz and biotite. Iron oxide and plagioclase occur as accessories. The marble is hard, compact, and massive, showing color and grain size variation. The marble is mostly serpentinised and contains tremolite needles in places. Amphilbolites are coarse-grained, dark grey, massive, hard, and non-foliated. The rock comprises hornblende, plagioclase, quartz, biotite, zircon, and opaques.

Talchir Formation of the Lower Gondwana Group tops the whole sequence. The rocks of Talchir formations exposed in the area are mainly conglomeratic bed, shale, and fine-grained sandstone units. It is observed in the northeastern portion of the area. The shales, at places, overlie directly on the granite of the Archean age. The shales are friable and purple, greenish grey and grey. Multiple joints traverse it. These joints have produced the feature of needle shale, where the rock has broken along joints into thin pencil-like prismatic fragments. At places, shales are interbedded with calcareous shale bands, usually less than 15 cm in thickness. The shales are overlain by sandstone. In places, sandstone is directly lying over the Archaean as an overlap. The sandstone is friable, fine to medium-grained, and is composed of quartz and feldspar. It is green, greenish yellow. Fig 3. B shows the detailed geological map of the area.
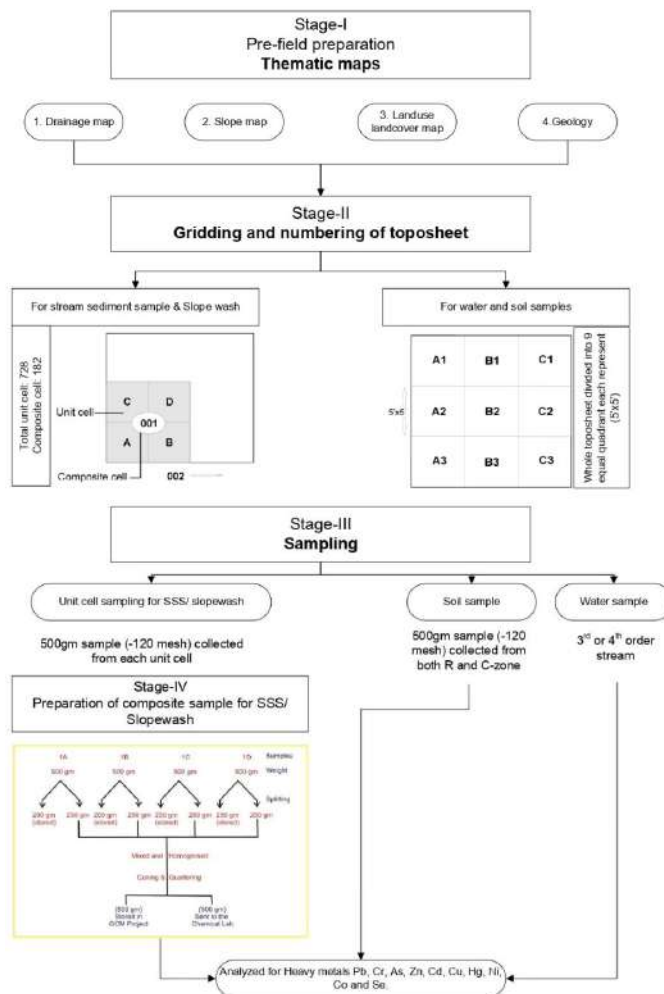


Fig. 4: Methodology flowchart showing different stages involved in geochemical mapping.

## MATERIALS AND METHODS

The methodology adopted to achieve the research objective begins with the preparation of different thematic maps such as a drainage map, slope, land-use land cover map, and detailed study of the area's geology. The drainage map on a 1:50,000 scale is divided into a small grid cell called the unit cell, each representing about 1 sq. km area, and tentative sample location points are placed in each small grid. It has been followed by collections of samples from each sq. km area in case of stream sediments and slope wash. For soil and water samples, the 728 sq. km area of the whole toposheet has been divided into 9 large squares having dimensions 9 km x 9 km, and samples have been collected from each of the 9 quadrants. The flow chart of the methodology followed has been illustrated in Fig. 4.

### Sampling and Preparation

Samples from different sampling media such as stream sediments/slope wash, regolith (R), and C-horizon of soil and stream water represent the most surface environment. For regional surveys, drainage sediment samples are an appropriate evaluation medium because they more accurately reflect the chemistry of a much larger area than soil samples (Appleton & Ridgway 1992). For the collection of stream sediment samples, the existing drainage in the toposheet 64J/01 has been digitized in a GIS environment and then divided in a 1 km×1 km cell grid (Fig. 1). A total of 728 nos. of samples has been collected from each grid which will represent an area of 1 sq. km. Samples were collected from each grid from the 1st and 2nd order channels. As these lower-order river-lets are non-perennial, most of the streams in plain areas don't have any water in flowing conditions, mainly during the post-monsoon season from September to March. Hence, most of the lower-order drainage in the area has been modified to agricultural land by the locals. At places where the streams are absent, samples have been collected from the slope wash based on the existing terrain gradient, representing the one sq. km area. Samples from four adjacent 1 km × 1 km cells have been mixed and homogenized through conning and quartering to make one composite sample (NGCM SOP 2011). 182 nos. of such composite samples were analyzed for heavy metal concentration in the area. Sample location points in the gridded drainage map superimposed on the geological map of the study area are shown in Fig. 1.

To assess the variation in heavy metal concentration in the uppermost layer of the earth's crust and to see its vertical distribution, soil samples have been collected from 9 different sites, each representing a grid of 9 × 9 km. In the vertical soil profile, samples have been collected from the topsoil/upper horizon (5-50 cm), referred to as Regolith (R), avoiding the top organic layer (0-5 cm). Samples are also being collected from the bottom C-horizon within a 50-200 cm depth range in each location. Comparison of a C-soil and regolith would give information about elemental behavior in weathering or pedogenic processes, environmental changes affecting the layers, and anthropogenic contamination of the top layer (R). Water sampling is done within the study area to study the interplay between the geosphere and hydrosphere. Nine water samples have been collected, representing the surface water quality. The surface water bodies in the area are the primary source of agricultural water available and are also occasionally used as drinking water in the area, directly affecting human health.

Each stream sediment/slope wash sample and the soil R- and C samples have been sun-dried, de-lumped with a wooden mortar and pestle, and finally sieved through 120 mesh size using a standard stainless steel sieve of ASTM standard. The sample was then conning and quartered, and 250 g samples were selected after homogenization following NGCM SOP 2011. These samples have been analyzed for heavy metal concentration through different analytical techniques.

All the samples were analyzed in the Geological Survey of India's laboratory at Chemical Division, Central Region, Nagpur, India. For stream sediments and soil samples, the heavy metals considered for the present investigation include Co, Cr, Cu, Ni, Pb, Zn, and Se, which are analyzed through XRF techniques; As through HG-AAS; Cd and Ag through GS-AAS and Hg through CV-AAS.

### Stream Sediment Samples and Analysis

The analytical results of heavy metals observed in the stream sediment samples were analyzed using basic statistics and spatial distribution maps. The elements considered for the present investigation are Pb, Cr, As, Zn, Cd, Cu, Hg, Ni, Co, and Se. Statistical methods were applied to comprehensively understand the elemental data set's concentrations, deviation, and distribution. The basic statistical parameters determined include mean, standard error, median, mode, standard deviation, sample variance, kurtosis, skewness, range, minimum, maximum, and count. Histograms for each element were also prepared to visualize the data distribution pattern and check for outliers. Elemental distribution maps are prepared using ArcGIS software, and the distribution pattern of each element represented by the contours is overlapped on the geological map of the area so that the anomaly zones can be easily interpreted in terms of the lithology.

### Soil Samples Analyses

A total of nine nos. of samples were collected from the area

such that each sample represents an area of 81 sq km so that a detailed representation of the nature and type of soil can be made. Two samples were taken from each location, one from the topsoil or Regolith/R-horizon (after removing the organic layer) and another from the bottom C-horizon. Both samples were analyzed for selective heavy metal concentrate as in the sediments/slope-wash sample case.

## Water Sample Analyses

Water samples have been collected from flowing streams to represent the elemental distribution of that particular drainage basin. 9 samples have been collected from the study area, as shown in Fig 1. Field measurements, including temperature (°C), electrical conductivity (EC), total dissolved solids (TDH), and pH, were carried out using standard field equipment. For IC ion analysis, five hundred milliliters of water samples were collected in a polyethylene bottle. The bottle was rinsed with sample water twice before filling it up by submerging it completely under water so that no air bubbles were left. Once the bottle is full, it has been closely tight below the water level.

To determine other heavy metals and trace elements through ICP-MS and ICP-AES analysis, another 100 mL filtered water sample was collected, and soon after collection, 1.0 mL of conc. $HNO_3$ has been added through a droplet bottle. The tightly closed bottle was shaken to mix the acid well with the sample water. TDS in the irrigation water was measured by weighting, the concentration of $Cl^-$ was measured by the colorimetric methods using a micro flux auto analyzer, the content of $SO_4^{2-}$ was determined by volume, the concentrations of $Mg^{2+}$, and $Ca^{2+}$ were dignified by the AAS, and the contents of $K^+$, $Na^+$ were determined by the flame emission spectroscopy, $HCO_3^-$, $CO_3^{2-}$. Alkalinity was determined by the acid titration method (NGCM SOP 2011).

The suitability of irrigation water was assessed using sodium adsorption ratio (Richards 1954), sodium percentage (Wilcox 1955), residual sodium bi-carbonate (Gupta & Gupta 1987), permeability index (Doneen 1964), magnesium hazard ratio (Paliwal 1972) and Kelley's ratio (Kelly 1963). They were computed using the following equations:

$$\text{Sodium Adsorption Ration (SAR)} = \frac{Na^+}{\sqrt{\frac{(Ca^{2+}+Mg^{2+})}{2}}}$$
$$\qquad\qquad\qquad …(1)$$

$$\text{Sodium percentage (Na\%)} = \frac{(Na^++K^+)\times100}{(Ca^{2+}+Mg^{2+}+Na^++K^+)}$$
$$\qquad\qquad\qquad …(2)$$

$$\text{Residual sodium bi} - \text{carbonate (RSBC)} = HCO3^- + Ca^{2+}$$
$$\qquad\qquad\qquad …(3)$$

$$\text{Permeability index (PI)} = \frac{Na^++\sqrt{HCO3^-}}{Ca^{2+}+Mg^{2+}+Na^+} \times 100$$
$$\qquad\qquad\qquad …(4)$$

$$\text{Magnesium hazard (MH)} = \frac{Mg^{2+}}{Ca^{2+}+Mg^{2+}} \times 100$$
$$\qquad\qquad\qquad …(5)$$

$$\text{Kelly index (KI)} = \frac{Na^+}{Ca^{2+}+Mg^{2+}}$$
$$\qquad\qquad\qquad …(6)$$

Where all ion concentrations are expressed in meq/L.

## RESULTS AND DISCUSSION

The details of the heavy metal concentrations observed in stream sediments and slope wash samples from the area are given in Table 1, with all the statistical parameters measured. The concentrations of heavy metals like Pb, Zn, Cu, and Co in stream sediments/slope-wash samples are observed to be higher than their upper continental crust (UCC) abundance. Other elements like Cr, Cd, Hg, Ni, and Se concentrations are below UCC value. Almost all the element's distributions are positively skewed, and apart from Cr, Ni, and Co, all have positive kurtosis. When compared with the globally acceptable permissible or critical limits of each element, it has been observed that the concentration of Pb, Cd, Cu, Hg, and Se is well within safe limits. Slightly higher concentrations are observed in Cr, As, Zn, and Co but not higher than the critical range. The Ni concentration in the area shows maximum values of 47.0 ppm, mainly in the southwestern part, and falls under a slight contamination range as per Alloway 1990.

The elemental distribution map for Ni has been superimposed over the geological map of the area (Fig. 5.viii) to observe any geogenic causes for these higher concentrations. Higher values of Ni with anomaly are present in and around Bharidand and south of Kodri village. The area is occupied by mainly granite gneiss of the Chhotanagpur Gneissic Complex. Cr values also show a slightly high concentration in these areas, mainly in the western part (Fig. 5.ii). High 'As' concentrations are observed in the southwestern part near Kudri village, similar to Ni (Fig. 5.iii). Similarly, Higher values of Cr with anomaly are present mainly north of Kodri and east of Bhaarridand village, where the litho unit is Granite gneiss of the CGC group. At the same time, Zn and Co show high concentration in Singarbahar, south of Kotmikalan, and near Pasan villages occupied by Granite gneiss (Fig. 5.iv & 5.ix).

Table 1: Values of statistical parameters calculated for different heavy metals (in ppm) in stream sediment samples and their permissible limits in soil.

| Elements | Statistical parameters | | | | | | | Permissible limits | Reference |
|---|---|---|---|---|---|---|---|---|---|
| | Maximum | Minimum | Mean | Skewness | Kurtosis | Threshold value | UCC abundance | | |
| Pb | 77.00 | 22.00 | 35.54 | 1.33 | 2.67 | 53.26 | 17.00 | 250-500 | Awasthi 2000 |
| Cr | 78.00 | 10.00 | 28.15 | 0.78 | -0.4 | 63.38 | 92.00 | 1-100 | Alloway 1990 |
| As | 11.21 | 1.00 | 4.50 | 0.72 | 0.28 | 9.09 | 9.00 | 0-30 | Alloway 1990 |
| Zn | 248.00 | 35.00 | 15.15 | 1.95 | 5.39 | 122.41 | 67.00 | 150-300 | Mushtaq & Khan 2010 |
| Cd | 0.137 | <0.1 | 0.053 | 4.38 | 18.03 | 0.08 | 0.09 | 1.0-3.0 | Mushtaq & Khan 2010 |
| Cu | 70.00 | 6.00 | 18.90 | 2.16 | 11.82 | 33.75 | 28.00 | 135-270 | Awasthi 2000 |
| Hg | 0.037 | <0.005 | 0.012 | 1.26 | 1.10 | 0.026 | 0.05 | 0-1 | Alloway 1990 |
| Ni | 47.00 | 5.00 | 20.71 | 0.73 | -0.01 | 38.57 | 47.00 | 0-20 | Alloway 1990 |
| Co | 26.00 | 8.00 | 15.28 | 0.30 | -0.46 | 23.07 | 17.30 | 1.0-40.0 | Alloway 1990 |
| Se | 0.82 | 0.10 | 0.30 | 0.61 | 0.75 | -0.02 | 0.90 | 0-1 | Alloway 1990 |
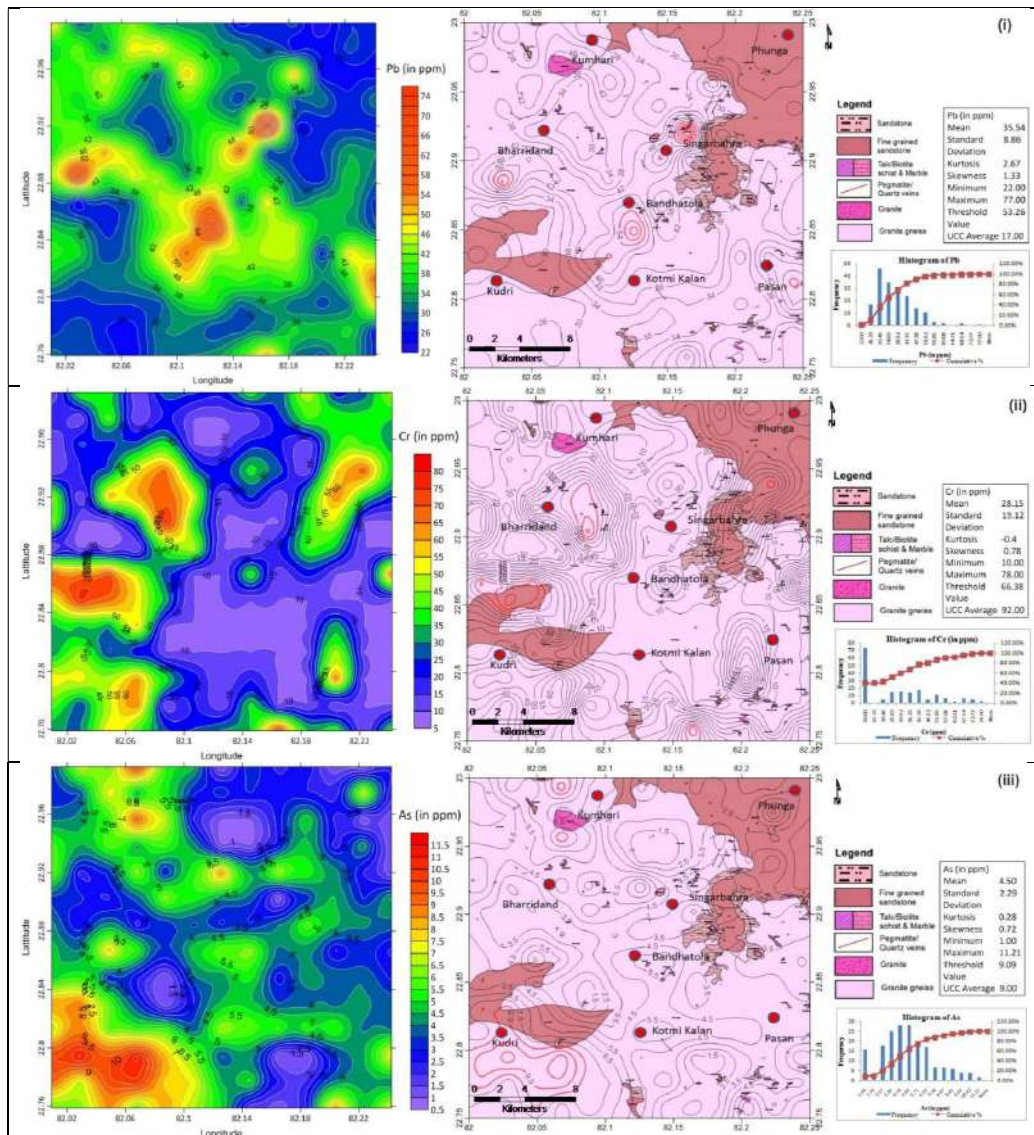


Figure Cont....
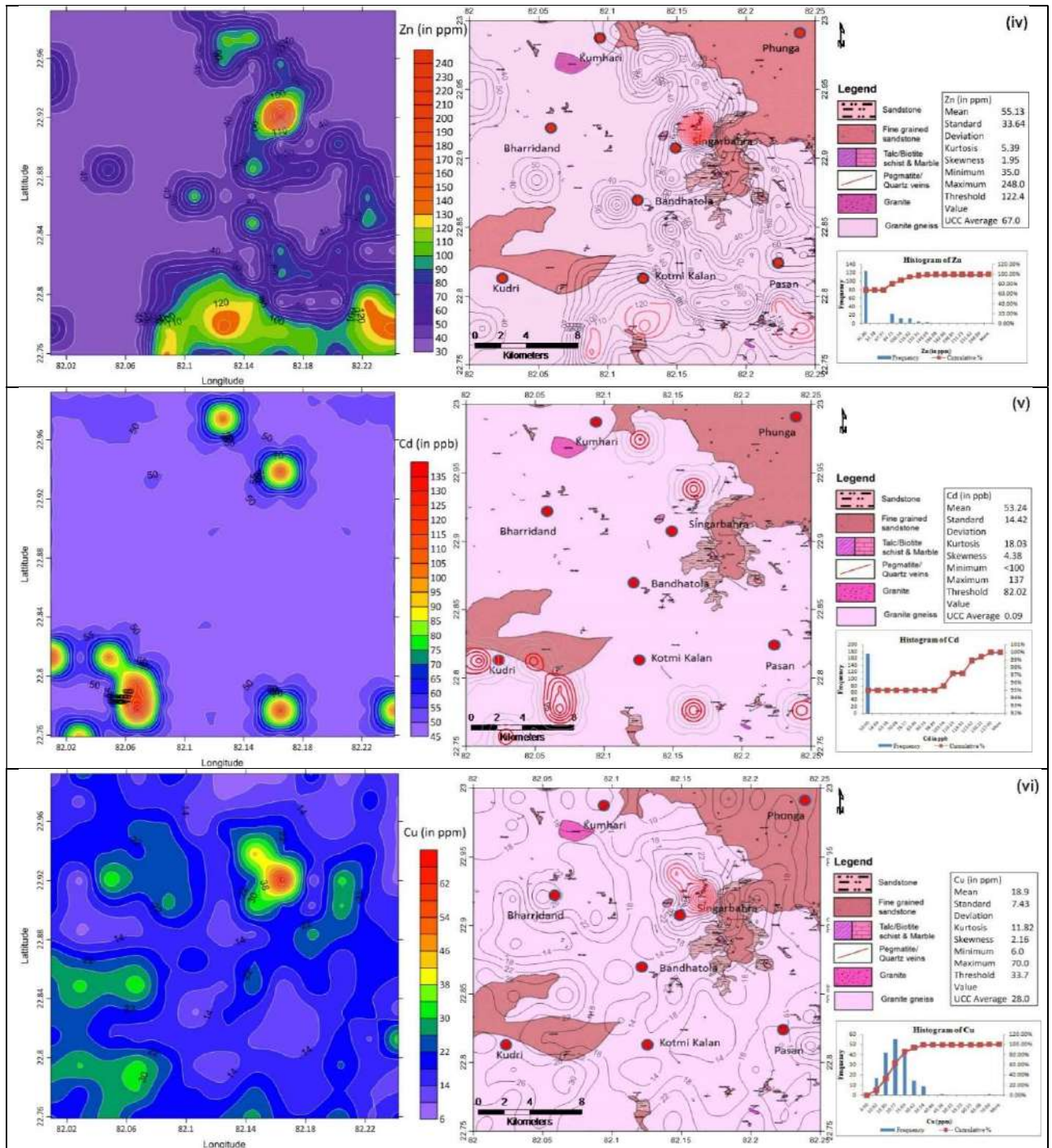
Figure Cont....
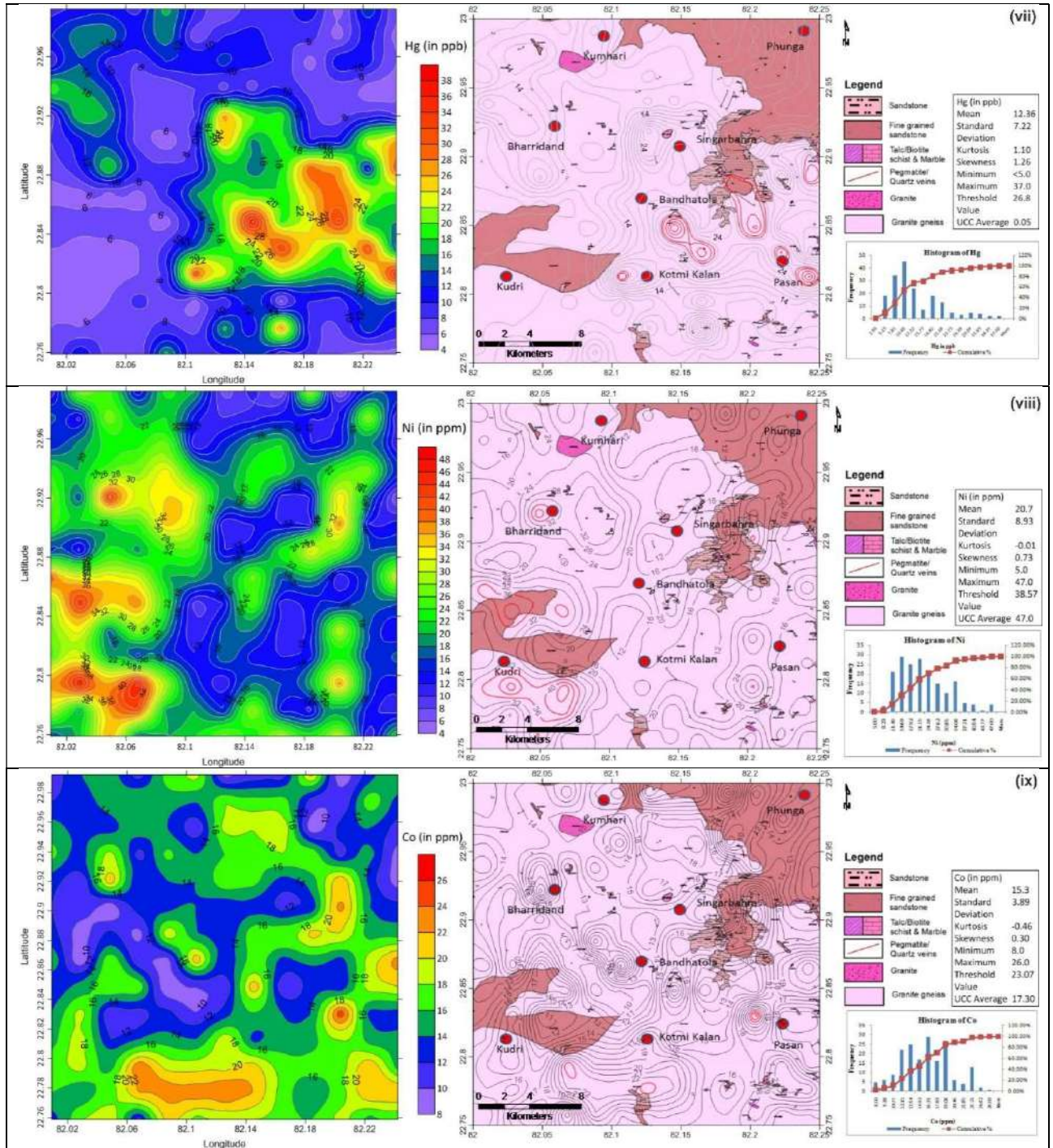
Figure Cont....
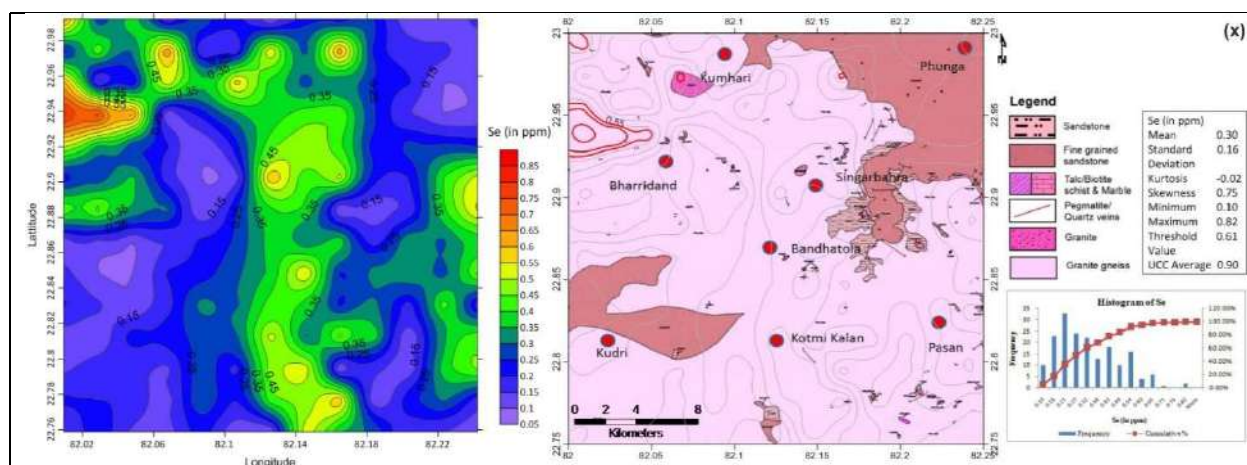
Fig. 5: Geochemical distribution map of heavy metals in stream sediments/slope wash samples in the area and contour diagram superimposed on the geological map of T.S. no 64J/01 for i. lead (Pb), ii. Chromium (Cr), iii. Arsenic (As), iv. Zinc (Zn), v. Cadmium (Cd), vi. Copper (Cu), vii. Mercury (Hg), viii. Nickel (Ni), ix. Cobalt (Co) and x. Selenium (Se).

The remaining heavy metals occur as minor concentrations in the area are Pb, within the granite gneiss of Chhotanagpur Gneissic Complex in the area mainly near Singarbahra and south of Bharridand village (Fig. 5.i). The abnormal value of Cd are observed in the north-east of Singarbahra and Bharridand village. The lithology of this area is mainly Granite Gneisss of the Chotanagpur Gneissic Complex (Fig. 5.v). Higher values of Cu are present in and around Singarbahra village, occupied by granite gneiss of the CGC group (Fig. 5.vi). The highly concentrated anomaly of Hg is observed in the southeast of Singarbahra, Bandhatola, and Pasan villages over Granite Gneisss of Chotanagpur Gneissic Complex and sandstone rocks of Lower Gondwana group (Fig. 5.vii). A highly concentrated anomaly for Se is observed northwest of Bharridand village, in the granite gneiss of Chhotanagpur Gneissic Complex (Fig. 5.x).

The vertical distribution of heavy metal concentrations in the area has been assessed through several soil samples from R- and C-horizon. Analytical results for nine such samples were shown graphically in Fig. 6. 'Pb' ranges from 26 to 46 ppm in the area where samples from the central portion of the area show high concentration. 'Cr' ranges from 15 to 87 ppm in R-horizon and 15 to 77 ppm in C-horizon. 'As' concentration in soil samples varies from 2.56 to 13.22 ppm in the R-horizon and 2.87 to 6.93 ppm in the C-horizon. 'Zn' concentration ranges from 60 to 107 ppm in both R and C- horizons. The 'Cd' value in the R-horizon is <100 ppb, whereas the maximum value of Cd is observed to be 147 ppb in the C-horizon. 'Cu' ranges from 8 to 34 ppm in the R-horizon, whereas in C-horizon, Cu ranges from 10 to 38 ppm. 'Hg' concentration ranges from 2.5 to 15 ppb and 7 to 17 ppb in the R- and C- horizons, respectively. 'Ni'

values range from 14 to 51 ppm in R-horizon and 14 to 61 ppm in C-horizon. 'Co' values range from 9 to 24 ppm and 5 to 25 ppm in R- and C-horizon, respectively, whereas the Se concentration in R-horizon ranges from 0.1 to 0.5 ppm and 0.2 to 0.75 ppm in C-horizon.

Fig 6 shows that almost all heavy metal concentrations are higher in the bottom C-horizon than in the top regolith zone, except for 'Zn' in samples no SS-06, 08, and 09. High-density heavy metals concentrate at the bottom of the soil profile, thus increasing the concentration in the C-horizon. A high Zn value in the R-horizon at the southeastern part of the area is mainly due to anthropogenic changes such as higher uses of fertilizer in agricultural lands. Higher values of Ni and Cr have also been observed in sample no SS-03, from the southwestern part where Ni: 31 ppm and 54 ppm and Cr: 64 ppm and 87 ppm in R and C-samples, respectively.

Higher concentrations of Ni-Cr are mainly seen in the area occupied by mafic or ultra-mafic rocks (Alloway 1990). Nickel is relatively more abundant than chromium and widely distributed in the earth's crust. Nickel concentrations in the soil largely depend on the parent rocks. The lowest contents are found in sedimentary rocks comprising clays, limestones, sandstones, and shales, while the highest concentrations exist in basic igneous rocks (Kabata-Pendias & Mukherjee 2007). Ultramafic rocks such as peridotite, dunite, and pyroxenite have the highest Ni concentrations, followed by mafic and intermediate rocks. However, in surface soils, its content also reflects pedogenic processes and pollution (Kabata-Pendias & Pendias 1992). In the present area of investigation, no such mafic or ultramafic bodies were observed, as shown in the lithological map of TS no 64J/01 (Fig. 3. B). The higher concentrations of Ni and Cr are mainly observed in

**Sample No: SS-01**

| | Se | Co | Ni | Hg | Cu | Cd | Zn | As | Cr | Pb |
|---|---|---|---|---|---|---|---|---|---|---|
| SS-01-R | 0.47 | 18 | 51 | 0.01 | 38 | 0.10 | 60 | 6.93 | 77 | 29 |
| SS-01-C | 0.22 | 25 | 61 | 0.02 | 44 | 0.10 | 65 | 8.63 | 76 | 36 |

**Sample No: SS-02**

| | Se | Co | Ni | Hg | Cu | Cd | Zn | As | Cr | Pb |
|---|---|---|---|---|---|---|---|---|---|---|
| SS-02-R | 0.37 | 9 | 17 | 0.01 | 11 | 0.15 | 65 | 3.86 | 15 | 39 |
| SS-02-C | 0.33 | 13 | 34 | 0.01 | 23 | 0.10 | 65 | 8.41 | 15 | 43 |

**Sample No: SS-03**

| | Se | Co | Ni | Hg | Cu | Cd | Zn | As | Cr | Pb |
|---|---|---|---|---|---|---|---|---|---|---|
| SS-03-R | 0.23 | 10 | 31 | 0.01 | 25 | 0.10 | 65 | 4.96 | 64 | 26 |
| SS-03-C | 0.3 | 11 | 54 | 0.01 | 31 | 0.10 | 65 | 9.14 | 87 | 26 |

**Sample No: SS-04**

| | Se | Co | Ni | Hg | Cu | Cd | Zn | As | Cr | Pb |
|---|---|---|---|---|---|---|---|---|---|---|
| SS-04-R | 0.41 | 13 | 14 | 0.01 | 12 | 0.13 | 65 | 3.45 | 15 | 38 |
| SS-04-C | 0.59 | 14 | 37 | 0.01 | 26 | 0.10 | 65 | 9.27 | 22 | 46 |

**Sample No: SS-05**

| | Se | Co | Ni | Hg | Cu | Cd | Zn | As | Cr | Pb |
|---|---|---|---|---|---|---|---|---|---|---|
| SS-05-R | 0.38 | 13 | 17 | 0.01 | 10 | 0.10 | 65 | 2.87 | 15 | 46 |
| SS-05-C | 0.43 | 18 | 30 | 0.01 | 20 | 0.10 | 70 | 6.64 | 15 | 38 |

**Sample No: SS-06**

| | Se | Co | Ni | Hg | Cu | Cd | Zn | As | Cr | Pb |
|---|---|---|---|---|---|---|---|---|---|---|
| SS-06-R | 0.7 | 20 | 24 | 0.01 | 24 | 0.10 | 96 | 5.53 | 27 | 38 |
| SS-06-C | 0.2 | 19 | 45 | 0.01 | 34 | 0.10 | 76 | 10.21 | 36 | 44 |

**Sample No: SS-07**

| | Se | Co | Ni | Hg | Cu | Cd | Zn | As | Cr | Pb |
|---|---|---|---|---|---|---|---|---|---|---|
| SS-07-R | 0.67 | 16 | 18 | 0.02 | 20 | 0.10 | 91 | 4.71 | 15 | 32 |
| SS-07-C | 0.51 | 18 | 25 | 0.01 | 26 | 0.10 | 107 | 9.06 | 15 | 34 |

**Sample No: SS-08**

| | Se | Co | Ni | Hg | Cu | Cd | Zn | As | Cr | Pb |
|---|---|---|---|---|---|---|---|---|---|---|
| SS-08-R | 0.65 | 24 | 22 | 0.01 | 28 | 0.10 | 107 | 4.78 | 22 | 28 |
| SS-08-C | 0.41 | 18 | 28 | 0.01 | 31 | 0.10 | 70 | 13.22 | 28 | 28 |

**Sample No: SS-09**

| | Se | Co | Ni | Hg | Cu | Cd | Zn | As | Cr | Pb |
|---|---|---|---|---|---|---|---|---|---|---|
| SS-09-R | 0.75 | 10 | 18 | 0.01 | 14 | 0.10 | 74 | 3.85 | 15 | 39 |
| SS-09-C | 0.1 | 5 | 14 | 0.00 | 8 | 0.10 | 65 | 2.56 | 15 | 30 |

Fig. 6: Heavy metal concentration in soil (both R- and C- horizon) samples collected from the study area.

the southwestern part of the area occupied by granitoid and granite gneisses (Fig 5. ii & viii). The concentration of Cr and Ni in granitic igneous rocks ranges from 2 to 90 mg kg$^{-1}$ for Cr and 2–20 mg kg$^{-1}$ for Ni (Krishna et al. 2011). The higher concentrations of Ni in stream sediments and soil mightn't be related to any geo-genic source but rather anthropogenic interference. Anthropogenic sources such as industrial waste materials, lime, fertilizer, and sewage sludge constitute the major sources of Nickel in soils (McIlveen & Negusanti 1994, Chauhan et al. 2008, Iyaka 2011). The study

area is mainly a rural-based agroecosystem with no industries or major townships. Therefore, the influence of industrial waste and sewage sludge is very negligible. Phosphate fertilizers are among the sources of heavy metal inputs to agricultural systems (Ramadan & Al-Ashkar 2007). The primary source of fertilizer-derived heavy metals in soils is phosphatic fertilizers manufactured from the phosphate rocks that contain various metals as minor constituents in the ores. Some fertilizers and soil amendments used in agriculture are important sources of Ni in soil. Rock phosphate, which is

used as a raw material for phosphatic fertilizers, is known to contain Ni ranging between 16.8 to 50.4 ppm, and other fertilizers like ammonium nitrate (<0.20 ppm) and triple super phosphate may also contain 15.6 to 25.2 ppm Ni (Raven & Loeppert 1997).

A few important observations can also be made from the land-use land cover map in Fig 2, where the southwestern part comprises active agricultural activity, villages, and other build-up areas. This area has the highest concentrations of heavy metals like Ni, Cr & As, etc., suggesting the anthropogenic influence mainly from the fertilizer source. Higher concentrations of 'As' are observed in stream sediments, mainly in the southwestern part, similar to Nickel. Whereas higher values of Zn are observed in the southern and south-eastern parts of the area and almost all soil samples. Higher concentrations of As and Zn can also be ascribed to the extensive use of fertilizer and soil amendments. Rock phosphate contains 16.5-20.5 ppm, and Triple superphosphate contains 15.3-16.2 ppm of As, whereas Zn concentrations vary from 78.8-382 ppm in rock phosphate and 61.3 in triple superphosphate (Raven & Loeppert 1997).

Similarly, poultry and swine manure contain an appreciable amount of Zn in the order 330-456 and 540-1200 ppm, respectively (Wolfgang & Dohler 1995). The other heavy metals like Pb, Cd, Cu, Hg, Co, and Se occurs below the permissible limits and have normal distribution pattern. Their anomalous concentrations are observed mainly over the granite gneiss of CGC. Instead of anthropogenic sources, erosion of granite may be the primary cause of heavy metals in granite-gneiss soils (Baltrenaite & Butkus 2004).

Twelve water quality parameters viz., temperature (T), pH, electrical conductivity (EC), total hardness (TH), total dissolved solids (TDS), sodium ($Na^+$), potassium ($K^+$), calcium ($Ca^{2+}$), magnesium ($Mg^{2+}$), bicarbonate ($HCO_3^-$), chlorides ($Cl^-$), sulfates ($SO_4^-$) were analyzed for quality of surface water for drinking purpose. Samples were also analyzed for concentration of heavy metals like lead (Pb), chromium (Cr), Arsenic (As), zinc (Zn), cadmium (Cd), copper (Cu), nickel (Ni), Cobalt (Co) and Selenium (Se), etc. The analytical results of all the water samples are given in Table 2.

In the current study, the pH ranges between 7.2 (minimum) to 8.2 (maximum); EC values ranged from 224 $\mu$S.cm$^{-1}$ to 412 $\mu$S.cm$^{-1}$. The desirable limit of EC for drinking purposes is 300 $\mu$S.cm$^{-1}$ (Chaurasia et al. 2021).TDS in the area varies from 112 to 206 mg.L$^{-1}$. The permissible limit of TDS in water is 2000 mg.L$^{-1}$, and the ideal TDS for drinking water is below 500 mg.L$^{-1}$ (Shiow-Mey et al. 2004). Due to the prevalence of sodium compounds in rocks and soils, which are easily dissolved, all surface water contains some sodium. The permissible limit of sodium is 200 mg.L$^{-1}$, and in the current study area, it varies from 21.0 to 40.0 mg.L$^{-1}$. Potassium is common in many rocks. The primary source of potassium in natural freshwater is the weathering of rocks, but the quantities increase in the polluted water due to wastewater disposal. Usually, natural surface waters have less than 5 mg.L$^{-1}$ of potassium (Skowron et al. 2018). The present study area K varies from 1.0 to 2.0 mg.L$^{-1}$ within the permissible limit (12 mg.L$^{-1}$). Hardness is directly correlated with calcium and magnesium. Calcium concentration ranged between 27.0 to 50 mg.L$^{-1}$ and was found below the permissible limit (200 mg.L$^{-1}$). The magnesium content in the investigated water samples ranged from 5 to 14 mg.L$^{-1}$, within the permissible limit (100 mg.L$^{-1}$). The permissible limit of total hardness as $CaCO_3$ is 600 mg.L$^{-1}$ for drinking water. In the current study, hardness ranges from 88 to 156 mg.L$^{-1}$, which is within the permissible. The effects of the carbonate equilibrium typically maintain natural waters' bicarbonate concentrations within a moderate range. Most surface streams had bicarbonate and carbonate concentrations below 200 mg.L$^{-1}$ but in groundwater, somewhat higher (Kumar et al. 2016). Bicarbonate concentration in the surface water samples ranges from 131 to 220 mg.L$^{-1}$, thus within the permissible limit (500 mg.L$^{-1}$) (WHO 2011). The most common natural form of chlorine is chloride, which is incredibly stable in water. The high concentration of chloride is considered to be an indication of pollution due to increased organic animal waste (Comly 1945). The desirable limit and permissible limit for chloride, according to the World Health Organization (WHO 2011) and Bureau of Indian Standards (BIS 1991), are 250 and 1000 mg.L$^{-1}$, respectively. In the present study, the concentration of Cl ranges from 10 to 15 mg.L$^{-1}$, thus within the limit. The sulfate concentration varied between 3 mg.L$^{-1}$ and 22 mg.L$^{-1}$, under the permissible limit (1000 mg.L$^{-1}$).

All the water samples have also been analyzed for heavy metals, and the results show that Pb concentration ranges from <0.5 to 5.4 ppb; Cr ranges from 4.6 to 10.2 ppb; Cu values range from 0.8 to 1.33 ppb; Co value ranges from 0.07 to 0.42 ppb. Heavy metals like As, Zn, Cd, Ni, and Se present below detectable limits in the water samples. All vales are below the permissible limit of drinking water norms as par BIS standards (BIS 1991).

**Correlation Analysis**

The correlation matrix has been prepared for the fifteen physical and chemical parameters to assess the inter-elemental relationship (Table 3). The correlation coefficient expresses numerically the extent to which two variables are statistically associated. A correlation coefficient

of <0.5 exhibits poor correlation, 0.5 indicates a good correlation, and >0.5 represents excellent correlation (Kumar et al. 2016).

Some significant correlations observed in the correlation matrix are discussed below. The correlation matrix shows that the pH shows moderate to good correlation with almost

Table 2: Analyzed physico-chemical water quality parameters of nine surface water samples collected from the study area.

| Sample No. | Temp. (°C) | pH | E.C. (µS.cm⁻¹) | TDS (mg.L⁻¹) | Na⁺ (mg.L⁻¹) | K⁺ (mg/l) | Ca²⁺ (mg.L⁻¹) | Mg²⁺ (mg.L⁻¹) | T.H. as CaCO₃ | HCO₃⁻ (mg.L⁻¹) | Cl⁻ (mg.L⁻¹l) | SO₄²⁻ (mg/l) | Pb (ppb) | Cr (ppb) | As (ppb) | Zn (ppb) | Cd (ppb) | Cu (ppb) | Ni (ppb) | Co (ppb) | Se (ppb) |
|---|---|---|---|---|---|---|---|---|---|---|---|---|---|---|---|---|---|---|---|---|---|
| 64J01/ A1/W/18 | 16.4 | 7.3 | 236 | 118 | 21.0 | 1.0 | 32.0 | 7.0 | 108 | 131 | 10 | 3 | 5.4 | 4.6 | <1 | <2 | <0.01 | 0.9 | <1 | 0.4 | <100 |
| 64J01/ A2/W/18 | 18.7 | 7.9 | 224 | 112 | 21.0 | 2.0 | 32.0 | 5.0 | 100 | 131 | 10 | 9 | 3.5 | 7.3 | <1 | <2 | <0.01 | 0.9 | <1 | 0.3 | <100 |
| 64J01/ A3/W/18 | 18.7 | 8 | 242 | 121 | 22.0 | 2.0 | 29.0 | 7.0 | 100 | 136 | 11 | 6 | 2.9 | 10.2 | <1 | <2 | <0.01 | 1.0 | <1 | 0.1 | <100 |
| 64J01/ B1/W/18 | 19.7 | 8.2 | 330 | 165 | 40.0 | 2.0 | 27.0 | 10.0 | 112 | 157 | 13 | 22 | 0.6 | 6.1 | <1 | <2 | <0.01 | 1.1 | <1 | 0.1 | <100 |
| 64J01/ B2/W/18 | 14.8 | 7.9 | 412 | 206 | 31.0 | 2.0 | 50.0 | 8.0 | 156 | 220 | 15 | 12 | <0.5 | 5.0 | <1 | <2 | <0.01 | 1.3 | <1 | 0.1 | <100 |
| 64J01/ B3/W/18 | 16.6 | 7.4 | 254 | 127 | 26.0 | 2.0 | 30.0 | 6.0 | 100 | 142 | 15 | 7 | 3.2 | 7.0 | <1 | <2 | <0.01 | 1.0 | <1 | 0.3 | <100 |
| 64J01/ C1/W/18 | 15.6 | 7.2 | 312 | 156 | 31.0 | 1.0 | 30.0 | 11.0 | 124 | 163 | 11 | 13 | <0.5 | 5.0 | <1 | <2 | <0.01 | 1.1 | <1 | 0.1 | <100 |
| 64J01/ C2/W/18 | 19.5 | 8.2 | 352 | 176 | 30.0 | 1.0 | 35.0 | 14.0 | 148 | 199 | 13 | 11 | <0.5 | 5.3 | <1 | <2 | <0.01 | 1.2 | <1 | 0.1 | <100 |
| 64J01/ C3/W/18 | 18 | 7.6 | 258 | 129 | 23.0 | 1.0 | 27.0 | 5.0 | 88 | 147 | 10 | 4 | <0.5 | 5.2 | <1 | <2 | <0.01 | 1.3 | <1 | 0.1 | <100 |

Table 3: Correlation matrix between various surface water quality parameters.
The bold values in the correlation matrix show that the element correlated with >0.50.

| | pH | E.C. | TDS | Na⁺ | K⁺ | Ca²⁺ | Mg²⁺ | Total hardness | HCO₃⁻ | Cl⁻ | SO₄²⁻ | Pb | Cr | Cu | Co |
|---|---|---|---|---|---|---|---|---|---|---|---|---|---|---|---|
| pH | 1 | | | | | | | | | | | | | | |
| E.C. | 0.37 | 1 | | | | | | | | | | | | | |
| TDS | 0.37 | 1.00 | 1 | | | | | | | | | | | | |
| Na⁺ | 0.37 | **0.74** | **0.74** | 1 | | | | | | | | | | | |
| K⁺ | 0.42 | 0.02 | 0.02 | 0.15 | 1 | | | | | | | | | | |
| Ca²⁺ | 0.17 | **0.70** | **0.70** | 0.12 | 0.19 | 1 | | | | | | | | | |
| Mg²⁺ | 0.31 | **0.64** | **0.64** | **0.64** | -0.36 | 0.14 | 1 | | | | | | | | |
| Total hardness | 0.30 | **0.89** | **0.89** | **0.50** | -0.08 | **0.80** | **0.71** | 1 | | | | | | | |
| HCO₃⁻ | 0.36 | **0.96** | **0.96** | **0.55** | -0.05 | **0.78** | **0.60** | **0.93** | 1 | | | | | | |
| Cl⁻ | 0.24 | **0.65** | **0.65** | **0.55** | 0.46 | **0.52** | 0.28 | **0.55** | **0.63** | 1 | | | | | |
| SO₄²⁻ | 0.48 | **0.61** | **0.61** | **0.93** | 0.31 | 0.07 | **0.55** | 0.41 | 0.40 | 0.41 | 1 | | | | |
| Pb | -0.35 | -0.73 | -0.73 | -0.69 | 0.12 | -0.18 | -0.52 | -0.46 | -0.68 | -0.33 | -0.58 | 1 | | | |
| Cr | 0.34 | -0.45 | -0.45 | -0.31 | **0.62** | -0.29 | -0.31 | -0.42 | -0.43 | -0.06 | -0.13 | 0.29 | 1 | | |
| Cu | 0.19 | **0.62** | **0.62** | 0.34 | -0.24 | 0.32 | 0.21 | 0.36 | **0.66** | 0.35 | 0.10 | -0.80 | -0.37 | 1 | |
| Co | -0.49 | -0.66 | -0.66 | -0.63 | 0.02 | -0.15 | -0.54 | -0.44 | -0.60 | -0.18 | -0.61 | 0.92 | 0.03 | -0.63 | 1 |

all parameters while negatively correlated with lead and cobalt. Electrical conductivity and total hardness (TDS) show a positive correlation with most of the parameters except with heavy metals like lead (-0.73), Cr (-0.45), and cobalt (-0.66). Sodium exhibits a poor positive correlation with potassium (0.15). A strong positive correlation between sodium and potassium indicates a geogenic source and suggests that sodium and potassium have been derived from the disintegration of silicate minerals (Hem 1991). As there is a poor correlation between sodium and potassium, it can be suggested that the source of sodium may not be geogenic but anthropogenic. Sodium strongly correlates with sulfate (0.93) but moderately with chloride (0.55). This suggests that the source of sodium may be sulfate compounds instead of chlorides. Mirabilite, associated with gypsum, halite, etc., is a geogenic source of sodium sulfate compounds (Wells 1923, Khalili & Torabi 2003).

Moreover, while exposed, pyrite and other sulfides associated with granite and granite gneisses are oxidized to sulphuric acid. This sulphuric acid immediately dissolves some basic oxides, producing soluble sulfates (Wells 1923). As in the study area, no such mineralized sulfide zones were observed during mapping, nor were any reported occurrences of gypsum or halite in the area, so the source of sodium may be anthropogenic. Calcium and magnesium show a strong positive correlation (0.93) and moderate positive correlation (0.60), respectively, with bicarbonates indicating

that calcium and magnesium have been derived from the dissolution of carbonate minerals. As the pH of the stream water ranges between 7-8, the carbonate ions formed due to the disassociation of the carbonate minerals are present in the stream water as bicarbonates (Fetter 2001).

Amongst the heavy metals, lead is negatively correlated with almost all parameters. A strong positive correlation is observed between Cr with K (0.62) and Co with Cr (0.90), while both Cr and Co show a negative correlation with rest.

## Water Quality Characteristics for Irrigation Purposes

To understand the relationship of the chemical components of water, data was plotted in Gibbs diagram (1970). Three fields of the Gibbs diagram, precipitation dominance, evaporation dominance, and rock-water interaction dominance, are used to determine the quality attributes of water (Kumar et al. 2016), where all ions are expressed in $meq.L^{-1}$.

$$\text{Gibbs ratio I (for anion)} = \frac{Cl^-}{(Cl^- + HCO_3^-)} \quad \dots(7)$$

$$\text{Gibbs ratio II (for cation)} = \frac{Na^+}{(Na^+ + Ca^{2+})} \quad \dots(8)$$

The Gibbs ratio of the water samples is plotted against their respective total dissolved solid concentration (TDS), as shown in Fig. 7. According to Gibbs equations I and II, all the surface water samples fall under the evaporation dominance field. It indicates that evaporation-sedimentation
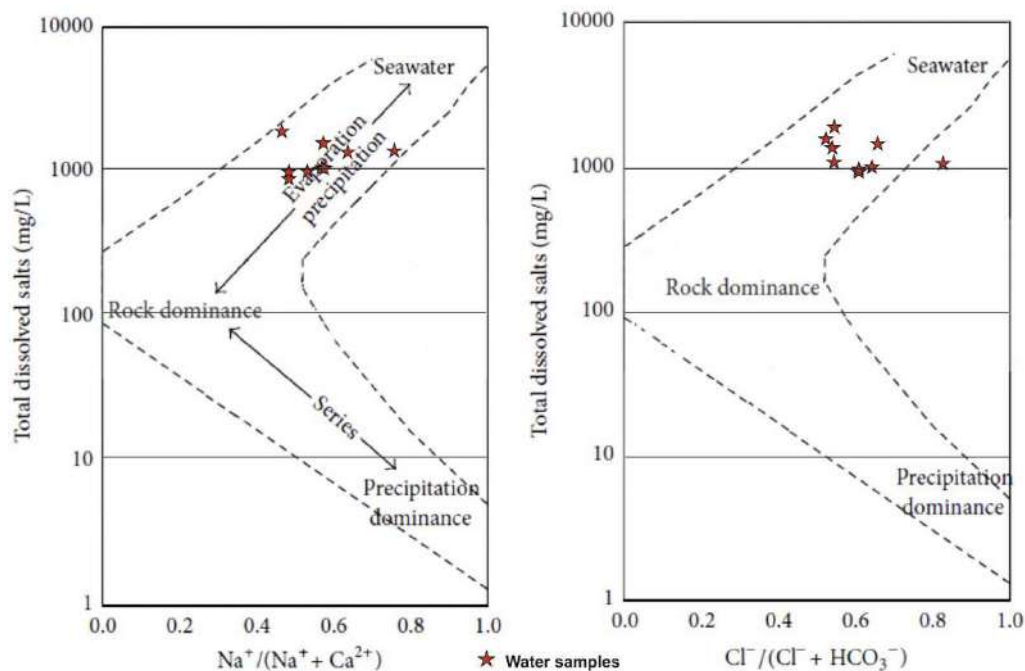


Fig. 7: Gibbs diagram illustrating the mechanism controlling the surface water chemistry.
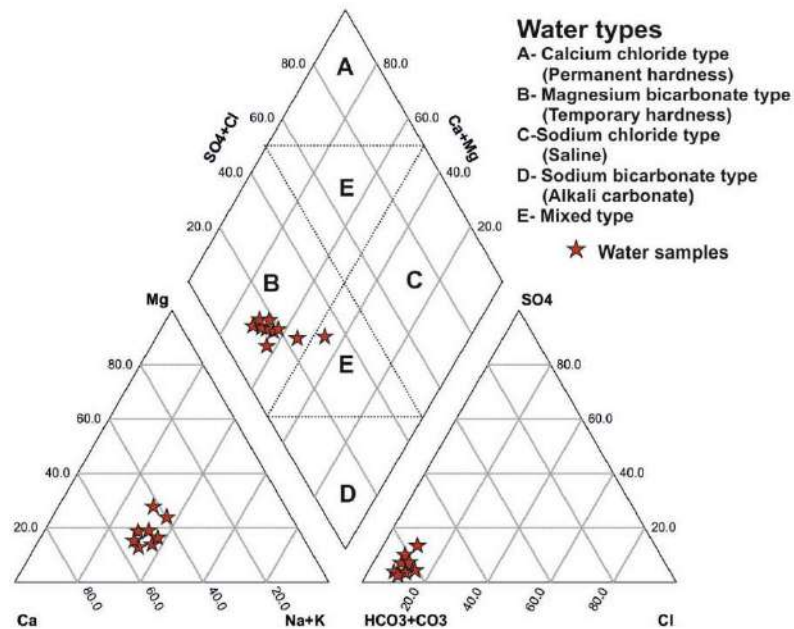
Fig. 8: Piper diagram showing water type in the study area (after Piper 1944).

is the main factor in the chemical composition of surface water bodies. Thus, the chemical weathering of rock-forming minerals doesn't control the surface water chemistry of the study area.

The groundwater type was characterized using the Piper trilinear diagram (1944) and is given in Fig. 8. This diagram shows five zones (Zone A, B, C, D & E). In zones A, B, C, and D, two groups of anions and cations dominate. For example, $SO_4^{2-}$- $Cl^-$ anions and $Ca^{2+}$- $Mg^{2+}$ cations dominate in zone A, HCO3 - CO32- anions and Ca2+- Mg2+ cations dominate in zone B, etc. Zone E represents a mixing zone where neither anions nor cations are dominant. The diagram shows that most of the water

samples are magnesium bicarbonate type, having temporary hardness.

The sodium hazard of irrigation water was definite by the relative proportion of sodium (Na+) to calcium ($Ca^{2+}$) and magnesium ($Mg^{2+}$) ions and was expressed in terms of SAR (sodium absorption ratio). High sodium concentration in water leads to the degradation of soil structure by reducing soil permeability, thus affecting the physical property of soil when used for irrigation purposes (Dhirendra et al. 2009). The SAR values are determined using Eq. 1 (Richards 1954) and varied from 0.88 to 1.67 (Table 4). SAR values >10 were not recommendable for water to be used for irrigation purposes (Siamak & Srikantaswamy 2009). In the present

Table 4: Statistical representation of irrigation water parameters.

| Sample No. | SAR | Na% | RSBC | PI | MH | KI |
|---|---|---|---|---|---|---|
| 64J01/A1/W/18 | 0.88 | 30.17 | 0.55 | 77.07 | 26.51 | 0.42 |
| 64J01/A2/W/18 | 0.91 | 32.45 | 0.55 | 81.41 | 20.49 | 0.45 |
| 64J01/A3/W/18 | 0.95 | 33.26 | 0.78 | 82.21 | 28.47 | 0.47 |
| 64J01/B1/W/18 | 1.67 | 45.21 | 1.23 | 85.52 | 37.92 | 0.80 |
| 64J01/B2/W/18 | 1.07 | 30.74 | 1.11 | 72.13 | 20.88 | 0.43 |
| 64J01/B3/W/18 | 1.13 | 37.26 | 0.83 | 85.10 | 24.80 | 0.57 |
| 64J01/C1/W/18 | 1.23 | 36.39 | 1.17 | 79.53 | 37.68 | 0.56 |
| 64J01/C2/W/18 | 1.08 | 31.46 | 1.51 | 74.01 | 39.74 | 0.45 |
| 64J01/C3/W/18 | 1.07 | 36.84 | 1.06 | 92.51 | 23.39 | 0.57 |
| Min | 0.88 | 30.17 | 0.55 | 72.13 | 20.49 | 0.42 |
| Max | 1.67 | 45.21 | 1.51 | 92.51 | 39.74 | 0.80 |
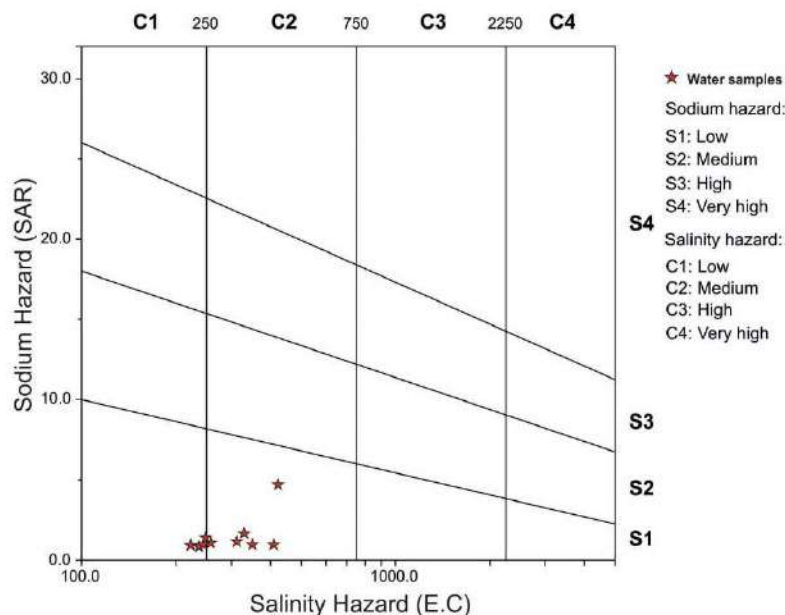
Fig. 9: Classification of irrigation waters using U.S. salinity diagram (USSL 1954).

area, all the surface water samples fall in the excellent category and are suitable for irrigation on almost all soil types with no sodium hazard.

The geochemical parameters of the water samples are plotted in the Salinity Hazards versus Sodium Hazards (USSL) diagram (Richards 1954) to assess the suitability of irrigation water using SAR and EC values. It is a scatter plot of Sodium Hazard (SAR) on the y-axis vs. Salinity Hazard (conductivity) on the x-axis. The sodium hazard of irrigation water is estimated by the sodium absorption ratio (SAR), which is related to the proportion of $Na^+$ to $Ca^{2+}$ and $Mg^{2+}$ (Kevin 2005). In this plot, the C1 zone represents 'low,' C2 represents 'medium,' C3 represents 'high,' and C4 represents 'very high' salinity hazard. S1 zone represents 'low,' S2 represents 'medium,' S3 represents 'high,' and S4 represents 'very high' sodium hazard. The USSL plot for the study area shows that most water samples have low to medium salinity hazard with low sodium hazard (C2-S1) (Fig 9). Fig. 9 shows that almost all the surface water bodies are suitable for irrigation in most of the soil types.

Another crucial element in assessing the sodium risk and the suitability of water for agricultural use is the sodium percentage (Na%). High Na% irrigation water will increase the exchange of sodium content in the soil, affecting the permeability and texture of the soil (Ghazaryan & Chen, 2016). The sodium percentage values in the study area were calculated by the formula in Eq. 2 (Wilcox 1955) and ranged from 30.17-45.21 % with a medium value of 33.25 % (Table 4). All water sample quality falls in the good to

permissible category for irrigation purposes (Wilcox 1955, Ayers & Westcot 1985).

Gupta & Gupta (1987) proposed the residual sodium bicarbonate (RSBC) calculation to assess the suitability of water. The water is considered safe, marginal, and unsatisfactory when the RSBC <5, 5-10, and >10 meq.$L^{-1}$, respectively (Tanvir Rahman et al. 2017). All the samples followed the satisfactory level of irrigation water.

The permeability index (PI) is also used to determine the suitability of the irrigation water. Long-term exposure to irrigation water containing high sodium, calcium, magnesium, and bicarbonate ions negatively impacts soil permeability (Ravikumar et al. 2011, Srinivasamoorthy et al. 2014). Doneen (1964) introduced the permeability index (PI) for assessing the suitability of irrigation water using Eq. 4. Based on the PI values, the irrigated water can be classified as Class I (>75%), Class II (25-75%) and Class III (<25%). The permeability index of the study area ranges from 72.13 to 92.51%. Only two samples out of nine fall under the Class II category, and the rest belong in the Class I category, indicating that the water is good for irrigation purposes (Table 4).

A higher concentration of Mg ions in water adversely affects the soil quality and crop yield (Shil et al. 2019). Paliwal (1972) developed an index called "magnesium hazard" to assess the adverse effects of magnesium in irrigation water and is calculated as magnesium ratio (MH) using the formula (Eq. 5) (Sundaray et al. 2009, Ravikumar et al. 2011). MH values above 50% adversely affect crop

yield and are unsuitable for irrigation (Sundaray et al. 2009). The magnesium ratio varied from 20.49 to 39.74 (Table 4); thus, all surface water bodies fall under the suitable irrigation category.

A high level of sodium in the water is indicated by Kelly's index, which compares sodium to calcium and magnesium (Kelly 1940) and is calculated using Eq. 6. Water with Kelly's index value less than one (KI < 1) is suitable for irrigation. In contrast, KI>1 indicates excess sodium in water, and KI < 2 indicates sodium deficiency in water (Kelly 1940, Sundaray et al. 2009). In this study, the values of Kelly's index range from 0.42 to 0.80, thus indicating that the water is safe for irrigational purposes.

## ACKNOWLEDGMENTS

## CONCLUSIONS

The study contributes to understanding heavy metals contamination of sediments, soils, and water due to anthropogenic activity, mainly in agriculture-based rural areas. Heavy metals like Pb, Zn, Cu, and Co concentrations in stream sediments/slope-wash samples are higher than their UCC abundance. In contrast, Cr, Cd, Hg, Ni, and Se concentrations are below UCC value. When compared with the globally acceptable permissible or critical limits of each element, it has been observed that the concentration of Pb, Cd, Cu, Hg, and Se is well within safe limits. Slightly higher concentrations are observed in Cr, As, Zn, and Co but not higher than the critical range. The Ni concentration in the area shows maximum values of 47.0 ppm, mainly in the southwestern part. The elements distribution map shows high concentration zones for Ni, Cr, and As over granite and granite gneiss, mainly in the southwestern part. Higher concentrations have also been observed in soil samples, where the bottom C-horizon is more enriched in heavy metals. This higher concentration of Ni-Cr might have come

from using phosphatic fertilizer, as agricultural lands occupy all high-value areas. Zn enrichment in the top part of the soil profile in R-horizon in the southern and south-eastern regions also indicates extensive use of fertilizer and soil amendments in the form of poultry and swine manure. Adequate measures should be taken by health and agricultural authorities in these areas for the betterment of the environment and society.

Water quality assessment of major streams in the study areas shows all parameters are well below the permissible limits of drinking water norms. Correlation analysis reveals a poor correlation between sodium and potassium, suggesting the anthropogenic source of sodium in water. Thus, the chemical weathering of rock-forming minerals doesn't control the surface water chemistry of the study area. The estimation of irrigation water quality of the surface water bodies indicates that these stream waters are suitable for irrigation on almost all soil types with no sodium hazard and low to medium salinity hazard.

This study also shows the importance of the country's geochemical mapping database, which will have much broader applications than conventional mineral exploration and geological mapping.

## REFERENCES

Abdu, N., Abdullahi, A.A. and Abdulkadir, A. 2017. Heavy metals and soil microbes. Environ. Chem. Lett., 15 (1): 65-84.

Acharyya, S.K. 2003. The nature of the Mesoproterozoic central Indian tectonic zone with exhumed and reworked older granulites. Gondwana Res., 6(2): 197-214.

Alloway, B.J. 1990. Heavy metals in soils. Wiley, New York.

Appleton. J.D. and Ridgway. J. 1992. Regional geochemical mapping in developing countries and its applications to environmental studies. Appl. Geochem. Suppl., 2: 103-110.

Awasthi, S.K. 2000. Prevention of food adulteration Act no 37 of 1954, Central and state rules as amended for 1999. Ashoka Law House, New Delhi.

Ayers, R.S. and Westcot, D.W. 1985. Water quality for agriculture, irrigation, and drainage (Paper No. 29). FAO, Rome.

Bakshi, S., Banik, C. and He, Z. 2018. The Impact Of Heavy Metal Contamination On Soil Health. In: Reicoskey, D. (ed) Managing Soil Health For Sustainable Agriculture. Taylor and Francis, Milton Park, pp. 63-95.

Baltrenaite, E. and Butkus, D. 2004. Investigation of heavy metals transportation from soil to the pine tree. Water Sci. Technol., 50: 239-244.

BIS 1991. Bureau of Indian Standards, 10500 Indian Standard drinking water specification, 1st rev., 1-8.

Central Ground Water Board, 2013. Groundwater brochure of Korba District, Chhattisgarh 2012-2013. Available online: ttps://cgwb.gov.in/District_Profile/Chhatisgarh/Korba.

Chauhan, S., Thakur, R. and Sharma, G. 2008. Nickel: its availability and reactions in the soil. J. Ind. Pollut. Control., 24(1): 1-8.

Chaurasia, A.K., Pandey, H.K., Tiwari, S.K., Pandey, P. and Ram, A. 2021. Groundwater vulnerability assessment using water quality index (WQI) under geographic information system (GIS) framework in parts of Uttar Pradesh, India. Sustain. Water Resour. Manag., 7(3): 1-15.

Chopra, A.K., Pathak, C. and Parasad, G. 2009. The scenario of heavy metal contamination in agricultural soil and its management. J. Appl. Nat. Sci., 1: 99-108.

Comly, H.H. 1945. Cyanosis in infants is caused by nitrates in well water. J. Am. Assoc., 129: 12-114.

Dhirendra, M.J., Kumar, A. and Agrawal, N. 2009. Assessment of the irrigation water quality of river Ganga in Haridwar District. Rasayan. J. Chem., 2: 285-292.

Doneen, L.D. 1964. Notes on water quality in agriculture. Water Science and Engineering, University of California, Davis.

Fetter, C.W. 2001. Applied Hydrogeology. Prentice-Hall, Inc., Hiscock, K.M. (ed), Hydrogeology: Principles and Practice. Blackwell Publishing, London, pp. 436-532.

Ghazaryan, K. and Chen, Y. 2016. Hydrochemical assessment of surface water for irrigation purposes and its influence on soil salinity in Tikanlik Oasis, China. Environ. Earth Sci., 75(5): 383.

Gibbs, R.J. 1970. Mechanism controlling world water chemistry. Sciences, 170: 795-840.

Gupta, S.K. and Gupta, I.C. 1987. Management of Saline Soils and Waters. Oxford and IBH Publishing Company, New Delhi

Hapke, H.J. 1996. Heavy Metal Transfer in the Food Chain to Humans. In Rodriguez-Barrueco, C. (ed), Fertilizers and Environment, Springer, Netherlands, pp. 431-486.

Hashim, M.A., Mukhopadhyay, S., Sahu, J.N. and Sengupta, B. 2011. Remediation technologies for heavy metal contaminated groundwater. J. Environ. Manage., 92(10): 2355-88.

He, Z., Shentu, J., Yang, X., Baligar, V.C., Zhang, T. and Stofella, P.J. 2015. Heavy metal contamination of soils: Sources, indicators, and assessment. J. Environ. Indic., 9: 17-18.

Hem, J.D. 1991. Study and Interpretation of the Chemical Characteristics of Natural Water. Third Edition. Scientific Publishers, Jodhpur, India, pp. 263.

Iimura, K., Ito, H., Chino, H., Morishita, M. and Hirta, H. 1977. The behavior of contaminant heavy metals in the soil-plant system. Proc. Inst. Sem., 11: 357.

Iyaka, Y.A. 2011, Nickel in soils: a review of its distribution and impacts. Sci. Res. Essays, 6(33): 6774-6777.

Jovanović, V.S., Mitić, V., Mandić, S.N., Ilić, M. and Simonović, S. 2015. Heavy Metals in the Postcatastrophic Soils. Sherameti, I. and Varma, A. (eds), Heavy Metal Contamination of Soils: Monitoring and Remediation, Springer International Publishing, New York, pp. 3-21.

Kabata-Pendias, A. 2011. Trace Elements in Soils and Plants. Fourth Edition. CRC Press, New York.

Kabata-Pendias, A. and Mukherjee, A.B. 2007. Trace Elements from Soil to Human. Springer- Verlag, Berlin.

Kabata-Pendias, A. and Pendias, H. 1992. Trace Elements in Soils and Plants. CRC Press, London.

Kaur, M., Soodan, R.K., Katnoria, J.K., Bhardwaj, R., Pakade, Y.B. and Nagpal, A.V. 2014. Analysis of physico-chemical parameters, genotoxicity, and oxidative stress-inducing potential of soils of some agricultural fields under rice cultivation. Trop. Plant Res., 1(3): 49-61.

Kelly, W.P. 1940. Permissible Composition and Concentration of Irrigated Waters. In: Proceedings of the ASCF 66, pp. 607.

Kevin, M.H., 2005. Hydrogeology Principles and Practice. Blackwell Science Ltd., London, pp. 202.

Khalili, M. and Torabi, H. 2003. The exploration of sodium-sulphate in Aran playa, Kashan, central Iran. Carbon. Evap., 18: 120-124.

Kools, S.A.E., Van Roovert, M., Van Gestel, C.A.M. and Van Straalen, N.M. 2005. Glyphosate degradation as a soil health indicator for heavy metal polluted soils. Soil Biol. Biochem., 37(7): 1303-1307.

Krishna, A.K., Rama Mohan, K. and Murthy, N.N. 2011. A multivariate statistical approach for monitoring heavy metals in sediments: a case study from Walipalli watershed, Nalgonda district, Andhra Pradesh, India. Res. J. Environ. Earth Sci., 3(2): 103-113.

Kumar, S.K., Babu, S.H., Rao, P.E., Selvakumar, S., Thivya, C., Muralidharan, S. and Jeyabal, G. 2016. Evaluation of water quality and hydrogeochemistry of surface and groundwater, Tiruvallur District, Tamil Nadu. India Appl. Water Sci., 7(5): 2533-2544.

Maji, A.K., Goon, S., Bhattacharya, A., Mishra, B., Mahato, S. and Bernhardt, H. J. 2008. Proterozoic polyphase metamorphism in the Chhotanagpur Gneissic Complex (India), and implication for transcontinental Gondwanaland correlation. Precamb. Res., 162: 385-402.

McIlveen, W.D. and Negusanti, J.J. 1994. Nickel in terrestrial environment. Sci. Total Environ., 148: 109-138.

Mohankumar, K., Hariharan, V. and Rao, N.P. 2016. Heavy metal contamination in groundwater around industrial estate vs. residential areas in Coimbatore, India. J. Clin. Diagn. Res., 10(4): BC05-7.

Mushtaq, N. and Khan, K.S. 2010. Heavy metals contamination of soils in response to wastewater irrigation in Rawalpindi region. Pak. J. Agrl. Sci., 47(3): 215-224.

NGCM SOP, 2011. Standard operating procedure for national geochemical mapping. Geological Survey of India, Central Head Quarter, Kolkata.

Notten, M.J.M., Oosthoek, A.J.P., Rozema, J. and Aerts, R. 2005. Heavy metal concentrations in a soil–plant–snail food chain along a terrestrial pollution gradient. Environ. Pollut., 138(1): 178-90.

Oliver, M.A. and Gregory, P.J. 2015. Soil, food security, and human health: A review. Euro. J. Soil Sci., 66(2): 257-76.

Paliwal, K.V. 1972. Irrigation with saline water. Monogram no. 2, new series. IARI, New Delhi, pp. 198.

Pepper, I.L. 2013. The soil health-human health nexus. Crit. Rev. Environ. Sci. Technol., 43(24): 2617-52.

Piper, A.M. 1944. A graphic procedure in the geochemical interpretation of water analysis. Trans. A.G.U., 25: 914-923.

Ramadan, M.A.E. and Al-Ashkar, E.A. 2007. The effect of different fertilizers on the heavy metals in soil and Tomato plants. Aust. J. Basic Appl. Sci., 1(3): 300-306.

Raven, K.P. and Loeppert, R.H. 1977. Trace Element composition of fertilizers and soil amendments. J. Environ. Qual., 26: 551-557.

Ravikumar, P., Somashekar, R.K. and Angami, M. 2011. Hydrochemistry and evaluation of groundwater suitability for irrigation and drinking purposes in the Markandeya River basin, Belgaum District, Karnataka State, India. Environ. Monit. Assess., 173: 459-487.

Rayment, G.E., Jeffery, A.J. and Barry, G.A. 2002. Heavy metals in Australian sugarcane. Commun. Soil Sci. Plant Anal., 33: 3203-3212.

Richards, L.A. 1954. Diagnosis and improvement of saline and alkali soils. Agric Handbook 60, USDA, Washington.

Sarwar, N., Imran, M., Shaheen, M.R., Ishaque, W., Kamran, M.A., Matloob, A., Rehim, A. and Hussain, S. 2017. Phytoremediation strategies for soils contaminated with heavy metals: Modifications and future perspectives. Chemosphere, 171: 710-21.

Shil, S., Singh, U.K. and Mehta, P. 2019. Water quality assessment of a tropical river using water quality index (WQI), multivariate statistical techniques, and GIS. Appl. Water Sci., 9 (7): 168.

Shiow-Mey, L., Shang-Lien, L. and Shan-Hsien, W. 2004. A generalized water quality index for Taiwan. Environ. Monit. Assess., 96: 35-52.

Siamak, G. and Srikantaswamy, S. 2009. Analysis of agricultural impact on the Cauvery River water around KRS dam. World Appl. Sci. J., 6(8): 1157-1169.

Skowron, P., Skowro´nska, M., Bronowicka-Mielniczuk, U., Filipek, T., Igras, J., Kowalczyk-Ju´sko, A. and Krzepiłko, A. 2018. Anthropogenic sources of potassium in surface water: the case study of the Bystrzyca river catchment, Poland. Agric. Ecosyst. Environ., 265: 454-460.

Srinivasamoorthy, K., Gopinath, M., Chidambaram, S., Vasanthavigar, M. and Sarma, V.S. 2014. Hydrochemical characterization and quality appraisal of groundwater from Pungar sub-basin, Tamilnadu, India. J. King Saud. Univ. Sci., 26: 37-52.

Sundaray, S.K., Nayak, B.B. and Bhatta, D. 2009. Environmental studies on river water quality with reference to suitability for agricultural purposes: Mahanadi river estuarine system, India—a case study. Environ. Monit. Assess., 155: 227-243.

Tanvir Rahman, M.A.T.M., Saadat, A.H.M., Islam, M.S., Al-Mansur, M.A. and Ahmed, S., 2017. Groundwater characterization and selection of suitable water type for irrigation in the western region of Bangladesh. Appl. Water Sci., 7: 233-243.

Tchounwou, P.B., Yedjou, C.G., Patlolla, A.K. and Sutton, D.J. 2012. Heavy metals toxicity and the environment. EXS, 101: 133-64.

USSL. 1954. Diagnosis and Improvement of Salinity and Alkaline Soil. USDA Hand Book no. 60, Washington.

Wells, C.R. 1923. Sodium sulfate: Its sources and uses. US Geol. Surv. Bull., 717:11214.

WHO 2011. WHO Guidelines for Drinking-Water Quality, Fourth Edition. World Health Organization, Washington DC.

Wilcox, L.V. 1955. Classification and Use of Irrigation Waters. USDA Circular No. 969, pp. 19.

Wolfgang, W. and Dohler, H. 1995. Heavy Metals in Agriculture. Springer, Germany.

Yang, J., Teng, Y., Wu, J., Chen, H., Wang, G., Song, L., Yue, W., Zuo, R. and Zhai, Y. 2017. Current status and associated human health risk of vanadium in soil in China. Chemosphere, 171: 635-43.

## ORCID DETAILS OF THE AUTHORS

Manash Protim Baruah: https://orcid.org/0000-0002-4398-6645

# Predictability Augmentation by In-silico Study to In-vivo and In-vitro Results of Lung Doses of Airborne Fine and Ultrafine Particles Inhaled by Humans at Industrial Workplaces

**M. Ali†** (iD)

Biosimulation and Aerosol Research Lab, Longview University Center, The University of Texas at Tyler, 3201 N. Eastman Road, Longview 75605, USA

†Corresponding author: M. Ali; mohammedali@uttyler.edu

## ABSTRACT

This study correlates computational predictions with in vivo and in vitro experimental results of inhaled fine and ultrafine particulate matter (PM) transport, dissemination, and deposition in the human respiratory airways. Epidemiological studies suggest that workplace exposure to anthropogenic pollutant PMs is a risk factor for increased susceptibility to acute broncho-pulmonary illnesses. However, investigations on detailed human inhalation and PM transport processes are restrictive from time, cost, and ethical perspectives. Computational simulation based on the Multiple Path Particle Dosimetry (MPPD) model was employed to quantify the risks associated with workplace exposure of these PMs. Here, the physical, mechanical, and electrical properties of PMs of carbon black (CB) and ultrafine particles (UFPs) from wire-cut electrical discharge machining (WEDM), with mass median aerodynamic diameter (CMAD) in the range of 1 nm to 1000 nm, were used as input parameters of MPPD. Additionally, it mimicked occupational workers' age, body mass index, and oronasal-combinational nose and mouth breathing exposure time. The deposition results were compared with several vivo and in vitro experimental data reported in the literature, and satisfactory agreements were found. For example, a total lung dose of CB-PMs of 100 nm is the highest (28%), while a 380 nm dose is the lowest (15%). Afterward, deposition increases with particle size, reaching 26% for 1000 nm. In the case of WEDM-UFPs, about 98% of all 1.0 nm inhaled particles remain in the lung. Subsequently, the deposition dose decreases with the particle size and reaches up to 28% for 100 nm particles. Approximately 51% of deposited WEDM-UFPs are of CMAD ≤ 5 nm. The images of lung geometry also observed the maximum deposited mass and mass flux rate in the head, tracheobronchial, and pulmonary airways.

## INTRODUCTION

It is a well-established concept that the human respiratory system represents a complicated air route with a defined structure-activity relationship. It is divided mainly into two regions: the conductive and respiratory regions. The conductive region comprises the nasal cavity, sinuses, nasopharynx, oropharynx, and larynx (combinedly "Head" airway), then the trachea, bronchi, and up to the terminal bronchioles (combinedly "TB" airway). The respiratory region comprises bronchioles, alveolar ducts, and alveolar sacs (combined "P" airway). The main functions of the conductive part are to filter, humidify, and warm the inhaled air, while the respiratory part functions as the place for oxygen and carbon dioxide gas exchanges (Douafera et al. 2020). However, the inhaled air and particulate matter (PMs), if carried along with it, will form an aerosol by mixing with airways' moisture. Fine particles are airborne smaller particles with an aerodynamic diameter ($d_{ae}$) of 2500 nm or less. The larger PMs (dia. > 2500 nm) deposit mostly in the conductive region, and the smaller ones will travel further into the respiratory region to cause systemic effects (either desirable or adverse).

Ultrafine particles (UFPs) are considered to have a $d_{ae}$ < 100 nm or 0.1 micrometer. The human eye can see debris and dust approximately 25 microns in size. The $PM_{10}$, $PM_{2.5}$ and UFPs are too small to be seen by the naked eye. More important, the origin and geometric size of PMs (100 nm ≤ $d_{ae}$ ≤ 100 μm) permit them to hold a diversity of physicochemical, electromechanical, and biological (PEB) properties. However, when PM enters the lung airways, their size, surface areas, and PEB properties play a major role in interacting materials with biological systems. Among

them, the medicinal particles provide expected desirable therapy effects, and the pollutant or carcinogen particles provide unexpected adverse effects or diseases. To our knowledge, the lung burden refers to the quantity of retained material within the lungs, which is a function of pulmonary deposition and retention of inhaled nanoparticles, and this PM deposition causes unexpected adverse effects or diseases (Seong Jo et al. 2020, Abraham et al. 2002).

Engineered UFPs are purposefully developed in many applications (e.g., carbon black, fumed silica, titanium dioxide [TiO2], iron oxide [FeOx], quantum dots, and carbon nanotubes (Ali 2014, Matsoukas et al. 2015). High-energy processes such as synthesis, spraying, machining, and industrial bagging are correlated with the release of large numbers of predominantly fine particles and UFPs. The wide application of engineered UFPs has induced increasing exposure to humans and the environment, which has led to substantial concerns about their biosafety. In an extensive review of the production of engineered particles, Ding et al. (2017) showed that process-based release potential can be ranked and tied with exposure assessment approaches, which can guide the implementation of workplace safety measures. Their study also suggested that significant exposures largely occur at industrial workplaces when industrial safeguards and personal protection schemes are not followed as recommended.

Major concerns exist regarding the potential consequences of human exposure to industrial-scale carbon black (CB) particles, but limited human toxicological data is currently available. The production of CB consists of a three-step process: reaction, pelletizing, and packaging (Kuhlbusch et al. 2004). In the reaction step, chemical reactions take place in a furnace reactor to produce the primary CB particles with particle sizes ranging from 1 to 500 nm, where the most common particles are in the range of 10 to 100 nm range. In the pelletizing step, large agglomerates (pellets) are formed by tumbling the newly made CB in a drum by mixing with water.

In the packaging step, workers pack the agglomerated CB pallet particles in 25-kg or 1000-kg bags for shipping. Here, the occupational workers are most susceptible to exposure by coming in close contact with inhalable particles, where the average mass concentration of PM with a dae from 100 nm to 1000 nm is on the order of 240 $\mu g.m^{-3}$, which is twenty times more concentrated than that of comparable but safe ambient sites (Kuhlbusch et al. 2004). The in vivo study at a CB production plant in Beijing, China, conducted by Zhang et al. (2014), showed that the CB particles are partially responsible for altered lung function and inflammation of packaging workers exposed to acetylene CB particles. Their

comparison sites maintained a PM level according to the guidelines recommended by the American Conference of Governmental Industrial Hygienists, the American Industrial Hygiene Association, and the German MAK Commission (Brook et al. 2004).

Exposure to UFPs in the metal industry workplaces is also a health concern to occupational workers, causing an increased risk of developing respiratory, cardiovascular, and neurological disorders. Wire-cut electrical discharge machining (WEDM) is very popular in die and mold manufacturing industries for producing delicate concave shape products. This process utilizes a high voltage between the wire electrode and the conductive metal pieces to cause flamboyant energy sparks, which remove material by melting and erosion, and the high-energy electrophysical process is the primary cause for generating nano-sized iron oxide particles (Tonshoff et al. 1996, Sivapirakasam et al. 2011). In a typical WEDM machine shop, nanoparticle number concentration is dominated by particles with $d_{ae} \leq 30$ nm, while particles with dae $\geq 60$ nm dominate mass and surface area concentration.

Tian et al. (2017) reported an in vitro inhalation study with realistic nasal and upper airway replicas and extrapolated the human lung tumor risk recommended exposure limits of WEDM-generated UFPs mass and number concentrations. However, their study could not show the effects of particle size distribution on deposition fraction or the implication to the human lung's regional airway in vivo dosages because such studies have health risks involved. Moreover, the investigations on detailed human inhalation and PM transport processes are restrictive from time, cost, and ethical perspectives. Also, in view of the health risks involved, individuals cannot be exposed to various toxic UFPs under different breathing scenarios and working conditions (Hofmann 2011, Nahar et al. 2013). Besides, these toxicities are inherent in the industrial workplace's ambient air.

To overcome this problem, in silico modeling and simulation can be an alternative way to computationally replicate the particle flow, distribution, and deposition. Understanding these limitations and opportunities, the present work adopted the Multiple Path Particle Dosimetry (MPPD) model based on a stochastic human lung morphology with realistic asymmetries at the airway branching structure. The novelty of this work is that the MPPD modeling technique closely fits reality due to its application of actual airway geometry (e.g., diameter, length, trachea-bifurcation angle, and intrabronchial angles) and the asymmetry of lung morphology (Bui et al. 2020). Moreover, the deposited PM concentration in each airway is calculated as a function of time for the proximal and distal ends.

There were two objectives of this work. Compare and fit MPPD model simulated data of the total lung deposition, regional deposition, and deposited mass of particles in regard to time and size distributions with (1) in vivo data on CB particles exposed workers' pulmonary function and pro-inflammatory cytokines conducted by Zhang et al. (2014) and (2) lung burden data of in vitro WEDM particles deposition investigation by Tian et al. (2017).

## MATERIALS AND METHODS

The present in silico study employed the MPPD simulation model computer software version 3.04, developed by Applied Research Associates (ARA) of Albuquerque, New Mexico, USA (ARA 2021). The MPPD is a software accepted by the inhalation toxicology scientific community. This computational model can estimate human and laboratory animal inhalation particle dosimetry. The model applies to risk assessment, research, and education, as reported elsewhere (Miller et al. 2016, Li et al. 2016, Backman et al. 2018, Manojkumar et al. 2019, Kuprat et al. 2021).

There have been confirmed cases and reports demonstrating the link between human pulmonary functional impairment and chronic exposure to various doses of metallic particles (Mayer-Baron et al. 2007, Nahar et al. 2013). In the MPPD simulation model, mechanistic modeling of local exposure can potentially speed up and improve the chances of successfully estimating inhaled particles. This multiscale computer model was designed to reasonably predict regional depositions of fine and UFP exposure following inhalation. Furthermore, these computer-based models are useful for comparing the available underpinning in vivo and in vitro data. Here, the physical, mechanical, and electrical properties of CB-PMs with a size range of 100 nm $\leq d_{ae} \leq$ 1000 nm and UFPs from WEDM, with mass median $d_{ae}$ in the range of 1 to 100 nm, were used as input parameters of the MPPD.

A flowchart of the Multiple Path Particle Dosimetry simulation sequence and implementation is given in Fig. 1. The model can run single or batch jobs with age-specific lung geometries, and plots can be drawn for mass flux or mass per surface area vs. lung generations or anatomical units. The MPPD user chooses various parameters of airway morphometry, inhalant properties, exposure boundary conditions, deposition, and clearance. The setting loop continues until the user accepts upon reviewing the simulation protocol.

In vitro experimental study indicated that the quantity of particles reaching the respiratory tract is directly proportional to the lung burden. However, the particle deposition in the lungs is also governed by other factors. For example, the diameter of the inhaled particles, the concentration of
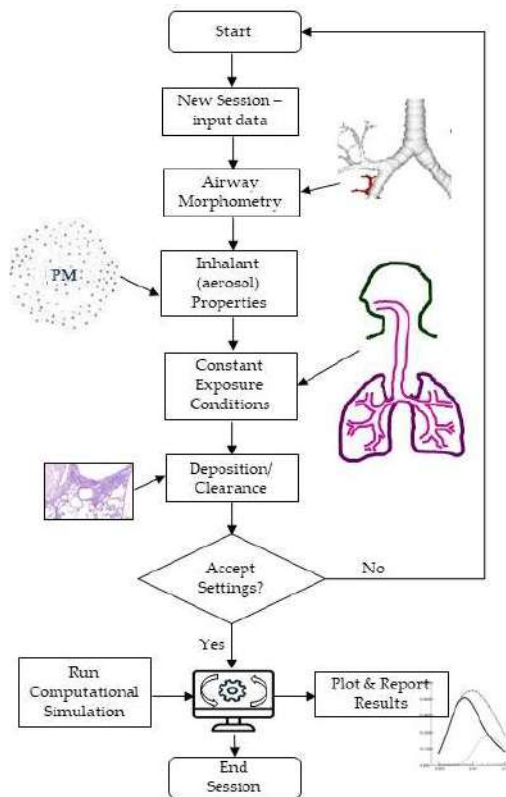


Fig. 1: The flowchart of the Multiple Path Particle Dosimetry simulation sequence and implementation.

particles per unit volume, and the inhalation rate constitute the determinant factors for their deposition in different parts of the respiratory tract (Yeh et al. 1976). This deposit interacts with different fundamental physical, aerodynamic, and electromechanical mechanisms. Among them, the inertial impaction, gravitational settling, Brownian diffusion, and the electrostatics forces are dominant processes (Ali et al. 2009, Hinds 2012). Asgharian et al. (2001) listed the original studies during the past six decades that were undertaken to develop the fundamental mathematical equations of these deposition mechanisms, and the MPPD computational model implemented these calculations in its software coding. Additional information on the MPPD model development and its features can be found elsewhere (Miller et al. 2016).

In the MPPD model, PM deposition computations are available for twenty-eight human respiratory airway anatomical units (Asgharian et al. 2001, Kuprat et al. 2021). Each anatomical unit is called a generation. Nevertheless, it is typical in most respiratory deposition studies to include twenty-four generations by counting the trachea as the first generation and the alveolar sacs as the last generation. Prior to the trachea, the MPPD considers four anatomical units, including the nose, mouth, esophagus, and larynx,

as the Head region. Thereafter, it considers the trachea to an additional fifteen anatomical units up to the terminal bronchioles as the tracheobronchial (TB) region and from the respiratory bronchioles to the alveolar sacs as the pulmonary (P) region.

The MPPD simulation assumes an average lung morphometry for the study population. There may be interindividual variability in airway structure, which may cause variations with in vitro studies. It also considered airway branching to be perfectly dichotomous. Furthermore, each airway branch is assumed to be cylindrical and straight, characterized by length, diameter, the angle the airway makes with its parent, and a gravity angle.

The model calculated the deposition fraction (DF) as the ratio of specific-size particles deposited in a particular region (Head, TB, and P) to the number of same-size particles entering the region. This notion is aligned with the reported literature (Cheng 1995). The PM, properties such as density, aspect ratio, diameter, or size, are necessary for calculation. In this model, the diameter can be specified to any of the three choices: count median diameter, mass median diameter, or mass median aerodynamic diameter. The DF can be estimated and visualized at simulation outputs for particles between 1 nm and 100 μm. The model offers morphometry of several species, such as humans, rhesus monkeys, rats, mice, pigs, and rabbits. Here, the human species was selected. The MPPD incorporated a stochastic model with asymmetries, representing the sixtieth percentile of lung-size population for Chinese adult airways to fit study objectives. Such airway branching structure provides more realistic flow and transport, eventually minimizing errors in deposition predictions.

To run the simulation software, input data such as airway morphometry, exposure conditions, and PM properties must be provided by default or user-specified values. Workers' lung airway morphometric parameters were as follows: gender was male, average age was forty-five years, BMI was 25 kg.m$^{-2}$, and the body was in an upright orientation while working. The user-specified values were given for the functional residual capacity (3174 mL), upper respiratory tract volume (50 mL), breathing frequency (16), and tidal volume (537.5 mL) to comply with the International Commission on Radiological Protection (ICRP) and model recommendations (ICRP 1994).

The fine or ultrafine particles generated from CB and WEDM are usually of irregular shapes, so the equivalent $d_{ae}$ was necessary to determine by the in situ scanning mobility particle spectrometer, as reported in both studies. These input data were applied in the MPPD to quantify the number and mass depositions of particles in the human airway, including the Head or extrathoracic, TB, and P regions of the exposed workers in the industrial workplace. PM size data was converted into mass data using the formula mass = density × volume. The mass, m, of each particle, was therefore calculated by the following equation:

$$m = \frac{\rho \pi d_{ae}^3}{6} \qquad \ldots(1)$$

P is the unit density, and $d_{ae}$ is the aerodynamic diameter or particle size. The MPPD calculates particle size distribution data, which can be analyzed by an Excel spreadsheet and develop the necessary plots. The model was developed for assessing deposition and clearance doses upon specifying all the input data.

## RESULTS AND DISCUSSION

Currently, too few examples in the literature combine a transparent presentation of key in vivo or in vitro UFPs as lung dosages. Therefore, epidemiological outcomes and mechanistic in silico model simulations are warranted to provide a sufficient database for validating and improving existing mathematical models. From this point of view, the adopted MPPD computational model in the present study provides necessary transparency regarding underlying assumptions, which may open the accessibility and acceptance by peer reviewers. Here, the simulation methodologies followed the same approaches as previously reported literature (Miller et al. 2016, Li et al. 2016, Backman et al. 2018, Manojkumar et al. 2019, Kuprat et al. 2021).

### Fit with Known Data of Zhang et al. (2014)

In their in vivo study on toxicological data of CB particles in the workplace, Zhang et al. (2014) found evidence of a link between human exposure to acetylene CB and long-term pulmonary effects. Their study focused on a work environment of CB production's packaging facility, where 51% of particles were less than 523 nm ($d_{ae} < 0.523$ μm), and the remaining were in the size range of 523 nm to 1000 nm. The mean particle concertation was 14.9 mg/m$^3$, 4.26 times higher than the NIOSH suggested threshold of 3.5 mg.m$^{-3}$ (Cassinelli and O'Connor 1994). The study subjects were 81 human volunteers with an average age of forty-five years at a CB production plant in Beijing, China, and the control was 104 nonexposed male workers.

In the experimental protocol, Zhang et al. (2014) evaluated clinical symptoms and lung functions of forced expiratory volume in 1 second (FEV1%), percent predicted peak expiratory flow (PEF%), and percent predicted maximal mid-expiratory flow (MMF%). These indicators were 5.54, 15.26, and 9.79 percent decrease compared with

the control workers. The pro-inflammatory cytokine levels in the serum of CB-exposed workers were 2.86 to 4.87 fold higher compared to controls. In summary, their study evidenced a link between human exposure to CB and lung functional impairments, which led to the toxicity of long-term respiratory distress.

To fit with the in vivo study, the present in silico MPPD modeling simulated CB exposure standard particle size distribution from 100 nm (0.1 μm) to 1000 nm (1 μm) and other PM properties as reported by Zhang et al. (2014). Also, their study subjects were male workers with an average age of forty-five years and an average BMI of 25 kg.m$^{-2}$. These values are considered as inputs of the MPPD's human physiological parameters. In addition, the PM exposure parameters include upright body orientation, 16 oronasal (nose and mouth combined) breathing frequency per minute, and 537.5 ml of tidal volume, as Roy et al. (1991) suggested. The breathing scenario was chosen as oronasal, a combination of nose and mouth breathing. The inspiratory fraction and tracheal mucous velocity were chosen to be 0.5 and 5.5 mm/min, respectively, to comply with ICRP and model recommendations.

The model also used the deposition and clearance approach because occupational workers usually breathe in this mode (Niinimaa et al. 1981). In a typical working day, a worker experiences a constant exposure of about six hours per shift except for lunch and other breaks. As such, each worker was assumed to be exposed for a period of six h/day, five days/week, and forty-four weeks/year. The model calculated lung deposition during exposure by the amount deposited in one breathing cycle.

The MPPD simulating human lungs' first ten generations of TB region is shown in Fig. 2. Even though the PM deposition calculation was done for all twenty-eight generations, Fig. 2 does not include respiratory bronchiole and P regions purposely because the entire lung geometry artifact will become an image of a black sponge where airway splitting will be invisible.

Notably, empirical and typical-path lung models are useful when quick calculations of regional and overall PM depositions are sought, but they produce limited information. Therefore, multiple-path and stochastic models are adopted in this study to determine more detailed site-specific deposition information like other computational fluid dynamics modeling techniques adopted by Kolanjiyila &Kleinstreuer (2017).

The conventional PM dosimetry recommendations are particles' either number or mass concentrations within a fixed aerodynamic size. So, as the present MPPD simulation model calculated both deposition and clearance of CB industrial workplace PM pollutants, Fig. 3 illustrates the particle size distributions deposited in various lung regions. Here, the total lung dose of 100 nm particles is the highest (28%), while 380 nm size particles are the lowest (15%). After that, the deposition increases with particle size again and reaches 26% for 1000 nm (1.0 μm). The size-segregated DF count of all inhaled particles is 20% in the entire respiratory airway of the lung. Out of these particles, about 27% are deposited in the Head airways. From the remaining 73% of particles, 32% and 41% deposit in the TB and P regions, respectively (Fig. 3).

The computed results demonstrated that the CB-PMs deposit highly in the TB and P regions. There is an important phenomenon that we will be going to explain here. As mentioned in the Introduction section, most CB particles leave the reactor in the 10 to 100 nm size range. Subsequently, large agglomerates (pellets) are formed by tumbling the newly made CB in a drum by mixing with water at the pelletizing step.

Moreover, Zhang et al. (2014) reported that these finished product particles with a 523 nm to 1000 nm size go for packaging, the last step of CB production. These particles



Fig. 2: Simulated lung geometry 1-10 airway generations or lung's anatomical units.
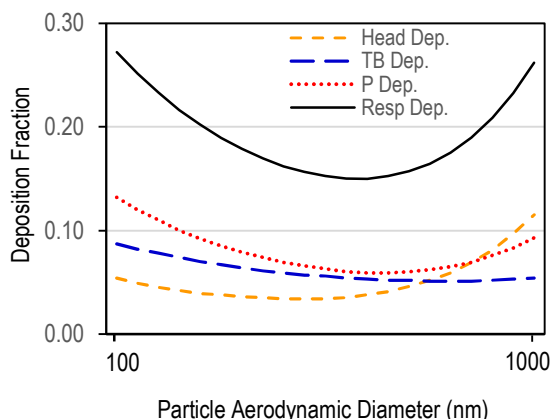


Fig. 3: Respiratory regional deposition fraction of inhaled carbon black PMs w.r.t particle size distribution. TB: tracheobronchial, P: pulmonary, Dep: deposition.

are heavier and neutral or carry no electrostatic charges. So, they tend to follow the inhaled fluid flow smoothly and move into the deeper lung to experience higher gravitational sedimentation and deposit superbly during each breath's pause moment.

Assessment of the total deposition of size-segregated PM fraction in the entire human lung airway is essential for further regional deposition investigations. The simulation model analysis showed that the total PM mass and count deposition in the human respiratory airways were 49% and 56% for 523 nm and smaller particles, respectively. Fine particles exhibited a higher mass deposition fraction (48%) in the Head and significantly (33%) in the P regions. Similar patterns are confirmed by the MPPD-generated images of deposited CB-PM mass at various lung lobes and mass flux per min (see Fig. 4a and 4b).

Fig. 4a shows the simulated visualizations of deposited CB-PM mass in the Head, TB, and P regions. It is found that PM mass concentration could reach as much as up to $2.23 \times 10^{-2}$ µg at the distal airways and the alveolar sacs. Fig. 4b depicts the simulated visualizations of deposited PM mass flux rate per unit area from the Head, TB, to P airways. It is also observed that the PM mass deposition rate could reach up to $2.72 \times 10^2$ µg/min/m$^2$. Observations in terms of DF in the line graphs confirm this trend.

To summarize, the in vivo study results of Zhang et al. (2014) and the present in silico MPPD simulations confirmed a relationship between CB-PMs as exposed in the workplace environment and altered lung functions of CB workers. However, it is difficult to further study the deposition characteristics using lung dissections following CB inhalation and the follow-up changes of lung inflammation in CB-exposed workers. Animal inhalation experiments

could be pursued to mimic the exposure conditions of CB workers.

### Fit with Known Data of Tian et al. (2017)

To determine the toxicity from exposure to UFPs in the WEDM process shop in Beijing, China, Tian et al. (2017) conducted an in vitro study. The UFPs were characterized in real-time at the production site, and this study found substantial emission of nano-pollutants by WEDM processes. The particle mass concentration was 27 mg/m$^3$, and the size distribution was in the range from 5.52 nm to 98.2 nm during a typical working day. Based on experimental data, the study found that particle dosimetry was extremely sensitive to real-time particle concentration and size distribution. To complement in vitro data, Tian et al. (2017) also carried out human inhalation simulations with realistic exposure conditions in a physiologically mimicked nasal and upper airway replica. Both study methodologies detected a substantial enhancement of WEDM respiratory DF with respect to UFP's number, mass, and surface area properties. For instance, study subjects' lungs acquired up to thirty-three-fold in mass, twenty-seven-fold in surface area, and eight-fold in number of dosages during working hours compared to controls.

A typical working day in the WEDM shop is from 8:00 a.m. to 5:30 p.m. The UFPs' exposure time is assumed to be 8 h, leaving 1.5 h for lunch and other activities. Mild physical activity was assumed because the machine operators perform their job responsibilities by mainly standing with the occasional walking to attend to the metal pieces. To fit with the in vitro study, the present in silico MPPD modeling simulated WEDM exposure standard particle size distribution from 1 nm to 100 nm and other UFP properties, as reported
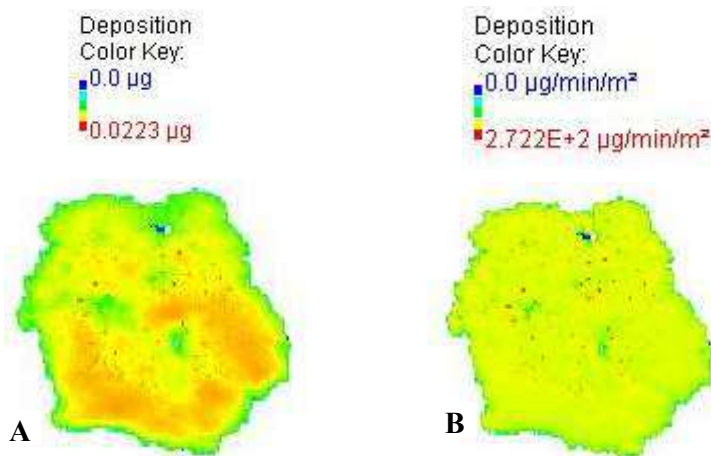


Fig. 4: Visualization of deposited CB-PMs at various lung lobes: (a) total mass; (b) mass flux per min per unit rate.

by Tian et al. (2017). In addition, it mimicked occupational workers' light breathing (12 L.min$^{-1}$) oronasal, a combination of nose and mouth breathing exposure. Here, it is notable that particle number counts are high for smaller particles, $d_{ae} <$ 20 nm, but their mass concentration is negligible. The mass concentration for larger than this size monotonically increases with particle size.

The MPPD model's human physiological parameters were employed, including an age of forty-five years and a BMI of 25 kg.m$^{-2}$. Moreover, the PM exposure parameters include upright body orientation, 16 oronasal (nose and mouth combined) positions, a breathing frequency per minute of 537.5 ml of tidal volume, and a pause and inspiratory fraction of 0.5, as Roy et al. (1991) suggested. The model also used a deposition and clearance approach because occupational workers usually breathe in this mode (Niinimaa et al. 1981). The typical constant exposure times at the WEDM packaging area are six hours per shift, five days a week, and forty-four weeks per year. Finally, the model output recommendations are in the total mass in number concentrations format. The MPPD model's human physiological parameters include an age of forty-five years and a BMI of 25 kg.m$^{-2}$. Fig. 5 illustrates the respiratory DF of inhaled WEDM UFPs with respect to the particle size distribution. In this simulation, inhaled UFP aerosol mass concentration and density were 27 mg.m$^{-3}$ and 2.7 g.cm$^{-3}$, respectively. Out of all deposited PMs, 50% of particle counts had an aerodynamic diameter of 5 nm or less. No particles smaller than 5 nm could reach the pulmonary region. The simulation also shows that 86% of all inhaled UFPs were deposited in the Head (mouth-throat) and tracheobronchial regions.
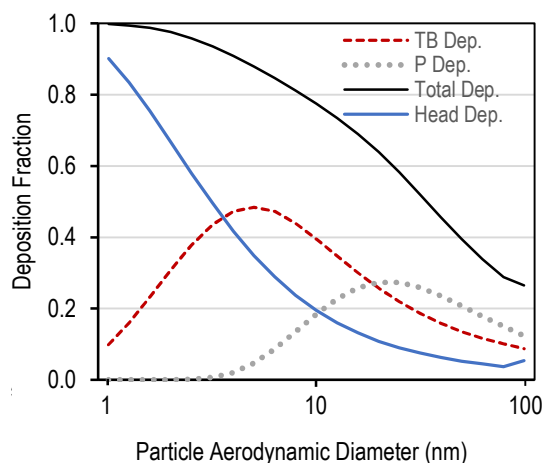
The present simulation calculated both deposition and clearance of WEDM industrial workplace UFP pollutants. The size-segregated DF count of all inhaled particles is 75% in the entire respiratory airway of the lung. Out of all deposited particles, about 44% settled in the Head airways. From the remaining 56% of particles, 38% and 18% were deposited in the TB and P regions, respectively (Fig. 5). The UFP tends to deposit highly in the Head and TB regions. Each particle's diffusive bombardment while wiggling in the lung's tabular airway can better explain this phenomenon. In addition, their Coulombic attraction (opposite charges between particles), due to electrostatic space charge force, and repulsion, due to same-charge polarity induced image charge forces, caused them to move toward the conductive airway walls and deposit subsequently.

In practice, the smaller the particle, the higher the charge-to-mass ratio and surface area. Therefore, the highest number of particles deposited in the Head region was smaller than 6.5 nm. In contrast, particles within the 25 to 35 nm size tend to deposit in the P region. This situation can be explained. As these particles pass conducting airways, they may lose charge by acquiring moisture from lung airways and become heavier and susceptible to deposit by gravitational sedimentation. Deposited mass per area in the lung's periphery or pulmonary regions is negligible for WEDM UFPs. See similar observations in the deposition line graphs of Fig. 6.

Tian et al. (2017) used industry-standard micro-nano-particle sizing, counting, and mobility analyzer instruments in their study. Their particle spectrometry detected 104/cc counts centration, which construed a mixture of iron, aluminum, copper, and trace elements of Mg, Mn, Mo, Zn, Ni, and Cr. These metallic components create larger (about



Fig. 5: Respiratory regional deposition fraction of inhaled wire-cut electrical discharge machining UFPs w.r.t particle size distribution. TB: tracheobronchial, P: pulmonary, Dep: deposition.
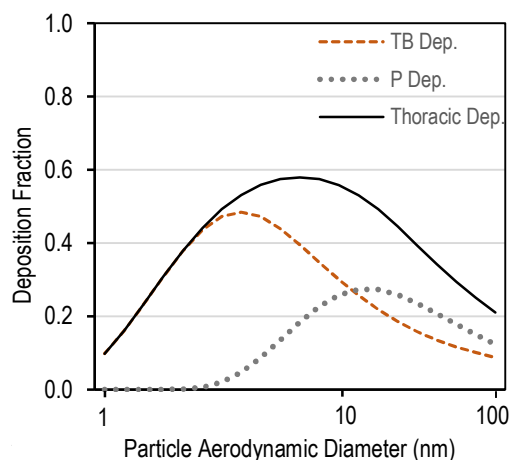


Fig. 6: Thoracic deposition fraction of inhaled wire-cut electrical discharge machining UFPs w.r.t particle size distribution. TB: tracheobronchial, P: pulmonary, Dep: deposition.
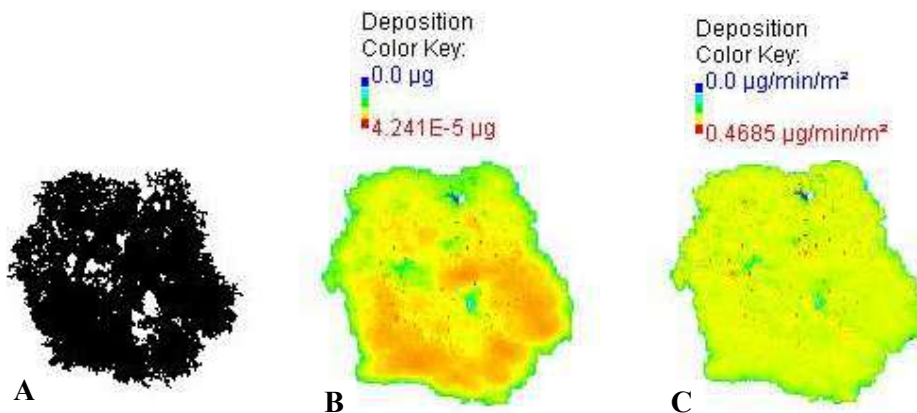
Fig. 7: Visualization of simulated lung geometry and deposited WEDM-UFPs at various lung lobes: (a) Stochastic lung morphological structure up to 16 generations; (b) Total mass deposition; (c) Mass flux per min per unit rate at various lobes.

2700 kg.m$^{-3}$) particle density. The MPPD used this value and calculated mass a deposition rate in 29.3 µg.m$^{-2}$.

Fig. 7a shows the simulated lung geometry or morphological structure up to sixteen generations. The remaining distal airways, including alveolar sacs, are not intentionally shown to prevent the image from becoming full solid black. Fig. 7b depicts the simulated visualizations of deposited UFP mass in the Head, TB, and P regions. It is found that the PM mass concentration could reach as much as up to 4.24 x 10$^{-5}$ µg at the distal airways and alveolar sacs.

Fig. 7c depicts the simulated visualizations of deposited UFPs mass flux rate per unit area from the Head, TB, to P airways. It is found that PM mass flux concentration could reach as much as up to 0.47 µg.min$^{-1}$.m$^{-2}$. Deposited mass per area in the lung's periphery or pulmonary regions is negligible for WEDM UFPs. See similar observations of depositions in line graphs in Fig. 5. This phenomenon can be explained by the fact that particles smaller than 50 nm experience higher surface charge-to-mass ratio, which caused them to deposit at the conductive Head and TB airways due to both space and image charge forces (Dumitran et al. 2008) because the particles' charge distributions are governed by their size and dielectric properties (Ali 2021, 2022).

All these studies have a good relationship with our present study results. Yet, our study's variation in deposition percentage is mainly due to the airway geometry, PM size, and unconsidered deposition mechanisms such as interception, van der Waals force, and adhesive force due to their negligible effects. More eminently, the MPPD mathematical equations considered all four crucial mechanisms that influence the PM depositions in airways, including (1) initial impaction, (2) gravitational sedimentation, (3) Brownian diffusion, and (4) electrostatic image/space charge forces.

Computational modeling and simulations can predict the UFP burden in the workers' lungs. However, the definitive evaluation of CB-induced carcinogenic effects is still insufficient, and more evidence from epidemiological studies in humans will help to understand the adverse effects of CB. Comparison of reported data (Zhang et al. 2014, Tian et al. 2017) versus model-predicted lung burdens in human lungs shows that the MPPD predictions are reasonably good. The simulated retained mass of poorly soluble fine and ultrafine particles in humans exposed to chronic inhalation occurs. To our knowledge, there is limited in vivo experimental data on regional-level deposition for CB- or WEDM-PM aerosols in human lungs.

Future work on additional model validation is needed for fine or ultrafine PMs of varying chemical characteristics. Such analyses would improve these particle doses' prediction for occupational safety and risk assessment.

**Study Limitations**

The computer-based models lack direct clinical validation beyond the first few airways (oropharynx and trachea) of the human lung's large conducting regions since available imaging methods (e.g., gamma scintigraphy) lack the required resolution (Backman et al. 2018). This drawback limits the full evaluation of deposition model robustness. Nevertheless, successful development and application of any pharmacokinetic modeling and simulation to predict regional exposure is likely to require at least an assessment of lung dose and, optimally, an assessment of deposition pattern, for example, distribution of particles in the lungs.

**CONCLUSIONS**

The present computational model has demonstrated the predictive power as a supplement to physical (either in

vivo or in vitro) models for assessing fine and ultrafine PM deposition in the realistic airways of extrathoracic, tracheobronchial tree, and pulmonary alveolar sacs like other models.

Compared with one in vivo and one in vitro source of experimental data in this work, satisfactory agreements are found regarding toxicity burdens and pulmonary function reduction. For example, a total lung dose of 100 nm CB-PMs is the highest (28%), while 380 nm is the lowest (15%). Afterward, deposition increases with particle size, reaching 26% for 1000 nm.

In the case of WEDM-UFPs, about 98% of all 1.0 nm inhaled particles remain in the lung. Subsequently, the deposition dose decreases with the particle size, reaching up to 28% for 100 nm size. Another notable point is that approximately 51% of deposited WEDM-UFPs are of CMAD $\leq$ 5 nm. Maximum deposited mass and mass flux rate in the Head, tracheobronchial, and pulmonary airways were also examined by the images of lung geometry.

Computational simulation of lung doses of harmful UFPs can overcome risks associated with investigations on detailed human inhalation, particle flow, and transport processes, which are restrictive from time, cost, and ethical perspectives. In conclusion, the practical application of this work demonstrated that the successful application of transparent mechanistic in silico models accompanied by robust experimental data on toxicity mechanisms could benefit the discovery of UFP inhalation toxicity to workers in chemical, steel, cement, and other industrial workplaces.

## ACKNOWLEDGMENTS

## REFERENCES

Abraham, J.L., Hunt, A. and Burnett, B.R. 2002. Quantification of non-fibrous and fibrous particulates in human lungs: twenty-year update on pneumoconiosis database. Ann. Occup. Hyg., 46(1): 397-401.

Ali, M. 2014. Engineered aerosol medicine and drug delivery methods for optimal respiratory therapy. J. Respir. Care, 59(10): 1608-1610. https://doi.org/10.4187/respcare.03634.

Ali, M. 2021. Computational fluid dynamics simulation of inhaled submicron bioaerosol particles flow and deposition in the human lung. Intl. J. Modern Engrg., 22(1): 5-11.

Ali, M. 2022. Multiple path particle dosimetry modeling employability to complement in-vitro ultrafine particle toxicity study. Current Trends Engrg. Sci., 2(2). DOI: 10.54026/CTES/1017.

Ali, M., Mazumder, M. K. and Martonen, T. B. 2009. Measurements of electrodynamic effects on the deposition of MDI and DPI aerosols in a replica cast of human oral-pharyngeal-laryngeal airways. J. Aerosol Med. Pulmon. Drug Del., 22(1): 35-44. https://doi.org/10.1089/jamp.2007.0637.

ARA (Applied Research Associates) 2021. Multiple Path Particle Dosimetry Model Version 3.04 [Computer Software]. Retrieved from https://www.ara.com/mppd. Retrieved 19 September 2021.

Asgharian, B., Hofmann, W. and Bergman, R. 2001. Particle deposition in a multiple-path model of the human lung. Aerosol Sci. Techno., 34(4): 332-339.

Backman, P., Arora, S. Couet, W., Forbes, B., Kruijf, W. and Paudel, A. 2018. Advances in experimental and mechanistic computational models to understand pulmonary exposure to inhaled particles. European J. Pharma. Sci., 113: 41-52. https://doi.org/10.1016/j.ejps.2017.10.030

Brook, R.D., Franklin, B., Cascio, W.E., Hong, Y., Howard, G., Lipsett, M., Luepker, R.V., Mittleman, M.A., Samet, J.M., Smith, S.C.J. and Tager, I.B. 2004. Air pollution and cardiovascular disease: A statement of the health care professionals from the expert panel on population and prevention science of the American Heart Association. Circulation, 109: 2655-2671.

Bui, V.K.H., Moon, J.Y., Chae, M., Park, D. and Lee, Y.C. 2020. Prediction of aerosol deposition in the human respiratory tract via computational models: a review with recent updates. Atmosphere, 11: 137-163. https://doi:10.3390/atmos11020137.

Cassinelli, M.E. and O'Connor, P.F. 1994. NIOSH manual of analytical methods. National Institute for Occupational Safety and Health. http://niosh.dnacih.com/nioshdbs/nmam/pdfs/5000.pdf. Retrieved 24 September 2021.

Cheng, K., Swift, D. L., Cheng, K. and Swift, D. L. 1995. Calculation of total deposition fraction of ultrafine aerosols in human extrathoracic and intrathoracic regions calculation of total deposition fraction of ultrafine aerosols in human extrathoracic and intrathoracic regions. Aerosol Sci. Technol., 22: 194-201. https://doi.org/10.1080/02786829509508887.

Ding, Y., Kuhlbusch, T.A.J., Tongeren, M. V., Jiménez, A. S., Tuinman, I., Chen, R. Alvarez, I.L., Mikolajczyk, U., Nickel, C., Meyer, J. Kaminski, H., Wohlleben, W., Stahlmecke, B., Clavaguera, S. and Riediker, M. 2017. Airborne engineered nanomaterials in the workplace- A review of release and worker exposure during nanomaterial production and handling processes. J. Hazard. Mater., 322: 17-28.

Douafera, H., Andrieub, V. and Brunela, J.M. 2020. Scope and limitations on aerosol drug delivery for the treatment of infectious respiratory diseases. J. Contr. Rel., 325: 276-292. https://doi.org/10.1016/j.jconrel.2020.07.002.

Dumitran, L.M., Blejan, O., Notingher, P., Samuila, A. and Dascalescu, L. 2008. Particle charging in combined corona-electrostatic fields. IEEE Trans. Ind. Appl., 44(5): 1385-1390. https://doi.org/10.1109/TIA.2008.2002935.

Hinds, W.C. 2012. Aerosol Technology: Properties, Behavior and Measurement of Airborne Particles. Second Edition. Wiley, New York.

Hofmann, W. 2011. Modelling inhaled particle deposition in the human lung: A review. J. Aerosol Sci., 4(10): 693-724. doi:10.1016/j.jaerosci.2011.05.007.

ICRP. 1994. Human Respiratory Tract Model or Radiological Protection. ICRP Publication 66. Ann. ICRP, 1-3. https://www.icrp.org/publication.asp?id=icrp%20publication%2066. Retrieved 24 September 2021.

Kolanjiyila, A.V. and Kleinstreuer, C. 2017. Computational analysis of aerosol dynamics in a human whole-lung airway model. J. Aerosol Sci., 114: 301-316. https://doi.org/10.1016/j.jaerosci.2017.10.001.

Kuhlbusch, T.A.J., Neumann, S. and Fissan, H. 2004. Number size distribution, mass concentration, and particle composition of PM1, PM2.5, and PM10 in bag-filling areas of carbon black production. J. Occup. Envir. Hygiene, 1(10): 660-671. DOI: 10.1080/15459620490502242

Kuprat, A.P., Jalali, M., Jan, T., Corley, R.A., Asgharian, B., Price, O., Singh, R.K., Colby, S. and Darquenne, C. 2021. Efficient bi-directional

coupling of 3D computational fluid-particle dynamics and 1D Multiple Path Particle Dosimetry lung models for multiscale modeling of aerosol dosimetry. J. Aerosol Sci., 151, https://doi.org/10.1016/j.jaerosci.2020.105647.

Li, X., Yan, C., Patterson, R.F., Zhu, Y., Yao, X., Zhu, Y., Ma, S., Qiu, X., Zhu, T. and Zheng, M. 2016. Modeled deposition of fine particles in the human airway in Beijing, China. Atmos. Environ., 124: 387-395. http://doi.org/10.1016/j.atmosenv.2015.06.045

Manojkumar, N., Srimuruganandama, B. and Nagendrab, S.M.S. 2019. Application of multiple-path particle dosimetry model for quantifying age-specified deposition of particulate matter in the human airway. Ecotoxicol. Environ. Safety, 168: 241-248. https://doi.org/10.1016/j.ecoenv.2018.10.091.

Matsoukas, T., Desai, T.G. and Lee, K. 2015. Engineered nanoparticles and their applications. J. Nanomatls, 2: 1-2. doi:10.1155/2015/651273.

Meyer-Baron, M., Schaper, M., Knapp, G. and Thriel, C.V. 2007. Occupational aluminum exposure: evidence in support of its neurobehavioral impact. Neurotoxicology, 28: 1068-1078.

Miller, F.J., Asgharian, B., Schroeter, J.D. and Price, O.T. 2016. Improvements and additions to the Multiple Path Particle Dosimetry model. J. Aerosol Sci., 99: 14-26.

Nahar, K., Gupta, N., Gauvin, R., Absar, S., Patel, B., Gupta, V., Khademhosseini, A. and Ahsan, F. 2013. In vitro, in vivo, and ex vivo models for studying particle deposition and drug absorption of inhaled pharmaceuticals. Euro. J. Pharma. Sci., 49: 805-818. https://doi.org/10.1016/j.ejps.2013.06.004.

Niinimaa, V., Cole, P. and Shephard, R.J. 1981. Oronasal distribution of respiratory airflow. Respir. Physiol., 43(1): 69-75. https://doi.org/10.1016/0034-5687(81)90089-X.

Roy, M., Becquemin, M.H. and Bouchikhi, A. 1991. Ventilation rates and lung volumes for lung modeling purposes in ethnic groups. Rad. Protect. Dosimet., 38(1-3): 49-55. https://doi.org/10.1093/rpd/38.1-3.49.

Seong Jo, M,. Kim. J.K., Kim, Y., Kim, H.P., Kim, H.S., Ahn, K., Lee, J.H., Faustman, E.M. Gulumian, M., Kelman, B. and Yu, J. 2020. Mode of silver clearance following 28-day inhalation exposure to silver nanoparticles determined from lung burden assessment, including post-exposure observation periods. Arc. Toxicol., 94: 773-784. https://doi.org/10.1007/s00204-020-02660-2

Sivapirakasam, S.P., Mathew, J. and Surianarayanan, M. 2011. Constituent analysis of aerosol generated from die sinking electrical discharge machining process. Process Safety Environ. Protec., 89(2): 141–50.

Tian, L., Shang, Y., Chen, R., Bai, R., Chen, C., Inthavong, K. and Tu, J. 2017. A combined experimental and numerical study on upper airway dosimetry of inhaled nanoparticles from an electrical discharge machine shop. Particle Fibre Toxicol., 14, Article 24. DOI 10.1186/s12989-017-0203-7.

Tonshoff, H.K., Egger, R. and Klocke, F. 1996. Environmental and safety aspects of electrophysical and electrochemical processes. CIRP J. Manufac. Sci. Techno., 45(2): 553-68.

Yeh, H.C., Phalen, R.F. and Raabe, G. 1976. Factors influencing the deposition of inhaled Particles. Environ. Health Perspect., 15: 147-156.

Zhang, R., Dai, Y., Zhang, X., Niu, Y., Meng, T., Li, Y., Duan, H., Bin, P., Ye, M., Jia, X., Shen, M., Yu, S., Yang, X., Gao, W. and Zheng, Y. 2014. Reduced pulmonary function and increased pro-inflammatory cytokines in nanoscale carbon black-exposed workers. Particle Fibre Toxicol., 11: 73. DOI 10.1186/s12989-014-0073.

## ORCID DETAILS OF THE AUTHORS

M. Ali: https://orcid.org/0000-0001-7255-5038

**Original Research Paper**  🔵 https://doi.org/10.46488/NEPT.2023.v22i04.018  **Open Access Journal**

# Multivariant Assessment of Metals Using Liverworts as an Appealing Tool in Catchment Sites of Uttarakhand, India

**Priyank Chaturvedi\*, Shivom Singh\*† and Kajal S. Rathore\*\***

\*Department of Environmental Sciences, ITM University, Gwalior, Madhya Pradesh, India
\*\*Department of Biotechnology, SMS Govt. Model Science College, Gwalior, Madhya Pradesh, India
†Corresponding author: Shivom Singh; shivomsingh101@gmail.com

## ABSTRACT

This study aimed to conduct a systematic review to analyze heavy metals seasonal concentrations in Uttarakhand tourist hotspot cities (Almora, Nainital, Ranikhet, Mussoorie, and Dhanaulti). A total of 45 samples of liverwort *Dumotiera hirsuta* were collected from five different cities during winter (Dry deposition) and monsoon (Wet deposition) in the year 2021. The concentrations of Zn, As, Cd, and Pb due to anthropogenic pollution load in the selected locations were analyzed by active biomonitoring using Inductive Coupled Plasma Mass Spectrometry (ICP-MS). Concentration loading of zinc, arsenic, cadmium, and lead was observed to be 79%, 71%, 48%, and 33%, respectively, higher during the dry (winter) season when compared with the monsoon dataset. Multivariant data were analyzed using Principal Component Analysis (PCA) with three components explaining maximum variation in data by factor loading through varimax rotation. The rapid growth and development have connected tourists to the mountain of the western Himalayas. Thus, a monitoring program is needed in these areas for further assessment. So that necessary action can be taken to conserve the eco-sensitive zones of Uttarakhand.

## INTRODUCTION

Heavy metals have become a global problem due to their toxicity and adverse environmental and human health effects (Fernandez et al. 2018). The presence of heavy metals in the atmosphere can be attributed to various many natural and human disturbances (Acharya et al. 2017). Metals such as Cd, Cu, Pb, Fe, and Zn are resistant to biological and chemical degradation and have instability and high toxicity, which have adverse effects on organisms. Therefore, a systematic study of these atmospheric elements of great interest (Zhu et al. 2008, Maleki et al. 2014, Singh et al. 2017).

Biomonitoring is a biological technique for measuring the extent of environmental pollution. One can assess the amount and impact of pollution on ecosystems by this method. This procedure is based on the examination of organisms that can accumulate environmental pollution. It provides an opportunity to obtain information on the quantitative and qualitative state of air pollution (Markert et al. 1999).

Heavy metals can break down some of our essential nutrients, and this can lead to lower immune defenses and many health issues. Complications such as headache, abdominal pain, dizziness, vomiting, diarrhea, reproductive problems failure, gastrointestinal cancer, disruption of hemoglobin biosynthesis and anemia, elevated blood pressure, kidney damage, miscarriage or minor miscarriage, the nervous system, brain damage, reduced learning ability in children, etc. have been observed in several studies (Irfan et al. 2013, Chakraborty et al. 2013, Jaishankar et al. 2014, Engwa et al. 2019).

The objective of the present research was to identify correlations between heavy metal concentrations determined in Liverwort and the seasonal variation of the atmospheric metal residue, which was used in active biomonitoring in the selected cities of Uttarakhand, India. The study was carried out in the western Himalayan region using Liverwort *Dumortiera hisuta* utilizing Inductive Coupled Plasma Mass Spectrometry to detect the following metals Zn, As, Cd, and Pb.

## MATERIALS AND METHODS

### Study Area

The study was conducted in five locations selected based on high tourist load during winter snowfall in the western Himalaya (Kumaon region), which covers the catchment sites of Nainital, Almora, and Ranikhet city and northwestern
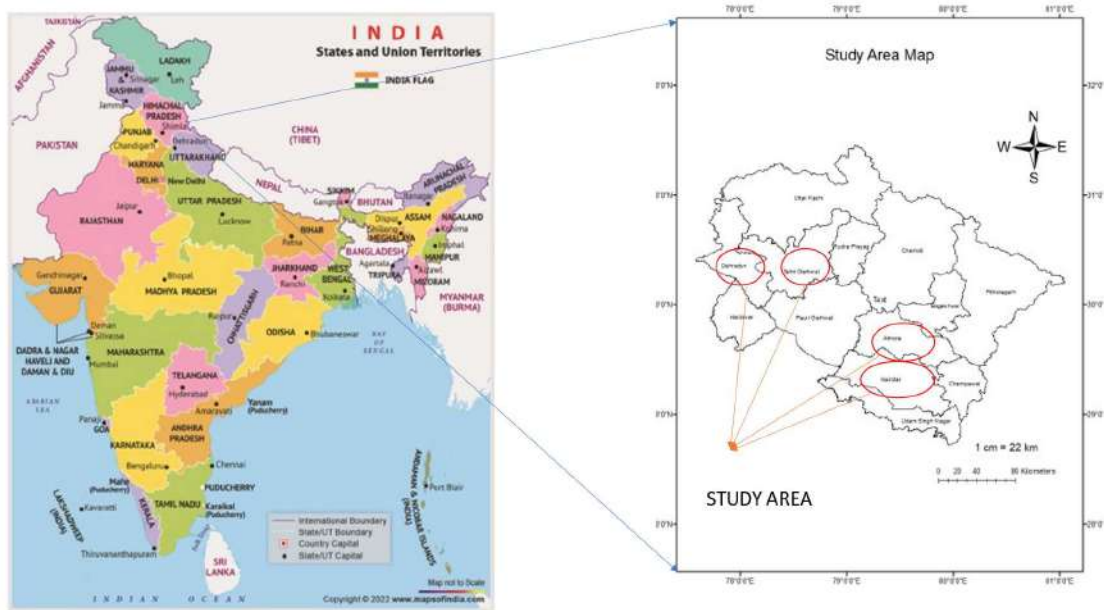
Fig. 1: Map showing different study locations (Almora, Ranikhet, Mussoorie, Nainital, Ranikhet, and Dhanaulti) of Uttarakhand, India.

Table 1: Showing meteorological data along with geo-coordinates of the sampling location.

| Sampling locations | Geo-coordinates | Temperature | Altitude |
|---|---|---|---|
| Mussoorie | 30°27'N 04°78'E | Max 20°C to 25°C<br>Min -1°C to 7°C | 6578 ft |
| Dhanaulti | 30°45' N 78°25' E | Max 20°C to 25°C<br>Min 1°C to 6°C | 7500 ft |
| Almora | 29°40' N 79°67' E | Max 15°C to 23°C<br>Min 0°C to 8°C | 5387ft |
| Ranikhet | 29°38' N 79°25' E | Max 13°C to 21°C<br>Min 0°C to °7C | 6132 ft |
| Nainital | 29°38' N 7945°' E | Max 16.6°C to 23.5°C<br>Min 1.7°C to 10.7°C | 6837 ft |

Himalaya (Garhwal region), which covers the city of Mussoorie and Dhanaulti (Fig. 1 and Table 1).

**Sample Collection**

Liverwort *Dumortiera hirsuta* was collected from the forest of Mukteshwar (control site), which is at an Altitude of 2300 meters (7545 ft). Twelve sampling sites in the city (Based on land use and land cover) at a distance of 0.5 km, 1 km, and 3 km were used for moss transplantation (Srivastava et al. 2014). Green moss was filled into a nylon bag and transplanted to study sites. Each moss bag was suspended 20 cm$^2$ above the ground in triplicate. For the dry season (November to February), samples were collected in the month of the first week of February 2021. For the wet season (July to October), samples were harvested in the first week of November 2021. Digestion and metal analysis

were performed on 0.5gm of moss samples to determine the concentration of specific metals using the ICPMS model (Agilent 7900) at IIT Delhi.

**Statistical Analysis**

Heavy metal concentration data analysis was performed with JMP (SAS) software to understand the statistical significance of the results. PCA was performed in MINITAB-18 to reduce the dimensionality of the data.

**RESULTS AND DISCUSSION**

The Zn, As, Cd, and Pb concentrations from the control site were found to be non-significant values when compared with the sampling cities dataset during both seasons monsoon 2021(Wet season) and winter 2021(Dry season). This analysis
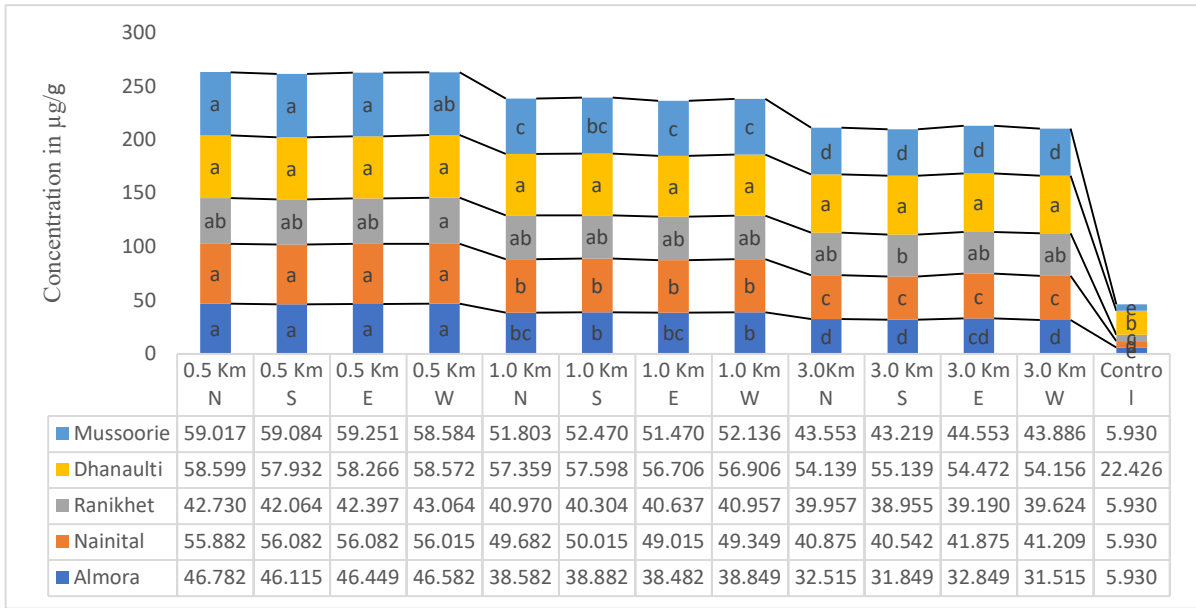
Fig. 2a: The concentration of zinc during Monsoon 2021 in Mussoorie, Dhanaulti, Ranikhet, Nainital, and Almora.

| | 0.5 Km N | 0.5 Km S | 0.5 Km E | 0.5 Km W | 1.0 Km N | 1.0 Km S | 1.0 Km E | 1.0 Km W | 3.0 Km N | 3.0 Km S | 3.0 Km E | 3.0 Km W | Control |
|---|---|---|---|---|---|---|---|---|---|---|---|---|---|
| Mussoorie | 59.017 | 59.084 | 59.251 | 58.584 | 51.803 | 52.470 | 51.470 | 52.136 | 43.553 | 43.219 | 44.553 | 43.886 | 5.930 |
| Dhanaulti | 58.599 | 57.932 | 58.266 | 58.572 | 57.359 | 57.598 | 56.706 | 56.906 | 54.139 | 55.139 | 54.472 | 54.156 | 22.426 |
| Ranikhet | 42.730 | 42.064 | 42.397 | 43.064 | 40.970 | 40.304 | 40.637 | 40.957 | 39.957 | 38.955 | 39.190 | 39.624 | 5.930 |
| Nainital | 55.882 | 56.082 | 56.082 | 56.015 | 49.682 | 50.015 | 49.015 | 49.349 | 40.875 | 40.542 | 41.875 | 41.209 | 5.930 |
| Almora | 46.782 | 46.115 | 46.449 | 46.582 | 38.582 | 38.882 | 38.482 | 38.849 | 32.515 | 31.849 | 32.849 | 31.515 | 5.930 |



Fig. 2b: The concentration of zinc during Winter 2021 in Mussoorie, Dhanaulti, Ranikhet, Nainital, and Almora.

| | 0.5 Km N | 0.5 Km S | 0.5 Km E | 0.5 Km W | 1.0 Km N | 1.0 Km S | 1.0 Km E | 1.0 Km W | 3.0 Km N | 3.0 Km S | 3.0 Km E | 3.0 Km W | Control |
|---|---|---|---|---|---|---|---|---|---|---|---|---|---|
| Mussoorie | 105.63 | 106.40 | 105.30 | 105.97 | 94.303 | 94.970 | 93.637 | 94.070 | 83.170 | 83.003 | 83.837 | 83.437 | 17.028 |
| Dhanaulti | 65.941 | 65.274 | 65.607 | 65.957 | 63.647 | 63.732 | 63.447 | 62.314 | 62.097 | 61.198 | 61.565 | 61.532 | 17.028 |
| Ranikhet | 74.231 | 73.898 | 73.997 | 74.228 | 72.895 | 72.228 | 72.562 | 73.362 | 71.028 | 71.362 | 71.695 | 71.495 | 17.028 |
| Nainital | 99.035 | 99.368 | 98.702 | 98.702 | 89.315 | 89.982 | 88.982 | 89.649 | 79.702 | 79.382 | 78.382 | 80.215 | 17.028 |
| Almora | 91.300 | 91.634 | 90.967 | 91.534 | 80.300 | 79.634 | 79.834 | 80.634 | 70.612 | 69.945 | 71.612 | 70.945 | 17.028 |

was conducted using the active biomonitoring method *Dumortiera hirsuta* samples collected at distances of 0.5 km, 1 km and 3 km in the east, west, north and south direction.

**Zinc**: Zinc results exhibited non-significant values at 0.5 km and 3 km during monsoon 2021 compared to its baseline (control) concentration (Fig. 2a). Zn is considered a biologically

active and living element, so it usually makes a complex with other environmental elements and can break down some essential nutrients (Stefanidou et al. 2006). The highest accumulation of zinc (59.251 µg.g-1 DW) was observed at 0.5 km in the Mussoorie catchment site, and non-significant values were also recorded at the same distance

to north (59.017 μg.g$^{-1}$) and south (59.084 μg.g$^{-1}$). Declining concentration was measured in Almora city of Kumaon region towards 3 km west (31.515 μg.g$^{-1}$), and non-significant values were observed at the north (32.515 μg.g$^{-1}$), south (31.849 μg.g$^{-1}$) and east (32.849 μg.g$^{-1}$) (Fig. 2a). However, researchers believed that Zn could originate from the abrasion of traffic lights and barriers (Carrero et al. 2012).



| | 0.5 Km N | 0.5 Km S | 0.5 Km E | 0.5 Km W | 1.0 Km N | 1.0 Km S | 1.0 Km E | 1.0 Km W | 3.0Km N | 3.0 Km S | 3.0 Km E | 3.0 Km W | Control |
|---|---|---|---|---|---|---|---|---|---|---|---|---|---|
| Mussoorie | 0.869 | 0.855 | 0.862 | 0.862 | 0.749 | 0.755 | 0.739 | 0.742 | 0.659 | 0.649 | 0.649 | 0.642 | 0.031 |
| Dhanaulti | 1.550 | 1.548 | 1.547 | 1.552 | 1.504 | 1.504 | 1.496 | 1.498 | 1.428 | 1.429 | 1.430 | 1.426 | 0.260 |
| Ranikhet | 0.829 | 0.822 | 0.826 | 0.831 | 0.800 | 0.796 | 0.801 | 0.797 | 0.774 | 0.772 | 0.773 | 0.775 | 0.031 |
| Nainital | 1.190 | 1.183 | 1.186 | 1.186 | 1.036 | 1.030 | 1.050 | 1.040 | 0.925 | 0.922 | 0.928 | 0.925 | 0.031 |
| Almora | 0.863 | 0.855 | 0.860 | 0.860 | 0.800 | 0.798 | 0.798 | 0.789 | 0.722 | 0.718 | 0.718 | 0.714 | 0.031 |

Fig. 3a: The concentration of arsenic during Monsoon 2021 in Mussoorie, Dhanaulti, Ranikhet, Nainital, and Almora.



| | 0.5 Km N | 0.5 Km S | 0.5 Km E | 0.5 Km W | 1.0 Km N | 1.0 Km S | 1.0 Km E | 1.0 Km W | 3.0Km N | 3.0 Km S | 3.0 Km E | 3.0 Km W | Control |
|---|---|---|---|---|---|---|---|---|---|---|---|---|---|
| Mussoorie | 1.665 | 1.672 | 1.652 | 1.655 | 1.510 | 1.507 | 1.503 | 1.520 | 1.408 | 1.415 | 1.398 | 1.402 | 0.212 |
| Dhanaulti | 1.634 | 1.640 | 1.650 | 1.652 | 1.610 | 1.614 | 1.612 | 1.612 | 1.555 | 1.552 | 1.557 | 1.554 | 0.212 |
| Ranikhet | 1.954 | 1.956 | 1.957 | 1.952 | 1.871 | 1.869 | 1.869 | 1.868 | 1.811 | 1.815 | 1.809 | 1.812 | 0.212 |
| Nainital | 2.645 | 2.655 | 2.659 | 2.662 | 2.495 | 2.475 | 2.482 | 2.489 | 2.355 | 2.342 | 2.349 | 2.352 | 0.212 |
| Almora | 1.965 | 1.952 | 1.955 | 1.958 | 1.765 | 1.768 | 1.755 | 1.745 | 1.530 | 1.529 | 1.531 | 1.532 | 0.212 |

Fig. 3b: The concentration of arsenic during Winter 2021 in Mussoorie, Dhanaulti, Ranikhet, Nainital, and Almora.

The highest concentration exhibited during winter 2021 was observed in Mussoorie of Garhwal region at 0.5 km south (106.400 µg.g$^{-1}$). Significant values were also observed at the same Km of north, east, and west. The maximum load of zinc was found in the Mussoorie region, which might be caused due to high traffic density and a major road component if the asphalt surface contains cobalt, nickel, zinc, etc. (Saxena et al. 2013). And lowest concentration was found in Dhanaulti at 3 Km south (61.198 µg.g$^{-1}$), and non-significant different values were observed at the same km of east (61.565 µg.g$^{-1}$) and west (61.532 µg.g$^{-1}$) (Fig. 2b). Zinc deposition in lichens was also discovered, which is frequently linked to increases in traffic along the roads that serve inner-city urban regions. Additionally, multiple studies discovered greater zinc concentrations in *Parmotrema* species found in metropolitan areas with high levels of automobile traffic (R Team 2015).

**Arsenic:** Compared to the baseline concentration, Arsenic (As) showed non-significant values in monsoon and winter 2021. The maximum concentration of As during monsoon 2021 was found in Mussoorie of Garhwal region at 0.5 km west (1.552 µg.g$^{-1}$), and non-significant values were also observed at the same distance north (1.550 µg.g$^{-1}$), south (1.548 µg.g$^{-1}$) and east (1.547 µg.g$^{-1}$). Minimum concentration was found in Almora of Kumaon region at 3 km west (0.714 µg.g$^{-1}$), and non-significantly different values were observed at the same distance in the north (0.722 µg.g$^{-1}$), south (0.718 µg.g$^{-1}$), and east (0.718 µg.g$^{-1}$) (Fig. 3a). Pollutant load decreased during monsoon could be attributed to two possible reasons, firstly, the low tourism load, and second, the less settlement time for atmospheric heavy metals.

The highest concentration of arsenic during winter 2021 was measured in Nainital of Kumaon region at 0.5 km west (2.662 µg.g$^{-1}$), and non-significant values were also observed at the same km in the north (2.645 µg.g$^{-1}$), south (2.655 µg.g$^{-1}$), east (2.662 µg.g$^{-1}$) respectively. The lowest concentration was found in Mussoorie of Garhwal region at 3 km west (0.714 µg.g$^{-1}$). Non-significantly different values were observed at the same distance of north (1.408 µg.g$^{-1}$), south (1.415 µg.g$^{-1}$), and west (1.402 µg.g$^{-1}$), respectively. Arsenic is mainly emitted from the mining industry, especially lead and zinc mining (Islam et al. 2015) (Fig. 3b). This could be because moss is frequently exposed to dust with airborne dust, which is rich in heavy metals (Markert & Weckert 2008).

**Cadmium:** During the monsoon of 2021, the highest concentration was found in the Dhanaulti catchment site of the Garhwal region at 0.5 km east (0.234 µg.g$^{-1}$), and non-significant values were also observed at the same distance in the north (0.233 µg.g$^{-1}$), south (0.230 µg.g$^{-1}$) and west (0.231 µg.g$^{-1}$). Cd is a substance that is primarily of anthropogenic origin and is released by the residential, industrial, and transportation sectors (Cuniasse & Glass 2020). Cd is probably also found in gasoline from the manufacture of cadmium compounds and colored plastic bags. An increase in vehicular pollution can be another factor for the rise in Cd level (Saxena et al. 2013). Declined concentration was observed in Mussoorie city at 3 km north (0.136 µg.g$^{-1}$), and non-significant values were observed at the same distance of south (0.138 µg.g$^{-1}$), east ((0.140 µg.g$^{-1}$), and west (0.141 µg.g$^{-1}$) (Fig. 4a). In addition, the transboundary pollution load of Cd-containing particles may travel far through wet and



| | 0.5 Km N | 0.5 Km S | 0.5 Km E | 0.5 Km W | 1.0 Km N | 1.0 Km S | 1.0 Km E | 1.0 Km W | 3.0 Km N | 3.0 Km S | 3.0 Km E | 3.0 Km W | Control |
|---|---|---|---|---|---|---|---|---|---|---|---|---|---|
| ■ Mussoorie | 0.173 | 0.175 | 0.174 | 0.174 | 0.157 | 0.155 | 0.158 | 0.154 | 0.136 | 0.138 | 0.140 | 0.141 | 0.014 |
| ■ Dhanaulti | 0.233 | 0.230 | 0.234 | 0.231 | 0.221 | 0.222 | 0.219 | 0.217 | 0.203 | 0.200 | 0.204 | 0.201 | 0.065 |
| ■ Ranikhet | 0.179 | 0.181 | 0.180 | 0.180 | 0.170 | 0.172 | 0.172 | 0.169 | 0.161 | 0.158 | 0.159 | 0.160 | 0.014 |
| ■ Nainital | 0.200 | 0.199 | 0.201 | 0.200 | 0.179 | 0.179 | 0.178 | 0.177 | 0.154 | 0.153 | 0.154 | 0.154 | 0.014 |
| ■ Almora | 0.195 | 0.193 | 0.197 | 0.193 | 0.179 | 0.177 | 0.178 | 0.178 | 0.163 | 0.164 | 0.163 | 0.166 | 0.014 |

Fig. 4a: The concentration of cadmium during Monsoon 2021 in Mussoorie, Dhanaulti, Ranikhet, Nainital, and Almora.

| | 0.5 Km N | 0.5 Km S | 0.5 Km E | 0.5 Km W | 1.0 Km N | 1.0 Km S | 1.0 Km E | 1.0 Km W | 3.0Km N | 3.0 Km S | 3.0 Km E | 3.0 Km W | Control |
|---|---|---|---|---|---|---|---|---|---|---|---|---|---|
| Mussoorie | 0.307 | 0.309 | 0.307 | 0.308 | 0.286 | 0.287 | 0.286 | 0.286 | 0.261 | 0.262 | 0.262 | 0.263 | 0.037 |
| Dhanaulti | 0.288 | 0.288 | 0.290 | 0.290 | 0.280 | 0.278 | 0.280 | 0.279 | 0.265 | 0.263 | 0.263 | 0.266 | 0.037 |
| Ranikhet | 0.312 | 0.313 | 0.312 | 0.311 | 0.299 | 0.297 | 0.300 | 0.298 | 0.281 | 0.279 | 0.280 | 0.283 | 0.037 |
| Nainital | 0.333 | 0.328 | 0.334 | 0.330 | 0.299 | 0.300 | 0.301 | 0.300 | 0.273 | 0.274 | 0.272 | 0.272 | 0.037 |
| Almora | 0.326 | 0.323 | 0.324 | 0.325 | 0.309 | 0.311 | 0.310 | 0.310 | 0.296 | 0.299 | 0.294 | 0.294 | 0.037 |

Fig. 4b: The concentration of cadmium during Winter 2021 in Mussoorie, Dhanaulti, Ranikhet, Nainital, and Almora.

dry deposition before settling on soil and aquatic systems (Sakata et al. 2008).

The maximum concentration loading of cadmium during winter 2021 was observed in the Nainital catchment of the Kumaon region at 0.5 km east (0.334 µg.g$^{-1}$), and non-significant values were also observed at distance to the north (0.333 µg.g$^{-1}$), south (0.328) and west (0.330). The concentration of cadmium was maximum in Dhanaulti during monsoon, possibly due to the influx of tourist visits to Tehri dam. Other sources include colored polyethylene bags, household waste, discarded plastics, utensils, etc., and the lowest concentration was found in Mussoorie of Garhwal

region at 3 km north (0.261 µg.g$^{-1}$). Non-significant different values were observed at the same distance in of south (0.261 µg.g$^{-1}$) and east (0.262 µg.g$^{-1}$) and (0.263 µg.g$^{-1}$), respectively (Fig. 4b). It is crucial to note that the emissions resulting from incinerated materials and their components, for example the quantity of dry batteries with varying Cd contents, will significantly differ based on how these materials are processed, whether they are segregated or burned.

**Lead:** The maximum concentration of lead during monsoon 2021 was found in Dhanaulti of Garhwal region at 0.5 km north (3.350 µg.g$^{-1}$), and non-significant values were also observed at the same distance south (3.347



| | 0.5 Km N | 0.5 Km S | 0.5 Km E | 0.5 Km W | 1.0 Km N | 1.0 Km S | 1.0 Km E | 1.0 Km W | 3.0Km N | 3.0 Km S | 3.0 Km E | 3.0 Km W | Control |
|---|---|---|---|---|---|---|---|---|---|---|---|---|---|
| Mussoorie | 2.559 | 2.565 | 2.542 | 2.545 | 2.372 | 2.359 | 2.362 | 2.365 | 2.169 | 2.175 | 2.175 | 2.185 | 0.112 |
| Dhanaulti | 3.350 | 3.347 | 3.340 | 3.343 | 3.281 | 3.279 | 3.271 | 3.274 | 3.226 | 3.224 | 3.223 | 3.221 | 0.711 |
| Ranikhet | 1.852 | 1.849 | 1.852 | 1.854 | 1.811 | 1.808 | 1.812 | 1.809 | 1.786 | 1.769 | 1.755 | 1.751 | 0.112 |
| Nainital | 2.147 | 2.133 | 2.140 | 2.157 | 1.967 | 1.973 | 1.963 | 1.969 | 1.796 | 1.787 | 1.778 | 1.771 | 0.112 |
| Almora | 2.134 | 2.130 | 2.131 | 2.130 | 2.044 | 2.039 | 2.040 | 2.042 | 1.935 | 1.932 | 1.935 | 1.929 | 0.112 |

Fig. 5a: The concentration of lead during Monsoon 2021 in Mussoorie, Dhanaulti, Ranikhet, Nainital, and Almora.

| | 0.5 Km N | 0.5 Km S | 0.5 Km E | 0.5 Km W | 1.0 Km N | 1.0 Km S | 1.0 Km E | 1.0 Km W | 3.0 Km N | 3.0 Km S | 3.0 Km E | 3.0 Km W | Control |
|---|---|---|---|---|---|---|---|---|---|---|---|---|---|
| Mussoorie | 4.984 | 4.964 | 4.971 | 4.978 | 4.878 | 4.864 | 4.864 | 4.871 | 4.754 | 4.764 | 4.744 | 4.751 | 0.589 |
| Dhanaulti | 3.747 | 3.750 | 3.744 | 3.745 | 3.705 | 3.703 | 3.702 | 3.704 | 3.667 | 3.662 | 3.660 | 3.661 | 0.589 |
| Ranikhet | 3.956 | 3.949 | 3.954 | 3.950 | 3.900 | 3.899 | 3.900 | 3.890 | 3.856 | 3.859 | 3.853 | 3.850 | 0.589 |
| Nainital | 4.317 | 4.330 | 4.324 | 4.327 | 4.107 | 4.144 | 4.134 | 4.147 | 3.940 | 3.954 | 3.960 | 3.964 | 0.589 |
| Almora | 4.332 | 4.352 | 4.345 | 4.342 | 4.142 | 4.132 | 4.135 | 4.138 | 3.830 | 3.845 | 3.846 | 3.856 | 0.589 |

Fig. 5b: The concentration of lead during Winter 2021 in Mussoorie, Dhanaulti, Ranikhet, Nainital, and Almora.

$\mu g.g^{-1}$), east (3.340 $\mu g.g^{-1}$) and west (3.343 $\mu g.g^{-1}$). The minimum concentration was found in Ranikhet of Kumaon region at 3 km west (1.751 $\mu g.g^{-1}$), and non-significantly different values were observed at the same distance in the north (1.786 $\mu g.g^{-1}$), south (1.769 $\mu g.g^{-1}$) and east (1.755 $\mu g.g^{-1}$) (Fig. 5a). Lead is derived from zinc, silver, and copper ores (MMSD 2010).

The highest concentration of lead during winter 2021 was found in Nainital of the Kumaon region at 0.5 km north (4.984 $\mu g.g^{-1}$), and non-significant values were also observed at the same km of the north (4.984 $\mu g.g^{-1}$), south (4.964 $\mu g.g^{-1}$) and east (4.971 $\mu g.g^{-1}$). The concentration loading of Lead was found to be maximum in Mussoorie due to industries located in Haridwar and Dehradun as well as emission of lead-based batteries (Sun et al. 2017b). The lowest concentration was found in Mussoorie of Garhwal region at 3 km east (3.660 $\mu g.g^{-1}$), and non-significantly different values were observed at the same distance in of north (3.667 $\mu g.g^{-1}$), south (3.662 $\mu g.g^{-1}$) and west (3.661 $\mu g.g^{-1}$) (Fig. 5b). Mining and other human activities discharge lead into the atmosphere, polluting soils and water (Makwe & Okobia 2020).

## Principal Component Analysis

The relationship between heavy metals and their association with winter (Dry season) and monsoon (Wet season) 2021 was done through a principal component with two components explaining maximum variation in data and followed by factor rotation through the varimax method.

The relationship between the cities and their correlation to heavy metal concentration. In the case of zinc (Zn), the first two components explained 99.9% of the total variance.

The factor loading for PC1, PC2, and PC3 indicated positive correlations with Nainital, Dhanaulti, and Mussoorie, and negative correlations with Almora and Ranikhet. The total variance of As in the cities explained by the first two components was 100.00%. The factor loading in PC1, PC2, and PC3 shows positive loading with Nainital and Ranikhet and negative loading with Almora, Dhanaulti, and Mussoorie. The total variance of Cd in cities explained by the first two components was 99.90%. The factor loading of Cd in PC1, PC2, and PC3 Almora and Mussoorie shows positive loading and negative loading with Nainital, Ranikhet, and Dhanaulti. The total variance of Pb between cities explained by the first two components was 100.00%. Factor loading of Pb for PC1, PC2, and PC3 varies greatly. All the components show positive loading with PC1 and Negative loading with PC2; in PC3, Almora, Dhanaulti, and Mussoorie show negative loading (Tables 2a and 2b). High vehicle traffic, the soil in the area, and the abrasion of brake pads, brake linings, car tires, paints, and other materials were all identified by the PCA as dust contributors' vehicle component varnishes and fuel combustion processes (Skorbiłowicz et al. 2020).

The relationship between the city with their correlation to heavy metal concentration. The total variance of Zn in the cities, explained by two components, was 100.00%. The factor loading of Zn for PC1, PC2, and PC3 was showed negative values for Nainital, Dhanaulti, and Mussoorie, while Almora and Ranikhet showed a positive loading. The total variance of arsenic between cities explained by the first two components was 100.00%. Factor loading of Pb for PC1, PC2 and PC3 varied significantly. All the components showed positive loading with PC1 and Negative loading with PC2; in PC3, Nainital and Ranikhet displayed negative loading, and Almora, Dhanaulti, and Mussoorie exhibited positive

Table 2a: The total variance of the Almora, Nainital, Ranikhet, Dhanaulti, and Mussoorie analyzed Liverwort during Monsoon 2021.

| Components | | Initial eigenvalues | | | Extraction sum of squared loadings | | | Rotation sums of squared loadings | | |
|---|---|---|---|---|---|---|---|---|---|---|
| | | Total | % of variance | Cumulative % | Total | % of variance | Cumulative % | Total | % of variance | Cumulative % |
| Zn | 1 | 4.841 | 96.800 | 96.800 | 4.841 | 96.800 | 96.800 | 2.618 | 52.400 | 52.400 |
| | 2 | 0.153 | 3.100 | 99.900 | 0.153 | 3.100 | 99.900 | 2.374 | 47.500 | 99.900 |
| | 3 | 0.004 | 0.100 | 100.000 | | | | | | |
| | 4 | 0.001 | 0.000 | 100.000 | | | | | | |
| | 5 | 0.000 | 0.000 | 100.000 | | | | | | |
| As | 1 | 4.927 | 98.500 | 98.500 | 4.927 | 98.500 | 98.500 | 2.518 | 50.400 | 50.400 |
| | 2 | 0.071 | 1.400 | 100.000 | 0.071 | 0.014 | 1.000 | 2.478 | 49.600 | 100.000 |
| | 3 | 0.001 | 0.000 | 100.000 | | | | | | |
| | 4 | 0.000 | 0.000 | 100.000 | | | | | | |
| | 5 | 0.000 | 0.000 | 100.000 | | | | | | |
| Cd | 1 | 4.972 | 99.400 | 99.400 | 4.972 | 99.400 | 99.400 | 2.518 | 50.400 | 50.400 |
| | 2 | 0.024 | 0.500 | 99.900 | 0.024 | 0.500 | 99.900 | 2.478 | 49.600 | 100.000 |
| | 3 | 0.001 | 0.000 | 100.000 | | | | | | |
| | 4 | 0.000 | 0.000 | 100.000 | | | | | | |
| | 5 | 0.000 | 0.000 | 100.000 | | | | | | |
| Pb | 1 | 4.963 | 99.300 | 99.300 | 4.963 | 99.300 | 99.300 | 2.536 | 50.700 | 50.700 |
| | 2 | 0.036 | 0.700 | 100.000 | 0.036 | 0.700 | 100.000 | 2.463 | 49.300 | 100.000 |
| | 3 | 0.000 | 0.000 | 100.000 | | | | | | |
| | 4 | 0.000 | 0.000 | 100.000 | | | | | | |
| | 5 | 0.000 | 0.000 | 100.000 | | | | | | |

Table 2b: Factor loadings for the Liverwort using (varimax rotation).

| Components | Zn | | | As | | | Cd | | | Pb | | |
|---|---|---|---|---|---|---|---|---|---|---|---|---|
| | PC1 | PC2 | PC3 | PC1 | PC2 | PC3 | PC1 | PC2 | PC3 | PC1 | PC2 | PC3 |
| Almora | 0.851 | 0.524 | -0.023 | 0.715 | 0.699 | -0.023 | 0.689 | 0.724 | 0.025 | 0.721 | -0.693 | -0.004 |
| Nainital | 0.798 | 0.602 | 0.038 | 0.779 | 0.627 | 0.016 | 0.774 | 0.633 | -0.009 | 0.626 | -0.780 | 0.008 |
| Ranikhet | 0.551 | 0.834 | -0.026 | 0.592 | 0.806 | 0.010 | 0.631 | 0.776 | -0.001 | 0.771 | -0.636 | 0.007 |
| Dhanaulti | 0.577 | 0.815 | 0.042 | 0.623 | 0.782 | -0.014 | 0.699 | 0.714 | -0.033 | 0.775 | -0.632 | -0.009 |
| Mussoorie | 0.788 | 0.614 | 0.026 | 0.808 | 0.588 | -0.010 | 0.747 | 0.664 | 0.020 | 0.655 | -0.755 | -0.015 |

loading. The total variance of Cd in the cities, explained by two components, was 100.00%. The factor loading of Cd for PC1 showed positive loading while in PC2, Nainital and Mussoorie show negative loading, and Almora, Dhanaulti, and Ranikhet showed positive loading. In PC3, Almora and Nainital, along with Ranikhet, Dhanaulti, and Mussoorie, showed negative loading. The total variance of Pb in the cities, explained by two components, was 100.00%. The factor loading of Pb is positive for all component in PC1 and negative for PC2 in PC3 Almora shows negative loading, and Nainital, Ranikhet, Dhanaulti, and Mussoorie shows positive loading (Table 3a and 3b). Source identification relies on correlation, which can confirm and explain PCA results (Jiang et al. 2019). The result of the PCA table, along with factor loading, indicates the source of metals and their association with other elements, and factor loading denotes their relation to other elements up to three components using varimax rotation.

## CONCLUSION

The study was designed to acquire information about the atmospheric heavy metals in the western Himalayan region. Mountains are a great site of attraction for tourists. Every year large population visits Uttarakhand for its natural beauty. The results imply that their simplicity, totipotency, high multiplication rate, and cost-effective tool make them excellent for pollution research. Research showed wet and dry metal contamination.

Table 3a: The total variance of the Almora, Nainital, Ranikhet, Dhanaulti, and Mussoorie for analyzed Liverwort during Winter 2021.

| Components | | Initial eigenvalues | | | Extraction sum of squared loadings | | | Rotation sums of squared loadings | | |
|---|---|---|---|---|---|---|---|---|---|---|
| | | Total | % of variance | Cumulative % | Total | % of variance | Cumulative % | Total | % of variance | Cumulative % |
| Zn | 1 | 4.880 | 97.600 | 97.600 | 4.880 | 97.600 | 97.600 | 2.649 | 53.000 | 53.000 |
| | 2 | 0.117 | 2.300 | 100.000 | 0.117 | 2.300 | 100.000 | 2.347 | 47.000 | 100.000 |
| | 3 | 0.001 | 0.000 | 100.000 | | | | | | |
| | 4 | 0.001 | 0.000 | 100.000 | | | | | | |
| | 5 | 0.000 | 0.000 | 100.000 | | | | | | |
| AS | 1 | 4.941 | 98.900 | 98.900 | 4.941 | 98.900 | 98.900 | 2.621 | 52.400 | 52.400 |
| | 2 | 0.056 | 0.100 | 100.000 | 0.056 | 0.100 | 100.000 | 2.375 | 47.500 | 100.000 |
| | 3 | 0.001 | 0.000 | 100.000 | | | | | | |
| | 4 | 0.000 | 0.000 | 100.000 | | | | | | |
| | 5 | 0.000 | 0.000 | 100.000 | | | | | | |
| Cd | 1 | 4.976 | 99.500 | 99.500 | 4.976 | 99.500 | 99.500 | 4.976 | 99.500 | 99.500 |
| | 2 | 0.022 | 0.400 | 100.000 | 0.022 | 0.400 | 100.000 | 0.022 | 0.400 | 100.000 |
| | 3 | 0.000 | 0.000 | 100.000 | | | | | | |
| | 4 | 0.000 | 0.000 | 100.000 | | | | | | |
| | 5 | 0.000 | 0.000 | 100.000 | | | | | | |
| Pb | 1 | 4.978 | 99.600 | 99.600 | 4.978 | 99.600 | 99.600 | 2.583 | 51.700 | 51.700 |
| | 2 | 0.021 | 0.400 | 100.000 | 0.021 | 0.400 | 100.000 | 2.415 | 48.300 | 100.000 |
| | 3 | 0.000 | 0.000 | 100.000 | | | | | | |
| | 4 | 0.000 | 0.000 | 100.000 | | | | | | |
| | 5 | 0.000 | 0.000 | 100.000 | | | | | | |

Table 3b: Factor loadings for the Liverwort using (varimax rotation).

| Components | Zn | | | As | | | Cd | | | Pb | | |
|---|---|---|---|---|---|---|---|---|---|---|---|---|
| | PC1 | PC2 | PC3 | PC1 | PC2 | PC3 | PC1 | PC2 | PC3 | PC1 | PC2 | PC3 |
| Almora | 0.828 | 0.561 | 0.003 | 0.595 | -0.803 | 0.006 | 0.998 | 0.057 | 0.021 | 0.643 | -0.766 | -0.005 |
| Nainital | 0.789 | 0.614 | -0.006 | 0.739 | -0.673 | -0.021 | 0.994 | -0.106 | 0.009 | 0.684 | -0.729 | 0.017 |
| Ranikhet | 0.566 | 0.824 | 0.018 | 0.784 | -0.621 | -0.023 | 0.999 | 0.038 | -0.009 | 0.760 | -0.650 | 0.003 |
| Dhanaulti | 0.612 | 0.790 | -0.03 | 0.803 | -0.596 | 0.007 | 0.998 | 0.062 | -0.008 | 0.762 | -0.648 | 0.001 |
| Mussoorie | 0.804 | 0.594 | -0.008 | 0.679 | -0.732 | -0.044 | 0.999 | -0.051 | -0.012 | 0.738 | -0.675 | 0.000 |

Additionally, bryophytes (mosses) are supportive and functional monitoring tools that could aid biomonitoring research around similar metal pollution sources and alert local inhabitants of potential metal deposition threats. A continuous monitoring program to understand pollution trends and protect the ecosystem and human health. Apart from it, future prospects reduce the pollution load and minimize the exposure of tourist sites. Public transport should be used, and the use of CNG and electrical vehicles should be encouraged.

## REFERENCES

Acharya, M.S., Satpathy, K., Panigrahi, S., Mohanty, A., Padhi, R. and Biswas, S. 2017. Concentration of heavy metals in the food chain components of the nearshore coastal waters of Kalpakkam, southeast coast of India. Food Contr., 72: 232-43.

Ayrault, S., Bonhomme, P., Carrot, F., Amblard, G., Sciarretta, M.D. and Galsomiès, L. 2001. Multianalysis of trace elements in mosses with inductively coupled plasma-mass spectrometry. Biol. Trace Elem. Res., 79(2): 177-184.

Carrero, J.A., Goienaga, N., Olivares, M., Martinez-Arkarazo, I. and Arana, G. 2012. Raman spectroscopy assisted with XRF and chemical simulation to assess the synergic impacts of guardrails and traffic pollutants on urban soils. J. Raman Spectros., 43: 1498-1503

Chakraborty, S., Dutta, A.R., Sural, S., Gupta, D. and Sen, S. 2013. Ailing bones and failing kidneys: a case of chronic cadmium toxicity. Ann. Clin. Biochem., 50(5): 492-495.

Cheng, K., Tian, H.Z., Zhao, D., Lu, L., Wang, Y., Chen, J. and Huang, Z. 2014. Atmospheric emission inventory of cadmium from anthropogenic sources. Int. J. Environ. Sci. Technol., 11(3): 605-616.

Cuniasse, B. and Glass, T. 2020. Emissions of greenhouse gases and atmospheric pollutants in France-Heavy Metals. CITEPA, Secten Report. https://www.citepa.org/wpcontent/uploads/1.3-ML_pdf. Accessed on 13 April 2021.

Engwa, G.A., Ferdinand, P.U., Nwalo, F.N. and Unachukwu, M.N. 2019. Mechanism and health effects of heavy metal toxicity in humans in poisoning in the modern world: New tricks for an old dog. Intech Open, 5: 577. DOI: http://dx.doi.org/10.5772/intechopen.82511.

Fernandez, M.R., Johnson-Restrepo, B. and Olivero-Verbel, J. 2018. Heavy metals in sediments and fish in Colombia's Caribbean coast: assessing the environmental risk. Inter. J. Environ. Res., 16: 1-13. https://doi.org/10.1002/jrs.4089.

Irfan, M., Hayat, S., Ahmad, A. and Alyemeni, M.N. 2013. Soil cadmium enrichment: Allocation and physiological manifestations. Saud. J. Biol. Sci., 20(1): 1-10.

Islam, M.S., Ahmed, M.K., Raknuzzaman, M., Habibulah-Al-Mamun, M. and Islam, M.K. 2015. Heavy metal pollution in surface water and sediment: A preliminary assessment of an urban river in a developing country. Ecol. Indic., 48: 282-291.

Jaishankar, M., Tseten, T., Anbalagan, N., Mathew, B.B. and Beeregowda, K.N. 2014. Toxicity, mechanism, and health effects of some heavy metals. Interdiscip. Toxicol., 7(2): 60-72. https://doi.org/10.2478/intox-2014-0009.

Jiang, N., Liu, X., Wang, S., Yu, X., Yin, S., Duan, S., Wang, S., Zhang, R. and Li, S. 2019. Pollution characterization, source identification, and health risks of atmospheric-particle-bound heavy metals in $PM_{10}$ and $PM_{2.5}$ at multiple sites in an emerging megacity in the central region of China. Aerosol Air Qual. Res., 19: 247-271. https://doi.org/10.4209/aaqr.2018.07.0275.

Makwe, E. & Okobia, E.L. 2020. Seasonal variation in accumulation of atmospheric heavy metals in bryophyte moss around the mining areas of Ebonyi state, Southeast Nigeria. GSJ., 8(4).

Maleki, A., Amini, H., Nazmara, S., Zandi, S. and Mahvi, A.H. 2014. Spatial distribution of heavy metals in soil, water, and vegetables of farms in Sanandaj, Kurdistan. Iran. J. Environ. Health. Sci. Eng., 12: 136.

Markert, B. and Weckert, V. 2008.Time and site-integrated long-term biomonitoring of chemical elements by means of mosses. Toxicol. Environ. Chem., 40(1-4): 43-56.

Markert, B., Wappelhorst, O., Weckert, V., Herpin, U., Siewers, U. and Friese, K. 1999. The use of bioindicators for monitoring the heavy-metal status of the environment. J. Radioanal. Nucl. Chem., 240: 425-429. DOI: 10.1007/BF02349387.

Ministry of Mines and Steel Development (MMSD). 2010. Lead-Zinc Exploration Opportunities in Nigeria. MMSD, The Federal Republic of Nigeria.

R Team. 2015. A Language and Environment for Statistical Computing. R Foundation for Statistical Computing., Vienna, Austria.

Sakata, M., Tani, Y. and Takagi, T. 2008. Wet and dry deposition fluxes of trace elements in Tokyo Bay. Atmos. Environ., 42: 5913-5922.

Saxena, D.K., Hooda, P.S., Singh, S., Srivastava, K., Kalaji, H.M. and Gahtori, D. 2013. An assessment of atmospheric metal deposition in Garhwal hills, India by moss *Rhodobryum giganteum* (Schwaegr.) Par. Geophytology, 43: 17-28.

Singh, S., Srivastava, K., Gahtori, D. and Saxena, D.K. 2017. Biomonitoring of atmospheric elements in *Rhodobryum giganteum* (Schwaegr.) Par., growing in the Uttarakhand region of the Indian Himalayas. Aerosol Air Qual. Res., 17(3): 810-820.

Skorbiłowicz, M., Skorbiłowicz, E. and Łapiński, W. 2020. Assessment of metallic content pollution and sources of road dust in the city of Białystok (Poland). Aerosol Air Qual. Res., 20(11): 2507-2518.

Srivastava, K. Singh, S. and Saxena, D K. 2014. Monitoring of metal deposition by moss *Barbula constricta* J. Linn., from Mussoorie Hills in India. Environ. Res. Eng. Manag., 62-54 :(1)67.

Stefanidou, M., Maravelias, C., Dona, A. and Spiliopoulou, C. 2006. Zinc: A multipurpose trace element. Arch. Toxicol., 80(1): 1-9.

Sun, C., Liu, J., Gong, Y., Wilkinson, D.P. and Zhang, J. 2017. Recent advances in all-solid-state rechargeable lithium batteries. Nano Energy, 33: 363-86.

Zhu, Y.G., Williams, P.N. and Meharg A. A. 2008. Exposure to inorganic arsenic from rice: a global health issue? Environ. Pollut., 154(2): 169-171.

# Removal of Brilliant Green Dye from Aqueous Solutions Using Multi-walled Carbon Nanotubes (MWCNTs): Linear and Nonlinear Isotherm Models and Error Analysis

**N. I. Mahdi\*, M.S. Falih\*, R. F. Abbas†\*, A. A. Waheb\* and A. A. Rahi\*\***

\*Department of Chemistry, College of Science, Mustansiriyah University, Baghdad, Iraq
\*\*Ministry of Oil/Iraq Drilling Company, Iraq
†Corresponding author: R. F. Abbas; rubaf1983@uomustansiriyah.edu.iq

## ABSTRACT

Current research explains the comparison of linear and nonlinear regression methods for finding the optimal isotherm study using experimental data for the adsorption of BG on multi-walled carbon nanotubes MWCNTs. BG dye maximum adsorption onto MWCNTs occurred at pH 2 and 35°C, with the apparent equilibrium reached after 15 min. In this study, five error functions were used: ERRS, Hybrid, Chi-square ($\chi^2$), ARE, and EABS. The values of error functions suggest that the Langmuir Linear type 3 is a suitable isotherm to describe the adsorption of BG on MWCNTs. The results showed that the Langmuir isotherm is a fit good isotherm to describe the adsorption process. The coefficient of non-determination ($K^2$) showed Hybrid, and ERRS were the preferable error functions used to predict the fit of linear and nonlinear isotherm models. Compared with other studies, MWCNTs can be used as a low-cost adsorbent with low contact time for the removal of BG dye from an aqueous solution.

## INTRODUCTION

Water pollution is one of the major causes of environmental pollution today. Dyes are colored organic compounds that are discharged into wastewater from many industries and cause serious pollution to the environment and humans (Al-Tohamy et al. 2022). Brilliant Green (BG) dyes are cationic, odorless green crystals and belong to the triphenylmethane family (Singh et al. 2022). This dye is dangerous and toxic to humans and animals, as it causes irritation in the digestive system and is a carcinogenic and mutagenic substance. When exposed for a long time, it leads to damage to organs, including the lungs (Mansour et al. 2021, 2020, Abbas 2020). It generates carbon dioxide, sulfur oxides, and nitrogen oxides during its decomposition. Therefore, removing this dye from the aqueous solution is very important because of its complete solubility (Salem et al. 2016, Rehman et al. 2013). It is used for a variety of purposes, including veterinary medicine, dyeing textiles, printing paper, and as an additive in poultry feed to prevent the formation of parasites and fungi (Mariah & Pak 2020, Fiaz et al. 2020). Adsorption is a common technique used to remove dyes and harmful substances from aqueous solutions. This technique has the advantages of low operating costs, simplicity, and

high efficiency (Mansour et al. 2021, 2020, Ali 2018). Many researchers used a variety of sorbents to remove this dye, such as red clay (Rehman et al. 2013), areca nut husk (Baidya & Kumar 2021), sawdust (Mane & Babu 2011), Luffa Cylindrical Sponge (Segun Esan et al. 2014), rice husk ash (Dahlan et al. 2019) and Ficus (Gul et al. 2023). Carbon nanotubes (CNTs) can be divided into two general types: single-walled carbon nanotubes(SWCNTs) and multi-walled carbon nanotubes (MWCNTs) (Alkaim et al. 2015). CNTs have properties similar to those reported for fullerenes, but other novels are of great importance in the fields of biology, electricity, and the environment (Rodríguez et al. 2020). CNTs have the potential to deliver drugs to cancer sites in a targeted and sustained manner (Raza et al. 2016). MWCNTs are inexpensive surfaces that have many properties as new and powerful adsorbents due to their large specific surface area, small size, and negative surface charge (Saxena et al. 2020, Abujaber et al. 2019). MWCNTs are more effective at removing cations due to the attractive force between the surface and the positively charged dye molecules with very short contact times, less amount, and high adsorption capacity (Karimifard & Alavi Moghaddam 2016, Ghaedi et al. 2016).

MWCNTs have gained great appeal due to unique properties such as electrical conductivity, large surface area, high mechanical strength, and chemical stability. Water-soluble functional groups such as carboxyl and amino groups are used for making the surface of MWCNTs hydrophilic due to their surface being hydrophobic (Hayat et al. 2022). It was widely used in electronic transistors (Gupta et al. 2009), biosensors (Crini et al. 2006), and optical components (Rida et al. 2013) because of its unique chemical, mechanical, and electronic properties (Wang et al. 2012). This study aimed to use MWCNTs as a low-cost, highly efficient, and available absorbent for the removal of BG dyes from aqueous solutions. The effect of different adsorption factors, such as solution pH, contact time, and temperature, was studied. In the present work, the initial behavior of BG dye removal onto MWCNTs was analyzed by the Langmuir and Freundlich isotherm models with linear and nonlinear regressions with error functions applied.

## MATERIALS AND METHODS

### Equipment

UV-visible (1800 Shimadzu) spectrophotometer, A shaking water bath (BS-11 digital, JETO Korea, TECH), and a pH meter (Hanna) were used in this study.

### Chemicals and Solutions

Multiwall Carbon Nanotubes (purity 90%) was obtained from Cheap Tubes Inc. (Grafton, VT 05146 USA) with a tube length of 10–30μm and outer diameter (o.d.) of 10–30 nm, brilliant green (BG) (Sigma-Aldrich), NaOH (BDH) and HCl (Fluka) were analytical reagent. 0.01 gm of BG dye was dissolved in 100 mL distilled water($100 \text{ mg.L}^{-1}$).

(0.5-3.5 mL) of BG dye were transferred from $100 \text{ mg.L}^{-1}$ solution BG dye followed by dilution using 25 ml of distilled water to prepare a series of various concentrations from 2 to $14 \text{ mg.L}^{-1}$. The pH effect study of BG solutions was adjusted using ($0.003 \text{ mol.L}^{-1}$) of HCl and NaOH.

### Adsorption Studies

A set of tubes containing 10 mL of $10 \text{ mg.L}^{-1}$ of BG dye solutions were used to carry out adsorption experiments. Three affected factors were investigated, namely: pH (2-9), temperature (35°C, 45°C, 55°C), and contact time (10-30 min.). The calibration curve of the BG solution showed that a maximum absorbance appeared at $\lambda_{max}$ of 624 nm and the molar absorptivity ($\epsilon = 0.131 \text{ L.g}^{-1}.\text{cm}^{-1}$). Three different temperatures (25°C, 35°C, 45°C, and 55°C) were tested as the isotherm for the adsorption of BG dye onto MWCNTs for 15 min. The efficiency adsorbed amount qe of adsorption BG dye and removal% defined as in equations (1) and (2) (Song et al. 2018, Das et al. 2018):

$$q_e = ((C_O - C_e) \times V/m \qquad \text{…(1)}$$
$$\text{Removal\%} = (C_o - C_e)/C_o \times 100 \qquad \text{…(2)}$$

Where Co and Ce are the initial and final concentrations of BG dye ($\text{mg.L}^{-1}$), respectively, m is the weight of MWCNTs surfaces (gm), and V is the volume of BG dye (L) (Rostamian & Behnejad 2018). The adsorption of a dye molecule onto a surface can be described by different models (like linear and nonlinear Langmuir and Freundlich), depending on the characteristics of the system being studied (Belhachemi & Addoun 2011). Langmuir isotherm described that there is a single layer of dye molecules on the surface and that the adsorption process is reversible and homogeneous. The Freundlich isotherm model is multilayer adsorption, where the adsorbate molecules form layers on top of each

Table 1: Equations of adsorption isotherm.

| Isotherm | Equation | Linearized form | Plot | Parameters |
|---|---|---|---|---|
| Langmuir type1 | $q_e = q_m K_L C_e/(1+KLCe)$ | $\dfrac{Ce}{qe} = \dfrac{1}{qmKL} + \dfrac{Ce}{qm}$ | (Ce/qe) vs. Ce | $qm = (\text{slope})^{-1}$, $K_L = (\text{slope/intercept})$ |
| Langmuir type2 | | $\dfrac{1}{qe} = \dfrac{1}{qmKLCe} + \dfrac{1}{qm}$ | $1/q_e$ vs.$1/Ce$ | $qm = (\text{intercept})^{-1}$, $K_L = (\text{intercept/slope})$ |
| Langmuir type3 | | $qe = qm - (\dfrac{1}{KL})\dfrac{qe}{Ce}$ | $qe$ vs. $qe/Ce$ | $qm = \text{intercept}$, $K_L = -(\text{slope})^{-1}$ |
| Langmuir type4 | | $\dfrac{qe}{Ce} = KLqm - Klqe$ | $qe/Ce$ vs. $qe$ | $qm = -(\text{intercept/slope})$, $K_L = -\text{slope}$ |
| Freundlich | $q_e = KFCe^{1/n}$ | Log $(q_e) = 1/n \log (C_e) + \log(K_F)$ | $Log q_e$ vs.$Log C_e$ | $K_F = \exp(\text{intercept})$, $n = (\text{slope})^{-1}$ |

$q_m$ ($\text{mg.g}^{-1}$) and $K_L$ ($\text{mL.mg}^{-1}$) are Langmuir constants; $K_F$ ($\text{mL.mg}^{-1}$) is the Freundlich constant, and n is the intensity of adsorption of the Freundlich isotherm model

Table 2: Equations of error functions.

| Error functions | Equations |
|---|---|
| Square error function (ERRS) | $\sum_{i=1}^{n} (q_{cal.} - q_{exp.})^2$ |
| Hybrid fractional error function(HYBRID) | $\dfrac{100}{n-p} \sum_{i=1}^{n} \dfrac{(q_{cal.} - q_{exp.})^2}{q_{cal.}}$ |
| Chi-square($X^2$) | $\sum_{i=1}^{n} \dfrac{(q_{cal.} - q_{exp.})^2}{q_{cal.}}$ |
| The average relative error (ARE) | $\dfrac{100}{p} \sum_{i=1}^{n} \dfrac{(q_{cal.} - q_{exp.})^2}{q_{cal.}}$ |
| the sum of the absolute errors (EABS) | $\sum_{i=1}^{n} \lvert (q_{cal.} - q_{exp.}) \rvert$ |

other. Freundlich supposed that the adsorption surface is heterogeneous (Table 1) (Sala et al. 2014).

## Error Analysis

Error functions are mathematical functions that are used to determine how well a particular isotherm model fits the experimental data. In this study, three error functions were calculated using Microsoft Excel and the origin lab® 16 (Table 2) (Subramanyam & Das 2014, McKay et al. 2014, Shahmohammadi-Kalalagh & Babazadeh 2014).

## RESULTS AND DISCUSSION

### Effect of pH

The acidity of the medium is the most important factor in adsorption (Machado et al. 2011). Different pH in the range (2-10) was studied (Fig. 1). All solutions were prepared at 0.003 mg of MWCNT dosage, 10 mg/L of initial BG dye concentration, and $35^oC$ for 15 min. The maximum percentage of BG dye removal when pH 2 was 92.8% (Fig. 2). An acidic medium (pH2) increases the removal of BG dye because of the electrostatic attraction between BG dye and the positive charge on the MWCNTs surface (Abualnaja et al. 2021).

### Effect of Contact Time and Temperature

The contact time influence of BG with 0.003 gm of MWCNTs was investigated for solutions with pH 2 and 10 $mg.L^{-1}$ concentration. The tests were achieved at 25, 35, 45, and 55°C (Fig. 3). The high removal percentage of BG onto the MWCNTs was achieved at 15 min and 35°C to sponsor the high adsorption and completed reaction. At first, the high rate of removal percentage is due to the greater number of active sites present on the surface of MWCNTs at 15 min and 35°C. After that, it becomes constant due to the lesser number of active sites left on the adsorbent surface (Figs. 4 and 5).

### Linear Isotherm Models

Five error functions- ERRS, HYBRID, Chi-square($\chi^2$), ARE, and EABS have been used as evidence to establish the best isotherm in this study. The linear forms type 2 of
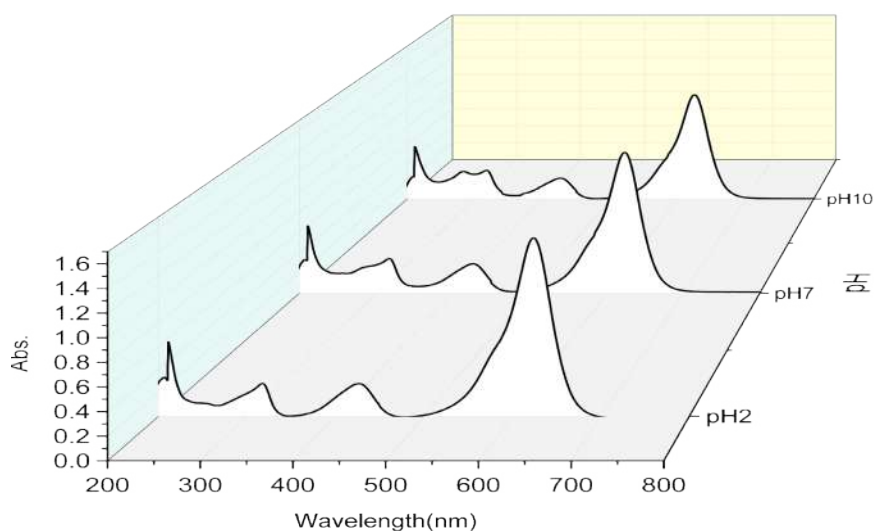


Fig. 1: pH stability of BG dye.
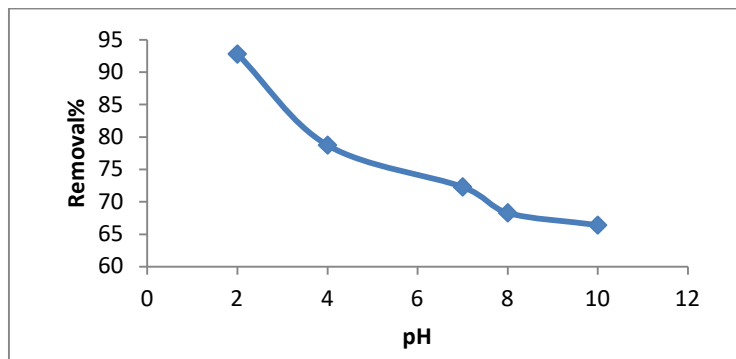
Fig. 2: Effect of pH on adsorption of BG dye onto MWCNTs.
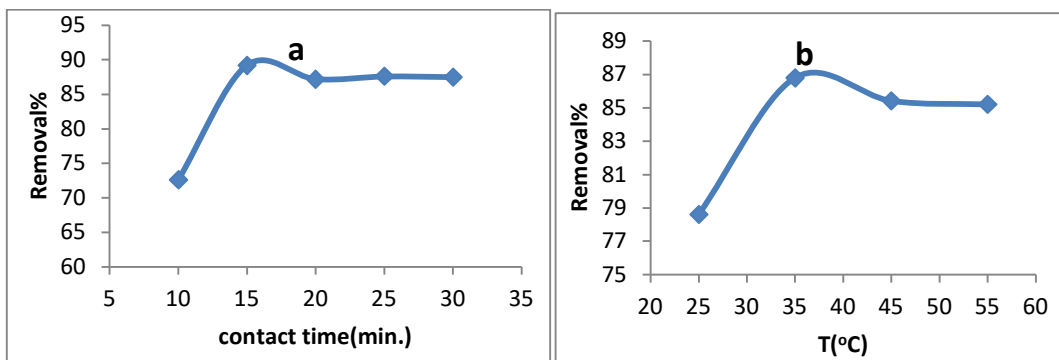


Fig. 3: Effect of (a) contact time and (b) temperature on adsorption of BG dye adsorption by MWCNTs.
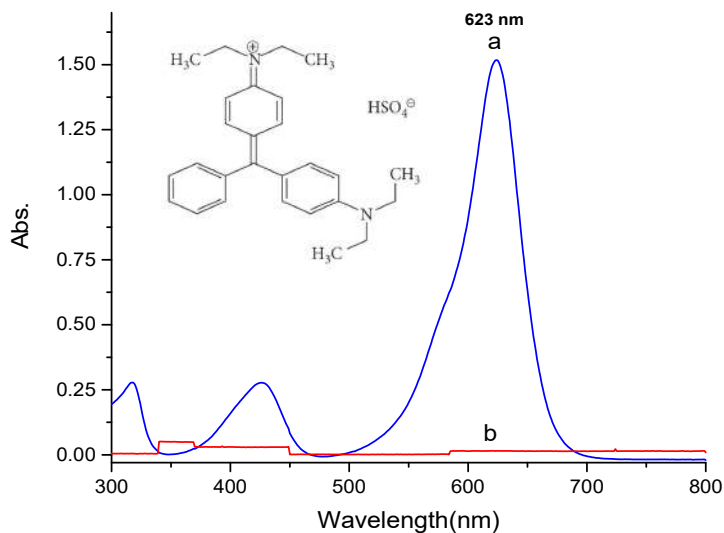


Fig. 4: UV-Vis absorption spectrum of 12 mg.L$^{-1}$ BG dye solution: a- before adsorption and b- after adsorption with 0.003 g of MWCNTs at pH 2, 15 min. and 35°C.

Langmuir isotherm models have shown a lower value of error function and the highest values of (R$^2$ 0.963) compared to other forms (Fig. 6). The low Langmuir error function value suggests that the adsorption of the BG dye onto the MWCNTs surface is a monolayer process. The surface is homogeneous with a limited number of identical adsorption sites, and the adsorption process is monolayer and reversible (Ayawei et al. 2017). According to the low value of the error
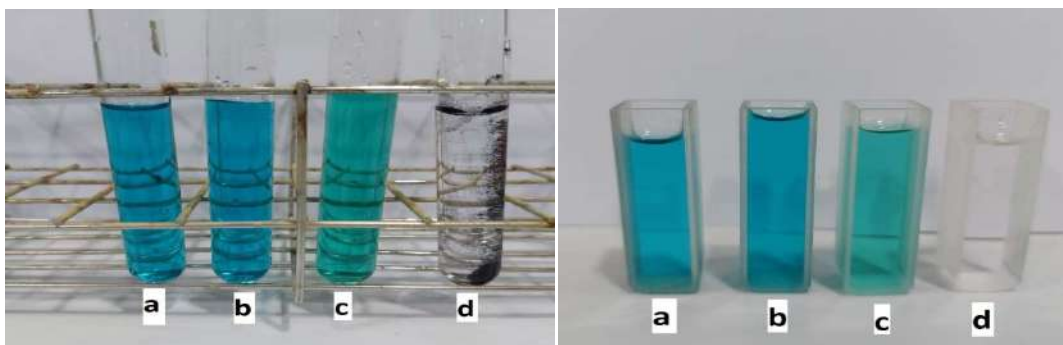
Fig. 5: photograph of 12 mg.L$^{-1}$ brilliant green dye before adsorption in a - pH 9, b - pH 7, c - pH 2, and d - after adsorption process with 0.003 g of MWCNTs at pH 2, 15 min, and 35°C.

functions, it could be considered that the linear Langmuir model is a more suitable isotherm for this study than the linear Freundlich model (Fig.7) (Table 3) (Piccin et al. 2011, Kumar & Sivanesan 2005, 2006).

**Nonlinear Isotherm Models**

Origenlab®16 was used to find the nonlinear forms of Langmuir and Freundlich isotherm (Fig. 8). Nonlinear
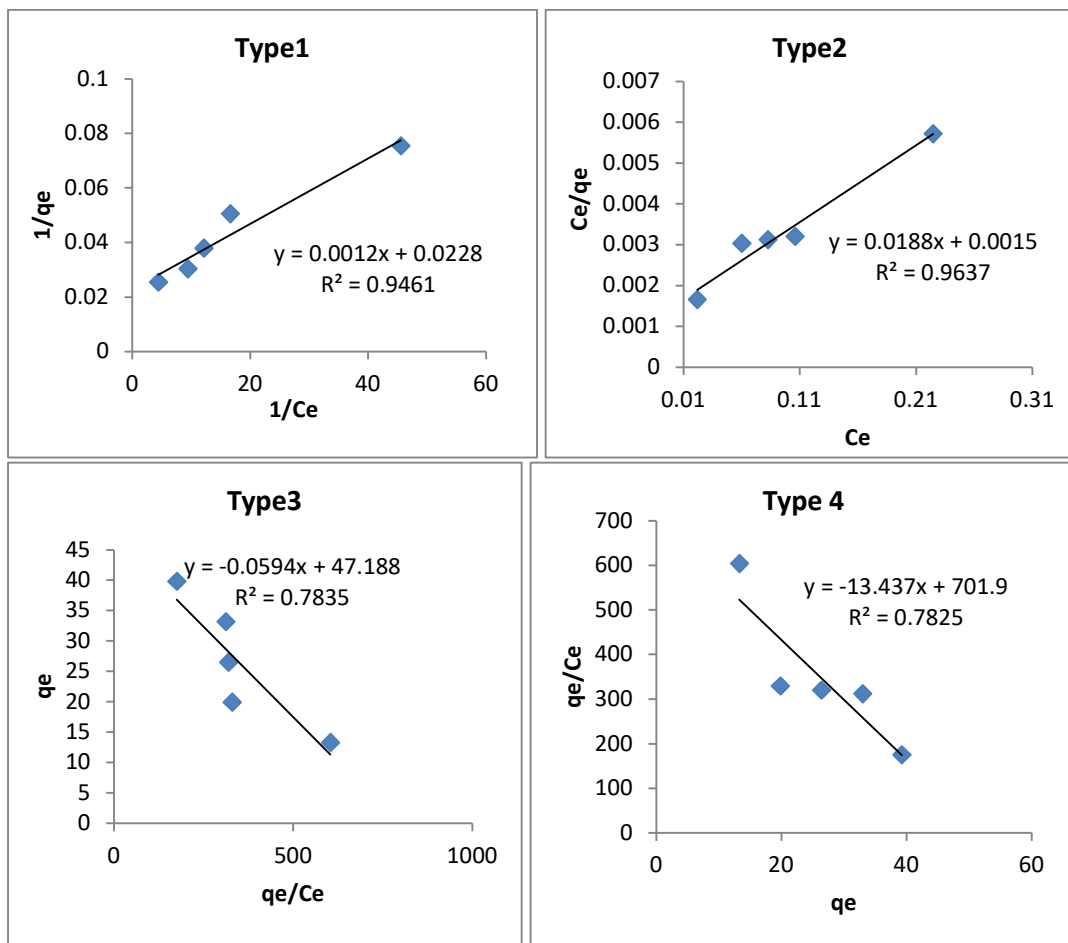


Fig. 6: Linear Langmuir isotherm models for removal of BG dye at 35°C.
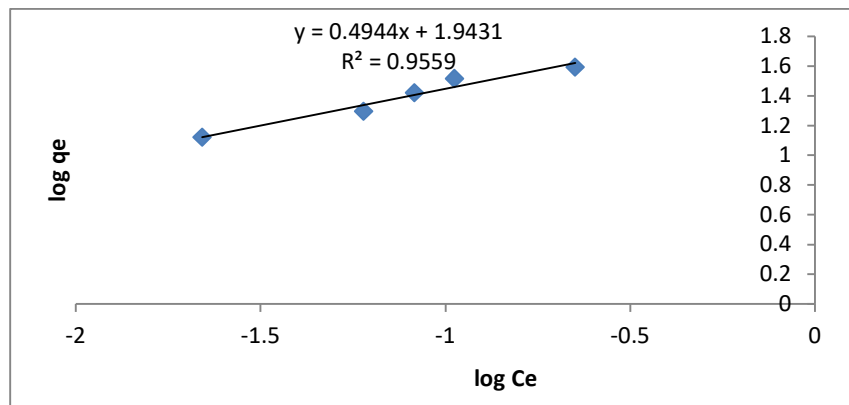
Fig. 7: Linear Freundlich isotherm models for removal of BG dye at 35°C.

Table 3: Adsorption parameters of BG dye onto MWCNT at 35°C for linear Langmuir and Freundlich isotherms.

| Adsorbent | Isotherm models | Parameters value | | ERRS | HYBRID | $\chi^2$ | ARE | EABS |
|---|---|---|---|---|---|---|---|---|
| MWCNTs | Langmuir Linear type1 | KL | 0.045 | 2.602 | **0.011** | 0.647 | 42.452 | 4.375 |
| | | $q_m$ | 1000 | | | | | |
| | | $R^2$ | 0.946 | | | | | |
| | Langmuir Linear type2 | $K_L$ | 0.055 | 3.892 | 81.643 | 79.624 | 49.997 | 5.267 |
| | | $q_m$ | 1000 | | | | | |
| | | $R^2$ | **0.963** | | | | | |
| | Langmuir Linear type3 | $K_L$ | 16.949 | 0.028 | 0.019 | **0.081** | 4.094 | **0.002** |
| | | $q_m$ | 47.18 | | | | | |
| | | $R^2$ | 0.783 | | | | | |
| | Langmuir Linear type4 | $K_L$ | 52.263 | **0.020** | 0.016 | 0.090 | **3.922** | 0.037 |
| | | $q_m$ | 13.430 | | | | | |
| | | $R^2$ | 0.782 | | | | | |
| | Freundlich linear | $K_f$ | 87.700 | 3.851 | 0.448 | 24.921 | 49.737 | 5.239 |
| | | n | 2.024 | | | | | |
| | | $R^2$ | 0.955 | | | | | |

Langmuir isotherm is the best nonlinear isotherm due to the higher value of $R^2$ and the lowest value of the error function compared to the nonlinear Freundlich isotherm (Table 4).

$R^2$ is limited in its ability to identify the better fitting of the models, essentially when the models under consideration have different numbers of variables or different functional forms. Therefore, the error function gives a good fitting of data to isotherm models. The isotherm models of this study could be arranged as follows: Langmuir Linear type 3>Langmuir Linear type 4>Langmuir non-linear> Langmuir Linear type 1> Freundlich nonlinear>Freundlich linear> Langmuir Linear type 2.

**The Relationship Between Error Functions**

The coefficient of non-determination ($K^2$) measures the amount of unexplained variance between two variables or between a set of predictors and an outcome variable (like error functions). When the relationship between the variables or the predictors and the outcome variable becomes weaker, the $K^2$ value is higher. On the other hand, when the relationship between the variables or the predictors and the outcome variable became stronger, the $K^2$ value is smaller (Hami et al. 2021, Sivarajasekar & Baskar 2019)

$$K^2 = \frac{\text{Unexplained variance}}{\text{Total variance}}$$

$$= 1 - \frac{Unexplained\,variance}{\text{Total variance}} = 1 - r^2$$

HYBRID had shown minimal unexplained isotherm for Langmuir linear type 1, 3, 4, and Freundlich linear,
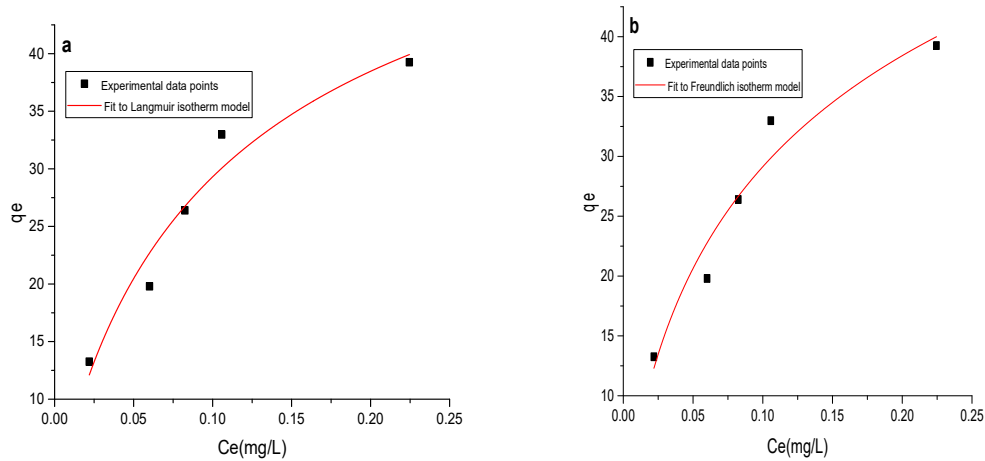
Fig. 8: Adsorption parameters of BG dye onto MWCNT at 35°C for nonlinear (a) Langmuir and (b) Freundlich isotherms.

Table 4: Adsorption parameters of BG dye onto MWCNT at 35°C for nonlinear Langmuir and Freundlich isotherms.

| Adsorbent | Isotherm | Parameters value | | ERRS | HYBRID | $\chi^2$ | ARE | EABS |
|---|---|---|---|---|---|---|---|---|
| MWCNTs | Langmuir nonlinear | $K_L$ | 6.3552 | 0.129 | **0.014** | 0. 082 | 10.350 | 0.932 |
| | | $q_m$ | 62.550 | | | | | |
| | | $R^2$ | **0.955** | | | | | |
| | Freundlich nonlinear | $K_f$ | 0.201 | 2.873 | **0.016** | 0.911 | 44.195 | 4.581 |
| | | n | 0.187 | | | | | |
| | | $R^2$ | 0.952 | | | | | |
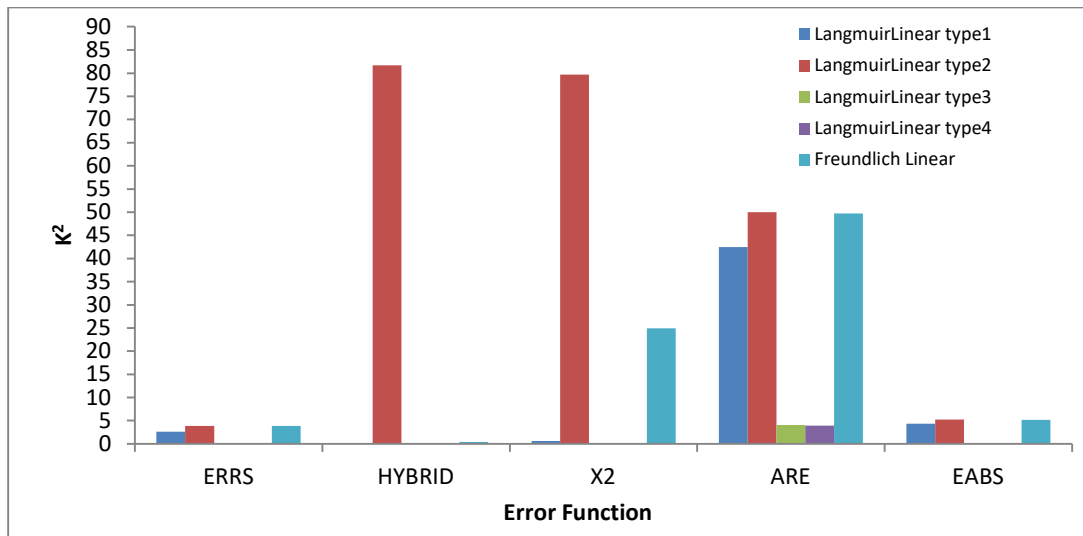


Fig. 9: The relationship between linear Langmuir and Freundlich isotherms with error functions of BG dye adsorption onto MWCNTs.
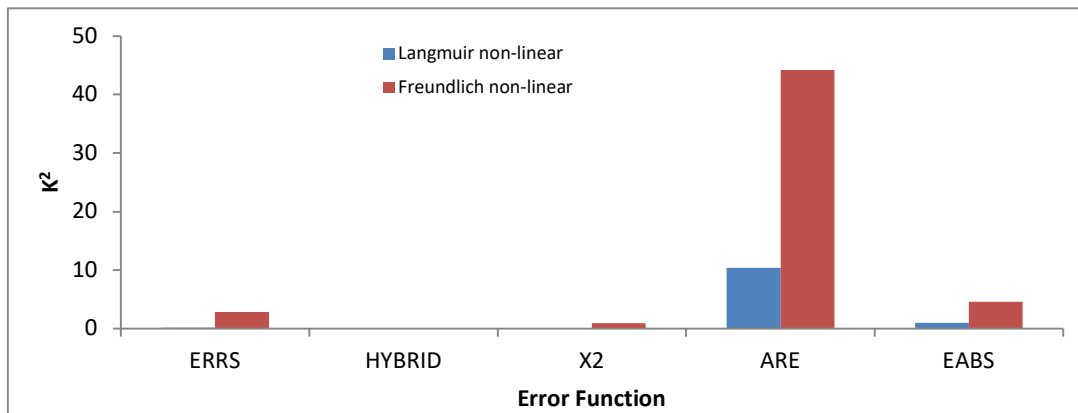
Fig. 10: The relationship between nonlinear Langmuir and Freundlich isotherms with error functions of BG dye adsorption onto MWCNTs.

Table 5: Comparison with other studies.

| Adsorbent | pH | Contact time | isotherm | Ref. |
|---|---|---|---|---|
| Red clay | 7 | 4 h | Redlich–Peterson | (Rehman et al. 2013) |
| Peat soil in Brunei Darussalam | 4.9 | 60 min. | Redlich–Peterson | (Chieng et al. 2015) |
| Activated carbon derived from guava tree wood | 7 | 20 min. | Freundlich | (Mansour et al. 2020) |
| Modified *Bambusa Tulda* | 7 | 60 min. | Langmuir | (Laskar & Kumar 2019) |
| Surfactant Doped Polyaniline/MWCNTs Composite | 3 | 240 min. | Langmuir | (Kumar et al. 2014) |
| MWCNTs | 2 | 15 min. | Langmuir Linear type 3 | This study |

but ERRS had shown minimal unexplained isotherm for Langmuir linear type 2 (Table 3) (Fig. 9). HYBRID was shown to minimize the distribution of error between the empirical and expected nonlinear isotherm (Table 4) (Fig. 10).

### Comparison with Other Studies

The adsorption of BG dye on the MWCNTs surface had a better contact time than other surfaces of other works (Table 5).

### CONCLUSION

In this work, the linear Langmuir isotherm type 3 performed better compared to the nonlinear isotherm model for the adsorption of BG dye onto MWCNTs. As a result, the optimal conditions for adsorption of BG dye with pH 2, 15 min of shaking time, and 35°C of temperature. The coefficient of non-determination ($K^2$) showed Hybrid, and ERRS were the preferable error functions used to predict the fit of linear and nonlinear isotherm models.

### ACKNOWLEDGEMENTS

We are grateful to Mustansiriyah University, the College of Science, and the Department of Chemistry for their valuable help.

### REFERENCES

Abbas, M. 2020. Removal of brilliant green (BG) by activated carbon derived from medlar nucleus (ACMN): Kinetic, isotherms, and thermodynamic aspects of adsorption. Adsorp. Sci. Technol., 38(9-10): 464-482.

Abualnaja, K.M., Alprol, A.E., Ashour, M. and Mansour, A.T. 2021. Influencing multi-walled carbon nanotubes for the removal of ismate violet 2R dye from wastewater: isotherm, kinetics, and thermodynamic studies. Appl. Sci., 11(11): 4786.

Abujaber, F., Ahmad, S.M., Neng, N.R., Martín-Doimeadios, R.R., Bernardo, F.G. and Nogueira, J.M.F. 2019. Bar adsorptive microextraction coated with multi-walled carbon nanotube phases: Application for trace analysis of pharmaceuticals in environmental waters. J. Chromatogr. A, 1600: 17-22.

Ali, I. 2018. Microwave-assisted economic synthesis of multi-walled carbon nanotubes for arsenic species removal in water: batch and column operations. J. Mol. Liq., 271: 677-685.

Alkaim, A.F., Sadik, Z., Mahdi, D.K., Alshrefi, S.M., Al-Sammarraie, A.M., Alamgir, F.M. and Aljeboree, A.M. 2015. Preparation, structure, and adsorption properties of synthesized multiwall carbon nanotubes for highly effective removal of maxilon blue dye. Korean J. Chem. Eng., 32: 2456-2462.

Al-Tohamy, R., Ali, S.S., Li, F., Okasha, K.M., Mahmoud, Y.A.G., Elsamahy, T. and Sun, J. 2022. A critical review on the treatment of dye-containing wastewater: Ecotoxicological and health concerns of textile dyes and possible remediation approaches for environmental

safety. Ecotoxicol. Environ. Saf., 231: 113-160.

Ayawei, N., Ebelegi, A.N. and Wankasi, D. 2017. Modeling and interpretation of adsorption isotherms. J. Chem., 2: 17.

Baidya, K.S. and Kumar, U. 2021. Adsorption of brilliant green dye from aqueous solution onto chemically modified areca nut husk. South Afr. J. Chem. Eng., 35: 33-43.

Belhachemi, M. and Addoun, F. 2011. Comparative adsorption isotherms and modeling of methylene blue onto activated carbons. Appl. Water Sci., 1: 111-117.

Chieng, H.I., Priyantha, N. and Lim, L. B. 2015. Effective adsorption of toxic brilliant green from aqueous solution using peat of Brunei Darussalam: isotherms, thermodynamics, kinetics, and regeneration studies. RSC Adv., 5(44): 34603-34615.

Crini, G. 2006. Non-conventional low-cost adsorbents for dye removal: A review. Bioresour. Technol., 97(9): 1061-1085.

Dahlan, I., Zwain, H.M., Seman, M.A.O., Baharuddin, N.H. and Othman, M.R. 2019. Adsorption of brilliant green dye in aqueous medium using magnetic adsorbents prepared from rice husk ash. AIP Conf. Proceed., 2124(1): 020017.

Das, M.P. and Rebecca, L.J. 2018. Removal of lead (II) by phyto-inspired iron oxide nanoparticles. Nat. Environ. Pollut. Technol., 17(2): 569-574.

Fiaz, R., Hafeez, M. and Mahmood, R. 2020. Removal of brilliant green (BG) from aqueous solution by using low-cost biomass Salix alba leaves (SAL): Thermodynamic and kinetic studies. J. Water Reuse Desal., 10(1): 70-81.

Ghaedi, A.M., Ghaedi, M., Pouranfard, A.R., Ansari, A., Avazzadeh, Z., Vafaei, A. and Gupta, V.K. 2016. Adsorption of Triamterene on multi-walled and single-walled carbon nanotubes: artificial neural network modeling and genetic algorithm optimization. J. Mol. Liq., 216: 654-665.

Gul, S., Gul, A., Gul, H., Khattak, R., Ismail, M., Khan, S. U. and Krauklis, A. 2023. Removal of Brilliant Green Dye from Water Using Ficus benghalensis Tree Leaves as an Efficient Biosorbent. Materials, 16(2): 521.

Gupta, V.K. 2009. Application of low-cost adsorbents for dye removal: A review. J. Environ. Manag., 90(8): 2313-2342.

Hami, H.K., Abbas, R.F., Azeez, S.A. and Mahdi, N.I. Azo Dye Adsorption onto Cobalt Oxide: Isotherm, Kinetics, and Error Analysis Studies. Indon. J. Chem., 21(5): 1148-1157.

Hayat, M., Shah, A., Hakeem, M.K., Irfan, M., Haleem, A., Khan, S.B. and Shah, I. 2022. A designed miniature sensor for the trace level detection and degradation studies of the toxic dye Rhodamine B. RSC Adv., 12(25): 15658-15669.

Karimifard, S. and Alavi Moghaddam, M. R. 2016. Removal of an anionic reactive dye from aqueous solution using functionalized multi-walled carbon nanotubes: isotherm and kinetic studies. Desal. Water Treat., 57(35): 16643-16652.

Kumar, K.V. and Sivanesan, S. 2005. Prediction of optimum sorption isotherm: Comparison of linear and nonlinear method. J. Hazard. Mater., 126(1-3): 198-201.

Kumar, K.V. and Sivanesan, S. 2006. Isotherm parameters for basic dyes onto activated carbon: Comparison of linear and nonlinear method. J. Hazard. Mater., 129(1-3): 147-150.

Kumar, R., Ansari, M. O. and Barakat, M. A. 2014. Adsorption of brilliant green by surfactant doped polyaniline/MWCNTs composite: evaluation of the kinetic, thermodynamic, and isotherm. Indust. Eng. Chem. Res., 53(17): 7167-7175.

Laskar, N. and Kumar, U. 2019. Removal of Brilliant Green dye from water by modified Bambusa Tulda: adsorption isotherm, kinetics and thermodynamics study. Int. J. Environ. Sci. Technol., 16: 1649-1662.

Machado, F.M., Bergmann, C.P., Fernandes, T.H., Lima, E.C., Royer, B., Calvete, T. and Fagan, S.B. 2011. Adsorption of reactive red M-2BE dye from water solutions by multi-walled carbon nanotubes and activated carbon. J. Hazard, Mater., 192(3): 1122-1131.

Mane, V.S. and Babu, P.V. 2011. Studies on the adsorption of Brilliant Green dye from aqueous solution onto low-cost NaOH-treated sawdust. Desalination, 273(2-3): 321-329.

Mansour, R.A.E.G., Simeda, M.G. and Zaatout, A.A. 2021. Removal of brilliant green dye from synthetic wastewater under batch mode using chemically activated date pit carbon. RSC Adv., 11(14): 7851-7861.

Mansour, R.A., El Shahawy, A., Attia, A. and Beheary, M.S. 2020. Brilliant green dye biosorption using activated carbon derived from guava tree wood. Int. J. Chem. Eng., 20: 1-12.

Mansoura, R., Simedab, G. and Zaatout, A. 2020. Adsorption studies on brilliant green dye in aqueous solutions using activated carbon derived from guava seeds by chemical activation with phosphoric acid. Desalin. Water Treat., 202: 396-409.

Mariah, G.K. and Pak, K.S. 2020. Removal of brilliant green dye from aqueous solution by electrocoagulation using response surface methodology. Mater. Today Proceed., 20: 488-492.

McKay, G., Mesdaghinia, A., Nasseri, S., Hadi, M. and Aminabad, M.S. 2014. Optimum isotherms of dyes sorption by activated carbon: Fractional theoretical capacity & error analysis. Chem. Eng. J., 251: 236-247.

Piccin, J.S., Dotto, G.L. and Pinto, L.A.A. 2011. Adsorption isotherms and thermochemical data of FD&C Red n 40 binding by chitosan. Brazil. J. Chem. Eng., 28: 295-304.

Raza, K., Kumar, D., Kiran, C., Kumar, M., Guru, S.K., Kumar, P. and Katare, O. P. 2016. Conjugation of docetaxel with multiwalled carbon nanotubes and codelivery with piperine: implications on pharmacokinetic profile and anticancer activity. Mol. Pharm., 13(7): 2423-2432.

Rehman, M.S.U., Munir, M., Ashfaq, M., Rashid, N., Nazar, M.F., Danish, M. and Han, J. I. 2013. Adsorption of Brilliant Green dye from aqueous solution onto red clay. Chem. Eng. J., 228: 54-62.

Rehman, R., Mahmud, T. and Irum, M. 2015. Brilliant green dye elimination from water using Psidium guajava leaves and Solanum tuberosum peels as adsorbents in an environmentally benign way. J. Chem., 65: 111-121.

Rida, J.F.A., Bhardwaj, A.K. and Jaswal, A.K. 2013. Preparing Carbon Nanotubes (CNTs) for Optical System Applications. Int. J. Nanotubes Appl., 3(2): 1-20.

Rodríguez, C., Briano, S. and Leiva, E. 2020. Increased adsorption of heavy metal ions in multi-walled carbon nanotubes with improved dispersion stability. Molecules, 25(14): 3106.

Rostamian, R. and Behnejad, H. 2018. Insights into doxycycline adsorption onto graphene nanosheet: A combined quantum mechanics, thermodynamics, and kinetic study. Environ. Pollut. Res., 25: 2528-2537.

Sala, L., Figueira, F.S., Cerveira, G.P., Moraes, C.C. and Kalil, S.J. 2014. Kinetics and adsorption isotherm of C-phycocyanin from Spirulina platensis on ion-exchange resins. Brazil. J. Chem. Eng., 31: 1013-1022.

Salem, M.A., Elsharkawy, R.G. and Hablas, M. F. 2016. Adsorption of brilliant green dye by polyaniline/silver nanocomposite: Kinetic, equilibrium, and thermodynamic studies. Europ. Poly. J., 75: 577-590.

Saxena, M., Sharma, N. and Saxena, R. 2020. Highly efficient and rapid removal of a toxic dye: adsorption kinetics, isotherm, and mechanism studies on functionalized multiwalled carbon nanotubes. Surf. Interf., 21: 100639.

Segun Esan, O., Nurudeen Abiola, O., Owoyomi, O., Olumuyiwa Aboluwoye, C. and Olubunmi Osundiya, M. 2014. Adsorption of brilliant green onto luffa cylindrical sponge: equilibrium, kinetics, and thermodynamic studies. Int. Schol. Res. Not., 6: 14.

Shahmohammadi-Kalalagh, S. and Babazadeh, H. 2014. Isotherms for the sorption of zinc and copper onto kaolinite: comparison of various error functions. International Journal of Environmental Science and Technology, 11: 111-118.

Singh, S., Gupta, H., Dhiman, S. and Sahu, N. K. 2022. Decontamination of cationic dye brilliant green from the aqueous media. Applied Water Science, 12(4): 61.

Sivarajasekar, N. and Baskar, R. 2019. Adsorption of Basic Magenta II onto $H_2SO_4$ activated immature Gossypium hirsutum seeds: Kinetics, isotherms, mass transfer, thermodynamics, and process design. Arab. J. Chem., 12(7): 1322-1337.

Song, G., Shen, M., Zhu, K. and Li, G. 2018. Adsorptive removal of methylene blue by mn-modified tourmaline. Nat. Environ. Pollut. Technol., 17(1): 243-247.

Subramanyam, B. and Das, A. 2014. Linearised and non-linearised isotherm models optimization analysis by error functions and statistical means. Journal of Environmental Health Science and Engineering, 12: 1-6.

Wang, S., Ng, C. W., Wang, W., Li, Q. and Hao, Z. 2012. Synergistic and competitive adsorption of organic dyes on multi-walled carbon nanotubes. Chem. Eng. J., 197: 34-40.

# Studies on the Contamination of Heavy Metals and Their Chemical Speciation in Sediment from Selected Locations of Pune District

**Parveen Hassanpourfard\*† iD , Ashish Vilas Mane\* and Kaushik Banerjee\*\***
\*Department of Environmental Science, Fergusson College (Autonomous), Pune, India
\*\*ICAR-National Research Centre for Grapes, Pune, Maharashtra, India
†Corresponding author: Parveen Hassanpourfard; parveenhfard@gmail.com

## ABSTRACT

The heavy metal speciation analysis in sediments helps us understand and evaluate essential and unavoidable issues in terms of both health and environmental hazards imposed by these metals in our lives. Analyzing the total content of heavy metals enables us to understand only the quantity of the contaminants. To understand the different species or the chemical forms of heavy metals available in the sediments, we must study their speciation. Speciation studies help us determine their possible sources as well as their environmental stability in terms of availability to plants and other organisms. The heavy metals in this study were specified using four-stage sequential extraction, also known as the BCR technique. This study mainly highlights the quantification of metal contamination of Cu, Zn, Pb, Ni, Cd & Cr, and chemical forms as species in sediment samples collected from different Pune District, Maharashtra sites. Heavy metal contamination from the collected samples was analyzed with the use of flame atomic absorption spectrometry. This study indicated that Zn and Ni are among the most abundant metals in the sediment samples; however, Cu and Cd belong to the least abundant category. The oxidizable and residual forms (immobile and cannot be used by the organisms readily) appeared dominant for most heavy metals. Very significant differences were observed in the speciation of heavy metals from sample to sample, which was probably due to differences in water/soil composition and the agrochemicals like pesticides, weedicides, and fertilizers used in agricultural practices; the wastewater generated from different pharmaceuticals, chemical processing and manufacturing industries as well as the improper wastewater treatment methods.

## INTRODUCTION

Heavy metals contribute to the vast spectrum of pollutants, causing chronic impacts on human health and the ecosystem. Various practices such as agricultural, medical, industrial, domestic, medical, and production-based technological activities result in the wide dispersion of heavy metals within the environment. Studying the impact of these contaminants on human health and the immune system has become an area of great interest among scholars due to their wide range of distribution and their careless use in most industries and our day-to-day lives (Guan et al. 2001, Yan et al. 2008, Christoforidis & Stamatis 2009). Heavy metals have earned the fame of being dreadful environmental pollutants due to their toxic ability to cause huge disruption and discord regarding nutritional, ecological, and environmental balances (Goyer & Clarkson 1996, Wang & Shi 2001). Numerous factors determine the toxicity of heavy metals, including the chemical type, source of contamination, the contaminant's distribution route, and the recipient's age, sex, genetics, and immunity or nutritional status.

As per the current global condition, arsenic, cadmium, chromium, mercury, and lead are on the list of the heavy metals studied due to their very high toxicity causing great worry for the public health sector. The study of heavy metal contamination of soil and sediments helps assess their quality and degree of contamination (Su & Wong 2004, Walter et al. 2006). The bioavailability and mobility of these contaminants depend on their species or chemical forms (Fuentes et al. 2004, Wang et al. 2006). The method commonly used to study the speciation of these metals is the three-step sequential extraction procedure, also known as the BCR technique (Community Bureau of Reference), a modified version of the Tessier method developed in 1979 (Tessier et al. 1979, Rauret et al. 2000, Álvarez et al. 2002). The commonly found heavy metals in wastewater include -Arsenic, Cadmium, Chromium, Copper, Lead, Nickel, and Zinc, which results in serious human health and environmental disruption by obtaining easy access to the ecosystem by both natural and man-made activities. (Beyersmann & Hartwig 2008). The wide distribution of these contaminants into the ecosystem ranges from natural

activities like soil erosion, and weathering of rocks to man-made activities like mining, industrial run-offs, sewage discharge, agricultural practices of using insecticides and pesticides, and so on (Arruti et al. 2010).

The procedure allows us to determine the contaminants in the soil and sediment samples, particularly the species in the bound form that can readily migrate from the sediment to the soil and then further become a part of the ecosystem. (Sutherland 2010, Rashed et al. 2011). The study's core objectives were to first analyze heavy metal concentration present in the water, soil, and sediment samples from different locations of Pune District in Maharashtra. Secondly, to investigate the species or chemical forms of the contaminants in the sediment samples from selected seven sites of Pune District using the BCR sequential extraction technique, which focuses on evaluating their bioavailability and mobility. Finally, to determine the quality of the soil and sediment for agrarian practices based on the degree of contamination by heavy metals in samples and their degree of toxicity.

## MATERIALS AND METHODS

### Total Content of Heavy Metals in Sediment

The sample preparation comprised air drying for 24 h at 24°C. Afterward, the sediment was crushed into a fine powder and subjected to digestion. A conventional aqua regia digestion technique was employed for this purpose. Firstly, a homogenously mixed sample of 0.5 g was shifted to a clean 250 mL glass beaker. The sample was digested on a hotplate for 3 h using 12 mL of aqua regia at 110°C. Once the sample was observed to have obtained near dryness consistency, it was reduced using 20 mL -Nitric Acid (2 % v/v, $H_2O$) & collected in a 100 mL flask, later filtering through Whatman 42 filter paper.

Further, it was watered down using 100 mL of deionized water. The total heavy metal content in the samples was analyzed using an Atomic Absorption Spectrometer, employing SpectraAA 220, VARIAN. When the metal concentration was observed to obtain a standard curve., Samples were further diluted with deionized water. All the assessments were carried out thrice for the sake of accuracy.

### Speciation of the Heavy Metals in Sediment

**Sequential extraction of heavy metals in sediment samples:** The speciation study was performed by the three-stage extraction, the modified BCR technique proposed by the European Community Bureau of Reference, which facilitates the evaluation of metal species present in the sample.

**Fraction 1** – Bound to Carbonates (Soluble in acids) – These are extracted using Acetic Acid ($CH_3COOH$) – applicable to bound to carbonates form that can readily pass to the soil and are among the most readily available forms, where they are bioavailable and migrates to water bodies very easily (transportable).

**Fraction 2** – Attached to Manganese and Ferrous oxides (Reducible) – These are concentrated using hydroxylamine hydrochloride ($NH_2OH$-$HCl$) – attached to Iron and Manganese oxide forms. Migration capacity and absorption are slower than Fraction 1 (transportable) forms.

**Fraction 3** – Attached to organic matter and sulfides (Oxidizable) – These are concentrated using hydrogen peroxide ($H_2O_2$)– applicable to bound to organic matter and sulfide forms. They are neither readily absorbed nor have the migration capacity as the forms observed in Fraction 1 and Fraction 2 (non-transportable).

**Fraction 4** – Residual Fraction – These are concentrated using aqua-regia (3 parts of HCl and 1 part of $HNO_3$) – applicable to the residual metal concentrate obtained after extraction from the previous fractions. They are practically inaccessible to the plants and hence have no capacity to migrate (non-transportable).

**BCR procedure:** The sample preparation for the metal speciation involved drying the sediment sample (48 h at 20°C, air-dried to obtain constant mass at 105°C) followed by grinding to obtain a fine powder of homogenously mixed sample. The sequential extraction of the heavy metal fractions of sediment samples was performed using the following steps:

**Step 1** – Fraction 1: Bound to Carbonates (Extraction of exchangeable fraction):

1 g of a homogenously mixed dried sample was digested by adding 40 mL, 0.11 mol acetic acid, in a 100 cm$^3$ centrifuge tube. This tube was stirred for 16 h at normal temperature, at 30 rpm, and then centrifuged at 3000 rpm for 20 min. The supernatant was obtained, then stored aside for testing. The leftover remainder was washed with 5 mL of deionized distilled water and centrifuged again. The supernatant was then discarded. This leftover residue was kept aside to be used in Step 2.

**Step 2** – Fraction 2: Attached to Mn and Fe Oxides (Reducible fraction):

40 mL 0.1 M hydroxylamine hydrochloride was added to the residue obtained in the first Step. This tube was again agitated for 16 hrs. at 24°C, at 30 rpm, and centrifuged later at 3000 rpm (20 min.). The supernatant obtained was stored aside for analysis. The leftover residue was washed with 5

mL of deionized distilled water and centrifuged again. The supernatant was discarded, and the leftover residue was kept aside for use in the next step.

**Step 3** – Fraction 3: Attached to Sulfides and Organic matters (Extraction of Oxidizable Form):

10 mL of 30% $H_2O_2$ was carefully added to the residue obtained from the previous extraction stage, transferred to transparent glassware, and left for 11 h at normal temperature with occasional stirring. The sample was then incubated at 85$^o$C for 1 h. The residue was combined with 50 mL of Ammonium acetate and centrifuged at 3000 rpm) for 20 min.). The supernatant was stored aside for analysis in a separate polyethylene container, followed by the procedure conducted in Step 1 and Step 2.

**Step 4** – Fraction 4: Extraction of Residual Fraction with aqua regia (mixture of 3 parts HCl + 1-part $HNO_3$):

5 mL of $HNO_3$ & 15 mL of HCl were mixed with residue obtained from the previous stage, then evaporated to dryness. On chilling, 5% of $HNO_3$ was used to dissolve the residue. The metal concentrations were analyzed using Flame Atomic Absorption Spectrometry, SpektraAA 220 VARIAN. All of the analyses were repeated thrice for the sake of accuracy.

## RESULTS AND DISCUSSION

### Physicochemical Properties of the Sediment Samples

Table 1 indicates that on examining the sediment samples for the heavy metal contaminants, namely, Cd, Cr, Cu, Co, Fe, Mn, Mg, Ni, Pb, and Zn, it was clearly found that almost all the heavy metals appeared to be above the permissible limits (WHO, ICMR, BIS) ranging from moderately toxic to highly toxic. We also observed that the levels of heavy metals increase as we move from the upstream to the central and the downstream regions. This table represents the total concentration of these metals in the sediment samples from different locations in Pune.

As per the available research data, the concentration of these metal contaminants present in the sewage sludge can be arranged as follows Zn > Cu > Cr > Ni > Pb > Cd (this order does not include Mn, Mg, Fe, Co) (Shrivastava & Banerjee 2004). The order we obtained after examining the Sediment Samples Ni > Mn > Pb > Cd > Cr > Cu > Zn > Co. In this study, we notice that the Ni ranges from 30 to 50 times more than the permissible limits. Likewise, Pb ranges more than 30 times; Mn more than 33 times; Cd more than 10 times; and Cr more than 4 times the permissible limits suggested by the World Health Organisation (WHO 2019).

Table 2 gives us an idea of the heavy metal speciation results of selected metals from Sediment samples from different sites in the Pune District. Fig. 1 explains the Zn Speciation (Heavy metal speciation) of sediment samples from Site 1 to Site 7 (Fraction 1 to Fraction 4). In this case, Fraction 3 (F-3) results appear to be in higher concentration than F-1, F-2 and F-3.

Fig. 2 describes the Cu Speciation of sediment samples from Site 1 to Site 7 (Fraction 1 to Fraction 4). Here, Fraction 3 outcomes indicate that F-3 exhibits higher concentration than F-1, F-2, and F-4.

Fig. 3 and Fig. 4 report about the concentration of Ni and Pb Speciation of sediment samples from Site 1 to Site 7 (Fraction 1 to Fraction 4). As far as Ni speciation is concerned, Fractions 1 and 2 seem to be the lowest, however, F-3 and F-4 indicate a slight increase than the former two. However, while studying the Pb speciation it is clearly understood that F-3 and F-4 species of the heavy metal is present in way higher concentration than F-1 and F-2. The arrangement of concentration of Pb metal species could be better explained like F-3 >F-4 > F-1 > F-2.

Table 1: Heavy metal analysis of sediment samples (upstream to downstream).

| Heavy Metals | Site-1 | Site-2 | Site-3 | Site-4 | Site-5 | Site-6 | Site-7 |
|---|---|---|---|---|---|---|---|
| Cd | 0.007 | 0.005 | 0.014 | 0.013 | 0.135 | 0.029 | 0.007 |
| Cr | 0.027 | 0.044 | 0.048 | 0.002 | 0.162 | 1.076 | 0.047 |
| Cu | 0.057 | 0.059 | 1.137 | 0.461 | 2.6 | 2.516 | 0.265 |
| Co | 0 | 0.002 | 0.572 | 0.222 | 0.328 | 1.031 | 0.274 |
| Fe | 0.004 | 0.012 | 111.6 | 45.6 | 489.6 | 715.3 | 113.4 |
| Mn | 0.015 | 0.008 | 18.969 | 4.563 | 11.502 | 22.94 | 11.738 |
| Mg | 1.661 | 13.487 | 81.72 | 51.41 | 71.66 | 40.58 | 15.82 |
| Ni | 1.14 | 0.488 | 2.448 | 2.625 | 5.57 | 15.11 | 1.954 |
| Pb | 0.13 | 0.09 | 0.2 | 0.34 | 0.72 | 0.62 | 0.22 |
| Zn | 0.009 | 0.016 | 1.181 | 0.76 | 2.556 | 3.471 | 0.607 |

Table 2: Heavy metal speciation results of selected metals from sediment samples

| Zn | S-1 | S-2 | S-3 | S-4 | S-5 | S-6 | S-7 |
|---|---|---|---|---|---|---|---|
| F-1 | 0.003 | 0.005 | 0.235 | 0.236 | 0.025 | 0.876 | 0.142 |
| F-2 | 0.004 | 0.006 | 0.096 | 0.315 | 0.621 | 0.93 | 0.203 |
| F-3 | 0.005 | 0.004 | 1.035 | 0.325 | 1.59 | 1.23 | 0.29 |
| F-4 | 0.001 | 0.003 | 0.181 | 0.124 | 0.325 | 0.423 | 0.216 |
| Cu | S-1 | S-2 | S-3 | S-4 | S-5 | S-6 | S-7 |
| F-1 | 0.014 | 0.019 | 0.26 | 0.128 | 0.23 | 0.56 | 0.032 |
| F-2 | 0.011 | 0.02 | 0.115 | 0.132 | 0.051 | 0.146 | 0.052 |
| F-3 | 0.019 | 0.023 | 0.45 | 0.15 | 1.268 | 1.058 | 0.125 |
| F-4 | 0.012 | 0.009 | 0.232 | 0.145 | 0.751 | 0.752 | 0.056 |
| Ni | S-1 | S-2 | S-3 | S-4 | S-5 | S-6 | S-7 |
| F-1 | 0.13 | 0.123 | 0.22 | 0.766 | 1.523 | 3.708 | 0.212 |
| F-2 | 0.023 | 0.056 | 0.048 | 0.042 | 0.326 | 0.19 | 0.025 |
| F-3 | 0.685 | 0.266 | 1.762 | 1.525 | 2.322 | 9.093 | 1.329 |
| F-4 | 0.0423 | 0.045 | 0.448 | 0.128 | 1.59 | 2.113 | 0.389 |
| Pb | S-1 | S-2 | S-3 | S-4 | S-5 | S-6 | S-7 |
| F-1 | 0.012 | 0.015 | 0.07 | 0.065 | 0.052 | 0.092 | 0.02 |
| F-2 | 0.006 | 0.023 | 0.02 | 0.0423 | 0.023 | 0.021 | 0.01 |
| F-3 | 0.052 | 0.042 | 0.09 | 0.142 | 0.422 | 0.321 | 0.152 |
| F-4 | 0.048 | 0.021 | 0.06 | 0.071 | 0.232 | 0.215 | 0.04 |
| Cd | S-1 | S-2 | S-3 | S-4 | S-5 | S-6 | S-7 |
| F-1 | 0 | 0.001 | 0.001 | 0.001 | 0.007 | 0.023 | 0.001 |
| F-2 | 0.001 | 0.003 | 0.002 | 0.003 | 0.009 | 0.062 | 0.001 |
| F-3 | 0.002 | 0.002 | 0.006 | 0.007 | 0.092 | 0.177 | 0.004 |
| F-4 | 0.004 | 0.001 | 0.004 | 0.002 | 0.032 | 0.048 | 0.002 |
| Cr | S-1 | S-2 | S-3 | S-4 | S-5 | S-6 | S-7 |
| F-1 | 0.005 | 0.005 | 0.007 | 0 | 0.023 | 0.009 | 0.011 |
| F-2 | 0.006 | 0.022 | 0.008 | 0.001 | 0.011 | 0.056 | 0.008 |
| F-3 | 0.009 | 0.009 | 0.011 | 0.0015 | 0.087 | 0.988 | 0.012 |
| F-4 | 0.007 | 0.012 | 0.023 | 0.0011 | 0.033 | 0.087 | 0.018 |

Note: Results are expressed in mean mg.kg$^{-1}$ (PPM); Each sample has been run thrice for accuracy.

Similarly, Fig. 5 and Fig. 6 explain the concentration of Cd and Cr Speciation of sediment samples from Site 1 to Site 7 (Fraction 1 to Fraction 4). Both Cd and Cr exhibit similar results, where F-1, F-2 and F-4 are noted as having lower concentration and F-3 represents higher concentration in the case of both heavy metals.

The obtained results of heavy metal speciation have been mentioned in the table above. The basic aim of the speciation analysis of the sediment samples was to analyze the bioavailability and migration capacity of these contaminants to the water and soil environment to assess their possible impacts directly or indirectly on the environment and the ecosystem. The total Concentration of the heavy metals at different sites was recorded as follows:

Site 1- Ni > Pb > Zn> Cr > Cu > Cd

Site 2- Ni > Zn > Cu > Pb > Cd > Cr

Site 3- Ni > Cu > Pb > Zn > Cd > Cr

Site 4 – Ni > Zn > Pb > Cu > Cd > Cr

Site 5 – Ni > Zn > Cu > Pb > Cd > Cr

Site 6 – Ni > Zn > Pb > Cu > Cr > Cd

Site 7 – Ni > Zn > Pb > Cu > Cr > Cd
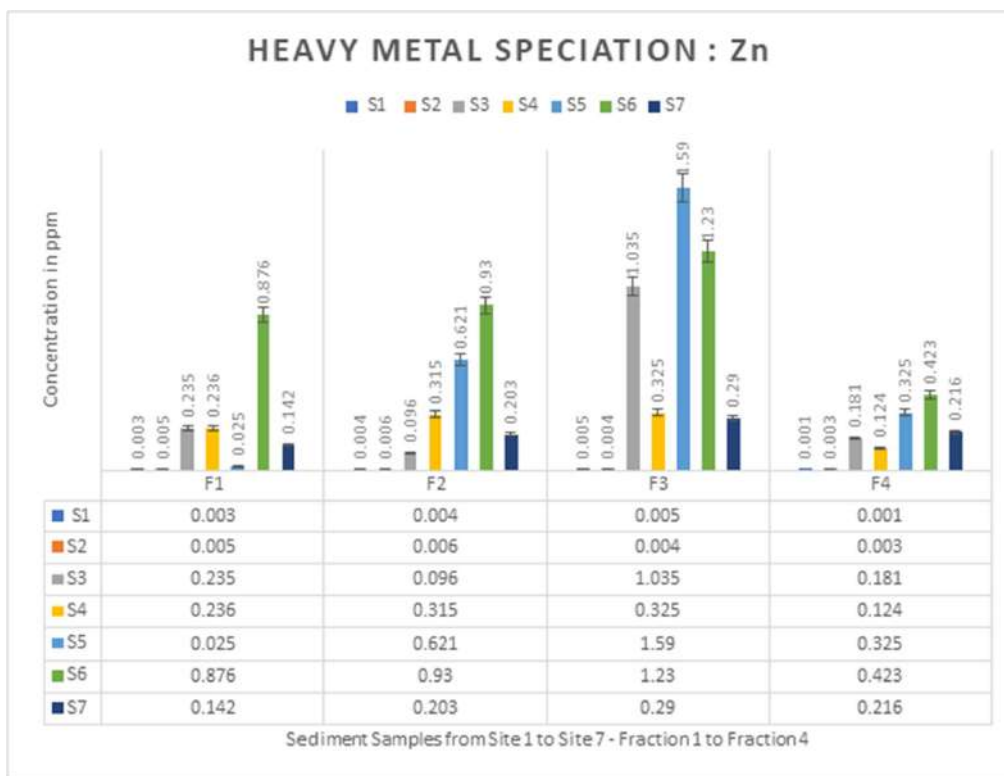
Fig. 1: Heavy metal (Zn) speciation of sediment samples from Site 1 to Site 7 (F1 to F4).

| | F1 | F2 | F3 | F4 |
|---|---|---|---|---|
| S1 | 0.003 | 0.004 | 0.005 | 0.001 |
| S2 | 0.005 | 0.006 | 0.004 | 0.003 |
| S3 | 0.235 | 0.096 | 1.035 | 0.181 |
| S4 | 0.236 | 0.315 | 0.325 | 0.124 |
| S5 | 0.025 | 0.621 | 1.59 | 0.325 |
| S6 | 0.876 | 0.93 | 1.23 | 0.423 |
| S7 | 0.142 | 0.203 | 0.29 | 0.216 |
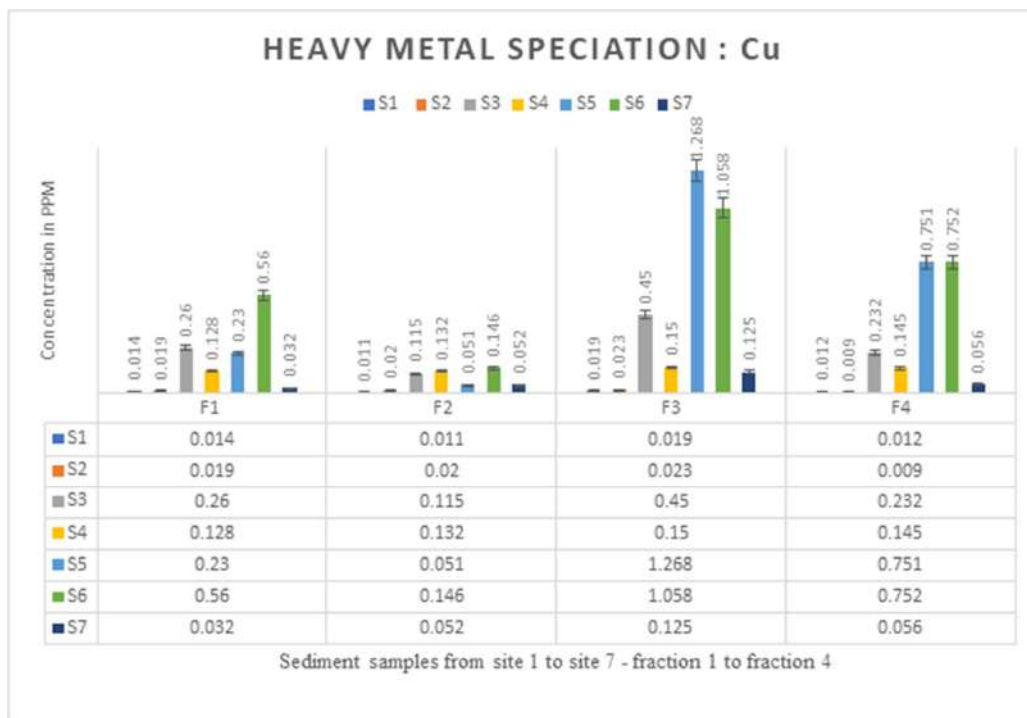


Fig. 2: Heavy metal (Cu) speciation of sediment samples from Site 1 to Site 7 (F1 to F4).

| | F1 | F2 | F3 | F4 |
|---|---|---|---|---|
| S1 | 0.014 | 0.011 | 0.019 | 0.012 |
| S2 | 0.019 | 0.02 | 0.023 | 0.009 |
| S3 | 0.26 | 0.115 | 0.45 | 0.232 |
| S4 | 0.128 | 0.132 | 0.15 | 0.145 |
| S5 | 0.23 | 0.051 | 1.268 | 0.751 |
| S6 | 0.56 | 0.146 | 1.058 | 0.752 |
| S7 | 0.032 | 0.052 | 0.125 | 0.056 |

HEAVY METAL SPECIATION: Ni

| | F1 | F2 | F3 | F4 |
|---|---|---|---|---|
| S1 | 0.13 | 0.023 | 0.685 | 0.0423 |
| S2 | 0.123 | 0.056 | 0.266 | 0.045 |
| S3 | 0.22 | 0.048 | 1.762 | 0.448 |
| S4 | 0.766 | 0.042 | 1.525 | 0.128 |
| S5 | 1.523 | 0.326 | 2.322 | 1.59 |
| S6 | 3.708 | 0.19 | 9.093 | 2.113 |
| S7 | 0.212 | 0.025 | 1.329 | 0.389 |

Sediment samples from site 1 to site 7 - fraction 1 to fraction 4
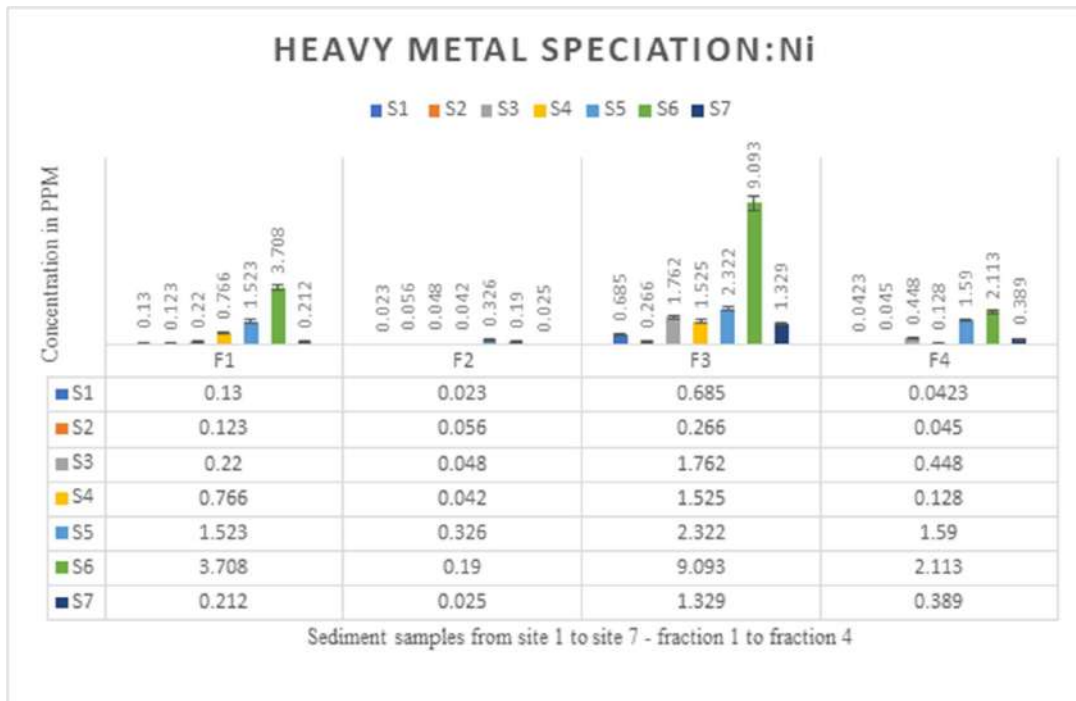
Fig. 3: Heavy metal (Ni) speciation of sediment samples from Site 1 to Site 7 (F1 to F4).



HEAVY METAL SPECIATION: Pb

| | F1 | F2 | F3 | F4 |
|---|---|---|---|---|
| S1 | 0.012 | 0.006 | 0.052 | 0.048 |
| S2 | 0.015 | 0.023 | 0.042 | 0.021 |
| S3 | 0.07 | 0.02 | 0.09 | 0.06 |
| S4 | 0.065 | 0.0423 | 0.142 | 0.071 |
| S5 | 0.052 | 0.023 | 0.422 | 0.232 |
| S6 | 0.092 | 0.021 | 0.321 | 0.215 |
| S7 | 0.02 | 0.01 | 0.152 | 0.04 |

Sediment samples from site 1 to site 7 - fraction 1 to fraction 4
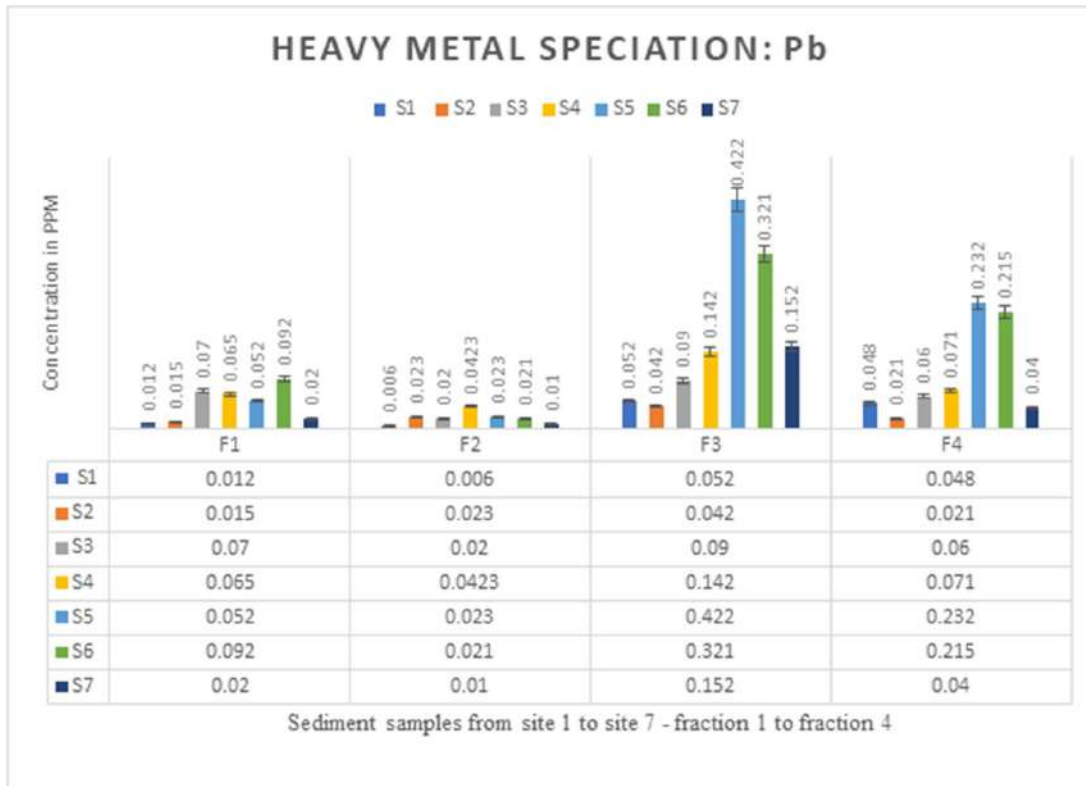
Fig. 4: Heavy metal (Pb) speciation of sediment samples from Site 1 to Site 7 (F1 to F4).
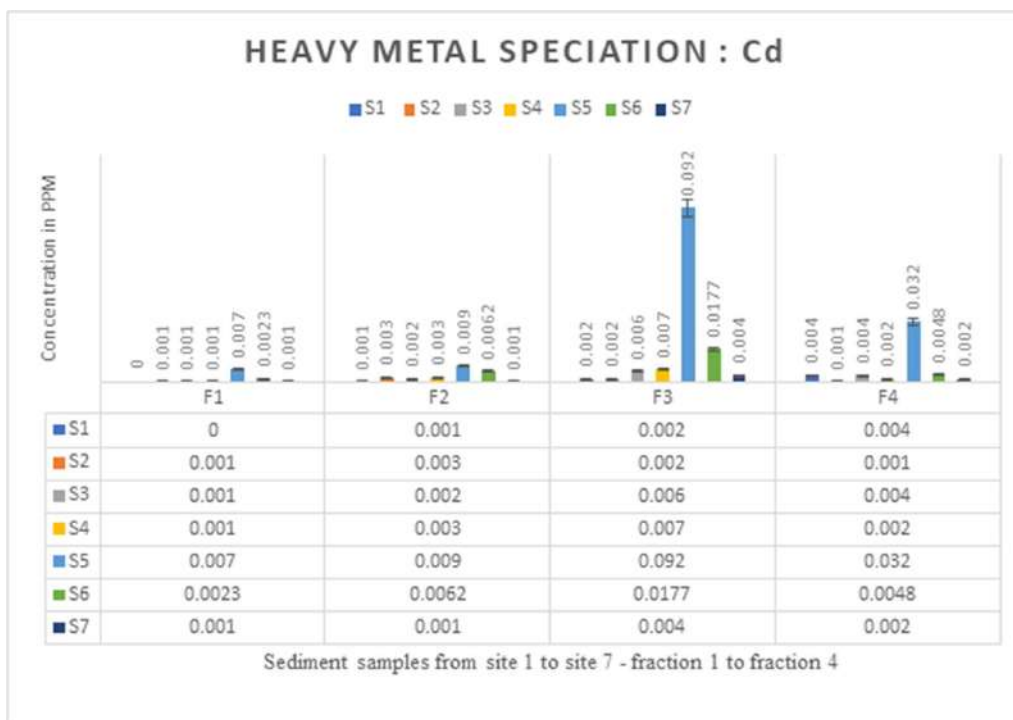
Fig. 5: Heavy metal (Cd) speciation of sediment samples from Site 1 to Site 7 (F1 to F4).
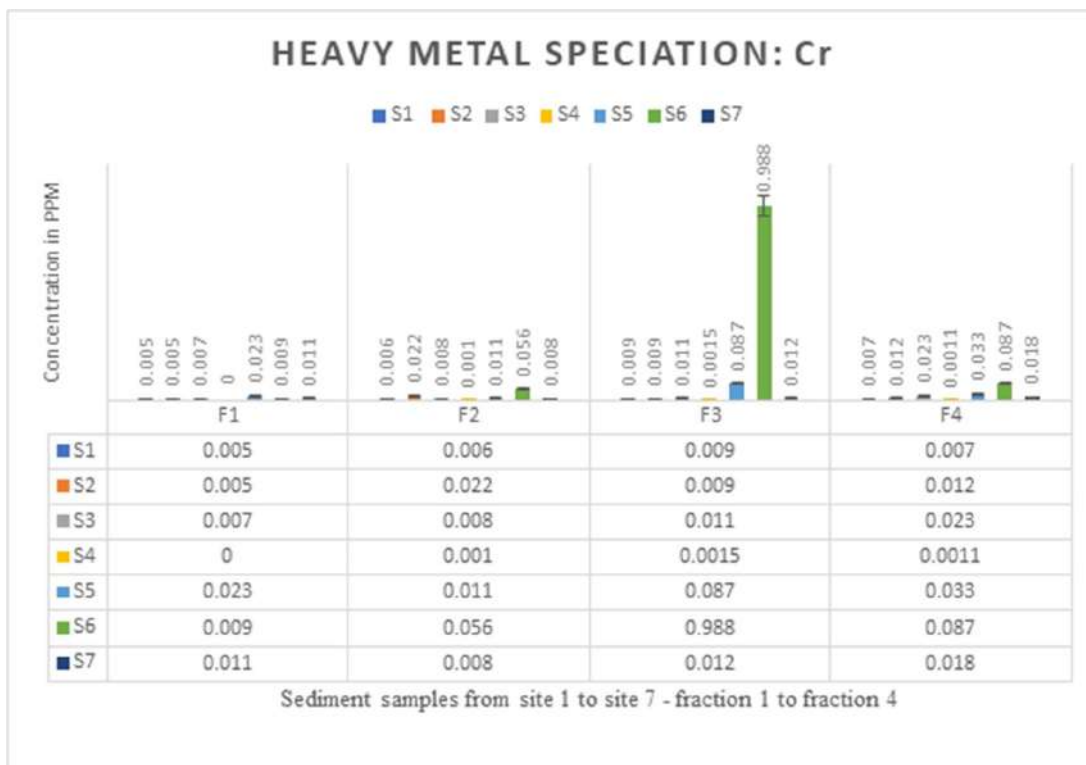


Fig. 6: Heavy metal (Cr) speciation of sediment samples from Site 1 to Site 7 (F1 to F4).

Considering the heavy metal distribution in the selected fractions (F1, F2, F3 and F4), it was recorded as follows:

**Site 1 –** Ni (F-3 > F-4 > F-1 > F-2), Pb (F-3 > F-4 > F-2 >F-1), Zn (F-3 > F-2 > F-1 > F-4), Cr (F-3 > F-4 > F-2 > F-1), Cu (F-3 > F-1 > F-4 > F-2), Cd (F-4 > F-3 > F-2 > F-1)

**Site 2 –** Ni (F-3 > F-1 > F-2 > F-4), Zn (F-2 > F-1 > F-3 > F-4), Cu (F-3 > F-2 > F-1 > F-4), Pb (F-3 > F-2 > F-4 > F-1), Cd (F-2 > F-3 > F-1 > F-4), Cr (F-2 > F-4 > F-3 > F-1)

**Site 3 –** Ni (F-3 > F-4 > F-1 > F-2), Cu (F-3 > F-1 > F-4 > F-2), Pb (F-3 > F-1 > F-4 > F-2), Zn (F-3 > F-2 > F-1 > F-4), Cd (F-3 > F-4 > F-2 > F-1), Cr (F-4 > F-3 > F-1 > F-2)

**Site 4 –** Ni (F-3 > F-1 > F-4 > F-2), Zn (F-3 > F-2 > F-1 > F-4), Pb (F-3 > F-4 > F-1 > F-2), Cu (F-3 > F-4> F-2 > F-1), Cd (F-3 > F-2 > F-4 > F-1), Cr (F-3 > F-4 > F-2 > F-1)

**Site 5 –** Ni (F-3 > F-4 > F-1 > F-2), Zn (F-3 > F-2 > F-4 > F-1), Cu (F-3 > F-4 > F-1 > F-2), Pb (F-3 > F-4 > F-1 > F-2), Cd (F-3 > F-4 > F-2 > F-1), Cr (F-3 > F-4 > F-1 > F-2)

**Site 6 –** Ni (F-3 > F-1 > F-4 > F-2), Zn (F-3 > F-2 > F-1 > F-4), Pb (F-3 > F-4 > F-1 > F-2), Cu (F-3 > F-4 > F-1 > F-2), Cr (F-3 > F-4 > F-2 > F-1), Cd (F-3 > F-2 > F-4 > F-1)

**Site 7 –** Ni (F-3 > F-4 > F-1 > F-2), Zn (F-3 > F-4 > F-2 > F-1), Pb (F-3 > F-4 > F-1 > F-2), Cu (F-3 > F-4 > F-2 > F-1), Cr (F-4 > F-3 > F-1 > F-2), Cd (F-3 > F-4 > F-2 > F-1).

Most sediment samples showed high concentrations of heavy metals species attached to residual and oxidizable and fractions (F-3 and F-4). Fractions 3 and 4 are immobile. Hence they are not readily absorbed by the Plants and move in the food chain from one trophic level to another. Among the mobile forms (F-1 and F-2), F-2 is a reducible form bound to Mn and Fe oxides is much higher than F-1. Other researchers observed similar relations on sludge (Jamali et al. 2007). Fractions 1 and 2 are mobile, meaning they can be quickly utilized by the producers (Plants) and have the capacity to move up in the food chain by leaping from one trophic level to the other as efficiently as possible, intoxicating the organisms that come under its influence directly or indirectly.

The distribution of the heavy metals (Fig. 7) was observed to be highest at the following sites: Zn at Site 1, Cu at Site 4, Ni at Site 5, Pb at Site 2, Cd at Site 2, and Cr at Site 2. However, the lowest distribution was recorded – Zn at Site 6, Cu at Site 5, Ni at Site 1, Pb at Site 1, Cd at Site 3, and Cr at Site 5. It should be noted that results could be impacted by factors such as diverse sample consistency, chemicals used, and the processes or changes taking place while the sample was being analyzed.

**Recovery Rate**

Table 2 describes the Heavy metal speciation results of the sediments obtained from different locations in the Pune district. The following mathematical operation did verification of the results.
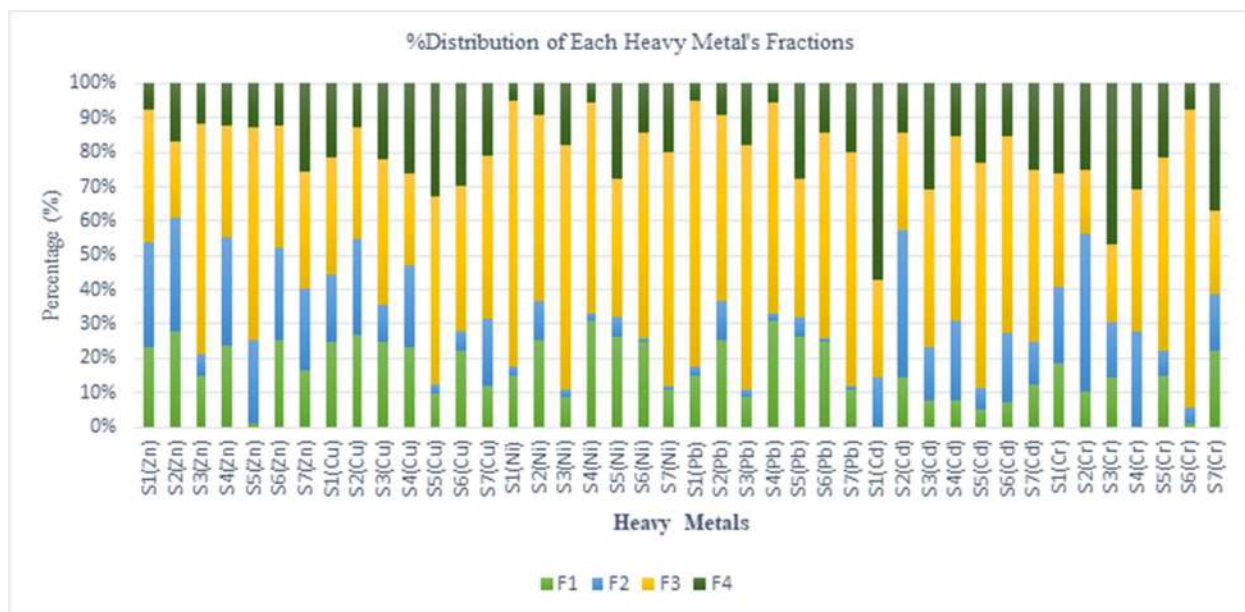


Fig. 7: % Distribution of each metal's fraction in sediment samples from Site 1 to 7.

Table 3: Recovery Rates of the Heavy Metals of the Sediment Samples.

| Heavy Metal | S1 | S2 | S3 | S4 | S5 | S6 | S7 |
|---|---|---|---|---|---|---|---|
| Zn | 144.4 | 112.5 | 130.99 | 131.57 | 100.19 | 99.65 | 140.19 |
| Cu | 98.24 | 120.33 | 92.96 | 120.39 | 88.46 | 100 | 100 |
| Ni | 77.21 | 100.40 | 101.22 | 93.75 | 103.42 | 99.96 | 100.05 |
| Pb | 90.76 | 112.22 | 120 | 94.20 | 101.25 | 104.67 | 100.90 |
| Cd | 100 | 140 | 92.85 | 100 | 103.70 | 106.89 | 114.28 |
| Cr | 100 | 109.09 | 102.08 | 180 | 95.06 | 105.94 | 104.25 |

$$R = [(F\text{-}1) + (F\text{-}2) + (F\text{-}3) + (F\text{-}4)]/TC \times 100\%$$

where,

R is the Recovery percentage of the heavy metal

$TC$ (mg.kg$^{-1}$) is the total concentration of heavy metals

F-1, F-2, F-3 & F-4 are the concentration of heavy metals concentrated in individual fractions.

Here, Table 3 depicts the recovery rates of six heavy metals namely Zn, Cu, Ni, Pb, Cd, and Cr from the sediment samples from different sites of Pune District. The recovery rate of Zn ranged from 99.65 % to 144.44 % for Sediment Samples from Site 1 to Site 7. Similarly, the recovery rate of Cu and Ni was observed between 88.46% to 120.39 % and 77.21 % to 103.42 %, respectively. Likewise, Pb, Cd, and Cr recovery rates ranged from 90.76% to 120.0 %, 92.85 % to 114.28%, and 95.06% to 109.09%, respectively.

## CONCLUSION

The total heavy metal concentration investigation was conducted to assess the total concentration of selected heavy metals in sediment samples collected from different locations of Pune (Upstream region to the Downstream Region). Nickel and lead were observed to be among the highest concentrations, while Zinc and Copper were of the lowest ones. In total, the sediment samples from the central part of Pune and the downstream regions (Ujani Backwaters) were recorded to have the highest concentration of heavy metals (Site 5 to Site 7). The heavy metal speciation study indicates that Ni and Zn are among the abundant heavy metals in sediment samples, while Cd and Cr are among the lowest concentrations. In the speciation study, the oxidizable and residual species were found to be leading for all heavy metals. A notable change in the speciation fashion was observed among the sediment samples from different sample collection sites. This could be due to differences in water/soil composition and the agrochemicals like pesticides, weedicides, and fertilizers used in agricultural practices, the wastewater generated from different pharmaceutical industries, chemical processing, and manufacturing industries, as well as the improper wastewater treatment methods.

## REFERENCES

Álvarez, E.A., Mochon, M.C., Sánchez, J.J. and Rodrıǵuez, M.T. 2002. Heavy metal extractable forms in sludge from wastewater treatment plants. Chemosphere, 47(7): 765-775.

Arruti, A., Fernández-Olmo, I. and Irabien, Á. 2010. Evaluation of the contribution of local sources to trace metals levels in urban PM2.5 and PM10 in the Cantabria region (Northern Spain). J. Environ. Monit., 12(7): 1451-1458.

Beyersmann, D. and Hartwig, A. 2008. Carcinogenic metal compounds: recent insight into molecular and cellular mechanisms. Archives of toxicology, 82: 493-512.

Christoforidis, A. and Stamatis, N. 2009. Heavy metal contamination in street dust and roadside soil along the major national road in Kavala's region, Greece. Geoderma, 151(3-4): 257-263.

Fuentes, A., Lloréns, M., Sáez, J., Soler, A., Aguilar, M.I., Ortuño, J.F. and Meseguer, V.F., 2004. Simple and sequential extractions of heavy metals from different sewage sludges. Chemosphere, 54(8): 1039-1047.

Goyer, R.A. and Clarkson, T.W. 1996. Toxic effects of metals. The McGraw-Hill Company, NY.

Guan, D.S., Chen, Y.J. and Ruan, G.D. 2001. Study on heavy metal concentrations and the impact of human activity on them in urban and suburb soils of Guangzhou. Acta Sci. Nat. Unv. Sunyatseni, 40(4): 93-6.

Jamali, M.K., Kazi, T.G., Afridi, H.I., Arain, M.B., Jalbani, N. and Memon, A.R. 2007. Speciation of heavy metals in untreated domestic wastewater sludge by time saving BCR sequential extraction method. J. Environ. Sci. Health Part A, 42(5): 649-659.

Klaassen, C.D., Casarett, L.J. and Amdur, M.O. 1986. Toxicology: The Basic Science of Poisons. Macmillan, NY.

Rashed, M.N., Soltan, M.E., Fawzey, E.M. and El-Taher, M.A. 2011. Impact of sewage sludge spreading on heavy metal speciation in ecosystem. Indian J. Environ. Protect., 1: 37-44.

Rauret, G., López-Sánchez, J.F., Sahuquillo, A., Barahona, E., Lachica, M., Ure, A.M., Davidson, C.M., Gomez, A., Lück, D., Bacon, J. and Yli-Halla, M. 2000. Application of a modified BCR sequential extraction (three-step) procedure for the determination of extractable trace metal contents in a sewage sludge amended soil reference material (CRM 483), complemented by a three-year stability study of acetic acid and EDTA extractable metal content. J. Environ. Monit., 2(3): 228-233.

Shrivastava, S.K. and Banerjee, D.K. 2004. Speciation of metals in sewage sludge and sludge-amended soils. Water, Air, and Soil Pollution, 152: 219-232.

Su, D.C. and Wong, J.W.C. 2004. Chemical speciation and phytoavailability of Zn, Cu, Ni, and Cd in soil amended with fly ash-stabilized sewage sludge. Environ. Int., 7)29): 895-900.

Sutherland, R.A. 2010. BCR®-701: A review of 10-years of sequential extraction analyses. Anal. Chim. Acta, 680(1-2): 10-20.

Tessier, A.P.G.C., Campbell, P.G. and Bisson, M.J.A.C. 1979. Sequential extraction procedure for the speciation of particulate trace metals. Anal. Chem., 51(7): 844-851.

Walter, I., Martinez, F. and Cala, V. 2006. Heavy metal speciation and phytotoxic effects of three representative sewage sludges for agricultural uses. Environ. Pollut., 3)139): 507-514.

Wang, C., Li, X.C., Ma, H.T., Qian, J. and Zhai, J.B. 2006. Distribution of extractable fractions of heavy metals in sludge during the wastewater treatment process. J. Hazard. Mater., 137(3): 1277-1283.

Wang, S. and Shi, X. 2001. Molecular mechanisms of metal toxicity and carcinogenesis. Mol. Cell. Biochem., 222: 3-9.

Yan, J., Ye, Z.X., Yan, Y. and Huang, X.P. 2008. Study on heavy metals distribution in atmospheric particulate matter on both sides of the Cheng-Ya Expressway. Sichuan Environ., 2)2): 19-21.

## ORCID DETAILS OF THE AUTHORS

Parveen Hassanpourfard: https://orcid.org/0000-0003-4171-4766

# Biodiesel from *Dunaliella salina* Microalgae Using Base Catalyzed Transesterification – An Assessment through GC/MS, FTIR and NMR Studies

**V. Hariram*†, M. Janarthanan*, R. Christu Paul**, A. Sivasankar*, M. Wasim Akram*, E. Sangeethkumar**, V. Ramanathan**, P. Sajid Khan* and S. Manikanta Reddy***

*Department of Mechanical Engineering, Hindustan Institute of Technology and Science, Padur, Chennai-603103, Tamil Nadu, India
**Department of Automobile Engineering, Hindustan Institute of Technology and Science, Padur, Chennai-603103, Tamil Nadu, India
†Corresponding author: V. Hariram; connect2hariram@gmail.com

## ABSTRACT

Algal biofuels are a promising renewable feedstock to produce energy that can supplement future energy demands greatly. The present study aims to utilize Dunaliella salina, a hypersaline, unicellular greenish-orange micro-algae, to produce bio-oil. F/2 nutrient media and trace metal and vitamin solution under carbon-dioxide-rich conditions were used to cultivate the microalgae. Ultrasonic extraction method at 60 Hz for 90 min isolated 650 mL of bio-oil. A single-stage based-catalyzed transesterification process with methanol and sodium hydroxide yielded 380 mL of Pure *Dunaliella salina* biodiesel at % an extraction efficiency of 87%. The Phytochemical screening on the cultivated *Dunaliella* sp. was performed to understand its feasibility to be used as a fuel for IC engines. Furthermore, the obtained biodiesel was characterized using Fourier Transform Infrared Spectrometer (FTIR), Gas Chromatography Mass Spectrometer (GCMS), and Nuclear Magnetic Resonance (NMR) spectral analysis.

## INTRODUCTION

Global warming and environmental pollution concerns have arisen as a universal problem mainly due to non-renewable petroleum reserves. Continuous growing population, impulsive scarcity of energy, food, unpredictable weather, and insufficiency of cultivable land threaten global economic development (Hariram et al. 2017). Improbability in the availability of petroleum reserves acts up to the above factor leading to economic crises. Notable biomedical, biotechnology, and biological improvements triggered the researchers to reconnoiter feedstocks for new and renewable sources, thereby replacing the petroleum reserves. Among the feedstocks for deriving the biofuel, micro-algal sources gained importance in recent times due to their scalable adaptation Algal omic approach in the abiotic and biotic adaptation environment to understand a micro-algal growth response in a diversified condition created a new pathway to generate algal feedstocks for biofuel preparation (John et al. 2018).

Among the available microalgae, marine algal strain is a prominent sustainable choice for bio-oil production. As it requires primary seawater with a nominal quantity of micro and macronutrients for large-scale production, the further marine micro-algal feedstock is more advantageous than terrestrial vegetable feedstock due to their higher liquid biomass production rate, Superior photosynthesis and lesser requirement of arable land. Marine micro-algal biofuel production focuses on the design of a photobioreactor, micro macronutrients for liquid and biomass enhancement, Techniques for harvesting the biomass, and finally, liquid extraction. Further, the transformation of the extracted bio-oil into its fatty acid methyl ester places a thorough transesterification technique along with Sodium hydroxide and Methanol place a role. Difficulties in estimating the free fatty acid content lead to unsuitable esterification technique selection and partial transesterification leading to soapy sludge development. The transesterification efficiency also depends upon various operational parameters like molar ratio, reaction temperature, reaction time, and catalyst concentration. The resultant biodiesel is also subjected to a few spectroscopic characterization studies like Gas chromatography Mass Spectrometry (GC-MS) analysis, Fourier Transform Infrared Spectrometry (FT-IR) analysis,

and Nuclear Magnetic Resonance (NMR) Spectrometry to understand its feasibility to be used as a substitute fuel in internal combustion engines.

Sarpal et al. (2016) investigated the potential of biomass productivity from *Spirulina* sp., *Chlorella* sp., and *Tetraselmis sp*. They employed the GC-MS and NMR techniques to identify its fatty acid content. Modified RM6, F/2, and WC micro nutrient mediums were employed in microalgae cultivation with nitrogen and phosphate-rich conditions. The laboratory scale cultivation used an ultrasonicator to extract the liquids and was esterified. The GC-MS analysis identified the presence of polar and neutral fatty acids, and NMR analysis revealed the presence of polyunsaturated fatty acids (C18 to C22). Mathimani et al. (2015) asserted an efficient methodology to transesterify chlorella sp. (marine microalgae) using homogenized acidic catalytic transesterification. A maximum of 60% biodiesel yield was noticed at a reaction time of 2.5 h, and 3.5% of sulphuric acid Prominent proportion of Oleic acid, Palmitic acid, and Palmitoleic acid were found in the biodiesel using the Gas Chromatogram. Chisti (2007) has thoroughly reviewed extracting biodiesel from microalgae. He has demonstrated that an increase in global need would be met only with the continuous supply of renewable biodiesel from microalgae. It was also evidenced that algae production from micro-algal feedstock was found to be many folds than the best oil-yielding vegetable crop.

Chailleux et al. (2013) carried out an algo-route investigation to identify various compounds present in microalgae and their rheological characterization. Thermal-dependent and chemical-dependent behavior was noticed in the microalgae characterized through Gas Chromatography, Mass spectrometry, Nuclear Magnetic resonance, and Infrared analysis. Shah and Veses (2016) derived biofuel from *Spirogyra* sp., a freshwater microalgae. The high-density energy fuel (bio-oil) was extracted through pyrolysis techniques (A thermal process without oxygen) in multi-steps. The operating temperature was increased from 25° Centigrade to 650° Centigrade at equal internal time, and the resultant product was characterized using GC-MS and FT-IR analysis. 2, 3, 5 Trimethyl Pyrazole, a long-chain hydrocarbon, was found in a notable proportion up to 20.086%. Yasir Al-Shikaili et al. (2022) used Fourier transform Infrared Spectrometry to analyze the quantity and quality of neutral liquids in Nannochloropsis Salina microalgae. Micro oven drying of 40% centigrade for 12 h and processing the algal sample with potassium bromide transformed the algal feedstock into the fillets. The neutral liquid was identified in the FT-IR spectrum due to its characteristic absorption band between 1742 cm$^{-1}$ and

2920 cm$^{-1}$. Sarpal et al. (2015) monitored the liquid content of the microalgal biomass by employing the Nuclear Magnetic Resonance technique throughout the cultivation and biodiesel production face.

Laboratorial strains of *Scenedesmus ecornis* and *Chlorella vulgaris* were employed in this study to assess polar and neutral liquids and fatty acid profiles in the microalgal biomass. The $^{13}$C and 'H NMR analyses were very effective in monitoring the enhancement in liquid productivity of the micro-algal samples. The fatty acid content using GC-MS analysis revealed a similar hydrocarbon structure as that of fish and vegetable oil with enhanced neutral liquid content in the micro-algal strains. Bisht et al. (2021) adopted the nuclear Magnetic Resonance approach to assess metabolic capabilities like lipidomics and metabolomics activities. Wahlen et al. (2013) derived biodiesel from oleaginous microalgae through the transesterification process from Bacteria, Yeast, and Microalgae. The feasibility of using biodiesel in a C. I engine was performed, and its effect on the exhaust emissions was evaluated.

Most of the reported literature above has analyzed the potential of micro-algal oil using various spectroscopic studies towards bio-oil yielding capability. In the present investigation *Dunaliella* sp., a marine single-cell algae, was cultivated in a controlled environment using an F/2 nutrient medium, and its liquid content was isolated using centrifugation. The bio-oil was expelled by employing an ultrasonicator. Characterization and phytochemical analyses were carried out on the expelled bio-oil and further trans-esterified. The feasibility of the derived biodiesel to be used as a substitute fuel in an IC engine was carried out by employing GC-MS, FT-IR, and NMR Spectral techniques.

## MATERIALS AND METHODS

*Dunaliella salina* is a unicellular greenish-orange halophile microalgae found abundant in the salina environment. *Dunaliella salina* belongs to the Division of Chlorophyta, class of Chlorophyceae, Order of Chlamydomonas, family of Dunaliellaceae Genes of Dunaliella, and Species of *Dunaliella salina* (Fig. 1). The biomass of *Dunaliella salina* was reported to comprise carotenoids and lipids in prominent proportions.

The National Institute of Ocean Technology, Chennai, Tamilnadu, India, provided the algal strain of Dunaliella Salina. The biomass cultivation of the *Dunaliella* sp. was organized in a lab scale model using three sets of Erlenmeyer flasks under acidic conditions. Each Erlenmeyer flask was filled with 200 mL of F/2 nutrient medium under nitrogen-deficient conditions. The F/2 nutrient medium was prepared
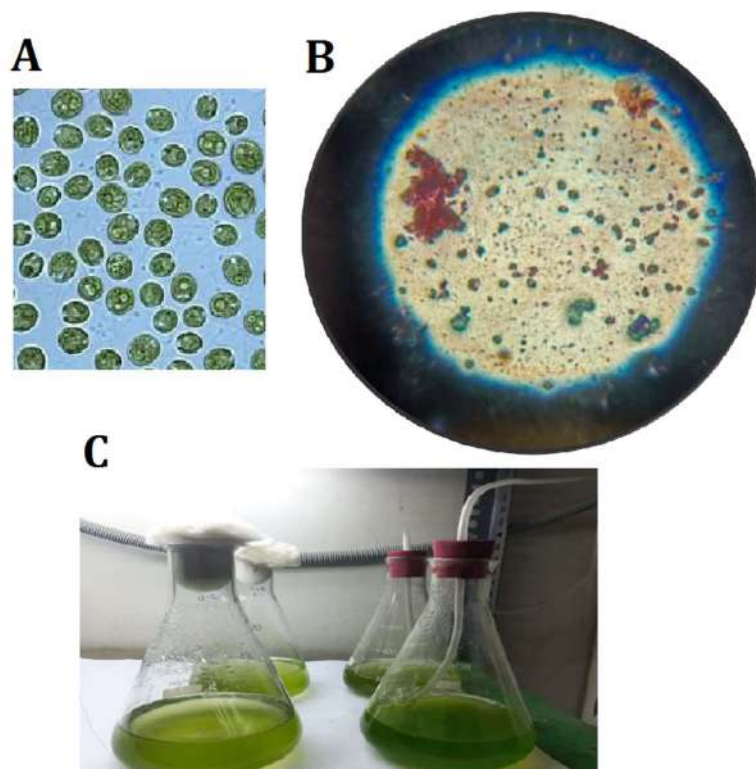
Fig. 1: *Dunaliella salina* – Morphology (A and B) and Growth (C).

in three stages. Stage one comprises the stock solution followed by trace metal and vitamin solutions. The stock solution comprises five different chemical mixtures that are 75 g.L$^{-1}$ of $NaNO_3$ in distilled $H_2O$, 5 g.L$^{-1}$ of $NaH_2PO_4$ in distilled $H_2O$, 30 g.L$^{-1}$ of $Na_2 CO_3$ in distilled $H_2O$ along with trace metal & vitamin solution. The trace metal solution is prepared by amalgamating the following trace metals with 950 mL of distilled water. 3.15 g of $FeCl_3$, 4.36 g of $Na_2 (EDTA)_2$, 9.8 g.L$^{-1}$ $CuSO_4$ in $DH_{2,6.3}$ g.L$^{-1}$ $Na_2 MoO_4$ 22.0 g $ZnSO_4$, 10:8 $CoCl_2$ and 180 g.L$^{-1}$ of $MnCl_2$ in $dH_2O$. The F/12 vitamin solution is prepared once again by mixing 950ml of $dH_2O$ with thiamine and the stock solution further by adding 200 mg of thiamine HCL, 10 mL of Biotin as 0.1 g.L$^{-1}$ in $dH_2O$ and 1 mL of Cyanocobalamin as 1 g.L$^{-1}$ in $dH_2O$. The Biomass cultivation was initiated in the laboratory scale with an illuminated fluorescent light intensity between 70μ mol.m$^{-2}$s$^{-1}$ and 90μ mol.m$^{-2}$s$^{-1}$. The Carbon dioxide was allowed to recirculate continuously with the cultivation temperature between 27±2° Centigrade. The growth face of *Dunaliella salina* was monitored continuously for up to 72 h, beyond which stationary growth face was attained. The wet biomass of *Dunaliella salina* was carefully harvested and subjected to freezing at less than 6°C in a refrigerator for pelleting and lyophilization.

## Extraction of Bio-Oil from *Dunaliella salina*

An ultrasonic Bio-oil extraction process was adopted to derive algal oil from harvested *Dunaliella salina* biomass. 100 g of *Dunaliella salina* biomass was mixed with 30 mL of a mixture containing methanol, chloroform, and double distilled water in the ratio of 1:2:0.4 to improve the extraction efficiency of the ultra-sonication process. The ultrasonicator was allowed to operate at 60 Hz for 90 min, during which the cell wall membranes of the *Dunaliella salina* were ruptured, thereby expelling out the algal oil. The extracted oil was then transferred into a beaker along with the sediments, and 10 mL of methanol was further added and thoroughly mixed. The Whatman filter paper was employed to remove the unwanted particles and isolate the algal oil. The resultant algal oil was treated with 6 mL acetone at an elevated temperature to remove the traces of $H_2O$ in the algal oil. This procedure was repeated 17 times to isolate 650 mL of algal oil from *Dunaliella salina*.

## Transesterification of Algal Oil

Since the free fatty acid content in the *Dunaliella salina* bio-oil was estimated as 1.82 single-stage transesterification process with sodium hydroxide methanol was adopted to

convert a tri-glyceride into its mono alkyl methyl esters. The transesterification conditions were set to the optimistic levels based on the literature as molar ratio 1:6, 0.6% by weight of NaOH as a catalyst, 70°C, and 120 min as reaction time, respectively. Initially, 1.2 g of Sodium hydroxide pellets were dissolved in 100 mL of methanol Solution in a beaker for 20 min and 450 rpm agitation speed for the formation of sodium methoxide solution. As stated earlier, the molar ratio between algal bio-oil and methanol was maintained at 1:6 by mixing 40 mL of sodium methoxide solution with 120 mL of algal oil in a single batch base catalyze transesterification process. The entire mixture was transferred into a flat bottom conical flask and maintained at 70°C for 120 min to initiate the transesterification reaction. A cooling period of 180 min was allowed after transferring the entire content into a separating funnel. A ring formation distinction between the glycerol and algal biodiesel as the lower and upper layers conformed to the completion of the transesterification process. The rotating knob of the separating funnel was turned on to remove the glycerol. Thereby, algal oil was isolated. The obtained algal oil was heated up to 60°C for 2 min after the addition of 5 mL acetone for the removal of trace elements and water molecules (John et al. 2017). This batch process was repeated 6 times, yielding 380 mL of pure Dunaliella salina biodiesel at a transesterification efficiency of 87%.

### Gas Chromatography-Mass Spectrometer (GCMS)

To identify the various Fatty Acid Methyl Esters in esterified bio-oil extracted from the *Dunaliella sp*. marine algae. The single quadruped 5977B mass spectrometer (8890) Agilent GC system was employed to identify the various FAME's through thermal stabilization. The GC system was equipped with an SSL injector and capillary columns with an inlet split ratio of 7500:1. The over temperature of the GC system can be raised to 450°C. A pre-heated monolithic hyperbolic quadrupole mass filter was employed in the chemical and electron impact ionization mode. The quadruple temperature and the ion source temperature were varied between 106°C -200°C and 150°C - 350°C respectively. HP5 MSUI and DB-WAX type of polar capillary column were used to identify the various FAME's.

### Fourier Transform Infrared Spectrometer (FTIR)

The phenomenon of total internal reflection was utilized to understand the transmittance of *Dunaliella sp*. biodiesel. A single reflection module by Bruker Alpha Platinum Total Attenuated Internal Reflectance FT-IR instrument was employed in this study. A transmittance vibration signal was obtained when an infrared beam was allowed to pass through the biodiesel sample and the crystal where the total internal reflection takes place, producing the angle of incidence. The spectral range of the Bruker Alpha Platinum spectrometer was between 500 cm$^{-1}$ and 4000 cm$^{-1}$ with a resolution of 2 cm$^{-1}$. One mL of the biodiesel sample was injected into the rock-solid Michelson Interferometer equipped with diamond and brazed Tung Carbide crystal and Deuterated triglycine Sulphate (DTGS) as the detector.

### Nuclear Magnetic Resonance (NMR)

Bruker AVANCE 3 HD 500 FT-NMR spectrometer was used to analyze the presence of Carbon and Proton observation and decoupling in the biodiesel sample. The spectrometer is equipped with ASCEND 500 MHz high-performance actively shielded Superconducting magnet with an operational field at 11.746 Tesla and 54 mm Standard bore. The lock Control unit (Shim) system has 36 orthogonal shim gradients and Bruker Smart Magnetic Control System. The electronic control system compresses a bi-directional connection with a compact AQS-IPSO 3 frequency channel and 1 gradient channel. Advanced pulse generating system with a time resolution of 12.5 ns and frequency generating System of 2 RF channels with a frequency range. 6-643 MHz was used to synchronize the frequency and amplitude. A 6-365 MHz ATR transmitter with 500 w pulse power, high dynamic, multi-nuclear, linear amplifier was used as the transmitter. 4 mm broadband cross-polarization Magic Angel Spinning (MAS) multi-nuclear probe was used to observe the decoupling of $^1$H nuclei, whereas a 1.7 mm Triple Inverse Probe (TIP) with gradient was used to observe the decoupling cross-polarization of $^{13}$C nuclei in the spectrometer.

## RESULTS AND DISCUSSION

### Qualitative Analysis and Phytochemical Analysis

The presence of alkaloids, carbohydrates, protein amino acids, flavonoids, phenolic compounds, tannin, carotenoid carboxylic acid, volatile oils, and fixed oil was identified by employing the phytochemical screening approach. Dragendroff's reagent and Barfoed's reagents were primarily used in a phytochemical screening process.

The Dragendroff's reagent is prepared in two stages: a stock solution and a working Solution. The stock solution is composed of Sodium iodide (4 g), Bismuth carbonate (5.2 g), and Glacial acidic acid (50 mL). The mixture was boiled for 20 min, and a 12 h cooling period was allowed, during which sodium acetate crystal precipitated 40 mL of the filtrate were was thoroughly mixed with ethyl acetate (160 mL) in 1 L of distilled water. The working solution (Dragendroff's reagent) was prepared by amalgamating 10 mL of stock solution, 20 mL of acidic acid, and 70 mL of double distilled water. Similarly, Barfoed's reagent was prepared by thoroughly mixing copper acetate (30.5 g) and
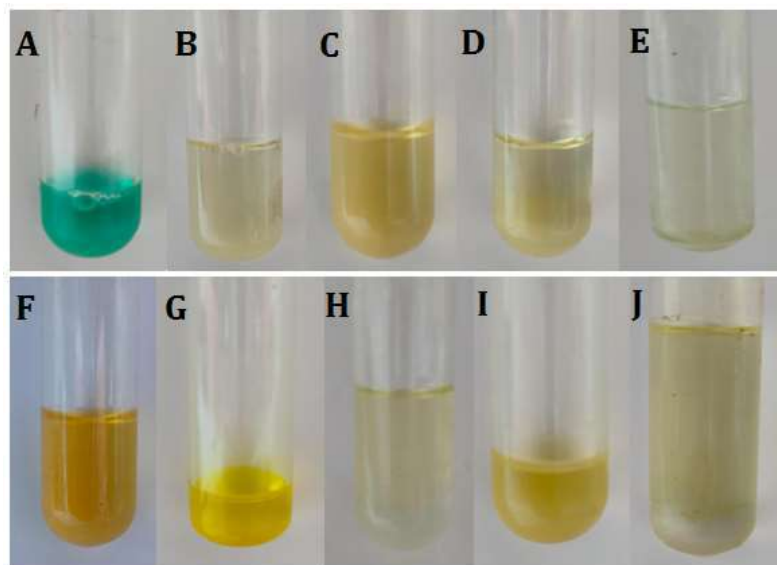
Fig. 2: *Dunaliella salina* – Phytochemical screening and analysis.

glacial acidic acid (1.8 mL) in 100 mL of distilled water (Shaikh & Patil 2020).

## Carotenoids Detection

Carr-Price reaction was used to detect the presence of Carotenoid in the *Dunaliella sp*. sample. In a glass plate, 10 mL of *Dunaliella* sp. algal extract was evaporated to dryness. A saturated chloroform and antimony dichloride solution was dropped on the glass plate. A transformation of bluish-green color to bright red confirmed the presence of carotenoids (Fig. 2A).

## Alkaloid's Detection

The Dragendroff's reagent was used to identify the presence of alkaloids. 2 mL of *Dunaliella sp*. sample extract was mixed with 2 mL of Dragendroff's reagent in a test tube under an aseptic condition. The appearance of radish brown indicated the presence of alkaloids (Fig. 2B).

## Carbohydrate Detection

1 mL of centrifuged *Dunaliella* sp. extract is mixed with 2 mL of Barfoed's reagent in a test tube and heated for 3 min. The disappearance of red precipitate confirms the absence of monosaccharide carbohydrates (Fig. 2C).

## Proteins and Amino Acid Detection

Biuret test with the *Dunaliella* sp. extract was employed to detect the amino acids and proteins. The test was performed with 2 mL of *Dunaliella* sp. sample extract, a drop of copper

sulfate solution (2%), and 1 mL of ethanol and potassium hydroxide fillets. The non-appearance of the pink-colored ethanolic layer indicated the absence of amino acids and proteins (Fig. 2D).

## Flavonoids Detection

A two-step alkaline reagent test was adopted to detect the presence of flavonoids. In the primary steps, 2% sodium hydroxide solution (2 mL) and 3 drops of dilute hydrochloric acid were mixed with 1 mL of *Dunaliella* sp. algal extract in a test tube. The solution's color transformation from, for instance, yellow to transparent and colorless liquid during dilute hydrochloric acid addition indicates the presence of flavonoids. The secondary step involved adding Ammonium hydroxide solution (10%) to the *Dunaliella* sp. algal extract turning the solution into a fluorescent yellow color liquid, confirming the presence of flavonoids (Fig. 2F).

## Phenolic Compounds Detection

The iodine test was adopted to identify the presence of Phenolic compounds. A few drops of dilute Iodine solution were mixed thoroughly with 1 mL of *Dunaliella* sp. algal extract. The color non-transformation into dark red confirmed the absence of phenolic compounds (Fig. 2E)

## Tannin Detection

A gelatin test was adopted to detect the presence of tannin. The base solution was prepared using 1% gelatin solution with 10% sodium chloride. The centrifuged *Dunaliella* sp.

algal extract was dissolved in 5 mL of distilled water and further thoroughly amalgamated with the base solution. A white precipitate formation after 10 min indicated the presence of Tannin in the algal strain.

## Carboxylic Acid Detection

A simplified effervescence test was used to identify the carboxylic acid. After a few minutes of mixing, 1 mL of sodium bicarbonate solution was mixed with an equal amount of centrifuged Dunaliella sp. extract in the effervescence, indicating the presence of carboxylic acid, as shown in Fig. 2J.

## Fixed Oil and Fat Detection

Stain/Spot tests were adopted to identify the presence of fat and fixed oils. A major quantity of centrifuged *Dunaliella* sp. algal extract was placed between two filter papers and pressed. Upon evaporation, the presence of an oil stain on the filter paper indicated its presence.

## Volatile Oil Detection

Fluorescence was used to detect the volatile oil presence in *Dunaliella* sp. Sample. 10 mL of the *Dunaliella* sp. algal extract was filtered till the saturation level and subjected to UV light rays. The non-observant of bright pinkish fluorescence indicated the absence of Volatile oils.

## Comparison of Physio-Chemical Properties – Diesel, *Dunaliella salina* Algal Oil and its Biodiesel

The physicochemical properties of *Dunaliella salina* algal oil and its biodiesel were compared with commercial diesel in Table 1. The density of *Dunaliella salina* algal biodiesel was slightly increased by 0.545% but was found to be within limits. The gross calorific value showed significant appreciation up to 24.89%, along with a notable increase in oxygen content. The transesterification process considerably

reduced the kinematic viscosity from 22.9875 cSt to 2.657 cSt, thus making it more suitable for CI engine usage (Hariram et al. 2018).

## Fourier Transform Infrared Spectrometer (FTIR)

The bending and stretching Vibration seen between 547.17 cm$^{-1}$ and 3008.32 cm$^{-1}$ in the FTIR spectrum of *Dunaliella* sp. biodiesel is showcased in Fig. 3, a strong signal compressing of stretching vibration at 1741.22 cm$^{-1}$ indicates the transformation of bio-oil from *Dunaliella* sp. into its fatty acid methyl ester. A group bending-stretching vibration was noticed between 1019.14 cm$^{-1}$ and 1460.99 cm$^{-1,}$ indicating long-chain hydrocarbon (C=H). Several weak signals were seen at 844.85 cm$^{-1}$, 914.1 cm$^{-1,}$ and 1437.12 cm$^{-1,}$ indicating a carboxylic group's presence. Strong signals were seen at 2853.91 cm$^{-1}$ and 2923.46 cm$^{-1,}$ along with the weak trailing signal 3008.32 cm$^{-1,}$ confirming the complete transformation of the bio-oil and its FAME's. No signal formation between 1750 cm$^{-1}$ and 2800 cm$^{-1}$ is one of the characteristic features of biodiesel obtained through a single state-based transesterification process (Hariram et al. 2017).

## Gas Chromatography-Mass Spectrometer (GCMS)

A single-stage base-catalyzed transesterification process with sodium hydroxide and methanol converted the bio-oil extracted from the *Dunaliella* sp. marine algae into its biodiesel. Gas Chromatography-Mass Spectrometer analysis was conducted on an esterified biodiesel sample to understand its transesterification efficiency and identify the presence of various fatty acid methyl esters. The mass chromatogram of the biodiesel reviewed the presence of nine different FAME's at retention time (RT) between 19.93 and 30.48 min (Fig. 4). A characteristic base Peak was noticed at m/z 74 in all the distinct fragmentation patterns to identify fatty acid methyl ester. It was noticed that the mass chromatogram and the fragmentation patterns of the algal bio-oil and the esterified biodiesel were in line with the McLafferty rearrangement process. Several mass

Table 1: Physio-chemical properties of *Dunaliella salina* algal oil, its biodiesel, and diesel.

| Property | *Dunaliella salina* algal oil | *Dunaliella salina* algal biodiesel | Diesel |
|---|---|---|---|
| Molecular formula | $C_{13} - C_{24}$ | - | $C_{12}H_{22}$ |
| Gross calorific value [kJ.kg$^{-1}$] | 30547 | 40547 | 42700 |
| Density [kg.m$^{-3}$] | 834.786 | 860 | 842 |
| Kinematic Viscosity [cSt] | 22.9875 | 2.657 | 2.82 |
| Sulfur content [% vol] | 0.34 | 0.20 | 0.04 |
| Flashpoint [$^{o}$C] | 270-280 | 48 | 69 |
| Cetane number | 36 | 45 | 48.5 |
| Oxygen content [% wt] | 5.678 | 9.871 | 0 |
| Ash content | 1.315 | 0.479 | 0 |
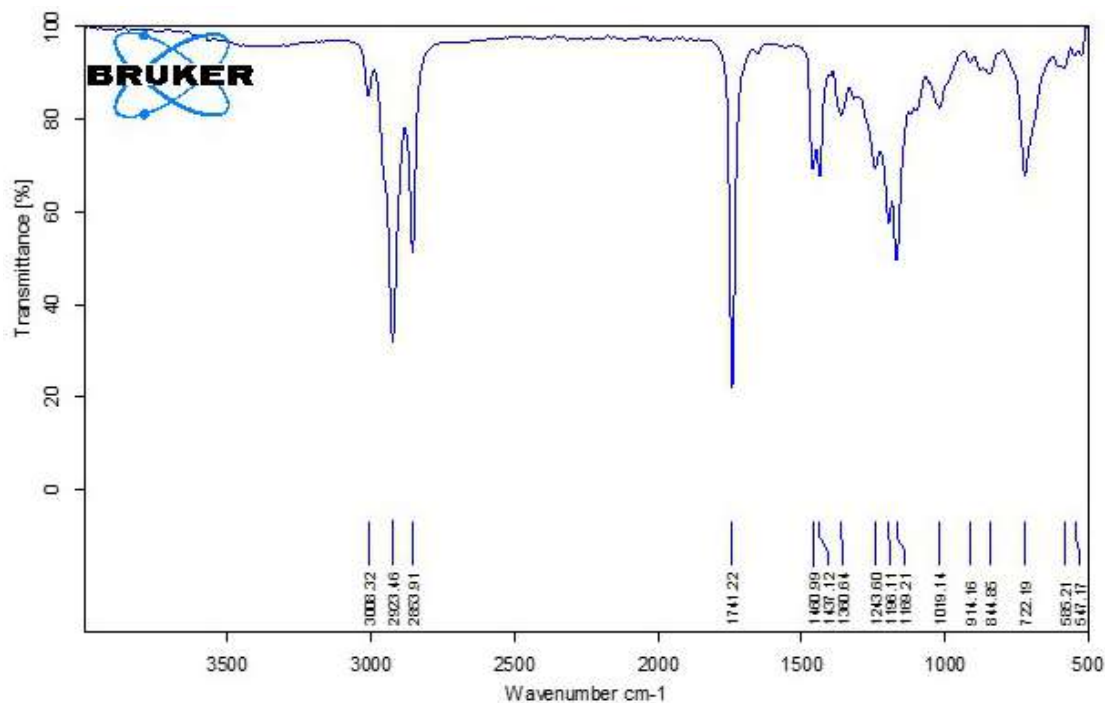
Fig. 3: *Dunaliella salina* biodiesel – FTIR Transmittance.
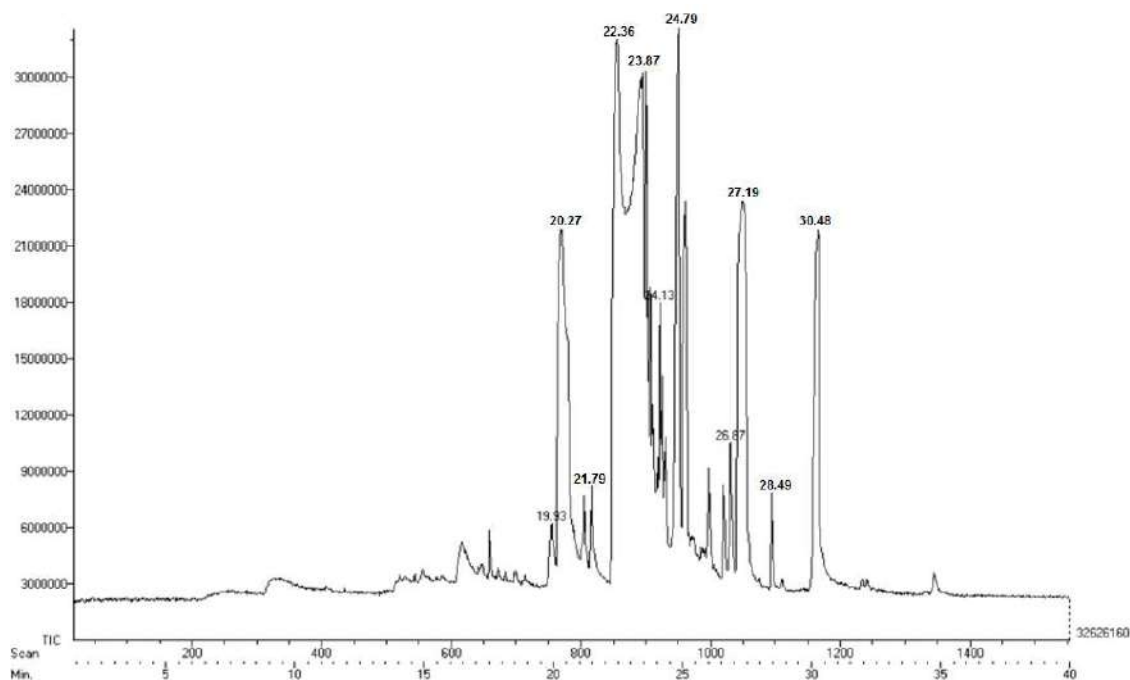


Fig. 4: *Dunaliella salina* biodiesel – GCMS chromatogram.

fragmentation patterns of the FAME showcase the loss of carbo-methoxy ions due to β cleavage. Multiple profusions were also noticed in a few of the mass fragmentation patterns, which may be due to the loss of the methoxy group and the rearrangement of carbon and hydrogen atoms during the transesterification process. The presence of unsaturated

fatty acids like 14, 17-Octadecadienoic acid methyl ester at RT 22.36 min is due to the repositioning and regrouping of the hydrogen ion in the Carbonyl group (Sarpal et al. 2016).

The various fatty acid methyl ester presenting the biodiesel sample was found to be 9-hexadecenoic acid methyl ester at RT 19.93, hexadecanoic acid methyl ester at RT 20.27, heptadecanoic acid methyl ester at RT 21.79, 14, 17-octadecadienoic acid methyl ester at RT 22.36, eicosanoic acid methyl ester at RT 24.79, 13-docosenoic acid methyl ester at RT 26.87, docosanoic acid methyl ester at RT 27.19, tricosanoic acid methyl ester at RT 28.49, and tetracosanoic acid methyl ester at RT 30.48.

### Nuclear Magnetic Resonance (NMR)

**Proton NMR (^{1}H NMR):** ^{1}H NMR solution was prepared by dissolving 7.5 mL of *Dunaliella salina* algal biodiesel with 0.8 mL of Deuterated methanol as a Solvent. The relaxation delay and the pulse during the Injection of the sample were maintained at 10 sec and 90°, respectively. The Proton NMR Spectrum of the *Dunaliella salina* biodiesel compresses mainly fatty acid esters along with alkaloids, alkanes, and steroids in minor proportions. The characteristic peak in the ^{1}H NMR spectrum of *Dunaliella salina* biodiesel spectrum was noticed at 3.669 ppm, which

is due to the functional group of fatty acid esters (Fig. 5). A prominent signal corresponding to the carbonyl functional group is seen at 5.387 ppm. Clustered peaks indicative of unsaturated long-chain hydrocarbons are evident in the range of 3.330 ppm to 2.108 ppm. Signals at 5.397 ppm and 5.408 ppm were apportioned to OCH and OCH$_2$ ester groups due to their transformation from triglyceride to mono-alkyl fatty acid ester. The ^{1}H NMR spectrum also exhibited a faint doublet peak at 3.336 ppm, possibly arising from alkenes in the excipient. The existence of the triplet peak at 1.377 ppm confirmed the presence of polyunsaturated fatty acid in the *Dunaliella salina* biodiesel Sample (Bisht et al. 2021).

### Carbon NMR (^{13}C NMR)

Similar to the sample injection Proton NMR, ^{13}C NMR analysis was also initiated with Deuterated methanol of solvent for profiling the unsaturated fatty acid composition. Since ^{13}C NMR possesses a relatively larger chemical shift range between 0 ppm to 200 ppm, sharper and distinctive peaks of monoglycerides, diglycerides, triglycerides, and epoxy ester were identified (Fig. 6). In the ^{13}C NMR spectrum of *Dunaliella salina* biodiesel, a characteristic singlet peak was noticed at 47.967 ppm due to the existence of mono-alkyl long-chain hydrocarbon. A cluster peak
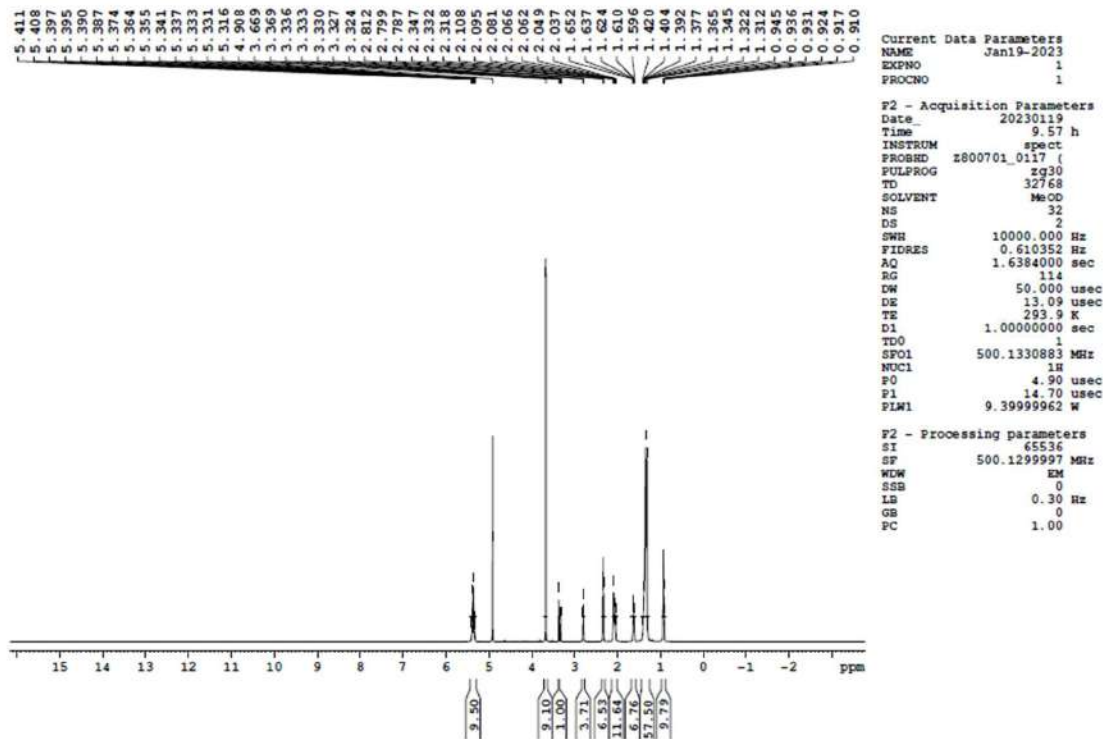


Fig. 5: *Dunaliella salina* biodiesel – ^{1}H NMR spectrum.
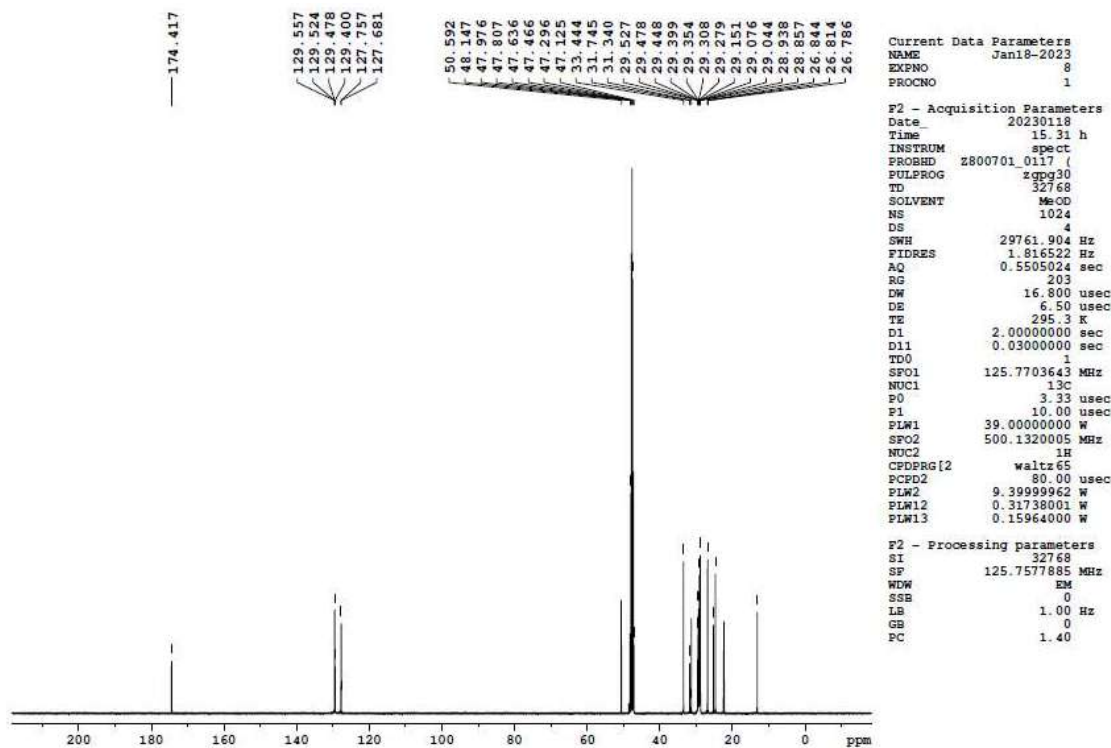
Fig. 6: *Dunaliella salina* biodiesel – $^{13}$C NMR spectrum.

between 127.681 ppm and 129.557 ppm showed the strong existence of carbonyl group unsaturated esters. A terminal peak at 174.417 ppm evidenced the completion of the transesterification reaction with the presence of long-chain hydrocarbons. A large group cluster peaks between 26.814 ppm and 33.444 ppm showed the presence of a carboxylic group. The presence of monoglycerides was also evidenced by a weak signal at 16. 442 ppm in the $^{13}$C NMR spectrum of *Dunaliella salina* biodiesel.

## CONCLUSION

This investigation aims at producing biodiesel from *Dunaliella salina* microalgae. The following conclusion was made at the outset.

- *Dunaliella salina,* hypersaline unicellular microalgae, was cultivated in an aseptic environment under carbon dioxide-rich conditions with F/2 as a nutrient medium.

- Ultrasonic-assisted bio-oil extraction process with the combination of methanol, chloroform, and double distilled water in ratios of 1:2:0.4 operating at 60 Hz for 90 min isolated 650 mL of *Dunaliella salina* bio-oil.

- Single-stage base-catalyzed transesterification process with a 1:6 molar ratio, 0.6% by weight of NaOH,

70°C reaction temperature, and 120 min reaction time yielded 380 mL of *Dunaliella salina* biodiesel at a transesterification efficiency of 87.2%.

- The phytochemical screening process with Dragendroff's and Barfoed's reagents revealed the presence of carotenoids, alkaloids, flavonoids, and carboxylic acid.

- The Fourier Transform Infrared transmittance evidenced the transformation of bio-oil into its FAME's by strong stretching vibrations at 1741 cm$^{-1}$ and 2853.91 cm$^{-1}$.

- The Gas Chromatography-Mass Spectrometry analysis revealed the presence of Octadecadienoic acid methyl ester at RT 22.36 in notable proportions.

- The Proton NMR ($^1$H NMR) with a characteristic peak at 3.669 ppm confirmed the presence of fatty acid esters. Further, signals at 5.397 ppm and 5.048 ppm apportioned to OCH and OCH$_2$ resulted from the transformation of mono-alkyl esters to FAME. The Carbon NMR ($^{13}$C NMR) spectrum also revealed long-chain hydrocarbon resulting from the transesterification reaction by cluster peaks between 127.681 ppm and 129.557 ppm.

Thus, with the above qualitative outcomes, it can be concluded that biodiesel derived from *Dunaliella*

*salina* could be a promising substitute for petro-diesel feedstock.

## REFERENCES

Bisht, B., Kumar, V., Gururani, P., Tomar, M.S., Nanda, M., Vlaskin, M.S., Kumar, S. and Kurbatova, A. 2021. The potential of nuclear magnetic resonance (NMR) in metabolomics and lipidomics of microalgae: A review. Arch. Biochem. Biophys., 710: 108987. https://doi.org/10.1016/j.abb.2021.108987

Chailleux, E., Audo, M., Bujoli, B., Queffelec, C., Legrand, J. and Lepine, O. 2013. Alternative binder from microalgae: Algoroute project. HAL, 11: 7-14.

Chisti, Y. 2007. Biodiesel from microalgae. Biotechnol. Adv., 25(3): 294-306. https://doi.org/10.1016/j.biotechadv.2007.02.001

Hariram, V., John, G. and Seralathan, S. 2017. Spectrometric analysis of algal biodiesel as a fuel derived through base-catalyzed transesterification. Int. J. Ambient Energy, 40(2): 195-202.

Hariram, V., Prakash, S., Seralathan, S. and Micha Premkumar, T. 2018. Data set on optimized biodiesel production and formulation of emulsified *Eucalyptus teriticornisis* biodiesel for usage in compression ignition engine. Data Brief, 20: 6-13. https://doi.org/10.1016/j.dib.2018.07.053

John, G., Hariram, V. and Seralathan, S. 2018. Emission reduction using improved fuel properties of algal oil biodiesel and its blends. Energy Sour. Part A, 40(1): 45-53.

John, G., Hariram, V., Seralathan, S. and Jaganathan, R. 2017. Effect of oxygenate on emission and performance parameters of a CI engine fuelled with blends of diesel-algal biodiesel. Int. J. Renew. Energy Res., 7(4): 2041-2047.

Mathimani, T., Uma, L. and Prabaharan, D. 2015. Homogeneous acid-catalyzed transesterification of marine microalga *Chlorella* sp. BDUG 91771 lipid e– an efficient biodiesel yield and its characterization. Renew. Energy, 81: 523-533. https://doi.org/10.1016/j.renene.2015.03.059

Sarpal, A.S., Costa, I.C.R., Teixeira, C.M.L.L., Filocomo, D., Candido, R., Silva, P.R., Cunha, V.S. and Daroda, R.J. 2016. Investigation of biodiesel potential of biomasses of microalgae *Chlorella*, *Spirulina*, and *Tetraselmis* by NMR and GC-MS techniques. J. Biotechnol. Biomater., 6(1): 1-15.

Sarpal, A.S., Teixeira, C.M.L.L., Silva, P.R.M., Vieira da Costa Monteiro, T., Itacolomy da Silva, J., Smarcaro da Cunha, V. and Daroda, R.J. 2015. NMR techniques for determination of lipid content in microalgal biomass and their use in monitoring the cultivation with biodiesel potential. Appl. Microbiol. Biotechnol., 1-15.

Shah, Z. and Veses, R.C. 2016. GC-MS and FTIR analysis of bio-oil obtained from freshwater algae (spirogyra) collected from Freshwater. Int. J. Environ. Agric. Res., 2(2): 134-141.

Shaikh, J.R. and Patil, M.K. 2020. Qualitative tests for preliminary phytochemical screening: An overview. Int. J. Chem. Stud., 8(2): 603-608. https://doi.org/10.22271/chemi.2020.v8.i2i.8834

Wahlen, B.D., Morgan, M.R., McCurdy, A.T., Willis, R.M., Morgan, M.D., Dye, D.J., Bugbee, B., Wood, B.D. and Seefeldt, L.C. 2013. Biodiesel from microalgae, yeast, and bacteria: engine performance and exhaust emissions. Energy & Fuels, 27(1): 220-228.

Yasir Al-Shikaili, T., Thomasson, J.A., Ge, Y., Brown, L. and Brown, Jola. 2022. FTIR transmission spectroscopy for measurement of algae-neutral lipids. Agriculturists Eng. Int., CIGR J., 24(4): 111-118.

# Ability of Water Lettuce (*Pistia stratiotes*) And Water Hyacinth (*Eichhornia crassipes*) To Remove Methylene Blue Anionic Surfactant (MBAS) From Detergent Wastewater

**N. Hendrasarie\*† iD and C. Redina\***

\*Department of Environmental Engineering, University of Pembangunan Nasional "Veteran" Jawa Timur, Indonesia
†Corresponding author: N. Hendrasarie; novirina@upnjatim.ac.id

## ABSTRACT

ABS was the first surfactant used in detergent formulations, but because its molecular structure is branched, it is difficult to decompose biologically, making ABS a toxic compound for the environment. This study aims to remove MBAS surfactant, using a combination of phytoremediation and filtration methods to remove surfactant (MBAS) Chemical Oxygen Demand (COD) from detergent wastewater by optimizing operating factors such as pH, contact time, plant type, and filter media. Water lettuce (*Pistia stratiotes*) and water hyacinth (*Eichhornia crassipes*) were selected as plant species and silica-activated carbon was used as filter media. Water lettuce and hyacinth were grown in a 10-liter reactor with detergent wastewater samples for 6 and 12 days. Filter media are placed in the reactor in use, and aeration is done. The efficiency for reducing COD was 81.73%, and the efficiency for surfactant was 99.42% for each experiment, which was thought to be because of plant adsorption and filtering processes. The water lettuce (*Pistia stratiotes)* plant had the maximum adsorption capability for all the qualities evaluated, with a surfactant content in the roots of 27543.24 (mg/kg MBAS), compared to the water hyacinth plant, which only absorbed 2597.95 (mg/kg MBAS).

## INTRODUCTION

Detergent is the highest pollutant in the water, along with world detergent production, which reached 2.7 million t.y$^{-1}$ with an increase of 5% annually. The active substance in this waste needed to be noticed because it could be a threat to the health and environment. Detergent wastewater is usually produced from washing and laundry waste and has a main content in the form of surfactant and builder in phosphate form. The waste continued to increase as the community grew. Most of the detergent wastewater is directly discharged into the water bodies without going through a treatment or appropriate process. This could lead to environmental damage (Suwandhi et al. 2022, Moondra et al. 2021, Saini et al. 2021).

People have less understanding of the adverse effects of detergent waste when it is directly discharged into the environment. This resulted in disturbance to the environment, even the community itself. The other environmental impact caused by detergent waste was also eutrophication in the waters. Aquatic plants consume oxygen in the water to decrease dissolved oxygen content and disrupt the lives of

other aquatic biota, such as fish and benthic invertebrates. Surfactants in detergent waste may harm humans, particularly with direct contact with the skin, and cause dryness, blister, easily peeled skin, allergies, and itch (Rebello et al. 2014, Simoni et al. 1996).

Detergent is a widely used surfactant. Detergent is used for both household and industrial purposes. The anionic type surfactant in the form of sulfonate (SO3) is the most widely used to produce detergent surfactants. The detergent class of sulfonates is divided into two types: branched chain types such as Alkyl benzene sulfonate (ABS) and straight-chain types such as Linear Alkylbenzene sulfonate (LAS) (Al Idrus et al. 2020, Correa dos Santos et al. 2022).

ABS was the first surfactant used in detergent formulations, but because of its branched molecular structure (Fig. 1), ABS is a toxic compound to the environment. Linear alkylbenzene sulfonate (LAS) is widely used to replace branch alkylbenzene sulfonate (ABS) in large quantities around the world because it is a detergent material with a straight molecular structure (Fig. 1) and is more biodegradable than ABS. (Lee 2013, Lundholm 2013, Parde
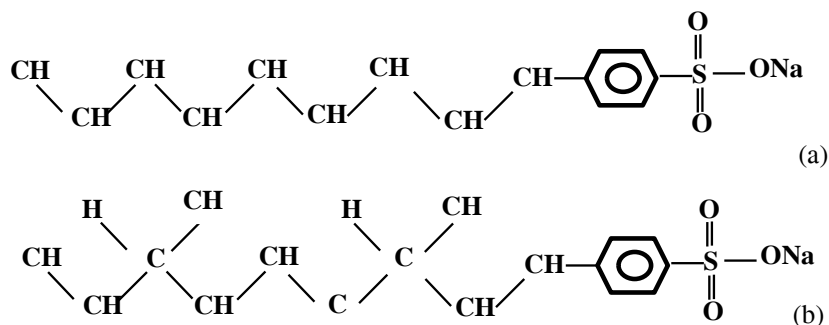
Fig. 1: Straight Chain and Branched Chain Detergent Molecule Structure.

et al. 2021). LAS can reduce surface tension and emulsify fat, making it useful as a fat solvent and for protein denaturation (Hudori & Soewondo 2009). LAS slows the diffusion of oxygen from the air into the waters, lowering dissolved oxygen (DO) (Suastuti et al. 2015).

In addition, the surfactant may cause slowing oxygen diffusion from the air to the water and lead to the reduction of dissolved oxygen (DO) in the water (Hendrasarie et al. 2021, Kataki et al. 2021).

Chemical Oxygen Demand (COD) is a benchmark for water pollution by organic substances, which could be naturally oxidized by microorganisms and cause depletion of dissolved oxygen in the water. Some organic materials in water are resistant to biodegradation. However, they would be degraded chemically through oxidation. There are several methods for treating detergent waste. Based on research, existing methods are the photocatalytic method of UV light, bio-sand filter (An &Verhoeve 2019), and activated carbon (Hendrasarie et al. 2021). One method that could be applied in treating this detergent waste is phytoremediation. Phytoremediation has been proven to reduce surfactant content in detergent waste (Fitrihidajati et al. 2022, Kettenring & Tarsa 2020). Water lettuce and hyacinth could be used as hyperaccumulator plants to treat laundry waste (Cooper 2005, Dong et al. 2005).

Phytoremediation is a technology that involves plants in the remediation processes. Some plants can absorb, transform, and degrade pollutants in waste (Heidari 2003, Hu et al. 2014). Plants used in the phytoremediation process are also called hyperaccumulator plants. Hyperaccumulator plants include water lettuce, water hyacinth, sunflower, bamboo, water kale, and others. Some types of aquatic plants can process organic or inorganic compounds in wastewater. Aquatic plants also have a group of microbes called rhizobacteria that surround the plant. This type of bacteria also can decompose organic and inorganic substances (Grime

1998, Khan & Bano 2016). Adding aeration will fulfill the oxygen demand for microbes found in plant roots and enhance the decomposing process of organic and inorganic substances.

Water lettuce is a common hyperaccumulator plant used for phytoremediation. This plant can treat heavy metals and inorganic and organic waste. This plant can be found floating in swamps or ponds. Known as a pond's protective plant, water lettuce is a monocot plant with thick leaves and strings like roses. The leaves could reach 14 cm and had no stems. The roots have long hair and are surrounded by air bubbles that increase the buoyancy of the plant (Knox et al. 2008, Shahid et al. 2018). Water hyacinth is a type of floated plant freely on the surface of the water and has dark green leaves attached to the spongy stems. The root has branches (fibers) in water and is dark in color. Water hyacinth is easy to grow and can cover all large water surfaces in a very short time. This plant is also widely used in phytoremediation to treat livestock, sugar mills, paper, and palm oil waste.

Filtration is a process of separating water and particles that are not settled during sedimentation and through porous media. Most media often used in filtration are sand, activated carbon, anthracite, and coconut shells. Filtration is divided into two types: rapid sand filter and slow sand filter. A rapid sand filter is often used for drinking water treatment. Types of this sand media are divided into two, namely single-media in the form of sand and multi-media, which consists of 2 media or more. Sand filter media could reduce pollutant content with effectiveness between 18-75% (Mohd Saad et al. 2021, Wang et al. 2019).

The process that occurred in the filtration could not be separated from the biological process that involved microorganisms. These microorganisms are found around the filter media and from wastewater itself, then will be accumulated in the filter media and transformed into biofilms. Biofilms may grow well due to their activity that

utilizes organic substances and converts organic compounds into simpler compounds, such as water, carbon dioxide, and biomass. In addition, biofilm may reduce the concentration of organic materials in the waste by lowering the concentration of organic wastewater (Sayadi et al. 2012, Rahman et al. 2020).

The main object of this study was to evaluate the ability of water lettuce and water hyacinth to decline the surfactant and COD concentration in detergent wastewater. The combined treatment of phytoremediation and filtration was used to enhance the remediation processes. In addition, the morphological parameters of the plant were also measured as a response to detergent wastewater exposure.

## MATERIALS AND METHODS

Water lettuce and water hyacinth were collected from a local pond in Surabaya City. The plants were transported to the laboratory for an acclimatization process in a 10 L tank for 7 days. The filter media used in this experiment were sand, silica sand, and active carbon. Detergent wastewater was collected from the drainage near densely populated areas and measured the water quality parameters (Table 1). The experiment was a laboratory scale, with a 1:10 scale comparison with the reactor's size of $26 \times 26 \times 30$ cm. The water level above the media was 9 cm.

The phytoremediation and filtration were conducted in the same reactor. The reactor consists of a plant and two-combined filter media with 3 cm for each filter media (Table 2). The control reactors were used with two-combined filter media only and without plants. The residence time was 6 days and 12 days, and the parameters used for removal were surfactant and COD. The pH and temperature were also measured during the experiment.

The morphological parameters measured in this experiment were plant height (cm), root length (cm), the number of leaves, leaf surface area ($cm^2$), and the number of new branches. Data on existing plant conditions were

Table 1: Water quality parameter of detergent wastewater.

| Parameter | Value |
|---|---|
| $BOD_5$ [mg.L$^{-1}$] | 1268 |
| COD [mg.L$^{-1}$] | 2884 |
| TSS [mg.L$^{-1}$] | 616 |
| Oil & Grease [mg.L$^{-1}$] | 64.00 |
| Surfactant (MBAS) [mg.L$^{-1}$] | 734.86 |
| Phosphate [mg.L$^{-1}$] | 249.42 |
| pH | 9.50 |

Table 2: The combination of a reactor for phytoremediation and filtration.

| Duration | Filter Media | Plant |
|---|---|---|
| 6 days | Sand-Active carbon | Water lettuce |
| | | Water hyacinth |
| | Sand-Silica sand | Water lettuce |
| | | Water hyacinth |
| 12 days | Sand-Active carbon | Water lettuce |
| | | Water hyacinth |
| | Sand-Silica sand | Water lettuce |
| | | Water hyacinth |

presented in graphical form of the average value of plant parts. The total plants used in this study were 16 water lettuce and 16 water hyacinths. At the time of the treatment, 16 plants would be divided into two parts, based on the variation in their 2-residence time, and then the average value of 8 plants was used.

## RESULTS AND DISCUSSION

### Surfactant and COD Removal

In general, using water lettuce and water hyacinth and a combination of media filters can reduce the concentration of surfactants in the range of 98-99%. The Highest percentage of the surfactant decreased was 99.42% in water hyacinth in combination with sand-active carbon for 6 days. Meanwhile, the lowest percentage of surfactant removal was 98.88% in water lettuce with sand-active carbon for 6 days. The decrease in surfactants in water can occur due to absorption by plants through the roots, which will then be transported to the plant's organs. In addition to the absorption mechanism, the existence of microorganisms that are usually in plant roots can also play a role in degrading organic compounds such as surfactants. Microorganisms that could help to decompose surfactants were rhizobacteria from the genus of Pseudomonas (Zhang et al. 2016, Yu et al. 2021). The surfactant breakdown by microorganisms was divided into three stages. First was the oxidation of the alkyl group at the end of the LAS chain, forming an intermediate in the form of alcohol. The process would occur until the chain had only 4-5 carbon atoms (Masoudian et al. 2020). Next, through the desulfonation stage, the sulfonate group was removed and catalyzed by a complex enzyme, NAD(P)H coenzyme, and oxygen formed phenolic hydroxides in the benzene ring. Then the final stage was the opening of the benzene ring through the meta or ortho pathway (Scholz et al. 2007, Wiegleb et al. 2017).

The result of COD Removal in Fig. 2 showed sand-active carbon for 12 days has the highest percentage, 81.73% in
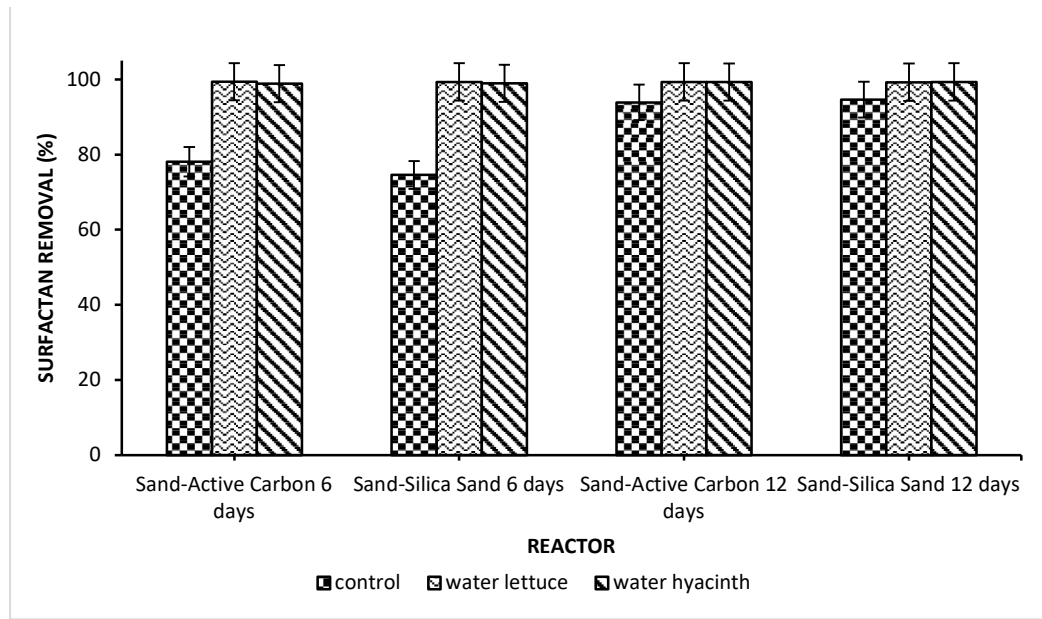
Fig. 1: Surfactant removal using plants and filter media.

water lettuce and 78.67% in water hyacinth. In addition to the degradation process of organic material by plants, the filtration process that uses sand-active carbon can increase the decrease in COD during treatment. The use of aeration intended to increase the aeration of oxygen in wastewater can help the existence of microorganisms in the roots of plants and microorganisms in the filter layer in the decomposition process. The use of slow sand filters was usually due to the

more optimum ability to remove organic materials(Scott et al. 2020). Besides, the contact time of wastewater with the media was longer. The longer the contact time, the more perfect the role of microorganisms in degrading organic material (Cong et al. 2021, Al-Idrus et al. 2020). A slow sand filter could be applied considering the time when the wastewater comes into contact with the filter media, drainage discharge, and filtration speed.
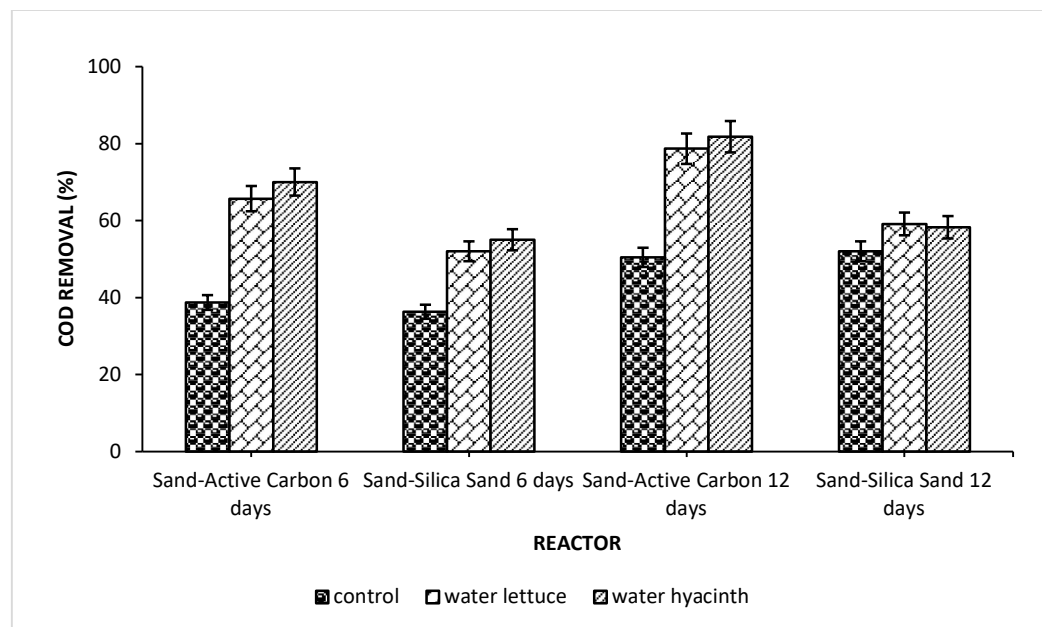


Fig. 2: COD removal using plants and filter media.

Anova One-Way statistical tests were performed to determine the relation between factorial value (residence time) toward the responses (percent of surfactant removal and COD). The test was carried out using a trust level of 95%. The Influence of residence time on surfactants and COD resulted in a P-value of 0.00 (P-value <0.05). This showed a relationship between the percentage decrease and residence time.

**Plants' Response to Surfactant Exposure**

The morphometric parameter shown first was the average plant height in Fig. 3. In the acclimatization stage, all parts of the plant grew normally. This could indicate that the plants had been acclimatized well for 7 days. After acclimatization, the average height of water hyacinth was 28-35.4 cm, and water lettuce was 16.2-18.8 cm at the initial stage of the experiment.

After 6 days' residence time, the plant's height of both plants experienced a decrease. At the second treatment with a residence time of 12 days, both plants showed a decrease in height from day 1 to day 6. Meanwhile, from day 7 to day 12, the plants' condition slightly improved. From day 1 until day 6, the plants may carry out maximum absorption and adapt to the new environment floating on the wastewater. From day 7 until day 12, the average height of the plants started to increase, which means the plants had been able to adapt and survive in wastewater.

The number of leaves in the initial experiment in water lettuce was 8.88-9.25 cm, and water hyacinth was 8-8.25 cm (Fig. 4). At 6 days' residence time, the number of leaves at both plants decreased. Whereas at 12 days' residence time, both plants showed a similar pattern. The average number of leaves in both plants gradually decreased until day 4 and day 5. However, water lettuce showed an increase in leaves until day 12. In contrast, the water hyacinth continued the decrease until day 10, then turned into arising until day 12 in Fig. 4. The changes of both plants to the circumstances also could be observed from the number of leaves. The first 6-day stage was the adaptation period, and the plants would experience physiological stress from the wastewater, which might be absorbed. After that period could be passed, the plants would continue to grow with the adapted condition. Leaves are an important part of plants, particularly for photosynthesis. Exposure to surfactants may change the enzyme for metabolism and cause chlorosis (Hu et al. 2014, Masoudian et al. 2020).

The root length of both plants showed a noticeable decrease at the 6 days of residence time. Meanwhile, at 12 days of residence time, both plants showed a slight decrease until day 6 and continued to grow until day 12 (Fig. 5). In aquatic plants, the root is essential, particularly to absorb nutrients. Moreover, in the polluted media exposed to wastewater, the root would be the first part that interacts directly with the pollutants. Therefore, the effect
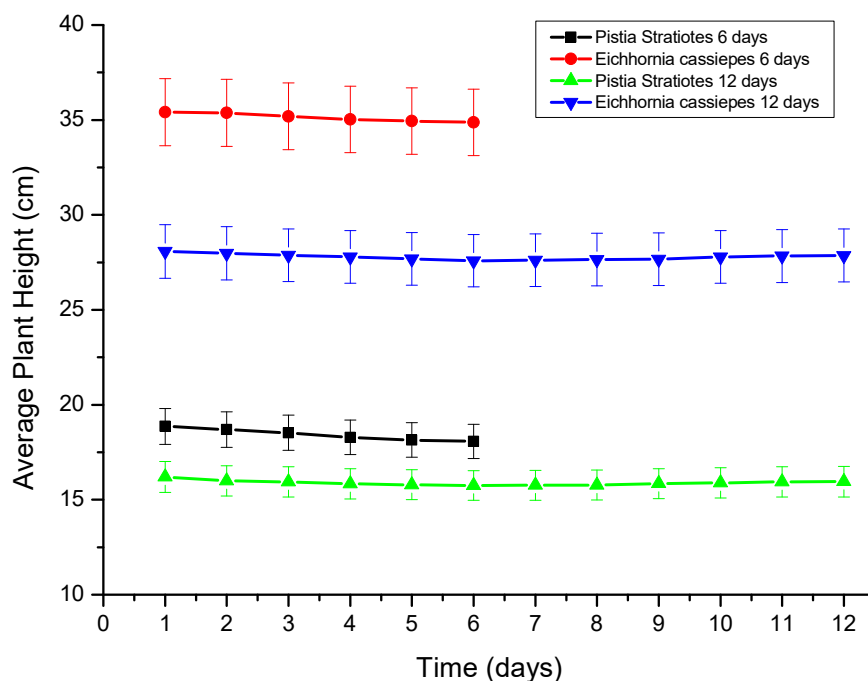


Fig. 3: Plant height of water lettuce and water hyacinth.
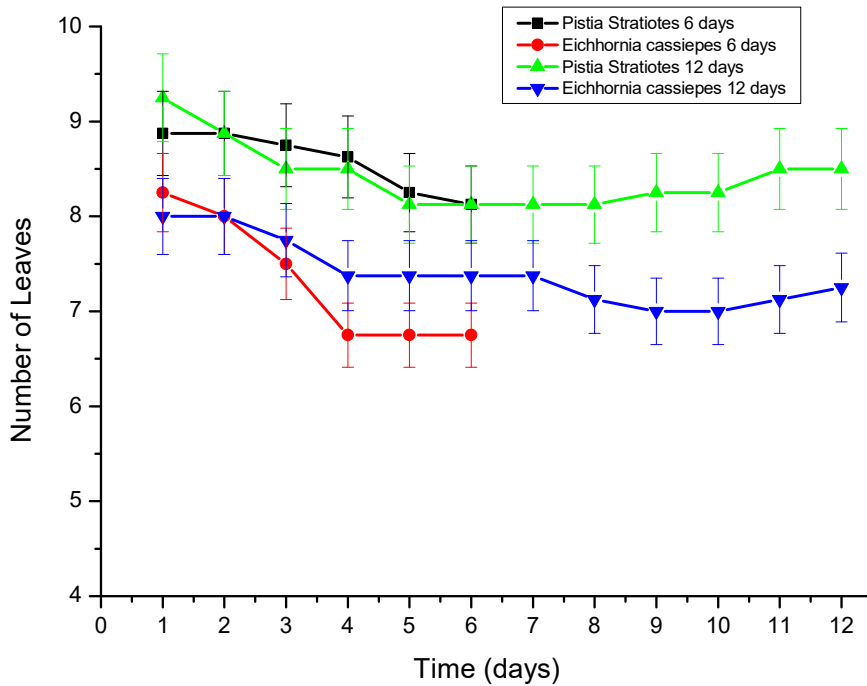
Fig. 4: The number of leaves of water lettuce and water hyacinth.
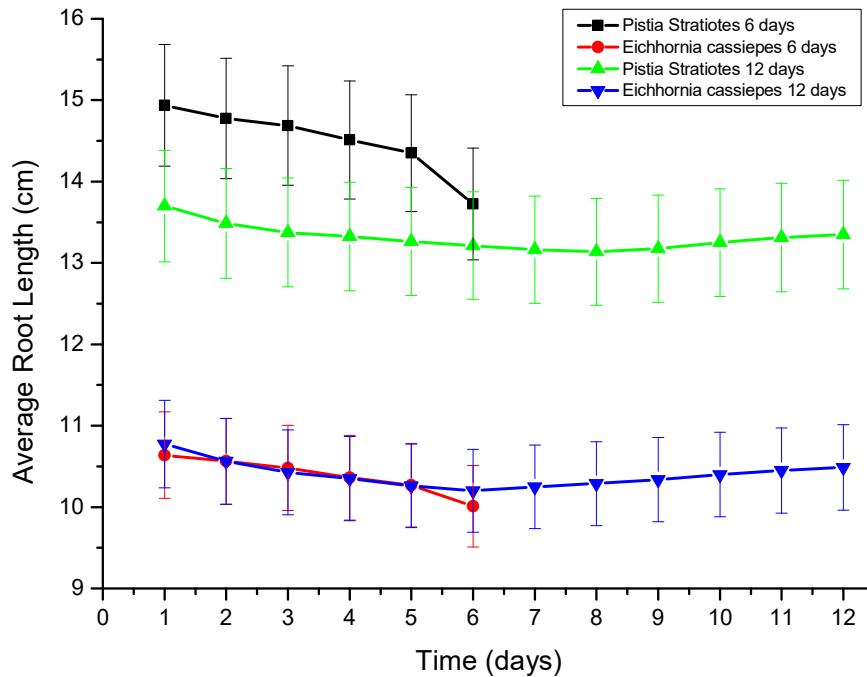


Fig. 5: Average root length of water lettuce and water hyacinth.

of wastewater could be responded to the changes in the root length. In certain conditions, the plant would be able to adjust to stress conditions and survive (Shahid et al. 2018).

A similar result also occurred in the leaf surface area. During 6 days of exposure to wastewater, as can be seen from Fig. 6, both plants showed a decrease in leaf surface
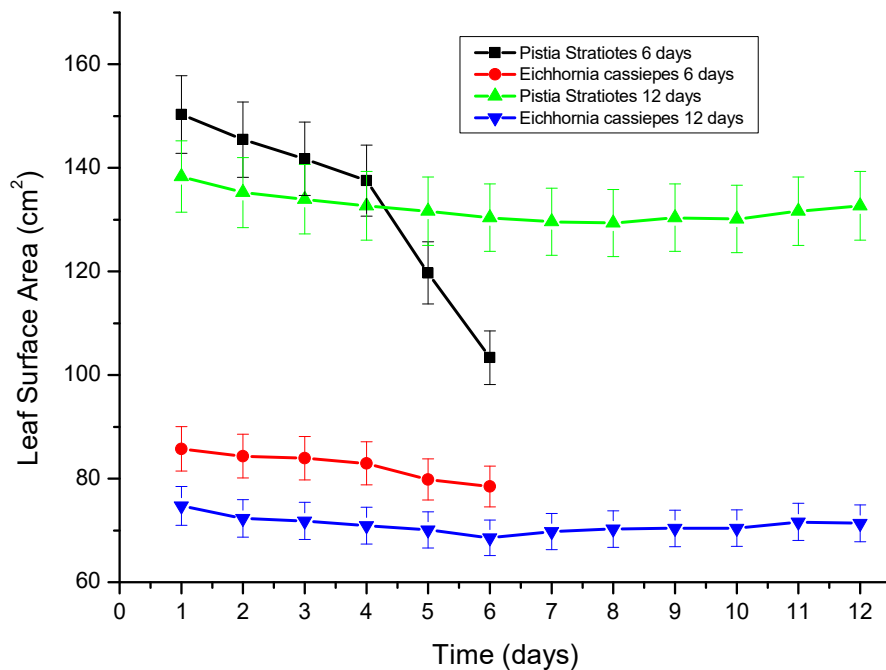
Fig. 6: Leaf surface area of water lettuce and water hyacinth.
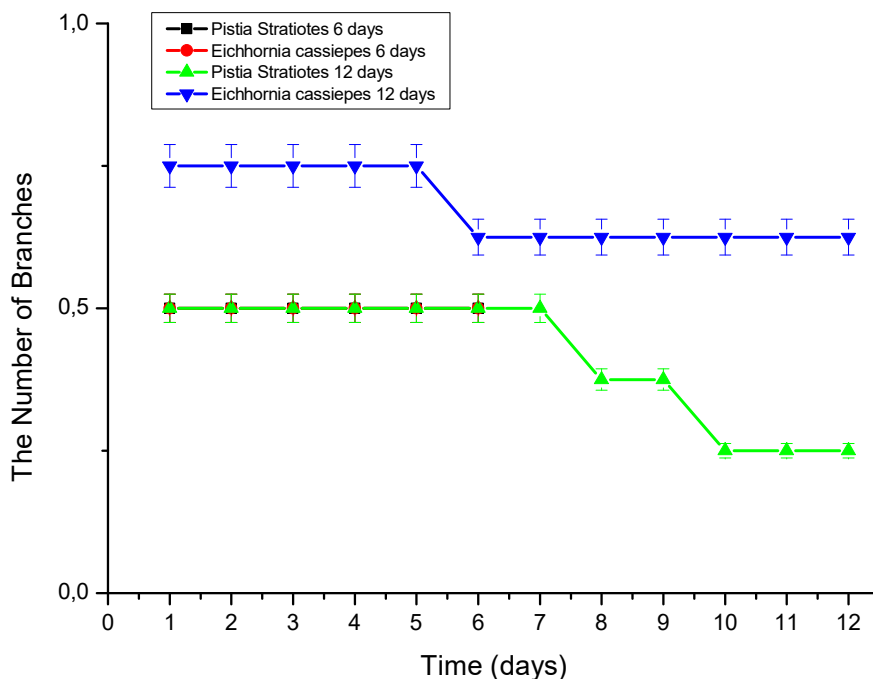


Fig. 7: The number of branches of water lettuce and water hyacinth.

area. However, water lettuce showed a considerable decrease on the last day. At 12 days of residence time, water hyacinth and water lettuce showed a moderate change in response to wastewater exposure. Based on the result, a significant decrease in the leaf surface area of water lettuce at day 6 might be attributed to the morphological factors, in which the leaf's position is relatively lower and has no stems. Therefore, the leaves were exposed directly to the wastewater

(Hasan et al. 2021, Correa dos Santos et al. 2022). Unlike water hyacinth, which has stems, it could keep the leaves from direct contact with wastewater.

The result of 6 days of residence time is shown in Fig. 7. Both plants had no additional branches. Meanwhile, at 12 days of residence time, both plants' branches decreased. Water hyacinth showed numerous decreases compared to water lettuce during the exposure. The plants also experienced symptoms such as yellowing of leaves, withered leaves, and shortened roots. The growth of new branches in poor conditions was difficult for plants. Mostly, the plants were attempting to adapt and survive in poor conditions. Some plants would survive and tend to meet their basic growth. In addition, growing new branches indicates that plants can adapt and survive without any environmental disturbance (Knox et al. 2008).

**Surfactant Accumulation in Plants**

The existence of surfactant in plants, shown in Table 3, indicates the plants were able to absorb and keep in the organ. As the photo process mechanism in plants, surfactant would be degraded and result from the lower concentration. In general, the concentration of surfactant in both plants at 6 days was greater than 12 days of residence time. Water lettuce and water hyacinth absorb a high amount of surfactant from the wastewater at the initial treatment. This was the mechanism of adaptation for the plants by adjusting to the new environment (Linh et al. 2021, Al-Idrus et al. 2020). Surfactants in plant tissues had not been completely transformed into simple forms which would be released into the air through the leaves. The surfactant concentration in 12 days' residence time was less than 6 days because the plants had done the process of phytovolatilization. This process changed the surfactant substances to a simpler form and then was released into the air through leaves tissue. Microorganisms also assisted the decrease in surfactant substances in the root. The longer microorganisms treat the waste, the more maximum and effective decomposition of surfactant substances.

**The Influence of pH and Temperature on Plants**

The pH of wastewater during the experiment ranged from 7.6 to 8.4. Water hyacinth could grow and develop well at pH 6-8 (Zhang et al. 2016). At first, the waste in the reactor had a pH above 8, causing the growth of water hyacinth plants to decrease. After a few days, the pH of the wastewater in the reactor decreased. Therefore, the plant turned to show increased growth. The lower pH would cause toxicity for the plants with a minimum threshold of pH 4.2. Moreover, if the plant lives in a toxic environment, it would cause a high death

Table 3: Surfactant the plant's parts (6 days and 12 days).

| Plants | Plant parts | Surfactant [mg.kg$^{-1}$] LAS | |
|---|---|---|---|
| | | 6 days | 12 days |
| Water hyacinth | Roots | 2597.95 | 164.11 |
| | Stems | 178.48 | 110.49 |
| | Leaves | 134.09 | 148.58 |
| Water lettuce | Roots | 27543.24 | 248.41 |
| | Leaves | 3158.92 | 126.61 |

probability for the plants (Hendrasarie et al. 2021, Ratnani et al. 2013). The results showed that the P-value of pH against COD and surfactant was greater than 0.05 (P-value> 0.05), meaning there was no relationship between pH and the test parameters of both surfactants and COD.

The temperature of wastewater in growth media for water hyacinth and water lettuce during the study ranged from 25-29°C. The temperature needed for plants to grow and develop properly was at a temperature of 20-30°C (Hendrasarie & Dieta 2019, Kataki et al. 2021).

The temperature at the time of the study was still in the range for plants to grow well. Therefore, both plants could survive until the end of the study, even though the morphological condition of the plants had decreased due to the accumulation of waste. The results showed that the temperature P-value toward COD and surfactants was greater than 0.05 (P-value > 0.05), meaning there was no relation between temperature and the test parameters of both surfactants and COD.

## CONCLUSION

The results of this study show that a combination of phytoremediation and filtration can effectively decompose the MBAS surfactants and COD found in detergent wastewater. With an aeration rate of 14 L/minute, a combination of the water lettuce (*Pistia stratiotes)* plant and activated carbon was able to remove 99.42% of MBAS surfactant for 6 days, meanwhile reducing COD for 12 days and achieve a reduction of 81.73%. The state of plants, plants started adjusting to their surroundings on the eighth day, especially the water lettuce and water hyacinth plants.

## ACKNOWLEDGMENTS

# REFERENCES

Al-Idrus, S., Rahmawati, W.R. and Hadisaputra, Q.S. 2020. Phytoremediation of detergent levels in waters using water plants: Eichornia crassipes, Ipomoea aquatica, Pistia stratoites and their combinations. Eur. J. Adv. Chem. Res., 1: 504.

An, S. and Verhoeven, J.T. 1991. Wetland Functions and Ecosystem Services: Implications for Wetland Restoration and Wise Use. In Bhatnagar, L. and Fathepure, B.Z. (eds), Wetlands: Ecosystem Services, Restoration and Wise Use, Springer, Cham, Switzerland, pp. 293-340.

Cong, N.V., Kim, D.T., Yen, N.T.H., Nguyen, P.Q., Hoang, N.X., Chiem, N.H. and Kieu, L.D. 2021. To produce compost from water lettuce (Pistia stratiotes L.) for planting water spinach (Ipomoea aquatic). Viet. J. Agric. Rural Dev., 421: 42-50.

Cooper, P.F. 2005. The performance of vertical flow constructed wetland systems with special reference to the significance of oxygen transfer and hydraulic loading rates. Wat. Sci. Technol., 51: 81-90.

Correa dos Santos, N.M.P.G., Monteiro, E.A., Ferreira, B.T.B., Alencar, C.M. and Cabral, J.B. 2022. Use of Eichhornia crassipes and Pistia stratiotes for environmental services: Decontamination of aquatic environments with atrazine residues. Aquat. Bot., 176.

Dong, H., Qiang, Z., Li, T., Jin, H. and Chen, W. 2012. Effect of artificial aeration on the performance of vertical-flow constructed wetland treating heavily polluted river water. J. Environ. Sci., 24: 596-601.

Fitrihidajati, H., Rachmadiarti, F. and Khaleyla, K. 2020. Effectiveness of Sagittaria lancifolia as detergent phytoremediator. Nat. Environ. Pollut. Technol., 19: 1723-1727.

Grime, J.P. 1988. The CSR Model of Primary Plant Strategies: Origins, Implications, and Tests. Springer, Dordrecht, The Netherlands, pp. 371-393.

Hasan, M.N., Altaf, M. M., Khan, N. A., Khan, A. H., Khan, A. A., Ahmed, S., Kumar, P. S., Naushad, M., Rajapaksha, A. U., Iqbal, J., Tirth, V. and Islam, S. 2021. Recent technologies for nutrient removal and recovery from wastewaters: A review. Chemosphere, 277: 130238.

Heidari, H. 2013. Effect of irrigation with contaminated water by cloth detergent on seed germination traits and early growth of sunflower (Helianthus annuus L.). Nat. Sci. Biol., 5: 86-89.

Hendrasarie, N. and Dieta, Y.A. 2019. Adsorption ability of Pb from industrial wastewater by Kayu Ambang (Lemna Minor), Kayu Apu (Pistia Stratiotes), and water hyacinth (Eichhornia Crassipes Solm). Jurnal Envirotek, 11: 54.

Hendrasarie, N., Nugraha, M. and Fadilah, K. 2021. Restaurant wastewater treatment with a two-chamber septic tank and a sequencing batch reactor. E3S Web Confer., 328: 010.

Hu, Y., Zhao, Y. and Rymszewicz, A. 2014. Robust biological nitrogen removal by creating multiple tides in a single bed tidal flow constructed wetland. Sci. Total Environ., 470: 1197-1204.

Kataki, S., Chatterjee, S., Vairale, M.G., Dwivedi, S.K. and Gupta, D.K. 2021. Constructed wetland, an eco-technology for wastewater treatment: A review on types of wastewaters treated and components of the technology (macrophyte, biofilm, and substrate). J. Environ. Manag., 283: 111986.

Kettenring, K.M. and Tarsa, E.E., 2020. Need to seed Ecological, genetic, and evolutionary keys to seed-based wetland restoration. Front. Environ. Sci., 8: 109.

Khan, N. and Bano, A. 2016. Role of plant growth promoting rhizobacteria and Ag-nano particle in the bioremediation of heavy metals and maize growth under municipal wastewater irrigation. Int. J. Phytoreme., 18: 211-221.

Knox, A.K., Dahlgren, R.A., Tate, K.W. and Atwill, E.R. 2008. Efficacy of natural wetlands to retain nutrients, sediment, and microbial pollutants. J. Environ. Qual., 37: 1837-1846.

Lee, J.H. 2013. An overview of phytoremediation as a potentially promising technology for environmental pollution control. Biotechnol. Bioprocess Eng., 18: 431-439.

Linh, L.N., Hoang, N.X., Thuan, N.C., Chiem, N.H. and Cong, N.V. 2021. Removal of ammonium from aliquots by water lettuce. J. Nat. Resour. Environ., 1: 28-30. (In Vietnamese).

Lundholm, J. 2015. The ecology and evolution of constructed ecosystems as green infrastructure. Front. Ecol. Evol., 3: 106.

Masoudian, Z.S.Y., Salehi-Lisar, A. and Norastehnia, Y. 2020. Phytoremediation potential of Azolla filiculoides for sodium dodecyl benzene sulfonate (SDBS) surfactant considering some physiological responses, effects of operational parameters, and biodegradation of surfactant. Environ. Sci. Pollut. Res., 27: 20358-20369.

Mohd Saad, F.N., Jamaludin, S.Z.A. and Tengku Izhar, T.N. 2021. Investigation of using a sand filter in treating grey water. IOP Conf. Ser. Earth Environ. Sci., 646: 12056.

Moondra, N., Christian, R.A. and Jariwala, N.D. 2021. Bibliometric Analysis of Constructed Wetlands in Wastewater Treatment. Springer, Singapore, pp. 1021-1028.

Parde, D., Patwa, A., Shukla, A., Vijay, R., Killedar, D.J. and Kumar, R. 2021. A review of constructed wetlands on type, treatment, and technology of wastewater. Environ. Technol. Innov., 21: 101261.

Rahman, M.E., Bin Halmi, M.I.E., Bin Abd Samad, M.Y., Uddin, M.K., Mahmud, K., Abd Shukor, M.Y., Sheikh Abdullah, S.R. and Shamsuzzaman, S.M. 2020. Design, operation, and optimization of constructed wetland for removal of pollutants. Int. J. Environ. Res. Pub. Health, 17: 8339.

Rebello, S., Asok, A.K., Mundayoor, S. and Jisha, M.S. 2014. Surfactants: Toxicity, remediation, and green surfactants. Environ. Chem. Lett., 12: 275-287.

Saini, G., Kalra, S. and Kaur. U. 2021. The purification of wastewater on a small scale by using plants and sand filters. Appl. Water Sci., 11: 1-6.

Sayadi, M.H., Kargar, R., Doosti, M.R. and Salehi, H. 2012. Hybrid constructed wetlands for wastewater treatment: A worldwide review. Proc. Int. Acad. Ecol. Environ. Sci., 2: 204.

Scholz, M., Harrington, R., Carroll, P. and Mustafa, A. 2007. The integrated constructed wetlands (ICW) concept. Wetlands, 27: 337-354.

Scott, B., Baldwin, A.H., Ballantine, K., Palmer, M. and Yarwood, S. 2020. The role of organic amendments in wetland restorations. Restore. Ecol., 28: 776-784.

Shahid, M.J., Arslan, M., Ali, S., Siddique, M. and Afzal, M. 2018. Floating wetlands: A sustainable tool for wastewater treatment. Clean-Soil Air Water, 46: 1800120.

Simoni, S., Klinke, S., Zipper, C., Angst, W. and Kohler, H.E. 1996. Enantioselective metabolism of chiral 3-phenyl-butyric acid, an intermediate of linear alkylbenzene degradation, by Rhodococcus rhodochrous PB1. Appl. Environ. Microbiol., 62: 749-755.

Suastuti, N.G., Suarsa, I.W. and Putra, R.D.K. 2015. Pengolahan Larutan Deterjen Dengan Biofilter Tanaman Kangkungan (Ipomoea crassicaulis) dalam Sistem Batch (Curah) Teraerasi. Jurnal Kimia, 9(1): 98-104.

Suwandhi, I.A.A., Hendrasarie, N. and Dewi, R. 2022. Constructed horizontal-type wetland subsurface flow using Odot Grass for Tofu WWTP effluent treatment. Serambi Eng., 7(3): 3252-3261.

Wang, G., Jiang, M., Wang, M. and Xue, Z. 2019. Natural revegetation during the restoration of wetlands in the Sanjiang Plain, Northeastern China. Ecol. Eng., 132: 49-55.

Wiegleb, G., Dahms, H.U., Byeon, W.I. and Choi, G. 2017. To what extent can constructed wetlands enhance biodiversity? Int. J. Environ. Sci. Dev., 8: 561-569.

Yu, G., Li, P., Wang, G., Wang, J., Zhang, Y., Wang, S., Yang, K., Du, C. and Chen, H. 2021. A review on the removal of heavy metals and metalloids by constructed wetlands: Bibliometric, removal pathways, and key factors. World J. Microbiol. Biotechnol., 37: 157.

Zhang, C., Ye, F., Liu, Y., He, W., Kong, C. and Sheng, K. 2016. Determination and visualization of pH values in anaerobic digestion of water hyacinth and rice straw mixtures using hyperspectral imaging with wavelet transform denoising and variable selection. Sensors, 16: 244.

## ORCID DETAILS OF THE AUTHORS

Arpita Ghosh: https://orcid.org/0000-0002-7651-1558

# Carbon Emissions from Energy Use in India: Decomposition Analysis

**Sebak Kumar Jana\*† and Wietze Lise\*\***

\*Department of Economics, Vidyasagar University, Midnapore-21102, West Bengal, India
\*\*Energy Markets, Management Consultancy Department, MRC Turkey, Ankara, Turkey
†Corresponding author: Sebak Kumar Jana; sebakjana@yahoo.co.in

## ABSTRACT

To become the fastest-growing large economy in the world, India has set a target growth rate of 9%, reaching an economy of $5 trillion by 2024-25. It is an immense challenge to meet the growth target and keep the $CO_2$ emissions under control. The present paper aims to discover the determinants for explaining $CO_2$ emissions in India by conducting a complete decomposition analysis, where the residuals are fully distributed to the determinants for the country from 1990-2018. The analysis reveals that the biggest contributor to the rise in $CO_2$ emissions in India is the expansion of the economy (scale effect). The intensity of $CO_2$ and the change in the composition of the economy, which nearly move in tandem, also contribute to the rise in $CO_2$ emissions, although more slowly. A declining energy intensity of the Indian economy is responsible for a considerable reduction in $CO_2$ emissions. As a typical result for an upcoming economy, this paper did not find evidence for an environmental Kuznets curve. This implies that continued economic growth will lead to increased $CO_2$ emissions.

## INTRODUCTION

With a population of 1.4 billion and a real GDP growth of 6.2% over the period 1990-2018, India has set a target growth rate of 9% for becoming the fastest-growing large economy in the world, reaching a $5 trillion economy by 2024-25 (IEA 2020). India's sustained economic growth, large population, and rapid urbanization are placing an enormous demand on its energy resources, systems, and infrastructure. Moreover, population density is high throughout most of the country.

The Government of India (GoI) aims to achieve 100 smart cities, LPG connections to all housing, and universal electricity access. Moreover, India's 2008 National Action Plan on Climate Change (NAPCC) set out eight national missions to promote India's sustainable development objectives, including the National Solar Mission, the National Mission for Enhanced Energy Efficiency, and the National Mission on Strategic Knowledge for Climate Change. At the Conference of the Parties (COP) 15 in Copenhagen in 2008, India announced voluntary targets to reduce the emissions intensity of its GDP by 20-25% against 2005 levels by 2020. In 2015, the Government of India submitted its Intended Nationally Determined Contributions (INDC) after the GoI ratified the Paris Agreement in 2016. India's Nationally Determined Contribution (NDC) focuses strongly on actions related to the energy sector, and some of the targets are:

- Reducing the emissions intensity of GDP by 33-35% from 2005 levels by 2030;
- Achieving 40% cumulative installed capacity of electric power from non-fossil fuel-based energy resources by 2030 with low-cost international finance and
- Creating an additional carbon sink of 2.5-3 billion tons of $CO_2$ equivalent through the creation of additional forest and tree cover by 2030.

At the United Nations Climate Summit in September 2019, Prime Minister Modi announced an increased ambition to promote renewable energy towards a 450 GW overall installed capacity target.

The world is progressing towards UN Goal 7, with an encouraging note that the energy sector is becoming more sustainable and widely accessible. Lack of access to energy may hamper the efforts to contain the current pandemic effects across many countries (UN 2021a). In India, about 300 million people lack access to electricity. Successfully addressing India's energy poverty and achieving sustainable development goals would require the reduction of poverty and social and economic inequality.

The power system of India is presently going through a major shift to higher shares of renewable energy. India's coal supply has increased rapidly since the early 2000s, and coal continues to be the largest domestic source of energy

supply for electricity generation, which leads to a higher $CO_2$ intensity. The government aims to increase the share of natural gas in the country's energy mix to 15% by 2030 from 6% today (IEA 2020). Natural gas consumption is 50% imported and 50% locally produced as of 2018.

Considering all these challenges India faces, the present paper aims to discover the determinants for explaining $CO_2$ emissions in India by carrying out a complete decomposition analysis for the country from 1990-2018. Here, the role of four factors, scale, composition, energy, and carbon intensity, explain changes in $CO_2$ emissions. The residuals are fully distributed to these four determinants in a complete decomposition analysis. In addition, changes in the economy's sectoral composition, technologies in the energy mix, energy and carbon intensity, and the link between national income and carbon emissions in India are also examined.

The outline of this paper is as follows. A literature survey is presented in Section 2. Section 3 presents the methodology used. Section 4 presents the results and discusses the changes in the energy situation in India, undertakes a complete decomposition analysis, and tests whether an environmental Kuznets curve (EKC) can be found in India. The final section concludes.

## PAST STUDIES

There is a good number of publications on decomposition analysis of emissions worldwide. However, work is lacking on the situation in India considering the current context of $CO_2$ emission reductions. A broad review of the literature is provided in this section.

Xu & Ang (2013) undertook a comprehensive survey of literature focusing specifically on emissions by various countries by reviewing eighty papers that appeared in peer-reviewed journals from reviews of studies conducted in developed and developing countries at national scales (and for various sectors, including national total emissions).

According to Ang (2004), practitioners must have a common understanding and consistency of the method used in decomposition analyses in empirical studies.

Ang & Choi (1997) proposed a refined Divisia index decomposition using a logarithmic function by replacing the arithmetic mean weight function with no residual.

Su & Ang (2012) highlighted novel new methods in structural decomposition analysis (SDA), namely structural decomposition analysis (SDA) and index decomposition analysis (IDA). They compared SDA and IDA using the latest available information.

According to Hoekstra et al. (2003), decomposition analysis is often used to understand changes in various indicators: energy use, $CO_2$ emissions, labor demand, and the value added to the economy. They considered SDA using an input-output model and IDA, which uses more aggregated sector data and provided a hypothetical numerical example.

Tiwari (2011) examined causality by considering energy consumption, $CO_2$ emissions, and economic growth in India. This study covered 1971-2007 using the Granger approach (VECM framework) and Dolado and Lütkepohl's approach. The study concluded that India's Energy consumption positively impacts $CO_2$ emissions and GDP, but its impact negatively impacts capital and population.

Wolde-Rufael & Idowu (2017) examined whether income inequality affects environmental degradation in India and China, where both countries are concerned about their unsustainable energy consumption. A long-run, statistically insignificant link between income inequality and $CO_2$ emissions has been observed in India and China.

Using a decoupling method, Kojima & Bacon (2009) found the decoupling of economic growth and emissions in India, an increasing share of the service sector in GDP, and falling energy intensity of industry as major contributors to achieving decoupling of economic growth and emissions.

Table 1 summarizes key characteristics of some important studies on applied studies using Decomposition Analyses. The main methods used are as follows:

- Index Decomposition Analysis (IDA),
- Structural Decomposition Analysis (SDA),
- Refined Laspeyres decomposition model (LASP),
- Logarithmic Mean Divisia Index (LMDI) and
- Other decomposition methods.

The countries covered vary from single countries, such as Brazil, China, Ethiopia, India, and Turkey, to various studies with multi-country coverage.

In summary, the studies presented try to untangle factors that cause $CO_2$ emissions and recommend ways to reduce these emissions. The so-called "scale effect" is often prominent in developing countries, where population growth and growth of the economy are often found to be the key contributing factors to rising $CO_2$ emissions. The present paper has as the main purpose to employ a recent data set (1990-2018) for India with a sectoral breakdown to numerically calculate the impact of four different components of growth, namely scale, composition, intensity of energy use, and carbon emissions and their contributions to increases in $CO_2$ emissions.

Table 1: Summary of the past studies.

| Author(s) | Years of Analysis | Method | Countries covered | Key results |
|---|---|---|---|---|
| Andreoni and Galmarini (2016) | 1995-2007 | Index Decomposition Analysis (IDA) | 33 world countries | They found economic growth as the main driving factor of energy-related increase in $CO_2$ emissions. |
| Wang and Zhou (2018) | 1995-2009 | Theil index and IDA | China and India | They examined global per capita consumption-based emission inequality in 1995–2009. |
| Su et al. (2020) | 1990-2015 | IDA | G7 and BRICS | They developed a framework for some countries' index decomposition of carbon dioxide. |
| Das and Paul (2014) | 1993-94 to 2006-07 | Structural Decomposition Analysis (SDA) | India | They used input-output analysis to estimate direct and indirect $CO_2$ emissions by households in India. |
| Pal et al. (2015) | 1994-1995 and 2006-2007 | SDA | India | They found that change in emission intensity negatively impacts India's greenhouse gas (GHG) emissions. |
| Tandon and Ahmed (2016) | 1993-94 to 2007-08 | SDA | India | They analyzed the sector-wise changes in production technology and its effect on the demand for direct and embodied energy. |
| Karstensen et al (2020) | 1996-2009 | SDA between years, which expands on the Kaya identity | India | They found that India's GHG emissions until 2009 economic growth and technological intervention have helped reduce emission growth. |
| Wang et al. (2020) | 2000 to 2014 | SDA | Group of Twenty (G20) countries | They concluded that reducing energy intensity in Russia, India, China, and South Korea has great potential to reduce global energy consumption and improve global energy efficiency. |
| Lise (2006) | 1980-2003 | Complete decomposition analysis and LASP | Turkey | They found that the major cause of the rise in $CO_2$ emissions in Turkey is the expansion of the economy (scale effect). |
| Ebohon and Ikeme (2006) | −1971 1998 | Refined Laspeyres decomposition model (LASP) | Sub-Saharan African countries | They found that $CO_2$ emission intensity has been attributable to energy consumption intensity. |
| Wang et al. (2005) | 1957 to 2000 | Logarithmic Mean Divisia Index (LMDI) | China | They analyzed the change in aggregated $CO_2$ in China. |
| Pachauri and Muller (2008) | 1980-2005 | LMDI | India | They analyzed the importance of different drivers by conducting a decomposition analysis of household electricity consumption in India. |
| De Freitas and Kaneko (2011) | 1970-2009 | LMDI | Brazil | They evaluated the changes in $CO_2$ emissions from energy consumption in Brazil. |
| Xu et al. (2014) | 1995-2011 | LMDI | China | They found that production is the major driver for reducing carbon emissions. |
| Chen and Yang (2015) | 1995-2011 | LMDI | China | They presented a coupled decomposition analysis of emissions in China. |
| Zhang and Da (2015) | 1996 to 2010 | LMDI | China | The authors found that the scale effect was the main driver of China's carbon emissions increase. |
| Dasgupta and Roy (2017) | 1990-91 to 2012-13 | Decoupling elasticity and LMDI | India | They found that the change in emission intensity of GDP is highest in agriculture (24%) and lowest in Industry (-23%), and India has achieved relative decoupling during the study period. |
| Kanitkar (2020) | 1971 and 2008 | LMDI and arithmetic mean Divisia index (AMDI) | India | They found that the improvements in energy efficiency are the main contributing factor to the reduction in the overall emission intensity of GDP. |

Table Cont....

| Author(s) | Years of Analysis | Method | Countries covered | Key results |
|---|---|---|---|---|
| Taka et al. (2020) | 1990 and 2017 | Kaya identity combined with the LMDI decomposition approach | Ethiopia | They found that the main drivers of energy-based $CO_2$ emissions are the economic effect (52%), population effect (43%), and fossil fuel mix effect (40%), while the emission intensity effect (14%) was not strongly pronounced. |
| Sun (1998) | 1973–1990 | complete decomposition model | World Energy | They applied a complete decomposition model for the decomposition of world energy consumption. |
| Nag and Parikh (2000) | 1970-1995 | Divisia decomposition technique | India | They found the increase in per capita emission after 1980 was due to a rise in per capita income. |
| Paul and Bhattacharya (2004) | 1980 and 1996 | decomposition method | India | Activity growth is a major cause of a rise in emissions, while energy intensity change contributes to the reduction of $CO_2$ emission, especially in industry and transport sectors. |
| Zhang et al. (2009) | 1991–2006 | decomposition analysis | China | They showed that economic activity has a major positive effect on changes in $CO_2$ emission in all the major economic sectors. |
| Reddy and Roy (2010) | 1992-2002 | Total decomposition analysis model | India | They showed that most intensity reductions are driven purely by structural effect rather than energy intensity. |
| Attari and Attaria (2011) | 1971-2008 | Decomposition Analysis | Pakistan, India, and China | The population contribution to $CO_2$ emission is high in Pakistan, and the contribution of energy intensity in reducing emissions is high in China. |

## MATERIALS AND METHODS

### Decomposition Analysis

In studies at the country level, it is of particular interest to decompose the elements that drive changes in $CO_2$ emissions (or energy consumption). This paper decomposes $CO_2$ emission amounts into four effects. Setting up the Kaya identity, as shown in Eq. (1), can do this:

$$CO_2 \text{ emissions}$$
$$= \underbrace{\frac{GDP}{}}_{\substack{\text{scale}\\\text{effect}}} \times \sum_i \left( \underbrace{\frac{\text{Added value}_i}{\text{GDP}}}_{\substack{\text{composition}\\\text{effect}}} \times \underbrace{\frac{\text{Energy use}_i}{\text{Added value}_i}}_{\substack{\text{energy intensity}\\\text{effect}}} \times \underbrace{\frac{CO_2 \text{ emissions}_i}{\text{Energy use}_i}}_{\substack{\text{carbon intensity}\\\text{effect}}} \right)$$
$$= P \times \sum_i (G_i \times I_i \times E_i)$$

...(1)

Where,

$CO_2$ emissions are the total for India, measured in million tons (Mtons)

GDP is the total for India, measured in trillion Indian Rupees in 2015 prices.

Added value$_i$ is the share of GDP for sector $i$.

Energy use$_i$ is the share of energy use for sector $i$, measured in billion tons of oil equivalent (btoe)

$CO_2$ emissions$_i$ is the share of $CO_2$ emissions for sector $i$, measured in Mtons.

Sectors $i$ are: Agriculture, Industry, Transport and Other.

$P$ is GDP (scale effect).

$G_i$ is Added value$_i$ divided by GDP (composition effect).

$I_i$ is Energy use$_i$ divided by Added value$_i$ (energy intensity effect).

$E_i$ is $CO_2$ emissions$_i$ divided by Energy use$_i$ (carbon intensity effect).

The total $CO_2$ emissions are fully equal to the product of total GDP ($P$), and the sum of the sectoral products of the added value per GDP ($G_i$), energy consumption per added value ($I_i$), and the $CO_2$ emissions per energy consumption ($E_i$).

To explain the changes in $CO_2$ emissions, let us define the differences ($\Delta P$, $\Delta G_i$, $\Delta I_i$, $\Delta E_i$) with respect to the base-year 1990, for instance, $\Delta P_{\text{current}} = P_{\text{current}} - P_{1990}$, and so on. Then, using the four factors from the Kaya identity as given in Eq. (1), it is possible to decompose the $CO_2$ emissions into four effects. First, the scale or activity effect represents additional emissions of $CO_2$, which is caused by economic growth. If the scale effect is found to be the dominating effect, then emissions of $CO_2$ increase linearly with the level of GDP. Second, the composition effect shows increased emissions due to economic changes. If the economy specializes in cleaner sectors, there will be fewer additions to $CO_2$ emissions. Third, the energy intensity effect shows that when the energy intensity goes down, the level of $CO_2$ emissions goes down, too. For example, the energy intensity may be improved by introducing energy-saving technologies. Fourth, the carbon intensity effect shows that

when the carbon intensity reduces, the level of $CO_2$ emissions reduces, too. For instance, switching to a cleaner fuel mix in energy consumption can lower the carbon intensity. The last two effects represent two types of technological change.

Eq. (2) presents the required formulas for complete decomposition analysis with LASP (Zhang & Ang 2001). This is implemented in EXCEL to do the calculations.

$$Peff_t =$$

$$\Delta P_t \sum_i \left[ G_{i,1} \left\{ I_{i,1}E_{i,1} + \frac{1}{2}\left(\Delta I_{i,t}E_{i,1} + I_{i,1}\Delta E_{i,t}\right) + \frac{1}{3}\Delta I_{i,t}\Delta E_{i,t} \right\} \right.$$
$$\left. + \Delta G_{i,t}\left\{ \frac{1}{2}I_{i,1}E_{i,1} + \frac{1}{3}\left(\Delta I_{i,t}E_{i,1} + I_{i,1}\Delta E_{i,t}\right) + \frac{1}{4}\Delta I_{i,t}\Delta E_{i,t} \right\} \right]$$

$$Geff_t =$$

$$P_1 \sum_i \Delta G_{i,t}\left\{ I_{i,1}E_{i,1} + \frac{1}{2}\left(\Delta I_{i,t}E_{i,1} + I_{i,1}\Delta E_{i,t}\right) + \frac{1}{3}\Delta I_{i,t}\Delta E_{i,t} \right\}$$
$$+\Delta P_t \sum_i \Delta G_{i,t}\left\{ \frac{1}{2}I_{i,1}E_{i,1} + \frac{1}{3}\left(\Delta I_{i,t}E_{i,1} + I_{i,1}\Delta E_{i,t}\right) + \frac{1}{4}\Delta I_{i,t}\Delta E_{i,t} \right\}$$

$$Ieff_t =$$

$$P_1 \sum_i \Delta I_{i,t}\left\{ G_{i,1}E_{i,1} + \frac{1}{2}\left(\Delta G_{i,t}E_{i,1} + G_{i,1}\Delta E_{i,t}\right) + \frac{1}{3}\Delta G_{i,t}\Delta E_{i,t} \right\}$$
$$+\Delta P_t \sum_i \Delta I_{i,t}\left\{ \frac{1}{2}G_{i,1}E_{i,1} + \frac{1}{3}\left(\Delta G_{i,t}E_{i,1} + G_{i,1}\Delta E_{i,t}\right) + \frac{1}{4}\Delta G_{i,t}\Delta E_{i,t} \right\}$$

$$Eeff_t =$$

$$P_1 \sum_i \Delta E_{i,t}\left\{ G_{i,1}I_{i,1} + \frac{1}{2}\left(\Delta G_{i,t}I_{i,1} + G_{i,1}\Delta I_{i,t}\right) + \frac{1}{3}\Delta G_{i,t}\Delta I_{i,t} \right\}$$
$$+\Delta P_t \sum_i \Delta E_{i,t}\left\{ \frac{1}{2}G_{i,1}I_{i,1} + \frac{1}{3}\left(\Delta G_{i,t}I_{i,1} + G_{i,1}\Delta I_{i,t}\right) + \frac{1}{4}\Delta G_{i,t}\Delta I_{i,t} \right\}$$

$$...(2)$$

Eq. (2) shows that to calculate the scale effect ($Peff_t$), we must consider the difference in P weighed by the other three factors presented in Kaya identity. However, this first term leaves a residual. The residual is then distributed by applying the principle of 'jointly created and equally distributed' (Zhang & Ang 2001). By fully distributing the residuals in the decomposition analysis, it becomes a complete decomposition analysis with LASP. This helps us explain the halves, thirds, and quarters in the formula, which has terms with two, three, and four deltas. The scale effect is obtained by adding all these terms. The other effects like $Geff_t$ (Composition effect), $Ieff_t$ ( Energy intensity effect), and $Eeff_t$ (Carbon intensity effect) have been derived similarly. By summing up the scale, composition, energy intensity, and carbon intensity effects, it is possible to derive the changes in $CO_2$ emissions with respect to the base year 1990. In this

process, there is no residual. This methodology has been used to decompose the changes in the emission levels of $CO_2$ over the period 1990–2018 in India.

### EKC Test

In addition, a test will be performed to verify whether an environmental Kuznets curve (EKC) can be found for India. To establish this, the following equation needs to be estimated with OLS:

$$ln(CO2) = \alpha + \beta_1 \, ln(GDP) + \beta_2 (ln(GDP))^2 \quad ...(3)$$

The coefficient of the quadratic term ($\beta_2$) must be negative and statistically significant. In this case, there will be a so-called inverted U relationship between GDP and $CO_2$ emissions, implying that as GDP grows, the rate of $CO_2$ emissions will slow down and ultimately even decrease; there will be a decoupling of $CO_2$ emissions from a growing economy. This is the EKC relationship (Stern 2004).

### Data

Data for the present work on India have been collected from various sources. These data comprise annual observations over the years 1990-2018, namely:

- Total population measured in millions,
- Gross domestic product (GDP) measured in trillion INR (Indian Rupees) in 2015 prices,
- Total supply of primary energy per technology measured in billion tons of oil equivalents (BTOE),
- Total consumption of primary energy per sector per technology in BTOE and
- Total emissions of $CO_2$ per sector measured in Mtons derived with the sectoral approach.

Energy data is collected from IEA (2021). The added value per sector has been collected from the UN (2021b). The economic liberalization process started in India in the early 1990s. We have started our analysis from the year 1990 and have taken the period of 1990 to 2018, which has been divided into three sub-periods: 1990-2000, 2000-2010, and 2010-2018. The reference year is 1990.

For preparing the data for analysis of complete decomposition, the Indian economy has been divided into four different sectors: the primary agricultural sector, the secondary industrial sector, the tertiary transport sector, and the services sector. The value added for agriculture and industry sectors are separately specified in the data and have been used immediately. However, the value added for transport is only available in combination with communication. In this paper, the value added of transport

Table 2: Emission factors of fuels (in tons carbon per TJ).

| Coal | Crude Oil | Oil Products | Natural gas |
|------|-----------|--------------|-------------|
| 26.8 | 20.0 | 19.5 | 15.3 |

Source: IPCC (2000).

and communication has been used as a proxy for the transport sector for lack of sufficient information. The remaining value added has been assigned to the services sector in the economy.

## RESULTS AND DISCUSSION

The level of $CO_2$ emissions in India is subjected to a decomposition analysis from 1990–2018. Energy use changes with technologies and sectors. Energy technologies have been divided broadly into two categories, namely fossil fuel (coal, lignite, oil, and gas) and renewable (wind, solar, hydro, and bioenergy) (Jana & Singh 2022, Jana 2022). The energy-using sectors considered in the present analysis are agriculture, industry, transport, and services.

Sectoral division for energy consumption has been done as for value-added. This has been done simply by taking the numbers published in IEA (2021a). It is also possible to derive the composition of different fuel types in the primary energy supply from these energy balances. Emissions from energy consumption have been calculated using emission factors given in IPCC guidelines II (Chapter I.6) (given in Table 2). Table 2 presents the emission factors (in tons carbon per TJ) per ton of used fuel type. The carbon content of coal is the highest, with 26.8 tons of carbon per TJ, while the carbon content is lowest for natural gas, with 15.3 tons of carbon per TJ. Emissions from energy sources like animal waste, wood, wind power, geothermal, hydro, nuclear, and traded electricity have not been considered.

Two ways to estimate $CO_2$ emissions from energy consumption exist, the reference and sectoral method (IPCC 2006). The reference method uses a carbon flow account (inputs and outputs of carbon fuels) and corrects for non-emitted carbon in fuels. The sectoral method uses consumption figures for different sectors. The outcomes of these two methods are generally different for various reasons, like different statistics sources. The difference between these two methods is, on average, about 2% of the data set used in this study. In the present paper, the level of emissions is based on the second method, i.e., the sectoral method. This method is preferred as it gives the required breakdown of $CO_2$ emissions per sector for the complete decomposition analysis with LASP.

In addition to the four sectors, namely agricultural, industrial, transport, and services, there is a fifth sector: power generation. This conversion sector has a relatively low value added to the national accounts; a separate consideration may probably yield a distorted image of the economy. Following Paul & Bhattacharya (2004), the emissions of $CO_2$ from power generation are assigned to four economic sectors proportional to their electricity consumption as given in the energy balances.

### GDP, $CO_2$ Emissions, and Population Growth in 1990-2018

To show structural changes in the Indian economy, Fig. 1 plots the development of GDP and population in India during the period 1990-2018. The economy has been growing at an
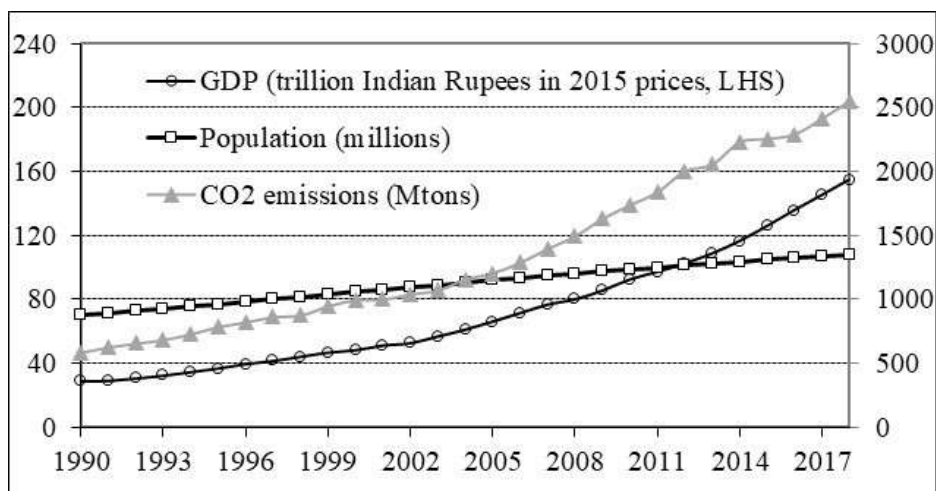


Source: Authors' estimation based on IEA(2021).

Fig. 1: GDP in real terms, $CO_2$ emissions, and population in India.

Table 3: The stages of development in India in the years 1990 and 2018 linked to a comparable stage of development of other selected countries in 2018.

|  | GDPPC in 2010 prices | Agricultural sector | Industrial sector | Services sector | Population [millions] |
|---|---|---|---|---|---|
| Ethiopia in 2018 | 571 | 31.1 | 27.3 | 41.6 | 109.2 |
| **India in 1990** | **581** | **40.3** | **27.9** | **31.8** | **873.3** |
| Mozambique in 2018 | 593 | 24.6 | 25.3 | 50.0 | 29.5 |
| Vietnam in 2018 | 1,964 | 14.7 | 34.2 | 51.1 | 95.5 |
| **India in 2018** | **2,086** | **16.5** | **29.7** | **53.8** | **1352.6** |
| Honduras in 2018 | 2,219 | 11.6 | 26.8 | 61.6 | 9.6 |

* Source: WDI (2021), whereas sectoral shares and population for India are derived as explained in the text.

average per capita annual growth rate of 4.6%, higher than average world long-term growth.

To assess the performance of the Indian economy, Table 3 compares the economic development situation in India in 1990 and 2018 with countries in 2018, similar in terms of GDP. This shows that based on GDP, in 1990, India was at a comparable level to Ethiopia and Mozambique in 2018. Thanks to economic growth, India is comparable to Vietnam and Honduras in 2018, a considerable improvement in 28 years.

**Energy Consumption in India by Sector and by Fuel**

Before analyzing the complete decomposition results, the data's nature is presented here. The real GDP in India has increased at an annual rate of 6.2%, and the population has increased at an annual rate of 1.6%. The development of the sectoral share of GDP during 1990-2018 of the four sectors is presented in Fig. 2.

Fig. 2 shows that the industrial sector (from 27.9% in 1990 to 29.7% in 2018) and transport sector (from 3.5% in 1990 to 8.9% in 2018) increased to some extent during 1990-2018. There is a substitution between an increasing share of the service sector (from 28.4% in 1990 to 44.9% in 2018) and a decreasing share of the agricultural sector (from 44.3% in 1990 to 16.5% in 2018). From a traditional viewpoint, one would expect an economy to move from a farm-based economy to an industrial economy and finally enter into an economy dominated by the services sector. Contrary to this traditional view, India's sectoral composition leapfrogged the industrial phase, where the services sector has substituted the agricultural sector.

The development over time of the sectoral energy consumption per value added (energy intensity) is presented in Fig. 3. The graph depicts the changes in energy intensity. Table 4 reveals that the overall energy intensity of the Indian economy decreased steadily by 53.7%, with decreases of 22.8% in 1990-2000, 20.7% in 2000-2010, and 24.3% in 2000-2018. Fig. 3 shows that the agricultural sector has become much more energy-intensive, with an increase of 53.6%. Moreover, there has been a substantial decrease in the energy intensity in services by 78.6%. The decrease in the services sector over the subperiods was stable. Furthermore, the energy intensity in the transport sector decreases substantially, with a rate of 63.9% from 1990–2018. The
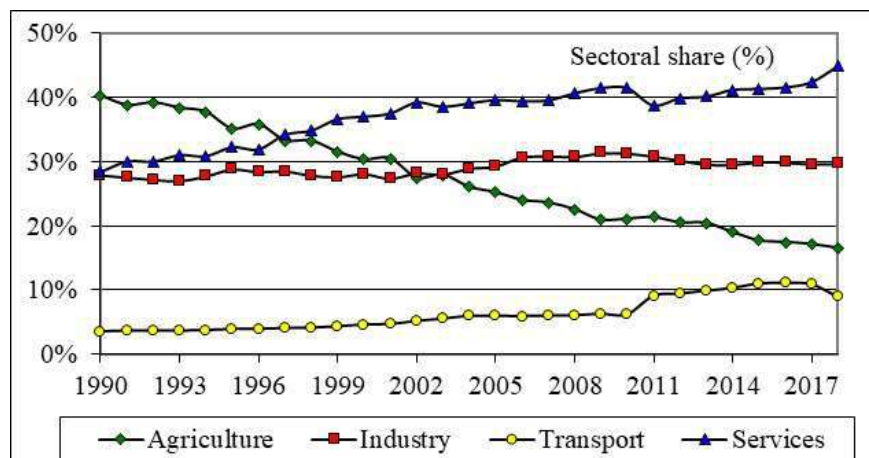


Fig. 2: Share in the Indian economy of four considered sectors.
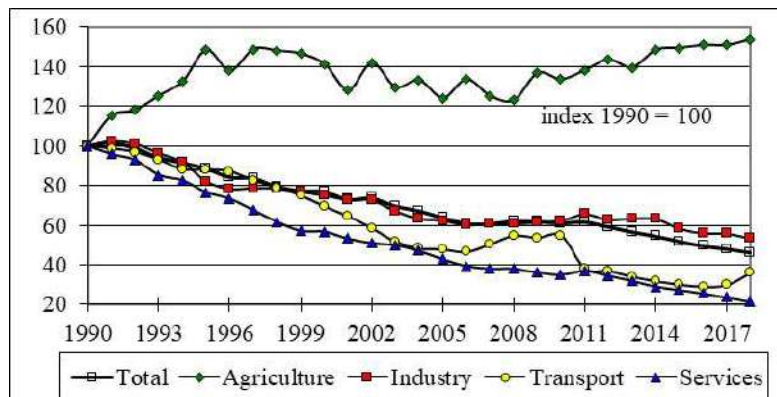
Fig. 3: Sector-wise growth of energy intensity (per value added) in India.

Table 4: Changes (%) in energy intensity from 1990 to 2018 in India.

|           | Agriculture | Industry | Transport | Services | Total  |
|-----------|-------------|----------|-----------|----------|--------|
| 1990-2000 | 41.2%       | -24.9%   | -30.5%    | -43.2%   | -22.8% |
| 2000-2010 | -5.4%       | -16.8%   | -21.0%    | -38.0%   | -20.7% |
| 2010-2018 | 15.0%       | -14.4%   | -34.3%    | -39.2%   | -24.3% |
| 1990-2018 | 53.6%       | -46.5%   | -63.9%    | -78.6%   | -53.7% |

Source: Authors' estimation

energy intensity in the industrial sector also decreased during the mentioned period by 46.5%, with the highest decrease of 24.9% in the first decade.

In interpreting the results of the changes in energy intensity (per value added), energy intensity has decreased except in the agricultural sector. This can be explained by focusing on the sectoral level. Due to mechanization, energy intensity mainly increased in the first decade when it shifted from animal to tractor power. The energy intensity is found to decrease overall subperiods in all other sectors. Historically, following various sector specifications and policy measures, especially after the Energy Conservation Act of 2001,

Integrated Energy Policy in 2005, and National Action Plan on Climate Change (NAPCC) in 2008, emissions per unit of output have been reduced considerably, especially in the industry sector leading to substantial relative decoupling (Das & Roy 2020).

India has been able to reduce $CO_2$ emissions through various policies, such as phasing out inefficient older thermal power units, deregulation of diesel prices by reducing subsidies and increasing taxes on fossil fuels like petrol and diesel, setting up a corpus, National Clean Environment Fund (NCEF); implementation of Renewable Purchase Obligation (RPO) where power distribution companies are
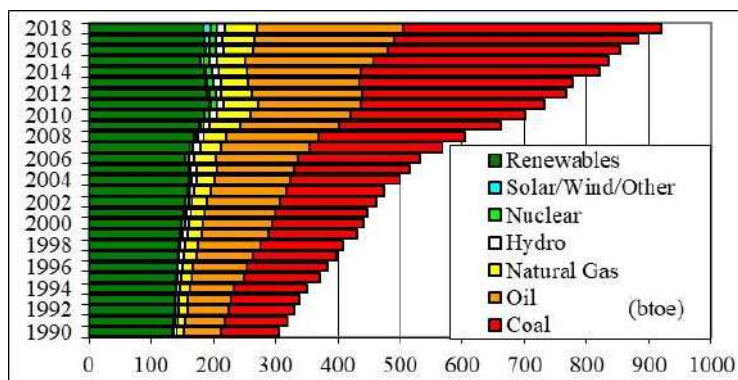


Source: Authors' estimation.

Fig. 4: Shares (%) of different fuels in primary energy supply in India.

Table 5: Shares (%) of different fuels in primary energy supply in India in 1990 and 2018.

| | Coal | Oil | Natural Gas | Hydro | Nuclear | Solar/Wind/ Other | Renewables (fuelwood) | Total btoe |
|---|---|---|---|---|---|---|---|---|
| 1990 | 30.3% | 20.0% | 3.5% | 2.0% | 0.5% | 0.0% | 43.7% | 306 |
| 2018 | 45.0% | 25.6% | 5.7% | 1.4% | 1.1% | 1.1% | 20.1% | 919 |
| Share Growth Factor | 1.48 | 1.28 | 1.65 | 0.70 | 2.05 | N.A. | 0.46 | 3.01 |

Source: Authors' estimation based on IEA(2021).
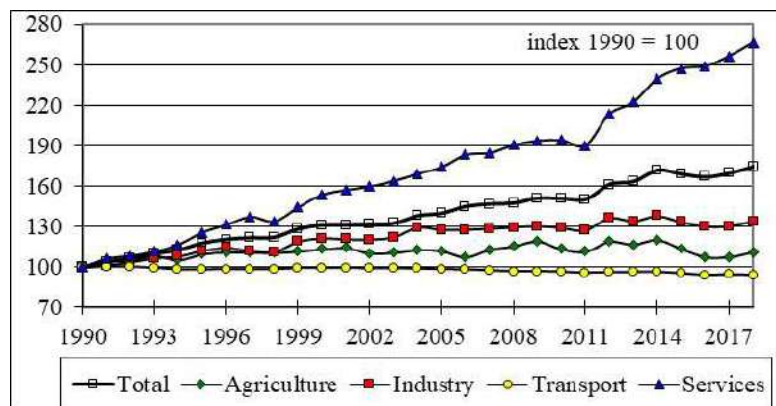


Source: Authors' estimation

Fig. 5: Sector-wise growth of carbon intensity (per energy consumption) in India.

Table 6: Change (%) in carbon intensity (per energy consumption) in India.

| | Total | Agriculture | Industry | Transport | Services |
|---|---|---|---|---|---|
| 1990-2000 | 31.0% | 13.4% | 21.4% | -0.6% | 53.7% |
| 2000-2010 | 15.1% | 0.1% | 6.3% | -2.9% | 26.3% |
| 2010-2018 | 15.7% | -1.9% | 3.9% | -2.4% | 37.2% |
| 1990-2018 | 74.5% | 11.4% | 34.1% | -5.7% | 166.1% |

Source: Authors' estimation.

obligated to buy at least 15% of electricity from renewable energy producers; and providing incentives to the producers of renewable energy and importing hydro-power from neighboring countries Bhutan (Das and Roy, 2020).

Fig. 4 presents the composition of fuel types in primary energy supply in India during the 1990–2018 period. Fig. 4 shows that the growing demand for energy in India is primarily met with an increase in the share of oil (factor 1.28) and coal (factor 1.48) in the energy supply. In 1990, coal contributed 30.3%, oil 20.0%, and renewables 43.7% to the primary energy supply in India (Table 5). In 2018, coal contributed 45.0%, oil 25.6%, natural gas 5.7%, and renewables 20.1% to the primary energy supply in India. The share of traditional renewables, e.g., fuelwood, has decreased at the expense of an increase in the share of coal in the energy supply.

The growth of $CO_2$ emissions per unit of energy consumed (carbon intensity) for different sectors is presented in Fig. 5. In parity with Fig. 3, the carbon intensity for all sectors is presented with respect to the base level of 100 in 1990. Table 6 shows the percent changes in carbon over three periods, showing that the carbon intensity has increased over time in all the sectors except the transport sector. Over the period 1990-2018, the carbon intensity increased by 74.5%. The increase in carbon intensity is the highest in the services sector, which shows an increase of +166% over the 1990–2018 period. The carbon intensity increased in the agricultural and industrial sectors by +11.4 and +34.1%, respectively.

Interpretation of the result in Fig. 5 indicates that the services and industrial sectors have become more carbon-intensive to a lesser extent. The 'gain' of a reduction in energy intensity in India is slightly more than offset by the 'loss' in an increased carbon intensity in the services sector. The main reason for increased carbon intensity in the services sector is electrification, which has seen the share
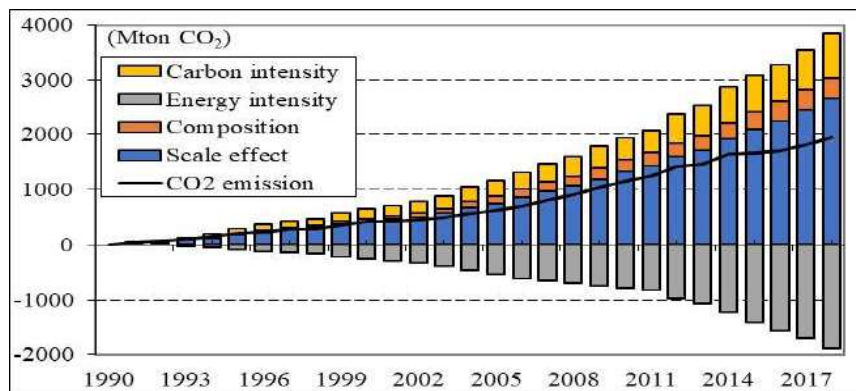
Fig. 6. Decomposition of the difference in the level of emissions $CO_2$ (in Mtons $CO_2$) with respect to the level of emissions in 1990.

of coal increase in the electricity generation mix, leading to a higher $CO_2$ emission factor of the Indian power grid. The aggregate effect of energy efficiency and carbon intensity gain is a gradual rise in $CO_2$ emissions. Hence, there was no significant reduction in carbon intensity in the various sectors of the Indian economy, except for transport.

### Decomposition Analysis

A complete decomposition analysis, as proposed by Sun (1998), has been presented in this section. Given the availability of data, changes in $CO_2$ emissions over time with respect to the base year 1990 can be decomposed into several factors. Fig. 6 presents the results of the (non-binding Kyoto) decomposition analysis for India. Fig. 6 presents a decomposition of the total national $CO_2$ emissions. The difference between the current amount of $CO_2$ emissions and the amount of $CO_2$ emissions in the base year 1990 is given in Fig. 6. For instance, the increase of 409.5 Mtons $CO_2$ emissions in 2000 with respect to 1990 is the sum of the scale (409.6 Mtons), composition (63 Mtons), energy

intensity (–250.3 Mtons) and carbon intensity (187.3 Mtons) effects.

Table 7 shows the level and percent changes over three periods. Fig. 6 shows that the scale effect is the main driver for increasing $CO_2$ emissions. More specifically, Table 7 reveals that the scale effect already accounts for +135.5% of rising emissions of $CO_2$ over the whole period. The carbon intensity (+41.8%) and composition effect (+18.6%) move in tandem. However, the carbon intensity effect varies more than the composition effect. Therefore, the composition of the Indian economy has become somewhat dirtier, where the $CO_2$ emissions have increased over time because of the carbon intensity effect. The opposite is true for the energy intensity effect, where carbon emissions decreased. From 1990–2018, the energy intensity effect accounts for a decrease of 95.9% in $CO_2$ emissions (Table 7).

### Link $CO_2$ Emissions and GDP

To verify the link between $CO_2$ emissions (CO2) and GDP in India, it is also possible to test whether there is an EKC for

Table 7: Decomposition of the change in the levels of $CO_2$ emissions (Mton) in India.

|            | Scale effect | Composition effect | Energy Intensity effect | Carbon Intensity effect | $CO_2$ emissions |
|------------|--------------|--------------------|-------------------------|-------------------------|------------------|
| 1990-2000  | 409.6        | 63.0               | -250.3                  | 187.3                   | 409.5            |
| 2000-2010  | 918.9        | 144.3              | -540.9                  | 218.6                   | 740.8            |
| 2010-2018  | 1327.4       | 157.7              | -1089.3                 | 414.6                   | 810.3            |
| 1990-2018  | 2655.8       | 365.0              | -1880.5                 | 820.4                   | 1960.6           |
| % share of effect |       |                    |                         |                         |                  |
| 1990-2000  | 100.0        | 15.4               | -61.1                   | 45.7                    | 100.0            |
| 2000-2010  | 124.0        | 19.5               | -73.0                   | 29.5                    | 100.0            |
| 2010-2018  | 163.8        | 19.5               | -134.4                  | 51.2                    | 100.0            |
| 1990-2018  | 135.5        | 18.6               | -95.9                   | 41.8                    | 100.0            |

India with respect to greenhouse gas emissions as measured by $CO_2$ emissions. The OLS regression results are as follows: the standard errors are presented in the parenthesis.

$$ln(CO2) = \underset{(0.05)}{3.48} + \underset{(0.013)}{0.873} \, ln(GDP) \, ; R_{adj}^2 = 0.994$$

...(4)

$$ln(CO2) = \underset{(0.50)}{3.32} + \underset{(0.243)}{0.954} \, ln(GDP)$$

$$- \underset{(0.0291)}{0.0097} (ln(GDP))^2 ; R_{adj}^2 = 0.994$$

...(5)

The variables are also tested for normality with the Jarque-Bera test, which did not give sufficient evidence to conclude that the dataset is not normally distributed. Two equations are estimated: a linear relationship between $CO_2$ emissions and GDP (4) and the quadratic equation to test whether there is an EKC. While the goodness of fit $(R_{adj}^2)$ of the estimated quadratic regression equation (5) is high. The estimation results reveal that EKC does not hold for India, as the regression coefficient of the quadratic term in the estimated regression equation is insignificant, though it possesses the right sign.

Therefore, the yearly data covering the period 1990–2018 show that the $CO_2$ emissions have been linearly increasing in the level of GDP, and no EKC can be observed in $CO_2$ emissions for India. Hence, in India, economic growth has not (yet) decoupled from carbon emissions during the studied period. This result is in parity with the conclusion derived from the decomposition analysis that GDP growth (scale effect) is the major determinant of the increase in $CO_2$ emissions in India.

## CONCLUSION

The present paper has decomposed the factors that drive $CO_2$ emissions in India through changes in four components: scale, composition, energy intensity, and carbon intensity. Changes in the sectoral composition of the economy over time were also considered. The study has also addressed the energy mix changes and the following questions: How has the energy and carbon intensity changed over time and across sectors in India? What is the link between national income and carbon emissions in India?

The study shows that India's overall energy intensity dropped from 1990–2018, with a decline in all sectors except agriculture. The agricultural mechanization process may explain the considerable increase in energy use in the agricultural sector in India. Despite declining overall energy intensity, the level of $CO_2$ emissions per energy unit consumption (carbon intensity) increased in India between 1990-2018. This increase in emission is found to be highest in the services sector, more than offsetting the gains achieved through an improved energy intensity.

The research shows that carbon emissions are increasing considerably in the Indian economy. The decomposition analysis demonstrates that, out of four effects, the scale effect is dominant, implying that $CO_2$ emissions in India are increasing due to the expansion of the economy (scale effect). The actual sectoral composition of the economy and the level of carbon intensity are also found to have a considerable contribution to increasing $CO_2$ emissions. The energy intensity of the Indian economy is found to be decreasing and is responsible for decreasing $CO_2$ emissions. Hence, without proper carbon policies, it is unlikely that emissions of $CO_2$ can be reduced in India. Although various policies adopted by the Government of India have helped achieve relative decoupling in these sectors, the current dominance of coal in the mix of primary energy remains a big hindrance in reducing pollution.

This paper has analyzed the causes of $CO_2$ emissions in a country with a high growth potential. Looking at the sectoral composition, the share of the agricultural sector is 16.5%, and that of the service sector is 53.8% in 2018. This shows that India is still in the middle of its transition toward a modern, developed economy. Moreover, India has skipped the industrialization phase, leapfrogging from an agricultural-dominated society to a services sector-dominated society. For the transition of India into a modern society, a path with a high level of carbon emissions is foreseen. Future policy research is necessary to further reduce these emissions in India.

India is playing an active role at the international level in the global fight against climate change. India's NDC under the Paris Agreement sets out targets to reduce emissions intensity and increase the share of non-fossil fuels, i.e., renewables, in its power generation capacity. Although the emissions intensity of the GDP of India is found to decrease in line with targeted levels, progress towards the supply of low-carbon electricity remains very challenging. The services sector in India is the fastest-growing sector. India is currently facing shortages of coal. Efficient use of energy, and a low carbon path are very much needed to achieve an average high level of growth.

## REFERENCES

Andreoni, V. and Galmarini, S. 2016. Drivers in $CO_2$ emissions variation: A decomposition analysis for 33 world countries. Energy, 103: 27-37.

Ang, B.W. 2004. Decomposition analysis for policymaking in energy: which is the preferred method? Energy Policy, 32(9): 1131-1139.

Ang, B.W. and Choi, K.H. 1997. Decomposition of aggregate energy and gas emission intensities for industry: A refined divisia index method. Energy J., 18(3): 59-73.

Attari, M.I.J. and Attaria, S.N. 2011. The decomposition analysis of $CO_2$ emission and economic growth in Pakistan, India, and China. Pak. J. Comm. Social Sci., 52: 330-343.

Chen, L. and Yang, Z. 2015. A spatio-temporal decomposition analysis of energy-related $CO_2$ emission growth in China. J. Clean. Prod., 103: 49-60.

Das, A. and Paul, S.K. 2014. $CO_2$ emissions from household consumption in India between 1993–94 and 2006-07: a decomposition analysis. Energy Econ., 41: 90-105.

Das, N. and Roy, J. 2020. India can increase its mitigation ambition: an analysis based on historical evidence of decoupling between emission and economic growth. Energy for Sustain. Dev., 57: 189-199.

Dasgupta, S. and Roy, J. 2017. Analysing energy intensity trends and decoupling of growth from energy use in Indian manufacturing industries during 1973–1974 to 2011-2012. Energy Eff., 104: 925-943.

De Freitas, L.C. and Kaneko, S. 2011. Decomposition of $CO_2$ emissions change from energy consumption in Brazil: challenges and policy implications. Energy Policy, 393: 1495-1504.

Ebohon, O.J. and Ikeme, A.J. 2006. Decomposition analysis of $CO_2$ emission intensity between oil-producing and n5on-oil-producing sub-Saharan African countries. Energy Policy, 3418: 3599-3611.

Hoekstra, R. and Van den Bergh, J.C.J.M. 2003. Comparing structural and index decomposition analysis. Energy Economics 25: 39-64.

IPCC. 2000. Special Report on Emissions Scenarios. Cambridge University Press, Cambridge p. 599.

International Energy Agency (IEA) 2020. India 2020: Energy Policy Review. www.iea.org. Accessed 17 March 2021.

International Energy Agency (IEA). 2021. Data and Statistics. Energy Tables for India. https://www.iea.org/data-and-statistics/data-tables. Accessed 17 March 2021.

IPCC. 2000. Special Report on Emissions Scenarios. Cambridge University Press, Cambridge, p. 599.

IPCC. 2006. Chapter 6 Reference Approach. https://www.ipcc-nggip.iges. or.jp/public/2006gl/pdf/2_Volume2/V2_6_Ch6_Reference_Approach. pdf. Accessed 13 April 2022.

Jana, S.K. 2022. Sustainable energy development in emerging economies: a study on BRICS. In: Chakraborty, C. and Pal, D. (eds), Environmental Sustainability, Growth Trajectory, and Gender: Contemporary Issues of Developing Economies. Emerald Publishing Limited, Bingley, UK, pp. 23-35.

Jana, S.K. and Singh, K. 2022. Progress and determinants of renewable energy development in india. In: Danis, M.S.S. and Senjyu, T. (eds), Eco-Friendly and Agile Energy Strategies and Policy Development. IGI Global, Pennsylvania, pp. 190-203.

Kanitkar, T. 2020. An Integrated Framework for Energy-Economy-Emissions Modeling: A Case Study of India. Springer, India.

Karstensen, J., Roy, J., Pal, B.D., Peters, G. and Andrew, R. 2020. Key drivers of Indian greenhouse gas emissions. Econ. Pol. Week., 55(15): 47.

Kojima, M. and Bacon, R. 2009. Changes in $CO_2$ Emissions from Energy Use. The World Bank, Washington DC.

Lise, W. 2006. Decomposition of $CO_2$ emission in Turkey over 1980-2003. Energy Policy, 34: 1841-1852.

Nag, B. and Parikh, J. 2000. Indicators of carbon emission intensity from commercial energy use in India. Energy Economics, 224: 441-461.

Pachauri, S. and Muller, A. 2008. A Regional Decomposition of Domestic Electricity Consumption in India: 1980-2005. Presented at IAEE Conference, Istanbul. https://vol10.cases.som.yale.edu/sites/default/files/cases/SELCO/Pachauri%26Mueller_Istanbul_June2008_Final.pdf. Accessed 12 November 2021.

Pal, B.D., Ojha, V.P., Pohit, S. and Roy, J. 2015. GHG Emissions and Economic Growth: A Computable General Equilibrium Model-Based Analysis for India. Springer, India.

Paul, S. and Bhattacharya, R.N. 2004. $CO_2$ emission from energy use in India: A decomposition analysis. Energy Policy, 325: 585-593.

Reddy, B.S. and Ray, B.K. 2010. Decomposition of energy consumption and energy intensity in Indian manufacturing industries. Energy Sustain. Dev., 141: 35-47.

Stern, D.I. 2004. The rise and fall of the environmental Kuznets curve. World Dev., 32(8): 1419-1439.

Su, B. and Ang, B.W. 2012. Structural decomposition analysis applied to energy and emissions: Some methodological developments. Energy Econ., 341: 177-188.

Su, W., Wang, Y., Streimikiene, D., Balezentis, T. and Zhang, C. 2020. Carbon dioxide emission decomposition along the gradient of economic development: The case of energy sustainability in the G7 and Brazil, Russia, India, China and South Africa. Sustain. Dev., 284: 657-669.

Sun, J.W. 1998. Changes in energy consumption and energy intensity: a complete decomposition model. Energy Econ., 20: 85-100.

Taka, G.N., Huong, T.T., Shah, I.H. and Park, H.S. 2020. Determinants of energy-based $CO_2$ emissions in Ethiopia: A decomposition analysis from 1990 to 2017. Sustainability, 1210: 4175.

Tandon, A. and Ahmed, S. 2016. Technological change and energy consumption in India: a decomposition analysis. Innov. Dev., 61: 141-159.

Tiwari, A.K. 2011. Energy consumption, $CO_2$ emissions, and economic growth: Evidence from India. J. Int. Bus. Econ., 121: 85-122.

United Nations (UN). 2021a. Ensure Access to Affordable, Reliable, Sustainable, and Modern Energy. United Nations, NY.

United Nations (UN). 2021b. Value Added by Economic Activity: At Constant 2015 Prices - National Currency. https://unstats.un.org/unsd/nationalaccount/, https://unstats.un.org/unsd/snaama/basic. Accessed 17 March 2021.

Wang, C., Chen, J. and Zou, J. 2005. Decomposition of energy-related $CO_2$ emission in China: 1957-2000. Energy, 301: 73-83.

Wang, H. and Zhou, P. 2018. Assessing global $CO_2$ emission inequality from consumption perspective: An index decomposition analysis. Ecol. Econ., 154: 257-271.

Wang, Y., Sun, M., Xie, R. and Chen, X. 2020. Multiplicative structural decomposition analysis of spatial differences in energy intensity among G20 countries. Appl. Sci., 108: 2832.

WDI 2021. World Development Indicators. https://databank.worldbank.org/source/world-development-indicators. Accesed date 17 March 2021.

Wolde-Rufael, Y. and Idowu, S. 2017. Income distribution and $CO_2$ emission: A comparative analysis for China and India. Renew. Sustain. Energy Rev., 74: 1336-1345.

Xu, S.C., He, Z.X. and Long, R.Y. 2014. Factors that influence carbon emissions due to energy consumption in China: Decomposition analysis using LMDI. Appl. Energy, 127: 182-193.

Xu, X.Y. and Ang, B.W. 2013. Index decomposition analysis applied to $CO_2$ emission studies. Ecol. Econ., 93: 313-329.

Zhang, F.Q. and Ang, B.W. 2001. Methodological issues in cross-country/region decomposition of energy and environmental indicators. Energy Econ., 23: 179-190.

Zhang, M., Mu, H., Ning, Y. and Song, Y. 2009. Decomposition of energy-related $CO_2$ emission over 1991-2006 in China. Ecol. Econ., 687: 2122-2128.

Zhang, Y.J. and Da, Y.B. 2015. The decomposition of energy-related carbon emission and its decoupling with economic growth in China. Renew. Sustain. Energy Rev., 41: 1255-12.

# Impact of Nanoplastics on Marine Life: A Review

**S. Das†**

Department of Chemistry, Sreegopal Banerjee College, Bagati, Mogra, Hooghly-712148, West Bengal, India
†Corresponding author: S. Das; sumitrasgb2022@gmail.com

## ABSTRACT

Minute plastic subdivisions like microplastics and nanoplastics have recently gained considerable attention because of their toxic effects on the environment and human health. Many plastics have been consumed worldwide regularly, and most are thrown away after a single use. They all end up in the sea and ocean, leading to a large debris of plastic garbage in the marine environment. Different physical and chemical processes occur in the marine ecosystem to degrade the macroplastics into micro- and nano-level plastics. Owing to their small size and large surface area, nanoplastics can easily be ingested into the tissues and organs of various marine species (both vertebrates and invertebrates) and accumulate more toxic materials in them than micro and macroplastics. Several reports have been obtained on the toxicity of plastics and microplastics on marine organisms. Still, till now, a cursory report has been found on the potential risk of nanoplastics in connection with marine life. This review highlights the origins of nanoplastics (NPs), their properties, characterization, and impact on marine ecosystems, along with their remediation and future aspects. The review will also untangle and specify the area of nanoplastics on which further research is urgently needed to better understand its toxic effect and eco-friendly restoration on the environment, especially on marine life.

## INTRODUCTION

Plastics, a widely used synthetic or semi-synthetic material, are mainly synthesized by the polymerization and polycondensation of different monomeric components like ethylene, styrene, propylene, vinyl chloride, tetrafluoroethylene, etc. (Eyerer et al. 2010). It was developed and marketized in the early 19$^{th}$ century, and in the middle of the 20$^{th}$ century, the globalization of plastics occurred due to its large production and applications worldwide (Geyer et al. 2020). One-third of the total plastic production is used for making plastic bags, another one-third for preparing housing components, and the rest for industrial and medical purposes. Plastics are generally lightweight, but many are hard, have high longevity, are easy to prepare, and are inexpensive (Stolbov et al. 2021). Harnessing these properties, the uses of plastics propagate very rapidly all over the world in the modern era, so geologists identify this age as the 'plastic age' (Blocker et al. 2020).

Along with the abrupt use of plastics, the hazards associated with plastics also increase daily. Plastic is inherently a chemically stable compound and non-biodegradable. Thereby, it can accumulate more toxic materials in the environment. Nowadays, during the production of plastics, various additives are incorporated

into them, which further increase their strength and durability (Jain et al. 2019). After the introduction of plastics, it has become a good substitute for wood, which reduces the cutting of trees and thereby helps the environment. However, improper disposal of plastics on the land causes loss of soil fertility and quality, and the plastic garbage in the aquatic environment decreases the survival rate of aquatic animals. Ingestion of plastics through food and water causes serious health problems in humans (Alabi et al. 2019).

According to famous environmentalists all over the world, plastic is the main litter in the marine environment as well as in the terrestrial area. Plastics thrown away end up in the sea or oceans through various draining systems, and these are the main sources of plastic waste in the marine environment. These macro-sized plastic garbages transform into small-sized nanoplastics (NPs) through UV irradiation (Mao et al. 2020), mechanical abrasion (Sun et al. 2022), and biodegradation (Jaiswal et al. 2020). Nanoplastics possess a wide range of interesting properties because of their small size and large surface area. Due to their large surface curvature, nanoplastics can easily be adsorbed and transferred into the tissues of marine organisms (Bhagat et al. 2021). Even during breathing, several tiny particles of nanoplastic are entered into various sea animals and accumulate in their respiratory tract. It is also incorporated

into the food chain and spreads rapidly within the ecosystem, endangering all marine life (Zaki & Aris 2022) (Fig. 1). The main problem encountered with that is that the degradation of plastics is not a controllable fact. In the micro- and nanoscale, PE (polyethylene), PVC (polyvinylchloride), PS (polystyrene), PET (polyethylene terephthalate), and PMMA (polymethylmethacrylate) were observed (Baig et al. 2022). Literature has illustrated the toxic effect of polystyrene (PS) and polymethylmethacrylate (PMMA) nanoplastics on marine animals. This review briefly describes the source, sampling, degradation procedure, effect of nanoplastic on different types of marine organisms, and some of its remediation procedures. The future aspects of this research are also discussed in this context, which will help the upcoming researchers explore nanoplastics more and find a suitable way out of the present situation.

## ORIGIN OF NANOPLASTICS IN MARINE ENVIRONMENT

The two primary origins of plastics (Liu et al. 2020) in the sea and ocean are (i) primary, i.e., plastic particles that are produced in a definite size range, and (ii) secondary, which indicates the smaller-sized plastics that are obtained from the degradation of the larger-sized plastics. Nanoplastics that are found in the marine environment are of secondary origin and mainly emerge from different household, industrial, anthropogenic, and public drainage systems, a variety of constructions on the coastal side, business and landfill waste, and different types of litter disposal from varieties of water transports, fishing fleets, and entertainment activities (Koelmans et al. 2015). Survey reports revealed that in 2010, 2.5 billion metric tons of solid waste were produced worldwide, of which 275 million metric tons were plastics, and out of this, 4.4 to 12.7 million metric tons were found in the sea and ocean (Jambeck et al. 2015). The nano-sized plastic particles are also discharged into the sea and ocean from the plastic production and processing industries during their manufacturing and carriages through the release of wastewater from various plastic industries. These tiny plastic particles have a size in the nanometer range and have been found primarily in the beach surroundings, coastal regions, and industrial belts, along with spreading secondarily in the remote non-industrial zone. A survey report reveals a high concentration of household and consumer goods plastics has been widely found in the various seaside areas. This plastic is then degraded through various methods into tiny particles on the nanometer scale (Fotopoulou & Karapanagioti 2017). It has also been observed that the nanoplastics found in this region are of lower density, indicating that the composition of the plastics has been altered near this beach area.

## DEGRADATION OF PLASTICS FROM MACRO TO MICRO TO NANO-SIZED PLASTICS

Generally, the fragmentation of macroplastics into meso, micro, and, ultimately, nanoplastics (Amobonye et al. 2021) occurs due to the weathering of plastics. Nowadays, environmental experts classify the degradation processes of plastics into six categories: thermal, hydrolytic, mechanical, thermo-oxidative, photo, and biodegradation (Isaacson et al. 2021, Elsawy et al. 2017, Ravishankar et al. 2018, Kumagai et al. 2022, Berenstein et al. 2022, Ahmed et al. 2018). The thermal method indicates the degradation of plastics due to in situ heat generation. Hydrolytic breakdown arises due to the breakage of bonds by adding water. Mechanical abrasion occurs with the hit of a wave or the force of water flow. In the thermo-oxidative process, the macro-sized plastics are degraded into tiny particles through a slow oxidation process. Photodegradation is induced by sunlight, and the breakdown of larger plastics influenced by various living organisms like bacteria is termed "biodegradation. Among them, hydrolytic and mechanical degradation are the two most common degradation processes that take place in the marine environment. Different degradation processes will result in plastics of various sizes, from the micro- to the nanometer range. This review mainly deals with plastics in the nanometer range that possess a large surface area and can effectively interact with marine organisms.

It has been observed that, by degradation, a plastic carrying bag produces nano-sized plastics with a surface area of 2600 $m^2$, which are very harmful to our environment. So, the indiscriminate use of plastic bags should be strictly prohibited.

## NANOPLASTIC PARTICLE TRANSPORTER OF OTHER CHEMICALS

The ability of nanoplastics to adsorb and transport various types of toxic materials is primarily responsible for their toxicity. Moreover, the ingredients of the nanoplastic itself contain many chemical additives such as bisphenol A, organotin, triclosan, phthalates, and brominated flame retardants (Baig et al. 2022). The high surface polarity of nanoplastics increases their affinity to adsorb different hydrophobic materials like persistent organic pollutants (POPs) like PCBs, nonylphenol, various pesticides, phenanthrene, etc., along with heavy metals, antibiotics, and the antibiotic resistance genes (ARGS) through different transport mechanisms (Alprol et al. 2021). Liu et al. have revealed from their studies that low concentrations of polystyrene nanoplastics in the saturated soil solution can effectively transport nonpolar pyrene and weakly polar 2,2′,4′-tetrabromodiphenyl ether but have no effect on the

transport of polar molecules like bisphenol A, bisphenol F, and 4-nonylphenol (Liu et al. 2018). All the soil and land nanoplastic litter finally ends up in the sea and ocean. Nanoplastics impart a large surface area, thereby adsorbing the chemicals above to a large extent. These nanoplastics can easily pass into the tissues of marine organisms from seawater, as can the transported chemicals that largely affect the lives of marine organisms.

## SPECIAL FEATURES OF NANOPLASTICS

The mode of interaction of nanoplastics with living organisms is distinctly different from that of macroplastics. The exceptional behaviors arise due to their nano-level size. The small size and large surface area help them pass easily into marine organisms' biological tissues and make the intercellular interaction and accumulation within the organ more feasible. The increased surface area greatly increases the reactivity of the plastic particles. Chemical composition, size heterogeneity, doping, surface modification, stability, solubility, biodegradability, duration of exposure, interaction with other nanoparticles, and behavior under electromagnetic radiation are some characteristics that distinguish them as unique environmental hazards (Cartraud et al. 2019).

## CHARACTERIZATIONS OF NANOPLASTICS IN MARINE ENVIRONMENT

Since nanoplastics contain very tiny particles, their identification, characterization, and quantification in the marine system have become a great challenge to researchers.

Still, it is very urgent to better understand its potential risk factors for marine life. Nanoplastics can be separated and identified from seawater by ultrafiltration or nanofiltration using membranes with pore sizes of 0.02–5 m. A dynamic light scattering technique further quantifies the separated particles (Zhang et al. 2022).

## EFFECT OF NANOPLASTICS ON MARINE ORGANISMS

Nanoplastic particles found in the marine ecosystem have been proven to affect more than 600 marine species all over the world (United Nations Environment Programme and Secretariat of the Convention on Biological Diversity 2012). Some of the special features of nanoplastics, including their hardness, high longevity, and non-degradability, are primarily responsible for making them severe environmental hazards. The adverse effects of nanoplastics on various living marine species are discussed thoroughly in the following sections.

### Effect of Nanoplastics on Primary Marine Producers

Algae are the initial producers and the initiators of the food web in the marine ecosystem. They appear in veritable shapes and sizes, ranging from nanometers to several meters. The major algae cell wall component is cellulose, which interacts with various particles in the water body. Still, its action towards plastic nanoparticles has been less explored to date. Wang et al. (2020) studied the effect of PS NPs of 70 nm size on *Platymonas shelgolandica,* a green marine microalga,
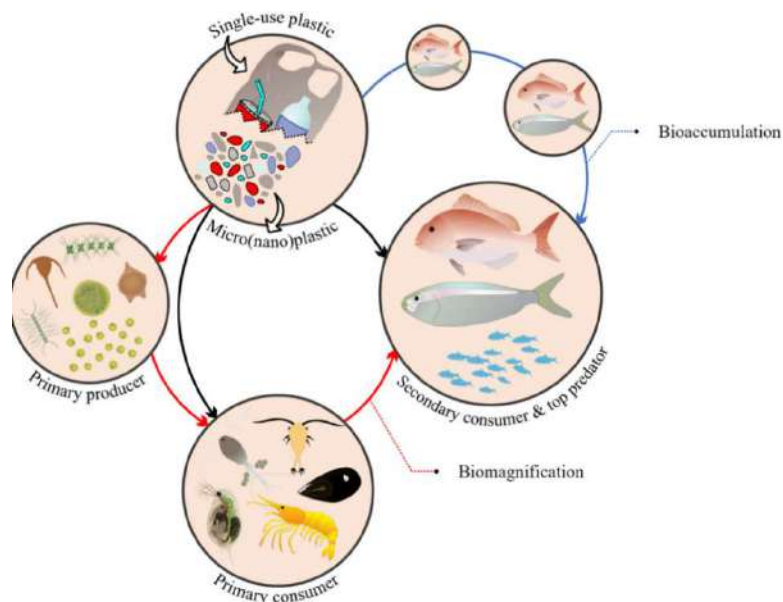


Fig. 1: Transfer of nanoplastics from primary producers to secondary consumers via primary consumers [adapted from Zaki et al. 2022].

upon explosions of 20, 200, and 2,000 g.L⁻¹ concentration for 6 days. After 3 days of exposure, algal growth decreased, and later, in 6 days, photosynthetic efficiency reduced significantly along with the rate of mortality, which increased abruptly. L. Hazeem et al. (2020) investigated the growth inhibition, reduced chlorophyll, and reactive oxygen species production effects of carboxyl-functionalized polystyrene nanoplastics of diameters 20–50 nm on microalgae named *Chlorella_vulgaris*. To understand the surface charge interaction of NPs with the marine microalgae, Sjollema et al. (2016) and Bergami et al. (2017) explored the effect of PS-NH$_2$ (50 nm) and PS-COOH (40 nm) on *Dunaliella tertiolecta* at a concentration level of 250 g.mL⁻¹ for 48 and 72 h, respectively. PS-COOH shows no effect, whereas PS-NH$_2$ exhibits a reduction of cellular growth and cell density. This is presumably due to the electrostatic interaction between the positively charged PS beads and the cellulose of the cell wall. The red microalgae, *Rhodomonas baltica,* was exposed to PMMA and PMMA-COOH (Gomes et al. 2020) of 50 nm size and 0.5-100 g.mL⁻¹ concentration for 72 h. PMMA-COOH inhibits cellular growth, whereas PMMA exposure causes multi-cellular malfunctions such as reduced lipid metabolism, photosynthetic efficiency, reactive oxygen species generation, etc. Venancio et al. (2020) examined the effect of PMMA nanoplastics on four marine algae and one rotifer. One algae named *Thalassiosira weissflogii* shows the highest sensitivity, and the rotifer species are far more sensitive than the marine algae. Their experiment's species sensitivity distribution curve shows that PMMA NPs are less harmful than PS NPs. Furthermore, the toxicity of nanoplastics increases to a great extent in aggregation with other toxic nanoparticles present in marine water. F.-F. Liu et al. (2022) revealed from their experiment that the hazards of CuO nanoparticles enhance significantly in combination with polystyrene NPs towards *Platymonas shelgolandica* var. *tsingtaoensis*. The combined effect of CuO and PS nanoparticles greatly influences cell oxidative stress and

cell membrane permeability compared to single CuO nanoparticles. In contrast to this observation, Natarajan et al. (2022) represented that PS NPs diminish the toxic effect of TiO$_2$ nanoparticles on one type of microalga, *Chlorella* sp. Some other observations related to marine algae have been summarized in Table 1.

The above case studies reveal that growth, rate of fertilization, photosynthetic ability, chlorophyll formation, and cell wall formation of the marine algae have been highly affected by the amide-containing PS nanoplastics. In contrast, PMMA NPs have a comparatively lesser effect on marine algae. The -COOH analog PS NPs have a very poor effect on marine algae. The toxicity of some suspended metal oxides increases to a far greater extent (Liu et al. 2022), whereas nanoplastics themselves can reduce the toxic effect of some other metal oxides (Natarajan et al. 2022). Still, further investigation should be carried out to better understand the interaction of NPS with marine algae.

**Effect of Nanoplastics on Marine Primary Consumers**

Primary consumers have an important role in maintaining stability among the primary producers and secondary consumers in the food chain of an ecosystem. They are mostly larvae of different vertebrates and invertebrates of marine organisms. Primary consumers are primarily herbivores but can also be omnivores, selective feeders, or passive feeders in an oceanic ecosystem. Depending on their omnipresence, nanoplastics are absorbed and transferred within the food web of the prevailing ecosystem. Primary marine consumers like rotifers, polychaetes, echinoderms like sea urchins, mollusks like mussels and oysters, and crustaceans like copepods, shrimp, barnacles, krill, and waterfowl experience severe adverse effects due to the adsorption of nanoplastics.

**Effect of nano plastic on marine feeders:** The feeders primarily consume different types of suspended marine

Table 1: Effect of nanoplastics on marine primary producers.

| Species | Type | Size (nm) | Concentrations (µg.L⁻¹) | Exposure time | Effect | References |
|---|---|---|---|---|---|---|
| *Phaeodactylum tricornutum* | PS | 50 | 0.1-50 | 24 and 72 h | After 24 h, cell size, and photosynthetic efficiency decrease, and after 72 hrs exposure mitochondrial membrane depolarisation occurs | Sendra et al. 2019 |
| *Thalassiosira pseudonana* | PS | 55 | 0.0001–250 | 48 h | Cellular stress increases severalfold in the phytoplankton species | Shiu et al. 2020 |
| *Karenia mikimotoi* | PS | 65 and 100 | 1 and 10 | 3 to 13 days | Increase the cellular stress, and the growth rate decreases abruptly | Zhao et al. 2020 |
| *Chlorella vulgaris* | PS-NH$_2$ | 90 | 25-100 | 24-72 h | Cellular aggregates take place, and cell size decreases significantly. | Khoshnamvand et al. 2021 |

Table 2: Effect of nanoplastics on marine filter feeders.

| Species | Type | Size | Concentrations | Effect | References |
|---|---|---|---|---|---|
| Blue Mussel *Mytilus edulis* | PS NPS | 30 nm | 100-300 $\mu g.mL^{-1}$ | Production of pseudofaces increases with an increase in the concentration of NPS. | Wegner et al. 2012 |
| *Mytilus galloprovincialis* | PS NPs + Cbz (carbamazepine) | 50 nm | 0.05 $mg.L^{-1}$ + 6.3 $\mu g.L^{-1}$ | A decrease in lysosomal membrane stability increases the rate of oxyradical generation, leading to cellular harm. | Brandts et al. 2018 |
| Gametes of the oyster *Crassostrea gigas* | PS-COOH | 500 nm | 4.9 $\mu g.mL^{-1}$ | Gammet and larva remain unaffected. | Tallec et al. 2018 |
| Gametes and embryo-larva of *C. gigas* | PS-NH$_2$ | 50 nm | 0.15 $\mu g.mL^{-1}$ | Highly affects the rate of the fertilization process and causes total malfunction of gametes and larva. | Tallec et al. 2018 |

matter. They help to keep the aquatic environment clean. The filter feeders primarily consume the aquatic nanoparticles, mostly combined with others. But, the effect of nanoplastics on the filter feeders has been rarely studied.

The aquatic feeders take up the plastic particles as they find them similar to their prey (like colorful plastic balloons or carrying bags), or they ingest foods that inherently contain nanoplastics. Marine filter feeders include clams, krill, sponges, and many fish, like different sharks. The effect of nanoplastics on marine filter feeders is described in Table 2.

**Rotifers:** Rotifers are marine planktonic species that mainly reside in marine water. It plays an important connector role between the primary producers and secondary consumers. They are very sensitive to different water contaminants, including nanoplastics, which prompted their selection as the test species. Manfra et al. (2017) examined the effect of PS-COOH and PS-NH$_2$ nanoplastics on the *Brachionus plicatilis*, a marine rotifer, at concentrations between 0.5 and 50 $mg.L^{-1}$ for 24-48 h. PS-COOH does not significantly affect the target species, even at higher concentrations and long-term exposure. However, PS-NH$_2$ nanoplastics result in a reduced survival rate even at lower concentrations and lower exposure times. It has also been observed that treating *B. plicatilis* with PMMA nanoplastics at a concentration of 4.69 $mg.L^{-1}$ for 48 hrs does not significantly affect the survival rate (Venancio et al. 2019). However, PMMA nanoplastics are far more toxic than PS nanoplastics. The result indicates that in the marine environment, several topological changes in nanoplastics occur that also affect the extent of their toxicity. Moreover, some special features of nanoplastics, like their large surface area and hydrophobic nature, enable them to absorb various organic pollutants suspended in the water bodies of the marine environment. Nanoplastics combined with these pollutants exhibit a greater toxic effect than their non-combined form, as observed in marine algae (Liu et al. 2022).

**Polychaetes:** Benthic species in marine environments are highly affected by nanoplastic pollution. The concentration of nanoplastics at the surface and inside the ocean's water column can be influenced by biological processes like biofouling and physical abrasion in the adjacent environment. Therefore, the nanoplastics in the sedimented water of the ocean become available for the adsorption of benthic species like polychaetes. They are mainly tested to identify the bioaccumulation of various water pollutants, including nanoplastics. The first effect of nanoplastic on polychaetes was first studied by Silva et al. (2020). They used a 100-nm PS nanoplastic on the polychaete *Hedistediversi color* at a concentration ranging from 0.005 to 0.5 $mg.L^{-1}$. It results in a neurotransmission change in the aforesaid polychaete species. Since The polychaetes play an important role in stabilizing the marine ecosystem, the ingested nanoplastics flow in the trophic level via the food web from them. Further investigation is needed to identify the toxic level in this polychaete species.

**Echinoderms:** Another important benthic species widely used for ecotoxicological studies in marine environments is the echinoderm, mainly found in the coral reef. It plays a pivotal role in stabilizing the reef ecosystem by providing shelter to small fish. Some reports (Trifuoggi et al. 2019, Oliviero et al. 2019) are found on the effect of microplastics on echinoderms, but investigation on the effect of nanoplastics on this species is very limited to date; only two such reports have been found using *Paracentrotus lividus* (Murano et al. 2021) and *Sterechinus neumayeri* (Bergami et al. 2019) as biomarkers. Murano et al. investigated the effect of PS-NH$_2$ and PS-COOH nanoplastics on *P. Vidus* for 48 hrs. PS-NH$_2$ treatment decreases cell viability for short-time exposure; this result is accompanied by the reduction of growth and development of its larva at 3.85 $mg.L^{-1}$ for long-term exposure. However, short-term exposure to PS-COOH nanoplastics has little effect, including a decrease

in the lysosomal membrane stability, whereas long-term treatment can hamper their immune system. Treatment of *Sterechinus neumayeri* with PS-NH$_2$ and PS-COOH gives rise to phagocytosis and chronic inflammation in response to oxidative stress after 24 h. The results indicate that the surface charge of nanoplastics increases their toxicity many times because they adhere to the cell walls of target species by electrostatic and van der Waal interactions. This is also influenced by external environmental factors and the species' physicochemical properties.

**Molluscs:** Naval mollusks are important biomarkers for evaluating the influence of nanoplastics in the marine environment, as they behave as excellent filter feeders. They can ingest suspended contaminants in the water body and nanoplastics by mistake, accumulating in their digestive tract and flowing into secondary consumers, including humans, through the food web. Wang et al. (2021) detected an accumulation and preservation of 70-nm PS nanoplastic in the digestive tract of *Mytilus coruscus*. Long-term exposure to PS nanoplastics (30 nm) on *M. edulis* decreases its filtering activity (Wegner et al. 2021). Capolupo et al. (2021) assessed a rise in general stress and a weakening of neurological and immunological function in the *Mytilus*

*galloprovincialis* after long-term exposure (21 days) to PS nanoplastics at a concentration of 1.5-150 mg.L$^{-1}$. In this study, the concentration of nanoplastics is very low, but it has had a long-term impact on the marine mollusk variety.

**Oysters:** Nano-sized plastic particles can harm oyster species in their early stages; however, adult oysters are rarely affected by nanoplastic exposure because self-immunity develops in the matured stage. Ingestion of 70 nm PS by *Crassostrea gigas* shows no significant effect on their growth rate (Cole & Galloway 2015). In contrast, a significant increase in cell size was observed due to the adherence of PS-COOH and PS-NH$_2$ nanoplastics on its gametes (González-Fernández et al. 2018). In the same manner, the embryonic development of *M. galloprovincialis* was restricted by PS-NH$_2$ exposure at concentrations of 2.5-10 mg.L$^{-1}$, and the effect became more pronounced with the increase in the concentration of the exposing nanoplastics (Balbi et al. 2017). Similarly, the embryo's development was further inhibited at higher exposure concentrations (e.g., 20 mg.L$^{-1}$). The above and other additional results have been summarized in Table 3.

The above study reflects that the adhesion also influences ingestion and toxicity regarding oysters. Through these two

Table 3: Effect of nanoplastics on marine primary consumers.

| Species | Type | Size | Concentrations | Effect | References |
|---|---|---|---|---|---|
| Daphnia magna | polystyrene NPS | 100 nm | 1 mg.L$^{-1}$ | Decrease in feeding capacity | Rist et al. 2017 |
| *Brachionus plicatilis* (Rotifers) | PS-NH$_2$ | 50 nm | 0.5-50 mg.L$^{-1}$ | High mortality | Manfra et al. 2017 |
| | PS-COOH | 40 nm | | No acute toxicity | Manfra et al. 2017 |
| *Brachionus plicatilis* | PMMA | 40 nm | 4.7-75.0 mg.L$^{-1}$ | Affect the survival rate | Venancio et al. 2019 |
| *Brachionus koreanus* | PS NPs | 50 nm, 500 nm | 10-20 mg.L$^{-1}$ | All sizes led to a decrease in growth rate and lifespan and longer reproduction time. | Jeong et al. 2016 |
| *Hediste diversicolor* | PS NPS | 100 nm | 0.005-50 mg.L$^{-1}$ | Inhibit neurotransmission behavior | Silva et al. 2020 |
| Sea Urchin | PS-NH$_2$ | 50 nm | 10 mg.L$^{-1}$ | Decrease in lysosomal membrane stability and apoptotic-like nuclear interaction. | Marques -Santos et al. 2018 |
| Blue mussel larvae | PS nanoplastics | 100 nm | 0.42 µg.L$^{-1}$ <br> 28.2 µg.L$^{-1}$ <br> 282 µg.L$^{-1}$ | Abnormal larval development and cellular malformation become significant with increased concentration. | Rist et al. 2019 |
| *Pecten maximus* | ^{14}C-radiolabeled nano polystyrene | 24 nm | 15 µg.L$^{-1}$ | Dispersed throughout the body, caused translocation of the epithermal membrane. | Al-Sid-Cheikh et al. 2018 |
| | | 250 nm | 15 µg.L$^{-1}$ | Accumulated in the digestive system hamper the feeding habit. | |

processes, adhesion and ingestion, the chemical additives are extracted from the nanoplastics to a water body that seems harmful to marine life.

## Effect of Nanoplastics on Marine Secondary Consumers

Various fish-like species are primarily considered secondary consumers of the marine ecosystem. Consumption and accumulation of nanoplastics within the secondary consumer's body due to consuming contaminated species as food in the marine environment. The ingestion of microplastic waste by different marine animals has become very harmful to sea turtles and marine mammals like seals (Rice et al. 2021). This causes physiological problems, such as decreased fitness, increased sinking tendency, decreased food-catching ability, and hampered fat formation in sea birds. The first evidence of plastic ingestion from marine debris was found in Fulmars (Feldkamp et al. 1989), a type of seabird. Between the mid-1980s and 1990s, the concentration of plastics in Fulmar and other sea animals increased significantly. To our surprise, some specific shapes or colors of plastic were found within some marine species, namely sea turtles and some fish. This occurred because those aquatic animals ingested those plastics as their target to feed by mistake; however, the adsorption of nanoplastics in marine secondary consumers has not been extensively studied. Investigation by Catraud et al. (2019) showed that an appreciable amount of nanoplastics has been ingested by a variety of sea birds, sea turtles, etc., which results in a decrease in the total amount of nanoplastics in the marine environment. These nanoplastics and the corresponding pollutants enter the food chain via these marine organisms,

endangering marine life. This process also increases the bioavailability of nanoplastics in sea animals; however, incorporating such materials into the food web has not been studied in depth. Cedervall et al. (2012) and Chae et al. (2018) used algae, zooplankton, and fish to characterize trophic stages in a fresh marine-water ecosystem, and it was discovered that fish species are severely impacted by nanoplastic exposure. Secondary consumers are critical in moving ingested nanoplastics up the food chain, as humans consume these as food ingredients. Zebrafish is one variety of marine fish that has been widely tested to examine the effect of nanoplastics on marine secondary consumers (Chen et al. 2017, Trevisan et al. 2019, Torres-Ruiz et al. 2021).

Kang et al. (2021) revealed the fact from their experiment that exposure of 10 mg.L$^{-1}$ of PS nanoplastics to medaka larvae, *Oryzias melastigma*, for 7 days causes rapid accumulation and dispersion within the larva's body, increasing oxidative stress. Longer induction times may cause severe toxicity as they readily penetrate the biological tissues. The harmful effect of nanoplastics on marine secondary consumers is related to the change in functional groups of the nanoplastics. Positively charged NH$_2$-containing nanoplastics seem more toxic to marine organisms' larvae than their negatively charged COOH-containing analog. Brandts et al. (2018) employed adult *Dicentrarchus labrax* to examine the impact of 45-nm PMMA nanoplastics for a short exposure time. The result is that the genes connected to lipid metabolism exhibit up-regulation, whereas genes related to the immune system and cell-tissue repair remain unchanged. This group further examined the exposure of *Sparus aurata* to 0.001 to 10 mg.L$^{-1}$ of nanoplastics for 24 to 96 hours; this resulted in

Table 4: Effect of nanoplastics on marine secondary consumers.

| Species | Type | Size | Concentrations | Effect | References |
|---|---|---|---|---|---|
| Seabream *Sparus aurata* | PMMA | 45 nm | 0-10 µg.mL$^{-1}$ | Increase in plasma cholesterol and tri glyceraldehyde | Brandts et al. 2021 |
| *Sparus aurata* | PMMA | 45 nm | 0.001-10 mg.L$^{-1}$ | Transcriptional level of genes and antioxidant response inhibited; increase the anti-inflammatory response. | Balasch et al. 2021 |
| *Larimichthys crocea* | PS | 100 nm | $5.5\times10^{-12}$-$5.50\times10^{-7}$ mg.L$^{-1}$ | Oxidative stress increases, survival rate decreases | Gu et al. 2020 |
| Zebra fish | PS | 50 nm | 1 mg.L$^{-1}$ | Upregulation of GFAP and α1-tubulin, nervous system related genes | Chen et al. 2017 |
| Zebra fish | PS NPs | <1 µm | 0.1-10 ppm | Mitochondrial dysfunction hamper ATP production, resulting in the reduction of energy production. | Trevisan et al. 2019 |
| Zebra fish | PS NPs + PAH | <1 µm | 0.1-10 ppm + 5.07-25.36 ppb | Agglomeration of PS NPs and PAH occurs, thereby minimizing the effect of single PAH exposure, only marginally affecting energy production. | |
| Zebra fish | PS NPS | 20-200 nm | 10 mg.L$^{-1}$ | Affects internal organs like the brain, eyes, heart, liver, and pancreas. | Torres-Ruiz et al. 2021 |
| | | >200 nm | 10 mg.L$^{-1}$ | Affects the guts, gills, and skin | |

the total malfunction of the lever and nervous system. Lai et al. (2021) observed the result of the exposure of nanoplastics (80 nm) to a large yellow croaker, *Larimichthys crocea*, a commercially available fish in China. They suggested that the increased accumulation level of nanoplastics in the lever system caused a total malfunction.

Similarly, Gu et al. (2020) examined the effect of nanoplastics accumulation on the intestines of marine species. Exposure of nanoplastics to *L. crocea* at a concentration level ranging from $5.50 \times 10^{-12}$ to $5.50 \times 10^{-7}$ mg.L$^{-1}$ for more than 14 days decreases survival and growth rate. The effect of NPs on marine secondary consumers is depicted in Table 4.

Overall, the experimental results indicate that secondary marine consumers have been severely affected by the NPS of different sizes, including loss of cell growth, lever malfunction, decrease in the rate of lipid metabolism, and other enzymatic action. It has also been observed that the juvenile species are worse affected than the adult organisms because of their better adaptation capacity to the environment. Furthermore, the effect of nanoplastics on adult marine species has been scarcely studied, whereas various experiments have been performed in the early stages of the life cycle of marine species.

## FUTURE CHALLENGES AND REMEDIATION

The accumulation of nanoplastics in the environment has now turned into something quite shocking as it is incorporated into the water bodies of the marine environment by some anthropogenic along with the effluents of different industrial and wastewater treatment activities. This, in turn, enters the bodies of marine organisms by ingestion, adsorption, and feeding. The accumulation of so much nanoplastic within marine creatures from low to high levels also affects human health indirectly through drinking water or the uptake of seafood. It has been proved that the accumulation of nanoplastics can hamper living marine organisms' growth, immune, and reproductive systems, affecting the human body.

Contemporary studies have established that the availability of nanoplastics is similar to that of microplastics because the fragmentation of microplastics produces them. But still, studies on the effects of nanoplastics on living beings are quite scarce compared to those on microplastics. This is due to the lack of advanced technologies and experimental methods for identifying and monitoring nanoplastics in environmental matrices. Besides, developing highly sensitive, optimal analytical methods and experimental setups is difficult and expensive. Therefore, concerning nanoplastic pollution in the marine environment, its source of exposure, quantification, detection, and provision in nature should be strictly identified. Secondly, the degradation process of macroplastics into nanoplastics should be assessed. Lastly, a more thorough investigation of the influence of nanoplastics on marine life will be urgently needed.

Recently, researchers have been developing new substitutes that are equally useful as plastics but can simultaneously reduce the toxic effects of nanoplastics. A safe, eco-friendly alternative to plastic, known as "bioplastic" (Muneer et al. 2021), is one such substitute, but its application is still limited. The sustainable, recycled, and biodegradable plastic alternatives synthesized from corn starch, bamboo fiber, weeds, and palm leaves (Dutta & Dutta, 2023) are now in various food packaging. A recent study explored how graphene oxide is used to minimize the toxic effect of PS nanoplastic on *Picochlorum* sp. (Yesilay et al. 2022). Gupta et al. (2022) highlighted methods like photocatalysis, adsorption on biochar, flocculation, eco-corona membrane, filtration, electrospun membrane, etc., to minimize the adverse effect of nanoplastics on marine life. However, a significant development of new technologies is strictly needed to make this remedial process more popular.

In the preceding sections, we have discussed the harmful effect of nanoplastics on marine life, which disturbs the whole ecosystem. Some remediation has also been deliberated to reduce this detrimental outcome (Yesilay et al. 2022, Gupta et al. 2022, Dutta & Dutta 2023). Since plastic has become indispensable to our daily life, I think a suitable alternative to plastic, namely bioplastic, should be introduced that possess similar properties to plastics but will be bio-degradable and eco-friendly. Shafqat et al. (2021) synthesize bioplastic using the banana peel, corn starch, rice starch, wood dust, potato peel, and two polysaccharides, glycerol, and sorbitol, as plasticizers in 1:1 molar ratios. The use of other vegetable starch (sugarcane, peas, lentils), bamboo fiber, and paper pulp mixed with different polysaccharides like glycerol, mannitol, etc. as plasticizers in different molar ratios can extend this work to form bioplastics in green maintainable method. Research on developing plant plastic derived from mushroom roots, baggase (by-product of sugarcane processing), wheat, and barley is urgently needed to reduce plastic hazards. Moreover, necessary steps must be taken to flourish jute and paper technology, which will become efficient substitutes for plastics.

## CONCLUSION

In the modern era of industrialization and globalization, nanoplastics have become alarming marine environmental pollutants. The sampling, quantification, distribution, and identification of nanoplastics in the environment, including the marine environment, has not been sufficiently

investigated compared to microplastics due to a lack of experimental and analytical methods. However, adequate research has been done to identify the toxicological effects of PS and PMMA nanoplastics on marine organisms. It has also been reported that some marine organisms accumulate nanoplastics in high concentrations, which flow into other species, including humans, through the food web. The exact mechanism for the transportation of nanoplastics at the trophic level has not been well established. For a better understanding of the potential risk aspect of nanoplastics, the occurrence, distribution, degradation procedure, and their fate in the environment should be thoroughly studied. This also increases the necessity of developing a reliable methodology to identify the origin of the risk factor of the nanoplastics and to sort out the probable pathways to minimize the problem if it arises. Keeping in mind the toxic effect of microplastics, an attempt has been made to examine the lethal effect of nanoplastics on marine environments. This review provides a brief overview of the harmful effects of nanoplastics on various types of marine organisms, supported by experimental evidence. The toxicity of marine organisms is highly dependent on their size, concentration, exposure time, and variety. Surface functionalization of nanoplastics also plays an important role in inducing toxic effects. Positively charged nanoplastics seem more harmful than negatively charged nanoplastics to marine organisms. Several organic contaminants adsorbed on nanoplastics enhance their toxicity far more.

Some bioremediation processes to reduce the effect of nanoplastics on them have also been highlighted in this aspect. Some marine organisms change their outer surfaces to inhibit themselves from the toxic effects of nanoplastics. Literature found to date demonstrates only the toxic effects of PS and PMMA nanoplastics. So, further investigation of other types of nanoplastics is required. This review also highlights the need for further thorough investigation and quantification of nanoplastics worldwide. It also includes the active involvement of authorities and the public in improving and properly implementing the existing policies to assess and reduce the risk factors related to nanoplastics in the environment. This review also opens the door for future researchers to explore new eco-friendly remedial processes to minimize the toxic effects of nanoplastics after thorough assessments of their adverse effects on marine life.

## ACKNOWLEDGEMENTS

## REFERENCES

Ahmed, T., Shahid, M., Azeem, F., Rasul, I., Shah, A.A., Noman, M., Hameed, A., Manzoor, I. and Muhammad, S. 2018. Biodegradation of plastics: current scenario and future prospects for environmental safety. Environ. Sci. Pollut. Res., 25: 7287-7298.

Alabi, O.A., Ologbonjaye, K.I., Awosolu, O. and Alalade, O.E. 2019. Public and environmental health effects of plastic waste disposal: A review. J. Toxicol. Risk Assess., 5(2): 1-13.

Alprol, A.E., Gaballah, M.S. and Hassaan, M.A. 2021. Micro and Nanoplastics analysis: Focus on their classification, sources, and impacts in marine environment. Reg. Stud. Mar. Sci., 42: 101625.

Al-Sid-Cheikh, M., Rowland, S.J., Stevenson, K., Rouleau, C., Henry, T.B. and Thompson, R.C. 2018. Uptake, whole-body distribution, and depuration of nanoplastics by the Scallop *Pecten maximus* at environmentally realistic concentrations. Environ. Sci. Technol., 52(24): 14480-14486.

Amobonye, A., Bhagwat, P., Raveendran, S., Singh, S. and Pillai, S. 2021. Environmental impacts of microplastics and nanoplastics: A current overview. Front. Microbiol., 12.

Baig, A., Zubair, M., Zafar, M.N., Farid, M., Nazar, M.F. and Sumrra, S.H. (ed.) 2022. Nano Biodegradation of Plastic Waste: Biodegradation, and Biodeterioration at the Nanoscale. Elsevier, Singapore, pp. 239-259.

Balasch, J.C., Brandts, I., Barría, C., Martins, M.A., Tvarijonaviciute, A., Tort, L., Oliveira, M. and Teles, M. 2021. Short-term exposure to polymethylmethacrylate nanoplastics alters muscle antioxidant response, development, and growth in *Sparus Aurata*. Mar. Pollut. Bull., 172: 112918.

Balbi, T., Camisassi, G., Montagna, M., Fabbri, R., Franzellitti, S., Carbone, C., Dawson, K. and Canesi, L. 2017. Impact of cationic polystyrene nanoparticles (PS-NH$_2$) on early embryo development of Mytilus galloprovincialis: effects on shell formation. Chemosphere, 186: 1-9.

Berenstein, G., Hughes, E.A., Zalts, A., Basack, S., Bonesi, S.M. and Montserrat, J.M. 2022. Environmental fate of dibutyl phthalate in agricultural plastics: Photodegradation, migration and ecotoxicological impact on soil. Chemosphere, 290: 133221.

Bergami, E., Krupinski Emerenciano, A., González-Aravena, M., Cárdenas, C.A., Hernández, P., Silva, J.R.M.C. and Corsi, I. 2019. Polystyrene nanoparticles affect the innate immune system of the Antarctic sea urchin *Sterechinusneumayeri*. Polar Biol., 42(4): 743–757.

Bhagat, J., Nishimura, N. and Shimada, Y. 2021. Toxicological interactions of microplastics/nanoplastics and environmental contaminants: Current knowledge and future perspectives. J. Hazard. Mater., 405: 123913.

Blöcker, L., Watson, C. and Wichern, F. 2020. Living in the plastic age - Different short-term microbial responses to microplastics addition to arable soils with contrasting soil organic matter content and farm management legacy. Environ. Pollut., 267: 114568.

Brandts, I., Barría, C., Martins, M. A., Franco-Martínez, L., Barreto, A., Tvarijonaviciute, A., Tort, L., Oliveira, M. and Teles, M. 2021. Waterborne exposure of gilthead seabream (Sparus aurata) to polymethylmethacrylate nanoplastics causes effects at cellular and molecular levels. J. Hazard. Mater., 403: 123590.

Brandts, I., Teles, M., Gonçalves, A.P., Barreto, A., Franco-Martinez, L., Tvarijonaviciute, A., Martins, M.A., Soares, A.M.V.M., Tort, L. and Oliveira, M. 2018. Effects of nanoplastics on *Mytilus galloprovincialis* after individual and combined exposure with carbamazepine. Sci. Total Environ., 643: 775-784.

Brandts, I., Teles, M., Tvarijonaviciute, A., Pereira, M.L., Martins, M.A., Tort, L. and Oliveira, M. 2018. Effects of polymethylmethacrylate nanoplastics on Dicentrarchuslabrax. Genomics, 110(6): 435–441.

Capolupo, M., Valbonesi, P. and Fabbri, E. 2021. A comparative assessment of the chronic effects of micro-and nano-plastics on the physiology of the Mediterranean mussel Mytilus galloprovincialis. Nanomaterials, 11(3): 649.

Cartraud, A.E., Corre, M.L., Turquetb, J. and Tourmetz, J. 2019. Plastic ingestion in seabirds of the western Indian Ocean. Mar. Pollut. Bull., 140: 308-314.

Cedervall, T., Hansson, L.A., Lard, M., Frohm, B. and Linse, S. 2012. Food chain transport of nanoparticles affects behavior and fat metabolism in fish. PLoS One, 7(2): e32254.

Chae, Y., Kim, D., Kim, S.W. and An, Y.J. 2018. Trophic transfer and individual impact of nano-sized polystyrene in a four-species freshwater food chain. Sci. Rep., 8(1): 1–11.

Chen, Q., Gundlach, M., Yang, S., Jiang, J., Velki, M., Yin, D. and Hollert, H. 2017. Quantitative investigation of the mechanisms of microplastics and nanoplastics toward zebrafish larvae locomotor activity. Sci. Total Environ., 584-585: 1022-1031.

Cole, M. and Galloway, T. S. 2015. Ingestion of nanoplastics and microplastics by Pacific oyster larvae. Environ. Sci. Technol., 49(24): 14625-14632.

Dutta, P. and Dutta, M. 2023. Microplastic hazards and possible mitigation. Eco. Environ. Cons., 29(1): 314-320.

Elsawy, M.A., Kim, K.H., Park, J.W. and Deep, A. 2017. Hydrolytic degradation of polylactic acid (PLA) and its composites. Renew. Sustain. Energy Rev., 79: 1346-1352.

Eyerer, P. 2010. Synthesis (Manufacture, Production) of Plastics: Polymers-Opportunities and Risks. Elsevier, Singapore, pp. 19-46.

Feldkamp, S.D., Costa, D. P. and Dekrey, G.K. 1989. Fish B. Noaa, 87(1): 85-94.

Fotopoulou, K.N. and Karapanagioti, H.K. (ed.) 2017. Degradation of Various Plastics in the Environment. Hazardous Chemicals Associated with Plastics in the Marine Environment. 78: pp. 71–92.

Geyer, R. (ed.) 2020. A Brief History of Plastics, Springer, NY, pp. 31-47.

Gomes, T., Almeida, A.C., and Georgantzopoulou, A. 2020. Characterization of cell responses in Rhodomonasbaltica exposed to PMMA nanoplastics. Sci. Total Environ., 726: 138547.

González-Fernández, C., Tallec, K., Le Goïc, N., Lambert, C., Soudant, P., Huvet, A., Suquet, M., Berchel, M. and Paul-Pont, I. 2018. Cellular responses of Pacific oyster (Crassostrea gigas) gametes exposed in vitro to polystyrene nanoparticles. Chemosphere, 208: 764-772.

Gu, H., Wang, S., Wang, X., Yu, X., Hu, M., Huang, W. and Wang, Y. 2020. Nanoplastics impair the intestinal health of the juvenile large yellow croaker Larimichthyscrocea. J. Hazard. Mater., 397: 122773.

Gupta, C., Kaushik, S., Jain, S., Dhanwani, I., Garg, S., Paul A., Pant, P. and Gupta, N. 2022. Bioaccumulation and toxicity of polystyrene nanoplastics on marine and terrestrial organisms with possible remediation strategies: A review. Environ. Advan., 8: 100227.

Hazeem, J.L., Yesilay, G., Bououdina, M., Perna, S., Cetin, D., Suludere, Z., Barras, A. and Boukherroub, R. 2020. Investigation of the toxic effects of different polystyrene micro-and nanoplastics on microalgae Chlorella vulgaris by analysis of cell viability, pigment content, oxidative stress, and ultrastructural changes. Mar. Pollut. Bull., 156: 111278.

Isaacson, K.P., Proctor, C.R., Wang, Q.E., Edwards, E.Y., Noh, Y., Shah, A.D. and Whelton, A.J. 2021. Drinking water contamination from the thermal degradation of plastics: implications for wildfire and structure fire response. Environ. Sci. Water Res. Technol., 7: 274-284.

Jain, A., Siddique, S., Gupta, T., Jain, S., Sharma, R.K. and Chaudhury, S. 2019. Fresh, strength, durability, and microstructural properties of shredded waste plastic concrete. Iran J. Sci. Technol, Trans. A Sci., 43: 455-465.

Jaiswal, J., Sharma, B. and Shukla, P. 2020. Integrated approaches in microbial degradation of plastics. Environ.Technol. Innov., 17: 100567.

Jambeck, J.R., Geyer, R., Wilcox, C., Siegler, T.R., Perryman, M. and Andrady, A. 2015. Plastic waste inputs from land into the ocean. Science, 347(6223): 768-771.

Jeong, C.B., Won, E.J., Kang, H.M., Lee, M.C., Hwang, D.S., Un, K.H., Zhou, B., Souissi, S., Jae L., Su, L. and Jae, S. 2016. Microplastic size-

dependent toxicity, oxidative stress induction, and p-JNK and p-P38 activation in the monogonont rotifer (Brachionus koreanus). Environ. Sci. Technol., 50: 8849-8857.

Kang, H.M., Byeon, E., Jeong, H., Kim, M.S., Chen, Q. and Lee, J.S. 2021. Different effects of nano-and microplastics on oxidative status and gut microbiota in the marine medaka Oryzias melastigma. J. Hazard. Mater., 405: 124207.

Khoshnamvand, M., Hanachi, P., Ashtiani, S. and Walker, T.R. 2021. Toxic effects of polystyrene nanoplastics on microalgae Chlorella vulgaris: changes in biomass, photosynthetic pigments and morphology. Chemosphere, 280: 130725.

Koelmans, A.A., Besseling, B. and Shim, W.J. 2015. Nanoplastics in the Aquatic Environment. Critical Review, Marine Anthropogenic Litter, 325-340.

Kumagai, S., Sato, M., Ma, C., Nakai, Y., Kameda, T., Saito, Y., Watanabe, A., Watanabe, C., Teramae, N. and Yoshioka, T. 2022. A comprehensive study into the thermo-oxidative degradation of sulfur-based engineering plastics. J. Anal. Appl Pyrolysis, 168: 105754.

Lai, W., Xu, D., Li, J., Wang, Z., Ding, Y., Wang, X., Li, X., Xu, N., Mai, K. and Ai, Q. 2021. Dietary polystyrene nanoplastics exposure alters liver lipid metabolism and muscle nutritional quality in carnivorous marine fish large yellow croaker (Larimichthyscrocea). J. Hazard. Mater., 419: 126454.

Liu, F.-F., Gao, Z.Y., Chu, W.C. and Wang, S.C. 2022. Polystyrene nanoplastics alleviate the toxicity of CuO nanoparticles to the marine algae Platymonashelgolandica var. tsingtaoensis, Front. Mar. Sci., 1-10.

Liu, J., Ma, Y., Zhu, D., Xia, T., Qi, Y., Yao, Y., Guo, X., Ji, R. and Chen, W. 2018. Polystyrene Nanoplastics-enhanced contaminant transport: Role of irreversible adsorption in glassy polymeric domain. Environ. Sci. Technol., 52(5): 2677-2685.

Liu, Y., Huang, J., Jin, J., Lou, S., Shen, C., Zang, H. and Wang, L. 2020. The classification of micro-plastics and biodegradation of plastics/micro-plastics. J. Eng. Technol Sci., 3(6): 181-190.

Manfra, L., Rotini, A., Bergami, E., Grassi, G., Faleri, C. and Corsi, I. 2017. Comparative ecotoxicity of polystyrene nanoparticles in natural seawater and reconstituted seawater using the rotifer Brachionusplicatilis. Ecotoxicol. Environ. Saf., 145: 557-563.

Mao, R., Lang, M., Yu, X., Wu, R., Yang, X. and Guo, X. 2020. Aging mechanism of microplastics with UV irradiation and its effects on the adsorption of heavy metals. J. Hazard. Mater.. 393: 122515.

Marques-Santos, L.F., Grassi, G., Bergami, E., Faleri, C., Balbi, T., Salis, A., Rist Damonte, G., Canesi, L. and Corsi, I. 2018. Cationic polystyrene nanoparticle and the sea urchin immune system: Biocorona formation, cell toxicity, and multixenobiotic resistance phenotype. Nanotoxicology, 17: 1-21.

Muneer, F., Nadeem, H., Arif, A. and Zaheer, W. 2021. Bioplastics from Biopolymers: An Eco-Friendly and Sustainable Solution of Plastic Pollution, Polym. Sci. Ser. C, 63: 47-63.

Murano, C., Bergami, E., Liberatori, G., Palumbo, A. and Corsi, I. 2021. Interplay between nanoplastics and the immune system of the Mediterranean Sea urchin Paracentrotuslividus. Front. Mar. Sci., 8: 234.

Natarajan, L., Jenifer, M.A., Chandrasekaran, N., Suraishkumar, G.K. and Mukherjee, A. (2022). Polystyrene nanoplastics diminish the toxic effects of Nano-TiO$_2$ in marine algae Chlorella sp. Environ. Res., 204: 112400.

Oliviero, M., Tato, T., Schiavo, S., Fernández, V., Manzo, S. and Beiras, R. 2019. Leachates of micronized plastic toys provoke embryotoxic effects upon sea urchin Paracentrotuslividus. Environ. Pollut., 247: 706-715.

Ravishankar, K., Ramesh, P.S., Sadhasivam, B. and Raghavachari, D. 2018. Wear-induced mechanical degradation of plastics by low-energy wet-grinding. Polym. Degrad. Stab., 158: 212-219.

Rice, N., Hirama, S. and Whiterington, B. 2021. High frequency of micro- and meso-plastics ingestion in a sample of neonate sea turtles from a major rookery. Mar. Pollut. Bull., 167: 112363.

Rist, S., Baun, A. and Hartmann, N.B. 2017. Ingestion of micro- and nanoplastics in *Daphnia magna* – Quantification of body burdens and assessment of feeding rates and reproduction, Environ. Pollut., 228: 398-407.

Rist, S., Baun, A., Almeda, R. and Hartmann, N.B. 2019. Ingestion and effects of micro- and nanoplastics in blue mussel (*Mytilus edulis*) larvae, Mar. Pollut. Bull., 140: 423-430.

Sendra, M., Staffieri, E., Yeste, M.P., Moreno-Garrido, I., Gatica, J.M., Corsi, I. and Blasco, J. 2019. Are the primary characteristics of polystyrene nanoplastics responsible for toxicity and ad/absorption in the marine diatom *Phaeodactylum tricornutum*? Environ. Pollut., 249: 610-619.

Shafqat, A., Al-Zaqri, N., Tahir, A. and Alsalme, A. 2021. Synthesis and characterization of starch based bioplastics using varying plant-based ingredients, plasticizers, and natural fillers. Saudi J. Biol. Sci., 28: 1739-1749.

Shiu, R.F., Vazquez, C.I., Chiang, C.Y., Chiu, M.H., Chen, C.S., Ni, C.W., Gong, G.C., Quigg, A., Santschi, P.H. and Chin, W.C. 2020. Nano- and microplastics trigger the secretion of protein-rich extracellular polymeric substances from phytoplankton. Sci. Total Environ., 748: 141469.

Silva, M.S.S., Oliveira, M., Valente, P., Figueira, E., Martins, M. and Pires, A. 2020. Behavior and biochemical responses of the polychaeta *Hediste diversicolor* to polystyrene nanoplastics. Sci. Total Environ., 707: 134434.

Sjollema, S.B., Redondo-Hasselerharm, P., Leslie, H.A., Kraak, M.H.S., and Vethaak, A.D. 2016. Do plastic particles affect microalgal photosynthesis and growth? Aquat. Toxicol., 170: 259-261.

Stolbov, D.N., Smirnova, A.I., Savilov, S.V., Shilov, M.A., Burkov, A.A., Parfenov, A.S. and Usol'tseva, N.V. 2021. Influence of different types of carbon nanoflakes on tribological and rheological properties of plastic lubricants. Fullerenes, Nanotubes, and Carbon Nanostructures. Proceedings of the 15th International Conference "Advanced Carbon Nanostructures". 177-184.

Sun, J., Zheng, H., Xiang, H., Fan, J. and Jiang, H. 2022. The surface degradation and release of microplastics from plastic films are studied by UV radiation and mechanical abrasion. Sci. Total Environ., 838: 156369.

Tallec, K., Huvet, A., Poi, C.D., González-Fernández, C., Lambert, C., Petton, B., Goïc, N. L., Berchel, M., Soudant, P. and Paul-Pont, I. 2018. Nanoplastics impaired oyster free-living stages, gametes, and embryos. Environ. Pollut., 242: 1226-1235.

Torres-Ruiz, M., Vieja, A.D.L., Gonzalez, M.D.A., Lopez, M.E., Calvo, A.C. and Portilla, A.I. C. 2021. Toxicity of nanoplastics for zebrafish embryos, what we know and where to go next. Sci. Total Environ., 797: 149125.

Trevisan, R., Voy, C., Chen, S. and Giulio, R.T.D. 2019. Nanoplastics decrease the toxicity of a complex PAH mixture but impair mitochondrial energy production in developing zebrafish. Environ. Sci. Technol., 53(14): 8405-8415.

Trifuoggi, M., Pagano, G., Oral, R., Pavičić-Hamer, D., Burić, P., Kovačić, I., Siciliano, A., Toscanesi, M., Thomas, P.J., Paduano, L., Guida, M. & Lyons, D.M. 2019. Microplastic induced damage in early embryonal development of sea urchin *Sphaerechinus granularis*. Environ. Res., 179: 108815.

United Nations Environment Programme and Secretariat of the Convention on Biological Diversity 2012. Impacts of Marine Debris on Biodiversity: Current Status and Potential Solutions. CBD Technical Series No. 67. Available at: https://wedocs.unep.org/20.500.11822/32622

Venâncio, C., Ferreira, I., Martins, M.A., Soares , A.M.V. M., Lopes, I. and Oliveira, M. 2019. The effects of nanoplastics on marine plankton: A case study with polymethylmethacrylate. Ecotoxicol. Environ. Saf., 184: 109632.

Wang, S., Hu, M., Zheng, J., Huang, W., Shang, Y., Fang, J.K.H., Shi, H. and Wang, Y. 2021. Ingestion of nano/microplastic particles by the mussel *Mytilus coruscus* is size-dependent. Chemosphere, 263: 127957.

Wang, S., Liu, M., Wang, J., Huang, J. and Wang, J. 2020. Polystyrene nanoplastics cause growth inhibition, morphological damage, and physiological disturbance in the marine microalga *Platymonas helgolandica*. Mar. Pollut. Bull., 158: 111403.

Wegner, A., Besseling, E., Foekema, E.M., Kamermans, P. and Koelmans, A.A. 2012. Effects of nanopolystyrene on the feeding behavior of the blue mussel (*Mytilus edulis* L.). Environ. Toxicol. Chem., 31: 2490-2497.

Yesilay, G., Hazeem, L., Bououdina, M., Cetin, D., Suludere, Z., Barras, A. and Boukherroub, R. 2022. Influence of graphene oxide on the toxicity of polystyrene nanoplastics to the marine microalgae *Picochlorum* sp. Environ. Sci. Pollut. Res., 29: 75870-75882.

Zaki, M.R.M. and Aris, A.Z. 2022. An overview of the effects of nanoplastics on marine organisms. Sci. Total Environ., 831: 154757.

Zhang, W., Wang, Q. and Chen, H. 2022. Challenges in Characterization of Nanoplastics in the Environment. Front. Environ. Sci. Eng., 16(1): 11.

Zhao, T., Tan, L., Zhu, X., Huang, W. and Wang, J. 2020. Size-dependent oxidative stress effect of nano/micro-scaled polystyrene on Kareniamikimotoi. Mar. Pollut. Bull., 154: 111074.

# Assessment and Characterization of Leather Solid Waste from Sheba Leather Industry PLC, Wukro, Ethiopia

**Desnet Gebrekidan Tegadye, Chhotu Ram† and Kibrom Alebel**

Department of Chemical Engineering, College of Engineering and Technology, Adigrat University, Adigrat 7040, Ethiopia

†Corresponding author: Chhotu Ram; chhoturao2007@gmail.com

## ABSTRACT

Leather manufacturing processes raw hides and skins into various finished leather products, generating huge amounts of untanned and untanned leather solid wastes (LSWs). The present study investigates the LSWs generation, characterization, and management practices of the Sheba leather industry in Ethiopia. Results revealed that LSWs are categorized as non-chrome solid waste, including de-dusted salt, raw trimming, hairs, fleshing waste, pickle trimming, and splitting wastes. Chrome-based wastes include chrome shaving waste, crust leather trimming waste, buffing dust waste, finished leather trimming waste, etc. Further, solid wastes were characterized for the physico-chemical parameters viz. moisture (31.5%), ash content (7.3%), pH (5.7), carbon content (14.7%), nitrogen content (0.3%), chromium content (2%), calorific value (20,107 $kJ.kg^{-1}$), VOCs (75.1%) and carbon to nitrogen ratio (52:1). Results obtained suggested various sustainable technological options for the effective LSWs management to preserve environment.

## INTRODUCTION

The leather industry plays a significant role in the present scenario's social development and global economy (Li et al. 2019). Leather solid waste (LSW) generated from the leather processing industry creates significant environmental problems due to the generation of huge amounts of solid waste and wastewater (Saira & Shanthakumar 2023). Thus, the leather processing industry is classified as a highly polluting manufacturing industry, adversely affecting the surrounding environment, i.e., soil, water, and air (Kanagaraj et al. 2006). Leather production utilizes about 85 percent chrome salts in processing raw hides or skins globally due to its low cost, easy availability, and easy use. Chromium-containing solid waste generates approximately 6,00,000 metric tons per year globally (Ocak 2012). On the other hand, one ton of hide processing in the leather industry consumes around 60 $m^3$ of water and generates a large quantity of wastewater (Fela et al. 2011). LSWs generated from industrial manufacturing processes contain chemicals, solvents, acids, and degraded products of the skins and hide, which are toxic. One previous work shows that processing one ton of wet salted hides or skins can generate approximately 200 kg of finished leather solid waste and 200 kg of solid waste lost in the effluents (Masilamani et al. 2016). The leather processing industry converts raw hides

or skins into physically and chemically stable end products using four major stages, i.e., beamhouse operations, tanning processes, re-tanning processes, and finishing processes (Muralidharan et al. 2022). These process further includes various chemical and mechanical processes (Ozgunay et al. 2007). During the entire leather manufacturing process, huge quantities of LSWs, i.e., tanned and untanned wastes, are generated. The chrome tanning process involves the chromium sulfate chemical, the most widely used tanning agent in leather manufacturing (Famielec 2020). As a result, the chrome-containing LSWs, like chrome shaving waste generated from leather production, are categorized as toxic and hazardous due to the presence of chromium and other chemicals (Fela et al. 2011). One estimation has shown that more than 60 percent of the produced leathers are utilized for footwear manufacturing (Koppiahraj et al. 2019). Another work depicts the production of 10 kg of final leather from processing 1000 kg of raw hides, generating about 850 kg of SWs. The tannery waste proportions from various processes are fleshing (50-60%), chrome shaving, splits, and buffing dust (35-40%), skin trimming (5-7%), and hairs (2-5%), etc. (Mushahary & Mirunalini 2017).

Various researchers carry out the characterization of solid wastes (SWs) from leather processing. LSWs were characterized for the various constituents, i.e., volatile matter,

pH, fats, soluble in dichloromethane, nitrogen, sodium chloride, sulfide content, and the Cr, Fe, Na, and Ca, etc. Results revealed that fleshing, shaving, and trimming waste have maximum proportions of protein and fat (Ozgunny et al. 2007). Another work highlighted the investigations on the physicochemical properties, i.e., pH, temperature (°C), alkalinity (mg.L$^{-1}$), moisture content (%), organic carbon (%), crude fiber (%) except chromium content from the chrome buffing dust of tannery (Emmanueul et al. 2014). Thus, it is further suggested to use fat liquoring oils and biodiesel from pre-fleshing wastes, ethane, and compost from the lime fleshings, re-tanning agents, and leather board from shaving wastes, etc. Literature suggests the various treatment methods/options for effectively managing tannery solid waste. In this connection, one report (Fela et al. 2011) suggested the thermal treatment for the huge amount of LSWs (tannery solid waste and sludge) generated from the tannery. The energy content estimated of solid wastes is equivalent to 20 MJ.kg$^{-1}$ as dry materials, which is higher in comparison to hard coal. Ram et al. (2021) proposed sustainable solutions and technologies through biochemical and thermal energy conversion. Further, the insights are useful in preserving natural resources, public health, and the environment.

Researchers developed a technique to remove chromium from wet blue waste with the recovery of high nitrogen solid collagen waste. Nitrogen content accumulations in plants and quantifications of nitrogen in soil were tested (Lima et al. 2010). One article (Famielec 2020) reviews the treatment technologies for the LSWs containing chromium with special emphasis on incineration in an experimentally designed tunnel incinerator. Chromium was present in a higher amount, i.e., 53 % (w/w), in the form of Cr (III) oxides in residual ash and can be recycled as a Crore substitute in the metallurgical or chemical industries. Chrome-containing solid waste generated from the leather-finished trimmings (LFT) and chrome shavings (CS) from tanneries observed higher calorific values of 15.77 MJ.kg$^{-1}$ and 19.97 MJ.kg$^{-1}$, respectively. Thus, these wastes could be suitably used for thermal treatment, mainly incineration and pyrolysis (Velusamy et al. 2020). Saira & Shanthakumar (2023) evaluated the existing techniques for the de-toxification of tannery wastes.

Further, they examined the possibility of solid waste management options to attain zero waste within the tannery industry. A recent review (Appala et al. 2022) highlighted the different routes of tannery solid waste conversion into biomass, a gamut of products, and energy. The primary organic resource is collagen, a natural protein in the skin hides. These are converted into useful composites such as adsorbents, adhesives, and renewable fuels such as biogas.

One recent estimation based on a global study shows that China is the leading leather exporter, followed by Italy (14.8%), Vietnam (11.6%), and Germany (5.3%) (Koppiahraj et al. 2019). The economic scenario of developing countries has also seen the contribution of leather manufacturing industries and their adverse impacts on the environment (Ministry of Agriculture and Rural Development 2009). Thus, the largest livestock population in Ethiopia has a strong input for leather manufacturing and is estimated to have about 26.5 million sheep, 55.6 million cattle, and 25 million goats. Ethiopia has 28 leather manufacturing industries, 16 large and medium-scale footwear processing, 15 garments and goods manufacturers, 3 gloves manufacturing, and 368 small and micro-scale leather products (Teklay 2018). As a result, huge amounts of tanned and untanned LSWs are generated in Ethiopian tannery industries, consequently a threat to the surrounding environment. A previous report (Framis 2018) carried out on the assessment of waste generation from the Sheba leather industry (Wukro, Ethiopia) under cooperation projects suggests utilizing the composting method for chrome-free wastes and recommended further research on solid waste generation and its effective management to protect the local environment. Therefore, we have planned a detailed study for the LSWs generation, characterization, and recommendations of technologies to reduce the challenges in waste management in an environmentally sustainable manner from the Sheba leather industry (Wukro), Ethiopia.

## MATERIALS AND METHODS

### Chemicals and Equipment

The present research is focused on the sample collection, sample preparation, and characterization of leather solid wastes from industrial collection to testing in the laboratory. All chemicals used are analytical grade throughout the experiments. Chemicals such as benzoic acid (for bomb calorimeter), nitric acid, sulphuric acid, perchloric acid, orthophosphoric aid (used for chromium content) and salicylic acid, sulphuric acid, and hydrogen peroxide used for the characterization of nitrogen content. The major equipment, such as the bomb calorimeter (Model IKA calorimeter C-4000) and UV-visible spectrophotometer (UV-1700, Shimadzu, Japan), are used for the calorific value and nitrogen content estimation, respectively. The oven and furnace are used for the estimation of the moisture content and volatile organic compounds, respectively.

### Assessment and Generation Rate of LSWs

Assessment of the practices of leather solid waste management (LSWM) was conducted by frequent visits

on-site and observations of the manufacturing processes. Auditing of the LSWM documentation, environmental policies, procedures, and waste disposal site nearby industry. The four major processes identified are i.e. beamhouse operations, tanning processes, re-tanning, and finishing processes as shown in Fig. 1. The tannery solid waste study was carried out between November 2020 to April 2021 a case study of the Sheba Leather Industry.

To determine the generation rate, a sample of ten pieces was taken, weighed before and after the unit operation of the process, and finally, calculated using the mass balance approach. The average value of waste generation in each stage is presented for ten samples. For example, in the case of de-dusted salt process generation rate (waste per tonne of raw wet salted sheep skin) was determined as follows (Framis 2018):

Mass of de-dusted salt waste (kg/ton of raw wet salted sheep skin) $= \dfrac{m1 - m2}{m1} \times 1000$ ...(1)

where $m_1$ is the initial mass of raw wet salted sheep skin before salt removal and $m_2$ is the final mass of raw wet salted sheep skin after salt removal.

The generation rate of untanned LSWs (de-dusted salt waste, raw sheep skin trimming waste, hair waste, fleshing waste, and pickle trimming waste) and tanned LSWs (chrome shaving waste, crust leather trimming waste, and finished leather trimming waste) were determined in the processing of raw wet salted sheep skin. Chrome-free SWs (raw hide
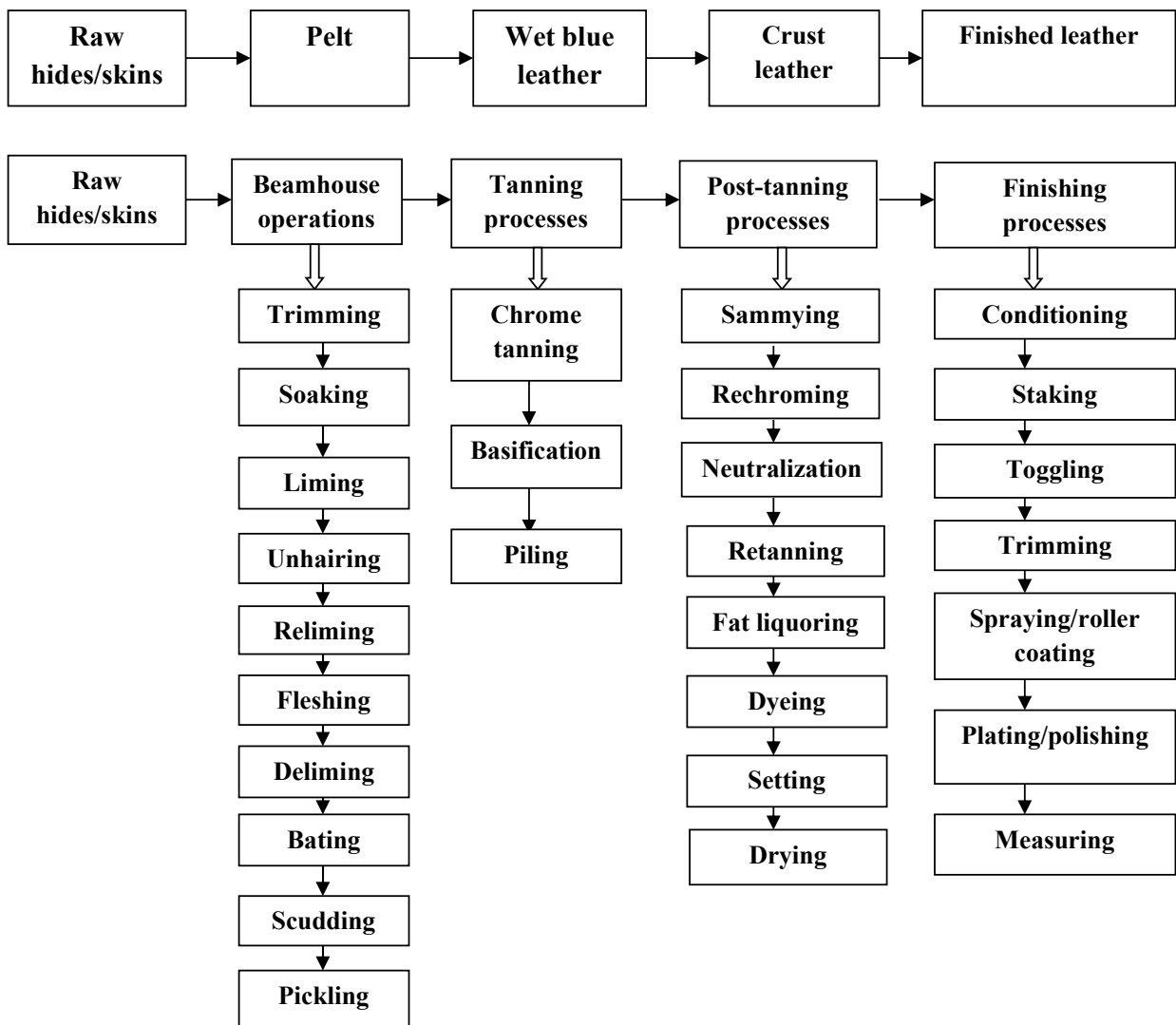


Fig. 1: Flow diagram of the leather production process in the Sheba leather industry.

trimming waste, fleshing waste, and splitting waste) and chrome-containing LSWs (chrome shaving waste, crust leather trimming waste, and finished leather trimming waste) were generated and estimated accordingly. Raw hide processing generates solid waste i.e. trimming waste, fleshing waste, splitting waste, chrome shaving waste, crust leather trimming waste, and finished leather trimming waste (Fig. 1).

Chrome shaving waste is generated by shaving the tanned sheep skins when the tanning process is over and the waste depends upon the required shaving thickness of the wet blue leather. The Beamhouse process is a major source of solid waste generation in the leather industry (Paul et al. 2015) and includes several sub-processes i.e. de-dusted salt, skin trimming, skin unhair, fleshing and pickle trimming, etc. (Hashem et al. 2014).

## Sources of Leather Solid Wastes

Leather processing involves four main stages viz. beamhouse operations (trimming, unhairing, fleshing, pickling, and splitting processes), tanning processes (shaving process), re-tanning processes (trimming and buffing processes), and finishing processes (trimming process). Various sources have been identified from the entire processing of the Sheba leather industry, which are the non-chrome containing LSWs viz. de-dusted salt waste, raw trimming waste, hair waste, fleshing waste, pickle trimming waste and splitting waste, and chrome containing wastes viz. chrome shaving waste, crust leather trimming waste, buffing dust waste and finished leather trimming waste. Thus, types and sources of LSWs were evaluated for the physical composition and nature of the wastes depending upon the unit operations. This will further help in the management of LSWs generated from the entire process. Table 1 shows the types of waste and their sources of samples collected from various processes in the industry.

## Characterization of LSWs

Physico-chemical parameters i.e. calorific value, ash content, volatile organic compounds content, moisture content, pH value, chromium content, carbon content, and nitrogen content were determined after collection from wastes. pH value was measured by a digital pH meter. To check the calorific value, 0.5 grams of waste sample was transferred into the sample holder which was placed in the bomb and the sample was burned using oxygen gas as activation energy. The following equations (2 and 3) were used to measure the (Onukak et al. 2017; Singh et al. 2022) calorific value on the dry basis.

$$\text{Calorific value (Kcal/kg)} = \frac{\Delta T * C - Qf}{m} \times F \quad \text{or} \quad \ldots(2)$$

$$\text{Calorific value (kJ/kg)} = \frac{\Delta T * C - Qf}{m} \times F \times 4.184 \quad \ldots(3)$$

Where $\Delta T$ represents the difference between the initial and final temperature measured (K), 'C' is the heat value of the water equivalent, 2183 calorie/Kelvin, '$Q_f^{'}$' is the heat value of nickel-chrome thread and the cotton thread, 19.1 calorie per Kelvin, 'm' is the mass of LSWs sample in gram and 'F' is the correction factor which is 1.033.

Ash content was determined by igniting 1 gram of sample in a furnace at $950^{o}$ C for 3 hours and ash was cooled in a desiccator for 1 hour and weighed and was determined (D2617 ASTM, 2001). Moisture content was estimated by the hot air oven method (D3790 ASTM, 2001) while pH by using a digital pH meter. Further, volatile organic compounds (D2617 ASTM, 2001) and chromium content were measured using a furnace (at temperature 950° C) and wet oxidation method (ASTM D2807) using titration, respectively. Fixed carbon content was estimated from its ash content, volatile organic compounds content, and moisture content (Onukak et al. 2017). Nitrogen presence was measured by using the three steps viz. digestion, filtration, and determination.

Table 1: The sources and types of leather solid waste generated by the Sheba leather industry.

| S. No. | Types of leather solid waste | Sources | Leather processing stage |
|---|---|---|---|
| 1. | De-dusted salt waste | Hand-shaking salt removal process from raw hides/skins | Preparation stage |
| 2. | Raw trimming waste | Raw skin/hide trimming process | |
| 3. | Hair waste | Sheep skin unhairing process | Beam house operation |
| 4. | Fleshing waste | Fleshing process | |
| 5. | Pickle trimming waste | Pickle trimming process | |
| 6. | Splitting waste | Hide splitting process | |
| 7. | Chrome shaving waste | Shaving process | Tanning process |
| 8. | Crust leather trimming waste | Crust leather trimming process | Re-tanning process |
| 9. | Buffing dust waste | Crust leather buffing process | |
| 10. | Finished leather trimming waste | Finished leather trimming process | Finishing process |

Finally, the sample was determined by using a UV-visible spectrophotometer at 570 nm wavelength as described elsewhere (Kruis 2014). Sample preparation was carried out using different operations viz. drying (oven drying), shredding (size reduction), crushing (using crusher) and milling (grinding mill), and the resulting powder samples were used for the laboratory analysis before chemical parameters (calorific value, ash content, volatile organic compounds, chromium content, and nitrogen content).

## RESULTS AND DISCUSSION

### Generation Rate of Leather Solid Wastes

Samples were collected to quantify the LSWs generated from different processes employed in the industry (Fig. 2). They used mass balance analysis techniques to estimate the processing of raw hides and sheep skins.

### Generation Rate from the Processing of Raw Sheep Skin

**Beamhouse operations:** Among all processes pickle trimming process generates minimum waste (13.6 kg.ton$^{-1}$), whereas the sheep skin hair process generates maximum waste (117.7 kg.ton$^{-1}$). This is mainly attributed to removing unwanted parts of raw sheep skin. After soaking operations, unhairing or liming by using chemicals such as lime $Ca(OH)_2$, sodium hydrosulfide (NaHS), and sodium sulfide ($Na_2S$) on sheep skins generates a large amount of waste (Ranjithkumar et al. 2017). Further, the fleshing process removes excess flesh and fats through a mechanical process. In the pickling process, skin is treated in a solution composed of salts and acids to lower the pH of 2.8-3.0.

**Chrome shaving, crust, and finished leather trimming waste:** The results obtained after estimation show an average of 39.7 kg of chrome shaving waste was generated per tonne of raw sheep skin processed. Crust leather is trimmed to obtain a uniform structure and remove the unnecessary parts of the leather by trimming. In addition, this type of solid waste is produced after the post-tanning process. Finished leather is trimmed to achieve uniform surface effects and improve the general appearance per the desired purpose of leather. Generation rates are calculated accordingly after the trimming process.

Therefore, LSWs from the Sheba leather industry during the entire processing of raw sheep skin. One tonne processing of raw sheep skin waste generation from four main processes, mainly i.e. beamhouse operations (de-dusted salt waste, raw sheep skin trimming waste, hair waste, fleshing waste and pickle trimming waste) is 188 kg.ton$^{-1}$ (73.52%), tanning process (chrome shaving waste) is 39.6 kg.ton$^{-1}$ (15.50%), re-tanning process (crust leather trimming waste) is 15.5 kg.ton$^{-1}$ (6.1%) and finishing process (finishing leather trimming waste) is 12. kg.ton$^{-1}$ (4.9%).

A study from Ethiopia's leather industry indicated that the total LSWs generated were 664.5 kg.ton$^{-1}$ of wet salted sheep skin (Teklay 2018). The present study shows the maximum percentage (73.5%) of LSWs are generated from the beamhouse operations (e. g. non-chrome based), whereas the minimum percentage (4.9%) of LSWs are generated from the finishing process (e.g., chrome-containing waste) (Fig. 3). The chrome based solid waste and its disposal are the biggest problems due to chromium a heavy metal in higher concentrations (Pati et al. 2014). On the other hand, a comparison between the individual processes indicates
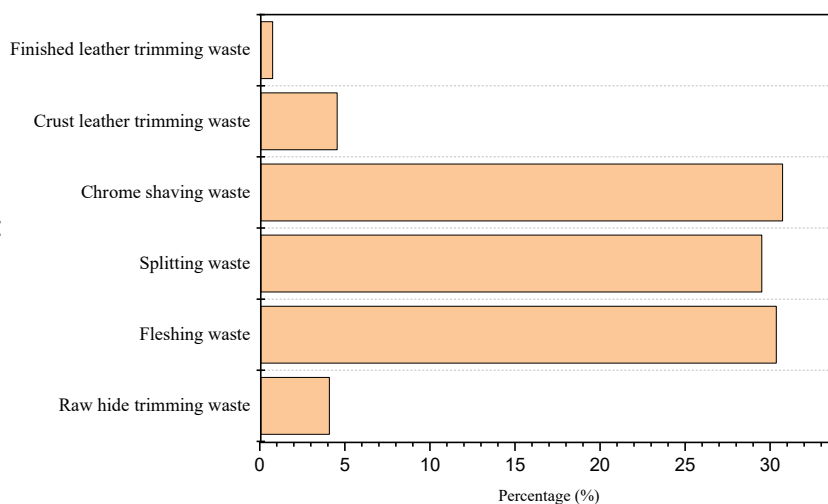


Fig. 2: Generation rate of leather solid wastes during the processing of raw hides involving various processes from finished leather trimming waste to raw hide trimming wastes.
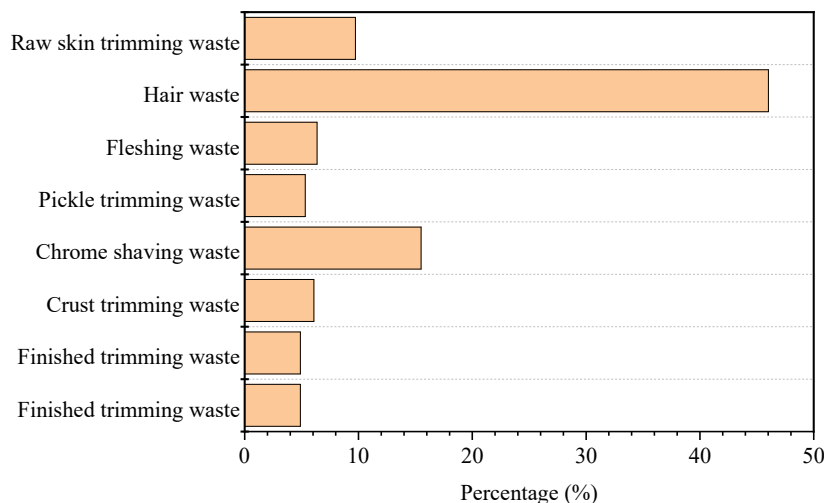
Fig. 3: Solid waste generation during the processing of raw sheep skin from skin trimming, hair, fleshing, pickle trimming, chrome saving, crust trimming, and finished wastes.
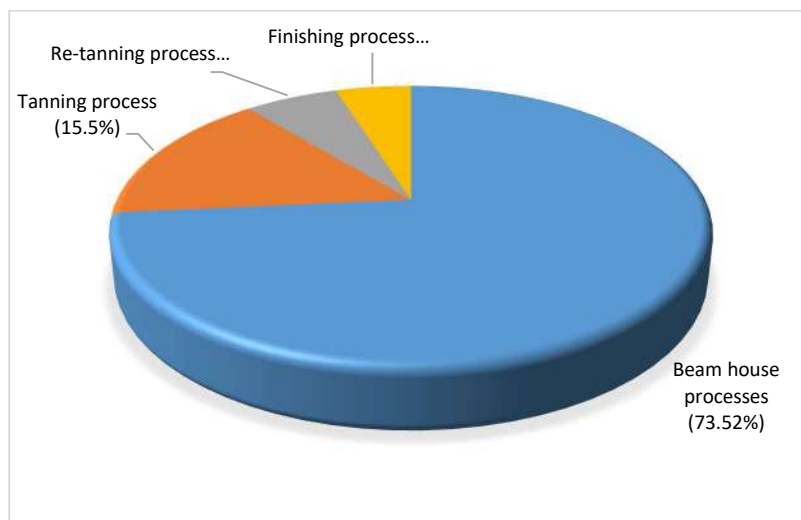


Fig. 4: Leather solid waste (%) generation rate from the four major production stages, such as beam house operations, tanning, re-tanning, and finishing processes.

the largest quantity (46%) of waste as hair waste and the lowest amount (4.9%) as finished leather trimming waste (Fig. 4). One report shows that one ton of wet salted sheep skin generates 262 kg of wastes which is around 26.2% of the total weight of sheep skin processed (Kanagaraj et al. 2006). Another observation for the Sheba leather industry, the daily maximum soaking capacity of raw sheep skins is 9000 kg, and the maximum raw sheep skin soaking capacity is 2700 tons per year.

**Generation of Solid Waste from Raw Hides Processing**

Trimming waste is generated by cutting the unnecessary

parts of the hide by the trimming process, and 28.4 kg.ton$^{-1}$ of average waste is generated. Trimmed hides are subjected to cleaning (fleshing process), generating the fleshing waste of around 211 kg.ton$^{-1}$ of hides processed. Further, hides are split into two or three layers by splitting process, and waste (205 kg.ton$^{-1}$) is generated by removing the hides' unnecessary layers as per the hide's intended use. Chrome shaving waste is generated by shaving the tanned hides; waste generation depends on the shaving thickness of the wet blue leather, which further depends on the end use of the finished leather (213.5 kg.ton$^{-1}$). Crust leather is trimmed to obtain a uniform structure and remove the leather's unnecessary parts by trimming.

Moreover, this type of solid waste is generated after the re-tanning process. Hence, an average of 31.6 kg.ton$^{-1}$ of crust-trimming waste of raw hides is processed. Finished leather is the final step in leather manufacturing and is trimmed to achieve a uniform finished surface as per the required quality of the final product. This process generates about 5.2 kg.ton$^{-1}$ of waste.

Table 2 systematically presents the waste generation from various processes involved in leather manufacturing. However, the generation rate of LSWs depends on the type and quality of raw material and operational technologies used during the manufacturing process of leather (Coară et al. 2016). Among all processes, the minimum quantity (5.2 kg.ton$^{-1}$) of waste is generated from finished leather trimming, whereas the maximum waste generated is 213.4 kg.ton$^{-1}$ from chrome shaving waste. In addition, beam house operations (rawhide trimming waste, fleshing waste, and splitting waste) generate waste of around 444 kg.ton$^{-1}$ (63.9%), tanning process (chrome shaving waste) is 213.4 kg.ton$^{-1}$ (30.7%), re-tanning process (crust leather trimming waste) is 31.6 kg.ton$^{-1}$ (4.5%). The finishing process (finishing leather trimming waste) is 5.2 kg.ton$^{-1}$ (0.7%). An earlier study shows that 75-80% of input raw wet salted hides or skins are generated as LSWs in the leather manufacturing industry (Oruko et al. 2014).

Another work cites the total solid waste generation of around 730 kg from the processing of one tonne of raw wet salted hides, which is further correlated to the major processes such as raw trimming, fleshing, chrome shaving, and buffing dust (Fela et al. 2011). The data depicted that the highest percentage (63.96%) of LSWs generation from the beamhouse operations and the lowest percentage (0.76%) from the finishing process (Fig. 5). Further, this shows that the largest quantity (30.7%) of LSWs generated as chrome shaving waste and the lowest quantity (0.76%) as finished leather trimming waste. Furthermore, the Sheba leather industry in the current scenario generates about 694 kg of waste from the processing of 1 tonne of raw hides, and it accounts for 69.4% of the LSWs from the raw wet salted hides. Besides these, the Sheba leather industry has the maximum daily soaking capacity of raw hides is 8,600 kg, and total waste generation is about 2,580 tonnes per year, taking 300 working days annually. Thus, the total waste generated from the processing of raw hides is 1,792 tons per year of LSW.

## Assessment of Current Practices of Leather Solid Waste Management

The assessment conducted on the leather solid waste management practices of the Sheba leather industry indicated that all the leather solid wastes generated during the entire leather manufacturing process are disposed of in the open dumping area nearby to the manufacturing compound. It was observed that the untanned leather solid wastes (de-dusted salt waste, raw trimming waste, hair waste, fleshing waste, pickle trimming waste, and splitting waste) and tanned leather solid wastes (chrome shaving waste, crust leather trimming waste, buffing dust waste and finished leather trimming waste) are disposed into the same dumping area without any proper segregation and treatment. Moreover, the Sheba leather industry has no leather solid waste management mechanism. However, the tanned leather solid wastes are chrome-based solid wastes categorized as toxic and hazardous that affect public health and create environmental pollution, viz. agricultural soil pollution, surface water pollution, groundwater pollution, and air pollution. Therefore, the chrome-free leather solid wastes and chromed-based leather solid wastes should be segregated, collected, treated, and dumped separately. In addition, the Sheba leather industry should construct its suitable landfill site per the type, quantity, characteristics, and environmental impact of the LSWs generated.

## Characterization of Leather Solid Waste

To check the characterization of LSW, various tests such as calorific value, ash content, volatile organic compounds, moisture content, pH, chromium content, fixed carbon content, nitrogen content, and carbon-to-nitrogen ratio were performed.

Table 2: Leather solid wastes generation rate during the processing of raw hides.

| S. No. | Types of leather solid wastes | Waste generation kg per kg of hide processed | Waste generation kg.ton$^{-1}$ of hides processed | Total solid waste generated (kg. ton$^{-1}$ of raw hides processed) |
|---|---|---|---|---|
| 1. | Raw hide trimming waste | 0.03 | 28.4 | 694.7 |
| 2. | Fleshing waste | 0.20 | 210 | |
| 3. | Splitting waste | 0.20 | 205 | |
| 4. | Chrome shaving waste | 0.21 | 213.5 | |
| 5. | Crust leather trimming waste | 0.03 | 31.6 | |
| 6. | Finished leather trimming waste | 0.005 | 5.2 | |
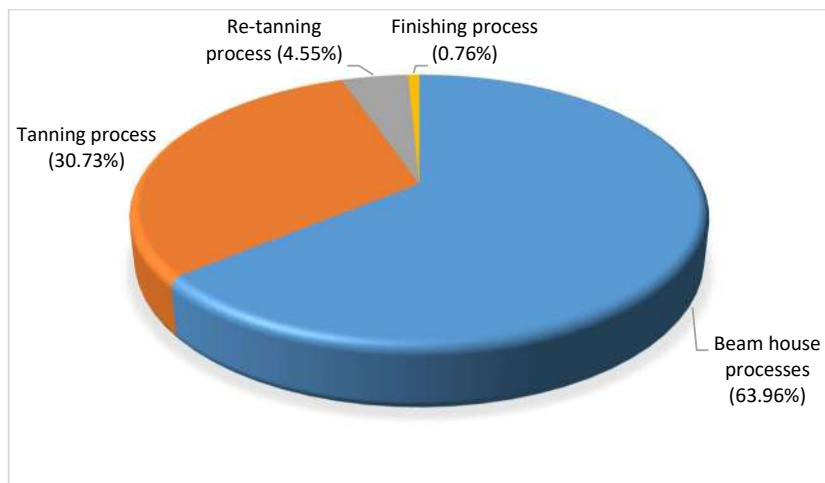
Fig. 5: Solid waste generation (%) from the four main of manufacturing leather from raw hides (Beamhouse operations, tanning, re-tanning, and finishing processes).

Table 3: Physico-chemical characterization of leather solid wastes from the Sheba leather industry.

| S. No. | Types of leather solid waste | Physico-chemical parameters | | | | | | | | |
|--------|------------------------------|-----------------------------|---|---|---|---|---|---|---|---|
| | | Calorific value [kJ.kg$^{-1}$] | Ash content % | VOC [%] | Moisture content [%] | pH | Cr [%] | C [%] | N [%] | C: N |
| 1. | Fleshing waste | 20,314 | 5.30 | 82 | 76.5 | 12.5 | NA | 12.4 | 0.26 | 47.7:1 |
| 2. | Chrome shaving waste | 16,899 | 13.3 | 7 | 42.0 | 3.9 | 1.6 | 14 | 0.26 | 54:1 |
| 3. | Crust leather trimming waste | 21,380 | 5.5 | 74.8 | 13.7 | 4.0 | 1.6 | 17.5 | 0.30 | 58.4:1 |
| 4. | Buffing dust waste | 21,575 | 6.5 | 77.7 | 7.8 | 4.0 | 1.6 | 12.8 | 0.27 | 47.5:1 |
| 5. | Finished leather trimming waste | 20,368 | 5.8 | 70 | 17.7 | 4.1 | 1.5 | 16.8 | 0.32 | 52.5:1 |

**Calorific value:** The calorific value represents the maximum amount of energy present in the LSWs and is affected by solid waste's ash and moisture content. Higher ash and moisture content of LSWs decreases the calorific value. Thus, the calorific value is the most important parameter to determine the suitability for energy recovery utilization (Onukak et al. 2017). Table 3 indicates the average calorific value of 20,107 kJ.kg$^{-1}$ ranges from a minimum value of 16,898 kJ.kg$^{-1}$ for chrome shaving waste up to a maximum value of 21,574 kJ.kg$^{-1}$ for buffing dust waste. The results obtained have a higher calorific value than the minimum required value of 5020 kJ.kg$^{-1}$ with MC greater than 45%. They agree with using solid waste for thermal applications (Alrikabi & Khaleefah 2005).

Overall LSWs generated having calorific values from chrome shaving waste (16,898 kJ.kg$^{-1}$), crust leather trimming waste (CT) (21,380 kJ.kg$^{-1}$), buffing dust waste (21,574 kJ.kg$^{-1}$), finished leather trimming waste (F) (20,367 kJ.kg$^{-1}$). Moreover, chrome shaving, crust leather trimming,

buffing dust, and finished leather trimming waste should be segregated and collected in separate areas to prevent mixing with other leather solid wastes with higher moisture content. Previous work (Onukak et al. 2017) investigated the tannery solid wastes (TSWs) in six briquettes, i.e., comprising varying ratios of chrome shavings (CS), flesh (FS), hair (HR), and buffing dust (BD) were characterized from Nigerian industry. The briquettes having calorific values from 18.6 to 24 MJ per kg were comparable to other fuel sources such as sub-bituminous coal (20-24.7 MJ.kg$^{-1}$). Author (Oyelaran et al. 2017b) assessed the energy and combustion efficiency of briquettes prepared from the TSWs for heating purposes. Among different types of TSWs, i.e., BD, CS, FS, and HR samples, their calorific values observed were between 18 and 21.8 MJ.kg$^{-1}$, where fleshing has better quality than the other three tannery wastes.

**Ash content:** Ash is an inorganic residue obtained after exposing LSWs to a particular temperature, and observance of higher ash content reduces the combustion efficiency

and heating value (Onukak et al. 2017). Results (Table 3) show that the minimum value of ash content was 5.3% from fleshing waste, whereas the maximum value was 13.3% from chrome shaving waste. The average value of ash content was found to be 7.3%, which indicates that more than 92% of LSWs are organic. The author performed a proximate analysis of various prepared briquettes, indicating 3.2% ash content in the HR briquette, whereas 4.2% ash content was observed in the BD briquettes (Oyelaran et al. 2017a). The permissible level of ash content from the LSWs was suggested to be around 35% in earlier work (Singh et al. 2011).

**Volatile organic compounds:** The flame's length estimates volatile organic compounds (VOCs) while burning LSWs and higher VOC content generates a longer and shorter flame that contains fewer VOCs. The observation shows a minimum value of 70% for finished leather trimming waste and a maximum value of 82% for fleshing waste. Results were further corroborated that the BD briquettes have the least volatile matter, an average of 1.6%, followed by CS briquettes, with an average of 1.7%. In comparison, HR briquettes have the highest value of an average of 4.5%, followed by FS with an average of 2%. This implies that more energy will be required to burn off the volatile matter in HR briquettes before releasing heat energy (Oyelaran et al. 2017b). One report indicated that VOC's presence is more than 40% suitable for solid waste's various thermal and biological treatments (Singh et al. 2011).

**Moisture content:** Moisture content (MC) is the weight loss measurement by drying at 100° C of the LSWs. MC is an important parameter to estimate the suitability of LSW options for various treatments and disposal. The result is shown (Table 3) that the MC in BD waste is 7.8%, while the maximum in the case of FW is 76.5%. The finding shows that the MC of FS is much higher than the other process due to the generation from the beam-house processing stage involving wet processing. Further, CT, BD, and F wastes have relatively low MC, 13.7%, 7.8%, and 17.6%, respectively, because of generation from tanning and re-tanning leather processing dry stages.

**pH value:** LSWs' pH greatly influences the surrounding environment if disposed of in open land unsafely. Besides, more alkaline or acidic wastes reduce soil fertility, water palatability, and crop productivity. It can be seen from Table 3. CS waste shows a minimum pH of 3.9. FS has a maximum pH of 12.5 and an average value of 5.7.

Further, FS waste is alkaline due to the unhairing and liming process performed before this stage. The remaining processes, i.e., CS, CL, BD, and F, pH in the acidic range (4-4.2), attributed mainly to tanning and re-tanning processes carried out in acidic media. Thus, it was recommended to segregate the wastes having higher alkalinity from the acidic media, and treatment is done accordingly.

**Chromium content:** Chrome tanning is used as a tanning material to provide unique features such as high thermal stability, flexibility, and high resistance for the finished leather. Chromium is applied in the tanning and re-tanning process with different percentages as chromium sulfate. Chromium has the potential to contaminate the surrounding environment (agricultural soil, surface water, and groundwater) and have negative impacts (Nigam et al. 2015). It was observed that LSWs range from the minimum value of 1.5% for F waste to the maximum value of 1.6% for CS waste, and thereby, average chromium was around 1.6%. It is further corroborated by the tanned LSWs, e.g., CS, CL, BD, and F, which have higher chromium content beyond the permissible limits in water (WHO 2011) and soil (Rahaman et al. 2016). The variation in chromium concentrations also depends upon the types of waste generated, and the tanning process used about 5.5 to 7.0% of chromium sulfate.

Therefore, the chrome-containing LSWs, viz. chrome shaving waste, crust leather trimming waste, buffing dust waste, and finished leather trimming waste, should be segregated, collected, treated, and disposed of separately from the non-chrome LSWs like fleshing waste. In addition, significant environmental problems (surrounding agricultural soil, surface, and groundwater pollution) are created due to the improper management of chrome-containing LSWs. Thus, to minimize environmental risks, tanned LSWs should be managed in a sustainable manner using waste-to-energy options, viz. thermal treatment technologies (incineration, pyrolysis, gasification, and plasma technology), anaerobic digestion and composting process after pre-treatment for chromium presence. Further manufacturing of various valuable products and end products or ash must be safely disposed of in a secured landfill area.

**Carbon content:** Carbon content is an important parameter to determine the suitability of LSWs to implement waste-to-energy technological options for solid waste management (Singh et al. 2011). The carbon content of LSWs generated ranges from the minimum value of 12.4% for fleshing waste up to the maximum value of 17.5% for crust leather trimming waste. The average carbon content of LSWs was found to be approximately 14.7%. A carbon content of less than 15 percent is considered to implement the thermal treatment methods (Alrikabi & Khaleefah 2005). Fleshing waste, chrome shaving, and buffing dust wastes contain carbon content of 12.4%, 14%, and 12.8%, respectively, which is less than 15%. Therefore, these wastes could be utilized for the waste to energy production in the industry. However,

fleshing waste contains higher moisture content (76.5%), and thermal treatment is not economically feasible due to high-temperature requirements.

In addition, crust and finished leather trimming waste containing carbon content of 17.5% and 16.8%, respectively, can be utilized for energy recovery applications by mixing with the other LSWs with low carbon.

**Nitrogen content:** Nitrogen content is a crucial parameter to know the carbon to nitrogen ratio of LSWs to evaluate their suitability to implement anaerobic digestion and composting process (waste to energy). Nitrogen is an important nutrient responsible for the growth of microorganisms, which is required for the effectiveness and productivity of the biological treatment system of LSWs (Kaosol & Wandee 2009). Table 3 presents the minimum nitrogen of 0.2% for fleshing waste up to the maximum value of 0.3% for finished leather trimming waste.

**Carbon to nitrogen ratio (C: N):** Carbon to nitrogen ratio is a key parameter to determine the suitability of solid waste to implement the waste-to-energy options, e.g., anaerobic digestion and composting processes. Carbon serves primarily as an energy source for microorganisms, and nitrogen is critical for microbial population growth. If nitrogen is limited, microbial populations will remain small and take longer to decompose the leather solid waste. Excess nitrogen, beyond the microbial requirements, is often lost from the system and can cause odor problems in the surrounding environment (Kaosol & Wandee 2009). Table 3 indicates that the carbon-to-nitrogen ratio of the leather solid wastes generated from the Sheba leather industry ranges from the minimum ratio of 47.4:1 for buffing dust waste up to the maximum ratio of 58.4:1 for crust process waste and the average carbon-to-nitrogen ratio of the solid waste was found to be 52:1. The carbon to nitrogen ratio requirement of the solid wastes to implement the anaerobic digestion and composting processes is 20-50:1 (Rastogi et al. 2020). The carbon to nitrogen ratio of fleshing waste and buffing dust waste was found as 47.7:1 and 47.4:1, respectively, which is within the range of the required value of 20-50:1. The laboratory result assures that fleshing waste and buffing dust waste are suitable to implement the anaerobic digestion and composting processes. On the other hand, the carbon to nitrogen ratio of chrome shaving waste, crust leather trimming waste, and finished leather trimming waste was 53.9:1, 58.4:1, and 52.4:1, respectively, which is above the range of required value 20-50:1. However, carbon to nitrogen ratio of solid waste can be adjusted to achieve the requirement 20-50:1 with additional nitrogen sources wastes such as manure, sewage sludge (biosolids), septic and urea. Therefore, the untanned and tanned LSWs (fleshing waste, chrome shaving waste, buffing dust waste,

crust leather trimming waste, and finished leather trimming waste) generated from the Sheba leather industry are suitable to implement the biological treatment options, e.g., anaerobic digestion and composting processes.

## CONCLUSIONS

The present research assessed and characterized leather solid waste (LSW) in the Sheba leather industry. Type of leather solid wastes generated from the unit operations of the four main leather processing stages (beamhouse operations, tanning processes, re-tanning processes, and finishing processes) are classified as chrome-free solid wastes, viz. de-dusted salt waste, raw trimming waste, hair waste, fleshing waste, pickle trimming waste and splitting waste and chrome containing solid wastes viz. chrome shaving waste, crust leather trimming waste, buffing dust waste and finished leather trimming waste. The annual generation amount of leather solid wastes during sheep skins and hides processing is 690 tonnes and 1,792 tonnes, respectively. As a result, the Sheba leather industry generates 2,482 tonnes of leather solid wastes per year while processing 5,280 tons of raw wet salted sheep skins and hides. Furthermore, the physico-chemical characterization results indicated that the average inorganic residue or ash content of the leather solid wastes is 7.3 %, ensuring that more than 90% of the leather solid wastes generated from the Sheba leather industry are organic. Average results obtained from the physico-chemical characterization of LSW were calorific value (20,107 kJ.kg kg.ton$^{-1}$), ash content (7.3%), volatile organic compounds content (75.1%), moisture content (31.5%), pH value (5.7), chromium content (1.6%), carbon content (14.7%), nitrogen content (0.3%) and carbon to nitrogen ratio (52:1).

## ACKNOWLEDGMENTS

## REFERENCES

Alrikabi, A.P. and Khaleefah, N. 2005. Sustainable solid waste management system. Ren. Energy, 17: 1391-1400.

Appala, V.N.S.G., Pandhare, N.N. and Bajpai, S. 2022. Biorefining of leather solid waste to harness energy and materials- A review. Biomass Conv. Bioenergy, 14: 456-463.

ASTM D2617 2001. Total Ash in Leather. 15: 4-5.

ASTM D3790 2001. Standard Test Method for Volatile Matter (Moisture) of Leather by Oven Drying.79: 1-2.

Coară, G., Florescu, M., Mocanu, C.R., Lăzăroiu, G. and Tonea, S. 2016. Green tannery- the leather processing unit. In: 5th International Conference of Thermal Equipment, Renewable Energy and Rural Development, pp. 447.

Emmanueul, S.D., Adamu, I.K., Ejila, A., Ja'afaru, M.I., Yabaya, A. and Habila, B. 2014. Characterization of chrome buffing dust (CBD) generated from NILEST tannery associated with pathogenic fungi. J. Toxicol. Environ. Heal Sci ., 6: 89-98.

Famielec, S. 2020. Chromium concentrate recovery from solid tannery waste in a thermal process. Materials, 13: 1533. https://doi.org/10.3390/ma13071533.

Fela, K., Wieczorek-Ciurowa, K., Konopka, M. and Woźny, Z. 2011. Present and prospective leather industry waste disposal. Polish J. Chem. Technol., 13: 53-55. https://doi.org/10.2478/v10026-011-0037-2.

Framis, C.P. 2018. Assessment of tannery solid waste management, A case of Sheba Leather Industry in Wukro (Ethiopia).

Hashem, M.A., Islam, A., Paul, S. and Nasrin, S. 2014. Generation of ammonia in deliming operation from tannery and its environmental effect: Bangladesh perspective. Proceedings of the 2nd International Conference Civil Engineering Sustainable Development (ICCESD-2014), 14-6 February 2014, KUET, Khulna, Bangladesh, pp. 17-23

Kanagaraj, J., Velappan, K.C., Chandra, Babu, N..K, and Sadulla, S. 2006. Solid wastes generation in the leather industry and its utilization for the cleaner environment: A review. J. Sci. Ind. Res. India, 65: 541-548. https://doi.org/10.1002/chin.200649273.

Kaosol, T. and Wandee, S. 2009. Cellulolytic Microbial activator influence on decomposition of rubber factory waste composting. Vol. 3, p. 306-11.

Koppiahraj, K., Bathrinath, S. and Saravanasankar, S. 2019. Leather waste management scenario in developed and developing nations. Int. J. Eng. Adv. Technol., 9: 852-857.

Kruis, F. 2014. Environmental Chemistry: Selected Methods for Water Quality Analysis. Delft, Netherland: UNESCO-IHE Institute for Water Education.

Li, Y., Guo, R., Lu, W. and Zhu, D. 2019. Research progress on resource utilization of leather solid waste. J. Leather Sci. Eng., 6: 1-17.

Lima, D.Q., Oliveira, L.C.A., Bastos, A.R.R. Carvalho, G.S., Marques, J.G.S.M. and Carvalho, J.G. et al. 2010. Leather industry solid waste as a nitrogen source for the growth of common bean plants. Appl. Environ. Soil Sci., 20: 1-7.

Masilamani, D.K., Madhan, B., Shanmugam, G., Palanivel, S. and Narayan, B. 2016. Extraction of collagen from raw trimming wastes of tannery: A waste to wealth approach. J. Clean. Prod., 13: 338-344. https://doi.org/https://doi.org/10.1016/j.jclepro.2015.11.087.

Ministry of Agriculture and Rural Development. 2009. The effect of skin and hide quality on the domestic and export market and evaluation of the campaign against ectoparasite of sheep and goat in Amhara, Tigray, and Afar region. Official Report to Region and Other Sectors, Ethiopia.

Muralidharan, V., Palanivel, S. and Balaraman, M. 2022. Turning a problem into possibility: A comprehensive review on leather solid waste intra-valorization attempts for leather processing. J. Clean. Prod., 367: 133021.

Mushahary, J. and Mirunalini, V. 2017. Waste management in leather industry - environmental and health effects and suggestions to use in construction purposes. Int. J. Civ. Eng. Technol., 8: 1394-1401.

Nigam, H., Das, M., Chauhan, S., Pandey, P. and Swati, P. 2015. Effect of chromium generated by the solid waste of tannery and microbial degradation of chromium to reduce its toxicity : A review. Adv. Appl. Sci. Res., 6(3): 129-136.

Ocak, B. 2012. Complex coacervation of collagen hydrolysate extracted from leather solid wastes and chitosan for controlled release of lavender oil. J. Eviron. Manag., 100: 22-28.

Onukak, I.E., Mohammed-dabo, I.A., Ameh, A.O., Okoduwa, S.I.R. and Fasanya, O.O (2017. Production and characterization of biomass briquettes from tannery solid waste. Recycling, Vol. 2, p. 17-36. https://doi.org/10.3390/recycling2040017.

Oruko, R.O., Moturi, W.N. and Mironga, J.M. 2014. Assessment of tannery-based solid wastes management in Asili. Nairobi Kenya, Int. J. Qual. Res., 8: 227-238.

Oyelaran, O.A., Balogun, O., Ambali, A.O. and Abidoye, J.K. 2017a. Characterization of briquette produced from tannery solid waste. J. Mater. Eng. Struct., 4: 79-86.

Oyelaran, O.A., Sani, F.M., Sansui, O.M., Balogun, O. and Fagbemigun, A.O. 2017a. Energy potentials of briquette produced from tannery solid waste. Makara J. Technol., 21: 122-128.

Ozgunny, H., Colak, S., Mutlu, M.M. and Akyuz, F. 2007. Characterization of leather industry wastes. Pol. J. Environ. Stud., 16: 867-873.

Pati, A., Chaudhary, R. and Subramani, S. 2014. A review on the management of chrome-tanned leather shavings: a holistic paradigm to combat the environmental issues. Environ. Sci. Pollut. Res., 21: 11266-11282. https://doi.org/10.1007/s11356-014-3055-9.

Paul, S., Mondal, N.R. and Ray, S.K. 2015. Minimization of solid waste generated during liming process in beamhouse operation through enzymatic treatment. WasteSafe 2015- 4th International Conference on Solid Waste Management in Developing Countries, KUET, 15-17 February 2015, Khulna, Bangladesh, pp. 1-6.

Rahaman, A., Afroze, J.S., Bashar, K., Ali, F. and Hosen, R. 2016. A comparative study of heavy metal concentration in different layers of tannery vicinity soil and near agricultural soil. Am. J. Anal. Chem., 7(12): 880-889. https://doi.org/10.4236/ajac.2016.712075.

Ram, C., Kumar, A. and Rani, P. 2021. Municipal solid waste management: A review of waste to energy (WtE) approaches. BioResources, 16(2): 4275-4320.

Ranjithkumar, A., Durga, J., Ramesh, R., Rose, C. and Muralidharan, C. 2017. Cleaner processing: A sulfide—free approach for depilation of skins. Environ. Sci. Pollut. Res., 24: 180-188. https://doi.org/10.1007/s11356-016-7645-6.

Rastogi, M., Nandal, M. and Khosla, B. 2020. Microbes as vital additives for solid waste composting. Heliyon, 6: e03343. https://doi.org/10.1016/j.heliyon.2020.e03343.

Saira, G.C. and Shanthakumar, S. 2023. Zero waste discharge in tannery industries - An achievable reality? A recent review. J. Environ. Manag., 335: 117508.

Singh, K., Lohchab, R.K., Dhull, P., Kumari, P., Choudhary, V. and Bala, J. 2022. Solid wastes generation at various zones of universities campus: Characterisation and its management approaches. Pollut. Res., 41(2): 557-568.

Singh, R., Roy, S. and Singh S. 2011. Energy recovery from waste: A review. Krish. Sansk., 11: 298-303.

Teklay, A. 2018. Quantification of Solid Waste Leather Generation Rate from the Ethiopian Leather Sector - A Contributing Perspective to Waste Management Approach Innovative Energy & Research Quantification of Solid Waste Leather Generation Rate from the Ethiopian Leather' https://doi.org/10.4172/2576-1463.1000208.

Velusamy, M., Chakali, B., Ganesan, S., Tinwala, F. and Venkatachalam, S.S. 2020. Investigation on pyrolysis and incineration of chrome-tanned solid waste from tanneries for effective treatment and disposal: An experimental study. Environ. Sci. Pollut. Res., 27: 29778-29790. https://doi.org/10.1007/s11356-019-07025-6.

World Health Organization (WHO) 2011. Guidelines for Drinking-water Quality.

# Assessment of SO₂ Emissions from Cement Industries Utilizing Limestone with High Pyritic Sulfur Content: Case Study of Cement Plants in the Jaintia Hills District, Meghalaya, India

**Arnab Mandal*†** [iD]**, M. K. Choudhury*, Nazimuddin** and Prashant Gargava****

*Central Pollution Control Board, Regional Directorate Shillong, BSNL CTO Building (GF), Shillong-793001, Meghalaya, India

**Central Pollution Control Board, Parivesh Bhawan, East Arjun Nagar, Delhi-110032, India

†Corresponding author: Arnab Mandal; mandalarnab.cpcb@gov.in

## ABSTRACT

In properly operated Cement Plants, $SO_2$ emissions are mostly caused by pyritic sulfur (sulfides) in the used limestones, accounting for approximately 85% of the raw mill in the plant. However, the pyritic sulfur content in limestones of the Jaintia Hills district of Meghalaya and their influence on the $SO_2$ Emission from cement industries of Meghalaya have not been studied so far.  The current study is conducted to perform an in-depth investigation of pyritic sulfur content in limestone reserves used by Meghalaya Cement Industries to assess the $SO_2$ emission in the cement industries using high pyritic sulfur limestones and review the existing technology for the recommendation of the most suitable technology to minimize the $SO_2$ Emissions. Random testing of collected limestone samples from various locations of Captive Mining sites in Cement Industries is performed to assess average pyritic sulfur concentration along different mining benches. Pyritic Sulfur Content (wt.%) in collected limestones varies from 0.15% to 3.5%. Polynomial Regression Analysis shows that Avg. $SO_2$ Emission(Y) from Klin Stack can be represented as a function of pyritic sulfur content (X) (wt.%) of used limestones in the process: $Y = 273.7X^2 + 21.46X + 422.76$. Based on the pyritic sulfur content in limestones, it is observed that "the more the Pyritic Sulfur content is, Darker the Limestone Samples are." Hence, A Colour Scale has been prepared to visualize higher pyritic sulfur content in limestones. For longer-term sustainability, installing a Flue-Gas Desulfurization (FGD) unit at the kiln stack outlet may be included in the manufacturing process of cement plants to reduce the $SO_2$ Emissions from Stack.

## INTRODUCTION

India is a multicultural nation with potentially valuable mineral resources. India produces over 90 different minerals, according to the Indian Mineral Yearbook Report (2013). There are 53 non-metallic minerals, 11 metallic minerals, 4 fuel minerals, and 23 minor minerals (building and other materials). This suggests that India's mining sector is vital to economic growth. Cement is a vital building material made from limestone, a non-metallic mineral necessary raw material. India has 184,935 million tonnes of estimated limestone resources across all types and grades. 14,926 million tonnes (or 8%) are classified as reserves, while 170,009 million tonnes (or 92%) are classified as residual resources. About 9% of India's entire limestone resources come from the northeastern states of India (Lamare & Singh 2016).

Meghalaya, one of the eight states that comprise India's Northeastern Region (NER), is located between latitudes 25°02'E and 26°07'N and longitudes 89°49'E and 92°50'E. The Khasi, Jaintia, and Garo, are three hilly regions. There

are currently 11 districts in the state. Limestone is Meghalaya's most frequently found and exploited mineral, second only to coal. The area's limestone rocks are found in various grades and sizes. The state's southern border stretches for around 200 Km from the east Jaintia Hills to the west Garo Hills. According to the Directorate of Mineral Resources, Government of Meghalaya (2022), the total deposit of limestone in the state is 15,100 MT, with 9,515 MT, 41,599 MT, and 3,986 MT being the proved, indicated & inferred deposits. Tripathi et al. (1996) claimed that there is reportedly a maximum limestone reserve in Jaintia Hills (~55%). Limestone is mostly found around the southern edge of the Meghalaya plateau and is a part of the Khasi, Jaintia, and Garo groups of Cretaceous-Tertiary sedimentary rocks (Sarma 2003).

Although Meghalaya is very rich in high-quality limestone (CaO wt.% varies from 40%-55%) deposits, the Pyritic Sulfur content is reportedly high in the very high-quality limestone available in Meghalaya. This has led to the

Table 1: Emission limits from rotary kiln cement industries.

| Industry | Parameter | Date of commissioning | Location | Concentration not to exceed in mg.Nm$^{-3}$ |
|---|---|---|---|---|
| Cement plant (Without coprocessing) Standalone Clinker Grinding plant or Blending plant (MoEFCC 2016) | $SO_2$ in mg.Nm$^{-3}$ | Irrespective of the date of commissioning, | Anywhere in the country | 100, 700, and 1000 when pyritic sulfur in the limestone is less than 0.25%, 0.25% to 0.5%, and more than 0.5%, respectively |

varying emission of $SO_2$ from the cement mills. The Ministry of Environment, Forests and Climate Change (MoEF&CC), Government of India, had notified the revised limits from emissions from cement industries on May 9, 2016. The new limits with respect to $SO_2$ emission from rotary kilns cement industries are represented as follows:

As seen from Table 1, the concentration of pyritic sulfur has been categorized into three broad categories viz less than 0.25%, 0.25% to 0.5%, and more than 0.5%, respectively. These are the general concentrations of pyritic sulfur in limestone across the world. However, the concentration is expected to be significantly higher in Meghalaya, especially in the East Jaintia Hills district. Various cement Industries in Meghalaya reported high concentrations of pyritic sulfur in the limestones of their captive mining. Therefore, compliance with the prescribed limit becomes a challenge for them. In this regard, this study is conducted to perform in-depth investigation of pyritic sulfur content in limestone reserves of Meghalaya Cement Industry, assess compliance w.r.t Regulatory Norms of $SO_2$ emission by cement industries using high pyritic sulfur limestones and review the existing technology for the recommendation of most suitable technology to counter-act the effect of high pyritic sulfur content in the manufacturing process, thereby reducing $SO_2$ Emissions to meet MoEF & CC Standards.

## MATERIALS AND METHODS

**Study Area:** The Jaintia Hills district of Meghalaya is home to many cement factories, largely owing to the region's plentiful limestone resources. Clusters of several cement manufacturing facilities surround the NH-44 road from Shillong to Katigara (see Fig. 1 (A&B)). Based on operating status and those that use their own captive limestone mining reserve, the following cement factories have been selected for this study.

Limestone samples from random sites & benches across these cement industries were collected to analyze the raw limestones' pyritic sulfur concentration (wt.%). Limestone Samples from the crushed limestone feeding system of cement industries were also collected to check the inlet pyritic sulfur concentration of the rotary kiln. Further, compliance with the prescribed limits of $SO_2$ Emission was

verified manually through stack monitoring during the field visits.

**Cement industry-process flow diagram:** A general flow diagram of the cement industry is shown in Fig. 2. All the cement industries under discussion share the same fundamental process design. Before the mixed flow is transferred to the preheater, crushed limestone from the limestone hopper and additives like clay, silica, or iron ore from the additives hopper are mixed in the raw mill section.

The material is heated, combined with coal from the coal mill in the rotary kiln, and then fed into the cement mill silo after cooling.

The main elements of a contemporary dry cement manufacturing process, including preheating, pre-calcination, burning, and clinker cooling, are shown in Fig. 2. The multistage cyclone preheater warms the raw mill materials. The raw meal is fed into the cyclone preheater at the top stage by being dispersed with the hot flue gas entering the cyclone inlet. The cold raw mill particles are separated in the cyclone following a direct heat transfer with the hot flue gas. The process is repeated until the final stage cyclone when the separated raw mill particles are put into the calciner. The raw mill particles are heated from about 100°C to 800°C after the typical counter current heat exchange through the cyclone preheater. Because of the calciner's comparatively

Table 2: Selected Cement Industries in Meghalaya for Study.

| Sl. No. | Name of the Cement Manufacturing Plants | Address |
|---|---|---|
| 1. | Dalmia Cements Bharat Limited (Adhunik Cements) | NH: 44, Thangskai, Meghalaya-793200 |
| 2. | Meghalaya Cements Limited (Topcem) | 693J+FWF, Thangskai, Lumshnong, Khliehriāt, Meghalaya-793210 |
| 3. | Star Cements Limited | 59HR+P8F, Lumshnong, Meghalaya 793200 |
| 4. | Hills Cements Limited | NH 44, Khliehriat, Jaintia Hills, Mynkree, Meghalaya-793200 |
| 5. | Goldstone Cements Limited | Umrasong, Meghalaya 793210 |
| 6. | Amrit Cements Limited | 69MH+89G, Lumshnong, Meghalaya-793210 |

Fig. 1 (A): Jaintia Hills District of Meghalaya (NH-44 Road Shillong to Katigara) (Reference:www.mapsofindia.com).



Fig. 1 (B): Distribution of Selected Cement Industries for study along NH-44 of East Jaintia Hills District (Reference: Google Maps).

high temperature of 900°C to 950°C, the limestone particles in the raw mill break down to generate CaO. The endothermic degradation of the limestone in the calciner requires additional heat, which is produced by burning fuels.

Following calcination, the calcinated raw meal is fed into the rotary kiln, where it is heated at a temperature of up to 1300°C to 1400°C to create cement clinker. Fuels are burned in the rotary kiln to provide heat. Finally, the newly formed cement clinker is cooled in a clinker cooler.

**Release and Capture of SO$_2$ in the Process:** Most SO$_2$ emissions occur in the preheater due to the oxidation of sulfides, primarily pyrites and organic sulfur (if any), in the raw mill. The remaining SO$_2$ emissions are produced in the pre-calciner and kiln by the oxidation of sulfides, primarily pyrites and organic sulfur in fuel, and the breakdown of sulfates from raw mill particles and fuel (Gossman 2011).

The raw mill, preheater, and pre-calciner all work as dry scrubbers to control SO$_2$ emissions because they use

kiln exhaust gas for drying, heating, and calcining the raw mill particles before they reach the kiln. The particle control system in the bag-house may additionally dry scrub some $SO_2$ (Horkoss 2008). As a result, $SO_2$ is released and captured at the same time. It is worth mentioning that the raw mill and preheater have insufficient $SO_2$ collecting capacity due to the slow reaction rate between $SO_2$ and $CaCO_3$. The bulk of $SO_2$ may be trapped when flue gas goes through the pre-calciner

because there is a lot of CaO there, and $SO_2$ and CaO react fast when they come into contact. Alkali and CaO in the kiln can also absorb $SO_2$, but during clinkerization, some amount of $CaSO_4$, the primary desulfurization product, will break down and release $SO_2$ again (Zhang et al. 2019).

Organic and inorganic sulfurs can be found in raw mills and fuel, primarily referring to sulfides (such as pyrite) and sulfates (gypsum). More than 80%-90% of the sulfur in
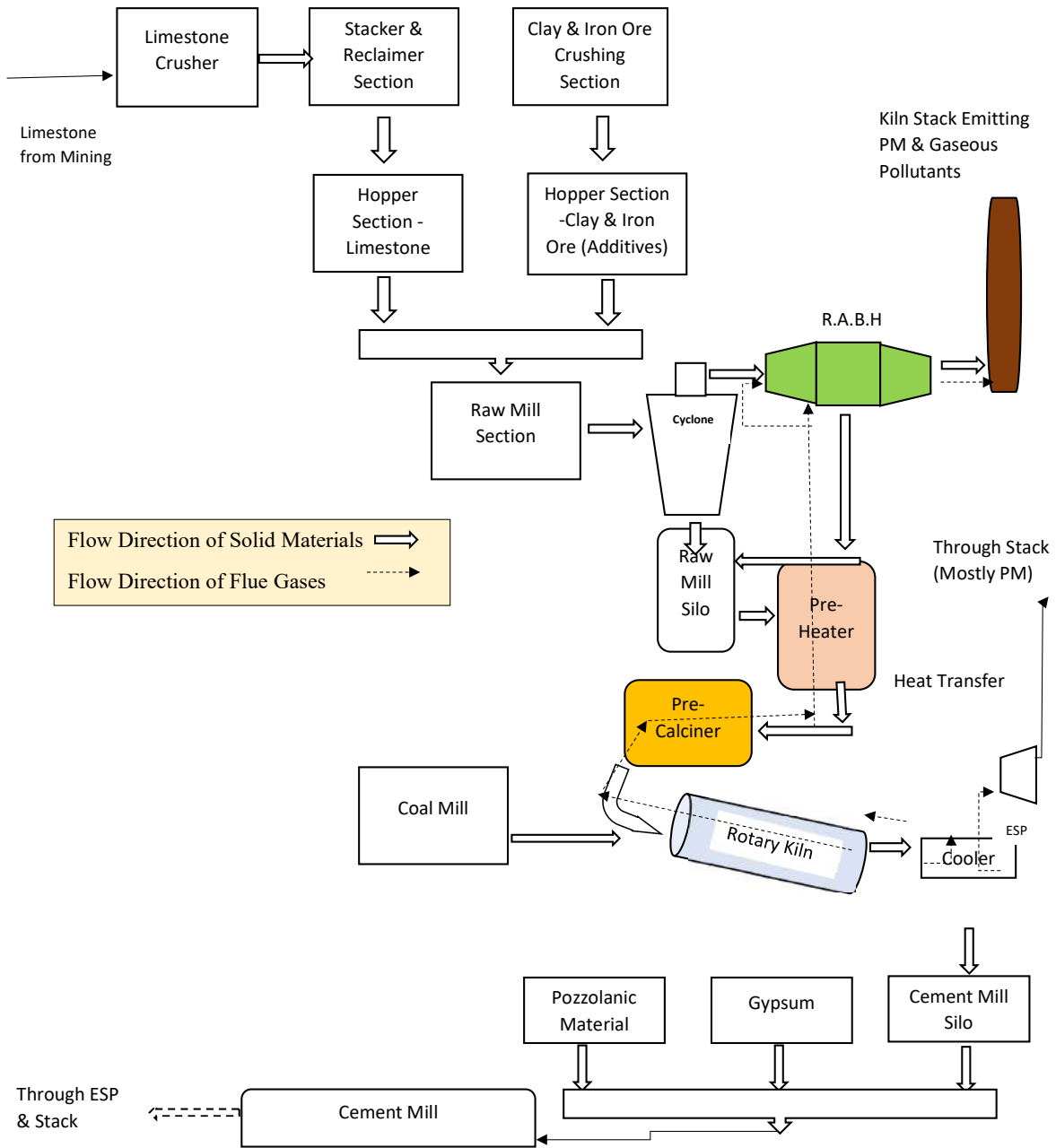


Fig. 2: Process Flow Diagram of Cement Plants.

coal is organic, with the rest primarily made up of pyrite (FeS$_2$), gypsum (CaSO$_4$), and a few ferric sulfates (Oliveira et al. 2011). Whether the coal is burned in the kiln or CaO may absorb the pre-calciner, the bulk of the SO2 released by the coal as the flue gas passes through the pre-calciner. On the other hand, the source of sulfur in limestone is purely inorganic: it primarily exists in the form of pyrite (Sulfide form) and gypsum/sulfate form. Because pyrite sulfur is more unstable than sulfate sulfur, pyrite sulfur would be released as SO$_2$ first compared with Sulfate decomposition.

Since the loading (wt.%) ratio of limestones& fuels (coal) ranges around 85:15, the minimal SO$_2$ Emission contributed by coal combustion in pre-calciner or kiln can be captured by CaO (forming CaSO$_4$) when the flue gas passes through the pre-calciner. Because the raw mill and preheater have a limited capacity for absorbing SO$_2$, any increase in the amount of pyritic sulfur in the raw limestones would eventually cause the preheater to oxidize the pyritic sulfur and release surplus SO$_2$, which the flue gas would then transport till stack emission. In light of this, the primary defining element for SO$_2$ emission from the stack associated with Kiln flue gas is the Pyritic Sulfur Content of limestones from raw limestones.

**Methodology**

Limestone samples were collected from different sites of mining benches (See Fig. 4) of the selected cement industries for analyzing the pyritic sulfur concentration (wt.%). Limestone Samples from the crushed limestone feeding system before the Kiln inlet were also collected from the selected plants to check the inlet pyritic sulfur concentration of the rotary kiln. The system adopted for minimizing pyritic sulfur in the kiln inlet was also deeply evaluated during field visits. Compliance with the prescribed limits of SO$_2$ Emission was verified manually during the field visits. The Methodology Adopted for this study is summarized in Fig. 3.

The collected samples were sent to M/s National Council for Cement and Building Materials, Haryana, India, for analysis of the pyritic sulfur content in the collected samples. Test Method *ASTM C-25: 2019* is used for reporting the
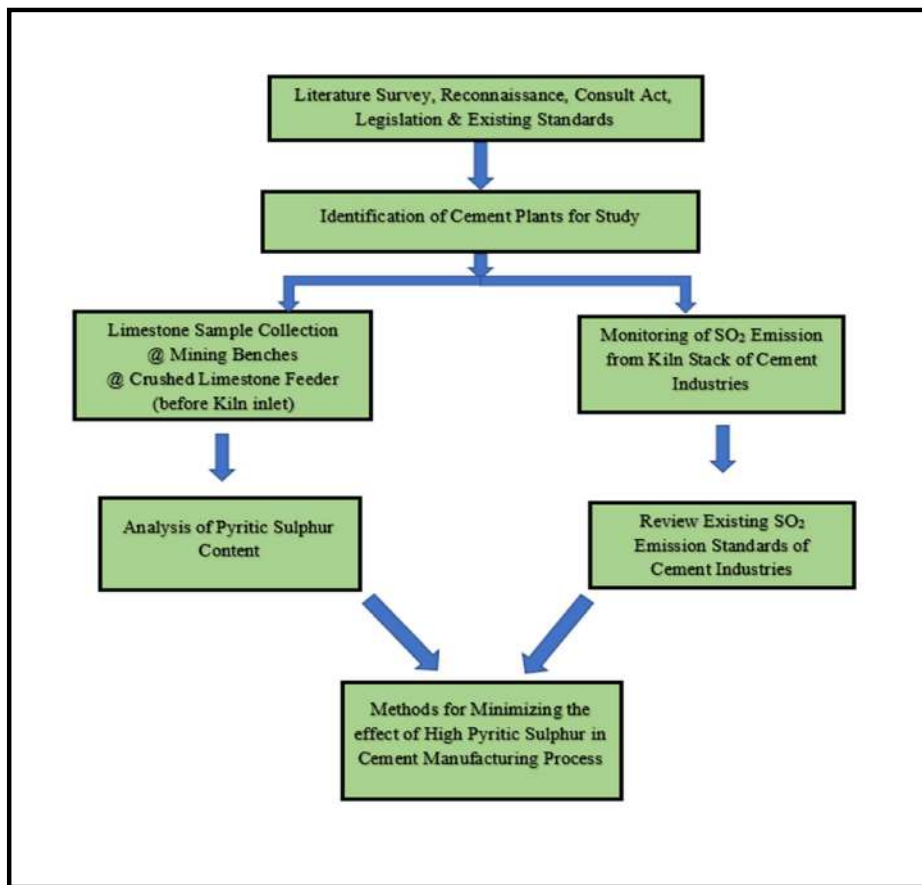


Fig. 3: Methodology of the study.

Fig. 4: Limestone mining bench @ Meghalaya Cements Ltd. (Topcem).

pyritic sulfur content (wt.%). There is no standard test method for directly determining pyritic sulfur in limestone. However, as per clause 24.1 (Scope) of ASTM C 25- 17, sulfur in limestone is chiefly, if not wholly, present as sulfide, usually as pyrite. If the total sulfur obtained in the Sodium carbonate fusion method is more than that present as soluble sulfate, the difference can be assumed to be iron disulfide." The concentration of pyritic sulfur in limestone samples is determined using this indirect technique.

## RESULTS AND DISCUSSION

**Comparison of pyritic sulfur content v/s $SO_2$ emission:** Limestone samples were collected from various limestone mining areas & processing sites of the selected cement industries to analyze the pyritic sulfur content (wt.%). Fuel Samples (Coal) were also collected from several Industries to assess the contribution of pyritic sulfur content (wt.%) at the Kiln inlet.

Fig. 5 depicts the variation of pyritic sulfur content (wt.%) in limestones across different Mining Benches of Cement Industries in Meghalaya. While most mining benches have Pyritic Sulfur content (wt.%) values ranging from 0.5% to 0.7%, Mining benches of Dalmia Cements show huge variation in the values of Pyritic Sulfur. Among the Four Benches (4) of Dalmia Cements Ltd., the limestones of the two benches have high pyritic sulfur (wt.%), i.e., 1.5% and 3.5%, respectively. Even limestone samples collected from Weigh Feeder before Kiln inlet is found to be higher (0.65%) for Dalmia Cements Ltd. (Fig. 6). High Pyritic Sulfur Content (wt.%) in limestones of mining benches at Dalmia Cements Ltd also contributes to the plant's relatively greater $SO_2$ Emission (941.3 µg.Nm³⁻) from Kiln Stack than others (Refer Fig. 7).

An attempt has been made to correlate the Average pyritic Sulfur concentration (wt.%) in limestones used by the cement plants in Meghalaya with their $SO_2$ emission from the kiln stack. Polynomial Regression Analysis (Refer Fig. 7) shows that Avg. $SO_2$ Emission(Y) from Klin Stack can be represented as a function of pyritic sulfur content (X) (wt.%) used limestones in the process:

$$Y = 273.7X^2 + 21.46X + 422.76$$

Although all the cement industries under investigation are complying with the standards notified by the Ministry of Environment, Forests and Climate Change, Government of India (GoI) (Standards can be referred from Table 1), $SO_2$ emission (941.3 µg.Nm³⁻) from M/s Dalmia Cements Ltd was found to be high compared to other plants & the value is almost touching the Maximum limits of 1000 µg.Nm³⁻. High pyritic sulfur content in the mining benches at Dalmia Cements Ltd is the main contributor to such a phenomenon. M/s Dalmia Cements Ltd. has adopted certain measures to counter-act the Average pyritic Sulfur concentration (wt.%) effects in their limestones. Selective mining from low pyritic sulfur Mining Benches and variation of Additives flow rate are practiced to tackle the rise in sulfur content in the feeder section & hence in $SO_2$ emission in the stack. The analytical Sulfur content of crushed limestones is checked hourly in the sample point of Limestone Hoppers. If the sulfur content exceeds the desired limit, the same is neutralized by the increase in additives flow rates from the additives hopper. Thus, the material in the Raw Mill, Sulfur content, is well within the desired limit. But this is a short-term preventive measure and a very tedious work.

**Color scale based on pyritic sulfur content in limestones:** We noticed color variation in crushed limestone samples collected from different mining benches. Increasing pyritic sulfur content in limestone samples has resulted in a color intensification trend (Fig. 8).

Notably, dark grey limestones have a higher pyritic sulfur than light grey limestones. In dark grey or dark
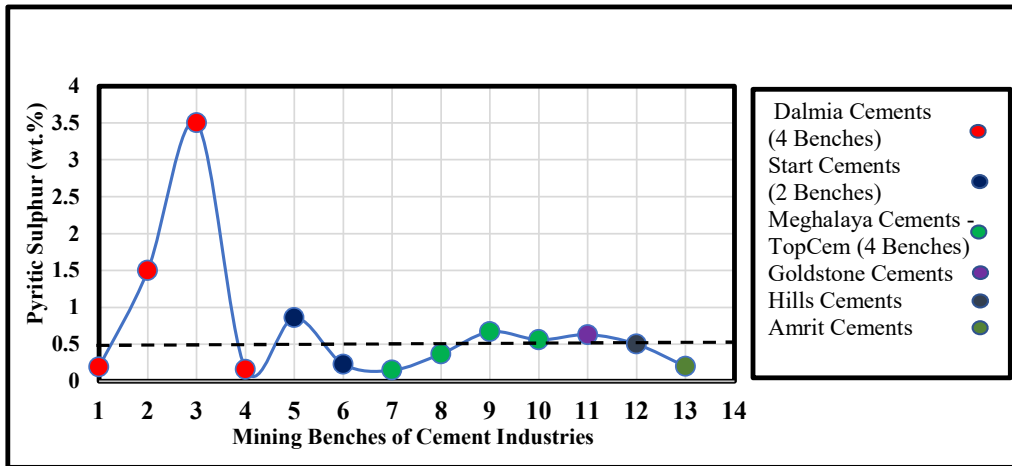
Fig. 5: Pyritic Sulphur Content in Limestones accross  Mining Benches.
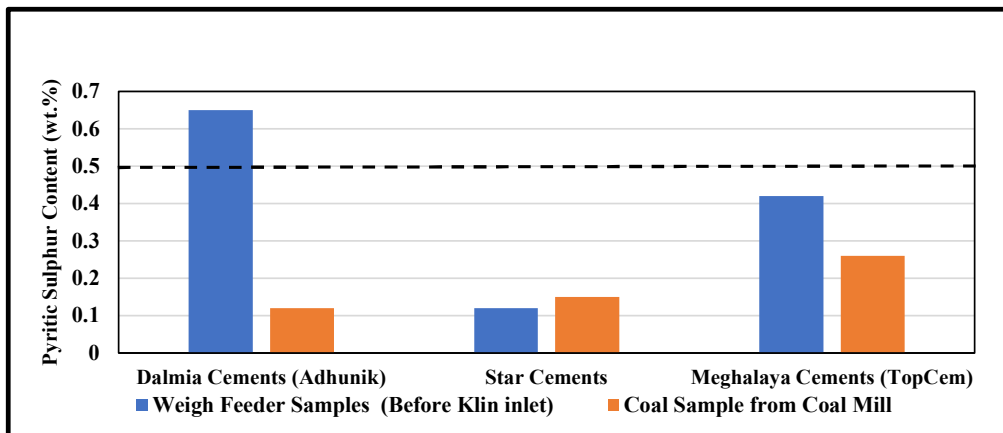


Fig. 6: Pyritic Sulphur Content in Limestone and Fuel Samples collected from Processing Sites.
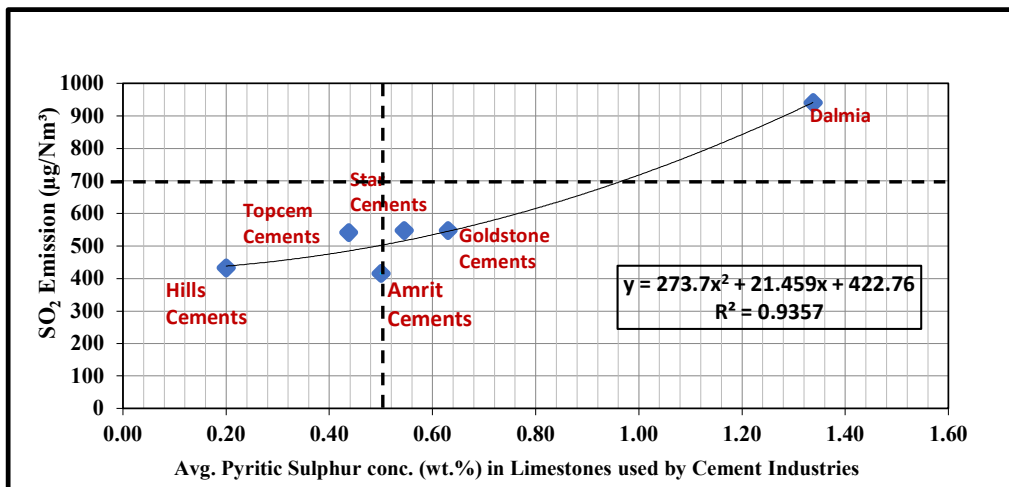


Fig. 7: Avg. SO$_2$ emission from klin stack v/s Avg. pyritic sulphur content in used limestones (Stack emission as on Oct. 2022).

brown limestones, bulk pyrites ($FeS_2$) are found layered and dispersed with impurities (In a reductive environment, metamorphic or sedimentary rocks typically develop). On the contrary, light yellow or light grey limestones, often calcite sedimentary rocks with trivalent iron oxides or hydroxides, hardly ever contain bulk pyrite. It is commonly known that trivalent iron oxides or hydroxides only form in oxidizing atmospheres, whereas pyrite only occurs in reducing atmospheres. As a result, light yellow or light grey limestones rarely contain pyrite and have substantially lower sulfur contents than dark grey limestones (Zhang et al. 2019).

Based on the color of the collected limestone samples and their pyritic sulfur content, a Colour Scale has been prepared to visualize higher pyritic sulfur content in limestones. (Fig.9) Colour Scale Can be easily used in fields to quickly understand pyritic sulfur in the limestone mining bench.

**Measures for Minimization of Effect from High Pyritic Sulfur in Cement Manufacturing Process:**

Pyritic sulfur in limestones is highly undesirable in the cement industry. It not only sets the stage for the significant $SO_2$ emissions from the kiln, but it also causes the production



Fig. 8: Colour Intensification Trend in Collected Limestones.
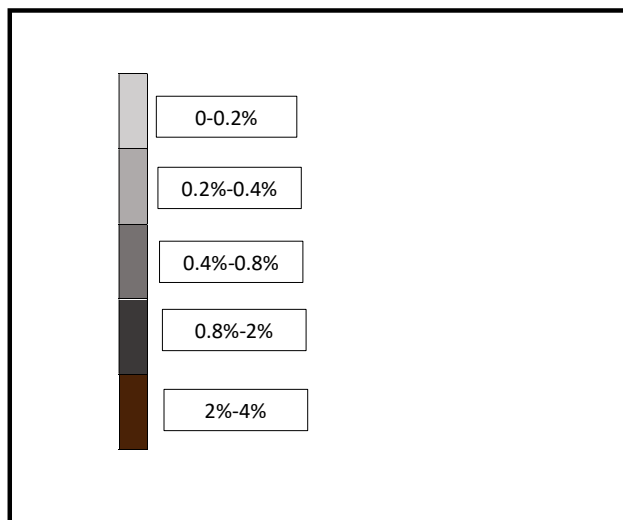
Fig. 9: Colour Scale for identification of pyritic sulphur (wt.%).

of golden rings inside the kiln skin, raising the system's maintenance costs. Several Steps are taken to minimize the effect of the same. We have made an effort to talk about a handful that emerged from the study and fieldwork.

**A. Short-Term Measures**

- **Selective mining and variation of additives flow rate** can be used to tackle the rise in sulfur content in the feeder section & and, hence, in SO$_2$ emission in the stack. As opposed to mining benches with high pyritic sulfur content, mining benches with low pyritic sulfur content can supply raw limestones in cement plants. After a proper sulfur distribution study in mining benches, a Minimal proportion of limestones from Mining benches with high pyritic sulfur content may also be blended with

limestones from mining benches with low pyritic sulfur content, keeping an eye on the pyritic sulfur content in the weigh feeder section. A case Study of Dalmia Cements Ltd. may depict a proper understanding of the blending ratios to get the required pyritic sulfur content in the Weigh Feeder (Refer to Table 3).

It is very much evident from Table 3 that About 80%-90% of the blended limestones should be from the mining benches with low pyritic sulfur content (wt.%) to get the desired kiln inlet pyritic sulfur value of 0.41%-0.64%. Moreover, the concerned ministry/department must investigate the distribution of pyritic sulfur content in captive mining benches of cement plants before giving any Environmental Clearance or Consent.

Table 3: Blending Proportions from Various Mining Benches of Dalmia Cements Ltd.

|        | Mining Benches | Pyritic Sulphur Content(wt.%) | Blending Proportions | Pyritic Sulphur in BlendedLimestones |
|--------|----------------|-------------------------------|----------------------|--------------------------------------|
| Case-1 | 1              | 0.19%                         | 0.4                  | 0.64%                                |
|        | 2              | 1.50%                         | 0.1                  |                                      |
|        | 3              | 3.50%                         | 0.1                  |                                      |
|        | 4              | 0.16%                         | 0.4                  |                                      |
| Case-2 | 1              | 0.19%                         | 0.2                  | 1.57%                                |
|        | 2              | 1.50%                         | 0.3                  |                                      |
|        | 3              | 3.50%                         | 0.3                  |                                      |
|        | 4              | 0.16%                         | 0.2                  |                                      |
| Case-3 | 1              | 0.19%                         | 0.45                 | 0.41%                                |
|        | 2              | 1.50%                         | 0.05                 |                                      |
|        | 3              | 3.50%                         | 0.05                 |                                      |
|        | 4              | 0.16%                         | 0.45                 |                                      |

- **The lime dosing system in the preheater** removes sulfur from the stream, and the produced $CaSO_4$ (Gypsum) is removed from the outlet of the kiln.

**B. Long Term Measures:**

- The cement plants may install **a Flue-gas desulfurization (FGD) unit** to treat the flue gas from the kiln. Because of the acidic nature of emitted $SO_2$ in flue gas, the typical alkaline sorbent slurries or other materials like $CaCO_3$ (limestone) slurry or $Ca(OH)_2$ (hydrated lime) slurry are used to remove the $SO_2$. The reaction produces $CaSO_3$ (calcium sulfite). Further, $CaSO_3$ (calcium sulfite) is oxidized to produce marketable $CaSO_4 \cdot 2H_2O$ (gypsum) used in wallboard and other products.

Being Capital-intensive, Industries are reluctant to adapt to this new technology. However, a proper techno-economic feasibility study may be performed before reaching any conclusion.

Being Capital-intensive in nature, Industries are reluctant to adopt this new technology. However, a proper techno-economic feasibility study may be performed before reaching any conclusion.

## CONCLUSION

The Pyritic Sulfur of limestones from the majority of cement industries in Meghalaya was found to be within values ranging from 0.5% to 0.7%, except Mining benches of Dalmia Cements show huge variation in the values of Pyritic Sulfur. Among the Four Benches (4) of Dalmia Cements Ltd., the limestones of the two benches are found to have high pyritic sulfur (wt.%), i.e., 1.5% and 3.5%, respectively. Even limestone samples collected from the Weigh Feeder before the Kiln inlet are higher (0.65%) for M/s Dalmia Cements Ltd than other plants. Although $SO_2$ emissions from kilns from cement industries were also within the acceptable range as notified by MoEF&CC, GoI, $SO_2$ emission from M/s Dalmia Cements Ltd is high compared to other plants. The cement industries may use selective mining from high and low pyritic limestone mining benches to tackle the rise in sulfur content in the feeder section. Installing a Flue-Gas Desulfurization (FGD) unit at the kiln stack outlet may be included for longer-term sustainability. The pyritic sulfur content of utilized coals is found to have relatively little effect on $SO_2$ emissions in Meghalaya cement factories. However, $SO_2$ released from the alternative fuels was not considered for this study. For example, co-processing high sulfur wastes, especially municipal solid waste, waste tires,

etc., may also create high $SO_2$ emissions in blocks of cement industries of Meghalaya. Therefore, the effects of sulfur characteristics of alternative fuels and treatment techniques for wastes containing sulfur should be further studied in the future.

## REFERENCES

Department of Mining and Geology, Government of Meghalaya 2022. Minerals of Meghalaya: http://www.megdmg.gov.in/minerals.html, Last Accessed on 5th March, 2023.

Directorate of Census Operations, Meghalaya 2014. Census of India 2011 - Meghalaya - Series 18 - Part XII A - District Census Handbook, South Garo Hills

Gossman, D. 2011. Process Compatible $SO_2$ Control in Cement Kilns. http://gcisolutions.com/gcitn0711.html.

Harries, D.D. 2008. A review of the biospeleology of Meghalaya India. Journal of Cave and Karst Studies,70.

Horkoss, S. 2008. Reducing the $SO_2$ emission from a cement kiln. Int. J. Nat. Soc. Sci., 1: 7-15.

Indian Bureau of Mines, Government of India. 2015. Indian Mineral Yearbook Report 2013, 52nd Edition: https://ibm.gov.in/writeread-ata/files/07302015125218IMYB2013_Diaspore.pdf. Accessed on 5th March 2023.

Lamare, R.E. and Singh, O.P. 2016. Limestone mining and its environmental implications in Meghalaya, India. ENVIS Bull. Himal. Ecol., 24: 116.

Ministry of Environment, Forests and Climate Change, Government of India 2016. The Gazette of India, Environment (Protection) Fourth Amendment Rules, 2016, G.S.R. 496(E).

Oliveira, M., Waanders, F., Silva, L., Jasper, A., Sampaio, C., McHabe, D., Hatch, R. and Hower, J. 2011. A multi-analytical approach to understand the chemistry of Fe minerals in feed coals and ashes. Coal Comb. Gasif. Prod., 3(1): 51-62.

Sarma, S. 2003. Meghalaya: The Land and Forest, a Remote Sensing Based Study. Geophil Publishing House, Guwahati, India, pp. 5-16.

Tripathi, R.S, Pandey H.N. and Tiwari B.K. 1996. State of Environment of Meghalaya. North–Eastern Hill University, Shillong.

Zhang, T., Wu, C., Li, B., Wang, J., Ravat, R., Chen, X., Wei, J., Yu, Q.2019. Linking the $SO_2$ Emission of cement plants to the sulfur characteristics of their limestones: A study of 80 NSP cement lines in China. Journal of Cleaner Production, 200-211.

## ORCID DETAILS OF THE AUTHORS

Arnab Mandal: https://orcid.org/0009-0000-9412-8440

# Decarbonization of the Building Sector in Morocco – A Systematic Review

**S. EL Majaty\*†, A. Touzani\* and Y. Kasseh\***
\*Mohammedia School of Engineering, Rabat, Morocco
†Corresponding author: S. EL Majaty: salma.elmajaty@gmail.com

## ABSTRACT

This article is a systematic review of the decarbonization of the building sector in Morocco. It explores the different approaches and technologies used to reduce greenhouse gas emissions and achieve decarbonization targets in this sector. The article examines the policies and regulations in place in Morocco to encourage decarbonization of the building sector, as well as the initiatives taken by key actors to reduce carbon emissions in their buildings. It also reviews sustainable building technologies and renewable energy systems currently used in the country. The systematic review concludes that while Morocco has put in place policies and regulations to encourage the decarbonization of the building sector, there is still much to be done to achieve the ambitious decarbonization targets set by the country. The authors of the article recommend greater investment in sustainable building technologies and renewable energies, as well as increased collaboration between public and private sector actors to accelerate the transition to low-carbon buildings.

## INTRODUCTION

According to the International Energy Agency (IEA) (Kober et al. 2020), the building sector is responsible for approximately 40% of energy consumption and 33% of global CO2 emissions. The global challenges of decarbonizing buildings are multiple and crucial to combat climate change and achieve the goals of the Paris Agreement. The building sector is indeed one of the largest emitters of greenhouse gases worldwide, responsible for around 40% of energy consumption and 33% of $CO_2$ emissions (Lowans et al. 2023).

In light of this reality, the need to decarbonize the building sector has become a priority for governments, businesses, and civil society. The challenges are even greater as the global population continues to grow, increasing the demand for housing and infrastructure. The rapid economic growth of emerging and developing countries such as China and India also significantly impacts construction and building demand (Gruenig & O'Donnell 2016).

Decarbonizing buildings also present significant economic opportunities, particularly in job creation in the construction, energy renovation, energy efficiency, and renewable energy sectors. Investments in these sectors can also generate long-term energy savings and reduce costs for households and businesses (Ugwu et al. 2022).

However, there are many challenges to be addressed in decarbonizing the building sector, including the high costs of innovative technologies and materials, the need for training and awareness-raising among construction stakeholders, the complexity of regulations and standards in different countries and regions, as well as the need to involve citizens and local communities in the energy transition (Sadeghian et al. 2021).

At the global level, initiatives have been launched to encourage the decarbonization of buildings, such as the Global Alliance for Buildings and Construction (GABC) and the Net Zero Carbon Buildings Commitment (González-Torres et al. 2022) initiative, which aims to achieve carbon neutrality in the building sector by 2050. However, more ambitious and concerted actions are needed to achieve the goals of the Paris Agreement and limit global warming to 1.5°C.

In Morocco (Ministry of Energy and Mines - Kingdom of Morocco 2020), the building sector accounts for about 25% of the country's final energy consumption. It is responsible for nearly 20% of the country's greenhouse gas emissions. This makes it a key sector for the country's energy transition. Despite Morocco's efforts and initiatives in renewable energy development, few studies have been conducted to evaluate specific efforts in the building sector. That's why this systematic literature review on decarbonizing buildings in Morocco is of great importance. It aims to identify the most effective practices for reducing GHG emissions in the building sector while highlighting the challenges and obstacles to overcome to support the energy transition. This study will thus identify benchmarks and numerical references in the field of decarbonizing buildings in Morocco based on

rigorous analysis of the available scientific literature on the subject. It will also determine the development opportunities and most effective practices to support the energy transition in the building sector. This information will be useful for policymakers, building professionals, and researchers who can rely on the results of this study to develop policies and programs aimed at reducing GHG emissions in the building sector. In summary, this systematic literature review on decarbonizing buildings in Morocco fills an important gap in the scientific literature on the subject. It will provide valuable information to support the country's energy transition and help achieve Morocco's ambitious goals for reducing GHG emissions.

## MATERIALS AND METHODS

The methodology used in this study is based on the analysis of several scientific references on decarbonization studies in the building sector (Othmani et al. 2022). We selected the most relevant elements of these methodologies to design a rigorous and appropriate methodology for this study (Nowell et al. 2022). This methodology, as shown in Fig.1, includes identifying data sources from bibliographic databases such as Scopus, Web of Science, and Google Scholar. Articles were then selected based on pre-defined criteria. Data were qualitatively analyzed using thematic analysis to identify trends, advancements, and challenges in the field of building decarbonization in Morocco. Two independent researchers validated The results by double-checking to ensure their coherence and accuracy. In summary, this rigorous methodology ensures a comprehensive and in-depth analysis of the available scientific literature on building sector decarbonization in Morocco, as well as providing a reliable and comprehensive synthesis of the advancements and challenges in this field.

**Data Source Identification:** The first step is to identify relevant data sources. This was done using bibliographic databases such as Scopus, Web of Science, and Google Scholar. Inclusion and exclusion criteria were pre-defined to select relevant articles specifically focused on decarbonization in the building sector in Morocco and published between 2012 and 2022. Exclusion criteria included irrelevant articles, non-scientific publications, and duplicates. This step allowed the selection of the most relevant articles for analysis.

**Data Analysis:** The second step involved analyzing the data. Relevant information was extracted from the selected articles, focusing on decarbonization initiatives in the building sector, benchmarks, and numerical references in similar countries. Thematic analysis was used to group the information into key categories. This step allowed the synthesis of data to extract key elements.

**Results Synthesis:** The third step was to synthesize the results. The results were synthesized by identifying trends, advancements, and challenges in building sector decarbonization in Morocco. Effective practices and development opportunities were highlighted while shedding light on obstacles and challenges to achieving decarbonization goals. This step provided an overview of the analysis results.

**Results Validation:** Finally, the fourth step involved validating the results. The results were validated using a double-checking method, where two independent researchers reviewed the results to ensure coherence and accuracy. This step ensured the reliability and validity of the study results.

In summary, this rigorous methodology ensured a comprehensive and in-depth analysis of the available scientific literature on building sector decarbonization in
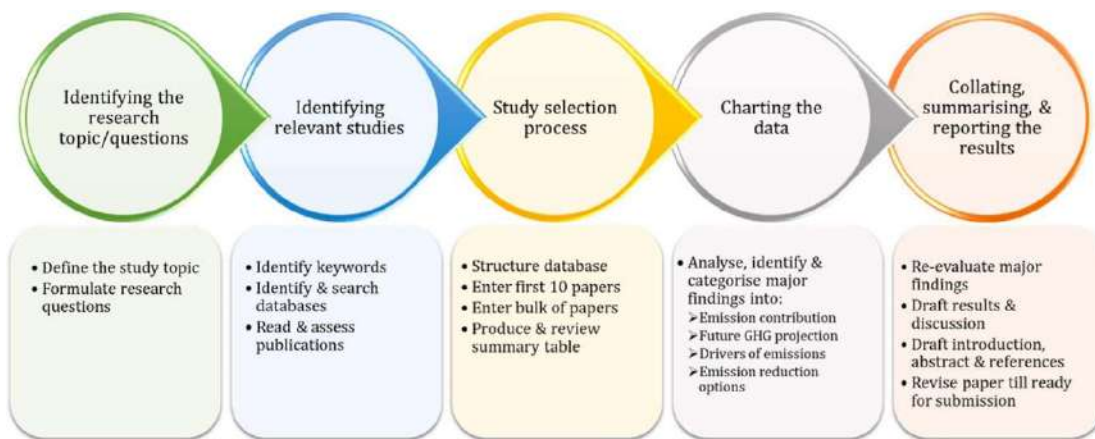


Fig. 1: The systematic quantitative review methodology applied in this study.

Morocco, as well as providing a reliable and comprehensive synthesis of the advancements and challenges in this field.

As part of our study on decarbonizing buildings in Morocco, we adopted a systematic approach to identify and select relevant articles. We formulated research questions related to the state of the art of building decarbonization, technological trends, conditions favoring this transition, as well as policy implications and future research prospects. Our research was conducted based on relevant keyword queries related to construction technologies, decarbonization, and scenarios. It was restricted to articles published between 2010 and 2023 to account for global energy and environmental policies. Studies were identified by conducting searches in electronic databases Scopus, Web of Science, and Google Scholar using a pre-defined keyword search string. Inclusion criteria for studies were: type of analysis: quantitative and qualitative; type of article: peer-reviewed and grey literature published in English; results: scenarios, decarbonization policies, and knowledge gaps; geography: Morocco; period: 2010-2021; scale: community, state, national, and regional; coverage of sub-sectors: residential, commercial, and institutional. Table 1 gives a synthesis of the systematic approach for the identification and selection of relevant papers.

In total, 30 studies were identified from electronic databases. After examining the inclusion criteria, 30 studies were included in the systematic review. These studies were evaluated for their methodological quality and relevance to the research questions. The included studies consisted of peer-reviewed journal articles, as well as working papers, research reports, and theses.

We reviewed a total of 623 articles from Scopus, 540 articles from Web of Science, and 470 articles from Google Scholar. The publications were then evaluated according to specific inclusion criteria, using the PRISMA (Preferred Reporting Items for Systematic Reviews and Meta-Analyses) flow diagram Fig. 2, including 30 publications (Becker & Thompson 2023).

The literature sources used were coded using a numerical index to facilitate their identification. The data was recorded in a table (Table 2) to document information on the authors, year of publication; country, sector studied, methods applied, scenarios explored, parameters, software, and data used (Table 4), emission projections, as well as technology-based reduction options, policies, and economic impact. The scenario analysis results allowed us to identify the factors contributing to greenhouse gas emissions and decarbonization policies that have been implemented to address them. This information was recorded in the results section and synthesized in our study. The authors checked and revised the data during weekly meetings before finalizing the systematic review.

Interestingly, most studies on decarbonizing the building sector in Morocco have been published recently, with a significant increase in the number of studies published from 2018 onwards. This suggests a growing awareness of the need to decarbonize the building sector in the country. Additionally, it is important to highlight that the majority of studies were research articles, indicating a growing interest in decarbonizing the building sector within the scientific community.

In terms of the geographical location of the studies, it is noteworthy that most studies were conducted by researchers based in Morocco (54%), while the remaining studies were conducted by researchers based in Europe (20%), Asia (18%),

Table 1: The systematic approach for identification and selection of relevant papers.

| Define the topic area | Drivers of the decarbonization of the building sector in Morocco |
|---|---|
| Formulate research questions | This review aims to systematically analyze the existing literature on the decarbonization of the building sector in Morocco, identify the main drivers of this transition, and draw political implications that could be implemented to accelerate this process in the country. |
| Research questions | • What is the state-of-art in the literature on building sector decarbonization in terms of geographical locus, methods, and emerging research areas?<br>• What are the technological trends, underlining drivers, and enabling conditions for decarbonization?<br>• What are the policy implications of the transport sector in Morocco?<br>• What are the research gaps and recommendations for future studies? |
| Keyword search string | ("building" OR "construction" OR "habitat" OR "housing") AND ("decarbonization" OR "low-carbon transition" OR "low-carbon emissions" OR "carbon neutrality") AND ("strategies" OR "scenarios" OR "policies" |
| Electronic database | Scopus, Web of Science, and Google Scholar |
| Inclusion criteria | Analysis type: quantitative and qualitative<br>Article type: peer-review and grey literature published in English  Findings: scenarios, decarbonization policies, and knowledge gaps  Geography: Morocco<br>Period: 2000–2021<br>Sub-sector coverage: Residential and Industrial |
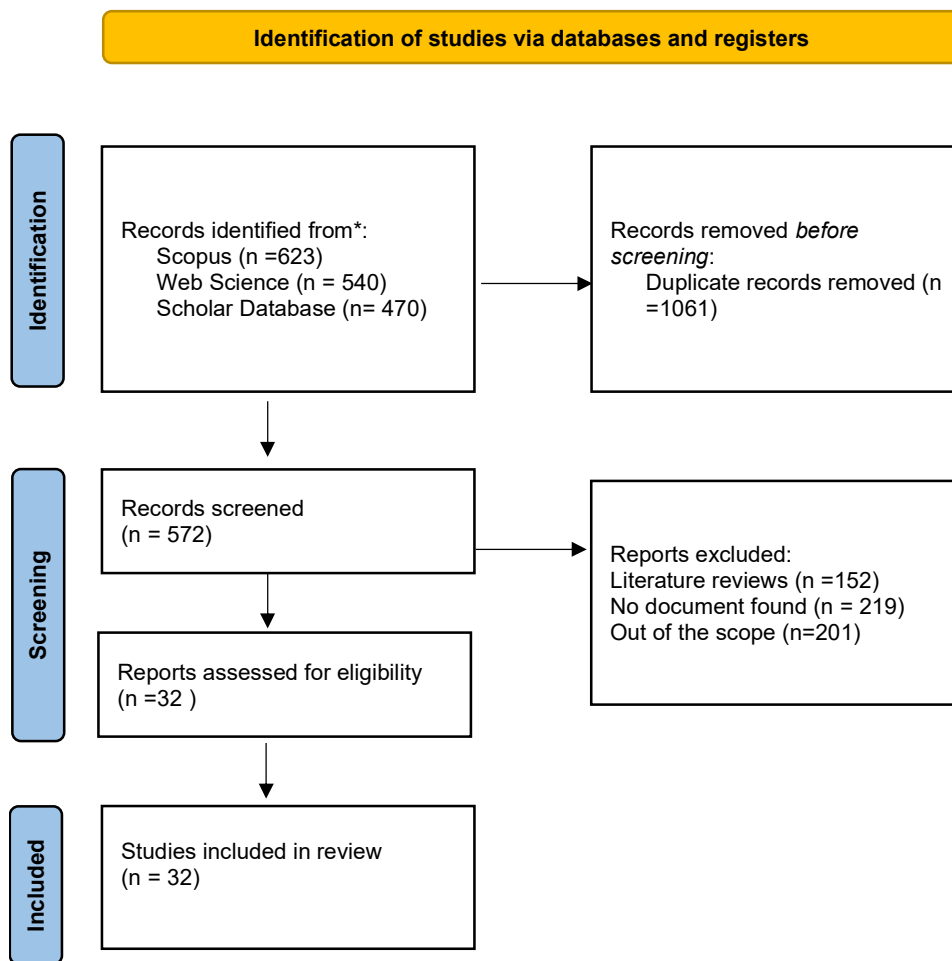
Fig. 2: PRISMA diagram for the systematic literature review.

and Africa (8%). This suggests a strong commitment of the Moroccan scientific community to research decarbonizing the building sector.

## RESULTS AND DISCUSSION

### Results

As part of the decarbonization of the building sector in Morocco, the characteristics of the identified studies reveal that the majority (60%) of studies focused on technical aspects such as emerging technologies and energy efficiency. Economic aspects were addressed in 30% of the studies, while social and behavioral aspects were addressed in only 10% of the studies. Additionally, nearly half of the studies (48%) used simulation models to evaluate the impact of different decarbonization policies and measures, while 26% conducted cost analyses. Renewable energy sources were studied in only 12% of the studies, indicating

significant potential for using alternative energy sources in decarbonizing the building sector. The use of multiple models in decarbonization research suggests that there is no universal approach to modeling the transition to a low-carbon economy. Instead, different models have been developed to serve various purposes and target different aspects of decarbonization. For example, some models focus on modeling the entire energy system, while others target specific sectors such as transportation, electricity, or industry. Additionally, some models are designed to simulate policy analysis scenarios, while others are better suited to studying technological solutions. The choice of model to use depends on the research question and study objectives.

The journals, as shown in Table 3, cover different areas related to the subject. The results show that the number of scientific publications in databases has significantly increased over the past 12 years, from 4 articles in 2010 to a peak of 12 articles in 2020. The trend shows an upward trend

Table 2: Details of published studies included in the review process.

| Index | Reference | Year | Research methods (model applied) | Model applied | Type of data | Publication Title | DOI |
|---|---|---|---|---|---|---|---|
| 1. | Nourdine & Saad 2021 | 2021 | Case studies | NA | Quantitative | Materials Today: Proceedings | 10.1016/j.matpr.2020.04.135 |
| 2. | Okpanachi et al. 2022 | 2022 | Case studies | NA | Quantitative | Futures | 10.1016/j.futures.2022.102934 |
| 3. | Cantoni & Rignall 2019 | 2019 | Case studies | NA | Quantitative | Energy Research & Social Science | 10.1016/j.erss.2018.12.012 |
| 4. | Choukri et al. 2017 | 2017 | Case studies | NA | Qualitative | Energy, Sustainability and Society | 10.1186/s13705-017-0131-2 |
| 5. | Makan et al. 2022 | 2022 | Modeling System | The PROMETHEE method | Quantitative | Environmental Science and Pollution Research | 10.1007/s11356-021-17215-w |
| 6. | Allouhi et al. 2022 | 2022 | Modeling System | Mathematical equations and simulations. | Qualitative | Energy Conversion and Management | 10.1016/j.enconman.2022.116261 |
| 7. | Dettner, F. and Blohm, M. 2021 | 2021 | | LCA approach with a health impact assessment (HIA) | Qualitative | Renewable and Sustainable Energy Transition | 10.1016/j.rset.2021.100002 |
| 8. | Eicke et al. 2021 | 2021 | Review | NA | Qualitative | Energy Research & Social Science | 10.1016/j.erss.2021.102240 |
| 9. | Almulla et al. 2022 | 2022 | Modeling System | Water Evaluation and Planning (WEAP) model to simulate water availability and use, as well as the Land Use and Cover Change (LUCC) model to project future land use changes. | Qualitative | Energy for Sustainable Development | 10.1016/j.esd.2022.08.009 |
| 10. | Saidi et al. 2023 | 2023 | Simulation Model | WRF-Chem | Quantitative | Atmospheric Environment | 10.1016/j.atmosenv.2022.119445 |
| 11. | Almulla et al. 2022a | 2022 | Modeling System | System dynamics model. | Quantitative | Energy for Sustainable Development | 10.1016/j.esd.2022.08.009 |
| 12. | Eicke et al. 2021 | 2021 | Review | NA | Qualitative | Energy Research & Social Science | 10.1016/j.erss.2021.102240 |
| 13. | Kasseh et al. 2023 | 2023 | Review | NA | Qualitative | Nature Environment and Pollution Technology | 10.46488/NEPT.2023.v22i01.015 |
| 14. | Almulla et al. 2022 | 2022 | Modeling System | Agriculture-Water-Energy Nexus analysis | Qualitative and quantitative data were collected through stakeholder consultations, field visits, and literature reviews. | Energy for Sustainable Development | 10.1016/j.esd.2022.08.009 |
| 15. | El Majaty et al. 2023 | 2023 | Review | NA | Qualitative | Materials Today: Proceedings | 10.1016/j.matpr.2022.07.094 |

| Index | Reference | Year | Research methods (model applied) | Model applied | Type of data | Publication Title | DOI |
|---|---|---|---|---|---|---|---|
| 16. | Essaghouri et al. 2023 | 2023 | Modeling System | LCA approach | Quantitative | Environmental Impact Assessment Review | 10.1016/j. eiar.2023.107085 |
| 17. | Fragkos 2023 | 2023 | Modeling System | TIMES-Morocco model | Quantitative | Energy Strategy Reviews | 10.1016/j. esr.2023.101081 |
| 18. | El Asri et al. 2022 | 2022 | Review | NA | qualitative | Energy Policy | 10.1016/j. enpol.2022.112944 |
| 19. | Eicke et al. 2021 | 2021 | Review | NA | qualitative | Energy Research & Social Science | 10.1016/j. erss.2021.102240 |
| 20. | Ouchani et al. 2022 | 2022 | Review | NA | Quantitative | Journal of Energy Storage | 10.1016/j. est.2022.105751 |
| 21. | Brunet et al. 2022 | 2022 | Modeling System | Multi-Criteria Decision-Making (MCDM) method | Quantitative | Energy Research & Social Science | 10.1016/j. erss.2021.102212 |
| 22. | Kettani & Bandelier 2020 | 2020 | Techno-economic assessment | NA | Quantitative | Desalination | 10.1016/j. desal.2020.114627 |
| 23. | Tahri et al. 2015 | 2015 | Modeling System | Geographic Information System (GIS) and Multi-Criteria Decision-Making (MCDM) | Quantitative | Renewable and Sustainable Energy Reviews | 10.1016/j. rser.2015.07.054 |
| 24. | Boussetta et al. 2017 | 2017 | Modeling System | Homer-pro | Quantitative | Sustainable Energy Technologies and Assessments | 10.1016/j. seta.2017.07.005 |
| 25. | Limami et al. 2023 | 2023 | Case studies | NA | Quantitative | Journal of Building Engineering | 10.1016/j. jobe.2023.106140 |
| 26. | Khouya 2020 | 2020 | Case studies | NA | Quantitative | International Journal of Hydrogen Energy | 10.1016/j. ijhydene.2020.08.240 |
| 27. | Laroussi et al. 2023 | 2023 | Case studies | NA | Quantitative | Materials Today: Proceedings | 10.1016/j. matpr.2022.07.323 |
| 28. | Adun et al. 2022 | 2022 | Modeling System | Artificial Neural Network model and a Gaussian Process Regression model for prediction analysis of the system's yield and efficiency. | Quantitative | Journal of Cleaner Production | 10.1016/j. jclepro.2022.133138 |
| 29. | Berrada & Laasmi 2021 | 2021 | Simulation Model | HOMER software | Quantitative | Journal of Energy Storage | 10.1016/j. est.2021.103448 |
| 30. | Wei et al. 2021 | 2021 | Modeling System | Geographic information system (GIS) modeling, statistical analysis | Quantitative | Environmental Impact Assessment Review | 10.1016/j. eiar.2021.106646 |

in publication production, and the number of publications on decarbonizing buildings is expected to increase beyond 2021.

Research has identified several technical and financial challenges to overcome to achieve these goals, such as improving the energy efficiency of existing buildings, promoting the use of renewable energy sources, optimizing heating and cooling systems, and establishing financing tailored to energy renovation projects. Additionally, studies have highlighted the importance of key policies and strategies to promote building decarbonization. These policies include stricter building standards, tax incentives for energy renovation projects, awareness-raising programs

Table 3: Scope of journals.

| Journal | ERA field of research | ERA field of research sub-category | No. |
|---|---|---|---|
| Energy for Sustainable Development | Sustainability Science | Energy and Climate Change | 5 |
| Energy Research & Social Science | Energy Systems Engineering | Energy Policy, Economics, and Social Sciences | 3 |
| Journal of Cleaner Production | Environmental Science and Management | Green and Sustainable Science and Technology | 2 |
| Journal of Energy Storage | Electrical and Electronic Engineering | Energy Storage | 2 |
| Materials Today: Proceedings | Materials Science and Engineering | Materials Science | 2 |
| Environmental Impact Assessment Review | Environmental Science and Management | Environmental Impact Assessment | 2 |
| Futures | Interdisciplinary Studies | Future Studies | 2 |
| Renewable and Sustainable Energy Reviews | Engineering | Renewable and Sustainable Energy | 2 |
| Energy Policy | Economics | Energy Economics | 2 |
| Energy Strategy Reviews | Energy Systems Engineering | Energy Strategy and Planning | 2 |
| Desalination | Engineering | Desalination and Water Treatment | 1 |
| Sustainable Energy Technologies and Assessments | Engineering | Sustainable Energy Technologies | 1 |
| Environmental Science and Pollution Research | Environmental Science and Management | Pollution Science and Technology | 1 |
| Energy Conversion and Management | Engineering | Energy Conversion and Management | 1 |
| Atmospheric Environment | Environmental Science and Management | Atmospheric Science | 1 |
| International Journal of Hydrogen Energy | Engineering | Hydrogen Energy | 1 |

Table 4: Simulation methodology applied in the reviewed papers over the study period.

| MODEL | 2015 | 2017 | 2019 | 2020 | 2021 | 2022 | 2023 | Total general |
|---|---|---|---|---|---|---|---|---|
| Mathematical equations and simulations. | | | | | | 1 | | 1 |
| TIMES-Morocco model | | | | | | | 1 | 1 |
| System dynamics model. | | | | | | 1 | | 1 |
| Geographic Information System (GIS) and Multi-Criteria Decision-Making (MCDM) | 1 | | | | | | | 1 |
| WRF-Chem | | | | | | | 1 | 1 |
| Geographic information system (GIS) modeling, statistical analysis | | | | | 1 | | | 1 |
| Artificial Neural Network model and a Gaussian Process Regression model for prediction analysis of the system's yield and efficiency. | | | | | | 1 | | 1 |
| Multi-Criteria Decision-Making (MCDM) method | | | | | | 1 | | 1 |
| HOMER software | | | | | 1 | | | 1 |
| The PROMETHEE method | | | | | | 1 | | 1 |
| Homer-pro | | 1 | | | | | | 1 |
| Water Evaluation and Planning (WEAP) model to simulate water availability and use, as well as the Land Use and Cover Change (LUCC) model to project future land use changes. | | | | | | 1 | | 1 |
| LCA approach | | | | | | | 1 | 1 |
| Agriculture-Water-Energy Nexus analysis | | | | | | 1 | | 1 |
| LCA approach with a health impact assessment (HIA) | | | | | 1 | | | 1 |

to encourage the adoption of sustainable practices, and the promotion of technological innovation to develop more effective decarbonization solutions. Finally, the review's results have emphasized the need for a comprehensive approach to encourage building decarbonization. This approach involves the participation of public and private stakeholders, coordination between different policies and strategies, as well as the establishment of a regulatory and financial environment conducive to stimulating innovation and the adoption of sustainable practices

## Discussion

The favorable conditions for the decarbonization of the building sector in Morocco are many. The Moroccan government has implemented a number of policies and programs to encourage the use of renewable energy sources and improve the energy efficiency of buildings. In addition, Morocco has a strong potential for renewable resources such as solar, wind, and hydro energy, which can be used to power buildings. The country also has a growing market for energy-efficient products and technologies in the construction sector, with more and more companies focusing on providing energy-efficient solutions for buildings. Finally, public awareness of environmental issues is constantly increasing, which may encourage building owners to opt for more environmentally friendly solutions. All of these conditions favor a successful transition to a decarbonized building sector in Morocco.

The building sector significantly contributes to greenhouse gas (GHG) emissions in Morocco, accounting for around 31% of total emissions. With increasing urbanization and demand for housing and commercial buildings, energy demand continues to grow, putting pressure on the energy system and GHG emissions. Although Morocco has implemented policies and measures to reduce building sector emissions, including through the National Energy Efficiency Program, challenges persist, such as a lack of funding, unclear regulations and standards, and a lack of awareness and training among market actors. To accelerate the transition to a decarbonized building sector, a coordinated and integrated approach is necessary, involving the participation of all actors, including governments, market actors, investors, and civil society.

**Advanced building demand management:** Adopting effective energy demand management practices is a cost-effective short-term measure that can quickly reduce greenhouse gas emissions in the building sector. Reviewed studies cited several options, including the use of high-efficiency lighting and air conditioning, green building design, energy needs reduction through effective insulation,

and the use of renewable energy sources for buildings. These practices can reduce greenhouse gas emissions while offering significant energy savings for building owners and occupants. However, implementing these practices often requires significant upfront investment and may require government policies to encourage widespread adoption. Policies can include subsidies, tax incentives, stricter building standards for new buildings, and energy renovation programs for existing buildings.

**Advanced technologies for building decarbonization:** Advanced technologies for building decarbonization can play a crucial role in reducing greenhouse gas emissions. According to the International Energy Agency (IEA), buildings are responsible for 28% of primary energy consumption worldwide and around 10% of $CO_2$ emissions. Advanced technologies, such as using durable and energy-efficient building materials, high-efficiency heating and cooling systems, installing solar panels to produce electricity, and using energy storage systems to optimize the use of renewable energy, could significantly reduce the carbon footprint of buildings. In fact, according to a study by the European Union, energy renovation of existing buildings could reduce the building sector's greenhouse gas emissions by 36% by 2030.

The decarbonization of the building sector can be achieved through the adoption of advanced technologies such as energy renovation of existing buildings, the use of low-carbon building materials, the use of high-efficiency heating, ventilation, and air conditioning systems, the installation of solar panels, and the use of geothermal energy. Governments can also promote building decarbonization by offering tax incentives and subsidies for energy renovation of buildings, introducing strict regulations on building energy efficiency and setting energy performance targets for new buildings. Advanced technologies for building decarbonization have significant potential to reduce greenhouse gas emissions in this sector, which can contribute to achieving the goals of the Paris Climate Agreement.

**Special mechanisms and public financing for the decarbonization of buildings in Morocco:** Special mechanisms and public financing for decarbonizing buildings in Morocco have the potential to stimulate the transformation of the construction sector toward a low-carbon future. However, a critical review of these mechanisms raises some concerns. Firstly, special mechanisms such as the Renewable Energy Development Fund (FDER) and the Fund for the Promotion of Energy Efficiency and Renewable Energy (FP2ER) can provide funding for renewable energy and energy efficiency projects in buildings. However, access to these funds can be difficult for businesses and individuals

who need financing for small or medium-sized projects. Additionally, changing government budget priorities may affect public financing for decarbonizing buildings. Investments in decarbonization programs can be reduced or canceled in times of budgetary pressure. This can compromise the financial viability of energy efficiency and renewable energy projects in buildings. Finally, the effective implementation of these mechanisms can be hindered by governance-related challenges, such as the complexity of application procedures, slow processing times, and a lack of transparency and accountability. In summary, while special mechanisms and public financing can provide crucial support for decarbonizing buildings in Morocco, additional measures may be needed to overcome potential obstacles to effective and large-scale implementation.

**Gaps in the literature and future research directions:** This systematic study provides an overview of the state of decarbonization in the building sector in Morocco. While several mechanisms and options for public financing have been implemented in Morocco, improvements are still possible. For example, the Green Investment Bank has only financed 10 projects, representing 40% of the total planned investments. Additionally, there is a need to expand financing options beyond energy efficiency projects and promote renewable energy sources, especially solar energy, in building design.

However, this study has highlighted 13 research gaps that need to be addressed to achieve the goal of net-zero emissions by 2050. First, only a few studies have considered the carbon budget when modeling decarbonization scenarios in the building sector. Second, long-term modeling studies are lacking that take into account the impact of renewable energy on building decarbonization. Third, most studies have ignored the impact of direct, indirect, and induced emissions on global warming, which can influence decarbonization policies. Fourth, economic variables, including prices, incomes, and employment, have not been adequately studied in decarbonization modeling studies of buildings. Fifth, there is a lack of research on the financing channels for sustainable construction options, with most studies assuming the availability of financing in the coming years. Finally, aspects related to consumer behavior, such as societal acceptance and lifestyle changes, need to be considered in modeling studies.

Overall, addressing these research gaps will enable the development of effective policies and strategies to decarbonize the building sector in member states.

**Strengths and limitations of the systematic review:** While the approach of the review was rigorous, the current study has some limitations. Firstly, the review strategy may suffer from language bias since the literature search was limited to articles published in the English language. Secondly, the number of search engines used was not exhaustive, and other databases may contain potentially interesting studies. Thirdly, the analysis did not focus on the social aspects of the transition. Finally, the review did not aim to evaluate the quality of the methodological approach or methods applied in the studies examined but to ensure that the selected documents used rigorous methods, a data search process, and a thorough analysis procedure. Therefore, the present study exhaustively examines the existing literature on the decarbonization of buildings in Morocco based on 73 studies published between 2010 and 2021.

## CONCLUSION

The energy transition of buildings is a significant issue in reducing greenhouse gas emissions. In academic and grey literature, studies on the decarbonization of the building sector have experienced significant growth in recent years. Publications are on an upward trend, reflecting the urgency of combating climate change. Studies focus on energy consumption modeling, energy efficiency evaluation, retrofitting of existing buildings, and the construction of new positive-energy buildings. The results show that policies aimed at encouraging energy efficiency improvement in buildings are the most effective in reducing greenhouse gas emissions. However, their implementation must be tailored to local contexts to take into account differences in building types, climatic conditions, and consumption habits. The energy transition of buildings requires the collaboration of all stakeholders, including governments, investors, building professionals, energy suppliers, and citizens. Public policies must be designed to encourage innovation, investment, and cooperation in the building sector to create more sustainable and resilient built environments in the face of the challenges of climate change.

## REFERENCES

Adun, H., Ishaku, H.P., Jazayeri, M., Adedeji, M., Shefik, A. and Dagbasi, M. 2022. Is the installation of photovoltaic/thermal for residential use in the MENA region feasible? A techno-economic and emission reduction discourse of the MENA region's commitment to the Paris Agreement. J. Clean Prod., 369: 133138. https://doi.org/10.1016/j.jclepro.2022.133138

Allouhi, H., Allouhi, A., Almohammadi, K.M., Hamrani, A. and Jamil, A. 2022. Hybrid renewable energy system for sustainable residential buildings based on solar dish stirling and wind turbine with hydrogen production. Energy Conv. Manag., 270: 116261. https://doi.org/10.1016/j.enconman.2022.116261

Almulla, Y., Ramirez, C., Joyce, B., Huber-Lee, A. and Fuso-Nerini, F. 2022. From participatory process to robust decision-making: An Agriculture-water-energy nexus analysis for the Souss-Massa basin in Morocco. Energy for Sustain. Develop., 70: 314-338. https://doi.org/10.1016/j.esd.2022.08.009

Becker, B.J. and Thompson, C.G. 2023. Meta-Analysis. Fourth Edition. Elsevier, The Netherlands, pp. 842-859. https://doi.org/10.1016/B978-0-12-818630-5.10092-2

Berrada, A. and Laasmi, M.A. 2021. Technical-economic and socio-political assessment of hydrogen production from solar energy. J. Energy Stor., 44: 103448. https://doi.org/10.1016/j.est.2021.103448

Boussetta, M., El Bachtiri, R., Khanfara, M. and El Hammoumi, K. 2017. Assessing the potential of hybrid PV–Wind systems to cover public facilities loads under different Moroccan climate conditions. Sustain. Energy Technol. Assess., 22: 74-82. https://doi.org/10.1016/j.seta.2017.07.005

Brunet, C., Savadogo, O., Baptiste, P., Bouchard, M. A., Cholez, C., Rosei, F., Gendron, C., Sinclair-Desgagné, B. and Merveille, N. 2022. Does solar energy reduce poverty or increase energy security? A comparative analysis of sustainability impacts of on-grid power plants in Burkina Faso, Madagascar, Morocco, Rwanda, Senegal and South Africa. Energy Res. Social Sci., 87: 102212. https://doi.org/10.1016/j.erss.2021.102212

Cantoni, R. and Rignall, K. 2019. Kingdom of the Sun: A critical, multiscalar analysis of Morocco's solar energy strategy. Energy Res. Social Sci., 51: 20-31. https://doi.org/10.1016/j.erss.2018.12.012

Choukri, K., Naddami, A. and Hayani, S. 2017. Renewable energy in emergent countries: lessons from energy transition in Morocco. Energy, Sustainability and Society, 7(1): 25.

Eicke, L., Weko, S., Apergi, M. and Marian, A. 2021. Pulling up the carbon ladder? Decarbonization, dependence, and third-country risks from the European carbon border adjustment mechanism. Energy Res. Social Sci., 80: 102240. https://doi.org/10.1016/j.erss.2021.102240

El Asri, N., Nouira, Y., Maaroufi, I., Marfak, A., Saleh, N. and Mharzi, M. 2022. The policy of energy management in public buildings procurements through the study of the process of delegated project management: The case of Morocco. Energy Pol., 165: 112944. https://doi.org/10.1016/j.enpol.2022.112944

El Majaty, S., Touzani, A. and Kasseh, Y. 2023. Results and perspectives of the application of an energy management system based on ISO 50001 in the administrative building: The case of Morocco. Mater. Today Proceed., 72: 3233-3237. https://doi.org/10.1016/j.matpr.2022.07.094

Essaghouri, L., Mao, R. and Li, X. 2023. Environmental benefits of using hempcrete walls in residential construction: An LCA-based comparative case study in Morocco. Environ. Impact Assess. Rev., 100: 107085. https://doi.org/10.1016/j.eiar.2023.107085

Fragkos, P. 2023. Assessing the energy system impacts of Morocco's nationally determined contribution and low-emission pathways. Energy Strat. Rev., 47: 101081. https://doi.org/10.1016/j.esr.2023.101081

González-Torres, M., Pérez-Lombard, L., Coronel, J. F., Maestre, I.R. and Yan, D. 2022. A review on buildings energy information: Trends, end-uses, fuels and drivers. Energy Rep., 8: 626-637. https://doi.org/10.1016/j.egyr.2021.11.280

Gruenig, M. and O'Donnell, B. 2016. Reshaping Equilibria: Renewable Energy Mega-Projects and Energy Security. In Lombardi, P. and Gruenig, M. (eds), Low-carbon Energy Security from a European Perspective. Academic Press, Cambridge, MA, pp. 109-134. https://doi.org/10.1016/B978-0-12-802970-1.00005-X

Kasseh, Y., Touzani, A. and EL Majaty, S. 2023. Exemplarity of the state for the energy efficiency of buildings institutional: The case of Morocco. Nature Environ. Pollut. Technol., 22(1): 169-177. https://doi.org/10.46488/NEPT.2023.v22i01.015

Kettani, M. and Bandelier, P. 2020. Techno-economic assessment of solar energy coupling with large-scale desalination plant: The case of Morocco. Desalination, 494: 114627. https://doi.org/10.1016/j.desal.2020.114627

Khouya, A. 2020. Levelized costs of energy and hydrogen of wind farms and concentrated photovoltaic thermal systems. A case study in Morocco. Int. J. Hydro. Energy, 45(56): 31632-31650. https://doi.org/10.1016/j.ijhydene.2020.08.240

Kober, T., Schiffer, H.W., Densing, M. and Panos, E. 2020. Global energy perspectives to 2060 – WEC's World Energy Scenarios 2019. Energy Strat. Rev., 31: 100523. https://doi.org/10.1016/j.esr.2020.100523

Laroussi, I., Huan, L. and Xiusheng, Z. 2023. How will the Internet of Energy (IoE) revolutionize the electricity sector? A techno-economic review. Mater. Today Proceed., 72: 3297-3311. https://doi.org/10.1016/j.matpr.2022.07.323

Limami, H., Manssouri, I., Noureddine, O., Erba, S., Sahbi, H. and Khaldoun, A. 2023. Effect of reinforced recycled sawdust-fibers additive on the performance of ecological compressed earth bricks. J. Build. Eng., 68: 106140. https://doi.org/10.1016/j.jobe.2023.106140

Liya, C. and Jianfeng, G. 2018. Scenario analysis of $CO_2$ emission abatement effect based on LEAP. Energy Procedia, 152: 965-970. https://doi.org/10.1016/j.egypro.2018.09.101

Lowans, C., Furszyfer Del Rio, D.D., Cameron, C., Ahmed, F., Al Kez, D., Brown, A., Hampton, H. and Foley, A.M. 2023. Energy Systems. In Garcia, J. (ed), Encyclopedia of Electrical and Electronic Power Engineering, Elsevier, The Netherlands, pp. 413-425. https://doi.org/10.1016/B978-0-12-821204-2.00004-0

Makan, A., Gouraizim, M. and Fadili, A. 2022. Sustainability assessment of wastewater treatment systems using cardinal weights and PROMETHEE method: A case study of Morocco. Environ. Sci. Pollut. Res., 29(13): 19803-19815. https://doi.org/10.1007/s11356-021-17215-w

Ministry of Energy and Mines - Kingdom of Morocco. 2020. National Energy Efficiency Strategy Horizon 2030.

Nourdine, B. and Saad, A. 2021. About energy efficiency in Moroccan health care buildings. Mater. Today: Proceed., 39: 1141-1147. https://doi.org/10.1016/j.matpr.2020.04.135

Nowell, L., Paolucci, A., Dhingra, S., Jacobsen, M., Lorenzetti, D. L., Lorenzetti, L. and Oddone-Paolucci, E. 2022. Interdisciplinary mixed methods systematic reviews: Reflections on methodological best practices, theoretical considerations, and practical implications across disciplines. Social Sci. Hum. Open, 6(1): 100295. https://doi.org/10.1016/j.ssaho.2022.100295

Okpanachi, E., Ambe-Uva, T. and Fassih, A. 2022. Energy regime reconfiguration and just transitions in the Global South: Lessons for West Africa from Morocco's comparative experience. Futures, 139: 102934. https://doi.org/10.1016/j.futures.2022.102934

Othmani, A., Kadier, A., Singh, R., Igwegbe, C.A., Bouzid, M., Aquatar, M.O., Khanday, W. A., Bote, M.E., Damiri, F., Gökkuş, Ö. and Sher, F. 2022. A comprehensive review of green perspectives of electrocoagulation integrated with advanced processes for effective pollutants removal from water environment. Environ. Res., 215: 114294. https://doi.org/10.1016/j.envres.2022.114294

Ouchani, F., Jbaihi, O., Alami Merrouni, A., Ghennioui, A. and Maaroufi, M. 2022. Geographic information system-based multi-criteria decision-making analysis for assessing prospective locations of pumped hydro energy storage plants in Morocco: Towards efficient management of variable renewables. J. Energy Stor., 55:105751. https://doi.org/10.1016/j.est.2022.105751

Sadeghian, O., Moradzadeh, A., Mohammadi-Ivatloo, B., Abapour, M., Anvari-Moghaddam, A., Lim, J.S. and Marquez, F.P.G. 2021. A comprehensive review on energy saving options and saving potential in low voltage electricity distribution networks: Building and public lighting. Sustain. Cities Soc., 72: 103064.

Saidi, L., Valari, M. and Ouarzazi, J. 2023. Air quality modeling in the city of Marrakech, Morocco using a local anthropogenic emission inventory. Atmos. Environ., 293: 119445. https://doi.org/10.1016/j.atmosenv.2022.119445

Tahri, M., Hakdaoui, M. and Maanan, M. 2015. The evaluation of solar farm locations applying geographic information system and multi-criteria decision-making methods: A case study in southern Morocco.

Renew. Sustain. Energy Rev., 51: 1354-1362. https://doi.org/10.1016/j.rser.2015.07.054

Dettner, F. and Blohm, M. 2021. External cost of air pollution from energy generation in Morocco. Renewable and Sustainable Energy Transition, 1: 100002.

Ugwu, J., Odo, K.C., Oluka, L.O. and Salami, K.O. 2022. A systematic review of renewable energy development, challenges, and policies in Nigeria with an international perspective and public opinions. Int. J. Renew. Energy Dev, 111, 287-308.

Wei, G., Zhang, Z., Ouyang, X., Shen, Y., Jiang, S., Liu, B. and He, B.J. 2021. Delineating the spatial-temporal variation of air pollution with urbanization in the Belt and Road Initiative area. Environ. Impact Assess. Rev., 91: 106646. https://doi.org/10.1016/j.eiar.2021.106646

# Ambient Air Quality Monitoring with Reference to Particulate Matter (PM$_{10}$) in Kolhapur City

C. S. Bhosale*, P. R. Mane***, J. S. Salunkhe***, V. M. Mothgare***, S. S. Sutar**, S. B. Manglekar*,
A. S. Jadhav* and P. D. Raut*†

*Department of Environmental Science, Shivaji University, Kolhapur, Maharashtra, India
**Yashwantrao Chavan School of Rural Development, Shivaji University, Kolhapur, Maharashtra, India
***Maharashtra Pollution Control Board, Kolhapur, Maharashtra, India
†Corresponding author: P. D. Raut; drpdraut@yahoo.co.in

## ABSTRACT

Air is an important medium for all living beings and is essential for the well-being of all. Monitoring of air is important to know the quality of air. The air quality monitoring was carried out in Kolhapur City under the National Air Monitoring Program. The present study involves the assessment of PM$_{10}$ as described in the National Ambient Air Quality Standards (NAAQS). The source apportionment study related to particulate matter was carried out in Kolhapur City. The study also determined the average PM$_{10}$ concentration in the city as it will be useful for preparing an action plan to reduce PM$_{10}$ concentration. PM$_{10}$ concentration was calculated as per the standard method adopted by CPCB. Sampling was carried out for 8 hours in three shifts twice a week at each sampling site for three consecutive years. Mahadwar Road (MR) and Dabholkar Corner (DC) were selected per the surrounding residential area, population density, and traffic conjunction. The third site Shivaji University (SUK), was selected as a control site. The results indicated that the PM$_{10}$ level has risen above the prescribed standards of NAAQS. The reason for the rise in PM$_{10}$ may be due to fossil fuel burning, construction activity, vehicles, and unpaved roads. The Analysis of Variance (ANOVA) technique is used to check the equality of the mean concentration of PM$_{10}$ at these three locations and found a significant difference between mean concentrations of PM$_{10,}$ suggesting increased particulate matter.

## INTRODUCTION

Determining the amount of particulate matter in the Earth's atmosphere was the initial focus of studies on atmospheric chemistry. Finding the sources, characteristics, and consequences of different chemical species in the clean and polluted air grew more important as air pollution became an increasing concern in many large cities. Urban air pollution is a significant issue in many countries throughout the world. According to the growing urbanization rates in Indian urban areas, poor air quality is essential to declining quality of life and negative consequences on people's wellness. Since crucial pollutants such as particulate matter (PM$_{10}$ and PM$_{2.5}$), NOx, SO$_2$, and O$_3$ are commonly found to exceed the National Ambient Air Quality Standard (NAAQS) limits and therefore, air quality monitoring has become increasingly important in recent decades (Guttikunda et al. 2014). The primary pollutant causing the decline in ambient air quality is particulate matter (PM) released from anthropogenic and natural sources.

The particulate matter is categorized as coarse (PM$_{2.5-10}$) and fine (PM$_{2.5}$) particles based on aerodynamic diameter. It was discovered that vehicular activity and associated emissions, including biomass burning, diesel generators, vehicles, and commercial coal burning, are the main PM sources. Vehicle exhaust and non-exhaust emissions were divided into two categories. Exhaust emissions come from a vehicle's tailpipe, whereas non-exhaust emissions come from the wear and tear of the vehicle, i.e. by abrasions of the brake, tire, clutch, and road dust re-suspension. These particles have been shown to harm human health and are released close to human activity (Buckeridge et al. 2002, Rissler et al. 2012).

In Indian cities, worsening urban air quality is a significant cause of health concerns. It was discovered that the amount of various dangerous contaminants and their concentration in the ambient environment exceeded health-based criteria. PM has been regarded as one of these pollutants' main public health issues. In the recent past, the

vehicular population in urban areas has taken up a hasty increase. It contributes a major part to declining ambient air quality in urban areas. Additionally, small-scale enterprises working inside urban communities were found to play a significant role in worsening the ambient air quality (Pant & Harrison 2013).

The current study area is Kolhapur City, a tourist place and industrial hub. Its increased urbanization and industrialization pose a threat to deteriorating the ambient air quality, especially from vehicular emissions. In Kolhapur alone, approximately 3 lakh commercial and private vehicles release 1 ton and more PM10 into the atmosphere daily. Thus, there is a compelling need to frame an air quality management plan to formulate effective strategies to control ambient air pollutants. National ambient air quality standards (NAAQS) have been established for the parameters particle matter ($PM_{2.5}$) of less than 2.5 microns and particulate of less than 10 microns ($PM_{10}$) (CPCB 2009, 2011).

## MATERIALS AND METHODS

Kolhapur city is known as Dakshin Kashi and Karveer Nagari, located on mountain ranges of the Western Ghats part of the Maharashtra state. The city has a network of 974.01 km of roads of different widths and types. It has a national highway of around 3.79 km, a state highway of around 29.41 km, other main district roads of around 1.87 km, and other roads of around 938.94 km.

There are 10,95,948 two-wheelers and 2,64,700 private and commercial vehicles registered in the city. The city Goddess Ambabai temple and 20 km away Shree Jotiba Temple is located, and all through the year, numerous festivals are celebrated in Kolhapur city. Therefore, the city is a popular tourist place all over the country. In the city, two industrial areas are Shivaji Udamnagar and Y. P. Powar Nagar. In those areas, foundries, showrooms, machine shops, and silver ornamental industries are situated. Many other developmental activities are increasing at a noticeable rate. Public transport facilities are also available in the city. In some villages, Kolhapur Municipal Transportation provides transportation for the city and around the city. CBS, Rankala Bus Stand, and Sambhaji Nagar Bus Stand are the state government's transport bus services hubs that provide inter-state and inter-district transport services for the public and freight. At the same time, roads and building construction activity, brick kilns, and increased road traffic, including private, commercial, and government vehicles, are responsible for the emission of particulate matter. A study was conducted to track the changes in ambient air quality from January to December of the years 2017, 2018, and 2019 to evaluate the ambient air quality in Kolhapur City. The

mean and standard deviation were used in the descriptive statistical analysis of $PM_{10}$ concentration, and a radar diagram and simple bar chart were used for the graphical presentation. to compare the mean $PM_{10}$ concentration at the chosen locations using the Analysis of Variance (ANOVA) method.

### Sampling Sites

The purpose of choosing the three sampling locations was to represent commercial, residential, and background site influences. Three places for sampling were chosen Dabholkar Corner (DC), Mahadwar Road (MR), and the Department of Environmental Science at Shivaji University (SUK). Dabholkar Corner is situated near the central bus stand, railway station, and private bus stand. In this area, many hotels, many shops, and lodges are situated. This area has dense traffic. Mahadwar Road is the main marketplace, and the goddess Ambabai temple is situated here. All pilgrims and local people visit the temple. The main clothing and vegetable market is here. Last few years in this area, lodges number has increased. Densely populated area situated around the Mahadwar Road site. Traffic congestion in these two; areas plays the main role in increasing air pollution. Shivaji University's location is at a minimum pollution level due to restricted activities in the university premises but in front of the university old Pune-Bangalore highway is situated. This road is one of the city's most important and busy roads. The locations of the sampling sites are shown in Fig. 1.

### Measurement Techniques

Particulate matter testing was carried out throughout 2017, 2018, and 2019. A sample of 24 hours is taken twice weekly at each sampling site. In Table 1, the details of sampling locations are given. Envirotech's calibrated APM 460DX and APM 460NL Respirable Dust samplers (RDS) were used for sampling at flow rates of 1.0 to 1.2 $m^3.min^{-1}$ as recommended by the CPCB on a pre-weighed 8 x 10-inch glass fiber filter paper. $PM_{10}$ was quantified using the gravimetric method (IS 5182 Part IV) and the HVS filtering method. The weight of the filter paper affects both the concentrations and quantity of dust collected. The sampling apparatus was set up three to ten meters above the ground. The collected samples were brought to Shivaji University's Environmental Science lab for further examination.

## RESULTS AND DISCUSSION

The $PM_{10}$ concentration was monitored at Shivaji University, Dabholkar Corner, and Mahadwar Road during 2017, 2018, and 2019. There were around 105 sampling days for each year. The $PM_{10}$ data varied from site to site, season to season,
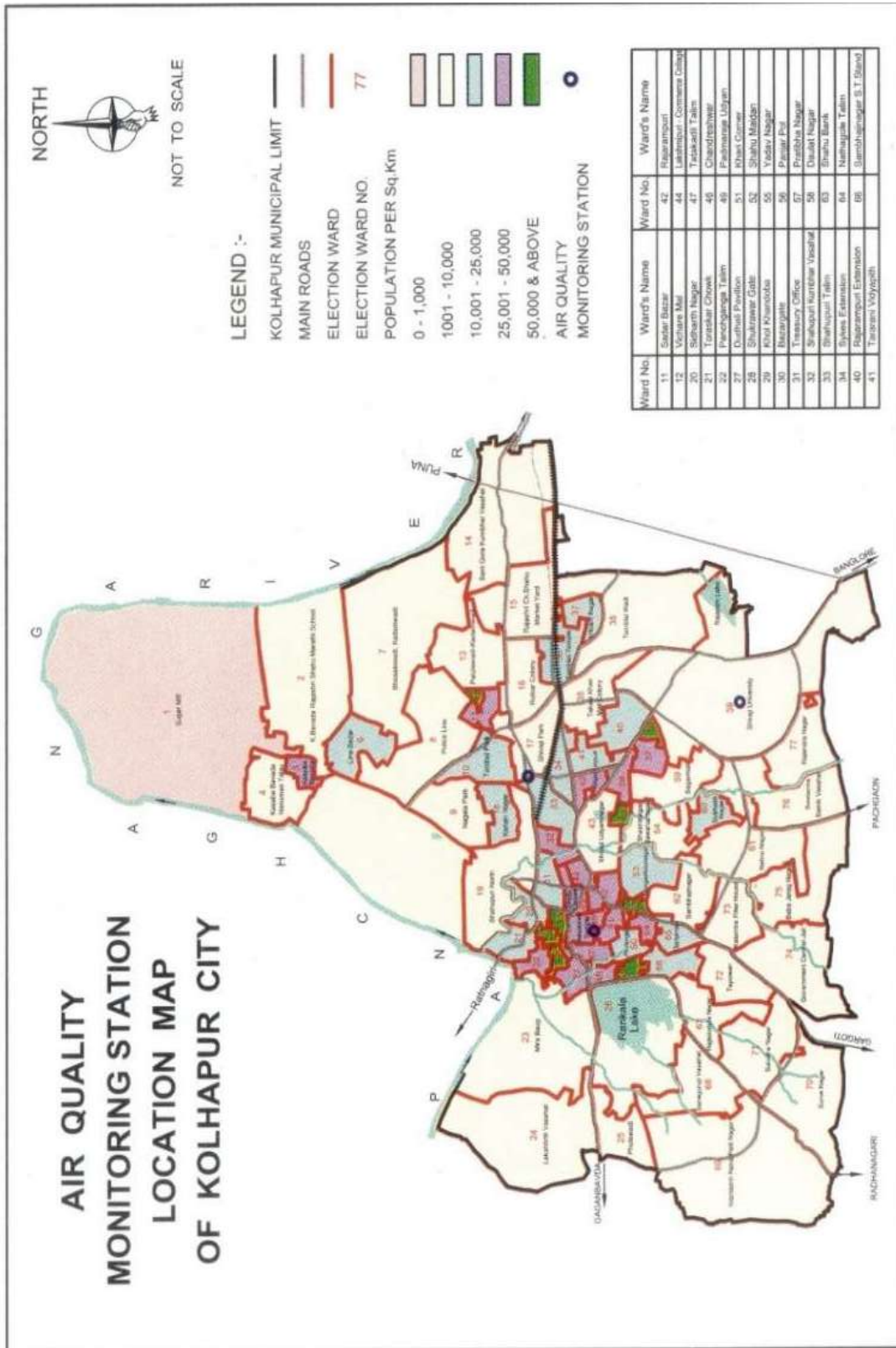
Fig. 1: Sampling Sites in Kolhapur City.

Table 1: Ambient Air Quality Monitoring Sampling Site of Kolhapur City.

| Sr. No. | Sampling site | Location | Status | Monitoring day and time |
|---------|---------------|----------|--------|-------------------------|
| 1. | Dabholkar Corner, Kolhapur | Longitude – 1615.35'42°" N | Ratnagiri highway, CBS, Railway station, main road to enter city, visitor's no is more, Commercial area | 2017, Monday 6 AM to Tuesday 6 AM |
| | | Latitude – 7430.25'14°" E | | 2018 -19, Wednesday 6 AM to Thursday 6 AM |
| | | Elevation – 1850 ft | | |
| 2. | Mahadwar Road, Kolhapur | Longitude - 1640.15'41°" N | Heavy traffic density, Vegetable and Cloth market, Goddess Ambabai temple, crowded area | 2017, Wednesday 6 AM to Thursday 6 AM |
| | | Latitude – 7418.40'13°" E | | 2018-19 Tuesday 6 AM to Wednesday 6 AM |
| | | Elevation – 1847 ft | | |
| 3. | Dept of Environmental Science, Shivaji University, Kolhapur | Longitude - 1636.00'40°" N | Educational Institute, less traffic, in front of University Old national highway is passes | 2017, Tuesday 6 AM to Wednesday 6 AM |
| | | Latitude – 7410.28'15°" E | | 2018-19 Monday 6 AM to Tuesday 6 AM |
| | | Elevation – 1956 ft | | |

i.e., from 30 to 150 and above. The frequency distribution of $PM_{10}$ concentration at these three locations, along with the standard, is shown in Fig. 3.

Fig. 3 shows that the maximum frequency of $PM_{10}$ concentration at the DC site where $PM_{10}$ exceeds the standard, i.e. $\mu g.m^{-3}$, was 72 times in 2017, 79 times in 2018, and 85 times in 2019. MR site where $PM_{10}$ exceeded the standard was 40, 34, and 49 times respectively. SUK site $PM_{10}$ concentration is not observed above the standard in all studied years.

The results of the study for locations SUK, DC, and MR are shown as a monthly mean concentration of $PM_{10}$ during 2017, 2018, and 2019 in Table 2. From the three locations studied, Dabholkar Corner's mean concentration of $PM_{10}$ exceeded the NAAQS limit, i.e., $100 \mu g.m^{-3}$ throughout the year except in monsoon season i. e. June, July, and August during 2017, 2018, and 2019. This location is near the central bus stand, railway station, and commercial area; hence, traffic intensity is maximum compared to other locations. The local sources found in metropolitan areas and the long-distance movement of the air pollutants play a significant role in assessing PM concentrations and sources. Developed nations have a greater variety of PM sources (Abulude 2016). This is followed by Mahadwar road $PM_{10}$ concentration which exceeded the NAAQS limit in January, February, March except 2018, April, May 2019, and December 2017, 2018, and 2019. Sometimes high air pollution load is observed at MR, a commercial area and one of the famous religious places in India. Hence, the large vehicular activity of the locals as well as tourists is observed in this place (Manglekar et al. 2015).

On the contrary, at the Shivaji University campus, $PM_{10}$ concentration was observed below the prescribed NAAQ standards in all seasons during 2017, 2018, and 2019, as it is located at the boundary of the city. The site has less

traffic density observed due to the educational institute and a large area covered by green plants. Trees absorb air pollution, reducing the concentration of contaminants in the air (Prajapat & Tripathi 2008). Due to their 'porous' nature, plants help remove and deposit airborne pollutants while influencing regional air pollutant dispersion patterns (Escobedo & Nowak, 2009, Fantozzi et al. 2015). Urban roadside plants' foliar surfaces serve as sinks for the deposition of PM, and as a result, they exhibit particular morphological, physiological, and biochemical responses. The deposition of PM particles on a leaf surface results in structural and functional alterations (Lalita & Kumar 2015).

The data analysis demonstrates unequivocally that $PM_{10}$ is becoming a crucial pollutant that requires special attention. Additionally, these particles are crucial in contributing to environmental issues, including climate change and reduced visibility (Gunasekaran et al. 2012). As $PM_{10}$ disperses over a wide area, it interacts chemically with respiratory system molecules, damaging the processes and causing unfavorable chemical changes. These might make people's lungs less capable (Ghose et al. 2005). It results in a negative relationship between precipitation and $PM_{10}$ concentration which can be explained by the well-known wet removal mechanism (Flossmann et al. 1985). The presence of $PM_{10}$ in the atmosphere has been linked to health problems, an increase in mortality, morbidity, and asthma (Dockrey et al. 1993). While drifting pollutants increase concentration per unit area in the summer, settling is the primary factor for reduced pollution levels during the rainy season (Patil et al. 2019). Because air pollutants, particularly $PM_{10}$, are washed off during precipitation, ambient pollutant concentration was at its lowest, with winter and summer recording the most significant levels (Manglekar et al. 2013).

Table 2: Month-wise average concentration (µg.m$^{-3}$) of Atmospheric PM$_{10}$ in Kolhapur City during 2017, 2018, and 2019.

| Sr. No. | Month | Year | Shivaji University | Dabholkar Corner | Mahadwar Road | NAAQS (2009) |
|---------|-------|------|--------------------|------------------|---------------|--------------|
| 1. | January | 2017 | 62.50 ±12.97 | **144.44** ±30.81 | **120.92** ±22.28 | 100 |
| | | 2018 | 80.86 ±12.07 | **146.45** ±28.02 | **126.70** ±24.71 | 100 |
| | | 2019 | 71.37 ±13.27 | **142.44** ±28.94 | **122.22** ±19.18 | 100 |
| 2. | February | 2017 | 59.11 ±11.69 | **140.36** ±31.27 | **104.25** ±22.58 | 100 |
| | | 2018 | 70.31 ±11.81 | **122.14** ±21.08 | **106.68** ±16.60 | 100 |
| | | 2019 | 70.05 ±10.22 | **135.07** ±20.94 | **118.92** ±16.11 | 100 |
| 3. | March | 2017 | 68.21 ±14.51 | **149.23** ±36.59 | **102.08** ±21.20 | 100 |
| | | 2018 | 70.10 ±12.29 | **116.74** ±19.97 | 97.76 ±11.64 | 100 |
| | | 2019 | 67.63 ±11.35 | **142.45** ±22.46 | **110.42** ±16.05 | 100 |
| 4. | April | 2017 | 78.56 ±12.25 | **150.78** ±30.67 | **109.80** ±16.21 | 100 |
| | | 2018 | 73.57 ±17.64 | **121.44** ±17.48 | **103.21** ±12.33 | 100 |
| | | 2019 | 70.23 ±12.75 | **138.12** ±20.90 | **118.13** ±18.02 | 100 |
| 5. | May | 2017 | 62.50 ±13.59 | **120.06** ±29.26 | 90.28 ±17.17 | 100 |
| | | 2018 | 63.50 ±10.07 | **112.15** ±21.78 | 88.27 ±17.47 | 100 |
| | | 2019 | 65.20 ±13.21 | **133.49** ±27.52 | **106.48** ±17.06 | 100 |
| 6. | June | 2017 | 51.93 ±17.83 | **104.05** ±17.91 | 75.91 ±16.66 | 100 |
| | | 2018 | 53.17 ±10.38 | 86.00 ±12.13 | 69.60 ±9.65 | 100 |
| | | 2019 | 53.14 ±14.55 | **103.17** ±11.40 | 83.81 ±11.82 | 100 |
| 7. | July | 2017 | 42.82 ±15.52 | 72.31 ±17.61 | 59.38 ±15.92 | 100 |
| | | 2018 | 47.07 ±7.40 | 97.52 ±15.86 | 74.11 ±10.85 | 100 |
| | | 2019 | 47.80 ±9.14 | 90.67 ±10.83 | 69.15 ±9.62 | 100 |
| 8. | August | 2017 | 39.66 ±13.32 | 80.56 ±19.79 | 62.58 ±16.35 | 100 |
| | | 2018 | 47.38 ±7.48 | **101.35** ±11.43 | 85.59 ±11.12 | 100 |
| | | 2019 | 50.52 ±10.90 | **100.42** ±12.55 | 78.53 ±12.37 | 100 |

Table Cont....

| Sr. No. | Month | Year | Shivaji University | Dabholkar Corner | Mahadwar Road | NAAQS (2009) |
|---------|-------|------|--------------------|------------------|----------------|--------------|
| 9. | September | 2017 | 43.19 ±12.80 | **102.62** ±23.09 | 73.96 ±17.90 | 100 |
| | | 2018 | 70.23 ±11.13 | **105.64** ±16.84 | 86.42 ±14.26 | 100 |
| | | 2019 | 60.01 ±7.74 | **120.79** ±16.54 | 83.33 ±11.36 | 100 |
| 10. | October | 2017 | 57.18 ±14.86 | **105.75** ±29.98 | 82.90 ±28.23 | 100 |
| | | 2018 | 52.16 ±9.29 | **107.72** ±10.43 | 86.34 ±8.38 | 100 |
| | | 2019 | 56.75 ±11.35 | **124.73** ±21.66 | 87.85 ±11.14 | 100 |
| 11. | November | 2017 | 57.41 ±10.85 | **109.64** ±17.95 | 95.99 ±15.42 | 100 |
| | | 2018 | 48.69 ±8.38 | **112.04** ±15.57 | 92.45 ±17.81 | 100 |
| | | 2019 | 53.70 ±10.29 | **111.81** ±18.68 | 95.14 ±13.96 | 100 |
| 12. | December | 2017 | 62.33 ±15.17 | **133.64** ±31.59 | **111.19** ±27.46 | 100 |
| | | 2018 | 66.32 ±10.24 | **135.11** ±24.88 | **114.12** ±16.47 | 100 |
| | | 2019 | 56.03 ±11.52 | **139.04** ±25.97 | **112.73** ±19.06 | 100 |

Note: Bold values show the concentration of $PM_{10}$ is above the NAAQS. Figures indicate Mean ± SD

Pollutants are transferred from the atmosphere to the surface of the ground through a process called deposition. Precipitation, scavenging, and sedimentation are its three constituent phenomena. The surface on which the particles are deposited is among the climatic factors and the characteristics of the particles that matter most (Damian 2019). Sharp edges, friction velocity, micro-scale roughness, and surface temperature significantly impact the deposition process, as demonstrated by Jonsson et al. 2008. Buildings and vegetation play a significant impact in metropolitan settings. According to earlier research, high winds frequently cause changes in vegetation density (Janhall 2015). It has been said that the primary factors governing the transport of air pollutants are wind speed and direction. These are all connected in some way to temperature. Put another way, the more wind there is, the more turbulence there is, and the more quickly and completely contaminants in the air disperse (Guttikunda & Gurjar 2012).

Fig. 2 shows the mean concentration of $PM_{10}$ below the NAAQS observed in SUK for 2017, 2018, and 2019. According to research on street canyons in central London (Jeanjean et al. 2017) and Leicester (Jeanjean et al. 2016), trees' aerodynamic effects outweighed their deposition effects. This is confirmed by the above results.

Mahadwar Road $PM_{10}$ concentration of January, February, and March, except for 2018, April, and May 2019, is above the NAAQ standards. Lack of road space and unplanned traffic hinder typical vehicular movements, which raises fuel consumption and exhaust emissions (Wijetileke & Krunatune 1995). In December every year, the $PM_{10}$ concentration is observed above the NAAQ standards, and Dabholkar corner represents the concentration of $PM_{10}$ always higher than the other locations except rainy season. Pollutant particulate matter in the sub-micron range, or $10^{-6}$ m diameter, is buoyant and stays suspended. A better knowledge of the relationship between particulates and morbidity points to the significance of sub-micron particles ($PM_{10}$), the primary source being motor vehicles (Anon 1995). A study on the assessment of ambient air quality concerning $PM_{10}$, $SO_2$, and $NO_2$ in the Bishnumati corridor, Kathmandu metropolis, found that heavy traffic and few roads without asphalt: perceivable mal-odor and the persistent stench emanating from the careless disposal and subsequent purification process, dense population, and increased commercial activities are other vital contributing sources to the end-result pollution of the corridor (Simkhada et al. 2005). People in Singapore, Japan, and Hong Kong are dealing with severe PM issues due to increased motorized
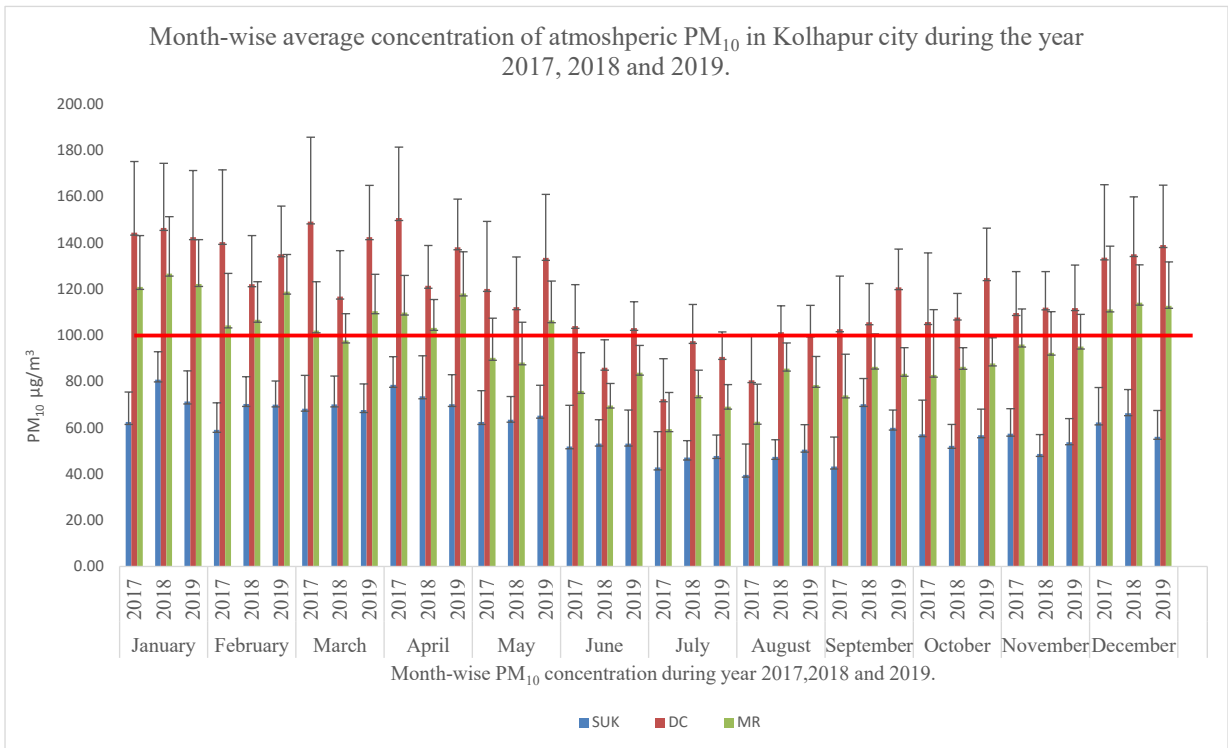
Fig. 2: Month-wise average concentration of atmospheric PM$_{10}$ in Kolhapur city during the years 2017, 2018, and 2019.
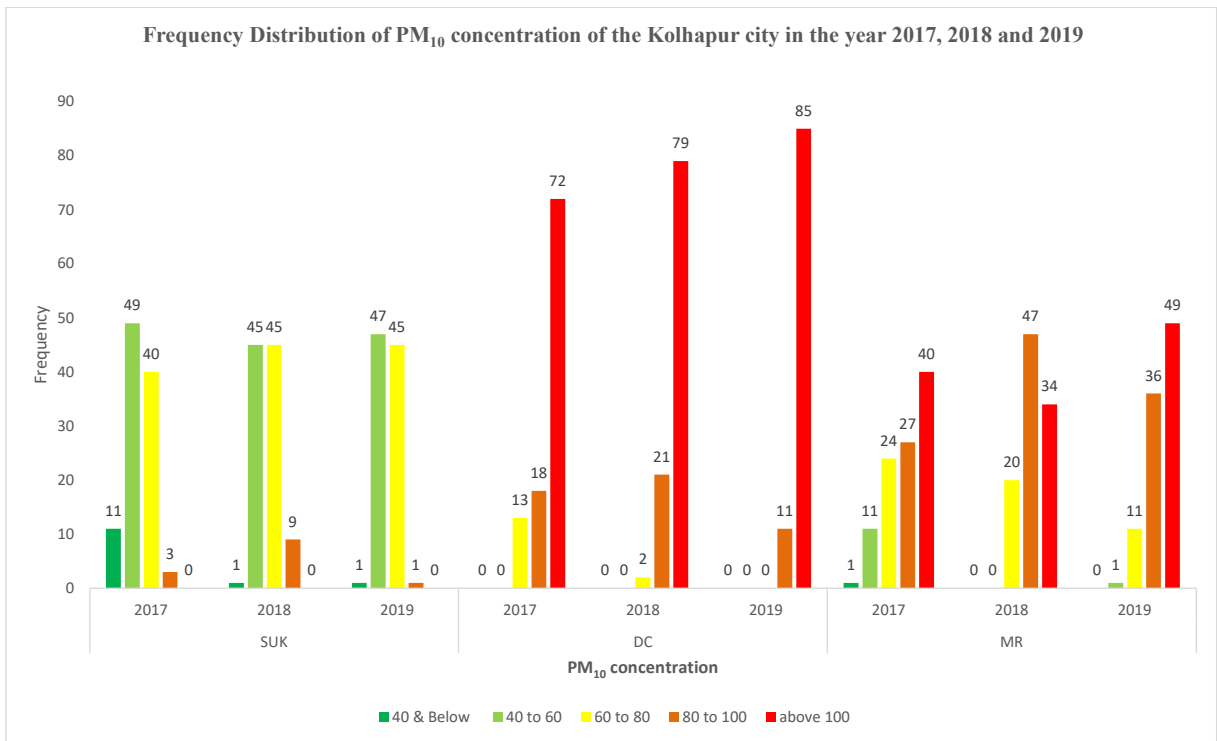


Fig. 3: Frequency distribution of PM$_{10}$ concentration of Kolhapur city in the years 2017, 2018, and 2019.

Table 3: One-way ANOVA test results for $PM_{10}$ based on different locations.

| The year 2017 | | | | | | | |
|---|---|---|---|---|---|---|---|
| Source | Sum of Squares | Degree of Freedom | Mean Square | F - Values | p- Value | F – critical value | Decision |
| Between locations | 22173.92 | 2 | 11086.96 | 27.2799 | $1.02 \times 10^{-7}$ | 3.2849 | Reject $H_0$: There is a significant difference between mean concentrations of $PM_{10}$ |
| Within locations | 13411.67 | 33 | 406.4141 | | | | |
| Total | 35585.58 | 35 | | | | | |
| The year 2018 | | | | | | | |
| Between locations | 16397.33 | 2 | 8198.663 | 36.5283 | $4.31 \times 10^{-9}$ | 3.28491 | Reject $H_0$ : There is a significant difference between mean concentrations of $PM_{10}$ |
| Within locations | 7406.756 | 33 | 224.4472 | | | | |
| Total | 23804.08 | 35 | | | | | |
| The year 2019 | | | | | | | |
| Between locations | 24446.62 | 2 | 12223.31 | 50.7384 | $8.57 \times 10^{-11}$ | 3.2849 | Reject $H_0$ : There is a significant difference between mean concentrations of $PM_{10}$ |
| Within locations | 7949.984 | 33 | 240.9086 | | | | |
| Total | 32396.6 | 35 | | | | | |

transportation (Edesess 2011). The study's multiple parameters have multiple sources for variation. They have to do with the variability of emissions from both point and non-point sources and potential changes in geographical factors such as mixed layer depth, wind speed, and relative humidity levels.

**Analysis by One-Way ANOVA Test**

The monthly mean concentration of $PM_{10}$ for the years 2017, 2018, and 2019 at three locations, namely Dabholkar Corner (DC), Mahadwar Road (MR), and Shivaji University (SUK) of Kolhapur City, was recorded. Interest is to test the equality of the mean concentration of $PM_{10}$ at three locations for a particular year. The claim was made with the help of one-way analysis of variance (ANOVA) technique. The null hypothesis ($H_0$) and alternative hypothesis ($H_1$) as $H_0$ were set. There is no significant difference between mean concentrations of $PM_{10}$ at three locations $H_1$: There is a significant difference between mean concentrations of $PM_{10}$ at three locations.

Now test $H_0$ against $H_1$ at a 5% level of significance (LOS). Table 3 reports the ANOVA results and shows that the p-values are significant for all three years. Thus, it can be concluded that there is a significant difference between mean concentrations of $PM_{10}$ at three locations for each year.

## CONCLUSION

Due to urbanization, an increase in the number of vehicles, industrialization, the use of fuel with poor environmental performance, and weak environmental legislation, ambient air quality has been steadily declining in India and other developing nations. The city of Kolhapur needs to control traffic pollution due to a higher level of $PM_{10}$ concentration at Dabholkar Corner than in the other two places. Shivaji University consistently has the lowest $PM_{10}$ concentration, ascribed to low traffic volume and rich canopy areas. The current study results show that greater transportation planning is required, with an awareness of the necessity for minimal automobile use and well-planned traffic routes. The Ambient Air Quality Network lays forth the fundamental guidelines for assessing the air quality of Kolhapur. Due to considerable traffic, particularly in the morning and evening, Dabholkar Corner has consistently displayed the highest $PM_{10}$ concentration. Shivaji University has low $PM_{10}$ concentrations, while Mahadawar Road has medium $PM_{10}$ concentrations. The concentration of $PM_{10}$ was found to be mostly associated with transportation and higher in the winter than in the summer or during the monsoon. ANOVA results indicate a significant difference between mean concentrations of $PM_{10}$ at these three locations. It is suggested that a sizable green plantation be established around the region. Alongside the highways, planting trees that are effective at retaining dust is recommended, and water should be sprayed continually where particulate matter is produced.

Some megacities in developed countries have recently shown signs of improvement in terms of PM. This is because the Urban Air Quality Management Plan (UAQMP) has been implemented (Gulia et al. 2015). According to a report from the European Environmental Agency (EEA), from 1990 to 2009, pollutants decreased by 16 percent ($PM_{10}$) and 21 percent, respectively ($PM_{2.5}$). It has also been noted that despite strenuous efforts, 18 to 49% of the populace in these nations is still in danger of exposure to $PM_{10}$ levels above the regulatory limits (EEA 2014). In US megacities, high PM concentration values from 1999 had decreased by

around 38% by 2010, yet in some places, the safety standards are being broken (USEPA 2012). But from 1997 to 2009, the average trend of $PM_{2.5}$ was more or less stable (Gulia et al. 2015).

## ACKNOWLEDGMENT

## REFERENCES

Abulude, F.O. 2016. Particulate Matter: An Approach to Air Pollution. Preprints, Basel, Switzerland, pp. 1-14.

Anon, S. 1995. Diesel Exhausts: A Critical Analysis of Emissions, Exposure, and Health Effects. Health Effect Institute, Cambridge, Massachusetts.

Buckeridge, D.L., Richard, G., Bart, J.H., Michael, E., Carl, A. and John, F. 2002. Effect of motor vehicle emissions on respiratory health in an urban area. Environ. Health Persp., 110(3): 293-300.

Central Pollution Control Board (CPCB). 2009. National Ambient Air Quality Standard. Gazette Notification, CPCB, New Delhi.

Central Pollution Control Board and Ministry of Environment (CPCB). 2011. Forest and Climate Change: Guidelines for the Measurement of Ambient Air Pollutants. Volume I. CPCB, New Delhi.

Damian, L. 2019, Landscape pattern as an indicator of urban air pollution of particulate matter in Poland. Ecol. Indic., 97: 17-24.

Dockery, D.W.C., Arden, P., Xiping, X.V., John, D., Spengler, J.H., Martha, E.F., Benjamin, G.F. and Frank, S. 1993. An association between air pollution and mortality in six US cities. N. Engl. J. Med., 329(24): 1753-1759.

Edesess, M. 2011. Roadside Air Pollution in Hong Kong: Why Is It Still So Bad? School of Energy and Environment, City University of Hong Kong, Kowloon, HK, pp. 1-19.

European Environment Agency (EEA). 2014. European Topic Centre on Air Pollution and Climate Change Mitigation. http://acm.eionet.europa.eu. Accessed January 2, 2014.

Escobedo F.J. and Nowak, D. 2009, Spatial heterogeneity and air pollution removal by an urban forest. Landsc. Urban Plan., 90: 102-110.

Fantozzi, F., Monaci, F., Blanusa, T. and Bargagli, R. 2015. Spatio-temporal variation of ozone and nitrogen dioxide concentrations under urban trees and in a nearby open area. Urban Clim., 12: 119-127.

Flossmann, A.I., Hall, W.D. and Purppacher, A. 1985. A theoretical study of the wet removal of atmospheric pollutants: Part I: The redistribution of aerosol particles captured through nucleation and impaction scavenging by growing cloud drops. Am. Meteorol. Soc., 42(6): 283-606.

Ghose, M.K., Paul, R. and Banerjee R.K. 2005, Assessment of the status of urban air pollution and its impact on human health in the city of Kolkatta. Environ. Monit. Assess., 108: 159.

Gulia, S., Shiva Nagendra, S., Khare, M. and Khanna, I. 2015. Urban air quality management: A review. Atm. Poll. Res., 6: 286-304.

Gunasekaran, R., Kumaraswamy, K., Chandrasekaran, P.P. and Elanchezhian, R. 2012. Monitoring of ambient air quality in Salem city, Tamilnadu. Int. J. Curr. Res., 4(3): 275-280.

Guttikunda, S.K. and Gurjar, B.R. 2012. Role of meteorology in the seasonality of air pollution in megacity Delhi, India. Environ. Monit. Assess., 184: 3199-3211.

Guttikunda S., Goel, R. and Pant, P. 2014. Nature of air pollution, emission sources, and management in the Indian cities. Atmos. Environ., 95: 501-510.

Janhall, S. 2015. Review on urban vegetation and particle air pollution: Deposition and dispersion. Atmos. Environ., 105: 130-137.

Jeanjean, A., Monks, P.S., and Leigh, R.J. 2016. Modelling the effectiveness of urban trees and grass on PM2.5 reduction via dispersion and deposition at a city scale. Atmos. Environ., 147: 1-10.

Jeanjean, A., Buccolieri, R., Eddy, J., Monks, P. and Leigh, R. 2017. Air quality affected by trees in real street canyons: the case of Marylebone neighbourhood in central London. Urban For. Urban Green., 22: 41-53.

Jonsson, L., Edvard, K. and Jonsson, P. 2008, Aspects of particulate dry deposition in the urban environment, J. Hazard. Mater., 153: 229-243.

Lalita, P. and Kumar, R.P. 2015. Roadside Plants: Study on Eco-Sustainability. Lambert Academic Publishing, London, UK, pp. 152.

Manglekar, S.B., Jadhav, A.S. and Raut, P.D. 2013. Ambient Air Pollution Monitoring: A Case Study of Kolhapur City, Maharashtra. National Conference of Aerobiology and Allergy (CANTAA), 29-30 November 2013, Pune, Maharashtra, pp. 29-30.

Manglekar, S.B., Jadhav, A.S. and Raut, P.D. 2015. Studies on ambient air quality status of Kolhapur city, Maharashtra, India during year 2013. Asian J. Water Environ. Pollut., 12(3): 15-22.

US Environmental Protection Agency (UEPA) 2009. National Ambient Air Quality Standards (NAAQS), EPA, USA.

Pant, P. and Harrison, R.M. 2013, Estimation of the contribution of road traffic emissions to particulate matter concentrations from field measurements: A review. Atmos. Environ., 77: 78-97.

Patil, V.N., Manglekar, S.B., Lad, R.J. and Raut, P.D. 2019. Ambient air quality monitoring and assessment of air pollution status at different locations in Kolhapur city. J. Res. Environ. Sci. Technol., 8(1): 47-49.

Prajapati, S.K. and Tripathi, D.B. 2008. Anticipated performance index of some tree species considered for green belt development in and around an urban area: A case study of Varanasi city, India. J. Environ. Manag., 88: 1343-1349.

Rissler, J., Swietlicki, E., Bengtsson, A, Boman, C., Pagels, J., Sandstrom, T., Blomberg, A. and Londahl, J. 2012. Experimental determination of deposition of diesel exhaust particles in the human respiratory tract. J. Aer. Sci., 48: 18-33.

Simkhada, K., Murthy, K. and Khanal, S.N. 2005, Assessment of ambient air quality in Bishnumati corridor, Kathmandu metropolis. Int. J. Environ. Sci. Tech., 3: 217-222.

US Environmental Protection Agency (USEPA). 2012. Our Nation's Air Status and Trends Through. Circular No. EPA-454/ R-12-001. USEPA, Washington, DC.

Wijetileke, I. and Krunatune, S.A.R. 1995. Air Quality Management Consideration for Developing Countries. Technical Paper No. 278. World Bank, Washington, DC, p. 77.

**Review Research Paper**       **Open Access Journal**

# Heavy Metal Remediation from Water/Wastewater Using Bioadsorbents - A Review

**Akhil Tewari\*, Dinesh S. Bhutada\*† and Vinayak Wadgaonkar\*\***

\*Department of Chemical Engineering, Dr. Vishwanath Karad MIT World Peace University, Pune-411038, India
\*\*Department of Petroleum Engineering, Dr. Vishwanath Karad MIT World Peace University, Pune-411038, India
†Corresponding author: Dinesh S Bhutada; dinesh.bhutada@mitwpu.edu.in

## ABSTRACT

This paper aims to emphasize heavy metals' impact on water and its removal mechanism with a focus on adsorption. Furthermore, factors affecting bio adsorption, such as temperature, pH, RPM, and initial heavy metal concentration, have been studied for different heavy metals and bioadsorbents. A comparison of their adsorption capacities and efficiencies has been made. This review reviewed different bioadsorbents for their suitability in removing cadmium, lead, and copper ions from water and wastewater, typically by using adsorption as a methodology. A suitable summary compares various heavy metal removal techniques and their advantages and limitations. For adsorption, the characteristics of bioadsorbents and their activation steps have been consolidated. Furthermore, the effects of operational parameters and adsorption mechanisms have been discussed in the review. Apart from assessing the suitability of bioadsorbent, a novel bioadsorbent has been suggested for copper ions removal. The findings shall be significantly useful in applying bioadsorbent in water/wastewater treatment fields to reduce heavy metal pollution. Thorough and well-planned research in this field can facilitate the creation of sustainable and durable technology for wastewater treatment, addressing the increasing demand for safe and dependable water resources, focusing on making it cost-effective and recyclable.

## INTRODUCTION

Water serves as an important raw material to most of the industries. Protection of this key component becomes a pivotal task for the present and future. Aside from industries, it is a vital food source for humans, animals, and other living beings, the basis for a wholesome environment. Water pollution due to heavy metals remains a key challenge, making it unsuitable for safe consumption (Malik et al. 2017, Sehyeong et al. 2021).

The inception of heavy metal pollution can be attributed to major operations such as smelting, foundries, mining the metal, and other operations in metal-based industries (Pham et al. 2019, Vaishnavi & Shelly 2015, Qasem et al. 2021). Common and toxic heavy metals in wastewater and sewage sludge include cadmium (Ca), chromium (Cr), mercury (Hg), copper (Cu), arsenic (As), nickel (Ni), silver (Ag), lead (Pb), and zinc (Zn). Each of these heavy metals has a detrimental effect on the health of living species, thus, these pollutants must be kept under limits (Pham et al. 2019, Malik et al. 2017).

Presently, significant work has been done for its removal using precipitation/coagulation, filtration, electrochemical treatment, and ion exchange treatment (Manisha et al. 2021,

Malik et al. 2017). Considering most of these methods, there are limitations to versatility in treatment, high cost of buildup, sludge disposal, and less technical maturity (Manisha et al. 2021, Malik et al. 2017, Naif et al. 2021).

Therefore, in this study, we will evaluate the work done on bio adsorbents (natural adsorbents) for removing heavy metals from wastewater with suitable operating conditions. The removal efficiency for different heavy metals (Pb, Cd, and Cu) will be compared using various agricultural waste-derived adsorbents.

## NEED OF HEAVY METAL REMOVAL FROM WATER

The presence of heavy metals poses a serious threat to human health. These metals are known to be lethal and carcinogenic, causing substantial damage to aquatic ecosystems and human health (Jamdade & Gawande 2015, Deniz et al. 2022). Contamination is a major challenge in modern times to provide quality potable water to mankind (Nadeem et al. 2021). Health disorders may range from nausea and skin irritation to neurological dysfunction and cancer (Vaishnavi & Shelly 2015, Qasem et al. 2021, WHO Guidelines for

Drinking Water Quality, 2011, 2017). Since these heavy metals are not biodegradable, there is a need for their removal by certain chemical/mechanical separation techniques (Mane et al. 2013). Data summarized below in Table 1 depicts the hazards associated with these heavy metals and their most prominent generation sources and limits defined by WHO.

As elucidated by Fig. 1, some heavy metals have their thresholds even at a concentration above 0.001 mg.L$^{-1}$. Studies have shown that apart from industrial wastewater, rivers, major water supply sources in cities & towns have particularly high heavy metal content (Vaishnavi & Shelly 2015, Jamdade & Gawande 2015).

## METHODS FOR HEAVY METAL REMOVAL

Various techniques have been developed to bring down the level of heavy metals in water. Broadly, there are three categories for reducing heavy metal concentration: physical, chemical, and biological, as shown in Fig. 2. There are certain techniques prominently used, currently being actively employed in industries/organizations, such as physical treatment: filtration (Zahra et al. 2023), sedimentation (Noureddine & Harvey 2020), coagulation/flocculation (Abujazar et al. 2022), adsorption (Nadeem et al. 2021), membrane filtration (Zahra et al. 2023), magnetic separation (Boruah et al. 2015), chemical treatment (Liang et al. 2020): chemical precipitation, ion exchange, reverse osmosis (Al-Alawy et al. 2017), electrochemical treatment (Trần et al. 2017), oxidation/reduction, co-precipitation, and biological treatment: advanced techniques like bioremediation (Monika & Surajit 2021), phytoremediation (Ram & Sangeeta 2010), biofiltration (Stefano et al. 2015), enzymatic treatment, microbial fuel cells (Wu et al. 2020) are employed.

Table 1: Heavy metals, WHO limit, and their effect.

| S.No. | Heavy Metal | WHO limit [mg.L$^{-1}$] | Primary Generation Source | Effect on humans | References |
|---|---|---|---|---|---|
| 1. | Cadmium | 0.003 | Batteries, paints, steel industry, plastic industries, metal refineries, and corroded galvanized pipes | Carcinogen, Kidney Dysfunction | (Vasihnavi & Shelly 2015, WHO Guidelines for Drinking Water Quality 2011,2017) |
| 2. | Chromium | 0.05 | Steel and pulp mills and tanneries | Carcinogen, Nausea, Diarrhea | (Vasihnavi & Shelly 2015, WHO Guidelines for Drinking Water Quality 2011,2017) |
| 3. | Mercury | 0.001 | Electrolytic chlorine and caustic soda production, runoff from landfills and agriculture, electrical appliances, Industrial and control instruments, laboratory apparatus, and refineries | Neurotoxin, Kidney dysfunction, Circulatory & Neurological Disorder | (WHO Guidelines for Drinking Water Quality 2011, 2017) |
| 4. | Copper | 2 | Corroded plumbing systems, electronic and cables industry | Liver Damage, Convulsions, Insomnia | (Vasihnavi & Shelly 2015, WHO Guidelines for Drinking Water Quality 2011, 2017) |
| 5. | Arsenic | 0.01 | Electronics and glass production | Skin Problems, Visceral Cancer | (WHO Guidelines for Drinking Water Quality 2011, 2017) |
| 6. | Nickel | 0.02 | Stainless steel and nickel alloy production | Carcinogen, Dermatitis, Gastrointestinal Disorder, Lung, Kidney Damage | (Vasihnavi & Shelly 2015, WHO Guidelines for Drinking Water Quality 2011, 2017) |
| 7. | Silver | 0.1 | electroplating, semiconductor manufacturing, photograph processing, and silver mining | bluish-gray discoloration of the skin, eyes, and mucous membranes, gastrointestinal symptoms, neurological effects, including tremors, seizures, and coma | (WHO Guidelines for Drinking Water Quality 2011, 2017) |
| 8. | Lead | 0.01 | Lead-based batteries, solder, alloys, cable sheathing pigments, rust inhibitors, ammunition, glazes, and plastic stabilizers | Central Nervous System Damage, Cerebral Disorders, Kidney and liver Reproductive System Dysfunction | (Vasihnavi & Shelly 2015, Qasem et al. 2021) |
| 9. | Zinc | 3 | Brass coating, rubber products, some cosmetics, and aerosol Deodorants | Skin irritation, nausea, depression, anemia, neurological symptoms | (Vasihnavi & Shelly 2015, WHO Guidelines for Drinking Water Quality 2011, 2017) |

Fig. 1: Graphical representation of WHO limit in mg.L$^{-1}$ for various heavy metals.
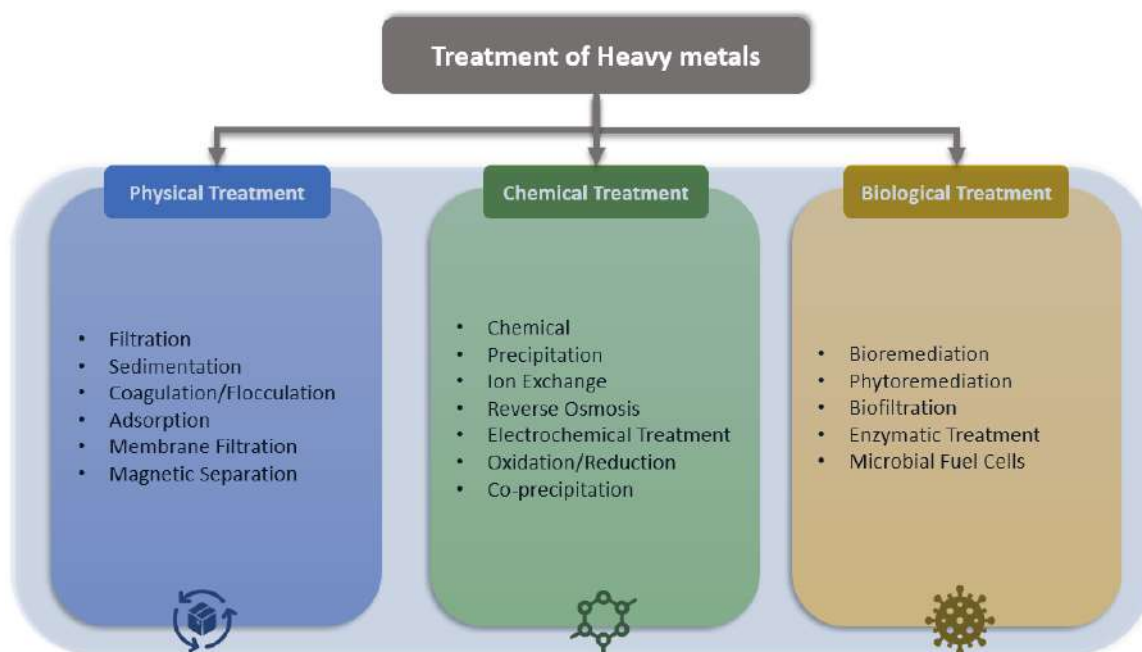


Fig. 2: Techniques available for heavy metal treatment in water/wastewater.

Despite significant efforts to remediate polluted environments using conventional techniques, many of these methods have proven ineffective in removing toxicants completely (WHO Guidelines for Drinking Water Quality 2011,2017, Abubakar et al. 2022). They often have significant drawbacks, including high energy requirements, production of secondary waste products, solvent loss, high operating and maintenance costs, operational complexity, phase separation difficulties, low efficiency, emulsion formation, and incomplete metal removal (Renu et al. 2017, Naseem 2012). Moreover, some traditional methods, such as electrodialysis, ultrafiltration, ion exchange, reverse osmosis, and precipitation, are not only expensive but also generate considerable amounts of sludge and secondary toxic waste products (Renu et al. 2017, Deen et al. 2021). Therefore, there is a need to consider a more efficient and sustainable remediation strategy to tackle the challenges of environmental pollution.

Considering the parameter mentioned earlier, as illustrated and summarized in Fig. 3, adsorption is found to be one of the most efficient methods in terms of cost, scalability, and operability (Manisha et al. 2021, Malik et al. 2017, Nadeem et al. 2021, Qasem et al. 2021).

**Suitability of Adsorption**

Adsorption has proven to be an efficient technique for the
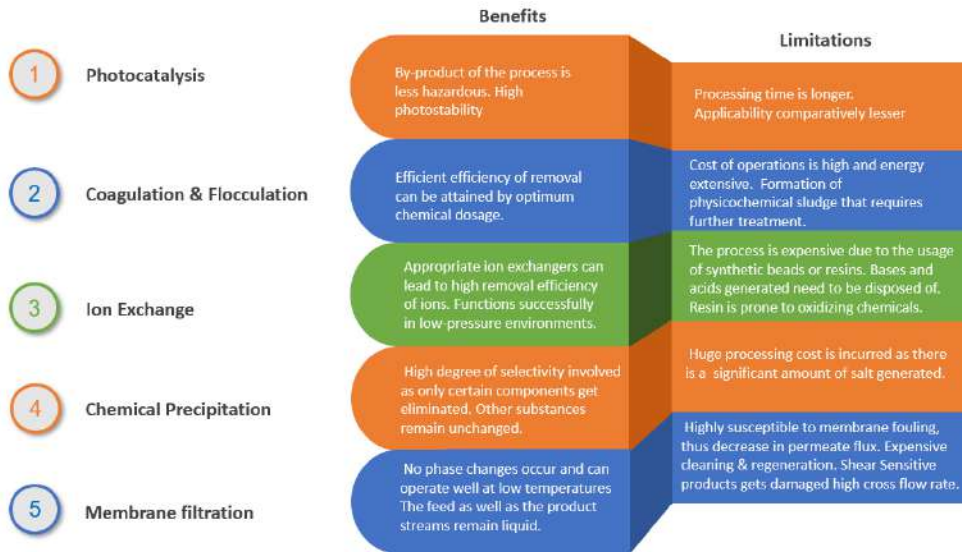
Fig. 3: Advantages and limitations of other treatment techniques.

removal of heavy metals due to multiple reasons. Various researchers have identified that high removal efficiency, even at low metal concentrations, can be obtained by adsorption techniques (Shahinur et al. 2015, Qasem et al. 2021, Deniz et al. 2022, Torres 2020). The rationale behind this is the mechanism by which adsorption works. Heavy metal ions attach to the adsorbent's surface (Malik et al. 2017, Gu et al. 2019).

We can choose and customize the adsorbent for each heavy metal, which makes this process highly selective (Sarthak et al. 2020, Gu et al. 2019). It allows us to target a specific heavy metal based on its functional group, surface charge, and pore size. The adsorption process is also versatile (Manisha et al. 2021) regarding operating parameters such as temperature, pressure, and pH (Naif et al. 2021). Additionally, it is found to produce minimum



Fig. 4: Factors affecting heavy metal adsorption.

waste and even offer great recyclability (Sarthak et al. 2020), thus making it a low-cost and sustainable technique, an ideal choice for the remediation of heavy metals. (Wai et al. 2021), Some commonly used adsorbents are activated carbon (Myalowenkosi et al. 2016), zeolites (Noureddine & Harvey 2020), chitosan (Zujin et al. 2019), clay mineral (Gu et al. 2019), like halloysite, bentonite, montmorillonite, vermiculite, organic water material derived material like biochar (Sarthak et al. 2020), and few advanced compounds such as nanoparticles (Boruah et al. 2015). All relevant factors which are found to have an impact on adsorption efficiency are shown in Fig. 4.

**Bio-Adsorbents as Suitable Adsorbent Media**

There is a certain limitation to the usage of chemical adsorbents. Among these, the primary issue is its high environmental impact and poor cost-effectiveness (Adewuyi 2020). As a sustainable alternative, bio-adsorbents can be utilized for similar purposes. There are many sources (refer to Fig. 5) and types of bio-adsorbents that can be customized for removing various heavy metals from water (Malik et al. 2017, Naif et al. 2021, Qasem et al. 2021). The source of generation can be plant-based, animal-based, microbial-based, algae and seaweed-based, or derived from fruit, vegetable, or food waste (Manisha et al. 2021, Nadeem et al. 2021, Abujazar et al. 2022, Deen et al. 2021). Several plants have lignin, cellulosic material, and other organic compounds normally utilized as bioadsorbent. Similarly, chitin and chitosan are derived from animal-based materials and have proven to have high adsorption capacities. Materials like eggshells (Carvalho et al. 2013, Zahir & Sheriff 2014) also can treat heavy metals. Aquatic plants such as algae and seaweed with high polysaccharides, protein, and other organic compounds also serve a similar purpose (Sarthak et al. 2020, Adewuyi 2020, Redha 2020). Food and fruits are proven adsorbents due to their abundance and organic content (Thachanan et al. 2018, Nadeem et al. 2021).

Apart from being eco-friendly, many properties make them typically suitable for such applications, which include large surface area, chemical composition, porosity, selectivity, low cost, and wider availability (Sabino et al. 2016). Generally, most of the bioadsorbents have substantial lignocellulosic content (refer Fig. 6), which provides them with a high surface area and porous structure, enabling a high number of active adsorption sites (Nadeem et al. 2021, Wu et al. 2020). This lignocellulosic structure contains multiple functional groups like amine, carboxyl, and hydroxyl, which enhances their affinity towards heavy metals (Naif et al. 2021).

Another important aspect is the elemental composition of bioadsorbent, which means the variety and content of elements present in the material. Testing methods, such as CHNS (Thachanan et al. 2018, Mohd et al. 2021), quantify this. Adsorption typically happens through chemical and electrostatic interactions (Naseem 2012, Sehyeong et al. 2021), where functional groups and metal ions interact on the surface of the adsorbent. Additional binding sites are made available if elements like sulfur, nitrogen, and oxygen are present, thus helping increase their adsorption capacity (Guat et al. 2022). These elements are even responsible for the structural stability of adsorbents, particularly phosphorus
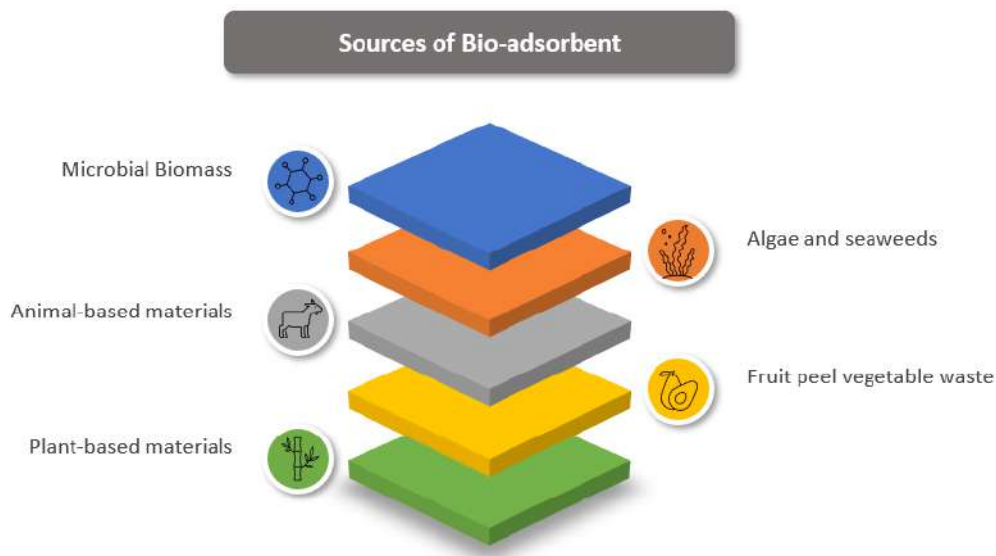


Fig. 5: Various sources of bio-adsorbent from nature.

Fig. 6: Lignocellulosic composition in different fruit waste (peels) (Nadeem et al. 2021, Kabenge et al. 2018, Wu et al. 2020, Pathak et al. 2017, Dammak et al. 2019).
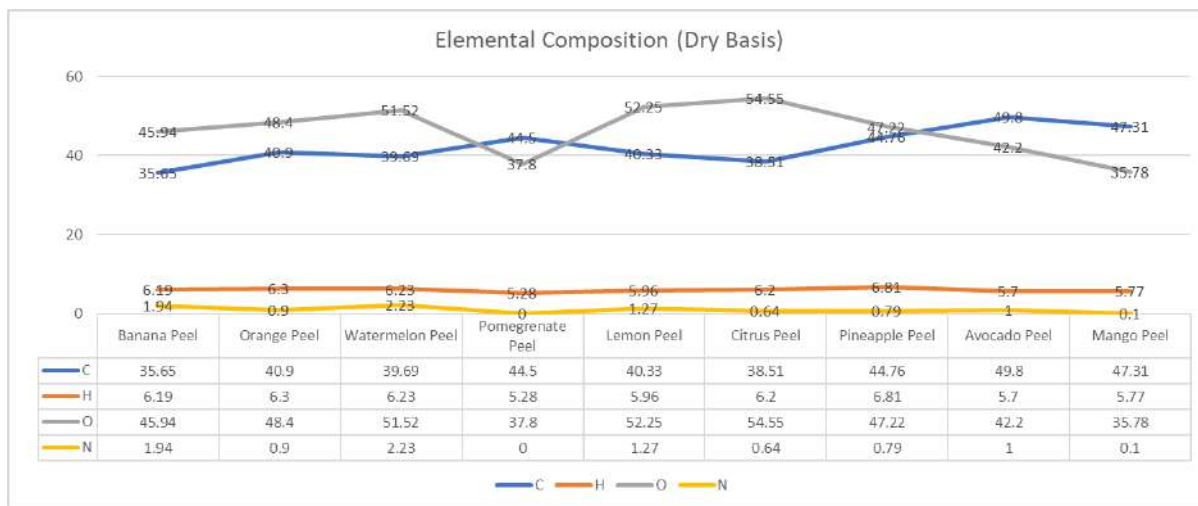


Fig. 7: Elemental composition in different fruit waste (peels) (Nadeem et al. 2021, Kabenge et al. 2018, Wu et al. 2020, Pathak et al. 2017, Dammak et al. 2019).

and silicon. In contrast, some elements like calcium and magnesium make them more resistant to degradation in acid or basic medium. Testing data of many agricultural wastes (Fig. 7) indicates a substantial presence of such elements, which makes them a suitable candidate for usage.

**Mechanism of Adsorption**

Adsorption is a process where ions, molecules, or atoms

from the first material (also known as adsorbate) form a thin layer on the second material (also known as adsorbent) due to forces of attraction that may be chemical or physical. The process can lead to single or multi-layer formation basis the external factors involved. It has varying applications, such as purification, separation, storage, etc. A few important terms that are associated with adsorption and are frequently used are adsorbate and adsorbent. Adsorbate is the material

being adsorbed, while adsorbent is the material on which it is adsorbed. The efficiency and interaction of adsorbate and adsorbent depend a lot on their characteristics and composition. There are two types of adsorptions: Physical adsorption (Sarthak et al. 2020) and Chemisorption (Thachanan et al. 2018). The adsorption process is majorly exothermic. Either physisorption or chemisorption, as the former causes a decrease in system entropy and free energy, while the latter involves the formation of new chemical bonds. As a result, physical adsorption is reversible, and chemisorption is not. Both adsorptions may occur concurrently in any given system, provided the process parameters are favorable. Thus, it can be said that entire bonding in adsorption happens by the bonding of adsorbates to the adsorbent surface via Van der Waals interactions, electrostatic interactions, and/or hydrogen bonds (Abujazar et al. 2022, Sabino et al. 2016, Sehyeong et al. 2021) (Maftouh et al. 2023).

The entire adsorption process depends on the concentration of adsorbate and adsorbent, surface area, pressure, temperature, and characteristics. While developing/design of any adsorption system, adsorption isotherm must be established. Prominently, Freundlich and Langmuir isotherms are developed. Both these isotherms determine how adsorption occurs in a system.

Mathematically, Freundlich isotherm can be written as

$$q = K_f \times Ce^{(1/n)}$$

Where,

q  = Amount of adsorbate adsorbed/ mass of adsorbent

Ce = Equilibrium concentration of the adsorbate in bulk phase

$K_f$ = Freundlich constant for determining adsorption capacity if the adsorbent

n  = Freundlich exponent for determining the intensity of adsorption

Langmuir adsorption isotherm can be written as

$$q = (q_{max} \times K \times Ce)/(1 + K \times Ce)$$

where

q = Amount of adsorbate adsorbed/ mass of adsorbent

Ce = Equilibrium concentration of the adsorbate in bulk phase

$q_{max}$ = is the maximum adsorption capacity of the adsorbent,

K = Langmuir constant related to the affinity of the adsorbent for adsorbate.

Isotherms are extensively explained in other research works (Sarthak et al. 2020, Pham et al. 2021, Shagufta et al. 2020, Jianlong & Can 2009), even though it is not detailed in this article.

## Preparation of Bio-adsorbent and Trials

The entire cycle of bioadsorbent application consists of multiple steps, starting from the selection of biomass to regeneration. First and foremost is the selection of biomass based on factors like their availability, cost, and efficiency for removing heavy metal. Post identification, the biomass is procured in raw form and is further prepared to make it fit for usage. In most cases, biomass is washed properly to remove external dust, contamination, or any other unwanted material, then dried and ground to a fine powder (Firomsa



Fig. 8: Typical bioadsorbent preparation and usage cycle.

et al. 2020, Jian et al. 2019, Gaurav et al. 2018). Drying temperature and time vary for every adsorbent.

In some cases, it is oven-dried, and in some, it is sun-dried (García-Vargas et al. 2020). The objective is to remove moisture and volatile content from the organic compounds without affecting their properties. Sometimes, the material is converted to carbon at very high temperatures if the objective is to use it in the same form (Sihem et al. 2012, Rajec et al. 2015, Opia 2018). In some cases, biomass is chemically treated to enhance its adsorption capacities (Rajkumar & Swati 2015, Adewuyi 2020). Fig. 8 depicts typical steps for the preparation of bioadsorbent followed and implemented by most researchers.

Once the adsorbent is ready, it is specifically characterized by determining its physical and chemical properties like surface area, composition, functional group, and porosity (Jian et al. 2019, Ali et al. 2019). These properties give a fair idea of the heavy metal impurities that can be removed and their optimization scope. Multiple tests are then performed to test the ability of the adsorbent prepared to remove heavy metals from the aqueous solution. This can be done by either mixing (for batch process) or just by contact through a packed column (for continuous process). The process is further optimized by varying parameters like the initial concentration of heavy metal, the dosage of adsorbent, pH, temperature, stirring time, or contact time to achieve the best removal efficiency (Maryam et al. 2020, Gregorio & Badot 2008). The biomass is sometimes regenerated by desorbing the heavy metal through an appropriate eluent, regenerated biomass and heavy metal removed can be utilized (Lata et al. 2015, Fouda-Mbanga et al. 2021). Based on the data points, the cost-effectiveness and efficiency of the adsorbent can be determined compared to other adsorbents.

For every trial, it is necessary to calculate adsorption efficiency. Typically, adsorption efficiency can be calculated as:

Adsorption efficiency % = $(C_i - C_f)/C_i \times 100$

where,

$C_i$ = Initial concentration of heavy metal in aqueous solution before adsorption

$C_f$ = Final concentration of heavy metal in aqueous solution after adsorption.

Similarly, in the case of regeneration, desorption percentage (%) is calculated, which can be given as:

Desorption percentage = (amount of adsorbate desorbed /amount of adsorbate adsorbed) x 100%

It is usually used to determine the effectiveness of the desorption process while regeneration and reusability of bioadsorbent are being considered. It indicates the extent to which heavy metals are removed from the surface of bioadsorbent. A higher value of desorption percentage is a positive indicator for recycling the adsorbent (Fouda-Mbanga et al. 2021, Redha 2020).

Additionally, the adsorption capacity (Opia 2018) of any bioadsorbent can be determined. It is mathematically written as

Adsorption capacity (mg/g) = $(C_i - C_f) \times (V/W)$

Where,

$C_i$ and $C_f$ are initial and final concentrations of heavy metal in water, V is the volume of solution, and W is the weight of the adsorbent. Adsorption capacity is a crucial parameter used to evaluate distinct adsorbents' usefulness in removing pollutants from water as it determines the amount of a pollutant that can be adsorbed per unit weight of the adsorbent.

## EFFECTIVENESS OF BIOADSORBENT IN HEAVY METAL REMOVAL

Existing studies have highlighted that different bio adsorbents, such as agricultural waste materials, algae, fungi, bacteria, and plant-based materials, can effectively remove heavy metals from contaminated water. Here, we will evaluate some of the work done to remove copper, lead, and cadmium using bioadsorbents.

### Removal of Copper (Cu) by Bioadsorbents

Copper (Cu) is among the toxic heavy metals introduced to water/wastewater due to industrial processes and natural deposits. Copper piping in plumbing systems is also a major source. The biosorption of copper has gained a lot of attention for its removal.

Table 2 shows the results of different studies on the adsorption of various components using different bioadsorbents. The adsorbents used in these studies include lentil shells, wheat shells, rice shells, papaya leaf powder, paddy straw powder, surfactant-modified laterite soil, powdered spent mushroom compost, banana peel, date pits, tea waste, dried marine algae (Hizikia fusiformis), and watermelon rind. The optimum pH, temperature, RPM, initial concentration, adsorption capacity, and removal efficiency for each study are also provided.

Data shows that the adsorbent's adsorption capacity and removal efficiency vary significantly depending on the adsorbate-adsorbent interaction. Date pits show a very high removal efficiency for an initial concentration of 1000 mg.L$^{-1}$, whereas banana peel is just 27.74% for an initial concentration of 5 mg.L$^{-1}$.

Table 2: Various sources of bio-adsorbent from nature for removal of copper.

| S. No. | Origin of adsorbent | Component used | Optimum pH | Temperature °C | RPM | Initial conc. mg.L⁻¹ or ppm | Adsorption capacity [mg.g⁻¹ or ppm] | Removal Efficiency | Reference |
|---|---|---|---|---|---|---|---|---|---|
| 1. | Lentil | Shells of the grains | 6 | 59.85 | 150 | 500 | 9.588 | 89.13% | (Haluk et al. 2008) |
| 2. | Wheat | Shells of the grains | 6 | 59.85 | 150 | 500 | 17.422 | 51.28% | (Haluk et al. 2008) |
| 3. | Rice | Shells of the grains | 6 | 59.85 | 150 | 100 | 2.954 | 35.43% | (Haluk et al. 2008) |
| 4. | Papaya | Leaf powder | 7 | Ambient | - | 20 | 24.63 | 85.00% | (Geetha & Anil 2016) |
| 5. | Paddy | Paddy straw powder | 7 | - | - | 20 | 37.17 | 65.00% | (Geetha & Anil 2016) |
| 6. | Laterite soil | Surfactant-modified laterite soil | 6 | 25+-2 | - | 10 | 185 | 91.56% | (Tien et al. 2017) |
| 7. | Mushroom compost - a mixture of mushroom mycelium, rubber tree sawdust, rice husk, and calcium carbonate | Powdered spent mushroom compost | 6 | ambient | 125 | 10 | 0.7 | 42.21% | (Kamarudzaman et al. 2022) |
| 8. | Banana | Banana peel | - | 50 | 100 | 5 | - | 27.74% | (Leong 2018) |
| 9. | Dates | Date pits | 7 | 25 | - | 1000 | - | 99.40% | (Thamer et al. 2015) |
| 10. | Tea | Tea waste | 7 | ambient | - | 200 | - | 94.62% | (Patrick et al. 2021) |
| 11. | Banana | Peels | <7 | 40 | - | 5 | - | 53.28% | (Leong 2018) |
| 12. | Dried marine algae | Hizikia fusiformis | 4 | 25 | - | 100 | 45.09 | 31.60% | (Pham et al. 2021) |
| 13. | Watermelon | Rind | 6.48 | 20 | - | 10 | 5.73 | 56.40% | (Liu et al. 2012) |

Table 3: Various sources of bio-adsorbent from nature for removal of Lead.

| S.No. | Origin of adsorbent | Component used | Optimum pH | Temperature °C | Initial conc. mg.L⁻¹ or ppm | adsorption capacity [mg.g⁻¹] | Removal efficiency | Reference |
|---|---|---|---|---|---|---|---|---|
| 1. | Orange | orange peels | 5-6 | Ambient | 10 | 0.97 | 97.87% | (Prasenjit et al. 2020) |
| 2. | Sugarcane | Bagasse | 6 | 30 | 0.8 | 1.61 | 89.31% | (Ezeonuegbu et al. 2021) |
| 3. | Polydopamine composite | - | - | - | 1 | 394 | 99.80% | (Daniel et al. 2018,) |
| 4. | Banana | Peels | <7 | 50 | 5 | - | 27.14% | (Leong 2018) |
| 5. | Banana | Peels | 13 | RT | - | 0.959 | 100.00% | (Rabiatul et al. 2019) |
| 6. | Dried Marine algae | Hizikia fusiformis | 4 | 25 | 100 | 167.73 | 10.90% | (Pham et al. 2021), |
| 7. | Biochar of pinewood or rice | Husk | 5 | 45 | 20 | 4.25 | 95.00% | (Zhengang and Fu-Shen 2009) |
| 8. | natural American bentonite | - | 5.5 | 25 | 200 | 427 | 95.00% | (Naeema 2014), |
| 9. | M. oleifera, | - | 6 | 27 | 10 | 5.6 | 86.00% | (Gautam et al. 2020) |
| 10. | Peanut | Shell | 6 | 27 | 10 | 1.7 | 78.00% | (Gautam et al. 2020) |
| 11. | P. juliflora | - | 6 | 27 | 10 | 1.4 | 72.00% | (Gautam et al. 2020) |
| 12. | Sugarcane | Bagasse | 6.0 | 30 | 0.8 | 1.61 | 89.31% | (Ezeonuegbu et al. 2021) |
| 13. | Papaya | Seed | - | Ambient | 100 | 8.5 | 85.00% | (Zahir & Sheriff 2014) |
| 14. | Chicken Egg | Shell | - | Ambient | 100 | 8.2 | 82.00% | (Zahir & Sheriff 2014) |
| 15. | Coconut | Leaf powder | - | Ambient | 100 | 9 | 90.00% | (Zahir & Sheriff 2014) |
| 16. | Tea | Brewed tea waste | 1.0 | 20 | 100 | 1.197 | 97.97% | (Hakan et al. 2020) |
| 17. | Tea | Tea waste | 5.0 | 25 | 100 | 33.49 | 85.00% | (Wan 2014), |
| 18. | Walnut | Walnut shell | 4.0 | 20 | 100 | 9.912 | 90.00% | (Çelebi & Gök 2017) |

Table 4: Various sources of bio-adsorbent from nature for removal of Cadmium.

| S. No. | Origin of adsorbent | Component used | Optimum pH | Temperature °C | Initial conc. mg.L$^{-1}$ or ppm | adsorption capacity [mg.g$^{-1}$] | Removal Efficiency | Reference Name |
|---|---|---|---|---|---|---|---|---|
| 1. | Natural phosphate | - | 5 | Ambient | - | - | 78.00% | (H.Yaacoubia et al. 2013) |
| 2. | Watermelon | Rind | 9.12 | 20 | 500 | 40.16 | 80.00% | (Husein et al. 2017) |
| 3. | Watermelon | Rind | 5 | Room temperature | 50-200 | 63.29 | - | (Lakshmipathy et al. 2013) |
| 4. | Orange | Dried orange peel powder [DOPP] is chemically modified with nano-silica (SiO$_2$) | 6.5 | Ambient | 50 | 142 | 95% (max) | (Jyoti et al. 2021) |
| 5. | Cork biomass | - | 6 | 40 | 10-100 | 14.77 | 64.48% | (Fouad et al. 2016) |
| 6. | Papaya | Seed | - | Ambient | 100 | 7.9 | 79.00% | (Zahir & Sheriff 2014) |
| 7. | Chicken Egg | Shell | - | Ambient | 100 | 8.6 | 86.00% | (Zahir & Sheriff 2014) |
| 8. | Coconut | Leaf powder | - | Ambient | 100 | 8.5 | 85.00% | (Zahir & Sheriff 2014) |
| 9. | Tea | Brewed tea waste | 4 | 20 | 100 | 1.163 | 84.74% | (Hakan et al. 2020) |
| 10. | Tea | Tea waste | 5 | 20 | 5 | 1.76 | 99.50% | (Ghasemi et al. 2017) |
| 11. | Tea | Tea waste | 5 | 25 | 20 | 16.87 | 45.00% | (Wan 2014) |
| 12. | Capparis decidua | branches and leaves | 6 | Room temperature | 249 | 248.62 | 80.00% | (Muhammad et al. 2021) |
| 13. | Ziziphus mauritiana | branches and leaves | 6 | Room temperature | 249 | 235.65 | 80.00% | (Muhammad et al. 2021) |
| 14. | Rice | Rice husk | 9 | Room temperature | 200 | - | 80-90% | (Salman & Khan 2015) |
| 15. | Wood | sawdust | 9 | Room temperature | 300 | - | 80-90% | (Salman and Khan 2015) |
| 16. | Dried Marine algae | Hizikia fusiformis | 4 | 25 | 100 | 42.08 | 14.90% | (Bich et al. 2021) |

The optimum pH for most cases is 6-7, with dried marine algae (*Hizikia fusiformis*) as the only exception (Pham et al. 2021, Haluk et al. 2008, Geetha & Anil 2016, Tien et al. 2017, Kamarudzaman et al. 2022, Leong 2018).

## Removal of Lead (Pb) by Bioadsorbents

Lead contamination must be removed critically to protect people's health and lives. Exposure to Lead while drinking water can have severe and prolonged health complications, particularly in women and children (Prasenjit et al. 2020, Ezeonuegbu et al. 2021). Even low concentrations of lead exposure can cause growth-related setbacks, reduced IQ, and behavioral challenges in children. For adults' kidney damage, reproductive problems, and high blood pressure are prominent diseases (Deen et al. 2021). Various industries, such as batteries, paint, plastic, automobile, steel, etc., contribute significantly to this increased level of lead in water (Salman & Khan 2015, Ezeonuegbu et al. 2021).

In Table 3, Lead removal data is compared using natural adsorbents and their corresponding adsorption capacities and removal efficiencies for water treatment. It can be observed that some adsorbents, such as polydopamine composite, have an outstanding adsorption capacity of 394 mg.g$^{-1}$, with a remarkable removal efficiency of 99.8%. Additionally, natural American bentonite displays an impressive adsorption capacity of 427 mg.g$^{-1}$, with a 95% removal efficiency. Sugarcane bagasse and banana peels exhibit moderate adsorption capacities, with sugarcane bagasse showing a capacity of 1.61 mg.g$^{-1}$ and banana peels ranging from 0.97 to 27.14 mg.g$^{-1}$, depending on pH and temperature. The removal efficiency of these adsorbents ranges from 78% to 89.31%. Other adsorbents, such as dried marine algae (Hizikia fusiformis), tea waste, and walnut shells, demonstrate good adsorption capacities, ranging from 1.197 to 167.73 mg.g$^{-1}$, with removal efficiencies ranging from 85% to 97.97%.

Adsorbents like papaya seeds, chicken eggshells, and coconut leaf powder exhibit moderate to good removal efficiencies, ranging from 82% to 90%. The optimum pH for most cases is within the range of 6-7.

## Removal of Cadmium (Cd) by Bioadsorbents

Like lead and copper, cadmium also possesses considerable health concerns. It can pile up in the body over time, leading to various health problems. Long-term exposure to cadmium-polluted drinking water can cause kidney damage, leading to kidney disease and failure (Lakshmipathy et al. 2013, Ghasemi et al. 2017) (Wan 2014). It can also affect the bones, causing osteoporosis and damage to the liver and lungs. There are various sources of cadmium in water: Natural sources of cadmium include the weathering of rocks and soils, while anthropogenic sources consist of manufacturing processes, mining activities, and improper disposal of waste materials (Vaishnavi & Shelly 2015, WHO Guidelines for drinking water quality 2011, 2017).

Different bioadsorbents have been tried for cadmium removals, such as natural phosphate, watermelon rind, orange peel powder, cork biomass, papaya seed, chicken eggshell, coconut leaf powder, tea waste, *Capparis decidua*, *Ziziphus mauritiana*, rice husk, sawdust, and dried marine algae. Data in Table 4 show that each adsorbent's adsorption capacity and efficiency vary based on the origin, component used, pH, temperature, initial concentration, and other factors. For instance, the highest removal efficiency was observed with orange peel powder chemically modified with nano-silica (Jyoti et al. 2021), with a maximum of 95%. Meanwhile, rice husk and sawdust showed an 80-90% removal efficiency for initial concentrations of 200 and 300 mg.L$^{-1}$, respectively. In contrast, dried marine algae showed a low removal efficiency of only 14.9%. The study highlights the potential of various natural adsorbents as an effective and eco-friendly solution for removing contaminants from water (Wan 2014, Muhammad et al. 2021). The results suggest that orange peel powder chemically modified with nano-silica, rice husk, and sawdust can be an efficient adsorbent for removing contaminants from water. The findings also emphasize the importance of considering the origin, component used, pH, temperature, and initial concentration while selecting an appropriate adsorbent for water treatment. (Yaacoubia et al. 2013, Husein et al. 2017, Lakshmipathy et al. 2013, Jyoti et al. 2021, Fouad et al. 2016).

## CONCLUSION

Minimizing pollutant and pollution sources in water is of utmost importance as fresh water is significantly scarce worldwide. Reiterating that these adsorbents are economical and environment friendly makes them quite a suitable option compared to traditional alternatives such as chemical precipitation & ion exchange. The alternatives have been generating residues that are difficult to dispose of. In this study, we learned that the efficacy of bio adsorbents is dependent on factors such as the type of bio adsorbent, its concentration and type of heavy metal ions in the solution, the pH of the solution, the contact time between the bio adsorbent and the solution, and the temperature of the solution. Conclusively, the data presented in this study shows bio adsorbents have an encouraging future as eco-friendly and economical alternatives to conventional water treatment methods and environmental remediation. Research in this direction can subsequently lead to various applications and increased efficiency.

## FUTURE OF BIOADSORBENT AND FURTHER SCOPE OF WORK

The multipronged benefits of bioadsorbent usage could play a significant role in addressing environmental challenges, an extreme area of concern, such as water pollution and air pollution. It can additionally pave the path for the development and acceptability of sustainable technologies for multiple industries. Evolutionary advances in Biotechnology and Materials Science can also be expected to contribute to developing innovative bio adsorbents. These adsorbents would certainly aid us with enhanced properties and performance. Principally, the future of bio adsorbents looks up and coming. This ingenuity has notable potential for important contributions to environmental safeguarding and sustainability. During the entire literature survey, it was identified that Lablab purpureus pod/seedcase (locally called Pavta in India) is not yet utilized as a bioadsorbent, particularly for copper removal. It is widely grown in Asia, Africa, and some of America. As a legume crop, *Lablab purpureus* is known to be a good source of lignocellulosic material. Thus, learning from data shows that it has the potential to become an adsorbent. Appropriate study and testing to be done further for its characterization and efficiencies.

## ACKNOWLEDGMENTS

## REFERENCES

Abujazar, M.S.S., Karaağaç, S.U., Abu Amr, S.S., Alazaiza, M.Y.D., Fatihah, S. and Bashir, M.J.K. 2022. Recent advancements in plant-based natural coagulant application in the water and wastewater coagulation-flocculation process: Challenges and future perspectives. DOI: 10.30955/gnj.004380.

Adewuyi, A. 2020. Chemically modified biosorbents and their role in the removal of emerging pharmaceutical waste in the water system. Water, 12(6): 1551. DOI: 10.3390/w1206155

Al-Alawy, M., Ahmed, S. and Salih, M. 2017. Comparative study between nanofiltration and reverse osmosis membranes for the removal of heavy metals from electroplating wastewater. Univ. Baghdad Eng. J., 23: 1-21.

Boruah, P., Borah, D., Handique, J., Sharma, P., Sengupta, P. and Das, M. 2015. Facile synthesis and characterization of fe3o4 nanopowder and fe3o4 reduced graphene oxide nanocomposite for methyl blue adsorption: A comparative study. J. Environ. Chem. Eng., 3: 414. DOI: 10.1016/j.jece.2015.06.030.

Carvalho, J., Ribeiro, A., Araújo, J. and Castro, F. 2013. Technical aspects of adsorption process onto an innovative eggshell-derived low-cost adsorbent. Mater. Sci. Forum. doi: 10.4028/www.scientific.net/MSF.730-732.648.

Çelebi, H. and Gök, O. 2017. Evaluation of lead adsorption kinetics and isotherms from aqueous solution using natural walnut shell. Int. J. Environ. Res., 11: 83-90.

Daniel, S.T., Peng, L., Reeder, W.S., Moosavi, S.M., Tiana, D., Britt, D.K. and Queen, W.L. 2018. Rapid, selective heavy metal removal from water by a metal–organic framework / polydopamine composite. ASCS, 1: 605. DOI: 10.1021/acscentsci.7b00605.

Deen, G.D., Alhazmi, A., Mohammad, A., Haque, S., Srivastava, N., Thakur, V.K. and Pal, D.B. 2019. Partial characterization and antitumor activity of a polysaccharide isolated from watermelon rinds. Int. J. Biol. Macromol., 136: 632-641. DOI: 10.1016/j.ijbiomac.2019.06.110.

Deniz, T., Bakhshpour, M., Akgönüllü, S., Asir, S. and Denizli, A. 2022. Heavy metal ions removal from wastewater using cryogels: A review. Front. Sustain., 11: 45-63. DOI: 10.3389/frsus.2022.765592.

Ezeonuegbu, B.A., Machido, D.A., Whong, C.M.Z., Japhet, W.S., Alexiou, A., Elazab, S.T. and Batiha, G.E. 2021. Agricultural waste of sugarcane bagasse as efficient adsorbent for lead and nickel removal from untreated wastewater: Biosorption, equilibrium isotherms, kinetics, and desorption studies. Biotechnol. Rep., 11: 71-83. DOI: 10.1016/j.btre.2021.e00614.

Firomsa, T., Karthikeyan, R. and Sahuc, O. 2020. Synthesized bioadsorbent from fish scale for chromium III removal. DOI: 10.1016/j.micron.2019.102817.

Fouad, K., Noureddine, A. and Mohamed. C.N. 2016. Adsorptive removal of cadmium from aqueous solution by cork biomass: Equilibrium, dynamic, and thermodynamic studies. Arab. J. Sci. Eng., 1: 661-671. DOI: 10.1016/j.arabjc.2011.12.013.

Fouda-Mbanga, B.G., Prabakaran, E. and Pillay, K. 2021. Carbohydrate biopolymers, lignin-based adsorbents for removal of heavy metals Cd2+, Pb2+, Zn2+ from wastewater, regeneration, and reuse for spent adsorbents including latent fingerprint detection: A review. Biotechnol. Rep., 30: e00609. DOI: 10.1016/j.btre.2021.e00609.

García-Vargas, M.C., Contreras, M.d.M. and Castro, E. 2020. Avocado-derived biomass as a source of bioenergy and bioproducts. Appl. Sci., 10(22): 8195. https://doi.org/10.3390/app10228195.

Gaurav, D.R., Bhoir, A., Raut, S. and Parkar, P. 2018. Removal of heavy metals by means of banana and orange peels. DOI: 10.15680/IJIRSET.2018.0704038.

Gautam, K., Markandeya, N.B., Singh, S.P. and Shukla, D. 2020. Lead removal efficiency of various natural adsorbents (*Moringa oleifera*, *Prosopis juliflora*, Peanut Shell) from textile wastewater. https://doi.org/10.1007/s42452-020-2065-0.

Geetha, V. and Anil, M.K. 2016. Copper contaminated wastewater – an evaluation of bioremedial options. J. Eng. Res., 16: 545. DOI 10.1177/1420326X16669397.

Ghasemi, S., Gholami, R.M. and Yazdanian, M. 2017. Biosorption of heavy metal from cadmium rich aqueous solutions by tea waste as a low-cost bio-adsorbent. Jundishapur J. Health Sci., 9: e37301.

Gregorio, C. and Badot, P.M. 2008. Application of chitosan, a natural aminopolysaccharide, for dye removal from aqueous solutions by adsorption processes using batch studies: A review of recent literature. Proceed. Eng., 16: 111-121.

Gu, S., Kang, X. and Wang, L. 2019. Clay mineral adsorbents for heavy metal removal from wastewater: A review. Environ. Chem. Lett., 17: 629-654. https://doi.org/10.1007/s10311-018-0813-9.

Guat.T., Gok, X.Y. and Yong, W.F. 2022. Adsorption of pollutants in wastewater via biosorbents, nanoparticles and magnetic biosorbents: A review. Environ. Res., 212: 113248. ISSN 0013-9351. https://doi.org/10.1016/j.envres.2022.113248.

Hakan, C., Gök, G. and Gök, O. 2020. Adsorption capability of brewed tea waste in waters containing toxic lead (II), cadmium (II), nickel (II), and zinc (II) heavy metal ions. Water, 15: 612-646. https://doi.org/10.1038/s41598-020-74553-4.

Haluk, A., Bulut, Y. and Yerlikaya, C. 2008. Removal of copper (II) from aqueous solution by adsorption onto low-cost adsorbents. J. Eng. Manag., 1: 1005, 10.1016/j.jenvman.2007.01.005.

Husein, D.Z., Aazam, E. and Battia, M. 2017. Adsorption of cadmium (II)

onto watermelon rind under microwave radiation and application into surface water from Jeddah, Saudi Arabia. Arab. J. Sci. Eng., 42(6): 2403-2415.

Jamdade, A.B. and Gawande, S.M. 2015. Analytical study of heavy metal in Pavana River and its effect on aquaculture. IJSR, 16: 555.

Jian, W., Liu, M., Duan, C., Sun, J. and Xu, Y. 2019. Preparation and characterization of cellulose-based adsorbent and its application in heavy metal ions removal. Carbohydrate Polymers, 206: 837-843. ISSN 0144-8617. https://doi.org/10.1016/j.carbpol.2018.11.059.

Jianlong, W. and Can, C. 2009. Biosorbents for heavy metals removal and their future. Biotechnology advances, 27(2): 195-226. doi: 10.1016/j.biotechadv.2008.11.002.

Jyoti, S, Garg, V.K. and Gupta, R.K. 2021. Cadmium removal from water by green synthesized nanobioadsorbent [SiO2@DOPP]: Mechanism, isotherms, kinetics, and regeneration studies. J. Sci. Eng. Res., 16: 202. https://doi.org/10.1016/j.scp.2020.100350.

Kabenge, I., Omulo, G., Banadda, N., Seay, J., Zziwa, A. and Kiggundu, N. 2018. Characterization of banana peels wastes as potential slow pyrolysis feedstock. J. Sustain. Dev., 11: 14-24.

Kamarudzaman, A.N., Che Adan, S.N.A., Hassan, Z., Ab Wahab, M.A., Makhtar, S.M.Z., Abu Seman, N.A. and Syafiuddin, A. 2022. Biosorption of copper (II) and iron (II) using spent mushroom compost as biosorbent. Water, 14(5): 778. DOI: 10.33263/BRIAC126.77757786.

Lakshmipathy, R., Vinod, A.V. and Sarada, N.C., 2013. Watermelon rind as biosorbent for removal of Cd2+ from aqueous solution: FTIR, EDX, and kinetic studies. J. Indian Chem. Soc., 90: 1147-1154.

Lata, S., Singh, P.K. and Samadder, S.R. 2015. Regeneration of adsorbents and recovery of heavy metals: A review. Int. J. Environ. Sci. Technol., 12: 1461-1478. https://doi.org/10.1007/s13762-014-0714-9

Leong, K.K. 2018. Adsorption of heavy metals using banana peels in wastewater treatment. Proceed. Sci. Technol. Eng., 2: 312-317

Liang, S., Cao, S., Liu, C., Zeb., S., Cui, Y. and Sun, G. 2020. Heavy metal adsorption using structurally preorganized adsorbent. RSC Adv., 10(12): 7259-7264. doi: 10.1039/d0ra00125b.

Liu, C., Ngo, H.H. and Guo, W. 2012. Watermelon rind: Agro-waste or superior biosorbent Appl. Biochem. Biotechnol., 167 (6): 1699-1715.

Maftouh, A., El Fatni, O., El Hajjaji, S., Jawish, M.W. and Sillanpää, M. 2023. Comparative review of different adsorption techniques used in heavy metals removal in water. DOI: 10.33263/BRIAC134.397.

Maleki, A., Hajizadeh, Z., Sharifi, V. and Emdadi, Z. 2019. A green, porous, and eco-friendly magnetic geopolymer adsorbent for heavy metals removal from aqueous solutions. J. Clean. Prod., 215: 1233-1245. DOI: 10.1016/j.jclepro.2019.01.084.

Malik, D.S., Jain, C.K. and Yadav, A.K. 2017. Removal of heavy metals from emerging cellulosic low-cost adsorbents: A review. Appl. Water Sci., 7: 2113-2136. DOI: 10.1007/s13201-016-0401-8.

Mane, P.C., Kadam, D.D. and Chaudhari, R.D. 2013. Status of Some Trace Metals in Water Samples from Manjara Dam of Maharashtra, India. Int. J. Curr. Microbiol. App. Sci., 2(10): 516-523.

Manisha, M., Manna, M., Sardar, M. and Sen, S. 2021. Heavy Metal Removal by Low-Cost Adsorbents. Proceedings of the International Conference on Environmental Science and Engineering, January 2021, pp. 474.DOI: 10.1007/978-3-030-47400-3_10

Maryam, S., Ghaemya, M. and Amininasab, S.M. 2020. Removal of NO3− ions from water using bioadsorbent based on gum tragacanth carbohydrate biopolymer. Carbohydr. Polym., https://doi.org/10.1016/j.carbpol.2019.115367.

Mohd, S.A., Dutta, R.K., Sen, A.K., Ram, S.S., Sudarshan, M., Naushad, Mu., Boczkaj, G. and Sadique, M. 2022. Chemical analysis of low carbon content coals and their applications as dye adsorbent. Chemosphere, 287(4): 0045-6535, https://doi.org/10.1016/j.chemosphere.2021.132286.

Monika, P. and Surajit, D. S. 2021. Biosorption and removal of toxic heavy metals by metal tolerating bacteria for bioremediation of metal contamination: A comprehensive review. J. Environ. Chem. Eng., 5: 331-346 https://doi.org/10.1016/j.jece.2020.104686.

Muhammad, B., Ihsanullah, I., Shah, M.U.H. and Younas, M. 2021. Enhanced removal of cadmium from water using bio-sorbents synthesized from branches and leaves of Capparis decidua and Ziziphus mauritiana. Environ. Technol. Innov., 75: 891-897. DOI: 10.1016/j.eti.2021.101922.

Myalowenkosi, S.I., Kunene, K., Kanchi, S., Xhakaza, N.M., Bathinapatla, A., Mdluli, P., Sharma, D., Bisetty, K. 2016. Removal of copper (II) from wastewater using green vegetable waste derived activated carbon: An approach to equilibrium and kinetic study. Arab. J. Chem., 15: 45-56. http://dx.doi.org/10.1016/j.arabjc.2016.06.001.

Nadeem, S.H., Kumar, J., Mazari, S.A., Ahmed, S., Fatima, N. and Mubarak, N.M. 2021. Development of fruit waste derived bio-adsorbents for wastewater treatment: A review. J. Hazard. Mater., 11: 414. https://doi.org/10.1016/j.jhazmat.2021.125848.

Naeema, H.Y. 2014. Removal of lead from wastewater by adsorption. Int. J. Curr. Microbiol. Appl. Sci., 3(4): 207-228.

Naef, A., Qasem, A., Mohammed, R.H., Lawal, D.U. 2021. Removal of heavy metal ions from wastewater: A comprehensive and critical review. Clean Water, 4: 36. https://doi.org/10.1038/s41545-021-00127-0.

Naseem, Z. N. 2012. Lead removal from water by low-cost adsorbents: A review. Pak. J. Anal. Environ. Chem., 13(1): 01-08.

Noureddine, E. and Harvey. A.G. 2020. The use of natural zeolite to remove heavy metals Cu (II), Pb (II) and Cd (II), from industrial wastewater. Cogent Eng., 16: 623, DOI: 10.1080/23311916.2020.1782623

Opia, B. 2018. The bio-adsorption of heavy metals from produced water using mango mangifera indica peel and corn zea mays cobs as bioadsorbents. Res. Rev. J. Ecol. Environ. Sci., 6(4): 511.

Pathak, P.D., Mandavgane, S.A. and Kulkarni, B.D. 2017. Fruit Peel Waste: Characterization and its Potential Uses. Current Sci., 113(3): 444-454. DOI: 10.2307/26294001.

Patrick, T.P.J., Wan Nur, W.O., Md Saad, J., Samsudin, M.F. and Hernández Yáñez, E. 2021. Factory tea waste biosorbent for Cu (II) and Zn (II) Removal from wastewater. Curr. Sci., 5: 11-23. DOI: 10.1051/e3sconf/202128704006.

Pham, B.N., Kang, J.K., Lee, C.-G. and Park, S.J. 2021. Removal of heavy metals Cd2+, Cu2+, Ni2+, and Pb2+ from aqueous solution using Hizikia fusiformis as an algae-based bioadsorbent. J. Eng. Tehcnol. Res., 15: 604. DOI: 10.3390/app11188604.

Pham, B.N., Kang, J.K., Lee, C.G. and Park, S.J. 2021. Removal of heavy metals (Cd2+, Cu2+, Ni2+, Pb2+) from aqueous solution using Hizikia fusiformis as an algae-based Bioadsorbent. Appl. Sci., 11: 8604. DOI: 10.3390/app11188604.

Prasenjit, M., Yadav, B.P. and Siddiqui, N.A. 2020. Removal of lead from drinking water by bioadsorption technique: An eco-friendly approach. Curr. Sci., 64: 1145. DOI: /10.46410/NEPT.2020.v19i04.036.

Qasem, N.A.A., Mohammed, R.H. and Lawal, D.U. 2021. Removal of Heavy Metal Ions from Wastewater: A Comprehensive and Critical Review. Npj Clean Water, 4: 36. DOI: 10.1038/s41545-021-00127-0.

Rabiatul, M. M., Norazlina, H., Suhaila, A., Nabihah, A. and Kaha Fakrul, M. 2019. Adsorption of heavy metals on banana peel bioadsorbent. Bioadsorbent. Appl. Sci., 3: 27-39. DOI: 10.1088/1742-6596/1532/1/012014.

Rajec, P., Galambosˇ, M., Danˇo, M., Rosskopfova´, O., Cˇaplovicˇova´, M., Hudec, P. and Cˇaplovic, Lˇ. 2015. Preparation and characterization of adsorbent based on carbon for pertechnetate adsorption. Water, 9: 54. 10.1007/s10967-014-3303-y.

Rajkumar, R. and Swati, P.S. 2015. Comparative Study on Efficiency of Natural Adsorbents in Removal of Chromium. URL: https://www.researchgate.com/publication/283664450.

Ram, C. and Sangeeta, S. 2010. Potential of typha angustifolia for phytoremediation of heavy metals from aqueous solution of phenol

and melanoidin. Ecol. Eng., 36(10): 1277-1284. DOI: 10.1016/j.ecoleng.2010.06.003.

Redha, A.A. 2020. Removal of heavy metals from aqueous media by biosorption. Arab J. Basic Appl. Sci., 27(1): 183-193. DOI: 10.1080/25765299.2020.1756177.

Renu, M., Agarwal, R. and Kailash, S. 2017. Methodologies for removal of heavy metal ions from wastewater: An overview. J. Clean. Prod., 22: 43-58. DOI: 10.1504/IER.2017.10008828.

Sabino, D.S., Lofrano, G., Grassi, M. and Notarnicola, M. 2016. Characteristics and Adsorption Capacities of Low-Cost Sorbents for Wastewater Treatment: A Review. Sustainable Materials and Technologies, 9: 10-40. DOI: 10.1016/j.susmat.2016.06.002.

Salam, A. and Khan, A.H. 2015. Efficiency of natural bio-adsorbents to remove heavy metal ions from artificially contaminated water. Bangl. J. Soil Sci., 37(1): 57-63.

Sarthak, G., Sireesha, S., Sreedhar, I., Patel, C.M. and Anitha, K.L. 2020. Latest trends in heavy metal removal from wastewater by biochar based sorbents. J. Water Process Eng., 38: 101561. DOI: 10.1016/j.jwpe.2020.101561.

Sehyeong, L., Kim, J.H., Park, H., Kwak, C., Yang, J., Kim, J. and Lee, J. 2021. Role of electrostatic interactions in the adsorption of dye molecules by Ti3C2-MXenes. IJSR, 54: 8176. DOI: 10.1039/d0ra10876f.

Shagufta, Z., Khan, M.I., Lashari, M.H., Khraisheh, M., Almomani, F., Mirza, M.L. and Khalid, N. 2020. Removal of copper ions from aqueous solution using NaOH-treated rice husk. DOI: 10.1007/s42247-020-00126-w.

Shahinur, A., Salam, A. and Khan, A.H. 2015. Efficiency of natural bio-adsorbents to remove heavy metal ions from artificially contaminated water. Bangl. J. Soil Sci., 37(1): 57-63. ISSN 0253-5440.

Sihem, A., Lehocine, B.M. and Miniai, H.A. 2012. Preparation and characterization of a natural adsorbent used for elimination of pollutants in wastewater. Energ. Procedia, 6: 434-456. DOI: 10.1016/j.egypro.2012.05.129.

Stefano, M., Parolini, M., Soave, C., Marazzi, F., Mezzanotte, V. and Binelli, A. 2015. Removal of metallic elements from real wastewater using zebra mussel bio-filtration process. J. Environ. Chem. Eng., 3(2): 915-921. DOI: 10.1016/j.jece.2015.01.017.

Thachanan, S., Deetae, P. and Wongpromrat, P. 2018. A study of atrazine adsorption by using the rice straw synthesized adsorbent. Curr. Sci., 36: 71-89. DOI: 10.1051/matecconf/201819203035.

Thamer, M.J., Azeez, R.A.A. and Lutffe, T. 2015. Biosorption of copper from synthesized wastewater using agriculture waste (roasted date pits). Int. J. Recent Sci. Res., 6(3): 3063-3068.

Tien, P.D., Nguyen, H.H., Nguyen, N.V. and Vu, T.T. 2017. Adsorptive Removal of Copper by Using Surfactant Modified Laterite Soil. Journal of Chemistry, 2017. DOI: 10.1155/2017/1986071.

Torres, E. 2020. Biosorption: A review of the latest advances. Processes, 8: 1584 https://doi.org/10.3390/pr8121584

Trần, T.K., Leu, H.J., Chiu, K.F. and Lin, C.Y. 2017. Electrochemical treatment of heavy metal-containing wastewater with the removal of COD and heavy metal ions. J. Chin. Soc., 64: 226. https://doi.org/10.1002/jccs.201600266

Vaishnavi, M.V.S. and Shelly, G. 2015. Study of levels of heavy metals in the river waters of regions in and around Pune City, Maharashtra, India. Department of Chemistry, JJT University, Rajasthan, India, G Moze College of Engineering, Pune, India.

Wai, W.S., Cheun, J.Y., Kumar, P.S., Mubashir, M., Majeed, Z., Banat, F., Ho, S.H. and Show, P.L. 2021. A review on conventional and novel materials towards heavy metal adsorption in wastewater treatment application. J. Clean. Prod., 8: 98-120. https://doi.org/10.1016/j.jclepro.2021.126589

Wan, S. 2014. Sorption of lead (II), cadmium (II), and copper (II) ions from aqueous solutions using tea waste. Indust. Eng. Chem. Res., 53: 3629–3635.

World Health Organization (WHO) 2011/2017. Guidelines for Drinking-Water Quality (4th ed.) World Health Organization.

Wu, Z., Soh, T., Chan, J.J., Meng, S., Meyer, D., Srinivasan, M. and Tay, C.Y. 2020. Repurposing of fruit peel waste as a green reductant for recycling of spent lithium-ion batteries. Environ. Sci. Technol., 54(15): 9681-9692. https://doi.org/10.1021/acs.est.0c02873

Yaacoubi, H., Zidani, O., Mouflih, M., Gourai, M. and Sebti, S. 2013. Removal of cadmium from water using natural phosphate as adsorbent. Proceed. Eng., 12: 24-39. doi: 10.1016/j.proeng.2014.09.039.

Zahir, H. and Sheriff, M.K. 2014. Removal of heavy metals from wastewater using low-cost adsorbents. Arch. Appl. Sci. Res., 6(6): 52-54.

Zahra S., Alireza, S., Pei, S.G., Ahmad, F.I. and Mohd, S.A. 2023. A comprehensive review of recent advances in nanofiltration membranes for heavy metal removal from wastewater, Chem. Eng. Res. Design, 189: 530-571.

Zhengang, L. and Fu-Shen, Z. 2009. Removal of lead from water using biochars prepared from hydrothermal liquefaction of biomass. J. Clean. Prod., 16: 511-537 doi: 10.1016/j.jhazmat.2009.01.085

Zujin, Y., Chai, Y., Zeng, L., Gao, Z., Zhang, J. and Ji, H. 2019. Efficient removal of copper ion from wastewater using a stable chitosan gel material. Molecules, 6: 43. https://doi.org/10.3390/molecules24234205

# Effects of Natural Radioactivity of Some Chemical and Organic Fertilizers on Gonads in Iraqi Kufa Markets

**Abdulhussein A. Alkufi\*** (iD)**, Shaymaa A. Kadhim\*\*\*†** (iD)**, Azhar S. Alaboodi\*\*** (iD) **and Shatha F. Alhous\*\*\*** (iD)

\*Education Directorate of Najaf, Ministry of Education, Iraq
\*\*Department of Physics, Faculty of Science, University of Kufa, Iraq
\*\*\*Department of Physics, Faculty of Education for Girls, University of Kufa, Iraq
†Corresponding author: Shaymaa A. Kadhim; shaymaa.alshebly@uokufa.edu.iq

## ABSTRACT

This study assessed the hazard indicators of common chemical and organic fertilizers widely available in the markets of Najaf Governorate, Iraq. The concentrations of natural radionuclides were measured in thirteen types of fertilizers by Gamma spectrum using NaI(Tl) (3*3) detector. The average radioactivity of the nuclides $^{226}$Ra, $^{232}$Th, and $^{40}$K was (48.91, 37.04, and 702.4675) Bq.kg$^{-1}$, respectively, for (Di-Aluminum Phosphate) the chemical fertilizers of the type (DAP) and the **(**nitrogen, phosphorus, and potassium**)** chemical fertilizers of the type (NPK) the average radioactivity of the nuclides $^{226}$Ra, $^{232}$Th, and $^{40}$K were (35.78, 42.356 and 1519.653) Bq.kg$^{-1}$, respectively, while the average radioactivity of the organic fertilizers (Orga.) were 55.153, 23.148 and 1451.258 for the three studied nuclei. As for the average values for radium equivalent were 155.967, 213.363, and 200.0023 (Bq.kg$^{-1}$) for (DAP), (NPK) and organic fertilizers, respectively. The values of the external severity index ($H_{ex}$), gamma radiation hazard index ($I_\gamma$), and representative alpha index ($I_\alpha$) were within the permissible limits determined by the UNCEAR 2000. The highest value of total annual effective dose equivalent(TAED) was 1.468 mSv.y$^{-1}$, the lowest value was 0.302 mSv.y$^{-1}$, and the mean values were 0.722 mSv.y$^{-1}$. In contrast, the highest value for annual gonadal dose equivalent(AGED) was 1392.527 µSv.y$^{-1}$, the lowest value was 275.361 µSv.y$^{-1}$, and the average values for all models were 672.135 µSv.y$^{-1}$. The Excess Lifetime Cancer Risk (ELCR), the highest value was 4.039 × 10$^{-3}$, the lowest value was 0.833× 10$^{-3}$, and the average value was 1.988× 10$^{-3}$ for all fertilizers. The Pearson correlation between radioactive variables and cluster analysis was recognized for the three types of fertilizer samples despite it not being widely accepted. The study can be considered preliminary data for subsequent studies.

## INTRODUCTION

Agricultural activities have expanded significantly in recent years. This led to a significant increase in chemical and organ fertilizers (Robinson & Sutherland 2002). Chemical fertilizers are chemical compounds that provide essential nutrients to plants, which have become essential for the agricultural field worldwide. The main raw material used to manufacture fertilizers is phosphate rock with potassium ores and nitrogenous compounds.

The concentration of $^{226}$Ra and its decomposition products tend to be higher in phosphate deposits of sedimentary origin (phosphorus is an essential element for plant growth) UNSCEARE200. Therefore, when these rocks are processed into phosphate fertilizers, radionuclides will naturally disperse in the fertilizer and thus become a source of radioactivity in food and the environment (Jibiri & Fasae 2012).

This process leads to potential radiation hazards due to the transfer of radionuclides from agricultural fertilizers to soils and plants, and through the food chain, to humans as this may lead to internal exposure through eating food grown in that agricultural soil.

In addition, some workers can get additional external exposure during the manufacture, packaging, and transportation of fertilizers Due to the high radioactive content of fertilizers, which may be for employees, producers, and farmers. Accordingly is crucial to determine the normal radioactivity in fertilizers.

These tests also give the foundational information needed to estimate how much radiation is in fertilizers and agricultural land. More than 30 million tons of phosphate fertilizers are used in Iraq each year to boost crop productivity and reclaim land.

The contamination of cultivated land with some naturally occurring radioactive material, however, is a potential drawback of fertilizer. Naturally Occurring Radioactive Materials (NORM) (Lambert et al. 2007). Calculating the radioactivity levels of organic and chemical fertilizers used in the Kingdom of Saudi Arabia, including the 226Ra and 232Th series, their decay products, and 40K. Inorganic fertilizer has a $Ra_{eq}$ of 34.07 to 102.19 Bq.kg$^{-1}$, while chemical fertilizer ranges from 100.37 to 161.43 Bq.kg$^{-1}$ (El-Taher & Althoyaib 2012).

Due to the importance of the topic from a health point of view, many studies have been conducted about radioactive contamination of fertilizers, where the quantities of $^{226}$Ra, $^{232}$Th, and $^{40}$K in chemical fertilizers led to the calculation of radiation hazard indicators in upper Egypt (Uosif et al. 2014). The average concentrations of $^{226}$Ra, $^{232}$Th, and $^{40}$K in the soil, organic (animal) and inorganic (chemical) as (granular fertilizers), (foliar fertilizers) and (animal fertilizers) were estimated, and the lowest values are observed of specific activities of the same radionuclides were in foliar fertilizer (Faweya et al. 2018).

Another study conducted in Saudi Arabia on fertilizers and obtained results showed significant differences in the radioactive content for $^{226}$Ra, $^{232}$Th, and $^{40}$K in different phosphate fertilizer samples (Khater & Al-Sewaidan 2008).

Based on the foregoing, the current study aims to compare some fertilizers widely spread in Iraq to find out their radioactivity levels. It opens the way for subsequent studies to establish a consistent radioactive database for the concentration of natural radionuclides in some types of local fertilizers used in agricultural soils in Najaf Governorate, Iraq.

## COMPONENTS AND TYPES OF FERTILIZERS

The chemical fertilizers available in the local markets are of two types in terms of composition (NPK) and (DAP). Fertilizer (NPK) is a crystalline fertilizer consisting of three main elements: nitrogen (18%) and phosphorus (46%), which is in the form of phosphorous and potassium pent oxide (36%), and these percentages change from one kind to another (Hignett 2018). This fertilizer is characterized by its slow release, granular shape, and easy dissolution, which leads to easy utilization by the plant and enables us to use it by agricultural machinery (Vincevica-Gaile et al. 2019). It is used for all crops and trees in rain-fed or irrigated areas. The second type is the fertilizer (DAP), an abbreviation for the phrase (Di-Aluminum Phosphate), this type consists of phosphorus and nitrogen, but it is free of potassium. These elements are also in different proportions (Knecht & Göransson 2004) .A third type is organic fertilizer, prepared from the remains of bones and blood, as well as animal manure (cow, poultry, and goat manure). Plant residues are also included in its ingredients because they contain important mineral elements, such as seaweed, which contains a decent amount of amino acids (Knecht & Göransson 2004). Table 1 represents the studied fertilizers' types, composition, and origin.

## SPECIFIC ACTIVITY AND HAZARD INDICES

### Specific Activity

Specific activity is the activity per unit mass for radioactive material.

It is measured in units Becquerel per kilogram (Bq.Kg$^{-1}$) or Curie per gram. The specific activity in Bq.Kg$^{-1}$ units were

Table 1: Types, origins, and components of studied fertilizers.

| Sample Code | Fertilizer Components | Origin | Type |
|---|---|---|---|
| F$_1$(Chem.$_{DAP}$) | (18%) nitrogen and (46%) phosphorous pentoxide, characterized as granular and easy to dissolve, leads to easy use by the plant, enables us to use it by agricultural machines, and is used for all crops and trees, whether in rain-fed or irrigated areas. | Jordan(DAP) | Chemical Fertilizer |
| F$_2$(Chem.$_{DAP}$) | | Iran(DAP) | Chemical Fertilizer |
| F$_3$(Chem.$_{DAP}$) | | China(DAP) | Chemical Fertilizer |
| F$_4$(Chem.$_{DAP}$) | | Egypt(DAP) | Chemical Fertilizer |
| F$_5$(Chem.$_{NPK}$) | NPK crystalline fertilizer is slow-release and water-soluble. Phosphorous (P) is derived from mono-ammonium phosphate, and potassium (K) is derived entirely from sulfate. Nitrogen is fixed in ammonia type with (Dicyandiamide DCD), a chemical nitrogen inhibitor. This process allows the ammonia ion (NH4) to exist for a longer period in the soil. | Jordan(Npk) | Chemical Fertilizer |
| F$_6$(Chem.$_{NPK}$) | | Egypt(Npk) | Chemical Fertilizer |
| F$_7$(Chem.$_{NPK}$) | | Jordan(Npk) | Chemical Fertilizer |
| F$_8$(Orga.) | The compost was prepared from the remains of bones and blood and animal manure ("cow, poultry, and goat dung). Its components also include plant residues, as they contain important mineral elements. And also seaweed, which contains the right amount of amino acids. | Iraq | Organic Fertilizer |
| F$_9$(Orga.) | | Iraq | Organic Fertilizer |
| F$_{10}$(Orga.) | | Iraq | Organic Fertilizer |
| F$_{11}$(Orga.) | | Iraq | Organic Fertilizer |
| F$_{12}$(Orga.) | | Iran | Organic Fertilizer |
| F$_{13}$(Orga.) | | Canada | Organic Fertilizer |

calculated by using equation 1 (Stenström 2011):

$$\mathcal{A}_n = \frac{(\mathcal{C}_n - \mathcal{C}_b)}{t\, \varepsilon_\gamma\, I_g\, m_s} \qquad \ldots(1)$$

where $\mathcal{A}_n$ Is the specific activity of each radionuclide in Bq.Kg$^{-1}$, $\mathcal{C}_n$ the count rate in cps for a sample, $\mathcal{C}_b$ the count rate in cps for background, $\varepsilon_\gamma$ and $I_g$ Are detection efficiency and representative level index, $t$ is the counting time and $m_s$ is the mass of the sample in kg.

## The Radium Equivalent Activity ($\mathcal{R}a_{eq}$)

The distribution of $^{226}$Ra, $^{232}$Th, and $^{40}$K nuclei in soil are not constant.

Radium equivalent activity ($\mathcal{R}a_{eq}$), which is defined as a weighted sum of the activity concentrations of the three radionuclides, including uranium $^{226}$Ra, thorium $^{232}$Th, and potassium $^{40}$K,

It was used as a common factor to compare its adverse effects. This factor was calculated using Equation 2.

$$\mathcal{R}a_{eq}(\text{Bq.}Kg^{-1}) = \mathcal{A}_{Ra} + 1.43\mathcal{A}_{Th} + 0.077\mathcal{A}_K$$
$$\ldots(2)$$

Where $A_{Ra}$ is the activity of $^{226}$Ra, $A_{Th}$ is the activity of $^{232}$Th, and $A_K$ is the activity of $^{40}$K, all in Becquerel per kilogram (Bq.Kg$^{-1}$) (Mohanty et al. 2004).

## External Hazard Index ($H_{ex}$)

The external risk index is an assessment of the natural gamma radiation risk calculated from equation 3 (Alhous et al. 2020).

$$H_{ex.} = \frac{A_{Bi}}{370} + \frac{A_{Th}}{259} + \frac{A_K}{4810} \leq 1 \qquad \ldots(3)$$

This coefficient must be less than one, and if it is equal to or greater than one, it indicates the presence of a radioactive hazard.

## Gamma Radiation Hazard Index ($I_\gamma$)

Index ($I_\gamma$) estimates the level of γ-radiation hazard associated with the natural radionuclides in specific activity for any matter studied. The derived formula calculates the value (Kadhim 2020).

$$I_\gamma = \frac{A_U}{150} + \frac{A_{Th}}{100} + \frac{A_K}{1500} \qquad \ldots(4)$$

Another hazard index, the Representative Level Index, $I_\gamma$, was determined from the above formula (Alam et al. 1999).

## Representative Alpha Index ($I\alpha$)

From the equation below, the alpha index was calculated for the samples by using equation 5 (Ziqiang et al. 1988, Adhab et al. 2020):

$$I_\alpha = \frac{A_{Ra}}{200} \qquad \ldots(5)$$

This hazard index is closely related to radium $^{226}$Ra.

## Total Annual Effective Dose Equivalent (TAED)

Exposure risk to any individual due to absorbed dose rate is estimated in terms of the TAED. The Outdoor and Indoor annual effective doses have been obtained, and the total annual effective dose equivalent (mSv.y$^{-1}$) was calculated using equation 6 (Alam et al. 1999, Aswood 2019).

$$TAED_{total}(\text{mSv.}y^{-1}) = D_{eff.out} + D_{eff.in} \qquad \ldots(6)$$

## Annual Gonadal Dose Equivalent (AGED):

The impacts of radiation on all living cells vary, which can lead to mutation or cell death. The AGED due to $^{226}$Ra, $^{232}$Th, and $^{40}$K was calculated by using the equation 7(Arafa 2004, Alkufi 2020):

$$AGED(\mu SV.y^{-1}) = 3.09A_{Ra} + 4.18A_{Th} + 0.314A_K$$
$$\ldots(7)$$

The gonads are considered organs of interest for dosimetry, according to UNSCEAR (2010). They are the basic reproductive organs. It is also known that an increase in AGED can impact the bone marrow, which makes red blood cells. Leukemia, a blood cancer that frequently results in death, could be resulted. The bladder, lungs, liver, colon, and thyroid are other radiosensitive organs.

## Excess Lifetime Cancer Risk (ELCR)

The equation below can be used to determine the increased lifetime cancer risk due to gamma radiation (Alhous et al. 2020).

$$ELCR = TAED * LS * RF \qquad \ldots(8)$$

where TAED (mSv.y$^{-1}$) presents the total annual effective dose equivalent. LS is a mean life span (approximately 70 years), and RF is the risk factor (Sv$^{-1}$) (Abbas et al. 2023), which reflects the fatal cancer risk per Sievert for stochastic effects. The ICRP determines the value of RF 0.05 for the public.

## MATERIALS AND METHODS

### Sample Description and Preparation

Thirteen types of chemical and organic fertilizers were collected from local markets. The types of examined samples were di-ammonium phosphate (DAP) fertilizer and four samples (Fig. 1). Nitrogen fertilizer for phosphorous-potassium (NPK) was three types, and organic fertilizer had six samples. The collected samples weighing about

500 grams were dried in an oven at about 110°C for 24 h to ensure complete dehumidification.

Then the samples were crushed, homogenized, and sieved through a 200 mm diameter, which is the optimal size enriched with heavy metals.

The samples were placed in a 350 cm³ polyethylene beaker. The beakers were completely closed for 4 weeks to reach temporal equilibrium when the daughters' rate of decay became equal to that of the parents.

This step is necessary to ensure that radon gas is contained within the volume and the daughters will remain in the sample (Kadhim 2020).

**Instrumentation and Calibration**

Samples were tested using gamma-ray spectroscopy because of the high penetrating intensity of gamma rays in materials.

A scintillation detector of the NaI(Tl) type with a dimension of 3"×3", provided by Alpha Spectra, Inc.-12I12/3, is the core of a gamma-ray spectrometer. It is connected via an interface to a multi-channel analyzer (MCA) of the ORTEC-Digi Base with a range of 4096 channels and an ADC (Analog to Digital Converter) unit. The laboratory PC's MAESTRO-32 software was used to carry out the spectroscopic measurements and analysis (Kadhim 2020), as shown in Fig. 2.

## RESULTS AND DISCUSSION

The measured activity concentrations of $^{226}$Ra, $^{232}$Th, $^{40}$K, and $Ra_{eq}$ in uniting (Bq.Kg$^{-1}$) for different fertilizer types were listed in Table 2.

From Table 2, the chemical fertilizers (chem. DAP) were noted to have an average concentration of $^{226}$Ra and



Fig. 1: Some of the chemical and organic fertilizer samples prepared for measurement in the laboratory.
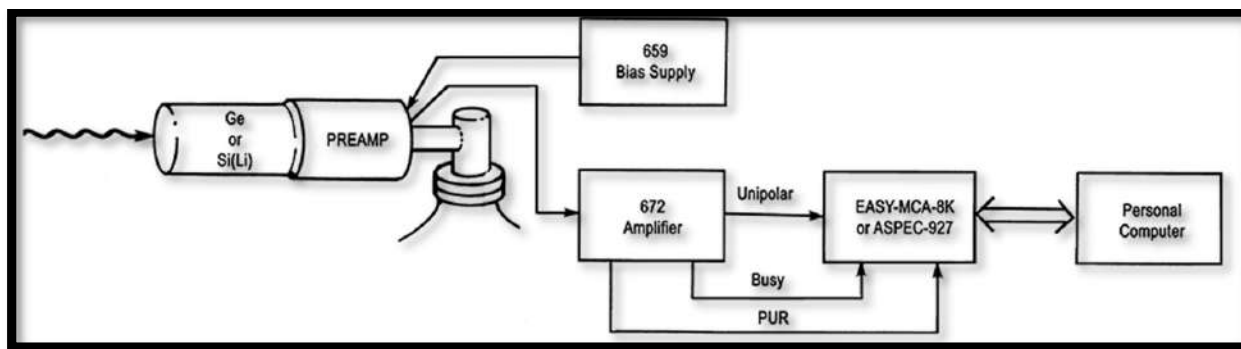


Fig. 2: Analog spectroscopy system block diagram (Constantin 2020).

Table 2: Specific activity of radium, thorium, potassium, and radium equivalent in the unit (Bq.Kg$^{-1}$) for all studied fertilizer samples.

| Sample Code | $^{226}$Ra | $^{232}$Th | $^{40}$K | Ra$_{eq.}$ |
|---|---|---|---|---|
| F$_1$(Chem.$_{DAP}$) | 50.72 | 34.56 | 660.6 | 151.000 |
| F$_2$(Chem.$_{DAP}$) | 41.26 | 52.41 | 130.25 | 126.235 |
| F$_3$(Chem.$_{DAP}$) | 11.15 | 23.40 | 455.72 | 79.7020 |
| F$_4$(Chem.$_{DAP}$) | 92.51 | 37.79 | 1563.30 | 266.923 |
| Min. | 11.15 | 23.40 | 130.25 | 79.7020 |
| Max. | 92.51 | 52.41 | 1563.30 | 266.923 |
| Average | 48.91 | 37.04 | 702.4675 | 155.967 |
| F$_5$(Chem.$_{NPK}$) | 26.32 | 79.41 | 168.11 | 152.820 |
| F$_6$(Chem.$_{NPK}$) | 66.39 | 28.23 | 977.100 | 181.995 |
| F$_7$(Chem.$_{NPK}$) | 14.63 | 19.43 | 3413.75 | 305.273 |
| Min. | 14.63 | 19.43 | 168.110 | 152.820 |
| Max. | 66.39 | 79.41 | 3413.75 | 305.273 |
| Average | 35.78 | 42.356 | 1519.653 | 213.363 |
| F$_8$(Orga.) | 31.29 | 24.24 | 944.610 | 138.688 |
| F$_9$(Orga.) | 23.69 | 23.34 | 640.590 | 106.391 |
| F$_{10}$(Orga.) | 36.20 | 10.78 | 861.730 | 117.968 |
| F$_{11}$(Orga.) | 39.10 | 26.10 | 3702.58 | 361.521 |
| F$_{12}$(Orga.) | 128.02 | 24.62 | 1612.01 | 287.351 |
| F$_{13}$(Orga.) | 72.62 | 29.81 | 946.030 | 188.092 |
| Min. | 31.29 | 10.78 | 640.590 | 106.391 |
| Max. | 128.02 | 29.81 | 3702.58 | 361.521 |
| Average | 55.153 | 23.148 | 1451.258 | 200.002 |
| Worldwide UNSCEAR2000 | 35 | 30 | 412 | 370 |

$^{40}$K higher than what was permitted globally (UNSCEAR 2000).

While $^{232}$Th is within the permissible limits due to the high concentration of potassium and uranium in sample F$_4$ Egypt (DAP).

The mean of the three radioactive nuclei was high for the second type of fertilizer(NPK). The reason is that the percentage of phosphorous for this type is 46%.

From the same table of organic fertilizers, it was noted that the average concentration of $^{40}$K is higher than what is recommended globally, and the reason is due to its high concentration in sample F$_{11}$(Iraq).

Because uranium levels were slightly higher than allowed, due to the high level in sample F12 Iran, the lowest concentration was in sample F8 Iraq, potassium in sample 9 was the lowest, and thorium was low in sample F$_{10}$ Iraq.

While it was concluded that the radium equivalent activity values are within the radiologically safe limits, Fig. 3 shows that (R$_{aeq}$) for $_{UNSCEAR}$ 2000 > NPK> Orga. > DAP respectively.

It can be seen that the values of activity concentrations in the studied fertilizers varied from 11.15 to 92.51, 130.250 to 1563.30, and from 23.40 to 52.41 (Bq.Kg$^{-1}$) for $^{226}$Ra, $^{40}$K, and $^{232}$Th, respectively, for DAP chemical fertilizers. As for the chemical fertilizers of the type (NPK), the average radioactivity of the nuclides $^{226}$Ra, $^{232}$Th, and $^{40}$K was 35.78, 42.356, and 1519.653 in the unit (Bq.Kg$^{-1}$), respectively.

Finally, the average radioactivity of the organic fertilizers was 55.153, 23.1483, and 1451.258333 for the $^{226}$Ra,$^{232}$Th, and $^{40}$ K nuclides, respectively. The difference in the concentration of radionuclides in the studied chemical and organic fertilizers is due to the different origins of the raw materials, the chemical treatment of the raw material during the manufacture of the fertilizers, animal feeding, and the type of plant algae. Also, the average values of radium equivalent for all types of fertilizer samples are less than the permissible activity levels, which was 370 (Bq.Kg$^{-1}$).

The average of the external hazard index values and the representative alpha index values were within the internationally acceptable limits. In contrast, the gamma radiation hazard index (I$_\gamma$) for most of the values was higher
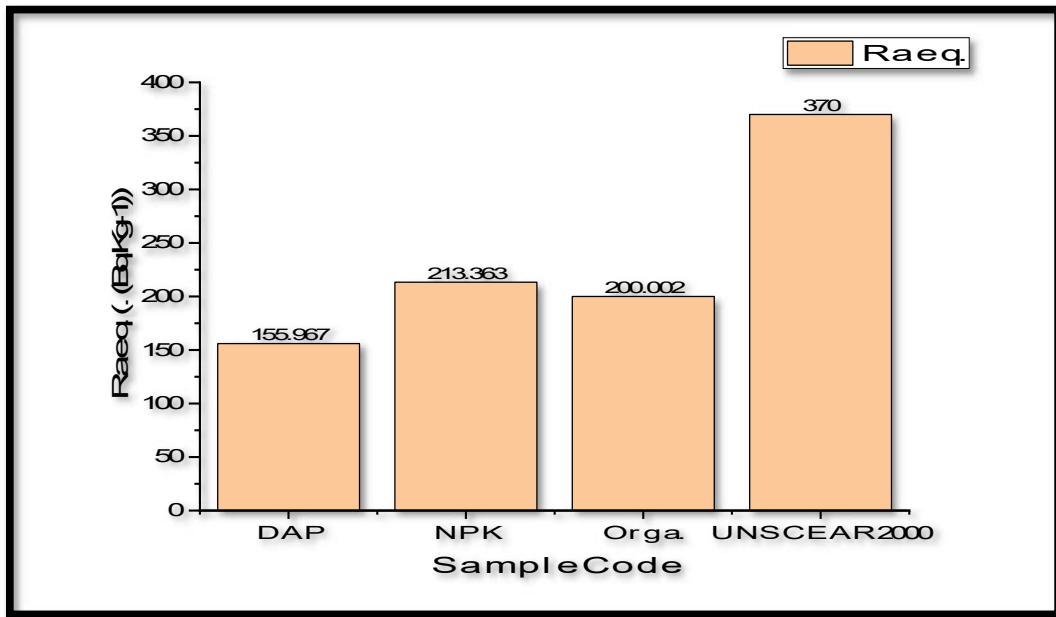
Fig. 3: Comparison of the three types of studied fertilizers with the worldwide value.

Table 3: Hazard indices for the studied samples.

| Sample Code | $H_{ex}$ | $I_\gamma$ | $I_\alpha$ | TAED (mSv.y$^{-1}$) | AGED ($\mu$Sv.y$^{-1}$) | ELCR*10$^{-3}$ |
|---|---|---|---|---|---|---|
| $F_1$(Chem. DAP) | 0.407 | 1.124 | 0.253 | 0.554 | 508.614 | 1.525 |
| $F_2$(Chem. DAP) | 0.340 | 0.886 | 0.206 | 0.440 | 387.465 | 1.210 |
| $F_3$(Chem. DAP) | 0.215 | 0.612 | 0.055 | 0.302 | 275.361 | 0.833 |
| $F_4$(Chem. DAP) | 0.720 | 2.036 | 0.462 | 1.001 | 934.694 | 2.754 |
| $F_5$(Chem. NPK) | 0.412 | 1.081 | 0.131 | 0.540 | 466.049 | 1.485 |
| $F_6$(Chem. NPK) | 0.491 | 1.376 | 0.331 | 0.677 | 629.955 | 1.862 |
| $F_7$(Chem. NPK) | 0.824 | 2.567 | 0.073 | 1.261 | 1198.342 | 3.469 |
| $F_8$(Orga.) | 0.374 | 1.080 | 0.156 | 0.532 | 494.616 | 1.464 |
| $F_9$(Orga.) | 0.287 | 0.818 | 0.118 | 0.403 | 371.908 | 1.110 |
| $F_{10}$(Orga.) | 0.318 | 0.923 | 0.181 | 0.453 | 427.501 | 1.247 |
| $F_{11}$(Orga.) | 0.976 | 2.990 | 0.195 | 1.468 | 1392.527 | 4.039 |
| $F_{12}$(Orga.) | 0.776 | 2.174 | 0.640 | 1.066 | 1004.665 | 2.933 |
| $F_{13}$(Orga.) | 0.508 | 1.412 | 0.363 | 0.695 | 646.055 | 1.911 |
| Min. | 0.215 | 0.612 | 0.055 | 0.302 | 275.361 | 0.833 |
| Max. | 0.976 | 2.990 | 0.640 | 1.468 | 1392.527 | 4.039 |
| Average | 0.511 | 1.468 > UNSCEAR 2000($\leq 1$) | 0.243 | 0.722 | 672.135 | 1.988 > UNSCEAR 2000(1.45) |

than the permissible limit, perhaps due to the high values of potassium in fertilizers in general, which means that they are not internationally accepted except the $F_2$(Chem. DAP) Iran, $F_3$(Chem. DAP) China, $F_9$(Orga.) Iraq and $F_{10}$ (Orga.) Iraq (Table 3).

Also noticed that the average total annual effective dose (TAED) values for all types of fertilizers are higher than the international safe limit of 0.48 (mSv.y$^{-1}$), the lifetime cancer risk (ELCR), was higher than the worldwide ($1.45 \times 10^{-3}$).

It can be noted that the values of the studied samples increased compared to USCEAR2000, as shown in Fig. 4. This means that there are risks when taking the average of all types.

## Radioactive Variable Correlation Study Using Pearson's Coefficient

Table 4 displays the results of Pearson correlation coefficients between all the radioactive factors examined for samples of both chemical and organic fertilizers. The relationship of $^{226}$Ra is weak, and it is not statistically significant with all other variables, except $I_\alpha$ For the fact that it depends on its calculation on $^{226}$Ra. Weak negative correlation between $^{232}$Th and all studied variables in fertilizer samples. The annual gonadal dose equivalent (AGED), excess lifetime cancer (ELCR), and external hazard indices ($H_{ex}$) have a high good positive correlation and high statistical significance.

Accordingly, were found to have a high good positive correlation coefficient of $^{40}$K. However, a slight negative correlation coefficient was found between the studied variables. Also, due to the reliance of these two variables on particular radioactivity, $H_{ex}$ has a substantial and statistically significant positive connection with the annual gonadal dose equivalent (AGED).

## Cluster Analysis

Cluster analysis determines the optimal set of observations or objects similar to each group (CA).

Using a dendritic diagram, a multivariate technique based on similarities divides system objects into categories
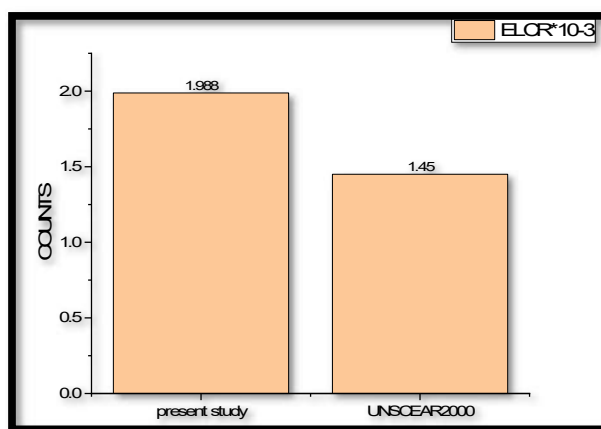


Fig. 4: Comparison of the current study with what is internationally accepted.

Table 4: Pearson correlation matrix among the radiological variables.

| Variables | Correlation | $^{226}$Ra | $^{232}$Th | $^{40}$K | $H_{ex}$ | $I_\alpha$ | AGED | ELCR |
|---|---|---|---|---|---|---|---|---|
| $^{226}$Ra | Pearson correlation | 1 | -.033- | 0.044 | 0.415 | 1.000** | 0.332 | 0.336 |
|  | P- value |  | 0.914 | 0.887 | 0.158 | 0 | 0.267 | 0.262 |
| $^{232}$Th | Pearson correlation |  | 1 | -.401- | -.124- | -.034- | -.206- | -.174- |
|  | P- value |  |  | 0.175 | 0.685 | 0.912 | 0.5 | 0.569 |
| $^{40}$K | Pearson correlation |  |  | 1 | .889** | 0.044 | .937** | .929** |
|  | P- value |  |  |  | 0 | 0.886 | 0 | 0 |
| $H_{ex}$ | Pearson correlation |  |  |  | 1 | 0.415 | .993** | .995** |
|  | P- value |  |  |  |  | 0.158 | 0 | 0 |
| $I_\alpha$ | Pearson correlation |  |  |  |  | 1 | 0.333 | 0.336 |
|  | P- value |  |  |  |  |  | 0.267 | 0.262 |
| AGED | Pearson correlation |  |  |  |  |  | 1 | .999** |
|  | P- value |  |  |  |  |  |  | 0 |
| ELCR | Pearson correlation |  |  |  |  |  |  | 1 |
|  | P- value |  |  |  |  |  |  |  |

** Correlation is significant at the 0.01 level (2-tailed).

* Correlation is significant at the 0.05 level (2-tailed).

## Dendrogram using Average Linkage (Between Groups)
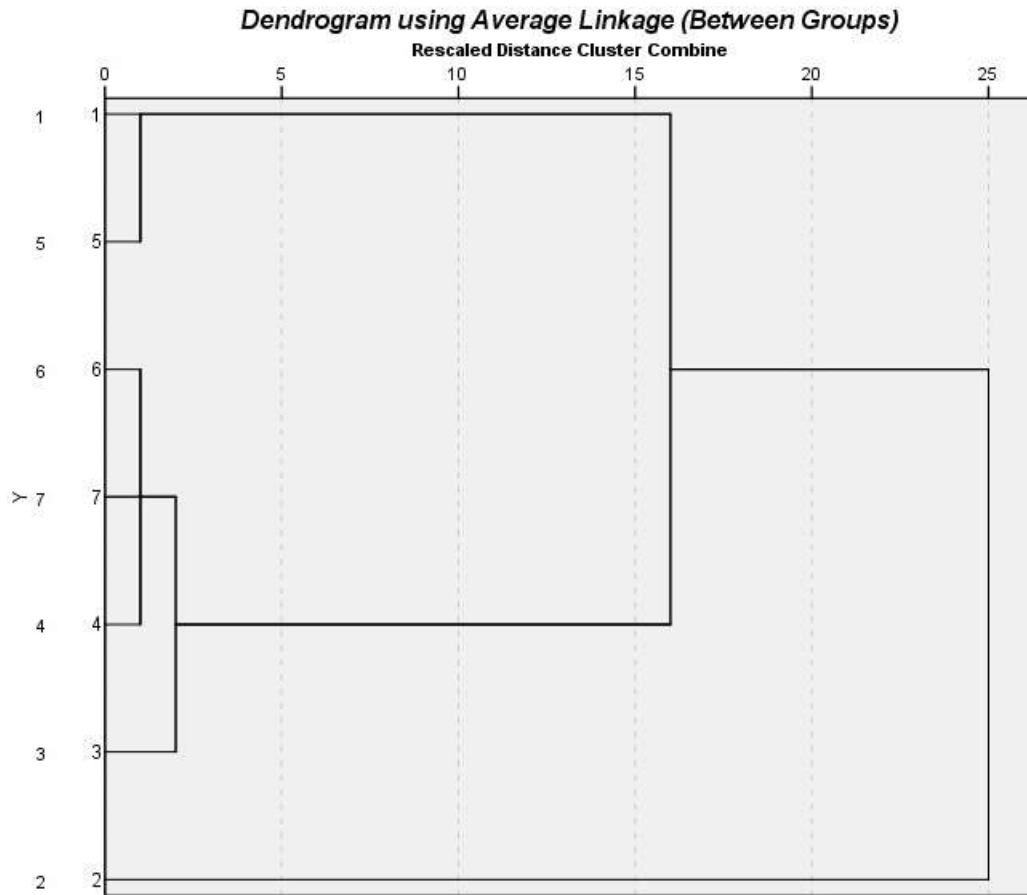### Rescaled Distance Cluster Combine



Fig. 5: Clusters of radionuclides and their radiological characteristics are displayed on a dendrogram.

or groups to visually show the order in which parameters or variables combine to produce groups with related qualities.

The first step is to group the most similar objects, and these initial groupings are created based on their shared characteristics. The maximum separation between any two individual variables and the separation between clusters are measures of similarity.

In contrast to a similarity of 0%, a similarity of 100% shows that the clusters were evenly spaced apart in the sample measurements (Guha et al. 2000). This study's cluster analysis calculates the Euclidean distance between the variables using the average linkage method. Fig. 5 displays the dendrogram that was derived. The seven parameters are arranged into three statistically significant groups in this dendrogram. Except for AGED, uranium, and thorium, all measured radiological parameters fall into Cluster 1; in contrast, Cluster 2 only includes the AGED, which is connected to uranium. Lastly, $^{40}K$ in cluster 3 has a large Euclidean distance. Based on already established commonalities, each cluster is created. The concentrations of $^{232}Th$ and $^{40}K$ are the principal radioactivity contributors from Clusters 1 and 2. Yet, the uranium content is what causes the annual gonadal dosage equivalent.

## CONCLUSION

The natural radioactivity and its risks were evaluated in samples of chemical and organic fertilizers by gamma-ray spectrometry.

It was the highest in radiation levels, Chem. NPK > Chem. Organic > Chem. DAP, Moreover, computed AGED was higher than $(300\,\mu Sv.y^{-1})$, which corresponded to a mean ELCR of $(1.988\times 10^{-3})$ that was higher than $(1.45\times10^{-3})$. Based on these results, more samples should be studied because they pose a threat to human health, as a foregone conclusion.

Among the statistical study results using Pearson's correlation factor and cluster analysis, there are variables with strong correlation and statistical significance and others with weak correlation.

Using the average linkage method, this study's cluster analysis calculates the Euclidean distance between the variables.

These fertilizers accumulate radioactivity in the soil, which can harm the health of farmers, workers, and consumers of products grown in soils overlaid with radiation.

## ACKNOWLEDGMENTS

## REFERENCES

Abbas, H.H., Kadhim, S.A., Alhous, S.F., Hussein, H.H., AL-Temimei, F.A. and Mraity, H.A.A. 2023. Radiation risk among children due to natural radioactivity in breakfast cereals. Nat. Environ. Pollut. Technol., 22(1): 527-533. https://doi.org/10.46488/NEPT.2023.v22i01.053

Adhab, H.G., Kadhim alshebly, S.A. and Alsabari, E.K. 2020. Assessment excess lifetime cancer risk of soils samples in Maysan neighborhood adjacent to the middle Euphrates cancer center in Najaf/Iraq. IOP Conf. Ser.: Mater. Sci. Eng., 928(7). https://doi.org/10.1088/1757-899X/928/7/072100

Alam, M.N., Chowdhury, M.I., Kamal, M., Ghose, S., Islam, M.N., Mustafa, M.N., Miah, M.M.H. and Ansary, M.M. 1999. The 226Ra, 232nd, and 40-K activities in beach sand minerals and beach soils of Cox's Bazar, Bangladesh. J. Environ. Radioact., 46(2): 243-250. https://doi.org/10.1016/S0265-931X(98)00143-X

Alhous, S.F., Kadhim, S.A., Alkufi, A.A., Muhmood, A.A. and Zgair, I.A. 2020. Calculation of radioactivity levels for various soil samples of Karbala-Najaf road (Ya-Hussein)/Iraq. IOP Conf. Ser.: Mater. Sci. Eng., 928(7): 072076. https://doi.org/10.1088/1757-899X/928/7/072076

Alkufi, A.A., Alhous, S.F. and Kadhim, S.A. 2020. Annual Committed Effective dose as a result of daily Consumption of Medicinal Herbs in Iraq. IOP Conf. Ser.: Mater. Sci. Eng., 928(7) 072054. https://doi.org/10.1088/1757-899X/928/7/072054

Arafa, W. 2004. Specific activity and hazards of granite samples collected from the Eastern Desert of Egypt. J. Environ. Radioact., 75(3): 315-327. https://doi.org/10.1016/j.jenvrad.2004.01.004

Aswood, M.S. 2019. Natural radionuclides in six selected fish consumed in south Iraq and their committed effective doses. SN Appl. Sci., 1(1): 1-5.

Constantin, F. 2020. A digital positron annihilation lifetime spectrometer. Rom. J. Phys., 65, 901.

El-Taher, A. and Althoyaib, S.S. 2012. Natural radioactivity levels and heavy metals in chemical and organic fertilizers used in the Kingdom of Saudi Arabia. Appl. Radiat. Isot., 70(1): 290-295. https://doi.org/10.1016/j.apradiso.2011.08.010

Faweya, E.B., Ayeni, M.J., Olowomofe, G.O. and Akande, H.T. 2018. Estimation of radiation exposure in soils and organic (animal) and inorganic (chemical) fertilizers using active technique. Int. J. Environ. Sci. Technol., 15(9): 1967-1982. https://doi.org/10.1007/s13762-017-1574-x

Guha, S.R., Rastogi, R. and Shim, K. 2000. ROCK: A robust clustering algorithm for categorical attributes. Inf. Syst., 25(5): 345-366. https://doi.org/10.1016/S0306-4379(00)00022-3

Hignett, T.P. 2018. Outlook, concepts, definitions, and scientific organizations for the fertilizer industry. Manual of fertilizer processing (pp. 1-33. Routledge.

Jibiri, N.N. and Fasae, K.P. 2012. Activity concentrations of 226Ra, 232nd, and 40K in brands of fertilizers used in Nigeria. Radiat. Prot. Dosim., 148(1): 132-137. https://doi.org/10.1093/rpd/ncq589

Kadhim, S.A. 2020. Estimated the concentration of 238U, 232nd and 40K in flour samples of Iraq markets. J. Phys.: Conf. Ser. IOP Publ., 47: 101421.

Khater, A.E.M. and Al-Sewaidan, H.A. 2008. Radiation exposure due to agricultural uses of phosphate fertilizers. Radiat. Meas., 43(8): 1402-1407. https://doi.org/10.1016/j.radmeas.2008.04.084

Knecht, M.F. and Göransson, A. 2004. Terrestrial plants require nutrients in similar proportions. Tree Physiol., 24(4): 447-460. https://doi.org/10.1093/treephys/24.4.447

Lambert, R., Grant, C. and Sauvé, S. 2007. Cadmium and zinc in soil solution extracts following the application of phosphate fertilizers. Sci. Total Environ., 378(3): 293-305. https://doi.org/10.1016/j.scitotenv.2007.02.008

Mohanty, A.K., Sengupta, D., Das, S.K., Saha, S.K. and Van, K.V. 2004. Natural radioactivity and radiation exposure in the high background area at Chhatrapur beach placer deposit of Orissa, India. J. Environ. Radioact., 75(1): 15-33. https://doi.org/10.1016/j.jenvrad.2003.09.004

Robinson, R.A. and Sutherland, W.J. 2002. Post-war changes in arable farming and biodiversity in Great Britain. J. Appl. Ecol., 39(1): 157-176. https://doi.org/10.1046/j.1365-2664.2002.00695.x

Stenström, K., Skog, G., Georgiadou, E., Genberg, J. and Mellström, A., 2011. A guide to radiocarbon units and calculations. (LUNFD6(NFFR-3111)/1-17/(2011)). Lund University, Nuclear Physics.

Uosif, M.A.M., Mostafa, A.M.A., Elsaman, R. and Moustafa, E. 2014. Natural radioactivity levels and radiological hazards indices of chemical fertilizers commonly used in Upper Egypt. J. Radiat. Res. Appl. Sci., 7(4): 430-437. https://doi.org/10.1016/j.jrras.2014.07.006

Vincevica-Gaile, Z., Stankevica, K., Irtiseva, K., Shishkin, A., Obuka, V., Celma, S., Ozolins, J. and Klavins, M. 2019. Granulation of fly ash and biochar with organic lake sediments–A way to sustainable utilization of waste from bioenergy production. Biomass Bioenergy, 125: 23-33. https://doi.org/10.1016/j.biombioe.2019.04.004

Ziqiang, P., Yin, Y. and Mingqiang, G. 1988. Natural radiation and radioactivity in China. Radiat. Prot. Dosim., 24(1-4): 29-38. https://doi.org/10.1093/rpd/24.1-4.29

## ORCID DETAILS OF THE AUTHORS

Abdulhussein A.Alkufi: https://orcid.org/0000-0002-4741-4409
Shaymaa A. Kadhim: https://orcid.org/0000-0002-3991-5318
Azhar S.Alaboodi: https://orcid.org/0000-0002-3029-1115
Shatha F. Alhous: https://orcid.org/0000-0001-9128-099x

Original Research Paper

doi https://doi.org/10.46488/NEPT.2023.v22i04.031

Open Access Journal

# Defluoridation of Water by Biowaste Material – A Study of Adsorption Kinetics and Isotherms

K. Kiran Kumar* iD, Ratnakaram Venkata Nadh**† iD, Kaza Somasekhara Rao*** and G. Krishnaveni* iD

*Department of Chemistry, KBN College, Vijayawada-520001, Andhra Pradesh, India
**Industrial Chemical Product Development and Analysis Centre, Department of Chemistry, GITAM Deemed to be University, Bengaluru Campus, Bengaluru-561203, Karnataka, India
***Department of Chemistry, Acharya Nagarjuna University, Nagarjuna Nagar, Guntur-522510, Andhra Pradesh, India
†Corresponding author: Ratnakaram Venkata Nadh; doctornadh@yahoo.co.in

## ABSTRACT

Human beings experience adversative effects due to the large fluoride concentrations present in potable water. Because of the low cost and simple operation, the extensively acknowledged process is adsorption. The objective of this study is to investigate the performance of some of the prepared carbons from bio-waste materials *viz., Citrus limon, Citrus nobilis, Pithecellobium dulce,* and *Bombax malabaricum* sheaths in defluoridation. Initial concentration, particle size, agitation time, adsorbent dose, and pH were the different parameters chosen to study their effect on adsorption. Studied the adsorption kinetics. Further suitability to adsorption isotherms was reviewed.

## INTRODUCTION

Prolonged exposure to fluoride at higher concentrations leads to disease – Fluorosis, a serious health concern in several portions of the world, wherever drinking water contains higher than the permissible limits (1 to 1.5 ppm) of fluoride (Choubisa 2018). Crippling fluorosis, dental fluorosis, and skeletal fluorosis are the various manifestations of fluorosis. Fluoride at higher levels affects bone mineralization and collagen synthesis (Antonarakis & Moseley 2014).

It involves diminishing the function of the soft tissue of the animals intoxicated by fluoride due to crossing the cell membrane and entering soft tissues. Inhibition of enzymes (involved in energy producing and transferring, synaptic transmission membrane transport) by it causes affecting the muscle and brain (Yan et al. 2016). It also inhibits enzymes associated with pathways (like myosin-ATPase and pentose) and antioxidant defense systems. In addition, deactivates glutathione peroxidase, superoxide dismutase, and other enzymes that scavenge the free-radical. A decrease in GSH levels and improved ascorbic acid and MDA activity causes elevated oxidative stress in three to ten-year-old children (Hamza et al. 2015).

Human beings are exposed to fluoride in many ways, like inhalation of fluorine-laden air, exposure to dental products, and consumption of fluoride-rich drinking water, food (fish, fruits, and vegetables), and beverages (tea). Out of the total fluoride exposure, air has minor responsibility. The production of phosphate fertilizers that burn coal containing fluoride contributes to fluoride concentration in the air (Choubisa & Choubisa 2016). Dental products are used for the demineralization of enamel (Dental varnishes) and to lessen dental caries in adults and children (fluoride-containing toothpaste, gels, and tablets) (Shen et al. 2016). Fluoride mounts up in the bones and protein concentrates of fish.

Similarly, vegetables and fruits cultivated in industrial areas with high emissions of fluoride. Leafy parts of plants are found to have more amounts of accumulated fluorine than roots. For example, high fluoride levels in tea leaves (400 mg.kg$^{-1}$ dry weight) (Zohoori & Duckworth 2016). The chief contribution of fluorosis is fluorine-laden laden drinking water. High amounts of fluoride were reported in potable water supplied in various countries (Balasubramanian & Umaranib 2014). In lakes' surface waters, fluoride hoards

up due to high evaporation and leaches from the lava, tephra, alkalic rocks, and minerals like fluorspar and fluorapatite (Bosshard-Stadlin 2017). The influence of contiguous rocks is responsible for high amounts of fluorine in groundwater compared to surface water. Other origins are seepage from proximate saline formations and low recharging of groundwater (Li et al. 2018). Higher fluoride concentrations recorded in rainwater samples were attributed to nearby industrial areas containing aluminum smelters and glass and ceramics manufacturing units (Rodrigues et al. 2017).

Various techniques used for defluoridation, like Precipitation/coagulation, Membrane processes (Reverse osmosis, Nano-filtration, Electrodialysis), Ion exchange, and adsorption, have their advantages and limitations. However, adsorption has a very good potential for defluoridation due to various factors like cost effectiveness, regeneration ability (to reuse the adsorbent), high elimination capacities, and simple operation (Yadav et al. 2018). For the defluoridation of water, different adsorption materials were used. For example, carbon adsorbent materials (derived from agricultural by-products), Waste carbon slurry, concrete adsorbent materials (Cement paste, Lightweight concrete materials, quick lime), biosorbent materials (chitosan adsorbent materials (Natural chitosan, Magnetic chitosan, Chitin), clay materials and other adsorbent materials (ligand exchange cotton cellulose loaded with iron(III), alum producing unit waste residue, novel Fe–Al–Ce tri-metal oxide, MgAl–CO$_3$ layered double hydroxides, Mg/Al hydrotalcite-like compounds as well as calcined products from them) (Mondal & George 2015). Continuous availability of raw materials and reduced cost of production/biowaste disposal (Wong et al. 2018, Mokkapati et al. 2015, Ramya et al. 2016a, 2016b, 2015) encouraged the researchers to explore the possibility of usage of biowaste (*Citrus limon, Citrus nobilis, Pithecellobium dulce,* and *Bombax malabaricum)* to prepare charcoals for their usage in defluoridation of water.

The prime objectives of the current research work are (i) to learn the influence of physico-chemical parameters such as carbon amount, initial fluoride concentration, pH, and agitation time in batch biosorption, (ii) to evaluate the adsorption efficiency of this carbon by employing adsorption kinetics and isotherm and (iii) to compare their adsorption potential with the already existing biomaterials.

## MATERIALS AND METHODS

Analytical reagent-grade chemicals were procured and used in the present research work. The apparatus used is the Elico UV-Visible Spectrophotometer (Model SL 171) and Elico pH Meter.

## Preparation of Activated Carbon from Biowaste

Bio-waste materials *viz.*, *Citrus limon, Citrus nobilis, Pithecellobium dulce,* and *Bombax malabaricum sheaths* were the starting materials to prepare the activated carbons and then utilized as adsorbents for defluoridation. Fruits vending shops and agriculture fields of Nuzvid Mandal, Andhra Pradesh, India, were the sources to collect the bio-waste materials of the current study. The adhered dust on the above-gathered bio-waste was removed by washing it with water and dried out by exposing it to sunlight for three days. Then crushed, the above-dried material was followed by carbonization at 600°C in an electrically heated horizontal tube furnace under the flow of nitrogen for 4 h for all conditions, followed by activation in the stream at 850°C; the activated sample was obtained directly under steam pyrolysis of 600°C to 700°C. Then these carbons were cooled to ambient temperature and collected as uniform particles by sieving. Mostly, the chemical or structural integrity of the biosorbents is modified by diverse methods, viz., chemical grafting, alkali or acid modification, and oxidation, to enhance the adsorption capacity (Li et al. 2010, Xue et al. 2012). Increased chemical reactivity and improved active surface area are due to the above activating techniques, which cause the creation of surface functional groups. Hence, chemical bonding with the ions in an aqueous solution occurs due to the chemical reactivity.

Hence, these carbons are treated with 1N HNO$_3$ and can settle for 2-3 h, filtered, and dried at 120°C for 2 h in an air oven. Then the above contents were brought to the ambient temperature. Clean air-tight vessels were used to store the above-prepared activated carbons and further used in the experiments with batch adsorption. The obtained acid-activated carbons are designated as *Citrus limon, Citrus nobilis, Pithecellobium dulce,* and *Bombax malabaricum* sheaths.

## Batch Adsorption Studies

Pipetted out 5 ppm fluoride standard aqueous solution (50 mL) into a flask. The batch mode was adopted by engaging ambient temperature (30 ± 1°C) and constant pH to carry out the adsorption studies. REMI shaker was used to maintain a mechanical stirring at 240 ppm after adding the above-prepared carbons at a 0.5 g.L$^{-1}$ dosage. Equilibrated the fluoride aqueous with these carbons in each experiment and then centrifuged the withdrawn solution. Then Zr-SPADNS method was employed to measure the final concentration of fluoride (Bellack & Schouboe 1958). The standard curve and the colored solution's absorbance value were used to learn the fluoride concentration in the defluoridized sample.

Each experiment was carried out by adopting the same procedure by changing the experimental conditions in the following ranges: (i) agitation time (from 10-120 min), (ii) adsorbent dosage (from 1.0 to 9.0 g.L$^{-1}$), (iii) pH of the initial standard fluoride solution (ranging from 3 to 9) (iv) initial concentration of fluoride solution (ranging from 1 to 7 ppm) and (v) carbon particle size (45 to 150 μ). The given below mathematical equations were used to get the % of defluoridation and adsorbed fluoride amount (in mg.g$^{-1}$)

$$q_e = \frac{(C_0 - C_e) \times V}{W} \qquad ...(1)$$

$$\text{Percent removal of nickel (II)} = \frac{(C_0 - C_e) \times 100}{C_0}$$

$$...(2)$$

In the present case, $C_0$ and $C_e$ are the initial and final concentrations of fluoride ions in aqueous solution before and after adsorption, $q_e$ (mg.g$^{-1}$) is the adsorption capacity of the adsorbent at equilibrium, V and W are the fluoride solution volume, and mass of carbons.

## RESULTS AND DISCUSSION

The adsorption potential of the prepared carbons from bio-waste materials for the defluoridation of water was studied by carrying out the adsorption experiments. The influence of various parameters (adsorbent dose, contact time, particle size, and initial fluoride concentration) was determined. Further studied the adsorption kinetics and isotherms.

### Effect of Adsorbent Dose

To appraise the sorption efficiency on the defluoridation, studied the adsorbent (CLC, CNC, PLDC, and BMC) dose effect on the fluoride ion removal. The increase in the adsorbent dose resulted in the exponential increase in % of fluoride removal (Fig 1.a.). It may be explained based on the improvement of available sites due to a hike in the effective surface area at larger adsorbent doses (Gupta & Sharma 2002).

Then, attained equilibrium after a certain dose. The relative percentage removal of fluoride after the doses of 5, 3, 3, and 3.5 g for CNC, BMC, PLDC, and CLC, respectively, are found to be insignificant and fixed as optimum doses. Overcrowding of biosorbent particles has resulted due to the biosorbent dosage escalation and hence observed an overlap of the adsorption sites (Garg et al. 2008). It is responsible for the decline in unit adsorption (Fig 1.b.).

### Effect of Agitation Time

A significant role is played by the contact time in the adsorption studies, which may be further experimental parameters that can influence the kinetics of adsorption. By changing the agitation time, i.e., contact time between adsorbent and fluoride water (5 - 120 min) at the constant conditions of other parameters like temperature (30 ± 0$^o$C), initial fluoride concentration (5 ppm), and adsorbent dose at optimum conditions, the extent of defluoridation was studied to learn about the dynamics and kinetics of fluoride adsorption by different adsorbents. Fig. 2 shows the extent of defluoridation due to a change in agitation time. The % of fluoride removal by the present adsorbent carbons is quick at the beginning. Still, its sluggishness was observed later and then nearly constant values with a further enhancement in the contact time. The availability of ample surface area of these carbons explains the higher rate of defluoridation at the initial time. A drop in adsorption rate with a rise in time can be attributed to the drop in the accessibility to the active sites. A hike in % of defluoridation with a surge of contact time can be understood from the known information
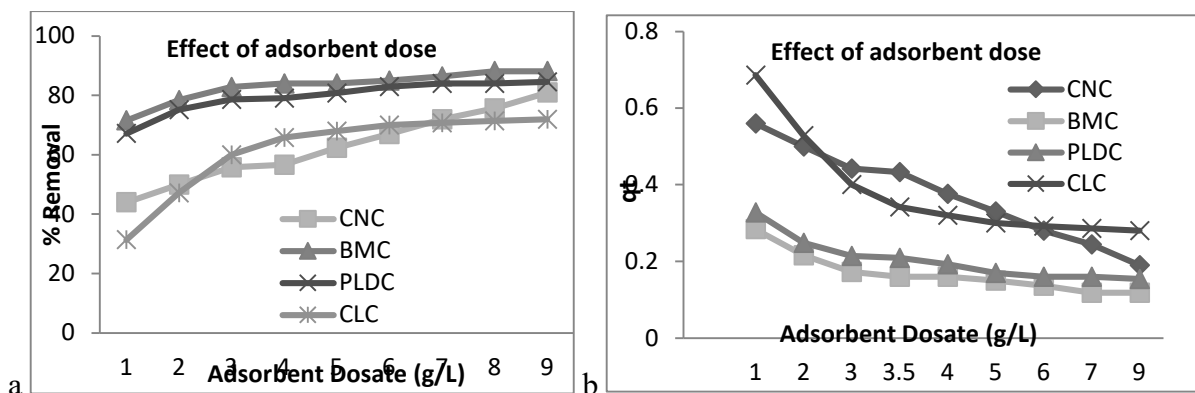


Fig. 1: Effect of biosorbent dose on (a) percent removal and (b) unit adsorption capacity in defluoridation.
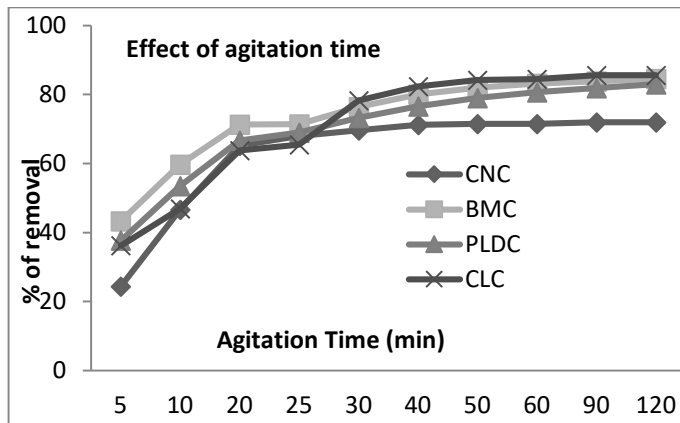
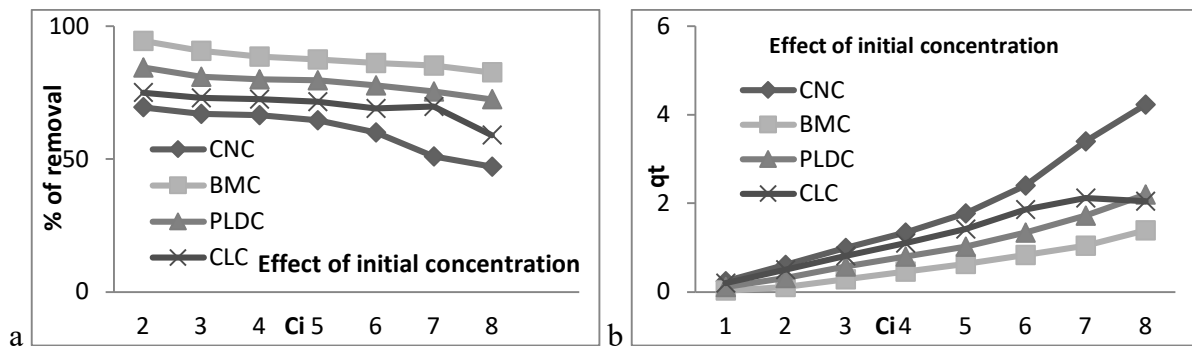Fig. 2: Effect of agitation time during defluoridation.



Fig. 3: Effect of initial fluoride ion concentration on (a) percent removal and (b) unit adsorption capacity in defluoridation.

that more time acquaints the fluorides to adsorb on these carbons (Bhattacharya et al. 2006). In the case of all carbons, forty minutes was when the highest % of adsorption was observed, and then a drop was noticed. Involvement of 3 steps can be proposed in the entire sorption mechanism from the observations in the % of defluoridation with time (Fig. 2). Those three steps can be listed as (i) film diffusion or molecular diffusion where an external mass transfer is involved, i.e., fluoride ions are transferred to the adsorbent's external surface from the aqueous solution (ii) fluoride ions adsorption takes place on the surface of particles; and (iii) intraparticle diffusion where the adsorbed fluoride ions transfer to the carbon particles internal surfaces (Li et al. 2010, Moradi 2011).

**Effect of Initial Concentration of Fluoride Ions**

A systematic study has been carried out to learn about the adsorption capacity of these four activated carbons with a variation in the fluoride ions' initial concentration. The prime factors involved in studying fluoride ions (adsorbate) concentration on these activated carbons are the untenanted adsorption spots and the accumulation of fluoride ions at

their upper concentrations (Min et al. 2004). In each case of these carbons, a firm fall in the % of defluoridation was detected with growth in opening fluoride ion concentration (Fig. 3a). The present trend of diminishing defluoridation can be made clear from an enhanced rivalry amongst the unadsorbed fluoride ions towards the leftover binding sites on these carbons' surface at the superior fluoride concentrations (Min et al. 2004). However, the value of $q_t$ (uptake capacity) of fluoride ions enhanced with an intensification of the initial concentration of fluoride (Fig. 3b). It can be understood from the disposal of larger fluoride ions in the aqueous solution towards adsorption, which is a motivating force to overwhelm resistance against the mass transfer between these activated carbons and fluoride ions. Consequentially improves the collision probability between the activated carbons and fluoride ions (Rao et al. 2008).

**Effect of pH**

A deci normal NaOH or HCl was used to maintain the fluoride-containing aqueous solution at various pH levels (3 to 9). Fig. 4 reveals the influencing nature of the pH of the medium on the defluoridation. An increase in the pH of
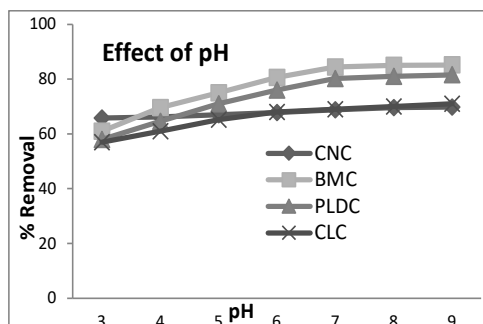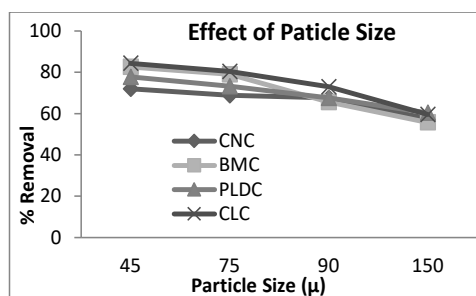
Fig. 4: Effect of pH on the % removal of fluoride.



Fig. 5: Effect of particle size on the % removal of fluoride.

the medium has resulted in an improved defluoridation up to pH 7 and then unchanged in the present investigation. The optimum pH is 7.

**Effect of Particle Size**

A decrease in these carbons' particle diameter resulted in improved fluoride ions uptake (Fig. 5). A diminished external mass transfer resistance and availability of a large surface area for defluroidation have resulted from the accessibility of

a high number of small-size particles with the same amount of biowaste adsorbent.

**Adsorption Kinetics**

Pseudo-first-order (Lagergren 1898) (Eq. 3) and pseudo-second-order (Ho & McKay 1999) (Eq. 4) kinetic equations are used to investigate the defluoridation mechanism using these four adsorbents.

$$ln\,(q_e - q_t) = ln\,q_e - k_1 t \tag{3}$$

$$\frac{t}{q} = \left(\frac{1}{k_2 q_e^2}\right) + \left(\frac{t}{q_e}\right) \tag{4}$$

In the above equation, the quantities of fluoride ions adsorbed on these carbons at equilibrium and time t are denoted by $q_e$ and $q_t$, respectively. $k_1$ and $k_2$ represent the corresponding rate constants of pseudo-first-order and second orders. Fig. 6a and 6b. respectively denote the linear plots of pseudo first and second-order kinetics and present the values of corresponding parameters in Table 1.

In the current study of fluoride removal by the prepared carbons, the kinetic data, i.e., determination coefficient ($R^2$) values, agree with the pseudo-second-order that of the pseudo-first-order. Further used the Elovich equation (Eq. 5) to learn about its suitability for the adsorption of fluoride ions (Sparks 1986). In equation 5, $q_t$, $\alpha$, and $\beta$ symbolize respectively the removed amount of fluoride at a time t, the rate of defluoridation at the beginning, and a constant pertaining to desorption (Table 1).

$$q_t = \frac{1}{\beta}\ln(\alpha\beta) + \frac{1}{\beta}\ln(t) \tag{5}$$

The significant interactions between these activated carbons and fluoride ions are intra-particle transport, pore diffusion, and film diffusion. Among the above three factors, the first and the latter are the prime steps in rate limiting. But, in a continuous flow system, film diffusion is the likely rate-
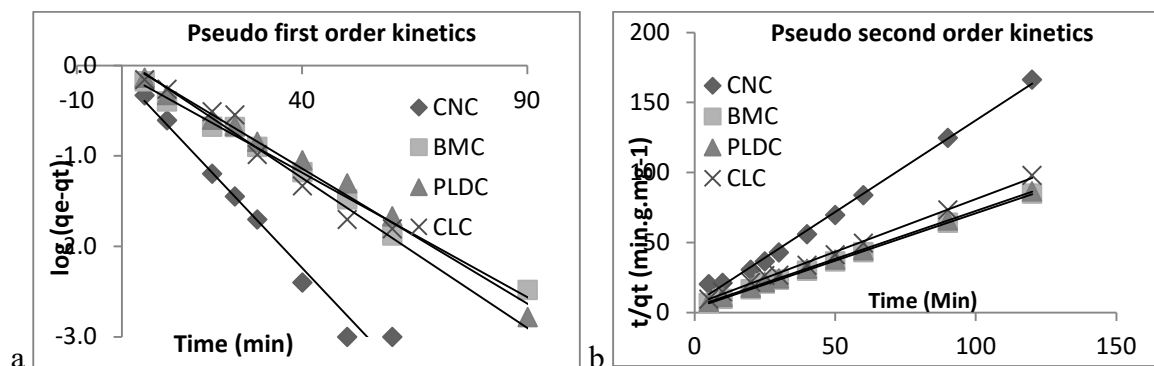


Fig. 6: Linear plots of (a) pseudo-first-order kinetics and (b) pseudo-second-order adsorption kinetics.

Table 1: Defluoridation kinetic parameters and values of kinetic models using 15 g.L$^{-1}$ CFP and SSP as biosorbents.

| Kinetic adsorption model | Parameter | CLC | CNC | PLDC | BMC |
|---|---|---|---|---|---|
| Pseudo-first-order | $q_e$ [mg.g$^{-1}$] | 1.0912 | 0.8835 | 1.0595 | 0.9234 |
| | $k_1$ [min$^{-1}$] | 0.0332 | 0.0528 | 0.0299 | 0.0276 |
| | $R^2$ | 0.9691 | 0.9761 | 0.9875 | 0.9906 |
| Experimental | $q_e$ [mg.g$^{-1}$] | 1.083 | 0.858 | 1.213 | 1.2 |
| Pseudo-second-order | $q_e$ [mg.g$^{-1}$] | 1.3243 | 0.7627 | 1.4613 | 1.4738 |
| | $k_2$ [g.mg$^{-1}$.min$^{-1}$] | 0.0995 | 0.2677 | 0.1111 | 0.1418 |
| | $R^2$ | 0.9966 | 0.9952 | 0.9998 | 0.9997 |
| Elovich's kinetic model | $\alpha$ [mg.g$^{-1}$.min$^{-1}$] | 0.478 | 0.398 | 1.010 | 2.049 |
| | $\beta$ [g.mg$^{-1}$] | 4.034 | 7.107 | 4.186 | 4.65 |
| | $R^2$ | 0.9067 | 0.7672 | 0.9299 | 0.9116 |
| Weber intraparticle diffusion model | $K_d$ [mg.g$^{-1}$.min$^{1/2}$] | 0.081 | 0.043 | 0.077 | 0.069 |
| | $\theta$ [$\mu\gamma.\gamma^{-1}$] | 0.518 | 0.369 | 0.689 | 0.798 |
| | $R^2$ | 0.750 | 0.543 | 0.760 | 0.743 |
| Boyd kinetic model | $R^2$ | 0.9691 | 0.9671 | 0.9875 | 0.9906 |

limiting step (Goswami & Ghosh 2005). Therefore, further analysis was forwarded with Weber's model concerned to intra-particle diffusion (Eq. 6). Table 1 shows the calculated concerned statistic parameters like ꭥ (a constant value with regard to the thickness of the boundary layer) and $K_d$ (a rate constant related to intra-particle transport) (Sousa et al. 2007).

$$q_t = K_d t^{1/2} + \theta \qquad (6)$$

In addition, the Boyd kinetics model (Eq. 7) was used to analyze the adsorption data. In this model, F denotes the fluoride ions fraction adsorbed at any time (t min), which tells about the deviance of the fluoride ions' occupation on the adsorbent from the aqueous system. It indicates that external mass transport governs the adsorption mechanism (Kumar et al. 2011).

$$B_t = -0.4977 - \ln(1 - F) \qquad (7)$$

**Adsorption Isotherms**

To understand the nature of the interaction of the fluoride ion on the surface of these carbons and to reveal the adsorption mechanism, adsorption isotherms are very useful. In the present study, to evaluate the adsorption of fluoride onto CNC, BMC, PDLC, and CLC, three adsorption isotherms (Langmuir, Freundlich, and Temkin models) were studied by variation of $C_i$ (initial fluoride ion concentration). It is a well-known fact that Langmuir and Freundlich's isotherms describe monolayer and multilayer adsorptions (Fig. 7a & 7b). Table 2 lists the coefficient of determination ($R^2$) values and parameter values ($K_D$, $K_L$, $K_F$, $A_T$, n, B, $q_D$, and $q_m$), which are characteristics of these three isotherms. $R_L$

is the Langmuir isotherms characteristic. It is denoted as an equilibrium parameter or separation factor, a dimensionless constant.

$R_L = 1/[1+K_L C_o]$ was the equation used to derive values of these parameters. In this equation, initial fluoride ions concentration and Langmuir constant are represented respectively by $C_o$ and $K_L$. The RL values give Langmuir adsorption isotherm characteristics. Irreversible, favorable, unfavorable, and linear adsorptions can be expected from $R_L$ values 0, 0 to 1, 1, and greater than 1, respectively (Tewari et al. 2005). $R_L$ parameter values for different adsorbents are found to be CNC (0.577, 0.327, 0.255, 1, 1, 1, 1, 1), BMC (0.304, 0.155, 0.264, 1, 1, 1, 1, 1), PDLC (0.573, 0.140, 0.26, 1, 1, 1, 1, 1) and CLC (0.814, 0.103, 0.369, 1, 1, 1, 1, 1) at different initial concentrations of 1 to 8 mg.L$^{-1}$ with one unit increment. These values show that defluoridation by these adsorbents is favorable at lower initial concentrations and linear higher concentrations. Additionally, the values of n > 1 from Freundlich isotherm also reflected the favorable adsorption conditions (Crini & Ndongo Peindy 2006).

$K_L$ is the sorption energy representing the Langmuir constant; $K_F$ and n are the interactions between fluoride ions and carbons at a given temperature measured by these Freundlich constants. T represents the Kelvin-measured absolute temperature; B is the heat of sorption related to the Temkin constant; and $A_T$ is the equilibrium binding constant for the Temkin isotherm.

Preferred monolayer adsorption is evident in CNC from the calculated $R^2$ values in the adsorption isotherms studied in Table 2. However, in the case of other adsorbents (BMC, PDLC, and CLC), both the mono and multilayer adsorptions
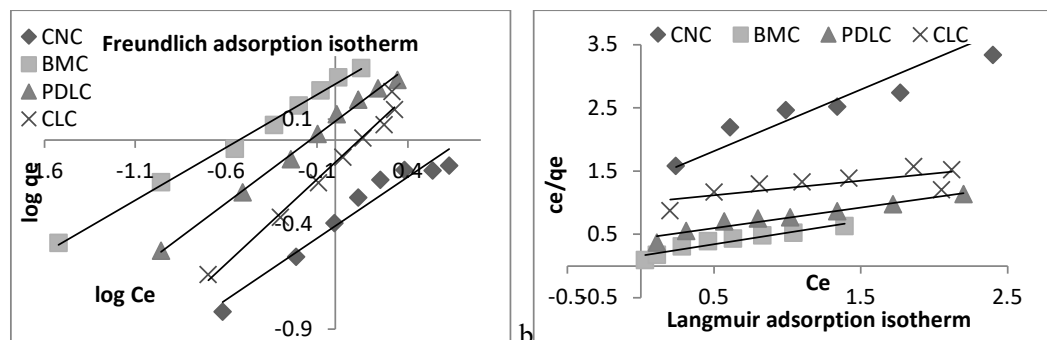
Fig. 7: Linear plots of (a) Langmuir adsorption isotherm and (b) Freundlich adsorption isotherm on fluoride adsorption.

Table 2: Fluoride ion adsorption isotherm parameters at 5.0 pH, 303 K, and 200 rpm agitation speed.

| Isotherm | Linear form of adsorption isotherm | Parameter | Parameter values for adsorbents | | | |
|---|---|---|---|---|---|---|
| | | | CLC | CNC | PDLC | BMC |
| Langmuir | $\dfrac{C_e}{q_e} = \dfrac{C_e}{q_m} + \dfrac{1}{K_L q_m}$ | $K_L$ [L.mg$^{-1}$] | 0.228 | 0.732 | 0.746 | 2.286 |
| | | $q_m$ [mg.g$^{-1}$] | 4.365 | 1.028 | 3.069 | 2.725 |
| | | $R^2$ | 0.570 | 0.972 | 0.948 | 0.927 |
| Freundlich | $\log q_e = \log K_F + \dfrac{1}{n}\, log C_e$ | n. | 1.243 | 1.711 | 1.541 | 1.988 |
| | | $K_F$ [mg.g$^{-1}$] [L.mg$^{-1}$]$^{1/n}$ | 0.784 | 0.389 | 1.228 | 1.849 |
| | | $R^2$ | 0.982 | 0.946 | 0.996 | 0.995 |
| Temkin | $q_e = B \ln A_T + B \ln C_e$ | B [J.mol$^{-1}$] | 0.56 | 0.23 | 0.57 | 0.49 |
| | | $A_T$ [L.g$^{-1}$] | 5.27 | 7.01 | 10.56 | 39.51 |
| | | $R^2$ | 0.84 | 0.95 | 0.93 | 0.90 |

can be considered with a preference for the latter. An even distribution of binding energies can be expected in all these carbon adsorbents with more inclination by CLC, as evident from Temkin isotherm (Kaewsarn & Yu 2001). For these models, the finest appropriate order can be concluded as given below.

Langmuir > Temkin > Freundlich : for CNC

Freundlich > Langmuir > Temkin: for BMC and PDLC

Freundlich > Temkin > Langmuir: for CLC

Compared to the adsorption capacities of some of the adsorbents like activated rice husk ash (0.426 mg.g$^{-1}$) (Mondal et al. 2012), banana peel (0.3123 mg.g$^{-1}$), and coffee husk (0.2946 mg.g$^{-1}$) (Getachew et al. 2015), the present study carbons – CNC (0.7 mg.g$^{-1}$) BMC (1.4 mg.g$^{-1}$), PDLC (1.3 mg.g$^{-1}$) and CLC (1.2 mg.g$^{-1}$) shown good defluoridation capacities. In view of the good sorption capacities of biomaterials in literature (Wong et al. 2018, Li et al. 2010, Ramya et al. 2015) and the present study, they can be effectively used to remove different pollutants.

## CONCLUSION

In the defluoridation of water using activated carbons prepared from bio-waste materials as adsorbents, the optimum dose for CNC, BMC, PLDC, and CLC are 5, 3, 3, and 3.5 g L$^{-1}$, the optimum time is 40min, the optimum pH is 7 at 30±1$^{o}$C. In the optimum pH conditions and dose of adsorbents, the percentage of defluoridation from synthetic samples is 71, 80, 76.6, and 82% for CNC, BMC, PLDC, and CLC, respectively. Different kinetic models (Elovich, Boyd, Webers) and kinetic orders (pseudo-first and second orders) were utilized to explore the adsorption mechanism. These results indicate that BMC and PLDC can be utilized as potential adsorbents for the defluoridation of water. Fluoride removal was 70 to 80% from potable water samples with 3-4.5 ppm fluoride under optimized conditions. The selected carbons successfully defluorinated potable water to the permissible limit. Hence, considering the fact that the selected biomaterials are abundantly available in nature and have a negligible cost involved in processing, these highly efficient carbons seem to have a rosy path for potable water

defluoridation and also can be practically used at household level by all populations including those who are without having any scientific knowledge.

## REFERENCES

Antonarakis, G.S. and Moseley, R. 2014. Waddington RJ. Differential influence of fluoride concentration on the synthesis of bone matrix glycoproteins within mineralizing bone cells *in vitro*. Acta. Odontol. Scand., 72(8): 1066-1069. doi: 10.3109/00016357.2014.882982.

Balasubramaniana, T. and Umaranib, R. 2014. A study on the health hazards of consuming high fluoride content potable water using fuzzy cognitive maps-A Data mining Approach. Women, 520: 52.

Bellack, E. and Schouboe, P.J. 1958. Rapid photometric determination of fluoride in water. Use of sodium 2-(p-sulfophenylazo)-1, 8-dihydroxynaphthalene-3, 6-disulfonate-zirconium lake. Anal. Chem., 30(12): 2032-2034. doi: 10.1021/ac60144a050.

Bhattacharya, A.K., Mandal, S.N. and Das, S.K. 2006. Adsorption of Zn(II) from aqueous solution by using different adsorbents. Chem. Eng. J., 123: 43-51. doi:10.1016/j.cej.2006.06.012.

Bosshard-Stadlin, S.A., Mattsson, H.B., Stewart, C. and Reusser, E. 2017. Leaching of lava and tephra from the Oldoinyo Lengai volcano (Tanzania): Remobilization of fluorine and other potentially toxic elements into surface waters of the Gregory Rift. J. Volcanol. Geother. Res., 332: 14-25. doi: j.jvolgeores.2017.01.009.

Choubisa, S.L. 2018. A brief and critical review of endemic hydrofluorosis in Rajasthan, India. Fluoride, 51(1): 13-33.

Choubisa, S.L. and Choubisa, D. 2016. Status of industrial fluoride pollution and its diverse adverse health effects in man and domestic animals in India. Environ. Sci. Pollut. Res., 23(8): 7244-7254. doi: 10.1007/s11356-016-6319-8.

Crini, G. and Ndongo Peindy, H. 2006. Adsorption of C.I. basic blue 9 on cyclodextrin-based material containing carboxylic groups. Dye Pigm., 70: 204-211. doi: 10.1016/j.dyepig.2005.05.004.

Garg, U.K., Kaur, M.P., Garg, V.K. and Sud, D. 2008. Removal of Nickel(II) from aqueous solution by adsorption on agricultural waste biomass using a response surface methodological approach. Bioresour. Technol., 99: 1325-1331. doi:10.1016/j.biortech.2007.02.011.

Getachew, T., Hussen, A. and Rao, V.M. 2015. Defluoridation of water by activated carbon prepared from banana (*Musa paradisiaca*) peel and coffee (*Coffea arabica*) husk. Int. J. Environ. Sci. Technol., 12(6): 1857-1866. doi: 10.1007/s13762-014-0545-8.

Goswami, S. and Ghosh, U.C. 2005. Studies on Cr (VI) adsorption behavior onto synthetic hydrous stannic oxide. Water SA, 31: 597-602. doi: 10.4314/wsa.v31i4.5150.

Gupta, V.K. and Sharma, S. 2002. Removal of cadmium and zinc from aqueous solutions using red mud. Environ. Sci. Technol., 36: 3612-3617. doi:10.1021/es020010v.

Hamza, R.Z, El-Shenawy, N.S. and Ismail, H.A. 2015. Protective effects of blackberry and quercetin on sodium fluoride-induced oxidative stress and histological changes in the hepatic, renal, testis, and brain tissue of male rat. J. Basic Clin. Physiol. Pharmacol., 26(3): 237-251. doi: 10.1515/jbcpp-2014-0065.

Ho, Y.S. and McKay, G. 1999. Pseudo-second order model for sorption processes. Process Biochem., 34: 451-465. doi: 10.10/16/S0032-9592(98)00112-5.

Kaewsarn, P. and Yu, Q. 2001. Cadmium(II) removal from aqueous solutions by pre-treated marine alga Padina sp biomass. Environ. Pollut., 112:209–213. doi: 10.1016/S0269-7491(00)00114-7.

Kumar, P.S., Ramalingam, S. and Kirupha, S.D. 2011. Adsorption behavior of nickel(II) onto cashew nut shell: Equilibrium, thermodynamics, kinetics, mechanism, and process design. Chem. Eng. J., 167: 122-131. doi:10.1016/j.cej.2010.12.010.

Lagergren, S. 1898. On the Theory of So-called Adsorption Solutes. The Royal Swedish Academy of Sciences, Handlingar, pp. 1-39.

Li, D., Gao, X., Wang, Y. and Luo, W. 2018. Diverse mechanisms drive fluoride enrichment in groundwater in two neighboring sites in northern China. Environ. Pollut., 237: 430-41. doi: 10.1016/j.envpol.2018.02.072.

Li, X., Zheng, W. and Wang, D.B. 2010. Removal of Pb (II) from aqueous solutions by adsorption onto modified areca waste: kinetic and thermodynamic studies. Desalination, 258: 148-153. doi: 10.1016/j.desal.2010.03.023.

Li, Xming., Zheng, W., Wang D.B., et al. 2010. Removal of Pb(II) from aqueous solutions by adsorption onto modified areca waste: kinetic and thermodynamic studies. Desalination, 258: 148-153. doi: 10.1016/j.desal.2010.03.023.

Min, S.H., Han, J.S., Shin, E.W. and Park, J.K. 2004. Improvement of cadmium ion removal by base treatment of juniper fiber. Water Res., 38: 1289-1295. doi:10.1016/j.watres.2003.11.016.

Mokkapati, R.P., Ratnakaram, V.N. and Mokkapati, J.S. 2018. Using agro-waste to remove toxic hexavalent chromium: surface interaction and mass transfer studies. Int. J. Environ. Sci. Technol., 15: 875-886. doi: 10.1007/s13762-017-1443-7

Mondal, N.K., Bhaumik, R., Banerjee, A., Datta, J.K. and Baur, T. 2012. A comparative study on the batch performance of fluoride adsorption by activated silica gel and rice husk ash. Int. J. Environ Sci., 2(3): 1643-1661.

Mondal, P. and George, S. 2015. A review on adsorbents used for defluoridation of drinking water. Rev. Environ. Sci. Biotechnol., 14(2): 195-210. doi: 10.1007/s11157-014-9356-0

Moradi, O. 2011. The removal of ions by functionalized carbon nanotube: Equilibrium, isotherms, and thermodynamic studies. Chem. Biochem. Eng Q., 25: 229-240.

Ramya, P.M., Jayasravanthi, Dulla, B.J. and Venkata Nadh, R. 2015. Chemical oxygen demand reduction from Coffee Processing wastewater – A comparative study on the usage of biosorbents prepared from agricultural wastes. Global NEST J., 17(2): 291-300.

Ramya, P.M., Jayasravanthi, M. and Venkata Nadh, R. 2016a. Kinetic, thermodynamic, and equilibrium studies on removal of hexavalent chromium from aqueous solutions using agro-waste biomaterials, *Casuarina equisetifolia L.* and *Sorghum bicolour*. Korean J. Chem. Eng., 33(8): 2374-2383. doi: 10.1007/s11814-016-0078-6.

Ramya, P.M., Jayasravanthi, M. and Venkata Nadh, R. 2016b. Kinetic, isotherm, and thermodynamics investigation on adsorption of divalent copper using agro-waste biomaterials, *Musa acuminate Casuarina equisetifolia* L. and *Sorghum bicolor*, Pol. J. Chem. Technol., 18(2): 68-77. doi: 10.1515/pjct-2016-0031.

Rao, K., Mohapatra, M., Anand, S. and Venkateswarlu, P. 2011. Review on cadmium removal from aqueous solutions. Int. J. Eng. Sci. Technol., 2: 81-103. doi:10.4314/ijest.v2i7.63747.

Rodrigues, A.A., Vasconcelos-Filho, S.C., Mendes, G.C., Rehn, L.S., Rodrigues, D.A., Rodrigues, C.L. and Muller, C. 2017. Fluoride in simulated rain affects the morphoanatomy and physiology of Eugenia dysenterica (Mart.) DC. Ecol. Indic., 82: 189-195. doi: 10.1016/j.ecolind.2017.07.005.

Shen, P., Bagheri, R., Walker, G.D., Yuan, Y., Stanton, D.P., Reynolds, C. and Reynolds, E.C. 2016. Effect of Calcium phosphate addition to fluoride containing dental varnishes on enamel demineralization. Aust. Dent. J., 61(3): 357-365. Doi: 10.1111/adj.12385.

Sousa, F.W., Rosa, M.F., Tropical-ce, E.A. et al. 2007. The use of green coconut shells as adsorbents in the removal of toxic metals. Quim. Nov., 30: 1153-1157. doi: 10.1590/S0100-40422007000500019.

Sparks, D.L. 1986. Kinetics of Reaction in Pure and Mixed Systems in Soil Physical Chemistry. CRC Press, Boca Raton.

Tewari, N., Vasudevan, P. and Guha, B.K. 2005. Study on biosorption of Cr(VI) by *Mucor hiemalis*. Biochem. Eng. J., 23: 185-192. doi: 10.1016/j.bej.2005.01.011.

Wong, S., Ngadi, N., Inuwa, I.M. and Hassan, O. 2018. Recent advances in applications of activated carbon from biowaste for wastewater treatment: A short review. J. Clean. Prod., 175: 361-375. doi: 10.1016/j.jclepro.2017.12.059.

Xue, Y., Gao, B. and Yao, Y. 2012. Hydrogen peroxide modification enhances the ability of biochar (hydrochar) produced from hydrothermal carbonization of peanut hull to remove aqueous heavy metals: Batch and column tests. Chem. Eng. J., 200-202: 673-680. doi: 10.1016/j.cej.2012.06.116.

Yadav, K.K., Gupta, N., Kumar, V., Khan, S.A. and Kumar, A. 2018. A review of emerging adsorbents and current demand for defluoridation of water: Bright future in water sustainability. Environ. Int., 111: 80-108. doi: 10.1016/j.envint.2017.11.014.

Yan, N., Liu, Y., Liu, S., Cao, S., Wang, F., Wang, Z. and Xi, S. 2016. Fluoride-induced neuron apoptosis and expressions of inflammatory factors by activating microglia in rat brain. Mol. Neurobiol., 53(7): 4449-4460. doi: 10.1007/s12035-015-9380-2.

Zohoori, F.V. and Duckworth, R.M. 2016. Fluoride: Intake and metabolism, therapeutic and toxicological consequences. Mol. Genet. Nutr. Aspects Major Trace Miner., 20: 539-550. doi: 10.1016/B978-0-12-802168-2.00044-0.

## ORCID DETAILS OF THE AUTHORS

K. Kiran Kumar: https://orcid.org/0000-0001-8612-5776
Ratnakaram Venkata Nadh: https://orcid.org/0000-0003-0925-1132
G. Krishnaveni: https://orcid.org/0000-0003-1589-2497

# Emerging Trends in Wastewater Treatment of Semiconductor Industry: A Review

**Hemant S. Sadafale†** iD **and R.W. Gaikwad** iD

Department of Chemical Engineering, Jawaharlal Nehru Engineering College, MGM University, Aurangabad-431003, Maharashtra, India

†Corresponding author: Hemant S. Sadafale; hemant.sadafale@rediffmail.com

## ABSTRACT

The semiconductor industry produces a lot of wastewater. These wastewaters can affect the environment if they are not treated. As a result, one of the semiconductor industry's primary concerns and duties is the treatment and disposal of wastewater from the industry. Many processes, including electrocoagulation, electro-adsorption, and coagulation-flocculation using both natural and synthetic coagulants, have been invented over the years for purifying semiconductor effluent. The long-term viability of this system is unknown although it generates solid by-products (sludge) and requires routine sludge disposal, both of which raise the operational expenses of effluent treatment. Thus, a sustainable alternative method of removing contaminants from the semiconductor industry is needed to advance toward pollution prevention and green innovation. The hydrodynamic cavitation technique has improved over time and is useful for treating water and wastewater. This article gives an insight into different wastewater technologies, so proper technology must be chosen.

## INTRODUCTION

One of the quickly expanding economic sectors is the semiconductor industry, which is anticipated to experience increased expansion in the future (Eng et al. 2019). High-quality semiconductor wafers must be produced using intricate and delicate processes such as wafer back polishing, cutting, device connection, wire bonding, encapsulating, cutting, shape, and labeling (Hollingsworth et al. 2005, Lai & Lin 200, Sun & Tay 2004). In these processes, there are more than 200 different kinds of natural and synthetic substances. Water is also essential for the fabrication of thin films, in addition to elements and materials that are manmade and natural. Investigation shows that the manufacturing processes for semiconductor wafers utilize about 60% of the water from the tap and 40% of ultra-pure water, which is then wasted (Drouiche et al. 2007). In the electronics sector, back grinding and chemical mechanical polishing (CMP) are the two main producers of wastewater (Teow et al. 2022, Lin & Yang 2004). CMP wastewater is produced when wafers are cleaned after a CMP operation when tiny surface particles mix with CMP slurry (Huang et al. 2011). The resulting effluent is dark in color and has a high level of turbidity in contrast to wastewater, which is created from back grinding operations where synthetic particles combine

with cleaning water (Yang et al. 2012). Chemicals and by-products from the semiconductor industry, including acidic, basic ions, volatile compounds, trace metals, minute scattered ionic compounds, and organic materials, are frequently found in the effluent (Eng et al. 2019). The semiconductor sector creates more wastewater due to the rising demand for semiconductor wafers. As a result, one of the semiconductor industry's primary concerns and duties is managing and disposing of wastewater from manufacturing. There have been a number of processes that have evolved for treating electronic effluent, namely electrocoagulation, electro-adsorption, and coagulation-flocculation using both natural and synthetic coagulants. (Mousazadeh et al. 2021). It is uncertain if this system will be financially feasible in the long term, although it generates solid by-products (sludge) and requires frequent scheduled disposal of the sludge. Therefore, a sustainable choice of treating wastewater from the electronic sector is required to move toward ecological safety and green manufacturing. One of the semiconductor industry's most water and energy-consuming processes is copper chemical mechanical planarization (Cu-CMP). Around 30 to 40 percent of the water utilized during the entire semiconductor production process is used in this phase alone, according to estimates (Golden et al. 2000). The wastewater produced contains a lot of copper, usually

Table 1: Characteristics of metal plating industrial wastewater.

| Characteristics | Units | Value |
|---|---|---|
| pH | - | 2.0 |
| Electric Conductivity | mS.cm$^{-1}$ | 560 |
| Zinc | mg.L$^{-1}$ | 25 |
| Copper | mg.L$^{-1}$ | 30 |
| DO | mg.L$^{-1}$ | 4 |
| Turbidity | (NTU) | 256 |
| TDS | mg.L$^{-1}$ | 1180 |
| TSS | mg.L$^{-1}$ | 100 |
| TOC | mg.L$^{-1}$ | 370 |
| COD | mg.L$^{-1}$ | 1430 |

between 5 and 100 mg.L$^{-1}$ of soluble copper (Maag et al. 2000). Semiconductor wastewater is distinguished by its strenuously dark color, high turbidity, high chemical oxygen demand (COD) concentration, non - biodegradable, and presence of both inorganic and organic pollutants. It may also contain a variety of solvents, acids, bases, salts, and fine oxide particles. Hussein and Abdel-Shafy (2022) collected samples from a plating industry and analyzed them for the metals shown in Table 1.

Many methods have been used to treat organics and heavy metals like Cu; the methodology selected will primarily depend on the characteristics of the influent being treated and the intended effluent properties. Considering the characteristics of the wastewater, it is possible to apply both physical-chemical and biological treatments.

## PHYSICO-CHEMICAL TREATMENT OF CMP EFFLUENTS

Cu-CMP wastewater treatment in the semiconductor sector involves a variety of physico-chemical techniques, most frequently utilizing coagulation and flocculation for wastewater preprocessing, led by micro or ultrafiltration, and then cation exchange for the removal of copper (Golden et al. 2000, Mendicino & Brown 1998).

The production of huge quantities of metal-bearing sludges or brines during the physico-chemical treatment of metals is one of the primary issues with this process and could lead to their eventual dumping in unsafe discarded locations (Golden et al. 2000).

### Chemical Coagulation-Flocculation

Chemical coagulation can remove heavy metals above 90% (Alazaiza et al. 2022). Research on electrocoagulation demonstrates excellent outcomes in eliminating copper ions and floating fragments (99% clearance) (Lai & Lin 2003).

Sun et al. (2020) produced a new dual-functional chitosan flocculant CMCTS-g-P(AM-CA) for the flocculation removal of heavy metal using UV-induced graft copolymerization using AM, CMCTS, and ammonium di-thio-carbamate as reaction monomers.

### Chemical Precipitation

Chemical precipitation is one way to remove the most frequently utilized heavy metals (Pohl 2020, Yan et al. 2020).

### Precipitation With Hydroxides

Precipitation with hydroxides is one of the most common techniques due to its low cost and very simple control by altering pH (Bilal et al. 2013, Veeken et al. 2003). The precipitate from hydroxide precipitation is a gelatinous sludge that is challenging to dewater, one of its main drawbacks (Pohl 2020). One major problem with chemical precipitation is that it lacks selection. Thus, even if pH is only raised, many metal hydroxides may precipitate at once (Bilal et al. 2013), making the resulting sludge useless for metal recovery (Veeken et al. 2003).

### Precipitation With Sulfides

The most significant benefits of employing sulfide as a ligand to precipitate heavy metals over hydroxide precipitation are greater removal efficiency and reduced reliance on chelating chemicals found in contaminated water (Prokkola et al. 2020). In reality, sulfide precipitation is an extra costly practice (in terms of chemical expenses), and too much sulfide in the effluent could cause hazardous and corrosion issues preventing it from being widely used as a physico-chemical approach, however (Kaksonen 2004).

### Ion Exchange

Unfavorable metal ions are exchanged for secure, environmentally beneficial ones using the ion exchange method, which employs a reversible chemical reaction. A heavy metal ion is removed from a wastewater solution by attaching it to an immobile solid particle and then replacing it with the solid particle cation. According to Bisht & Agarwal (2017), the ion-exchange approach may eliminate target (all or some) heavy metal ions from wastewater, including lead, mercury, cadmium, nickel, chromium, copper, and zinc. According to Zhang et al. (2021), when comparing SiAcyl resin to other commercially available resins, it showed good stability, reusability, and cost-effectiveness for potential use in industrial applications.

## BIOLOGICAL APPROACHES

Microbial processes usually focus on immobilization strategies to remove metals from aqueous streams, the more prominently biosorption by microorganisms; metal reduction to less soluble forms; and chemical precipitation with biogenic products, such as oxalates, phosphates, or sulfides (Schiewer & Volesky 2000, White et al. 1995, Gadd 2000). There haven't been many attempts to use biological methods to treat CMP wastewater.

### Biosorption

In research to eradicate cadmium from wastewater by the blue-green alga, Abdel et al. (2013) achieved high biosorption. By partially or completely esterifying the carboxylic sites on its cell wall, sargassum biomass was found to be able to biosorbent cadmium and lead cations (Abdi & Kazemi 2015).

## RECENT TRENDS IN WASTEWATER TREATMENT

### Membrane Technology

Ahmed and Yossor (2016) found that industrial effluent containing nickel, lead, and copper ions can be effectively treated using reverse osmosis (RO) membrane technologies to save water and protect the environment. The outcomes demonstrated that the RO process could efficiently remove heavy metals, with removal efficiencies for Ni(II), Pb(II), and Cu(II) ions of 98.5%, 97.5%, and 96%, respectively. Teow et al. (2022) evaluated the performance of commercial ultrafiltration (UF) ceramic and polymeric membranes when treating three different types of wastewater from the semiconductor industry: diluted back grinding wastewater (DBGW), diluted chemical mechanical polishing wastewater (DCMPW), and collection tank wastewater. In this study, two types of polymeric membranes and one type of ceramic membrane were assessed. Due to its high porosity, hydrophilicity, and permeability, the ceramic membrane produced the maximum permeate flux (131.23-308.98 $L.m^{-2}h^{-1}$) for all three types of wastewaters and was least prone to fouling, as seen by the lowest relative flux reduction (RFR) (8.22-57.59%).

### Advanced Oxidation Process

In advanced treatment methods, degrading promising intractable components with membrane and bioremediation is difficult. Owing to its capacity to decompose a variety of natural micro-pollutants, the advanced oxidation process (AOP) has drawn a lot of interest in solving this issue (Sievers 2010, Bethi et al. 2016).

### Photocatalysis

Some semiconductors for purifying water are $TiO_2$, ZnO, $Fe_2O_3$, CdS, and ZnS (Diya'Uddeen et al. 2011, Hasan et al. 2012). To detect and adsorb heavy metal ions in water, a unique titania nanomaterial was modified with a sulfhydryl group (nano $TiO_2$-SH) and properly quantified the adsorption process utilizing Surface-Enhanced Raman Spectroscopy (SERS) and other useful testing methods by Chen et al. (2023). For the three heavy metal ions, $Hg^{2+}$, $Cd^{2+}$, and $Pb^{2+}$, the maximum adsorption efficiency of nano $TiO_2$-SH was 98.3%, 98.4%, and 98.4%, respectively. Furthermore, the adsorption efficiency of nano $TiO_2$-SH for these three metal ions remains above 96% after five adsorption and desorption cycles. These findings demonstrated the nano $TiO_2$-SH adsorbent's considerable potential for removing water pollutants in real-world applications.

## GAPS OR LIMITATIONS IDENTIFIED

Removing nutrients from wastewater is commonly acknowledged as an affordable and practical procedure called biological treatment. However, due to the high amount of hazardous chemicals in semiconductor wastewater, which can prevent microbe movement in the organic handling procedure, biological procedures may not be practical for the treatment of semiconductor wastewater (Kim et al. 2009). Although the electro-dialytic approach may effectively remove fluoride from an aqueous solution (Keri et al. 2011), it is challenging to apply this technology to the management of semiconductor effluent owing to the difficulty of wastewater. The effluent from semiconductor manufacturing is frequently treated alternatively by precipitation using calcium salts. However, the presence of $PO_4^{-3}$, $SO_4^{-2}$, and $NH^{4+}$ in the wastewater fast prevents this procedure from removing the TAN and $PO_4^{-3}$ concurrently, which lowers the recapture issue of $CaF_2$ for a variety of manufacturing uses (Aldaco et al. 2007).

Furthermore, flocculants like polyferric sulfate and polyaluminum chloride must speed up the solid separation process since the chemical precipitation creates extremely small $CaF_2$ precipitates (Liu & Liu, 2016). Copper concentrations in semiconductor effluent can reach 100 $mg.L^{-1}$ (Lai & Lin 2004). $Cu^{2+}$ can now be detached through a range of techniques and technologies, as well as chemical precipitation, ion exchange, sorption, membrane filtering, and electrochemical treatment (Awual 2015). Copper removal from the trash from semiconductors using the coagulation-flocculation method followed by sedimentation is one of them. The generation of excessive mud and/or the use of copious quantities of coagulants and/or coagulant aids

Table 2: Identified drawbacks in the treatment of semiconductor wastewater.

| Sr. No. | Treatment | Limitations/Drawbacks Identified | Reference |
|---|---|---|---|
| 1. | Biological Process | Inhibit the Microorganisms' activity in a biological system | Kim et al. (2001) |
| 2. | Eletrodialetic Method | Difficult to apply to Semiconductor Wastewater due to the complexity of wastewater | Keri et al. (2011) |
| 3. | Precipitation Process | This process can not eliminate the TAN & Po4 Since it is quickly intercepted by the presence of $PO_3$, $SO_4$ & $NH_4$ | Aldaco et al. (2007) |
| 4. | Coagulation – Flocculation Process | Creation of surplus sludge and use of huge amounts of coagulation or conjugate aids | Awual (2015) |
| 5. | Ion Exchange | Require Regular regeneration, and hence treatment cost increases | Fang et al. (2010) |
| 6. | Adsorption | Requires regular regeneration and hence difficult to recover chemicals from Waste. | Crini (2005) |
| 7. | Physico-Chemical Treatment of CMP Effluents | Large-scale production of metal-containing sludges that would need to be disposed of in hazardous waste sites in the future | Golden et al. (2000) |
| 8. | Hydroxide precipitation | Gelatinous mud, which is not easy to get rid of water | Lanouette (1977) |
| 9. | Sulfide precipitation | It is a more expensive process (chemical costs), and too much sulfide in the effluent can cause toxicity and corrosion issues. | Kaksonen (2004), Humberto et al. (2021), and Veeken et al. (2003) |
| 10. | Biosorption | The price of supplying nutrition and the harm that heavy metals do to living cells | Schiewer and Volesky (2000) |
| 11. | Dissolved air flotation | High initial energy and capital costs. High costs for operations and maintenance. | Chuang et al. (2002) |
| 12. | Membrane filtration, Microfiltration (MF), Ultrafiltration (UF), Nanofiltration (NF) Reverse osmosis, Dialysis Electrodialysis (ED) Electro-electrodialysis (EED) Emulsion liquid membranes (ELM) | For small and medium-sized businesses, investment expenses are frequently too expensive, and they have large energy needs. Membrane filtering system designs can vary significantly. High operating and maintenance costs rapidly clog membranes (fouling with high concentrations). Little throughput, Restricted flow rates Low solute feed concentrations are uninteresting. The particular application determines the membrane choice. | Sharma & Sanghi (2012) Sonawane and Ghate (2004) |
| 13. | Advanced oxidation processes (AOP) Photolysis | Laboratory scale Insufficiently profitable for small and medium-sized businesses | Parsons (2004) Sharma (2015) |
| 14. | Electrochemical reduction | Passivation of the anode and sludge buildup on the electrodes can prevent the electrolytic process from running continuously. | Chen (2004) |

are the process's main downsides, though. Ion exchange and sorption are now regarded as efficient and affordable approaches. However, regeneration is necessary to have a repeatable response using this strategy after equilibrium is reached. Chemical coagulation, electrocoagulation, flotation, membrane filtering, and adsorption are traditional methods for removing silica particles from CMP or BG wastewater (Fang et al. 2010). Adsorption technologies are possibly the most alluring of the previously discussed treatment methods because of their effectiveness, affordability, and ease of use (Crini 2005). Table 2 gives the different wastewater treatment technologies and identified drawbacks.

## COMMENTS ON THE TREATMENT MODALITIES AND PROSPECTIVE OUTCOMES

The information above shows that any technique used to remove metal ions is not universally favorite and has pros and cons. Adsorption has received the greatest attention recently among all approaches. It demonstrated simple to use, low expense, and a large sorption capacity. The present study trend is to create affordable, eco-friendly adsorbents from the garbage. To reduce environmental concerns, disposing of such adsorbents after the adsorption process is a significant task.

Membrane techniques are important in the treatment of wastewater and are now seen as a more viable solution. Some separation applications, like desalination, already suit them the best. High effectiveness in the extraction of metal ions is a characteristic of membrane processes. Membrane fouling and biofouling, low recovery for the volume of feed wastewater, process complexity, pre-treatment, frequent membrane cleaning, and high cost are further downsides

of this strategy. Future industrial wastewater treatment requires the growth of innovative membrane resources with improved thermal and chemical stability to achieve superior anti-fouling capabilities and increase membrane selectivity for the target metals. The autonomous operation of industrial facilities requires more implementation and development for both adsorption and membrane techniques. Chemical-based separations have been used widely for heavy metal removal due to their simplicity and low cost. However, chemicals are used to adjust pH levels and improve ion accumulation. There is a huge amount of sludge created that desires additional action.

The electrochemical treatment benefits from being quick, and well-controlled sludge removal is made simple, and there are fewer chemicals used. However, the main issues with this approach are the high cost of anodes and cathodes, low throughput, and excessive energy consumption. To solve this problem, combining several electrochemical treatment techniques powered by renewable energy sources may be effective. Aerated electrochemical oxidation (EC) and electrochemical oxidation technologies were the best choices to be integrated with other approaches since they can remove both organic and inorganic contaminants from wastewater.

Small sludge is formed by the flotation method. Therefore, this technique is a great candidate to be incorporated into creating a successful and affordable electrochemical treatment system.

The stability and reusability issues with the ion exchange method are comparable to those with adsorption techniques, where further research may be necessary. With minimal chemical use and no sludge generation, the photocatalyst approach enables straightforward treatment. It is still being researched, is pH-dependent, has low throughput, and is useless when different metals are present.

## CONCLUSION

The most effective way to remove heavy ions from sewage depends on a number of important criteria, including the cost of operation, the metal ions' initial concentration, the effect on the environment, the pH levels, the chemicals used, the effectiveness of the removal, and the viability from an economic standpoint. These procedures can be broken down into four groups: adsorption treatments (using different adsorbents, including carbon-based, carbon-composites, minerals, CS, magnetic, biosorbents, and MOFs), membrane treatments (such as UF, nanofiltration, microfiltration, reverse osmosis, and electrodialysis), chemical treatments (such as chemical precipitation, coagulation-flocculation, and flotation), and electric treatments.

Adsorption is the most promising technology for removing heavy metal ions from wastewater that has undergone substantial research because of its simple operation, broad applicability, high removal rate, and economical reusability. Nevertheless, the key factors influencing this desire are the choice of inexpensive materials, high uptake, and effective regeneration procedures.

Technically sophisticated and useful are the chemical-based approaches, particularly chemical precipitation. They are also regarded as economical techniques. They depend on the chemical consumed, as opposed to the electrochemical technique, which also depends on electrodes, electrical energy, and other fixed expenditures. However, they produce a lot of sludge and require sedimentation separation.

Because electrodes are passivated, and a lot of electrical energy is used during the electrochemical process, it is a relatively costly technology. In addition, electric approaches are the least developed compared to photocatalytic ones. The photocatalytic process has the advantage of being ecologically friendly because it utilizes fewer chemicals and generates less sludge.

Because the majority of research used synthetic wastewater that contained just one or a small number of metal types, it has been noted that there is a glaring information gap about the effectiveness of treatment strategies for the removal of heavy metal ions from actual wastewater. Therefore, more studies on treating different toxins should be conducted using actual wastewater. The development of low-cost components and methods for heavy metal removal from wastewater should be further researched. The pilot-scale procedure should be the focus of future research as well. Future research should consider the best techniques for obtaining effective metal recovery with minimal environmental harm and at a reasonable cost.

## REFERENCES

Abdel Aty, A.M., Ammar, N.S., Abdel Ghafar, H.H. and Ali, R.K. 2013. Biosorption of cadmium and lead from aqueous solution by fresh water alga *Anabaena sphaerica* biomass. J. Adv. Res., 4(4): 367-374.

Abdi, O. and Kazemi, M. 2015. A review study of biosorption of heavy metals and comparison between different biosorbents. J. Mater. Environ. Sci., 6(5): 1386-1399.

Ahmed, H.A. and Yossor, R.A.M. 2016. Removal of heavy metals from industrial wastewater by using RO membrane. Iraq. J. Chem. Petrol. Eng., 17(4): 125-136.

Alazaiza M.Y.D., Albahnasawi A., Al Maskari O., Al Maskari T., Abujazar M.S.S., Abu Amr S.S., and Nassani D.E. 2022. Role of natural coagulants in the removal of heavy metals from different wastewaters: Principal mechanisms, applications, challenges, and prospects, Glob. NEST J., 24(4): 594-606.

Aldaco, A., Garea, A. and Irabien, M. 2007. Calcium fluoride recovery from fluoride wastewater in a fluidized bed reactor. Water Res., 41(4): 810-818.

Awual, M.R. 2015. A novel facial composite adsorbent for enhanced copper (II) detection and removal from wastewater. Chem. Eng. J., 266: 368-375.

Bethi, B., Sonawane, S.H., Bhanvase, B.A. and Gumfekar, S.P. 2016. Nanomaterials-based advanced oxidation processes for wastewater treatment: A review. Chem. Eng. Process. Process Intensif.,109: 178-189.

Bilal, M., Shah, J.A. and Ashfaq, T. 2013. Waste biomass adsorbents for copper removal from industrial wastewater–A review. J. Hazard Mater. Journal of Hazardous Materials, 263: 322-333.

Bisht, R. and Agarwal, M. 2017. Methodologies for removal of heavy metal ions from wastewater: An overview. Interdiscip. Environ. Rev., 18: 124-142.

Chen, B., Li, L., Liu, L. and Cao, J. 2023. Effective adsorption of heavy metal ions in water by sulfhydryl-modified nano titanium dioxide. Front. Chem. 10: 1072139. doi: 10.3389/fchem.2022.1072139

Chen, G. 2004. Electrochemical technologies in wastewater treatment. Sep. Purif., 38(15): 11-41.

Chuang, T., Huang, C. and Jane, J.C. 2002. Treatment of semiconductor wastewater by dissolved air flotation. J. Environ. Eng., 128(10): 974-980.

Crini, G. 2005. Recent developments in polysaccharide-based materials used as adsorbents in wastewater treatment, Prog. Polym. Sci., 30(1): 38-70.

Diya'Uddeen, B.H., Daud, W.M.A.W. and Abdul Aziz, A.R. 2011. Treatment technologies for petroleum refinery effluents: A review. Process Saf. Environ. Protect., 89(2): 95-105.

Drouiche, N., Ghaffour, N., Lounici, H. and Mameri, M. 2007. Electrocoagulation of Chemical Mechanical Polishing Wastewater. Desalination, 214(1-3): 31-37.

Eng, C.Y., Yan, D., Withanage, N., Liang, Q. and Zhou, Y. 2019. Wastewater treatment and recycle from a semiconductor industry: A demo-plant study. Water Pract. Technol., 2)14): 371-379.

Fang, Y., Gong, J.L., Zeng, G.M., Niu, Q.Y., Zhang, H.Y., Niu, C.G., Deng, J.H. and Yan, M. 2010. Adsorption of Cd (II) and Zn (II) from aqueous solutions using magnetic hydroxyapatite nanoparticles as adsorbents. Chem. Eng. J., 162: 487-494.

Gadd, G.M. 2000. Bioremedial potential of microbial mechanisms of metal mobilization and immobilization. Curr. Opin. Biotechnol., 11(3): 271-279.

Golden, J.H., Small, R., Pagan, L., Shang, C. and Raghavan, S. 2000. Evaluating and treating CMP wastewater. Semicond. Int., 23: 85-98.

Hasan, D.B., Abdul Aziz, A.R. and Daud, W.M.A.W. 2012. Oxidative mineralisation of petroleum refinery effluent using a Fenton-like process. Chem. Eng. Res. Des., 90(2): 298-307.

Hollingsworth, J., Sierra-Alvarez, R., Zhou, M., Ogden, K.L. and Field, J.A. 2005. Anaerobic biodegradability and methanogenic toxicity of key constituents in copper chemical mechanical planarization effluents of the semiconductor industry. Chemosphere, 59(9): 1219-1228.

Huang, C.J., Yang, B.M., Chen, K.S., Chang, C.C. and Kao, C.M. 2011. Application of membrane technology on semiconductor wastewater reclamation: A pilot-scale study. Desalination, 278(1): 203-210.

Humberto, E., Barros, L. and Troncoso, E. 2021. Metal sulfide precipitation: Recent breakthroughs and future outlooks. Minerals, 11: 1385.

Hussein, I. and Abdel-Shafy, M. 2022. Treatment of industrial electroplating wastewater for metals removal via electrocoagulation continuous flow reactors, Water Pract. Technol., 17(2): 555-566.

Kaksonen, A.H. 2004. The performance, kinetics, and microbiology of sulfidogenic fluidized-bed reactors treating acidic metal- and sulfate-containing wastewater. Tampere University of Technology, Tampere, Finland.

Keri, R.S., Hosamani, K.M., Seetharama Reddy, H.R., Nataraj, S.K. and

Aminabhavi, T.M. 2011. Application of the electrodialytic pilot plant for fluoride removal. J. Water Chem. Tech., 33: 293.

Kim, J.H., Wong, S.L. and Kim, B.G. 2001. Optimization of staphylokinase production in Bacillus subtilis using inducible and constitutive promoters. Biotechnol. Bioprocess. Eng. 6: 167.

Lai, C.L. and Lin, S.H. 2003. Electrocoagulation of chemical mechanical polishing (CMP) wastewater from semiconductor fabrication. Chemical Engineering Journal 95(1- 3): 205-211.

Lai, C.L. and Lin, S.H. 2004. Treatment of chemical mechanical polishing wastewater by electrocoagulation: System performances and sludge settling characteristics. Chemosphere, 54(3): 235-242.

Lanouette, K.H. 1977. Heavy metals removal. Chem. Eng., 84: 73-80.

Lin, S.H. and Yang, C.R. 2004. Chemical and physical treatments of chemical mechanical polishing wastewater from semiconductor fabrication. J. Hazard. Mater., 108(1-2): 103-109.

Liu, C.C. and Liu, J.C. 2016. Coupled precipitation-ultrafiltration for treatment of high fluoride-content wastewater. Journal of the Taiwan Institute of Chemical Engineers, 58: 259-263.

Maag, B., Boning, D. and Voelker, B. 2000. Assessing the environmental impact of copper CMP. Semicond. Int., 23(12): 101-114.

Mendicino, L. and Brown, P.T. 1998. The environment, health, and safety side of copper metalization. Semicond. Int., 21(6): 105-110.

Mousazadeh, M., Alizadeh, S.M., Frontistis, Z., Kabdaşlı, I., Karamati, E., Qodah, Z., Naghdali, Z., Mahmoud, A.E.D., Sandoval, M.A., Butler, E. and Emamjomeh, M.M. 2021. Electrocoagulation as a promising defluoridation technology from water: A review of the state of the art of removal mechanisms and performance trends. Water (Switzerland), 13(5): 101-121.

Parsons, S. (ed) 2004. Advanced oxidation process for water and wastewater treatment. IWA Publishing, London

Pohl, A. 2020. Removal of heavy metal ions from water and wastewaters by sulfur-containing precipitation agents. Water Air Soil Pollut., 23: 503.

Prokkola, H., Nurmesniemi, E. and Lassi, U. 2020. Removal of metals by sulfide precipitation using Na2S and HS solution. Chem. Engi., 4(3): 1-10.

Schiewer, S. and Volesky, B. 2000. Biosorption Processes for Heavy Metal Removal. In Lovley, D.R. (ed), Environmental Microbe-Metal Interactions, ASM Press, Washington, D.C., pp. 329-362.

Sharma, S.K. (ed) 2015. Green Chemistry For Dye Removal From Wastewater. Scrivener Publishing LLC Wiley, Beverley

Sharma, S.K. and Sanghi R, (eds) 2012. Advances in Water Treatment and Pollution Prevention. Springer, Dordrecht

Sievers, M. 2010. Advanced oxidation processes. Treat. Water Sci., 11: 377-408.

Sonawane, A. and Ghate R 2004. Developments in wastewater treatment methods. Desalination 167: 55-63.

Sun, Y., Zhou, S. and Sun, W. 2020. Flocculation activity and evaluation of chitosan-based flocculant CMCTS-g-P(AM-CA) for heavy metal removal. Sep. Purif. Technol., 241: 116737.

Sun, D. and Tay, J.H. 2004. Process-to-process recycling of high-purity water from semiconductor wafer back grinding wastes. Resour. Conserv. Recycl., 41(2): 119-132.

Teow, Y.H., Chia, Y.H., Ho, K.C. and Mahmoudi, E. 2022. Treatment of semiconductor-industry wastewater with the application of ceramic membrane and polymeric membrane. J. Clean. Prod. 337: 130569.

Veeken, A.H.M., de Vries, S., van der Mark, A. and Rulkens, W.H. 2003. Selective precipitation of heavy metals as controlled by a sulfide-selective electrode. Sep. Sci. Technol., 38(1): 1-19.

White, C., Wilkinson, S.C. and Gadd, G.M. 1995. The role of microorganisms in biosorption of toxic metals and radionuclides. Int. Biodeter. Biodegrad., 35(1-3): 17-40.

Yan, F.L., Wang, Y. and Wang, W.H. 2020. Application of biochars obtained through the pyrolysis of Lemna minor in the treatment

of Ni-electroplating wastewater. J. Water Process Eng. 37: 101464.

Yang, B.M., Huang, C.J., Lai, W.L., Chang, C.C. and Kao, C.M. 2012. Development of a three-stage system for the treatment and reclamation of wastewater containing nanoscale particles. Desalination, 284: 182-190.

Zhang, S., Ning, S. and Liu, H. 2021. Preparation of ion-exchange resin via in-situ polymerization for highly selective separation and continuous removal of palladium from electroplating wastewater. Sep. Purif. Technol., 258: 117670.

## ORCID DETAILS OF THE AUTHORS

Hemant S. Sadafale: https://orcid.org/0000-0002-5550-560X
R.W. Gaikwad: https://orcid.org/0000-0001-9195-2055

# Assessment of the Vulnerability of Groundwater to Biological Contamination in the Khartoum State, Sudan

**H. B. Abbas\*, A. E. Elmanssury\*\*, S. A. Dafaalla\*\*\* and S. Arif Pasha\*\*\*\*†**

\*Department of Environmental Health, Ministry of Health, Khartoum State, Sudan

\*\*Department of Public Health, College of Public Health and Health Informatics, Qassim University, Al-Bukayriyah, Kingdom of Saudi Arabia

\*\*\*Department of Public Health, College of Public Health and Health Informatics, University of Hail, Hail, Kingdom of Saudi Arabia

\*\*\*\*Department of Health Administration, College of Public Health and Health Informatics, Qassim University, Al-Bukayriyah, Kingdom of Saudi Arabia

†Corresponding author: S. Arif Pasha; sa.pasha@qu.edu.sa

## ABSTRACT

This study aims to determine how vulnerable groundwater in Khartoum is to contamination. For this purpose, the DRASTIC Index idea was used. A descriptive cross-sectional analytical analysis is designed in this study. A total of 279 boreholes were sampled from a total of 1015 boreholes (27.5 percent). The following criteria were utilized to define the DRASTIC Index: depth, net recharge, aquifer media, soil texture, terrain, video media, and soil conductivity. Standard bacteriological test methodologies were used for groundwater. The biological data from the 279 boreholes revealed that total coliform, thermo-tolerant coliform, and E. coli were found in 34.4 percent, 18.6 percent, and 0.36 percent of the boreholes, respectively. Bacteriological contamination is common in Sharge Elnile, although only a few cases have been reported in Khartoum. According to the study, the bulk of boreholes in Khartoum State were built without any criteria. Many sources of contamination were discovered within a radius of less than 120 meters, which was deemed to violate Khartoum State's Environmental Health Law of 2002. For this reason, bacteriological contamination is common in Sharge Elnile, although only a few cases have been reported in Khartoum.

## INTRODUCTION

Because of the spatial heterogeneity of aquifers and the many physical processes and chemical reactions that occur in the soil, unsaturated, and saturated zones, managing groundwater contamination is a complex undertaking. Because of this intricacy, a contaminant's physical condition or chemical form may vary, resulting in a change in the degree of contamination in an aquifer (Massimo & Civita 2010)

For potable drinking water, the majority of people in underdeveloped countries rely on untreated groundwater supplies. The rising demand for water from these sources has created concerns that some groundwater sources may not be as safe as they appear, putting people's lives at risk. Boreholes (tube wells) that are often rig-drilled >20 meters deep and potentially tap deeper aquifers; and shallow wells (hand-dug wells) that are typically dug 20 meters deep and often tap unconfined aquifers (Macdonald & Davies 2000).

Water is a basic necessity of life, an inevitable resource available underneath the surface and in soil pores, not the only constituent of life. Groundwater is a vital foundation of drinkable freshwater on the planet, and it theaters a key part in human survival and growth. Groundwater pollution is an important environmental hazard from various sources and is costly to human health. For example, nitrate groundwater pollution may result in health issues such as (blue baby syndrome), cancer risks), and high drinking water treatment costs (Schneider & Lechevallier 2017).

Boreholes and protected shallow wells are commonly associated with a few possible concerns in Sudan. For starters, their proximity to township latrines exposes them to infectious adulteration. Second, their proximity to the use points (houses) necessitates laborious transportation from the beginning until the end of water storage within the households. Water in storage facilities in houses can have a poorer microbiological quality than water at the beginning, implying that contamination occurs before consumption,

during collection, transit, storage, and drawing from containers (Schneider & Lechevallier 2017). As a result, Pollution may limit the water's potential health advantages. Rather than closeness to toilet facilities, poor borehole features, such as hygienic seals, can be water quality risk factors and cause microbial contamination of groundwater sources (Wright et al. 2004). The studies showed that the presence of the virus (COVID-19) in the stool had been significantly reported in the literature. The presence of stool in sewage drains leading to groundwater contamination can be an emerging threat to water pollution and could lead to the spread of COVID-19 (Cronin et al. 2006).

Freshwater testing methods aren't done regularly. This is a third possible issue. It is exceedingly expensive to freshen up contaminated groundwater and might take an extended recovery period. Furthermore, groundwater observation is both time-wasting and expensive, making it impossible to accurately quantify the topographical extent of pollution on a regional basis. As a result, identifying the longitudinal dissemination of regions in danger of pollution and zones susceptible to pollution is the best strategy for managing groundwater pollution (Huo et al. 2021, Mimi & Assi 2009). Danger and susceptibility charts are effective for allocating imperfect observing efforts toward the most critical locations. In these places, a significant effort is necessary to avoid or ameliorate the environmental impact of human activity (Lahr & Kooistra 2010, Thapinta & Hudak 2003).

The map of where the resource is vulnerable to pollution from surface operations is often produced as part of a groundwater vulnerability assessment. Vulnerability evaluations identify areas that need more research, protection, and monitoring. Vulnerability evaluations are also effective

instructional tools for improving public knowledge about the importance of groundwater protection, which is a constant requirement (Almasri 2008). Groundwater vulnerability maps are essential for protecting groundwater properties and assessing the possibility of improved growth in food techniques and landscape use affecting water quality (Rivera & Bouchard 2005). The rationale behind groundwater potential modeling is that certain geographical areas seem more susceptible to underground pollutants than others (Babiker et al. 2005). An evaluation of shallow groundwater quality in the Beni Mellal region ranges from medium to poor, with 14% and 20% of samples rated as poor and bad water quality, respectively (Gogu & Dassargues 2000).

Most underdeveloped countries, like Sudan, continue to focus their research on groundwater contamination on the outcome of actual solutions to filter intake water (Barakat et al. 2020). Nevertheless, little effort has been made to demystify underground pollution from a specific hydrogeology and sociological perspective. This allows professionals to create efficient groundwater protection methods from perceived pollution and review the method to scale up pathogenically infested groundwater bases. As a result, this study was carried out to determine the state of Khartoum's groundwater's vulnerability to contamination.

## MATERIALS AND METHODS

### Study Area and Climate

Geographically, the study area is approximately 28.165 square kilometers and is located within longitudes 31.5-34 East and latitude 15-16 North. The River Nile Region borders it on the north and east, the Northern Region on the north,
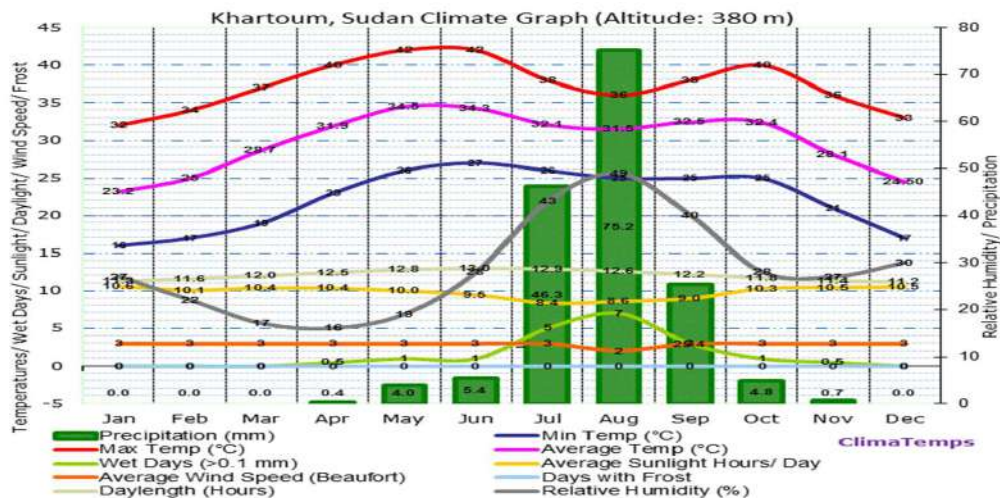


Fig. 1: Graph showing Khartoum climate in metric units.

Table 1: Online calculator to determine the sample size.

| Determine Sample Size | |
| --- | --- |
| Confidence Level: | 95% |
| Confidence Interval: | 5 |
| Population: | 1015 |
| Sample size needed: | 279 |

and the states of Kassala, Gedaref, and Gezira on the east and south-east.

The population of Khartoum state is projected to be around five million people, according to the 2008 population data representing different parts they engaged in economic activities like agriculture, workers, and officers.

The annual average temperature in Sudan's Khartoum state is 29.9 degrees Celsius (85.8 degrees Fahrenheit). The average monthly temperature varies by only 11.3 degrees Celsius (20.3 degrees Fahrenheit), which is a small variation. The average diurnal temperature variation/range is 15.1 degrees Celsius (27.2 degrees Fahrenheit). With an average temperature of 34.5 degrees Celsius, May is the warmest time (very, very hot) (94.1 degrees Fahrenheit). With an average temperature of 23.2 degrees Celsius, the coolest month (January) is also the hottest (73.76 degrees Fahrenheit.) Fig. 1.

**Sampling Techniques**

The sample size for the study area was determined by using a online calculator (Table 1)

**Biological Tests for Water**

Water samples were collected in sterile bottles for bacteriological testing. The samples' site, date, time, and location were carefully labeled. The water samples were then taken to the Ministry of Health's public health laboratory in Khartoum for analysis using the following tests: When positive results are known to be uncommon, presence-absence tests may be suitable. They are not measurable, and their title suggests that they indicate whether the required indication exists. In nations or situations where contamination is frequent, such results are of little utility, and the goal of the study is to assess the grade of pollution rather than to signal its occurrence. As a result, occurrence-absenteeism assays are not advised for use in the study of surface water and raw small-scale community resources in places where there may be concerns with maintenance and upkeep.

Before deciding whether or not to apply the presence-absence test to analyze a water source, the test's results should be compared to those obtained using a well-known, quantitative method of analysis. Both procedures should be used to evaluate approximately 100 samples (Pruss-Ustun and WHO 2008). When evaluating a 50 mL sample, the medium employed for the presence-absence test for coliform bacteria was lauryl tryptose sulfate broth, which was double strength.

- The dehydrated lauryl tryptose sulfate broth was dissolved in water in stages without being heated.
- 50 mL of the medium to be poured into 250-300 mL screw-cap glass dilution bottles. It's vital to have a fermentation tube.
- The samples were autoclaved for 12 min at 121 degrees Celsius, with a total time in the autoclave of no more than 30 min.
- After autoclaving, the pH of the medium was determined; it should be 6.8.

**Presumptive Test**

- The sample was mixed carefully by inverting the sample bottle sometimes.
- 50 mL of the sample was added to the dilution bottle.
- Samples were incubated at 35°C and examined after 48 h.
- A positive result is indicated by the production of gas and turbidity and is regarded as a positive presumptive test (WHO 1997).

**Confirmative Test**

- Each gas-positive presumptive tube was infected with an inverted Durham tube into a tube containing 5ml of vivid green bile broth.
- All tubes were incubated for 24 hours at 44-45 degrees Celsius to identify fecal coliform. The presence of negative tubes was observed, and the results were recorded. Gas output and turbidity appearance were used to identify positive tubes.

*E. coli* **Test (Completed Test)**

A loop of vivid green positive tubes was inoculated into 5ml peptone water and incubated at 44-45 degrees for 24 h before adding a drop of Kovac's reagent (0.2-0.3ml). The surface culture's intense red color showed a positive indole test. E. coli is the only coliform bacteria capable of generating indole from tryptophan-containing media at 44-45 degrees Celsius.

**Confirmativ*e E. coli* Test**

EMB media were incubated where *E.coli* created green metallic cheen (WHO 1997) .Two commonly employed methods of testing water are the membrane filtration technique for its sensitivity and the MPN method due to its accuracy and applicability.

## Membrane Filtration

- A membrane filter filters a 100 mL water sample or a diluted sample in this approach. The membrane was then cultivated on a pad of sterile selective broth containing lactose and an indicator with the coliform organisms on it.

- The number of coliform colonies was counted after incubation. The estimated number of E. coli in a 100-milliliter water sample

## Multiple Tube/Most Probable Number (MPN)

- One 50 mL sample, five 10 mL samples, five 1 mL samples, and five 0.1 mL samples were inoculated into an appropriate broth to determine the (MPN) in water samples.

- When coliforms were found, a Durham tube captured any gas produced.

- Following incubation, the number of samples generating a positive reaction (coliforms, turbidity, acid, and gas generation in the case of coliforms) is counted, and the most likely number of bacteria in the original sample is calculated using published MPN tables (Pruss-Ustun and WHO 2008).

- In this scenario, the 50 mL sample and all 10 mL samples, four 1 mL samples, and one 0.1 mL sample are positive.

## Membrane Filtration Methods

Bacteria were collected using membrane filters with porosities ranging from 0.22 to 0.45 nm and a diameter of 47 mm. Membrane filters were incubated in solid media, while pads were immersed in liquid media or enrichment broth as an MPN system (WHO 2003).

**Method:** The filtration unit and suction device were assembled according to membrane instructions by antiseptic blunted-ended forceps. Antiseptic membrane filter grid-side. The unit was reassembled with the highest on the filter base (positioned centrally). The taster of water was mixed thoroughly, upsetting the flask many times.

## Testing the Water to Make Sure That it is Safe to Drink

Although bacteriological testing of water is done regularly, it is not necessary to do biological testing on drinking water. It's difficult to culture many lab viruses that cause water-borne diseases. They might also last longer in water than bacterial fecal indicator species.

Test water samples have been inoculated into tissue cultures and then examined for panel growth or an exact cytopathic impact, although these procedures are limited to specialized laboratories. To get around these issues, it's been suggested that bacteriophages may operate as virus indicators, highlighting water that could be infected with viruses. Observing drinking water for viruses is not a common practice. Maybe this is an area where molecular genetics techniques such as PCR could be useful. However, caution is suggested when analyzing the results of such tests.

The existence of virus nucleic acid in a specimen does not necessarily imply the existence of infectious virus particles. The European Community has established a set of guidelines for the concentration of virus particles in water sources (Evans 2004). The first case for COVID-19 also experienced diarrhea before pneumonia was examined by Providence Regional Medical Center Everett in Washington. In many studies, authors reported that infectious/carrier visions could exist in human feces (Pritchard et al. 2010, Quilliam et al. 2020). Also, this virus can sustain in feces for up to 33 days. Afterward, the carrier has a negative test for respiratory viral ''RNA'' (Xu et al. 2020). This is an alarming threat because most gastrointestinal diseases are caused by contaminated water.

## RESULTS

Table 2 shows that the boreholes were mostly owned by private individuals (81.4 percent), and no metering system was discovered. Nearly half of the boreholes were linked to other systems, 78.5 percent of the borehole samples were drilled, and the rest were driven or bored.

According to our findings, the capacity of water sources exceeded the maximum daily demand by 88.2% (not considering the losses of the non-accounted-for). It was discovered that 71 percent of the boreholes were encased in bedrock. At the same time, 59.9% were found filling annular spaces with grout or bentonite surrounding them, 50.9 percent had adequate sealing, and 54.8 percent had casing extensions at least 30 cm above the slab.

Table 3 shows total coliform bacteria were found in 34.4 percent of boreholes as positive results, 54.2 percent of samples showed positive results in thermotolerant coliform, 92.3 percent for Presumptive *E. coli* test, and 37.5 percent for Confirmative E. coli test, according to bacteriological analysis of groundwater samples.

Table 4 shows no significant association between the type of construction of the borehole and the presence of bacteria. The study discovered that total coliform was present in 97 out of 279 boreholes, thermotolerant bacteria in 52 boreholes, presumptive *E. coli* was positive in 48 boreholes, and the confirmative E. coli test yielded 18 positive results.

Table 2: Characteristic of sources of groundwater in Khartoum State.

| Variables | Categories | Frequency | Percent % |
|---|---|---|---|
| Ownership of boreholes | Publicly | 52 | 18.6 |
| | Privately | 227 | 81.4 |
| Metering of services | Metered | 2 | .7 |
| | Not metered | 277 | 99.3 |
| Number of customers | Less than 250 | 14 | 5.0 |
| | 251-500 | 18 | 6.5 |
| | 501-750 | 21 | 7.5 |
| | 751 -1000 | 11 | 3.9 |
| | More than 1000 | 72 | 25.8 |
| | Unknown | 143 | 51.3 |
| Interconnection of the system with neighboring systems | Interconnected | 116 | 41.6 |
| | Not interconnected | 162 | 58.4 |
| Groundwater source capacity | Equal / exceed | 246 | 88.2 |
| | Not equal / exceed | 33 | 11.8 |
| Borehole encased into bedrock. | Yes | 198 | 71 |
| | No | 81 | 29.0 |
| Filling the annular space around the borehole casing with grout or bentonite clay | Filled | 167 | 59.9 |
| | Not filled | 112 | 40.1 |
| Sealing of the borehole at the surface | Properly sealed | 142 | 50.9 |
| | Not properly sealed | 137 | 49.1 |
| Extension of the casing for at least 30 cm above the borehole slab | Extended | 154 | 55.2 |
| | Not Extended | 125 | 44.8 |

Table 3: Results of the bacterial tests of groundwater samples.

| Types of bacterial tests | Results | Frequency | Percentage % |
|---|---|---|---|
| Coliform test | + | 96 | 35.8 |
| | – | 172 | 64.2 |
| Thermo-tolerant coliform test | + | 52 | 54.2 |
| | – | 44 | 45.8 |
| Presumptive *E. coli* test | + | 48 | 92.3 |
| | – | 4 | 7.7 |
| Confirmative *E. coli* test | + | 18 | 37.5 |
| | – | 30 | 62.5 |

Table 4: Relationship between the type of construction of the borehole and the presence of bacteria.

| Types of Testing / Types of Construction | Coliform test (n = 279) | | Thermotolerant coliform test (n = 97) | | Presumptive E.coli test (n = 52) | | Confirmative E.coli test (n = 48) | |
|---|---|---|---|---|---|---|---|---|
| | + | - | + | - | + | - | + | - |
| Dug | 16(36.4) | 28(63.6) | 8(50) | 8(50) | 7(87.5) | 1(12.5) | 3(42.9) | 4(57.1) |
| Drilled | 74(33.8) | 145(66.2) | 39(52.7) | 35(47.3) | 37(94.9) | 2(5.1) | 13(35.1) | 24(64.9) |
| Bored | 0 (00.0) | 2(100) | 0 | 0 | 0 | 0 | 0 | 0 |
| Driven | 7(50) | 7(50) | 5(71.4) | 2(28.6) | 4(80) | 1(20) | 2(50) | 2(50) |
| Total | 97(34.8) | 182(65.2) | 52(53.6) | 45(46.4) | 48(92.3) | 4(7.7) | 18(37.5) | 30(62.5) |
| p. value | 0.451 | | 0.606 | | 0.430 | | 0.802 | |
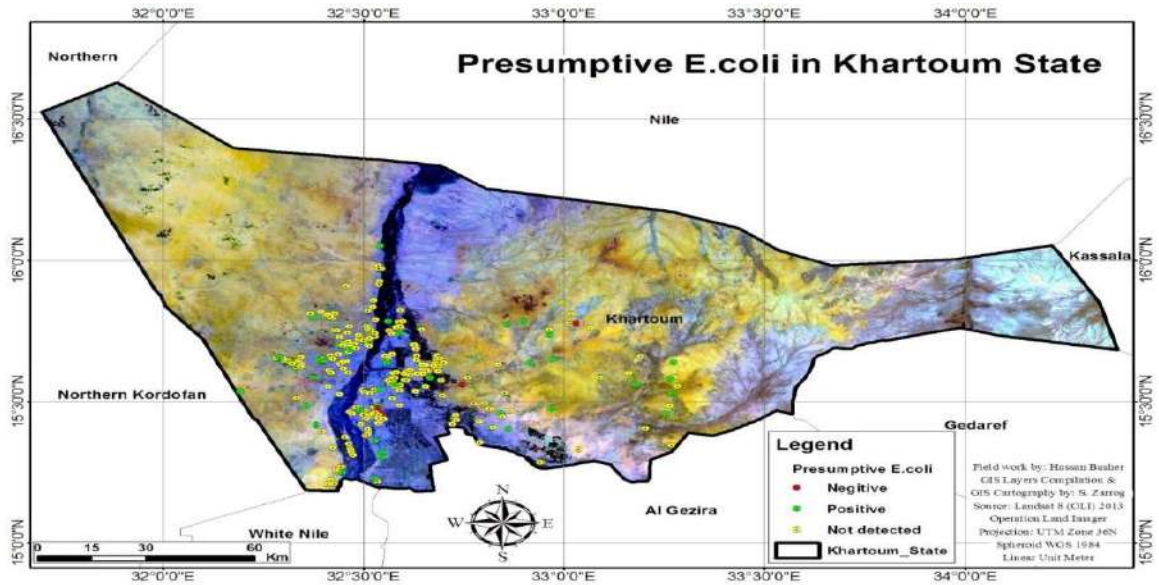
Fig. 2: The presence of presumptive *E. coli* in groundwater in Khartoum State.
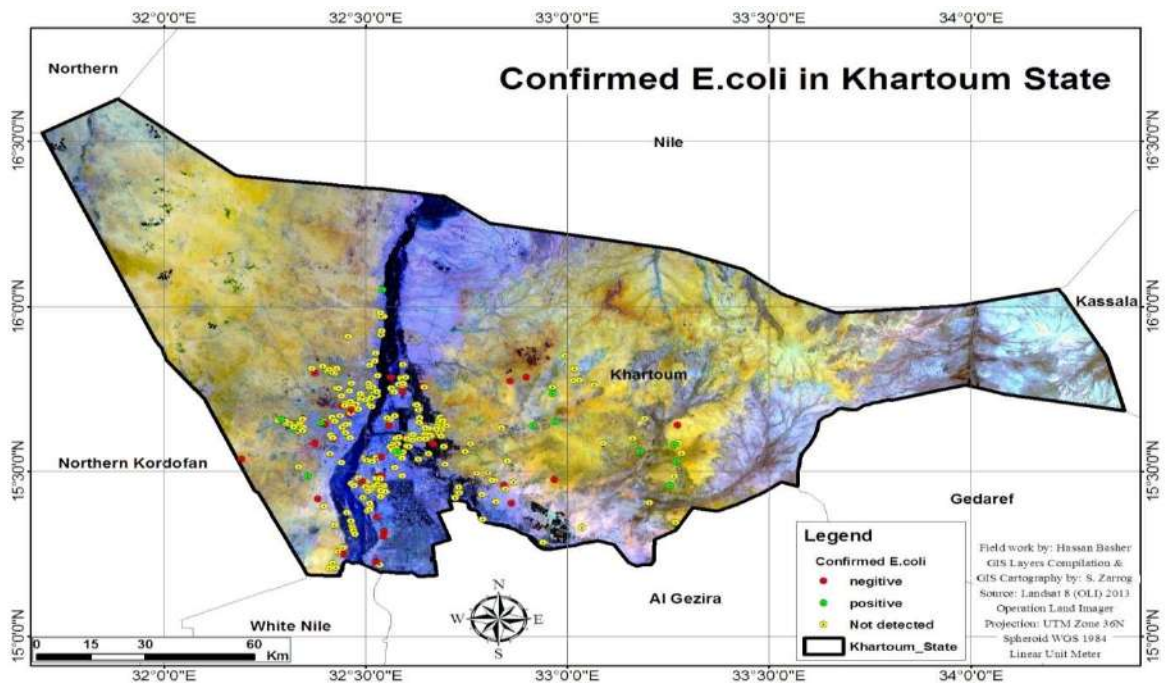


Fig. 3: The presence of confirmed *E. coli* in groundwater in Khartoum State.

The quality of Khartoum State groundwater was assessed using bacteriological and chemical tests. It was discovered that total coliform was present in 96 out of 279 boreholes, thermotolerant bacteria in 52 boreholes, and presumptive E. coli was positive in 48 boreholes (Fig. 2). The confirmative E. coli test yielded 18 positive results, indicating that the

boreholes were contaminated due to the current environment being surrounded by contaminants (Fig. 3).

## DISCUSSION

All parts of the base soil and substrate are equally powerful in pollution mitigation when it comes to the security of

groundwater from contaminants. Groundwater pollution is most commonly associated with what we refer to as free, unconfined springs, especially when the air circulation zone isn't thick and the free surface of the groundwater sow. Still, it can also occur in semi-bound springs. The holding layers are thick and permeable in general.

A pollutant column is frequently discharged into the aquifer due to the contaminant. Pollutants are dispersed over a larger region as a result of water movement and distribution inside the aquifer. The approaching boundary, the emission edge, can collide with surface water, such as leaks and streams or groundwater wells, putting human and wildlife's water supplies at risk. A hydrological transport or groundwater model can analyze the vertical emission movement, known as the vertical emission interface. Soil features, in situ geology, hydrogeology, hydrology, and the nature of pollutants may all be included in a groundwater pollution analysis. Physical, inorganic, chemical, organic, bacteriostatic, and radioactive characteristics are all present in groundwater contaminants. Essentially, many of the same chemicals are found in polluted surface water. Polluted groundwater contains these as well, though their relevance varies (Ling et al. 2019).

Dr. McDonough said it was important to understand what caused high DOC concentrations in groundwater. "An increase in groundwater DOC concentration impacts the ability and cost to make groundwater drinkable," she said. For example, we projected a 16 percent increase in annual household water costs in some parts of the United States because of rising water treatment costs due to the need to implement additional water treatment measures to remove increased DOC concentrations. The decrease in groundwater quality and substantial increase in water treatment costs will also compound existing constraints on groundwater resources, including availability (Owens et al. 2019).

The limit of the water sources exceeded the largest everyday interest by 88.2 percent, according to our investigation (considering unaccounted misfortunes). Lack of cleanliness, incorrect drainage, and unprotected groundwater sources may make groundwater resources more vulnerable to microbial pollution. According to our findings, 71 percent of the wells were shrouded in shale, while 59.9% occupied the annular space with gypsum or betonies around it, 50.9 percent had an acceptable fitting, and 54.8 percent of the wells had a packaging augmentation of around 30 cm over the chunk. Another study on groundwater quality in rural North Central Nigeria found that poor management of groundwater resources can lead to E. coli and Enterobacter aerogenes pollution (McDonough et al. 2020).

This was evident in the investigation's aftermath, which showed a link between the well's development and

the presence of germs. The bacteriological and compound tests were used to determine the nature of groundwater in Khartoum State. It was discovered that all E. coli forms were present in 96 (35.8%) of the 279 wells, while heat-safe microbes were found in 52 (54.2%). The putative E. coli was positive in 48 (92.3%) of the wells, and the corroborative test for E. coli yielded 18 (37.5%) positive results, implying that Usher 2007.91. This indicates that the boreholes were contaminated either due to the current environment's existence of contaminants or due to the boreholes' construction (Sojobi 2016). Len Ritter said loading of contaminants to surface waters, groundwater, sediments, and drinking water occurs via two primary routes, point-source pollution, and non-point-source pollution. Point-source pollution originates from discrete sources whose inputs into aquatic systems can often be defined spatially explicitly. Non-point-source pollution, in contrast, originates from poorly defined, diffuse sources that typically occur over broad geographical scales (McDonald et al. 2016).

Five of the six groundwater samples examined for fecal coliform exceeded the drinking water requirements, with concentrations as high as 13,000 per 100 mL (Ritter et al. 2002), discovered microbial contamination in ten of the 24 wells tested due to total coliform, E. coli, and enterococci. Enterococci had the highest volume and identification frequency, with enterococci pollution found in 40-48 percent of the wells. Although bacteriological testing of water is routine, organic testing of drinking water is less usual. Various infections that cause aquatic illnesses are difficult to purify in a laboratory setting. They may also survive longer in water than trash bacterial life forms. The study found that the amount of drinking water produced by the Khartoum State Water Corporation (KSWC) in Khartoum ranges between 1,500,000 and 1,700,000 $m^3.day^{-1}$, with 50% coming from groundwater (1015 producing boreholes). The private sector owns most of the sampled boreholes (81.4%), although the law assigns KSWC responsibility for all water sources. This was obvious in the construction methods, which included dug, drilling, driven, and bored wells with no metering system for all services (99.3%). According to the study, 41.6 percent of boreholes had linkage with neighboring systems, implying that contaminants could be transferred through the distribution network. The extension of the casing at least 30 cm above the borehole slab and the design of encased boreholes into the bedrock and filling the annular area around the borehole played a part in protecting boreholes from contamination.

In theory, locations with a low slope are more sensitive to groundwater pollution Because water can collect for extended periods, increased penetration and, thus, pollutant

migration are possible (Yolcubal et al. 2016). Groundwater contamination is a risk when water sources are located in low-lying wet areas, partly because reservoirs are likely to be in close physical contact with surface water in such areas. Our research found a link between E. coli bacteria and borehole casing, as well as between E. coli bacteria and boreholes encased in bedrock or unweathered subterranean rock strata. Boreholes that aren't protected against vandalism and accidents can become contaminated with bacteria (there's a link between the presence of *E. coli* and borehole protection). This agrees with a study conducted by Syampadzi, using E. Coli parameters as a representation of pollution risk where the results exceed 85% of total samples that a value exceeds the standard of quality >0 MPN/100 mL (Rahman 2008). Pathogen concentrations in groundwater samples can vary significantly, so time-spaced samples might not accurately represent the microbial biota present in groundwater (Nurroh et al. 2020).

Specific diagnostic information assessments and applying the DRASTIC approach alone will not be enough to pinpoint the causes of drinking water pollution. Observational evidence on the position of water sources vs. latrines, low-lying wet regions, slope features, and knowledge of the local hydrogeological environment provided additional information to advise the optimum siting of water sources and sanitation services. This agrees with Robins (2007).

The presence of thermotolerant bacteria and the suitability of the cooling system demonstrated a significant association between the presence of thermotolerant bacteria and the appropriateness of the cooling system. The safety distance between the source of contamination and the boreholes protects the groundwater from contamination. Khartoum state legislation keeps the distance between the source of contamination and the boreholes in the range of not less than 120m. The results revealed that 161 boreholes were within the range of 120 m and less to the source of contamination, and there was a strong relationship between total coliform bacteria presence and the distance of 120 m and less.

Although disinfectants (chlorine, ozone, and ultraviolet) are used to protect groundwater supplies from contamination, only ten boreholes employed disinfectants (chlorine, ozone, and ultraviolet) without employing disputed online monitoring.

## CONCLUSION

According to the report, to protect subterranean aquifers from pollution, land use, solid and liquid waste disposal techniques must be restricted, and general restrictions on land use and liquid waste disposal must be implemented.

Inoculating test water samples in tissue cultures and then examining plaque growth or the specific effect of cell pathology has been done. Still, these tests are only available in specialized laboratories. To get around these issues, it's been hypothesized that phages could operate as virus indicators, recognizing water that's probable to be infected.

## ACKNOWLEDGMENT

## REFERENCES

Almasri, M.N. 2008. Assessment of intrinsic vulnerability to contamination for Gaza coastal aquifer, Palestine. J. Environ. Manag., 88(4): 577-593.

Babiker, I.S., Mohamed, M.A.A. and Hiyama, T.A. 2005. GIS-based DRASTIC model for assessing aquifer vulnerability in Kakamigahara Heights, Gifu Prefecture, Central Japan. Sci. Tot. Environ., 345(1): 127-140.

Barakat, A., Hilali, A. and Baghdadi, M.E. 2020. Assessment of shallow groundwater quality and suitability for drinking purposes near the Béni-Mellal wastewater treatment lagoon (Morocco). Hum. Ecol. Risk Asses., 26(6): 1476-1495.

Cronin, A.A., Breslin, N. and Gibson, J. 2006. Monitoring source and domestic water quality parallel with sanitary risk identification in northern Mozambique to prioritize protection interventions. J. Water Health, 4(3): 333-345.

Evans, G. 2004. Mundo Maya: from Cancún to city of culture. World heritage in post-colonial Mesoamerica. Current Issues in Tourism, 7(4-5): 315-329.

Gogu, R.C. and Dassargues, A. 2000. Sensitivity analysis for the EPIK method of vulnerability assessment in a small karstic aquifer, southern Belgium. Hydrogeol. J., 8(3): 337-345.

Huo, C., Ahmed Dar, A. and Nawaz, A. 2021. Groundwater contamination with the threat of COVID-19: Insights into CSR theory of Carroll's pyramid. J. King Saud Univ. Sci., 33(2): 101295.

Lahr, J. and Kooistra, L. 2010. Environmental risk mapping of pollutants: State of the art and communication aspects. Sci. Total Environ., 408(18): 3899-3907.

Ling, Y., Xu, S. and Lin, Y. 2020. Persistence and clearance of viral RNA in 2019 novel coronavirus disease rehabilitation patients. Chin. Med. J., 133(9): 1039-1043.

Macdonald, A.M. and Davies, J.A. 2000. A Brief Review Of Groundwater for Rural Water Supply in Sub-Saharan Africa. British Geological Survey, UK, pp. 1-30.

Massimo, R. and Civita, V. 2010. The combined approach when assessing and mapping groundwater vulnerability to contamination. J. Water Resour. Protect., 2(1): 14-28.

McDonald, S., Gbondo-Tugbawa, S. and Prabhu, C. 2016. Groundwater

impacts on surface water and sediment-Gowanus Canal, Brooklyn, New York. Remediation, 26(4): 53-71.

McDonough, L.K., Santos, I.R. and Andersen, M.S. 2020. Changes in global groundwater organic carbon driven by climate change and urbanization. Nature Commun., 11(1): 1279.

Mimi, Z.A. and Assi, A. 2009. Intrinsic vulnerability, hazard and risk mapping for karst aquifers: A case study. J. Hydrol., 364(3): 298-310.

Nurroh, S., Gunawan, T. and Kurniawan, A. 2020. Assessment of groundwater pollution risk potential using the DRASTIC Model in Yogyakarta City, Indonesia. E3S Web Conf., 200: 02002.

Owens, D.W., Hunt, R.J. and Firnstahl, A.D. 2019. Automated time series measurement of microbial concentrations in groundwater-derived water supplies. Ground Water, 57(2): 329-336.

Pritchard, M., Craven, T. and Mkandawire, T.A. 2010. A study of the parameters affecting the effectiveness of Moringa oleifera in drinking water purification. Phys. Chem. Earth Parts A/B/C, 35(13): 791-797.

Pruss-Ustun, A. and World Health Organization, 2008. Safer water, better health: costs, benefits and sustainability of interventions to protect and promote health. World Health Organization.

Quilliam, R.S., Weidmann, M. and Moresco, V. 2020. COVID-19: The environmental implications of shedding SARS-CoV-2 in human feces. Environ. Int., 140: 105790.

Rahman, A.A. 2008. GIS-based DRASTIC model for assessing groundwater vulnerability in shallow aquifer in Aligarh, India. Appl. Geogr., 28(1): 32-53.

Ritter, K.S., Paul, S., Ken, H., Patricia, K., Gevan, M. and Beth, L.L. 2002. Sources, pathways, and relative risks of contaminations in surface water and groundwater: A perspective prepared for the Walkerton inquiry. J. Toxicol. Environ. Health Part A, 65(1): 1-142.

Rivera, A. and Bouchard, N. 2005. How well do we understand groundwater in Canada? A science case study. Buried Treasure - Groundwater Permitting and Pricing in Canada. pp. 1-41.

Robins, N.S., Chilton, P.J. and Cobbing, J.E. 2007. Adapting existing experience with aquifer vulnerability and groundwater protection for Africa. J. Afr. Earth Sci., 47(1): 30-38.

Schneider, O.D. and Lechevallier, M.W.A. 2017. The cost-effective treatment process for producing high-quality drinking water. J. Am. Water Works Assoc., 109(3): 39-47.

Sojobi, A.O. 2016. Evaluation of groundwater quality in a rural community in North Central Nigeria. Environ. Monit. Assess., mental Monitoring and Assessment, 188(3): 1-17.

Thapinta, A. and Hudak, P.F. 2003. Use of geographic information systems for assessing groundwater pollution potential by pesticides in Central Thailand. Environ., 29(1): 87-93.

World Health Organization (WHO) 1997. Guidelines for drinking-water quality. In: Surveillance and Control of Community Supplies, Vol. 3, 2nd ed. Geneva.

World Health Organization (WHO) 2003. Assessing Microbial Safety of Drinking Water. Published, by OECD.

Wright, J., Gundry, S. and Conroy, R. 2004. Household drinking water in developing countries: a systematic review of microbiological contamination between source and point-of-use. Trop. Med. Int. Health, 9(1): 106-117.

Xu, Y., Li, X. and Zhu, B. 2020. Characteristics of pediatric SARS-CoV-2 infection and potential evidence for persistent fecal viral shedding. Nature Med., 26(4): 502-505.

Yolcubal, I., Gündüz, Ö.C. and Sönmez, F. 2016. Assessment of the impact of environmental pollution on groundwater and surface water qualities in a heavily industrialized district of Kocaeli (Dilovası), Turkey. Environ. Earth Sci., 75(2): 1-23.

# Influence of Yeast Bioinoculant Isolated from Indian Date Palm Tree (*Phoenix sylvestris*) Sap on the Health of Wheat Crop and Soil

**M. S. Ambawade*†, N. V. Manghwani*, P. R. Madhyani*, A. M. Shaikh**, D. D. Patil* and G. R. Pathade***
*The P. G. K. Mandal's, Haribhai V. Desai College, Pune, Maharashtra India
**LMK College of Horticulture, Kadegaon, Pune, Maharashtra India
***Krishna Institute of Allied Science, KVVDU, Karad, Maharashtra India
†Corresponding author: M. S. Ambawade; ambawade2014@gmail.com

## ABSTRACT

In this study, three promising yeast isolates were isolated from the sap of the Indian date palm tree (*Phoenix sylvestris*) and characterized by biochemical tests and 18S rRNA gene sequencing. They were confirmed as *Saccharomyces cerevisiae* and were designated as strains PYS-1, PYS-2, and PYS-3. These confirmed strains were used for the preparation of bioinoculants. Bioinoculant was prepared and applied to wheat crops, and the effect of Bioinoculant. Statistical analysis is carried out using analysis of variance (ANOVA), and it is found that the absorbance of chlorophyll, protein, and Indole Acetic Acid (IAA) content is significantly increased. The treatment of bioinoculant showed that crops significantly increased chlorophyll, protein, and IAA content. Further, we applied bioinoculant on the soil and measured the soil's humus content before and after the treatment of bioinoculant. Then, a paired t-test was applied to check the effectiveness of the treatment, and it was found to significantly increase humus content in the soil. The use of bioinoculants is an economically feasible and eco-friendly method.

## INTRODUCTION

Since the inception of mankind, human beings have been using traditional plants to manage several ailments. One traditional plant, *Phoenix sylvestris*, is widely known as wild date palm. *Phoenix sylvestris* is commonly known as Indian date and is native to India and Southern portions of Pakistan. *P. sylvestris* is widely distributed in India, Pakistan, Myanmar, Nepal, Bhutan, Bangladesh, Mauritius, China, and Sri Lanka. Currently, the pest is reported in c. 15% of the coconut-growing countries and nearly 50% of the date palm-growing countries (Faleiro 2006). It is mostly found in Rajasthan, Gujarat, Himachal Pradesh, and Haryana states in India. It is traditionally important and known for its nutritional values worldwide (Barh & Mazumdar 2008). It is a rich source of carbohydrates, phenols, amino acids, tannins, flavonoids, alkaloids, terpenoids, dietary fibers, essential vitamins, and minerals. Sap is a Phloem, or sieve-tube sap, which is the fluid carrying sugar from roots to other parts of plants. Sap is a watery fluid of plants. Most tapped palm trees give a sap rich in sugar (10-20%). The farmers achieve the palm mainly for sap production, with which sugar-based secondary goods are manufactured. The sap is used fresh as a drink or after some processing as molasses

and/or alcoholic beverages (Francisco & Scott 2013). Seven diversified sites support the palm as its territory; most palms (20.40%) occur in orchards (Chowdhury et al. 2008). Sap can be used for fermentation as it contains sugar. Sweet sap is consumed fresh, processed into syrup or sugar, or fermented into alcohol or vinegar. Yeasts are eukaryotic, single-celled microorganisms classified as members of the fungus kingdom. Yeast sizes vary greatly, depending on species and environment, typically measuring 3–4 μm in diameter, although some yeast can grow to 40 μm in size. The yeast species *Saccharomyces cerevisiae* converts carbohydrates to carbon dioxide and alcohol through fermentation. Microbial inoculants, or bioinoculants, are agricultural alterations that use beneficial rhizospheric or endophytic microbes to promote plant health. Bioinoculant may consist of either a single or consortium of mixed microbial populations, which are substances containing live microorganisms, which, when applied to plant surfaces, seeds, roots, or soil, colonize the rhizosphere or the interior of plants and help to improve soil fertility while also stimulating plant growth by increasing the availability of plant nutrients and growth substances to the host crops (Suyal et al. 2016, Vessey 2003) like *Triticum aestivum*. Wheat (*Triticum aestivum*) is a crop widely cultivated for its seed, a cereal grain that is a worldwide

staple food. The many species of wheat together make up the genus *Triticum*; the most widely grown is common wheat (*T. aestivum*). Wheat is an important source of carbohydrates. Indole acetic acid (IAA) is one of the greatest physiologically active auxins. IAA is a common product of L- L-tryptophan metabolism produced by several microorganisms, including Promoting Rhizobacteria (PGPR). The plant growth parameters were found to be enhanced by the mixed inoculation of two groups of R and E bacteria compared to individual inoculations (respectively 33.7 and 37.8% increase in root and shoot dry weight), suggesting that PGP rhizobacteria acted synergistically with PGP endophytes in phosphate solubilization (Emami et al. 2019). IAA helps produce longer roots with more root hairs and root laterals involved in nutrient uptake. Soil fertility refers to the capability of soil to sustain agricultural plant growth, *i.e.*, to provide plant habitat and result in sustained and consistent yields of high quality. The organic matter (OM) content influences many soil properties, such as the capacity of soil to supply N, P, S, and trace elements; infiltration and retention of water; degradation of aggregation; and overall soil structure. Cation exchange capacity, soil color.

## MATERIALS AND METHODS

**Collection of sap sample:** The sap was extracted and collected by tapping. The sap sample was collected from Bhor, Pune.

**Isolation of yeast isolates from sap:** Sap was collected, and 2-5mL of the sample was transferred into Sabouraud's dextrose broth (SD) and Yeast extract broth (YE) for the enrichment and incubated at 30°C for 48h on a rotatory shaker. YE agar plates and SD agar plates were inoculated with enriched broth (Anyanwu et al. 2020). Then, plates were incubated at 30°C for 48 hours. The yeast nature of isolates was confirmed by microscopy.

**Microscopic examination of isolates:** Isolates were observed microscopically. The yeast was characterized for colony characters and gram nature.

**Biochemical characterization of yeast isolates:** The biochemical tests viz. sugar fermentation and utilization, oxidase, catalase, nitrate reduction, and IMViC tests were used for the characterization of promising isolates (Bergey & Holt 1994).

**Preparation of bioinoculant:** Promising isolates ($10^8$CFU/mL of each) were inoculated in sterile Yeast extract broth (100 mL). Enriched broth was kept on a rotatory shaker at 30°C for 48h incubation. Dilutions were prepared from incubated broth, spread on YE plates, incubated at 300°C for

48h, and colonies were counted of each isolate inoculated to study their compatibility.

**Growth curve:** Yeast growth is measured in a shaken conical flask by determining the optical density (OD) at 600 nm. Then, a growth curve is built by plotting OD versus time. Each of the four flasks of yeast extract broth of 100 mL, one as control. The three different isolates were then inoculated in each broth. The OD of each flask was recorded hourly from zero hour onwards. The graph was then plotted as a growth curve.

**Estimation of photosynthetic pigment (Chlorophyll) content:** The chlorophyll (a and b) content of the mature leaves of the test plant *Triticum aestivum* was estimated by the method of (Liang et al. 2017, Sadasivam & Manickam 1996)

**Estimation of protein of test plant:** Estimation of protein content was done by Lowry's method (Lowry et al. 1951).

**Quantification of Indole Acetic Acid (IAA) of isolates by spectrophotometric method:** It was quantified by Salkowski's method (Emami et al. 2019).

**Estimation of the soil fertility- humus content of soil:** It was determined by rapid dichromate oxidation technique (Walkley & Black 1934).

**18S rRNA gene sequencing:** The promising yeast isolates were identified presumptively per Bergey's Manual of Determinative Bacteriology based on physical, biochemical, and microbiological characteristics. All were further identified based on 18S rRNA gene sequencing using universal primers. Pure cultures were given to NCMR-Pune, India, and NCBI server (http://www.ncbi.nlm.nih.gov/BLAST) to check the similarity.

## RESULTS AND DISCUSSION

**Isolation of yeast:** Yeast was isolated on Sabouraud's dextrose agar and yeast extract agar. Three promising yeast isolates were selected for further studies (Fig. 1).

**Biochemical characterization of Yeast isolates:** Three promising isolates were biochemically characterized with reference to (Bergey & Holt 1994) using eleven biochemical tests (sugars, IMViC, Amylase, Catalase, and Oxidase). From Table 1, it is observed that two (PYS-1 and PYS-2) isolates showed positive for Sugars, MR, Catalase, and Oxidase and negative for Indole, VP Citrate and Amylase whereas One (PYS-3) isolate showed positive for Sugars like Glucose, Sucrose, Fructose and negative for maltose, MR, Catalase, and Oxidase positive and negative for Indole, VP, Citrate and Amylase. These isolates were identified as *Yeast* spp. at the genus level.

**Photoplate 1: PYS – 1**



**Photoplate 2: PYS - 2**



**Photoplate 3: PYS - 3**

Fig. 1: Growth of yeast isolates on Sabouraud's dextrose agar at 30°C for 48 h incubation.

Table 1: Biochemical characterization of selected isolates.

| Sr. No. | Biochemical tests | Isolates | | |
|---------|-------------------|----------|-------|-------|
| | | PYS-1 | PYS-2 | PYS-3 |
| 1. | Glucose | + | + | + |
| 2. | Sucrose | + | + | + |
| 3. | Fructose | + | + | + |
| 4. | Maltose | + | + | - |
| 5. | Indole | - | - | - |
| 6. | MR | + | + | + |
| 7. | VP | - | - | - |
| 8. | Citrate | - | - | - |
| 9. | Amylase | - | - | - |
| 10. | Catalase | + | + | + |
| 11. | Oxidase | + | + | + |

+ Positive test and – Negative test

**18S rRNA gene Sequence:** The 18S rRNA sequences of all three promising isolates confirm that isolates were *Saccharomyces cerevisiae* strains.

### *Saccharomyces Cerevisiae* Strain PYS-1

AGAGATGGAGAGTCCAGCCGGGCCTGCGCT-
TAAGTGCGCGGTCTTGCTAGGCTTGTAAGT-
TTCTTTCTTGCTATTCCAAACGGTGAGAGAT-
TTCTGTGCTTTTGTTATAGGACAATTAAAACCGT-
TTCAATACAACACACTGTGGAGTTTTCATATCT-
TTGCAACTTTTTCTTTGGGCATTCGAGCAATCGG-
GGCCCAGAGGTAACAAACACAAACAATTTTAT-
TTATTCATTAAATTTTTGTCAAAAACAAGAAT-
TTTCGTAACTGGAAATTTTAAAATATTAAAAACT-
TTCAACAACGGATCTCTTGGTTCTCGCATCGAT-
GAAGAACGCAGCGAAATGCGATACGTAATGT-
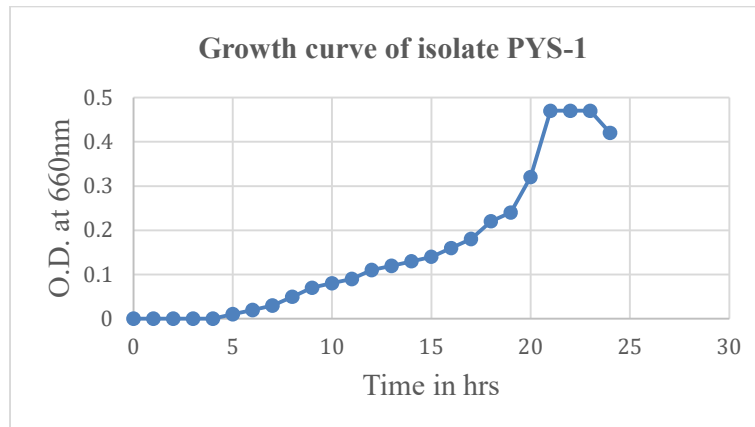GAATTGCAGAATTCCGTGAATCATCGAATCTTT-

GAACGCACATTGCGCCCCTTGGTATTCCAGGG-
GGCATGCCTGTTTGAGCGTCATTTCCTTCTCAAA-
CATTCTGTTTGGTAGTGAGTGATACTCTTTGGAGT-
TAACTTGAAATTGCTGGCCTTTTCATTGGATGT-
TTTTT

### *Saccharomyces Cerevisiae* **Strain PYS-2**

GGCAAGAGCATGAGAGCTTTTACTGGGCAAGAA-
GACAAGAGATGGAGAGTCCAGCCGGGCCTG-
CGCTTAAGTGCGCGGTCTTGCTAGGCTTGTAA-
GTTTCTTTCTTGCTATTCCAAACGGTGAGAGAT-
TTCTGTGCTTTTGTTATAGGACAATTAAAAC-
CGTTTCAATACAACACACTGTGGAGTTTTCAT-
ATCTTTGCAACTTTTTCTTTGGGCATTCGAG-
CAATCGGGGCCCAGAGGTAACAAACACAAA-
CAATTTTATTTATTCATTAAATTTTTGTCAAAAA-
CAAGAATTTTCGTAACTGGAAATTTTAAAATAT-
TAAAAACTTTCAACAACGGATCTCTTGGTTCTCG-

CATCGATGAAAAACGCAGCGAAATGCGATA-
CATATTTTTTTTTTTGCAGAATTCCGAGAAT-
CATCGAATCTTTGAATA

### *Saccharomyces Cerevisiae* **Strain PYS-3**

CTTTTACTGGGCAAGAAGACAAGAGATGGA-
GAGTCCAGCCGGGCCTGCGCTTAAGTGCGCG-
GTCTTGCTAGGCTTGTAAGTTTCTTTCTTGCTAT-
TCCAAACGGTGAGAGATTTCTGTGCTTTTGT-
TATAGGACAATTAAAACCGTTTCAATACAA-
CACACTGTGGAGTTTTCATATCTTTGCAACT-
TTTTCTTTGGGCATTCGAGCAATCGGGGCCCA-
GAGGTAACAAACACAAACAATTTTATTTAT-
TCATTAAATTTTTGTCAAAAACAAGAATTTTCG-
TAACTGGAAATTTTAAAATATTAAAAACT-
TTCAACAACGGATCTCTTGGTTCTCGCATCGAT-
GAAGAACGCAGCGAAATGCGATACGTAATGT-
GAATTGCAGAATTCCGTGAATCATCGAATCTTT-



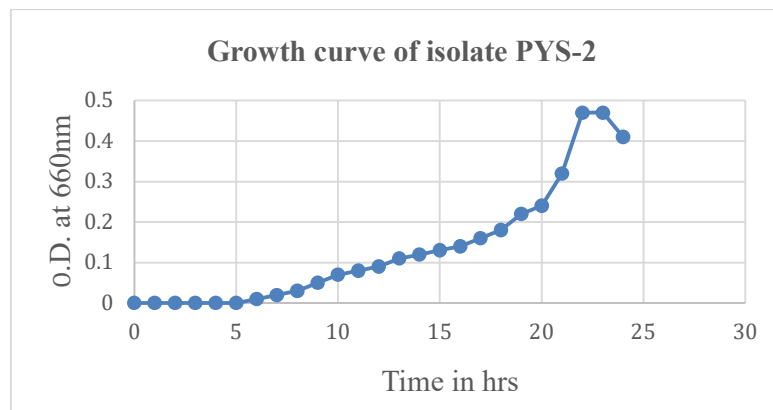Fig. 2: Growth curve of promising isolate PYS -1.
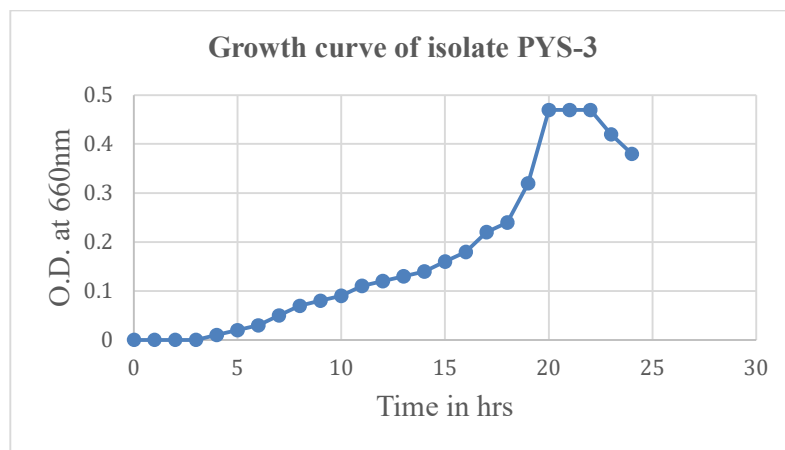


Fig. 3: Growth curve of promising isolate PYS -2.

Fig. 4: Growth curve of promising isolate PYS-3.

GAACGCACATTGCGCCCCTTGGTATTCCAGGG-
GGCATGCCTGTTTGAGCGTCATTTCCTTCTCAAA-
CATTCTGTTTGGTAGTGAGTGATACTCTTTGGAGT-
TAACTTGAAATTGCTGGCCTTTTCATTGGATGT-
TTTTTTTTCCAAAGAGAGGTTTCTCTGCGTGCTT-
GAGGTATAATGCAAGTACGGTCGTTTTAGGT-
TTTACCAACTGCGGCTAATCTTTTTTATACTGAG-
CGTATTGGAACGTTATCGATAG

**Growth curve of promising isolates (PYS-1, PYS-2, and PYS-3):** The growth of yeast isolates is observed in shaken conical flasks by determining the optical density (OD) at 660 nm. Then, a growth curve is a sigmoid graph built by plotting OD versus time, which allows identification and selection of the exponential phase and is fitted with the exponential growth equation to obtain kinetic parameters. Low specific growth rates with higher doubling times generally represent respiratory growth. Conversely, higher specific growth rates with lower doubling times indicate fermentative growth. In the growth curve of three (PYS-1, PYS-2, and PYS-3) promising isolates, found that up to 8, 5, and 4h time for PYS-1, PYS-1, and PYS-3 isolates, respectively, were in the log phase, indicating further ranged in between 4 to 8 h of incubation and there was no drastic difference in their growth pattern and could be compatible with each other in co-cultivation (Figs. 2, 3 and 4).

Bioinoculant (PYS-1, PYS-2, and PYS-3) was formulated as mentioned in Table 2. The bioinoculant was prepared in higher volume (in liters) for further studies (Fig. 5). This Bioinoculant was used as a biofertilizer, resulting in significant plant growth and soil fertility.

**Effect of Bioinoculant on the growth of wheat *Triticum aestivum* and soil fertility:** Bioinoculant was prepared from all three promising isolates (PYS 1, PYS 2, and PYS 3) and given to the crops and soil. The effect of bioinoculant was studied on the wheat crop (*Triticum aestivum*) compared to control. A positive effect on the crop is seen, as there is an increase in shoot length and root length for all three isolates and a mixture of them. Among the single treatments, the best upsurge for most growth parameters
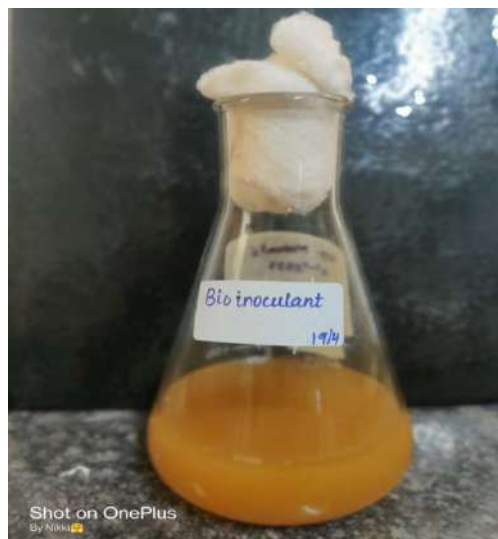
**Preparation of Bioinoculant of promising isolates**



Fig. 5: Bioinoculant.

Table 2: Formulation of Liquid Bioinoculant.

| Sr. No. | Isolates | No. of CFU.mL$^{-1}$ |
|---------|----------|---------------------|
| 1. | PYS-1 | $10^8$ |
| 2. | PYS-2 | $10^8$ |
| 3. | PYS-3 | $10^8$ |

Fig. 6: Effect of bioinoculant on crop (*T. aestivum*).

(chlorophyll, protein, and IAA contents) was shown by *Triticum aestivum* plants compared to the control crop (Fig. 6).

**Estimation of photosynthetic pigment (Chlorophyll) of *Triticum aestivum*:** The total chlorophyll content of the wheat crop was measured by taking absorbance at 620nm
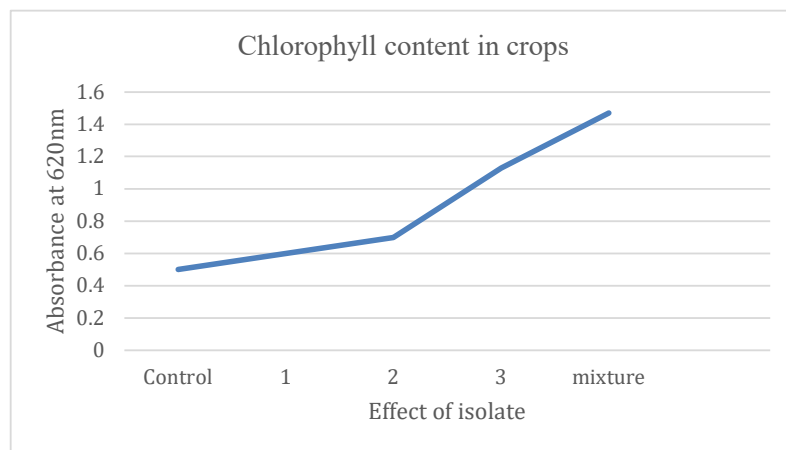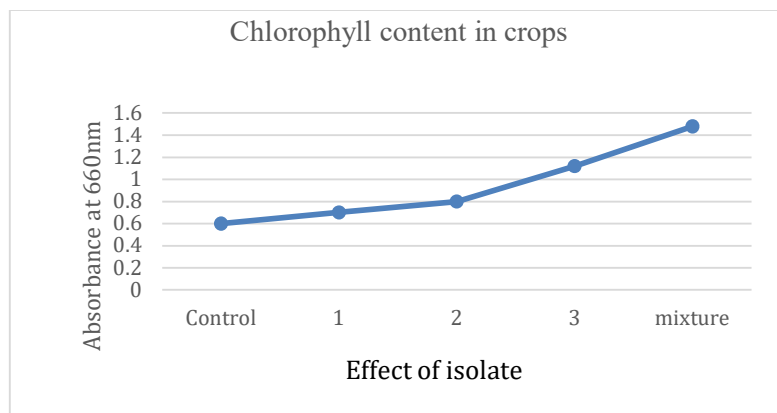


Fig. 7: Chlorophyll content at 620nm.



Fig. 8: Chlorophyll content at 660nm.

Table 3: Tukey's honest significant difference (HSD) test statistic for different pairs of isolates.

| Pairs of isolates | | q value at 620 nm | q value at 660 nm |
|---|---|---|---|
| Control | YS-1 | 1.326473065 | 1.543646179 |
| Control | YS-2 | 4.863734571 | 5.196942137 |
| Control | YS-3 | 8.224133002 | 7.975505259 |
| Control | Mixture | 13.0436518 | 13.5326315 |

and 660nm using a calorimeter. Results are plotted on the graphs as shown in Fig. 7 and Fig. 8, respectively.

The increasing chlorophyll in the inoculated crops probably resulted in higher photosynthetic rates and thus improved plant biomass. It has been shown in the study that total chlorophyll is more than that was reported earlier. The increase of chlorophyll that could lead to higher rates of photosynthesis is dependent.

Further analysis of variance (ANOVA) (Scheffe 1999) is carried out to test whether there is a significant difference in mean absorbance of chlorophyll at 620 nm and at 660 nm between the control isolates YS-1, YS-2, YS-3, and a mixture of these three isolates at 5% level of significance (l. o. s.) ($\alpha$), $i.e.\ \alpha = 0.05$. The p-values are 0.0032 and 0.0030 for 620nm and 660 nm, respectively, which are less than $\alpha$. So, there is sufficient evidence to conclude that the absorbance of chlorophyll is significantly different at 620 nm and 660 nm.

Hence, checking which isolate is more significant (effective) than others is necessary. To fulfill this requirement, we carried out Tukey's honest significant difference (HSD) test (Tukey 1949) and checked the significance difference between the control and other isolates. The values of test statistic q of Tukey's HSD test for control and different isolates are reported in Table 3, where the test statistic q is

$$q = \frac{\text{Abs(mean of control group} - \text{mean of isolate})}{\sqrt{\frac{1}{2}} \times \text{SE of residual} \times \left(\frac{1}{n_1} + \frac{1}{n_2}\right)}$$

From the values of test statistic q, q value is highest for the pair Control and mixture. Therefore, a mixture of isolates is most effective, followed by isolates YS-3 and YS-2 at both 620 nm and 660 nm with respect to the extraction of chlorophyll.

**Estimation of protein in *Triticum aestivum*:** The protein content of enzyme extract is usually determined by Lowry's Method (Lowry et al. 1951) as amino acids give the exact quantification- the method developed by Lowry Reading was taken at 660nm, and a graph is plotted using the standard protein graph as shown in Fig. 9.

The results show that plant protein content significantly increased with bioinoculant injection compared to the control. Total protein content was determined according to the Lowry protein assay (Lowry et al. 1951), with reduced Folin reagent and subsequent colorimetric determination at 660nm.

Further analysis of variance (ANOVA) (Scheffe 1999) is carried out to test whether there is a significant difference in mean protein absorbance between Control isolates YS-1, YS-2, YS-3, and a mixture of these three isolates at 5% l. o. s. ($\alpha$), $i.e.,\ \alpha = 0.05$. The p-values are found to be 0.02171, which is less than $\alpha$. So, there is sufficient evidence to conclude that protein absorbance is significantly different.

Hence, to check which isolate is more significant (effective) than others. The values of test statistic q of Tukey's HSD test (Tukey 1949) for control and different isolates are reported in Table 4.
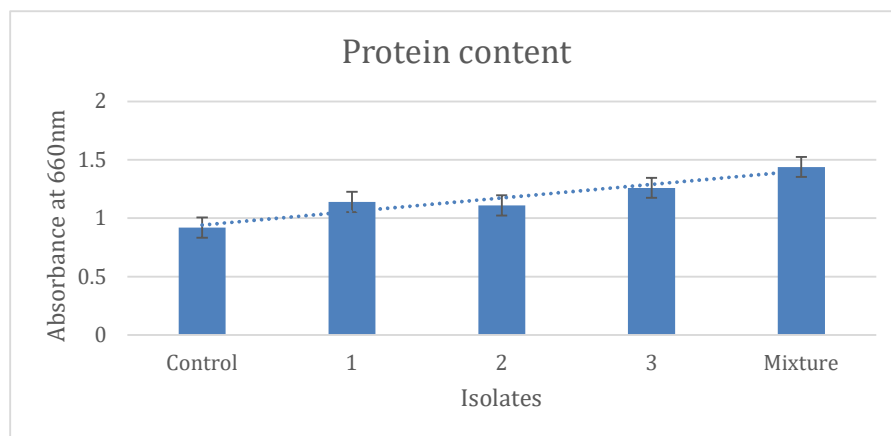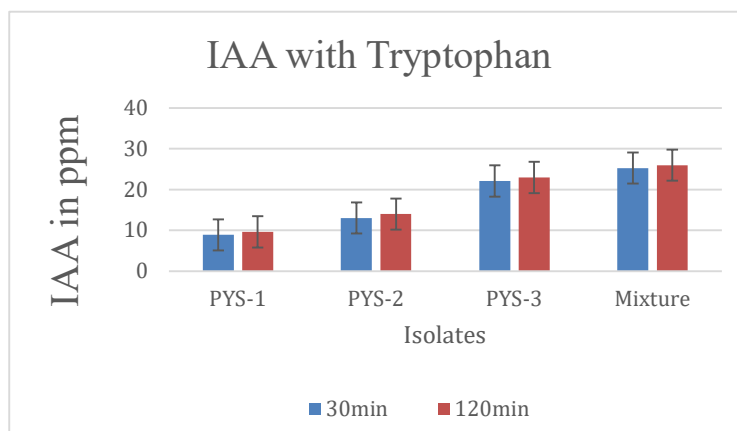


Fig. 9: Protein analysis chart.

Fig. 10: IAA with Tryptophan analysis chart.

From the values of test statistics q, q value is highest for the pair Control and mixture. Therefore, a mixture of isolates is most effective, followed by isolates YS-3 and YS-2 with respect to the extraction of protein.

**Estimation of Indole Acetic Acid (IAA) on *Triticum aestivum:*** The significance of the study could be stated as the potential of these IAA-producing isolates will flourish the growth and ultimately IAA production in the field and prevent environmental pollution by avoiding excessive applications of chemical fertilizers. The IAA analysis chart is shown in Fig. 10.

All three isolates and their mixture were screened out for their productivity of IAA on a spectrophotometer. They all showed the ability to produce IAA with Tryptophan supplemented in the medium at 30 minutes and 120 minutes. These Endophytic bacteria are also helpful in developing liquid bioinoculants for economically convenient and sustainable agriculture. (Emami et al. 2019).

Further analysis of variance (ANOVA) (Scheffy 1999) is carried out to test whether there is a significant difference in mean absorbance of IAA at 30 minutes and 120 minutes between Control isolates YS-1, YS-2, YS-3, and a mixture of these three isolates at a 5% level of significance (l. o. s.) ($\alpha$), *i.e.* $\alpha = 0.05$. The p-values are found to be $6.98 \times 10^{-11}$ and $6.62 \times 10^{-10}$ for 30 and 120 min, respectively, which are less than $\alpha$. So, there is sufficient evidence to conclude that the absorbance of IAA is significantly different at 30 minutes and 120 min.

Hence, checking which isolate is more significant (effective) than others is necessary. We, therefore, carried out an HSD test and checked the significance difference between controls and other isolates. The values of test statistic q of Tukey's HSD test (Tukey 1949) for control and different isolates are reported in Table 5.

From the values of test statistics q, q value is highest for the pair Control and mixture. Therefore, a mixture of isolates is most effective, followed by isolates YS-3 and YS-2 at both 30 minutes and 120 minutes with respect to extraction of IAA.

**Effect of bioinoculant on soil (Organic matter):** The humus content of soil before and after applying bioinoculant (treatment) is reported in Table 6.

Table 4: Tukey's honest significant difference (HSD) test statistic for different pairs of isolates.

| Pairs of isolates | | q value |
|---|---|---|
| Control | YS-1 | 4.914942619 |
| Control | YS-2 | 4.839328117 |
| Control | YS-3 | 7.107763172 |
| Control | Mixture | 10.20795775 |

Table 5: Tukey's honest significant difference (HSD) test statistic for different pairs of isolates.

| Pairs of isolates | | q value at 30 minutes | q value at 120 minutes |
|---|---|---|---|
| Control | YS-1 | 3.841463511 | 1.140572822 |
| Control | YS-2 | 14.35357865 | 12.24590758 |
| Control | YS-3 | 36.76841271 | 28.30056821 |
| Control | Mixture | 43.49648101 | 34.17095266 |

Table 6: Estimation of organic matter.

| Observation No. | Organic matter in mg.mL$^{-1}$ (Before treatment) | Organic matter in mg.mL$^{-1}$ (After treatment) |
|---|---|---|
| 1 | 4.9 | 15 |
| 2 | 5.5 | 15.7 |
| 3 | 6.0 | 16.25 |

To check whether the treatment is effective or not, statistically, we carry out the paired t-test, and the corresponding p-value is found to be 0.000778, which is less than l.o.s. 0.05. Hence, it is concluded that the humus content of soil is increased in the soil after treatment of bioinoculant in comparison with control soil.

## CONCLUSIONS

Three dominant yeast strains were screened out from the sap of wild date palm tree (*Phoenix sylvestris*) for preparation of bio-inoculant. All the isolates were characterized with their morphological characterization and genetically confirmed strains as *Saccharomyces cerevisiae* Strain PYS-1, *Saccharomyces cerevisiae* Strain PYS-2, *Saccharomyces cerevisiae* Strain PYS-3. Based on observed data, statistical analysis is carried out using ANOVA and paired t-tests. The results are reported in the respective sections. Regarding biochemical analysis like photosynthetic pigment, protein content, and hormone (IAA), it was clear that crop health (Triticum aestivum) has been increased with consortia. Also, concluding that there was an increase in the organic content of soil proving/ stating that this bio-inoculant is preferable. Microbial inoculants can minimize the negative impact of chemical input and consequently increase the quantity and quality of farm produce.

## REFERENCES

Anyanwu, N.O., Isitua, C.C. and Egbebi, A. 2020. Isolation and identification of yeast cells from palm wine in Ado Ekiti Southwest Nigeria. J. Sci. Res., 9(12): 1282-1286.

Bergey, D.H. and Holt, J.G. 1994. Bergey's Manual of Determinative Bacteriology. 9th Edition, Lippincott Williams and Wilkins, Baltimore.

Barh, D. and Mazumdar, B.C. 2008. Comparative nutritive values of palm saps before and after their partial fermentation and effective use of wild date (*Phoenix sylvestris* Roxb.) sap in treatment of anemia research. J. Med. Med. Sci., 3(2):173-176.

Chowdhury, H., Muhammed, H. and Koike, M. 2008. Traditional utilization of wild date palm (*Phoenix sylvestris*) in rural Bangladesh: an approach to sustainable biodiversity management. J. Forest. Res., 19(1): 245-251.

Emami, A., Etesami, S. and Motessharezadeh, F. 2019. Effect of rhizospheric and endophytic bacteria with multiple plant growth promoting traits on wheat growth. Environ Sci Pollution Res., 26: 19804-19813.

Francisco, O. and Scott, M. 2013. Sweet sap from palms, a source of beverages, alcohol, vinegar, syrup, and sugar. VIERAEA, 41: 91-113.

Faleiro, J. 2006. A review of the issues and management of the red palm weevil *Rhynchophorus ferrugineus* (Coleoptera: Rhynchophoridae) in coconut and date palm during the last one hundred years. Int. J. Trop. Insect Sci., 154-135 :(3)26.

Liang, U., Liao, H. and Jones, G. 2017. Non-destructive plant method estimation of chlorophyll content of Arabidopsis seedlings. Springer, 13(26): 13-26.

Lowry, O.H., Rosebrough, N.J., Farr, A.L. and Randall, R.J. 1951. Protein measurement with folin phenol reagent. J. Biol. Chem., 193: 256-275.

Sadasivam, S. and Manickam, A. 1996. Biochemical Methods. New Age International (P) Ltd., Publishers, India.

Scheffe, H.. 1999. Analysis of Variance, Wiley, New York.

Suyal, D.C., Ravindra, S., Santosh, S. and Reeta, G. 2016. Microbial inoculants as biofertilizers. Sustain. Agric. Product., 15: 311-318.

Tukey, J. 1949. Comparing individual means in the analysis of variance. Biometrics, 5(2): 99-114, JSTOR 3001913.

Vessey, P. 2003. Plant growth promotes rhizobacteria as biofertilizers. Plant Soil J., 255(2): 571–586.

Walkley, A. and Black, I.A. 1934. An examination of the Degtjareff method for determining soil organic matter and a proposed modification of the chromic acid titration method. Soil Sci., 37: 29-37.

# Production of a Database on Short-Lived Climate Pollutants (SLCP) and the Elaboration of Projection Scenarios of these Emissions Using the LEAP Software - The Case of Morocco

**Y. Kasseh†** (ID)**, A. Touzani** (ID) **and S. EL Majaty** (ID)

Mohammedia School of Engineers, Avenue Ibn Sina B.P 765, Agdal, Rabat 10090, Morocco

†Corresponding author: Y. Kasseh; youssefkasseh.emi@gmail.com

## ABSTRACT

Short-lived climate pollutants (SLCPs) have significant effects on climate, human health, and the environment. In Morocco, steps are being taken to reduce SLCP emissions, but effective policymaking requires a thorough understanding of emission sources and trends. In this paper, we present a study on the production of a database on SLCP emissions in Morocco, as well as the development of scenarios to project these emissions using LEAP software. The results of this analysis allow us to better understand the emissions sources and evaluate the impact of different emission reduction policies.

## INTRODUCTION

Short-lived climate pollutants (SLCPs) are gases and particles that remain in the atmosphere for a short period but have a significant impact on climate, air quality, and human health The main SLCPs are methane, black carbon, HFCs, PFCs, and SF6. SLCP emissions are mainly caused by human activities such as fossil fuel combustion, agriculture, and chemical production and consumption. According to the United Nations Environment Programme (UNEP), SLCPs account for about one-third of global warming and are responsible for 7 million premature deaths each year worldwide. In Morocco, a recent study by the Ministry of Environment found that SLCP emissions increased by nearly 70% between 1990 and 2014, with a projected 5% annual growth by 2030 (Saidi et al. 2023). This alarming trend can be attributed to the country's rapid economic growth, increasing population, rapid urbanization, and increased industrialization (Al Wachami et al. 2023).

Morocco is committed to reducing its greenhouse gas emissions in line with the Paris Climate Agreement. It adopted a National Sustainable Development Strategy (NSSD) 2017 to guide its emission reduction efforts (Kasseh et al. 2023). Morocco also joined the CCW in 2014, demonstrating its strong commitment to managing

and reducing short-lived pollutants (Ministry of Energy and Mines - Kingdom of Morocco, 2020). The Kingdom of Morocco joined the Sustainable Development Goals (SDGs) program in 2015 after participating in its development with the United Nations. Morocco considers the SDGs as levers to structure its development model and achieve its sustainable development objectives (Dettner & Blohm 2021).

However, national climate action faces challenges related primarily to limited funding and technology transfer (Liya & Jianfeng 2018). These challenges have been exacerbated by the combination of climatic elements, notably the drought experienced by the country, with the COVID-19 pandemic, which has taken a heavy human toll and constituted an additional financial burden (Sun et al. 2022). To face the challenges related to climate and health crises, Morocco advocates the adoption of a development model oriented toward sustainability and the resilient development of populations and territories (Boulakhbar et al. 2020).

It is also important to note that some air pollutants, such as black carbon, tropospheric ozone, or HFCs in particular, which contribute to climate change, are not considered in mitigation plans or the NDC. These pollutants, which are the subject of this study, are called "short-lived air pollutants" and have been the subject of particular attention since 2012 in

the framework of a Climate and Clean Air Coalition (CCAC) (Duan et al. 2022).

The proposed paper fills a gap in producing a database on SLCPs in Morocco and developing scenarios to project these emissions using LEAP (Liya & Jianfeng 2018). In addition, the paper addresses the challenges Morocco faces in climate action, including limitations in financing and technology transfer, exacerbated by the COVID-19 pandemic and the drought that has affected the country. Ultimately, the paper proposes a solution to address these challenges by promoting a sustainable and resilient development model for Morocco.

Therefore, this paper is structured around three key issues. Firstly, the elaboration of an SLCP database, indeed, to define efficient air pollution control policies and, in the absence of structuring of data by activity and by sector, seemed to us relevant for the continuation of the study. Secondly, the realization of an inventory of emissions of SLCP and air pollutants, which are generally associated with them, is the 1st inventory of emissions in polluting gases and/or SLCP by groups of activities in Morocco. Finally, this work will provide projection scenarios of these emissions using the LEAP-IBC software. These results are presented for the selected base year and the emission projection horizon (2014 and 2040).

## MATERIALS AND METHODS

### Inventory of GHG, SLCP and Pollutant Gases

A first inventory of GHGs, SLCPs, and polluting gases has been carried out in Morocco. Activities were classified into two categories: energy and non-energy. Gases emitted by activities in the energy category are mainly from combustion, while emissions in the non-energy category are generated by the decomposition of raw materials (such as the production of lime and cement), fugitive emissions (such as the production of PVC or paints) or biochemical reactions (such as the methanization of waste).

The emissions of a given gas (Qgaz) are calculated as follows:

For energy activities: $Qgaz = G \times Ie \times Fe$

G: Characteristic size of the activity

Ie: energy consumption per unit of the characteristic quantity

Fe: emission factor of the energy used

For non-energy activities: $Qgaz = G \times Fe$

G: Characteristic size of the activity

Fe: emission factor of the energy used

The results of our study are presented and analyzed in the following paragraphs. We have included in our analysis the greenhouse gases, which are also part of the polluting gases. We have presented the greenhouse gas emissions for each activity to compare our results with those of the BUR2, which includes the revised emissions of the Third National Communication. The results for each activity are organized as follows:

- Cumulative greenhouse gas emissions expressed in $tEqCO_2$
- Total emissions of polluting gases modeled by LEAP
- Emissions and analysis of short-lived gases (SLCP)

### Tool Used

A GHG emissions analysis for Morocco was conducted using LEAP software. LEAP, or Long-range Energy Alternative Planning System, is a widely used software tool for energy policy analysis and GHG mitigation assessments developed by the Stockholm Environment Institute (SEI) (Dettner & Blohm 2021).

LEAP is an integrated modeling tool that can be used to track energy consumption, production, and resource extraction in all sectors of an economy. It can be used to account for GHG emissions sources and sinks in both the energy and non-energy sectors. In addition to tracking GHGs, LEAP can also be used to analyze local and regional pollutant emissions and to perform cost-benefit assessments of scenarios (Gebremeskel et al. 2023).

LEAP is not a model of a particular energy system but rather a tool that can be used to create models of different energy systems, each of which requires its particular data structures. It supports a range of different modeling methodologies. On the demand side, it offers bottom-up/end-use accounting techniques and top-down/macro modeling. On the supply side, it offers a range of accounting and simulation methodologies and has optimization modeling capabilities.

LEAP's modeling operates at two conceptual levels. LEAP's built-in calculation formulas at the first level support all non-controversial energy accounting and emissions calculations. At the second level, the user enters spreadsheet-like expressions that can be used to specify time-varying data or to create multi-variable models (Fig. 1).

LEAP-IBC was the preferred tool for estimating emissions of gaseous pollutants and SLCPs and modeling their impacts.

Several activities emit polluting gases or SLCPs due to fossil or alternative energy consumption. We present the emissions of the three families of gases: i) Air pollutants, ii) Short-lived pollutants, and iii) Greenhouse gases. The independence between these three families is illustrated in Fig. 2.
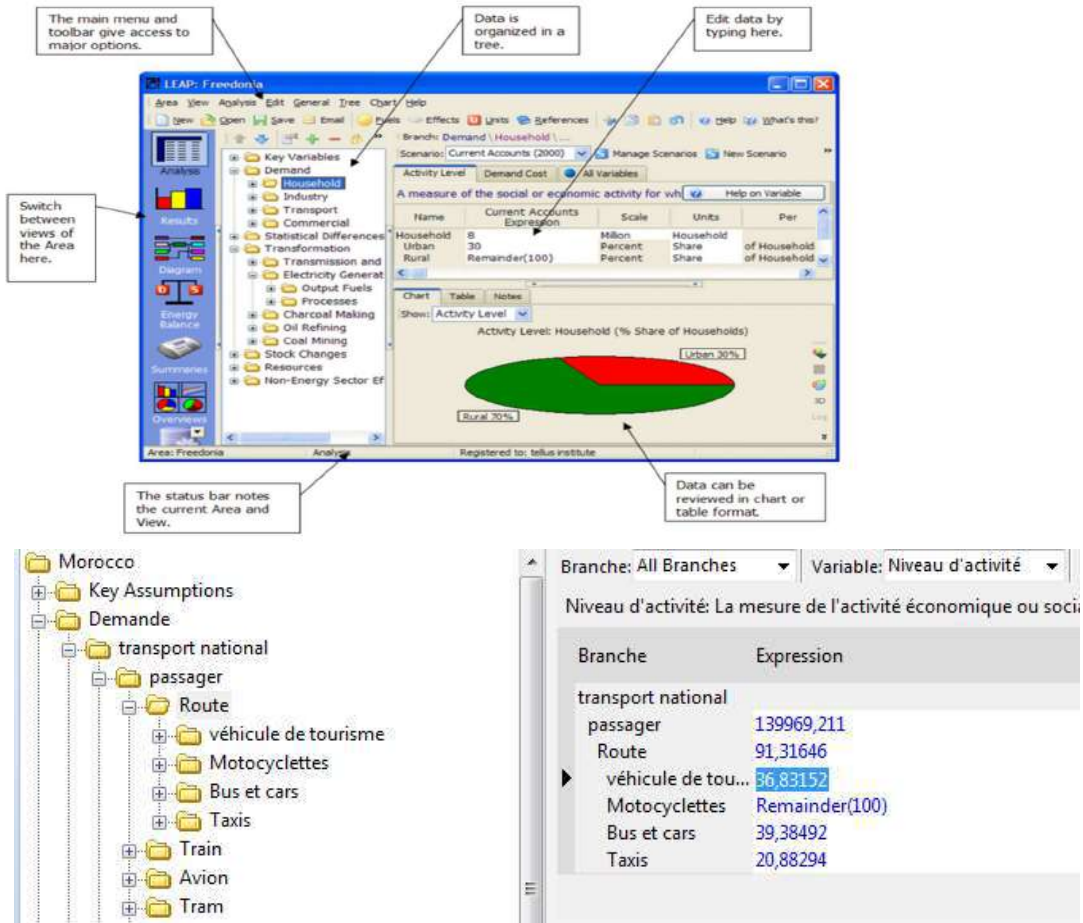
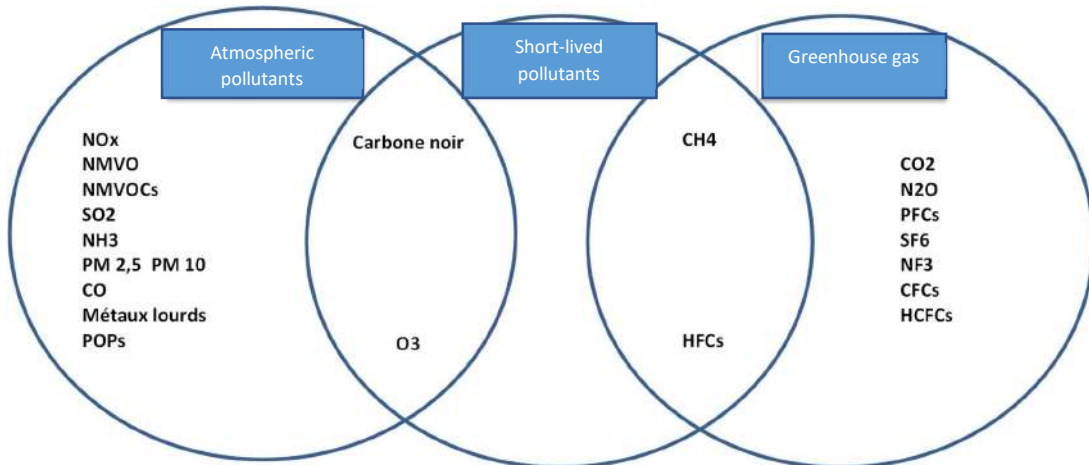Fig. 1: General view of the LEAP software interface.



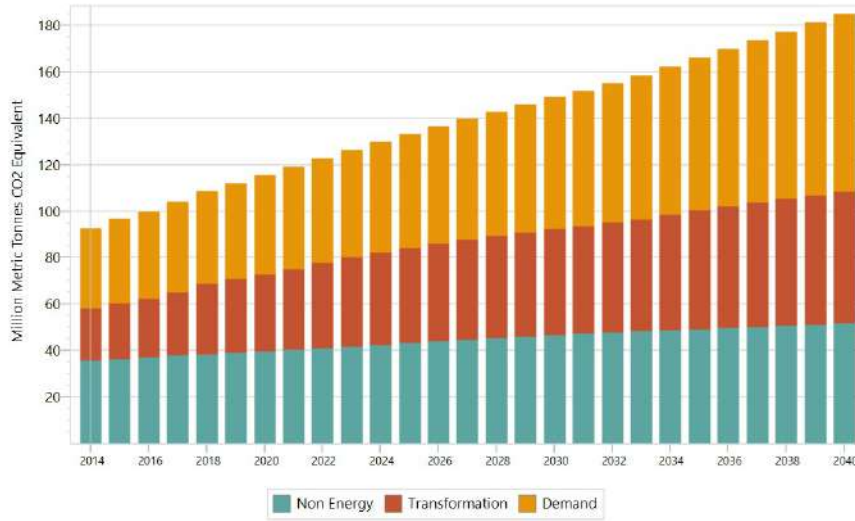Fig. 2: Independence of the three gas families.

Fig. 3: Global GHG emissions.

## RESULTS AND DISCUSSION

### Summary of Emissions in Morocco

Global GHG emissions: The GHG emissions at the level of Morocco (BAU) evolved from 92.44 Million tons of $CO_2$ equivalent in 2014 to 184.63 Million in 2040. The non-energy sector represented 38.8% in 2014, followed by the demand sector at 37.1% and the transformation sector at 24.0%. (Fig. 3).

By fuel type, the non-energy part represents 38.8%, followed by diesel at 19.4%, coal at 17.0%, LPG at 6.9%, and heavy fuel oil at 5.1%. The rest of the fuels contribute with percentages < 5%. (Fig. 4). The graphs (Fig.5, Fig. 6) show the emissions by sub-sector and by activity.

In comparison with the TCN and the CDN, we can notice that our baseline is between the emissions of the TCN and the CDN. The evolution of the GHG of the TCN seems exaggerated from 2030.
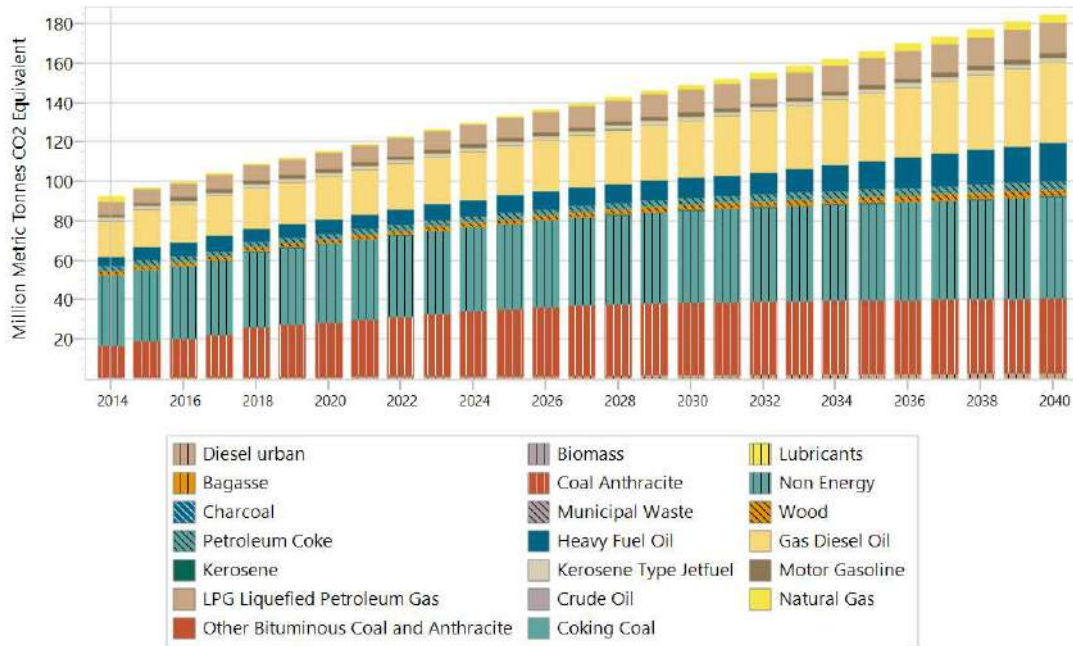


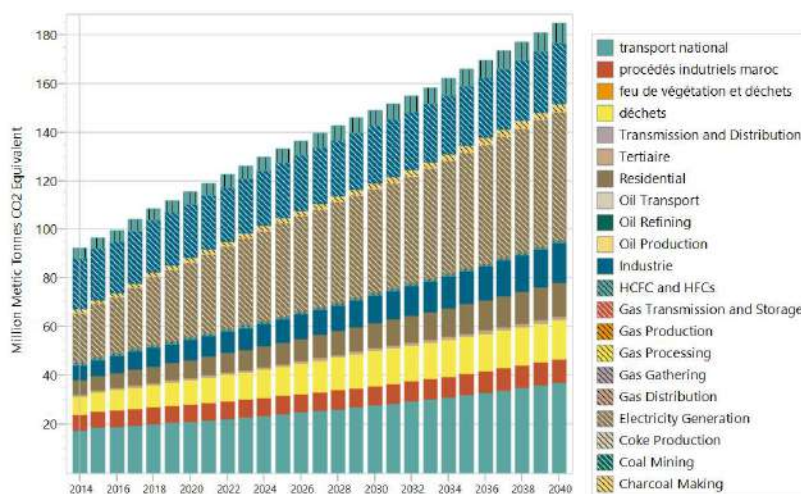Fig. 4: Global GHG Emissions by fuel type.
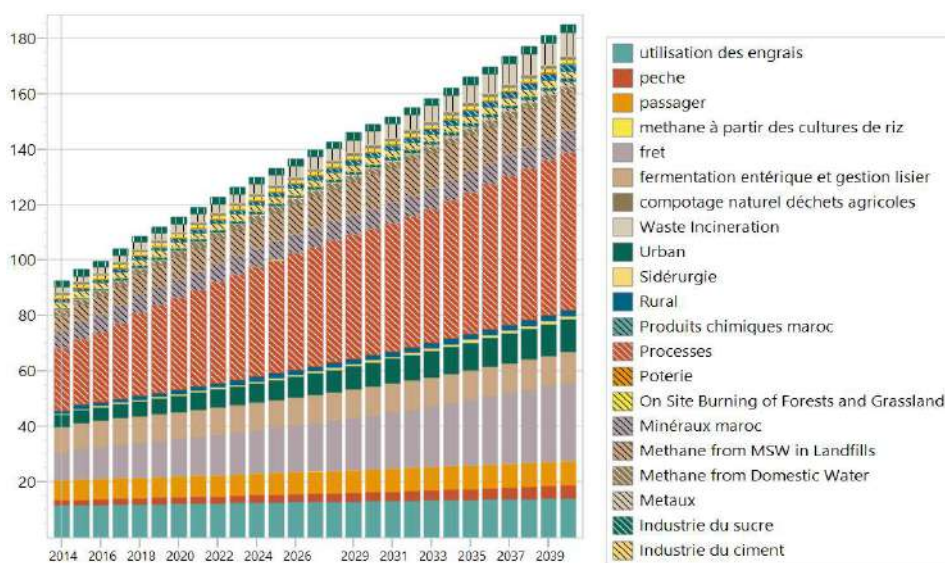
Fig. 5: Overall GHG emissions by sub-sector.



Fig. 6: Global GHG emissions by activity.

Note that the NDC does not consider emissions from HCFCs and HFCs, which is considered in our baseline (Fig. 7).

The details of the emissions of the 3 basic lines are summarized in the Table 1:

**Global SLCP emissions:** Overall, SLCP (Methane and Black Carbon) emissions changed from 899,907 tons in 2014 to 1,480,746 tons in 2040. Methane represents more than 99.25% of the total emissions. (Fig. 8)

**Global emissions of polluting gases:** The overall emissions of pollutant gases evolved from 26.63 Million tons in 2014 to 45.54 Million tons in 2040. NMVOCs represent more than 46.3%, followed by PM10 with 41.2%,

PM2.5 with 4.3%, and CO with 3.7%. The other pollutants contribute with a percentage of < 1%. (Fig. 9).

## CONCLUSIONS

A trend analysis of air quality (AQI) and GHG emissions in the energy sector was conducted for Morocco. The results showed that total GHG emissions have increased over the years due to economic growth and increased energy consumption. However, there has been a downward trend for some air pollutant criteria in some Moroccan cities in recent years, likely due to emission control measures and the implementation of environmental policies. Morocco has committed to a target of reducing its GHG emissions
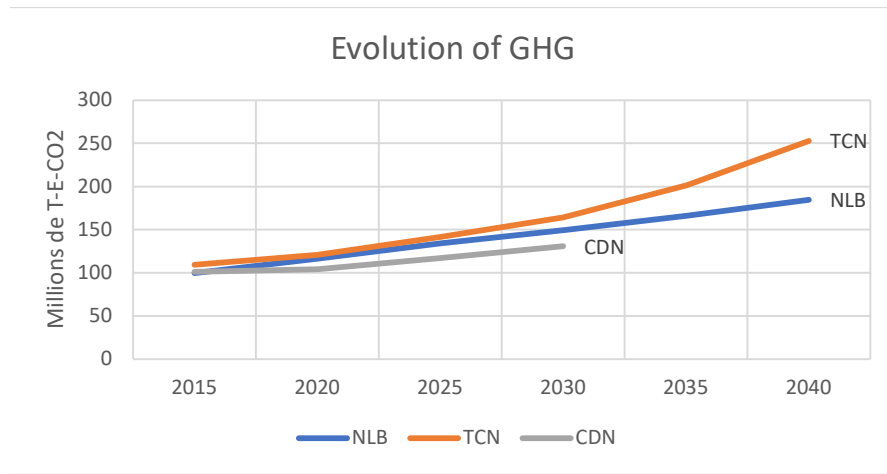
Fig. 7: Comparison of baseline with TCN and CDN.

Table 1: Evolution of GHG emissions of the 3 scenarios, NLB, TCN, and CDN (in Millions of tons $CO_2$ equivalent)

| TCN | 2010 | 2015 | 2020 | 2025 | 2030 | 2035 | 2040 |
|---|---|---|---|---|---|---|---|
| Households | 5,98 | 8,68 | 10,25 | 11,94 | 13,94 | 16,03 | 18,52 |
| Industry | 6,87 | 7,77 | 8,45 | 9,15 | 10,05 | 11,09 | 12,44 |
| Transportation | 13,86 | 18,25 | 23,88 | 30,39 | 38,69 | 49,27 | 62,76 |
| Tertiary | 0,38 | 0,46 | 0,58 | 0,72 | 0,90 | 1,15 | 1,47 |
| Agriculture and fisheries | 4,16 | 4,86 | 5,67 | 6,57 | 7,61 | 8,83 | 10,23 |
| Processing | 19,86 | 23,87 | 22,43 | 26,25 | 25,52 | 29,72 | 33,44 |
| Non-energy Industrial processes | 9,29 | 9,29 | 10,46 | 11,42 | 12,42 | 13,60 | 14,98 |
| Non-energy Agriculture | 22,02 | 22,60 | 23,37 | 27,83 | 36,55 | 52,19 | 79,29 |
| No energy Forestry | 4,51 | 4,34 | 4,25 | 3,85 | 3,07 | 1,82 | 0,00 |
| No energy waste | 7,03 | 9,13 | 11,34 | 13,61 | 15,64 | 17,64 | 19,66 |
| **Total** | **93,94** | **109,26** | **120,67** | **141,72** | **164,38** | **201,36** | **252,81** |
| **NLB** | **2010** | **2015** | **2020** | **2025** | **2030** | **2035** | **2040** |
| Households | | 5,97 | 7,46 | 8,94 | 10,34 | 12,05 | 13,72 |
| Industry | | 9,07 | 10,43 | 11,98 | 13,9 | 16,33 | 19,4 |
| Transportation | | 18,53 | 19,25 | 21,96 | 25,05 | 28,73 | 33,09 |
| Tertiary | | 0,39 | 0,45 | 0,52 | 0,6 | 0,69 | 0,8 |
| Agriculture and fisheries | | 4,51 | 4,7 | 5,21 | 5,78 | 6,45 | 7,24 |
| Processing | | 24,8 | 34,04 | 42,04 | 46,86 | 52,56 | 58,41 |
| Non-energy Industrial processes | | 6,66 | 7,03 | 7,46 | 8 | 8,69 | 9,61 |
| Non-energy Agriculture | | 20,97 | 21,91 | 22,73 | 23,55 | 24,37 | 25,2 |
| No energy Forestry | | 0,01 | 0,01 | 0,01 | 0,01 | 0,01 | 0,01 |
| No energy waste | | 7,91 | 9,98 | 12,14 | 14,44 | 15,23 | 16,04 |
| No energy HCFCs and HFCs | | 0,94 | 0,93 | 0,92 | 0,9 | 0,9 | 0,89 |
| **Total** | | **99,76** | **116,19** | **133,91** | **149,43** | **166,01** | **184,41** |
| **CDN** | **2010** | **2015** | **2020** | **2025** | **2030** | **2035** | **2040** |
| **Total** | | **100,96** | **103,9** | **117,34** | **130,78** | | |
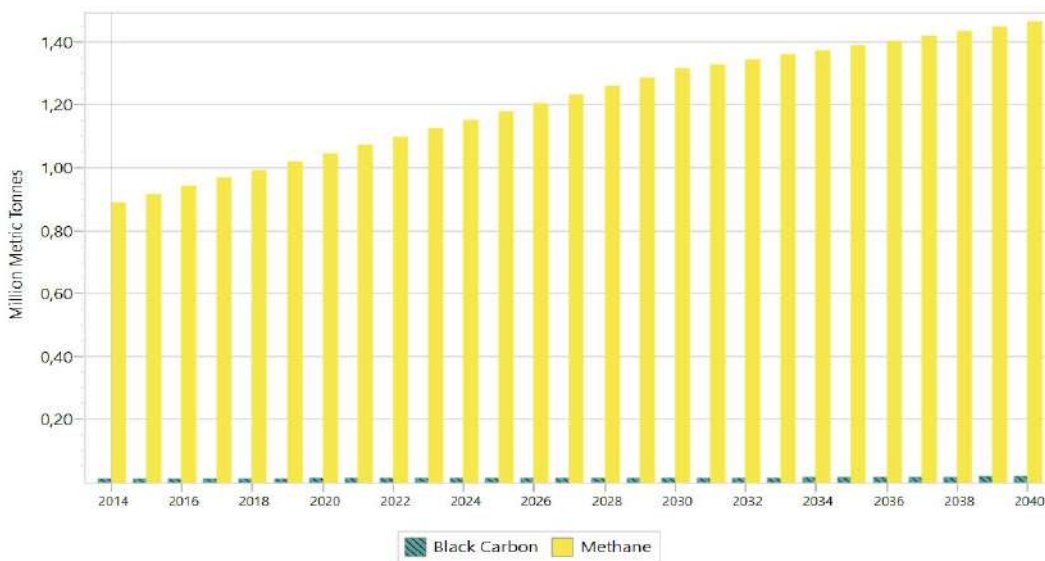
Fig. 8: Global SLCP emissions.
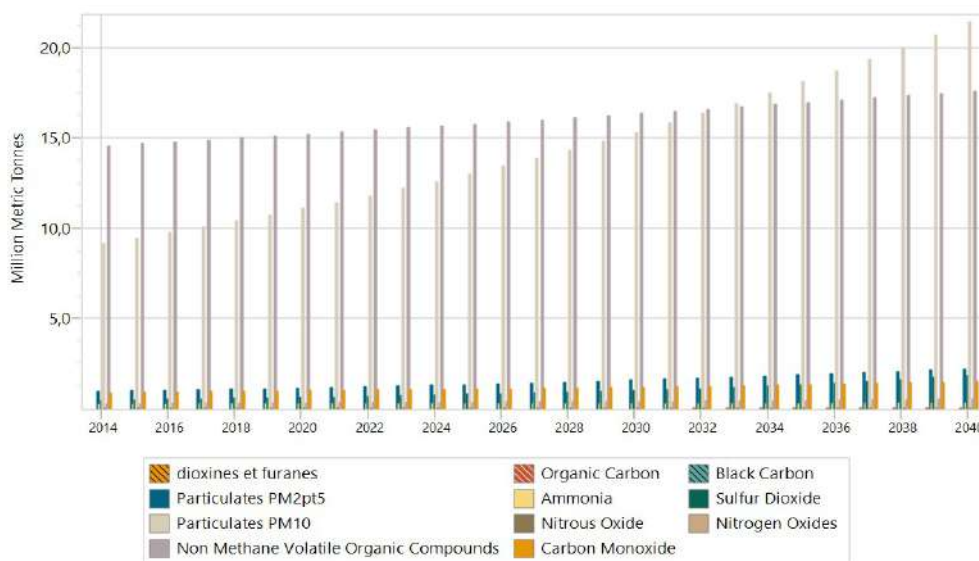


Fig. 9: Global air pollutant emissions.

by 17% by 2030 from 2010 levels in accordance with the Paris Agreement on Climate Change. To achieve this goal, the Moroccan government has implemented several policies, including the National Energy Strategy, which aims to increase the share of renewable energy in electricity generation and promote energy efficiency in all economic sectors. Morocco must continue to implement effective policies and measures to reduce GHG emissions and improve air quality. This requires international cooperation to facilitate technology and knowledge transfer, as well as financial investments to support sustainable development initiatives. By meeting its GHG emission reduction targets, Morocco can contribute to the global fight against climate change while improving the quality of life of its population.

## REFERENCES

Al Wachami, N., Louerdi, M., Iderdar, Y., Boumendil, K. and Chahboune, M. 2023. Chronic obstructive pulmonary disease (COPD) and air pollution: The case of Morocco. Mater. Today Proceed., 72: 3738-3748. https://doi.org/10.1016/j.matpr.2022.09.249

Boulakhbar, M., Lebrouhi, B., Kousksou, T., Smouh, S., Jamil, A., Maaroufi, M. and Zazi, M. 2020. Towards a large-scale integration of renewable energies in Morocco. J. Energy Storage, 32: 101806. https://doi.org/10.1016/j.est.2020.101806

Dettner, F. and Blohm, M. 2021. External cost of air pollution from energy generation in Morocco. Renew. Sustain. Energy Trans., 1: 100002. https://doi.org/10.1016/j.rset.2021.100002

Duan, H., Hou, C., Yang, W. and Song, J. 2022. Towards lower CO2 emissions in iron and steel production: Life cycle energy demand-LEAP based multi-stage and multi-technique simulation. Sustain. Prod. Consump., 32: 270-281. https://doi.org/10.1016/j.spc.2022.04.028

Gebremeskel, D.H., Ahlgren, E.O. and Beyene, G.B. 2023. Long-term electricity supply modeling in the context of developing countries: The OSeMOSYS-LEAP soft-linking approach for Ethiopia. Energy Strat. Rev., 45: 101045. https://doi.org/10.1016/j.esr.2022.101045

Kasseh, Y., Touzani, A. and Majaty, S. 2023. Exemplarity of the state for the energy efficiency of buildings institutional: A case of Morocco. Nat. Environ. Pollut. Technol., 22(1): 169-177. https://doi.org/10.46488/NEPT.2023.v22i01.015

Liya, C. and Jianfeng, G. 2018. Scenario analysis of $CO_2$ emission abatement effect based on LEAP. Energy Proced., 152: 965-970. https://doi.org/10.1016/j.egypro.2018.09.101

Ministry of Energy and Mines-Kingdom of Morocco 2020. National Energy Efficiency Strategy Horizon 2030.

Saidi, L., Valari, M. and Ouarzazi, J. 2023. Air quality modeling in the city of Marrakech, Morocco, using a local anthropogenic emission inventory. Atmos. Environ., 293: 119445. https://doi.org/10.1016/j.atmosenv.2022.119445

Sun, X., Wang, P., Ferris, T., Lin, H., Dreyfus, G., Gu, B.H., Zaelke, D. and Wang, Y. 2022. Fast action on short-lived climate pollutants and nature-based solutions to help countries meet carbon neutrality goals. Adv. Clim. Change Res., 13(4): 564-577. https://doi.org/10.1016/j.accre.2022.06.003

## ORCID DETAILS OF THE AUTHORS

Y. Kasseh: https://orcid.org/0000-0001-7776-5034
A. Touzani: https://orcid.org/0000-0002-5987-455X
S. El: https://orcid.org/0000-0002-4408-4969

# Reducing the Carbon Footprint of Clinical Trials: Implementing Sustainable Practices in Clinical Research

**Aditi Nidhi†**

Gujarat National Law University, Gandhinagar, Gujarat, India

†Corresponding author: Aditi Nidhi; aditinidhirmlnlu@gmail.com

## ABSTRACT

Sustainable clinical trials involve conducting trials in a socially conscious and environmentally responsible manner. This involves considering the effects of clinical trials on the environment and the populations engaged in the studies. The pharmaceutical sector, particularly clinical research, is a large contributor to greenhouse gas emissions. The need for a legal framework considering the environmental impact of hundreds of global clinical trials cannot be overstated. Clinical trials' carbon footprint is a complex subject that calls for cooperation from various parties, including researchers, trial sponsors, healthcare providers, and regulatory organizations. The waste generated during clinical trials, including packaging materials, laboratory supplies, and hazardous waste from the disposal of clinical samples, can adversely affect public health and the environment. Therefore, addressing this issue is essential to ensure that clinical trials are conducted in an environmentally and socially responsible manner. The purpose of this study is to discuss potential strategies to cut down on carbon emissions, discuss the challenges in setting up clinical trials in an environmentally sustainable way, and highlight the importance of a precautionary approach during the various phases of conducting clinical trials. Although there is limited research on greenhouse gas emissions generated by clinical trials, it is evident that more work needs to be done in this field.

## INTRODUCTION

Clinical trials are an essential component of medical research because they provide evidence that can be used to support the development of novel medicines and treatments to improve healthcare quality (Subbiah 2023). However, conducting clinical trials has significant environmental implications, as they generate substantial amounts of waste and carbon emissions. Although the healthcare sector is vital for saving lives, it has a significant ecological footprint (Lenzen et al. 2020). As a result of climate change, it is imperative to reduce carbon emissions and waste generation. It is essential to explore how clinical trials impact the environment and develop solutions to mitigate their environmental impact while continuing to advance medical research (Clark et al. 2019).

It has been established for quite some time that social, biological, and environmental factors can affect or cause diseases, and numerous clinical trials have been conducted to ascertain the impact of environmental factors on a range of outcomes (Manisalidis et al. 2020). Among other topics, these trials investigated the effect of environmental factors on drug efficacy in treating dry-eye syndrome, the relationship between diet and obesity and cardiovascular disease, and the environmental impact on autoimmune diseases (Fugger et al. 2020). Despite the fact that the healthcare business has prevented the loss of millions of lives, it has had a substantial influence on the environment as a result of its operations (Clarke 2014).

The healthcare sector ranks among the most carbon-intensive industries in the developed world, contributing between 4.4 and 4.6 percent of global greenhouse gas emissions and a comparable amount of harmful air pollutants (Parkins 2022). Healthcare must undergo sustainability revamp, including clinical trials, to reach the target of net-zero carbon emissions by 2030 (Singh et al. 2022). In terms of carbon emissions, a recent study found that over 350,000 national and worldwide clinical trials produce 27.5 million tonnes of greenhouse gas emissions (Cuffari 2021). The Declaration of Helsinki calls for research processes to minimize harm to the environment (Halonen et al. 2021). Still, clinical trials have a negative environmental impact due to greenhouse gas emissions from shipping and transport, as well as waste production, which is an underexplored contributor to greenhouse gas emissions (WHO 2005).

Hence, the healthcare industry must address its environmental impact and take a sustainable approach to clinical trials, which are essential for advancing medical research. By reducing carbon emissions and waste production in clinical trials, we can minimize the environmental impact of healthcare while improving public health outcomes. Thus, this paper will examine the environmental impact of clinical trials, including their carbon footprint and waste production, and propose strategies to promote sustainable clinical trials.

## ENVIRONMENTAL IMPACT OF CLINICAL TRIALS

Clinical trials are vital for the development of novel pharmaceuticals and medical treatments, thereby contributing to the improvement of global health and well-being (Inan et al. 2020). However, the conduct of clinical trials can also have environmental impacts that need to be carefully considered and addressed.

The environmental impacts of clinical trials can be direct or indirect (Selby 2011). Direct environmental impacts may include energy and water consumption, hazardous waste generation, air and noise pollution, and land use change (Drew et al. 2022). These impacts can be associated with the construction and operation of clinical trial facilities and the transportation of participants, staff, and equipment. Indirect environmental impacts (WHO 2021) may include the production and transportation of pharmaceuticals and medical devices, as well as impacts on local communities, global health, and animal welfare.

Given the potential negative environmental impacts of clinical trials, it is important for researchers and sponsors to incorporate sustainable practices into clinical trial design and implementation (Alemayehu et al. 2018). This can include strategies such as reducing energy and water consumption, minimizing waste generation, using renewable energy sources, and engaging with local communities to address concerns related to the trial (Edenhofer et al. 2011). By considering the environmental impacts of clinical trials and taking steps to mitigate these impacts, researchers and sponsors can help to ensure that the development of new medical treatments is consistent with environmental sustainability.

Clinical trials can have various environmental impacts, including:

a) Resource consumption: Clinical trials require significant resources such as energy, water, and materials for equipment and supplies, which can contribute to environmental degradation (Rajadhyaksha 2010).

b) Waste generation: Clinical trials generate large amounts of waste, including hazardous waste such as chemicals and biological materials. The disposal of this waste has the potential to have an adverse effect on the surrounding ecosystem.

c) Transportation: Clinical trials often involve the transportation of study participants, clinical staff, and equipment, which can contribute to air pollution and greenhouse gas emissions (Rissman et al. 2020).

d) Land use: Clinical trials may require the use of land for study sites, which can result in habitat destruction, deforestation, or other forms of land use change (OECD 2019).

e) Animal testing: Some clinical trials involve animal testing, which can have ethical implications and contribute to animal welfare concerns.

f) Energy consumption: Clinical trials require the use of energy for powering equipment, heating and cooling facilities, and lighting (De Franco et al. 2017). The energy consumed during clinical trials can contribute to greenhouse gas emissions and other pollutants.

g) Air pollution: The transportation of study participants, clinical staff, and equipment can contribute to air pollution and greenhouse gas emissions. Some medical procedures may also generate air pollutants, such as anesthetic gases.

h) Noise pollution: Clinical trials may generate noise from equipment and machinery used in medical procedures, which can harm the health of humans and wildlife (Belay et al. 2021).

i) Use of non-renewable resources: Clinical trials may require using non-renewable resources, such as fossil fuels, for transportation and electricity generation (Avtar et al. 2019). This can contribute to climate change and other environmental problems associated with the extraction and use of non-renewable resources.

j) Soil contamination: Clinical trials involving hazardous chemicals or biological agents can lead to soil contamination if these substances are not properly disposed of (Ashraf et al. 2014). This can have negative impacts on soil quality and ecosystem health.

k) Landfill waste: Clinical trials may generate large amounts of non-hazardous waste, such as packaging materials and single-use medical supplies, that end up in landfills (Padmanabhan & Barik 2019). This can contribute to the environmental problems associated with landfill waste, such as greenhouse gas emissions and contamination of soil and water.

The magnitude of these direct effects on the environment is highly variable. It is determined by several factors,

including the size and scope of the clinical trial, the location of the study site, and the sort of medical procedures and equipment utilized (Manisalidis et al. 2020). However, by implementing sustainable practices and considering the environmental impacts of their work, researchers and sponsors can help minimize the negative effects of clinical trials on the environment.

Clinical trials may also have indirect environmental impacts, such as the effects of producing and transporting pharmaceuticals or medical devices used in the trials (Boxall 2004). The manufacturing process of these products may require significant amounts of energy, water, and raw materials and may generate greenhouse gas emissions and other pollutants. In addition to this, after the completion of clinical trials, the disposal of unused or expired medicines and medical devices can also have an effect on the surrounding environment (Smale et al. 2021). These products may end up in landfills, where they can leach chemicals and other harmful substances into the soil and water (Salam & Nilza 2021). The indirect environmental impacts of clinical trials may include:

a) Manufacturing and shipping of drugs and medical devices: Significant environmental impacts can be caused by the manufacturing and distribution of drugs and medical devices utilized in clinical trials (Gaw et al. 2014). The production of these items may demand substantial amounts of energy and raw materials and emit greenhouse gases and other pollutants.

b) Impact on local communities: Clinical trials may impact the quality of life of local communities by increasing traffic and noise levels, affecting access to natural resources, and altering the local landscape (Halperin 2014). This can have indirect environmental impacts, such as biodiversity or air quality changes.

c) Impact on global health: The results of clinical trials can have significant impacts on global health, including the treatment and prevention of diseases that may have environmental causes, such as air pollution-related illnesses (Turner et al. 2020). By improving human health, clinical trials can indirectly contribute to environmental sustainability by reducing disease burden and improving quality of life.

d) Use of animal models: Some clinical trials involve the use of animals, which can have indirect environmental impacts related to animal welfare and ethical concerns (Soulsbury et al. 2020). This includes using animal models to study environmental health effects, such as pollution exposure or other environmental stressors.

e) Impact on healthcare systems: The results of clinical trials can impact healthcare systems and healthcare policy, which in turn can affect the environmental sustainability of healthcare (Samuel & Lucassen 2022). For example, developing new medical treatments may increase demand for medical resources and energy use.

Overall, the indirect environmental impacts of clinical trials can be complex and multifaceted. By considering the full range of environmental impacts associated with clinical research, researchers and sponsors can take steps to minimize their negative effects and promote sustainable practices in developing new medical treatments. This includes considering the lifecycle impacts of pharmaceuticals and medical devices, engaging with local communities, and exploring alternative research methods.

Thus, clinical trials can have significant environmental impacts throughout their lifecycle, from developing and manufacturing study drugs to disposing of hazardous waste generated during the study. The main areas of concern include using resources such as water and energy, generating waste and emissions, and impacting ecosystems and biodiversity (Subbiah 2023). To reduce the environmental impact of clinical trials, researchers can implement measures such as using eco-friendly materials and manufacturing processes, reducing waste generation and energy consumption, and selecting study sites with minimal impact on local ecosystems. Collaboration between stakeholders such as pharmaceutical companies, regulators, and research institutions can also help promote sustainable clinical trial practices (Dănescu & Popa 2020). Hence, it is important to consider the environmental impact of clinical trials alongside their scientific and ethical considerations and to strive for more sustainable and responsible practices in clinical research.

## CARBON FOOTPRINTS OF CLINICAL TRIALS

The carbon footprint is the total amount of greenhouse gases (GHGs) emitted by human activities like transportation, energy generation, and manufacturing. Clinical trials are a vital component of the process of developing new medicines, and they are also a contributor to the emissions of greenhouse gases (Tennison et al. 2021). The production and transportation of study medications, medical equipment, and supplies, travel of study employees, and energy usage in clinical trial facilities are all examples of activities that contribute to the emission of greenhouse gases (GHGs) during clinical trials. All of these activities have a substantial effect on the carbon footprint of clinical trials.

The carbon footprint of clinical trials has become a growing concern in recent years, as the pharmaceutical industry is one of the major contributors to GHG emissions (Belkhir & Elmeligi 2019). Pharmaceutical companies are

now recognizing the importance of reducing the carbon footprint of clinical trials to reduce their environmental impact and meet sustainability goals. The use of electric vehicles and public transportation, as well as a reduction in air travel and the increased use of remote monitoring equipment, are all part of this effort to lessen the environmental impact of clinical trials (Holmner et al. 2014). In addition, pharmaceutical companies are also exploring the use of sustainable materials in clinical trial supplies, as well as improving energy efficiency in clinical trial facilities. These initiatives not only help to cut emissions of greenhouse gases (GHG), but they also lead to cost savings and an improvement in public health.

Clinical trials are an essential step in the development of new drugs and treatments. They help ensure the safety and efficacy of these products before they are released to the public. However, clinical trials can also have a significant carbon footprint, which can have a negative impact on the environment.

A study by researchers at the University of California, San Francisco, looked at the carbon footprint of a Phase III clinical trial for a cancer drug (Lazar et al. 2018). The trial involved 200 patients from 20 different countries, and the researchers estimated that the trial generated approximately 15,000 metric tons of carbon dioxide equivalents ($CO_2e$) over a period of three years. Another case study on carbon footprints of clinical trials is the IMPACT (Intensive Management of Patients with Advanced Chronic Kidney Disease) trial, conducted in the United Kingdom (Sanchez et al. 2021). The trial aimed to evaluate the effectiveness of a new treatment approach for patients with advanced chronic kidney disease. The trial involved 2,746 patients from 57 different hospitals across the UK and lasted five years. An analysis of the trial's carbon footprint showed that it generated approximately 4,500 metric tons of $CO_2e$.

The largest contributor to the trial's carbon footprint was patient travel to and from study visits, which accounted for approximately 80% of the total emissions. Other significant sources of emissions included the production and transportation of study drugs, as well as the energy and resources required to manage and analyze the trial data. To reduce the trial's carbon footprint, the researchers implemented several strategies, including:

a) Using telemedicine and other remote technologies to reduce the need for patient travel.

b) Encouraging patients to use low-carbon modes of transportation, such as public transport or carpooling.

c) Using digital tools to collect and manage study data reduces the need for paper-based records and data transportation.

d) Encouraging hospitals and study sites to implement sustainable practices, such as using renewable energy and minimizing waste.

e) The trial reduced its carbon footprint by approximately 30% by implementing these strategies.

The IMPACT trial is an example of how clinical trials can take steps to reduce their carbon footprint, even when involving a large number of patients and sites. The strategies employed in the trial demonstrate that it is possible to prioritize sustainability without compromising the quality and integrity of the trial data. The total amount of greenhouse gas emissions produced during the lifetime of a clinical trial is referred to as its "carbon footprint." These emissions come from various sources, including the production and transportation of trial materials, the consumption of energy in clinical facilities, and the travel of study participants and staff.

Some case studies from around the world have explored the carbon footprint of clinical trials: The UK Clinical Research Collaboration (UKCRC) conducted a study in 2009 to estimate the carbon footprint of clinical trials in the UK. The study found that clinical trials accounted for approximately 2.5% of the National Health Service's (NHS) carbon footprint. In 2015, researchers at the University of California, San Francisco (UCSF) conducted a case study of a clinical trial for prostate cancer. They found that the trial's carbon footprint was primarily due to participant travel, accounting for 59% of its total emissions. A study conducted in 2017 by researchers at the University of Sydney in Australia found that clinical trials for a new drug to treat hepatitis C had a significant carbon footprint, primarily due to the production and transportation of the drug. In 2018, researchers at the University of Edinburgh in Scotland studied the carbon footprint of clinical trials for five different diseases, including diabetes and heart disease. They found that the carbon footprint varied widely depending on the disease and the trial's design. A 2020 study by researchers at the University of Copenhagen in Denmark estimated the carbon footprint of a phase 3 clinical trial for a new cancer drug. They found that the trial's carbon footprint was primarily due to energy use in clinical facilities and the manufacture and transportation of trial materials. These case studies illustrate that the issue of clinical trials' carbon footprint is a complicated one that varies considerably depending on the trial's design, the trial, the location of the trial, and the ailment being examined. However, they also state that there are chances to lessen the carbon footprint of clinical trials by implementing more environmentally friendly routines, like remote monitoring, virtual participant recruitment, and using renewable energy sources in clinical facilities.

Lowering clinical trials' carbon impact is a significant step toward sustainability and ethical corporate citizenship. As the demand for more sustainable practices continues to grow, clinical trial sponsors will likely increasingly incorporate sustainability criteria into study design and implementation.

## CLIMATE CHANGE: A HEALTHCARE CHALLENGE

The emissions caused by the healthcare industry account for around 4 to 5 percent of the total emissions made worldwide (Prater 2019), making it the equivalent of the fifth most polluting country in the world behind Russia, India, USA, and China (Evans 2022). Health systems are being tested as they try to keep up with the growing demand for treatment in the face of demographic shifts like an aging population, an increase in chronic non-communicable diseases, and fast urbanization (Jarzebski et al. 2021). All stakeholders must work together to reduce emissions while enhancing health outcomes to reach net zero, including regulatory organizations, legislators, governments, manufacturers, health authorities, and payers.

To successfully decarbonize intricate healthcare systems, cutting emissions at every level of the value chain will be necessary, including research and development, the supply chain, and patient care. While most healthcare sector emissions are created in the upstream supply chain and patient care settings, trial emissions represent up to 100 million tons of $CO_2$e per year, equivalent to a midsize country like Belgium (Fig. 1).

## POSSIBLE SOLUTIONS TO REDUCE CARBON EMISSIONS

Digital solutions play an increasingly important role throughout the healthcare value chain in driving efficiencies, delivering superior patient outcomes, and reducing costs and emissions (Mondejar et al. 2021) (Fig. 2).

Digital solutions are a key enabler to reduce emissions related to clinical research. Because trials touch upon many aspects of the broader health system (including healthcare facilities, staff and patient travel, drug manufacturing, and delivery), examining how digitalization reduces emissions in
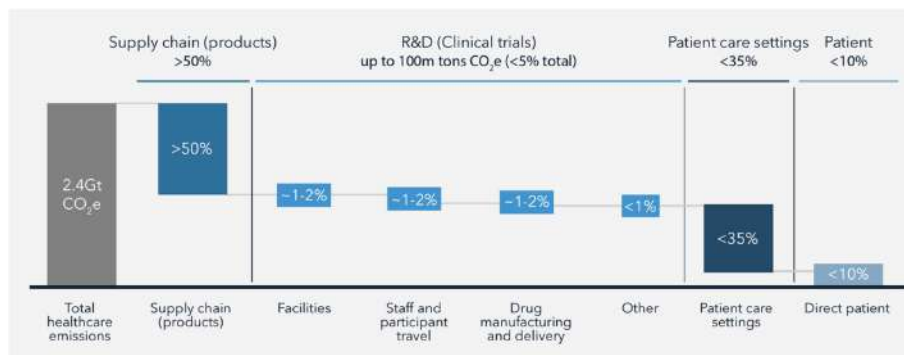


Source: Sustainable Market Initiative 2022

Fig. 1: Clinical trials drive up to ~100 million tons of $CO_2$e emissions per year.



Note: AI: artificial intelligence; RWE: real-world evidence; Source: Sustainable Market Initiative 2022

Fig. 2: Digital solutions can be used all along the healthcare value chain.

clinical trials provides a good proxy for the benefits of digital in the broader healthcare system. Digitalization refers to using digital technologies to improve the efficiency, effectiveness, and sustainability of various processes, including clinical research. By embracing digitalization, researchers can reduce their reliance on paper-based processes, physical meetings, and travel, all contributing to the carbon emissions associated with clinical research.

For example, electronic data capture (EDC) allows researchers to collect data electronically, reducing the need for paper forms and reducing the carbon footprint associated with paper production and transportation (Mishra 2022). Similarly, virtual clinical trials and remote monitoring allow researchers to conduct studies without requiring participants to travel to clinical trial sites, reducing the carbon emissions associated with transportation.

Cloud computing and electronic communications can also significantly reduce the carbon footprint of clinical research. Cloud computing allows researchers to store and share data without requiring physical servers, which consume much energy. Electronic communications, such as email, video conferencing, and instant messaging, can replace in-person meetings and reduce the carbon emissions associated with travel.

Hence, digitalization has the potential to significantly reduce the carbon footprint of clinical research while still ensuring high-quality studies. By embracing digital technologies, researchers can make clinical research more sustainable and environmentally friendly, helping protect the planet for future generations.

## BARRIERS TO DIGITALIZING CLINICAL TRIALS

While COVID-19 accelerated digitalization across clinical trials by limiting options for on-site travel and creating a high unmet need for COVID-19 treatments (Vara 2022), further efforts can be made across four key areas to increase the scale of digital solutions deployed for emissions benefits in clinical trials (Fig. 3).

1. **Regulatory Hurdles**

    In recent years, there have been significant advances in regulatory framework, driven by the COVID-19 pandemic, that have made it possible for clinical trials to make increasing use of digital technology.

    - For example, The US Food and Drug Administration (FDA) has a specific regulatory process to address the use of digital biomarkers (and their components) and is currently piloting a program that further streamlines product-level approvals (Coravos et al. 2019). Meanwhile, the European Medicines Agency (EMA) has a set of qualification criteria companies must follow to use a digital biomarker in a trial (Human Medicines Division 2020).

    - The FDA's 2021 draft guidance details requirements for remote data acquisition from patients in clinical trials, enabling decentralization (CDER 2021).

    - The Digital Health Centre of Excellence at the FDA also offers advice on Software as a Precertification of Digital Health Software, Wireless Medical Devices, Mobile Medical Applications, and Medical Devices (Lievevrouw et al. 2021).



Source: Sustainable Market Initiative 2022

Fig. 3: Four areas where further work is required to scale digital solutions in clinical trials.

- The FDA and EMA published guidelines for good clinical practice that enable greater use of risk-based monitoring principles, paving the way for more remote clinical trial data monitoring. The FDA has also confirmed that sponsors switched to remote monitoring during the pandemic do not need to re-monitor on-site.

- Despite these developments, further guidance and acceptance from regulators are still required for digital solutions to be used widely in clinical trials and drive emissions benefits:

**Requirements for digital tools are still evolving**: Experts are still debating topics such as using patient-relevant endpoints (in place of clinical outcomes) to indicate efficacy and identify patients that can be included in synthetic control arms. The FDA and EMA do not have official guidance on using digital twins and synthetic control arms in trials. However, the FDA has issued an RWE framework, and the EMA has recently issued a draft qualification on a statistical method (Prognostic Covariate Adjustment) that supports the use of synthetic control arms (Detela et al. 2022).

**Guidance on digital tools in clinical trials varies across geographies, limiting the ability of sponsors to implement global approaches**: Where clinical trials are intended to produce globally representative results, different regulator guidance on digital tools across geographies can be inefficient for sponsors of multicenter trials. For instance, the European Medicines Agency's (EMA) guidance on electronic consent (eConsent) makes conducting cross-broader trials with digital solutions difficult because it requires the sponsor to clarify legality and compliance with each country's ethics committees and national regulatory authorities (Minisman et al. 2012).

2. **Lack of Interoperability Between Digital Solutions**

To reap the benefits of digital solutions, they must work seamlessly together (Kerber & Schweitzer 2017). However, digital tools remain complex to set up and are not always interoperable – with data often captured in nonstandard formats using local codes. This increases the difficulty for trial managers and negatively impacts patient user experience. Furthermore, it may include errors that bias assessments, especially when working with the large 19 Sustainable Markets Initiative Health Systems Task Force, in collaboration with BCG, November 2022 data sets, which erodes trust in digital health solutions (Sustainable Markets Initiatives 2020). Although interoperability does not reduce trial emissions, it facilitates adopting and accepting digital solutions that enable emissions savings.

3. **Ingrained Culture, Behavior and Beliefs**

All those involved in trials—trial sponsors, providers, technology platform providers, CROs, and patients—must learn how to work with new digital systems and devices. Major stumbling blocks in realizing the benefits of these new digital tools include a reluctance to change behaviors and embed digital tools in running clinical trials, concerns about data privacy and security, a lack of access to technology, and insufficient technical literacy (Rosa et al. 2021).

4. **Cost and Range of Digital Solutions**

Although digital solutions are expected to drive down the cost of clinical trials, technology remains expensive (particularly the initial investment). With so many options, many providers are unsure which to invest in (DiMasi et al. 2022). A survey of 231 clinical trial sites finds that cost, complexity, and the right technology are the key challenges associated with digital adoption (Rosa et al. 2015).

## CONCLUSION

In conclusion, clinical trials can have positive and negative consequences on the surrounding ecosystem. It is essential to find a middle ground between medical research's possible benefits and potential costs to the surrounding environment. Researchers and sponsors of clinical trials should consider ways to minimize the environmental impact of their trials by reducing resource use, waste generation, and greenhouse gas emissions. Additionally, they can explore alternative methods to animal testing and promote sustainable practices in clinical trial design and implementation. By doing so, we can ensure that clinical trials continue to advance human health while promoting environmental sustainability for the benefit of current and future generations. In addition to the aforementioned measures, there are additional strategies to minimize the environmental impact of clinical studies. One way is to incorporate sustainability considerations into the study design and protocol development process. For example, researchers can use eco-friendly materials and equipment, choose study locations that minimize transportation and energy use, and use electronic data capture systems to reduce paper usage. Another approach is to use virtual clinical trials, which rely on remote data collection and monitoring, reducing the need for in-person visits and travel. This approach can help minimize the environmental impact of clinical trials while making them more accessible to participants who may have difficulty traveling to a study site.

Lastly, regulatory and policy measures can encourage sustainability in clinical trials. For example, funding agencies and regulatory bodies can require environmental impact assessments to approve the study. They can also incentivize researchers and sponsors who implement sustainable practices in their clinical trials. In conclusion, there are many strategies for lessening the negative effects of clinical trials on the surrounding ecosystem, and sustainability should be factored into every step of the scientific method. By doing so, we can advance medical research while minimizing our impact on the environment and promoting a healthier planet for all.

## REFERENCES

Alemayehu, C., Mitchell, G. and Nikles, J. 2018. Barriers for conducting clinical trials in developing countries - a systematic review. Int. J. Equity Health, 17: 37. https://doi.org/10.1186/s12939-018-0748-6

Ashraf, M., Maah, M.J. and Yusoff, I. 2014. Soil contamination, risk assessment, and remediation. Intech eBooks. https://doi.org/10.5772/57287

Avtar, R., Sahu, A., Chakraborty, K., Yunus, D. and Kurniawan, S. 2019. Exploring renewable energy resources using remote sensing and GIS - A review. Resources, 8(3): 149. https://doi.org/10.3390/resources8030149

Belay, S., Giday, M. and Manyazewal, T. 2021. Harnessing clinical trial capacity to mitigate zoonotic diseases: The role of expert scientists in Ethiopia. Front. Public Health, 9: 621433. https://doi.org/10.3389/fpubh.2021.621433

Belkhir, L. and Elmeligi, A. 2019. Carbon footprint of the global pharmaceutical industry and relative impact of its major players. J. Clean Prod., 214: 185-194. https://doi.org/10.1016/j.jclepro.2018.11.204

Boxall, ABA 2004. The environmental side effects of medication. EMBO Rep., 5(12): 1110-1116. https://doi.org/10.1038/sj.embor.7400307

CDER 2021. United States Department of Health and Human Services, Food and Drug Administration, Center for Drug Evaluation and Research. Digital health technologies for remote data acquisition in clinical investigations. https://www.govinfo.gov/content/pkg/FR-2021-12-23/pdf/2021-27894.pdf (Accessed March 10, 2023)

Clark, L.T., Watkins, L., Piña, I.L., Elmer, M., Akinboboye, O., Gorham, M., Jamerson, B., McCullough, C., Pierre, C., Polis, A.B., Puckrein, G. and Regnante, J.M. 2019. Increasing diversity in clinical trials: Overcoming critical barriers. Curr. Probl. Cardiol., 44(5): 148-172. https://doi.org/10.1016/j.cpcardiol.2018.11.002

Clarke, R.A. 2014. The Challenge of Going Green. Harvard Business Review. Retrieved from https://hbr.org/1994/07/the-challenge-of-going-green (Accessed March 9, 2023)

Coravos, A., Khozin, S. and Mandl, K.D. 2019. Developing and adopting safe and effective digital biomarkers to improve patient outcomes. Digit. Med., 2(1): https://doi.org/10.1038/s41746-019-0090-4

Cuffari, B. 2021. The carbon footprint of clinical trials. News-Medical. https://www.news-medical.net/health/The-Carbon-Footprint-of-Clinical-Trials.aspx (Accessed March 19, 2023)

Dănescu, T. and Popa, M.A. 2020. Public health and corporate social responsibility: Exploratory study on pharmaceutical companies in an emerging market. Glob. Health, 16(1): 117. https://doi.org/10.1186/s12992-020-00646-4

De Franco, A., Shaker, M., Kalubi, D. and Hostettler, S. 2017. A review of sustainable energy access and technologies for healthcare facilities in the Global South. Sustain. Energy Technol. Assess., 22: 92–105. https://doi.org/10.1016/j.seta.2017.02.022

Detela, G., Inacio, P., Saragoussi, D. and Schaumberg, D. 2022. Registries for Regulatory Decision-Making: Comparing EMA and FDA Guidance on Real-World Evidence Insights Hub. https://www.ppd.com/blog/comparing-ema-fda-real-world-evidence-guidance/ (Accessed March 10, 2023).

DiMasi, J.A., Smith, Z., Oakley-Girvan, I., Mackinnon, A., Costello, M., Tenaerts, P. and Getz, K.A. 2023. Assessing the financial value of decentralized clinical trials. Ther. Innov. Regul. Sci., 57(2): 209–219. https://doi.org/10.1007/s43441-022-00454-5

Drew, J., Christie, S.D., Rainham, D. and Rizan, C. 2022. HealthcareLCA: An open-access living database of healthcare environmental impact assessments. Lancet Planet. Health, 6(12): e1000–e1012. https://doi.org/10.1016/S2542-5196(22)00257-1

Edenhofer, O., Pichs-Madruga, R., Sokona, Y., Seyboth, K., Kadner, S., Zwickel, T., Eickemeier, P., Hansen, G., Schlömer, S., von Stechow, C. and Matschoss, P. (eds.) 2011. Renewable energy sources and climate change mitigation: Special report of the intergovernmental panel on climate change. Cambridge University Press.

European Medicines Agency 2020. Questions and answers: qualification of digital technology‑based methodologies to support approval of medicinal products.

Evans, S. 2022. Analysis: which countries are historically responsible for climate change? https://www.carbonbrief.org/analysis-which-countries-are-historically-responsible-for-climate-change/ (Accessed March 29, 2023).

Fugger, L., Jensen, L.T. and Rossjohn, J. 2020. Challenges, progress, and prospects of developing therapies to treat autoimmune diseases. Cell, 181(1): 63-80. https://doi.org/10.1016/j.cell.2020.03.007

Gaw, S., Thomas, K.V. and Hutchinson, T.H. 2014. Sources, impacts, and trends of pharmaceuticals in the marine and coastal environment. Philos. Trans. R. Soc. Lond. B Biol. Sci., 369(1656): 20130572. https://doi.org/10.1098/rstb.2013.0572

Halonen, J.I., Erhola, M., Furman, E., Haahtela, T., Jousilahti, P., Barouki, R., Bergman, Å., Billo, N.E., Fuller, R., Haines, A., Kogevinas, M., Kolossa-Gehring, M., Krauze, K., Lanki, T., Vicente, J.L., Messerli, P., Nieuwenhuijsen, M., Paloniemi, R., Peters, A. and Antó, J.M. 2021. A call for urgent action to safeguard our planet and health in line with the Helsinki Declaration. Environ. Res., 193: 110600. https://doi.org/10.1016/j.envres.2020.110600

Halperin, D. 2014. Environmental noise and sleep disturbances: A threat to health? Sleep Sci., 7(4): 209-212. https://doi.org/10.1016/j.slsci.2014.11.003

Hirsch, I.B., Martinez, J., Dorsey, E.R., Finken, G., Fleming, A., Gropp, C., Home, P., Kaufer, D.I. and Papapetropoulos, S. 2017. Incorporating site-less clinical trials into drug development: A framework for action. Clin. Ther., 39(5): 1064-1076. https://doi.org/10.1016/j.clinthera.2017.03.018

Holmner, A., Ebi, K.L., Lazuardi, L. and Nilsson, M. 2014. The carbon footprint of telemedicine solutions – Unexplored opportunity for reducing carbon emissions in the health sector. PLoS ONE, 9(9): e105040. https://doi.org/10.1371/journal.pone.0105040

Inan, O.T., Tenaerts, P., Prindiville, S.A., Reynolds, H.R., Dizon, D.S., Cooper-Arnold, K., Turakhia, M., Pletcher, M.J., Preston, K.L., Krumholz, H.M., Marlin, B.M., Mandl, K.D., Klasnja, P., Spring, B., Iturriaga, E., Campo, R., Desvigne-Nickens, P., Rosenberg, Y., Steinhubl, S.R. and Califf, R.M. 2020. Digitizing clinical trials. Digit. Med., 3(1): 101. https://doi.org/10.1038/s41746-020-0302-y

Jarzebski, M.P., Elmqvist, T., Gasparatos, A., Fukushi, K., Eckersten, S., Haase, D., Goodness, J., Khoshkar, S., Saito, O., Takeuchi, K., Theorell, T., Dong, N., Kasuga, F., Watanabe, R., Sioen, G.B., Yokohari, M. and Pu, J. 2021. Aging and population shrinking: Implications for sustainability in the urban century. Npj Urban Sustain., 1(1): https://doi.org/10.1038/s42949-021-00023-z

Kerber, W. and Schweitzer, H. 2017. Interoperability in the digital economy. SSRN Electron. J. https://doi.org/10.2139/ssrn.2922515

Lazar, A.A., Schulte, R., Faddegon, B., Blakely, E.A. and Roach, M. 2018. Clinical trials involving carbon‑ion radiation therapy and the path forward. Cancer, 124(23): 4467-4476. https://doi.org/10.1002/cncr.31662

Lenzen, M., Malik, A., Li, M., Fry, J., Weisz, H., Pichler, P.P., Chaves, L.S.M., Capon, A. and Pencheon, D. 2020. The environmental footprint of health care: A global assessment. Lancet Planet. Health, 4(7): e271-e279. https://doi.org/10.1016/S2542-5196(20)30121-2

Lievevrouw, E., Marelli, L. and Van Hoyweghen, I. 2022. The FDA's standard-making process for medical digital health technologies: co-producing technological and organizational innovation. BioSocieties, 17(3): 549-576. https://doi.org/10.1057/s41292-021-00232-w

Manisalidis, I., Stavropoulou, E., Stavropoulos, A. and Bezirtzoglou, E. 2020. Environmental and health impacts of air pollution: A review. Front. Public Health, 8: 14. https://doi.org/10.3389/fpubh.2020.00014

Minisman, G. and Bhanushali, M. and Conwit, R. and Wolfe, G.I. and Aban, I. and Kaminski, H.J. and Cutter, G. 2012. Implementing clinical trials on an international platform: Challenges and perspectives. J. Neurol. Sci., 313(1-2), 1-6. https://doi.org/10.1016/j.jns.2011.10.004

Mishra, S.V. 2022. Utilization of digital technology in conduction of clinical trials in India: Issues and perspectives. Int. J. Sci. Res. Pub., 12(5): 93. https://doi.org/10.29322/IJSRP.12.05.2022.p12514

Mondejar, M.E., Avtar, R., Diaz, H.L.B., Dubey, R.K., Esteban, J., Gómez-Morales, A., Hallam, B., Mbungu, N.T., Okolo, C.C., Prasad, K.A., She, Q. and Garcia-Segura, S. 2021. Digitalization to achieve sustainable development goals: Steps towards a Smart Green Planet. Sci. Total Environ., 794: 148539. https://doi.org/10.1016/j.scitotenv.2021.148539

OECD 2019. Biodiversity: Finance and the Economic and Business Case for Action, OECD Publishing, Paris, https://doi.org/10.1787/a3147942-en (Accessed March 6, 2023).

Padmanabhan, K.K. and Barik, D. 2019. Health hazards of medical waste and its disposal, In: Energy from Toxic Organic Waste for Heat and Power Generation. pp. 99-118. https://doi.org/10.1016/b978-0-08-102528-4.00008-0

Parkins, K. 2022. Healthy patients, healthy planet: tackling the carbon footprint of clinical trials. Clinical Trials Arena. https://www.clinicaltrialsarena.com/features/healthy-patients-healthy-planet-tackling-the-carbon-footprint-of-clinical-trials/ (Accessed March 15, 2023).

Prater, T. 2019. Healthcare in world's largest economies 'accounts for 4%' of global emissions. Carbon Brief. https://www.carbonbrief.org/Healthcare-In-Worlds-Largest-Economies-Accounts-For-4-Of-Global-Emissions/ (Accessed March 10, 2023)

Rajadhyaksha, V. 2010. Conducting feasibilities in clinical trials: An investment to ensure a good study. Perspect. Clin. Res., 1(3): 106-109. https://doi.org/10.4103/2229-3485.71767

Rissman, J., Bataille, C., Masanet, E., Aden, N., Morrow, W.R., Zhou, N., Elliott, N., Dell, R., Heeren, N., Huckestein, B., Cresko, J., Miller, S.A., Roy, J., Fennell, P., Cremmins, B., Koch Blank, T., Hone, D., Williams, E.D., de la Rue du Can, S. and Helseth, J. 2020. Technologies and policies to decarbonize global industry: Review and assessment of mitigation drivers through 2070. Appl. Energy, 266: 114848. https://doi.org/10.1016/j.apenergy.2020.114848

Rosa, C., Campbell, A. N. C., Miele, G. M., Brunner, M. and Winstanley, E. L. 2015. Using e-technologies in clinical trials. Contemporary Clinical Trials, 45: 41-54. https://doi.org/10.1016/j.cct.2015.07.007

Rosa, C.B., Narsch, L.A., Winstanley, E.L., Brunner, M. and Campbell, A.N.C. 2021. Using digital technologies in clinical trials: Current and future applications. Contemp. Clin. Trials, 100: 106219. https://doi.org/10.1016/j.cct.2020.106219

Salam, M.D. and Nilza, N.C. 2021. Hazardous components of landfill leachates and its bioremediation. Intechopen, 577: 948. https://doi.org/10.5772/intechopen.94890

Samuel, G. and Lucassen, A.M. 2022. The environmental sustainability of data-driven health research: A scoping review. Dig. Health, 8: 20552076221111297. https://doi.org/10.1177/20552076221111297

Sanchez, J.A. 2021. Treatments for chronic kidney disease: A systematic literature review of randomized controlled trials. Adv. Ther., 39(1): 193-220. https://doi.org/10.1007/s12325-021-02006-z

Selby, P. 2011. The impact of the process of clinical research on health service outcomes. Ann. Oncol., 22(7): 2-4. https://doi.org/10.1093/annonc/mdr418

Singh, H., Eckelman, M., Berwick, D.M. and Sherman, J.D. 2022. Mandatory reporting of emissions to achieve net-zero health care. N. Engl. J. Med., 387(26): 2469-2476. https://doi.org/10.1056/NEJMsb2210022

Smale, E.M. and Egberts, T.C.G. and Heerdink, E.R. and van den Bemt, B.J.F. and Bekker, C.L. 2021. Waste-minimizing measures to achieve sustainable supply and use of medication. Sustain. Chem. Pharm., 20: 100.

Soulsbury, C. D., Gray, H. E., Smith, L. M., Braithwaite, V., Cotter, S. C., Elwood, R. W., Wilkinson, A. and Collins, L. M. 2020. The welfare and ethics of research involving wild animals: A primer. Methods in Ecology and Evolution, 11(10): 1164-1181. https://doi.org/10.1111/2041-210X.13435

Subbiah, V. 2023. The next generation of evidence-based medicine. Nature Medicine, 29(1): 49-58. https://doi.org/10.1038/s41591-022-02160-z

Sustainable Markets Initiative 2022. The digital solution for sustainability in clinical research. Sustainable Markets Initiative Health Systems Task Force, in collaboration with BCG. https://a.storyblok.com/f/109506/x/42119be232/smi-hstf-digital-health-whitepaper.pdf (Accessed March 9, 2023).

Sustainable Markets Initiatives 2020. Health systems task force. https://www.sustainable-markets.org/taskforces/health-systems-taskforce/ (Accessed March 8, 2023).

Tennison, I, Roschnik, S., Ashby, B., Boyd, R., Hamilton, I, Oreszczyn, T., Owen, A., Romanello, M., Ruysevelt, P., Sherman, J. D., Smith, A. Z. P., Steele, K., Watts, N. and Eckelman, M.J. 2021. Health care's response to climate change: A carbon footprint assessment of the NHS in England. Lancet. Planet. Health, 5(2): e84-e92. https://doi.org/10.1016/S2542-5196(20)30271-0

Turner, M.C., Andersen, Z.J., Baccarelli, A., Diver, W.R., Gapstur, S.M., Pope, C.A., Prada, D., Samet, J., Thurston, G. and Cohen, A. 2020. Outdoor air pollution and cancer: An overview of the current evidence and public health recommendations. Cancer J. Clin., 70(6): 460-479. https://doi.org/10.3322/caac.21632

Vara, V. 2022. Ensuring Data Authenticity, Integrity, And Confidentiality Biggest Barrier to Using Digital Technologies in Clinical Trials: Poll. https://www.clinicaltrialsarena.com/news/ensuring-data-authenticity-integrity-and-confidentiality-barrier-to-digital-technologies-in-clinical-trials/ (Accessed March 1, 2023)

World Health Organization (WHO) 2021. Climate Change and Health. https://www.who.int/news-room/fact-sheets/detail/climate-change-and-health (Accessed February 18, 2023)

World Health Organization (WHO) 2005. Handbook for Good Clinical Research Practice (GCP): Guidance for Implementation. World Health Organization.

**Original Research Paper**    doi   https://doi.org/10.46488/NEPT.2023.v22i04.037    **Open Access Journal**

# An Eco-friendly Solution for Oil Spill Absorption

**Ahmad Arquam, Minal Deshmukh† iD and Aadil Pathan iD**

School of Petroleum Engineering, MIT World Peace University, Paud Road, Kothrud, Pune, 411038, India

†Corresponding author: Minal Deshmukh; minal.deshmukh@mitwpu.edu.in

## ABSTRACT

It is extremely difficult to clean up accidental oil spills in water since conventional oil sorbents absorb much more water in addition to the oil. Alternatively, cleanup techniques might lead to secondary contamination. This study examines and measures the oil absorption capacities of two hydrophobic natural fibers: water hyacinth (*Eichhornia crassipes*) and lotus (*Nelumbo nucifera*). At the laboratory scale, the absorption of engine oil, vegetable oil, and diesel oils onto various dry biomass materials, including water hyacinth and lotus with different particle sizes (BSS-44, BSS-60, BSS-100, BSS-120, BSS-160, and BSS-200), was investigated. Water hyacinth shows a higher absorption efficiency for all samples as compared to the lotus.

## INTRODUCTION

The environment has been exposed to oil for years since it is a naturally occurring element (Kingston 2002). Oil production and consumption are rising day by day due to the industrial economy's fast rise. When manufactured, used, stored, or transported, oil can leak or discharge, severely damaging the environment and depleting energy supplies (Cao et al. 2016). When oil spills on the sea's surface, it goes through several processes at once, including spreading, emulsification, evaporation, dispersion, biodegradation, sinking, photo-oxidation resurfacing, and tarball creation (Al-Majed et al. 2012). So, it has an impact on marine life. The number of oil pollutants that penetrate the ecosystem of the seas is large, difficult to degrade, and greatly complicates the cleanup procedure.

Additionally, it endangers public safety and seriously harms fishing, tourism, and the aquatic environment (Suleman 2012). Consequently, controlling oil spills has been a research focus (Yu et al. 2019). On May 27, 2020 an uncontrolled oil and gas spill happened in the Baghjan village of Assam owing to failing pressure mechanisms in an oil well operated by the state-owned Oil India Limited (OIL). The water eventually caused the gas-emitting mist to condense, which in turn caused hazardous floods to occur in neighboring houses and fields, harming crops and damaging the soil. Similarly, in Nagaland, the district's Changpang and Tsorri villages were badly damaged by spills from Oil and Natural Gas Company (ONGC) drill sites, as shown in Fig. 1. More than 2,000 individuals have experienced the contamination of their farmlands, woods, and water supplies as a result of the leak.

Several techniques are used to remove oil from water surfaces where it has been spilled. This falls into one of five categories (Jarrah et al. 2018): mechanical processes. Booms are often used to encircle and control the oil spreading from water surfaces, whereas skimmers are typically used to remove liquid oil from the water's surface (Ramanathan et al. 2022, Ansari et al. 2003). This method is time-consuming and costly, necessitates many mechanical tools, and is ineffective when the oil spill is far from the beaches. Internal burning this approach, which may eliminate 600 to 1,800 barrels of oil every hour and decrease its impact on aquatic plants and animals, is one of the most affordable ways to remove oil from the water's surface (Gote et al. 2023). However, this approach has drawbacks related to spill settings and pollutes the atmosphere by producing several hazardous substances, including polycyclic aromatic hydrocarbons, sulfur dioxide, and carbon monoxide. Chemical spreaders cause oil to coalesce due to the chemical solidifiers, where it either floats on the water's top or sinks to the bottom. The surfactants reduce liquid oil's surface tension, increasing its water solubility. Both approaches are costly, unfriendly,

Fig. 1: Oil spillage in Nagaland.

and detrimental to marine environmental systems (Alaa El-Din et al. 2018). Biological procedures, specifically fungus, bacteria, algae, and yeasts, break down oil off the water's surface (Atlas & Hazen 2011). Only thin oil layers may be removed using this process; most oil sorbents must be removed using other techniques. Oil spill cleaning and recovery utilizing various sorbent materials are some of the most effective ways currently used. This technique also demonstrates the qualities of recyclability (Jarrah et al. 2018).

The best oil sorbents will likely have excellent hydrophobic-oleophilic properties to draw liquid oil into the fibrous structure, quick sorption kinetics to make cleanup of spills easier and prevent leakage, good buoyancy and stability in water to facilitate collection, and recyclability and biodegradation potential (Zhang et al. 2017). Many types of sorbent materials have been employed to date for the cleaning and recovery of oil spills. These sorbents either operate by adsorption or absorption. When used with less viscous oils, absorbents function similarly to sponges and absorb oil through capillary action or suction. Conversely, adsorbents are most effective for heavy, sticky oils because they have a wide surface area, high porosity, and strong chemical affinity for spilled oil. Certain sorbents may sequester oil by acting in both ways. Several methods based on sorbent materials have recently been created as potentially effective remedies for the oil leak issue (Shang et al. 2016). These sorbents may be correctly divided into synthetic polymeric materials, inorganic mineral products, and organic natural materials (Wang et al. 2012). Due to their capacity to absorb large amounts of oil, several synthetic polymers, including poly

(dimethylsiloxane), polystyrene fiber, polypropylene fiber, polyester fiber, polyurethane sponge, and several carbon-based materials, have been utilized for oil spill cleanups (Zhang et al. 2017). However, synthetic materials' inability to degrade naturally is a serious problem.

Additionally, the preparation process frequently calls for lengthy, complex synthesis processes, which raises the cost of production. Applications for cleaning up oil spills using inorganic mineral materials such as zeolites, silica, vermiculite, sepiolite, and perlite have been investigated. According to studies, these materials' insufficient buoyancy and inadequate oil-absorbing capabilities render them ineffective at cleaning up oil spills (Zheng et al. 2017). Numerous fibers from plants, including cattail, nettle, cotton, milkweed, kapok, sunflower seed, and Metaplexis japonica fiber, are examples of organic natural materials (Yu et al. 2019, Viju et al. 2021, 2019). Natural cellulosic fiber-based oil sorbents have recently attracted more attention because of their beneficial qualities, including oil absorbency equivalent to synthetic sorbent materials, sustainability and environmental friendliness, and affordability. Oil may bind to cellulosic fiber surfaces through interactions with waxes and oils or be physically trapped on its surface due to its shape. The porous internal structure of the fiber's porous structure may allow the oil to become trapped there. Oil may diffuse through the fiber more easily thanks to its porous core, improving its sorption capabilities (Wang et al. 2012, Cao et al. 2016).

This research study aims to examine studies on natural fiber-based oil sorbents, summarize the status of the science,

and highlight recent advancements in oil spill cleaning gear. The current work examines the sorption of organic oils onto the dry biomass water hyacinth (*Eichhornia crassipes*), a freshwater aquaphyte with the necessary buoyancy, hydrophobicity, and biodegradability for oil sorption (Jansi Rani et al. 2014). It may be found in ponds and rivers. It is regarded as the worst aquatic plant and develops and reproduces rapidly (El-Sayed 2003). The thick mats of water hyacinth float on the water's surface, obstructing navigation and causing problems with irrigation, fishing, recreation, and power production.

Additionally, these mats block sunlight from entering and lessen water aeration, which causes an oxygen shortage. They decrease biological diversity by competitively excluding submerged plants. Removing water hyacinth dumps requires expensive mechanical collection and disposal methods, creating a solid waste problem. Much study has been done on the optimum use of discarded water hyacinth. This study has aimed to explore the possibility of the aquaphyte as a low-cost option for treating oil effluents and spills.

The two-level hierarchical surface structure of lotus leaves gives super hydrophobic and self-cleaning capabilities. This study examines how well water hyacinth and lotus plants can absorb oil and calculated oil separation through these natural fibers for different particle sizes (Zeiger et al. 2016).

## Water Hyacinth (*Eichhornia crassipes*) Characteristics

Lignin, crystalline cellulose, and hemicellulose polymers are structural carbohydrates that make up water hyacinth (Zhang et al. 2020). Due to important functional groups on its surface, specifically carboxyl, hydroxyl, and carbonyl, water hyacinth serves as a catalyst for the adsorption of water pollutants onto plant-based adsorbents (Brown et al. 2020). Functional groups $PO_4$, $C = O$, and C–H are found in the water hyacinth roots (Milke et al. 2020). Water hyacinth fibers include a sizable quantity of cellulose in the form of hemicellulose (33%), cellulose (25%), and lignin (10%). These water hyacinth characteristics encourage researchers to look into the potential use of invasive species for water restoration (Amalina et al. 2022). Using cellulose from water hyacinth to remove impurities from water has also been the subject of several research-based studies (Emam et al. 2020, Salahuddin et al. 2021). This is mostly because the cellulose backbone of this aquatic plant has several hydroxyl groups (Singh & Chandra 2019). These hydroxyl groups were chemically adjusted to make generation easier and are the main determinants of adsorption.

## Lotus (*Nelumbo nucifera*) Characteristics

The large aquatic rhizomatous plant lotus (*Nelumbo nucifera*) has a creeping stem that is thin, elongated, and covered in nodal roots. With floating and floating orbicular leaves, the lotus is a perennial plant (Mukherjee et al. 2009, 1996). On a biological level, lotus possesses characteristics that set it apart from other plant species and those typical of water plants (Paudel & Panth 2015). These characteristics include flower thermoregulation, leaf ultra hydrophobicity, and seed life span. The "lotus effect" is the ultra-hydrophobicity in lotus leaves (Darmanin & Guittard 2015). The leaf's top epidermis might be protected from water by this ultra-hydrophobicity trait, preserving the stomata's ability to open
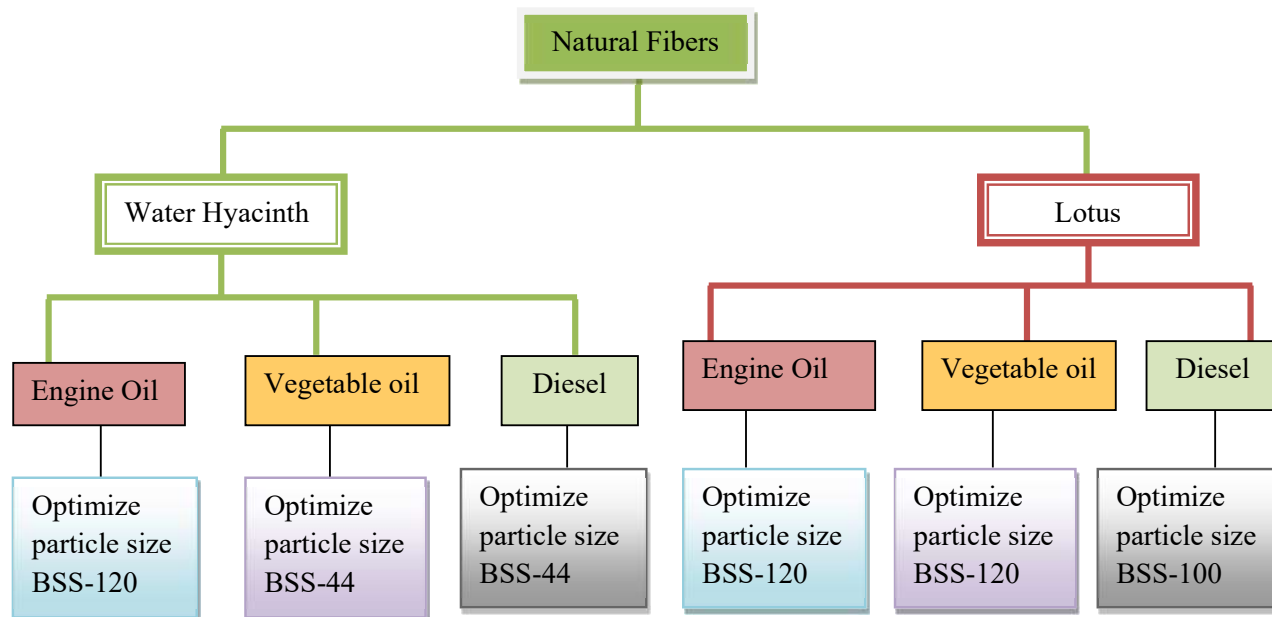
and close normally (Ensikat et al. 2011). Because of this, ultra hydrophobicity is thought to have served the lotus well in its evolutionary process. A unique thick coating of waxy papillae on the surface of the lotus leaf has been proven in studies to be responsible for this (Zhang et al. 2012, Lin et al. 2019).

## MATERIALS AND METHODS

Research has been carried out using two different hydrophobic natural fibers, namely Water hyacinth, and Lotus, with three different types of oils, including engine oil, vegetable oil, and diesel. For each oil sample, six different particle sizes of water hyacinth and lotus were taken to remove oil from the water.

### Materials

The study examined two distinct natural fibers, water hyacinth, and lotus fiber. The two eco-friendly hydrophobic materials, lotus and water hyacinth, have been used for oil spill removal. Lotus flowers have been taken from Swargate, Pune. Locally grown water hyacinth was collected from Khadakwasla Lake in Pune. For water hyacinth and lotus, BSS-44, BSS-60, BSS-100, BSS-120, BSS-160, and BSS-200 particle sizes were screened out. Castrol engine oil, vegetable oil, and diesel are used in this research study.

### Methods

Water hyacinth and lotus have been dried with the help of a hot air oven for 72 hours at 55 $^0$C. Dried water hyacinth and lotus materials have been crushed into fine particles with the help of a lab-scale grinder (spice & herb grinder). With the help of different sieves, BSS-44, BSS-60, BSS-100, BSS-120, BSS-160, and BSS-200, crushed powder of water hyacinth and lotus were screened into different particle sizes.

Sample solution of engine oil, vegetable oil, and diesel with water has been made on a volumetric ratio of 1:1.



Fig. 2: Experimental setup-1.



Fig. 3: Experimental setup-2.



Fig. 4: Water Hyacinth treatment samples for engine oil.



Fig. 5: Lotus treatment samples for engine oil.

Buchner funnel of diameter 100mm has been taken for the filtration process with different natural fiber particle sizes of 1.5 g. The 30 mL of oil and water was passed through

Fig. 6: Water hyacinth treatment samples for vegetable oil and diesel.



Fig. 7: Lotus treatment samples for vegetable oil and diesel.

different particle sizes of water hyacinth and lotus for 24 hours through the Buchner funnel. Fig. 2 and Fig. 3 show the experimental setup of oil spill removal through water hyacinth and lotus with different particle sizes. Fig. 4, Fig. 5, Fig. 6, and Fig. 7 show the separation of oil and water for different particle sizes of water hyacinth and lotus.

## RESULTS AND DISCUSSION

The absorbent material must reject water and absorb oil to produce effective oil spill cleaning on the water through selective oil absorption materials (Zeiger et al. 2016). The lotus and water hyacinth floating plants completely satisfy this requirement. Due to the design of their surface and the presence of wax on their surface, they are extremely hydrophobic and retain an air layer when submerged in water (Jansi Rani et al. 2014). Due to their super hydrophobic and super oleophilic qualities, water hyacinth and lotus quickly and selectively absorb oil from water. We calculated the water hyacinth and lotus plants' absorption rates. Initially, we used Castrol engine oil to assess the sorption capacity of water hyacinth (1.5 gm) with six different particle sizes. Graphs show the results, which show that water hyacinth has a better capacity to absorb oil than lotus. For 1 ton liter of oil removal, 4 kg of water hyacinth is required. On the other hand, approximately 5 kg of lotus is required to remove 1 ton liter of oil from water.

In Fig. 8, water hyacinth gives a higher oil absorption efficiency of 92% for particle size of BSS-120 compared to other particle sizes of water hyacinth. As shown in Fig. 8, the optimized particle size for removing the oil spill from the water hyacinth is BSS-120.
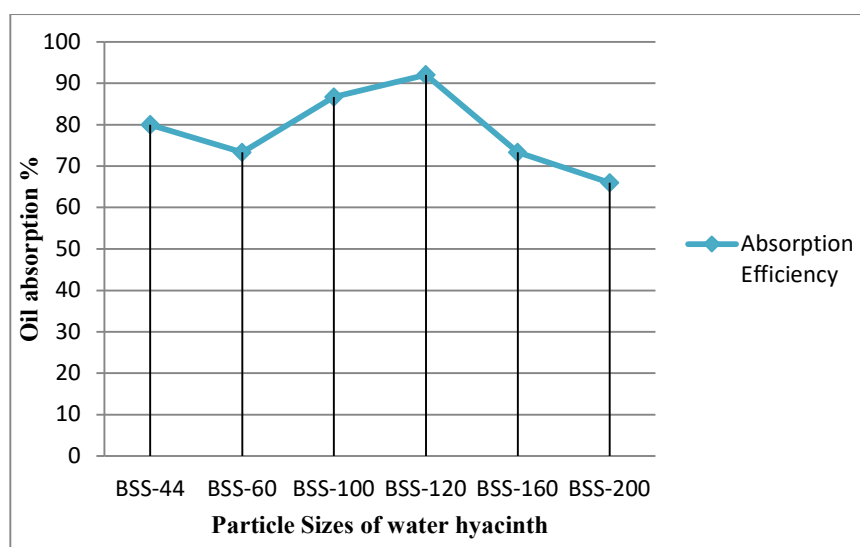


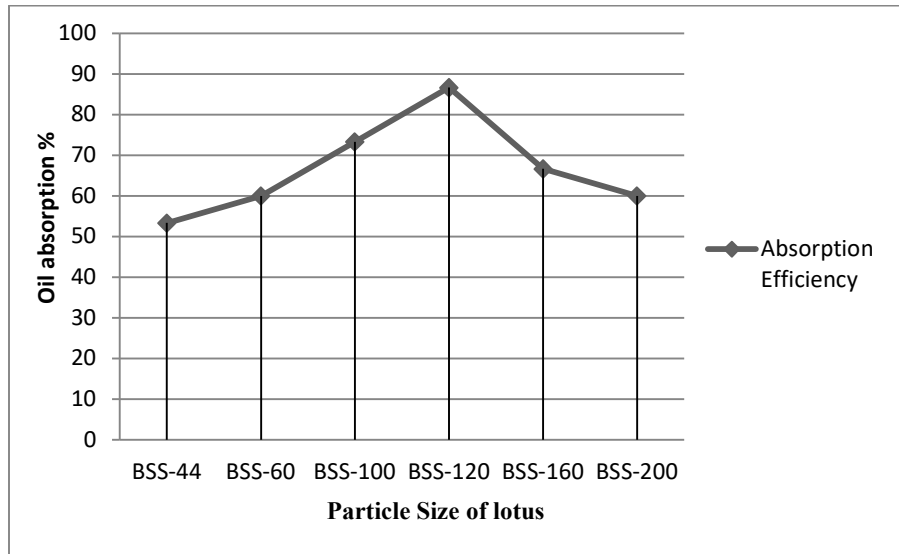Fig. 8: Oil absorption efficiency of water hyacinth for engine oil.

Fig. 9: Oil absorption efficiency of lotus for engine oil.

As shown in Fig. 9, the particle size of BSS-120 lotus provides a higher efficiency of 86.67%. From BSS-44 to BSS-120, absorption efficiency increases; after that, the efficiency decreases for BSS-160 and BSS-120.

In Fig. 10, water hyacinth gives a higher oil absorption efficiency of 86.66% for vegetable oil for particle size of BSS-44 compared to other particle sizes of water hyacinth. The optimized particle size for removal of an oil spill for water hyacinth is BSS-44 in a vegetable oil solution. After BSS-44, the absorption efficiency decreases for other particle sizes.

As shown in Fig. 11, for particle size of BSS-120, lotus gives a higher efficiency of 70% for vegetable oil. From BSS-44 to BSS-120, absorption efficiency increases. After that, the efficiency decreases for BSS-160 and BSS-120.

The optimized particle size for removal of oil spill for lotus is BSS-120 in a vegetable oil solution.
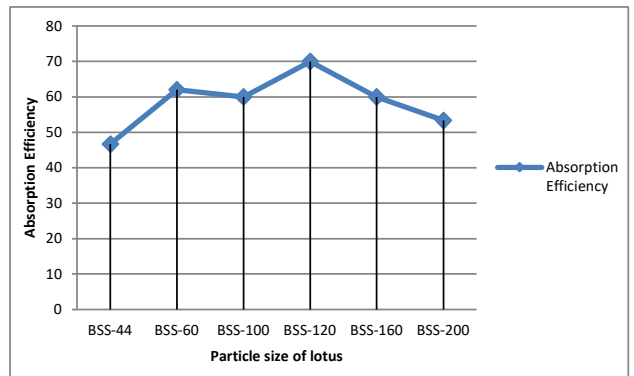


Fig. 11: Oil absorption efficiency of lotus for vegetable oil.



Fig. 10: Oil absorption efficiency of water hyacinth for vegetable oil.



Fig. 12: Oil absorption efficiency of water hyacinth for diesel.

Fig. 13: Oil absorption efficiency of lotus for diesel.

As per Fig. 12, particle size of BSS-44 shows higher oil absorption efficiency, with 80% for water hyacinth for diesel solution. BSS 44 optimizes the particle size of water hyacinth for diesel solution. The graph shows that absorption efficiency decreases for other particle sizes.

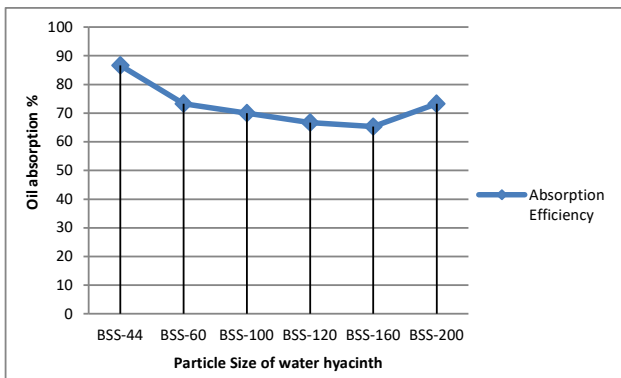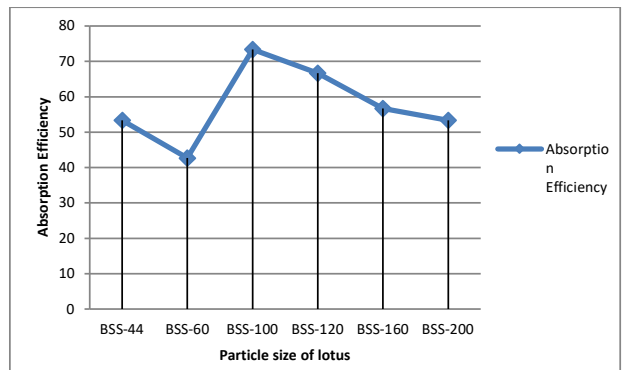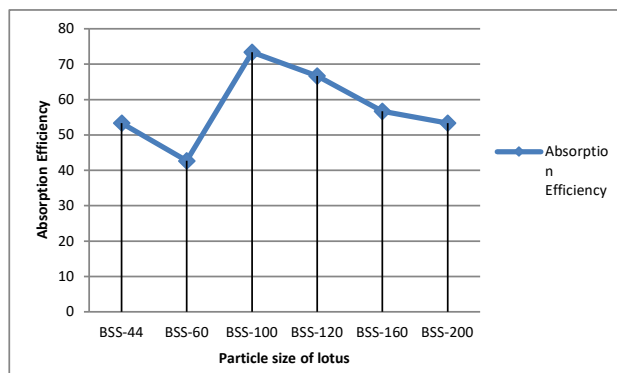In Fig. 13 for diesel solution, the lotus particle size of BSS-100 gives a higher oil absorption efficiency of 73.33%. The optimized particle size to separate diesel and water for lotus is BSS-100.

## CONCLUSION

The findings of this investigation demonstrated that biomass water hyacinth has a better ability to absorb oil than lotus. Water hyacinth is a potential replacement for conventional synthetic oil absorbents used to recover oil in the absence or presence of water due to the bio material's high absorption capacity, high degree of hydrophobicity, and low water absorption. The material is cheap and easily available in tropical areas. Hence, based on the research, it can be concluded that biomass water hyacinth is a low-cost yet effective oil absorbent.

### Future Scope

Another hydrophobic natural fiber could be used for oil spill removal based on their different particle size. A simulation study of the present work will help to choose the efficient absorbent for oil spill removal.

## REFERENCES

Al-Majed, A.A., Adebayo, A.R. and Hossain, M.E. 2012. A sustainable approach to controlling oil spills. J. Environ. Manag., 113: 213-227. https://doi.org/10.1016/j.jenvman.2012.07.034

Alaa El-Din, G., Amer, A.A., Malsh, G. and Hussein, M. 2018. Study on the use of banana peels for oil spill removal. Alex. Eng. J., 57(3): 2061-2068. Elsevier B.V. https://doi.org/10.1016/j.aej.2017.05.020

Amalina, F., Razak, A. S. A., Krishnan, S., Zularisam, A. W. and Nasrullah, M. 2022. Water hyacinth (Eichhornia crassipes) for organic contaminants removal in water – A review. J. Hazard. Mater., 7: 100092. https://doi.org/10.1016/j.hazadv.2022.100092

Ansari, I.A., East, G.C. and Johnson, D.J. 2003.Structure–property relationships in natural cellulosic fibers: Part III: Flax—an oil sorbent. J. Text. Inst., 94(1–2): 1-15. https://doi.org/10.1080/00405000308630590

Atlas, R. M. and Hazen, T. C. 2011. Oil biodegradation and bioremediation: A tale of the two worst spills in U.S. history. Environmental Science and Technology, 45(16): 6709-6715. https://doi.org/10.1021/es2013227

Brown, A.E., Adams, J.M.M., Grasham, O.R., Camargo-Valero, M.A. and Ross, A.B. 2020. An assessment of different integration strategies of hydrothermal carbonization and anaerobic digestion of water hyacinth. Energies, 13(22): 465

Cao, S., Dong, T., Xu, G. and Wang, F. 2016. Study on structure and wetting characteristics of cattail fibers as natural materials for oil sorption. Environ. Technol., 37(24): 3193–3199.

Darmanin, T. and Guittard, F. 2015. Superhydrophobic and superoleophobic properties in nature. Mater. Today, 18(5): 273-285.

El-Sayed, A.F.M. 2003. Effects of fermentation methods on the nutritional value of water hyacinth for Nile tilapia Oreochromis niloticus (L.) fingerlings. Aquaculture, 218: 10456.

Emam, A.A., Abo Faraha, S.A., Kamal, F.H., Gamal, A.M. and Basseem, M. 2020. Modification and characterization of Nano cellulose crystalline from Eichhornia crassipes using citric acid: An adsorption study. Carbohydr. Polym., 240: 1415-1422

Ensikat, H.J., Ditsche-Kuru, P., Neinhuis, C. and Barthlott, W. 2011. Superhydrophobicity in perfection: The outstanding properties of the lotus leaf. Beilstein J. Nanotechnol., 2(1): 152-161.

Gote, M.G., Dhila, H.H. and Muley, S.R. 2023. Advanced synthetic and bio-based sorbents for oil spill cleanup: A review of novel trends. Nat. Environ. Pollut. Technol., 22(1): 39-61.

Jansi Rani, M., Murugan, M., Subramaniam, P. and Subramanian, E. 2014. A study on water hyacinth Eichhornia crassipes as oil sorbent. J. Appl. Nat. Sci., 6(1), 134-138.

Jarrah, K., Hisaindee, S. and Al-Sayah, M.H. 2018. Preparation of oil sorbents by solvent-free grafting of cellulose cotton fibers. Cellulose, 25(7): 4093-4106.

Kingston, P.F. 2002. Long-term environmental impact of oil spills. Spill Sci. Techno. Bull., 7(1-2): 53-61. https://doi.org/10.1016/S1353-2561(02)00051-8

Lin, Z., Zhang, C., Cao, D., Damaris, R. N. and Yang, P. 2019. The latest studies on lotus (Nelumbo nucifera)-an emerging horticultural model plant. Int. J. Mol. Sci., 20(15): 680. https://doi.org/10.3390/ijms20153680

Milke, J., Gałczyńska, M. and Wróbel, J. 2020. The importance of biological and ecological properties of Phragmites Australis (Cav.) Trin. Ex steud., in phytoremediation of aquatic ecosystems: The review. Water, 12(6): 1770. https://doi.org/10.3390/w12061770

Mukherjee, P.K., Balasubramanian, R., Saha, K., Saha, B.P. and Pal, M. 1996. A review on nelumbo nucifera gaertn. Ancient Sci. Life, 4: 23-32

Mukherjee, P.K., Mukherjee, D., Maji, A.K., Rai, S. and Heinrich, M. 2009. The sacred lotus (Nelumbo nucifera) - phytochemical and therapeutic profile. J. Pharm. Pharmacol., 61(4): 407-422. https://doi.org/10.1211/jpp/61.04.0001

Paudel, K.R. and Panth, N. 2015. Phytochemical profile and biological activity of Nelumbo nucifera. Evid. Based Complement. Alternat. Med., 16: 54

Ramanathan, R., Abdullah, L., Mohamed, M.S.S. and Fauadi, M.H.F.M. 2022. A Review of User-Centred Design Methods for Designing a Portable Oil Spill Skimmer. Nat. Environ. Pollut. Technol., 21(4): 1519-1529.

Salahuddin, N., Abdelwahab, M.A., Akelah, A. and Elnagar, M. 2021. Adsorption of Congo red and crystal violet dyes onto cellulose extracted from Egyptian water hyacinth. Nat. Hazards, 105(2): 1375-1394.

Shang, B., Wang, Y., Peng, B. and Deng, Z. 2016. Bioinspired polydopamine particles-assisted construction of superhydrophobic surfaces for oil/water separation. J. Colloid Interface Sci., 482: 240-251.

Singh, A.K. and Chandra, R. 2019. Pollutants released from the pulp paper industry: Aquatic toxicity and their health hazards. Aquat. Toxicol., 211: 202-216.

Suleman, S. 2012. Oil spills: Law on liability with special reference to the Indian regime. SSRN Electron. J., 15: 611-623

Viju, S., Brindha, R. and Thilagavathi, G. 2021. Surface modification of nettle fibers by grafting to improve oil sorption capacity. J. Ind. Textiles, 50(8): 1314-1329.

Viju, S., Thilagavathi, G., Vignesh, B. and Brindha, R. 2019. Oil sorption behavior of acetylated nettle fiber. J. Textile Inst., 110(10): 1415-1423.

Wang, J., Zheng, Y. and Wang, A. 2012. Effect of kapok fiber treated with various solvents on oil absorbency. Ind. Crops Prod., 40(1): 178-184.

Yu, M., Wang, Q., Yang, W., Xu, Y., Zhang, M., Deng, Q. and Liu, G. 2019. Facile fabrication of magnetic, durable, and superhydrophobic cotton for efficient oil/water separation. Polymers, 11(3): 54-63.

Zeiger, C., Rodrigues Da Silva, I.C., Mail, M., Kavalenka, M.N., Barthlott, W. and Hölscher, H. 2016. Microstructures of superhydrophobic plant leaves - Inspiration for efficient oil spill cleanup materials. Bioinsp. Biomimetics, 11(5): 614.

Zhang, C., Ma, X., Chen, X., Tian, Y., Zhou, Y., Lu, X. and Huang, T. 2020. Conversion of water hyacinth to value-added fuel via hydrothermal carbonization. Energy, 197: 47-56.

Zhang, X., Wang, C., Chai, W., Liu, X., Xu, Y. and Zhou, S. 2017. Kapok fiber is a natural source for the fabrication of oil absorbent. J. Chem. Technol. Biotechnol., 92(7): 1613-1619.

Zhang, Y., Wu, H., Yu, X., Chen, F. and Wu, J. 2012. Microscopic observations of the lotus leaf for explaining the outstanding mechanical properties. J. Bionic Eng., 9(1): 84-90.

Zheng, Y., Cao, E., Tu, L., Wang, A. and Hu, H. 2017. A comparative study for oil-absorbing performance of octadecyl trichlorosilane treated Calotropis gigantea fiber and kapok fiber. Cellulose, 24(2): 989-1000.

## ORCID DETAILS OF THE AUTHORS

Minal Deshmukh: https://orcid.org/0000-0002-6534-5005
Aadil Pathan: https://orcid.org/0000-0002-9974-8881

# Effect of Fulvic Acid on the Denitrification in Deep Subsurface Wastewater Infiltration System

**Jingjing Lv\*, Jingjing Li\*\*, Yanyan Dou\*, Guoke Chen\*, Yubing Ye\*\*\* and Li'an Hou\*\*\*\*†**

\*College of Energy and Environmental Engineering, Zhongyuan University of Technology, Zhengzhou 450007, China
\*\*CSCEC Zhongyuan Architectural Design Institute Co. Ltd., Zhengzhou 450004, China
\*\*\*Shanghai Municipal Engineering Design Institute Co. Ltd., Shanghai 200092, China
\*\*\*\*College of Environmental Science and Engineering, Tongji University, Shanghai 200092, China
†Corresponding author: Li'an Hou; houla@cae.cn

## ABSTRACT

This work aims to explore the impact of fulvic acid (FA) on denitrification within the purification process of sewage in the deep subsurface wastewater infiltration system (DSWIS). In the system, an organic glass column (height = 2.40 m; radius = 0.30 m) was filled with several layers of soil. Simulated domestic wastewater and extracted FA from landfill leachate were used in the experiments. It was found that before and after the addition of FA, COD, and $NH_4^+$-N were efficiently removed when a hydraulic load was 8 cm·d$^{-1}$. Moreover, after FA addition, the removal efficiency of TN was enhanced from 67.74% to 78.01%. Organic matter transformation analysis indicated that in the under part, the shortage of carbon sources limited the denitrification prior to FA addition, resulting in a low TN removal efficiency. However, after adding FA, more FA-like substances were transferred into protein-like matters than before the addition of FA, which has helped produce more easily biodegradable organics for denitrification. So, the addition of FA could enhance the denitrification process in the system of DSWIS.

## INTRODUCTION

It has been proved that a soil wastewater infiltration system (SWIS) could be an efficient and cost-on-site alternative advanced strategy to deal with wastewater (Chen et al. 2021, Lv et al. 2019, Zheng et al. 2018a, Yang et al. 2020). Nowadays, SWIS has been largely implemented to treat wastewater in various countries, like China, Japan, and the United States (Lv et al. 2020, Yuan et al. 2016, Xu et al. 2020, Eregno & Heistad 2019, Kawasaki 2019.). In SWIS, traditional biological or physical-chemical approaches are firstly applied to treat wastewater; afterward, the treated wastewater is penetrated through an aerated unsaturated zone; during the penetration, wastewater is purified via a series of processes, including adsorption, chemical reaction, filtration, and biodegradation. Compared to the traditional process of the activated sludge, SWIS exhibits various advantages, covering easy operation and maintenance, low cost of manufacture and execution, and excellent performance in removing total phosphorus (TP) and chemical oxygen demand (COD) (Li et al. 2021a, Yamaguchi et al. 1996). In addition, more than 80% removal efficiencies were achieved for TP, suspended solids, and organic compounds

(Payne et al. 2017, Christianson et al. 2017, Yang et al. 2021, Bieber et al. 2018).

However, it was previously reported by many studies that SWIS was not sufficient to remove nitrogen. Depending on the operation conditions, wastewater composition, and environmental conditions, 10-90% removal efficiency of total nitrogen (TN) could be yielded (Gu et al. 2019, Jia et al. 2023, Qin et al. 2021, Li et al. 2021b, Yang et al. 2022, Li et al. 2023).

Additionally, it has been indicated that in the subsurface infiltration systems, denitrification and nitrification serve as the two primary reactions involved in eliminating nitrogen from sewage water, while other processes, including ammonia volatilization, grass uptake, and substrate adsorption, are generally of less significance (Li et al. 2021a, Perujo et al. 2017, Yu et al. 2019). However, during the percolation process, denitrification and nitrification can occur in the same unit of soil infiltration. Nitrification and decomposition of organic substrates typically appear in the upper area containing enough oxygen. However, denitrification primarily occurs in the lower area where organic matter barely remains and oxygen is strictly absent.

Therefore, in the lower part, the shortage of carbon sources greatly contributes to the low elimination of TN and low denitrification (Jia et al. 2019, Shokri et al. 2021, Su et al. 2023).

Different research has been conducted to solve this problem. Zheng et al. (2018b) demonstrated that shunt-distributing wastewater promoted decreased oxygen concentration in the system, establishing a good environmental condition for denitrification. According to the study of Nakhla and Farooq (2003), it was found that in the slow sand filters, slowly biodegradable COD and particulate could be used for denitrification. Ye et al. (2008) designed a system of a two-stage anaerobic tank integrated with a soil trench. In the system, 60% and 40% of the raw sewage was individually transferred into the first and second anaerobic tanks. In the soil trench, 40% of raw sewage provided the necessary carbon source, leading to a high nitrogen removal rate.

Moreover, various research has demonstrated that successful denitrification was associated with the depth of the SWIS. It has been proved that in a DSWIS, the optimal depths for the reactions of denitrification and nitration were 0.70-1.50 m and 0.30-0.70 m, individually (Li et al. 2021). However, for the traditional SWISs, the optimal depths were < 1.2 m (varying between 0.6 and 1.2 m), where the process of denitrification was prevented due to the presence of an anaerobic environment (Ye et al. 2008). It was also revealed that the optimal depth to remove the total nitrogen (TN) in SWIS was 1.55 m, where TN was effectively eliminated (Li et al. 2021). Zhang et al. (2015) also achieved good performance of nitrogen removal in the soil column with a 2.00 m depth, and 83.68 and 99.77% removal efficiencies were obtained for TN and $NH_4^+$-N. Furthermore, it has been observed that the refractory organics, fulvic acid-like (FA-like) substances, were partly degraded at 1.05-1.30m and transferred into protein-like substances, which led to a leap of TN elimination. It might indicate that the FA-like substances were able to serve as carbon sources for denitrification.

Hence, we checked if FA could be used as the biodegradable carbon source to facilitate removing nitrogen in DSWIS. Furthermore, we investigated the impact of FA on nitrogen removal efficiency. A soil column with a depth of 2.00 m was utilized to simulate a subsurface soil infiltration system. Nitrogen and organic matter variations in the whole percolation process will be studied. Then, the nitrogen and organics removal performances before and after the addition of FA would be compared. Moreover, the exact effect mechanisms of FA on denitrification will be analyzed.

## MATERIALS AND METHODS

### Description of the Pilot System

The material of the pilot system column is organic glass. The height and radius of the column are 2.40 m and 0.30 m. It is composed of four segments connected using flanges. From the top to the bottom, the lengths of segments are 0.50, 0.50, 0.70, and 0.70 m, respectively. Before securing each segment together, a gasket is located between the two segments to keep a watertight seal. Three parallel experiments were conducted. Fig.1 displays the schematic of the soil column.

### Materials

In this study, the soil was obtained from the Shunyi District of Beijing. To simulate the real soil condition, the soil depth in the organic glass column was the same as in the original soil location. From top to bottom, the soil densities in the column were 1.43, 1.56, 1.63, and 1.76 g·cm$^{-3}$ at 0~0.50,
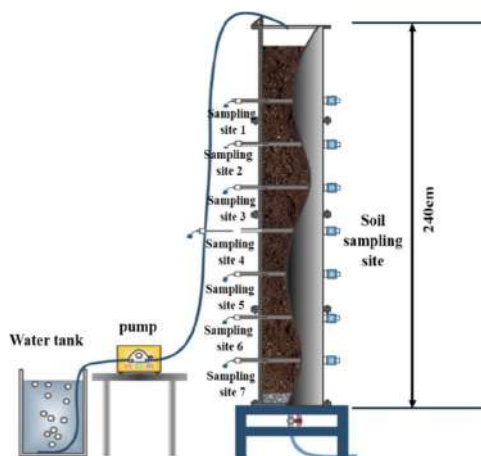


Fig. 1: Setup of the soil column. There are seven sampling sites. They are set at 0.20, 0.50, 0.80, 1.10, 1.40, 1.70, and 2.00 m, where water samples would be obtained using in-situ soil solution samplers.

Table 1: The exacted components from the sewage.

| Drag names | Concentration (mg·L$^{-1}$) |
|---|---|
| Sucrose | 200.0 |
| Peptone | 220.0 |
| ammonium chloride | 117.0 |
| ferric chloride | 0.4 |
| magnesium sulfate heptahydrate | 62.0 |
| dipotassium phosphate | 44.0 |
| boric acid | 10.0 |
| copper sulfate pentahydrate | 0.8 |
| potassium iodide | 1.9 |
| manganese sulfate dihydrate | 7.8 |
| sodium molybdate dihydrate | 4.0 |
| zinc sulfate heptahydrate | 7.8 |
| calcium chloride dihydrate | 1.9 |
| sodium nitrate | 91.0 |

0.50~1.00, 1.00~1.50, and 1.50~2.00 m. Once filled with soil, the column was thoroughly covered by black plastic tarps to avoid the growth of algae and the effect of light during operation.

The sewage in the experiment was used to simulate domestic wastewater. The components extracted from the sewage are listed in Table 1. A silicone tube transferred wastewater into the column using a variable-speed peristaltic pump.

The FA used in the experiment was extracted from landfill leachate of A Su Wei landfill field in Beijing, China. XAD-8 and hydrogen-type cation exchange resin were used to isolate and purify the FA (Stevenson & Cole 1999). Then, the purified FA solution was dehydrated by a freezer dryer, and the FA powder was preserved in valve bags.

After the column was set up, tap water was transferred to the soil column to eliminate the original pollutants in the soil for 3 months. Afterward, the 24-hour composite percolate was analyzed for sequential three days. The results indicated that there are no constituents leached (TP < 0.01 mg·L$^{-1}$, TN < 1 mg·L$^{-1}$, and COD < 10 mg·L$^{-1}$). Subsequently, simulated wastewater was delivered into the soil column for three months for the start-up and domestication of the system. At last, a hydraulic load was set as 8 cm·d$^{-1}$ and the detailed experiments were performed in the continuous feeding mode for one year.

### Test of Soil Adsorption

Batch adsorption tests were carried out to evaluate the adsorption capacities of $NH_4^+$-N by the soils. A constant weight of soil samples was obtained by drying at 105°C.

Prior to sterilization for 30 min at 121°C and 1.1 MPa, 5 g of dried soil sample was taken out from different depths (0-0.50, 0.50-1.00, 1.00-1.50 and 1.50-2.00 m) and transferred in 250 mL conical flasks. Certain volumes of solution containing various levels of $NH_4^+$-N were placed into each flask. The samples in the flasks were agitated at the seed of 160 rpm for 24 h at 25°C. When equilibrium was observed in adsorption, the solution was filtered through a membrane (0.45 μm). According to Zhang et al. (2020), the following formula could be employed to compute the adsorption capacity of NH4+-N by the soil:

$$q = (C_0 - C)V/M \qquad \ldots (1)$$

Where q represents the soil adsorption capacity, mg·g$^{-1}$; M represents the soil dry weight, g; $C_0$ and C individually represent the initial and equilibrium levels of the target component in the solution of mixed soil, mg·L$^{-1}$; and V represents the solution volume, L.

### Sample and Data Analysis

After the soil system ran stably, samples at the influent, effluent, and seven sampling points of the system were collected weekly. A dichromate approach was employed to determine the concentration of COD. The Multin N/C 2100 TOC/TN tester was implemented for the quantification of the total organic carbon (TOC). Standard approaches according to E.P.A. (2002) were applied to measure the levels of TN, nitrate nitrogen ($NO_3^-$-N), nitrite nitrogen ($NO_2^-$-N), and ammonia nitrogen ($NH_4^+$-N). All samples were tested on the same day when they were sampled. The organic composition and stabilization of samples were evaluated by using fluorescence spectroscopy.

Each sample was conducted at ambient temperature (~25°C) by 3D excitation-emission matrix (3D-EEM) fluorescence spectroscopy using a luminescence spectrophotometer (F-7000 FL spectrophotometer, Hitachi, Japan). Samples were continuously scanned with the speed of 2400 nm·min-1 at 5 nm intervals. The emission and excitation wavelengths were 260 to 550 nm and 200 to 450 nm, individually (Elliotts et al. 2006, Chen et al. 2003). The width of the slit was 10 nm for emission and excitation monochromators. Before the fluorescent measurement, the samples would be diluted below 10 mg·L$^{-1}$.

3D-EEM integrated with parallel factor (PARAFAC) analysis was comprehensively used to evaluate the change of dissolved organic matter (DOM), which could help to obtain the DOM variation regularity (Urban-Rich et al. 2006). Over the past two decades, it has been widely reported that PARAFAC could be successfully utilized to decompose EEMs of complex mixtures into their individual fluorescent components (Mazivila et al. 2020, Zhang et al. 2020). The

Table 2: This was Langmuir's model of adsorption isotherms of ammonia nitrogen.

| Model | Soil depth (cm) | Fitted equations | y, x | Correlation coefficient ($R^2$) |
|---|---|---|---|---|
| Langmuir | 0-50 | y=3.24x+149.6 | y=Ce/qe | 0.94 |
| | 50-100 | y=3.06x+97.2 | x=Ce | 0.99 |
| | 100-150 | y=2.19x+101.7 | Ce: Equilibrium concentration | 0.98 |
| | 150-200 | y=3.17+187.4 | Qe: Equilibrated adsorption capacity | 0.95 |

PARAFAC model of EEMs was elucidated by Markager et al. (2011). Before PARAFAC modeling, FL solution 4.0 and DOM Flour toolbox (MATLAB 2009a) were used to wipe off the influence of Raman and Rayleigh scattering.

## RESULTS AND DISCUSSION

### Ammonia Nitrogen Adsorption Process

The observed data were fitted to the Langmuir isothermal adsorption model based on the study reported by Zhang et al. (2015).

The saturated adsorption capacities of the soils in various depths were 0.32, 0.37, 0.34, and 0.26 mg·g$^{-1}$ from the top to the bottom (Table 2). Considering the densities of different layers, the total adsorption capacities were 16.16, 20.38, 19.57, and 16.16 g, respectively.

The ammonia nitrogen removal efficiencies were above 98% during all the experiments at 1.10 m depth. Therefore, the soil at 0~1.10 m played the most important role in ammonia nitrogen elimination. Moreover, the maximal ammonia nitrogen adsorption capacity at 0~1.50 m was

16.16 + 20.38 + 19.57 = 56.11 g. Since the average level of ammonia nitrogen flowed in was 35.33 mg·L$^{-1}$, the load of influent ammonia nitrogen was 35.33 × 0.08 × 3.14 × 0.32 = 0.8g·d$^{-1}$, and the maximal saturation adsorption time was 56.11/0.8 = 70.14 d. Nevertheless, the start-up and domestication time of the system was three months (90 d), and the operation time lasted one year. Therefore, the soil adsorption exhibited no impact on the removal of nitrogen.

### Performances Before and After the Addition of FA

As shown in Fig. 2, trends in COD changes before and after the addition of FA were similar, and the organic matter degradation process could be divided into three parts. In part, at the depth of 0~0.20 m, 40.72% and 39.29% of COD were rapidly degraded before and after adding FA, which mainly contributed to the aerobic decomposition process of organic matter. Certainly, the nitrifying process of ammonia nitrogen, which was restricted because of the high concentration of oxygen and organic matter, and other possibly existing processes consumed a small amount of organic matter. In part II, at a depth of 0.20~1.10 m, due to the gradually decreasing dissolved oxygen concentration, the removal rate of COD
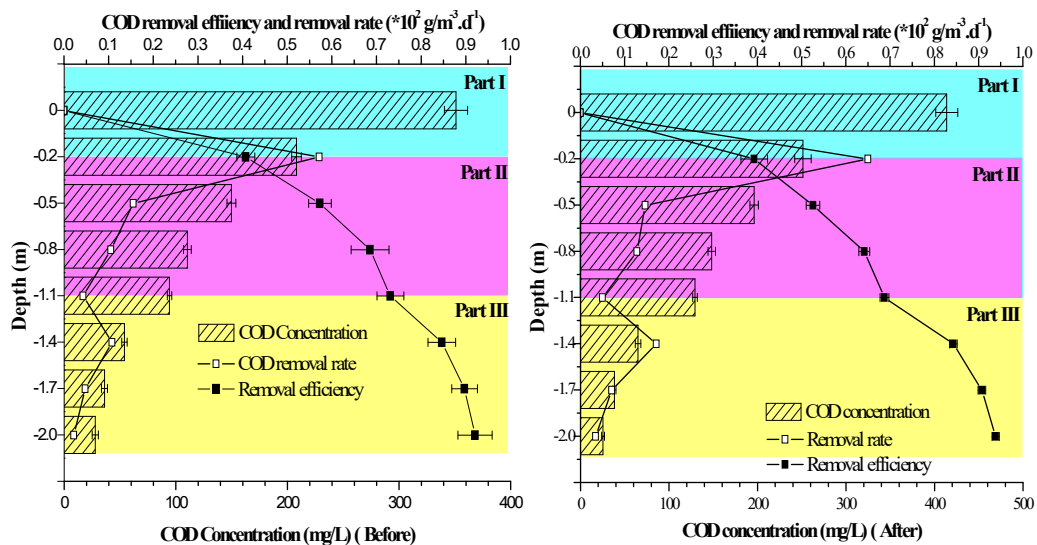


Fig. 2: Variation of COD along the depth before and after the addition of FA. Variation of COD concentration, COD removal efficiency, and removal rate before the addition of FA (left); Variation of COD concentration, COD removal efficiency, and removal rate after the addition of FA. In the figures, error bars were the values of standard deviations (right).

Fig. 3: Variation of TN, $NO_2^-$-N, $NO_3^-$-N, and $NH_4^+$-N along with the depth of soil column. Variation of TN, $NO_2^-$-N, $NO_3^-$-N, $NH_4^+$-N concentration, removal efficiency, and removal rate before the addition of FA (left); Variation of TN, $NO_2^-$-N, $NO_3^-$-N, $NH_4^+$-N concentration, removal efficiency, and removal rate after the addition of FA. In the figures, error bars were the values of standard deviations (right).
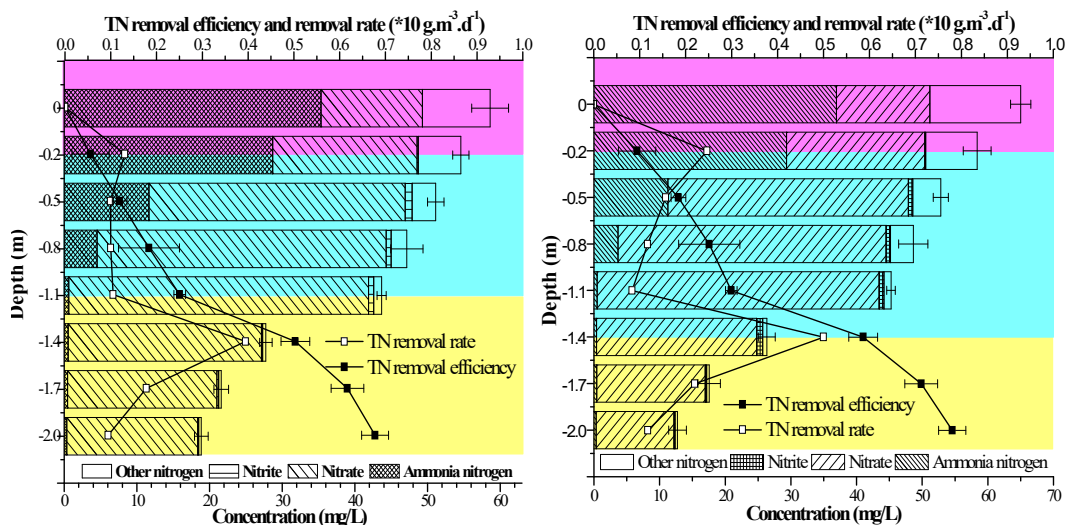
was reduced gradually. In part III, the COD removal rate experienced a rise and then fell. Especially at 1.10~1.40 m, the COD removal rate had a shape rise, which meant some reactions that consumed a great amount of organic matter occurred.

In general, the addition of FA promoted the nitrogen removal process. TN removal efficiency increased to 78.01% after the addition of FA from 67.74%. The nitrogen removal amount was also improved from 39.70 to 50.95 mg·L$^{-1}$.

Nitrification and denitrification were reported to be mainly related to the removal of TN. The nitrification mainly occurred in parts I and II, where more than 98% of ammonia nitrogen was eliminated, so the shape rises of the COD removal rate in part III had little relation with ammonia nitrogen variation. Meanwhile, as shown in Fig. 3, nitrate nitrogen accounted for more than 93% of TN in part III, and the elimination of TN was mainly due to the degradation of nitrate nitrogen, which demonstrated the occurrence of denitrification. That was to say. It was the denitrification process that caused the COD variation in part III.

In part I, before the addition of FA, the nitrification process was seriously limited at 0~0.20 m. The reason might be attributed to the shortage of carbon sources. As described above, nitrification was greatly restricted because of the high concentration of oxygen and organic matter in part I. As organic nitrogen was decomposed and another possible denitrification process was presented, only a small amount of TN was eliminated. Nevertheless, in part II, the nitrification rate reached the maximum at 0.20~0.50 m and then gradually

decreased because of the gradually decreasing concentration of dissolved oxygen and the existence of organic matter. The ammonia nitrogen removal efficiency reached 98.25% at 1.10 m, and only 25.06% of TN was eliminated at 0~1.10 m. In part III, at 1.10~1.40 m, the average TN removal rate was sharply promoted to 3.95 g·m$^{-3}$·d$^{-1}$ and 14.67 mg·L$^{-1}$ nitrate nitrogen was eliminated in this area. However, at 1.40~1.70 and 1.70~2.00 m, the removal rate was reduced to 1.78 and 0.94 g·m-3·d$^{-1}$, suggesting that the denitrification process was limited. Taking the COD variation in part III into consideration, the COD/TN ratio were respectively 2.85, 2.68, and 2.34 mg COD·(mg TN)$^{-1}$ at 1.10~1.40, 1.40~1.70 and 1.70~2.00 m, which were lower than the literature value (Pochana & Keller 1999). It is possible that some refractory organic matter was utilized during the denitrification process due to the lack of biodegradable organics. However, the standard COD determination method could not detect this refractory organic matter. It seemed that during the process of denitrification, the shortage of biodegradable organic matter restricted the elimination of TN.

After adding FA, the nitrogen variation trend was similar to before adding FA. However, the denitrification process was improved to a certain extent. 31.40 mg·L$^{-1}$ of TN was eliminated in part three after the addition of FA, 6.39 mg·L$^{-1}$ higher than before. Meanwhile, the COD removal rate was respectively 14.23, 7.10, and 3.73 g·m$^{-3}$·d$^{-1}$ at 1.10~1.40, 1.40~1.70, and 1.70~2.00 m, which were all higher than before. Also, 103.98 mg.L$^{-1}$ COD was degraded after adding FA, which was 37.43 mg.L$^{-1}$ higher than before. We could conclude that adding FA could provide a high level of carbon

source for denitrification, resulting in the enhancement of TN elimination.

However, the variation of COD could demonstrate the changes in total organic matter. More details about the change rules in organic matter should be studied.

## Fluorescence Spectrum Analysis

The current work elucidated and distinguished the transformation and alteration of organic matter in the SWIS. The analysis of 3DEEM integrated with PARAFAC was comprehensively utilized to quantify the variation of dissolved organic matter (DOM).

The spectra of 72 samples were applied to form the model components. Before PARAFAC modeling, FL solution 4.0 and DOM Flour toolbox were used to wipe off the influence of Raman and Rayleigh scattering. Moreover, all fluorescent data of samples were normalized by dividing by the TOC of each sample. 3-5 component models with non-negativity restrictions were performed. The loadings were converted to positive values and plotted. It was found that a 3-component model was sufficient to depict the dataset and minimize the residuals. Fig. 4 illustrates the position of maximum intensities of PARAFAC components.

The maximum intensity of C1 was located at Ex245/Em410 (Fig. 4), which was associated with fulvic acid-like components (Region III) (Wünsch et al. 2019). The maximum intensities of C2 were located at Ex235/ Em275 and Ex235/ Em340, which were related or correlated to protein-like (such as tryptophan- and tyrosine-like) components (Regions I, II, and IV) (Arellano & Coble 2015, Ishii & Boyer 2012). The locations of maximum intensities of C3 were Ex270/ Em335 and Ex270/ Em460 due to the presence of humic acid-like organic matters (Region V) (Nebbioso & Piccolo 2012, Lyu et al. 2021).

As shown in Tables 3 & 4, there is no significant difference in the change of organic matter between with and without FA addition. At 0~1.10 m, organic matter (mainly protein-like substance, C2) was greatly consumed due to its aerobic degradation and nitrification process. Parts of them were utilized and adsorbed by microorganisms, while others were transformed into refractory substances (such as fulvic acid- and humic acid-like substances (C1, C3)), resulting in a decrease in biodegradability. The result was consistent with the variation of COD. However, at 1.10~1.40 m, the biodegradability increased because of the decrease of C1 and C3 and the increase of C2. It seemed that C1 and C3 were transformed into C2. As described above, the denitrification
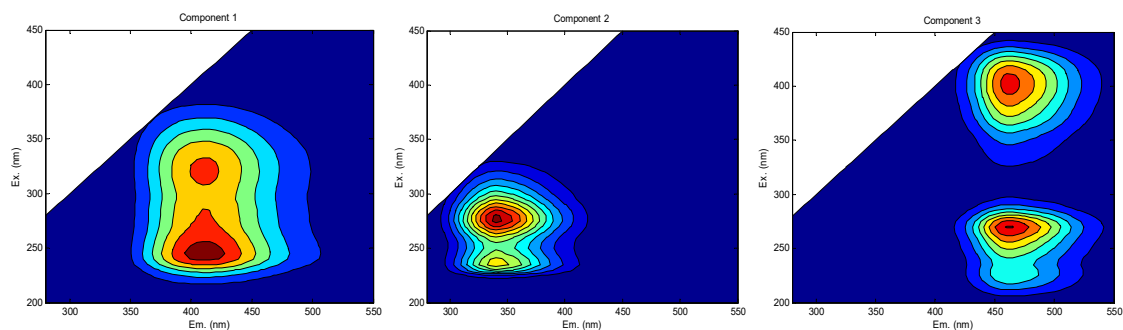


Fig. 4: Fluorescence spectra of three components distinguished by PARAFAC analysis. Component 1 (C1) location of maximum peak: Ex/Em=245/410, in Region III similar to peak fulvic acid-like (left); Component 2 (C2) location of maximum peak: Ex/Em=235,275/340, in Region I, II and IV similar to peak protein-like(middle); Component 3 (C3) location of maximum peak: Ex/Em=270/335,460, in Region V similar to peak humic acid-like (right).

Table 3: This was the biodegradability variation of organic matter before adding FA.

| Dept [m] | C1 (fulvic acid-like) | C2 (protein-like) | C3 (humic acid-like) | Biodegradablity* |
|----------|----------------------|-------------------|----------------------|------------------|
| 0 | 0.0201 | 0.9771 | 0.0028 | 0.0234 |
| 0.20 | 0.1603 | 0.7562 | 0.0835 | 0.3224 |
| 0.50 | 0.1903 | 0.6964 | 0.1133 | 0.4360 |
| 0.80 | 0.2314 | 0.6493 | 0.1193 | 0.5401 |
| 1.10 | 0.2399 | 0.6384 | 0.1217 | 0.5664 |
| 1.40 | 0.2312 | 0.6456 | 0.1232 | 0.5489 |
| 1.70 | 0.2476 | 0.6163 | 0.1361 | 0.6226 |
| 2.00 | 0.2538 | 0.6029 | 0.1433 | 0.6586 |

Table 4: This was the biodegradability variation of organic matter after adding FA.

| Dept [m] | C1 (fulvic acid-like) | C2 (protein-like) | C3 (humic acid-like) | Biodegradablity* |
|---|---|---|---|---|
| 0 | 0.1165 | 0.8790 | 0.0045 | 0.1377 |
| 0.20 | 0.1798 | 0.7338 | 0.0864 | 0.3628 |
| 0.50 | 0.2242 | 0.6769 | 0.0989 | 0.4773 |
| 0.80 | 0.2375 | 0.6425 | 0.1200 | 0.5564 |
| 1.10 | 0.2466 | 0.6235 | 0.1299 | 0.6038 |
| 1.40 | 0.2230 | 0.6565 | 0.1205 | 0.5232 |
| 1.70 | 0.2518 | 0.6121 | 0.1361 | 0.6337 |
| 2.00 | 0.2627 | 0.5948 | 0.1425 | 0.6812 |

*Biodegradablity = (C1+C3)/C2, which represents the biodegradability of organic matter. The smaller the biodegradability is, the easier the organic matter to be utilized by microorganisms.

process occurred at 1.10~2.00 m. Especially at 1.10~1.40 m, the denitrification rate was the highest. We could conclude that parts of refractory organic matter were degraded into biodegradable ones at 1.10~1.40 m, then implemented as carbon sources for denitrification. A similar result was reported by Nakhla and Farooq (2003). They demonstrated that the refractory organics were not able to be implemented as the carbon source for denitrification until the refractory organics were degraded into easily biodegradable organics. Moreover, after the addition of FA, 104.98 mg·L$^{-1}$ of COD was degraded for the denitrification process, 57.75% higher than that before the addition of FA, which eliminated 31.40 mg·L$^{-1}$ of TN, 28.64% higher than that before the addition of FA. It indicated that more FA-like matter was translated into protein-like matter after adding FA.

Overall, we could conclude that adding FA helped produce more easily degradable organic matter for denitrification, which enhanced the denitrification performance in the deep SWIS.

## CONCLUSION

When a hydraulic loading was set as 8 cm·d$^{-1}$ in DSWIS, the ammonia nitrogen, and COD could be efficiently removed before and after the FA addition. However, in the lower part, the removal efficiency of TN was insufficient due to the shortage of carbon sources which hindered the process of denitrification. Nevertheless, adding FA could facilitate the production of more easily degradable organics for denitrification, resulting in the enhancement of denitrification and the elimination of total nitrogen in the DSWIS.

## ACKNOWLEDGEMENT

## REFERENCES

Arellano, A.R. and Coble, P.G. 2015. Assessing carbon and nutrient inputs in a spring-fed estuary using fluorescence spectroscopy and discriminatory classification. Limnol. Oceanogr., 60 (3): 789-804.

Bieber, S., Snyder, S. A., Dagnino, S., Rauch-Williams, T. and Drewes, J.E. 2018. Management strategies for trace organic chemicals in water: A review of international approaches. Chemosphere, 195: 410-426.

Chen, F.M., Li, G.W., Li, X.G., Wang, H.Q., Wu, H.B., Li, J.X., Li, C.L., Li, W., Zhang, L.Y. and Xi, B.D. 2021. The cotreatment of old landfill leachate and domestic sewage in rural areas by deep subsurface wastewater infiltration system (SWIS): Performance and bacterial community. Environ. Pollut., 274(24): 115800.

Chen, W., Westerhoff, P., Leenheer, J.A. and Booksh, K. 2003. Fluorescence excitation–emission matrix regional integration to quantify spectra for dissolved organic matter. Environ. Sci. Technol., 37(24): 5701-5710.

Christianson, L.E., Lepine, C., Sibrell, P.L. and Penn, C. and Summerfelt, S.T. 2017. Denitrifying woodchip bioreactor and phosphorus filter pairing to minimize pollution swapping. Water Res., 121: 129-139.

E.P.A. (4th ed.) 2002. Standard methods for the examination of water and wastewater, China Environmental Science Press, pp.210.

Elliotts, S., Lead, J.R. and Baker, A. 2006. Characterisation of the fluorescence from freshwater, planktonic bacteria. Water Res., 40(10): 2075-2083.

Eregno, F.E. and Heistad, A. 2019. On-site treated wastewater disposal systems – The role of stratified filter media for reducing the risk of pollution. Environ. Int., 124: 302-311.

Gu, Y.F., Wei, Y., Xiang, Q.J., Zhao, K., Yu, X.M. Zhang, X.P., Li, C.N., Chen, Q., Xiao, H. and Zhang, X.H. 2019. C:N ratio shaped both the taxonomic and functional structure of microbial communities in livestock and poultry breeding wastewater treatment reactor. Sci. Total Environ. 651:625-633.

Ishii, S.K.L. and Boyer, T.H. 2012. Behavior of reoccurring PARAFAC components in fluorescent dissolved organic matter in natural and engineered systems: A critical review. Environ. Sci. Technol., 46(4): 2006-2017.

Jia, L.P., Cheng, X. L., Fang, L.C. and Huang, X. G. 2023.Nitrogen removal in improved subsurface wastewater infiltration system: Mechanism, microbial indicators and the limitation of phosphorus. J. Environ. Manage., 335: 117456.

Jia, L.P., Jiang, B.H., Huang, F. and Hu, X.M. 2019. Nitrogen removal mechanism and microbial community changes of bioaugmentation subsurface wastewater infiltration system. Bioresour. Technol., 294: 22-140.

Kawasaki, K. 2019. Paleomagnetism of the Mn wad deposit at Niimi hot springs, Hokkaido, Japan. Can. J. Earth Sci., 56(9): 973-982.

Li, W., Liang, C.L., Dong, L., Zhao, X. and Wu, H.M. 2021a.Accumulation and characteristics of fluorescent dissolved organic matter in loess soil-based subsurface wastewater infiltration system with aeration and biochar addition. Environ. Pollut., 269: 16100.

Li, Y.H., Peng, L.L., Zhang, Y., Li, H.B., Wang, Y.Y., Su, F. and Qian. J. 2023. Simultaneous removal of typical antibiotics and nitrogen by SWIS assisted by iron carbon micro-electrolysis. Chem. Eng. Res. Des.,192: 289-298.

Li, Y.H., Yang, L., Peng L.L., Liu, D.Z. and Li, H.B. 2021b. How does the operation time affect the performance and metabolomics of the subsurface wastewater infiltration bed? Desalin. Water Treat., 223: 146-153.

Lv, J.J., Dou, Y.Y., Gong, W.J., Duan, X.J., Hou, L.A., Zhang, L.Y., Xi, B.D. and Yu, S.L. 2019. Characterization of Dissolved Organic Matter in Hybrid Constructed Wetlands Using Three-Dimensional Excitation-Emission Matrix Fluorescence Spectroscopy. J. Water Chem. Techno., 41(2): 113-118.

Lv, J.J., Gong, W.J., Dou, Y.Y., Duan, X.J., Liu, H.F., Zhang, L.Y., Xi, B.D., Yu, S.L. and Hou, L.A. 2020. Spectroscopy and microbiological analysis of soil infiltration clogging in treating aged swine wastewater. Spectrosc. Spect. Anal., 40(5): 1541-1546.

Lyu, C., Liu, R., Li, X.J., Song, Y.H. and Gao, H.J. 2021. Degradation of dissolved organic matter in the effluent of municipal wastewater plant by a combined tidal and subsurface [flow] constructed wetland. J. Environ. Sci., 106: 171-181.

Markager, S., Stedmon, C.A. and Sondergaard, M. 2011. Seasonal dynamics and conservative mixing of dissolved organic matter in the temperate eutrophic estuary Horsens Fjord. Estuar. Coast. Shelf S., 92(3): 376-388.

Mazivila, S.J., Castro, R.A.E., Leitão, J.M.M. and da Silva, J.C.G.E. 2020. At-line monitoring of the salification process of the antiretroviral lamivudine-saccharinate salt using FT-MIR spectroscopy with multivariate curve resolution. Vib. Spectrosc., 106:102992.

Nakhla, G. and Farooq, S. 2003. Simultaneous nitrification-denitrification in slow sand filters. J. Hazard. Mater. 96(2-3): 291-303.

Nebbioso, A. and Piccolo, A. 2012. Molecular characterization of dissolved organic matter (DOM): a critical review. Anal. Bioanal. Chem. 405(1): 109-124.

Payne, E.G.I., Pham, T., Cook, P.L.M., Deletic, A., Hatt, B.E. and Fletcher, T.D. 2017. Inside story of gas processes within stormwater biofilters: Does greenhouse gas production tarnish the benefits of nitrogen removal? Environ. Sci. Technol., 51(7): 3703-3713.

Perujo, N., Sanchez-Vila, X., Proia, L. and Romaní, A.M. 2017. Interaction between Physical Heterogeneity and Microbial Processes in Subsurface Sediments: A Laboratory-Scale Column Experiment. Environ. Sci. Technol., 51(11): 6110-6119.

Pochana, K. and Keller, J. 1999. Study of factors affecting simultaneous nitrification and denitrification (SND). Water Sci. Technol., 39(6): 61-68.

Qin, S.N., Huang, F., Jiang, B.H. and Jia L.P. 2021.Evaluation of the removal performance in the long-term operation of bioaugmented subsurface wastewater infiltration systems under a high hydraulic loading rate. Environ. Technol. Inno.24: 101918.

Shokri, M., Kibler, K.M., Hagglund, C., Corrado, A., Wang, D.B., Beazley, M. and Wanielista. M. 2021. The hydraulic and nutrient removal performance of vegetated filter strips with engineered infiltration media for treatment of roadway runoff. J. Environ. Manag., 300: 113747.

Stevenson F. and Cole M. 1999. Cycles of soils: Carbon, nitrogen, phosphorus, sulfur, micronutrients, 2nd ed. John Wiley& Sons Inc., pp. 26.

Su, F., Li, Y.H., Qian, J., Wang, Y.Y. and Zhang, Y. 2023. Does the repeated freezing and thawing of the aerobic layer affect the anaerobic release of $N_2O$ from SWIS? Sci. Total Environ., 859(2): 160313.

Urban-Rich, J., McCarty, J.T., Fernández, D., Acuña, J.L. 2006. Larvaceans and copepods excrete fluorescent dissolved organic matter (FDOM). J. Exp. Mar. Biol. Ecol., 332(1): 96-105.

Wünsch, U., Bro, R., Stedmon, C., Wenig, P. and Murphy, K. 2019. Emerging patterns in the global distribution of dissolved organic matter fluorescence. Anal. Methods, 11: 616 doi:10.1039/c8ay02422g.

Xu, J.J., Wu, X.H., Zhu, N.W., Shen, Y.W. and Yuan, H. P. 2020. Anammox process dosed with biochars for enhanced nitrogen removal: Role of surface functional groups. Sci. Total Environ., 748: 141367.

Yamaguchi, T., Moldrup, P., Rolston, D.E., Ito, S. and Teranishi, S. 1996. Nitrification in porous media during rapid, unsaturated water flow. Water Res., 30(3): 531-540.

Yang, L., Li, Y.H., Su, F. and Li, H.B. 2020. Metabolomics study of subsurface wastewater infiltration system under fluctuation of organic load. Curr. Microbiol., 77(2): 261-272.

Yang, P., Hou, R.R., Yuan, R.Y., Wang, F., Chen, Z.B., Zhou, B.H. and Chen, H.L. 2022. Effect of intermittent operation and shunt wastewater on pollutant removal and microbial community changes in subsurface wastewater infiltration system. Process Saf. Environ., 165: 255-265.

Yang, S.L., Zheng, Y.F., Mao, Y.X., Xu, L., Jin, Z., Zhao, M., Kong, H.N., Huang, X.F. and Zheng, X.Y. 2021.Domestic wastewater treatment for single household via novel subsurface wastewater infiltration systems (SWISs) with NiiMi process: Performance and microbial community. J. Clean. Prod., 279: 123434.

Ye, C., Hu, Z.B., Kong, H.N. Wang, X.Z. and He, S.B. 2008. A new soil infiltration technology for decentralized sewage treatment: Two-stage anaerobic tank and soil trench system. Pedosphere, 18(3): 401-408.

Yu, G.L., Peng, H.Y., Fu, Y.Q., Yan, X.J., Du, C.Y. and Chen, H. 2019. Enhanced nitrogen removal of low C/N wastewater in constructed wetlands with co-immobilizing solid carbon source and denitrifying bacteria. Bioresour. Technol., 280: 337-344.

Yuan, H.P., Nie, J.Y., Gu, L. and Zhu, N.W. 2016. Studies on affecting factors and mechanism of treating decentralized domestic sewage by a novel anti-clogging soil infiltration system. Environ. Technol., 37(23): 3071-3077.

Zhang, J., Song, F.H., Li, T.T., Xie, K.F., Yao, H.Y., Xing, B.S., Li, Z.Y. and Bai. Y.C. 2020. Simulated photo-degradation of dissolved organic matter in lakes revealed by three-dimensional excitation-emission matrix with regional integration and parallel factor analysis. J. Environ. Sci., 90(1): 310-320.

Zhang, L.Y., Ye, Y.B., Wang, L. Xi, B.D., Wang, H.Q. and Li, Y. 2015. Nitrogen removal processes in deep subsurface wastewater infiltration systems. Ecol. Eng., 77: 275-283.

Zheng, F.P., Tan, C.Q., Hou, W.Y., Huang, L.L., Pan J. and Qi S.Y. 2018a. Does the influent COD/N ratio affect nitrogen removal and $N_2O$ emission in a novel biochar-sludge amended soil wastewater infiltration system (SWIS)? Water Sci. Technol., 78(2): 347-357.

Zheng, F.P., Zhao, Y., Li, Z.Q., Tan, C.Q., Pan, J., Fan, L.L., Xiao, L. and Hou, W.Y. 2018b. Nitrogen removal and $N_2O$ emission by shunt distributing wastewater in aerated or non-aerated subsurface wastewater infiltration systems under different shunt ratios. Water Sci. Technol., 78(2): 329-338.

# Potassium Solubilizing Bacteria (KSB) and Osmopriming Mediated Morphological Changes and Triggers in Yield of Green Gram (*Vigna radiata* L.) Under Water-Limiting Conditions

## A. Kalangutkar and A. Siddique†

Department of Agronomy, School of Agriculture, Lovely Professional University, Phagwara-144 411, Jalandhar, Punjab, India

†Corresponding author: A. Siddique; anaytullahsiddique@gmail.com

## ABSTRACT

A field-based experiment was conducted to know the relevance of potassium solubilizing bacteria (KSB), and Osmo-priming mediated morphological changes and yielded recovery in green gram (*Vigna radiata* L.) under water-limiting conditions. Hence, the experiment was carried out at the research farm of Lovely Professional University. The characters like plant height, number of leaves, leaf area plant$^{-1}$, and LAI were considered to track the morphological changes, while the primary branches, nodules, pods plant$^{-1}$, seeds pod$^{-1}$, the average length of the pod, test weight, biological yield, grain yield, and harvest index (HI) were used to determine the recovery of yield as compared to control. Among the treatments, $T_8$ was recorded as one of the best treatments for all the morphological parameters studied, *i.e.,* plant height (51.80 cm), number of leaves (42 plant$^{-1}$), leaf area (577.27 cm$^2$.plant$^{-1}$) and LAI (1.92) while most of the yield contributing characters were found better in $T_6$ *i.e.* nodules (8.3 plant$^{-1}$), seeds pod$^{-1}$ (10) and length of the pod (7.65 cm) except for the primary branches and the number of pods plant$^{-1}$ which was remain recorded maximum in $T_8$ (6.0 and 22). The yield of green gram and its biological yield were recorded as highest in $T_6$ and $T_2$ (6.83 and 24.23 g.plant$^{-1}$), while HI and test weight were also noted in $T_6$ (32.0% and 5.90 g). This study has concluded that the KSB, combined with $KNO_3$ showed a strong potential to modify the morphological structure while the yield of green gram was in KSB + $Ca(NO_3)_2$ under water scarcity.

## INTRODUCTION

The green gram (*Vigna radiata* L.) is a Leguminosae (Fabaceae) family member, widely grown as a pulse crop in arid and semi-arid regions. It is highly protein, easily digested, and can fix nitrogen with a symbiotic association with Rhizobia (Khiangte & Siddique 2022). India is the world's largest producer of green gram, producing 1.5 to 2.0 million tonnes of green gram from 3 to 4 million hectares of area annually (Pandey et al. 2019). Around 42% of India's land is under drought, thus simultaneously impacting agriculture production and yield. For several years, such conditioned priming has been a widely used technique for reviving seeds to increase agronomic production. Seed priming is a method of controlled hydration that exposes seeds to low water potentials, allowing pre-germinative physiological and biochemical changes that boost stand establishment and yield (Anaytullah & Bose 2007, Devika et al. 2021). In seed priming, seeds are treated with a variety of organic and inorganic compounds, *i.e.,* hydropriming,

halopriming, osmo-priming, hormone priming, and solid-matrix priming for a predetermined amount of time under controlled conditions before sowing, which then causes biochemical changes by adjusting the temperature and moisture content of the seeds bringing them closer to germination before being dried back to its original moisture content (Singh et al. 2020, Zulfiqar 2021, Eshkab et al. 2021, Pawar & Laware 2018, Rhaman et al. 2022).

Osmo-priming is a pre-sowing approach that helps in maintaining the plasma membrane, which allows the osmo-primed seeds to germinate more rapidly, which is why seedlings grow more quickly, more aggressively, and better in complicated situations under specific physiological, biochemical, cellular, and molecular variations. Additionally, it solubilizes storage proteins, boosts antioxidant activity, and lowers lipid peroxidation (Marthandan et al. 2020).

Potassium is an essential nutrient that plants need for a wide range of processes, including antioxidative defense mechanisms. This element is present in the soil in bound

form, and only 1%–2% of the total potassium in the earth's crust is available to plants (Meena et al. 2016). Many strains of soil microorganisms show efficiency in converting the insoluble form of potassium to solubilize or mobilize it into a usable form (Choudhary & Siddique 2020). Hence, in the present study, we used KSB in combination with osmopriming agents to overcome the impact of drought on green gram.

## MATERIALS AND METHODS

An experiment was planned and executed over the Research Farm of Lovely Professional University, Punjab, in the summer of March 2020, wherein the SML-668 variety of green gram was used. The entire experiment was executed in Randomized Block Design (RBD) with three replications and eight treatments, while the total treatments were used in combinations of potassium solubilizing bacteria (KSB) and priming agents. The priming treatments were employed using nitrates of Ca and K in two different concentrations, i.e., Ca $(NO_3)_2$, 7.0 and 10 mM and $KNO_3$, 12.0 and 15 mM, by considering eight hours of priming duration. The culture of potassium solubilizing bacteria was used as a soil application in two concentrations, which were used as per the recommended dose of 3 to 5 L.acre$^{-1}$, respectively. Standard agronomic and cultural practices were followed during the entire growth period of the crop, like field preparation, sowing, weeding, fertilizer application, and plant protection measures. However, one irrigation was skipped before flowering in all treatments, including the control, to create water-limiting conditions. After the establishment of the plant over the field, randomly 5 plants were tagged from each plot to record morphological observations like plant height, number of leaves, number of primary branches plant$^{-1}$, and number of nodules plant$^{-1}$ while the leaf area plant$^{-1}$ was measured through the leaf area meter (Model No. 211) and the leaf area index (LAI) was derived as per the (Watson 1947).

$$\text{Leaf Area Index (LAI)} = \frac{\text{Leaf area (cm}^2)}{\text{Ground area (cm}^2)}$$

The estimation of yield and yield attributing characters, i.e., the number of pods plant$^{-1}$, the number of seeds pod$^{-1}$, the length of pod plant$^{-1}$, biological yield, and grain yield, were measured at the maturity stage by considering the tagged plants of each plot. The formula given by (Donald & Hamblin 1976) was used to calculate HI% while 100 seeds were used to record the test weight.

$$\text{Harvest Index (\%)} = \frac{\text{Grain yield}}{\text{Biological yield}} \times 100$$

SPAD reading was measured using a SPAD meter (Model No-SPAD-502 Plus), which measures the greenness of chlorophyll in field conditions.

## RESULTS

### Morphological Changes due to KSB and Osmopriming Treatments

The impact of potassium solubilizing bacteria (KSB) and osmo-priming with nitrate-based salts Ca and K were studied in green grams under water-limiting conditions. Data depicted from (Table 1) revealed that the $T_8$ ($KSB_2$ + $KNO_3$, 15 mM) was recorded as significantly highest (p<0.05%) plant height (cm), the number of leaves plant$^{-1}$, leaf area (cm$^2$) and LAI (51.80, 42, 577.27 and 1.924) compared to control set (39.5, 32.67, 483.30 and 1.61) while the second most significantly highest was recorded in $T_4$ ($KSB_1$ + $KNO_3$, 15 mM) for the plant height (cm) and the number of leaves plant$^{-1}$ (50.93 and 41.33) and $T_6$ ($KSB_2$ + Ca($NO_3$)$_2$, 12 mM) for leaf area cm$^2$ and LAI (562.77 and 1.87) which T7 followed for plant height and the number of leaves plant$^{-1}$ (50.23 and 40) and $T_4$ for leaf area and LAI (549.17 and 1.83). The data % increase/decrease over the control was presented in parenthesis, which justifies the performance of the treatment concerning parameters. The % increase/decrease over the control showed that the treatment $T_8$ has maximum gain in growth for plant height, number of leaves plant$^{-1}$, leaf area (cm$^2$), and LAI (23.62, 22.22, 16.28, and 16.28). The scrutiny of the data for the performance of KSB revealed that $KSB_2$ is better than $KSB_1$ for most of the parameters (Table 1).

### Influence of KSB and Osmopriming Treatments on Yield Attributes

Data presented in (Table 2) reveals the significance of KSB and Osmo-priming-based salts of nitrates, i.e., Ca and K, under water-limiting conditions. Out of all the combinations of the treatment, again $T_8$ was recorded as one of the best combinations which was significantly highest (p<0.05%) for the number of primary branches and pods plant$^{-1}$ (6.0 and 22), while $T_6$ for the nodules, length of pod plant$^{-1}$ (cm) and seeds pod$^{-1}$ (8.33, 7.65 and 10.0) compared to control set (3.67, 4.33, 16.0, 6.63 and 6.10). The second most significantly highest number of primary branches and pods plant$^{-1}$ was recorded in $T_6$ (5.0 and 21), while nodules, length of pod plant$^{-1}$, and seeds pod$^{-1}$ were recorded in $T_8$ (7.33, 7.37, and 9.13). The computed data of % increase/ decrease over the control presented in (Table-2) justified the impact of treatment. They found that the highest % increase was recorded in $T_8$ for primary branches and pods plant$^{-1}$

Table 1: KSB and Osmo-priming-based changes on plant height (cm), number of leaves, leaf area plant[-1,] and LAI under water-limiting conditions.

| Treatments | PH at harvest | No. of leaves plant[-1] | Leaf area plant[-1] | LAI |
|---|---|---|---|---|
| $T_0$ | 39.57 ± 2.46 | 32.67 ± *1.45* | 483.30 ± 6.36 | 1.611 ± 0.02 |
| $T_1$ | 46.07 ± 1.79 [8.13%] | 33.33 ± *1.45* [2.00%] | 523.27 ± 5.39 [7.64%] | 1.744 ± 0.01 [7.64%] |
| $T_2$ | 41.80 ± 2.93 [9.67%] | 35.00 ± *1.15* [6.67%] | 535.67 ± 24.18 [9.78%] | 1.786 ± 0.08 [9.78%] |
| $T_3$ | 46.40 ± 2.75 [14.73%] | 35.33 ± *1.20* [7.55%] | 490.83 ± 5.28 [1.53%] | 1.636 ± 0.01 [1.53%] |
| $T_4$ | 50.93 ± 3.39 [20.76%] | 41.331.38± [20.97%] | 549.17 ± 4.98 [11.99%] | 1.831 ± 0.02 [11.99%] |
| $T_5$ | 47.23 ± 3.67 [16.23%] | 38.33 ± *3.38* [14.78%] | 488.53 ± 3.21 [1.07%] | 1.628 ± 0.01 [1.07%] |
| $T_6$ | 49.87 ± 1.07 [20.66%] | 40.00 ± *1.52* [18.33%] | 562.77 ± 18.12 [14.12%] | 1.876 ± 0.06 [14.12%] |
| $T_7$ | 50.23 ± 0.86 [21.70%] | 40.00 ± 1.15 [19.67%] | 526.43 ± 17.09 [8.19%] | 1.755 ± 0.05 [8.19%] |
| $T_8$ | 51.80 ± 1.34 [23.62%] | 42.00 ± *2.40* [22.22%] | 577.27 ± 22.44 [16.28%] | 1.924 ± 0.07 [16.28%] |
| CD at (p<0.05) | 7.58 | 6.55 | 44.25 | 0.14 |

**Notes:** 1. $T_0$ = Control, $T_1$ = $KSB_1$ + Ca $(NO_3)_2$ [7.0 mM], $T_2$ = $KSB_1$+ Ca $(NO_3)_2$ [10.0 mM], $T_3$ = $KSB_1$+ $KNO_3$ [12.0 mM], $T_4$ = $KSB_1$ + $KNO_3$ [15.0 mM], $T_5$ = $KSB_2$ + Ca $(NO_3)_2$ [7.0 mM], $T_6$ = $KSB_2$ + Ca $(NO_3)_2$ [10mM], $T_7$ = $KSB_2$ + $KNO_3$ [12mM], $T_8$ = $KSB_2$ + $KNO_3$ [15mM]

2. Data in parenthesis represent % increase/decrease over control.

Table 2: KSB and Osmo-priming-based changes on primary branches, nodules, pods plant[-1], seeds pod[-1] and length of pods plant[-1] in green gram under water-limiting conditions.

| Treatments | Primary branches Plant[-1] at harvest | Nodules plant[-1] at harvest | Pods plant[-1] at harvest | Seeds pod[-1] | Length of pod plant[-1] [cm] |
|---|---|---|---|---|---|
| $T_0$ | 3.67 ± 0.33 | 4.33 ± 0.33 | 16.00 ± 1.52 | 6.63 ± 0.32 | 6.10 ± 0.02 |
| $T_1$ | 3.67 ± 0.33 [0.00%] | 5.67 ± 0.33 [23.53%] | 17.33 ± 0.88 [7.69%] | 7.31 ±0.27 [9.22%] | 6.47 ± 0.14 [5.77%] |
| $T_2$ | 4.33 ± 0.33 [15.3%] | 7.33 ± 0.33 [40.91%] | 20.00 ± 0.57 [20.00%] | 8.37 ±0.18 [20.72%] | 7.26 ± 0.17 [16.06%] |
| $T_3$ | 4.33 ± 0.33 [15.38%] | 5.67 ± 0.33 [23.53%] | 17.17 ± 0.33 [6.80%] | 7.80 ±0.25 [14.96%] | 6.90 ± 0.19 [11.60%] |
| $T_4$ | 5.0 ± 0.57 [26.67%] | 5.67 ± 0.33 [23.53%] | 20.17 ± 0.44 [20.66%] | 7.90 ± 0.20 [16.03%] | 7.20 ± 0.21 [15.28%] |
| $T_5$ | 4.33 ± 0.33 [15.38%] | 5.67 ± 0.33 [23.53%] | 18.17 ± 0.33 [11.93%] | 8.17 ± 0.16 [18.78%] | 7.11 ± 0.01 [14.29%] |
| $T_6$ | 5.0 ± 0.57 [26.67%] | 8.33 ± 0.33 [48.00%] | 21.00 ± 0.28 [23.81%] | 10.00 ±0.57 [33.67%] | 7.65 ± 0.09 [20.31%] |
| $T_7$ | 4.00 ± 0.00 [8.33%] | 7.33 ± 0.33 [40.91%] | 19.83 ± 1.16 [19.33%] | 9.00 ± 0.57 [26.30%] | 7.29 ± 0.14 [16.33%] |
| $T_8$ | 6.00 ± 0.00 [38.89%] | 7.33 ± 0.33 [40.91%] | 22.00 ± 0.57 [27.27%] | 9.13 ± 0.59 [27.37%] | 7.37 ± 0.21 [17.24%] |
| CD at (p<0.05) | 1.10 | 1.06 | 2.31 | 1.18 | 0.48 |

(38.89 and 27.27) while $T_6$ for nodules, length pod plant[-1,] and seeds pod[-1] (48, 23.31, and 33.67). Scrutiny about the impact of KSB showed that $KSB_2$ is performing well in combination with osmo-priming treatment compared to the combinations of $KSB_1$.

### Influence of KSB and Osmopriming Treatments on Yield

Data presented in Table 3 was found significant (p<0.05%) for biological yield (g.plant[-1]), grain yield (g.plant[-1]), HI (%),

and test weight (g) at harvest. The highest biological yield, g.plant$^{-1}$, was obtained in $T_2$ (24.23), while the highest grain yield (g plant$^{-1}$), HI (%), and test weight(g) were found in $T_6$ (6.83, 32, and 5.90). The second highest value for biological yield was recorded in $T_4$ (21.87), and grain yield, HI (%), and test weight (g) were observed in $T_6$ (6.67, 67.72, and 5.67). The value of % increase/decrease over control was also found in $T_2$ for biological yield (21.60) while $T_6$ was detected for grain yield (27.80), HI and test weight (18.88 and 29.42)

over control (Fig. 1). Close analysis of the data for the grain yield, HI and Test weight indicated that the combinations of the $KSB_2$ and osmopriming agent in combinations of osmopriming agents performed better than combinations of $KSB_1$.

**Trigger in SPAD Reading Due to KSB and Osmopriming Treatments**

The impact of KSB in combination with osmo-priming agents showed a significant difference at ($p<0.05$%) for the SPAD

Table 3: KSB and Osmo-priming-based triggers on biological yield, grain yield, harvest index (%), and test weight (g) in green gram under water-limiting conditions.

| Treatments | Biological yield [g. plant$^{-1}$] | Grain yield [g.plant$^{-1}$] | HI % | Test weight [g] |
|---|---|---|---|---|
| $T_0$ | 19.0 ± 0.58 | 4.93 ± 0.29 | 25.95 ± 0.12 | 4.17 ± 0.12 |
| $T_1$ | 20.10 ± 0.64 [5.47] | 5.33 ± 0.17 [7.50] | 26.54 ± 0.42 [2.21] | 4.42 ± 0.06 [5.80%] |
| $T_2$ | 24.23 ± 0.41 [21.60] | 6.33 ± 0.07 [22.10] | 26.16 ± 0.70 [0.78] | 4.50 ± 0.13 [7.48%] |
| $T_3$ | 21.60 ± 0.38 [12.04] | 5.87 ± 0.12 [15.91] | 27.20 ± 1.04 [4.57] | 4.28 ± 0.04 [2.72%] |
| $T_4$ | 21.87 ± 1.13 [13.11] | 6.27 ± 0.07 [21.28] | 28.78 ± 1.22 [9.83] | 4.64 ± 0.06 [10.14%] |
| $T_5$ | 20.97 ± 0.78 [9.38] | 6.00 ± 0.12 [17.78] | 28.70 ± 1.26 [9.56] | 5.53 ± 0.01 [24.61%] |
| $T_6$ | 21.40 ± 0.55 [11.21] | 6.83 ± 0.09 [27.80] | 32.00 ± 1.25 [18.88] | 5.90 ± 0.01 [29.42%] |
| $T_7$ | 21.13 ± 0.43 [10.09] | 6.17 ± 0.18 [20.0] | 29.18 ± 0.61 [11.06] | 5.12 ± 0.01 [18.57%] |
| $T_8$ | 21.83 ± 1.04 [12.98] | 6.67 ± 0.13 [26.0] | 30.72 ± 1.98 [15.52] | 5.67 ± 0.01 [26.51%] |
| CD at ($p<0.05$) | 2.23 | 0.46 | 3.73 | 0.21 |
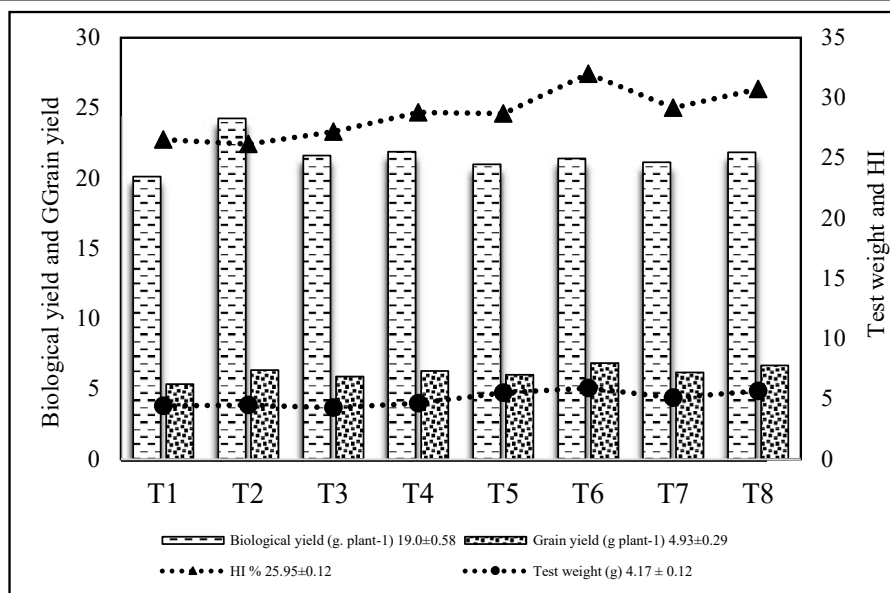


Fig. 1: KSB and Osmo-priming-based triggers on biological yield, grain yield, harvest index (%), and test weight (g) in green gram under water-limiting conditions.

Table 4: KSB and Osmo-priming-based triggers on SPAD reading in green gram under water-limiting conditions.

| Treatments | SPAD Chlorophyll at 20 DAS | SPAD Chlorophyll at 40 DAS | SPAD Chlorophyll at harvest |
|---|---|---|---|
| $T_0$ | 35.43 ± 0.40 | 46.63 ± 0.96 | 25.23 ± 0.95 |
| $T_1$ | 36.43 ± 0.37 [2.74%] | 50.90 ± 0.75 [8.38%] | 27.40 ± 0.25 [7.91%] |
| $T_2$ | 38.53 ± 0.88 [8.04%] | 51.60 ± 0.11 [9.63%] | 27.53 ± 0.99 [8.35%] |
| $T_3$ | 35.53 ± 0.63 [0.28%] | 52.63 ± 0.41 [11.40%] | 28.47 ± 0.94 [11.36%] |
| $T_4$ | 39.77 ± 0.26 [10.90%] | 53.83 ± 0.46 [13.37%] | 30.20 ± 1.42 [16.45%] |
| $T_5$ | 40.33 ± 0.06 [12.15%] | 52.47 ± 1.46 [11.12%] | 28.43 ± 2.11 [11.25%] |
| $T_6$ | 40.23 ± 0.86 [11.93%] | 54.90 ± 0.83 [15.06%] | 31.77 ± 0.84 [20.57%] |
| $T_7$ | 37.30 ± 0.55 [5.00%] | 53.17 ± 1.03 [12.29%] | 31.13 ± 0.88 [18.95%] |
| $T_8$ | 43.57 ± 0.57 [18.67%] | 58.63 ± 0.53 [20.47%] | 34.23 ± 0.24 [26.29%] |
| C.D at (p<0.05). | 1.61 | 2.50 | 3.28 |

unit. The SPAD reading was recorded at regular intervals of 20, 40, and at the harvest stage, wherein the highest reading was recorded at 40 DAS in all the sets of treatment compared to 20 and at the harvest stage. Among the treatments, the highest SPAD reading was recorded in $T_8$ (43.57, 58.63, and 34.23), which represents the % increase/decrease over control of 18.67, 20.47, and 26.29% as compared to control at the regular intervals of 20, 40, and at harvest stage of the crop (Table 4). However, data depicted from (Fig. 1) also showed that the second highest SPAD reading was in $T_6$ (54.90 and 31.77) at 40 DAS and the harvest stage of the crop with % increase/decrease over control (15.06 and 20.57) as compared to controls. The response of KSB in combinations of priming treatment revealed $KSB_2$ support better than $KSB_1$ for SPAD reading.

## Influence of the Treatments among the Studied Parameters

Relationships among the parameters were studied in the present work under water-limiting conditions. It seems from the data presented in (Table 5) that the arrows in the upward direction indicating parameters had a high level of positive correlation with each other and downward arrows indicating a high level of negative correlation among them, while the horizontal direction of arrows indicated that the parameters were positively correlated with a low level of significance due to the impact of KSB based osmopriming treatments under water limiting conditions.

## DISCUSSION

The importance of nutrients is well known to regulate several metabolic processes in, which photosynthesis, respiration, transpiration, nutrients, and water uptakes are some. It also acts as a cofactor responsible for activating many enzymes for several other metabolic processes. Moreover, potassium and calcium play a vital role in water-limiting conditions, a kind of drought (Guo et al. 2019). The data pertaining in (Table 1) reveals that the morphological parameters like PH, Number of leaves, leaf area, and LAI studied in the present work were positively influenced by $T_8$ ($KSB_2$ + $KNO_3$, 15mM) concentration followed by $T_6$ ($KSB_2$ + $Ca(NO_3)_2$, 10mM) for most of the morphological parameters except to PH compared to a control set while $KSB_2$ was common in both the treatment. Archana et al. (2012) reported that the potassium-solubilizing bacteria (KSB) is capable of releasing the K from the inorganic source, while seed priming with potassium nitrate was well documented by (Siddique & Bose 2015, Moaaz et al. 2020, Zrig et al. 2022) and (Arun et al. 2016) who reported that priming treatment with $KNO_3$ and $Ca(NO_3)_2$ not only triggers seed germination but also influence the further morphological growth in plants. Therefore, the combined effect of KSB-based osmopriming agents reflected their impact on PH, number of leaves, leaf area, and LAI. It seems from the data presented in (Tables 2 and 3) that most of the yield and yield attributes like grain yield, HI, test weight, nodules plant[-1], seeds pod[-1], and length of pod plant[-1] were found to be highest in $T_6$ and primary branches pods plant[-1] were slightly higher in

Table 5: Correlation among the characters studied in green gram under water-limiting conditions.

| | PH | No. of leaves plant-1 | Leaf area plant-1 | LAI | Primary branches plant-1 | Nodules plant-1 | Pods plant-1 | Seeds pod-1 | Length of pod plant-1 | Biological yield | Grain yield plant-1 | HI % | Test weight (g) | SPAD reading |
|---|---|---|---|---|---|---|---|---|---|---|---|---|---|---|
| PH | 1 | | | | | | | | | | | | | |
| No. of leaves plant-1 | 0.896 | 1.000 | | | | | | | | | | | | |
| Leaf area plant-1 | 0.642 | 0.684 | 1.000 | | | | | | | | | | | |
| LAI | 0.642 | 0.684 | 1.000 | 1.000 | | | | | | | | | | |
| Primary branches plant-1 | 0.674 | 0.796 | 0.771 | 0.770 | 1.000 | | | | | | | | | |
| Nodules plant-1 | 0.512 | 0.568 | 0.749 | 0.749 | 0.523 | 1.000 | | | | | | | | |
| Pods plant-1 | 0.701 | 0.839 | 0.916 | 0.916 | 0.826 | 0.839 | 1.000 | | | | | | | |
| Seeds pod-1 | 0.670 | 0.740 | 0.706 | 0.706 | 0.633 | 0.945 | 0.851 | 1.000 | | | | | | |
| Length of pod plant-1 | 0.697 | 0.808 | 0.689 | 0.689 | 0.690 | 0.869 | 0.885 | 0.929 | 1.000 | | | | | |
| Biological yield | 0.151 | 0.305 | 0.458 | 0.459 | 0.428 | 0.594 | 0.611 | 0.469 | 0.679 | 1.000 | | | | |
| Grain yield plant-1 | 0.694 | 0.814 | 0.773 | 0.773 | 0.797 | 0.867 | 0.929 | 0.920 | 0.982 | 0.688 | 1.000 | | | |
| HI % | 0.824 | 0.860 | 0.672 | 0.672 | 0.734 | 0.688 | 0.761 | 0.867 | 0.779 | 0.107 | 0.795 | 1.000 | | |
| Test weight (g) | 0.672 | 0.754 | 0.552 | 0.550 | 0.638 | 0.687 | 0.708 | 0.848 | 0.748 | 0.135 | 0.745 | 0.912 | 1.000 | |
| SPAD reading | 0.863 | 0.849 | 0.779 | 0.778 | 0.890 | 0.692 | 0.863 | 0.783 | 0.814 | 0.461 | 0.866 | 0.801 | 0.726 | 1.000 |

$T_8$ while biological alone was recorded maximum in $T_2$ compared to the rest of the treatments. A similar trend was also found for the SPAD reading, whereas T8 was slightly higher than $T_6$ at all the intervals (Table 4). The results were similar to the outcomes received by Ghasemi-Golezani et al. (2013), who reported that seed priming is an innovative technique to accelerate and synchronize the establishment of plant population over the field even under water stress conditions and subsequent gain of morphological growth, yield attributes, and yield of pulse crops. The additional availability of K through the action of KSB in the soil helps in channelizing stress-related processes because K is an osmoregulatory compound in the plant (Tavakol et al. 2022, Cochrane & Cochrane 2009, Prajapati & Modi 2016, Meena et al. 2016.). The availability of Ca in the appropriate amount at the time of drought helps in maintaining the turgor pressure, improving the rate of photosynthesis, water use efficiency, and coordinating with ABA because Ca acts as a signaling molecule during the drought (Ali et al. 2020, Cardoso et al. 2020, Naeem et al. 2018, Hosseini et al. 2018). Moreover, the correlation studies presented in Table 5 also indicate the positive relevance of the treatments, *i.e.,* KSB + $KNO_3$ and $Ca(NO_3)_2$, which enabled the plant to survive and helped cover the yield loss due to wastewater-limiting conditions.

## CONCLUSION

The present study was focused on finding out the impact of KSB and osmopriming-mediated morphological changes and triggers in the yield of green gram. As far as our findings are concerned, the combinations of $KSB_2$ and + $KNO_3$,15mM were among the best combinations for the morphological character studies. At the same time, most of the yield attributes and yield of green were better in $T_6$, which were combinations of $KSB_2$ and $Ca(NO_3)_2$. However, the SPAD reading was marginally better in $T_8$, followed by $T_6$, compared to the rest of the treatments. A remarkable result was that the $KSB_2$ greatly influences combinations of priming agents for all the characters studied in the present work compared to combinations of $KSB_1$.

## REFERENCES

Ali, S., Hayat, K., Iqbal, A. and Xie, L. 2020. Implications of abscisic acid in the drought stress tolerance of plants. Agronomy, 10: 1323.

Anaytullah, M. and Bose, B. 2007. Nitrate-hardened seeds increase germination, amylase activity, and proline content in wheat seedlings at low temperatures. Physiol. Mol. Biol. Plants, 13: 199-207.

Archana, D.S., Nandish, M. S., Savalagi, V.P. and Alagawadi, A.R. 2012. Screening of potassium solubilizing bacteria (KSB) for plant growth promotional activity. Bioinfo. Quart. J. Life Sci., 9: 627-630.

Arun, M.N., Bhanuprakash, K., Hebbar, S.S. and Senthivel, T. 2016. Effect of seed priming with various chemicals on germination and vigor in cowpea (*Vigna unguiculata* (L.) Walp). Prog. Res. Int. J., 11: 2113-2117.

Cardoso, A.A., Gori, A., Da-Silva, C.J. and Brunetti, C. 2020. Abscisic acid biosynthesis and signaling in plants: Key targets to improve water use efficiency and drought tolerance. Appl. Sci., 10: 6322.

Choudhary, P. and Siddique, A. 2020. Role of potassium solubilizing bacteria in crop production: An overview. Int. J. Chem. Stud., 9: 542-544.

Cochrane, T.T. and Cochrane, T.A. 2009. The vital role of potassium in the osmotic mechanism of stomata aperture modulation and its link with potassium deficiency. Plant Sig. Behavior, 4: 240-243.

Devika, O.S., Singh, S., Sarkar, D., Barnwal, P., Suman, J. and Rakshit, A. 2021. Seed priming: a potential supplement in integrated resource management under fragile intensive ecosystems. Front. Sustai. Food Syst., 654001 :5.

Donald, C.M. and Hamblin, J. 1976. The biological yield and harvest index of cereals as agronomic and plant breeding criteria. Adv. Agron., 28: 361-405.

Eshkab, I.A. and Harris, P.J. 2020. Seed priming: Factors affecting efficacy. Int. J. Basic Appl. Sci., 8: 31-52.

Ghasemi-Golezani, K., Japparpour-Bonyadi, Z., Shafagh-Kolvanagh, J. and Nikpour-Rashidabad, N. 2013. Effects of water stress and hydro-priming duration on-field performance of lentil. Int. J. Farm. Allied Sci., 2: 922-925.

Guo, J., Jia, Y., Chen, H., Zhang, L., Yang, J., Zhang, J. and Zhou, Y. 2019. Growth, photosynthesis, and nutrient uptake in wheat are affected by differences in nitrogen levels, forms, and potassium supply. Sci. Rep., 12-9:1.

Hosseini, S.A., Réthoré, E., Pluchon, S., Ali, N., Billiot, B. and Yvin, J.C. 2019. Calcium application enhances drought stress tolerance in sugar beet and promotes plant biomass and beetroot sucrose concentration. Int. J. Mol. Sci., 20: 3777.

Khiangte, Z. and Siddique, A. 2022. Response of rhizobium inoculation and boron application on yield and its attributes and root morphology in Pea (*Pisum sativum* L.). Ann. Biol., 38: 188-192.

Marthandan, V., Geetha, R., Kumutha, K., Renganathan, V. G., Karthikeyan, A. and Ramalingam, J. 2020. Seed priming: A feasible strategy to enhance drought tolerance in crop plants. Int. J. Mol. Sci., 21: 8258.

Meena, V.S., Maurya, B.R., Verma, J.P. and Meena, R.S. 2016. Potassium Solubilizing Microorganisms for Sustainable Agriculture. Volume 331. Springer, New Delhi.

Moaaz Ali, M., Javed, T., Mauro, R.P., Shabbir, R., Afzal, I. and Yousef, A.F. 2020. Effect of seed priming with potassium nitrate on the performance of tomato. Agriculture, 10: 498.

Naeem, M., Naeem, M.S., Ahmad, R., Ihsan, M.Z., Ashraf, M.Y., Hussain, Y. and Fahad, S. 2018. Foliar calcium spray confers drought stress tolerance in maize via modulation of plant growth, water relations, proline content, and hydrogen peroxide activity. Arch. Agron. Soil Sci., 64: 116-131.

Pandey, O.P., Shahi, S.K., Dubey, A.N. and Maurya, S.K. 2019. Effect of integrated nutrient management of growth and yield attributes of green gram (*Vigna radiata* L.). J. Pharmacog. Phytochem., 8: 2347-2352.

Pawar, V.A. and Laware, S.L. 2018. Seed priming a critical review. Int. J. Sci. Res. Biol. Sci., 5: 94-101.

Prajapati, K. and Modi, H. 2016. Growth promoting effect of potassium solubilizing *Enterobacter hormaechei* (KSB-8) on cucumber (Cucumis sativus) under hydroponic conditions. Int. J. Sci. Res. Biol. Sci., 3: 168-173.

Rhaman, M.S., Tania, S.S., Imran, S., Rauf, F., Kibria, M.G., Ye, W. and Murata, Y. 2022. Seed priming with nanoparticles: An emerging technique for improving plant growth, development, and abiotic stress tolerance. J. Soil Sci. Plant Nutri., 4062-4047 :22.

Siddique, A. and Bose, B. 2015. Effect of seed invigoration with nitrate salts on morpho-physiological and growth parameters of wheat

crop sown on different dates in its cropping season. Vegetos, 28: 76-85.

Singh, V., Sharma, M., Upadhyay, H. and Siddique, A. 2020. Ameliorative effect of seed priming on germination, vigor index, and tolerance index against short-term moisture stress in maize (Zea mays L.). Indian J. Agric. Res., 382-378 :54.

Tavakol, E., Jákli, B., Cakmak, I., Dittert, K. and Senbayram, M. 2022. Optimization of potassium supply under osmotic stress mitigates oxidative damage in barley. Plants, 11: 55.

Watson, D. J. 1947. Comparative physiological studies on the growth of field crops: I. Variation in net assimilation rate and leaf area between species and varieties and within and between years. Ann. Bot., 76-41 :11.

Zrig, A., Saleh, A., Hamouda, F., Okla, M. K., Al-Qahtani, W.H., Alwasel, Y.A. and AbdElgawad, H. 2022. Impact of sprouting under potassium nitrate priming on nitrogen assimilation and bioactivity of three Medicago species. Plants, 11: 71.

Zulfiqar, F. 2021. Effect of seed priming on horticultural crops. Sci. Hort., 110197 :286.

Original Research Paper

Open Access Journal

# Intellectual Property Rights Regime in Green Technology: Way Forward to Sustainability

**Z. A. Khan\*** (iD) **and Shireen Singh\*†** (iD)

*University School of Law and Legal Studies, Guru Gobind Singh Indraprastha University, New Delhi-110078, India
†Corresponding author: Shireen Singh; shireensingh17@gmail.com

## ABSTRACT

Climate change crises and environmental imbalances have been a significant concern globally in recent times. The climatic changes give rise to various issues such as global warming, depletion of the ozone layer, deterioration of natural resources, soil erosion, deforestation, and more. Many international and national agreements and policies have been created to protect the environment, from the UNFCCC to the recent Paris Agreement, aiming to control rising environmental issues. However, developed and developing countries must achieve desirable results in combating climate change. Industrial and technological developments are critical reasons for environmental pollution and degradation. Progress is necessary for planned developing countries, but growth and expansions shall also consider ecological sustainability. Technology shall be novel in adapting to the changes, considering the effects it can produce on the environment. Green technology combines technology with the environment, also called environmental technology, clean technology, or sustainable technology. It is a combination of science and technology together to mitigate climatic changes and protect the environment. Green technology is the modern sustainable solution to pressing environmental concerns. India is one of the countries globally showing rapid green technology developments. The authors of this paper have tried to highlight the dire need to modify technological developments vis-a-vis environmental sustainability to protect the environment. The research paper delves into and understands the interface between clean technology's importance and relevance for ecological sustainability and the role of patent law, particularly in dealing with issues of the environment. The paper shall also establish a harmonious relationship between patent law and its role in ensuring environmental sustainability.

## INTRODUCTION

Green technology means a technology that is environmentally friendly and sustainable. It is also sometimes referred to as clean technology. It means creating ecologically friendly, sustainable products. It aims to promote a sound and healthy environment. Therefore, green technologies are more appropriately called clean, environmental, or eco-friendly technologies. The adoption of green technologies is simply due to the community's global challenges against ecological crises. The harsh greenhouse gas emissions, unjustified use of fossil fuels, and carbon emissions lead to creating an imbalance in the environment, threatening the ecosystem as a whole, wherein there are repercussions such as depletion of the ozone layer, heat waves, forest fires, extinction of certain life forms of birds and animals they are the result of the extreme loss caused to our environment. Green technology is one such step taken to combat climate change. Rapid climate deterioration is one of the driving forces for the launch of green technology, so going green is the need of the hour to address the global climate crisis. Green technology includes production and consumption technologies that would function to preserve the environment. Green technology uses the three R's, i.e., reuse, recycle, and reduce.

The importance of green technologies for climate change can be understood through its aims and objectives. First, green technology seeks to cater to society's needs by making it aware of the urgency to adapt to green technology (Su 2017). Second, the overconsumption of exhaustible resources like fossil fuels is aiding the influx of green technologies. Green technology has become essential for conserving natural resources. Green technology and sustainability sometimes mean two sides of the same coin, as both target environmental preservation (Wira & Abadi 2017). Sustainable development can be understood as the foundation of the evolution of green technology. Sustainable development is the judicial use of resources so future generations can benefit. Green

technology is the eco and environment-friendly processes and methods aiming to conserve the natural resources in the ecosystem, indirectly protecting our environment. Therefore, as the name suggests, green technology is a tool to reduce harmful environmental impacts by adopting environment-friendly products. The technologies work with the agenda for environmental preservation; they are the future of technologies by employing green energy sources to promote the environment. The 'clean tech' technology covers four major areas: energy, transportation, water, and materials. It focuses on limiting exhaustible non-renewable energy sources and reducing hazardous gaseous emissions. Green technologies can be referred to as 'environment sound technologies' by using products and equipment that are less polluting, adapting to sustainable usage of resources, recycling the products, and handling wastes more judiciously and responsibly. Green technology has a broad connotation to cover all these aspects. It is a general term that includes innovative ways to make environment-friendly technology. It works in a way that conserves natural resources. Incentives provided by intellectual property rights stimulate the growth of such technologies, leading to the expansion and improvement of such technologies, which will further contribute to developing green innovations. The combination of IPRs & green technology encourages & incentivizes innovations (Mustafi 2021). The TRIPS agreement acknowledges IPRs' contribution to innovation and growth, taking care of sustainability.

The enforcement of IPRs will help encourage and promote high-tech advancement and technology transfer that benefits end-users of technological knowledge, assists in socioeconomic welfare, and brings a balance between rights & duties (Article 7 of the TRIPS agreement). IPRs foster economic growth, inventions, and innovations by giving them monopoly rights over such creations. It generates investments in such innovations and inventions, and green intellectual property rights grant protection to environment-friendly technologies that protect green technology. The combination of IPR with technology is referred to as 'green intellectual property'; broadly, the term green intellectual property (from now on referred to as green IPR) covers legally the innovations that are beneficial to the preservation of the environment. The green IPRs are initiatives in the field of invention and science that can help mitigate climate crises. Green IP is quite a recent phenomenon, and it helps incentivize an eco-friendly environment, which further helps in the growth of research and development in this field. However, green intellectual property will shape how the resources and the technology will be used judicially to care for environmental concerns (Deren 2022). One of the essential facets of green intellectual property is 'green patents.'

Green patents provide for the patenting of green technology in environmental protection (Chanda and Rao (2019). They are the technological answer to ecological problems. Patents are the exclusive monopoly rights granted to the owner of the invention. It is a protection granted upon the invention. Green patents are the legal right or protection given to the technologies that provide an environmental benefit, specifically to environment-friendly technology. Green patents are granted on technologies dealing with wastes, wind power, geothermal energy, solar energy, tidal energy, etc. Green patents are grabbing attention and importance due to the ongoing crises the world faces. Granting green patents to such technologies encourages innovation and promotion and is influential in the growth and expansion of green technologies. Since the issues and concerns regarding climate change are in the news, it is vital to consider these technologies. Green patents are a relatively new concept, with more debate. Green patents are granted to environmentally sound technologies; patents help attract investments in eco-innovations that further stimulate economic development (Lima 2013).

There have been initiatives at the global level, such as the WIPO Green, which is a global marketplace or a network place for green technology, innovation, and diffusion. WIPO Green aims to provide environmentally sustainable solutions with technology in developing countries. WIPO Green works through a network of companies, SMEs, investors, and government institutions, aiming to collaborate on activities relating to environmental sustainability. In addition, the Organisation for Economic Cooperation and Development (OECD) has been working to maintain green growth indicators. Containing data on environmental innovations, economic opportunities, and policy responses, it supports statistical patent data–analysis of patents in ecological technologies. In the Indian context, the Environment Protection Act of 1986 is a core legislation to provide for the protection and promotion of the environment that strives for mechanisms to uphold environmental protection by providing for penal provisions in case of deviations from any of the provisions of the act; the act aims to prohibit activities harming the environment. Furthermore, the Indian patent regime has adequate provisions to foster technical knowledge, innovations, and technology transfer (The Patents Act, 1970). Therefore, there is a requirement to develop a strategy for the advantage of end users of technological expertise and encourage socioeconomic benefit for society.

## GREEN TECHNOLOGY AND SUSTAINABLE DEVELOPMENT

Green technology is eco-friendly, which results in social,

economic, and environmental sustainability. These are ecological technologies because these technologies can significantly improve environmental concerns compared to other technologies. Green technologies are often considered a combination of science and human activities that aid in balancing both. Developing resources for the current generation without depletion is known as sustainable development. Sustainable development favors a healthy and stable environment and allows the resources to be used judiciously for future generations. According to the Brundtland Commission, sustainable development is "that satisfies present demands without compromising the capacity of future generations to meet their requirements." With the rapid increase in the deterioration of the environment, including climate change and depletion of resources, there is pressure on the countries, be it developing or developed countries, to employ the technologies that are prone to less risk to the environment; it is not a choice anymore, but a necessity, the precipitated rise of the harm and damage has made it implied to bring about environment-friendly mechanisms. Green technology is one such mechanism where the countries would launch products and technologies that are more sustainable and eco-friendly. Now, growth and economic development have to be taken consciously with concepts such as eco-innovations. Green technology and sustainable development can now be called two interlinked concepts; nevertheless, green technology could be a means to attain sustainable development.

The countries aim to achieve 'green growth,' according to OECD; green growth refers to promoting economic expansion and development while preserving the ability of the environment to benefit from natural resources. It shall encourage investments and innovation, leading to economic expansions and sustainable evolutions. Green growth is essential as it helps maintain a check on the rising growth of the environment. It makes sure that the development does not erode natural wealth. Green growth management helps create, use, and acquire green technologies, leading to sustainable development. Green, sustainable, and environmental technologies allow companies or firms to develop sustainable innovations. Sustainable innovations are high-quality products or machinery that efficiently reduce ecological footprints (Deren 2022). Green technology is not just limited to having sustainable and eco-friendly technology; it works through a series of green technology strategies, including green product strategy, green pricing strategies, availability of green products, green promotion strategies, and green consumer behavior strategies (Das 2018).

## COP 27: THE UNITED NATIONS CLIMATE CHANGE CONFERENCE

The Conference of Parties (COP) 27 contemplates various nuances of the adverse effects of climate change on food security and agriculture. It also focuses on an action plan for climate empowerment and appropriate preventive measures against damage incurred due to climate change. The parties' conference invites the Least Developed Countries to process, create, and effectively implement adaptation plans and progress in implementing national adaptation plans in one of its reports on National Adaptation Policies. The Sharm El Sheikh Climate Implementation Summit, commonly known as COP 27, took place in Egypt in November 2022. The COP is also known as the "Implementation COP." wherein many effective mechanisms for climate change have been discussed. One round table on "Investing in the future of energy: Green Hydrogen." The COP mentions Green Energy playing a significant role. Energy has been a primary focus in the transition process, making a shift towards clean and green energy. COP 27 focuses on green energy development in transitions and encourages a healthy exchange of energy, proposing sustainable solutions to numerous climate-related challenges.

## THE INTERFACE BETWEEN GREEN TECHNOLOGY AND IPR: DIFFUSION AND COOPERATION

Clean or green technology is environment-friendly technology or innovation, also called ecological technology (Wira & Abadi 2017). With the constant climatic changes, there has been growth in what is called 'green intellectual property. It is a broad term that combines green technology and IPRs. As already discussed, IPRs promote innovation and incentives in technological development. It is crucial for the recognition and growth of innovations and technological elopement. It is essential for the recognition and growth of innovations. The patent law is significant for the development and recognition of innovations. The ongoing rise in environmental degradation is climate change, a severe crisis the earth faces. Earlier intellectual property rights were only concerned with innovations or aspects that usually had some business perspectives; however, this is not the case anymore, and there is a shift toward protecting environmental sustainability. Clean technology is concerned with improving environmental quality and ensuring sustainability by launching environmentally sound and safe technologies, which could add to the measures taken to ensure environmental protection (Kumar & Kumar 2009). The new term coined to promote environmental protection and maintain the innovation business is 'green intellectual property. Green IPR includes granting rights to environment-friendly innovations (Sultana 2019). This

combination incentivizes innovation while internalizing ecological degradation. The role of green IPR is strengthened by the TRIPS agreement that seeks to promote the creation and technological dissemination for the benefit of end-users & creators of specific technical knowledge, which is also compatible with the socioeconomic advantage of the society (Sharma 2021).

IPRs grant monopoly rights to invention, and green intellectual property gives protection and rights to environment-friendly technologies. The significance of intellectual property in promoting and disseminating green technologies will be thoroughly discussed in this study; in a broad spectrum, green intellectual property legally protects the environmental innovations that contribute towards sustainability. Green IPR, is a relatively new concept encompassing the needs of the current crises to safeguard ecological sustainability and promote businesses through eco-friendly innovations. It is a recent phenomenon but not a completely alien concept; the backdrop of the green IPR in every industry and firm would relate. It is making innovations that support the environment. It is the way forward toward achieving sustainability. With the ongoing climate crises, there is a need for realization towards going green. The concern for protecting the environment is not limited to one domain but extends to a few other departments like government agencies, corporate bodies, and consumers; the responsibility is divided amongst all. Green IPR, therefore, is needed for the interplay between IPR and sustainability.

In its 2030 Sustainable development agenda, the World Intellectual Property Organization (WIPO) reaffirmed the significance of IP protections for green technology and sustainability, noting that IP and its supporting innovation are linked to a country's capability towards innovation, investment-friendly FDI and encourage commercial products and services on the worldly horizon. For green technology to succeed, they need to have strong IP protection. Therefore, high-green technological innovations must be developed as a top priority, and a robust framework must be encouraged so that green development includes innovations.

## GREEN PATENTS AND THEIR ROLE IN PROMOTING SUSTAINABILITY

Patents grant the proprietor the 'sole authority' to prohibit others from exploiting the invention. The inventor's request to protect the specified innovation is granted. Patents are an individual right or a privilege because they promote the inventor's interest in investing, advertising, and selling his patented design. The invention acquires the right that nobody except him would have the right or a claim upon the invention. It is not only from the legal point of view but also helps in the expansion of the business of the invention; granting patents is also referred to as creating incentives for investment. Incentives for investment mean that any company interested in investing in any green technology would examine a strong patent portfolio of the green technology, which includes their patent filing strategy and their patent positions in a particular market. Companies seek to invest in any specific green technology by assessing the financial, political, and associated risks associated with the technology. Since green technology is developing, patenting these technologies would help build these companies' confidence before investing in green technology (Hall & Helmers 2010). Green patents are an appropriate tool to incentivize and encourage investments in green technologies (Ring 2021).

Green patents are a mechanism to combat climate change and promote sustainability. It refers to patenting the technology that fosters environmental growth and development (Chanda & Rao 2019). Green patenting, therefore, promotes green innovations, those that seek to work for the environment. Although green patents cannot fit into a straight definition since the ambit of the term is quite broad, it means innovation in environment-friendly technologies that promote environmental sustainability (Mohan 2021). Green patents protect green technology globally, i.e., patenting technologies or inventions that enable ecological growth. Green patents are also referred to as green tech patents. Green patents provide a platform for innovations to promote their idea of a sustainable business. Green patents are crucial in incentivizing these technologies' business, allowing companies to stay alert for their environmental imprints. Even though green patents are a relatively new concept, countries have made efforts to recognize the role of green patents in promoting sustainability. Green patents are the patents to be given to the inventors of green technologies, which are the central component of green intellectual property; green patents determine the rights to be given to the inventors' playing field in green technology. Green patents are to be considered as the only alternative if economic and environmental incentives are to be considered. Although, as most understood, climate change is mainly considered an environmental law issue, contentions are there as to why to include it as an IPR issue. Still, there is a need to understand that current environmental problems also include many technological interventions. Hence, technological problems require technological solutions, and IPRs are the most technologically advanced law (Grajales et al. 2012). Green patents are one of the initiatives of the IPR regime for addressing environmental problems by allowing patenting of green technologies. Green patents work through green patent databases such as IPC Green Inventory, WIPO Green, etc. These databases maintain data on green patent inventions,

making it easier for the countries to connect with inventors and investors in green technologies.

## THE ESG CONNECT WITH GREEN PATENTING

ESG is a concept that transcends environmental issues; it aims to look at sustainability from a broader perspective. ESG stands as an acronym for environment, social, and governance. It is a combination of all the aspects contributing towards sustainability. The concept of ESG is mainly associated with the corporate entities, companies, and organizations' financial activities that impact the environment. It deals with the company's activities that may have environmental impacts. ESG affects companies' investments to make sure that companies make sustainable investments (Cohen et al. 2021). ESG comes under the concept of sustainable financing. ESG works through the environmental, social, and governance pillars (Raghu & Savitha 2019). The components under the ecological pillars are greenhouse gas emissions, water, air, and land pollution companies engaging in recycled goods, whether the company causes soil erosion or deforestation. The social pillar covers the company's responsibilities towards the public; companies should be sure about the safety, quality, and health standards, how far the company provides services to underprivileged people, and whether the company is following ethical labor practices.

Finally, the governance pillar includes the internal organization of the company. It generally consists of corporate governance activities like shareholders' rights, corruption prevention, and other ethical behavior. Broadly, to sum up how the ESG works for a company is to determine the company's efforts for protecting the climate, addressing human rights issues and conditions, and workplace equality and opportunities (sustainable working conditions). The whole idea of ESG is that companies follow this strategy while engaging in business. Therefore, a company should be accountable for ESG. Today, because of the growing environmental concerns worldwide, investors also invest in a company that promotes activities that promote sustainability and adhere to climate change mitigation regulations. It is stated that investors in a company following an ESG strategy are guided more by the environmental benefits than the monetary ones. They want to put their contribution to environmental preservation and protection rather than profit sharing. The strategy for ESG was first incorporated in the "United Nations Principles for Responsible Investment" (UNPRI). At the latest COP 27, deliberations have been made regarding climate financing; the PRI focuses on achieving long-term and ambitious global climate financing. These targets must be met in keeping line with the Paris Agreement.

ESG is primarily concerned with enterprises working out in the field of environment as well as carrying out corporate works. The enterprises are working out by fulfilling the goals of the environment and time putting out CSR policies. This helps in the overall development of the companies. The enterprises or companies consider the CSR rules. ESG policies state the goals of achieving sustainable economic development. Although the concept of ESG in firms is still in the infancy stage, gradual developments are being undertaken; the idea of the companies is to improve the status of the economy for a sustainable position by focusing not just on economic development but also on green development. In the study conducted in China in the research paper (Zhang & Qin 2020), non-financial companies listed in the Shanghai and Shenzhen stock exchanges between 2012 and 2018 were taken as samples; after conducting analysis and empirical tests, it was held that green innovations could hasten and push economic benefits.

## INTERNATIONAL EFFORTS IN PROMOTING PATENTING OF GREEN TECHNOLOGY

WIPO Green is a global network or marketplace developed by WIPO that promotes green technology. It is an online platform for technology exchange. WIPO Green aims to bring together the key players of green technology innovation and diffusion. The USPTO launched the green pilot program in 2009; this program was an initiative by the United States to fast-track green patent applications. The program's task was to accelerate the process of green patenting by examining the green patent applications before the general applications. The Green Channel program is an initiative by the UKIPO in the year 2009 that provides for accelerated processing of patent applications for an invention that offers any environmental benefit. The green channel scheme provides for accelerated processing of patent applications if they intend to benefit the environment; this scheme also seeks to promote prompt communications from the UKIPO to accelerate the grant of patents on such applications. Japan has recently joined the line to encourage green patenting by joining the WIPO Green program. Japan has partnered with WIPO Green to promote the utilization of green technologies, and the JPO intends to work with WIPO to facilitate the spread of green technology. After partnering with WIPO, Japan has published the Green Transformation Technologies Inventory (GXTI), which will help enterprises explain their green transformation efforts. GXTI shows a way to categorize GX technologies and how to search for patent documents pertinent to respective GX technology. The inventory works with the recommendations of the Taskforce on /climate-related Financial Disclosures (TCFD). Companies must demonstrate the value created by

them that contributes to solving climate change issues. The GX inventory tries to make an effort to shift the economic, social, and industrial structures that have depended upon fossil fuels towards clean energy.

## COMPULSORY LICENSING OF GREEN TECHNOLOGY

Compulsory licensing is a license given to a person to use a patented invention by paying a royalty to the inventor without the patentee's permission. Compulsory licensing is an essential concept in IPR law. It is a statutorily created license allowing access to the invention's third party. TRIPS agreement and the Indian Patent regime also have a relevant discussion on the basic features of compulsory licensing. The TRIPS agreement allows products under compulsory licensing to be available in the market for further use. However, the TRIPS agreement does not mention compulsory licensing but discusses the invention's use without the right holder's authorization (Article 31 of the TRIPS agreement). However, the benefit under this clause has only been permitted if attempts have been made to secure consent from the right holder on acceptable commercial conditions, provided such attempts have not been successful within a reasonable time. The exception to this rule is a national emergency, a situation of extraordinary urgency, or a public non-commercial purpose. The period of such use shall be limited to the authorized purpose. In addition, the patent holder or the patentee has to be paid proper remuneration for the use by the third party. The most crucial point about compulsory licensing under TRIPS is that it can be allowed only in a 'national emergency' (Nanda 2009). What national emergency, though, is not specified by the TRIPS agreement? Environmental degradation can be considered a national emergency. The severity of the environment, like resource depletion and climate change, accelerates the degradation. These are the pressing issues adding up to the catastrophic consequences. There have been deliberations that if climate change is considered a national emergency, granting compulsory licenses on green inventions can elucidate the problem of climate change and environmental degradation (Fair 2020). Under the backdrop of climate change, compulsory licensing of green technologies would not be prohibited by TRIPS because it is silent on what constitutes public interest or a national emergency. Nonetheless, it is up to the countries or member states to demonstrate the presence of such an emergency or urgency; it is up to the member states to show that a given circumstance qualifies as a national emergency or an extremely urgent matter.

Article 27 of the TRIPS agreement allows the member states to exclude from the domain of the patentability inventions those inventions the commercial exploitation of which is necessary to protect public order and morality or to avoid severe prejudices to the environment; however, again, no clear explanations are given to understand these. Speaking of patents and environment both fields are now interconnected and interlinked, by now few green technology litigations have also been there. A crucial green technology litigation was Paice LLC v. Toyota Motor Corp (609 F. Supp. 2d 620, 623 (ED Tex. 2009), In this US case, the defendant used the plaintiff's hybrid automobile technology and gave him a royalty of twenty-five dollars in exchange for that technology. However, the defendant company argued that they should not be restricted from using that technology as that would be antithetical to the public interest. Again, in the case of eBay v. Merc Exchange (LLC, 547 US 388, 391-92 (2006), this case said that public interest is one of the factors to be contemplated by the courts while determining the injunction cases. These two cases underpin the patentability and granting of compulsory licensing of green technologies.

The General Electric Co. v. Mitsubishi Heavy Industries (No. 3:10-CV-00276-F, 2013 BL 141580 (ND Tex. May 28, 2013). This was another litigation for clean technology. General Electric (from now on referred to as GE) had obtained a patent for creating a wind turbine operating system that could function at variable speeds at disparate wind conditions. GE and Mitsubishi entered a dispute as GE brought an infringement action against Mitsubishi. The defendants counter-filed by accusing GE of dominating the sector by making these turbine machines; these cases were showcasing green technology.

However, the countries or the member states should prove the existence of such an emergency or urgency. It should entirely be upon the member states to prove that a particular situation is a national emergency or extreme speed. Compulsory licensing is thus considered an important tool to tackle the problem of diffusion of green technology. Furthermore, since green technology prices are very high, especially in low-income countries, compulsory licensing can be considered a measure to solve this problem. Thus, if a law complies with the requirements outlined in Article 31, it may be passed in a member state that allows or supports compulsory licensing for green technology. For example, compulsory licensing of green technology is permitted if each case of green technology is a separate and individual one, the authorization has been sought from the patent holder, the scope and duration should specifically be for green technology, the use of such compulsory licensing fits the interests of green technology transfer, following these conditions compulsory licensing could be made use for green technology transfer.

All do not favor compulsory licensing as sometimes they are detrimental to the inventor or the country where a patent is deemed to be granted on the product. Some authors argue that compulsory licensing abridges the rights of the patentees if there is unauthorized use of the patentee's invention. Compulsory licensing is also harmful to the countries they are granted because it obstructs the growth of an independent and research-based country as it would obstruct its ability to innovate something of its own. It is also challenging to determine whether the recipient country has enough infrastructure to accommodate the technology in their country; if it does, then the idea of compulsory licensing would fail.

## INDIAN LANDSCAPES OF GREEN TECHNOLOGY

India is swiftly attempting to overhaul the energy industry to achieve zero carbon emissions by 2070. Green energy is crucial in altering the current energy landscape for sustainable development. Goal 7 of the Sustainable development goals, which must be accomplished by 2030, is affordable and clean energy. According to the Ministry of New and Renewable Energy's year and review of 2022, India's action plan for promoting green technology is quite effective. India is ranked fourth in the world for installed renewable energy capacity, which includes massive hydro, wind, and solar generating capacity. In the nation, 172.72 GW of power derived from non-fossil fuel will soon be operational. Therefore, a sustainable shift towards green technology is the need of the hour.

In addition to the statistics, India has also launched numerous national initiatives to support green technology and innovations, such as the introduction of AGNI, a program by the Indian government and a mission under the Prime Minister's Science, Technology, and Innovation Advisory Council (PM-STAIIC); it is a platform that aids in the commercialization of technological innovation. There have also been other initiatives, such as Climate Launchpad 17, the world's largest green company ideas competition that the European Union co-founded. They want to realize the clean tech potential of the planet to combat climate change. In addition, the National Science and Technology Entrepreneurship Development Board (NSTEDB) encourages knowledge-based, technologically advanced businesses that advance environmentally friendly innovations.

Furthermore, to ensure robust and sustainable systems for addressing climate change challenges, the Department of Science and Technology has been launching the year-by-year climate change program under the auspices of the Ministry of Science and Technology, Government of India. In addition, the department launched the National Action Plan on Climate Change, a flagship program with numerous initiatives to address climate change challenges. Indian inventors have patents on their green inventions; in August 2022, PI Green Innovations was granted a patent for its carbon cutter technology. This carbon cutter technology creates retrofit devices to reduce particulate matter from the air. The company has already obtained patents in countries like the USA, China, and Singapore and has now secured a patent for its technology in India. SunHydrogen, a developer of green technology has received patents in India on its "Multi-junction artificial photosynthetic cell with enhanced photo-voltages." The company already holds patents in the USA, China, Europe, and Australia but has not received patents from the Indian Patent Office as well. These are, again, some remarkable developments being made by India in the field of green patenting and green technology. The companies developing green technology are being granted patents on their technologies and will raise the Indian patent landscapes on green technologies.

## CONCLUSION

The world is moving at an unprecedented pace with the need for technology, which has to be updated; it is impossible to take steps backward, but what can be done is to prevent further harm. Therefore, it is essential to address the environmental and climate change problems with specific academic or practical policies so that development can occur and the environment should not be harmed. Green technology is being adopted as an effective technologically advanced mechanism to address environmental concerns as well as to achieve the levels of technological advancements; green patenting, therefore, becomes an important concept because it deals with the protection of these green technologies; it means that the technologies which would be launched should be granted their recognition and the inventors should also enjoy the safety of their inventions. However, some things still need to be clarified about the easy transfer of these technologies, as the process could be more streamlined. The green technology transfer, regulated through compulsory licensing, and the related provisions still need to be clarified. There are other uncertainties associated with the legal aspects of green patenting, such as the concept of inherent participation, which makes patenting of green technologies complicated as deciding the novelty of the green inventions becomes strenuous because numerous inventors launch multiple inventions related to environmental technologies, so there has to be a streamlined and explicit provision for that since green technology is vast. In an emerging concept, there becomes a dire need to update or modify some of

the existing preconditions at the end; the efforts must be collaborative and aligned to achieve the goals. It is time for countries worldwide to work towards a common direction: achieving sustainable development goals.

Climate change-induced environmental pollution and other environmental concerns of the global community result in the sustainable degradation of the whole ecosystem. Thus, international legal instruments and organizations must acknowledge the adverse effect of climate change as a severe global emergency. Undoubtedly, such a complex problem can be addressed through the diffusion of green technology followed by an innovation-based partnership between technology producers and national members of such international legal organizations. Global patent regimes must acknowledge and promote the recognition of climate-friendly technologies and their further dissemination and transfer for sustainable, innovative growth and preventive action against environmental harm. Apart from compulsory licensing, it is also crucial that the state adopt other regulatory practices associated with the relaxation of trade barriers and the inclusion of a fast-track patent prosecution process for environmental-oriented inventions.

## REFERENCES

Chanda, S. and Rao, P. 2019. Green patents. J. Emerg. Technol. Innov. Res., 6(3): 56-69.

Cohen, L., Gurun, U. and Nguyen., Q. 2021. The ESG - Innovation Disconnect: Evidence from Green Patenting. European Corporate Governance Institute – Finance Working Paper No. 744/2021. ECGI, pp. 1-61 https://ssrn.com/abstract=3718682 or http://dx.doi.org/10.2139/ssrn.3718682.

Das, B. 2018. Green technology for attaining environmental safety and sustainable development. Int. J. Mech. Eng. Technol., 9(3): 45-56.

Deren, A. 2022. Green intellectual property is a strategic resource in the sustainable development of an organization. Sustainability, 14: 4758.

Fair, R. 2010. Does climate change justify compulsory licensing of green technology? Int. Law Manag. Res., 16: 414-426.

Grajales, D., Soto, P. and Switzer, D. 2012. Green patents as a way of addressing environmental issues. Food Clim. Change Intell. Prop. Define. Issue, 1(2): 434.

Hall, B. and Helmers, C. 2010. The role of patent protection in (clean/green) technology transfer. Santa Clara High Technol. Law J., 26(4): 35-49.

Kumar, H.D. and Kumar, E. 2009. Cleaner Production; Sustainable Trade & Industrial Ecology. Vitasta Publishing Pvt. Ltd, New Delhi, pp. 1-28.

Lima, N. 2013. Scenario-patent protection compared to climate change: the case of green patents. Int. J. Social Ecol. Sustain. Dev., 4(3): 14-35.

Mohan, A. 2021. Tackling environmental issues through green patents. Taxmann, 130: 109.

Mustafi, R. 2021. Intellectual property rights vis a vis green technology with a special focus on the corresponding developments in international patent regime: A comprehensive study. In Sharma, L. (ed). 2021. Green Intellectual Property and Climate Change Mitigation Technologies: Road Ahead. Bharti publications, pp.133-144.

Nanda, N. 2009. Diffusion of climate-friendly technologies: Can compulsory licensing help? J. Intellectual Prop. Rights, 14: 17-36.

Raghu, N. and Savitha, R. 2019. Green technology: Innovation status and challenges in India. J. Emerg. Technol. Innov. Res., 6(3):121-136.

Ring, C. 2021. Patent law and climate change: Innovation policy for a climate in crises. Harvard J. Law Technol., 35: 141.

Sharma, L. (ed.). 2021. Green Intellectual Property and Climate Change Mitigation Technologies: Road Ahead. Bharti Publications, New Delhi.

Su, H.N. 2017. Does innovation respond to climate change? Empirical evidence from patents and greenhouse gas emissions. Technol. Forecast. Social Change, 122: 49-62.

Sultana, S.M. 2019. Green technology: An emerging trend. Int. J. Res. Eng. Technol., 6(3): 78.

The Patents Act 1970. The Patents Act. Universal Law Publishing, Delhi, India.

Wira, S. and Abadi, H. 2017. The importance of green technologies and energy efficiency for environmental protection. Int. J Appl. Environ. Sci., 12(5): 76.

Zhang, F. and Qin, X. 2020. The interaction effect between ESG and green innovation and Its impact on firm value from the perspective of information disclosure. Sustainability, 12(5): 465.

## ORCID DETAILS OF THE AUTHORS

Z. A. Khan: https://orcid.org/0000-0003-3681-333X

Shireen Singh: https://orcid.org/0009-0008-9104-0695

**Original Research Paper**  |  https://doi.org/10.46488/NEPT.2023.v22i04.041  |  **Open Access Journal**

# Saccharification of Various Wastepaper Materials by Cellulase from Brown Garden Snail (*Cornu aspersum*) at Different Incubation pH Values

**T. M. Ndlovu and J. P. H. van Wyk†** 

Department of Pharmacology and Therapeutics, School of Medicine, Sefako Makgatho Health Sciences University, Garankuwa, South Africa

†Corresponding author: J. P. H. van Wyk; bioenergy.res@gmail.com

## ABSTRACT

Increased solid waste pollution and the negative effect of fossil fuel consumption on the environment are issues that would require more scientific attention and application to deal effectively with these phenomena. Wastepaper, a major component of solid waste, is classified as organic waste due to the presence of cellulose, a glucose-based biopolymer that is part of its structural composition. The saccharification of cellulose into glucose, a fermentable sugar, can be achieved with a hydrolytic enzyme known as cellulase. Although cellulase from fungal species such as *Trichoderma*, *Aspergillus,* and *Penicillium* are well described, knowledge about cellulase isolated from the brown garden snail is limited as it has not been the subject of many research endeavors. The waste paper has been described as a suitable resource for bio-energy development due to cellulose, a structural component of this bio-material that can be degraded into glucose, a fermentable sugar. Although paper materials such as newspaper, office paper, filter paper, Woolworths and Pick and Pay (retailers) advertising paper, as well as foolscap paper, were saccharified by different cellulases, the degradation of these paper materials by garden snail cellulase is a novel investigation from our laboratory. With the effects of temperature and incubation time on this cellulase action when degraded paper materials have already been investigated and reported, this study dealt with the garden snail cellulase action when degraded paper materials at different pH values. Most of the paper materials were degraded optimally at a pH value of 6.0, while optimum saccharification was observed at pH 4.5 when newspaper and brown envelope paper were degraded, with office paper showing maximum bioconversion at pH 7.0. The difference in the structural composition of the paper materials also affects the degree of saccharification, as the amount of sugar released from the various paper materials at optimum pH values is not similar. Together with other catalytic parameters, the pH value of this enzymatic catalysis is also to be considered when designing the development of waste paper as a bio-product resource, with limiting environmental pollution as an additional advantage of this process.

## INTRODUCTION

The bio-conversion of biomass to valuable bioproducts, biofuels, and biochemicals has become an important area of current research. Biomass can include agricultural waste, natural herbaceous plants, forest residues, and industrial and municipal wastes. Also included as biomass derivatives or cellulose-related products are paper materials, and it was reported (Loelovich 2014) that the world pulp and paper industries produced about 300-350 million tons of various types of paper and board. This statement was supported by (Tiseo 2021), who indicated that in 2018, the global production of paper and cardboard stood at 419.72 million metric tons. With such an enormous volume of paper produced annually, it can be concluded that the amount of wastepaper is also extremely high and that this waste cellulose material should

be considered a potential resource for developing renewable substances. The use of organic waste materials as a resource for the biotechnological production of biofuels should be economically and environmentally advantageous, and the development of lignocellulosic matter as raw materials for the hydrolytic production of fermentable sugars has already become a feasible option (Vladimir et al. 2014).

Snails are organisms that can use cellulose as an energy resource since they can produce cellulase enzymes by bacteria in their digestive tract, and the cellulase can decompose cellulose into simple sugars such as glucose by breaking the chemical bonds between glucose units in the cellulose polymer. These chemical bonds are known as β-1,4-glycosidic bonds and can be broken by the cellulase enzyme components known as endoglucanase, exoglucanase, and

ꞵ-glucosidase (Dini et al. 2019). The degradation of cellulose into sugars can also be done by exposing the cellulose material to high temperatures or treating it with acidic or alkaline agents, which are not environmentally friendly. As an alternative, an environmentally friendly procedure like an enzyme-based treatment of cellulose with a cellulase enzyme as the biocatalyst has become a major focus of research (Navarro et al. 2018).

The in-situ pH, oxygen, and hydrogen profiles of the helicid snails (gastropoda: pulmonata) gut microenvironment have been described by Charrier & Brune (2003), who concluded that the degradation of cellulose by snails is subjected to two factors that link all animals feeding on a lignocellulosic diet. The first of these two variables is the enlarged gut region, and the second is the gut microbiota that provides the host with a battery of digestive enzymes to hydrolyze plant food, mainly its lignocellulosic components. The pH profiles of *Cornu aspersum* (commonly known as the brown garden snail) investigated by Charrier and Brune were discovered to be acidic in the crop, close to neutrality in the distal intestine, and above pH 7 in the glands. The pH of the digestive system of slugs and snails decreases shortly after they have been fed, with the main change in pH after feeding in the crop, which is significantly more acidic than the digestive gland and salivary gland (Walker et al. 1996). The crop pH values of snails were 7.7 when empty and 5.8 when full, whereas the corresponding values for the digestive gland were 7.0 and 6.3, respectively, reflecting information of the pH value when the cellulase is saccharifying cellulose in the digestive system of the snail. It was suggested that the gut pH in slugs is characteristic of mollusks rather than determined by their diet preferences, and the proteolytic activity of crude gut homogenates of snails and slugs has been reported to have a pH far from the physiological pH (Walker et al. 1996). In comparison, a close relationship between the pH optimum for proteolytic activity and the in-situ pH of the alimentary tract for crude gut homogenates has been reported to be pH $6.0 \pm 0.1$ (Evans & Jones 1961).

The saccharification of cellulose by cellulase enzymes is a process investigated for the degradation of various types of waste celluloses by cellulases from different origins. Different types of waste paper, such as newspaper (Mokatse & Van Wyk 2017), office paper (Van Wyk & Sibiya 2016), foolscap paper (Mokatse et al. 2016), and filter paper (Van Wyk et al. 2000) have been investigated as a possible resource for bioenergy development as it has been subjected to the saccharification action of cellulase from *Trichoderma viride* and *Aspergillus niger* (Zhao et al. 2020). The hydrolytic action of cellulase from garden snails on cellulose has not yet been investigated in detail or depth,

as is the case with cellulases from fungal resources. All enzymatically catalyzed reactions are sensitive to changes in many catalytic properties, such as pH, and to ensure an optimum yield of the reaction product, these properties must be optimized. Due to the cellulase enzyme's complexity and the structural differences of the various waste cellulose materials, it cannot be accepted that the enzyme would act optimally at the same pH value when degrading the paper materials. This investigation attempted to determine the bioconversion of various waste paper materials at different incubation pH values and to conclude the pH value for optimum saccharification of each paper by a cellulase enzyme isolated from garden snails.

## MATERIALS AND METHODS

### Isolation of the Cellulase Enzyme from Garden Snail

The isolation of cellulase from the brown garden snail was carried out according to the method described by Ndlovu and Van Wyk (2019). A dialysis tube (Sigma, St Louis, Switzerland) was soaked in water and cooled in the fridge at 4°C for four hours. A snail's foot was removed, and the organs inside the shell were cut into small pieces. Tris-buffer (0.005M, 30mL; Merck, Darmstadt, Germany) was added to form a homogeneous mixture by stirring the mixture for one hour on a magnetic stirrer. The snail sample and tris-buffer mixture were centrifuged (Beckman, Indianapolis, United States) at 4000 rpm for 30 min. The supernatant was collected and transferred into the soaked dialysis tube that was immersed into a glass container filled with water and left for 24 h in a cold room at 4°C with the water continuously stirred. After 24 h of stirring, the dialyzed cellulase sample was transferred from the dialysis tube into a clean glass container. Samples of this dialyzed enzyme solution have been used to saccharify various waste paper materials at different pH values.

### Incubation of Wastepaper Materials with Brown Garden Snail at Different pH Values

Filter paper, office paper, newspaper, foolscap paper, brown envelope paper, Pick 'n Pay, and Woolworth's advertising paper were cut into round discs with a diameter of 6 mm (Woolworths and Pick 'n Pay are two local retailers). Twenty pieces of each paper were transferred in triplicate into separate test tubes and mixed with 800 μL tris-buffer at different pH-values of 3.5; 4.0; 4.5; 5.0; 5.5; 6.0; 6.5, 7.0 adjusted with 32% hydrochloric acid (HCl) or 0.5M potassium hydroxide (KOH). A fixed volume of the dialyzed garden snail cellulase solution (200 ul) was added to each test tube with the well-mixed content. The filled test tubes were incubated for 2 hours at 50°C and centrifuged for 15

minutes at 4000 rpm. The supernatant was transferred into a clean test tube to determine the sugar released from each paper material when saccharified at different pH values with cellulase from the brown garden snail.

## Sugar Determination and Percentage Saccharification

The amount of sugar released from each paper material when saccharified with garden snail cellulase at different pH values was determined according to a method described by Miller (1959). During this analysis, 1500 µL of dinitrosalicylic acid solution (DNS) was added to each tube. The tubes were placed in a boiling water bath for 10 minutes; whereafter it was cooled in ice water. The cooled samples were read on a spectrophotometer (Shimadzu, Kyoto, Japan) at 520 nm to determine the concentration of the produced reducing sugars from each paper material using a calibration curve constructed with glucose standards solutions prepared at different concentrations. To determine the percentage saccharification of each paper material, the mass of the paper disks incubated with the cellulase enzyme was determined (weighed) before the paper was saccharified. With the sugar concentration determined after the bioconversion of the paper materials, the total mass of sugar in the incubation mixture was determined. This mass of sugar produced during the degradation of the paper materials was expressed as a percentage of the total mass of paper material incubated with the garden snail cellulase.

## Statistical Analysis

All the experimental analyses were performed in triplicate, and the mean values with standard deviations were determined with Microsoft Excel.

## RESULTS AND DISCUSSION

The pH of a biological environment is an important parameter that could affect the activity of enzymes operating in this milieu by changing the shape and structure of these bio-catalysts. Each enzyme, irrespective of its nature or action, performs optimally at specific pH values, and to ensure maximum catalysis, these pH values must be maintained while enzymes are in contact with substrates. Certain enzymes could exhibit optimum activity over a broad pH range, such as extracellular alkaline protease from *Bacillus licheniformis* NCIM-2042 (Bhunia et al. 2011), while peak activity of others could be executed at narrower pH values as described for the maximum activity of the enzyme, phosphoserine aminotransferase from *Bacillus alcalophilus* at a pH-value of 9.0 (Dubnovitsky et al. 2005). With enzyme-like reactions responsible for the conversion of substrates into products, a change in the pH value of these reactions

will influence the yield of the reaction. Cellulase-catalyzed reactions do not differ and are also pH-dependent for optimum bioconversion of cellulose into glucose.

Snails are rich in a wide range of digestive enzymes, particularly carbohydrates, of which cellulases are a major component (Okeniyi et al. 2015). Although the pH of the gut of snails is important for the optimum activity of its cellulases producing maximum glucose as an energy resource from cellulose, the acid-base balance can be changed by chemical substances produced during bacterial fermentation (Dar et al. 2017). Thus, mechanisms must exist within the gut of snails to maintain a pH value that would ensure a relatively high cellulase activity. Cellulose is a major component of organic waste, such as waste paper. If this bio-polymer could be resolved effectively into glucose by cellulase enzymes, many cellulose-related waste materials could be developed as a resource of bio-energy. During this investigation, the effect of changing pH values on the degradation of various wastepaper materials into glucose by cellulase isolated from the brown garden snail has been concluded.

Fig. 1 reflects the concentration of sugar released from filter paper when degraded with cellulase from the brown garden snail at different incubation pH values as well as the percentage saccharification of this paper material. The saccharification of filter paper showed a gradual increase in sugar production from pH 3.5 and reached the highest amount of sugar production and saccharification at pH 6.0. The highest level of filter paper bioconversion was at pH 6.0 with 6.35% saccharification, while a 65 % increase in sugar concentration was observed from pH 3.5 (0.70 mg.mL$^{-1}$) to pH 6.0 (1.98 mg.mL$^{-1}$). Filter paper is regarded as pure cellulose, and the maximum concentration of sugar produced from this material (1.98 mg.mL$^{-1}$) at pH 6 was the lowest sugar concentration compared to the amount of sugar released from the other paper materials degraded with cellulase from the brown garden snail. During the saccharification of office paper (Fig. 2) at different pH values, a maximum sugar concentration of 3.39 mg.mL$^{-1}$ was obtained at pH 7.0, while at the same pH value, the highest percentage of saccharification was calculated at 9.11%. The amount of sugar released from this paper material when degraded with cellulase from garden snails increased by 34% as the incubation pH increased from 3.5 (2.25 mg.mL$^{-1}$) to pH 7.0 (3.39 mg.mL$^{-1}$).

Fig. 3 reflects the extent of sugar production and percentage saccharification of foolscap paper when degraded with brown garden snail cellulase. The profiles reflected in Fig. 3 indicate that this paper material was increasingly degraded as the incubation pH value increased from a value of 3.5 to 6.0, with a decrease in the degradation when the pH value was increased to higher pH values. At the incubation
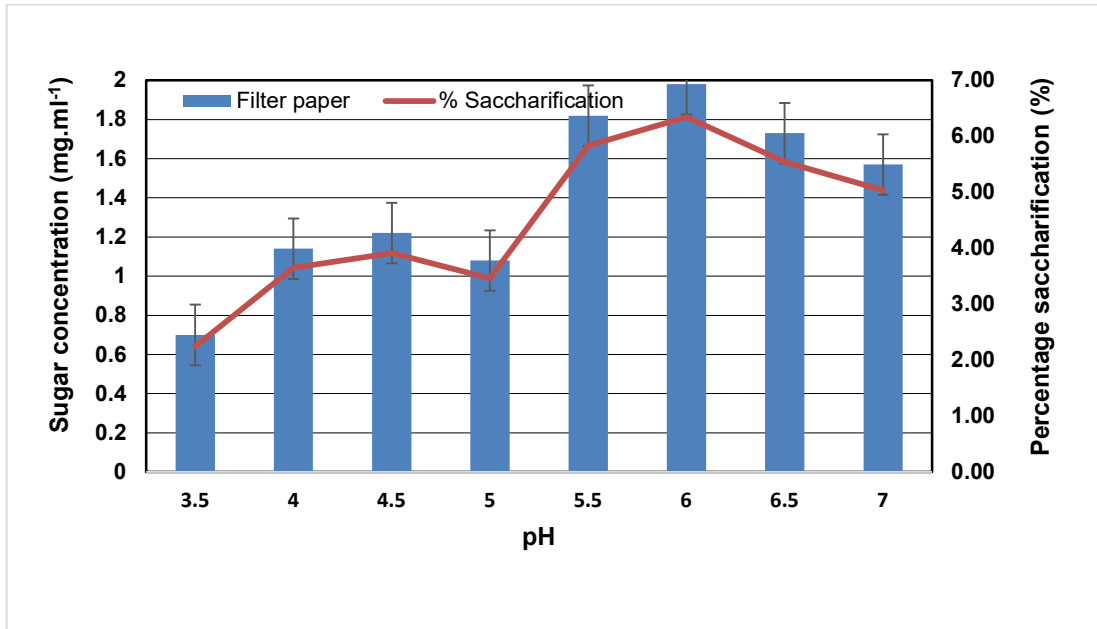
Fig. 1: Concentration of sugar (mg.mL$^{-1}$) produced from and percentage saccharification (%) of filter paper when degraded with cellulase from the brown garden snail (*Cornu aspersum*) at different pH-values.
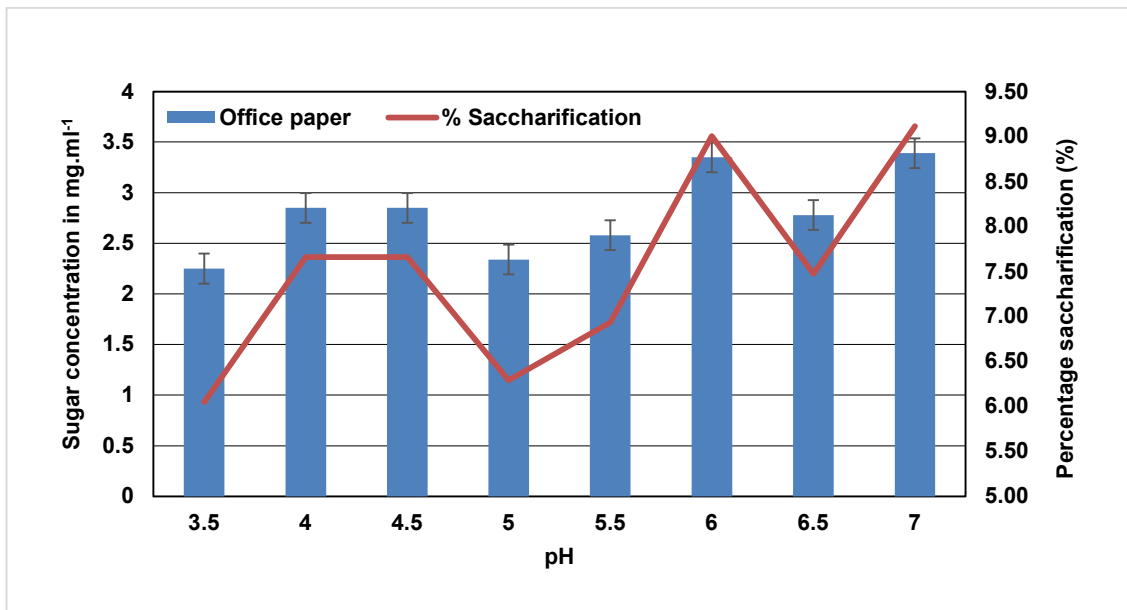


Fig. 2: Concentration of sugar (mg.mL$^{-1}$) produced from and percentage saccharification (%) of office paper when degraded with cellulase from the brown garden snail (*Cornu aspersum*) at different pH-values.

pH-values less than 6.0, the amount of sugar produced varies between concentrations of 2.13 mg.mL$^{-1}$ and 2.35 mg.mL$^{-1}$, while the maximum sugar concentration at pH 6.0 was calculated at a concentration of 2.92 mg.mL$^{-1}$. At pH-values higher than 6.0, the amount of sugar decreased to a value of 2.49 mg.mL$^{-1}$ and 2.62 mg.mL$^{-1}$ at the pH-values of 6.5 and 7.0, respectively. The percentage saccharification at the pH value of maximum saccharification was 10.81%, while the lowest degree of saccharification was obtained at 7.89%, calculated at an incubation pH of 4.0. The degree of saccharification increased by 37% from the lowest sugar yield to the maximum amount of sugar produced.
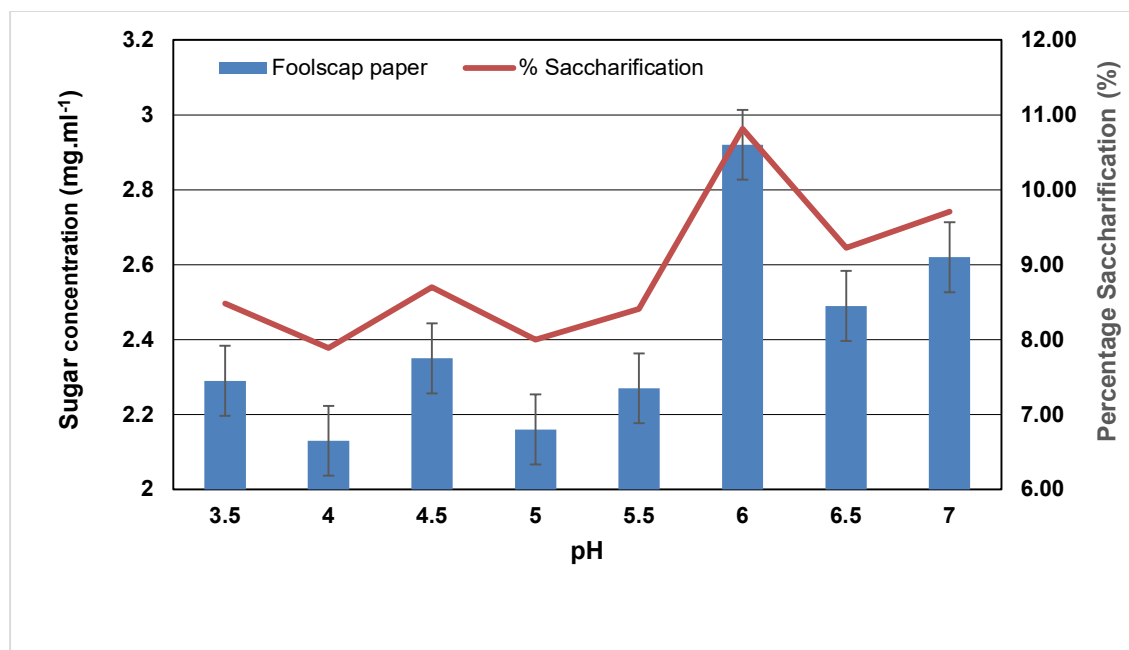
Fig. 3: Concentration of sugar (mg.mL$^{-1}$) produced from and percentage saccharification (%) of foolscap paper when degraded with cellulase from the brown garden snail (*Cornu aspersum*) at different pH-values.

Saccharification of newspaper (Fig. 4) at different pH values yielded the highest amount of sugar at a concentration of 2.18 mg.mL$^{-1}$ when degraded at a pH of 4.5, with the second highest amount of sugar released at a concentration of 2.11 mg.mL$^{-1}$ obtained at a pH-value of 6.0. The lowest amount of sugar was released at a pH of 3.5 when the produced sugar concentration was 1.5 mg.mL$^{-1}$, and this amount was increased 1.45 times to produce the maximum concentration of 2.18 mg.mL$^{-1}$. When incubated at pH values higher than pH-6.0, the amount of sugar released from the newspaper decreased with a concentration of 1.77 mg.mL$^{-1}$ produced during incubation at a pH of 7.0. The degree of saccharification at the optimum pH value of saccharification was 9.60%.
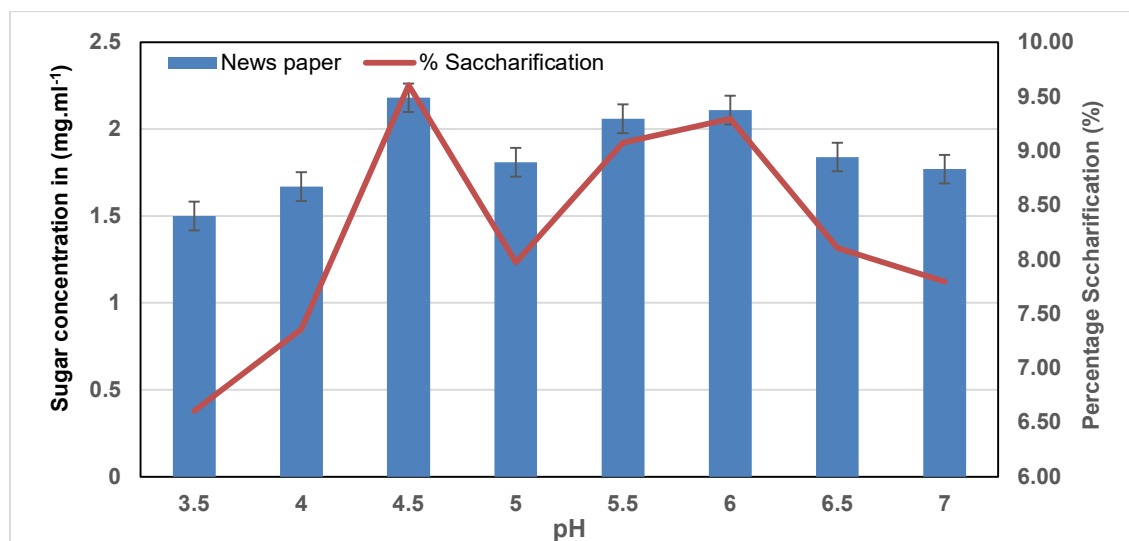


Fig. 4: Concentration of sugar (mg.mL$^{-1}$) produced from and percentage saccharification (%) of the newspaper when degraded with cellulase from the brown garden snail (*Cornu aspersum*) at different pH-values.
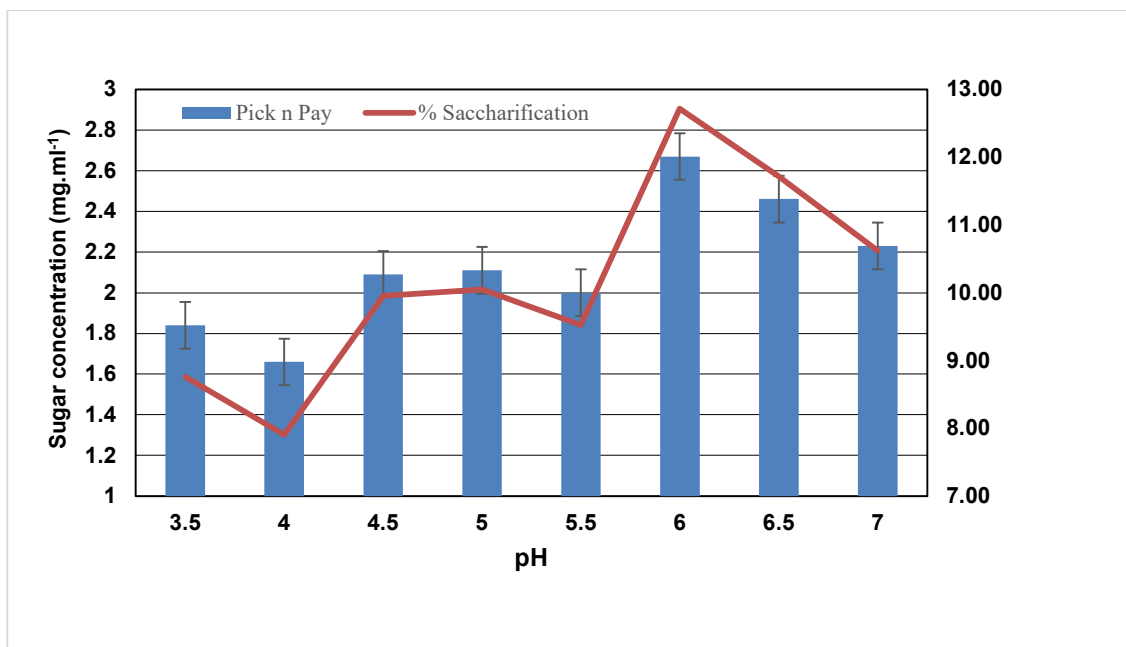
Fig. 5: Concentration of sugar (mg.mL$^{-1}$) produced from and percentage saccharification (%) of Pick 'n Pay advertising paper when degraded with cellulase from the brown garden snail (*Cornu aspersum*) at different pH-values.

In comparison, the lowest extent of saccharification was 7.36% when degraded at an incubation pH-value of 4.0, with a 7.80% saccharification when degraded at a pH-value of 7.0.

When Pick 'n Pay (Fig. 5) advertising paper was saccharified with cellulase from the brown garden snail, the maximum amount of sugar was released at a pH of 6.0, producing a sugar concentration of 2.67 mg.mL$^{-1}$ and a percentage of saccharification equal to 12.71%. The degradation of this paper material at pH values higher than 6.0 was more than the amount of sugar produced at pH values less than 6.0. The lowest degree of saccharification was calculated at a concentration of 1.66 mg.mL$^{-1}$ and 7.90% saccharification at an incubation pH of 4.0. At the pH-values higher than 6.0, the rate of saccharification was 11.71% and 10.62 % at pH-values of 6.5 and 7.0, respectively, while the corresponding sugar concentrations were 2.46 mg.mL$^{-1}$ and 2.23 mg.mL$^{-1}$. The highest amount of sugar produced during the degradation at pH 6.0 was 60.8% higher than the lowest amount of sugar released at the pH value of 4.0.

Other than degradation of the other paper materials was, the saccharification of Woolworth's paper highly pH-specific, and maximum bioconversion was observed at a pH-value of 6.0 with a strong decline in sugar production at pH-values higher and lower than the optimum pH-value of cellulase action. When maximally degraded, the sugar concentration

was 3.86 mg.mL$^{-1}$ with a degree of saccharification of 8.85%. At pH values higher and lower than the optimum pH value for saccharification of this paper material, the amount of sugar produced varied between 2.67 mg.mL$^{-1}$ and 2.97 mg.mL$^{-1}$, with the percentage saccharification varied between 6.12% and 6.81% (Fig. 6). The increase in saccharification from the lowest yield of 2.67 mg.mL$^{-1}$ to the highest concentration was 44.5%.

No unique optimum pH value was identified for the degradation of brown envelope paper (Fig. 7) as the amount of sugar produced varied between 5.29 mg.mL$^{-1}$ and 5.91 mg.mL$^{-1}$ during incubation between pH values of 3.5 and 6.5. Incubation at a pH value of 7.0 resulted in the lowest sugar production from this paper material at a concentration of 4.76 mg.mL$^{-1}$ and 8.90% saccharification. In contrast, the percentage of saccharification at the lower pH values varied between 9.89% and 11.05%.

These findings of changing pH values on the catalytic effect of cellulase from garden snails are supported by work done by Gautam et al. (2011), who concluded that the optimum pH for cellulase activity is at pH 6.5 and also noted that the enzyme activity was stable at pH range between 5.0 and 8.0. During the current investigation, the optimum degradation of brown envelope paper was obtained at pH values of 4.5 as well as pH 6.0, which supports the findings of Mokatse and Van Wyk (2017), who concluded that certain paper materials could be saccharified optimally by
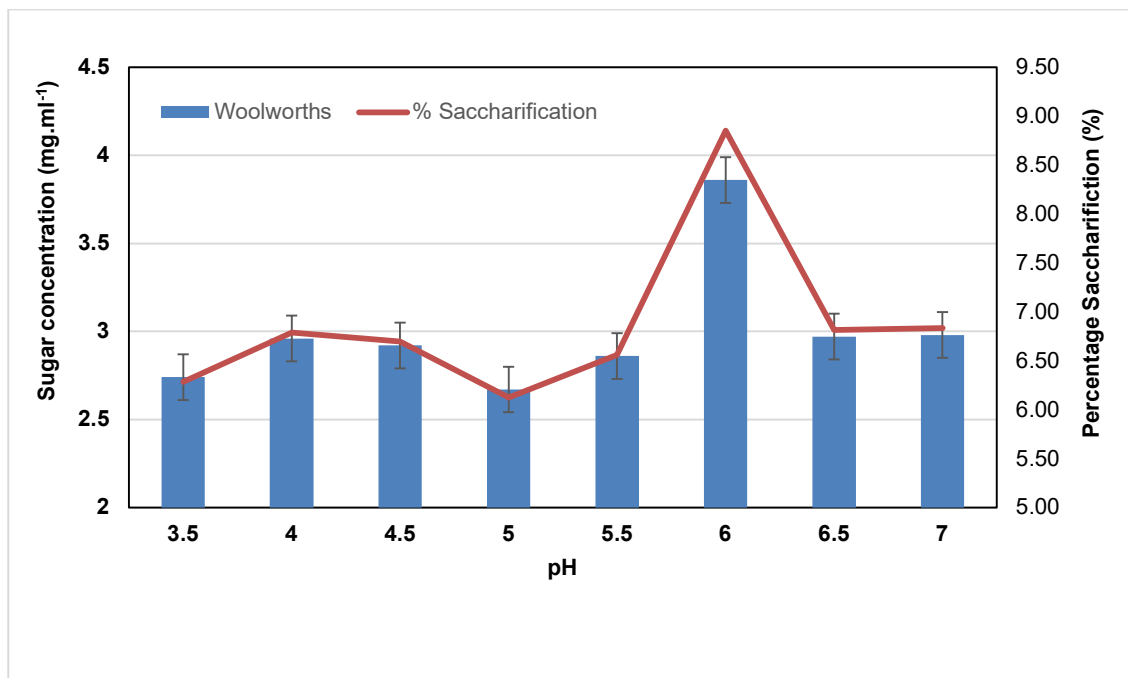
Fig. 6: Concentration of sugar (mg.mL$^{-1}$) produced from and percentage saccharification (%) of Woolworth's advertising paper when degraded with cellulase from the brown garden snail (*Cornu aspersum*) at different pH values.
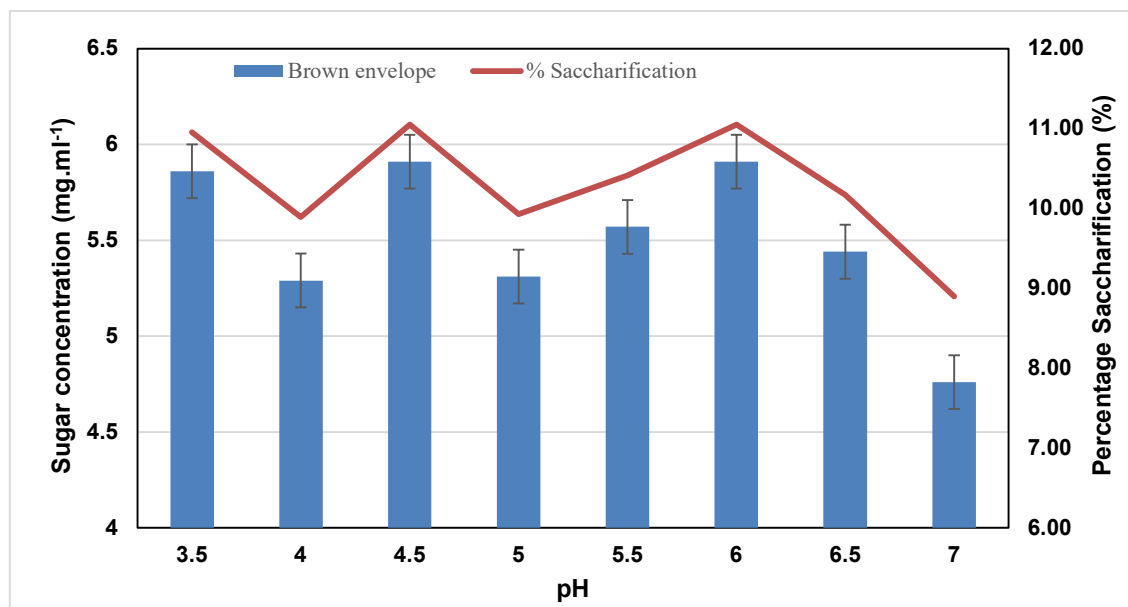


Fig. 7: Concentration of sugar (mg.mL$^{-1}$) produced from and percentage saccharification (%) of brown envelope paper when degraded with cellulase from the brown garden snail (*Cornu aspersum*) at different pH values.

cellulase enzymes at two different pH-values. The optimum pH value of 6.0 is also consistent with the value published by Abdulsattar et al. (2020) when performing a cellulase-related investigation.

Cellulose is described as the most abundant renewable substance on the planet, and it is present in many waste substances, such as paper materials, kitchen and garden waste, and agricultural waste. With the rate at which

solid waste is produced daily without an effective waste management system in place, the accumulation of solid waste is already a major environmental concern to many countries, and the future effects of waste on the environment do not appear to be very positive. Dumping at landfills, incineration, and illegal burning are still popular ways of dealing with organic waste, including cellulose-derived materials. Chemically, cellulose is described as a biopolymer composed of glucose units that have the potential to be developed as a resource for bio-energy production. Waste cellulose could also be used as an alternative feedstock to fossil fuels for the biosynthesis of bioproducts. To utilize waste cellulose effectively as a resource with renewable potential, it must be degraded into glucose, a fermentable sugar. This saccharification process could be performed with a hydrolytic enzyme system such as cellulase, which exhibits the ability to break the chemical bonds between glucose units in the cellulose molecule, releasing free glucose units. The degradation of cellulose by cellulase enzymes from bacteria (Hosny & El-Sheshtawy 2022) and mostly fungi (Sarsaiya et al. 2018) are well described with many references to the optimum catalytic properties such as pH, temperature, enzyme as well and substrate concentration. The saccharification effect of cellulase from *Trichoderma reesei* and *Aspergillus niger* on various paper materials has been published to a great extent by laboratories where the current research is performed.

Information regarding cellulase isolated from brown garden snails is not available to the same extent as information related to other cellulase enzymes, as the scientific community has not studied this cellulase extensively. A method to isolate cellulase from brown garden snails has been described, as well as its hydrolytic effect on the degradation of certain waste paper materials (Ndlovu et al. 2019). To secure maximum cellulose conversion into glucose, it is essential that the catalytic parameters, such as the pH of the enzyme action, be optimized. The various paper materials have non-identical structural compositions. They would exhibit different susceptibilities towards the cellulase enzyme, thus the observed difference in relative sugar production from the different paper materials when saccharified with cellulase from the brown garden snail. The pH value of an enzyme-catalyzed reaction is a catalytic parameter that would affect the effective catalysis of the reaction, and such is the case with the bioconversion of waste paper into sugars by cellulase from the brown garden snail. This investigation found that maximum saccharification was obtained at pH 6 with almost all the paper materials. However, the sugar-releasing patterns at higher and lower pH values than 6.0 differ for the various materials. The pH-value of 6 for optimum activity is more acid than the

pH-value of 7.4 observed for the cellulase isolated from *B. licheneniformis* used to degrade carboxymethyl cellulose (Zanab et al. 2022). A more acidic pH value of 4.8 was recorded for the degradation of corn straw, wheat straw, and sugarcane bagasse by cellulase from *Aspergillus niger* (De Aguiar et al. 2022). Cellulase with a wide optimum pH range between pH 5.0 to pH 9.0 has also been reported for the degradation of cellulose by cellulase from *Geobacillus* sp. isolated from hot spring water (Khadka et al. 2022).

Although waste paper is rich in cellulose, not all types treated with the garden snail cellulase have been degraded with cellulase from other bacterial or fungal cellulases. The degradation of Woolworths and Pick 'n Pay paper is a unique attempt by researchers in our laboratories, as any other researchers have not reported its bio-conversion potential. These two paper materials have been bio-converted into sugars by cellulase from *Trichoderma viride,* and both were maximally degraded to a value of pH 4.5. During the same investigation, it was concluded that newspaper and foolscap paper also showed maximal degradation into sugars by the same cellulase at pH 4.5. Brown envelope paper, office paper, and filter paper showed optimum degradation by the *T. reesei* enzyme at a pH of 5.0 (Mokatse & Van Wyk 2017). Of the paper materials, filter paper is the utmost studied, mostly to demonstrate the action of cellulase and at optimum values of pH 5.5 when degraded with *T. viride* cellulase (Rathman et al. 2015) and pH 4.8 when treated with *T. reesei* cellulase (Chu et al. 2012). The presence of dyes or ink on paper material is a physical factor that needs to be considered when degrading the cellulose content of used paper with cellulase enzymes. Ink or dyes covering the paper materials act as a barrier between the enzyme and the cellulose substrate, thus preventing the effecting interaction between enzyme and substrate. This observation was made during an investigation in our laboratory when paper covered to different extents was degraded with cellulase from *T. viride*. It can be assumed that cellulase from the garden snail would experience the same difficulty (Van Wyk & Sibiya 2014).

Environmental pollution is a global concern, and associated with this singularity is climate change, whose effects are already experienced by many countries in terms of excessive heat, drought, and flooding. The use of fossil fuels is a major contributor to this change in natural processes, and replacing this energy resource as a fuel and feedstock in many chemical syntheses with an environmentally friendly substance becomes more urgent. Bioenergy is classified as environmentally friendly, and waste cellulose materials such as wastepaper contain cellulose as a structural component that could be resolved into glucose by cellulase, a biological catalyst. Glucose is a fermentable sugar that can be used as a feedstock for synthesizing bioethanol (Byadgi &

Kalburgi 2016). To optimize the saccharification of different wastepaper materials effectively, catalytic parameters such as incubation pH must be optimized, and this writing does not only reveal the effect of pH on cellulase-catalyzed degradation of various wastepaper materials but also describes the action of a cellulase isolated from brown garden snails an enzyme which has not received much scientific attention during the past.

## CONCLUSIONS

Environmental pollution and climate change are two issues that already influence global activities, and corrective scientific procedures will have to be investigated and applied more aggressively to counteract these occurrences. Developing organic waste as a renewable energy resource and utilizing it as a feedstock for the biosynthesis of chemical commodities could assist in controlling the negative environmental forces caused by pollution and climate change. Using cellulase isolated from garden snails as biocatalysts contributes further to the value of the waste bioconversion process, as snails are regarded by many communities, such as farmers, as a pest due to the destructive effect of snails on their crops. The development of wastepaper as a renewable energy resource is contributing to the process of dealing with solid waste in an environmentally friendly manner, and the optimization of incubation pH-values for various paper materials when degraded by garden snail enzyme is contributing to the effectiveness of the process. The observation that most paper materials are optimally degraded at a pH value of 6.0 indicates the similarity between these materials. However, the difference in relative sugar yield, From the investigation, it can be concluded that cellulase isolated from garden snails can degrade the cellulose component of various wastepaper materials into glucose. That waste cellulose can be developed as a renewable feedstock for producing glucose-related fermentation bio-products. Identifying the optimum incubation pH values is also an important catalytic parameter for optimizing bioconversion.

## ACKNOWLEDGEMENT

## REFERENCES

Abdulsattar, M.O., Abdulsattar, J.O., Greenway, G.M., Welham, K.J. and Zein, S.H. 2020. Optimization of pH as a strategy to improve enzymatic saccharification of wheat straw for enhancing bioethanol production. J. Anal. Sci. Technol., 11(17): 217. https://doi.org/10.1186/s40543-020-00217-7.

Bhunia, B., Dutta, D. and Chaudhuri, S. 2011. Extracellular alkaline proteases from Bacillus licheniformis NCIM-2042: Improving enzyme activity assay and characterization. Eng. Life Sci., 11(2): 207-215. DOI: 10.1002/elsc.201000020.

Byadgi, S. and Kalburgi, P.B. 2016. Production of bioethanol from a waste newspaper. Proc. Environ. Sci., 35: 555-562.

Charrier, M. and Brune, A. 2003. The gut microenvironment of helicid snails (Gastropoda: Pulmonata): in-situ profiles of pH, oxygen, and hydrogen determined by microsensors. Can. J. Zool., 81: 928-935. https://doi.org/10.1139/z03-071.

Chu, D., Deng, H., Zhang, X., Zhang, I. and Bao, J. 2012. A simplified filter paper method of cellulase enzyme based on HPLC-analysis. Appl. Biochem. Biotechnol., 167: 190-196.

Dar, M.A., Pawar, K.D. and Pandit, R.S. 2017. Gut Microbiome Analysis of Snails: A Biotechnological Approach. Intech Open, NY. http://dx.doi.org/10.5772/68133.

De Aguiar, C.M., Rufino, A.R., Hasan, S.D.M. and Lucena, S.L. 2019. Effects of pH and temperature on the enzymatic hydrolysis of crop residue by fungal cellulase. Int. J. Sci. Eng. Res., 10(11): 1109-1112.

Dini, I.R., Restuhadi, F. and Silaturahmi, K. 2019. The effect of purification on Snail (Achatina fulica) cellulase enzyme characteristics. IOP Conf. Ser. Earth Environ. Sci., 250: 012051. doi:10.1088/1755-1315/250/1/012051.

Dubnovitsky, A.P., Kapetaniou, G. and Papageorgiou, A.C. 2005. Enzyme adaptations to alkaline pH: atomic resolution 1.08 A structure of phosphoserine aminotransferase from Bacillus alcalophilus. Protein Sci., 14(1): 97-110: doi: 10.1110/ps.041029805.

Evans, W.A.L. and Jones, E.G. 1961. A note on the proteinase activity in the alimentary tract of the slug Arion ater L. Comp. Biochem. Physiol., 5: 223–225. https://doi.org/10.1016/0010-406X(62)90108-1.

Gautam, S.P., Bundela, P.S., Pandey, A.K., Khan, J., Awasthi, M.K. and Sarsaiya S. 2011. Optimization for the production of cellulase enzyme from municipal solid waste residue by two novel cellulolytic fungi. Biotechnol. Res. Int., 11: 412. doi:10.4061/2011/810425.

Hosny, M. and El-Sheshtawy, H.S. 2022. Effect of biosurfactant on the hydrolysis of municipal waste by cellulases producing bacteria for bioethanol production. Curr. Res. Green Sustain. Chem., 5: 100294.

Khadka, S., Khadka, D., Poudel, R.C., Bhandari, M., Baidya, P., Sijapati, J. and Maharjan, J. 2022. Production optimization and biochemical characterization of cellulase from Geobacillus sp. KP43 is isolated from the hot spring water of Nepal. Biomed Res. Int., 11: 614. https://doi.org/10.1155/2022/6840409.

Loelovich, M. 2014. Wastepaper is a promising feedstock for the production of biofuel. J. Sci. Res. Rep., 3(7): 905-916. DOI: 10.9734/JSRR/2014/8025.

Miller, G. 1959. Use of di-nitrosalicylic acid reagent for determination of reducing sugar. Anal. Chem., 31: 426-428.

Mokatse, K.M.P., Mhlanga, H.S. and Van Wyk, J.P.H. 2016. Relative saccharification and initial degradation rates of different waste paper materials by cellulase from Trichoderma viride. J. Appl. Biosci., 105(1): 10183-10190. DOI: 10.4314/jab.v105i1.14.

Mokatse, K.M.P. and Van Wyk, J.P.H. 2017. pH-values for optimum saccharification of various wastepaper materials by cellulase from Trichoderma viride. J. Basic Appl. Sci. Res., 7(9): 18-26.

Navarro, R.R., Otsuka, Y., Nojiri, M., Ishizuka, S., Nakamura, M., Shikinaka, K., Matsuo, K., Sasaki, K., Kimbara, K., Nakashimada, Y. and Kato, J. 2018. Simultaneous enzymatic saccharification and comminution for the valorization of lignocellulosic biomass toward natural products. BMC Biotechnol., 18(79): 487. https://doi.org/10.1186/s12896-018-0487-1.

Ndlovu, T.M. and Van Wyk, J.P.H. 2019. Isolation of cellulase enzyme from brown garden snail (Cornus aspersum) for the saccharification of waste paper materials. MethodsX, 6: 1030-1035.

Okeniyi, F.A., Osinowo, O.A., Ladokun, O.A., Akinloye, A.K., Bamidele, and Sanni, D.M. 2015. Bacteria and digestive enzymes in the alimentary tract of the giant African land snails, *Archachatina marginata*, and *Achatina achatina*. Niger. Soc. Anim. Prod., 42: 28-36.

Rathnan, R.K., Balasaravanan, S.M., Tony, A.K., Anamika, P. and Ambili, M. 2015. Bioconversion of waste paper by co-cultures of fungi isolated from lignocellulosic waste. Int. J. Curr. Microbiol. Appl. Sci., 4: 326-333.

Sarsaiya, S., Awasthi, S.K., Awasthi, M.K., Awasthi, A.K., Mishra, S. and Chen, J. 2018. The dynamic of cellulase activity of fungi inhabiting organic municipal solid waste. Bioresour. Technol., 251: 411-415. https://doi.org/10.1016/j.biortech.2017.12.011.

Tiseo, I. 2021. Global paper industry – statistics and facts. Statista Dossier. https://www.statista.com/topics. Accessed on 10 April 2023.

Van Wyk, J.P.H. and Sibiya, J.B.M. 2014. Effect of ink on the saccharification of waste office paper during the biodegradation with cellulase from *Trichoderma viride* at different temperatures. Int. Res. J. Biol. Sci., 3(8): 40-45.

Van Wyk, J.P.H. and Sibiya, J.B.M. 2016. Saccharification of ink-covered office paper by different concentrations of cellulase from *Trichoderma viride*. J. Chem. Pharm. Res., 6(10): 9-17.

Van Wyk, J.P.H., Mogale, M.A. and Seseng, T.A. 2000. Saccharification of used paper with different cellulases. Biotechnol. Lett., 22: 491-494.

Vladimir, B., Tomas, J., Viliam, H., Jirina, O., Ladislav, B., Petr, G. and Petr, S. 2014. Enzymatic hydrolysis of pretreated wastepaper – Source of raw material for the production of liquid biofuels. Bioresour. Technol., 152: 543-547. http://dx.doi.org/10.1016/j.biortech.2013.11.030.

Walker, A.J., Miller, A.J., Glen, D.M. and Shewry, P.R. 1996. Determination of pH in the digestive system of the slug *Deroceras reticulatum* (Müller) using ion-selective microelectrodes. J. Molluscan Stud., 62: 387-390. https://doi.org/10.1093/mollus/62.3.387.

Zainab, E.E., Samir, H.A., Ibrahim, A.M., Guirgis, A.A. and Dawwam, G. 2022. Purification, biochemical characterization, and molecular cloning of cellulase from Bacillus licheniformis strain Z9 isolated from soil. J. Genet. Eng. Biotechnol., 20(34): 10317. Doi: 10.1186/s43141-022-00317-4.

Zhao, X., Zheng, Z., Cai, Y., Zhao, Y., Zhao, Y., Zhang, Y., Gao, Y., Cui, Z. and Wang, X. 2020. Accelerated biomethane production from lignocellulosic biomass: Pretreated by mixed enzymes secreted by *Trichoderma viride* and *Aspergillus* sp. Bioresour. Technol., 309: 123378. http://doi.org/10.1016/j.biortech.2020.123378.

## ORCID DETAILS OF THE AUTHORS

J. P. H. van Wyk: https://orcid.org/0000-0002-8950-2490

# Household Energy Fuel Choice in Nigeria Residential Urban Area

**O. J. Ubani†** iD **, A. Okosun, G. Chukwurah and Ivo Henry**

Department of Urban and Regional Planning, University of Nigeria, Enugu Campus, Enugu, Nigeria
†Corresponding author: O. J. Ubani; obinna.ubani@unn.edu.ng

## ABSTRACT

In most Nigerian cities, there have been an increased number of trading in charcoals, firewood, and sawdust. Yet, the fast citing of cooking gas refilling stations in these areas requires much to be studied since their increasing number suggests great demand for cooking gas. The knowledge of the different household fuel choices and the drivers of this choice was lacking in Nigerian cities, thus the inability of energy policymakers to predict and plan household fuel agenda in Nigeria. The thrust of this paper was to analyze the household energy fuel choice and the pattern of consumption as well as analyze the household socioeconomic factors that influenced the fuel choice in the Abakaliki urban area of Ebonyi State, Nigeria. Stratified and simple random sampling was adopted in the study. Regression was used to consider the relationship between energy fuel choice and household socioeconomic factors. It was revealed that there was a mixture of traditional and modern energy fuel choices in the study area, with the modern energy fuel choices (gas and electricity) having higher patronage. There was a significant relationship between energy fuel choice and household socioeconomic factors. It was recommended, among others, that a clear energy fuel policy that will adopt the identified explorable household socioeconomic factors that influence the choice of energy fuel be developed.

## INTRODUCTION

Heating, lighting, and cooking are part of basic human needs that involve energy consumption. The various energy forms required for lighting and heating, cooking, and other like tasks, according to UNDP & WHO (2009), are gas, coal, electricity, charcoal, dung, and wood, among others. Unfortunately, though, there is still much dependency on traditional biomass fuels from persons in various third-world and developing countries. These biomass fuels are mainly used for light sources such as kerosene, and candles have also been used for cooking. It has been an enormous challenge to expand access to modern energy services, especially in third-world countries. As of 2019, about three million people in developing countries of the world depend on solid fuels for cooking, while 1.2 persons do not have access to electricity (UNDP & WHO 2009).

Figures have it that the annual firewood consumption in Nigeria stands at 50 million metric tons, and this exceeds the replenishment rate through the reforestation program (ICCDD 2000). With the ongoing situation of consumption of fuel wood in Nigeria, it is important to find alternative ways of cooking without exhausting our forest resources. Degradation of forest resources is increasing daily, which has affected the Nigerian economy as a result of the loss of

properties due to flooding and arable farmland in the process. The multiplier effect of this has already become clear, as seen in different ecological spheres in the country, and that has resulted in great economic losses (Sambo 2009). Studies also indicate that 74% of households in Asia rely on traditional energy sources like biomass. This, according to the World Bank (2007), is contrary to the situation in Nigeria, where 65% of urban household still depends on charcoal, fuel wood, and waste wood to meet the energy demand of households for their cooking. This was collaborated by the study by Madukwe (2014) on domestic energy usage patterns in Enugu State of Nigeria. He found out that while most rural dwellers in Nigeria depend on biomass fuel, a substantial number in urban areas use wood fuel also.

Ebonyi State of Nigeria has Abakaliki as its capital city, and various households in the city have varying energy fuels for lighting and cooking. In Abakaliki urban, the rate of urbanization, industrialization, and increased economic development seems to have caused changes in the consumption patterns of households, which has ultimately led to margin changes in the household energy sector. The seeming shift from modern fuel products to charcoal and saw specks of dust in some parts of the area has raised some concern among urban planners and energy experts. There has been an increased number of trading in

charcoals, firewood, and sawdust in the study area, and this has remained unregulated. Yet, the fast citing of cooking gas refilling stations in the State capital requires much to be studied since this indicates great demand for cooking gas. The understanding of the varying household fuel choices has been seemingly minimal in most Nigeria cities, and the inability of energy policymakers to estimate and propose household fuel agenda in the area is grossly worrisome even at the national level (Nnaji et al. 2012, Energy Commission of Nigeria 2003). The perceived apathy by the Nigerian government in tackling household energy challenges has been linked to the nonexistence of baseline data on energy consumption, and this has seriously affected energy planning and policy-related studies. Various literature searches suggest that in most of Nigeria's newly created State capital cities, no detailed study has been conducted to establish patterns of household energy consumption (Madukwe 2014).

Furthermore, household drivers on these cooking fuel preferences have not been robustly determined, especially as it relates to residential densities. Hence, understanding household fuel choice and its drivers will serve as the basis for formulating a sustainable household fuel agenda. The thrust of this paper was to analyze the household cooking energy fuel choice in the Abakaliki urban area. This is to evolve policy design and interventions that will serve as the basis for a sustainable household fuel agenda in the State and ensure improved quality lives of households in Nigeria. The study also considered the household socioeconomic factors that drive energy fuel choice in the study area. It was hypothesized that the household socioeconomic factors did not influence different household cooking energy fuel consumption.

## PAST STUDIES

### Energy consumption Effect on the Users

The various energy resources have different impacts on their users. Traditional biomass has the most hazardous effect as it produces excessive smoke, which has an adverse effect on its users. Indoor air pollution that emanates from the use of solid waste, according to the World Health Organization (WHO 2010), has been linked to the premature death per annum of an estimated 1.5m globally. In developing nations, there is over-dependency on biomass fuel as a result of the low standard of living that exists there. The impact of socio-cultural and gender inequality has made more women victims of energy choices made by households in the world as they are the major users, followed by little children who are, at one point or the other, charged with the responsibility of cooking household meals. Women and children who are predominant

users of biomass in traditional stoves are prone to high levels of indoor air pollution (Dzioubinski & Chipman 1999).

The importance of clean fuels cannot be over-emphasized as it is crucial in the health of households that give very little or no smoke. The health of the users is as important as the entire household, which therefore means that more attention should be given to selecting household fuels so as to reduce health crises that may surround their users. This is crucial since, according to studies done by Toole (2015) and Muller & Yan (2016), it was revealed that the consumption of traditional biomass is linked to indoor air pollution and greenhouse gas emissions.

However, the presence of clean fuel services in homes opens better economic opportunities to the end users who have been identified as women and children in that it improves their political, economic, and social status, thereby reducing the effort and time they are engaged in domestic chores, thus, providing better educational and health conditions as well as increasing generating opportunities (UNDP 2006). Among the various household energy sources, the most effective are electricity and gas, which do not produce smoke. However, most people in developing nations choose not to use it simply because they are expensive and scarce in some localities. Apart from the direct impact it has on users, it also affects the water in which we drink due to deforestation. Deforestation affects water as plants have been cut down, and the tendency for erosion also increases as water washes the uppermost surface of the earth into a nearby river or water bodies. The content that has been washed might have some fertilizer and insecticide content, which might be poisonous to man, thereby causing water pollution.

### The Concept of Household Energy Consumption Pattern

Right from the inception of man into this world, energy has been a key factor in his existence as it helps in providing fundamental needs such as lighting, cooking, and heating, which is a fundamental requirement in sustaining human life. Generally, the amount of energy resources consumed by homes in different appliances in the home is referred to as household energy consumption. A nation's stage of economic growth and development, as well as its social status, is always a function of its pattern of energy consumption. The increase in population has been traced to be the underlying factor for the rise in household energy consumption, along with growth in the economy and a rise in per capita income. Bhattacharyya (2011), however, posited that the use of energy fuel differs from country to country, and this difference could be attributed to the country's level of economic growth, certain government policies, and varied climatic conditions.

Among the various sectors (industrial, household, commercial, etc., Wang et al. (2011) noted that the household sector was rated the most important in the energy consumption sector. Swan and Ugursal (2008) posited that energy consumption of the residential sector accounts for approximately 30% of the total world energy consumption. The importance of energy in the world cannot be over-emphasized because of its fundamental usefulness to every mankind in every sector. Table 1 below represents household energy consumption from a few of the world countries in which Nigeria has the highest rate of energy consumed by her residential sector at 65%. This was adopted by Swan & Ugursal (2008). The statistics show how important household energy consumption is to Nigeria compared to other sectors.

Studies have shown that 2.5 billion people depend on nuclear fuels in developing countries for their domestic use. (IEA 2006). In the same vein, it was recorded that 3 billion people rely on solid fuels globally for their domestic needs. In Nigeria, a developing economy, the major sources of cooking fuel are kerosene, cooking gas, electricity (electric cookers, electric stoves, electric heaters), charcoal, and firewood (fuel wood). Expectedly, though, Maduka (2011) stated that Nigeria depends on more traditional sources of energy like fuel wood, crops, and plant residues, as well as firewood for their regular energy needs. This is despite the abundance of great natural resources like gas and oil. He further estimated that 55% of Nigeria's primary energy demand comes from animal waste, biomass, firewo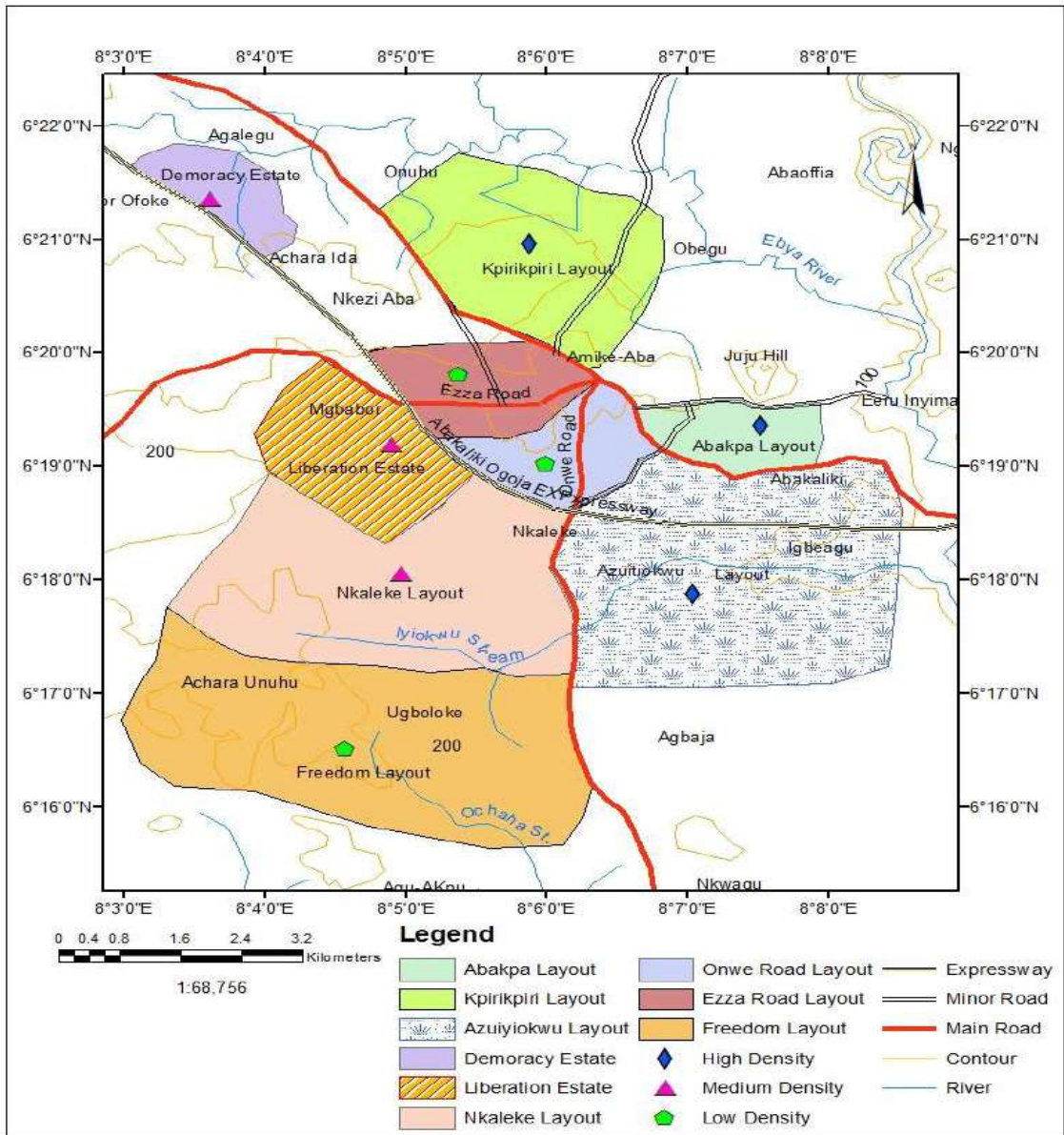od, and charcoal. He concluded that this fuel is used for cooking and heating homes. There is pressure on forests as a major source of firewood for cooking because of the low standard of living among the populace and the ever-growing population. Globally, there is this continued increase in energy demand observed in both developing and developed countries of the world, and this increased demand has been attributed to an improved standard of living among the populace, a growing number of manufacturing industries, a high urbanization rate, as well as increased population (Adedayo et al. 2008).

## Study Area - Abakaliki Urban

Abakaliki is among the new State capitals in Nigeria. It is the capital city of Ebonyi state, which is in the eastern part of Nigeria. It is located on latitude 06°18' North and longitude 08°07' East; It is situated on a seemingly highland located in the lower belt of Niger, covering a land mass of about 2463 hectares (2.8 km radius). Since the elevation of Abakaliki Local Government Headquarters to the Ebonyi State capital, the town has witnessed a substantial influx of population and economic activities. The population of Abakaliki urban center in the 2006 census was 276,909; this was projected to be 383,443, with a gross density of 742 persons per hectare in 2022. Also, Abakaliki city, due to rural-urban migration, urbanization, and industrialization, has experienced a steady and speedy increase in her population. There has been an increased number of trading in charcoals, firewood, and sawdust in this area, yet there are increased citing of cooking gas refilling stations in and around this city center. Abakaliki has many higher educational institutions and many housing estates located in it, which indicates a great demand for cooking gas.

The Abakaliki urban has a combination of highland and scarp land terrains. The mineral deposits made the topography slightly undulating. The dominant land uses in Abakaliki are commercial, residential, industrial, institutional, transportation, and recreational land uses. Residential land uses represent the ubiquitous and largest land use within the core area. The various residential neighborhoods in the study area are seen in Fig. 1. The labor force in Abakaliki Capital Territory is made up of skilled, semi-skilled, and unskilled personnel. The majority of the labor force is engaged in agriculture, agro-based industries, hawking, and petty trading. The rest are engaged in mining, processing, and other self-employed activities. The private sector dominates the employment structure within the planned area. These private sectors employ semi-skilled workers in order to maximize their profit. Only very few are employed by the government in different ministries, schools, and parastatals.

Table 1: Residential energy consumption for some countries.

| Country | Percentage of Energy Consumption by Residential Sector (%) |
|---|---|
| Saudi Arabia | 50 |
| Malaysia | 19 |
| Japan | 26 |
| Jordan | 29 |
| Turkey | 31 |
| Italy | 17 |
| Norway | 21 |
| Sweden | 19 |
| Finland | 16 |
| Brazil | 26 |
| Mexico | 23 |
| Usa | 25 |
| Canada | 24 |
| Nigeria | 65 |
| World | 31 |

Source: Adapted from Swan and Ugursal (2008)

Fig. 1: Map of Abakaliki urban showing the residential neighborhoods.

## MATERIALS AND METHODS

### Research Methodology

This study employed an analytic cross-sectional survey and descriptive research design. Data collected were cross-sectional data which were collected from primary sources. The population was drawn from the neighborhoods in the metropolis of Abakaliki, and the study population comprises residents who have lived more than one year in the city. Williams, 1978 Sample Determination Size formula was used

to get 585 respondents for the study. Abakaliki was stratified into low, medium, and high residential density areas, and simple random sampling techniques were further used to select the respondents from nine neighborhoods in the study area. The study was analytic since the a priori hypothesis, which sought to ascertain the relationship between household energy fuel choices and household socioeconomic variables in the study area, was proposed. Five hundred and forty (540) copies of questionnaires were successfully received from the study area out of the 585 that were randomly distributed

in the selected neighborhoods. Inferential and descriptive statistics were used to analyze the collected data using the SPSS 25 version. Frequency count and percentage were normally used to analyze the demographic data and personal information of the respondents. These descriptive statistical tools are necessary for such analytical study. Regression statistical techniques were used to test the hypothesis (the dependent variable was the quantity of use of each energy fuel resource while the socioeconomic attitudes (age, number of years in school, income, sex, and marital status) were the independent variable. Some of the variables, like sex and marital status, were measured as dummy variables of either 0 or 1. Equally, educational attainment was measured as a dummy variable – illiterates = 0 and others = 1).

## RESULTS

### Data Analysis and Results

Table 2 summarises the socioeconomic features of the 540 respondents that were used for the study. The study revealed respondents who were household heads and those who were not. Household heads were 54% of the respondents. This balanced sampled respondents ratio increases the internal validity of the study. Furthermore, 55% were female household heads, while 45% were males. This shows the absence of bias in respondents' representativeness in the study. However, it was not surprising that the former constitutes the majority because female folks are traditionally associated with the use of this household fuel energy use in most African cities. It is always assumed that the kitchen is made for women (Anyim et al. 2021). The study revealed the various types of kitchens of the sampled respondents in the study area. 55.0% of the respondents use an in-house kitchen type, 24.4% use an outdoor kitchen type, and 20.6% use a separate-house kitchen. The study further revealed the various kitchen floor materials used by the various respondents in the study area. 40.6% of the sampled population uses cemented floors, 36.1% uses tiles, 12.2% of the respondent uses terrazzo, 5.6% uses un-cemented floors, and 3.9% of the sampled population uses mud. In comparison, 1.7% of the respondent uses woodwork on their kitchen floors.

The study made some further interesting revelations, as presented in Table 2. The study, as seen in Table 2, shows that 95.0% of the respondents do not use charcoal as a household fuel for cooking, while only 5.0% do. Again, only 34.4% use kerosene for cooking, as against 65.6% of the sampled population that do not. The study also revealed that 40.6% use gas as their source of energy for cooking, which was the highest. Summarily, the percentage of energy consumption usage aside from gas was 34.4%, 20.6%, 7.8%, and 5.0% for

Table 2: Respondents' socioeconomic data.

| Features | (540) | % |
|---|---|---|
| **Respondents** | | |
| *Household head* | 422 | 54 |
| *Not household head* | 118 | 46 |
| Sex of the household head | | |
| *Male-headed household* | 190 | 45 |
| *Female-headed household* | 232 | 55 |
| **Age** | | |
| 20-40 Years | 237 | 43.9 |
| 41-60 | 198 | 36.7 |
| Above 60 | 105 | 19.4 |
| **Marital status** | | |
| *Married* | 482 | 89.2 |
| *Never married* | 43 | 8 |
| *Widowed* | 3 | 0.8 |
| *Divorced* | 12 | 2. |
| **Dwelling categories** | | |
| *Block/corrugated iron roof* | 418 | 77.3 |
| *Block/grass roof* | 82 | 15.1 |
| *Other types* | 40 | 7.6 |
| **Educational level** | | |
| *Illiterate* | 72 | 13.3 |
| *Primary education* | 32 | 5.9 |
| *Secondary education* | 263 | 48.7 |
| *Above secondary education* | 173 | 32.1 |
| **Main occupation** | | |
| Public servant | 98 | 18.1 |
| *Employee* | 82 | 15.2 |
| *Causal labourer* | 17 | 3.2 |
| *Artisan* | 52 | 9.6 |
| *Herder/cultivator/agriculturist* | 201 | 37.2 |
| *Others* | 90 | 16. |
| **Ownership of dwelling** | | |
| *Rented* | | 84 |
| *Owned* | | 484 |
| **Income month-1 (Naira)** | N | % |
| <=₦18,000 | 168 | 31.1 |
| ₦18,500-₦30,000 | 114 | 21.1 |
| ₦30,500-₦70,000 | 72 | 13.3 |
| ₦70,500-₦130,000 | 30 | 5.6 |
| ₦130,500-₦200,000 | 111 | 20.6 |
| Above ₦200,000 | 45 | 8.3 |
| **Type of material used in your kitchen floor** | | |
| Tiles | 195 | 36.1 |
| Woodwork | 9 | 1.7 |
| **Mud** | | |
| *Terrazzo* | 66 | 12.9 |
| *Cement floor* | 219 | 40.6 |
| *Un-cemented floor* | 30 | 5.6 |
| **Kitchen type** | | |
| In-house kitchen | 297 | 55.0 |
| Outdoor kitchen | 132 | 24.4 |
| Separate house kitchen | 111 | 20.6 |

Table 3: Total fuel energy choice.

| S/N | Energy sources | Frequency | Percentage |
|-----|----------------|-----------|------------|
| 1. | Charcoal | 27 | 5.0 |
| 2. | Firewood | 42 | 7.8 |
| 3. | Gas | 219 | 40.6 |
| 4. | Kerosene | 186 | 34.4 |
| 5. | Electricity | 111 | 20.6 |

Source: Researcher's Field Survey (2022)

kerosene, electricity, firewood, and charcoal, respectively. In view of the above statement, charcoal has the lowest used in the study area, as shown in Table 3

The study considered the reasons for the various household cooking fuel choices, which are diverse. The major reasons for people's choice have been found to be associated with the time factor, in which 41.1% of the sampled respondents said they preferred energy fuel that is time efficient. Other reasons adduced were cost efficiency (18.3%), easy to use (13.9%), safety (5.0%), neatness, 5.0%, manageable (8.8%), affordability (3.3%), convenience (2.8%) and comfort (1.7%)

The research revealed some of the challenges encountered by fuel users: 20.0% of the respondents posited that the matter of high risk of fire accident, 11.1% stated that it causes indoor air pollution, 7.8% declared it causes deforestation, 2.8% stated it is usually inconvenient to use. In comparison, 1.1% agreed that it was usually scarce.

The study further presented the regression result of the hypothesis, which sought to ascertain the relationship between household energy fuel choices and household socioeconomic variables. The result is presented in Table 3 below.

## DISCUSSION

Electricity, gas, and kerosene were the major alternative energy sources that were consumed by households in Abakaliki. The study shows a descriptive analysis indicating

Table 3: Regression Analysis.

| No. | Energy choice/type | Household socioeconomic factors | T value | P-sig | Remarks |
|-----|--------------------|----------------------------------|---------|-------|---------|
| 1. | Charcoal | Age | 2.003 | 0.046* | **Significant** |
| | | Sex | -0.401 | 0.688 | Insignificant |
| | | Marital | 2.232 | 0.026* | **Significant** |
| | | School Completion | 2.536 | 0.012* | **Significant** |
| | | Monthly income | -1.024 | 0.030* | **significant** |
| 2. | Firewood | Age | 0.446 | 0.656 | Insignificant |
| | | Sex | 0.778 | 0.437 | Insignificant |
| | | Marital | 1.887 | 0.060 | Insignificant |
| | | School Completion | 1.251 | 0.011* | Insignificant |
| | | Monthly income | -3.595 | 0.000* | **Significant** |
| 3. | Gas | Age | 0.120 | 0.904 | Insignificant |
| | | Sex | -0.950 | 0.342 | Insignificant |
| | | Marital | 1.334 | 0.183 | Insignificant |
| | | School Completion | 3.876 | 0.000* | **Significant** |
| | | Monthly income | 0.325 | 0.745 | Insignificant |
| 4. | Kerosene | Age | -2.904 | 0.004* | **Significant** |
| | | Sex | 1.211 | 0.227 | Insignificant |
| | | Marital | -0.677 | 0.499 | Insignificant |
| | | School Completion | -3.816 | 0.000* | **Significant** |
| | | Monthly income | -3.447 | 0.001* | **Significant** |
| 5. | Electricity | Age | 2.211 | 0.027* | **Significant** |
| | | Sex | 0.637 | 0.525 | Insignificant |
| | | Marital | -0.259 | 0.795 | Insignificant |
| | | School Completion | -1.198 | 0.032* | **Significant** |
| | | Monthly income | 6.067 | 0.000* | Significant |

Source: SPSS Regression Output

that families use a mixture of modern and traditional energy fuel choices and consumption patterns. It was observed that the modern energy choices, which comprise gas and electricity, were more pronounced in the usage than the traditional sources.  It was also noted that greater patrons of these modern sources of energy were younger couples, youths, and students. The use of kerosene was seen as a temporary and emergency alternative to electricity and gas. Multiple fuel use has been revealed by many studies as prominent in most urban areas of developing countries (Taylor et al. 2011, Ngui et al. 2011, Mekonnem & Kohlin 2008). Taylor et al. (2011) stated in their study that despite the nearly universal ownership of stoves by many households in Guetamelia, 77% maintained the use of fuel wood as their main fuel energy source. This agreed with the finding of Ngui et al. (2011), which revealed in their study that most households in Kenya use multiple fuel energy. The situation was not different from the study by Mekonnem & Kohlin (2008), which was conducted in Ethiopia, where they concluded that the best way to describe the choice of energy use by households was multiple.  These findings contradict the popular thought, which theoretically would assume that sources of energy fuel that are inconveniencing – charcoal and firewood are usually the source of energy for low-expenditure households, which were generally believed to live mostly in high-density areas.

 Surprisingly, this study revealed that modern energy sources dominated household energy choices despite the seemingly increased trading of charcoal and sawdust in some precincts in the study area. The implication of this is rather encouraging as it portends minimal environmental damage (Meried 2021). In other words, environmental issues like declining agricultural productivity, felling of trees, soil erosions, and distortion of natural habitat for the wildlife in the area would be seemingly reduced and avoided (Ehirim & Emeka 2020). Thus, this trend is quite good as it depicts that Abakiliki city was accepting modern fuel as a substitute for traditional energy sources, which the area was known for before its status as a State capital.

The study further revealed the household socioeconomic factors that influenced the individual fuel choice and consumption in the study area. Table 3 shows the households' socioeconomic variables that significantly influenced the different fuel energy choices.

Some striking revelations from the study show that in the case of gas used for cooking, it was apparent that only one of the five household socioeconomic variables had a significant relationship with gas, which was educational attainment or number of school years. In the case of the use of kerosene as a household energy choice, it was noticed

that three variables out of five had significant relationships, and these were age, number of years in school, and average household head income. Also, in the case of firewood used for cooking, it was observed that only household head income and educational attainment had a significant relationship with the choice of firewood energy fuel. These findings were not in accordance with the findings by Emagbetere et al. (2016), which posited that socioeconomic variables like household size, income, prices of fuel wood, and prices of fuel wood substitutes were significant to firewood used for cooking in his study. However, in the case of charcoal used for cooking, it was apparent that four of the five independent variables had a significant relationship with it, and these include age, marital status, educational attainment (Number of years in school), and monthly income. Whereas, in the case of electricity used for cooking, it was apparent that only age, school completion - education, and monthly income had a significant relationship. This agrees with the study of Abdullahi et al. (2017), where they posited that explanatory indicators like economic status, household demographic profile, social factors, and public campaign (awareness) are significant determinants for household fuel consumption choices in Nigeria. It was noted from this study that in line with the theoretical propositions of the energy ladder model, households whose socioeconomic status threshold was low were the most likely to patronize the fuel wood as their household fuel energy choice. However, Adamu et al. (2020) revealed that beyond income, there are intricate webs of closely interrelated socioeconomic factors that drive household energy choice and transition. It was obvious from this study that educational attainment had a positive significant influence on the choice of all energy choices by households. This portrays the importance of education as an explorable variable in the study. It is little wonder why Chambwera & Folmer (2007) posited that education is a veritable and significant variable that must be considered while evolving policies to manage and handle the demand for household energy choices on a long-term basis. More enlightened household heads are normally more educated to understand the peril of using biogas fuels, and this thereby increases their desire to demand modern fuel use due to its convenience and safety.

Furthermore, the revelation from this study was in accordance with the findings of Ajao (2011) and Demurger & Fournier (2011), who posited that in households that use firewood as an energy fuel choice, wealth and income have a significant though negative influence in determining their household firewood energy choice. They found out that aside from the matter of household wealth, residents are seen to be generally reluctant to leave traditional cooking habits that they have been used to. Their findings further noted that

floor effect may decrease firewood fuel consumption since households on higher floors in high-rise buildings most times will not prefer firewood usage due to inconveniences. They posited that besides the income effect, own-price effects have significant effects on firewood consumption behavior. They also said that age and academics influence energy choice. In the same vein, the outcome of this study was in sync with the study by Farsi et al. (2007), where they posited that several other socioeconomic demographic variables like education and the gender of the household heads were observed to have the most significant influence in household fuel choice.

## CONCLUSION

The study concluded that the choice of household energy fuel and consumption pattern indicates that there was a mixture of traditional and modern energy fuel choices, and the modern energy fuel choice (gas and electricity) had higher patronage in the study area. Again, the paper concluded that the household socioeconomic factors that determined the cooking fuel choice by the household were the age of the head of household, number of years in schools – educational attainment, marital status, and income level of the household. These energy fuel choice parameters are needed for the framework of the policies for cooking fuel choice models in Nigerian cities. Basically, these socioeconomic and demographical factors have significantly yielded an effect on the use of household cooking fuel choice among households. The government should, therefore, develop a clear energy fuel policy that will adopt the identified household socioeconomic factors that influence the choice of energy fuel, as revealed by the study. The study showed that educational attainment, age, and income were the most pronounced factors that drive people to use gas as their source of energy for cooking. Thus, in areas where youths and working-class citizens were found, there should be availability of those gas-based appliances needed.

Furthermore, there should be policies that should discourage using firewood fuel and ashes for cooking. The policy of any country is geared towards making an enabling environment conducive for the people and, as such, for the overall well-being of the present and future generations yet unborn. Thus, policies to dissuade the public from the use of wood should be put in place, but this should come after a cheaper energy source has been made available to the public. There is a need for a price decrease in cooking gas appliances, for example, cooking gas cylinders, gas stoves, and hoses, since many households choose gas as the prominent energy source. There is a need by the government, therefore, to reduce the cost of all appliances that are linked to gas stoves and their appliances in order to make them more affordable. In achieving this, there is a need for an urgent policy effectuation for the betterment of the households that use gas as energy fuel.

## REFERENCES

Adamu, M., Adamu, H., Ade, S. and Akeh, G. 2020. Household energy consumption in Nigeria: A review on the applicability of the energy ladder model. J. Appl. Sci. Environ. Manag., 24(2): 237-244.

Abdullahi, B., Musa, A., Idi, A. and Adamu, Jibir. 2017. Socioeconomic determinants of household fuel consumption in Nigeria. Int. J. Res. Granthaalayah, 10)5): 348-360.

Adedayo, A.G., Sale, M. and Koleh, O. 2008. Rural Household Wood Energy Utilization Pattern and Its Impact on Deforestation in Akoko South-West L.G.A., Ogun State, Nigeria. Proceedings of the 1st National Conference of the Forests and Forest Produce Society, April 16-18, 2008, Nigeria, pp 15-164.

Ajao, B. 2011. Factors associated with contraceptive ideation among urban men in Nigeria. Adv. Family Plan., 1(3): 3. 56-61.

Anyim, C., Odoemelam, L. and Okorie, N. 2021, Women Participation in fish processing and packaging in rural communities of Delta State, Nigeria. Journal of Agricultural Extension and Rural Development, 3(1): 34-43.

Chambwera, M. and Folmer, H. 2007. Fuel switching in Harare: An almost ideal demand system approach. Energy Policy, 35: 2538-2548.

Bhattacharyya, S.C. 2012. Energy economics: concepts, issues, markets and governance. Int. J. Energy Sect. Manag., 6(1): 145-149.

Démurger, S. and Fournier, M. 2011. Rural households' decisions towards income diversification: Evidence from a township in northern China. J. Chem. Eng., 5: 007 https://doi.org/10.1016/j.chieco.2010.05.007.

Dzioubinski, O. and Chipman, R. 1999. Trends in Consumption and Production: Household Energy Consumption. Discussion Paper of the United Nations Department of Economic and Social Affairs, NY, US p. 21.

Ehirim, C. and Emeka, E. 2020, Demand Analysis for Solid Fuel and Its Substitutes as `Energy in Imo State, Nigeria. Fin. Econ. Rev., 8: 13-25.

Emagbetere, E., Odia, J. and Oreko, B.U. 2016. Assessment of household energy utilized for cooking in Ikeja, Lagos State, Nigeria. Nigeria. J. Technol., 35(4): 796-804.

Energy Commission of Nigeria. 2003. National Energy Policy. Federal Republic of Nigeria, Abuja.

Farsi, M., Filippini, M. and Pachauri, S. 2007. Fuel choices in urban Indian households. Environ. Dev, Exon., 12: 757-774.

Food and Agriculture Organization (FAO). 2008. State of the World's Forests 1997, Rome: Food and Agriculture Organization.

Inter-Ministerial Committee on Combating Deforestation and Desertification (ICCDD). 2000. Handbook on Nigeria Environment. Ministry of Environment, Nigeria.

International Energy Agency (IEA). 2006. World Energy Outlook 2006. Organization for Economic Cooperation and Development and IEA, Paris.

Maduka, J.O. 2011. Popularizing the use of Liquefied Petroleum Gas (LPG) as a substitute for fuelwood among women in Nigeria. Proceedings of the 3rd Int. Conf. of the African Renewable Energy Alliance on Renewable Energy and Gender, June 29-July 1, 2011, Abuja, Nigeria.

Madukwe, C.E. 2014. Domestic Energy Usage Pattern of Households in Selected Urban and Rural Communities of Enugu State. Unpublished M.Sc. Project. Department of Institution for Development Studies, University of Nigeria, Enugu Campus, pp. 21-26.

Mekonnen, A. and Kohlin, G. 2008. Determinants of household fuel choice in major cities in Ethiopia. Working Papers in Economics No. 399, University of Gothenburg, Sweden.

Meried, E. 2021. Rural household preferences in transition from traditional to renewable energy sources: The applicability of energy ladder hypothesis in North Gondar Zone. Heliyon, 7(11): 34-45.

Muller, C. and Yan, H. 2016. Household fuel use in developing countries: Review of theory and evidence. Energy Econ., 70: 429-439.

Ngui, D., Mutua, J., Osiolo, H. and Aligula, E. 2011. Household energy demand in Kenya: An application of the linear approximate almost ideal demand system (LA-AIDS). Energy Pol., 39: 7084-7094.

Nnaji, C.E., Ukwueze, E.R. and Chukwu, J.O. 2012. Determinants of household energy choices in rural areas; Evidence from Enugu State, Nigeria. Cont. J. Soc. Sci., 5(2): 1.

Sambo, S.A. 2009. Strategic developments in renewable energy in Nigeria. Int. Assoc. Energy Econ., 3: 46.

Swan, G. and Ugursal, V. 2008. Modeling of end-use energy consumption in the residential sector: A review of modeling techniques. Renew. Sust. Energy Rev., 13: 1819-1835.

Taylor, M.J., Moran-Taylor, M., Castellanos, E.J. and Elías, S. 2011: Burning for sustainability: Biomass energy, international migration and the move to cleaner fuels and cookstoves in Guatemala. Ann. Assoc. of Amer. Geog., 101(4): 918-928.

Toole, R. 2015. The Energy Ladder: A Valid Model for Household Fuel Transition in Sub-Saharan Africa? MSc thesis. The Department of Urban and Environment Planning and Economica, Tufts University, USA.

United Nations Development Program (UNDP). 2006, Fact Sheet on Energy, Gender and Sustainable Development, Energia. UNDP, New York.

UNDP and WHO. 2009. The Energy Access Situation in Developing Countries: A Review on the Least Developed Countries And Sub-Saharan Africa. New York, USA.

Wang, Z., Zhang, B., Yin, J. and Zhang, Y. 2011. Determinants and policy Implication of household electricity saving behavior: Evidence from Beijing China. Energy Policy, 39: 3550-3557.

World Health Organization (WHO). 2010. Household Air Pollution and Health. Fact Sheet No 292. WHO, Geneva.

World Bank. 2007. Household Energy Use in Developing Countries. WB, Washington D.C., USA.

## ORCID DETAILS OF THE AUTHORS

O. J. Ubani: https://orcid.org/0000-0003-0396-254X

# Economic Impact of Climate Change on Agriculture: A Study of India and its Neighbouring Countries Using ARDL Approach

**Mashud Ahmed\*†** and **Paramita Saha\*\***

\*Department of Economics, Tripura University & Khairun Nessa Begum Women's College, Badarpur, Assam, India
\*\*Department of Economics, Tripura University. Tripura, India
†Corresponding author: Mashud Ahmed; hmashud786@gmail.com

## ABSTRACT

This study aims to analyze the association between the share of agriculture in GDP and changes in climatic variables, notably per capita $CO_2$ emissions and temperature change, using time series data of India, Bangladesh, and Nepal for the period 1961-2018. The ARDL bounds testing method was applied to analyze the relationships among the research variables for both short-term and long-term. The results revealed that in the long run, per capita $CO_2$ emissions and temperature change have no statistically significant relationship with India and Nepal's share of agriculture in GDP. However, temperature change has demonstrated a positive and statistically significant relationship with the share of agriculture in Bangladesh's GDP. Temperature change has a significant and adverse impact on the share of agriculture in India's GDP in the short run, whereas $CO_2$ has no significant effect. In the short run, $CO_2$ shows a positive and significant connection with the share of agriculture in Bangladesh's GDP. Still, temperature change is negatively and significantly associated with the proportion of agriculture in the nation's GDP. Different lag values of both $CO_2$ and temperature change have significant relationships with the share of GDP in agriculture in the short run in Nepal. As agriculture is a key source of GDP for all three countries, it is vital to implement suitable policies and make plans and strategies to mitigate climate change's harmful consequences in agriculture.

## INTRODUCTION

Climate change's impact on agriculture has received a lot of attention since it is linked to food security and poverty for a major portion of the population in the world (Dinar et al. 1998). By raising food prices and reducing food production, it will directly contribute to future food insecurity. Climate change decreases agricultural productivity directly by causing crop damage and indirectly by changing cropping choices (Trinh et al. 2021). The agriculture sector is highly susceptible to the change of climate in the world since it relies on adequate temperature ranges and rainfall patterns to produce crops and cattle (Nastis et al. 2012, Mendelsohn & Dinar 2009).

In agricultural production, climatic factors interact directly with input variables, including land, water, fertilizer, and pesticides. As a result, empirical research on climate change and agricultural production has shown that poor nations are negatively affected (Cline 2007, Xie et al. 2019). In India, a large number of people are engaged in farming activities. Climate change is having a detrimental impact on agriculture, hydropower, forest management, and

biodiversity (Senapati et al. 2013). According to research, climate change would reduce agricultural productivity in India by 4.5 to 9 percent between 2010 and 2039 (Guiteras 2009). A gradual increase in global temperature over the past few years seems to have a visible effect on agriculture all across the world. Nepal's agricultural production has already been impacted by rising temperatures, which has an impact on food security and agrarian communities (Karki & Gurung 2012). Climate change's impact on agriculture poses a huge danger to Bangladesh's national food security, as agriculture is vital to people's lives and livelihoods (Sikder & Xiaoying 2014).

The Indian Prime Minister promised to decrease India's total predictable carbon emissions by 1 billion tonnes within 2030, decrease the carbon concentration of the country's economy by fewer than 45 percent by the end of the decade, and reach net-zero carbon emissions by 2070 at the 26th UN climate change conference (COP26) summit in Glasgow, held in November 2021. The Prime Minister of Bangladesh, on the other hand, has urged wealthy countries to follow through on their pledges to diminish greenhouse

gas emissions and to provide the promised $100 billion in annual financial aid to less developed countries to help them to mitigate and adapt to climate change. Nepal committed to reaching net zero emissions by 2045, and 15 percent of total energy demand to be supplied from clean energy sources.

In the above context, the current study aims to look at the associations between changes in the share of agriculture in GDP and climatic variables in India, Bangladesh, and Nepal from 1961 to 2018. These countries are immediately neighboring each other and vulnerable to climate change in different manners because of their diverse geographical characteristics as well as low per capita GDPs as compared to developed countries. Temperature changes, changes in rainfall and weather patterns, an increase in the frequency of extreme weather events, sea level rise, changes in $CO_2$ levels, etc., over a long period are important indications of climate change (WMO 2022). Due to the non-availability of sufficient data on all climate factors during the study period, this study is confined only to the temperature change and per capita $CO_2$ emissions which are very pertinent to the international level.

The observed data plots of natural log values of the research variables for India are demonstrated in Fig. 1.

Fig. 1 and Fig. 2 show almost stable growth in the share of agriculture in GDP in the long run, both in India and Bangladesh, with some fluctuations in the short run. However, during the 1980s, a deep decrease in the graph was observed for both countries. This may result from the farm crisis in both countries during the 1980s. In India, a gradual increase in $CO_2$ emission and temperature change is seen over the period. For Bangladesh, except for a deep decline in the early 1980s, a continuous increase in $CO_2$ emission and temperature change is also noticeable. From Fig. 3, it is visible that all three variables are gradually increasing simultaneously at different rates. The concentration of $CO_2$ in a country rises due to the Industrial Revolution and the rise in manufacturing activity. The burning of fossil fuels, destruction of forests, and raising of livestock all have a rising impact on the climate and temperature of the planet (European Commission 2022).

The observed data plots of Bangladesh's natural log values for study variables are presented in Fig. 2. The
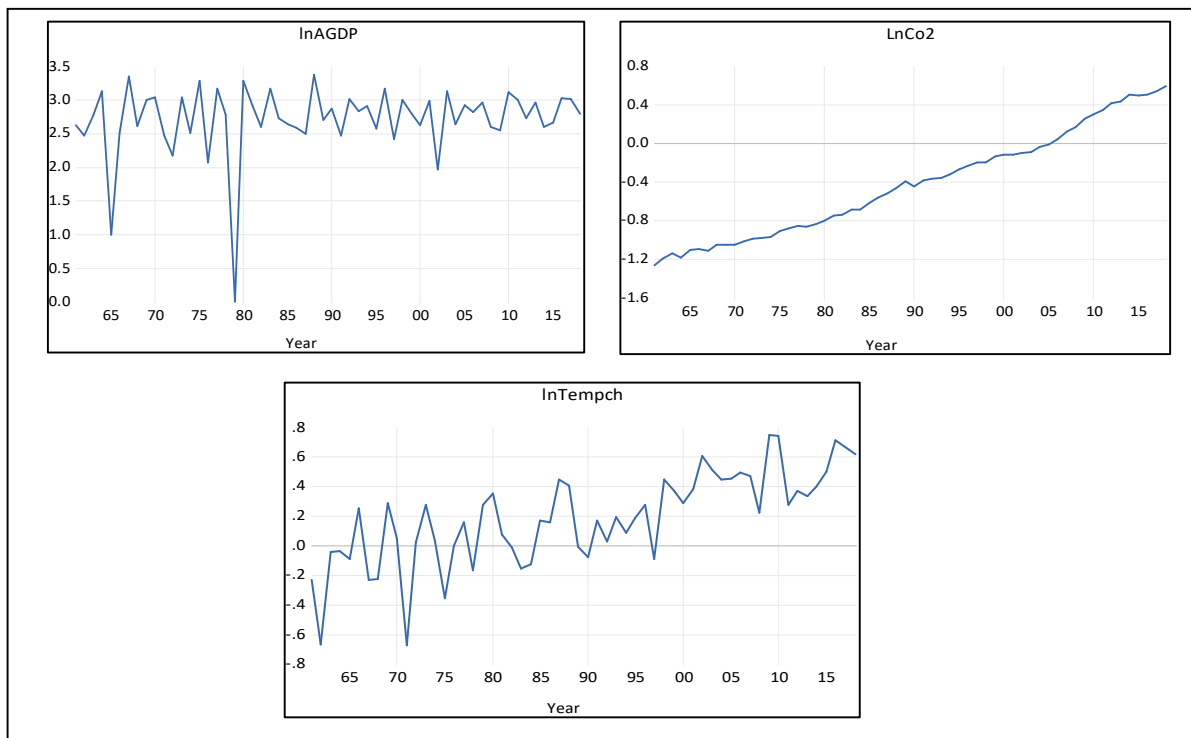


Note: lnAGDP, lnCO$_2$, and lnTempch denote the natural log value of the share of agriculture in GDP, carbon emissions, and temperature change, respectively.

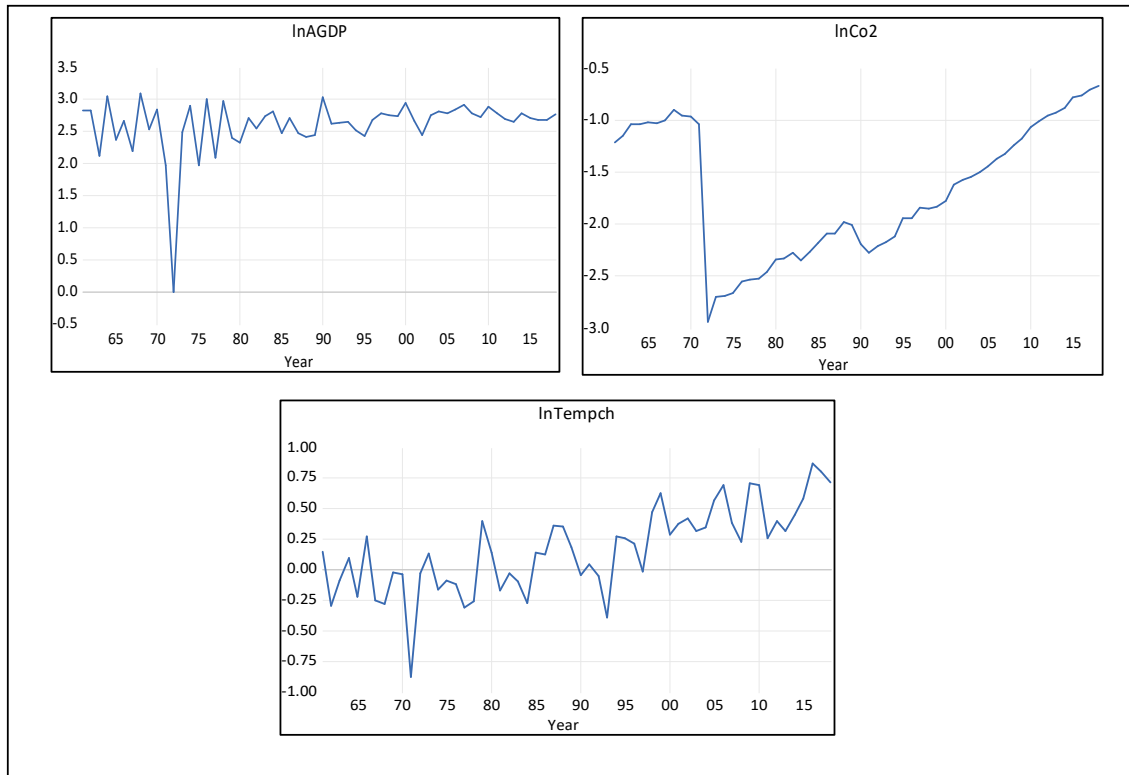Fig. 1: Data plots of variables (India).
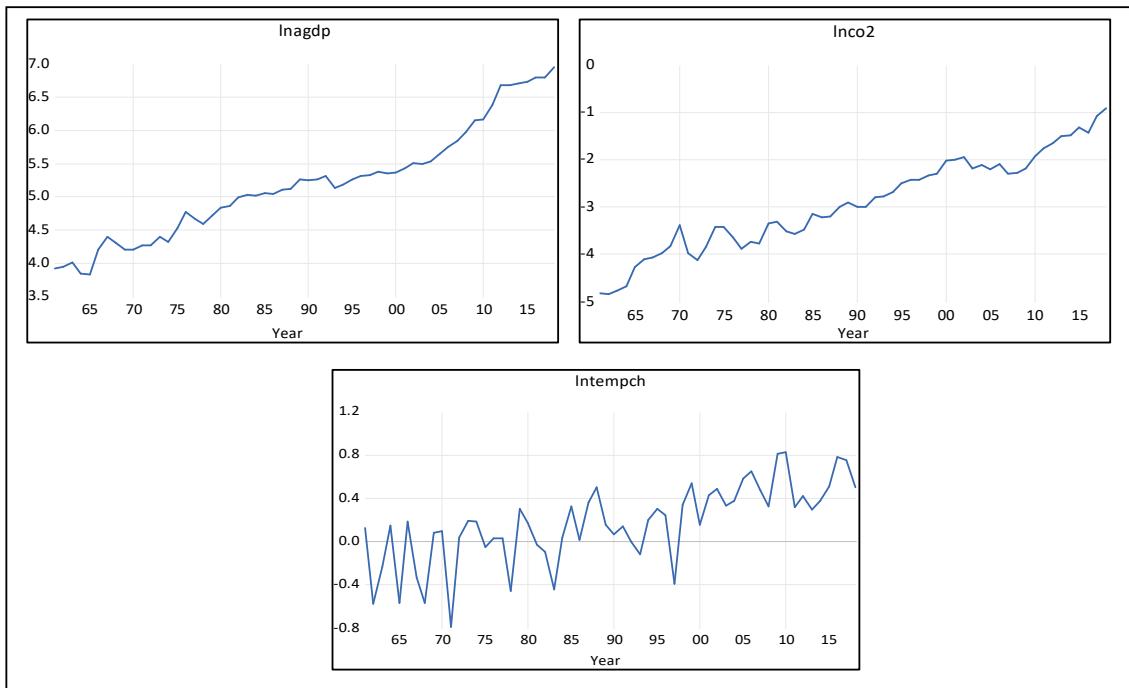
Fig. 2: Data plots of variables (Bangladesh).



Fig. 3: Data plots of variables (Nepal).

observed data plots of the natural log values of study variables for Nepal are presented in Fig. 3.

## MATERIALS AND METHODS

### Data Sources

The data on per-head carbon dioxide ($CO_2$) emission in metric tons and the share of agriculture in GDP (percentage growth) were obtained from the World Bank's data portal (https://data.worldbank.org/). In contrast, the data on temperature change (°C) are collected from the Food and Agricultural Organisation (https://www.fao.org/faostat/) for the period spanning from 1961 to 2018.

### Methodology

Climate change's impact on agriculture may be studied using a variety of methodologies. To estimate the long-run relationship between the percentage share of agriculture in GDP and climatic conditions, we used the Auto-regressive Distributed Lag (ARDL) bounds method. Eviews12's automatic lag section option uses the Akaike information criterion (AIC) to determine the best lag sequence. Charemza and Deadman (1992) introduced the ARDL test, which was further developed by Pesaran and Shin (1999) and Pesaran et al. (2001). This approach is advantageous as compared to other methods in some cases. First, even when independent variables have different integration orders, the ARDL approach can be used. Secondly, it gives more consistent results for small samples as compared to other techniques.

To study the relationship between the percentage of agriculture in GDP and climatic variables, notably temperature change and carbon dioxide emissions in India, Bangladesh, and Nepal from 1961 to 2018, a model can be expressed as given in the equation (1).

$$AGDP_t = f \ (Tempch, CO_2) \qquad \ldots(1)$$

In equation (1), $AGDP_t$ indicates the share of agriculture in GDP for a specific country over time, Tempch represents the temperature change, and $CO_2$ denotes per capita carbon dioxide emissions. Equation (1) can also be written as:

$$AGDP_t = \beta_0 + \beta_1 Tempch + \beta_2 CO_2 + \mu_t \qquad \ldots(2)$$

To decrease multicollinearity and instability in the time series data, the study used all variables in their natural logarithmic form. The natural logarithm is applied to equation (2) to create a log-linear model as given below:

$$LnAGDP_t = \beta_0 + \beta_1 LnTempch + \beta_2 LnCO_2 + \mu_t \qquad \ldots(3)$$

There are two steps in the ARDL method. The initial step is to check the long-run cointegrating connection using either the Wald-coefficient test or F-statistics, as suggested by Pesaran et al. (2001). Lower limits and upper bounds are two sorts of critical values, according to Pesaran et al. (2001). Lower-level critical values are assigned to the I (0) variables, whereas upper-level critical values are assigned to the I (1) variables. Suppose the estimated value of the F-Statistic is greater than the upper boundaries. In that case, the null hypothesis of no co-integration among the variables will be rejected, suggesting a long-run cointegration connection, irrespective of their integration order. We cannot reject the null hypothesis if the estimated value of the F-statistic is below the lower bound crucial value, showing the absence of a long-run equilibrium connection. A clear inference cannot be made if the computed F-statistic comes between the lower and upper-level bound. The mathematical representation of the ARDL bounds-testing model for this study can be expressed as follows:

$$\Delta \, LnAGDPti \ = \beta_0 + \beta_1 \sum_{i=1}^{n} \Delta \, LnAGDPt_{t-i}$$
$$+ \beta_2 \sum_{i=1}^{n} \Delta \, LnTempch_{t-i} + \beta_3 \sum_{i=}^{n} \Delta \, LnCO2_{t-i} +$$
$$\gamma_1 LnAGDP_{t-1} + \ \gamma_2 \, LnTepch_{t-1} + \gamma_3 LnCO2_{t-1} + \varepsilon_t$$
$$\ldots(4)$$

Where $\Delta$ means change, $\beta_0$ is the intercept, n denotes the lag order and $\varepsilon_t$ Reflects the error term. The significance of the lagged levels of the study variables is evaluated using the F-statistic to see if there is a cointegration connection between variables from Equation (4). Pesaran et al. (2001) recommend the test: $H_0$: $\gamma_1 = \gamma_2 = \gamma_3 = 0$, which indicates we can't rule out the hypothesis of no cointegration, but we can rule out the alternative hypothesis $H_1$: $\gamma_1 \neq \gamma_2 \neq \gamma_3 \neq 0$, which means the possibility of such a connection can't be ruled out. The error correction model (ECM), based on the ARDL approach, is used to examine the short-term connections between the variables shown in the equation (5).

$$\Delta LnAGDPt = \gamma_0 + \gamma_1 \sum_{i=1}^{n} \Delta \, LnAGDPt_{t-i} +$$
$$\gamma_2 \sum_{i=1}^{n} \Delta \, LnTempch_{t-i} + \gamma_3 \sum_{i=1}^{n} \Delta \, LnCO2_{t-i} +$$
$$\gamma_4 ECM_{t-1} + \varepsilon_t \qquad \ldots(5)$$

Where, $ECM_{t-1}$ is the residual lagged value in the model from which the long-term connection is derived? $ECM_{t-1}$ is expected to be a negative value for the speed of adjustment parameter.

## RESULTS AND DISCUSSION

### Unit Root Tests

A pre-requisite condition for the ARDL test is to check the stationarity and the integration order for study variables. The Augmented Dickey-Fuller (ADF) test was employed in the present study to determine the stationarity and the integration order. As stated in Table 1, the stationarity test was applied by taking a natural log to each variable in level and first

Table 1: Results of Unit Root Tests.

| India | | | |
|---|---|---|---|
| Variables | ADF Unit Root Test | | Order of integration |
| | Level | First Difference | |
| LNAGDP | -9.863573* (-3.490662) | - | I (0) |
| LNCO$_2$ | -1.591749 (-3.490662) | -9.694125* (-3.492149) | I (1) |
| LNTEMPCH | -7.475508* (-3.492149) | - | I (0) |
| **Bangladesh** | | | |
| LNAGDP | -7.491959* (-3.490662) | - | I (0) |
| LNCO$_2$ | -1.675092 (-3.490662) | -7.969308* (-3.492149) | I (1) |
| LNTEMPCH | -5.685645* (-3.492149) | - | I (0) |
| **Nepal** | | | |
| LNAGDP | -3.864800* (-3.508508) | - | I (0) |
| LNCO$_2$ | -3.350035 (-3.504330) | -6.824868* (-3.495295) | I (1) |
| LNTEMPCH | -7.160386* (-3.492149) | - | I (0) |

Note: 0 represents critical values in the t-statistic of the intercept and trend model with a 5% significance level; *indicates statistical significance at a 5% level of significance.

difference forms. The integration order is a combination of I (0) and I (1).

## Cointegration Testing Results

Table 2 shows the results of the ARDL bound test. At a 5 percent level of significance, the estimated F statistic values are determined to be above the critical values. The F statistic values for India, Bangladesh, and Nepal are 24.02841,

Table 2: Cointegration Test Results of ARDL (1, 0, 1), ARDL (3, 4, 4), and ARDL (3, 2, 3) for India, Bangladesh, and Nepal, respectively.

| Test statistic | Estimated Values | | k |
|---|---|---|---|
| F Statistics | 24.02841* | AGDP of India | 2 |
| | 11.17842* | AGDP of Bangladesh | |
| | 6.28523* | AGDP of Nepal | |
| Critical Values of Bounds | | | |
| Significance | Lower Bound (I0) | | Upper Bound (I1) |
| 10% | 2.63 | | 3.35 |
| 5% | 3.1 | | 3.87 |
| 1% | 4.13 | | 5 |

Note: * refers to the rejection of the null hypothesis at a 5% significance level.

11.17842, and 6.28523, respectively, whereas the critical value is 3.87 at a 5 percent level of significance. These results suggest a long-term association among the variables for all three countries from 1961 to 2018.

## Long-Run ARDL Estimates

Table 3 displays long-term coefficients obtained using the estimation results of the ARDL (1, 0, 3), ARDL (3, 4, 4), and ARDL (3, 2, 3) models for India, Bangladesh, and Nepal, respectively. The results show that per capita $CO_2$ emission and temperature change have a positive but statistically insignificant association with the percentage of agriculture in the GDP of India in the long term. However, $CO_2$ has a significant and positive association with the share of agriculture in Bangladesh's GDP, whereas temperature change has a significant and positive association with the share of agriculture in Bangladesh's GDP in the long run. In the case of Nepal, both $CO_2$ and temperature changes do not show any statistically significant relationship with the share of agriculture in GDP. The coefficient of temperature change for Bangladesh indicates that a 1% increase in temperature would result in a 0.31 percent growth in the percentage of agriculture in GDP over time. These results are also supported by Fig. 1 and Fig. 2, where time series data are plotted.

## Short-Run ARDL Estimates

Table 4 shows the results of the short-run ARDL estimations and the coefficients of error terms. The computation of the

Table 3: Long-Run ARDL estimates.

| India | | | |
|---|---|---|---|
| Dependent variable: D(LNAGDP), ARDL (1, 0, 3) | | | |
| Regressor | Coefficient | T-statistics | P- value |
| LNCO$_2$ | 0.101384 | 0.440994 | 0.6612 |
| LNTEMPCH | 0.198494 | 0.363848 | 0.7176 |
| C | 2.744065 | 14.09615* | 0.0000 |
| Bangladesh | | | |
| Dependent variable: D(LNAGDP), ARDL (3, 4, 4) | | | |
| LNCO$_2$ | -0.007592 | -0.207120 | 0.8370 |
| LNTEMPCH | 0.319830 | 3.583387* | 0.0009 |
| C | 4.162481 | 6.045027* | 0.0000 |
| Nepal | | | |
| Dependent variable: D(LNAGDP), ARDL (3, 2, 3) | | | |
| LNCO2 | -0.395185 | -0.333304 | 0.7405 |
| LNTEMPCH | 5.981115 | 1.055079 | 0.2971 |
| C | 4.090269 | 1.203129 | 0.2354 |

* Indicates significance at a 5 % level of significance.

Source: Authors' own calculation using EViews12.

ECM (-1) coefficient is an important result of the short-run dynamics. For all three nations, the ECM coefficients are negative and significant. For example, the coefficient of ECMt-1 for the percentage of agriculture in the GDP of India is -1.253095. This means that in the current year, about 125 percent of the disequilibria from the prior year's shock have adjusted back to the long-term equilibrium. Similarly, the coefficient of ECMt-1 for Bangladesh's percentage of agriculture in GDP is -1.641099, meaning that the short-run disequilibria are correcting back to the long-run equilibrium at a pace of 164 percent in the current year. For Nepal, the

coefficient of ECMt-1 is -0.059861, which means that the short-run disequilibria are correcting back to the long-run equilibrium at a rate of 5 percent.

In the short run, temperature change has a significant and negative association with a share of agriculture in GDP, but $CO_2$ has no significant relationship with this in India. In the case of Bangladesh, $CO_2$ has a significant and positive association with the share of agriculture in GDP. For Nepal, different $CO_2$ and temperature change lag values have significant relationships with the share of GDP in agriculture.

## CONCLUSION

In recent years, climate change has become popular in agricultural research, as climate change is predicted to adversely impact agricultural productivity and the share of agriculture in GDP across different countries. The present study investigated the long-run associations and short-run dynamics of the share of agriculture in GDP and climate variables, particularly temperature change and $CO_2$ emission, in India, Bangladesh, and Nepal. The study finds the presence of long-run association among the study variables over the period spanning from 1961 to 2018 for all three nations. The results indicate that per capita $CO_2$ emission and temperature change have a positive but insignificant association with agriculture's contribution to India's GDP in the long run. However, a positive and significant connection is observed between temperature change and the percentage of agriculture in Bangladesh's GDP in the long run. In Nepal, $CO_2$ and temperature changes do not show any statistically significant relationship with the share of agriculture in GDP in the long run. In the short run, temperature change has a negative and significant association with the share of agriculture in India's GDP, but $CO_2$ has no significant impact. The $CO_2$ emission is positively and significantly connected with the percentage of agriculture in the GDP, while the temperature is negatively and significantly related to the contribution of agriculture to Bangladesh's GDP in the short run. For Nepal, Different lag values of both $CO_2$ and temperature change have significant relationships with the share of GDP in agriculture in the short run. The agriculture sector is the major source of GDP for all three countries. Therefore, governments need to make suitable mitigation policies and encourage farmers to take appropriate adaptation approaches to combat the adverse effects of climate change on agriculture.

Table 4: Short-run ARDL estimate.

| INDIA | | | |
|---|---|---|---|
| Dependent variable: D(LNAGDP), ARDL (1, 0, 3) | | | |
| Variable | Coefficient | T-statistics | P- value |
| D(LNTEMPCH) | -0.940106* | -3.401473 | 0.0014 |
| D (LNTEMPCH (-1)) | 0.006901 | 0.027163 | 0.9784 |
| D (LNTEMPCH (-2)) | -0.802004* | -3.123978 | 0.0030 |
| ECM (-1) | -1.253095* | -10.10548 | 0.0000 |
| Bangladesh | | | |
| Dependent variable: D(LNAGDP), ARDL (3, 4, 4) | | | |
| Variable | Coefficient | T-statistics | P- value |
| D (LNAGDP (-1)) | 0.410331* | 2.155088 | 0.0372 |
| D (LNAGDP (-2)) | 0.334046* | 2.893972 | 0.0061 |
| D (LNCO$_2$) | 1.330953* | 11.05392 | 0.0000 |
| D (LNCO$_2$ (-1)) | 0.2269772 | 1.305786 | 0.1991 |
| D (LNCO$_2$ (-2)) | 0.088597 | 0.453282 | 0.6528 |
| D (LNCO$_2$ (-3)) | 0.566551* | 3.203279 | 0.0027 |
| D (LNTEMPCH) | -0.071907 | -0.654086 | 0.5168 |
| D (LNTEMPCH (-1)) | -0.753033* | -4.925982 | 0.0000 |
| D (LNTEMPCH (-2)) | -0.353038* | -2.288117 | 0.0275 |
| D (LNTEMPCH (-3)) | -0.418429* | -3.237696 | 0.0024 |
| ECM (-1) | -1.641099* | -6.933051 | 0.0000 |
| Nepal | | | |
| Dependent variable: D(LNAGDP), ARDL (3, 2, 3) | | | |
| D (LNAGDP (-1)) | 0.036537 | 0.309789 | 0.7582 |
| D (LNAGDP (-2)) | -0.354683* | -3.085855 | 0.0035 |
| D (LNCO2) | 0.068902 | 0.968849 | 0.3379 |
| D (LNCO2 (-1)) | 0.163920* | 2.437778 | 0.0189 |
| D (LNTEMPCH) | 0.009992 | 0.209020 | 0.8354 |
| D (LNTEMPCH (-1)) | -0.321236* | -4.884497 | 0.0000 |
| D (LNTEMPCH (-2)) | -0.165443* | -3.2463333 | 0.0022 |
| ECM (-1) | -0.059861* | -5.182189 | 0.0000 |

* Indicates significance at a 5 % level of significance.

Source: Authors' own calculation using EViews12.

## REFERENCES

Charemza, W.W. and Deadman, D.F. 1992. New Directions in Econometric Practice: General to Specific Modelling. Cointegration and Vector Autoregressions, Edward Elgar Publication, England.

Cline, W.R. 2007. Global Warming and Agriculture: Impact Estimates by Country. Centre for Global Development and Peterson Institute for International Economics, Washington, DC.

Dinar, A., Mendelsohn R., Evenson R., Parikh J., Sanghi A., Kumar K. and Lonergan S. 1998. Measuring the Impact of Climate Change on Indian Agriculture. WB Technical Paper no. 402, The World Bank, Washington DC.

European Commission (EC) 2022. Causes of Climate Change. https://ec.europa.eu/clima/climate-change/causes-climate-change_en (Accessed 15 June 2022)

Guiteras, R. 2009. The impact of climate change on Indian agriculture. Manuscript, Department of Economics, University of Maryland, College Park, Maryland.

Karki, R. and Gurung, A. 2012. An overview of climate change and its impact on agriculture: A review from least developing country, Nepal. Int. J. Ecosyst., 2(2): 19-24. DOI: 10.5923/j.ije.20120202.03

Mendelsohn, R.O. and Dinar, A. 2009. Climate Change and Agriculture: An Economic Analysis of Global Impacts, Adaptation, and Distributional Effects. Edward Elgar Publishing. Cheltenham, UK.

Nastis, S.A., Michailidis, A. and Chatzitheodoridis, F. 2012. Climate change and agricultural productivity. Afr. J. Agric. Res., 7(35): 4885-4893.

Pesaran, M.H. and Shin, Y. 1998. An autoregressive distributed-lag modeling approach to cointegration analysis. Econ. Soc. Monogr., 31: 371-413.

Pesaran, M.H., Shin, Y. and Smith, R.J. 2001. Bounds testing approaches to the analysis of level relationships. J. Appl. Econ., 16(3): 289-326.

Senapati, M.R., Behera, B. and Mishra, S.R. 2013. Impact of climate change on Indian agriculture & its mitigating priorities. Am. J. Environ. Protect., 1(4): 109-111.

Sikder, R. and Xiaoying, J. 2014. Climate change impact and agriculture of Bangladesh. J. Environ. Earth Sci., 4(1): 35-40.

Trinh T.A., Feeny S. and Posso A. 2021. The Impact of Natural Disasters and Climate Change on Agriculture: Findings from Vietnam – Economic Effects of Natural Disasters. Academic Press, Cambridge, MA, pp. 261-280. https://doi.org/10.1016/B978-0-12-817465-4.00017-0.

WMO 2022. Climate Data. https://climatedata-catalogue.wmo.int/climate_indicators (Accessed 20 June 2022).

Xie, B., Brewer, M.B., Hayes, B.K., McDonald, R.I. and Newell, B.R. 2019. Predicting climate change risk perception and willingness to act. J. Environ. Pyschol., 65: 101331.

## ORCID DETAILS OF THE AUTHORS

Mashud Ahmed: https://orcid.org/0000-0002-0092-7282

# The Role of Stakeholders in Achieving Sustainable Agriculture: A Case Study in Sragen Regency, Indonesia

**R. C. Sartika†, Y. Purwaningsih, E. Gravitiani and P. Nitiyasa**

Department of Economics and Business, Sebelas Maret University, Surakarta 57126, Indonesia

†Corresponding author: R. C. Sartika; rebeccacindy09@student.uns.ac.id

## ABSTRACT

Rice farming plays a crucial role in maintaining national resilience and stability. However, its sustainability is faced with complex and multidimensional challenges. One of the challenges agricultural sustainability faces is the reduction of farmland due to the construction of toll roads. The development of the Solo-Mantingan-Ngawi toll road has significantly impacted the reduction of agricultural land in Sragen Regency, the second-largest rice-producing area in Central Java after Grobogan. This issue will threaten national food security if left unaddressed without further intervention. The development of sustainable agriculture is expected to be a solution to promoting food resilience. However, stakeholder involvement is necessary for successful development. This research aims to identify the stakeholders involved in developing sustainable agriculture to promote food resilience in Sragen Regency. This study adopts a mixed-method approach with data collection through in-depth interviews. The analytical tool used in this research is MACTOR (Matrix of Alliance and Conflict: Tactic, Objectives, and Recommendation). The study identified the stakeholders influencing the development of sustainable agriculture in Sragen Regency as Farmer Groups, Farmers, Village Heads, Agriculture Extenders, and the Department of Agriculture and Food Security. These findings serve as a basis for developing collaborative patterns among all stakeholders required to develop sustainable agriculture to achieve food resilience in the Sragen Regency.

## INTRODUCTION

Infrastructure development plays a vital role in fulfilling people's rights. It influences increasing community access and the productivity of existing resources to encourage economic growth (Ardiyono et al. 2018). Development in infrastructure aspects that require more space or large land is the construction of toll roads. The structure of toll roads cannot be separated from society's physical and non-physical aspects. The physical part is related to the environment, while the non-physical element is a social problem for the community. Of course, these two aspects are felt directly by the people affected by the toll road construction (Siswoyo 2020).

Although the construction of toll roads provides many benefits, such as accelerating the movement of people and goods, increasing accessibility to certain areas, and boosting the economy, there are also negative impacts (Dwiputri et al. 2022). One negative impact was a change in land use around the toll road construction area. The construction of toll roads requires quite a large area of land. It is usually carried out in areas with high economic value, such as agricultural land (Salim & Faoziyah, 2022). Construction of

toll roads can change the land use from agriculture to non-agriculture, thereby reducing the available agricultural land and disrupting the sustainability of agricultural production in the area (Makbul et al. 2019). In addition, agricultural land is divided into 2 (two) parts because the construction of a toll road separates it. It is a constraint for farmers regarding irrigation. The impact is on the economic rights of the community related to their rights as citizens to obtain prosperity from the state as follows: the amount of income from agriculture has decreased because the land used for agricultural activities is decreasing. Value and compensation process (Sudiyarto & Indah 2019).

Meanwhile, human life is inseparable from the need for food, so food matters is an essential need for humans. Food is everything that comes from biological and water sources, both processed and unprocessed, which is intended as food or drink for human consumption, including food additives, food raw materials, and other materials used in the process of preparing, processing, and manufacturing food or beverages (FAO et al. 2021). The United Nations (UN) noted that at the end of 2018, there were still more than 821 million people worldwide, or one in nine people suffering from hunger (Kılıç

2022). The Asian Development Bank (2019) records that as many as 22 million people in Indonesia experience chronic hunger, which means the hunger level is still relatively serious. This issue is a challenge for stakeholders to achieve the zero hunger target by 2030 as the second goal of the SDGs (Sustainable Development Goals) (Manurung et al. 2022).

The issue of food security arises because of the problem of food insecurity, where this food insecurity is impacted due to reduced agricultural land. The land is one of the most important aspects of life. In agricultural production, the role of land as the primary input is irreplaceable. Economically, land is the most efficient wealth-generating asset for farmers (Muyanga et al. 2013, Sitko & Jayne 2014) and an essential factor for economic growth (Li 2014). However, the finite and non-renewable nature of land supply creates fierce competition for land use, usually between the agricultural and non-agricultural sectors. It has given rise to land use change, which has significantly increased from year to year. If this situation continues, it is feared that it could threaten food security in Indonesia. Central Java Province is a province on the island of Java that functions as a national food buffer zone (BPS 2022). One of the areas in Central Java Province that are experiencing the problem of reduced paddy fields is Sragen Regency. Sragen Regency is one of the potential areas and the second largest rice producer in Central Java after Grobogan (Prihartini et al. 2018, Anggraini et al. 2021). Rice production in the five highest districts in Central Java Province can be seen in Table 1.

Rice production in Sragen Regency in 2020 has decreased from the previous year to 723,671.68 tons. This situation is due to reduced agricultural land due to the Solo-Mantingan-Ngawi toll road construction project (Anggraini et al. 2021). If thousands of hectares of agricultural land, especially paddy fields in Sragen Regency, are converted into business and residential areas and offices, production in the farm rice sector will undoubtedly decrease. On the other hand, as a national rice storage area, paddy fields in the Sragen Regency should be maintained to fulfill national food needs and create food security. Sustainable agricultural development is needed to realize food security and sovereignty.

Table 1: The highest rice production in the five districts of Central Java Province in 2019.

| No | Regency | Rice Production (Tonnnes) |
|---|---|---|
| 1. | Grobogan | 772521.47 |
| 2. | Sragen | 766012.30 |
| 3. | Cilacap | 699964.69 |
| 4. | Demak | 666141.30 |
| 5. | Pati | 592099.74 |

Source: Anggraini et al. (2021)

The 1990 US Livestock Bill, as discussed in Velten et al. (2015), defines sustainable agriculture as a holistic approach that encompasses various plant and animal production practices tailored to specific locations. Its long-term objectives include meeting human food and fiber needs, enhancing environmental quality, optimizing resource utilization, incorporating natural biological cycles and controls, ensuring the economic viability of agricultural operations, and improving the overall well-being of farmers and society. Sustainable farming systems strive to minimize environmental impact, maintain agricultural productivity, increase farmers' income, and enhance rural areas' stability and quality of life. However, achieving sustainable agricultural development and improving food security requires the involvement of multiple stakeholders.

The involvement of stakeholders is crucial as an essential aspect in decision-making and development planning because stakeholders are parties that influence or are influenced by those plans. The challenges in sustainable agriculture development can be overcome through collaborative and integrated development with the support and participation of all stakeholder actors within a mutually beneficial partnership framework. This aligns with Velten et al. (2021), who state that collaboration among stakeholders is crucial for the success of sustainable agriculture. Therefore, an analysis of stakeholder roles is necessary to understand their strengths, competitiveness, and attitudes toward the intended goals of this development project. The results of this stakeholder analysis are useful in determining the power map, support, and potential conflicts that may arise. Stakeholder support is vital for sustainable agriculture development (Syahyuti et al. 2021).

The idea of stakeholder involvement in the agricultural sector has grown due to the belief that such involvement can generate positive impacts on sustainable agriculture and support participation, empowerment, and inclusive stakeholder engagement (Adil et al. 2022). Based on the background of these issues, this research is designed to identify the stakeholders involved in developing sustainable agriculture in Sragen Regency, Indonesia. The findings of this research will be highly valuable in determining appropriate programs and action plans related to stakeholder engagement in developing the agricultural potential of Sragen Regency in a participatory and sustainable manner.

## MATERIALS AND METHODS

### Method of Collecting Data

This research uses a mixed method paradigm that combines qualitative and quantitative approaches in all stages of

the research process to obtain a holistic picture of the characteristics of stakeholders in the agricultural sector, especially in the Sragen Regency, about other stakeholders. The research location is in Sragen Regency, especially in the areas most affected by the construction of the Solo-Mantingan-Ngawi toll road, namely Jetak Village, Singopadu Village, Purwosuman Village, Karangmalang Village, and Kebonromo Village. The primary data collected consists of qualitative data from 26 informants, including the Head of the Department of Food Security in Sragen Regency, Village Heads, Agricultural Extenders, Farmer Groups, and Farmers. This study uses data collection techniques in in-depth interviews to strengthen the analysis and discussion. In-depth interviews were conducted with key informants who were determined purposively based on the informants' involvement and understanding of sustainable agriculture. Interviews were conducted by visiting the location of the informant. The consultation asked about the informant's knowledge of agricultural potential in Sragen Regency and the problems that arise.

**Data Analysis Method**

All data in this study were analyzed using Mactor software (Matrix of Alliances and Conflicts Tactics, Objectives, and Recommendations). Mactor is a software developed by Michel Godet in 1991 to deeply analyze power relations between actors, actors' competitiveness, and actors' attitudes towards goals. Mactor's work is based on inter-actor influence, distinguished as direct, indirect, and potential. Direct influence occurs when actor A affects actor B. In contrast, indirect influence occurs when actor A influences actor B and B affects actor C. With the transitivity process, actor C is indirectly influenced by A. Potential influence occurs when influence should have had actor A to B. Mactor works based on a structural analysis approach (Isa 2021).

The initial stages in Mactor's analysis are 1) determining system actors, 2) determining a set of goals, and 3) building a matrix of direct influence or MDI (Matrix of Direct Influence) and MAO (Matrix of Actor Objective). The MDI matrix describes the influence between actors on other actors, which is indicated by a score of 0 to 4. The greater the value suggests, the more significant the influence, while the MAO matrix shows the actor's attitude toward goals. The actor's attitude and judgment reflect the actor's role toward this goal on whether to support or reject the plan. This matrix is filled with a value of 0 (the goal has a dismal outcome), 1 (pursuit interferes with the actor's operational procedures), 2 (plan interferes with the success of the actor's work), 3 (goal interferes with the achievement of the actor's mission, and 4 (pursuit interferes with the actor's existence)
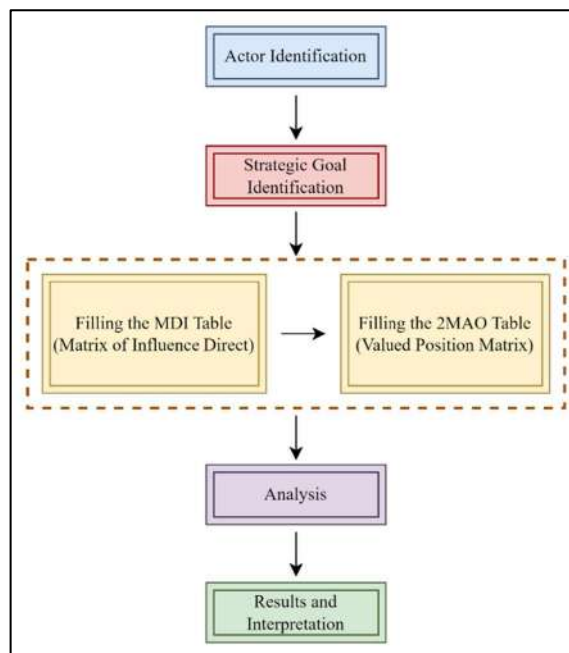


Fig. 1: The stages of Mactor analysis.

(Gravitiani et al. 2022). The stages of MACTOR analysis are summarized in Fig. 1.

## RESULTS AND DISCUSSION

The initial step in MACTOR analysis is to identify key actors and determine their objectives in the effort to develop sustainable agriculture in the Sragen Regency. Based on preliminary observations, several actors have shown their interest in sustainable agriculture development in Sragen Regency, as described in Table 2. In addition, several objectives were also identified which were grouped in Table 3.

In the next stage, the positioning of the actors involved in sustainable agricultural development in the region is mapped. The position of each actor is assessed based on their level of influence and dependency on other actors. The results obtained from questionnaires and in-depth interviews

Table 2: Identification of actors/stakeholders related to sustainable agriculture development in Sragen Regency.

| No | Actor/Stakeholder | Code |
|---|---|---|
| 1. | Department of Agriculture and Food Security | DAFS |
| 2. | Village Heads | VH |
| 3. | Farmer Groups | FG |
| 4. | Agriculture Extenders | AE |
| 5. | Farmers | FAR |

Table 3: Identification of objectives related to sustainable agriculture development in Sragen Regency.

| No | Objectives | Code |
|---|---|---|
| 1. | The Application of an Environmentally Friendly Rice Farming System | Farming |
| 2. | An increase in Farmers' Access to Finance | Finance |
| 3. | Providing Subsidies and Incentives to Farmers | Subsidies |
| 4. | An increase in Farmers' Income | Income |
| 5. | Increase the Availability of Agricultural Facilities and Infrastructure | Facilities |
| 6. | Build Rice Supply Connectivity Between Regions | Supply |

with the actors are entered into a Matrix of Direct Influence (MDI) in Table 4 and a Matrix of Valued Position (2MAO) in Table 5. Both matrices serve as inputs for the overall MACTOR analysis. Table 4 (MDI) provides an overview of the level of influence of each actor on others, while Table 5 (2MAO) illustrates the position of each actor in relation to the objectives of this development.

Mactor provides various tools and analyses helpful in getting a comprehensive and aggregate picture of a situation from a few simple inputs to the actor's role in problem-solving. Actors are essential in determining the strategy for formulating sustainable agricultural development policies, especially in the Sragen Regency. Stakeholder analysis is vital in mapping the roles and relationships between actors/stakeholders and understanding how stakeholders behave towards various sustainable agricultural development goals in the Sragen Regency. The first result of Mactor's analysis is a map of actor influence and dependency. Actor influence describes the actor's ability to influence other actors and design, plan, and implement the development of a project. The sources of the power of actor influence are determined by the ownership of material resources, social position, and the actors' knowledge of the future of a system (Tronvoll 2017). Based on their strength, actors are positioned in the actor's influence and dependency map. They are divided into dominant actors (strong influence), dominated actors (high dependency), isolated actors (low power and dependency), and relay actors (strong influence and dependency) (Elmsalmi & Hachicha 2014). The map of the impact and dependence of agricultural stakeholder actors in Sragen Regency is shown in Fig. 2.

Fig. 2 shows that the Farmer Group (FG), Farmer (FAR), and Village Head (VH) are the dominant actors, namely the most influential actors because the power to influence other actors is high while their dependency is low. This position is

Table 4: Direct influence between actors (MDI).

| | Department of Agriculture and Food Security (DAFS) | Village Head (VH) | Farmer Group (FG) | Agriculture Extender (AE) | Farmer (FAR) |
|---|---|---|---|---|---|
| Department of Agriculture and Food Security (DAFS) | 0 | 3 | 2 | 1 | 2 |
| Village Head (VH) | 4 | 0 | 4 | 3 | 2 |
| Farmer Group (FG) | 2 | 4 | 0 | 3 | 4 |
| Agriculture Extender (AE) | 3 | 2 | 2 | 0 | 2 |
| Farmer (FAR) | 4 | 3 | 3 | 4 | 0 |

Source: Primary Data Analysis, 2022.

Table 5: Attitudes of actors towards goals (2MAO).

| | The Application of an Environmentally Friendly Rice Farming System (Farming) | An increase in Farmers' Access to Finance (Finance) | Providing Subsidies and Incentives to Farmers (Subsidies) | An increase in Farmers' Income (Income) | Increase the Availability of Agricultural Facilities and Infrastructure (Facilities) | Build Rice Supply Connectivity Between Regions (Supply) |
|---|---|---|---|---|---|---|
| Department of Agriculture and Food Security (DAFS) | 3 | 4 | 3 | 2 | 2 | 4 |
| Village Head (VH) | 4 | 3 | 4 | 1 | 4 | 4 |
| Farmer Group (FG) | 2 | 3 | 4 | 3 | 4 | 4 |
| Agriculture Extender (AE) | 2 | 3 | 4 | 3 | 4 | 4 |
| Farmer (FAR) | 3 | 3 | 3 | 3 | 2 | 4 |

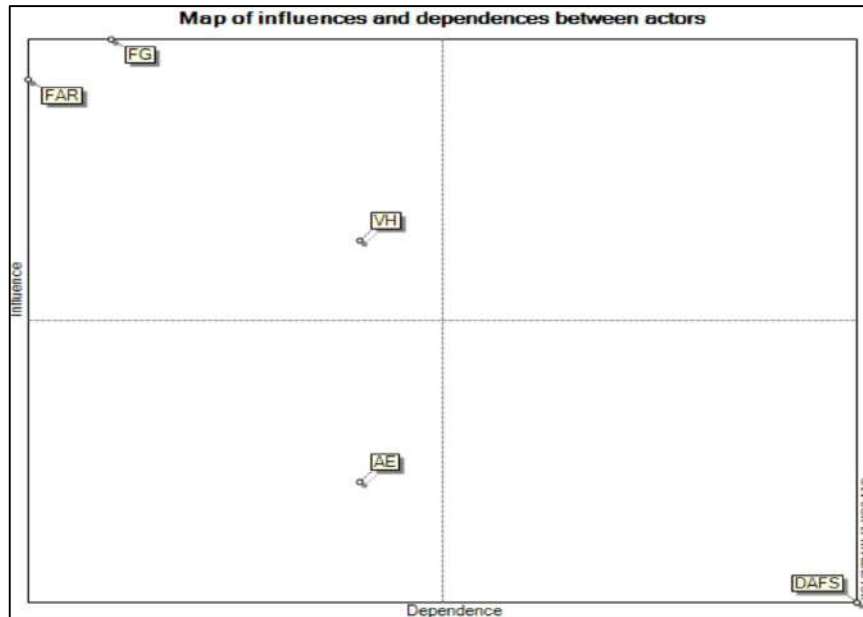Source: Primary Data Analysis, 2022.

Fig. 2: Actor influence and dependence map.

controlled by the roles of these three actors, which are very important in the development of sustainable agriculture, as stated in the table. The dominant part of the three actors also shows their ability as leaders in determining future sustainable agricultural development policies. Agriculture Extender (AE) is an isolated actor because it has low influence and dependency. At the same time, the Department of Agriculture and Food Security (DAFS) is a dominant actor who is highly influenced and dependent on other actors.

The second result of Mactor's analysis is a map of actor competitiveness. Actor competitiveness describes the intensity of an actor's influence on other actors, which is determined by direct effect, direct dependence, indirect impact, and indirect dependence. The competitiveness map simultaneously shows the actors' willingness to use their power to control other actors (Elmsalmi & Hachicha 2014). Fig. 3 shows that Farmer Group and Farmer are actors who have the highest competitiveness. This mapping is exact because the Farmer Group is a group that has the most authority and responsibility for sustainable agricultural development.

In contrast, Farmers are a source of ideas and strength in sustainable agricultural development. With this great competitiveness, these two actors have enormous potential in determining sustainable agricultural development plans. In addition, the Department of Agriculture and Food Security is the actor with the weakest competitiveness. At the same time, other actors are in a moderate position.

The following analysis is related to the development objective map. One that determines stakeholder support or
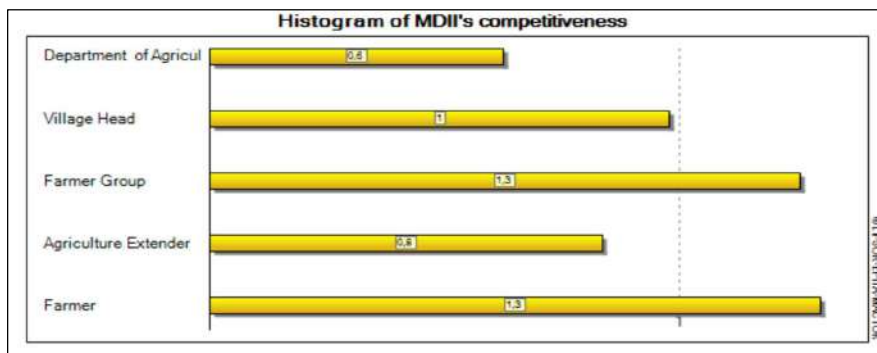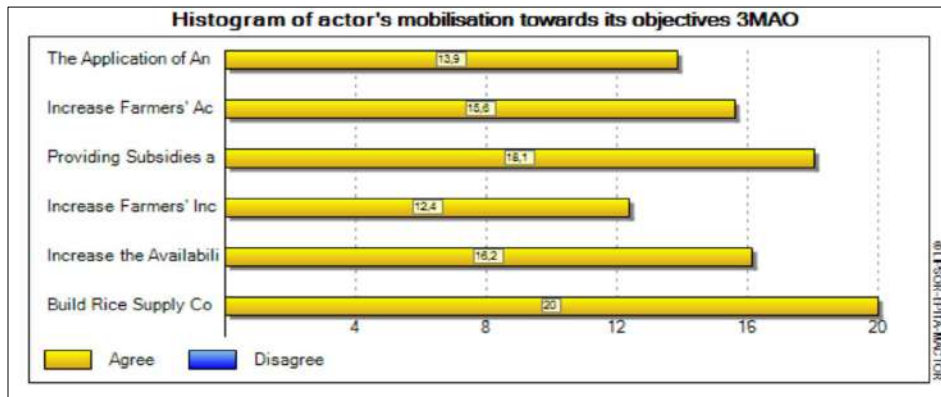


Fig. 3: Actor competitiveness.

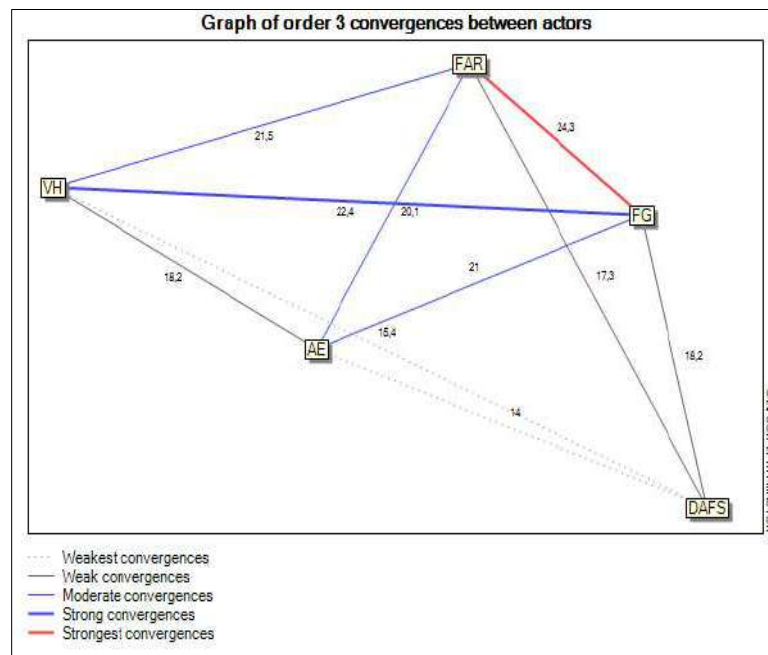Fig. 4: Objective strength map.



Fig. 5: Actor convergence map.

resistance in development is how appropriate the goals of the plot are to the actor's mission (Fuentes 2013). To find out the actor's support map for development goals, a group of goals to be achieved is mapped out on their level of importance. The more critical a plan describes, the stronger the actor supports that goal. Fig. 4 presents a map of the objectives of a sustainable agricultural development project.

Fig. 4 shows that all actors support or are not resistant to all the goals set. This situation can be seen as having no blue color on the goal bar graph. The highest support intensity is on the Build Rice Supply Connectivity Between Regions objective. This situation is appropriate because it

can guarantee the availability of rice and price stability in all regions, increasing the farming community's welfare.

The next goal strongly supported by actors is providing subsidies and incentives to farmers and increasing the availability of agricultural facilities and infrastructure. Providing subsidies or incentives in the form of fertilizers and seeds is an essential factor in determining agricultural production. Seed is a characteristic of production and the foundation of agriculture, while fertilizer is a critical element in productivity. Seed and fertilizer subsidies are intended to ease the burden on farmers and transfer technology to farmers to use superior seeds and balanced fertilization at affordable

prices so that production and productivity increase. The increase in food production is expected to lead to a rise in the welfare of farmers.

One of the factors that can increase agricultural production is the support of farming facilities and infrastructure. Food is the primary basic need for humans that must be met at any time. The right to obtain food is one of the human rights. If food availability is less than needed, it can impact economic instability and various social and political upheavals. This issue happens when food security is disrupted. Support for agricultural infrastructure and facilities aims to increase productivity and production through efforts to expand agricultural land in food crop areas to offset land conversion. Then make efforts to rehabilitate irrigation networks, optimize land, increase the availability of farming tools and machinery, and improve the distribution of subsidized fertilizers so they are targeted.

The results of the subsequent analysis focus on the actor convergence map. Actor convergence describes the similarity of actors' attitudes toward goals. Actors with the same mindset will converge, while those with different perspectives will diverge. Convergence analysis is intended to discover the points of potential alliances of potential actors. Convergence maps can be used to determine which actors can work together to avoid potential conflicts. A description of possible actor alliances/cooperation in sustainable agricultural development projects can be seen in Fig. 5. It shows that Farmer Groups and Farmers are groups of actors that can form strong alliances to successfully develop sustainable agricultural potential.

## CONCLUSION

Based on the MACTOR analysis of stakeholders in the sustainable agriculture development project in Sragen Regency, it can be concluded that farmer groups, farmers, and village heads are dominant actors with high influence in determining agricultural development policies. Their active involvement and knowledge play a crucial role in the success of the sustainable agriculture project. Policy recommendations to be considered include strengthening the role and support for farmer groups, enhancing the competitiveness and capacity of farmers, fostering collaboration between farmer groups and individual farmers, allocating adequate budget for agricultural infrastructure, involving the Department of Agriculture and Food Security, and conducting regular monitoring and evaluation. By empowering these key actors, sustainable agriculture development in Sragen Regency is expected to improve farmers' welfare, environmental sustainability, and food security.

## REFERENCES

Adil, A., Syarief, R., Widiatmaka & Najib, M. 2022. Stakeholder analysis and prioritization of sustainable organic farming management: A case study of Bogor, Indonesia. Sustainability, 14(24): 1-16. https://doi.org/10.3390/su142416706

Anggraini, D.P., Sutrisno, J. and Barokah, U. 2021. The impact analysis of rice field conversion on food security in Sragen Regency. E3S Web Conf., 316: 1-7. https://doi.org/10.1051/e3sconf/202131602035

Ardiyono, S.K., Parenrengi, N.P.A. and Faturachman, F. 2018. How does toll road impact accessibilities, trades, and investments in the short term? A case study of Cipali toll road in West Java, Indonesia. Journal of Infrastructure, Policy Dev., 2(2): 226-247. https://doi.org/10.24294/jipd.v2i2.673

BPS. 2022. Statistik Indonesia 2022. Badan Pusat Statistik. https://www.bps.go.id/publication/2020/04/29/e9011b3155d45d70823c141f/statistik-indonesia-2020.html

Dwiputri, I.N., Allo, A.G., Yusida, E. and Seprillina, L. 2022. The effect of the operational exit tolls on the welfare of the local community. Sign. J. Econ., 11(1): 73-82. https://doi.org/10.15408/sjie.v11i1.22108

Elmsalmi, M. and Hachicha, W. 2014. Risk mitigation strategies according to the supply actors' objectives through the MACTOR method. 2014 International Conference on Advanced Logistics and Transport, ICALT 2014, May 1-3 2014, Hammamet, Tunisia, IEEE, Manhattan, NT, US, pp. 362-367. https://doi.org/10.1109/ICAdLT.2014.6866339

FAO, IFAD, UNICEF, WFP and WHO. 2021. The State of Food Security and Nutrition in the World 2021. Transforming food systems for food security, improved nutrition, and affordable healthy diets for all. In: In Brief to The State of Food Security and Nutrition in the World 2021. FAO. https://doi.org/10.4060/cb5409en

Fuentes, C.D. 2013. Governance for the tourism sector and its measurement. UNWTO Statistics and TSA Issue Paper Series. World Tourism Organization, Madrid Spain. https://doi.org/https://doi.org/10.18111/9789284415632

Gravitiani, E., Sasanti, I.A., Sartika, R.C. and Cahyadin, M. 2022. The role of stakeholders in sustainable tourism using mactor analysis: Evidence from Kragilan's Top Selfie, Magelang, Indonesia. Equal. Sci. J. Econ., 17(2): 102-109. https://doi.org/10.24269/ekuilibrium.v17i2.%y.pp102-109

Isa, M. 2021. Strengthening the institutional capacity of guitar cluster: Implementation of DEA and MACTOR. Equal. Sci. J. Econ., 16(2): 107-116.

Kılıç, R. 2022. The problem of hunger in the world and a new model proposal to solve this problem. Balk. J. Social Sci., 11(21): 63-68. https://doi.org/https://doi.org/10.55589/bsbd.1107538

Li, J. 2014. Land sale venue and economic growth path: Evidence from China's urban land market. Habitat Int., 41: 307-313. https://doi.org/10.1016/j.habitatint.2013.10.001

Makbul, Y., Faoziyah, U., Ratnaningtyas, S. and Kombaitan, B. 2019. Infrastructure development and food security in Indonesia: The impact of the trans-Java toll road on rice paddy farmers' desire to sell farmland. J. Reg. City Plan., 30(2): 140-156. https://doi.org/10.5614/jpwk.2019.30.2.4

Manurung, E.T., Maratno, S.F.E., Permatasari, P., Rahman, A.B., Qisthi, R. and Manurung, E. M. 2022. Do village allocation funds contribute towards alleviating hunger among the local community (SDG#2)?

An insight from Indonesia. Economies, 10(155): 1-20. https://doi.org/10.3390/economies10070155

Muyanga, M., Jayne, T.S. and Burke, W.J. 2013. Pathways into and out of poverty: A study of rural household wealth dynamics in Kenya. J. Dev. Stud., 49(10): 1358-1374. https://doi.org/10.22004/ag.econ.202603

Prihartini, S., Yuliantoro., M. and Gunarto, S. 2018. The Role of land deed officials in the conversion of agriculture land function related land social function in Sragen Regency. J. Akta, 5(3): 573-579. https://doi.org/10.30659/akta.v5i3.3235

Salim, W. and Faoziyah, U. 2022. The effect of transport infrastructure on land-use change: The case of toll road and high-speed railway development in West Java. J. Reg. City Plan., 33(1): 53-70. https://doi.org/10.5614/jpwk.2022.33.1.3

Siswoyo, M. 2020. The impact of toll roads development: Ecology of public administration perspective. Syst. Rev. Pharm., 11(11): 152-157. https://doi.org/10.31838/srp.2020.11.22

Sitko, N.J. and Jayne, T.S. 2014. Structural transformation or elite land capture? The growth of "emergent" farmers in Zambia. Food Policy, 48: 194-202. https://doi.org/10.1016/j.foodpol.2014.05.006

Sudiyarto, M. and Indah, P.N. 2019. The impact of agricultural land conversion to toll roads on farmers "perception and welfare." Asian J. Manag. Sci. Edu., 8(1): 40-49.

Syahyuti, K.I., Swastika, D.K.S., Susilowati, S.H. and Suharyono, S. 2021. The role of stakeholders is to support the implementation of modern agricultural programs. IOP Conf. Ser. Earth Environ. Sci., 892(1): 1-8. https://doi.org/10.1088/1755-1315/892/1/012024

Tronvoll, B. 2017. The actor: The key determinator in service ecosystems. Systems, 5(2): 1-14. https://doi.org/10.3390/systems5020038

Velten, S., Jager, N. W. and Newig, J. 2021. Success of collaboration for sustainable agriculture: a case study meta-analysis. Environ. Dev. Sustain., 23(10): 14619-14641. https://doi.org/10.1007/s10668-021-01261-y

Velten, S., Leventon, J., Jager, N. and Newig, J. 2015. What is sustainable agriculture? A systematic review. Sustainability, 7(6): 7833-7865. https://doi.org/10.3390/su7067833.

# Assessment of Particulate and Gaseous Fluoride in Phosphate Fertilizer Industry

**S. Jawahar\*(\*\*)† [iD], K. Shridhar\* [iD], V. Dhananjayan\* [iD], K. Panjakumar\*, B. Ravichandran\*, A. Ravinder Nath\*\*\* and Nirmala Babu Rao\*\*\*\***

\*Industrial Hygiene & Toxicology Division, ICMR-Regional Occupational Health Centre (Southern), Kannamangala, Devanahalli Taluk, Bangalore-562110, Karnataka, India
\*\*Department of Environmental Science, University College of Science, Osmania University, Hyderabad-500007, India
\*\*\*School of Life Sciences, Central University of Karnataka, Gulbarga-585367, Karnataka, India
\*\*\*\*Department of Botany, University College of Science, Osmania University, Hyderabad-500007, India
†Corresponding author: Salavath Jawahar; jawahar.nin@gmail.com

## ABSTRACT

Fluorides are emitted in both gaseous and particle forms in the industrial sector. However, studies usually only report total fluoride content. Therefore, the study aimed to assess the particulate, gaseous fluoride and correlate it with the respirable dust particles in Single Super Phosphate (SSP), Granular Single Super Phosphate (GSSP), and administration divisions of the industry. Respirable dust particles, particulate fluoride, and hydrogen fluoride in the work environment were collected on a filter cassette containing an MCE filter paper (0.8 micron 37-mm) and $Na_2CO_3$ impregnated backup pad, respectively, using a personal sampler. The fluoride samples were analyzed using Ion Selective Electrode (ISE) and expressed as milligrams per meter cube ($mg.m^{-3}$). The respirable dust, particulate, and gaseous fluoride content were found to have statistically significant differences ($p<0.001$) between the divisions (SSP, GSSP, and administration) in the static monitoring, whereas, in the case of personal monitoring, no significant differences were observed. Average airborne respirable, particulate, and gaseous fluoride levels in static monitoring were 1.37, 1.03, 0.20 $mg.m^{-3}$, 0.018, 0.008, 0.001 $mg.m^{-3}$, and 0.808, 0.403, 0.026 ppm in SSP, GSSP and administration respectively, whereas in personal monitoring the average respirable, particulate and gaseous fluoride concentrations were 1.18, 0.85, 0.30 $mg.m^{-3}$, 0.0013, 0.007, 0.002 $mg.m^{-3}$ and 0.356, 0.258, 0.011 ppm in SSP, GSSP and administration respectively. The present study observed that the levels of fluoride decreased with an increase in distance from SSP, followed by GSSP and administration. It indicates that the fluoride exposure was inversely proportional to the distance of the source. This study outcome will help to design a policy and intervention to mitigate fluoride exposure among workers.

## INTRODUCTION

Fluorine (F) is the most electronegative and reactive non-metal element. Therefore, the elemental form of fluorine never occurs in nature, and fluoride pollution mostly occurs through anthropogenic activities in the industrial sector (Jawahar et al. 2022, Wang et al.2019, Sunitha et al. 2022, Torres-Sánchez et al. 2020, Cui et al. 2021). In the fertilizer industry, phosphate fertilizers are produced by adding sulphuric acid to digest rock phosphate, which is necessary to maintain agricultural production worldwide (Millán-Becerro et al. 2022). During this industrial process, particulate and gaseous fluorides are generated. In 2012, hydrofluoric acid (HF) spilled from a chemical plant in Gumi City, South Korea. As a result, many people were injured,

and five workers died on-site due to exposure to hydrofluoric acid (Jung & Park 2016, Lee et al. 2016). The exposure to hazardous chemicals in the working environment causes adverse health effects to the workers. Therefore, the workers should be aware of the preventive measures to control the accidents.

Anthropogenic activities, fossil fuel combustion processes, manufacturing operations, and biogenic sources can contribute to the ambient $PM_{2.5}$ particles. In addition to primary released particles, ambient $PM_{2.5}$ contains secondary inorganic particulate fluoride and organic aerosols (Anastasopolos et al. 2022, Fadel et al. 2021). According to Pawar et al. (2014), the mutagenic nature of F was revealed as an increase in the chromosomal aberrations (CA) and sister

chromatid exchanges (SCE) frequencies in the lymphocytes of the subjects. Meng & Zhang (1997) showed that the workers chemically exposed to the fumes containing fluoride in the phosphate fertilizer industry could associated with increased Chromosomal aberrations (CA) and micronuclei (MN) frequencies in their blood lymphocytes. Among welders, the relationship between welding fume exposure and respiratory symptoms appears more influenced by fluorides than other particles (Sjögren 2004). Ma et al. (2009) found that the concentrations of serum osteocalcin (OCN) and calcitonin (CTN) increased simultaneously in a Fluoride-exposed worker population.

The SSP and GSSP are the major units in phosphate fertilizer production. In the SSP plant, the single super phosphate is produced by the addition of sulfuric acid to ground or pulverized rock phosphate (insoluble in water) to produce single super phosphate (SSP) with a phosphorus content of 16-21% as phosphorus pentoxide (soluble in water). This process involves mixing the sulphuric acid and the rock phosphate in a reactor. The mixture goes onto a moving conveyor in a den, and the semisolid mixture produced from the den is termed a single super phosphate, which is allowed to cure for 10 to 20 days. After curing the product, the cured SSP is taken further to produce a granulated form of single super phosphate (GSSP) in the granulation circuit of the GSSP plant. The fumes containing silicon tetrafluoride ($SiF_4$) and hydrogen fluoride (HF) gasses generated from the reactor (mixer) and den. Workers' exposure to these fumes containing fluoride compounds released during the industry's processing and handling of fertilizer might be through inhalation or dermal contact. These fumes might pose adverse health effects to the workers working in the industry. We know that no literature is available regarding assessing particulate and gaseous fluoride levels in the phosphate fertilizer industry. Therefore, this study aimed to assess the particulate and gaseous fluoride levels in the working environment of the phosphate fertilizer industry. This study will be useful to evaluate the key sources of the pollutants in various work environments of the phosphate fertilizer industry.

## MATERIALS AND METHODS

### Samples Collection

The samples of airborne respirable dust, particulate, and gaseous fluoride (static n = 71 and personal n = 36) were collected from various divisions' phosphate fertilizer production industry. Respirable dust, aerosol-containing particulate, and gaseous fluoride were sampled by following NIOSH method 7902, using personal respirable dust sampler

SIDEKICK Ex 51 and universal sample pump 224-PCXR4 (make SKC, USA) through filter cassette flitted with 37mm mixed cellulose ester (0.8µm pore size) filter paper and backup impregnated pad at the flow rate of 2.2 L.min$^{-1}$ and 2.0 L.min$^{-1}$ respectively. Initial and final weights of the MCE filter paper were measured using the analytical balance (make Shimadzu). Respirable dust samplers pump for sampling were tagged to the waist of the workers working in the different sections in the industry, whereas the respirable dust samplers filter cassette and cyclone inlet set were kept in the breathing zone of each worker for the entire shift duration of 8 h. For the static monitoring, the samplers were positioned in the breathing zone (periphery of 1.2 to 1.8 m) of the dust-producing source inside the plant with the help of a tripod stand. After sampling, the filter papers and pads were stored and transported to the laboratory for further analysis.

### Measurement of Personal and Static Respirable Dust (PM$_{2.5}$) Concentration

All the collected samples were processed for determination of dust content. The concentrations were computed from the gravimetric weight for the respirable dust (PM$_{2.5}$) evaluation, the differences of filter paper weights before and after sampling for an entire shift. The dust concentration was expressed in mg.m$^{-3}$.

Respirable dust concentration (mg.m$^{-3}$) =

$$\frac{W1 - W2 \text{ (mg)} \times 10^3}{\text{Flow rate (L/min)} \times \text{Time (min)}}$$

Where, W1= Initial weight of the filter paper (mg)
W2 = Final weight of the filter paper (mg)

### Estimation of Particulate and Gaseous Fluoride

The method 7902 was used to analyze particulate and gaseous fluoride (NIOSH 1994). Fluoride concentration in particulate and gaseous mist samples was analyzed using a pH/ISE benchtop meter (Model: ORION 4 STAR, Thermo Scientific). Before sample analysis, the fluoride Ion Selective Electrode was calibrated using freshly prepared 0.01, 0.1, 1, 10, and 100 ppm working standard concentrations(Orion 940907).

**Particulate fluoride:** The particulate fluoride collected on mixed cellulose ester (MCE) filter papers was conditioned in the laboratory before analysis. The post-weighed filter papers were transferred to a nickel crucible containing 5 mL of 20% NaOH for fusion. It was kept in the muffle furnace for 1 to 2 minutes at 600-650°C. After this, the residues were cooled and dissolved in a plastic beaker containing 40 mL of deionized water, filtered solution, and added 50 mL TISAB-II solution (Orion 940907) to each aliquot. Adjusted

the pH to 5.5 ± 0.2 using 1-2 mL of con. HCl and made up the volume up to 100ml with the deionized water. The equal volume of the sample & TISAB-II solution was maintained, and the ISE electrode was inserted in the beaker containing samples, and measured the fluoride levels in it. The blank and known standards were measured between sample analyses to check quality control. In the spiked samples, recovery observed was 98±2%.

**Gaseous fluoride:** The absorbed gaseous fluoride in the alkali-impregnated cellulose pads were transferred to 100-mL plastic beakers. Equal aliquots of distilled water and TISAB-II solution were added and kept for 30 min until reduced to pulp. Stirred and mixed continuously on a magnetic stirrer at room temperature for 2-3 min, and then the readings were measured in ppm using an ion-selective electrode.

### Data Analysis

The data was analyzed using Statistical Package for Social Sciences (SPSS) software (version 26).

### RESULTS AND DISCUSSION

During the monitoring, 107 airborne particulate and gaseous mist samples (static n = 71 and personal n = 36) were collected using personal samplers at three different divisions in the phosphate fertilizer factory. In the static monitoring, the maximum particulate fluoride concentration of 0.074 mg.m$^{-3}$ was obtained in the single super phosphate (SSP) division, whereas in the case of respirable dust, the maximum concentration of 4.72 mg.m$^{-3}$ was observed in

granular single super phosphate (GSSP) division, however, the highest mean level of respirable dust was found in SSP division (Table 1). Due to rock phosphate digestion takes place in the SSP division.

In personal monitoring, the highest respirable dust and particulate fluoride concentrations were observed in the SSP division, followed by GSSP and administration (Table 1). In the SSP division, maximum respirable dust and particulate fluoride concentrations were observed as 1.18 and 0.013 mg.m$^{-3}$, respectively. Overall, the respirable dust and particulate fluoride level was higher in static monitoring than in personal monitoring. The reason is that in the static monitoring, the sampler was fixed in one place for 8 hours at workplaces. Whereas in the personal monitoring, the sampler was attached to the workers for 8 hours, these workers moved here and there for their job requirements. Therefore, exposure load may be less compared to static monitoring.

Correlation analysis was performed to test the relationship between fluoride concentrations and respirable dust concentration. A significant positive correlation ($r > 0.36$, $p < 0.01$) was found between the particulate fluoride and respirable dust collected in the industrial area. This indicates that the anthropogenic fluoride is higher in industry compared to the periphery of the industry.

Table 2 shows that varied levels of gaseous fluoride concentration were observed in the different divisions in static and personal monitoring methods. Generally, the maximum gaseous fluoride concentration was observed in the SSP division have to remove at 2.44 ppm in the static and personal monitoring, followed by GSSP and administration

Table 1: Respirable dust and particulate fluoride concentration (mg.m$^{-3}$) at different divisions in the fertilizer industry.

| Monitoring type | Static Monitoring n = 71 | | | Personal Monitoring n = 36 | | |
|---|---|---|---|---|---|---|
| Divisions | SSP n = 30 | GSSP n = 30 | Administration n = 11 | SSP n = 16 | GSSP n = 16 | Administration n = 4 |
| Respirable dust Concentration (mg.m$^{-3}$) Mean ± SD (Range) | 1.37 ± 0.83 (0.27-4.09) | 1.03 ± 0.90 (0.13-4.72) | 0.20 ± 0.12 (0.02-0.34) | 1.18 ± 1.12 (0.24-4.56) | 0.85 ± 0.51 (0.9-2.06) | 0.30 ± 0.11 (0.17-0.41) |
| Particulate Fluoride Concentration (mg.m$^{-3}$) Mean ± SD (Range) | 0.018 ± 0.015 (0.004-0.074) | 0.008 ± 0.008 (0.001-0.043) | 0.001 ± 0.0001 (0.001-0.002) | 0.013 ± 0.013 (0.002-.046) | 0.007 ± 0.003 (0.004-.014) | 0.002 ± 0.002 (0.001-0.006) |

Table 2: Gaseous fluoride concentration (ppm) at different divisions in the fertilizer industry.

| Monitoring type | Static Monitoring n = 71 | | | Personal Monitoring n = 36 | | |
|---|---|---|---|---|---|---|
| Divisions | SSP n = 30 | GSSP n = 30 | Administration n = 11 | SSP n = 16 | GSSP n = 16 | Administration n = 4 |
| Gaseous Fluoride (HF) Concentration (ppm) Mean ± SD (Range) | 0.808 ± 0.758 (0.069-2.444) | 0.403 ± 0.263 (0.069-1.187) | 0.026 ± 0.022 (0.007-0.071) | 0.356 ± 0.340 (0.084-1.146) | 0.258 ± 0.187 (0.077-0.550) | 0.011 ± 0.004 (0.009-0.017) |

Table 3: Exposure limits for fluoride by different regulatory bodies at the workplace.

| Regulatory bodies | Particulate fluoride | Hydrogen Fluoride | Respirable dust |
|---|---|---|---|
| OSHA PEL*<br>8-hour TWA | 2.5 mg.m$^{-3}$ | 3 ppm | 5 mg.m$^{-3}$ |
| NIOSH REL**<br>Up to 10-hour TWA | 2.5 mg.m$^{-3}$ | 3 ppm | 5 m.m$^{-3}$ |
| ACGIH TLV***<br>8-hour TWA | 2.5 mg.m$^{-3}$ | 0.5 ppm | 5 mg.m$^{-3}$ |
| Indian Factories Act 1948-PEL<br>8-hour TWA | 2.5 mg.m$^{-3}$ | 3 ppm | 10 mg.m$^{-3}$ |

*Occupational Safety and Health Administration Permissible Exposure Limits (OSHA 2017)
**National Institute for Occupational Safety and Health Recommended Exposure Limit (NIOSH 2019)
***American Conference of Governmental Industrial Hygienists Threshold Limit Values (ACGIH 2023)

(Table 2). The maximum gaseous fluoride concentration in static monitoring was observed in the single super phosphate division, which was lower than the OSHA PEL and Indian Factories Act 1948, 8-hour TWA standard value of 3 ppm (Table 3) (OSHA 2017). In the SSP division in the static monitoring, the gaseous fluoride mean concentration was 0.808 ppm, which is higher when compared to the ACGIH TLV- 8 hrs time-weighted average standard of 0.5 ppm (Table 3) (ACGIH 2003). A significant difference (p<0.001) in gaseous fluoride levels was found between the divisions in static monitoring, whereas in personal monitoring, no significant differences were observed.

According to Schwarz et al. (2020) study, the maximum particulate and gaseous fluoride levels in the primary aluminum industry (Slovakia) were reported as 10.29 and 6.21 mg.m$^{-3}$, respectively, whereas in our investigations, the maximum particulate fluoride level was 0.074 mg.m$^{-3}$

and 2.44 ppm respectively. In the US, a study by Seixas et al. (2000) reported total fluoride 4.07 mg.m$^{-3}$ and hydrogen fluoride 0.74 mg.m$^{-3}$ personal airborne exposure in the aluminum smelting industry. The current study found a lower level of particulate and gaseous fluoride compared to aluminum smelting industry workers.

Figs. 1 & 2 showed that the percentage of particulate fluoride concentration was present in the respirable dust concentration among the different divisions in the static and personal monitoring. The percentage of particulate fluoride concentration was distributed considerably higher in the SSP division, followed by GSSP and administration. Ramteke et al. (2018) conducted a study on selected commercial phosphate fertilizers and reported higher levels of fluoride content. The phosphate fertilizer industrial environment could be contaminated by fluoride. Dartan et al. (2017) study says that the surrounding area of the phosphate fertilizer
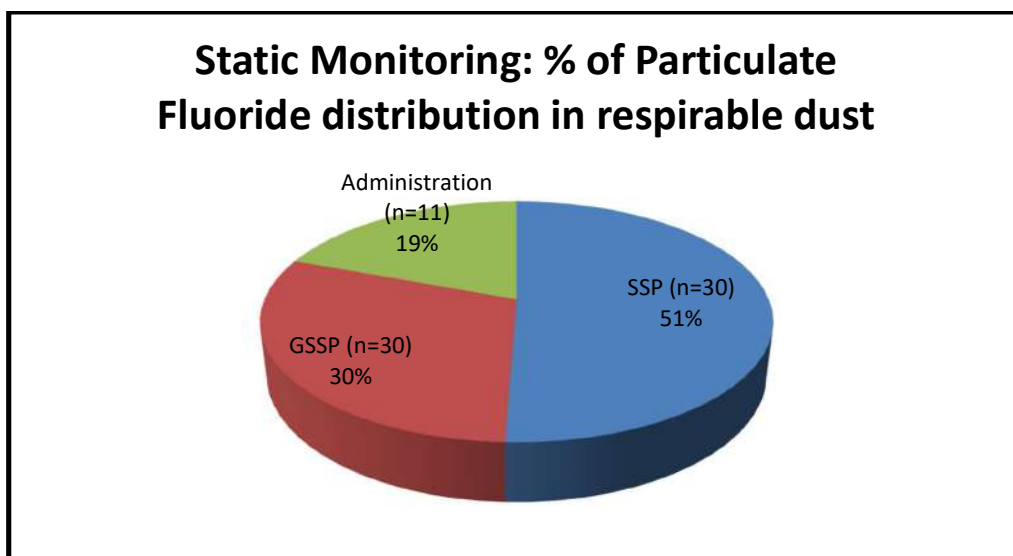


Fig. 1: Percentage distribution of particulate fluoride in the respirable dust (static monitoring).
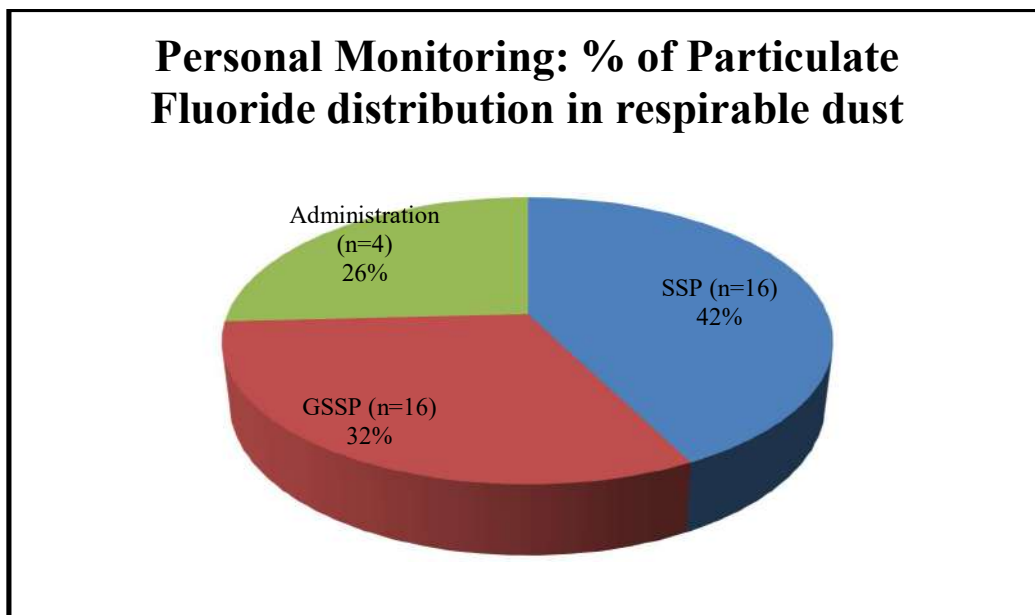
Fig. 2: Percentage distribution of particulate fluoride in the respirable dust (personal monitoring).

industry has serious fluoride contamination. Several previous studies state that chronic fluoride exposure causes adverse effects on bones, skeletal fluorosis, teeth; dental fluorosis, and organs (kidney, liver, thyroid gland, and gastrointestinal); non-skeletal fluorosis in humans and animals (Ghosh et al. 2013, Bhat et al. 2015). Therefore, the workers working in the industry have to avoid fluoride exposure by using personal protective equipment, and rotating the workers' duties from one division to another by the management may help in less exposure.

## CONCLUSION

In the present study, we discussed fluoride exposure in the workplace environment in the different divisions of the phosphate fertilizer industry. The results revealed that the concentration of fluoride decreased with the increase of distances from SSP, followed by GSSP and administration. It indicates that the fluoride exposure was indirectly proportional to the distance of the source. The respiratory dust, particulate, and gaseous fluoride concentrations, significant differences ($p < 0.001$) were found between the divisions (SSP, GSSP, and administration) of static monitoring. In contrast, in the case of personal monitoring, no significant differences were observed. The percentage distribution of particulate fluoride in the respirable dust in static (51% SSP, 31% GSSP, and 19% administration) and personal monitoring (42% SSP, 32% GSSP, and 26% administration) was observed, respectively. The particulate and gaseous fluoride concentrations obtained were within permissible exposure limits of OSHA, NIOSH, and the Indian Factories Act 1948. Although, we observed a maximum concentration of gaseous fluoride close to the permissible exposure limit in the SSP division. An awareness program was conducted among employees about the effects of excess fluoride exposure and the importance of PPEs in avoiding fluoride exposure in the workplace. Further studies are required on environmental and biological monitoring in the industry and as well as surrounding areas.

## REFERENCES

ACGIH 2023. ACGIH® Threshold Limit Values for Chemical Substances in the Work Environment. Adopted by ACGIH® with Intended Changes. http://www.acgih.org/.

Anastasopolos, A.T., Hopke, P.K., Sofowote, U.M., Zhang, J.J. and Johnson M. 2022. Local and regional sources of urban ambient PM2.5 exposures in Calgary, Canada. Atmos. Environ., 290: 119383.

Bhat, N., Jain, S., Asawa, K., Tak, M., Shinde, K., Singh, A., Gandhi, N. and Gupta, V.V. 2015. Assessment of fluoride concentration of soil and vegetables in the vicinity of zinc smelter, Debari, Udaipur, Rajasthan. J. Clin. Diag. Res., 9(10): ZC63.

Cui, S.F., Fu, Y.Z., Zhou, B.Q., Li, J.X., He, W.Y., Yu, Y.Q. and Yang, J.Y. 2021. Transfer characteristics of fluorine from atmospheric dry deposition, fertilizers, pesticides, and phosphogypsum into soil. Chemosphere, 278: 130432.

Dartan, G.U., Taspinar, F.A. and Toroz, I. 2017. Analysis of fluoride pollution from fertilizer industry and phosphogypsum piles in agricultural areas. J. Ind. Pollut. Control., 33(1): 662.

Fadel, M., Ledoux, F., Farhat, M., Kfoury, A., Courcot, D. and Afif, C. 2021. PM2.5 characterization of primary and secondary organic aerosols in two urban-industrial areas in the East Mediterranean. J. Environ. Sci., 101: 98-116.

Ghosh, A., Mukherjee, K., Ghosh, S.K. and Saha, B. 2013. Sources and toxicity of fluoride in the environment. Rev. Chem. Intermed.,39(7): 2881-2915.

Jawahar, S., Nath, A.R., Rao, N.B., Venugopal, D., Kondhalkar, S., Yadav, R.K., Karunamoorthy, P. and Ravichandran, B. 2022. Biological monitoring of urinary fluoride among phosphate fertiliser production industrial workers. Indian J. Sci. Technol., 15(45): 2451-2457.

Jung, K. and Park, H.W. 2016. Tracing inter-organizational information networks during emergency response period: A webometric approach to the 2012 Gumi chemical spill in South Korea. Gov. Inf. Q., 33(1): 133-141.

Lee, K., Kwon, H.M., Cho, S., Kim, J. and Moon, I. 2016. Improvements in safety management systems in the Korean chemical industry after a large chemical accident. J. Loss Prev. Process Ind., 42: 6-13.

Ma, J., Li, M., Song, Y.E., Tu, J., Liu, F. and Liu K. 2009. Serum osteocalcin and calcitonin in adult males with different fluoride exposures. Fluoride, 42(2): 133.

Meng, Z. and Zhang, B. 1997. Chromosomal aberrations and micronuclei in lymphocytes of workers at a phosphate fertilizer factory. Mutat. Res. Genet. Toxicol. Environ. Mutagen., 393(3): 283-288.

Millán-Becerro, R., Macías, F., Cánovas, C.R., Pérez-López, R. and Fuentes-López, J.M. 2022. Environmental management and potential valorization of wastes generated in passive treatments of fertilizer industry effluents. Chemosphere, 295: 133876.

National Institute for Occupational Safety and Health (NIOSH). 1994. Filter T. Fluorides, aerosol, and gas by Ion Selective Electrode 7902.

National Institute for Occupational Safety and Health (NIOSH). 2019. NIOSH Pocket Guide to Chemical Hazards. Department of Health and Human Services. Centers for Disease Control and Prevention. National Institute for Occupational Safety and Health (NIOSH). Available at https://www.cdc.gov/niosh/npg

Occupational Safety and Health Administration (OSHA). 2017. Air Contaminants. 29 CFR 1910.1000 82 FR 2735, January 9, 2017. Available at https://www.osha.gov/laws regs/regulations/standardnumber/1910/1910.1000

Pawar, A.C,, Naik, S.J. and Kumari, S.A. 2014. Cytogenetic analysis of human lymphocytes of fluorosis-affected men from the endemic fluorosis region in Nalgonda district of Andhra Pradesh, India. Fluoride, 47(1): 78-84.

Ramteke, L.P., Sahayam, A.C., Ghosh, A., Rambabu, U., Reddy, M.R., Popat, K.M., Rebary, B., Kubavat, D., Marathe, K.V. and Ghosh, P.K. 2018. Study of fluoride content in some commercial phosphate fertilizers. J. Fluor. Chem., 210: 149-55.

Schwarz, M., Salva, J., Vanek, M., Rasulov, O. and Darmová, I. 2020. Fluoride exposure and the effect of tobacco smoking on urinary fluoride levels in primary aluminum workers. Appl. Sci., 11(1): 156.

Seixas, N.S., Cohen, M., Zevenbergen, B., Cotey, M., Carter, S. and Kaufman, J. 2000. Urinary fluoride as an exposure index in aluminum smelting. Am. Ind. Hyg. Assoc. J., 61(1): 89-94.

Sjögren, B.2004. Fluoride exposure and respiratory symptoms in welders. Int. J. Occup. Environ. Health., 10(3):310-312.

Sunitha, V., Reddy, Y.S., Suvarna, B. and Reddy, B.M. 2022. Human health risk assessment (HHRA) of fluoride and nitrate using pollution index of groundwater (PIG) in and around hard rock terrain of Cuddapah, AP South India. J. Environ. Chem. Ecotoxicol., 4: 113-123.

Torres-Sánchez, R., Sánchez-Rodas, D., de la Campa, A.S. and de La Rosa, J.D. 2020. Hydrogen fluoride concentrations in the ambient air of an urban area based on the emissions of a major phosphogypsum deposit (SW, Europe). Sci. Total Environ., 714: 136891.

Wang, M., Li, X., He, W.Y., Li, J.X., Zhu, Y.Y., Liao ,Y.L., Yang, J.Y. and Yang, X,E. 2019. Distribution, health risk assessment, and anthropogenic sources of fluoride in farmland soils in phosphate industrial area, southwest China. Environ. Pollut., 249: 423-33.

WHO. 2000. Fluorides. In: Air quality guidelines for Europe, 2nd ed. Copenhagen, World Health Organization Regional Office for Europe, pp. 143-146.

## ORCID DETAILS OF THE AUTHORS

S. Jawahar: https://orcid.org/0009-0004-7805-9501

K. Shridhar: https://orcid.org/0000-0002-6170-2941

V. Dhananjayan: https://orcid.org/0000-0002-9977-4609

# Pattern of Lead Accumulation in Two Vegetable Plants Due to EDTA Treatment

**A. Rosyidah\*** (iD) **, M.W. Lestari\*** (iD) **and N. Syam\*\***

\*Department of Agrotechnology, Faculty of Agriculture, University of Islam Malang, Malang, East Java, Indonesia
\*\*Department of Agrotechnology, Faculty of Agriculture, University of Moeslim Indonesia, Makasar, Indonesia
†Corresponding author: A. Rosyidah; ard@unisma.ac.id

## ABSTRACT

Phytoextraction and phytostabilization are the most consistent patterns or mechanisms of action of phytoremediation. One of the elements influencing the mechanism of action of heavy metal absorption by plant species is Ethylene Diamine Tetraacetic Acid (EDTA). Therefore, this study aimed to determine the pattern of phytoremediation in water spinach and spinach due to the addition of EDTA in the soil. The treatments tested by factor 1 were water spinach (T1) and spinach (T2), and factor 2 was the concentration of EDTA consisting of 3 levels, 0, 3, and 6 g/polybag. Each treatment was repeated three times on five sample plants. Furthermore, growth evaluation was carried out in the first six days after planting and conducted every 3 days. It was carried out on variables such as changes in plant height, leaves area, total root length, Pb content in the soil, fresh and dry weight of shoots and roots, shoot, seeds, and Translocation Factor (TF). The results showed that water spinach and spinach had different mechanisms of action due to the application of EDTA in Pb-contaminated media. Furthermore, water spinach and spinach have a mechanism of phytoextraction and phytostabilization, respectively. Therefore, spinach is safer than water spinach when grown in Pb-polluted land.

## INTRODUCTION

Lead (Pb) is one of the numerous heavy metals that can easily contaminate agricultural soil. This contaminant can come from garbage, liquid waste, and other pollutants from agricultural activities, such as using fertilizers and pesticides. Heavy metal pollution remains a world problem (Sigua et al. 2005, Fu & Wang 2011) because of its effect on crop yields, biomass, and soil fertility, resulting in bioaccumulation of metals in the food chain (n.d.) (Rajkumar et al. 2009, Wong 2003 and Sivarajasekar & Baskar 2014). Therefore, heavy metal needs to be removed from the soil for agro-ecological sustainability and the carrying capacity of human health, Mittal et al. 2016, Alqadami et al. 2017, Bushra et al. 2017, Daneshvar et al. 2017, Kumar et al. 2017, and Naushad et al. 2017).

Various soil removal methods are expensive, labor intensive, and cause soil disturbance (Khan et al. 2004, Bhargava et al. 2012). Scientists are more interested in phytoremediation methods, which clean the soil of heavy metal pollutants using plants (Chaudhary et al. 2016). An example is phytoremediation technology, which has been a cheaper option until now. Its mechanism consists of several basic concepts, such as phytoextraction, phytovolatilization, phytodegradation, phytostabilization, rhizofiltration, and interaction with pollutant-degrading microorganisms (Marques et al. 2009, Glick 2003). Furthermore, it depends on several factors, including the accumulation of plants for various pollutants and concentrations.

Many studies demonstrated that water spinach and spinach absorb heavy metals from the soil. Therefore, they were classified as hyperaccumulators because they can accumulate potentially phytotoxic elements at 50 to 500 times higher than the average plants (Gupta et al. 2004, Yang et al. 2006, Reeves et al. 2018, Gratão et al. 2005).

The absorption of metal by plants can be increased by inducing a phytoextraction process using chelate compounds. The application of this compound to the soil can stimulate the availability and transfer of metal from the roots to the canopy. In the chelating mechanism, it is believed that plants absorb metal elements as metal-chelate complexes, which are more easily absorbed by roots and translocated to the canopy. A chelating compound commonly used to optimize phytoremediation is EDTA (*Ethylene Diamine Tetraacid*). This compound has a strong chelating ability for different heavy metals, specifically for Pb (Katoh et al. 2012, Zou et al. 2009, Finzgar et al. 2014, Hu et al. 2014, García et al. 2017).

Many studies also discussed various aspects of phytoremediation in water spinach and spinach. However,

there is conflicting evidence regarding whether water spinach and spinach have the same phytoremediation mechanism and how the presence of EDTA in the soil influences the phytoremediation pattern.

## MATERIALS AND METHODS

This study was conducted from September to December 2020 at the Greenhouse, Faculty of Agriculture, Islamic University of Malang, with an altitude of 540 meters above sea level and a temperature of 21-30°C. The media used include soil and sand at a ratio of 4:1 and then a 10 kg polybag. The soil was analyzed to ensure that the Pb content in the ground was low. Afterward, Pb was added to each polybag at 350 mg.kg$^{-1}$ soil (1.75 g.polybag). It was applied 1 week before planting and mixed with the prepared media until homogeneous. EDTA was then dissolved with 100 ml of distilled water, mixed with 1 kg of media, and combined with other substances. EDTA was applied 1 week before planting. Furthermore, 15-day-old Spinach and water spinach seedlings were planted in polybags containing Pb and EDTA.

This study adopted the randomized block design. The treatments tested in factor 1 were water spinach (T1) and spinach (T2), and factor 2 was the concentration of EDTA consisting of 3 levels, namely 0 (K1), 3 (K2), and 6 (K3) g/polybag. Each treatment was repeated three times with five sample plants. Growth evaluation was carried out every three days for the first six days after planting. Furthermore, the variable evaluated includes changes in plant height, leaves area, fresh and dry weight of shoots and roots, total root length, Pb levels in soil, shoots, roots, and Translocation Factor (TF).

## RESULTS AND DISCUSSION

### Plant Growth

Several abiotic stress factors severely limit plant growth, including heavy metal contamination. This study showed different growth responses on water spinach and spinach grown on Pb-contaminated media. Furthermore, water spinach plant media without EDTA tended to give the best plant height gain value at various ages of observation, as shown in Fig. 1. The average plant height decreased from 21 DAT, but the leaf area declined to 24 DAT. Water spinach planted on media supplemented with 6 g/polybag EDTA experienced the greatest decrease in plant height. Those planted on media supplemented with 6 g/polybag EDTA experienced the highest rate of reduction in plant height, accounting for 71%. Meanwhile, in spinach, the rate of decrease in plant height was not significantly different between all treatments.
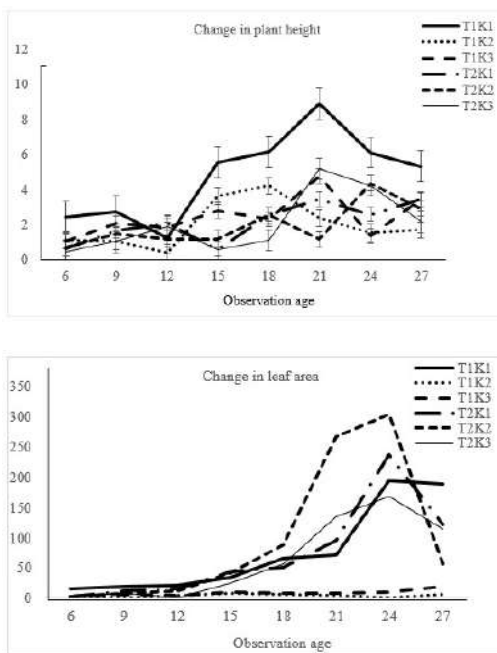


Fig. 1: Changes in plants' height and leaves area.

The highest decrease in leaf area occurred in spinach treated with EDTA at a 3 g/polybag dose. The rate of change in leaves area on water spinach was insignificant among all treatments. Furthermore, Pb is tightly bound to minerals and soil organic matter, making it difficult for plants to absorb through the roots. It is mainly absorbed through the roots. Hence, it will easily form complex bonds with nutrients, limiting plants' ability to translocate it to the canopy. Pb accumulator plants managed to translocate no more than 30% to the shoot. The application of EDTA facilitates this translocation from roots to shoots, accumulating as Pb-EDTA complex bonds resulting in a higher Pb. In addition, it induces physiological and morphological changes in certain concentrations, reducing plants' height and leaf area.

Water spinach and spinach were grown on Pb-contaminated media without EDTA and had the highest fresh and dry weight of roots and shoots, as shown in Fig. 2. The administration of EDTA at 3 and 6 g/polybag reduced the fresh and dry weight of roots and shoots. Furthermore, the reduction rate in the new weight of roots and shoots in water spinach was 89% and 93%, respectively, while in spinach, it was 49% and 25%. The rate of roots and shoots dry weight reduction in kale was 89% and 94%, respectively, while in spinach, it was 23% and 19%.

Water spinach and spinach productivity is related to the mass content of the plant, both fresh and dry weight. According to Fattahi et al. (2019), plants dry weight decreased in response to increasing lead concentrations at 0,
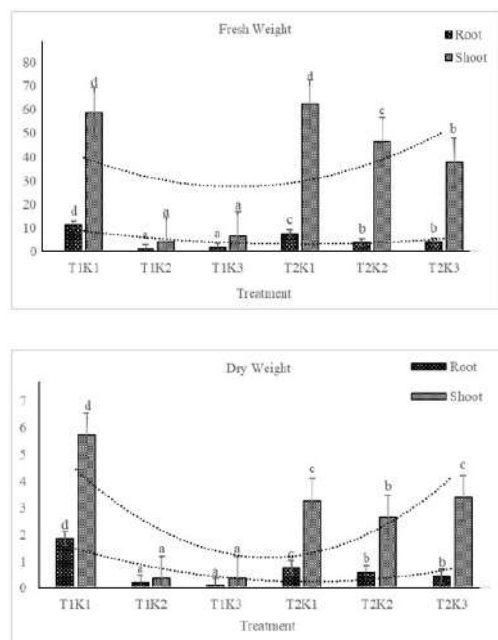
Fig. 2: Fresh weight and dry weight of plants in various treatments.

100, 200, and 400 mg.kg$^{-1}$ soil. Therefore, it is concluded that physiological reactions related to the primary metabolism of plants, which are responsible for growth and development, are affected by Pb stress.

The roots length of water spinach decreased to 77% due to the administration of EDTA at various doses in the media, while spinach had no significant changes, as shown in Fig. 3. The roots are the first organs in plants that are in contact with the different rhizosphere environments. They are one of the most important plant organs to absorb nutrients and heavy metals (Li et al. 2009). The roots also play an important role in accumulating heavy metals in plants' organs. In line with the results of (Xia et al. 2016), the correlation between root surface area, volume, and heavy metal concentrations in mustard shoots was statistically significant.
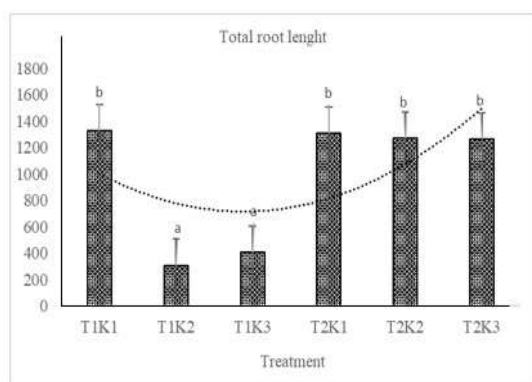


Fig. 3: Total root length.

Some commonly used growth performance indicators for plants exposed to heavy metals such as Pb include total plant biomass, growth rate, root, and shoot length. In addition, the presence of Pb in the environment can act as a stress-triggering factor that induces physiological changes or total plant growth inhibition. Every plant is different in its ability to accumulate heavy metals. Therefore, it determines the mechanism of action or pattern of accumulation.

Phytoextraction is the process where plants absorb pollutants from water or soil through the roots, which are then stored in the plant's canopy (Jacob et al. 2018, Yoon et al. 2006). Translocation of metals to shoots is an important and desirable biochemical activity, but it is ineffective for phytoextraction because harvesting root biomass is generally impossible (Tangahu et al. 2011).

Phytostabilization uses metal-tolerant plant species to immobilize heavy metals underground and reduce their bioavailability. This prevents their migration into the ecosystem and reduces the possibility of metals entering the food chain (Wong 2003, Marques et al. 2009). Furthermore, phytostabilization occurs through the deposition of heavy metal or reduction of valence in the rhizosphere, absorption, and sequestration in root tissues or onto the cell walls (Ginn et al. 2008, Kumpiene et al. 2012, Gerhardt et al. 2017).

EDTA is one of the most potent chelating agents to artificially increase the solubility, absorption, and complexation of metals, including Pb ions, in soil (Guo et al. 2014, Najeeb et al. 2017). Its application produces a synergistic effect in Pb uptake and increases roots' uptake and translocation. This study showed that water spinach and spinach decreased the plant's height, leaves area, fresh and dry weight of both shoots and roots, as well as total root length. This is due to the application of EDTA, which increases Pb absorption by plants, thereby causing stress.

**Pb Content in Soil and Plant**

One of the key factors for the success of phytoremediation in metal-contaminated soils is the high accumulation of metal in plants and its availability in the soil. However, the increased tolerance of the selected plants can ensure normal growth. To compensate for the ineffectiveness of metal in the soil, organic chelating chemicals such as EDTA can be used to increase metal uptake and delivery to plant parts (Seth et al. 2011, Guo et al. 2014, Shahid et al. 2014).

Fig. 4 shows a significant difference in the concentration of Pb in the soil after water spinach, and spinach were harvested at 28 days. The media used for water spinach contains Pb concentrations, which decrease with the addition of EDTA. The higher the dose of EDTA, the less Pb is left in the soil. On the other hand, the administration of EDTA at
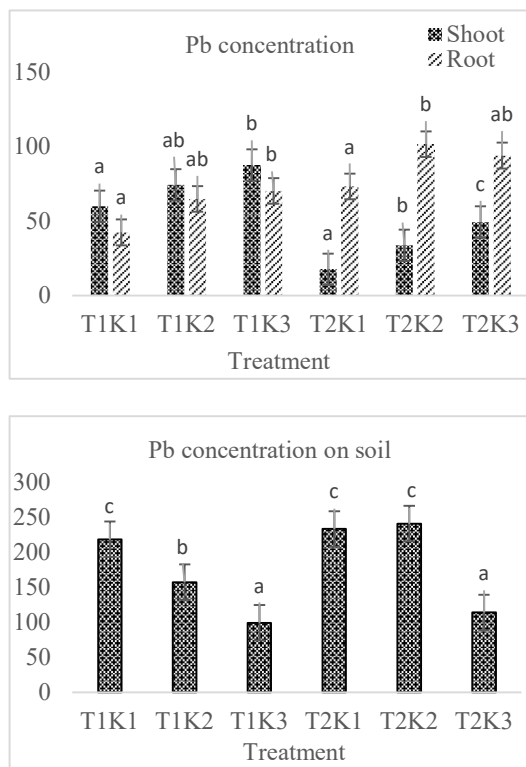
Fig. 4: Pb content in soil, roots, and shoot.

a dose of 3 g/polybag in spinach did not show a significant change in the concentration of soil Pb. At a quantity of 6 g/polybag, EDTA can reduce the concentration of soil Pb. This shows that the application of EDTA in Pb-polluted soil can increase the absorption of Pb by plants. Hence, only a small amount is left.

Fig. 4 shows that the administration of EDTA significantly affected the total Pb of the plant's roots and shoots. In water spinach, the concentration of Pb at the shoot and root is 125.3 and 111.32 ppm, respectively. Similarly, spinach has values of 61.57 ppm and 161.08 ppm. Therefore, it can be concluded that water spinach accumulates Pb in the shoots, while spinach is in the roots. The difference in Pb concentration indicated that both plants had different Pb absorption mechanisms.

Pb stress has direct and indirect effects on plant development, metabolism, and several physiological processes (Hasanuzzaman et al. 2011). Furthermore, plant biomass and height are the best indices to evaluate response to Pb toxicity (Zulfiqar et al. 2019). Reduction of biomass results in lower nutrient absorption, changes in hormonal status and cell membrane permeability, impaired respiration, inhibition of cell division at root tips, and decreased photosynthetic activity. These negative effects of EDTA are due to the high mobility of metal in soil solution

(Epelde et al. 2008). EDTA also dissolves Pb attached to soil particles (Katoh et al. 2012) and increases Pb transfer to roots by diffusion or mass flow. Israr & Sahi (2008) reported a significant reduction in the growth of *Sesbania drummondii* with EDTA. According to (Barrutia et al. 2011), the application of lower doses of EDTA to avoid a considerable decrease in biomass effectively increased the phytoremediation tolerance of water spinach and spinach.

**Translocation Factor (TF)**

TF shows the efficiency of plants in translocating accumulated metals from underground parts, such as roots and rhizomes, to stems and leaves (Bonanno & Vymazal 2017). The TF value generally characterizes the ability of phytoremediation (Srivastava et al. 2006, Yoon et al. 2006, Usman & Mohamed 2009). Furthermore, plants with a TF value greater than 1 are classified as highly efficient for metal translocation from roots to shoots. In this study, the highest TF value was found in water spinach grown on media with EDTA 6 g/polybag (1.25) and was significantly different from the control treatment (1.05). This value increased in response to the addition of EDTA. TF value of spinach was not significantly different between the treatment and control groups, as shown in Fig. 5 (Chunilall et al. 2005) stated that the accumulation of metals varies greatly among plant species. Element uptake depends on plant species and the quality of growth.

The low level of translocation from roots to shoots indicates that spinach is a good candidate for Pb phytostabilization. Meanwhile, EDTA stimulated Pb translocation from the soil to the roots (Wang et al. 2007), as indicated by TF = 0.32 <1 for the treatment without EDTA at a dose of 3 g/polybag. The analysis of Pb concentrations in plants showed that spinach stored higher Pb in the roots. The EDTA treatment effectively increased the Pb content in spinach roots. These results are consistent with (Tammam et al. 2021) on *Glebionis coronaria* L.
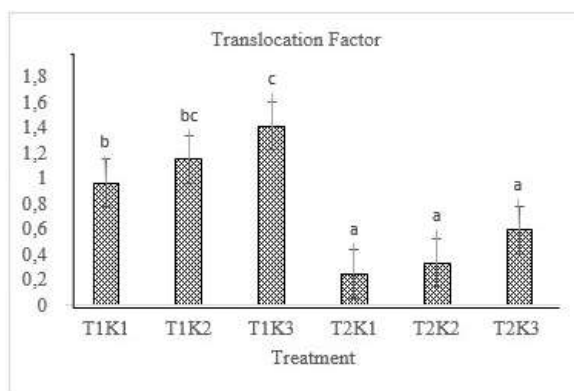


Fig. 5: Translocation factor.

TF value > 1 indicates that the plants translocate the absorbed contaminants to their upper organs. Furthermore, TF is defined by the ratio of the contaminant number in the upper organs of the plants to the roots (Maldonado-Magaña et al. 2011, Branzini & Zubillaga 2013). The results of this study indicated that water spinach had a TF > 1, which is consistent with the analysis of Pb concentrations in the shoots and roots, which is higher in the canopy of kale. This is thought to be due to the role of EDTA in increasing the absorption of Pb ions by plant roots and increasing their transport, which may be due to the formation and action of metal-EDTA complexes (Doncheva et al. 2013, García et al. 2017).

## CONCLUSIONS

The results indicated that water spinach and spinach are potential phytoremediators in Pb-contaminated soil due to their strong tolerance and ability to accumulate Pb. However, these plants have different working mechanisms due to the application of EDTA. The concentration of Pb absorbed by the roots increased significantly for water spinach and accumulated in the canopy. Therefore, it possesses a phytoextraction mechanism of action. In spinach, the concentration of Pb is higher in the roots, indicating that it has a phytostabilizing mechanism. Therefore, when grown on Pb-polluted land, spinach is safer than water spinach.

## REFERENCES

Alqadami, A.A., Naushad, M., Abdalla, M.A., Ahamad, T., AlOthman, Z.A., Alshehri, S.M. and Ghfar, A.A. 2017. Efficient removal of toxic metal ions from wastewater using a recyclable nanocomposite: A study of adsorption parameters and interaction mechanism. J. Clean. Prod., 156: 426-436.

Awual, M.R., Hasan, M.M., Eldesoky, G.E., Khaleque, M.A., Rahman, M.M. and Naushad, M. 2016. Facile mercury detection and removal from aqueous media involving ligand impregnated conjugate nanomaterials. 2016. J. Chem. Eng., 290: 243-251.

Barrutia, O., Artetxe, U., Hernández, A., Olano, J.M., García-Plazaola, J.I., Garbisu, C. and Becerril, J.M. 2011. Native plant communities in an abandoned Pb-Zn mining area of northern Spain: implications for phytoremediation and germplasm preservation. Int. J. Phytoremed., 13(3): 256-270.

Bhargava, A., Carmona, F.F., Bhargava, M. and Srivastava, S. 2012. Approaches for enhanced phytoextraction of heavy metals. J. Environ. Manage., 105: 103-120.

Bonanno, G. and Vymazal, J. 2017. Compartmentalization of potentially hazardous elements in macrophytes: insights into capacity and efficiency of accumulation. J. Geochem. Explor, 181: 22-30.

Branzini, A. and Zubillaga, M.S. 2013. Phytostabilization as soil remediation strategy. Plant-Based Remediation Processes, pp.177-198.

Bushra, R., Naushad, M., Sharma, G., Azam, A. and Alothman, Z.A. 2017. Synthesis of polyaniline-based composite material and its analytical applications for the removal of highly toxic Hg 2+ metal ion: Antibacterial activity against E. coli. Korean J. Chem. Eng, 34(7): 1970-1979.

Chaudhary, K., Jan, S. and Khan, S. 2016. Heavy metal ATPase (HMA2, HMA3, and HMA4) genes in the hyperaccumulation mechanism of heavy metals. Plant Metal Interac., 16: 545-556.

Chunilall, V., Kindness, A. and Jonnalagadda, S.B. 2005. Heavy metal uptake by two edible Amaranthus herbs grown on soils contaminated with lead, mercury, cadmium, and nickel. J. Environ. Sci. Health, 40(2): 375-384.

Daneshvar, E., Vazirzadeh, A., Niazi, A., Kousha, M., Naushad, M. and Bhatnagar, A. 2017. Desorption of methylene blue dye from brown macroalga: effects of operating parameters, isotherm study, and kinetic modeling. J Clean Prod.,152: 443-453.

Doncheva, S., Moustakas, M., Ananieva, K., Chavdarova, M., Gesheva, E., Vassilevska, R. and Mateev, P. 2013. Plant response to lead in the presence or absence of EDTA in two sunflower genotypes (cultivated *H. annuus* cv. 1114 and interspecific line *H. annuus × H. argophyllus*). Environ. Sci. Pollut. Res., 20(2): 823-833.

Epelde, L., Becerril, J.M., Hernández-Allica, J., Barrutia, O. and Garbisu, C. 2008. Functional diversity as an indicator of the recovery of soil health derived from *Thlaspi caerulescens* growth and metal phytoextraction. Appl. Soil Ecol., 39(3): 299-310.

Fattahi, B., Arzani, K., Souri, M.K. and Barzegar, M. 2019. Effects of cadmium and lead on seed germination, morphological traits, and essential oil composition of sweet basil (Ocimum basilicum L.). Ind. Crops Prod., 138: 111584.

Finzgar, N., Jez, E., Voglar, D. and Lestan, D. 2014. Spatial distribution of metal contamination before and after remediation in the Meza Valley, Slovenia. Geoderma, 217-218: 135-143.

Fu, F. and Wang, Q. 2011. Removal of heavy metal ions from wastewaters: a review. J. Environ. Manage., 92(3)0: 407-418.

García, S., Zornoza, P., Hernández, L.E., Esteban, E. and Carpena, R.O. 2017. Response of Lupinus albus to Pb–EDTA indicates relatively high tolerance. Toxicol. Environ. Chem., 99(9-10): 1378-1388.

Gerhardt, K.E., Gerwing, P.D. and Greenberg, B.M. 2017. Opinion: Taking phytoremediation from proven technology to accepted practice. Plant Sci., 256: 170-185.

Ginn, B.R., Szymanowski, J.S. and Fein, J.B. 2008. Metal and proton binding onto the roots of Fescue rubra. Chem. Geol., 253(3-4): 130-135.

Glick, B.R. 2003. Phytoremediation: synergistic use of plants and bacteria to clean up the environment. Biotechnol. Adv., 21(5): 383-393.

Gratão, P.L., Prasad, M.N.V., Cardoso, P.F., Lea, P.J. and Azevedo, R.A. 2005. Phytoremediation: green technology for the clean up toxic metals in the environment. Braz. J. Plant Physiol., 17: 53-64.

Guo, J., Feng, R., Ding, Y. and Wang, R. 2014. Applying carbon dioxide, plant growth-promoting rhizobacterium, and EDTA can enhance the phytoremediation efficiency of ryegrass in a soil polluted with zinc, arsenic, cadmium, and lead. J. Environ. Manage., 141: 1-8.

Gupta, D.K., Tohoyama, H., Joho, M. and Inouhe, M. 2004. Changes in the levels of phytochelatins and related metal-binding peptides in chickpea seedlings exposed to arsenic and different heavy metal ions. J. Plant Res., 117(3): 253-256.

Hasanuzzaman, M., Hossain, M.A. and Fujita, M. 2011. Nitric oxide modulates antioxidant defense and the methylglyoxal detoxification system and reduces salinity-induced damage to wheat seedlings. Plant Biotechnol. Rep., 5(4): 353-365.

Hu, P., Yang, B., Dong, C., Chen, L., Cao, X., Zhao, J., Wu, L., Luo, Y. and Christie, P. 2014. Assessment of EDTA heap leaching of agricultural soil highly contaminated with heavy metals. Chemosphere, 117: 532-537.

Israr, M. and Sahi, S.V. 2008. Promising role of plant hormones in translocation of lead in Sesbania drummondii shoots. Environ. Pollut., 153(1): 29-36.

Jacob, J.M., Karthik, C., Saratale, R.G., Kumar, S.S., Prabakar, D., Kadirvelu, K. and Pugazhendhi, A. 2018. Biological approaches to tackle heavy metal pollution: a survey of the literature. J. Environ. Manage., 217: 56-70.

Katoh, M., Masaki, S. and Sato, T. 2012. Single-step extraction to determine soluble lead levels in the soil. Int. J. Geomate, 3(6): 375-380.

Khan, F.I., Husain, T. and Hejazi, R. 2004. An overview and analysis of site remediation technologies. J. Environ. Manage., 71(2): 95-122.

Kumar, A., Sharma, G., Naushad, M., Kumar, A., Kalia, S., Guo, C. and Mola, G.T. 2017. Facile hetero-assembly of superparamagnetic Fe3O4/BiVO4 stacked on biochar for solar photo-degradation of methyl paraben and pesticide removal from soil. J. Photochem. Photobiol. A Chem., 337: 118-131.

Kumpiene, J., Fitts, J.P. and Mench, M. 2012. Arsenic fractionation in mine spoils 10 years after aided phytostabilization. Environ. Pollut., 166: 82-88.

Li, T., Yang, X., Lu, L., Islam, E. and He, Z. 2009. Effects of zinc and cadmium interactions on root morphology and metal translocation in a hyperaccumulating species under hydroponic conditions. J. Hazard. Mater., 169(1-3): 734-741.

Maldonado-Magaña, A., Favela-Torres, E., Rivera-Cabrera, F. and Volke-Sepulveda, T.L. 2011. Lead bioaccumulation in Acacia farnesiana and its effect on lipid peroxidation and glutathione production. Plant and Soil, 339(1-2): 377-389.

Marques, A.P., Rangel, A.O. and Castro, P.M. 2009. Remediation of heavy metal contaminated soils: phytoremediation as a potentially promising clean-up technology. Crit. Rev. Environ. Sci. Technol., 39(8): 622-654.

Mittal, A., Naushad, M., Sharma, G., Alothman, Z.A., Wabaidur, S.M. and Alam, M. 2016. Fabrication of MWCNTs/ThO2 nanocomposite and its adsorption behavior for the removal of Pb (II) metal from aqueous medium. Desalin. Water Treat., 57(46): 21863-21869.

Najeeb, U., Ahmad, W., Zia, M.H., Zaffar, M. and Zhou, W. 2017. Enhancing the lead phytostabilization in wetland plant Juncus effusus L. through somaclonal manipulation and EDTA enrichment. Arab. J. Chem., 10: S3310-S3317.

Naushad, M., Ahamad, T., Al-Maswari, B.M., Alqadami, A.A. and Alshehri, S.M. 2017. Nickel ferrite bearing nitrogen-doped mesoporous carbon as an efficient adsorbent for the removal of highly toxic metal ions from aqueous medium. J. Chem. Eng., 330: 1351-1360.

Rajkumar, M., Vara Prasad, M.N., Freitas, H. and Ae, N. 2009. Biotechnological applications of serpentine soil bacteria for phytoremediation of trace metals. Crit. Rev. Biotechnol., 29(2): 120-130.

Reeves, R.D., Baker, A.J., Jaffré, T., Erskine, P.D., Echevarria, G. and van Der Ent, A. 2018. A global database for plants that hyperaccumulate metal and metalloid trace elements. New Phytol., 208(2): 407-411.

Seth, C.S., Misra, V., Singh, R.R. and Zolla, L. 2011. EDTA-enhanced lead phytoremediation in sunflower (Helianthus annuus L.) hydroponic culture. Plant and Soil, 347(1-2): 231-242.

Shahid, M., Austruy, A., Echevarria, G., Arshad, M., Sanaullah, M., Aslam, M., Nadeem, M., Nasim, W. and Dumat, C. 2014. EDTA-enhanced phytoremediation of heavy metals: A review. Soil Sed. Contam. Int. J., 23(4): 389-416.

Sigua, G., Adjei, M. and Rechcigl, J. 2005. Cumulative and residual effects of repeated sewage sludge applications: forage productivity and soil quality implications in South Florida. Environ. Sci. Pollut. Res., 12(2): 80-88.

Sivarajasekar, N. and Baskar, R. 2014. Adsorption of basic red 9 on activated waste Gossypium hirsutum seeds: process modeling, analysis and optimization using statistical design. J. Ind. Eng. Chem., 20(5): 2699-2709.

Srivastava, M., Ma, L.Q. and Santos, J.A.G. 2006. Three new arsenic hyperaccumulating ferns. Sci. Total Environ., 364(1–3): 24-31.

Tammam, A., El-Aggan, W., Abou-Shanab, R. and Mubarak, M. 2021. Improved growth and phytostabilization potential of lead (Pb) in Glebionis coronaria L. under the effect of IAA and GA3 alone and in combination with EDTA by altering the biochemical attributes of stressed plants. Int. J. Phytoremed., 23(9): 958-968.

Tangahu, B.V., Sheikh Abdullah, S.R., Basri, H., Idris, M., Anuar, N. and Mukhlisin, M. 2011. A review on heavy metals (As, Pb, and Hg) uptake by plants through phytoremediation. Int. J. Chem. Eng., 21: 1-31.

Usman, A.R.A. and Mohamed, H.M. 2009. Effect of microbial inoculation and EDTA on the uptake and translocation of heavy metal by corn and sunflower. Chemosphere, 76(7): 893-899.

Wang, H.Q., Lu, S.J. and YAO, Z.H. 2007. EDTA-enhanced phytoremediation of lead-contaminated soil by Bidens maximowicziana. J. Environ. Sci., 19(12): 1496-1499.

Wong, M.H. 2003. Ecological restoration of mine degraded soils, with emphasis on metal contaminated soils. Chemosphere, 50(6): 775-780.

Xia, S., Deng, R., Zhang, Z., Liu, C. and Shi, G. 2016. Variations in the accumulation and translocation of cadmium among pak choi cultivars as related to root morphology. Environ. Sci. Pollut. Res., 23(10): 9832-9842.

Yang, R.Y., Chang, L.C., Hsu, J.C., Weng, B.B., Palada, M.C., Chadha, M.L. and Levasseur, V. 2006. Nutritional and functional properties of Moringa leaves–From germplasm to plant, food, and health. Moringa leaves: Strategies, standards, and markets for a better impact on nutrition in Africa. Moringa News, 2: 1-9.

Yoon, J., Cao, X., Zhou, Q. and Ma, L.Q. 2006. Accumulation of Pb, Cu, and Zn in native plants growing on a contaminated Florida site. Sci. Total Environ., 368(2-3): 456-464.

Zou, Z., Qiu, R., Zhang, W., Dong, H., Zhao, Z., Zhang, T., Wei, X. and Cai, X. 2009. The study of operating variables in soil washing with EDTA. Environ. Pollut., 157(1): 229-236.

Zulfiqar, U., Farooq, M., Hussain, S., Maqsood, M., Hussain, M., Ishfaq, M., Ahmad, M. and Anjum, M.Z. 2019. Lead toxicity in plants: Impacts and remediation. J. Environ. Manage., 250: 109557.

## ORCID DETAILS OF THE AUTHORS

A. Rosyidah: https://orcid.org/0000-0003-2103-2741

M.W. Lestari: https://orcid.org/0000-0002-6456-9357

# Effect of Soil and Foliar Application of Humic Acid and Brassinolide on Morpho-physiological and Yield Parameters of Black Gram (*Vigna mungo*)

**More Kiran Narayan*** iD **, Anita Jaswal*†** iD **and Arshdeep Singh*** iD

*Department of Agronomy, School of Agriculture, Lovely Professional University, Phagwara 144 411, Punjab, India
†Corresponding author: Anita Jaswal; anita.27139@lpu.co.in

## ABSTRACT

During the Kharif season of 2022-2023 at Lovely Professional University, Jalandhar, Punjab, a field experiment was conducted to investigate the "Effect of soil and foliar application of humic acid and brassinolide on morpho-physiological and yield parameters of Black gram (*Vigna mungo*)." The experiment was designed using a Randomised Block Design (RBD) with three replications and eight treatments. Compared to the other treatments, RDF + humic acid 0.1% + brassinolide 0.1ppm (foliar application) was the optimal treatment for most morphological and yield parameters. Plant height (cm), number of primary branches per plant, number of secondary branches per plant, dry matter accumulation (g), chlorophyll Index (SPAD), and leaf area (cm$^2$) were highest under $T_7$- RDF + humic acid 0.1%+brassinolide 0.1ppm (foliar applied) conditions. Minimum phenological observations were recorded for soil and foliar applications of brassinolide, including days to first flowering, days to 50 percent flowering, and days to pod initiation. Number of pods /plant, pod length(cm), pod weight (g), no. of seeds /pod, test weight (g), seed yield (q/ha), stover yield (q/ha), and harvest index (%) were significantly influenced by the $T_7$ and recorded higher values. The increased seed yield may be attributable to plants treated with growth regulators remaining physiologically more active to accumulate sufficient food reserves for developing blossoms and seeds.

## INTRODUCTION

Pulses are commonly rich in protein, fiber, vitamins, and minerals and have been designated as the primary source of protein for humans. After cereals, it is the second most essential component of the Indian diet. By fixing atmospheric nitrogen, pulses enhance soil fertility. In India, pulses are cultivated on an area of approximately 28.83 million hectares, with an annual production of approximately 25.72 million tonnes and a productivity of approximately 892 kg/ha (Rajender et al. 2020). Cultivating black gram (*Vigna mungo*) is vital to Indian agriculture. Black gram has 2n=22 chromosomes and belongs to the Leguminaceae and Papilionaceae families. Black gram is a short-duration pulse crop with a yield of 32.84 lakh tonnes and a productivity of 652 kg/ha (Ministry of Agriculture and Farmer Welfare, India). In Punjab, black gram is grown on 2,000 hectares during the 2019-20 season, with a total production of 1,200 tonnes and an average crop yield of 5.78 quintals per hectare.

Crop yield depends on the soil's nutrient content to provide humans with essential nutrients. Several techniques, such as rotation planting, various plowing techniques, and applying fertilizers, can be used to increase the organic matter content of soils for crop production. In addition to

these methods, organic mineral fertilizers have increased in agriculture in recent years. Humic acid is one of the commonly used organic mineral fertilizers. Humic acid is one of the humic substances' primary components. The humic matter is produced through the chemical and biological humification of plant and animal matter and the biological activity of microorganisms. Both humic and fulvic acids play vital functions in soil fertility and plant nutrition (Lavanya et al. 2020, Patial et al. 2020). Humic compounds are composed of humic and fulvic acids. Humic acid (HA), a key component of most organic fertilizers and one of the most active soil and organic matter components, may be beneficial in overcoming these production limitations in pulse crops. Humic acid promotes plant development by enhancing oxygen absorption. Improved root growth leads to enhanced nutrient and water absorption. According to Sani (2014), foliar application of humic acid may reduce nitrogen administration to the soil. Humic acid stimulates plant growth and yield by increasing nutrient uptake and influencing various processes, including cellular respiration, photosynthesis, protein synthesis, and enzyme activity. Despite abundant flowering, the crop suffers from excessive vegetative growth, a low harvest index, and a low yield due primarily to inadequate pod setting (Badhe et al. 2021).

Flower and pod loss is common in this legume crop, as sink realization indicates. If these prospective yield barriers could be eliminated, yield enhancement and quality improvement of black gram could be accomplished. It has been known for a long time that pollen is rich in hormones and other growth substances; consequently, hormones play an essential role in plant reproduction. Numerous plant growth regulators have been shown to increase crop yields. Brassinolide, a newly discovered plant growth-promoting steroidal lactone isolated from rape pollen, exhibited distinct plant growth responses under various test conditions. Brassinolide (BR), a plant-based steroidal hormone derived from the pollen of the *Brassica napus* plant, is widely used in agriculture to increase crop yield. Although the significance of NPK in plant metabolism is well-documented, the role of BR on NPK content in plants and nutritional components of seeds is not. Brassinolide-induced plant growth has been correlated with increased metabolic activities such as photosynthesis, nucleic acid, and protein synthesis (Matwa et al. 2017). A growth-regulating substance is known to influence a wide variety of physiological parameters, including plant architecture modification, assimilate partitioning, photosynthesis promotion, nutrient uptake (mineral ions), nitrogen metabolism enhancement, flowering promotion, uniform pod formation, increased mobilization of assimilates to defined sinks, induction of synchrony in flowering and delayed senescence of leaves, and improved seed quality (Sharma et al. 2002). Therefore, examining the impact of brassinolide and humic acid on the development and yield of black gram was deemed beneficial.

## MATERIALS AND METHODS

### Preliminary Information

The field investigation was conducted at Lovely Professional University in Phagwara, India, during Kharif 2022. At 31.25°N75.7°E was the experimental location. It has a subtropical monsoon climate with an average annual precipitation of 600 millimeters and is situated in the central plains of Punjab. The experimental design consisted of a randomized block with eight treatments and three replications. The total number of plots was 24, with plot dimensions of 5 × 4 m and row-to-row and plant-to-plant distances of 30 cm and 10 centimeters, respectively. The natural soil type at the experimental site was sandy loam. The initial nutrient status of the soil was determined by analyzing the soil before the experiment. On August 15, 2022, the MASH-114 variety was planted. The treatments were: $T_0$-Control, $T_1$-(100% RDF), $T_2$-RDF + humic acid 20 kg.ha$^{-1}$ (soil-applied), $T_3$-RDF + humic acid 0.1% (foliar applied), $T_4$-RDF + brassinolide 0.25ppm (soil-applied), $T_5$-RDF +

brassinolide 0.1ppm (foliar applied), $T_6$- RDF + humic acid 20 kg.ha$^{-1}$ + brassinolide 0.25ppm (soil-applied), $T_7$-RDF + humic acid 0.1%+ brassinolide 0.1ppm (foliar applied). The recommended fertilizer ratio for black gram is 25:50:25 (N: $P_2O_5$: $K_2O$) (kg.ha$^{-1}$). Urea, SSP, and MOP were the sources of NPK in that order.

### Time and Method of Application

At 25 DAS and 15 days after the initial spray, humic acid was applied as soil and foliar, while Brassinolide was applied at 30 DAS and 45 DAS. The soil application of humic acid and brassinolide was carried out using the soil drench method with a knapsack sprayer, and the foliar application of humic acid and brassinolide was also carried out with a knapsack sprayer.

### Morpho-Physiological Attributes

Standard protocol was used to measure the different morphological and physiological observations, such as plant height, number of primary branches, number of secondary branches, fresh weight of the plant, dry weight of the plant, and leaf area. Five randomly chosen plants from each plot were used to measure the morphological attributes, and the average value was used to determine what the data meant concerning the treatments.

**Chlorophyll index:** The Soil Plant Analysis Development (SPAD) meter was used to determine the chlorophyll index by looking at the green leaves. The fully grown leaf was chosen to measure the amount of chlorophyll. Take the value from a single leaf with the SPAD meter three times, then take the average of these three numbers as the chlorophyll content (Arregui et al. 2006).

**Crop growth rate (CGR, g.m$^{-2}$.day):** CGR is the increase in dry weight of plant materials per unit area per unit time. It can be calculated by formulae given by Watson (1952).

**Relative growth rate (RGR, g.g$^{-1}$day$^{-1}$):** The RGR term was coined by Williams in 1946. It is the total growth in a plant's dry weight between two points in time. It can be written as one unit of dry weight per unit of dry weight per unit of time (g.g$^{-1}$.day$^{-1}$).

### Phenological Parameters

Days to first flowering, days to 50% flowering, and days to pod initiation were also recorded.

### Yield Attributes

Yield attributing traits, i.e., number of pods per plant, number of seeds per pod, pod length, pod weight, test weight, seed yield, straw yield, and harvest index (%), were recorded at the maturity stage using the standard procedures.

## Statistical Analysis

With the SPSS 22 version of the software, the generalized linear model under univariate techniques with two factors was used to determine the differences between the means. A mean separation method was used to find the best treatment with a probability of $p < 0.05$ and Duncan's multiple range test (DMRT). Fisher's LSD test was used as a posthoc test to see if there was a big difference between the means. The calculations were based on the LSD (least significant difference) at a 5% significance level.

## RESULTS AND DISCUSSION

### Growth Attributing Parameters

The results obtained from the above study in terms of growth studies are presented in Table 1.

**Plant height:** The highest plant height (62.78 cm) was recorded in RDF + humic acid 0.1%+ brassinolide 0.1ppm (foliar applied), followed by (59.40 cm) in $T_6$-RDF + humic acid 20 kg.ha$^{-1}$ + brassinolide 0.25 ppm (soil-applied). Minimum height (41.69 cm) was observed in $T_0$-control. This rise in plant height could have been caused by humic acid and the right amount of nutrients, which helped the plant absorb more nutrients and grow at the top. Brassinolide causes plants to grow taller because it makes plant cells grow longer and divide, boosts the activity of DNA polymerase and RNA polymerase, and speeds up the production of nucleic acids and proteins in legumes. It also helps symbiotic nitrogen fixation. Similar results have been reported by Netwal et al. (2022), Dixit and Elamathi (2007), and Umar et al. (2008).

**Number of primary and secondary branches per plant:** Maximum no. of primary branches (12.5) and secondary branches (43.33) recorded in $T_7$-RDF + humic acid 0.1%+ brassinolide 0.1ppm (foliar applied) which was at par with $T_6$- RDF + humic acid 20 kg.ha$^{-1}$ + brassinolide 0.25 ppm (soil-applied) with (11.3, 42.00) branches. Minimum no. of primary and secondary branches (7.4, 29.04) recorded in $T_0$-Control. The rise in the number of branches on plant$^{-1}$ may have been caused by humic acid, which sped up the plant's metabolic and physiological processes. This led to more growth from the main nutrients and, in the end, more branches. The results of this study agree with Tripura et al. (2016) and Padghan et al. (2018). These results match those of Netwal et al. (2022), who found that giving the Indian bean brassinolide at a concentration of 1.0 ppm greatly impacted the number of shoots on each plant. This could be because brassinosteroid speeds up the process of cell division and cell growth. Similar results were found by Bera et al. (2013), who said that the highest branches were found in crops that were sprayed twice with homo-brassinolide at the pre-flowering and pod growth stages.

**Chlorophyll Index (SPAD):** In the present investigation, it was observed that plant growth regulators and micronutrients had profound effects on chlorophyll content. Significant differences were noticed among the treatments with respect to mean total chlorophyll at all growth stages in black gram. There was significant variation recorded in the chlorophyll index. $T_7$-RDF + humic acid 0.1%+ brassinolide 0.1ppm (foliar applied) recorded the highest value (52 SPAD). The minimum chlorophyll index (24.56 SPAD) was recorded in $T_0$ - Control. When humic acid is given, the amount of chlorophyll in the plant increases because of increased oxygen consumption. It has been said that brassinolide may have made more assimilates available, which may have caused chlorophyll production to last longer. The results of the present investigation conform with the findings of Maity and Bera (2009) in green gram and Rao et al. (2016) in mung bean.

**Dry matter accumulation (g):** The plants' build-up of dry matter indicates how they use light to make food. When dry matter output goes up, nutrients are used better, and more solar energy is produced. The maximum dry matter accumulation (18.41g) was recorded in $T_7$- RDF + Humic acid 0.1%+ Brassinolide 0.1ppm (Foliar applied). The second highest dry matter accumulation (16.08 gm) was recorded in $T_6$- RDF + Humic acid 20 kg.ha$^{-1}$ + Brassinolide 0.25 ppm (soil-applied). Whereas the remaining treatments showed statistically significant variations among themselves. The minimum dry matter accumulation (8.86g) was recorded in $T_0$-Control. Boosted dry matter production might be attributed to soil and foliar nutrient delivery, which boosted the pace of the photosynthetic process, resulting in greater dry matter production by the plant at each stage of growth. Increased plant height, more trifoliate leaves, and a larger leaf area index because of foliar fertilizer administration may have increased dry matter accumulation per plant. Similar results were also recorded by Surender et al. (2013) in black gram, Sengupta & Tamang (2015) in green gram, and Marimuthu & Surendran (2015) in black gram.

**Leaf area (cm$^2$):** The highest leaf area (157.3 cm$^2$) was recorded in $T_7$- RDF + Humic acid 0.1%+ Brassinolide 0.1ppm (foliar applied) followed by $T_6$- RDF + Humic acid 20kg/ha + Brassinolide 0.25ppm (soil-applied) with (151.86 cm$^2$). The minimum leaf area (121.56 cm$^2$) was observed in $T_0$-Control. Results confirm the findings made by Maity and Bera (2009) in green gram and Surender et al. (2013) in black gram. The results align with Sani (2014), who observed that leaf area increased significantly by 1 ppm foliar spray of brassinolide over control in (*Vigna radiata*).

**CGR (gm$^2$.day$^{-1}$) and RGR (g.g$^{-1}$.day$^{-1}$):** The maximum

CGR (0.343 g.m$^{-2}$.day$^{-1}$) was recorded in T$_7$- RDF + Humic acid 0.1% + Brassinolide 0.1 ppm (foliar applied) followed by T$_6$- RDF + Humic acid 20 kg.ha$^{-1}$ + Brassinolide 0.25 ppm (soil-applied) with (0.253 g.m$^{-2}$.day$^{-1}$). The lowest CGR (0.113 g.m$^{-2}$.day$^{-1}$) was recorded in T$_4$-RDF + Brassinolide 0.25 ppm (Soil applied). The highest RGR (0.053 g.g$^{-1}$.day$^{-1}$) was recorded in T$_1$-100% RDF. The minimum RGR (0.018 g.g$^{-1}$.day$^{-1}$) was observed in T$_2$-RDF + Humic acid 20 kg.ha$^{-1}$ (Soil applied). Rajavel and Vincent (2009) and Sengupta and Tamang (2015) also reported that the foliar application of growth regulators and nutrients significantly increased the mean RGR in black gram.

**Phenological Parameters**

The results obtained from the above study regarding phenological parameters are presented in Fig. 1.

**Days to first flowering:** There was significant variation observed in days to first flowering. The first flowering (32 days) was observed in T$_7$- RDF + humic acid 0.1%+ brassinolide 0.1ppm (foliar applied). The maximum days required for first flowering (39 days) was observed in T$_0$-Control depicted in Fig. 1. This result conforms with the findings of Maity & Bera (2009) who reported that foliar application of BR (0.25 ppm) and SA (1000 ppm) on green gram plant once at pre-flowering (30 DAS) and second time at flowering stage (40 DAS) could be beneficial for improving the nutritional quality of green gram and thus hold promise for farmers.

**Days to 50% flowering and days to pod initiation (days):** Days to 50% flowering is the number of days required to initiate flowering, not less than 50% of plants. The 50% flowering (34 days) was first observed in T$_7$-RDF + humic acid 0.1%+ brassinolide 0.1ppm (foliar applied). The maximum number of days required for 50% flowering was (42 days) observed in T$_0$-Control. The pod initiation (45 days) was observed in RDF + humic acid 0.1%+ brassinolide 0.1ppm (foliar applied), which was at par with T$_6$- RDF + Humic acid 20 kg.ha$^{-1}$ + Brassinolide 0.25 ppm (Soil applied) with 46 days respectively. The maximum days required for pod initiation (55 days) were observed in T$_0$-Control. The results conform with Ananthi & Gomathy (2011), who reported that foliar application of 0.1% humic acid with 0.1 ppm brassinosteroid improved blooming days to 50% in green gram. Sumathi et al. (2018) reported that among different PGRs tested, the application of BR induces pollen tube growth and germination, which induces early flowering and fruit set, proving its worthiness in days to 50% blooming.

**Yield Attributing Parameters**

The results obtained from the above study regarding yield parameters are presented in Table 2.

**Number of pods/plants:** The highest no. of pods/plant (25.33) was recorded in T$_7$-RDF + Humic acid 0.1%+ Brassinolide 0.1ppm (Foliar applied). The minimum no. of pods/plant (12.84) was recorded in T$_0$-control. These findings could be attributable to humic acid, a rich supply of nitrogen and phosphorus for early-stage growth, increased blooming, and increased pod number. These results conform with the findings of Sritharan et al. (2015) and Jeyakumar et al. (2008) reported that among the treatments, brassinolide @ 0.1 ppm resulted in a greater number of pods per plant in black gram.
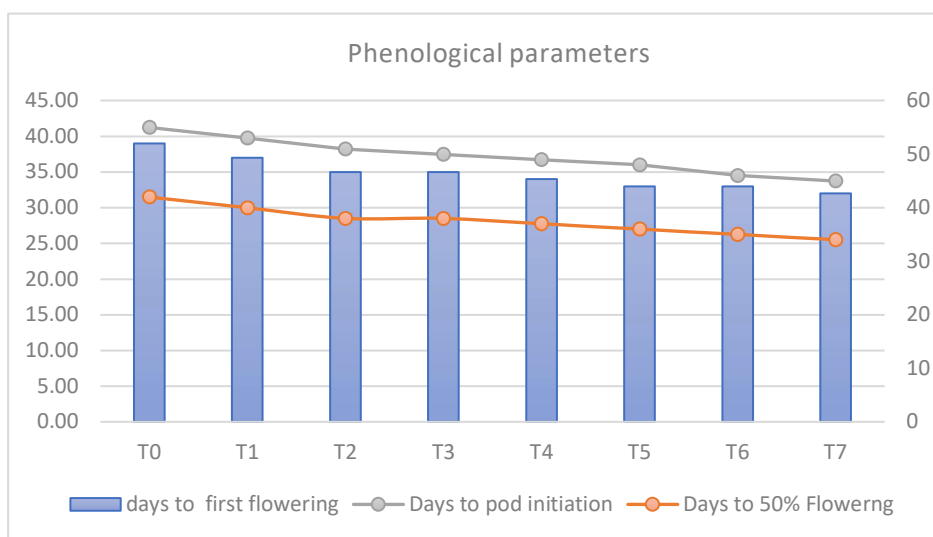


Fig. 1. Phenological response of black gram towards humic acid and brassinolide.

Table 1: Effect of humic acid and brassinolide on growth parameters of black gram.

| Treatments | Plant height [cm] | No. of primary branches per plant | No. of secondary branches per plant | Dry matter accumulation [g] | Chlorophyll Index (SPAD) | Leaf Area [cm$^2$] | CGR [gm$^2$.day$^{-1}$] | RGR [g.g$^{-1}$. day$^{-1}$] |
|---|---|---|---|---|---|---|---|---|
| T$_0$-Control | 41.69±0.92g | 7.40±0.44e | 29.04±0.41f | 8.86±0.36g | 24.56±0.73f | 121.56±0.87g | 0.182±0.028bc | 0.046±0.007a |
| T$_1$-(100%RDF) | 46.57±0.78f | 8.33±0.47de | 32.33±0.47e | 10.81±0.49f | 28.60±0.86e | 131.06±1.19f | 0.254±0.050ab | 0.053±0.010a |
| T$_2$-RDF + Humic acid 20 kg.ha$^{-1}$ (Soil applied) | 53.81±0.95d | 8.80±0.21cd | 35.33±0.47cd | 13.59±0.75de | 38.56±0.77d | 137.36±0.94e | 0.125±0.025c | 0.018±0.004b |
| T$_3$-RDF + Humic acid 0.1% (Foliar applied) | 54.97±0.26 cd | 9.40±0.57cd | 36.66±0.47c | 15.75± 0.74bc | 46.60±1.23c | 142.53±0.54d | 0.156±0.050bc | 0.019±0.006b |
| T$_4$-RDF + Brassinolide 0.25 ppm (Soil applied) | 51.73± 0.66e | 8.73±0.53cd | 34.33±1.25d | 12.83± 0.41e | 39.06±1.03d | 132.60±0.77f | 0.113±0.063c | 0.018±0.010b |
| T$_5$-RDF + Brassinolide 0.1 ppm (Foliar applied) | 56.57±0.84c | 9.83±0.84c | 38.95±0.07b | 14.56± 0.38cd | 49.79±1.23b | 145.20±0.77c | 0.160±0.029bc | 0.021±0.004b |
| T$_6$-RDF + Humic acid 20 kg.ha$^{-1}$ +Brassinolide 0.25 ppm (Soil applied) | 59.40±0.36b | 11.33±0.47b | 42.00± 1.41a | 16.08± 0.33b | 47.73±1.30bc | 151.86±0.33b | 0.253±0.028ab | 0.027±0.02b |
| T$_7$-RDF + Humic acid 0.1%+ Brassinolide 0.1 ppm (Foliar applied) | 62.78±0.35a | 12.50±0.46a | 43.33±1.25a | 18.41±0.45a | 52.66±1.19a | 157.30±0.65a | 0.343±0.048a | 0.031±0.006b |

*The mean followed by different letters was significantly different at p<0.05 according to DMRT (Duncan's multiple range test).

Table 2: Effect of humic acid and brassinolide on yield parameters of black gram.

| Treatments | No. of pods / plant | Pod length [cm] | Pod weight [g] | No. of seeds /pod | Test weight [g] | Seed Yield [q.ha$^{-1}$] | Stover yield [q.ha$^{-1}$] | Harvest index [%] |
|---|---|---|---|---|---|---|---|---|
| T$_0$-Control | 12.84±0.60f | 4.1±0.132e | 12.84±0.60f | 4.55±0.35e | 41.44±0.67f | 6.51±0.295e | 14.69±0.55d | 30.70±1.42a |
| T$_1$-(100%RDF) | 14.19±0.34e | 4.3±0.094e | 14.19±0.34e | 5.53±0.49d | 44.53±0.47e | 7.11±0.458d | 15.68±0.31c | 31.15±0.95a |
| T$_2$-RDF + Humic acid 20 kg.ha$^{-1}$ (Soil applied) | 19.17±0.36d | 4.8±0.085cd | 19.17±0.36d | 6.02±0.13cd | 48.03±0.62d | 8.13±0.132c | 19.17±0.54b | 29.78±0.84a |
| T$_3$-RDF + Humic acid 0.1% (Foliar applied) | 22.41±0.53c | 5.1±0.205bc | 22.41±0.53c | 7.19±0.08b | 51.27±0.65c | 8.44±0.151bc | 19.44±0.23b | 30.26±0.43a |
| T$_4$-RDF + Brassinolide 0.25 ppm (Soil applied) | 18.47±0.74d | 4.7±0.205d | 18.17±0.74d | 6.48±0.45c | 47.65±0.44d | 8.08±0.142c | 19.21±0.25b | 29.60±0.12a |
| T$_5$-RDF + Brassinolide 0.1 ppm (Foliar applied) | 23.44±0.19bc | 5.2±0.272bc | 23.44±0.19bc | 7.38±0.06b | 52.10±1.09c | 8.66±0.159bc | 19.47±0.24b | 30.63±0.43a |
| T$_6$-RDF + Humic acid 20 kg.ha$^{-1}$ +Brassinolide 0.25 ppm (Soil applied) | 24.43±0.54ab | 5.4±0.094ab | 24.43±0.54ab | 7.41±0.21b | 53.93±0.47b | 8.81±0.215ab | 20.34±0.15a | 30.23±0.42a |
| T$_7$-RDF + Humic acid 0.1%+ Brassinolide 0.1 ppm (Foliar applied) | 25.33±0.57a | 5.7±0.124a | 25.33±0.57a | 8.18±0.47a | 55.48±0.57a | 9.28±0.162a | 20.55±0.24a | 31.104±0.62a |

*The mean followed by different letters were significantly different at p<0.05 according to DMRT (Duncan's multiple range test).

The increased pods and seeds could be attributed to improved nutrition and assimilation transfer to reproductive areas.

**Pod length (cm) and pod weight (g):** Pod length is the main yield contributing character. There was a significant difference recorded in the case of pod length. Maximum pod length (5.7 cm) recorded in $T_7$-RDF + Humic acid 0.1%+ Brassinolide 0.1 ppm (foliar applied). Minimum pod length (4.80 cm) recorded in $T_0$-Control. The highest pod weight (27.2 gm) was recorded in $T_1$-RDF + humic acid 20 kg.ha$^{-1}$ (Soil applied). The lowest pod weight (14.5 gm) was recorded in $T_0$-Control. The increase in pod length and weight might be due to more translocation of nutrients from source to sink. These results conform with the findings of Sritharan et al. (2015)**.**

**Number of seeds/pods:** A significant variation was recorded in no. of seeds/pods. At the same time, all treatments showed superiority over control. The maximum (8.18 seeds/pod) recorded in $T_7$-RDF + Humic acid 0.1%+ Brassinolide 0.1 ppm (Foliar applied). The second highest (7.41 seeds/pod) was recorded in $T_6$- RDF + Humic acid 20 kg.ha$^{-1}$ + Brassinolide 0.25ppm (Soil applied). The minimum number of seeds/pod was recorded (4.55 seeds/pod) in $T_0$- Control. More seeds per pod may be linked to growth regulators since plants treated with growth regulators remained physiologically more active to build sufficient food reserves for growing blooms and seeds (Hamed & Abdullah 2022).

**Test weight (g):** The highest test weight (55.48 g) was recorded in $T_7$- RDF + humic acid 0.1%+ brassinolide 0.1 ppm (foliar applied). Followed by $T_6$- RDF + Humic acid 20 kg.ha$^{-1}$ + Brassinolide 0.25 ppm (soil-applied). The lowest test weight (41.44 gm) was recorded in $T_0$- Control. This might be due to the use of humic acid as soil and foliar spray, which boosted seed weight by improving nutrient mobilization (Jat et al. 2012)

**Seed yield and stover yield (q.ha$^{-1}$):** There was significant variation in the seed yield. All treatments showed superiority over control. The maximum seed yield (9.28 q.ha$^{-1}$) was recorded in $T_7$- RDF + humic acid 0.1%+ brassinolide 0.1ppm (foliar applied). The second maximum seed yield (8.81 q.ha$^{-1}$) was recorded in $T_6$- RDF + humic acid 20 kg.ha$^{-1}$ + brassinolide 0.25 ppm (soil-applied). Minimum seed yield (6.51 q.ha$^{-1}$) was recorded in $T_0$-Control. The highest stover yield (20.55 q.ha$^{-1}$) was recorded in $T_7$- RDF + humic acid 0.1%+ brassinolide 0.1ppm (foliar applied), which was statistically non-significant with $T_6$- RDF + humic acid 20 kg.ha$^{-1}$ + brassinolide 0.25 ppm (soil-applied). The minimum stover yield (14.69 q.ha$^{-1}$) was recorded in $T_0$-Control. This could be attributable to increased photosynthetic activity and rapid photosynthesis or nutrient transfer to the grain (Mishra 2016, Padghan et al. 2018)**.** Similarly, Hamed and Abdullah (2022) reported that plants sprayed with 1.5 mg.L$^{-1}$ concentration of brassinolide achieved the highest weight of total seed yield of sunflowers. There was non-significant variation recorded in the harvest index.

**Regression Analysis**

The impact of plant height (cm), number of pods per plant, and number of days to 50% flowering on black gram seed yield were predicted using quadratic response regression analysis, and the results showed that increasing these parameters significantly improved black gram seed yield, as shown in Figs. 2, 3, 4 with the $R^2$ value and polynomial equation. The final crop yield is the sum of the effects of growth qualities, and treatments that change favorable
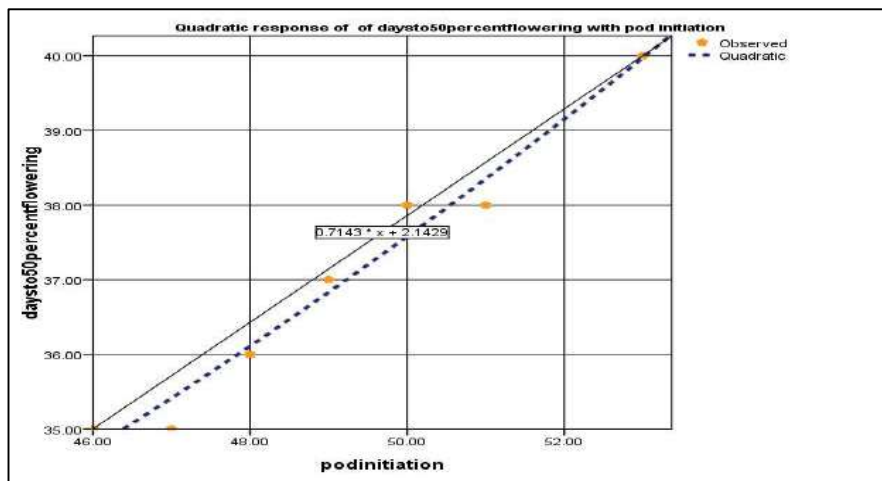


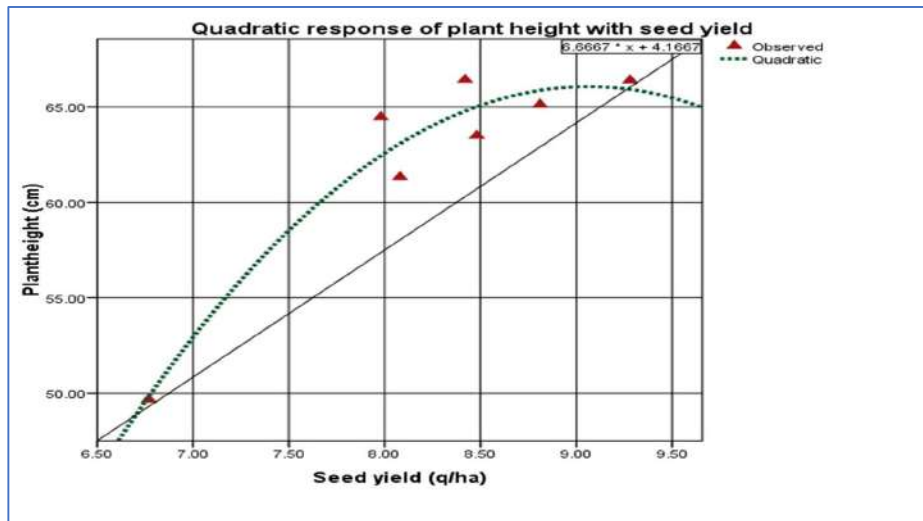Fig. 2: Regression analysis of pod initiation vs. days to 50% flowering.

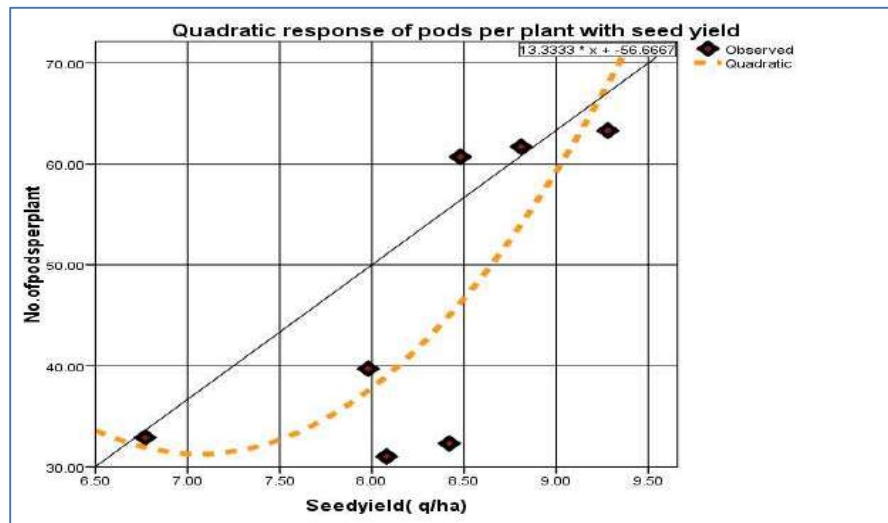Fig. 3: Regression analysis of plant height vs. seed yield.



Fig. 4: Regression analysis of No. of pods vs. seed yield.

parameters may result in a positive association with increased productivity, as demonstrated in the current study.

## CONCLUSION

The current study concluded that humic acid and brassinolide are key components in organic fertilizers and plant growth regulators. Applying humic acid and brassinolide improved black gram's overall crop performance and productivity in this study. Among the several treatments, foliar application of humic acid and brassinolide was the most effective. As a result, T7- RDF + Humic acid 0.1%+ Brassinolide 0.1 ppm (foliar applied) may be the best alternative for enhancing black gram productivity and quality.

## REFERENCES

Ananthi, K. and Gomathy, M. 2011. Effect of bio-regulators on the yield of green gram. International Journal of Forestry and Crop Improvement, 2(1): 12-15.

Arregui, L.M., Lasa, B., Lafarga, A., Irañeta, I., Baroja, E. and Quemada, M. 2006. Evaluation of chlorophyll meters as tools for N fertilization in winter wheat under humid Mediterranean conditions. Europ. J. Agron., 2)24):140-148. https://doi.org/10.1016/j.eja.2005.05.005

Badhe, N.P., Shende, P.V. and Wadhai, M.K. 2022. Physiological Response of Homobrassinolide on Growth and Yield Component of Black Gram (Vigna Mungo L.). Int, J. Agric. Animal Prod., 2(05): 16-25. https://doi.org/10.55529/ijaap.25.16.25

Bera, A.K., Pramanik, K. and Panda, D. 2013. Response of biofertilizers and homo-brassinolide on growth, relative water content and yield of lentil (Lens culinaris Medik). J. Crop Weed, 9(2): 84-90.

Dixit, P.M. and Elamathi, S. 2007. Effect of foliar application of DAP, micronutrients, and NAA on growth and yield of green gram (*Vigna radiata* L.). Legume Res. Int. J., 30(4): 305-307.

Hamed, M.A. and Abdullah, B.H. 2022. The Effect of Brassınolıde on the Yıeld Components, Seed and Oıl Yıelds of some Sunflower Cultıvars. J. Plant Prod., 6)13): 215-218. https://dx.doi.org/10.21608/jpp.2022.245281

Jat, G., Bagdi, D.L., Kakralya, B. L., Jat, M. L. and Shekhawat, P. S. 2012. Mitigation of salinity-induced effects using brassinolide in cluster bean (*Cyamopsis tetragonoloba* L.). Crop Res., 44(1&2): 45-50

Jeyakumar, P., Velu, G., Rajendran, C., Amutha, R., Savery, M. A. J. R. and Chidambaram, S. 2008. Varied responses of black gram (Vigna mungo) to certain foliar-applied chemicals and plant growth regulators. Legume Res. Int. J., 31(2): 105-109.

Lavanya, S. A., Vanniarajan, C. and Souframanien, J. 2022. Study of chlorophyll and macro mutations induced by physical mutagens in black gram [*Vigna mungo* (L.) hepper]. Legume Res. Int. J., 45(3): 311-314. http://dx.doi.org/10.18805/LR-4200

Maity, U. and Bera, A. K. 2009. Effect of exogenous application of brassinolide and salicylic acid on green gram's physiological and biochemical aspects (*Vigna radiata* L. Wilczek). Indian J. Agric. Res., 43(3): 194-199.

Marimuthu, S. and Surendran, U. 2015. Effect of nutrients and plant growth regulators on growth and yield of black gram in sandy loam soils of Cauvery new delta zone, India. Cogent Food & Agriculture, 1(1): 1010415. https://doi.org/10.1080/23311932.2015.1010415

Matwa, D., Rao, K.P., Dhewa, J.S. and Rajveer, R. 2017. Effect of plant growth regulators (PGRs) and micronutrients on flowering and yield parameters of green gram (*Vigna radiata* L.). Int. J. Curr. Microbiol. App. Sci, 6(4): 2350-2356.

Mishra, B.P. 2016. Effects of nitrogen and growth regulators on yield Phaseolus mungo L. Int. J. Adv. Res. Dev., 1: 39-42

Netwal, M., Choudhary, M. R., Jakhar, R. K., Garhwal, O. P. and Choudhary, G. 2022. Growth attributes of Indian bean (*Lablab purpureus* L. var. *typicus*) as influenced by bio-regulators and plant growth-promoting bacteria. TPI Int. J., 11(1): 227

Padghan, G.A., Deotale, R.D., Jayde, V.S., Mohurle, N.A. and Meshram, S.D. 2018. Responses of humic acid and NAA on morpho-physiological and yield attributes of pigeon pea. J. Soils Crops, 28(1):, 108-114.

Patial, R., Mittal, R.K., Sood, V. K. and Ahmed, S. 2022. Studies on combining ability for seed yield and its related traits in blackgram [*Vigna mungo* (L.) hepper]. Legume Res. Int. J., 45(3): 292-298. http://dx.doi.org/10.18805/LR-4187

Rajavel, M. and Vincent, S. 2009. Influence of nutrients and hormones on yield maximization of black gram. J. Ecobiol., 4)24): 387-394.

Rajender, B., Tiwari, A. K. and Chaturvedi, S. K. 2021. Pulses revolution in India through rice-fallows management. Scaling-up Solutions for farmers. Technol. Partner. Converg., 16: 229.

Rao, D.S.N., Naidu, T.C.M. and Rani, Y.A. 2016. Effect of foliar nutrition on physiological and biochemical parameters of mung bean (*Vigna mungo* (l.) Hepper) under irrigated conditions. Int. J. Res, Appl. Nat. Social Sci., 10(4): 101-104.

Sani, B. 2014. Foliar application of humic acid on plant height in canola. APCBEE Proced., 8: 82-86. https://doi.org/10.1016/j.apcbee.2014.03.005

Sengupta, K. and Tamang, D. 2015. Response of green gram to foliar application of nutrients and brassinolide. J. Crop Weed, 1)11): 43-45.

Sharma, P., Sardana, V. and Sukhvinder Singh, K. 2013. Dry matter partitioning and source-sink relationship as influenced by foliar sprays in groundnut. Bioscan, 8(4): 1171-1176.

Sritharan, N., Rajavel, M. and Senthilkumar, R. 2015. Physiological approaches: Yield improvement in black gram. Legume Res. Int. J., 38(1): 91-95. http://dx.doi.org/10.5958/0976-0571.2015.00015.6

Sumathi, A., Prasad, V. and Vanangamudi, M. 2018. Influence of plant growth regulators on yield and yield components in pigeon pea. Legume Res. Int. J., 41(3): 392-398. http://dx.doi.org/10.18805/lr.v40i04.9010

Surendar, K.K., Vincent, S., Wanagamundi, M. and Vijayaraghavan, H. 2013. Physiological effects of nitrogen and growth regulators on crop growth attributes and yield of black gram (*Vigna mungo* L.). Bull. Env. Pharmacol. Life Sci., 2(4): 70-76.

Watson, D.J. 1952. The physiological basis of variation in yield. Adv. Agron., 4: 101-145.

## ORCID DETAILS OF THE AUTHORS

More Kiran Narayan: https://orcid.org/0009-0006-9742-8565
Anita Jaswal: https://orcid.org/0000-0002-7214-8747
Arshdeep Singh: https://orcid.org/0000-0001-8199-3494

Original Research Paper

Open Access Journal

# Wastewater Treatment Technologies Selection Using Analytical Hierarchy Process and VIKOR Methods: A Case Study

**Gnanasekaran Sasikumar*†, A. Sivasangari** and S. Ravibabu***

* Department of Mechanical Engineering, GMR Institute of Technology, Rajam, Srikakulam District, 532 127, Andra Pradesh, India

**Department of Electronics and Communication Engineering, GMR Institute of Technology, Vizianagaram, Andhra Pradesh, India

†Corresponding author: Gnanasekaran Sasikumar; sasikumar.g@gmrit.edu.in

## ABSTRACT

Due to the ever-increasing water scarcity problem across the globe, the treatment of wastewater is an important public health and socio-economic issue. Treating wastewater through proper technology is vital to protect the ecosystem from unsafe and contaminated matter available in wastewater. Identification of suitable wastewater treatment technologies is a complex Multi-Criteria Decision Making (MCDM) problem since it includes many conflicting assessment criteria. The objective of the paper is to construct an integrated model using the Analytical Hierarchy Process (AHP) and VIseKriterijumska Optimizacija I Kompromisno Resenje (VIKOR) for evaluating wastewater treatment technologies (WWTTs). AHP is applied to calculate criteria weights, and the VIKOR method is applied to prioritize and select the best WWTTs. The proposed model is applied to selecting the best WWTT among four alternatives and seven criteria. It is found that the proposed model yields better results when compared with other MCDM solutions.

## INTRODUCTION

Water treatment plants are constructed for efficient treatment of harmful and toxic elements found in wastewater to protect humans and the ecosystem. These plants are designed to process the wastewater to ensure the purification of water and its discharge to the environment. Due to the constant increase in the number of industries and people moving to cities, water contamination is becoming worse by the discharge of poisonous elements into water bodies. Additionally, growth in domestic and industrial activities increased the amount of wastewater that will be discharged to sewage systems. Hence, wastewater treatment is necessary to increase the availability of water.

AHP and Grey Relational Analysis methods were developed to compute criteria weights based on and rank the wastewater treatment technologies (Sasikumar et al. 2022). A combined AHP and ANP model is developed to evaluate WWTT performance (Bottero et al. 2011). Green and sustainable wastewater technologies are introduced by the investigators for wastewater treatment (Paruch et al. 2019). The discharge of heavy metals from industrial effluents of processing industries into the atmosphere has increased notably (Francis Xavier et al. 2022). The membrane and biological treatment methods are evaluated based on the removal of organic matter (Gutu et al. 2021). The implementation of natural coagulants to remove pharmaceutical products from water sources is discussed (Alazaiza et al. 2022). The AHP method is integrated with VIKOR to evaluate the performance of solar panels and rank them as per the performance score (Sasikumar et al. 2022, Sasikumar & Sivasangari 2022).

Many solutions for Agricultural recycling of water were suggested (Hidalgo et al. 2007). The fuzzy TOPSIS model is developed to evaluate wastewater treatment sites (Kim et al. 2013). Ranade and Bhandari (2014) proposed an industrial wastewater treatment by ELECTRE model. A fuzzy AHP model is recommended to rank optimal wastewater treatment and validated by empirical study (Ouyang et al. 2015). The application of DSS to choose proper wastewater treatment technology was described (Yahya et al. 2020). The AHP method was applied to choose the best Sewage Treatment Technology using thirteen selection criteria (Chaisar & Garg 2022). A model based on AHP and ANP is considered to prioritize the various technologies of wastewater treatment (Marta et al. 2011). An integrated decision-making approach by linear diophantine fuzzy sets is developed to decide on the best treatment technique (Samayan et al. 2022). A model

based on the Choosing-by-advantages method is proposed to prioritize WWTTs and compare the results with AHP (Arroyo & Molinos-Senante 2018).

This paper is aimed to assess WWTTs to find out the most suitable one. WWTT selection problem contains many contradictory criteria, including ambiguity and fuzziness. This paper deals with the development of the AHP-VIKOR approach to identify the best WWTT choice.

## COMBINED AHP-VIKOR MODEL FOR WASTEWATER TREATMENT TECHNOLOGIES (WWTTS) SELECTION

The selection of suitable WWTTs is an MCDM problem that can be selected by the VIKOR method. Firstly, the criteria AHP estimates weights, and VIKOR is applied to analyze and evaluate the WWTT options. Fig. 1 shows the WWTT selection by the proposed method:

## APPLICATION OF AHP TO ESTIMATE CRITERIA WEIGHTS

The AHP is an MCDM technique that works on the Eigenvalue approach. It includes the standardization of numeric scales for measuring quantitative and qualitative performances. The scale covers the entire range of the comparison. The AHP offers a simple and ideally effective multi-criteria method to assess alternatives in a structured way considering contradictory multi-criteria involved in the selection.
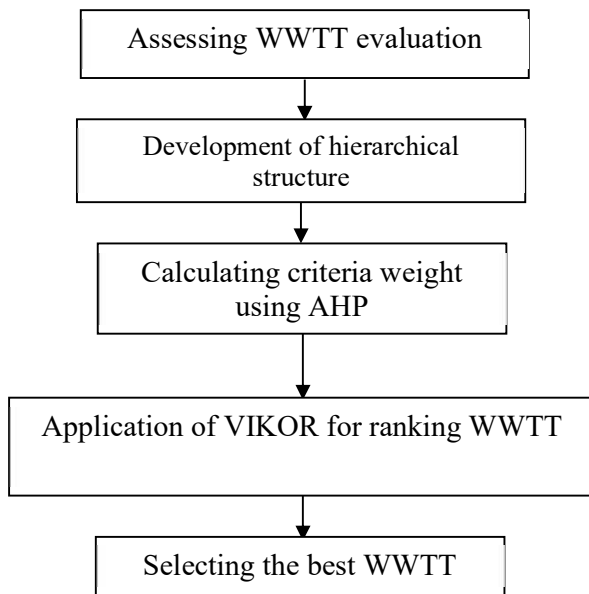


Fig. 1: Steps to be adopted for selection of best WWTT by VIKOR method.

This AHP model starts with the calculation of criteria weights that have the following phases:

Phase-1: Defining assessing criteria for selecting WWTTs

Phase 2: Determining an ordered structure by solving WWTT selection into an order of organized decision domains

Phase-3: Determining the pairwise comparison matrix $A_P$ using the following procedure:

All evaluators build a pairwise comparison of elements and assign comparative scores. $C_1$, $C_2$, ..., $C_n$ Indicates criteria, while $a_{ij}$ denotes a calculated decision on a set of criteria $C_i$ and $C_j$. The relative importance of two factors is evaluated by a scale as shown in Table 1 (Saaty 2000) and shown as matrix $A_P$ as presented in equation 1:

$$A_P = [a_{ij}] = \begin{array}{c} \\ C_1 \\ C_2 \\ \vdots \\ C_n \end{array} \begin{array}{cccc} C_1 & C_2 & \cdots & C_n \\ \left[ \begin{array}{cccc} 1 & a_{12} & \cdots & a_{1n} \\ 1/a_{12} & 1 & \cdots & a_{2n} \\ \vdots & \vdots & \ddots & \vdots \\ 1/a_{1n} & 1/a_{2n} & \cdots & 1 \end{array} \right] \end{array} \ldots(1)$$

Where $a_{ij}$ is equal to one and $a_{ij}$ is the reciprocal of $a_{ij}$.

Phase-4: Calculating the weight of pairwise comparison matrix by additive normalization technique for arriving priority vector $w$. It is calculated by dividing all column elements of $A$ by the total of columns, later summing up the elements of all resulting rows, and lastly dividing the value by a number of rows.

Phase-5: Checking the consistency of the comparison matrix by equations 2 and 3.

Saaty (1980, 2008) has used consistency index (CI) and Eigenvalue ($\lambda_{max}$) to compute the consistency ratio (CR), which is presented below:

$$\text{Consistency index} = (\lambda_{max} - m)/(m-1) \qquad \ldots(2)$$

Consistency ratio= Consistency index/Random index …(3)

Where m represents matrix size, the random index is chosen from Table 1. The CR is suitable if it is not more than 0.10. It becomes inconsistent if CR is greater than 0.10. In order to get consistency, judgments will be examined continuously Saaty (1980).

Phase-6: Aggregating the comparative scores by Geometric mean method.

## VIKOR METHOD

The VIKOR method was established by Opricovic & Tzeng

Table 1: Random Index values.

| Matrix dimension | 1 | 2 | 3 | 4 | 5 | 6 | 7 | 8 | 9 | 10 |
|---|---|---|---|---|---|---|---|---|---|---|
| Random consistency | 0 | 0 | 0.6 | 0.9 | 1.1 | 1.2 | 1.3 | 1.4 | 1.45 | 1.5 |

(2004 & 2007) to resolve MCDM problems with ambiguous and disproportionate criteria. It assumes that compromise is tolerable for resolving conflict, a solution that is closest to the ideal. In the VIKOR approach, alternative ranking is obtained based on the regret value of each alternative, which has inconsistent criteria. VIKOR method focuses on resolving a possible solution nearest to the ideal solution. VIKOR provides a maximum group utility of the majority and a minimum of the individual regret of the opponent. VIKOR method is applied in Design and manufacturing management, Business and marketing management, Environmental resources and energy management, Supply chain management, Construction management, and risk management. The ranking is done based on the criteria weights obtained by AHP, and the VIKOR method is used for discrete choice issues with conflicting standards by trade-off positioning strategy based on distinguishing the quantity of closeness with best choices.

The computational steps in VIKOR are stated as follows:

**Stage-1:**
Compute the best and worst ($f_i^+$ & $f_i^-$) scores of criterion functions, i = 1,2,...,n; $f_i^+$ = max $(f_{ij})$, $f_i^-$ = min $(f_{ij})$, j=1,2...,j). If i$^{th}$ function is beneficial, then $f_i^+$ = max $(f_{ij})$ and $f_i^-$ = min $(f_{ij})$, j=1,2...,j) . If i$^{th}$ function is cost, then $f_i^+$ = min $(f_{ij})$ and $f_i^-$ = max $(f_{ij})$.

**Stage-2:**
Calculation of $S_j$ and $R_j$, j=1,2,...,j, using Equations 4 and 5:

$$S_j = \sum_{i=1}^{n} w_i(f_i^+ - f_{ij})/(f_i^+ - f_i^-) \qquad …(4)$$

$$R_j = \max \left[ w_i(f_i^+ - f_{ij})/(f_i^+ - f_i^-) \right] \qquad …(5)$$

where $w_i$ Indicates criteria weights.

**Stage-3:** Estimation of $Q_j$ by equation 6:

$$Q_j = \left[ v \frac{(S_j - S^*)}{(S^- - S^*)} \right] + \left[ (1 - v) \frac{(R_j - R^*)}{(R^- - R^*)} \right] \qquad …(6)$$

where $S^*$ = min $(S_j)$, $S^-$ = max $(S_j)$, j=1,...,j), $R^*$ = min $(R_j)$, $R^-$ = max $(R_j)$, j=1,...,j),.; and k and (1-k) represent the weight of maximum group utility and individual regret, respectively. k varies from 0 to 1.

**Stage-4:** Grading the options by classification of S, R, and Q from smallest value.

**Stage-5:** Proposing a compromise solution the alternative A1, which is the best ranked by the measure Q (minimum) on satisfactory fulfillment of the below condition:

C1. "Acceptable Advantage": Q (A2) − Q (A1) ≥ 1/(N-1), A2 is the alternative with second position by Q;

C2. "Acceptable Stability in decision making": The alternative A1 should also be the greatest ranked by S or/ and R. This compromise solution is found to be good for the MCDM problem.  (Opricovic & Tzeng 2004, 2007).

## CASE STUDY

The integrated AHP and VIKOR methods deal with the implementation of the AHP method to get the criteria weights by different evaluators, followed by the application of the VIKOR method to evaluate and compare the performance of four wastewater treatment technologies and seven parameters, namely manpower requirement, Durability, Aesthetics, Power consumption, Removal Efficiency,
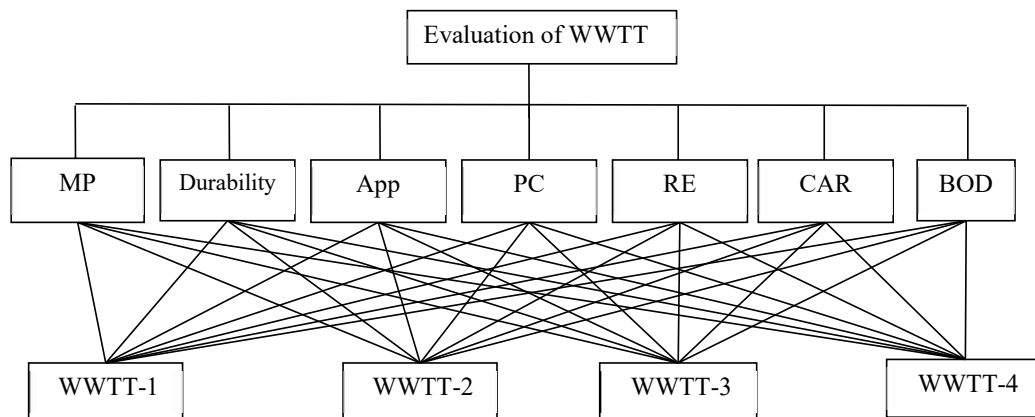


Fig. 2: Combined AHP-VIKOR model for WWTT selection.
MPR-Manpower requirement, D-Durability, App-Aesthetics, PC- Power consumption, RE-Removal Efficiency, CAR- Construction area requirement and BOD- Biochemical Oxygen Demand

Table 2: Salty's 9- Point Scale.

| Amount of comparative importance | Description of importance |
|---|---|
| 1 | Identical |
| 3 | Low |
| 5 | High |
| 7 | Very high |
| 9 | Absolute |
| 2,4,6,8 | Intermediate values |

Construction area requirement, and Biochemical Oxygen Demand.

Fig. 2 depicts the proposed AHP-VIKOR model for WWTTs selection.

### Applying AHP for Calculating Criteria Weights

The AHP is started by interviewing the decision makers and taking their inputs for pairwise comparison. To simplify the evaluation process, a program is written in EXCEL to compute the weights. The judgment matrix size is 7×7, and its consistency ratio is computed as 0.07,

which is less than 0.1, which shows the consistency of the judgment matrix. The AHP is applied to find out the criteria weight. Table 2 shows Saaty's 9-point scale (Saaty 2000).

The criteria weights are estimated by the method explained in this section, and the details are given in Table 3.

As shown in Table 3, it is evident that BOD has higher importance than other criteria in WWTTs ranking. The data on four alternative WWTTs with respect to eight criteria are collected and shown in Table 4.

### Application of the VIKOR Method

**Step 1:** Computation of best $f_i^+$ and worst $f_i^-$ values of all criterion functions, i = 1,2,...,n; $f_i^+$ = max $(f_{ij}$, j=1,...,J), $f_i^-$ = min $(f_{ij}$, j=1,...,J). Among the seven criteria for WWTT selection, Durability, manpower, Aesthetics, Removal Efficiency, and BOD are considered beneficial criteria that higher values are assigned. Power consumption and CAR are non-beneficial criteria, and lesser values are assigned, as depicted in Table 5.

Table 3: Criterion weights for WWTTs selection.

| Criteria | MPR | Durability | APP | Power consumption | Removal Efficiency | CAR | BOD |
|---|---|---|---|---|---|---|---|
| Weight | 0.13 | 0.16 | 0.05 | 0.14 | 0.22 | 0.04 | 0.26 |

Table 4: Alternatives and criteria for WWTTs.

| WWTT | MPR | Durability | APP | Power consumption | Removal Efficiency | CAR | BOD |
|---|---|---|---|---|---|---|---|
| AS | 2 | 5 | 5 | 3 | 87 | 0.4 | 88 |
| WSPs | 5 | 3 | 3 | 4 | 83 | 0.46 | 86 |
| CWs | 1 | 2 | 4 | 5 | 91 | 0.5 | 83 |
| MBR | 4 | 1 | 5 | 3 | 82 | 1.4 | 81 |

Table 5: Best $f_i^+$ and the worst $f_i^-$ values.

| Parameter | MPR | Durability | APP | Power consumption | Removal Efficiency | CAR | BOD |
|---|---|---|---|---|---|---|---|
| $f_i^+$ | 45 | 220 | 5 | 3 | 90 | 0.3 | 90 |
| $f_i^-$ | 0.8 | 20 | 4 | 4 | 80 | 1.2 | 80 |

Table 6: Values of $S_j$ and $R_j$.

| WWTT | 1 | 2 | 3 | 4 | 5 |
|---|---|---|---|---|---|
| $S_j$ | 0.695 | 0.292 | 0.789 | 0.105 | 0.389 |
| $R_j$ | 0.270 | 0.156 | 0.186 | 0.075 | 0.171 |

Table 7: Values of $Q_j$ for different k values.

| k | WWTT1 | WWTT2 | WWTT3 | WWTT4 |
|---|---|---|---|---|
| 0 | 0 | 0.0716 | 0.3368 | 1 |
| 0.2 | 0 | 0.2212 | 0.3513 | 1 |
| 0.4 | 0 | 0.3708 | 0.3656 | 1 |
| 0.6 | 0 | 0.5204 | 0.3800 | 1 |
| 0.8 | 0 | 0.6700 | 0.3945 | 1 |
| 1 | 0 | 0.8196 | 0.4089 | 1 |

**Step 2:** Calculation of $S_j$ and $R_j$, j=1,2,...,J, using equations 4 and 5 (Table 6).

**Step 3:** Computation of $Q_j$ for various k values

The values of $Q_j$ for k=(0 to 1) are computed by equation 6, and Table 7 shows the $Q_j$ values.

**Step 4:** Rank the WWTTs by arranging S, R, and Q from the minimum value

"Acceptable Advantage": Q (A2) – Q (A1) ≥ 1/ (N-1), A2 is the alternative with second position in the ranking list by Q

Ranking the WWTTs by the proposed AHP-VIKOR method, Q (S3) – Q (S1) = 0.3656-0 = 0.3656 ≥ 1/ (4-1) = 0.3656 ≥ 0.33   (here, N=4)

The WWTT 4 is best ranked by Q, and conditions C1 and C2 are satisfied as this alternative is also best ranked by S and R and Q (S3) – Q (S1) ≥ 1/(N-1).

The final ranking of WWTTs is WWTT1> WWTT3> WWTT2> WWTT4.

The final ranking of WWTTs is shown in Table 7 for the corresponding $Q_j$ And k (k varies from 0 to 1). WWTTs 1 and 3 are better than other WWTTs (2 and 4). With subsequent consideration of other criteria, it is concluded that WWTT1 is evaluated better than the other three WWTTs.

## CONCLUSION

The selection of wastewater treatment technology includes both subjective and objective criteria, which makes the problem a complex MCDM problem. Choosing the suitable wastewater treatment technology is a key factor for optimizing the wastewater treatment process by the following factors:

- A number of criteria
- Contradictory criteria
- Availability of various alternatives

The AHP-VIKOR model is developed for the selection of WWTTs by computing criteria weights using the AHP method and ranking of WWTTs by the VIKOR method. The criteria considered in the model are Workforce requirement, Durability, Aesthetics, Power consumption, Removal Efficiency, Construction area requirement, and Biochemical Oxygen Demand.

Based on the case study, it is found that BOD has more weight vector and has more importance than other criteria. It is observed that WWTT 1 is preferred over the remaining WWTTs.

The proposed model has the following features for WWTT selection:

(i) The model computes the weights of the criteria efficiently.

(ii) Subjective evaluation of intangible sub-criteria is removed.

(iii) The model considers the comparative value of the criteria

(iv) The VIKOR gives better results than other MCDM methods

The results of the AHP-VIKOR method shall be compared with the results of other methods in terms of the calculation of the weights and their utilization for selection and ranking. In addition to WWTTs, the AHP-VIKOR method is suitable for other MCDM problems. To simplify the calculation procedure of the AHP-VIKOR model and obtain faster results, a decision support system can be developed.

## REFERENCES

Alazaiza, M., Albahnasawi, A., Ali, G., Bashir, M., Nassani, D., Al Maskari, T., Amr, S. and Abujazar, M. 2022. Application of natural coagulants for pharmaceutical removal from water and wastewater: A review. Water, 14: 140.

Arroyo, P. and Molinos-Senante, M. 2018. Selecting appropriate wastewater treatment technologies using a choosing-by-advantages approach. Sci. Total Environ., 625: 819-827.

Bottero, M., Comino, E. and Riggio, V. 2011. Application of the analytic hierarchy process and the analytic network process for the assessment of different wastewater treatment systems. Environ. Modell. Softw., 26(10): 1211-1224.

Chaisar, M. and Garg, S.K. 2022. Selection of sewage treatment technology using analytic hierarchy process. Mater. Today Proc., 56(6): 3433-3440.

Francis Xavier, L., Money, B.K., John, A. and Rohit, B. 2022. Removal of cadmium heavy metal ion using recycled black toner powder. Mater. Today Proc., 59(1): 649-654.

Gutu, L., Basitere, M., Harding, T., Ikumi, D., Njoya, M. and Gaszynski, C. 2021. Multi-integrated systems for treatment of abattoir wastewater: A review. Water, 13: 2462.

Hidalgo, D., Irusta, R, Martinez, L., Fatta, P. and Papadopoulos, A. 2007. Development of a multi-function software decision support tool for the promotion of the safe reuse of treated urban wastewater. Desalination, 215(1): 90-103.

Kim, Y., Chung, E.S., Jun, S.M. and Kim, S.U. 2013. Prioritizing the best sites for treated wastewater instream use in an urban watershed using fuzzy TOPSIS. Resour. Conserv. Recycl., 73(1): 23-32.

Marta, B., Comino, E. and Riggio, V. 2011. Application of the analytic hierarchy process and the analytic network process for the assessment of different wastewater treatment systems. Environ. Modell. Softw., 26(10): 1211-1224.

Opricovic, S. and Tzeng, G.H. 2004. The compromise solution by MCDM methods: a comparative analysis of VIKOR and TOPSIS. Eur. J. Oper. Res., 156(2): 445-455.

Opricovic, S. and Tzeng, G.H. 2007. Extended VIKOR method in comparison with outranking methods. Eur. J. Oper. Res., 178(2): 514-529.

Ouyang, X., Guo, F., Shan, D., Yu, H. and Wang, J. 2015. Development of the integrated fuzzy analytical hierarchy process with multidimensional scaling in the selection of natural wastewater treatment alternatives. Ecol. Eng., 74: 438-447.

Paruch, A.M., Mæhlum, T., Eltun, R., Tapu, E. and Spinu, O. 2019. Green wastewater treatment technology for agritourism business in Romania. Ecol. Eng., 138: 133-137.

Ranade, V.V. and Bhandari, V.M. 2014. Industrial Wastewater Treatment, Recycling and Reuse. Elsevier, Oxford, United Kingdom, pp.1-80.

Saaty, T.L. 1980. The Analytic Hierarchy Process, McGraw-Hill, New York.

Saaty, T.L. 2000. Fundamentals of Decision Making and Priority Theory with AHP. RWS Publications, Pitsburg.

Saaty, T.L. 2008. Decision-making with the analytic hierarchy process. Int. J. Serv. Sci., 1(1): 83-98.

Samayan, N., Brainy, J.V., Sulaiman, R., Ferrara, M., Ahmadian, A. and Kang, D. 2022. An integrated decision-making approach for selecting a sustainable wastewater treatment technology. Chemosphere, 301: 134568.

Sasikumar, G. and Sivasangari, A. 2022. Multi-criteria decision-making for solar panel selection using an integrated analytical hierarchy process and VIKOR approach: a case study. Int. J. Bus. Inform. Sys., 40(2): 285-298.

Sasikumar, G., Sudhakar, U., Jodhi, C., and Sivasangari, A. 2022. Evaluation of wastewater treatment technologies by combined analytical hierarchy process and grey relational analysis, Glob. NEST J., 24(4): 607-612.

Yahya, M.N., Gökçekuş, H., Ozsahin, D.U. and Uzun, B. 2020. Evaluation of wastewater treatment technologies using TOPSIS. Desal. Water Treat., 177: 416-422.

# Fuzzy Indicators of the Forecast of Environmental Safety Taking into Account the Impact of Natural and Technosphere Factors

**Alexey Gordienko\*, Eduard Tshovrebov\*, Boris Boravskiy\*\* and Filyuz Niyazgulov\*\*\*†**

\*Federal State Budgetary Establishment, All-Russian Scientific Research Institute for Civil Defence and Emergencies of the EMERCOM of Russia (Federal Science and High Technology Center), Moscow, 121352, Russia
\*\*Innovative Environmental Fund LLC (INECO LLC), Moscow, 105066, Russia
\*\*\*Russian University of Transport (RUT MIIT), Moscow, 127994, Russia
†Corresponding author: Filyuz Niyazgulov; filyuz1989@yandex.ru

## ABSTRACT

The emergence and uncontrolled development of environmental hazards in the processes of life in the absence of appropriate response measures in many cases leads to the emergence of man-made emergencies with dangerous consequences for public health and the environment. It is proposed to evaluate the results of complex monitoring and forecasting of these dangerous processes in a new format of creating a fuzzy scale of indicators of the level of environmental safety of life support of territories based on the theory of fuzzy sets. The study aims to develop a fuzzy scale of indicators for predicting the state of environmental protection. Protection of the population and territories from environmental threats and possible man-made emergencies. Within the framework of the purpose of the study, a fuzzy scale of threshold levels of environmental safety of territories and economic objects has been developed based on the theory of fuzzy sets and the mathematical apparatus of soft computing. The practical significance of the developments is confirmed by the successful application of the proposed scale of indicators and indicators in assessing the environmental hazard of life support systems of settlements and industrial enterprises affecting the environment.

## INTRODUCTION

The analysis of information on emergencies (emergencies) with dangerous environmental consequences has shown that natural disasters, as well as dangerous technogenic processes and accidents, are the main causes of emergencies and pose a significant threat to the environmental safety of the world community, the population, socio-economic development (Oltyan et al. 2020). In this regard, achieving Sustainable Development Goals determines the relevance of scientific and methodological tasks to substantiate mechanisms for improving the forecasting of environmental threats and emergencies for timely prevention. The most important task is the development of effective environmental safety systems that ensure the protection of the natural environment, population, and territories from the negative impact of technosphere objects, the main ones being toxic waste, emissions, and discharges into the natural environment (Tshovrebov et al. 2018a).

As a positive example of preventing environmentally hazardous situations associated with the formation and placement of life results in solid toxic waste, the experience of the Southeast Asian countries should be highlighted. For a long time, such waste has served as a dangerous socio-ecological problem for the environment and the health of the population of these countries (Liu et al. 2000, Bredel 1995).

To gradually solve the current urgent problem, in 2010, the States of the Pacific zone (China, Indonesia, and Australia) created the Asian Coal Ash Association (Asian Coal Ash Association), which was then joined by other countries. As a result, through joint efforts, a well-structured strategy, an effective legal framework, and management models for achieving the task were formed. The legislation of India and other countries provides for a dynamically changing value, depending on economic conditions, for the mandatory use of fuel slag as the main material for the construction of embankments, in road works, the production of wall materials, block structures at facilities located within a radius of 25-100 km from thermal power plants and CHP. A similar legal norm regulates the use of waste in other areas. As a result of environmentally and economically justified actions over the past decade in India, China, and

the countries of Southeast Asia, the level of ash and slag processing from the total volume of such waste generation has reached over 75-80%.

In 2014-2019 India successfully implemented a nationwide program to clean the country of garbage, "Swah Bharat", to popularize a resource-saving and environmentally friendly lifestyle. In Panaji and Alappuzha, facilities have been liquidated, and the territories of former waste disposal have been recultivated. Effective implementation of systems for the selective collection of municipal waste is underway, considering that their composition contains over 60% organic matter. New and innovative biocomposting technologies are being introduced as part of this initiative. Similar decisions are being made in the world regarding the disposal and recycling of waste from electronic and household equipment (Baldé et al. 2017, Zeng et al. 2018), solid municipal and construction waste (Sereda & Kostarev 2021, Sereda et al. 2022), and a number of other hazardous technosphere objects from products used in the life process. Such solutions serve as the basis for the prevention of natural hazards, hydrometeorological and other processes: smog, dust storms, landslides, subsidence of soils, loss of forests, shortage of drinking water as a result of water poisoning, and destruction of biological resources irretrievably lost for water supply of underground aquifers (Hertwich et al. 2020, Liu et al. 2016, Omar et al. 2019, Varughese 2017).

The adoption of scientifically sound system management, organizational, technical, and technological solutions to reduce technosphere hazards contributes to the comprehensive solution of social problems, ensuring environmental, economic, and food security, availability of necessary drinking water supplies, and groundwater purification (Bhagawati et al. 2017, He et al. 2017, Rosalia & Hakim 2021), the implementation of a closed-cycle economy, the return of safe, natural resources to the environment (Domenech et al. 2019, Hart & Adam 2019, Kirchherr et al. 2017).

In 2015, the Prime Minister of India and the Head of the Ministry of Emergency Situations of Russia reached agreements on cooperation in the field of emergency prevention and response, exchange of information on hazards and threats, including environmental ones, obtained using space monitoring methods. The main threats to natural and man-made nature include the death of forests, desertification of territories, smog, reduction of biodiversity, dangerous effects of agrochemicals, and toxic waste on soils and water bodies.

In the given context of the pressing issue, the utilization of advanced forecasting techniques for environmental threats and emergencies is of paramount importance. This approach aims to assess the likelihood of emergencies' emergence, occurrence, and progression by systematically analyzing potential causes and conditions that could lead to an uncontrolled escalation of environmental hazards, thereby reaching hazardous levels.

However, at present, the formation of a forecast can be based only on a limited set of incomplete data that make up information in the field of protection of the population and territories from emergencies, the composition of which is determined by the framework of information exchange between the Ministry of Emergency Situations of Russia, other agencies, and at the international level - with other countries. At the same time, the effectiveness of emergency forecasting largely depends on the accuracy of related forecasts of the state, dynamics of changes in natural and man-made factors, and sources of environmental hazards, which are not always and not fully provided. The revealed contradiction formed the need to develop a new approach to forecasting environmental hazards based on the application of fuzzy set theory and fuzzy logic.

The issues of using artificial intelligence in forecasting environmental threats and assessing the state of technosphere security of territories based on a systematic analysis of monitoring data are relevant in solving global problems of socio-economic development that do not have state borders.

## MATERIALS AND METHODS

The research methods are based on the application of system analysis, the theory of fuzzy sets, realizing the possibilities of soft computing when calculating the levels of environmental safety of the population and territories, thereby providing an opportunity for a comprehensive assessment and analysis of trends and interrelated processes of the state of protection of the natural environment and vital human interests from the dangerous impacts of technosphere objects, taking into account various factors, conditions, and restrictions.

The strategy of this study correlates with the concepts accepted in the world community: "Zero waste" (Elgizawy et al. 2016, Murray 2002), "Circular economy" based on the materials of many years of research, the results of the author's own research in the field of environmental safety, environmental protection, prevention of environmentally hazardous situations at life support facilities technosphere territories (Tshovrebov et al. 2018b, 2021).

## RESULTS AND DISCUSSION

In the course of the study, the authors took into account the materials of generalization, analysis of the scientific and practical results achieved in the world in the subject

area under study (Anisimov et al. 2017, Oltyan et al. 2020, Saurenko et al. 2018), indicating the following features and trends.

Firstly, the existing methods of assessing the state of technosphere danger of an object or territory and forecasting possible adverse consequences are insufficiently interconnected in a single system, which, in turn, reduces the effectiveness, validity, and reliability of the forecast, as well as the completeness, timeliness, and effectiveness of management decisions to prevent man-made emergencies based on the establishment of causal investigative links.

Secondly, the starting point of the vector of the development of an emergency situation from an unfavorable one has not been established and characterized.

Thirdly, the totality of various factors, limitations, conditions, and causes of the origin, course, and development of environmentally hazardous processes is not sufficiently taken into account, and consequently, the ability to make a reliable forecast of the assessment of hazardous environmental consequences is limited.

The presence of not fully researched aspects of the subject area that do not allow the effective use of accurate forecasting methods in solving state tasks of preventing man-made emergencies required the development of a fundamentally new approach to the methodology of forecasting the occurrence and development of environmental hazards.

Taking into account that in the formation of environmental forecasts, there are no strict approaches that allow for obtaining an unambiguous result for the optimal time in vaguely expressed conditions for the preparation of project, organizational, technical, and managerial decisions, the research methodology is based on the theory of soft computing using inaccurate and mathematically not strictly conditioned methods, algorithms that implement the achievement of goals and research tasks.

The use of the theory of fuzzy sets and the method of soft computing provides an analytical platform for the presence of a threshold for estimating changes in the studied indicators in the interval {0;1}. In other words, the formed threshold model of environmental forecasting (*EF*) assumes the presence of a threshold (level) below or above which the factor studied in the course of forecasting does not function:

$$EF = F\left(P_f/P_p\right), \qquad \ldots(1)$$

$P_p$ - is a safe limiting threshold level of exposure (permissible, background or temporarily agreed concentration, the volume of allocated pollution during the operation of an object, process in normal mode, or the amount of discharge, emission as a function of these indicators;

$P_f$ - actual impact taking into account changing factors and conditions;

$F$ is the Heaviside function ($F(P_f - P_p) = 0$ at $(P_f - P_p) \leq 0$ and $F(P_f - P_p) = 1$ at $(P_f - P_p) > 0$).

An acceptable information and analytical basis for the proposed approach can serve as a restrictive system of maximum permissible concentrations (MPC) of pollutants in the components of the natural environment: waters, soils, and atmospheric air. Firstly, compliance with the level of safety in relation to public health and the natural environment is guaranteed when using this system. Secondly, the threshold principle is fully implemented, which applies to all factors of a negative impact, and thirdly, the level of danger of the pollutant, the effects of summation, and the joint presence of various substances are taken into account. Taking into account the limiting indicators of the harmfulness of various groups of pollutants.

Taking into account that the MPC of pollutants has been approved to assess the safety of three groups of components of the natural environment, we present a classification of the potentially possible threshold impact of various technosphere emergencies on these natural components (Table 1).

According to the criteria adopted in Russia, an emergency is characterized by a ratio $(R_f/R_p) = 5$ or 50 when exposed to chemicals on soils and atmospheric air or water resources. Such gradation does not fully reflect the level of both danger and toxicity of specific pollutants, the effects of summation, the conditions and intensity of pollution, and the types and severity of the consequences.

For a more complete and accurate justification of the processes and phenomena under consideration, within the framework of a conditionally deterministic approach, modeling of the predictive state of changing stepwise processes characterizing the dynamics of environmental hazard of the technosphere objects under study can be characterized by a function of the form:

$$P(T) = \sum_{j=1}^{n} \cdot \sum_{i=1}^{n} \Delta ij \, n(T - Tij) \qquad \ldots(2)$$

$P(T)$ – forecast of the hazard level of the object (territory) by time $T$;

$\Delta ij$ – the predicted magnitude of the negative impact on the $i$-th component of the natural environment (a. water, b. soil, c. atmospheric air), which determines the threshold of the $j$-th event or situation (a. regular (normative, safe); b. unfavorable (potentially dangerous); c. emergency (extreme));

$Tij$ – the predicted (expected) moment of occurrence of the $j$-th event due to the time-continuing impact on the $i$-th component of the natural environment;

Table 1: Threshold impact of technospheric emergencies on natural components.

| Technosphere emergencies | Threshold effect on natural components | | |
|---|---|---|---|
| | Water ($\kappa e$) | Soil quality ($ke$) | Atmospheric air ($ko$) |
| Accidents of freight and passenger trains with the release, spillage, scattering, and dumping of hazardous chemicals | 1 | 1 | 1 |
| Accidents of cargo and passenger ships | 1 | 1 | 0 |
| Aviation disasters | 0 | 1 | 1 |
| Major car accidents | 0 | 1 | 0 |
| Accidents on oil pipelines | 1 | 1 | 1 |
| Accidents on main gas pipelines | 0 | 0 | 1 |
| Accidents on electric power systems | 0 | 1 | 0 |
| Accidents on utility systems | 1 | 1 | 1 |
| Accidents on heating networks | 0 | 0 | 1 |
| Hydrodynamic accidents | 1 | 0 | 0 |
| Accidents with the release (threat of release) of chemically hazardous substances | 0 | 0 | 1 |
| Accidents at agricultural facilities | 1 | 1 | 0 |
| Explosions in buildings in populated areas | 0 | 1 | 1 |
| Explosions at industrial facilities | 0 | 1 | 1 |
| Explosions on communications | 1 | 1 | 1 |
| Sudden collapse of buildings | 0 | 1 | 1 |
| Sudden collapse of rocks, dumps, embankments | 0 | 1 | 1 |
| Poisoning and pollution of water bodies | 1 | 0 | 0 |
| Forest fires and forest arson | 0 | 0 | 1 |
| Fires in landfills | 0 | 0 | 1 |
| Infiltration is the translocation of toxicants from the body of landfills and landfills into the environment | 1 | 1 | 1 |

$n(T\text{-}Tij)$ – fuzzy view function:

$$n(T\text{-}Tij) = \begin{cases} 1, \text{if } (T\text{-}Tij) > 0 \\ 0, \text{if } (T\text{-}Tij) \leq 0 \end{cases} \quad I = \{1;3\}, \; j = \{1;3\}$$

...(3)

Depending on (2), a relationship is achieved between the specific forms of manifestation of environmental hazards, their quantitative expression, and the intensity of propagation in time and space.

The process of the origin, formation, accumulation, and impact of dangerous factors and their development in dangerous situations has certain stages (stages). The accumulation of dangerous environmental and related factors to a certain level precedes the emergence of a dangerous environmental situation, which, in turn, if proper preventive measures are not taken, precedes the occurrence of all these types of accidents, catastrophes, and emergencies. The accumulation of dangerous factors, their development into dangerous situations and further into environmental emergencies can be schematically represented as follows:

Dangerous factor (+ Dangerous Factor) + Conditions that create (generate) danger → Danger → Unfavorable (environmentally dangerous, threatening) situation → Environmental emergency

Taking into account this causal relationship scheme, a model of a composite criterion for the environmentally safe (*ES*) condition of the territories of enterprises and regions in relation to potential sources of ecologic impact has been formed (Fig. 1).

The formation of these indicators into a composite criterion is carried out through a system of sequential transformations:

$ke^0\,ko^0\,k\text{в}^0 \Rightarrow ke^0\,ko^1\,k\text{в}^0 \Rightarrow ke^1\,ko^0\,k\text{в}^0 \Rightarrow ke^0\,ko^2\,k\text{в}^0 \Rightarrow ke^2\,ko^0\,k\text{в}^0$

$ke^0\,ko^0\,k\text{в}^0 \Rightarrow ke^1\,ko^0\,k\text{в}^0 \Rightarrow ke^0\,ko^0\,k\text{в}^1 \Rightarrow ke^2\,ko^0\,k\text{в}^0 \Rightarrow ke^0\,ko^0\,k\text{в}^2$

$ke^0\,ko^0\,k\text{в}^0 \Rightarrow ke^0\,ko^1\,k\text{в}^0 \Rightarrow ke^0\,ko^0\,k\text{в}^1 \Rightarrow ke^0\,ko^2\,k\text{в}^0 \Rightarrow ke^0\,ko^0\,k\text{в}^2$

As a result, the composite *ES* criterion is defined as follows:
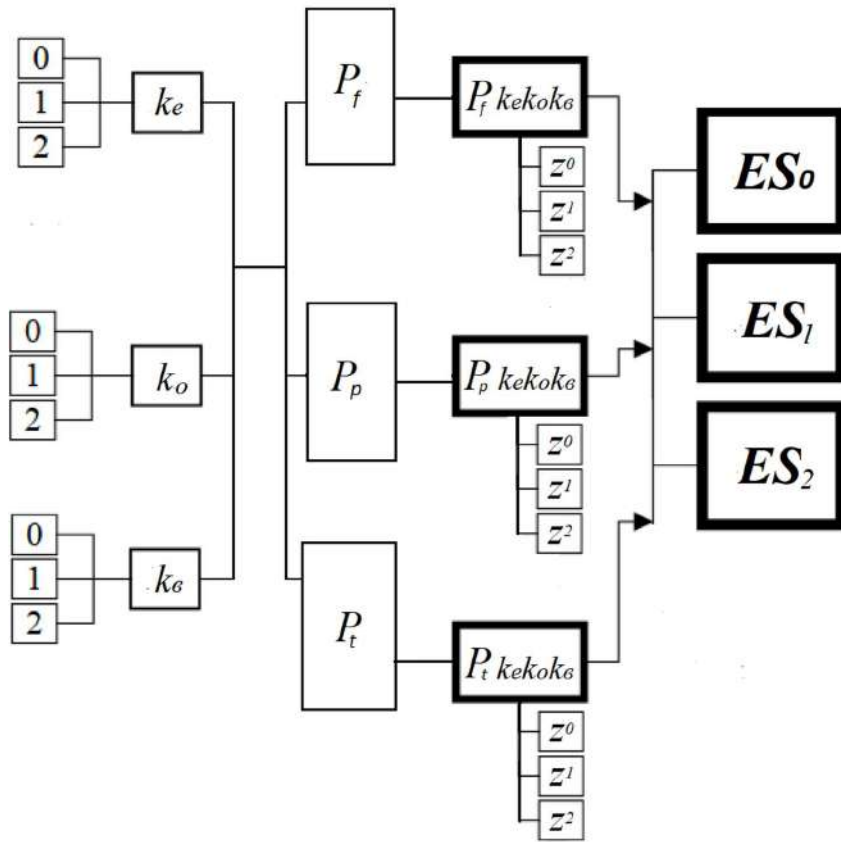
Fig. 1: Scale of composite criteria for assessing the level of environmental hazard.

$$ES^0 \qquad | \qquad ES^1 \qquad | \qquad ES^2$$

$$\mathbf{ke^0\,ko^0\,k\text{в}^0} \Rightarrow ke^0\,\mathbf{ko^1}\,k\text{в}^0\,| \Rightarrow \mathbf{ke^1}\,ko^0\,k\text{в}^0 \Rightarrow ke^0\,ko^0\,\mathbf{k\text{в}^1} \Rightarrow$$
$$ke^0\,\mathbf{ko^2}\,k\text{в}^0\,| \Rightarrow \mathbf{ke^2}\,ko^0\,k\text{в}^0 \Rightarrow ke^0\,ko^0\,\mathbf{k\text{в}^2}$$

Each of the criteria is determined by a set of characteristics determined by a set of parameters or a specific parameter. The initial set of alternatives is described by three indicators ($Pf$, $Pp$, $Pt$) and weight features ($ke$, $ko$, $k\text{в}$) having ordered threshold scales of discrete estimates: $P_f = \{0,1,2\}$; $P_p = \{0,1,2\}$; $P_t = \{0,1,2\}$ and their products as resultant indicators expressing both factors ($Z^0$; $Z^1$; $Z^2$).

Many alternatives are grouped into three ordered classes: $ES_0$, $ES_1$, $ES_2$ - "Environmental safety" with assessments of levels: 0 – (safe); 1 – unfavorable; 2 - extreme (dangerous), corresponding to the gradations of the scale of the composite criterion of the upper-level $Z = \{Z^0, Z^1, Z^2\}$. The indicators of the fuzzy assessment scale correspond to the above three composite criteria for predictive assessment of the possible escalation of a standard (regular situation) through an unfavorable one into an emergency and form a fuzzy scale of the level of environmental safety of territories. For the quantitative interpretation of the fuzzy assessment

of the level of environmental safety, a point assessment of the weight of indicators is proposed, followed by a ranking of threshold levels by the sum of the assigned points as a result of an expert assessment based on an analysis of the environmental situation (Fig. 2).

The factors determining the "critical" indicator are assigned a numerical value of "-0.2", "unacceptable – "-0.04", "normative" - "0", comfortable – "0.2", taking into account the transition from one threshold level to another within the boundaries of the fuzzy rating scale [-1;1] with the designations: a – lower the boundary of the critical level (-1); b – unfavorable (-0.2); c - normative (0); d – safe (1). The permissible zero level determines the starting point of the safe state of the life support system. It is assumed that the total balance of indicators determining the minimum level of environmentally safe condition of the territory, the object should have a positive value, satisfactory - exceed the value of "0.2", average – "0.5", high – "0.7", the highest - one. In this case, the environmentally safe level will correspond to finding an indicator of the state of the territory in the range of fuzzy estimates [0;1] according to the proposed fuzzy scale.
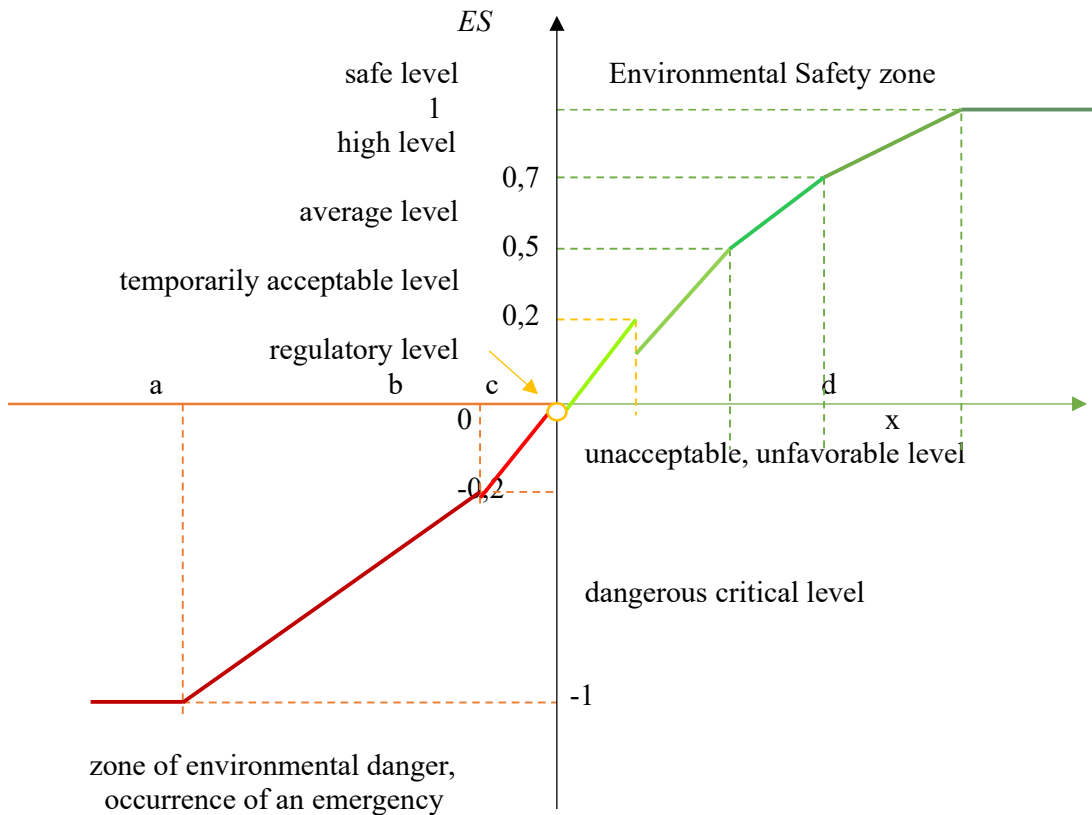
Fig. 2: Graphical interpretation of the membership function of assessments of environmental safety indicators of a fuzzy point scale.

Operational, medium- and long-term forecasts of the state of protection of the natural environment from the effects of technosphere objects are proposed to be carried out based on the use of mathematical logic methods to assess groups of environmental conditions: safe, unfavorable, dangerous, catastrophic (emergency) in accordance with the developed indicators.

## CONCLUSION

A fuzzy scale of indicators is presented, which makes it possible to apply the numerical apparatus of soft computing. It displays in a formalized form the current state, development scenarios, and forecast of environmentally safe life support of territories based on a fuzzy scale of levels reflecting the quantitative interpretation of the weight of the established indicators using a point assessment.

The scientific and applied significance of the developed fuzzy scale of environmental safety indicators is confirmed by a wide range of practical implementation possibilities: when assessing the safety of facilities; within the framework of updating legal acts in the field of forecasting and prevention of emergencies; as criteria for both technospheric emergencies and environmental assessment of territories; analyzing the effectiveness of government agencies and business by introducing a fuzzy indicator, reflecting the situation and the measures taken in the field of environmental safety and emergency prevention.

Forecasting of the five emergency levels adopted in many countries of the world (federal, interregional, regional, municipal, facility), in the format of the proposed fuzzy system for assessing environmental safety indicators in scientific and methodological terms should be based on the possibilities of the use of integrated monitoring databases that allow you to monitor the development of the situation at all territorial levels at once; work with large data sets, detailing the numerical values of factors of natural and man-made sources of emergencies, as well as with the maximum number of characteristics of protected objects of the economy; construction of mathematically calculated digital models of the prospects and visualization of the development of emergencies in relation to state information systems and emergency warning systems.

# REFERENCES

Anisimov, V.G., Zegzhda, P.D., Anisimov, E.G., Saurenko, T.N. and Prisyazhnyuk, S.P. 2017. Indices of the effectiveness of information protection in an information interaction system for controlling complex distributed organizational objects. Autom. Contr. Comp. Sci., 51(8): 824-828.

Baldé, C.P., Forti, V., Gray, V., Kuehr, R. and Stegmann P. 2017. The Global E-waste Monitor. United Nations University (UNU), International Telecommunication Union (ITU) & International Solid Waste Association (ISWA), Bonn/Geneva/Vienna. p. 53.

Bhagawati, R., Bhagawati, K., Jini, D., Alone, R.A., Singh, R., Chandra, A., Makdoh, B., Sen, A. and Shukla, K.K. 2017. Review on climate change and its impact on agriculture of Arunachal Pradesh in the Northeastern Himalayan region of India. Nat. Environ. Pollut. Technol., 6(2): 535-539.

Bredel, G. 1995. Tackling India's coal ash problem. Mining Eng., 10: 51.

Domenech, T. and Bahn-Walkowiak, B. 2019. Transition Towards a Resource Efficient Circular Economy in Europe: Policy Lessons from the EU and the Member States. Ecological Economics, 155: 7-19.

Elgizawy, S., El-Haggar, S. and Nassar, K. 2016. Slum development using zero waste concepts: Construction waste case study. Proceed. Eng., 145: 1306-1313.

Hart, J. and Adam, K. 2019. Barriers and drivers in a circular economy: the case of the built environment. Procedia CIRP, 80: 619-624.

He, X., Wada, Y., Wanders, N. and Sheffield, J. 2017. Intensification of hydrological drought in California by human water management. Geophys. Res. Lett., 44(4): 1777-1785. https://doi.org/10.1002/2016GL071665/

Hertwich, E., Lifset, R., Pauliuk, S. and Heeren, N. 2020. Resource Efficiency and Climate Change: Material Efficiency Strategies for a Low-Carbon Future. A Report of the Int. Resource Panel. United Nations Environment Programme, Kenya; https://www.unep.org/resources/report/resource-efficiency-and-climate-change-material-efficiency-strategies-low-carbon.

Kirchherr, J., Reike, D. and Hekkert, M. 2017. Conceptualizing the circular economy: An analysis of 114 definitions. Resources, Conservation & Recycling, 127: 9.

Liu, H., Yuan, F. and Yang, D. 2000. The strength varieties of the seibsurface made of lime and fine coal ash of the Hingwaj from Changba to Baichengt. Dongbei linye daxue. J. Nort-East Forest. Univ., 28(1): 45.

Liu, X.F., Wang, S.X., Zhou, Y., Wang, F.T., Yang, G. and Liu, W.L. 2016. Spatial analysis of meteorological drought return periods in China using Copulas. Natural Hazards, 80(1): 367-388. https://doi.org/10.1007/s11069-015-1972-7/

Murray, R. 2002. Zero waste. Greenpeace Environ. Trust. 11: 211

Oltyan, I.Y., Arefyeva, E.V. and Kotosonov, A.S. 2020. Remote assessment of an integrated emergency risk index. IOP Conference Series: Materials Science and Engineering. International Conference on Construction, Architecture and Technosphere Safety, ICCATS 2020. Sochi. 1: 042053.

Omar, P.J., Gaur, S., Dwivedi, S.B. and Dikshit, P.K.S. 2019. Groundwater modeling using an analytic element method and finite difference method: An insight into Lower Ganga river basin. J. Earth Syst. Sci., 128(7): 195. https://doi.org/10.1007/s12040-019-1225-3.

Rosalia, A.C. and Hakim, L. 2021. Spatial analysis of the impact of flood and drought on food security index. Nature Environ. Pollut. Technol., 20(2): 721-727. https://doi.org/10.46488/NEPT.2021.v20i02.031

Saurenko, T., Anisimov, E., Anisimov, V. and Levina, A. 2018. Comparing Investment Projects of Innovative Developing Strategies of Municipalities, Based on a Set of Indicators. MATEC Web of Conferences: International Science Conference (SPbWOSCE-2017): Business Technologies for Sustainable Urban Development, 20-22 December 2017, St. Petersburg, Russia, Curan Associates, Inc., NY, US, pp. 01038.

Sereda, T.G. and Kostarev, S.N. 2021. Development of the automated workstation for the operator of the solid municipal waste landfill. IOP Conference Series: Earth and Environmental Science, 677(4): 042107.

Sereda, T.G., Kostarev, S.N., Novikova, K.O.V. and Ivanova, I.E. 2022. Study of solid municipal waste accumulation rates in penitentiary facilities in Perm Krai during the pandemic of 2020. IOP Conf. Ser. Earth Environ. Sci., 1043(1): 012005.

Tshovrebov, E. Velichko, E. and Shevchenko, A. 2018b. ethodological approaches to a substantiation resource - and energetically effective economic model of the object of placing of a waste. Adv. Intell. Syst. Comp., 692: 1296-1305.

Tshovrebov, E., Velichko, E. and Niyazgulov, U. 2018a. lanning measures for environmentally safe handling of extremely and highly hazardous wastes in industrial, building, and transport complexes. Mater. Sci. Forum, 945: 988-994.

Tshovrebov, E.S., Velichko, E.G., Kostarev, S.N. and Niyazgulov, U.D. 2021. Mathematical model of environmentally friendly management of construction waste and waste of urban economy. IOP Conf. Ser. Earth Environ. Sci., 937(4): 042062.

Varughese, A. 2017. Analysis of historical climate change trends in Bharathapuzha River Basin, Kerala, India. Nature Environ. Pollut. Technol., 16(1): 237-242.

Zeng, X., Mathews, J.A. and Jinhui, L. 2018. Urban mining of e-waste is becoming more cost-effective than virgin mining. Environ. Sci. Technol. Publ., 4: 121-125.

# The Impact of Climate Change on the City of Padang, Indonesia

**Widya Prarikeslan*(**)†** iD **, Nofi Yendri Sudiar*(***), Gema Anugrah**, Deski Beri*(****),**
**Dezi Handayani*(*****), Irma Leilani Eka Putri*(*****) and Mohammad Isa Gautama*(******)**

*Research Center for Climate Change, Universitas Negeri, Padang, Indonesia
**Department of Geography, Faculty of Social Science, Universitas Negeri, Padang, Indonesia
***Department of Physics, Faculty of Mathematics and Natural Sciences, Universitas Negeri, Padang, Indonesia
****Department of Chemistry, Faculty of Mathematics and Natural Sciences, Universitas Negeri, Padang, Indonesia
*****Department of Biology, Faculty of Mathematics and Natural Sciences, Universitas Negeri, Padang, Indonesia
******Department of Sociology, Faculty of Social Science, Universitas Negeri, Padang, Indonesia
†Corresponding author: Widya Prarikeslan; widya_geo@fis.unp.ac.id

## ABSTRACT

The impact of global warming is climate change which affects elements of society. This condition causes a decrease in the level of community welfare and increases the level of community vulnerability. Some climate change impacts are floods, droughts, landslides, and shoreline changes. In this study, we will focus on landslides. Landslides are among the most dangerous natural disasters that often occur in mountainous areas, especially during the rainy season. Various factors influence events involving landslides. This study aims to utilize GIS to identify landslide-prone areas in Padang. The method used in this study is the Zuidam and Concelado criteria overlay method for the level of landslide hazard and the broken method (jenks). The natural break (jenks) classification method reduces within-class variation and maximizes between-class variation. This study shows that the level of landslide vulnerability in Padang City is low, with a total area of 288854.38173 ha with a percentage of 42.21%. We need to consider more factors and experiment with training and validating data in more detail to gain insight into the physical contributions of the factors to landslide occurrences.

## INTRODUCTION

Human activities have led to an increase in Greenhouse Gas (GHG) emissions which has led to the phenomenon of global warming and resulted in climate change. Climate change is happening slowly but surely. In addition, climate change has an impact on all sectors of life. As a country vulnerable to climate change, Indonesia in the Asian region is predicted to see an increase in temperature of 2-6$^{\circ}$C and more rainfall. Low <20 mm within 10 days with a 70% chance (Herawaty 2007). This climate change provides opportunities for vulnerability to climatic disasters such as drought and floods caused by changes in temperature and rainfall patterns. These changes provide opportunities for increasing climatic disasters, such as droughts and floods caused by changes in temperature and rainfall patterns. The second is to protect functions such as the danger of erosion and landslides and reduce the danger of fire and pest attack by mixing various plants. The third is the function of utilizing renewable energy with fuelwood-producing plants. The community has not recognized these roles so far, especially in the

regions. Along with the increasingly ongoing issue of global warming and climate change, people are gradually starting to understand that they have felt the negative effects of global warming.

Natural disasters can occur anytime, anywhere, bringing tangible and intangible losses to people's lives. Landslides are among the most dangerous natural disasters frequent in mountainous places, particularly during the rainy season. It might lead to a loss of injuries and damage to other facilities and property infrastructures like housing, business, and agricultural property (Rotigliano et al. 2012, Yu & Chen 2020, Yang & Chen 2010, Chen et al. 2019). Additionally, it can significantly impact society, the neighborhood, and the local economy in the affected regions (Abdurrohim & Firman 2018).

Numerous researchers have investigated landslide-prone regions worldwide (Mersha & Meten 2020, Roodposhti et al. 2014, Nurdin & Kubota 2018).

The primary areas of concentration for research studies include the inventory of landslides, the influence of

geographic, topographical, hydrological, and environmental elements on the occurrences of landslides, and the participation of triggering factors such as precipitation and earthquake (Gian Quoc et al. 2018, Ya'acob et al. 2019). Events involving landslides are influenced by a variety of causal elements, which can be divided into several categories, including geomorphology, geology, soil, land cover, and hydrological conditions (Huqqani et al. 2021).

Padang is a coastal city with a population of more than 900,000 people, making it the largest city in West Sumatra. Situated in hilly terrain, the city is prone to landslides due to its unique geographical position. The soil is composed of clay, silt, and sand, making it highly susceptible to erosion and landslides. In addition, the city experiences high-intensity rainfall, which can trigger landslides, especially during the rainy season.

To address this issue, there is a need for a comprehensive approach that integrates technology, scientific knowledge, and community participation. One such approach is using Geographic Information Systems (GIS) for landslide hazard analysis (Mukhlisin et al. 2010, Nahayo et al. 2019, Bai et al. 2010, Cao et al. 2016, Lee 2005). GIS technology is a powerful tool that can be used to combine multiple layers of data, such as slope, geology, land use, and precipitation, to identify areas at risk of landslides.

Landslide dangers have been evaluated using remote sensing techniques and GIS. The landslide hazard maps were created using a variety of mathematical techniques, from more traditional advanced intelligence techniques like artificial neural network (ANN) (Shahri et al. 2019, Alkhasawneh et al. 2013, 2014, Lee et al. 2001) to more recent conventional statistic methods like frequency ratio (Regmi et al. 2014, Chen et al. 2020), statistical index and weights-of-evidence.

Most study studies have only used these two data configurations of the landslide data, and many researchers have examined landslide hazard mapping utilizing original data or frequency ratio data (Catani et al. 2013, Liu et al. 2019). We emphasize the major disparities in the generated landslide danger maps and suggest the most effective data configurations.

GIS technology for landslide hazard analysis in Padang has several benefits. First, it provides a cost-effective and efficient approach to identifying areas at risk of landslides (Sukrizal et al. 2019). Traditional approaches, such as field surveys, are time-consuming and expensive and do not provide a comprehensive picture of the area under consideration. Second, GIS-based analysis can be used to inform land use planning decisions, ensuring that vulnerable areas are not developed or that appropriate mitigation measures are taken. Third, the analysis can be used to develop an early warning system that can warn people living in high-risk areas of impending landslides (Miswar et al. 2022). This study aims to utilize GIS to identify landslide-prone areas in Padang. Based on the explanations above, the results of this analysis will provide valuable insights for decision-makers to develop effective disaster prevention and mitigation strategies in urban areas.

## MATERIALS AND METHODS

### Study Area

This research was conducted in the city of Padang. According to the Central Bureau of National Statistics, On the whole, the area of Padang Municipality was 694,96 Km2. Padang city is geographically located between $0^o44'$ and $01^o08'$ south latitude and between $100^o05'$ and $100^o34'$ East Longitude. Based on data from the National Disaster Mitigation Agency (BNPB), landslides in Padang City occurred due to high rainfall, a very steep slope > 70 (100-150%), and an area classified as prone to ground movement (red zone) (Gemilang et al. 2017).

The data for this study includes 10 landslide failure points obtained from exploratory activities. This study indicates that almost all landslides and most ground failures occur in the loess layer and that rock mass is the rock mass of the entire region and the sliding bed of the loess rock interface landslide (Li et al. 2021).

### Methods

To achieve the purpose of this study, we collected and organized data, created a landslide inventory dataset, constructed and applied a database of landslide causative factors, and created and validated a landslide susceptibility map. Data collection and organization: The data required for this study was collected from various sources. This includes gathering relevant literature from published literature, a Data Elevation Model from BIG, a regional geological map from ESDM at a scale of 1:250000, and a soil map from (Badan Penelitian Dan Pengembangan Pertanian Kementerian Pertanian).

During fieldwork, data collection was carried out on different rock types by describing their steepness, soil texture, and landslide inventory mapping on both active landslide and scarp areas by measuring their length, width, accumulation zone, and depth (if possible) (Mersha & Meten 2020). After compiling the actual field investigation, the data was systematically processed and analyzed first in ArcGIS, then in Microsoft Excel, and finally in ArcGIS.

### Method of Mapping

To assess the vulnerability of classified landslides to determine

the level of landslide hazard (Zuidam & Concelado 1979) with GIS Arc View 10.1. Data scores and maps are needed to obtain data and maps of the potential for avalanche hazard using the method of overlaying the Zuidam and Concelado criteria for the level of landslide hazard (Jumardi & Nurfalaq 2019). The results of landslide vulnerability zoning are further classified into 5 classes: not vulnerable, slightly vulnerable, moderately vulnerable, vulnerable, and very vulnerable. The classification is done using the natural break method (jenks). According to ESRI (2010), the natural break (jenks) classification method tries to reduce within-class variation and maximize between-class variation (Nugroho 2020).

## RESULTS AND DISCUSSION

**Physical Factors of Landslide**

**Lithology:** Because different lithology units have variable levels of landslide risk, lithology is the most crucial factor in this study of landslides (Cuesta et al. 1999, Dai et al. 2001, Nurdin & Kubota, 2018). According to geology and development centers, the lithological units depicted on the surface geologic maps were reclassified. A broad geology map was the outcome. Lithology shows a great influence on landslide development since different lithological units may be affected by different landslide types (Trisnawati et al. 2022). Moreover, soil cover deposits, mostly exposed to weathering, may influence land permeability and the landslide type, as known from thematic literature (Henriques et al. 2015). In the study area, based on the mapping results, there are 5 lithological units that have different characteristics (Fig. 1).
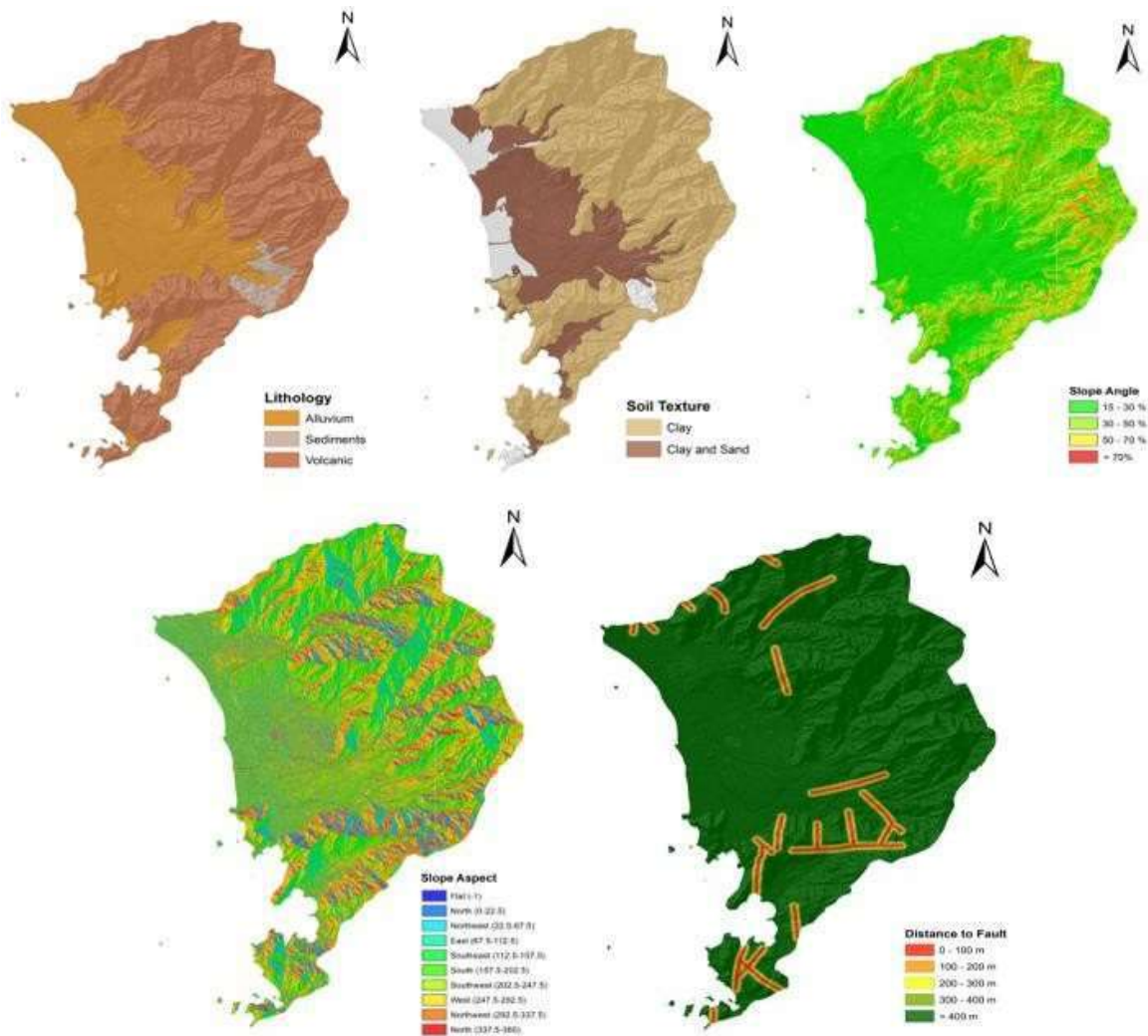


Fig. 1: Thematic maps used in this study, (a) Litologhy; (b) Soil Texture; (c) Slope Angle; (d) Slope Aspect; (e) Distance to Fault.
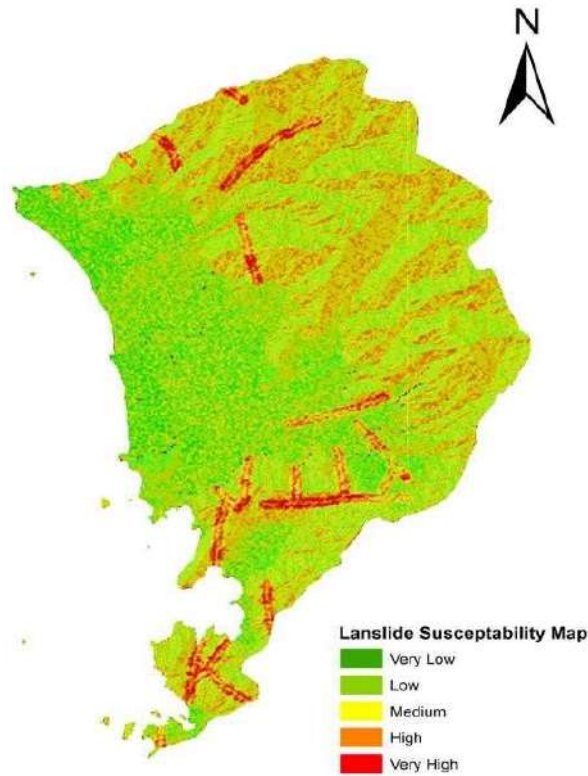
Fig 2: Landslide Susceptibility Map.



Fig. 3: (a) (A road settled at the slope affected by a landslide; (b) Forest carried by a mass movement.

**Slope Angle:** Every investigation into the likelihood of landslides takes slope into account because the slope is frequently utilized to study landslide probability (Dai et al. 2001, Lee & Talib 2005, Nurdin & Kubota, 2018). The direct sunshine that strikes heavily sloped slopes and cleared terrain dries the soil and raises the risk of landslides. The slope angle affects the shear pressures operating on hill slopes, so it's generally regarded as one of the most important parameters for

landslide modeling (Dai et al. 2001). Landslides increased in the study area as slope steepness increased. 20% of all landslides happened on slopes between 30 and 45 degrees (Fig. 1).

**Slope Aspect:** The degree of vegetation coverage, surface weathering, and surface evaporation are all impacted by the varying solar radiation that the surface receives depending on the slope's aspect, which also affects the likelihood of landslides. According to the slope aspect, the DEM data can be categorized into 9 types: 0° to 40, 40" to 80", 80-120", 120-160", 200-240", 240-280", and 320- 360". Landslides in the research area typically occur between 160 and 200 of slope aspect (Fig. 1), and those with this slope aspect account for the biggest share (21%), according to the slope aspect backdrop (Li et al. 2021).

**Fault:** In fault zones, rock and soil structures are prone to collapse and weathering, which has a certain impact on the occurrence of landslide disasters. ArcGIS calculates the Euclidean distance for fault data in your study area. Due to the fault distance, the landslide disasters in the study area are mainly concentrated in the fault distance of 0-2361m, and the landslide disaster in the fault distance of 0-1127m is the most frequent, accounting for 29% (Fig. 1) (Sun et al. 2020, Li et al. 2021).

**Soil Texture:** With the application of a probabilistic approach to soil texture, the physical characteristics of soil are frequently used for parameter analysis of landslides. Other physical soil characteristics like water infiltration, porosity, water permeability, and groundwater's ability to pass can be impacted by soil texture. The Food and Agricultural Organization (FAO) of the United Nations (, the Centre for Soil and Agroclimatic Research, and the United States Department of Agriculture system are used to classify soil in Indonesia. The three varieties of soil in the study area-Dystrandepth, Dystropepts, and Tropaquepts-all belong to the Andosol family (Fig. 1). The soil type of Dystrandepts is where the majority of landslides occur (77, 25%). This might be related to the location of Dystrandepts deposition, mostly found at higher altitudes. This class accounts for the largest proportion of the areas (Nurdin & Kubota 2018).

**Landslide Vulnerability Area**

Based on the landslide vulnerability analysis results, five levels of landslide vulnerability were obtained in the Padang City area: very low, low, medium, high, and very high. The distribution of landslide vulnerability levels can be presented in Fig. 2.

Based on Table 1, the area of landslide vulnerability in the city of Padang is obtained as follows:

The data above shows that the level of landslide

Table 1: Landslide vulnerability in the city of Padang.

| landslide hazard level | Wide (ha) | % of Area |
|---|---|---|
| Very Low | 10069.4283 | 14.73 |
| Low | 28854.38173 | 42.21 |
| Medium | 20284.87757 | 29.67 |
| High | 7605.009513 | 11.12 |
| Very High | 1550.376236 | 2.27 |
| Total | 68364.07335 | 100 |

vulnerability in Padang City is low, with a total area of 288854.38173 ha with a percentage of 42.21%. However, the government must not be complacent about this, bearing in mind that other areas have very high, high, and medium levels of vulnerability. Fig. 3 shows a road settled at the slope affected by a landslide and a forest carried by a mass movement.

Mitigation measures for landslides can include structural and non-structural approaches. Structural measures include the construction of retaining walls, slope stabilization, and drainage systems. Non-structural measures include land-use planning, zoning, and early warning systems. The effectiveness of these measures depends on the specific characteristics of the landslide and the local conditions (Assilzadeh et al. 2010).

Identifying and mitigating the landslide vulnerability area is critical for reducing slide risks. However, there are challenges associated with this process. One of the significant challenges is the lack of accurate data on landslide occurrences and their causes. In many regions, landslides are not well documented, and the historical data may not be comprehensive or reliable. This makes it difficult to develop accurate landslide susceptibility maps, and identify areas requiring mitigation measures.

Another challenge is the difficulty in predicting landslides. Landslides can occur suddenly and without warning, making developing effective early warning systems challenging. Additionally, the occurrence of landslides is influenced by various factors, including climate, geology, and human activities, making it difficult to predict their occurrence accurately.

Despite these challenges, identifying and mitigating the landslide vulnerability area are essential for reducing landslide risks. In addition to protecting communities and infrastructure, these measures can also have economic benefits. Landslides can cause significant damage to property and infrastructure, leading to economic losses. These losses can be reduced by identifying and mitigating the landslide vulnerability area, and the region's long-term economic viability can be maintained.

## CONCLUSION

This study aims to utilize GIS to identify landslide-prone areas in Padang. From this utilization, the result is that the level of landslide vulnerability in Padang City is still low, with a total area of 288854.38173 ha with a percentage of 42.21%. The accuracy of the model might have been affected by the distribution of the random points (factors) used in this study. Therefore, we need to consider more factors and experiment with training and validating data in more detail to gain insight into the physical contributions of the factors to landslide occurrences.

## REFERENCES

Abdurrohim, H. and Firman, H. 2018. Mapping of landslide hazards prediction using geographic information system in Solok District. MATEC Web Conf., 229: 1-6. https://doi.org/10.1051/matecconf/201822904003

Alkhasawneh, M. S., Ngah, U. K., Tay, L. T. and Isa, N. A. M. 2014. Determination of importance for comprehensive topographic factors on landslide hazard mapping using artificial neural network. Environ. Earth Sci., 72(3): 787-799. https://doi.org/10.1007/s12665- 013-3003-x

Alkhasawneh, M.S., Ngah, U.K., Tay, L.T., Mat Isa, N.A. and Al-Batah, M.S. 2013. Determination of important topographic factors for landslide mapping analysis using MLP network. The Scientific World Journal, 2013(415023): 1-12. https://doi.org/10.1155/2013/415023.

Assilzadeh, H., Levy, J.K. and Wang, X. 2010. Landslide catastrophes and disaster risk reduction: A GIS framework for landslide prevention and management. Remote Sensing, 2(9): 2259-2273. https://doi.org/10.3390/rs2092259

Bai, S.B., Wang, J., Lü, G. N., Zhou, P.G., Hou, S.S. and Xu, S.N. 2010. GIS-based logistic regression for landslide susceptibility mapping of the Zhongxian segment in the Three Gorges area, China. Geomorphology, 115(1-2): 23-31. https://doi.org/10.1016/j.geomorph.2009.09.025

Cao, C., Wang, Q., Chen, J., Ruan, Y., Zheng, L., Song, S. and Niu, C. 2016. Landslide susceptibility mapping in vertical distribution law of precipitation area: Case of the Xulong hydropower station reservoir, Southwestern China. Water, 8(7): https://doi.org/10.3390/w8070270

Catani, F., Lagomarsino, D., Segoni, S. and Tofani, V. 2013. Landslide susceptibility estimation by random forests technique: Sensitivity and scaling issues. Natural Hazards Earth System Sci., 13(11): 2815-2831. https://doi.org/10.5194/nhess-13-2815-2013.

Chen, W., Fan, L., Li, C. and Pham, B.T. 2020. Spatial prediction of landslides using hybrid integration of artificial intelligence algorithms with frequency ratio and index of entropy in Nanzheng county, China. Appl. Sci., 10(1): 29. https://doi.org/10.3390/app10010029.

Dai, F.C., Lee, C.F., Li, J. and Xu, Z.W. 2001. Assessment of landslide susceptibility on the natural terrain of Lantau Island, Hong Kong. Environ. Geol., 40(3): 381-391. https://doi.org/10.1007/s002540000163

Gemilang, W. A., Husrin, S., Wisha, U. J. and Kusumah, G. 2007. Coastal

vulnerability to landslide disasters in Bungus, West Sumatra and surrounding areas using the storie method. Geoscience Journal, 3(1): 37. https://doi.org/10.12962/j25023659.v3i1.2954

Gian Quoc, A., Duc-Tan, T., Nguyen Dinh, C. and Tien Bui, D. 2018. Flexible configuration of wireless sensor network for monitoring of rainfall-induced landslide. Indon. J. Electr. Eng. Comp. Sci., 12(3): 1030-1036. https://doi.org/10.11591/ijeecs.v12.i3.pp1030-1036

Henriques, C., Zêzere, J.L. and Marques, F. 2015. The role of the lithological setting on the landslide pattern and distribution. Eng. Geol., 189: 17-31. https://doi.org/10.1016/j.enggeo.2015.01.025

Herawaty, H.S. 2007. Policy and Development Challenges: Adaptation to the 16 Hazards of Future Ground Motion Due to the Effects of Climate Change. Report of the First Dialogue Meeting on Soil Movements and Climate Change.

Huqqani, I.A., Tien, T.L. and Mohamad-Saleh, J. 2021. Landslide hazard analysis using a multilayered approach based on various input data configurations. Geosfera Indon., 6(1): 20. https://doi.org/10.19184/geosi.v6i1.23347

Jumardi, A. and Nurfalaq, A. 2019. Application of GIS in the analysis of landslide-prone areas: Case study along the shaft roads between districts of Wara Barat District, Palopo City). Semantic Proceed., 1: 10-17.

Lee, C.F., Li, J., Xu, Z.W. and Dai, F.C. 2001. Assessment of landslide susceptibility on the natural terrain of Lantau Island, Hong Kong. Environ. Geol., 40(3): 381-391

Lee, S. 2005. Application of logistic regression model and its validation for landslide susceptibility mapping using GIS and remote sensing data. Int. J. Remote Sens., 26(7): 1477-1491. https://doi.org/10.1080/01431160412331331012

Lee, S. and Talib, J.A. 2005. Probabilistic landslide susceptibility and factor effect analysis. Environ. Earth Sci., 47(7): 982-990. https://doi.org/10.1007/s00254-005-1228-

Li, B., Wang, N. and Chen, J. 2021. GIS-Based landslide susceptibility mapping using information, frequency ratio, and artificial neural network methods in Qinghai Province, Northwestern China. Adv. Civ. Eng., 21: 806. https://doi.org/10.1155/2021/4758062

Liu, L., Li, S., Li, X., Jiang, Y., Wei, W., Wang, Z. and Bai, Y. 2019. An integrated approach for landslide susceptibility mapping by considering spatial correlation and fractal distribution of clustered landslide data. Landslides, 16(4): 715-728. https://doi.org/10.1007/s10346- 018-01122-2.

Mersha, T. and Meten, M. 2020. GIS-based landslide susceptibility mapping and assessment using bivariate statistical methods in the Simada area, northwestern Ethiopia.

Geoenviron. Dis., 7(1): 155. https://doi.org/10.1186/s40677-020-00155-x

Miswar, D., Wahono, E.P., Aristoteles, S.A., Yarmaidi, D.R.Y., Zakaria, W.A. and Sugiyanta, I. G. 2022. The landslide spatial modeling in Limau District, Tanggamus Regency. Atlantis Press, 17: 236-250. https://doi.org/10.2991/assehr.k.220102.030

Mukhlisin, M., Idris, I., Salazar, A.S., Nizam, K. and Taha, M.R. 2010. GIS-based landslide hazard mapping prediction in Ulu Klang, Malaysia. ITB J. Sci., 42A(2): 163-178. https://doi.org/10.5614/itbj.sci.2010.42.2.7

Nahayo, L., Kalisa, E., Maniragaba, A. and Nshimiyimana, F.X. 2019. Comparison of analytical hierarchy process and certain factor models in landslide susceptibility mapping in Rwanda. Model. Earth Syst. Environ., 5(3): 885-895. https://doi.org/10.1007/s40808-019-00575-1

Nugroho, H. 2020. Analysis of landslide vulnerability using the frequency ratio method in West Bandung Regency, West Java. Geoid, 16(1): 8. https://doi.org/10.12962/j24423998.v16i1.7680

Nurdin, P.F. and Kubota, T. 2018. Gis-based landslide susceptibility assessment and factor effect analysis by certainty factor in upstream of Jeneberang River, Indonesia.

Geoplann. J. Geomat. Plan., 5(1): 75. https://doi.org/10.14710/geoplanning.5.1.75-90

Regmi, A.D., Devkota, K.C., Yoshida, K., Pradhan, B., Pourghasemi, H.R., Kumamoto, T. and Akgun, A. 2014. Application of frequency ratio, statistical index, and weights-of-evidence models and their comparison in landslide susceptibility mapping in Central Nepal Himalaya. Arab. J. Geosci., 7(2): 725-742. https://doi.org/10.1007/s12517-012-0807-z.

Roodposhti, M.S., Rahimi, S. and Beglou, M.J. 2014. PROMETHEE II and fuzzy AHP: An enhanced GIS-based landslide susceptibility mapping. Natural Hazards, 73(1): 77-95. https://doi.org/10.1007/s11069-012-0523-8

Rotigliano, E., Cappadonia, C., Conoscenti, C., Costanzo, D. and Agnesi, V. 2012. Slope units- based flow susceptibility model: Using validation tests to select controlling factors. Natural Hazards, 61(1): 143-153. https://doi.org/10.1007/s11069-011-9846-0

Shahri, A.S., Spross, J., Johansson, F. and Larsson, S. 2019. Landslide susceptibility hazard map in southwest Sweden using artificial neural network. Catena, 183(C): 104225. https://doi.org/10.1016/j.catena.2019.104225.

Sukrizal, S., Fatimah, E. and Nizamuddin, N. 2019. Analysis of landslide hazards area using geographic information system in Gayo Lues district. Int. J. Multicul. Multirelig. Understand., 6(3): 193. https://doi.org/10.18415/ijmmu.v6i3.807

Sun, X., Chen, J., Han, X., Bao, Y., Zhan, J. and Peng, W. 2020. Application of a GIS-based slope unit method for landslide susceptibility mapping along the rapidly uplifting section of the upper Jinsha River, South-Western China. Bull. Eng. Geol. Environ., 79(1): 533-549. https://doi.org/10.1007/s10064-019-01572-5

Trisnawati, D., Najib, Hidayatillah, A.S. and Najib, M. 2022. The relationship of lithology with landslide occurrences in Banyumanik and Tembalang Districts, Semarang City. IOP Conf. Ser. Earth Environ. Sci., 1047(1): 012026. https://doi.org/10.1088/1755-1315/1047/1/012026

Ya'acob, N., Tajudin, N. and Azize, A.M. 2019. Rainfall-landslide early warning system (RLEWS) using TRMM precipitation estimates. Indonesian J. Electr. Eng. Comp. Sci., 13(3): 1259-1266. https://doi.org/10.11591/ijeecs.v13.i3.pp1259-1266

Yang, X. and Chen, L. 2010. Using multi-temporal remote sensor imagery to detect earthquake-triggered landslides. Int. J. Appl. Observ. Geoinform., 12(6): 487-495. https://doi.org/10.1016/j.jag.2010.05.006

Yu, C. and Chen, J. 2020. Application of a gis-based slope unit method for landslide susceptibility mapping in Helong city: Comparative assessment of ICM, AHP, and ARF model. Symmetry, 12(11): 1-21. https://doi.org/10.3390/sym12111848

## ORCID DETAILS OF THE AUTHORS

Widya Prarikeslan: https://orcid.org/0000-0002-2974-8472

# Evaluation of Organic Pollution Using Algal Diversity in Rivers of Cotabato City, Bangsamoro Autonomous Region in Muslim Mindanao (BARMM), Mindanao Island, Philippines

**Nancy C. Alombro\*, Raisah C. Guiamadil\*, Warda U. Datumama\*, John Paul A. Catipay\*(\*\*) and Peter Jan D. de Vera\*\*\*†**

\*Natural Sciences Department, College of Arts and Sciences, Notre Dame University, Cotabato City, Bangsamoro Autonomous Region in Muslim Mindanao (BARMM), Philippines
\*\*Science Department, Senior High School, Notre Dame University, Cotabato City, Bangsamoro Autonomous Region in Muslim Mindanao (BARMM), Philippines
\*\*\*Natural Sciences Department, College of Arts and Sciences, Mindanao State University-Maguindanao, Dalican, Datu Odin Sinsuat, Maguindanao del Norte, Bangsamoro Autonomous Region in Muslim Mindanao (BARMM), Philippines
†Corresponding author: Peter Jan D. de Vera; peterjandevera0302@gmail.com

## ABSTRACT

This study investigated the water quality and the organic pollution level of rivers in Cotabato City, specifically the Rio Grande de Mindanao, Matampay, Esteros, and Tamontaka rivers. The physicochemical characteristics of water in these rivers were determined in the laboratory, and the level of organic pollution was determined using Palmer's algal pollution index. Water quality assessment showed that the dissolved oxygen (DO) in Matampay River and the biological oxygen demand (BOD) in Esteros River exceed the minimum standard set by the Department of Environment and Natural Resources (DENR) for water quality in class C rivers. Results also showed that there were thirty (30) algal genera belonging to twelve (12) classes were observed in Cotabato City rivers. Algal genera belonging to *Chlorophyceae* and *Bacillariophyceae* were found to be the most abundant in these rivers. Using Palmer's algal pollution index, the Rio Grande de Mindanao showed a probability of high organic pollution, while the rest of the rivers indicated a lack of organic pollution. For a more thorough assessment of the Cotabato City rivers, it is advisable to consider more comprehensive measures, such as extending the sampling duration and expanding the number of sampling stations.

## INTRODUCTION

Among the freshwater ecosystems, rivers are among the most productive and diverse ecosystems, representing below a percent of the Earth's surface (Opperman et al. 2015). This ecosystem has been utilized for domestic and personal purposes (Tickner et al. 2017). However, rivers that are situated near urban areas have been negatively affected by anthropogenic activities such as sewage discharge and industrialization (Khatri & Tyagi 2015). This leads to the degradation of rivers, worsening their water quality and adversely affecting the living organisms that depend on them (Bassem 2020).

Algae has an important role in a freshwater environment. It yields oxygen, consumes carbon dioxide, and serves as the foundation of the aquatic food chain (Stevenson 2014). These organisms are recognized as excellent reflectors of water quality due to their rapid life cycle and fast response to a wide range of pollutants. Nowadays, eutrophication and freshwater quality are assessed using microalgae as bioindicators and standards (Parmar et al. 2016). The nutrient condition of water bodies, such as eutrophication, is reflected by the increasing number of blue-green algae.

In contrast, oligotrophic conditions are highlighted by the abundance of diatoms and green algae (El-Serehy et al. 2018). This makes the algae population reliable bioindicators of freshwater environments such as streams and rivers since they represent the status of an ecosystem through their distribution and type. Furthermore, freshwater monitoring is much easier using algae as bioindicators due to the ease of sample collection, and most species are easy to identify (Omar 2010).

The growth and responses of freshwater algae have a positive response to variations in water quality. The

abundance of organic nutrients in a freshwater body could lead to a sudden increase in the algal population and has been considered a detrimental environmental problem (Paerl et al. 2018). Several studies evaluated the level of organic pollution in freshwater bodies using algae in rivers (Bhatnagar & Bhardwaj 2013, Noel & Rajan 2015, Salem et al. 2017). Algal communities can serve as biological indicators of environmental changes in freshwater ecosystems, such as in rivers (Omar 2010). Palmer's algal pollution index is a tool that has been used to provide descriptive characteristics of the level of organic pollution in freshwater bodies using algal communities (Palmer 1969). Several studies have used the index in determining the water quality of various freshwater bodies, particularly in rivers. Shahare (2017) used this index in assessing the organic pollution level of the Chudband River in Gondia District, India. Results showed the different physicochemical parameters of a water sample have a direct relationship with pollution-tolerant algal genera. Salem et al. (2017) also utilized Palmer's algal pollution index in evaluating the surface water quality of the middle Nile Delta in Egypt. The results of their study showed that the index is a reliable and convenient method for detecting organic pollution. In the Philippines, an assessment of water quality in rivers using Palmer's algal pollution index has also been conducted (Lacdan et al. 2014, Galinato & Evangelio 2016, Martinez 2017, Seriño & Belonias 2020).

Cotabato City is an urban area situated in the Bangsamoro Autonomous Region in Muslim Mindanao (BARMM) that is located between the Rio de Grande de Mindanao and Tamontaka River, making it a catch basin of floodwater from the Ligawasan marshland in Maguindanao. The study of Corcoro et al. (2012) pointed out that these rivers are very important to residents aboding along these rivers as they provide a wide range of services such as irrigation,

source of drinking water, and domestic purposes. To date, hydrological and biological studies in these urban rivers are very little to none. Hence, this study aims to determine the organic pollution in select areas of rivers in Cotabato City using different algal genera.

To our knowledge, there was no assessment regarding the determination of the probability of organic pollution based on algal diversity conducted in the rivers in Cotabato City. The data from this study will provide a valuable contribution to the knowledge about the diversity of algal diversity in rivers within an urban area in the country. Moreover, data on algal diversity indicating organic pollution may be utilized by policymakers and the community to come up with plans and programs that may help protect and conserve the rivers in Cotabato City.

## MATERIALS AND METHODS

### Study Sites

For this study, water samples were collected from three (3) sampling stations within the Rio de Grande Mindanao, Matampay, Esteros, and Tamontaka rivers in Cotabato City (Fig. 1) last August 2022. These rivers were classified as class C based on the classification set by the Department of Environment and Natural Resources (DENR). Class C rivers are intended to be used only for fish growth and propagation, recreational and agricultural purposes, and are not recommended for public water supply (DENR 2016). Sampling stations were established 10-15 meters from the river banks of each river and were at least 500 meters from each other. Proximity to the nearest household areas and access roads were the bases for establishing the sampling stations in each river. The abundance of *Eichornia crassipes* is highly notable in these rivers.
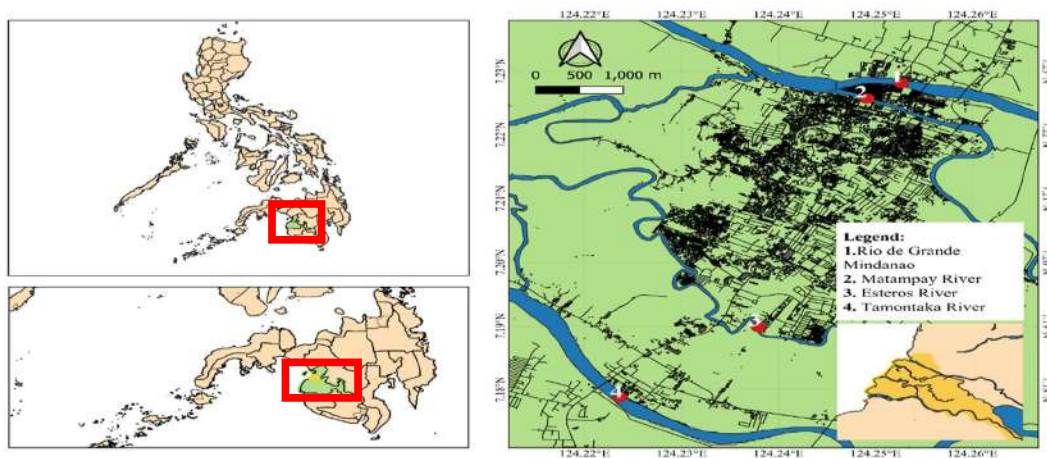


Fig. 1: Map showing the rivers in Cotabato City, BARMM, Philippines. (QGIS v3.24.1, PJdeVera).

## Water Sampling

The physicochemical parameters of the water in the rivers, such as pH, dissolved oxygen (DO), biological oxygen demand (BOD), total dissolved solids (TDS), and nitrates, were determined in the laboratory. The temperature of the three (3) sampling stations in each river was determined on-site. Sampling stations were at least 500 meters from each other. Water samples were collected and placed in empty plastic bottles (labeled with river and station numbers). The empty plastic bottles were rinsed three times with the river water before collection. All water samples were taken at an average depth of at least twelve (12) inches from the surface water and were collected on the same schedule as the collection of algal samples. The samples were placed in a styrofoam box with ice and were brought to a third party for analysis. The temperature was determined using a mercury-filled thermometer *in situ*. The pH was determined through the electrometric method. DO was determined using the glass electrode. The BOD was determined through the respirometric method. TDS was evaluated through the gravimetric method. Nitrates were determined through a closed reflux cell test. All physicochemical parameters were determined following the standard methods for the examination of water and wastewater (WEF 2022).

## Algal Collection and Identification

Algal samples were collected from the water surface of the same sampling stations where the water samples were taken. A plankton net was used to collect 250 mL of water from each river. Water samples were fixed using Lugol's solution and were brought to Notre Dame University, Cotabato City - Biology laboratory for identification of algal genera. All water samples were allowed to settle for 24 h in the Biology laboratory, and the supernatant was decanted until 20 mL of the liquid was left. One (1) mL of decanted water samples was placed in a Segdwick-Rafter counting chamber (Suther et al. 2009) and was examined under the microscope at higher magnification using an Olympus microscope cx23. Three replicates of 1 mL aliquot in each sampling station were used for the identification of algal genera. Only algal genera that are present at a density of more than fifty (50) cells in a one-ml sample were recorded for this study (Salem et al. 2017). Identification of algae down to the genus level was done using references by Palmer (1979) and Bellinger and Sigee (2005). The online database AlgaeBase (Guiry & Guiry 2018) was also consulted.

## Level of Organic Pollution Using Palmer's Algal Pollution Index

The organic pollution level of the study areas was determined using Palmer's algal pollution index (Palmer 1969) (Table 1). Only algal genera that are present at a density of more than fifty (50) cells in a one-ml sample will be recorded and included in the index (Salem et al. 2017). All the algal genera identified and used for the analysis in this study were present in all three sampling stations established in each river. The recorded algal genera were compared with the list of pollution-tolerant genera listed in Palmer's algal pollution index. Index scores designated in each algal pollution-tolerant genera were added to obtain each river's total pollution index score. A score lower than 15 means that the river lacks moderate organic pollution; 15-19 indicates a high probability of organic pollution in the river, and 20 or more signifies high pollution in the river.

## Data Analysis

Data collected from the physicochemical parameters were analyzed using the SPSS (version 26). One-way analysis of variance (ANOVA) was used to determine if there were significant differences ($p < 0.05$) among the rivers in Cotabato City. Tukey post hoc test was used to differentiate between means.

## RESULTS AND DISCUSSION

### Physicochemical Characteristics of Water Samples From Cotabato City Rivers

The mean values of the physicochemical parameters of water in rivers where water samples were taken are shown in Table 2. All the rivers assessed in this study were designated as class C based on the classification of water bodies by the Department of Environment and Natural Resources (DENR), Philippines. Results showed that these rivers had passed the minimum standard of water quality set by the DENR except for the dissolved oxygen (DO) in Matampay River and the

Table 1: Pollution-tolerant algal genera as listed in Palmer's algal pollution index.

| Genus | Index Score | Genus | Index Score |
|---|---|---|---|
| *Anacystis* | 1 | *Micractinium* | 1 |
| *Ankistrodesmus* | 2 | *Navicula* | 3 |
| *Chlamydomonas* | 4 | *Nitzchia* | 3 |
| *Chlorella* | 3 | *Oscillatoria* | 5 |
| *Closterium* | 1 | *Pandorina* | 1 |
| *Cyclotella* | 1 | *Phacus* | 2 |
| *Euglena* | 5 | *Phormidium* | 1 |
| *Gomphonema* | 1 | *Scenedesmus* | 4 |
| *Lepocinclis* | 1 | *Stigeoclonium* | 2 |
| *Melosira* | 1 | *Synedra* | 2 |

biological oxygen demand (BOD) in Esteros River. Data analysis showed that there is no significant difference in the DO in the Matampay River compared to other rivers such as Rio de Grande Mindanao and Tamontaka Rivers. However, the BOD in the Esteros River is significantly different from other rivers being studied (Table 2). High BOD levels were also observed in other class C rivers within an urban area in the country, such as the Carangan Estero in Ozamiz City (Enguito et al. 2013), Meycauayan River in Bulacan (Pleto et al. 2020) and the Guadalupe River in Metro Cebu (Claudio et al. 2019). High BOD may indicate high domestic discharges in the river system (Aniyikaye et al. 2019). However, this study is only limited to one sampling season. Thus, it is suggested that further monitoring of the water quality of Cotabato City rivers in different seasons shall be conducted to assess further the status of these freshwater bodies.

**Algal Genera Present in the Rivers**

A total of thirty (30) algal genera represented by twelve (12) classes were observed in the rivers in Cotabato City (Table 3). Algal genera observed in this study, such as *Asterionella*, *Cocconies*, *Eunotia*, *Gomphonema*, *Navicula*, *Nitzchia*, *Synedra*, *Ankistrodesmus*, *Oedegonium*, *Synura*, *Cryptomonas*, *Kumanoa*, *Ulothrix*, and *Spirogyra* were also found in other rivers in the country (Galinato & Evangelio 2016, Martinez 2017, Seriño & Belonias 2020, Arguelles & Monsalud 2021). However, the algal genera observed in this study are slightly lower compared to the algal genera noted in the Banahao (39 against 30 genera) and Biasong (32 against 30 genera) rivers in Leyte (Galinato & Evangelio 2016) and Pagbanganan river (39 against 30 genera) in Baybay City, Leyte (Seriño & Belonias 2020).

Algal genera belonging to *Chlorophyceae* and *Bacillariophyceae* were found to be the most abundant Cotabato City rivers. A high number of genera from *Chlorophyceae* and *Bacillariophyceae* in these rivers can be attributed to the vast number of genera under these classes (John et al. 2011).

Moreover, the genera of *Bacillariophyceae* noted in this study were also present in the Banahao-Palhi rivers in Leyte (Galinato & Evangelio 2016). Among the six (6) genera included in Chlorophyceae, only the *Rhizoclonium* was present in all rivers. This may suggest that species from these genera were likely to be well-distributed in freshwater ecosystems.

**Level of Organic Pollution in the Rivers**

Among the twenty (20) pollution genera in Palmer's algal pollution index, there were ten (10) genera documented in this study. The number of pollution genera detected was similar to the number of pollution genera encountered in the Pagbanganan River in Baybay City, Leyte (Seriño & Belonias 2020). Moreover, the pollution genera observed in this study were slightly higher compared to algal pollution genera observed in the Banahao-Palhi River (9 against 10 genera) in Leyte (Galinato & Evangelio 2016) and in Ylang-Ylang River (4 against 10 genera) in Cavite (Martinez 2017).

Using Palmer's algal pollution index, all water samples collected from rivers in Cotabato City indicated a lack of organic pollution except in Rio Grande de Mindanao (Table 4). Out of the twenty (20) genera listed as indicators of possible organic water pollution, six (6) genera were documented in Rio Grande de Mindanao, namely *Anacystis*, *Synedra*, *Navicula*, *Nitzchia*, *Oscillatoria*, and *Euglena*. Based on Palmer's pollution index, this river yields a score of eighteen (18), which is interpreted as having a high probability of organic pollution.

The algal genus *Nitzchia* is common in all rivers except the Tamontaka River. It is considered an organic tolerant diatom that serves as a good indicator of organic pollution in both marine and freshwater ecosystems (Xia et al. 2020). This algal pollution genus was also observed in other rivers in the country (Galinato & Evangelio 2016, Martinez 2017, Seriño & Belonias 2020, Arguelles & Monsalud 2021). The presence of nutrients and organic substrates in freshwater regulates the relative abundance of these diatoms (Kim et al. 2019). This

Table 2: Physicochemical characteristics of rivers in Cotabato City.

| Physicochemical Parameters (unit) | Water Quality Standard | Rivers Surrounding Cotabato City | | | |
|---|---|---|---|---|---|
| | | Rio Grande de Mindanao | Matampay | Esteros | Tamontaka |
| Temperature [°C] | 25-31 | 28.77 ± 0.59 | 28.6 ± 0.61 | 28.75 ± 0.67 | 28.87 ± 0.59 |
| pH | 6.5-9.0 | 7.78 ± 0.07[a] | 7.73 ± 0.03[a] | 7.48 ± 0.06[b] | 7.75 ± 0.05[a] |
| Dissolved Oxygen - DO [mg.L$^{-1}$] | 5 | 4.83 ± 0.32[a] | 5.03 ± 0.15[a] | 2.78 ± 0.06[b] | 4.63 ± 0.12[a] |
| Biological Oxygen Demand – BOD [mg.L$^{-1}$] | 7 | 3.1 ± 0.80[a] | 2.2 ± 0.61[a] | 9 ± 2.78[b] | 1.97 ± 0.96[a] |
| Total Dissolved Solid – TDS [mg.L$^{-1}$] | 500 | 114 ± 4.0[a] | 118.33 ± 1.53[a] | 123.33 ± 4.16[a] | 125.33 ± 4.73[b] |
| Nitrates [mg.L$^{-1}$] | 45 | 0.94 ± 0.09[a] | 0.57 ± 0.04[b] | 0.66 ± 0.04[b] | 1.17 ± 0.15[a] |

Values are expressed as mean ± standard deviation (n = 3). Means having identical superscript in the same row are not statistically significant ($p < 0.05$). Water quality standards were based on the Department of Environment and Natural Resources (DENR) – Philippines Water Quality Guidelines of 2016.

Table 3: Distribution of algal genera in Cotabato City rivers.

| Algal Classes | Algal Genera | Rivers in Cotabato City | | | |
|---|---|---|---|---|---|
| | | Rio Grande de Mindanao | Matampay | Esteros | Tamontaka |
| *Bacillariophyceae* | *Asterionella* | + | - | - | - |
| | *Cocconeis* | - | + | - | - |
| | *Eunotia* | - | - | - | + |
| | *Gomphonema* | - | - | + | - |
| | *Navicula* | + | - | - | - |
| | *Nitzchia* | + | + | + | - |
| | *Synedra* | + | - | - | - |
| *Chlorophyceae* | *Ankistrodesmus* | - | - | - | + |
| | *Carteria* | - | + | - | - |
| | *Chlamydomonas* | - | - | + | - |
| | *Chlorogonium* | - | - | - | + |
| | *Crucigenia* | - | - | + | + |
| | *Oedogonium* | + | + | - | + |
| *Chrysophyceae* | *Dinobryon* | - | + | - | - |
| | *Synura* | - | + | - | - |
| *Conjugatophyceae* | *Cosmocladium* | - | - | + | - |
| | *Zygnema* | - | + | - | - |
| *Cryptophyceae* | *Cryptomonas* | - | - | + | + |
| *Cyanophyceae* | *Oscillatoria* | + | - | - | - |
| *Dinophyceae* | *Ceratium* | - | + | - | - |
| *Euglenophyceae* | *Euglena* | + | + | - | + |
| *Florideophyceae* | *Bostrychia* | - | + | - | + |
| | *Kumanoa* | - | + | - | + |
| | *Polysiphonia* | + | - | + | - |
| | *Sterrocladia* | - | - | - | + |
| *Ulvophyceae* | *Rhizoclonium* | + | + | + | + |
| | *Ulothrix* | + | - | - | - |
| | *Ulva* | - | - | + | + |
| *Xanthophyceae* | *Excentrochloris* | - | - | + | - |
| *Zygnematophyceae* | *Spirogyra* | + | - | - | - |

diatom can be used as a pollution index in rivers for assessing pesticide contamination (Rimet & Bouchez 2011). In the study conducted by Xia et al. (2020), *Nitzchia* indicated the high presence of organic pollutants and pesticides in the river, which may exacerbate if not controlled.

This study also noted the presence of *Navicula* and *Synedra* in the Rio de Grande de Mindanao, which were also present in the Ylang-Ylang River in Cavite (Martinez 2017), and in Pagbanganan River in Baybay City, Leyte (Seriño & Belonias 2020). These genera were noted as two of the most abundant genera in the Pagbanganan River (Labonite & Belonias 2013). The genus *Euglena* is another algal bioindicator recorded in the Rio Grande de Mindanao, Tamontaka, and Matampay rivers.

This genus was also noted in the Ylang-Ylang River (Martinez 2017) and was used to calculate the organic pollution of the river based on Palmer's algal pollution index. Rastogi et al. (2015) stated that *Euglena* is a highly pollution-tolerant genus that can be used to detect eutrophication. However, the current study only accounted for the presence of the algal genera and not the frequency. Thus, continuous monitoring of algal diversity, as well as the frequency of the pollution-tolerant genera in the rivers of Cotabato City, is recommended to be conducted in future studies.

## CONCLUSION

Among the rivers in Cotabato City, the Rio Grande de

Table 4: Palmer's pollution index values in rivers surrounding Cotabato City

| Genera | Index Value | Esteros | Tamontaka | Matampay | Rio Grande de Mindanao |
|---|---|---|---|---|---|
| *Anacystis* | 1 | - | - | 1 | 1 |
| *Ankistrodesmus* | 2 | - | 2 | - | - |
| *Chlamydomonas* | 4 | 4 | - | - | - |
| *Chlorella* | 3 | - | - | - | - |
| *Closterium* | 1 | - | - | - | - |
| *Cyclotella* | 1 | - | - | - | - |
| *Euglena* | 5 | - | 5 | 5 | 5 |
| *Gomphonema* | 1 | 1 | - | - | - |
| *Lepocinclis* | 1 | - | - | - | |
| *Melosira* | 1 | 1 | 1 | - | - |
| *Micratinium* | 1 | - | - | - | - |
| *Navicula* | 3 | - | - | - | 3 |
| *Nitzchia* | 3 | 3 | - | 3 | 3 |
| *Oscillatoria* | 4 | - | - | - | 4 |
| *Pandorina* | 1 | - | - | - | - |
| *Phacus* | 2 | - | - | - | - |
| *Phormidium* | 1 | - | - | - | - |
| *Scenedesmus* | 4 | - | - | - | - |
| *Stigeoclonium* | 2 | - | - | - | - |
| *Synedra* | 2 | - | - | - | 2 |
| Total | | 8 | 8 | 9 | 18 |

Mindanao, particularly in Cotabato City, exhibited a high probability of organic pollution. At the same time, the Esteros, Tamontaka, and Matampay Rivers indicated a lack of organic pollution. The results of this study show that Palmer's algal pollution index can be utilized in detecting the levels of organic pollutants. Moreover, this index can be used as part of monitoring the health of the rivers along with the physicochemical characterization of the rivers. For further research, it is recommended to increase the sampling duration, both wet and dry seasons, in assessing the levels of organic pollution using algal diversity in Cotabato City rivers. The number of sampling stations in each river should be increased to capture the entire algal diversity in Cotabato City rivers.

## ACKNOWLEDGEMENT

## REFERENCES

Arguelles, E.D.L.R. and Monsalud, R.G. 2021. Taxonomy and species composition of epiphytic algae in Sta. Cruz River, Laguna (Philippines). J. Microbiol. Biotechnol. Food Sci., 11(3): 1-8.

Aniyikaye, T.E, Oluseyi, T., Odiyo, J. and Edokpayi, O. 2019. Physicochemical analysis of wastewater discharge from selected paint industries in Lagos, Nigeria. Int. J. Environ. Res. Public Health., 16(1235): 1-17.

Bassem S.M. 2020. Water pollution and aquatic biodiversity. Biodivers. Int. J., 4(1):10-16.

Bellinger, E.G. and Sigee, D.C. 2005. Freshwater Algae: Identification and Use as Bioindicators. John Wiley & Sons, NY.

Bhatnagar, M. and Bhardwaj, N. 2013. Biodiversity of algal flora in river Chambal at Kota, Rajasthan. Nat. Environ. Pollut. Tech., 12(3): 547-549.

Claudio, L.E., Pepito-Ochea, C., Secuya, M.F.R., Abe, J.C., Molina, M.J.B. and Orit, J.K.T. 2019. Regional state of the brown environment report. DENR-EMB., 11: 27-64.

Corcoro, T., Alombro, A.C. and Herrera, W. 2012. Water analysis of Cotabato City rivers and its implication to human and aquatic life. Am. Inter. J. Contemp. Res., 7(2): 82-89.

Department of Environment and Natural Resources (DENR). 2016. Water Quality Guidelines and General Effluent Standards of 2016. Environmental Management Bureau, US.

El-Serehy, H., Abdallah, H.S., Al-Misned, F., Al-Farraj, S.A. and Al-Rasheid, K.A. 2018. Assessing the water quality and classifying trophic status for scientifically based management of the water resources of Lake Timsah, the lake with salinity stratification along the Suez Canal. Saudi J Biol Sci., 25(7): 1247- 1256.

Enguito, M.R.C., Matunog, V.E., Bala, J.J.O. and Villantes, Y.L. 2013. Water quality assessment of Carangan estero in Ozamis City, Philippines. J. Multi. St., 1(1): 19-44.

Galinato, M.I. and Evangelio, J.C. 2016. Dynamics of plankton community in Banahao-Palhi river in Leyte, Philippines. Annal. Trop. Res., 38(2): 130-152.

Guiry, M.D. and Guiry, G.M. 2018. AlgaeBase. World-Wide Electronic Publication, University of Ireland, Galway.

John, D.M., Whitton, B.A. and Brook, A.J. 2011. The Freshwater Algal Flora of the British Isles. Cambridge University Press, Cambridge, pp. 878.

Khatri, N. and Tyagi, S. 2015. Influences of natural and anthropogenic factors on surface and groundwater quality in rural and urban areas. Front. Life Sci., 8:1. 23-39.

Kim, H.K., Cho, I.H., Kim, Y.J. and Kim, B.H. 2019. Benthic diatom communities in Korean estuaries: Species appearances in relation to environmental variables. Int. J. Environ. Res. Public Health., 16(2681): 1-22.

Labonite, E.K. and Belonias, B.S. 2013. Community structure of planktonic algae in Pagbanganan River, Baybay City, Leyte. Sci. Humananit., 10: 54-82.

Lacdan, N.F., Javier, L.M.V., Pagaddu, J.V.A. and Su, G.L.S. 2014. Assessing water quality of Dao River, Baybay City, Batangas using phytoplankton monitoring. Int. J. Curr. Sci., 12: 98-102.

Martinez, K.S. 2017. Developing a river health index: a study in Ylang-Ylang River, Cavite, Philippines. 4th International Research Conference on Higher Education, KnE Social Sciences, pp. 774-788.

Noel, S.D. and Rajan, M.R. 2015. Evaluation of organic pollution by Palmer's algal genus index and physicochemical analysis of Vaigai river at Madurai India. Nat. Res. Con., 3(1): 7-10.

Omar, 2010. Perspective on the use of algae as biological indicators for monitoring and protecting aquatic environments, with special reference to Malaysian freshwater ecosystems. Trop. Life Sci Res., 21(2): 51-67.

Opperman, J. Gunther, G. Hartmann, J. Angarita, H. Bara P. Delgado, J. Harrisson, D. Higgins, J. Martin, E. Newsock, A. Petry, P. Roth, B. Sotomayor, L. Torres, J. and Vazquez, D. 2015. The power of rivers: Finding a balance between energy and conservation in hydropower development. Nature Conserv., 6: 1-55.

Paerl, H.W., Otten, H. and Kudela, R. 2018. Mitigating the expansion of harmful algal blooms across the freshwater-to-marine continuum. Environ. Sci. Technol., 52(10): 5519-5529.

Palmer, C.M. 1969. A composite rating of algae tolerating organic pollution. J. Physiol., 65: 111-126.

Palmer, C.M. 1979. Algae and Water Pollution: An Illustrated Manual on the Identification, Significance, and Control of Algae in Water Supplies and in Polluted Water. Municipal Environmental Research Laboratory, Office of Research and Development, US Environmental Protection Agency, Ohio.

Parmar, T. Rawtani, D. and Agrawal, Y.K. 2016. Bioindicators: the natural indicator of environmental pollution. Front. Life Sci., 9(2): 110-118.

Pleto, J.V.R., Migo, V.P. and Arboleda, M.D.M. 2020. Preliminary water and sediment quality assessment of the Meycuayan river segment of the Marilao-Meycuayan-Obando river system in Bulacan, Philippines. J. Health. Pollut., 10(26): 1-9.

Rastogi, R., Madamwar D. and Incharoensakdi, A. 2015. Bloom dynamics of cyanobacteria and their toxins: environmental health impacts and mitigation strategies. Front. Microbiol., 6(1254): 1-22.

Rimet, F. and Bouchez, A. 2011. Use of diatom life-forms and ecological guilds to assess pesticide contamination in rivers: Lotic mesocosm approach. Ecol. Indic., 11(2): 489-499.

Salem, Z., Ghobara, M. and El-Nahwary, A.A. 2017. Spatiotemporal evaluation of the surface water quality in the middle Nile Delta using Palmer's algal pollution index. Egypt. J. Basic Appl. Sci., 4(3): 219-226.

Shahare, P.C. 2017. Phytoplankton as pollution indicator using Palmer index of Chulband river, Gondia District, India. Int. J. Res. Biosci. Agric. Tech., 5(1): 72-75.

Stevenson, J. 2014. Ecological assessments with algae: A review and synthesis. J. Physiol., 50(3): 437-461.

Seriño, E.K.L. and Belonias, B.S. 2020. Planktonic algae as bioindicators of water quality in Pagbanganan River, Baybay City, Leyte. Annal. Trop. Res., 42(2): 43-51.

Suthers, I., Bowling, L., Kobayashi, T. and Rissik, D. 2009. Sampling Methods for Plankton: In Suther, I. and Rissik, D. (eds), Plankton: A Guide to their Ecology and Monitoring of Water quality. Cambridge University Press, Cambridge, pp 73-114.

Tickner, D., Parker, H., Moncrieff, C., Oates, N., Ludi, E. and Acreman, M. 2017. Managing rivers for multiple benefits – A coherent approach to research, policy, and planning. Front.Environ. Sci., 5 (4): 1-8.

Xia, L., Zhu, Y. and Zhao, Z. 2020. Understanding the ecological response of planktonic and Benthic epipelic algae to environmental factors in an urban river system. Water, 12(5): 1311.

Water Environment Federation (WEF). 2022. Standard Methods for the Examination of Water and Wastewater. 24th edition. American Public Health Association, Washington DC.

# Leachate Characterization and Assessment of Soil Pollution Near Some Municipal Solid Waste Transfer Stations in Baghdad City

**Nabaa S. Hadi**

Department of Environmental Engineering, College of Engineering, University of Babylon, Babylon, Iraq
†Corresponding author: Nabaa S. Hadi; nabaa.hadi@uobabylon.edu.iq

## ABSTRACT

This study is conducted to determine the extent to which transfer stations in the Karkh neighborhood of Baghdad, Iraq, contribute to physicochemical and heavy-metal contamination of the soils in the immediate area. The concentrations of physicochemical primary indicators (pH, OC, OM, $Ca^{+2}$, $Mg^{+2}$, $Na^{+1}$, $NO_3^{-1}$, $Cl^{-1}$, $SO_4^{-2}$) and heavy metals (Pb, Cd, and Cu) were measured during July 2022 at four investigation sites that were located at distances of 5 m (Site 1), 10 m (Site 2), 15 m (Site 3), and 20 m (Site 4) from the edges of the mentioned transfer stations (Al-Rasheed, Al-Mansour, Al-Shula, and Al-Dora). The concentrations of the physico-chemicals and heavy metals were compared to the standards of the Food and Agriculture Organization (FAO) and the Consensus-Based Sediment Quality Guidelines (CBSQG). Based on the data collected, it was determined that Site 1 had the greatest physico-chemical and heavy metal concentrations, whereas Site 4 had the lowest. The metals tested were found to accumulate in the following order: Cu > Pb > Cd. Additionally, it was noticed that all the measured concentrations of metals were higher than the limitations of the CBSQG. The presence of $Ca^{+2}$, $Mg^{+2}$, $Na^{+1}$, Pb, Cd, and Cu in soil suggests that leachate percolation is having a major impact on the soil.

## INTRODUCTION

The most environmentally friendly method of solid waste disposal is still a problem in virtually all industrialized nations due to many political, environmental, economic, and social restrictions (Adani et al. 2000, Glewa & Al-Alwani 2013). Numerous studies in recent years have looked at how solid waste leachate affects soil (Eyankware et al. 2016, Okeke et al. 2019, Ruth et al. 2021, Hussieny et al. 2022, Rysul et al. 2022). Assessing soil and groundwater pollution has been done in a variety of ways. It may be evaluated either by experimental detection of contaminants or through computational simulations of their concentrations (Saarela 2003, Moo-Young et al. 2004, Mirbagheri et al. 2009, Bilgili 2011, Siddique et al.2021, Liu & Wang 2022).

After Cairo, Baghdad is the biggest city in the Arab world and the capital of Iraq. The population was counted at 8,780,422. Located in a mostly agricultural zone, the Tigris River provides considerable irrigation for a diverse variety of crops. Unfortunately, most soil quality is harmed by leachate that enters the soil via seepage and infiltration. The city of Baghdad has a widespread problem with open dumping. The contamination of soil and groundwater systems by leachate from these sites is a major threat to the local ecosystem.

Water percolates into a landfill, interacting with refuse and absorbing Calcium, magnesium, potassium, nitrogen, and ammonia are common elements found in leachate, as are trace metals like iron, copper, manganese, chromium, nickel, and lead, and organic compounds like phenols, polyaromatic hydrocarbons, acetone, benzene, toluene, chloroform, and so on (Freeze & Cherry1979). Both leachate and water contain varying concentrations of these substances, which are affected by the wastes' makeup (Alker et al. 1995). During a leachate's travel through the soil, some of the contaminants may be adsorbed onto the medium. In essence, the trace elements and contaminants are particularly adsorbed onto the fine soil and sediment particles with more surface area (Varkouhi 2009).

Municipal solid waste (MSW) has become a big challenge for environmental authorities since it not only pollutes subsurface waterways and surface water bodies with a diverse variety of organic and inorganic pollutants (Idowu et al. 2019, Ding et al. 2021, Xu et al.2022) but also significantly pollutes the surrounding soils. In addition, landfills emit greenhouse gases that contribute to global warming, resulting in environmental disasters and increased water consumption (Zubaidi et al. 2018, Liu et al. 2021, Nhien & Giao 2022). In Iraq, the published literature

indicates that the generation of the MSW has also rapidly increased during the last 15 years and, unfortunately, it still follows an increasing trend (Chabuk et al. 2015, Abdulredha et al. 2017, Zubaidi et al. 2019, Abdulredha et al. 2020). Therefore, this study aims to evaluate the impacts of solid waste leachate on soil.

## MATERIALS AND METHODS

### Leachate

Due to the lack of a leachate collector on-site, four independent samples of leachate were taken from waste compactor trucks destined for each transfer station (Al-Rasheed, Al-Mansour, Al-Shula, and Al-Dora). They mixed all samples before being subjected to analysis for various elements (APHA 2005).

### Soil

Sixteen drill holes were brought from four transfer stations to measure soil pollution. In July 2022, soil samples were collected from four different locations (1, 2, 3, and 4) at 5, 10, 15, and 20 meters from each transfer station. These samples were taken using a soil drill at a depth of 50 centimeters. As soon as soil samples were obtained, they were sealed in plastic bags, labeled, and sent to the lab to prevent the spread of any microorganisms. The obtained samples were treated and prepared according to the method of soil analysis (Page et al. 1982, Khan et al. 2008). All powdered samples were sieved through a 2 mm screen to get rid of any larger stones or pebbles.

### Physical Properties

With the use of a pH meter, we were able to figure out what the pH level of the saturation paste extract was obtained according to (APHA 2005). Analyzing the soil's main particle size by sieving as well as its particle-size distribution after air-drying soil samples are both possible. The dried samples are soaked in water on a tray and then combined with either 1 gram of sodium hydroxide or 1 gram of sodium carbonate per litter of water as a dispersing agent before being transferred to a 1000-ml jar for hydrometer measurement (Das 1989).

### Chemical Properties

The soil was chemically analyzed using the Standard Method of Soil Analysis (Page et al. 1982). Soil's chemical was analyzed after being extracted from its solid (the soil) form into a liquid (the solvent). Different elements need different extraction techniques. However, the saturation extract may be used to quantify several components, such as $Ca^{+2}$, $Mg^{+2}$,

$Na^{+1}$, $NO_3^{-1}$, $Cl^{-1}$, $SO_4^{-2}$, Pb, Cd, and Cu.

### (EDS, SEM)

Energy Dispersive X-ray Spectroscopy (EDS or EDX) is an analytical technique used to identify and characterize the elemental composition of four samples of soil taken from transfer stations. Using a scanning electron microscope (SEM) equipped with an X-ray detector, atoms within soil samples are excited by an electron beam.

### Study Area

The Municipality of Baghdad has been responsible for the civil works within its implementation of the project to establish nine transfer stations in Baghdad City, four of which are on the Karkh side (Al-Rasheed, Al-Mansour, Al-Shula, and Al-Dora) and five on the Rusafa side (Al-Sadr, Al-Shaab, Al-Rusafa Center, Al-Ghadir, and Al-Karrada). All the municipal departments transport municipal waste from the transfer stations to only one landfill site in the Al-Nabai area, outside the borders of the Baghdad governorate and near the district of Tarmiyah, which is a random site and does not have environmental approval.

The purpose of this type of station is to collect and compress waste into closed containers and then transfer it by specialized mechanisms to sanitary landfill sites in a way that helps reduce the volume of waste by an average of one-third. The design capacity of one station is 500 "tonnes" per day, and in exceptional cases, it reaches 1000 "tonnes" per day. The transfer stations are intermediate places for solid waste collection. They contain scales to weigh the collected waste and compress it by pistons to be then unloaded into tankers (trailers) of large sizes designated for this purpose to be transported to sanitary landfill sites. Domestic garbage such as food scraps, paper, plastic, glass, cardboard, and clothing are all accepted in these dumps. Sand, bricks, and concrete blocks from demolition and construction projects are also discarded.

The lands adjacent to the transfer stations (Al-Rasheed, Al-Mansour, Al-Shula, and Al-Dora) are virgin (untouched, not plowed), not lands of agricultural use. There are no major industrial sites or other objects that might have an impact on soil quality close to the transfer stations.

## RESULTS AND DISCUSSION

### Leachate Characterization

Characterization of leachate has been done, and the results are shown in Table 1 to help us comprehend the effect leachate quality has on the soil.

The composition of the solid waste and the amount of water in the trash as a whole are the two most important

Table 1: Characterization of leachate quality.

| No. | Parameter | Value |
|-----|-----------|-------|
| 1 | pH | 7.33 |
| 2 | EC [dS.m$^{-1}$] | 17.4 |
| 3 | TSS [g.L$^{-1}$] | 14.48 |
| 4 | TDS [mg.L$^{-1}$] | 10561 |
| 5 | Hardness | 8.04 |
| 6 | HCO$_3$ [meq.L$^{-1}$] | 7.65 |
| 7 | Na$^{+1}$ [meq.L$^{-1}$] | 16.59 |
| 8 | Ca$^{+2}$ [meq.L$^{-1}$] | 87.05 |
| 9 | Mg$^{+2}$ [meq.L$^{-1}$] | 59.31 |
| 10 | K [meq.L$^{-1}$] | 5.03 |
| 11 | SAR | 1.54 |
| 12 | Cl$^{-1}$ [meq.L$^{-1}$] | 145.01 |
| 13 | Cu [ppm] | 35.2 |
| 14 | Zn [ppm] | 65.2 |
| 15 | Pb [ppm] | 44.29 |
| 16 | Fe [ppm] | 102.45 |
| 17 | Cd [ppm] | 0.00124 |

factors influencing the leachate's physical and chemical properties. After testing, it was determined that the pH of the obtained sample was 7.33. Both the EC (17.4 dS.m$^{-1}$) and TDS (10,561 mg.L$^{-1}$) are quite high, suggesting the presence of inorganic matter in the samples. Because of the high concentration of Fe (102.45 ppm) in the leachate sample, it is possible that steel scrap and other ferrous metals were also deposited at the site. The dark brown color of the leachate is mostly due to ferrous oxidation to ferric and the subsequent formation of ferric hydroxide colloids and complexes with fulvic/humic material (Chu et al. 1994). A Zn reading of 65.2 ppm in leachate suggests that the landfill has been polluted by waste from batteries and CFLs. The presence of lead (44.29 ppm) in the leachate samples indicates that lead-acid batteries, lead-based paints, and lead-based pipes were discarded in the landfill (Moturi et al. 2004, Mor et al. 2006). The lead levels are between the threshold effect levels (TEL) and the probable effect level (PEL), indicating that adverse effects on biota are predicted to occur occasionally (Varkouhi 2009). Cu (35.2 ppm) and Cd (0.00124 ppm) values were also detected in leachate samples. The very low concentrations of Cd are consistent with significantly reduced effects of mining land-use practices in urban areas (Varkouhi 2007).

## Soil Characterization

Soil physicochemical characteristics at the location of the transfer stations are listed in Table 2. According to Table 2, this kind of soil is called loamy sand. A grain size study showed that sand ranged from 752 to 872 milligrams per kilogram of soil, silt from 100 to 200 milligrams per kilogram of soil, and clay from 28 to 68 milligrams per kilogram of soil. Higher levels of moisture in the garbage and landfill are correlated with more microbial activity and more organic material (Akinbile 2012).

## Energy Dispersive Spectroscopy (EDS) of Soil Samples

Acidity levels in soil samples ranged from 7.42 to 7.41 and 7.09 to 6.99, indicating the soil's exceptional buffering ability. The soils were categorized as loamy sand soils based on particle-size distributional analysis. Fig. 1 shows the energy dispersive x-ray spectroscopy (EDS) curve for soils, which shows that Si, Ca, K, S, Cl, Mg, Al, Na, Mg, Sb, and Fe are present in relatively high amounts.

## Scanning Electron Microscopy (SEM) of Soil Samples

The soil at transfer stations was characterized using scanning electron microscopy (SEM) images of soil particles and pore architecture. Soil from Al-Mansour, Al-Rasheed, Al-Shula, and Al-Dora was enlarged to 20 m using scanning electron microscopy (SEM) near transfer stations. Fig. 2 displays the soil samples' morphological properties according to (Wang et al. 2017). The white coating on the soil's surface in Fig. 2 (a, b, c, and d) is owing to the pollution residues that have saturated the soil's particles. As a result of this decreased sorption, no more contaminants will be taken up by the soil (Rashid & Faisal 2018, Safia et al. 2021).

## Soil Analysis

Soil samples were taken from four locations, five to twenty meters from the edge of each of the transfer stations under study, as described above. From what can be seen

Table 2: Physical properties of soil class in the transfer Stations Baghdad city (%).

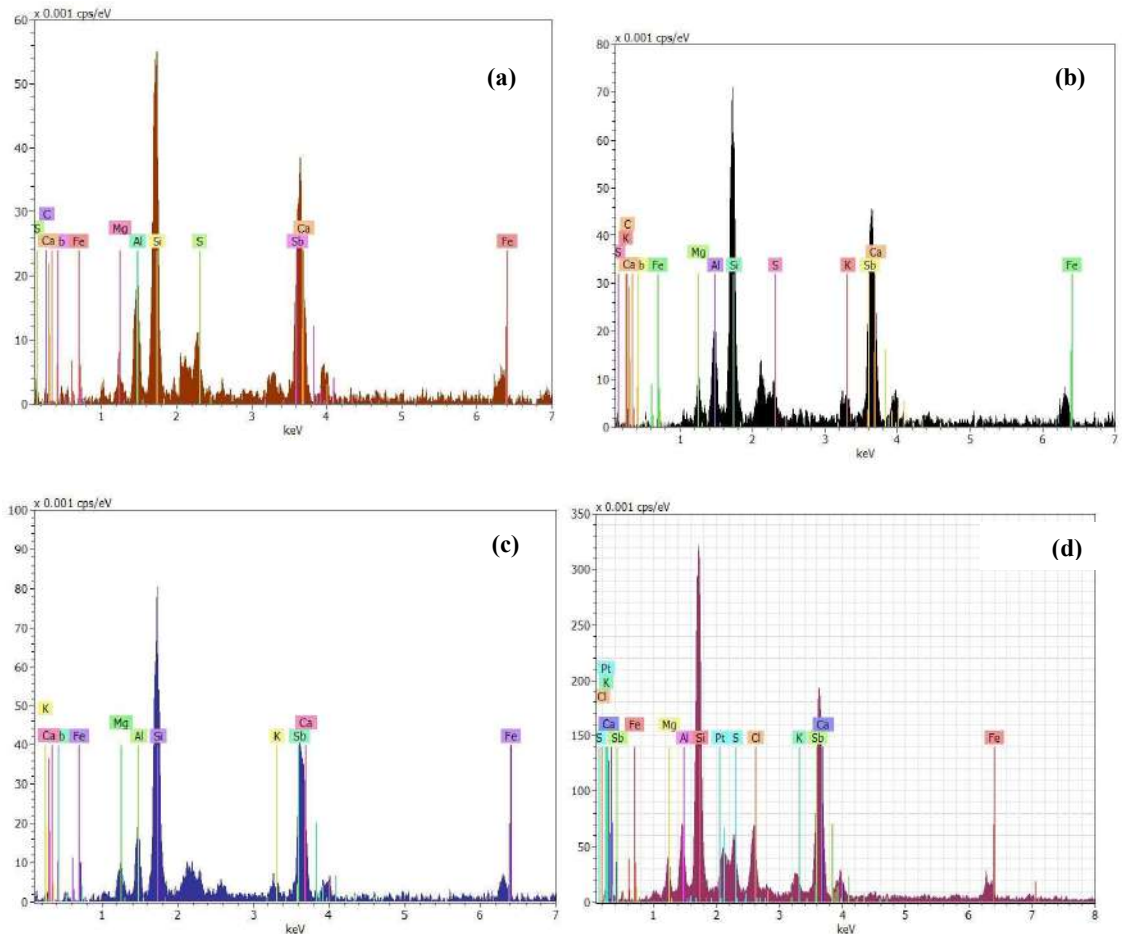| Locations | Moisture content [%] | Porosity [%] | Grain size analysis [g.kg$^{-1}$.soil$^{-1}$] | | | |
|-----------|----------------------|--------------|------|------|------|--------------|
| | | | Sand | Clay | Silt | Tissue class |
| Al-Mansour | 3.3 | 0.42 | 772 | 48 | 180 | Loamy Sand |
| Al-Rasheed | 1.7 | 0.41 | 792 | 68 | 140 | Loamy Sand |
| Al-Shula | 2.9 | 0.46 | 752 | 48 | 200 | Loamy Sand |
| Al-Dora | 4.3 | 0.48 | 872 | 28 | 100 | Loamy Sand |

Fig. 1: EDS for the composition of the soil sample:
(a) Al-Mansour soil, (b) Al-Rasheed soil, (c) Al-Shula soil, (d) Al-Dora soil.

in Figs. 3-14, it seems that when distance is put between a certain location and the transfer stations, concentrations of the various physicochemical and heavy metals under study diminish. There may be many causes for the correlation between distance and physiochemical and metal concentrations.

The first is a condition known as "seepage," in which the pollutants are concentrated in a small area around the transfer station locations because the leached water from the collected MSW is insufficient to spread over great distances.

Secondly, recent years have seen less rainfall and more dryness, which has reduced the amount of surface runoff that may leak into the landfill and wash contaminants into the soil and water sources nearby.

Third, the concentrations of the studied physicochemical ($Ca^{+2}$, $Mg^{+2}$, $Na^{+1}$) and heavy metals (Pb, Cu, and Cd)

Were higher than the stated limits by the (FAO 2012, CBSQG 2003), the limit values for $Ca^{+2}$ (0.5988 meql), $Mg^{+2}$ (0.0822 meql), and $Na^{+1}$ (0.0260 meql), and Pb (0.036 ppm), Cu (0.032 ppm), and Cd (0.001 ppm).

Finally, Cu was found to have the concentration that exceeded the limit values the most, followed by Pb and Cd, the one that exceeded the least. It is possible that the chemical composition of the dumped MSW and the makeup of the soil under study are to blame for the observed fluctuation in the content of the heavy metals under study (Jawad et al. 2021). Soil fertility, as well as the capacity to farm it, may be negatively impacted by metal pollution (Hill 2005). Crops grown in polluted soil may provide a significant health risk due to heavy metals and other toxins being absorbed by the plant (Sidra 2009).

The findings emphasized the pressing need for more study into the fluctuation of heavy metals in the examined
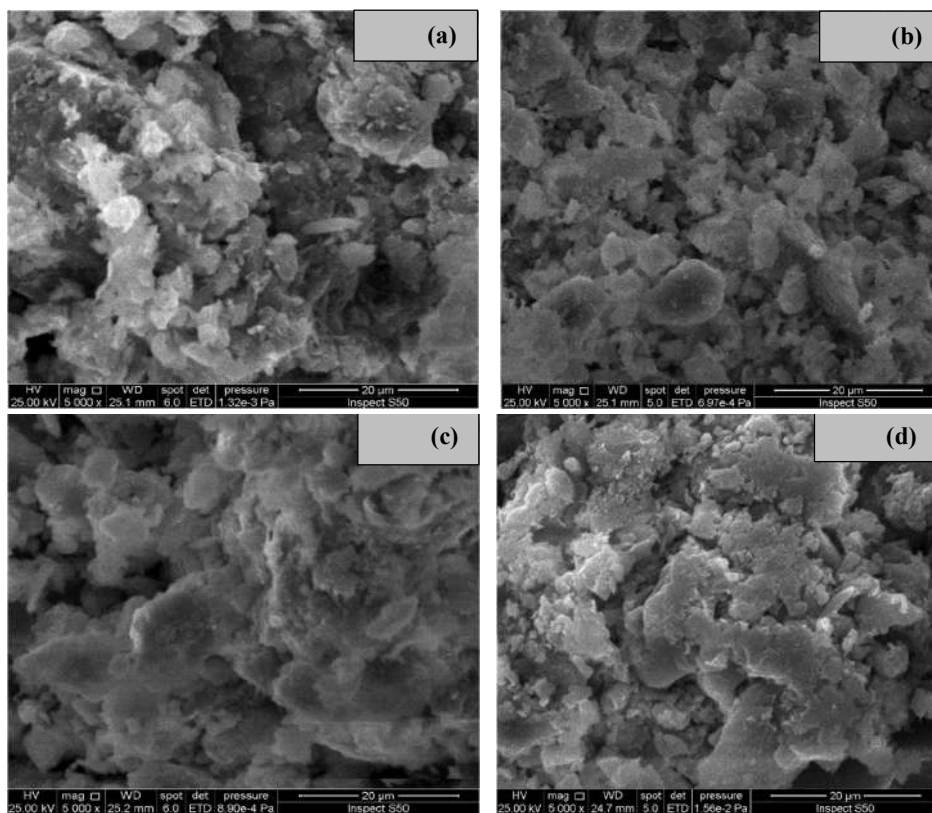
Fig. 2: SEM images for the samples:
Al-Mansour soil, (b) Al-Rasheed soil, (c) Al-Shula soil, (d) Al-Dora soil.

soil and the methods by which heavy metals are transported from transfer stations to the neighboring soils. Several studies should be undertaken throughout the rainy season to track how heavy metals are distributed around the landfill and how their concentration changes as surface runoff increases (Gkantou et al. 2019, Teng et al. 2019).

## CONCLUSIONS

The current study sought to assess the physiochemical and heavy metal concentration effects of municipal transfer stations on the soils surrounding them. It was shown that the concentration of all pollutants investigated decreased with
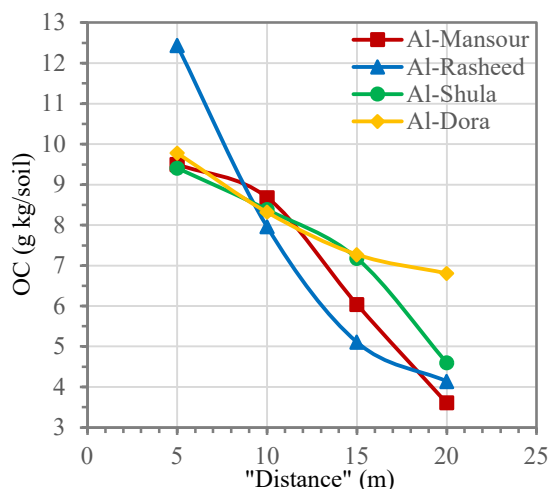


Fig. 3: Concentration of "OC" at various soil distances.
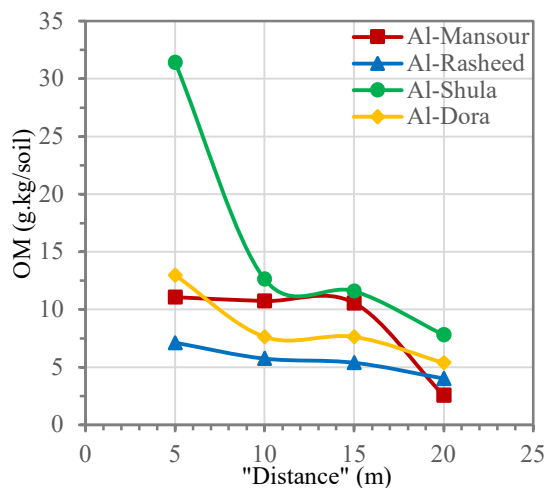


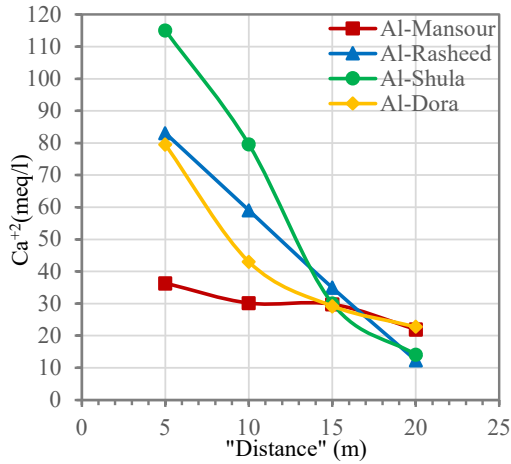Fig. 4: Concentration of "OM" at various soil distances.

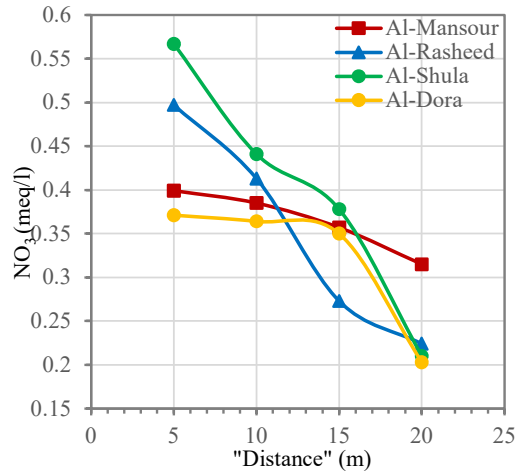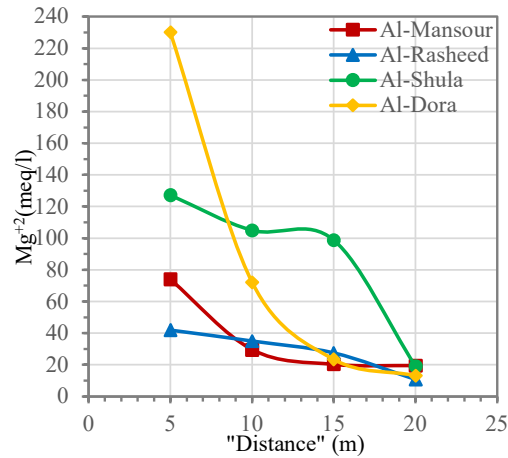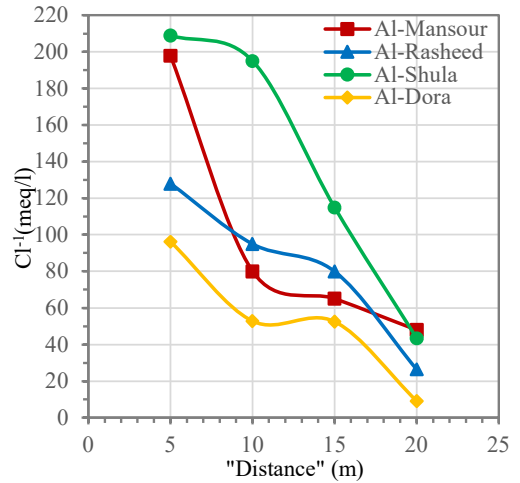Fig. 5: Concentration of "$Ca^{+2}$" at various soil distances.



Fig. 6: Concentration of "$Mg^{+2}$" at various soil distances.



Fig. 7: Concentration of "$Na^{+1}$" at various soil distances.



Fig. 8: Concentration of "$NO_3$" at various soil distances.



Fig. 9: Concentration of "$Cl^{-1}$" at various soil distances.



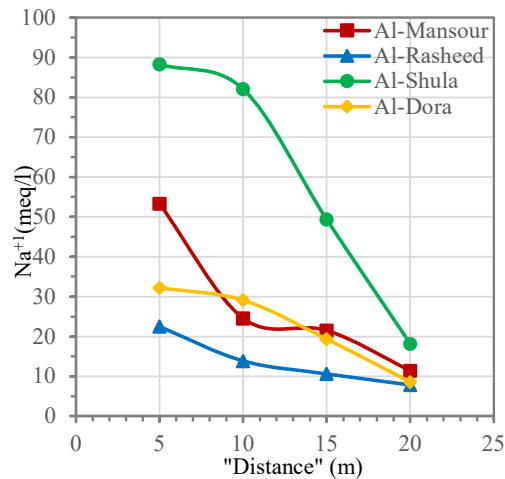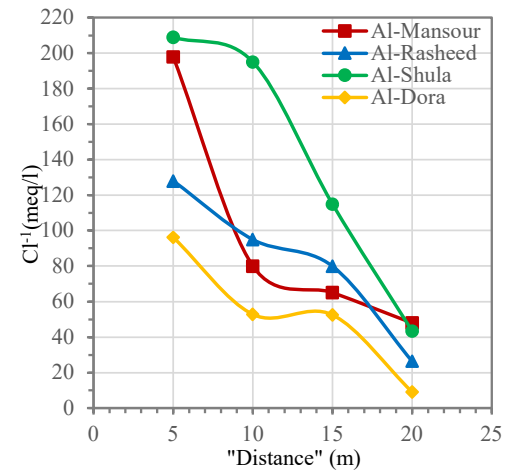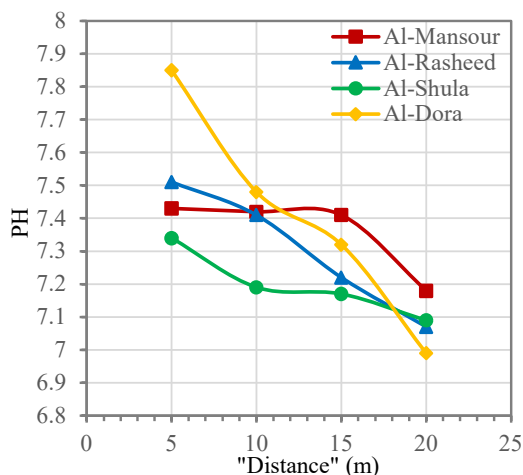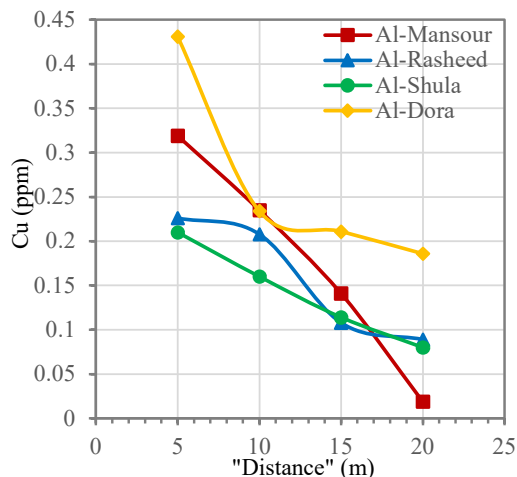Fig. 10: Concentration of "$SO_4$" at various soil distances.

Fig. 11: Concentration of "PH" at various soil distances.



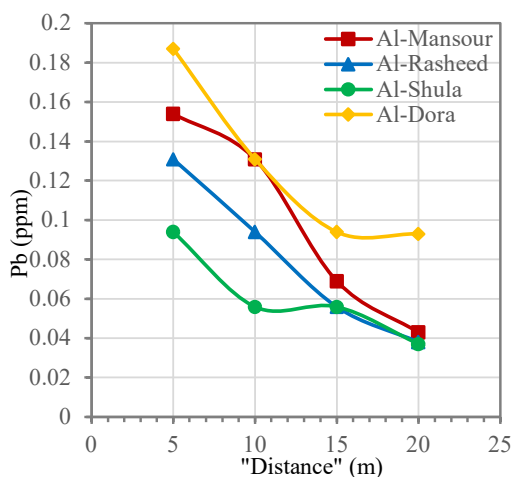Fig. 12: Concentration of "Pb" at various soil distances.



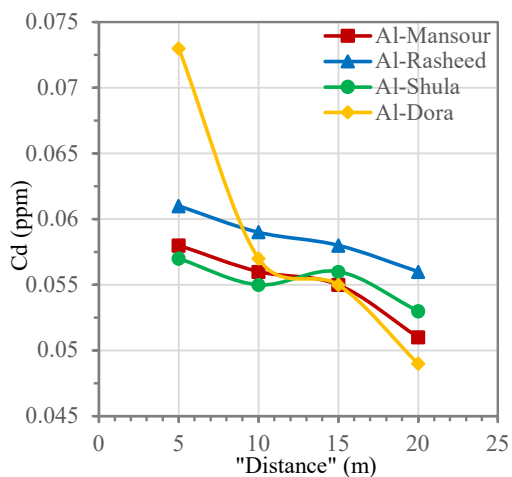Fig. 13: Concentration of "Cd" at various soil distances.



Fig. 14: Concentration of "Cu" at various soil distances.

increasing distance from the transfer stations. Furthermore, the observed concentrations of the studied ions ($Ca^{+2}$, $Mg^{+2}$, $Na^{+1}$) and heavy metals ( exceeded the FAO and CBSQG recommended limits. In the areas we looked at, copper was by far the most prevalent heavy metal, whereas cadmium was by far the least. Multiple studies are needed to understand the geological and meteorological effects of heavy metal distribution in the landfill area, including an investigation of the effects of wet weather on pollutant leaching and an analysis of the chemical composition of both the disposed MSW and the landfill's natural soil.

## ABBREVIATIONS

MSW     Municipal Solid Waste
APHA    American Public Health Association
FAO     Food and Agriculture Organization
CBSQG   Consensus-Based Sediment Quality Guidelines
SAR     Sodium Adsorption Ratio
SEM     Scanning Electron Microscope
EDS     Energy Dispersive Spectroscopy
OC      Organic Content
OM      Organic Matter

## ACKNOWLEDGEMENTS

## REFERENCES

Abdulredha, M., Al Khaddar, R., Jordan, D. and Hashim, K. 2017. The development of a waste management system in Kerbala during major pilgrimage events: determination of solid waste composition. J. Proced. Eng., 196 (7): 79-84.

Abdulredha, M., Kot, P., Al Khaddar, R., Jordan, D. and Abdulridha, A. 2020. Investigating municipal solid waste management system performance during the Arba'een event in the city of Kerbala, Iraq. Environ. Dev. Sustain., 22: 1431-1454.

Adani, F., Scatigna, L. and Genevini, P. 2000. Biostabilization of mechanically separated municipal solid waste fraction. J. Waste Manag. Res., 18(5): 471-477. https://doi.org/10.1177/0734242X0001800508

Akinbile, C.O. 2012. Environmental impact of landfill on groundwater quality and agricultural soils in Nigeria. J. Soil Water Res., 7(1):18–26

Alker, S.C., Sarsby, R.W. and Howell, R. 1995. Composition of leachate from waste disposal sites. Proceed. Waste Disp. Landfill-Green, 93: 215-221.

American Public Health Association/American Water Works Association/Water Environment Federation (APHA) 2005. Standard Methods for the Examination of Water and Wastewater. 21st Edition. APHA, Washington DC.

Bilgili, M. 2011. Migration behavior of landfill leachate contaminants through alternative composite liners. Sci. Tot. Environ., 409: 3183-3196.

Consensus-Based Sediment Quality Guidelines of Wisconsin (CBSQG). 2003. Consensus-Based Sediment Quality Guidelines; Recommendations for Use and Application Interim Guidance. Department of Natural Resources, Wisconsin, p. 35

Chabuk, A., Al-Ansari, N., Hussain, H., Knutsson, S. and Pusch, R. 2015. Present status of solid waste management at Babylon governorate, Iraq. Engineering, 7: 408–423.

Chu, L.M., Cheung, K.C. and Wong, M. H. 1994. Variations in the chemical properties of landfill leachate, Environ. Manag., 18: 105-117.

Das, B. 1989. Soil Mechanics Laboratory Manual, 3$^{rd}$ ed, California, Engineering.

Ding, Y., Zhao, J., Liu, J.W., Zhou, J., Cheng, L., Zhao, J., Shao, Z., Iris, Ç., Pan, B., Li, X. and Hu, Z.T. 2021. A review of China's municipal solid waste (MSW) and comparison with international regions: Management and technologies in treatment and resource utilization. J. Clean. Prod., 293: 126144.

Eyankware, M., Eyankware, O. and Ulakpa, R. 2016. Assessment of impact of leachate on soil physicochemical parameters in the vicinity of Eliozu dumpsite, Port Harcourt, Nigeria. Basic Resour. J. Soil Environ. Sci., 4(2): 15-25.

Food and Agriculture Organization (FAO). 2012. Investing in Agriculture for a Better Future. Food and Agriculture Organization, UN, Rome, Italy.

Freeze, R.A. and Cherry, J. A. 1979. Ground Water. Englewood Cliffs, NJ: Prentice-Hall.

Gkantou, M., Muradov, M., Kamaris, G.S., Hashim, K., Atherton, W. and Kot, P. 2019. Novel electromagnetic sensors embedded in reinforced concrete beams for crack detection. Sensors, 19(23): 5175. https://doi.org/10.3390/s19235175

Glewa, S.M. and Al-Alwani, M. 2013. Evaluation of the effect of solid waste leachate on soil at Hilla City. Babylon J. Eng. Sci., 3(21): 894-906.

Hill, M. J. 2005. Role of Gut Bacteria in Human Toxicology and Pharmacology. Taylor & Francis published, UK.

Hussieny, M., Morsy, M., Ahmed, M., Elagroudy, S. and Abdelrazik, M. 2022. Municipal solid waste and leachate characterization in the Cairo metropolitan area. Resources, 11: 102. https:// doi.org/10.3390/resources11110102.

Idowu, I.O., Atherton, W., Hashim, K.S., Kot, P., Alkhaddar, R.M., Alo, B.I. and Shaw, A. 2019. An analysis of the status of landfill classification systems in developing countries: Sub-Saharan Africa landfill experiences. J. Waste Manag., 87: 761-771. https://dx.doi.org/10.1016/j.wasman.2019.03.011

Jawad, M., Suad, M., Saheb, K., Saad, A., David, Y., Mawada, A. and Ahmed, A. 2021. Assessment of the effects of municipal landfills on the metal pollution in the surrounding soils: A case study in Iraq.

IOP Conf. Series: Mater. Sci. Eng., 15: 1058. doi:10.1088/1757-899X/1058/1/012008

Khan, S., Cao, Q., Zheng, Y., Huang, Y. and Zhu, Y. 2008. Health risks of heavy metals in contaminated soils and food crops irrigated with wastewater in Beijing, China. J. Environ. Pollut., 152(3): 686-692. http://10.1016/j.envpol.2007.06.056

Liu, X, Chen, S., Yan, X., Liang, T., Yang, X., El-Naggar, A., Liu, J. and Chen, H. 2021. Evaluation of potential ecological risks in potential toxic elements contaminated agricultural soils: Correlations between soil contamination and polymetallic mining activity. J. Environ. Manag., 300: 113679.

Liu, X. and Wang, Y. 2022. Identification and assessment of groundwater and soil contamination from an informal landfill site. Sustainability,14:16948. https://doi.org/10.3390/su142416948.

Mirbagheri, S., Monfared, S. and Kazemi, H. 2009. Simulation modeling of pollutant transport from leachate in Shiraz landfill. J. Environ. Earth Sci., 59: 287-296.

Moo-Young, H., Johnson, B., Johnson, A., Carson, D., Lew, C., Liu, S. and Hancock, K. 2004. Characterization of infiltration rates from landfills: Supporting groundwater modeling efforts. Environ. J. Monit. Assess., 96(1-3): 283-311. https:// 10.1023/b:emas.0000031734.67778.d7.

Mor, S., Ravindra, K., Vischher, A., Dahiya, R.P. and Chandra, A. 2006. Municipal solid waste characterization and its assessment for potential methane generation at Gazipur Landfill Site, Delhi: A case study. Sci. Tot. Environ., 371: 1-10. https://doi.org/10.1016/j.scitotenv.2006.04.014

Moturi, M.C.Z., Rawat, M. and Subramanian, V. 2004. Distribution and fractionation of heavy metals in solid waste from selected sites in the industrial belt of Delhi, India. J. Environ Monit Assess., 95(1-3): 183-199. https://10.1023/b:emas.0000029900.86810.85.

Nhien, H.T. and Giao, N.T. 2022. Assessment of pollution levels and ecological potential risk of the soil influenced by landfilling in a Vietnamese Mekong Delta province. Sci. Total Environ., 845:157263.

Okeke, I., Okagu, T., Okonkwo, V. and Ezeagu, A. 2019. Effect of municipal solid waste leachate on the geotechnical properties of soil. Int. J. Eng. Sci. Inv., 8(7): 40-52.

Page, A., Millers, R. and Keeney, D. 1982. Methods of soil analysis part 2: Chemical and microbiological properties. Am. Soc. Agro., 1159: 6105.

Rashid, H.M. and Faisal, A.H. 2018. Removal of dissolved cadmium ions from contaminated wastewater using raw scrap zero-valent iron and zero-valent aluminum as locally available and inexpensive sorbent wastes. Iraqi J. Chem. Petrol. Eng., 19(4): 39-45. https://doi.org/10.31699/IJCPE.2018.4.5

Ruth, O., Wisdom, C. and Moses, O. 2021. Quantitative analysis of physical and chemical attributes of soil around power-line dumpsite at Boji-Boji Owa, Delta State, Nigeria. World News Nat. Sci., 35: 118-134.

Rysul, H., Bakar, S., Ahedul, A., Aftab, A. and Mostafizur, R. 2022. Impacts of Landfill Leachate on the Surrounding Environment: A Case Study on Amin Bazar Landfill, Dhaka (Bangladesh). J. Soil Syst., 6(4): 90. https://doi.org/10.3390/soilsystems6040090

Saarela, J. 2003. Pilot investigations of surface parts of three closed landfills and factors affecting them. J. Environ Monit Assess., 84(1-2): 183-192. https://10.1023/a:1022859718865.

Safia, M.K., Hassan, F., Abdelazim, N. and Ahmed T. 2021. Measuring the engineering properties of landfill leachate-contaminated soil in Egypt. Euro-Mediterr. J. Environ. Integr., 6(23): 1-12.

Siddique, A.B., Islam, A.R., Hossain, S., Khan, R., Akbor, A., Sajid, W.M., Mia, Y., Mallick, J. and Rahman, M.S. 2021. Multivariate statistics and entropy theory for irrigation water quality and entropy-weighted index development in a subtropical urban river, Bangladesh. J. Environ. Sci. Pollut. Res., 29: 8577-8596.

Sidra K. 2009. Distribution and fractionation of heavy metals in solid waste from selected sites. J. Sci. Technol. Dev., 28(14): 65-73.

Teng, K.H., Kot, P., Muradov, M., Shaw, A., Hashim, K., Gkantou, M. and Al-Shamma'a, A. 2019. Embedded smart antenna for non-destructive testing and evaluation (NDT&E) of moisture content and deterioration in concrete. Sensors, 19(3): 547-559. https://doi.org/10.3390/s19030547

Varkouhi, S. 2007. Geochemical Evaluation of Lead Trace Element in Streambed Sediments. Proceedings of the WSEAS Int. Conf. on Waste Management, Water Pollution, Air Pollution, Indoor Climate, Arcachon, France, pp. 262-268.

Varkouhi, S. 2009. Lead in Sarbaz river basin sediments, Sistan and Baluchestan, Iran. J. Integr. Environ. Assess. Manag., 5(2): 320-330. https://doi.org/10.1897/IEAM_2008-077.1

Wang, H., Liu, T., Feng, S. and Zhang, W. 2017. Metal removal and associated binding fraction transformation in contaminated river sediment washed by different types of agents. PloS ONE, 12(3): e0174571. https://doi.org/10.1371/journal.pone.0174571

Xu, X., Li, G., Ni, D., Feng, C. and Xu, S. 2022. Laboratory model tests of leachate drawdown using vertical drainage wells with vacuum pumping in municipal solid waste landfills with high leachate levels. Sustainability., 14(13): 8101. https://doi.org/10.3390/su14138101

Zubaidi, S.L., Al-Bugharbee, H., Muhsen, Y.R., Hashim, K., Alkhaddar, R.M., Al-Jumeily, D. and Aljaaf, A.J. 2019. The prediction of municipal water demand in Iraq: A case study of Baghdad governorate. Int. Conf. Dev. Sys. Eng., 116: 789.

Zubaidi, S.L., Kot, P., Alkhaddar, R.M., Abdellatif, M. and Al-Bugharbee, H. 2018. Short-Term Water Demand Prediction in Residential Complexes: Case Study in Columbia City, USA. In: 11th International Conference on Developments in eSystems Engineering (DeSE), University of Cambridge, UK, IEEE, NY, pp. 15-42.

# Carbon Emission and Industrial Structure Adjustment in the Yellow River Basin of China: Based on the LMDI Decomposition Model

**J. Song \*†, W. J. Du\*\* and F. Wang\*\*\***

\*School of Humanities, Political Science and Law, Henan University of Engineering, Xinzheng, 451191, China
\*\*School of Public Policy and Administration, Nanchang University; Nanchang, 330031, China
\*\*\*School of Information Engineering, Henan University of Animal Husbandry and Economy, Zhengzhou, 450044, China
†Corresponding author: Jie Song; songjie@haue.edu.cn

## ABSTRACT

In the context of promoting high-quality development in the Yellow River Basin (YRB) of China, urgent action is needed to achieve the "Dual Carbon" goal through energy savings, emission reductions, and industrial upgrading. This study measures carbon emissions from eight types of energy consumption across 43 industries from 2000 to 2019. Using the Kaya-LMDI model, factors affecting carbon emissions are analyzed, and the relationship between industrial structure and carbon emissions is explored through the coefficient of variation (CV). The findings reveal that coal consumption remains significantly higher than other energy sources, and the effect of energy structure adjustment on carbon emission reduction is limited compared to the impact of energy consumption increase on carbon emission growth. Moreover, the economic output effect is identified as the primary driving factor of carbon emissions, while energy utilization rate is crucial in achieving energy savings and emission reductions. Finally, the CV of carbon emissions across 43 industries is increasing. Based on these results, we suggest several policy recommendations, including prioritizing ecological concerns, developing comprehensive and scientifically sound plans, optimizing energy consumption structure, improving energy utilization efficiency, and adjusting industrial structure to promote sustainable development in the YRB.

## INTRODUCTION

In the new era, China's YRB faces multiple opportunities, such as the new development pattern of "Double Cycle," the strategy of ecological protection and high-quality development, and the coordinated development of regions. In September 2020, General Secretary Xi Jinping stated that "China will strive to achieve a carbon peak by 2030 and strive to achieve carbon neutrality by 2060." "Dual Carbon" is a strategic move to achieve high-quality development, which brings about profound changes in the economy and society. The economic activities in the YRB should be limited to the sustainable range of resources and environment; new emerging industries should be developed to promote clean production for sustainable, high-quality development. The principles for functional positioning and governance systems in the YRB are "water conservation priority" and "integrated planning, coordinated promotion." On the one hand, 9 provinces along the YRB are subject to the dilemma of water shortage and a fragile ecological environment; on the other hand, they face challenges such as the slow transformation

of industry upgrading and backward development of strategic emerging industries (Song 2021). Under the "Dual Carbon" goal, the YRB should urgently replace the old drivers, improve energy utilization, upgrade the industry, and implement an innovation-driven development strategy.

In terms of industrial structure and carbon emissions, from the existing research results, there are significant regional differences in the relationship between industrial structure and carbon emissions, and the way and intensity of industrial structure in different regions are different. There was an obvious inconsistency between carbon emission efficiency and the industrial structure upgrade in China from the aspect of regional dynamic distribution in 1997-2016 (Zhou & Wang 2019). The upgrading industrial structure effectively restrained carbon emissions at the national level and in the eastern region, while the central and western regions increased carbon emissions in 2004-2008 (Wang & Wang 2019). Industrial structure upgrades and carbon emissions efficiency in the central region of China have not yet formed a two-way interaction. Carbon emissions

efficiency has insufficient impetus to improve industrial structure upgrades (Liu et al. 2022). The distortion of the industrial structure will lead to increased local carbon emission intensity and produce reverse spillover to adjacent areas (You et al. 2022). Research on the correlation between carbon emissions and industrial structure in the Yellow River Basin shows that industries have shown high energy consumption and high emissions for a long time in YRB (Zhao et al. 2023, Ren & Dou 2022), and the carbon emission efficiency of 9 provinces in YRB is significantly different (Zhang & Xu 2022).

LMDI is the most widely used factor decomposition model. ANG Beng Wah analyzed and studied decomposition methods in the energy field and compared them with specific examples, concluding that LMDI is more suitable for decomposition research of problems in the field of energy (Ang 2004, 2015). Related research includes carbon emissions of a specific industry, such as the steel industry (Pan et al. 2023), transportation industry (Yang et al. 2022), and carbon emissions in a certain region, such as a national region, a certain province (Liu. et al. 2023) or the Yellow River Basin (Chen et al. 2022), the Yangtze River (Hu et al. 2022), etc. It is considered that the LMDI method is very suitable for the decomposition analysis of energy consumption and carbon emissions (Su et al. 2023).

Through a review of previous studies, we found that the existing studies have made some achievements in coordinating the contradiction between the development of the economy and emission reduction. Still, there are some gaps in the literature. Firstly, existing studies have mainly focused on overall industrial structure, rationalization of industrial structure, advanced industrial structure, and a specific industry or province and region. Still, few have examined the carbon emissions from energy consumption in the different industries. Secondly, fewer studies have paid high attention to the YRB. Thirdly, the existing research on carbon emissions in the YRB is mainly about the emission characteristics of a certain industry while ignoring the carbon emission characteristics of the different industries in the YRB.

To fill the gap, this paper takes 43 industries of the five major industries in the YRB as research objects from the perspective of industry segmentation, which can reflect the distribution of carbon emissions of industries in the upstream, midstream, and downstream of the YRB. Our paper could be conducive to effectively formulating industrial development policies to control carbon emissions. Based on previous relevant studies, this paper constructs the LMDI model. It decomposes the carbon emission influencing factors of energy consumption into the energy structure effect, energy intensity effect, industrial structure effect, economic output effect, and population size effect. We analyze its contribution rate to carbon emission, respectively, and the regional differences and reasons for carbon emission intensity of industries in the YRB according to the CV method.

**Actuality of Energy Consumption in the YRB**

As a whole, from 2000 to 2019, the total energy consumption (converted into standard coal, similarly hereinafter) of the YRB increased from 17267.99 million tons to 54094.51 million tons with an average annual growth of 13.53%, reaching its highest value in 2012, and then showed a downward trend (see Fig. 1). In the energy consumption structure, coal accounted for the largest proportion, accounting for 77.29% on average, oil accounted for 21.82% on average, and natural gas accounted for 0.89% on average. The proportion of coal consumption gradually and slowly decreased in the fluctuation, with an average annual decrease of 0.13%; the proportion of petroleum consumption continued to rise slowly, with an average annual increase of 0.15%; the proportion of natural gas consumption grew fastest, with an annual increase of 6.53%.

Specifically, the raw coal consumption was more than 50% in 2000~2009, and in 2010, the proportion began to decline year by year and maintained at about 41% in 2016~2019. Coke consumption showed a slow growth trend in 2000~2016, with an average annual growth rate of 11.08%, and a downward trend in 2017, 2018, and 2019. Crude oil consumption decreased by 2.65% annually in 2000~2019. Gasoline consumption fluctuated slightly, with an average annual growth rate of 5.04%. Kerosene consumption showed a slow upward trend, with the highest proportion of 1.84% in 2017, and began to decline after 2017. Diesel consumption increased slowly, with an average annual growth of 8.53%. Fuel oil consumption decreased slowly, with an average annual decline of 4.93%. Natural gas consumption accounted for the least, increasing with an annual growth of 12.55%. It can be seen that after the "Action Plan for the Prevention and Control of Air Pollution" issued by China's State Council in 2013, which emphasized that "Coal consumption must be strictly controlled," nine provinces along the YRB promulgated the "Regulations on the Prevention and Control of Air Pollution" in 2018. The total coal consumption in the YRB has been reduced to a certain extent.

## MATERIALS AND METHODS

### Data Sources and Theoretical Models

**Study area:** The Yellow River basin covers 7 provinces (Gansu, Shangxi, Shanxi, Henan, Shandong, Sichuan, and 2 autonomous regions (Inner Mongolia, Ningxia). We use the
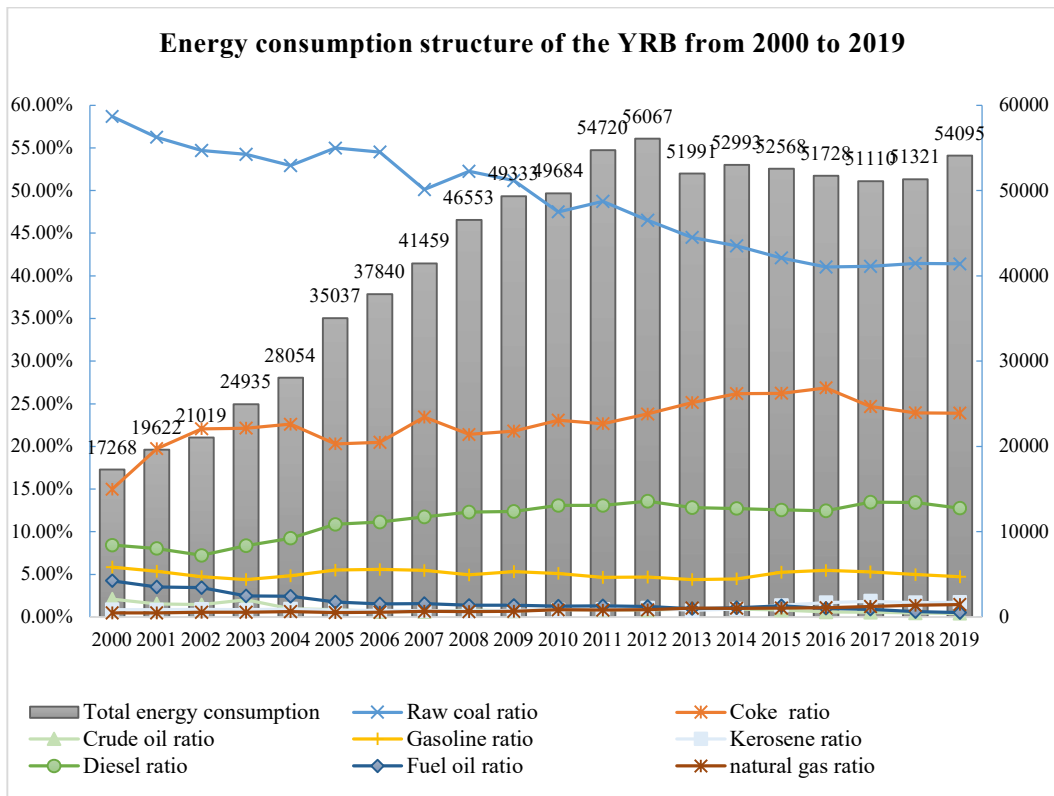
Fig. 1: Energy consumption structure of the YRB from 2000 to 2019.

word "province" to refer to these study areas throughout the rest of the paper. Upstream includes Gansu, Inner Mongolia, Ningxia, Qinghai, and Sichuan; midstream Qinghai) and includes Shangxi and Shaanxi; downstream includes Henan and Shandong. As shown in Fig. 2. The data are derived from the China Statistical Yearbook (2001-2020), China's Energy Statistical Yearbook (2001–2020), Provincial Statistical Yearbook (2001-2020), and Carbon Emission Accounts & Dataset.

**Data source and data processing:** The research objects of this paper include five industries (agriculture, the secondary industry, construction industry, transportation, post and telecommunications and software industry, wholesale and retail, and accommodation and catering industries involving 43 departments of carbon emission (see Table 1) and 8 major fossil energy sources (coal, coke, crude oil, gasoline, kerosene, diesel, fuel oil, and natural gas). According to the method provided by the Intergovernmental Panel on Climate Change (IPCC 2006) (Ren et al. 2019, He et al. 2021, Tang & Zhang 2022), the net calorific value (NCV) of energy and $CO_2$ emission factor (CEF) of each kind of fossil energy refer to Cheng Yeqing's research result (Cheng et al. 2014).The

carbon emissions from energy consumption in the YRB are estimated (see Equation (1)).

$$C = \sum_i Qf_i \times NCV_i \times CEF_i \times 10^{-9} \qquad ...(1)$$

Here, C is the total carbon emissions from energy consumption; $Qf_i$ is the consumption of the energy type i; $NCV_i$ is the net calorific value of the energy type i; $CEF_i$ is the carbon dioxide emission factor of the energy type i; i denotes energy type, i=1,2, …8.

**Kaya-LMDI Model:** The Japanese scholar Kaya Yoichi creatively proposed the Kaya identity and rewrote the Kaya identity in order to facilitate the analysis of different energy carbon emissions in different industries (see Equation (2)) (Kaya 1989).

$$C=\sum_{ij} C_{ij}=\sum_{ij} \frac{C_{ij}}{E_{ij}} \times \frac{E_{ij}}{E_i} \times \frac{E_i}{Q_i} \times \frac{Q_i}{Q} \times \frac{Q}{P} \times P \qquad ...(2)$$

Here, C is the total carbon emissions from energy consumption; $C_{ij}$ is the carbon emissions from the energy type j in the industry sector i; $E_{ij}$ is the consumption of energy type j in the industry sector i; $E_i$ is the total energy consumption in the industry sector i; $Q_i$ is the output value

Fig. 2: The research areas of the Yellow River Basin.

Table 1: Departments of carbon emission.

| Industry number | Industry name | Industry number | Industry name |
|---|---|---|---|
| 1 | Agriculture, forestry, animal husbandry and fishery | 23 | Chemical Fiber |
| 2 | Coal Mining and Dressing | 24 | Rubber Products |
| 3 | Petroleum and Natural Gas Extraction | 25 | Plastic Products |
| 4 | Ferrous Metals Mining and Dressing | 26 | Nonmetal Mineral Products |
| 5 | Nonferrous Metals Mining and Dressing | 27 | Smelting and Pressing of Ferrous Metals |
| 6 | Nonmetal Minerals Mining and Dressing | 28 | Smelting and Pressing of Nonferrous Metals |
| 7 | Other Minerals Mining and Dressing | 29 | Metal Products |
| 8 | Food Processing | 30 | Ordinary Machinery |
| 9 | Food Production | 31 | Equipment for Special Purpose |
| 10 | Wine, beverage, and refined tea manufacturing | 32 | Transportation Equipment |
| 11 | Tobacco processing | 33 | Electric Equipment and Machinery |
| 12 | Textile industry | 34 | Electronic and Telecommunications Equipment |
| 13 | Garments and Other Fiber Products | 35 | Instruments, Meters, Cultural and Office Machinery |
| 14 | Leather, Furs, Down, and Related Products | 36 | Other Manufacturing Industry |
| 15 | Timber Processing, Bamboo, Cane, Palm & Straw Products | 37 | Scrap and waste |
| 16 | Furniture Manufacturing | 38 | Electric Power, Steam, and Hot Water Production and Supply |
| 17 | Papermaking and Paper Products | 39 | Gas Production and Supply |
| 18 | Printing and Record Medium Reproduction | 40 | Tap Water Production and Supply |
| 19 | Cultural, Educational, and Sports Articles | 41 | Construction |
| 20 | Petroleum Processing and Coking | 42 | Transport, Storage, Postal & Telecommunications Services |
| 21 | Raw Chemical Materials and Chemical Products | 43 | Wholesale, Retail Trade and Catering Service |
| 22 | Medical and Pharmaceutical Products | | |

in the industry sector i; Q is the gross domestic product; P is the population size; i denotes different industry types, i=1, 2, 3, ..., 43; j denotes different energy types, j=1, 2, 3,..., 8.

Based on this, drawing on previous studies (Chen et al. 2022, Li & Wang 2008, Zhou et al. 2020, Wu et al. 2023, Jiang et al. 2021, Lai et al. 2021), this paper decomposes the carbon emission impact factors of energy consumption into carbon emission factor effect $(\Delta C_{\frac{C_{ij}}{E_{ij}}})$, energy structure effect $(\Delta C_{\frac{E_{ij}}{E_i}})$, energy intensity effect $(\Delta C_{\frac{E_i}{Q_i}})$, industrial structure effect $(\Delta C_{\frac{Q_i}{Q}})$, economic output effect $(\Delta C_{\frac{Q}{P}})$ and population size effect $(\Delta C_P)$. Based on Equation (2), according to the LMDI decomposition method (additive model), the total effect of carbon emissions is expressed as:

$$\Delta C_{tot} = C^t - C^0 = \sum_i \sum_j \ (\Delta C_{\frac{E_{ij}}{E_i}} + \Delta C_{\frac{E_i}{Q_i}} + \Delta C_{\frac{Q_i}{Q}} + \Delta C_{\frac{Q}{P}} + \Delta C_P)$$

...(3)

$C^0$ is the total carbon emissions in the base period; $C^t$ is the total carbon emissions in the period t; carbon emission factor effect is $\Delta C_{\frac{C_{ij}}{E_{ij}}}=0$ (The CV of carbon emission from various energy sources remains unchanged.) The contribution value and contribution rate of each decomposition factor are shown in Table 2:

## LMDI Decomposition of Carbon Emissions from Energy Consumption

The carbon emission of the YRB is calculated according to Equation (1), and Equation decomposes the influencing factors (4) ~ (13). The empirical results are shown in Fig. 2. On the whole, the total effect of carbon emissions in the YRB increased by 5174.58 million tons annually from 2000 to 2019, of which 13699.45 million tons increased

annually due to the growth of population scale and the improvement of economic output, and 8524.87 million tons decreased annually due to the reduction of industrial structure, the reduction of energy intensity and the adjustment of energy structure.

## RESULTS AND DISCUSSION

### Energy Structure Effect

The average value of the energy structure effect was (-586.01) million tons from 2000 to 2019, and the average contribution to carbon emissions from energy consumption in the YRB was (-11.32%). Hence, the structure effect was not very obvious. The impact of structural effects on carbon emissions in 2001~2004, 2005~2007, 2008~2010, 2011~2013, and 2014~2019 was mainly negative. The change in the energy consumption structure in the YRB mainly causes this situation. The proportion of raw coal consumption in the total energy consumption in the YRB decreased by 5.89% in 2004, 8.87% in 2007, 9.10% in 2010, 8.64% in 2013, and 4.92% in 2019, respectively, compared with 2001, 2005, 2008, 2011 and 2014. The energy structure effect was positive in 2000~2001, 2004~2005, 2007~2008, 2010~2011, and 2013~2014, indicating that the energy structure was not reasonable during this period, which led to the increase of carbon emissions in the YRB. During this period, the consumption of raw coal and coke increased significantly. The proportion of raw coal consumption increased by 3.84% in 2005, 4.28% in 2008, and 2.58% in 2011, respectively, compared with 2004, 2007, and 2010, and the proportion of coke consumption increased by 4.27% in 2011 compared with 2010. Because the carbon emission coefficients of raw coal and coke are the largest, the consumption of coal and coke has the most significant impact on carbon emissions when other coefficients remain unchanged. So, the role of

Table 2: Contribution value and contribution rate.

| Decomposition factors | Contribution value | Contribution rate |
|---|---|---|
| energy structure | $\Delta C_{\frac{E_{ij}}{E_i}} = \frac{c_{ij}^t - c_{ij}^0}{\ln c_{ij}^t - \ln c_{ij}^0} \cdot \ [\ln\left(\frac{E_{ij}}{E_i}\right)^t - \ln\left(\frac{E_{ij}}{E_i}\right)^0]$ (4) | $r_{\frac{E_{ij}}{E_i}} = \frac{\Delta C_{\frac{E_{ij}}{E_i}}}{\Delta C_{tot}}$ (9) |
| energy intensity | $\Delta C_{\frac{E_i}{Q_i}} = \frac{c_{ij}^t - c_{ij}^0}{\ln c_{ij}^t - \ln c_{ij}^0} \cdot \ [\ln\left(\frac{E_i}{Q_i}\right)^t - \ln\left(\frac{E_i}{Q_i}\right)^0]$ (5) | $r_{\frac{E_i}{Q_i}} = \frac{\Delta C_{\frac{E_i}{Q_i}}}{\Delta C_{tot}}$ (10) |
| industrial structure | $\Delta C_{\frac{Q_i}{Q}} = \frac{c_{ij}^t - c_{ij}^0}{\ln c_{ij}^t - \ln c_{ij}^0} \cdot \ [\ln\left(\frac{Q_i}{Q}\right)^t - \ln\left(\frac{Q_i}{Q}\right)^0]$ (6) | $r_{\frac{Q_i}{Q}} = \frac{\Delta C_{\frac{Q_i}{Q}}}{\Delta C_{tot}}$ (11) |
| economic output | $\Delta C_{\frac{Q}{P}} = \frac{c_{ij}^t - c_{ij}^0}{\ln c_{ij}^t - \ln c_{ij}^0} \cdot \ [\ln\left(\frac{Q}{P}\right)^t - \ln\left(\frac{Q}{P}\right)^0]$ (7) | $r_{\frac{Q}{P}} = \frac{\Delta C_{\frac{Q}{P}}}{\Delta C_{tot}}$ (12) |
| population size | $\Delta C_P = \frac{c_{ij}^t - c_{ij}^0}{\ln c_{ij}^t - \ln c_{ij}^0} \cdot \ [\ln P^t - \ln P^0]$ (8) | $r_P = \frac{\Delta C_P}{\Delta C_{tot}}$ (13) |

energy improvement in the YRB in emission reduction needs to be further improved over a long period of time.

**Energy Intensity Effect**

The average energy intensity effect was (-6401.24) million tons from 2000 to 2019, and the average contribution to the carbon emissions from energy consumption in the YRB was (-123.71%). Energy intensity reflects the efficiency of energy economic activities, and the decrease indicates the improvement of energy utilization efficiency (Adewale et al. 2023). The energy structure effect was positive in the five time periods of 2000~2001, 2002~2003, 2004~2005, 2008~2009, and 2018~2019. To some extent, it can be seen that the energy utilization technology in the YRB still has a large room for improvement. Further analysis shows that industrial energy intensity had the greatest impact on energy intensity in 2000~2001, 2002~2003, and 2018~2019, while transportation energy intensity had the greatest impact in 2004~2005 and 2008~2009. So, the industry and transportation urgently need to innovate energy application technology, and the most important way to save energy and reduce emissions is to improve energy efficiency in the YRB.

**Industrial Structure Effect**

The average value of industrial structure effect was (-1537.61) million tons from 2000 to 2019, and the average contribution to the carbon emissions from energy consumption in the YRB was (-29.71%), which is not a high percentage. The effect of industrial structure in the YRB harmed carbon emissions in 2000~2001 and 2009~2019, while it had a positive effect in 2002~2008. The secondary industry is the largest energy-consuming profession. The average proportion of the secondary industry output value to GDP in the YRB in 2000~2019 was about 40%, and its average annual proportion to total energy consumption was 78.42%. In contrast, the proportion of the secondary industry output value to GDP showed a downtrend after 2008, with an average annual decline of 0.23%. We find that the change in the proportion of the secondary industry output value in the YRB significantly impacts the industrial structure effect. Therefore, the YRB should focus on controlling carbon emissions from the secondary industry, actively adjusting industrial structure, and developing the tertiary industry.

**Economic Output Effect**

The average economic output effect was 12490.04 million tons from 2000 to 2019, with an average contribution of 241.37%. The growth of carbon emissions caused by economic growth in 2010~2011 was 22991.67 million tons. It can be seen that the economic output effect is the most important driving factor for the growth of carbon emissions and has a positive contribution to the YRB. Concurrently, the rapid and sustained economic growth has led to a large
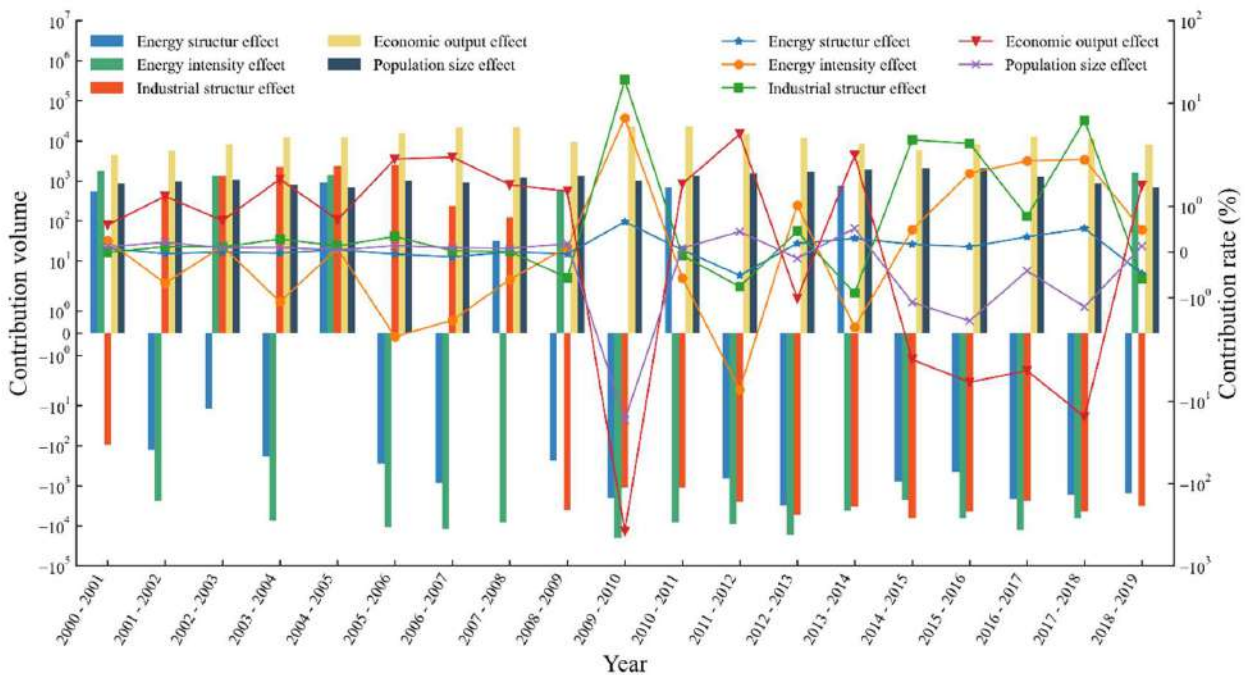


Fig. 3: Influencing Factors of Carbon Emissions in the YRB from 2000 to 2019. (contribution volume: million tons /contribution rate).

consumption of energy and increasing carbon emissions. For example, the per capita GDP of the YRB increased from 51535 yuan to 497258 yuan from 2000 to 2019, with an average annual growth of 12.67%. The cumulative economic output effect was 126203.59 million tons from 2000 to 2019, accounting for 53.18% of the total economic output effect. Therefore, the YRB should change its development concept, take resource-carrying capacity as a constraint, change from quantity growth to quality improvement, and explore the green and low-carbon development path (Xu et al. 2022).

**Population Size Effect**

The population size effect of the YRB is positive, so the increase in population size leads to the growth of carbon emissions. The average population size effect was 1209.41 million tons, and the average contribution to carbon emissions from energy consumption in the YRB was 23.37% from 2000 to 2019.

**Analysis of Regional Differences in Carbon Emission of 43 Intensities**

Based on China's goal of a green, low-carbon circular economic system by 2025, public policies have supported

green finance, the investment and financing system compatible with the "Double Carbon" goal. The government strictly controls high-carbon industries such as steel, coal, electrolytic aluminum, cement, and petrifaction through various measures to enhance the application level of low-carbon technology, which is conducive to the restructuring of energy consumption structure and the upgrading of industrial structure. However, due to the huge differences in regional ecological resources in China, the spatial layout and utilization level of land are different, so eastern, central, and western China have different missions and responsibilities of ecological civilization. At this stage, there are obvious regional differences in carbon emissions from 43 industries in the YRB (see Fig. 3). Therefore, the industrial division planning of the YRB should consider the differential characteristics of production factors, natural endowment, and ecological carrying capacity in the upstream, midstream and downstream, and try to avoid industrial isomorphism and disorderly competition, to improve energy production efficiency.

(1). The CV ranges of carbon emission in 43 industries were 7.09%~35.71% in 2000, 25.45%~83.54% in 2005, 26.62%~69.34% in 2010, 23.3%~101.45% in



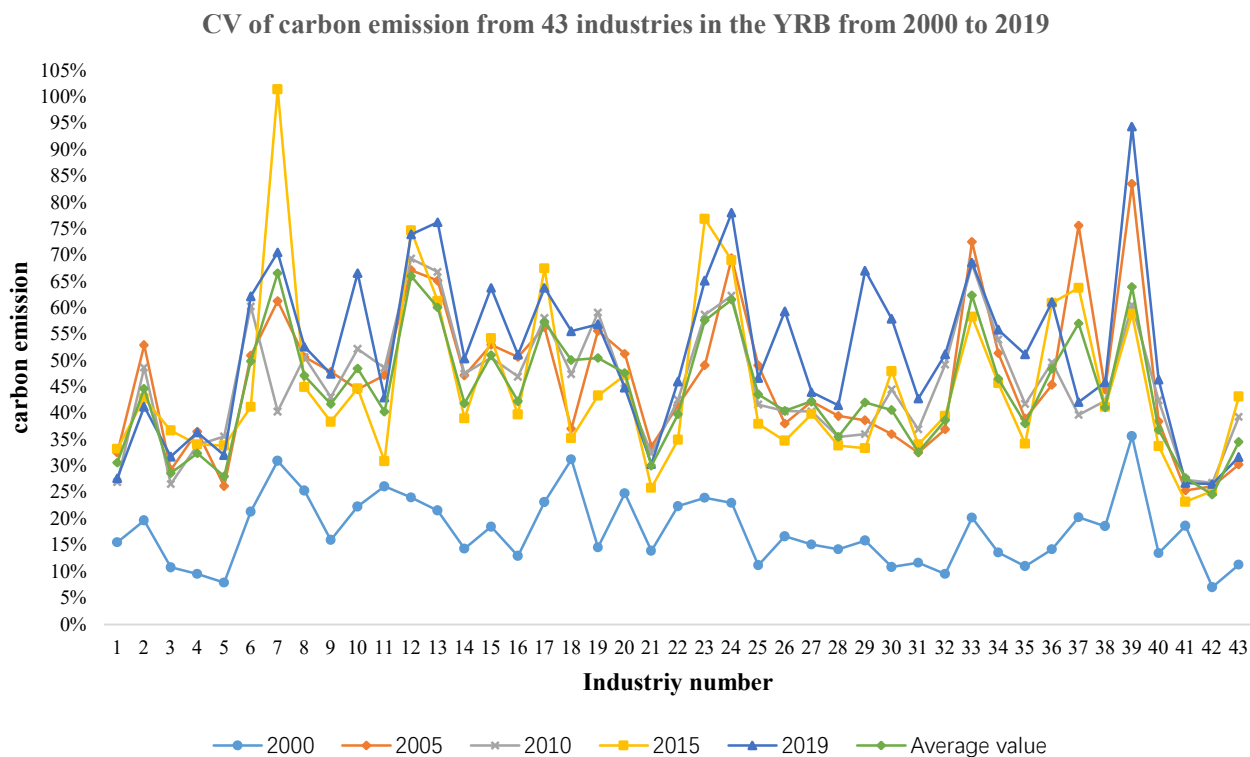**CV of carbon emission from 43 industries in the YRB from 2000 to 2019**

Fig. 4: CV of carbon emission from 43 industries in the YRB from 2000 to 2019.

2015, 26.62%~94.38% in 2019. To a certain extent, the improvement of the CV reflects the irrationality of the industrial structure in the YRB. In the future, the YRB should actively reduce industrial carbon emissions through reasonable industrial spatial layout and scientific regional industrial planning.

(2). The CV of carbon emissions in 43 industries were significantly higher in 2001 compared with 2000, and especially "Petroleum and Natural Gas Extraction," "Cultural, Educational and Sports Articles," "Smelting and Pressing of Ferrous Metals" have increased more than twice. The CV of carbon emissions from "Other Minerals Mining and Dressing," "Textile industry," "Garments and Other Fiber Products," "Rubber Products," "Electric Equipment and Machinery," and "Gas Production and Supply" were more than 60% on average in 2000~2019. The CV of carbon emission from "Scrap and waste" reached 104.5% in 2011. This means the range of carbon emission intensity of these industries varies greatly. So, the 9 provinces in the YRB should further strengthen the coordination. For example, industrial planning should be carried out according to regional carbon productivity, and the regions with low carbon emission intensity can relatively increase the industrial scale to reduce the industrial scale of regions with high carbon emission intensity.

(3). In 2000~2019, the CV of carbon emission in "Agriculture, forestry, animal husbandry, and fishery," "Coal Mining and Dressing," "Petroleum and Natural Gas Extraction," "Other Minerals Mining and Dressing," "Papermaking and Paper Products," "Petroleum Processing and Coking," "Chemical Fiber," "Scrap and waste," "Wholesale, Retail Trade, and Catering Service" showed a downward trend; the CV of carbon emission in "Ferrous Metals Mining and Dressing," "Smelting and Pressing of Ferrous Metals," "Construction," "Transport, Storage, Postal & Telecommunications Services" remains stable; the CV of carbon emission in 30 industries including "Nonferrous Metals Mining and Dressing," "Nonmetal Minerals Mining and Dressing," "Food Processing," "Food Production," "Wine, beverage and refined tea manufacturing," etc. had an upward trend. It can be seen that the regional difference in carbon production efficiency of 69.77% of the 43 industries has a trend of expanding, which indicates that there are problems such as incompatibility between industrial development planning and local resource conditions, low industrial production efficiency, low energy utilization, and waste of resources in different regions of the YRB.

## CONCLUSIONS

Our paper aimed to analyze the characteristics of energy consumption from 43 industries in the YRB and provide a scientific basis for formulating differentiated carbon emission reduction policies. In this paper, the LMDI model was employed to decompose influencing factors of carbon emissions in the YRB, and the CV method was introduced to dynamically analyze the regional differences in carbon emission of 43 intensities. The main conclusions are as follows.

(1) From the energy consumption in the YRB (see Fig. 1), the proportion of coal in the energy consumption structure of the YRB is the highest, with a slight decline trend; the proportion of oil and natural gas is limited. The total carbon emissions of the YRB showed an increasing trend in 2000~2012, especially with a rapid growth rate in 2000~2006 and a slight downward trend in 2013-2019.

(2) The empirical analysis of factor decomposition of carbon emissions in the YRB shows that, on the whole, the economic output effect and population size effect have a positive impact on the carbon emissions from energy consumption, and the economic output effect is the most important driving factor of carbon emissions in the YRB. The energy structure effect, energy intensity effect, and industrial structure effect have a negative impact on carbon emissions. Still, the energy structure and industrial structure effects have a limited inhibiting effect, while reducing energy consumption per unit GDP has a strong inhibiting effect. In recent years, the YRB has actively transformed industrial structures to promote green development, inhibiting carbon emissions. Still, the inhibition effect is limited due to the path dependence on high energy-consuming industries. Therefore, the carbon emissions of the YRB show a trend of robust increase at this stage.

(3) From the fluctuation of the CV of carbon emission (see Fig. 3), we can see that the regional differences in carbon emission intensity of 43 industries in the YRB are significant. The regional difference in carbon production efficiency of 69.77% of industries had an expanding trend. So, many problems must be solved, such as incompatibility between industrial development planning and local resource conditions, low industrial production efficiency, low energy utilization, and waste of resources in different regions of the YRB.

## SUGGESTIONS

In this paper, the LMDI model is used to illustrate the macro impact of the changes of various factors on the carbon

emission of provinces in the YRB. Still, it is difficult to quantitatively describe the spatial correspondence between carbon emission and the changes in various factors and their coupling mechanism, which is also an issue we must study in depth in the future. Therefore, some suggestions are based on this paper's research object, method, and content.

**Adhering to the principle of ecological priority and planning scientifically:** Our study shows that coal accounts for the largest share of energy consumption in the YRB. On the one hand, the YRB should always adhere to the principle of "Deciding production by water," strengthen water environment governance, promote water conservation projects, carry out water and soil loss control, promote intensive water, implement the strictest ecological protection system, and establish ecological compensation mechanism (Wei et al. 2023). On the other hand, the YRB should keep a close watch on the national special planning and strive to incorporate more projects into the national strategic planning. The development planning of the 9 provinces in the YRB should be differentiated and connected so that the spatial layout of urban agglomeration can be scientifically arranged. After that, the YRB can lead the adjustment of energy structure, ecological governance, and industrial layout through spatial planning and form a community of shared future in the YRB (Song & Feng 2022).

**Optimizing energy consumption structure and improving energy utilization efficiency:** From the energy intensity effect, the energy utilization technology in the YRB still has room for improvement. Authorities in the YRB should strengthen source control, strictly control high coal-consuming projects, strictly control total coal consumption, and increase the proportion of natural gas, photovoltaic, wind power, biomass, and other energy consumption. The upper reaches of the YRB should rationally use abundant water resources and vigorously develop new energy sources, such as wind and solar energy, to promote energy complementarity. The middle and lower reaches have a certain industrial foundation and geographical advantages, and they should develop clean energy sources such as natural gas, wind energy, and solar energy to enhance the renewable energy consumption ratio. In addition, economic and social development is highly dependent on high-coal consumption industries, and the development of strategic emerging industries and new energy industries lack enough support, which leads to the fact that it still takes some time to adjust the energy structure. Therefore, the 9 provinces should further replace fossil energy with electric energy and strengthen the application of ecological technology to improve energy efficiency.

**Adjusting the industrial structure and raising the quality of economic development:** This research finds that the contribution of the industrial structure effect to the carbon emissions in the YRB is not high. The industrial structure of the YRB is mainly resource-intensive industries such as coal and steel, and its economic development is highly dependent on resource-based industries. So transforming traditional industries, achieving energy conservation and efficiency improvement, and improving the green production level of traditional industries such as coal, steel, non-ferrous metals, petrochemical, and chemical industries, are important ways to achieve reducing emissions (Wang et al. 2022). Therefore, the YRB should actively promote the deep integration of information and artificial intelligence technology with traditional industries and use digital technology to empower traditional industries such as coal, petroleum, chemical, electricity, building materials, metal smelting, and equipment manufacturing in the upper and middle reaches of the YRB. At the same time, it is necessary to further promote the rapid development of modern service industries such as financial business, tourism, energy-saving environmental protection industry, science and technology services, and other modern service industries. For example, Jinan, Xi'an, Qingdao, and Zhengzhou should develop high-end manufacturing by building industrial innovation chains and value chains in combination with artificial intelligence, blockchain, and life science. The resource-based cities in the YRB should also further promote the transformation of the energy production base to the energy service center, strengthen the brand building, and extend to the high-end value chain.

**Integrating innovative resources within the watershed and strengthening technological support:** Local governments in the YRB should take more responsibility for integrating, opening, and sharing scientific and technological resources. They should further make full use of 9 double first-class universities, 3 national laboratories, 5 national innovation demonstration zones (Xi'an, Chengdu, Shandong Peninsula, Zheng-luo-xin, and Lanbai), as well as scientific research institutes, enterprise scientific research facilities, key laboratories and other scientific and technological resources in the YRB to improve the utilization efficiency of existing innovation resources. The YRB still needs to actively cooperate with the comprehensive national science centers (such as Huairou Beijing, Zhangjiang Shanghai, Greater Bay Area, and Hefei Anhui) and establish local, regional scientific and technological innovation centers to improve the overall scientific and technological innovation capacity. In addition, national or regional central cities such as Chengdu, Zhengzhou, Xi'an, Jinan, and Qingdao should seize opportunities in the new round of national innovation resource layout and strive for the construction of high-end

innovation platforms such as national science centers, national laboratories, comprehensive national industrial innovation centers, national technology innovation centers, and national manufacturing innovation centers. Moreover, 9 provinces should increase investment in innovation and promote the transformation and application of green technology services and achievements. Based on improving the investment mechanism for scientific and technological innovation and increasing financial investment, the governments should increase tax deductions and incentives and increase the proportion of R&D expenses deducted by enterprises to encourage and support enterprise innovation. At the same time, the 9 provinces should jointly establish a technology transfer and cooperation network in the YRB as soon as possible to promote collaborative cooperation and common development in terms of high-quality supply of scientific and technological achievements, precise integration of technology supply and demand, talent cultivation for technology transfer, and ecological construction for technology transfer and transformation.

## ACKNOWLEDGMENT

## REFERENCES

Adewale, A.A., Olabisi, O.I. and Ibrahim, S.M. 2023. Examining the drivers of alternative energy in leading energy sustainable economies: The trilemma of energy efficiency, energy intensity, and renewables expenses. Renew. Energy, 202: 1190-1197.

Ang, B W. 2015. LMDI decomposition approach: A guide for implementation. Energy Policy, 86: 233-238.

Ang, B.W. 2004. Decomposition analysis for policymaking in energy. Energy Policy, 32(9): 1131-1139.

Chen, F., Zhang, J., Ren, J., Xiang, Y.Y. and Li, Q. 2022. Spatiotemporal variations and influencing factors of carbon emissions in the Yellow River Basin based on LMDI model. J. Earth Environ., 13(4): 418-427.

Cheng, Y.Q., Wang, Z.Y., Ye, X.Y. and Wei, Y.H. 2014. Spatiotemporal dynamics of carbon intensity from energy consumption in China. J. Geogr. Sci., 24(4): 631-650.

He, Y., Q., Zhu, S.Y., Zhang, Y. and Zhou, Y.C. 2021. Calculation, elasticity, and regional differences of agricultural greenhouse gas shadow prices. Sci. Total Environ., 790: 148061.

Hu, H.M., Zuo, W. and Xu, S.Y. 2022. Decoupling effect and driving factors of transportation energy carbon emission in Yangtze River economic belt. Resour. Environ. Yangtze Basin, 31(4): 862-877.

Intergovernmental Panel on Climate Change (IPCC) 2006. 2006 IPCC Guidelines for National Greenhouse Gas Inventories. IPCC/IGES, Hayama, Japan.

Jiang, H.J., Geng, Y., Tian, X., Zhang, X., Chen, W. and Gao, Z.Y. 2021. Uncovering CO2 emission drivers under regional industrial transfer in China's Yangtze River Economic Belt: A multi-layer LMDI decomposition analysis. Front. Energy, 15(2): 292-307.

Kaya, Y. 1989. Impact of carbon dioxide emission control on GNP growth : Interpretation of proposed scenarios. Intergovernmental Panel on Climate Change/Response Strategies Working Group, May, pp. 842. https://cir.nii.ac.jp/crid/1570291225678384256.

Lai, W.W., Hu, Q.L. and Zhou, Q. 2021. Decomposition analysis of PM2.5 emissions based on LMDI and Tapio decoupling model: Study of Hunan and Guangdong. Environ. Sci. Pollut. Res., 28(32): 43443-43458.

Li, G.Z. and Wang, S. 2008. Regional Factor Decompositions in China's Energy Intensity Change: Base on LMDI Technique. J. Fin. Econ., 8: 52-62.

Liu, M.H., Zhai, H.X., Liu, S.N., Yue, Y.Y., Yang, D.K. and Li, J. 2023. Comparative analysis of carbon emissions in Tianjin based on the LMDI method and STIRPAT model. J. Environ. Eng. Technol., 13(1): 63-70.

Liu, Z.H., Xu, J.W. and Zhang, C.H. 2022. Technological innovation, industrial structure upgrading and carbon emissions efficiency: An analysis based on PVAR model of panel data at the provincial level. J. Nat. Resour., 37(2): 508-520.

Pan, C.C., Wang, B.W., Hou, X.W., Gu, Y.Q., Xing, Y., Liu, Y.S., Wen, W. and Fang, J. 2023. Carbon peak path of the Chinese iron and steel industry based on the LMDI–STIRPAT model. Chin. J. Eng., 45(6): 1034-1044.

Ren, B.P. and Dou, Y.B. 2022. Restrictive factors and path of industrial structure adjustment in the Yellow River Basin under the goal of carbon neutralization. Inner Mongolia Social Sciences, 43(1): 121-127+2.

Ren, Z.W., Wang, J.Q., Hu, S.H. and Huang, Z.F. 2019. Estimation of methane emission from agricultural activities in Jiangxi Province. J. Hefei Univ. Technol. Nat. Sci., 42(11): 1551-1556.

Song, J. 2021. The logic and path of the "domestic and international circulation" of the high-quality development of the Yellow River Basin under the new development pattern. Contemp. Econ. Manag., 43(7): 69-76.

Song, J. and Feng, Y. 2022. The characteristics and enlightenment of sci-tech innovation policies in the Yellow River area: A study based on 837 provincial policy texts from 2006 to 2020. J. Henan Univ. Eng. Social Sci., 37(3): 33-40.

Su, D.G., Tan, B., Zhang, A.B. and Hou, Y.K. 2023. Analysis of the influencing factors of power demand in Beijing based on the LMDI Model. Sustainability, 15(10): 7913.

Tang, Y. and Zhang, M.T. 2022. Research status and development trend of carbon emission standards and specifications. Stand. Sci., 12: 73-76+104.

Wang, J.S., Cheng, Y. and Wang, C.X. 2022. Environmental regulation, scientific and technological innovation, and industrial structure upgrading in the Yellow River Basin, China. Int. J. Environ. Res. Pub. Health, 19(24): 16597.

Wang, Z. and Wang, L.H. 2019. A study on the relationship among R&D input, upgrading industrial structure, and carbon Emission. J. Ind. Technol. Econ., 38(5): 62-70.

Wei, H.B., Wang, Y., Liu, J. and Zeng, R. 2023. Heavy Metal in River Sediments of Huanghua City in Water Diversion Area from Yellow River, China: Contamination, Ecological Risks, and Sources. Water, 15(1): 58.

Wu, X.T., Zhang, K., Wang, Q.B., Wang, D.Y. and Ku, G.Y.N. 2023. Analysis of carbon emission drivers of secondary industries in the Energy "Golden Triangle" area based on LMDI and two-dimensional decoupling model. Environ. Sci. Pollut. Res. Int., 30(3): 8154-8169.

Xu, J.J., Wang, H.J. and Tang, K. 2022. The sustainability of industrial structure on green eco-efficiency in the Yellow River Basin. Econ. Anal. Policy, 74: 775-788.

Yang, S.H., Zhang, Y.Q. and Geng, Y. 2022. An LMDI-based investigation of the changes in carbon emissions of the transportation sector in the Yangtze River Economic Belt. China Environ. Sci., 42(10): 4817-4826.

You, J.S., Ding, G.H. and Zhang, L.Y. 2022. Heterogeneous dynamic correlation research among industrial structure distortion, two-way FDI, and carbon emission intensity in China. Sustainability, 14(15):15.

Zhang, Y. and Xu, X. Y. 2022. Carbon emission efficiency measurement and influencing factor analysis of nine provinces in the Yellow River basin: based on SBM-DDF model and Tobit-CCD model. Environmental Science and Pollution Research International, 29(22).

Zhao, Y., Sun, H., Xia, X., and Ma, D. 2023. Can R&D intensity reduce carbon emissions intensity? Evidence from China. Sustainability, 15(2): 1619.

Zhou, D. and Wang, X.Q. 2019. Research on coupling degree and coupling path between China's carbon emission efficiency and industrial structure upgrade. J< Nat. Resour., 34(11): 2305-2316.

Zhou, D. and Wang, X.Q. 2019. Research on coupling degree and coupling path between China's carbon emission efficiency and industrial structure upgrade. J. Nat. Resour., 34(11): 2305-2316.

Zhou, Y.N., Yang, Y., Cheng, B. and Huang, J.X. 2020. Regional differences in the coupling relationship between Chinese economic growth and carbon emissions based on the decoupling index and LMDI. J. Univ. Chin. Acad. Sci., 37(3): 295-307.

# A Comprehensive Study of Variation in Water Quality Parameters to Design a Sustainable Treatment Plant

**Shifana Fatima Kaafil\*†** [iD] **and Shamim Shaukat Khan\*\*** [iD]

\*Hekma School of Design and Architecture, Dar Al-Hekma University, Jeddah, Kingdom of Saudi Arabia
\*\*General Education, Dar Al-Hekma University, Jeddah, Kingdom of Saudi Arabia
†Corresponding author: Shifana Fatima Kaafil: skaafil@dah.edu.sa

## ABSTRACT

In this paper, greywater samples are collected from the kitchens of different types of buildings (residential and commercial) located in different districts within the city of Jeddah, Saudi Arabia. The collected samples are analyzed and compared with the potable water from the same region. The parameters investigated are pH, conductivity, total solids (TS), total dissolved solids (TDS), total suspended solids (TSS), total hardness, temporary hardness, permanent hardness, alkalinity, chloride, and biochemical oxygen demand (BOD). It was found that the amount of total suspended solids is very high in the greywater samples. It shows the presence of both temporary and permanent hardness. Their alkalinity values are greater than hardness. It may be due to the number, lifestyle, age of the occupants, presence of children, and social and cultural behavior of residents. The concentration of BOD level is very low, which shows that the greywater samples have lower concentrations of organic compounds. Design details of the greywater treatment plant are suggested based on the results of the analysis. This includes a screening chamber, grit chamber, settling tank, and filtration unit. The treated greywater is recommended for reuse for gardening, landscaping, and toilet flushing purposes.

## INTRODUCTION

Saudi Arabia is an arid region and depends for its water supply mainly on desalination. Water processed from the Red Sea is used for domestic and commercial purposes. Baig (2014) mentioned that the per capita water consumption rate is higher in Jeddah, and the water demand is increasing drastically. Al-Juaidia & Attiahb (2020) and Anjum et al. (2019) mentioned that Saudi Arabia might face a significant water shortage without water conservation. Hence, it is the right time to recycle greywater and conserve water. The treated water replaces potable water for toilet flushing, fighting fires, gardening, washing cars, and other possible purposes.

The percentage of greywater generated varies regionally between households and depends on how efficiently and effectively the water is used. In addition, it contains fewer impurities compared to black water (Oteng-Peprah et al. 2018, Gross et al. 2015). In Saudi Arabia, greywater and black water are collected through a single pipe system in most buildings, requiring intense and vigorous treatment.

This paper aims to suggest a cost-effective treatment plant for greywater. To achieve this objective, the characteristics of greywater collected from kitchen lines of different buildings in three districts, namely Al-Fayha, Al-Bawadi, and Al-Aziziyah in Jeddah, Saudi Arabia, are analyzed.

## MATERIALS AND METHODS

The samples are stored, preserved, and tested per the specifications of the Central Pollution Control Board (CPCB) (2011).

### Collection of Samples

The greywater and tap water samples are collected from different buildings at different locations with minimum volumes varying from 500 mL to 1000 mL. The samples are collected at different times and days. It is assumed that they are of the same nature and are collected manually and randomly. The point of collection, date, hour, and time are recorded for the samples. The results of all samples obtained from the Al Fayha district are collectively mentioned under Area 1, from Al Bawadi as Area 2, and Al-Aziziyah as Area 3. The results of greywater are compared with the potable water of the same locations and with established data to study the variation in the pollutant level.

## Preservation of Samples

Samples are collected in glass bottles of a minimum of 500 mL and are analyzed immediately at the site for pH and within 2-3 hours at the lab for total solids, total dissolved solids, and alkalinity. Chloride is measured within 2-3 days for refrigerated samples. Hardness is measured by adjusting the pH of the collected samples to two or less by adding sulfuric acid ($H_2SO_4$), and then it is refrigerated and measured within 2-3 days. The samples are collected by overflowing the BOD bottles for BOD and dissolved oxygen and are analyzed immediately.

## Analysis of Samples

The various characteristics of the samples analyzed in this paper are pH, conductivity, total solids (TS), total dissolved solids (TDS), total suspended solids (TSS), total hardness, temporary hardness, permanent hardness, alkalinity, chloride, dissolved oxygen and Biochemical oxygen demand (BOD). The methods and the details of the equipment used for the analysis of the different characteristics are as per Khan and Kaafil (2020).

**pH and alkalinity:** pH is measured using a pH meter (Denver Instrument model # 215) and it is calibrated using laboratory-supplied buffers of pH = 4 (HACH), pH =7 (Panreac), and pH=10 (Panreac). usual precautions calibrate pH meters. The alkalinity of the samples is measured by the potentiometric method. Total alkalinities are calculated in milligrams (mg) of calcium carbonates ($CaCO_3$) and calcium hydrogen carbonate per L.

**Total solids, total dissolved solids, and total suspended solids:** To measure total solids (TS), 50 $cm^3$ of greywater sample was evaporated and dried in temperature temperature-controlled electric oven at 103-104°C for 24 h. Total dissolved solids (TDS) were measured using a TDS/EC meter at 25.6°C (Hanna instrument model # hi 98312). Total suspended solids (TSS) were the difference between total solids and total dissolved solids.

**Total hardness:** A mixture of cations and anions causes the hardness of the water. Total hardness is expressed as the concentration of calcium and magnesium ions ($Ca^{2+}$ and $Mg^{2+}$), and it is measured in terms of calcium carbonate ($CaCO_3$) as mg per L (US EPA 2000). In this paper, the hardness of samples is determined by EDTA titration using Eriochrome Black T after buffering 25 mL of the acidified sample with 2 mL of buffer solution ($NH_3 + NH_4Cl$).

**Chloride:** The collected samples are neutral and are made slightly alkaline before titrating against standardized silver nitrate ($AgNO_3$) to find the amount of chloride ($Cl^-$). At the end of the titration, it changes the orange color

of potassium dichromate to a red precipitate of silver chromate (VI).

**Dissolved oxygen (DO) and Biochemical Oxygen Demand (BOD):** The Biochemical Oxygen Demand (BOD) of the sample is the difference between the dissolved oxygen (DO) at zero days with DO after incubation of the sample for 3 days at 27.5°C, which is equivalent to $BOD_5$ (CPCB 2011).

Dilution water was prepared from aerated distilled water that added 1 mL of phosphate buffer of pH 7.2 (AppliChem Panreac), 1 mL of magnesium sulfate ($MgSO_4$ 0.091M),1 mL of calcium chloride ($CaCl_2$ 0.247 M) and 1 mL of Iron(III) chloride ( $FeCl_3$ 0.09M) and then diluted to 1 L (US EPA 2000). The prepared dilution water is tested immediately to ensure that the DO concentration is around 7.5 mg.L$^{-1}$, and it is used for diluting the greywater samples. Greywater samples are tested for residual chlorine by the iodometric titration method (US EPA 2000), which is found to be absent. Different dilutions tried for samples are 20%, 50%, 70%, 90%, 95%, 98%, and 99%. BOD results are obtained with 98 % dilution for most samples and a few with 99% dilution. Quality check for dilution water is also carried out as it may cause significant alteration in results.

## RESULTS AND DISCUSSION

The analysis results of the greywater samples collected from the kitchen line of the buildings located in the Al-Fayha district are mentioned under Area 1, and those samples are from the Al-Bawadi district as Area 2 and from Al-Aziziyah district as Area 3. The pH of potable water (tap) and greywater samples of area 1 is neutral and very weakly acidic for areas 2 and 3 (Fig. 1). The average pH value of the collected greywater samples is 6.53. The electrical conductivity of the greywater generated from different areas is compared with the potable (tap) water of the corresponding area (Fig. 2). The percentage increase in the electrical conductivity of the greywater samples compared to potable water is 58%, 35% and 36% for area 1, 2 and 3 respectively. The temporary and permanent hardness is found from the samples' alkalinity (Fig.3a) and total hardness (Fig. 3b). Area 1 includes the samples collected from a commercial kitchen, which shows very high percentage increase in hardness of grey water with respect to potable water samples of that area(Fig.3b). The hardness of the potable water in area 1 is less than the total alkalinity in-terms of carbonate ($CO_3^{-2}$) and hydrogen carbonate ($HCO_3^-$) which shows the absence of permanent hardness. However, the other areas' greywater samples and potable water (tap) samples show both temporary and permanent hardness as their alkalinity values are greater than hardness. The percentage increase in hardness compared to their potable water is 70% for Area 1, 15% for Area 2,

and 20% for Area 3. Area 2 and Area 3 include the samples collected from residential buildings alone

The total solids (Fig. 4a) of the greywater samples of different areas are very high compared to potable water and are mostly in the form of suspended solids (Fig. 4b). Also, it is noticed that the total dissolved solids (Fig. 4c) are very less in all the three areas. It may be due to greywater generated from the kitchen, which normally contains food particles that remain suspended solids. The chloride content of greywater samples is higher than the potable water of all three areas (Fig. 5), and it is found that the samples with more hardness have more chloride content (areas 2 and 3). The greywater samples of areas 2 and 3 show permanent hardness in the form of chlorides of calcium and magnesium ions. BOD is an indicator of bio-degradable organic matter and is given in Fig. 6.

The concentration of BOD in greywater samples is very low, indicating that greywater samples have lower concentrations of organic compounds. The characteristics of the potable and greywater of the different areas are summarized in Table 1. It is found that the amount of total suspended solids is very high in the samples, and the number,

Table 1: Characteristics of potable and greywater of different areas.

| Parameters | Area 1 | | Area 2 | | Area 3 | |
|---|---|---|---|---|---|---|
| | Potable water | Grey water | Potable water | Grey water | Potable water | Grey water |
| pH | 7.45 | 7.10 | 6.10 | 5.81 | 6.14 | 6.68 |
| EC $\mu$Siemens/cm | 82.29 | 206 | 361 | 550 | 76 | 120 |
| Alkalinity mg of $HCO_3^-.L^{-1}$ | 51.24 | 46.66 | 29.28 | 42 | 58.56 | 70.76 |
| Alkalinity mg of $CaCO_3^{-2}.L^{-1}$ | 42.00 | 38.25 | 24.00 | 34.43 | 48.00 | 58.00 |
| Total Hardness mg as $CaCO_3^{-2}.L^{-1}$ | 36.00 | 123.20 | 134.40 | 159.26 | 88.52 | 114.90 |
| Temporary Hardness | 36.00 | 38.25 | 24.00 | 34.43 | 48.00 | 58.00 |
| Permanent Hardness | 0 | 84.95 | 110.40 | 124.83 | 40.52 | 56.90 |
| TS $mg.L^{-1}$ | 200 | 2900 | 350 | 6000 | 200 | 500 |
| TSS $mg.L^{-1}$ | 140 | 2740 | 140 | 5710 | 140 | 400 |
| TDS $mg.L^{-1}$ | 60.00 | 170 | 210 | 280 | 60 | 100 |
| $Cl^-$ $mg.L^{-1}$ | 29.41 | 49.20 | 203.91 | 406 | 29.20 | 230 |
| $DO_0$ $mg.L^{-1}$ | 8.12 | 13.00 | 10.15 | 11.87 | 9.12 | 11.25 |
| $DO_3$ $mg.L^{-1}$ | 6.00 | 2.75 | 9 | 1.37 | 6.62 | 3.20 |
| BOD $mg.L^{-1}$ | 2.12 | 10.25 | 1.15 | 10.50 | 2.50 | 8.05 |
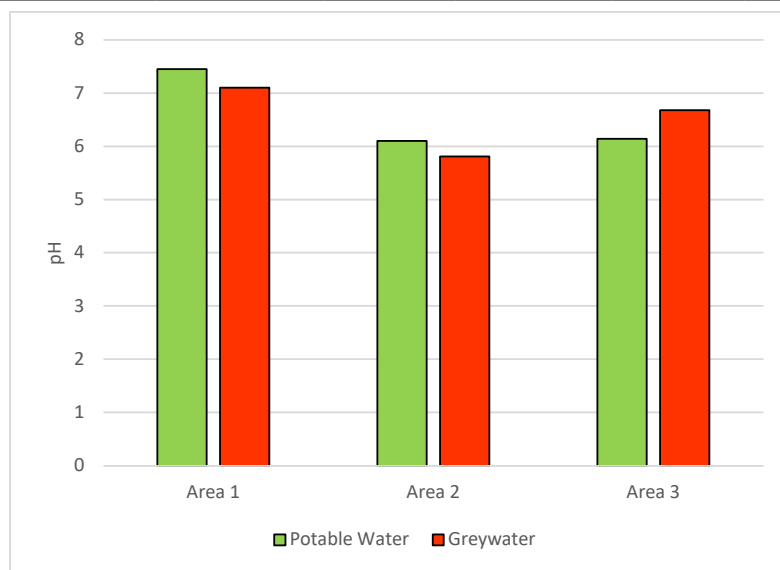


Fig. 1: pH of the different water samples.
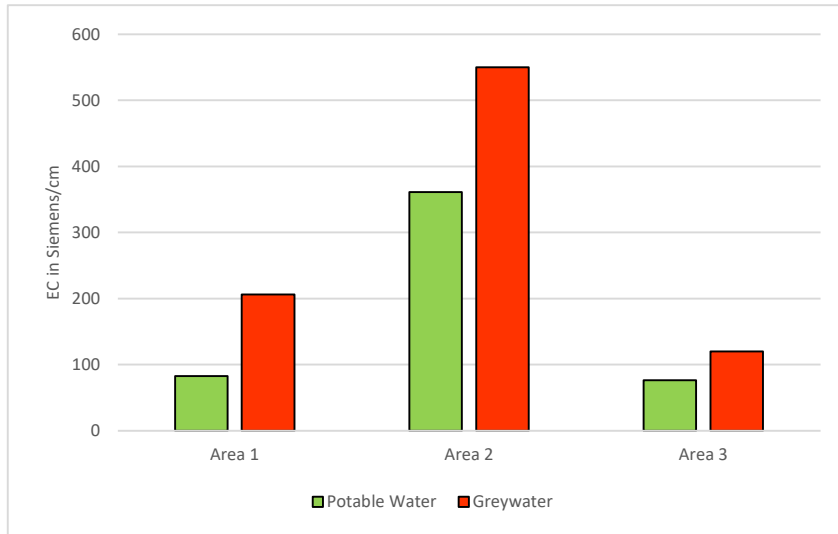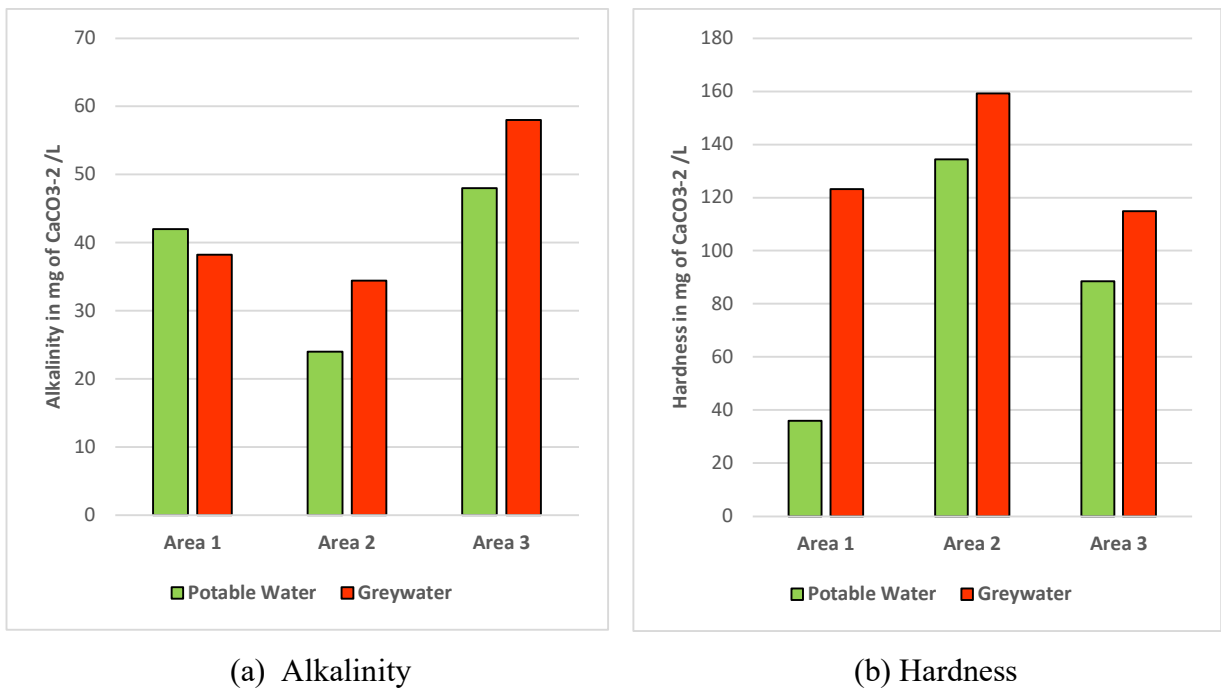
Fig. 2: Electrical conductivity of different water samples.



(a)  Alkalinity                                    (b) Hardness

Fig. 3: Alkalinity and hardness of different water samples.

lifestyle, age of the occupants, presence of children, social and cultural behavior of residents, and water usage patterns of the occupants influence the variations in the results. It is found that the samples with more hardness than potable water(tap) show higher concentrations of hard ions, and higher values of chlorides and electrical conductivity support it.

**Comparison with Established Data**

The average values of the characteristics of the greywater samples collected from different areas are compared with the established data (Pescod 1992) and are listed in Table 2.

It is found that alkalinity and total dissolved solids are weak, and it depends on the usage pattern of the water, and correspondingly, the treatment process will change. The

(a)   Total solids        (b)   Total suspended solids      (c)   Total dissolved solids
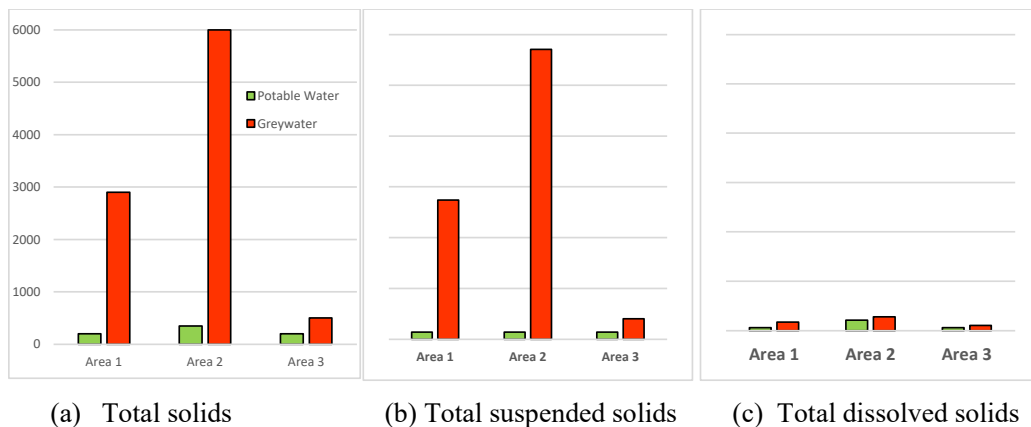
Fig. 4: Total solids, total suspended solids, and total dissolved solids of different water samples.
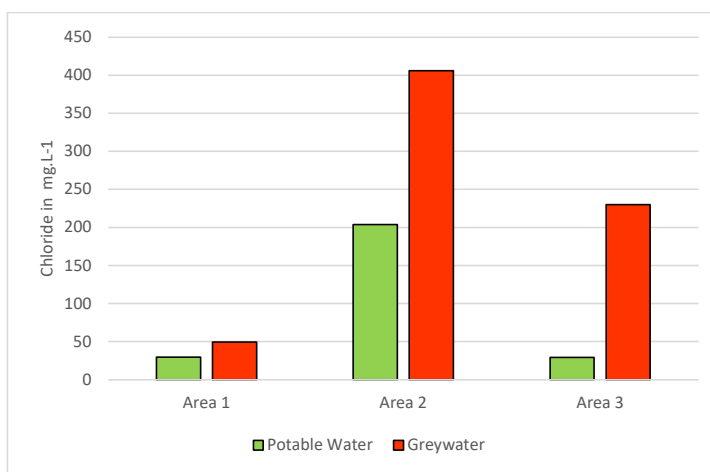


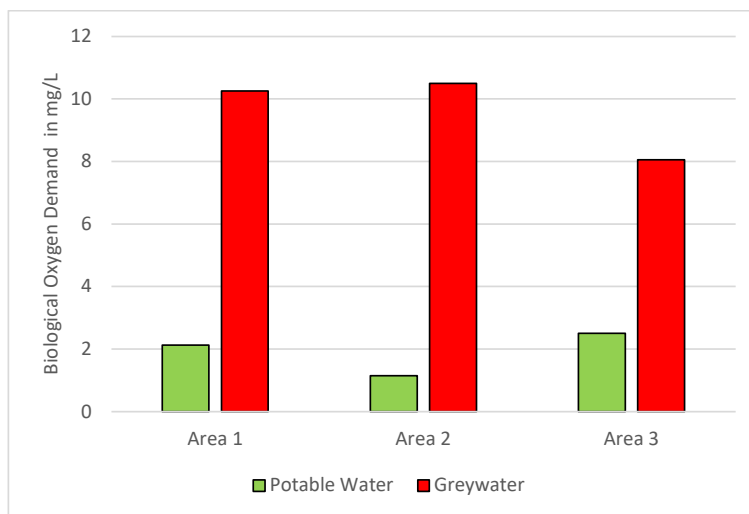Fig. 5: Chloride values of the different water samples.



Fig. 6: BOD of different water samples.

Table 2: Comparison of results with established data (Pescod, 1992).

| Constituents | strength | | | Test results |
|---|---|---|---|---|
| | Strong | Medium | Weak | |
| Alkalinity as $CaCO_3$ in mg.L$^{-1}$ | 200 | 100 | 50 | 43.56 |
| Total solids g.L$^{-1}$ | 1.2 | 0.7 | 0.35 | 3.1 |
| Total dissolved solids g.L$^{-1}$ | 0.85 | 0.5 | 0.25 | 0.18 |
| Total suspended solids g.L$^{-1}$ | 0.35 | 0.2 | 0.1 | 2.95 |
| Total hardness as mg $CaCO_3$/L | 180 | 120 | 60 | 132.45 |
| BOD mg.L$^{-1}$ | 300 | 200 | 100 | 12 |
| Chloride mg.L$^{-1}$ | 100 | 50 | 30 | 228 |

suspended solids are very high, whereas total hardness is found to be medium. Chloride is one of the anions causing permanent hardness, and it is found to be medium, 228 mg.L$^{-1}$ when compared with established data. The level of BOD was found to be very weak, 12 mg.L$^{-1}$, which shows a low pollution level. This comparative study gives an idea to the author to choose the greywater treatment process.

**Quality of Water for Reuse**

Water quality parameter for urban reuse is assessed by comparing the results with normative references and guidelines followed in different countries (US EPA 2004 & ANQIP 2011) and is reported in Table 3. The possible urban reuse is landscape irrigation, toilet flushing, fire protection, commercial air conditioners, and gardening. It is found that the pH, TDS, and BOD of the greywater samples are within the acceptable range for urban reuse without any treatment. It is recommended to do physical-chemical treatment to remove TSS before its reuse.

**Design of Greywater Treatment Plant**

The different technologies used to treat greywater depend on guidelines and standards (Gross et al. 2015, CPCB 2011) and include physical, chemical, and biological processes. One of the biggest prospects of reusing treated grey water is reducing desalinated water usage. The factors that influence the

Table 3: Water quality parameters for urban reuse.

| Parameters | Range | Results obtained |
|---|---|---|
| PH | 6-9 (US EPA 2004) | 6.53 |
| TSS [mg.L$^{-1}$] | ≤ 30 (ANQIP 2011) ≤ 30 (Ministry of Health Canada 2010) | 2950 |
| TDS [mg.L$^{-1}$] | 500-2000 (US EPA 2004) | 180 |
| BOD | ≤ 10 (US EPA 2004) ≤ 20 (Ministry of Health Canada 2010) | 12 |

selection of different types of treatment include the volume of greywater to be treated, characteristics of the greywater, and reuse applications. Also, reducing the volume of greywater generation through various water conservation technologies and decreasing the pollutant load is recommended. It is well established by Wurochekke et al. (2016) that the greywater intended for treatment and reuse should not be stored for longer periods as this encourages the growth of the microbial population present in it.

An extensive literature survey is conducted to study different physicochemical and biological methods to treat greywater. Physicochemical methods include screening, grit removal, sedimentation, sludge thickener, ion exchange, multimedia filtration, adsorption, reverse osmosis, and ultra-filtration. Biological methods are broadly classified as aerobic and anaerobic. Aerobic methods are divided into suspended growth (viz. Activated sludge process, Aerated lagoon, Waste stabilization pond, etc.) and attached growth (viz. Tricking filter, Rotating bio discs, Constructed wetlands, etc.). Anaerobic treatments comprise contact beds, up-flow anaerobic sludge blanket reactors, sludge digesters, and anaerobic ponds (Droste & Gehr 2018).

Filtration removes the particulate matter. During filtration, turbidity, colloidal matter of non-settleable type protozoan cysts, and helminth eggs are removed. The protozoa are stopped in the gravel, the bacteria by the medium gravel, and the viruses by the sand (Couto et al. 2014). However, this considers only the physical process of solids removal. In these systems, both physical and biological processes remove solids (Vuppaladadiyam et al. 2019).

It is suggested to set up a sustainable treatment plant based on the results obtained from the analysis. It includes a screening chamber, grit chamber, sedimentation tank, and filtration tank. It is recommended to use the two-pipe system to separate greywater from blackwater. The outlet of greywater is passed through a screening chamber to remove floating solids and then to the grit chamber to remove the grease and oil. The greywater samples contain high
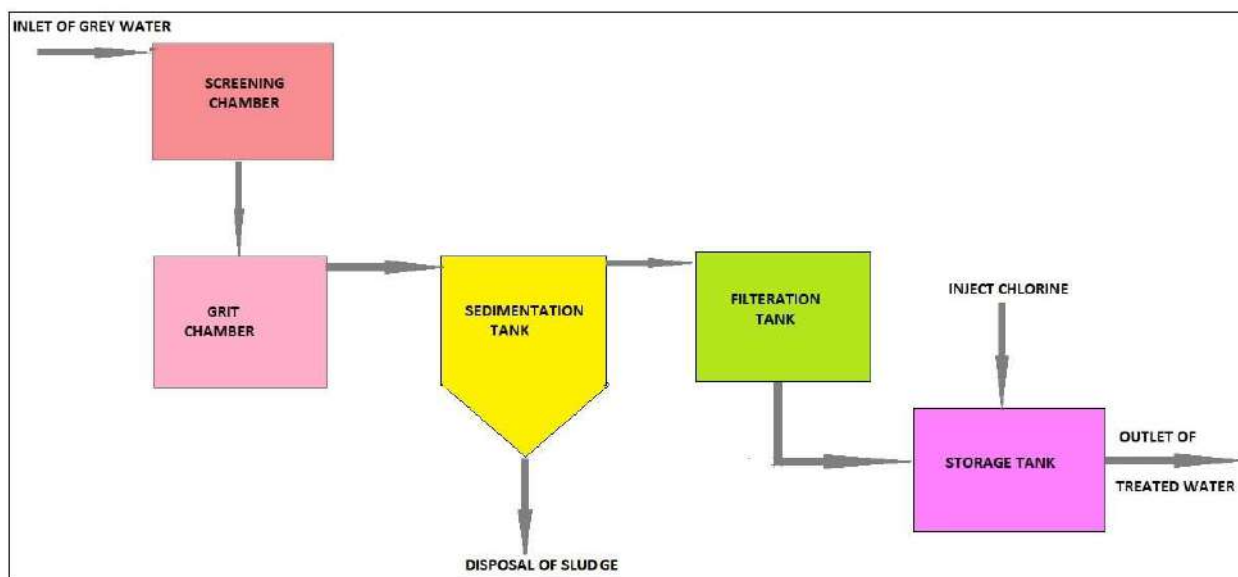
Fig. 7: Schematic view of sustainable treatment plant.

levels of suspended solids, so it is recommended to use a sedimentation tank with a coagulant to settle the suspended solids under gravity. The detention time is approximately 2 to 4 hours for the sediments to settle. The clear water collected from the top of the sedimentation tank is passed to the filtration tank to remove the microbes. The hardness of greywater samples is due to soluble calcium and magnesium chloride so it won't cause a scaling problem.

The capacity of the filtration tank designed in this paper is 20-L filled with locally available materials, marble, and gravel, acting as a drain with a size range of 2-16 mm to a height of 100 mm from the bottom of the unit. Sand is placed on top of the gravel to a height of 500 mm. The sand screens off particles larger than their pore size, while the marbles and gravel act as a drainage system to let off filtered greywater. The filtered greywater is collected from the bottom of the tank and sent to the storage tank. Chlorine is added to the storage tank as disinfection depends on the urban reuse option. The schematic view of the recommended treatment plant is shown in Fig. 7.

## CONCLUSIONS

The research is conducted on the greywater samples collected from households in three different districts within the city of Jeddah, Saudi Arabia. The results show that the quality of greywater with respect to PH, TDS, and BOD is within the acceptable range for reuse as toilet flush, gardening, landscape, and irrigation without any further treatment. Also, it is recommended to pass the greywater to a sedimentation

tank with coagulants before reuse to remove the suspended solids. The greywater samples generated from the kitchen have low pollution levels, so it is recommended to set up primary stages of treatment with sustainable material, a cost-effective treatment method.

## ACKNOWLEDGEMENTS

## REFERENCES

Al-Juaidia, A.E.M. and Attiahb, A.S. 2020. Evaluation of desalination and groundwater supply sources for future water resources management in Riyadh city. Desal. Water Treat., 175: 11-23. http:// doi: 10.5004/dwt.2020.24892

Anjum, M., Miandad, R., Waqasa, M., Gehanya, F. and Barakat, M.A. 2019. Remediation of wastewater using various nano-materials. Arab. J. Chem., 12(8): 4897-4919. https://doi.org/10.1016/j.arabjc.2016.10.004

ANQIP 2011. Technical Specification for Predial Systems of Gray Water Reuse and Recycling. ETA 0905.

Baig, M.B. 2014. KSA's water consumption rate is twice the world average. Arab News, 28 February 2014. http://www.arabnews.com/news/532571. Accessed: 12 May 2023

Central Pollution Control Board (CPCB). 2011. Guide Manual for Water and Wastewater Analysis for Hydrology Project II, Ministry of Water Resources, Government of India (2011). http://cpcb.nic.in/openpdffile.php?id=UmVwb3J0RmLsZXMvMjA0XzE1MjQ2NTA4OTNfb-WVkaWFwaG90bzEyODI3LnBkZg Accessed: 12 May 2023)

Couto, E.A., CallJuri, M.L., Assemany, P.P., Santlago, A.F. and Lopes L.S. 2014. Greywater treatment in airports using anaerobic filter followed by UV disinfection: an efficient and low-cost alternative. J. Clean. Prod., 106: 372-379. https://doi.org/10.1016/j.jclepro.2014.07.065

Droste, R.L. and Gehr, R.L. 2018. Theory and Practice of Water and Wastewater Treatment. Second Edition. Wiley, New Jersy.

Gross, A., Maimon, A., Alfiya, Y. and Friedler, E. 2015. Grey Water Reuse, CRC Press, Boca Raton, Florida.

Khan, S.S. and Kaafil, S.F. 2020. A comparative study of grey water generated from commercial and Residential buildings. Int. J. Environ. Waste Manag., 25(4): 487-497. https://doi.org/10.1504/IJEWM.2020.107568

Ministry of Health Canada. 2010. Water Quality Parameters. https://www.hc-sc.gc.ca/ Accessed 10 Dec 2022.

Oteng-Peprah, M., Acheampong, M.A. and Nanne K. DeVries. 2018. Greywater characteristics, treatment systems, reuse strategies, and user perception: A review. Water Air Soil Pollut., 229(8): 255. https://doi: 10.1007/s11270-018-3909-8

Pescod, M.B. 1992. Wastewater Treatment and Use in Agriculture: Wastewater Characteristics and Effluent Quality Parameters. FAO irrigation and drainage paper 47, Food and Agricultural Organization of United Nations, Italy.

US EPA 2000. Aggregate organic constituents (5000). https://beta-static.fishersci.com/content/dam/fishersci/en_US/documents/programs/scientific/technical-documents/white-papers/apha-biochemical-oxygen-demand-white-paper.pdf (Accessed: 12 May 2023).

US EPA 2004. EPA/625/R-04/108 Guidelines for Water Reuse. US Environmental Protection Agency, Washington DC USA.

Vuppaladadiyam, A.K., Merayo, N., Prinsen, P., Luque, R., Blanco, A. and Zhao, M. 2019. A review on greywater reuse: quality, risks, barriers, and global scenarios. Rev. Environ. Sci. Biotechnol., 18: 99-77. https://doi.org/10.1007/s11157-018-9487-9

Wurochekke, A.A., Mohamed, R.M.S., Al-Gheethi, A.A., Atiku, H., Amir, H.M. and Matias-Peralta, H.M. 2016. Household greywater treatment methods using natural materials and their hybrid system. J. Water Health, 14(6): 914-928. https://doi.org/10.2166/wh.2016.054

## ORCID DETAILS OF THE AUTHORS

Shifana Fatima Kaafil : https://orcid.org/0000-0003-1165-2277
Shamim Shaukat Khan : https://orcid.org/0000-0002-1981-7585

**Original Research Paper**    doi https://doi.org/10.46488/NEPT.2023.v22i04.055    **Open Access Journal**

# Risk Perception of Healthcare Workers Regarding Polymer Medical Waste Management

**Jasneet Kaur†** (iD) **, Sheela Upendra** (iD) **and Shital Barde** (iD)

Symbiosis College of Nursing, Symbiosis International (Deemed University), Pune, India
†Corresponding author: Jasneet Kaur; jasneetkaur@scon.edu.in

## ABSTRACT

Despite the relatively small amounts produced, medical waste is a significant issue for the government and the healthcare industry primarily because it poses threats to persons and the environment. Healthcare wastes pose threats to the environment and public health, but knowledge of these concerns and how they relate to management techniques is still lacking. Evaluating waste management practices and healthcare staff expertise is critical to identify shortcomings and lower risk levels. The study was conducted at three selected private hospitals. These three hospitals contain 462 beds, all together with 184 healthcare workers. The study was designed as a descriptive cross-sectional study, and three private healthcare institutions in the study region were evaluated. These 100 healthcare workers were chosen by purposive sampling. The hospitals under consideration include general surgical, Gynecological, pediatric, and various specialty treatments. Data was gathered for the study utilizing a quantitative questionnaire, which includes closed-ended structured questionnaires. The results showed that most healthcare workers practice waste segregation at source. Chemical cross-linking was very poor. However, waste shredding technology is being used substantially. Risk perception among Healthcare workers regarding polymer help waste management showed more of average to high risk. The study concluded that despite the existence of policies and plans, execution is still subpar at private healthcare institutions. The creation of guidelines for hospital waste management, their distribution to other institutions, and their encouragement to do a critical self-evaluation should all be required by the government.

## INTRODUCTION

Polymers are substances connected with energy-intensive manufacturing processes, along with environmental deterioration and severe loss of precious resources due to excessive waste generation (Evode et al. 2021). Furthermore, polymer items are extremely susceptible to rapidly shifting environmental conditions. Globally, the consumption and production of all forms of polymers have been increasing at a virtually consistent rate of roughly 6-7% each year (Balla et al. 2021). In India, main polymers such as plastics, rubber, and so on account for barely 4-5% of world consumption. According to a study, the plastic sector has risen at an annual growth rate of 10% in volume terms, with 8.33 million metric tonnes per year  (Jaiswal & Mishra 2019).

Despite the relatively small amounts produced, medical waste is a significant issue for the government and the healthcare industry, primarily because it poses threats to persons and the environment (Wei et al. 2021). Previous research has demonstrated that medical waste is poorly managed in impoverished countries, and India is no different. Some have researched the related dangers, but few have looked into risk awareness among healthcare workers, especially in this setting (Ferreira & Teixeira 2010).

Healthcare wastes may be harmful because they include infectious agents, poisonous or hazardous chemicals or medications, sharps, teratogenic or radioactive, among other things. Most incidents recorded in the literature have been linked to infectious medical wastes, especially sharps (Prem Ananth et al. 2010). The design and execution of waste management techniques decrease health and environmental concerns, according to several studies undertaken in various situations to evaluate healthcare waste management methods. There have also been reports of persistent shortcomings in handling medical waste (Azouz et al. 2019).

A committed waste leadership team, effective administration, careful planning, excellent organization, supporting legislation, sufficient funding, and complete

employee engagement are all necessary to manage polymer waste in a hospital (WHO 2019). Healthcare wastes pose threats to the environment and public health, but knowledge of these concerns and how they relate to management techniques is still lacking (Kenny & Priyadarshini 2021). Evaluating waste management practices and healthcare staff expertise is critical to identify shortcomings and lower risk levels. The objective of the study includes identifying the practices among healthcare workers regarding polymer health waste management, and identifying the risk perception among healthcare workers regarding polymer health waste management

## MATERIALS AND METHODS

A study was conducted at three selected private hospitals. These three hospitals contain 462 beds, all together with 184 healthcare workers. The study was designed as a descriptive cross-sectional study, and three private healthcare institutions in the study region were evaluated. These 100 healthcare workers were chosen by purposive sampling. The hospitals under consideration include general, surgical, gynecological, pediatric, and specialty treatments. Data was gathered for the study utilizing quantitative questionnaires, including closed-ended structured questionnaires. It contains three parts. The questionnaire's first component evaluated Socio-demographic characteristics, while the second part evaluated the practices for handling polymer-based medical waste. The third part was risk perception, measured by a 10-point Likert scale and evaluated the risk grading as low, average, and high.

## RESULTS

### Section 1: Socio-Demographic Characteristics

Table 1 shows the social demographic variables of the participants. 28% of them belong to the medical area, 22% belong to the surgical area, 11% belong to the obstetrics and gynecological area, 9% belong to the pediatric area, 12% belong to the operation theatre area, 7% belong to laboratory area, 6% belongs to radiology area whereas other were 5%.

44% of them knew the waste management policy, and 56%, that is, the majority, were unaware of it. 82% have already received training regarding waste management, whereas only 18% did not get any training.

### Section II: Practices Regarding Polymer Waste Management

Table 2 describes the practices regarding polymer waste management among healthcare workers. 68% of the healthcare workers practice waste segregation at source, 22% are not practicing, whereas 10% do it sometimes. Chemical cross-linking was very poor, as 72% were not practicing. Rather, only 28% were practicing. Regarding waste shredding Technology, only 69% were used, whereas 31% were not used. 94% claimed to be using incinerators, whereas only 6% were not using them. 88% practiced burning and landfills, whereas 12% did not use them. 92% said they disinfected the sharps before disposal, whereas 8% did not.

### Section III: Risk Perception Among Healthcare Workers Regarding Polymer Health Waste Management

Fig. 1 represents the risk perception among healthcare workers regarding polymer help waste management. 28% showed low risk, 58% were on average risk, whereas 16% represented high risk

## DISCUSSION

This study evaluated private hospitals' procedures for managing healthcare waste. It was found that the hospitals

Table 1: Socio-demographic characteristics.

| Characteristics | N | Frequency |
|---|---|---|
| Type of Area | | |
| Medical | 28 | 28% |
| Surgical | 22 | 22% |
| Obstetrics and Gyane | 11 | 11% |
| Pediatric | 9 | 9% |
| OT | 12 | 12% |
| Laboratory | 7 | 7% |
| Radiology | 6 | 6% |
| Others | 5 | 5% |
| Know the waste management policy | | |
| Yes | 44 | 44% |
| No | 56 | 56% |
| Got training regarding waste management | | |
| Yes | 82 | 82% |
| No | 18 | 18% |

Table 2: Practices regarding polymer waste management.

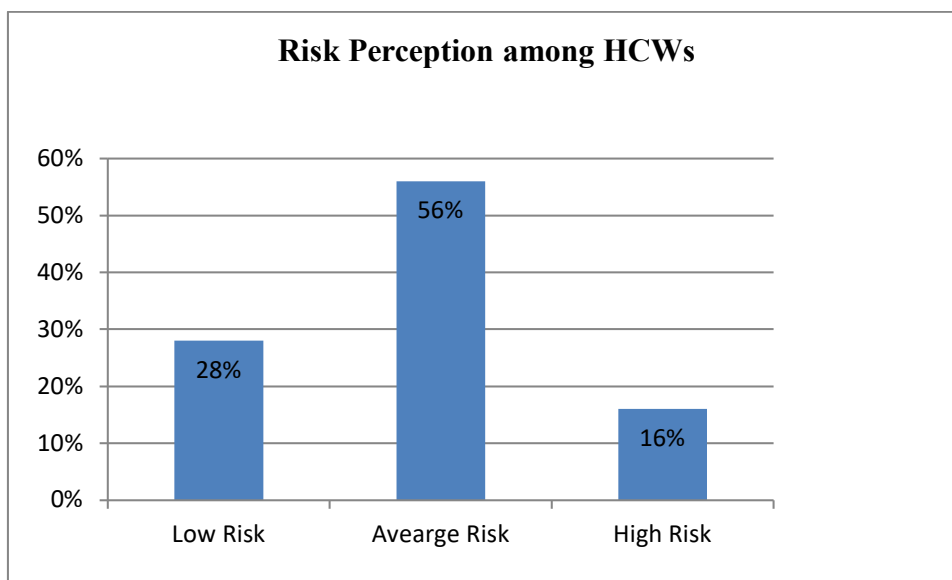| Characteristics | N | Frequency |
|---|---|---|
| Waste segregation at the source | | |
| Yes | 68 | 68% |
| No | 22 | 22% |
| Sometimes | 10 | 10% |
| Practicing Chemical cross Linking | | |
| Yes | 28 | 28% |
| No | 72 | 72% |
| Practicing waste shredding technology | | |
| Yes | 69 | 69% |
| No | 31 | 31% |
| Incinerator | | |
| Yes | 94 | 94% |
| No | 6 | 6% |
| Burying and Landfills | | |
| Yes | 88 | 88% |
| No | 12 | 12% |
| Disinfection of sharps before disposal | | |
| Yes | 92 | 92% |
| No | 8 | 8% |



Fig. 1: Risk Perception among healthcare workers.

had well-framed waste management policies, but 56% were unaware of that. Healthcare workers are the main task force dealing with health waste management, and it has been observed that more than 50% were unaware of the policy. Most of them practice waste-shredding Technology, whereas chemical cross-linking is the rarest. To minimize the volume of hospital trash and render it unidentifiable, waste-shredding techniques have previously been integrated with other waste treatment practices such as autoclaves, microwaves, and chemical treatment techniques (Mukhtar et al. 2018).

However, the shredding and compression techniques may be integrated with landfill and incinerator technologies in the chemical cross-linking approach because the shredding technique alone does not fulfill the objective of preventing hospital polymer waste recycling. A crucial component of effective waste management is separating trash at the source. However, maximum (68%) said they separated garbage at the source, which is substantially greater than the results described by Oli et al. where according to the study, 37 (12.3%) and 66 (21.4%) of the survey participants who

worked in government and private hospitals, respectively, consistently separated trash at the site of creation (Oli et al. 2016) The majority of respondents believed they were at risk, 58% were on average risk whereas 16% were representing high risk. Only a few people adopted protective measures. This discrepancy between risk perception and personal safety may be due to a lack of knowledge, personal protective equipment, and even the hazards of polymer waste (Koelmans et al. 2017). Such an assessment's results will help respond to the current public worry in a balanced way and allow policymakers to take measures for scientifically sound reasons.

## CONCLUSION

According to the study, adequate resources are often available for waste segregation at the point of creation. However, healthcare employees do not follow safety regulations, and there is no awareness of waste management policy. Despite the existence of policies and plans, execution is still subpar at private healthcare institutions. Most individuals are very aware of the dangers involved with managing polymer health waste, yet risk perception is relatively poor. The creation of guidelines for hospital waste management, their distribution to other institutions, and their encouragement to do a critical self-evaluation should all be required by the government. These concepts can be further developed toward technical guidance documents, and then actual risk assessments for plastic debris of all sizes will be within reach. The results of such an assessment will inform policymakers and reduce the present ignorance and uncertainty about ecological and human health risks.

## REFERENCES

Azouz, S., Boyll, P., Swanson, M., Castel, N., Maffi, T. and Rebecca, A.M. 2019. Managing barriers to recycling in the operating room. Am. J. Surg., 217(4): 634-638. https://doi.org/10.1016/j.amjsurg.2018.06.020

Balla, E., Daniilidis, V., Karlioti, G., Kalamas, T., Stefanidou, M., Bikiaris, N.D., Vlachopoulos, A., Koumentakou, I. and Bikiaris, D.N. 2021. Poly(lactic acid): A versatile biobased polymer for the future with multifunctional properties-from monomer synthesis, polymerization techniques, and molecular weight increase to PLA applications. Polymers, 13(11): 1822. https://doi.org/10.3390/POLYM13111822

Evode, N., Qamar, S.A., Bilal, M., Barceló, D. and Iqbal, H.M.N. 2021. Plastic waste and its management strategies for environmental sustainability. Case Stud. Chem. Environmental Eng., 4: 100142. https://doi.org/10.1016/J.CSCEE.2021.100142

Ferreira, V. and Teixeira, M.R. 2010. Healthcare waste management practices and risk perceptions: Findings from hospitals in the Algarve region, Portugal. Waste Manag., 30(12): 2657-2663. https://doi.org/10.1016/J.WASMAN.2010.07.012

Jaiswal, V. and Mishra, M. 2019. Polymer waste management: A review. Int. J. Pure Appl. Biosci., 7(2): 544-556. https://doi.org/10.18782/2320-7051.7509

Kenny, C. and Priyadarshini, A. 2021. Review of current healthcare waste management methods and their effect on global health. Healthcare, 9(3): 284 https://doi.org/10.3390/HEALTHCARE9030284

Koelmans, A.A., Besseling, E., Foekema, E., Kooi, M., Mintenig, S., Ossendorp, B.C., Redondo-Hasselerharm, P.E., Verschoor, A., Van Wezel, A.P. and Scheffer, M. 2017. Risks of plastic debris: Unravelling fact, opinion, perception, and belief. Environ. Sci. Technol., 51(20): 11513-11519. https://doi.org/10.1021/ACS.EST.7B02219/ASSET/IMAGES/LARGE/ES-2017-02219Z_0003.JPEG

Mukhtar, S., Khan, H., Kiani, Z., Nawaz, S., Zulfiqar, S. and Tabassum, N. 2018. Hospital waste management: Execution in Pakistan and environmental concerns: A review. Environ. Contam. Rev., 1(1): 18-23. https://doi.org/10.26480/ecr.01.2018.18.23

Oli, A.N., Ekejindu, C.C., Adje, D.U., Ezeobi, I., Ejiofor, O.S., Ibeh, C.C. and Ubajaka, C.F. 2016. Healthcare waste management in selected government and private hospitals in Southeast Nigeria. Asian Pac. J. Trop. Biomed., 6(1): 84-89. https://doi.org/10.1016/j.apjtb.2015.09.019

Prem Ananth, A., Prashanthini, V. and Visvanathan, C. 2010. Healthcare waste management in Asia. Waste Manag., 30(1): 154-161. https://doi.org/10.1016/J.WASMAN.2009.07.018

Wei, Y., Cui, M., Ye, Z. and Guo, Q. 2021. Environmental challenges from the increasing medical waste since the SARS outbreak. J. Clean. Prod., 291: 125246. https://doi.org/10.1016/J.JCLEPRO.2020.125246

World Health Organization. (WHO). 201. WASH in Healthcare Facilities: Practical Steps to Achieve Universal Access to Quality Care. https://www.who.int/publications/i/item/9789241515511

## ORCID DETAILS OF THE AUTHORS

Jasneet Kaur: https://orcid.org/0000-0001-6897-9137
Sheela Upendra: https://orcid.org/0000-0003-2413-1219
Shital Barde: https://orcid.org/0000-0003-1777-0629

**Original Research Paper**  https://doi.org/10.46488/NEPT.2023.v22i04.056  **Open Access Journal**

# Microbiological Quality of Drinking Water and Food in a Rural Community

**Y. Rapeepan*†, P. Piyabhorn**, P. Phatcharaporn* and S. Theethawat****

*Faculty of Public Health, Kasetsart University Chalermphrakiat Sakon Nakhon Campus, 59/7 Chiangkrua, Mueang Sakon Nakhon District, Sakon Nakhon, 47000, Thailand

**Faculty of Science, Udon Thani Rajabhat University, Udon Thani, 41000, Thailand

†Corresponding author: Y. Rapeepan; rapeepan.y@ku.th

## ABSTRACT

Safe water and food are essential for good human health. The contamination of water with infected fecal bacteria is common in areas with poor standards of hygiene and sanitation. This study investigated total coliform bacteria, fecal coliform bacteria, and *E.coli* in drinking water and food stalls using water from a rural community, where the rural living conditions increase the risk of water-related diseases. In total, 40 samples of bottled drinking water, 50 water samples from vending machines, 30 samples of household drinking water, 30 food samples were collected from household food, and 60 food samples were collected from food stalls, and coliform bacteria contamination was determined using the most probable number (MPN) technique. The results revealed that all the water and food samples contained coliform bacteria contamination, while all the water samples and 50% of the food samples contained fecal coliform bacteria. The numbers of household food samples contaminated with coliform bacteria and *E.coli* were 29 (97%) and 12 (40%), respectively. Entrepreneurs should be regularly maintaining clean drinking water vending machines. The government sector should be urgently solving the problem of drinking water standards to ensure suitable consumer safety.

## INTRODUCTION

Drinking water quality and food quality are two important factors affecting human health. The human body needs sufficient nutrients to grow and help develop and repair worn parts to keep them in perfect condition and remain strong. Consequently, the human consumption of water and food that are clean and safe must be a priority as well. If water and food become contaminated by dirt, this may cause foodborne diseases. Common symptoms of foodborne diseases include diarrhea, nausea, abdominal cramps, headache, dizziness, and fever (DDC 2020). Centers for Disease Control and Prevention (CDC 2020) indicate that each year, foodborne diseases cause about 48 million cases of illness, with 128,000 requiring hospitalization and 3,000 deaths. The annual incidence levels of foodborne or waterborne diseases in Thailand, such as diarrhea, food poisoning, dysentery, cholera, and typhoid fever or typhus, were 271, 933, 25, 640, 679, 1 and 153 cases, respectively (DDC 2020). In addition, in the 2020 Annual Report, Health Area 8 reported the sickness rate in Sakon Nakhon province, where diarrhea was identified as the disease most requiring monitoring with a morbidity rate of 569.33 per 100,000 population, followed by pneumonia, pneumonitis, dengue fever, influenza, and food

poisoning with morbidity rates of 131.63, 96.07, 78.83 and 49.96, respectively, per 100,000 population (Office of Health District 2020). Foodborne illness occurs when people eat or drink beverages contaminated with bacteria and their toxins, parasites, viruses, chemicals, or other agents. The symptoms include severe stomach cramps, diarrhea, fever, nausea, and vomiting (Administration FDA 2020). Foodborne disease reported all over the world has confirmed the fact that many foodborne disease outbreaks result from improper food handling, such as the use of leftover ingredients, improper food storage, and poor personal hygiene (Campos et al. 2009, FAO 2013, Hejar et al. 2011, Ryu et al. 2011).

Thailand's hot weather alternating with rain compounds the problems of contamination, as these climatic conditions are suitable for the growth of many pathogens, especially for diseases caused by food and water. This has been compounded by the coronavirus 2019 epidemic (COVID-19), as most people are restricted to their homes to reduce the spread and infection. Therefore, many people are preparing their food, which can cause sickness from food and water-borne diseases if not made properly, use unhygienic conditions, or involve undercooked or unheated food or easily spoiled food. Therefore, morbidity due to diarrhea

caused by unsafe food and water consumption requires much attention and surveillance. Consequently, this study investigated the biological quality of food and drinking water samples to develop guidelines to prevent poor food and drinking water consumption as basic data for government sectors to control and monitor the food and drinking water quality.

## MATERIALS AND METHODS

In total, 40 water samples were collected from bottled drinking water, 50 water samples were collected from vending machines, 30 water samples from households, 30 food samples from households, and 60 food samples were collected from food stalls, using a standard method (APHA 2017) and examined for total coliform bacteria and fecal coliform bacteria using the most probable number (MPN) method and *Escherichia coli* using the streak plate method.

### Drinking Water Analysis

The drinking water samples were analyzed in the laboratory for total coliform bacteria, and fecal coliform bacteria were determined with the MPN method. All parameters were determined according to the standard methods for examining water and wastewater, 23$^{rd}$ edition (APHA 2017).

### Food Analysis

All food samples were detected for the presence of total

coliform bacteria was carried out using a rapid test kit (SI-2) and *Escherichia coli* (*E. coli*) using the MPN method according to the standard methods and streak plate method according to the Clinical Microbiology Procedures Handbook, 4$^{th}$ Edition (Leber 2020).

## RESULTS

### Drinking Water Quality

**Household drinking water quality**: The 30 household drinking water samples used to analyze the biological drinking water quality had levels of total coliform bacteria (TCB) and fecal coliform bacteria (FCB), as presented in Table 1.

Analysis of the biological quality of the drinking water from households showed that all household drinking water samples contained TCB, and half were contaminated with FCB. The drinking water quality analysis indicated the samples did not meet the standards with the World Health Organization value, which requires that no TCB and FCB be detected in drinking water.

**Bottled drinking water quality:** Forty samples were taken from bottled drinking water sold in shops and analyzed for TCB and FCB in the laboratory. The results are shown in Table 2.

The results of the microbiological analysis show that the bottled drinking water quality was very poor, as all samples

Table 1: Biological characteristics based on total coliform bacteria (TCB) and fecal coliform bacteria (FCB) of drinking water quality from household drinking water (N = 30).

| Drinking water sample | TCB [MPN.100 mL$^{-1}$] | FCB [MPN.100 mL$^{-1}$] | Drinking water sample | TCB [MPN.100 mL$^{-1}$] | FCB [MPN.100 mL$^{-1}$] |
|---|---|---|---|---|---|
| 1 | ≥ 2,400 | 2.87 | 16 | **< 2.2** | 0 |
| 2 | 7.17 | 0 | 17 | **< 2.2** | 0 |
| 3 | **< 2.2** | **< 2.2** | 18 | **< 2.2** | 0 |
| 4 | **< 2.2** | 0 | 19 | **< 2.2** | **< 2.2** |
| 5 | **< 2.2** | **< 2.2** | 20 | 5.20 | **< 2.2** |
| 6 | ≥ 2,400 | 3.43 | 21 | **< 2.2** | **< 2.2** |
| 7 | **< 2.2** | **< 2.2** | 22 | 4.26 | **< 2.2** |
| 8 | **< 2.2** | 0 | 23 | **< 2.2** | 0 |
| 9 | 2.77 | **< 2.2** | 24 | **< 2.2** | **< 2.2** |
| 10 | **< 2.2** | **< 2.2** | 25 | **< 2.2** | 0 |
| 11 | **< 2.2** | 0 | 26 | **< 2.2** | 0 |
| 12 | 2.72 | **< 2.2** | 27 | ≥ 2,400 | 4.26 |
| 13 | 4.35 | **< 2.2** | 28 | **< 2.2** | 0 |
| 14 | **< 2.2** | 0 | 29 | **< 2.2** | 0 |
| 15 | **< 2.2** | 0 | 30 | **< 2.2** | 0 |

MPN = most probable number; Drinking water quality with the World Health Organization was established for TCB and FCB to be undetected (WHO 2017).

had total coliform bacteria and fecal coliform bacteria that exceeded the standard (In drinking water, TCB and FCB must not be found).

The results of the microbiological analysis show that the bottled drinking water was very poor, as all samples had total coliform and fecal coliform bacteria that exceeded the WHO standard value.

**Drinking water vending machines:** In the laboratory, 50 water samples were taken from Drinking water vending and analyzed for TCB and FCB. The results are shown in Table 3.

Out of 50 samples tested from drinking water vending machines. The results were reported of all drinking water vending machine samples containing TCB and FCB. Indicated that it exceeded the standard for drinking water with the World Health Organization value, which requires that no TCB and FCB be detected in drinking water.

**Biological Characteristics of Food Quality**

**Household food:** Coliform bacteria were detected using a rapid test kit (SI-2), and *E. coli* using streak plates of 30 household food samples. The results are shown in Table 4.

Coliform bacteria were detected in 29 (97%) of the samples of household food, and 12 (40%) of the samples were contaminated with *Escherichia coli*. Of all the food samples analyzed, only one passed the standard (3%), and 29 (97%) did not meet the standard.

**Food stall:** Sixty food samples were taken from the food stall, and the detection of *E. coli* in the laboratory by using streak plates. The results are shown in Table 5.

The results of the *Escherichia coli* analysis show that the quality of the food stall was very poor, 40 (66.67 %) samples had levels of *E. coli* that exceeded the standard, and 20 (33.33 %) did not meet the standard with the Ministry of Public Health guideline value indicated of food uncleanness caused by unsanitary sanitation of food stalls.

## DISCUSSION

Contamination of drinking water by TCB and FCB is an important hazard indicator. Bacteria may contaminate the soil, water influenced by surface water, and human or animal waste (Yongyod 2018). The World Health Organization has stipulated that such bacteria must never be detected in drinking water. Contaminated drinking water and poor

Table 2: Biological characteristics based on total coliform bacteria (TCB) and fecal coliform bacteria (FCB) of drinking water quality from bottled drinking water (N = 40)

| Drinking water sample | TCB [MPN.100 mL$^{-1}$] | FCB [MPN.100 mL$^{-1}$] | Drinking water sample | TCB [MPN.100 mL$^{-1}$] | FCB [MPN.100 mL$^{-1}$] |
|---|---|---|---|---|---|
| 1 | < 2.2 | < 2.2 | 21 | 41 | 4 |
| 2 | 6 | < 2.2 | 22 | 17 | 3 |
| 3 | 8 | 4 | 23 | 12 | 4 |
| 4 | 3 | < 2.2 | 24 | 9 | < 2.2 |
| 5 | 3 | < 2.2 | 25 | 25 | 6 |
| 6 | 4 | < 2.2 | 26 | 28 | 27 |
| 7 | 68 | < 2.2 | 27 | 36 | 16 |
| 8 | 9 | 3 | 28 | ≥ 2,400 | ≥ 2,400 |
| 9 | < 2.2 | < 2.2 | 29 | 6 | 4 |
| 10 | 8 | 6 | 30 | 6 | 4 |
| 11 | < 2.2 | < 2.2 | 31 | 19 | 12 |
| 12 | < 2.2 | < 2.2 | 32 | 4 | < 2.2 |
| 13 | 3 | 3 | 33 | ≥ 2,400 | ≥ 2,400 |
| 14 | 16 | 10 | 34 | 107 | 107 |
| 15 | 3 | 3 | 35 | ≥ 2,400 | 8 |
| 16 | ≥ 2,400 | < 2.2 | 36 | 23 | 8 |
| 17 | ≥ 2,400 | 71 | 37 | ≥ 2,400 | 18 |
| 18 | 18 | 3 | 38 | ≥ 2,400 | ≥ 2,400 |
| 19 | 3 | < 2.2 | 39 | 4 | < 2.2 |
| 20 | < 2.2 | < 2.2 | 40 | ≥ 2,400 | ≥ 2,400 |

Table 3: Biological characteristics based on total coliform bacteria (TCB) and fecal coliform bacteria (FCB) of drinking water vending machines (N = 50).

| Drinking water sample | TCB [MPN.100 mL$^{-1}$] | FCB MPN.100 mL$^{-1}$] | Drinking water sample | TCB [MPN.100 mL$^{-1}$] | FCB [MPN.100 mL$^{-1}$] |
|---|---|---|---|---|---|
| 1 | ≥ 2,400 | 22 | 26 | 21 | 7.8 |
| 2 | ≥ 2,400 | 4 | 27 | ≥ 2,400 | ≥ 2,400 |
| 3 | 540 | < 2.2 | 28 | 540 | 217 |
| 4 | 4.5 | < 2.2 | 29 | 32 | 15 |
| 5 | 21 | 8.2 | 30 | < 2.2 | < 2.2 |
| 6 | 7.8 | < 2.2 | 31 | ≥ 2,400 | ≥ 2,400 |
| 7 | 140 | < 2.2 | 32 | ≥ 2,400 | ≥ 2,400 |
| 8 | 3.6 | < 2.2 | 33 | ≥ 2,400 | 350 |
| 9 | ≥ 2,400 | < 2.2 | 34 | 4 | < 2.2 |
| 10 | 17 | < 2.2 | 35 | < 2.2 | < 2.2 |
| 11 | ≥ 2,400 | 3.6 | 36 | < 2.2 | < 2.2 |
| 12 | 540 | 11 | 37 | 31 | < 2.2 |
| 13 | 4 | < 2.2 | 38 | 43 | < 2.2 |
| 14 | 26 | 23 | 39 | 7.8 | < 2.2 |
| 15 | ≥ 2,400 | 13 | 40 | 70 | < 2.2 |
| 16 | 920 | 33 | 41 | 6.1 | 5.6 |
| 17 | 5 | < 2.2 | 42 | < 2.2 | < 2.2 |
| 18 | < 2.2 | < 2.2 | 43 | ≥ 2,400 | < 2.2 |
| 19 | 5.5 | 3.7 | 44 | 6.1 | < 2.2 |
| 20 | < 2.2 | < 2.2 | 45 | < 2.2 | < 2.2 |
| 21 | < 2.2 | < 2.2 | 46 | < 2.2 | < 2.2 |
| 22 | ≥ 2,400 | 3.7 | 47 | < 2.2 | < 2.2 |
| 23 | ≥ 2,400 | 14 | 48 | < 2.2 | < 2.2 |
| 24 | < 2.2 | < 2.2 | 49 | < 2.2 | < 2.2 |
| 25 | 23 | 7.8 | 50 | < 2.2 | < 2.2 |

MPN = most probable number; Drinking water quality with the WHO value for TCB and FCB to be not detected (WHO 2017).

Table 4: Detection of coliform bacteria and *E. coli* in household food samples (N=30).

| Food sample number | Coliform bacteria | *E. coli* | Food sample number | Coliform bacteria | *E. coli* |
|---|---|---|---|---|---|
| 1 | + | + | 16 | + | + |
| 2 | + | - | 17 | + | - |
| 3 | + | + | 18 | + | + |
| 4 | + | - | 19 | + | + |
| 5 | - | - | 20 | + | - |
| 6 | + | - | 21 | + | + |
| 7 | + | - | 22 | + | - |
| 8 | + | - | 23 | + | + |
| 9 | + | - | 24 | + | + |
| 10 | + | - | 25 | + | + |
| 11 | + | - | 26 | + | + |
| 12 | + | - | 27 | + | - |
| 13 | + | - | 28 | + | - |
| 14 | + | - | 29 | + | + |
| 15 | + | - | 30 | + | + |

The standard for food from the Ministry of Public Health (2020). + = Positive  - = Negative

Table 5: Detection of *E. coli* in food stall samples (N=60).

| Food sample number | *E. coli* | Food sample number | *E. coli* | Food sample number | *E. coli* |
|---|---|---|---|---|---|
| 1 | + | 21 | + | 41 | - |
| 2 | + | 22 | + | 42 | - |
| 3 | - | 23 | + | 43 | + |
| 4 | - | 24 | + | 44 | + |
| 5 | - | 25 | - | 45 | - |
| 6 | + | 26 | + | 46 | + |
| 7 | + | 27 | + | 47 | + |
| 8 | + | 28 | - | 48 | + |
| 9 | + | 29 | - | 49 | + |
| 10 | + | 30 | + | 50 | + |
| 11 | + | 31 | + | 51 | + |
| 12 | + | 32 | + | 52 | + |
| 13 | + | 33 | - | 53 | + |
| 14 | - | 34 | - | 54 | + |
| 15 | + | 35 | + | 55 | + |
| 16 | - | 36 | + | 56 | + |
| 17 | - | 37 | - | 57 | + |
| 18 | - | 38 | - | 58 | + |
| 19 | - | 39 | + | 59 | + |
| 20 | - | 40 | - | 60 | + |

The standard for food from the Ministry of Public Health (2020). + = Positive  - = Negative

sanitation are linked to the transmission of contaminating bacteria. Poor quality drinking water is a significant factor affecting the health of consumers (WHO 2018). Causes of bacterial contamination in bottled drinking water may result from a drinking water factory that does not meet the standards, especially from poor production processes and poor worker hygiene, such as not wearing gloves, masks, and hats. There was no hand washing after going to the toilet before filling the water (Bereda et al. 2016, Li & Wu 2019, Phusomya & Yongyod 2022).

Additionally, bacterial contamination can occur in the home due to the incorrect storage location of drinking water bottles, such as near the toilet, garbage disposal point, on the ground, or in a corner that may be the habitat of animals, insects, diseases, germs, and bacteria. Bacterial contamination from drinking water vending machines may be due to insufficient cleaning and sanitation of the water vending machines. Low quality of membrane filtration and lack of disinfection may contribute to bacteria re-growth after water treatment (Phusomya & Yongyod 2022). High coliform bacteria present in drinking water also indicate that the water treatment system in vending machines is not being sanitized and maintained regularly (Tan et al. 2016).

Coliform bacteria and *E. coli* in household foods and food stalls can be linked to contamination resulting from inappropriate processing, incomplete heating, using contaminated water during preparation and washing, or secondary contamination due to contact with contaminated materials such as chopping boards, knives, and serving utensils. These bacteria in foods could induce potential health problems for consumers. Poor personal hygiene, improper handling and storage practices of foods, and poor knowledge of safe cooking methods are associated risk factors that must be properly managed to reduce the potential for food contamination by foodborne diseases (Bereda et al. 2016). Food safety public awareness and control measures must be continually addressed to reduce and limit *E. coli*. Proper hand washing, preventing cross-contamination while preparing food, storage of meat below 4.4°C, and using a thermometer to confirm an internal temperature of 71°C during cooking are considered necessary steps to take for preventing foodborne illnesses (Baker et al. 2016, FSIS 2011, Vogt & Dippold 2005). The potential negative effects of contamination include food poisoning, diarrhea, or, in severe cases, even death (Daud et al. 2017, Pratum & Khananthai 2017).

## CONCLUSION

The biological quality of drinking water in the household and in purchased bottled water indicated that the major problem in the drinking water was total coliform bacteria and fecal coliform bacteria. Household food samples and food stall samples indicated that the major contamination was coliform bacteria and *Escherichia coli*. Consequently, suitable factory and household raw materials should be utilized along with strict compliance with sanitary principles to obtain quality drinking water and food that are not harmful to human health.

The findings of this study advised that the government sectors should monitor the drinking water factories in addition to monitoring drinking water and food quality to ensure the water and food produced are of acceptable quality. The government should improve consumer knowledge about food safety, foodborne diseases, and good personal hygiene and sanitation to improve the health quality of household food.

## ACKNOWLEDGEMENTS

## REFERENCES

Administration FDA. 2020. Foodborne pathogens. Food and beverages. Food and Drug Administration, Silver Springs, MD, USA.

American Public Health Association (APHA) 2017. Standard Methods for the Examination of Water and Wastewater. 23rd ed. American Public Health Association Inc, Washington DC, The USA.

Baker, C.A., Rubinelli, P.M., Park, S.H., Carbonero, F. and Ricke, S.C. 2016. Shiga toxin-producing *Escherichia coli* in food: Incidence, ecology, and detection strategies. Food Cont., 59: 407-419.

Bereda, T.W., Emerie, Y.M., Reta, M.A. and Asfaw, H.S. 2016. Microbiological safety of street vended foods in Jigjiga City, Eastern Ethiopia. Ethiop. J. Health Sci., 26(2): 163-172.

Campos, A.K.C., Cardonha, Â.M.S., Pinheiro, L.B.G., Ferreira, N.R., de Azevedo, P.R.M. and Stamford, T.L.M. 2009. Assessment of personal hygiene and practices of food handlers in municipal public schools of Natal, Brazil. Food Contr., 20(9): 807-810.

Center for Disease Control (CDC). 2020. Foodborne Germs and Illnesses. Available at: https://www.cdc.gov/foodsafety/foodborne-germs.html (Accessed May 9, 2021).

Daud, M.K., Nafees, M., Ali, S., Rizwan, M., Bajwa, R.A., Shakoor, M.B., Arshad, M.U., Chatha, S.A.S., Deeba, F., Murad, W. and Malook, I. 2017. Drinking water quality status and contamination in Pakistan. BioMed Res. Int., 17: 651.

Department of Disease Control (DDC). 2020. Ripe, hot, clean: preventing food and water communicable diseases. Thailand. Available at: https://ddc.moph.go.th/brc/news.php?news=12792&deptcode=brc (Accessed May 14, 2021).

Food and Agriculture Organization (FAO) 2013. Foodborne disease monitoring and surveillance systems. Available at: http://www.fao.org/3/J2381E/J2381E.htm (Accessed May 30, 2021).

FSIS. 2011. Shiga toxin-producing *Escherichia coli* in certain raw beef products. Fed. Reg., 76(182): 2010-0023.

Hejar, A., NorAfiah, M., Hayati, K., Salmiah, S., Yusma, M. and Titi, R. 2011. Cleanliness of food premises in Bahau. Malay. J. Pub. Med., 11(3): 31.

Leber, A.L. 2020. Clinical microbiology procedures handbook. Fourth Edition. John Wiley & Sons, American Society of Microbiology, Washington, DC, USA.

Li, P. and Wu, J. 2019. Drinking water quality and public health. Exp. Health, 11(2): 73-79.

Ministry of Public Health. 2020. Notification of Ministry of Public Health (No 414) B.E. 2563, Issued by virtue of the Food Act B.E.2522, Re: Standards for Contaminants in Food. Ministry of Public Health, Thailand.

Office of Health District. 2020. Annual Report 2020, Office of Health District 8. Strategy and Information Group, Ministry of Public Health, Thailand.

Phusomya, P. and Yongyod, R. 2022. Application of hazard analysis and critical control points concept for rural bottled drinking water production process. Urban Water J., 19(10): 1060-1065.

Pratum, C. and Khananthai, N. 2017. Assessment of factors affecting drinking water quality from free water dispensers in the higher education institution. IJESE, 12: 787-797.

Ryu, J.H., Ko, J., Park, H., Yang, S. and Kim, H. 2011. Microbial examination of nonheated foods served in feeding programs of elementary schools, Iksan City, Jeonbuk Province, Korea. J.Food Protect., 74(9): 1564-1568.

Tan, E.Y., Arifullah, M. and Soon, J.M. 2016. Identification of *Escherichia coli* strains from water vending machines of Kelantan, Malaysia, using 16S rRNA gene sequence analysis. Exp. Health, 8: 211-216.

Vogt, R.L. and Dippold, L. 2005. *Escherichia coli* O157: H7 outbreak associated with consumption of ground beef, June-July 2002. Pub. Health Rep., 120(2): 174-178.

World Health Organization (WHO). 2017. Guidelines for Drinking Water Quality. Fourth Edition incorporating the first addendum, World Health Organization, Geneva, Switzerland.

World Health Organization (WHO) 2018. Drinking Water. World Health Organization fact sheets, Available at: https://www.who.int/en/news-room/factsheets/detail/drinking-water (Accessed June 15, 2021).

Yongyod, R. 2018. Drinking water quality and evaluation of environmental conditions of water vending machines. Asia-Pac. J. Sci. Technol., 23(1): 1-5.

*... Continued from inner front cover*

- The text of the manuscript should run into Abstract, Introduction, Materials & Methods, Results, Discussion, Acknowledgement (if any) and References or other suitable headings in case of reviews and theoretically oriented papers. However, short communication can be submitted in running with Abstract and References. The references should be in full with the title of the paper.

- The figures should preferably be made on a computer with high resolution and should be capable of withstanding a reasonable reduction with the legends provided separately outside the figures. Photographs may be black and white or colour.

- Tables should be typed separately bearing a short title, preferably in vertical form. They should be of a size, which could easily be accommodated in the page of the Journal.

- References in the text should be cited by the authors' surname and year. In case of more than one reference of the same author in the same year, add suffix a,b,c,.... to the year. For example: (Thomas 1969, Mass 1973a, 1973b, Madony et al. 1990, Abasi & Soni 1991).

## List of References

The references cited in the text should be arranged alphabetically by authors' surname in the following manner: (Note: The titles of the papers should be in running 'sentence case', while the titles of the books, reports, theses, journals, etc. should be in 'title case' with all words starting with CAPITAL letter.)

Dutta, A. and Chaudhury, M. 1991. Removal of arsenic from groundwater by lime softening with powdered coal additive. J. Water Supply Res. Techno. Aqua., 40(1) : 25-29.

Hammer, D.A. (ed.) 1989. Constructed Wetlands for Wastewater Treatment-Municipal, Industrial and Agricultural. Lewis Publishers Inc., pp. 831.

Haynes, R. J. 1986. Surface mining and wetland reclamation. In: Harper, J. and Plass, B. (eds.) New Horizons for Mined Land Reclamation. Proceedings of a National Meeting of the Ameri can Society for Surface Reclamation, Princeton, W.V.

## Submission of Papers

- The paper can be submitted by e-mail as an attachment in a single WORD file at **contact@neptjournal.com**
- The paper can also be submitted online in a single WORD file through the online submission portal of journal's website: **www.neptjournal.com**

## Attention

1. Any change in the authors' affiliation may please be notified at the earliest.
2. Please make all the correspondence by e-mail, and authors should always quote the manu script number.

**Note:** In order to speed up the publication, authors are requested to correct the galley proof immediately after receipt. The galley proof must be checked with utmost care, as publishers owe no responsibility for mistakes. The papers will be put on priority for publication only after receiving the processing and publication charges.

For further details of the Journal, please visit the website. All the papers published on a particular subject/topic or by any particular author in the journal can be searched and accessed by typing a keyword or name of the author in the 'Search' option on the Home page of the website. All the papers containing that keyword or author will be shown on the home page from where they can be directly downloaded.

## www.neptjournal.com